



# X-RAYS IN PRACTICE





# X-RAYS IN PRACTICE

---

BY

WAYNE T. SPROULL, PH. D.

*Physicist, Research Laboratories Division  
General Motors Corporation*

*First Edition*

*Third Impression*

*New York*

*London*

McGRAW-HILL BOOK COMPANY, INC.

1946

# X-RAYS IN PRACTICE

COPYRIGHT, 1946, BY THE  
MCGRAW-HILL BOOK COMPANY, INC.

---

PRINTED IN THE UNITED STATES OF AMERICA

*All rights reserved. This book, or  
parts thereof, may not be reproduced  
in any form without permission of  
the publishers.*

## PREFACE

The publication of this book very nearly coincides with the fiftieth anniversary of the discovery of x-rays and with the hundredth anniversary of the birth of their discoverer, W. C. Röntgen. The knowledge that has been accumulated about these rays, and the ways in which they have been applied for the benefit of mankind during the past fifty years, comprise the broad subject which we have tried to present to the reader within the confines of a volume of ordinary size.

Special effort has been made to index the book so completely that it will serve the needs of the person desiring a ready reference giving quick answers to specific questions about x-rays. Extensive bibliographical footnotes have been included so that this type of reader will usually find key references serving as a starting point for more extensive reading in the scientific literature. The tables in the Appendix should prove helpful to all types of reader.

On the other hand, a serious endeavor has been made to arrange the material in a logical sequence and to make it sufficiently readable so that the student interested in x-rays and their applications will find the book convenient as a text. The student with little or no previous training in physics or mathematics will find the treatment of some of the quantitative aspects difficult in places, but an effort has been made to interpret such mathematical passages in words so that their chief significance is readily grasped. If one skips over a portion that seems too involved or uninteresting, it should not be difficult to resume the thread of the story farther on. Before reading beyond Chap. 13, it would be definitely advisable for one unacquainted with trigonometry to consult a trigonometry book to become acquainted with the concept of the sine of an angle. The questions at the end of each chapter should help the student to check the thoroughness of his reading as he proceeds.

The inclusion of only a single chapter on medical applications, as contrasted to the numerous chapters on diffraction, is not to be construed as an indication of the relative importance of the two fields. This circumstance arises from the fact that x-ray diffraction theory has been extensively developed in a quantitative manner. It is inseparably interwoven through the modern theories of solids and crystallography. On the other hand, x-ray techniques have infiltrated into medical science in a somewhat supplementary way not involving such extensive mathematical treatment.

# CONTENTS

	PAGE
PREFACE . . . . .	V
CHAPTER	
1. HISTORY OF X-RAYS. . . . .	1
2. FUNDAMENTALS OF X-RAY TUBES. . . . .	6
3. THE CONTINUOUS X-RAY SPECTRUM. . . . .	20
4. CHARACTERISTIC X-RAY SPECTRA. . . . .	45
5. ABSORPTION AND SCATTERING; SECONDARY X-RAYS . . . . .	71
6. REFRACTION OF X-RAYS AND THEIR DIFFRACTION BY RULED GRATINGS . . . . .	96
7. X-RAY GENERATING EQUIPMENT . . . . .	105
8. RUDIMENTS OF RADIOACTIVITY . . . . .	157
9. X-RAY DETECTION, MEASUREMENT, AND REGISTRATION . . . . .	168
10. PROTECTION . . . . .	198
11. X-RAYS IN THE MEDICAL FIELD (RADIOLOGY) . . . . .	211
12. INDUSTRIAL RADIOGRAPHY. . . . .	239
13. MISCELLANEOUS APPLICATIONS. . . . .	285
14. CRYSTALLOGRAPHY BEFORE THE DISCOVERY OF X-RAY DIF- FRACTION . . . . .	299
15. LAWS OF X-RAY DIFFRACTION IN A CRYSTAL. . . . .	320
16. THE BRAGG METHOD OF CRYSTAL ANALYSIS AND SOME PERTI- NENT PROPERTIES OF ACTUAL CRYSTALS. . . . .	331
17. THE LAUE METHOD, THE ROTATION METHOD, AND OTHER METHODS FOR A SINGLE CRYSTAL. . . . .	371
18. THE HULL-DEBYE-SCHERRER POWDER METHOD . . . . .	391
19. CHEMICAL ANALYSIS BY X-RAY DIFFRACTION. . . . .	420
20. GRAIN SIZE AND PREFERENTIAL ORIENTATION . . . . .	438
21. THE MEASUREMENT OF STRESS AND STRAIN BY X-RAY DIF- FRACTION; DIFFUSE REFLECTIONS. . . . .	468
22. X-RAY DIFFRACTION BY AMORPHOUS SOLIDS, LIQUIDS, AND GASES	496
23. ADDITIONAL APPLICATIONS OF X-RAY DIFFRACTION . . . . .	514
24. ELECTRON DIFFRACTION AND ITS APPLICATIONS. . . . .	536
APPENDIX. . . . .	561
INDEX . . . . .	593

It is a pleasant obligation to acknowledge that this book could never have been written at all without the aid of the vast literature on x-rays already existing. Among the books from which figures, tables, and information have been borrowed, special mention is due to the following: W. H. Bragg and W. L. Bragg, "The Crystalline State," George Bell & Sons, Ltd., and the Macmillan Company; A. H. Compton and S. K. Allison, "X-rays in Theory and Practice," D. Van Nostrand Company, Inc.; M. J. Buerger, "X-ray Crystallography," John Wiley & Sons, Inc.; G. W. Files, "Medical Radiographic Technic," Charles C. Thomas, Publisher; C. D. Hodgman, "Handbook of Chemistry and Physics," Chemical Rubber Publishing Co.; L. G. H. Sarsfield, "Electrical Engineering in Radiology," Chapman & Hall, Ltd.; M. Siegbahn, "X-ray Spectroscopy," Oxford University Press; G. P. Thomson and W. Cochran, "Theory and Practice of Electron Diffraction," the Macmillan Company; R. W. G. Wyckoff, "Structure of Crystals," Reinhold Publishing Corporation; also, such McGraw-Hill books as G. L. Clark, "Applied X-rays"; W. P. Davey, "A Study of Crystal Structure and Its Applications"; and F. K. Richtmyer and E. H. Kennard, "Introduction to Modern Physics."

Equally important are the numerous figures, tables, and information secured from a large number of periodicals. Of these, most are acknowledged in legends and footnotes.

Special mention is also due to General Motors Corporation for permission to publish numerous radiographs, diffraction patterns, and other material, and for excellent library facilities and other kind cooperation. The photographs and diagrams of x-ray equipment have been generously furnished by the General Electric X-ray Corporation, Machlett Laboratories, Inc., North American Philips Co., Inc., Picker X-ray Corp., Victoreen Instrument Co., and Westinghouse Electric & Mfg. Co., X-ray Division.

Much of the material for the final chapter on electron diffraction was taken from the work of Dr. W. W. Beeman, carried out while he worked with the author at General Motors. Thanks are also due to Prof. J. T. Norton of Massachusetts Institute of Technology and to Dr. E. J. Martin and A. E. Roach of General Motors for reviewing the manuscript and for helpful suggestions. Finally, the assistance and encouragement of my wife, Ethel, have greatly lightened the task.

WAYNE T. SPROULL.

DETROIT, MICH.,  
*January, 1946.*



## CHAPTER 1

### HISTORY OF X-RAYS

About 1890 the basic outline of the science of physics appeared to be practically complete. That is, it appeared that the general extent of the final structure was fairly well delineated by the portion already erected. Newton's laws of motion and gravitation, the concept of conservation of energy, the inverse square laws of magnetism and electrostatics, the kinetic theory of gases, Maxwell's equations, and Faraday's laws fully accounted for everything from the motion of the planets and the operation of an engine to the Brownian movement. The design of a telephone system, a bridge, or an electric power station was based on the same known fundamentals.

This physics of 1890 is now known as "classical physics." In 1890 it accounted for practically all known natural phenomena except a few obscure academic curiosities like the photoelectric effect and the spectral distribution of black-body radiation.

This happy picture of a science so complete that only minor details remained to be filled in did not long endure, however. The photoelectric effect was discovered in 1887. In rapid succession there followed the discovery of x-rays in 1895, radioactivity in 1896, and the electron in 1897. To cap the climax, in 1900 Planck succeeded in accounting for the spectral distribution of black-body radiation by assuming that the radiation consisted of integral indivisible "quanta" rather than continuous electromagnetic waves.

All these new developments were disconcerting. They not only failed to fit into the classical picture but often forced one to conclusions contradictory to it. Thus the discovery of x-rays is to be regarded as not merely another scientific discovery but one of a small group that initiated a new scientific era.

Late in 1895 some experiments on the properties of cathode rays were being conducted at the University of Würzburg in Germany by Wilhelm Conrad Röntgen, professor of physics. Many other scientists such as Hittorf, Crookes, and Lenard had been studying the properties of cathode rays for several years, but Röntgen noticed an effect that had escaped all the others. Since he was studying the fluorescence caused by the cathode rays, he was working in a dark room, and he was led to cover the cathode-ray tube with a black cardboard box, which of course prevented any visible light or ultraviolet radiation from escaping. In



spite of this, however, Röntgen observed that a screen coated barium platinocyanide glowed brilliantly when brought near the cathode tube. He made this epochal discovery on Nov. 8, 1895.<sup>1</sup>

Investigating this phenomenon, he soon concluded that it was caused by the generation of some hitherto unknown type of radiation from the cathode-ray tube, the new rays being invisible but ab-

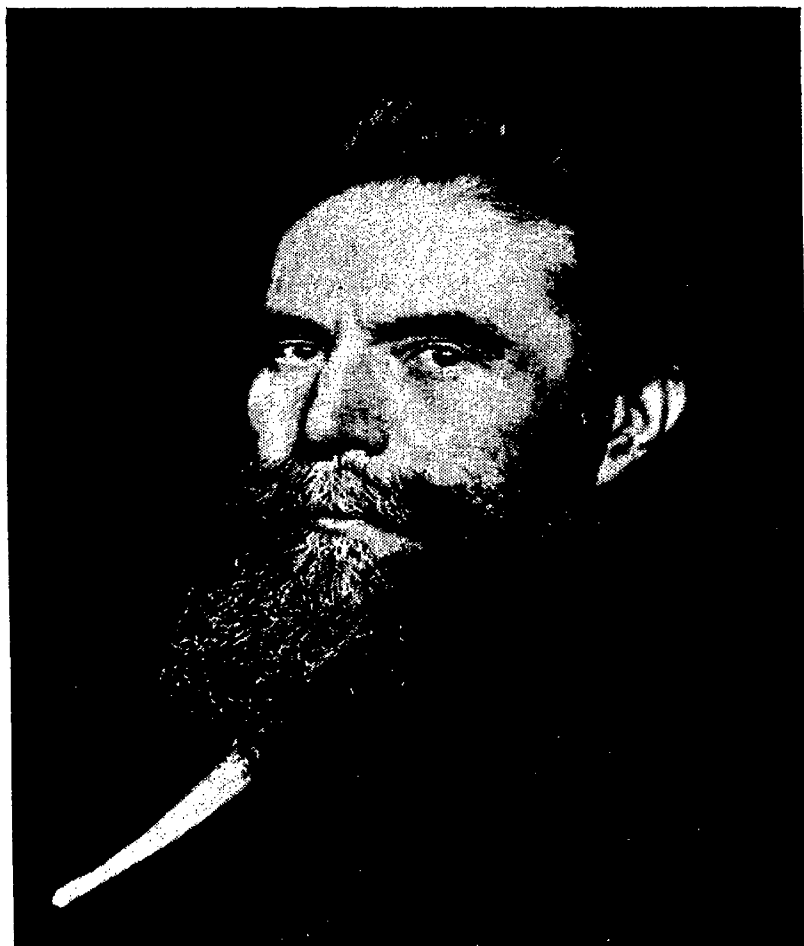


FIG. 1-1.—W. C. Röntgen. (Mar. 27, 1845–Feb. 10, 1923.)

cause visible fluorescence in certain materials such as barium platinocyanide. In his first published paper<sup>2</sup> describing the new rays, he called x-rays, he mentioned that they would penetrate a thousand-page book, a sheet of aluminum  $3\frac{1}{2}$  millimeters thick, and lead. He also mentioned that when he held his hand in front of the screen coated with barium platinocyanide the outlines of the bones in his hand could be seen on the screen. He stated that the rays acted like a photographic plate and suggested that this opened the possibility of

<sup>1</sup> See Otto Glasser, "Wilhelm Conrad Röntgen and the Early History of Roentgen Rays," Charles C. Thomas, Publisher, Springfield, Ill., 1934.

<sup>2</sup> W. C. Röntgen, *Ann. Physik*, **64**, 1 (1898), reprinted from an earlier publication in 1895.

taking pictures in a light room by enclosing the photographic plate in a lighttight holder, or "cassette," as he called it.

Many others immediately began experiments with these strange, new, penetrating rays, but it was not until 1912 that any really significant advance was made in the scientific understanding of their fundamental nature. Between 1895 and 1912 medical men learned to use x-rays as a powerful new tool in diagnosis. Almost immediately they were used as a means of photographing the bones of living people and animals, for detecting and setting fractures, and for detecting and locating foreign objects such as bullets and swallowed pins. This use of x-rays is known as *radiography*. The terms "radiography" and "radiograph" are analogous to the terms "photography" and "photograph," except that x-rays or gamma rays (to be discussed later) play the role played by light in photography. As the technique was improved, medical men eventually learned to recognize such phenomena as tubercular lesions, etc., in a radiographic picture.

During this period many of the pioneer experimenters suffered severe x-ray burns, which were found to be incurable in many cases; often fingers, hands, and arms were lost. Eventually, physicians learned to make use of this ability of the x-rays to kill living tissues by directing the rays at tumors and other diseased regions that they desired to destroy. It was found that such diseased tissues could be killed by a smaller dose of x-rays than that required to kill normal healthy tissue. Thus the technique of *x-ray therapy* was gradually developed, in which the basic idea is to apply a lethal dose of x-rays to diseased regions without exceeding the tolerance limit of the adjacent healthy tissue.

From the scientific point of view, however, the first milestone in the history of x-rays was their discovery by Röntgen in 1895. The next was the discovery of x-ray diffraction by crystals by M. Laue, W. Friedrich, and P. Knipping<sup>1</sup> in 1912.

Earlier experimenters had often tried to produce interference and diffraction effects with x-rays but had met with only indifferent success. However, they were able to conclude that x-rays consisted of waves having a length of the order of  $10^{-9}$  centimeter. On the other hand, crystallographers as early as 1850 had concluded that the atoms in a crystal must be arranged in a geometric space lattice in which the spacing between atoms was of the order of  $10^{-8}$  cm. Apparently Laue was the first to whom these two considerations suggested the idea that a crystal should serve as a diffraction grating for x-rays. Laue, being a theoretical physicist, asked Friedrich and Knipping, two experimental physicists, to try to observe the diffraction of x-rays by a single crystal. They

<sup>1</sup> M. Laue, W. Friedrich, and P. Knipping, *Ann. Physik*, **41**, 971 (1913), reprinted from an earlier publication in 1912.

set up suitable apparatus and soon discovered that diffraction patterns of the type predicted by Laue were indeed produced by crystals of copper sulfate (blue vitriol), zinc blende, rock salt, and galena.

This discovery immediately provided a powerful new method for investigating the nature of x-rays by diffracting them with crystals and, perhaps even more important, for investigating the nature of solids (most of which are composed of crystals) by using them to diffract x-rays. New possibilities and applications of this method are still being discovered and invented, and the work already done in this field is so extensive as to constitute a whole new branch of physics entirely unknown 30 years ago. Although hundreds of workers have made their names well known in the field of x-ray diffraction, there are two whose work is so extensive and important as to deserve special mention—W. H. Bragg and W. L. Bragg.

The next milestone in the history of x-rays was the invention of the Coolidge tube by W. D. Coolidge.<sup>1</sup> From 1895 to 1913, all x-ray tubes were of the so-called "gas-filled" type. These were suitable for certain types of work at less than 50,000 volts and are still widely used today in diffraction work, but they were very awkward for radiographic work and impractical for the higher voltages such as 100 or 200 kilovolts now used for many common types of radiographic work. Except for a few special types of tubes for diffraction work, all modern x-ray tubes are of the Coolidge type. These tubes are exhausted to the best vacuum obtainable and the cathode consists of an incandescent tungsten filament.

Another milestone in the history of x-rays was also established in 1913 by H. G. J. Moseley,<sup>2</sup> who discovered that a portion of the x-rays radiated from the target of an x-ray tube has a wave length characteristic of and dependent upon the atomic number of the target material. Thus the elements chromium, manganese, iron, cobalt, nickel, copper, and zinc, having atomic numbers 24, 25, 26, 27, 28, 29, and 30, respectively, strongly emit x-rays having the following wave lengths, respectively, when they are bombarded with cathode rays: 2.3, 2.1, 1.9, 1.8, 1.7, 1.5, and 1.4 angstrom. This discovery led to the establishment of a satisfactory theory of the origin of characteristic x-ray spectra and also helped theoretical physicists such as Bohr and Rutherford to arrive at a fundamentally correct theory of the structure of the atom. The important and extensive research of A. H. Compton also deserves special mention.

During the 30 years that have elapsed since Moseley's discovery, there have been remarkable developments in the application of x-rays to many important new types of work. At the same time, techniques

<sup>1</sup> W. D. Coolidge, *Phys. Rev.*, **2**, 409 (1913).

<sup>2</sup> H. G. J. Moseley, *Phil. Mag.* **26**, 1024 (1913), **27**, 703 (1914).

have been vastly improved in many of the older fields. For example, today steel parts 6 inches thick and weighing many tons are radiographed for defects in a routine manner with million-volt equipment as quickly and as easily as Röntgen radiographed his own hand 50 years ago.

Quite recently, however, a new invention has appeared that appears likely to rank with the Coolidge tube as another important milestone in the history of x-rays. This is the electron induction accelerator invented and developed by D. W. Kerst,<sup>1</sup> which has already generated x-rays of great intensity with an energy of 100 million volts. This device has also been called a "betatron" and a "rheotron," and the theory of its operation has been worked out by Kerst and Serber.<sup>2</sup>

### QUESTIONS

1. What is meant by classical physics?
2. Can x-rays be seen directly? Are they dangerous or harmful without proper protection?
3. Distinguish between radiography, x-ray diffraction, and x-ray therapy.
4. What are the two features that distinguish a Coolidge tube from gas-filled x-ray tubes?
5. What is a cassette?

<sup>1</sup> D. W. Kerst, *Phys. Rev.*, **60**, 47 (1941); *Rev. Sci. Instruments*, **13**, 387 (1942).

<sup>2</sup> D. W. Kerst and R. Serber, *Phys. Rev.*, **60**, 53 (1941).

## CHAPTER 2

### FUNDAMENTALS OF X-RAY TUBES

**1. Generation of X-rays.** Let us visualize a machine gun bullets in rapid succession against the face of a large, heavy block of iron. A person standing near the spot where the bullets strike the block would be able to hear a plinking noise, indicating that sound-waves are generated by the bullets striking the block.

The generation of x-rays is very similar to this except that electrons are substituted for the bullets, the x-rays being analogous to the sound waves.

**2. Cathode Rays.** Electrons moving rapidly in a stream like machine gun bullets are called "cathode rays." Of course, the electrons are incomparably lighter than bullets, and their motion is very much swifter.

Obviously, it would be impossible to produce a satisfactory stream of machine-gun bullets by firing the gun down a long hall filled with baseballs to the ceiling with baseballs. In a similar way, if one wishes to produce cathode rays, he would naturally choose a vacuum in which to fire rather than the open air, because the molecules in ordinary air obstruct the passage of electrons much as a hall full of baseballs obstructs the passage of bullets.

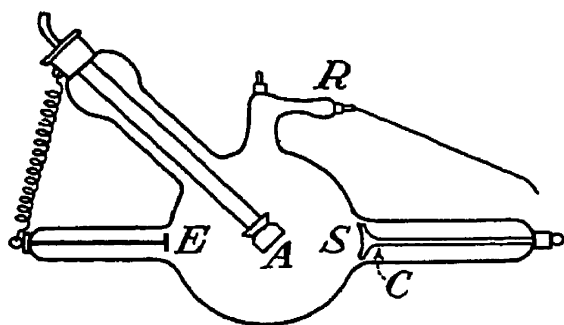


FIG. 2-1.—Diagram of early gas-filled x-ray tube.

**3. Gas-filled X-ray Tubes.** I shall now consider how one obtains the electrons. Before 1913, all x-ray tubes were of the "gas-filled" type. Gas-filled tubes are still used today for some types of diffraction work. The cathode rays are produced in a gas-filled tube somewhat as follows:

Figure 2-1 is a diagram of one of the early gas-filled x-ray tubes. A block of aluminum *C*, having a concave surface *S*, is located near one end of the partly evacuated glass tube, and a block of metal *A* is located near the center of the tube. These two pieces of metal are connected to a high-voltage electrical supply, and hence they are called "electrodes."

The concave aluminum electrode is negatively charged and hence is called the "cathode." The block of metal in the center is called the anticathode, or target from our machine-gun analogy. These early tubes were constructed with a third electrode *E* off to one side, which was positively charged (being directly connected to the anticathode) and is called the "anode."

The tube is evacuated to a pressure of about  $10^{-4}$  millimeter of mercury. Ordinary atmospheric pressure is about 760 mm. of mercury, so  $10^{-4}$  mm. of mercury is about  $10^{-7}$  atmosphere. Under these conditions, each cubic centimeter of space inside the tube still contains about  $3\frac{1}{2}$  trillion molecules, but even so the mean free path is about 50 centimeters, which means that a molecule of nitrogen or oxygen in the tube can travel more than a foot in a straight line, on the average, before it will collide with another molecule.

Owing to such causes as the presence of minute radioactive impurities and cosmic rays, there are always a few stray electrons present here and there in the tube. When a high voltage is applied, so as to make the cathode negative and the anode and anticathode positive, these electrons will be attracted to the latter and repelled by the former and hence will rush at high speed through the gas present, toward the anticathode. In so doing, a few of them will collide with some of the atoms of oxygen or nitrogen of which the air molecules are composed, and in many cases the collisions will be sufficiently violent to wrench an electron loose from the atom. (Atoms consist of a swarm of electrons electrically attached to a central positively charged nucleus.) The atoms thus bereft of one of their usual complement of electrons are called *ions*, and they carry a net positive charge. For example, a normal neutral nitrogen atom consists of a swarm of 7 electrons (each negatively charged) surrounding a central nucleus having a positive charge of 7 units just sufficient to neutralize the 7 negative electronic charges. When one of the 7 electrons is wrenched loose from the atom, the ion that is left consists of the nucleus with a charge of  $+7$  and the 6 remaining electrons with a charge of  $-6$ , leaving a net charge of  $+1$  for the ion.

Thus electrons rushing through the air at high speed produce more electrons by ejecting them from the atoms composing the air, and at the same time positive ions are produced. The electrons ejected from the atoms add to those initially present, and these, in turn, rush through the gas and produce by collision still more electrons and more ions. Thus the process is cumulative, and soon an enormous number of electrons is rushing toward the anticathode and a huge swarm of ions is rushing at a slower, yet very great speed toward the cathode.

In this manner, an electric discharge (similar to the one seen in the familiar neon signs) starts, and the large number of electrons streaming through the gas away from the cathode toward the anticathode constitutes the cathode rays needed to generate the x-rays when they strike the target, which is the general name given to the anticathode or anode or other metallic object (depending upon the construction of the tube) that most of the cathode rays strike. The positive ions likewise strike the cathode with great energy, where they pick up an electron and so

become neutral atoms again. This positive-ion bombardment of the cathode causes it to emit additional electrons, which also contribute to the electron stream constituting the cathode rays. The concave shape of the cathode distributes the high-voltage electrostatic field so as to focus the cathode rays upon a limited "focal spot" on the target.

Although the general operation of a gas-filled x-ray tube has been described here in only a brief qualitative way, enough has been said to indicate that the phenomena involved are of considerable complexity although the fundamental idea is merely to hurl electrons at high speed against a block of metal.

**4. Practical Operation of Gas-filled X-ray Tubes.** The electrons rushing through the tube away from the cathode and the positive ions rushing toward the cathode constitute an electric current passing through the tube, commonly called the "tube current." The magnitude of the current and the voltage between the electrodes is largely determined by the gas pressure in the tube. If the pressure is as great as  $10^{-3}$  mm. of mercury, so that the mean free path is only 5 cm., it will be found that a current of perhaps 50 or 100 milliamperes will flow through the tube when a potential difference as low as perhaps only two or three thousand volts is applied. It will be found impossible to build up a potential difference of, say, 20 kilovolts across the tube because the cumulative nature of the ionization process discussed in Sec. 3 causes a very great increase in the current when only a slight increase is made in the applied voltage.

If the pressure in the tube is as low as  $10^{-5}$  mm. of mercury, on the other hand, it will be found that a current of only a few microamperes can be forced through the tube, regardless of whether the applied potential is 5 kv. or 50 kv. This is due to the fact that the mean free path of the ions and electrons<sup>1</sup> in the gas is now about 5 meters so that very few of the electrons or ions strike any gas atoms in passing from one electrode to the other, and so there is no cumulative ionization process.

Between these two extremes, there is a limited critical range of pressure around  $10^{-4}$  mm. of mercury, in which the potential drop and tube current can both be maintained at suitable values to produce x-rays of desirable intensity and penetration. Regulation of the high voltage supply and the pressure of the gas in the tube will then permit one to maintain any tube current desired in the range of, say, 3 to 30 ma. and 5 to 50 kv.

If the tube is connected to a high-vacuum pumping system that is capable of exhausting it to a pressure of  $10^{-5}$  mm. of mercury, it will be found that a properly designed leak valve connected so as to permit a

<sup>1</sup> The mean free path of electrons is probably five or six times that of molecules of the gas.

to leak in at a very slow but accurately adjustable rate will afford accurate and rapid control over the tube current and voltage.

In medical work, however, it is impractical to have the tube rigidly connected by a glass or metal tube to a vacuum system; prior to 1913, therefore, the gas-filled tubes used in such work were exhausted to the desired pressure and then sealed off so as to be portable. The pressure in these tubes decreased slowly as they were used, with a current of perhaps 5 ma. passing through the tube, probably because of adsorption of the gas by the glass and metal surfaces of the tube. Consequently the tube potential increased as the tube was used, causing a change in the character of the x-rays generated; if not corrected, the pressure would soon drop to a value making further operation impossible. Various devices were incorporated in these early tubes to permit the operator to restore the gas pressure to a suitable value. In some types, a discharge was passed through a "gasifier" (such as asbestos, mica, or glass wool) in a small side tube *R* (Fig. 2-1). Some of these early x-ray tubes operated with hydrogen in them instead of air because this reduced the sputtering of the metal parts, and in these the pressure was regulated by means of palladium tubes, which could be heated to let a little hydrogen diffuse in. These disadvantages in a sealed-off gas tube are overcome by the Coolidge type of tube, now used for most purposes.

Gas tubes are still used for diffraction work to a considerable extent, and therefore the practical details of their operation are of some interest. These modern gas tubes are used permanently connected to a vacuum system, however, and equipped with a leak valve.

It is clear that ordinary gas-filled tubes must be supplied with high voltage of the correct polarity. That is, the cathode must be negative and the anode positive. The use of an alternating electric voltage cannot ordinarily be tolerated because electrons would bombard the cathode instead of the anode when the polarity is opposite to that intended by the tube designer. However, in recent years, those using gas-filled

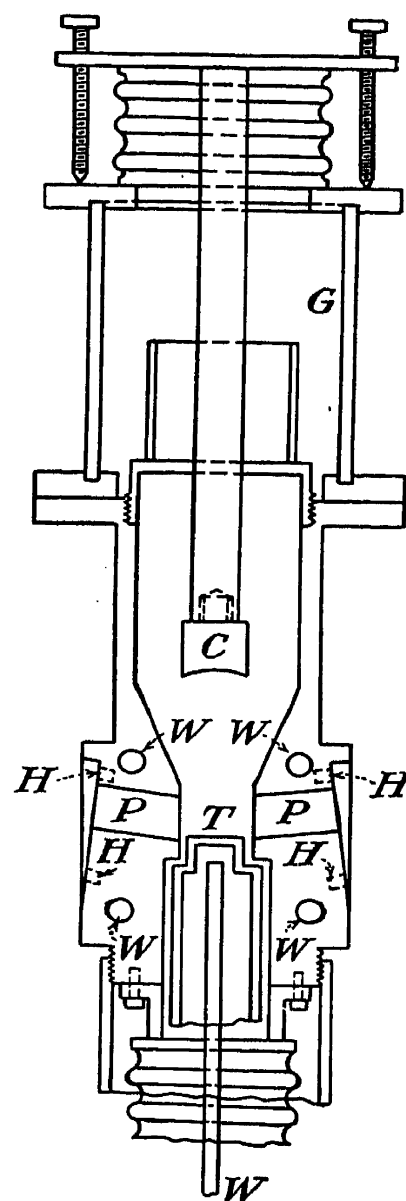
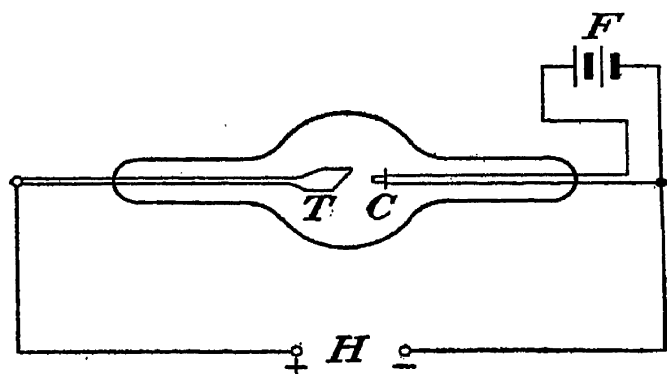


FIG. 2-2.—Self-rectifying water-cooled gas-type x-ray tube for diffraction work. *C*, cathode; *T*, target; *P*, ports for x-rays; *W*, water passages; *H*, screw holes for attaching diffraction cameras. (Wyckoff and Lagsdin; courtesy of American Institute of Physics.)



tubes in diffraction work have discovered that they can be so designed that they may be directly connected to a high-voltage electrical supply of alternating polarity, such as a transformer. Gas-filled tubes of such modern design (Fig. 2-2) will rectify their own current, like a Coolidge tube.



*Coolidge tube*

*C=Cathode cup    T=Target*  
*F=Filament battery*  
*H=High voltage source*

FIG. 2-3.

Ordinary gas tubes will rectify their own current, like a Coolidge tube. Ordinary gas tubes will not rectify their own current and therefore must be operated from an electrical supply having a rectifier or other provision for supplying direct current.

**5. The Coolidge X-ray Tube.** Reference to the Coolidge tube has already been made in Chap. 1.<sup>2</sup> The great majority of the x-ray tubes used today are of this type. The tube is evacuated to the best vacuum attainable. Before it is sealed from the pumps, it is operated under full power for several hours to drive the gas out of the portions which

get hot, so that, when it is sealed off, subsequent operation will not cause any appreciable amount of gas to be released inside the tube.

The cathode of this tube is not a block of aluminum, as in the ordinary tube, but consists instead of a spiral tungsten wire filament, inside a small metal cup. The filament can be heated to incandescence by passing an electric current through it, just like the filament of an ordinary incandescent lamp. The surrounding metal cup causes the electric field between the anode and cathode, set up by the high voltage applied to the tube, to distribute itself in such a way that electrons emitted from the hot filament inside the cup will be focused into a narrow beam of cathode rays, which will strike the anode within a small definite spot on its surface (called the "focal spot"). Without the focus cup, the electrons would diverge from the filament. A Coolidge tube ordinarily has only two electrodes, cathode and anode, the anode serving as target.

In the Coolidge tube, the electrons needed to provide the cathode rays are emitted from the surface of the hot tungsten filament. This will be explained in greater detail in the next section.

**6. Free Electrons and Thermionic Emission.** A normal tungsten atom consists of a central massive nucleus carrying a positive charge exactly sufficient to neutralize the negative charges of the surrounding swarm of 74 electrons. In a tungsten wire, the tungsten atoms will

<sup>1</sup> R. W. G. Wyckoff and J. B. Lagsdin, *Rev. Sci. Instruments*, **7**, 35 (1936).

<sup>2</sup> W. D. Coolidge, *Phys. Rev.*, **2**, 409 (1913).

compose it are fixed in a rigid framework in such a way that each one may vibrate with a small amplitude to and fro in any direction about its fixed central equilibrium position in the framework to which it is figuratively "attached" by the electrical forces of interaction with its neighboring atoms. However, each atom keeps to itself only 73 of its electrons<sup>1</sup> instead of the 74 present in a neutral atom. The seventy-fourth electron of each atom is not constrained to remain attached to its parent atom like the other 73 but instead goes wandering off freely through the space between atoms. Since this is true of all the atoms, there are as many free electrons as there are atoms, and these swarm about inside the metal much as the molecules of a gas swarm about, as visualized in the kinetic theory of gases.

This internal "gas" of free electrons is what distinguishes a metal, like copper, from a nonmetal, like sulfur. When an electric current is sent through a wire, these free electrons slowly migrate through the framework of atoms composing the wire. In fact, it is this slow migration of the electrons which is the current in the wire. As an example, if 6 amperes from a battery is passed through a piece of No. 17 copper wire, the free electrons in the wire are migrating along it at a rate of somewhat over a centimeter per minute, or let us say an inch every two minutes.

One may visualize the enormous number of collisions these electrons will make with each other and with the atoms composing the wire as they drift through 1 in. of it under the urging influence of the electric potential difference supplied by the battery. The energy supplied by the battery in driving the electrons through the wire is used to increase the average velocity of their rapid random thermal motion (which is much faster than that of a rifle bullet), just as the molecules of air in a room speed up when the temperature rises. Part of this is handed on to the atoms by elastic collisions, causing the atoms to vibrate more and more violently about their fixed equilibrium positions in the wire; in other words, the wire gets hot.

If enough energy is supplied, the random thermal motion of the free electrons becomes great enough, as the wire heats up, so that a small fraction of them acquire sufficient energy to fly completely out of the metal, by overcoming the restraining electric potential, which ordinarily holds the free electrons within the metal. One may see, in a qualitative way, that the free electrons, as a whole, must be firmly bound to the positive ions among which they circulate, and the kinetic energy which is required to enable an electron to escape against this restraining influence is called the "thermionic work function," or sometimes the "heat

<sup>1</sup> This figure is not to be taken too literally. The number of free electrons is certainly of the same order of magnitude as the number of atoms, however. For further details, see U. Dehlinger, *Z. Elektrochem.*, **38**, 150 (1932).

of evaporation of electrons," in analogy with the evaporation of water for example. Thus the electrons "evaporate" from a hot metal much as water evaporates from a wet cloth in the sunshine.

The theory of this process, which is called "thermionic emission," was first worked out by O. W. Richardson,<sup>1</sup> who derived the equation

$$I = AT^{\frac{1}{2}}e^{-\frac{b}{T}} \quad (2-1)$$

from theoretical considerations. At present, it is generally conceded that the correct equation is more probably

$$I = AT^2e^{-\frac{b}{T}} \quad (2-2)$$

which was later derived by Dushman.<sup>2</sup> Actually, the choice between the two equations is of theoretical interest only; for  $e^{-\frac{b}{T}}$  is such a powerful factor that it overwhelms the  $T^{\frac{1}{2}}$  or  $T^2$  factor, and consequently the experimental data fit either equation equally well. In these equations,

$$A = \frac{4\pi me k^2}{h^3} S \quad (2-3)$$

where  $S$  is the area of the emitting surface,  $m$  and  $e$  are the mass and charge of an electron [ $e$  in (2-1) and (2-2) is of course Napierian log base  $k$  is Boltzmann's constant,<sup>3</sup>  $h$  is Planck's constant,<sup>3</sup>  $T$  is the absolute temperature, and

$$b = \frac{10^7 E_w e}{k} \quad (2-4)$$

where  $E_w$  is the thermionic net work function, or "latent heat of evaporation of the electrons" (in ergs per electron).

The operator of a Coolidge tube soon learns that no appreciable emission of electrons from the filament occurs until it is hot enough to glow brightly. Once the temperature is reached at which a measurable current passes between the electrodes, a very slight increase in the filament heating current causes a very great increase in the high-voltage "tube" current carried by the emitted electrons. This rapid variation is represented by the  $e^{-\frac{b}{T}}$  term in equation (2-2).

The tube current and voltage in the Coolidge tube are thus regulated by means of the filament heating current, much as these factors are controlled in a gas tube by means of a leak valve. Enough has been

<sup>1</sup> O. W. Richardson, *Phil. Mag.*, **28**, 633 (1914).

<sup>2</sup> S. Dushman, *Phys. Rev.*, **21**, 623 (1923); see also L. A. DuBridge, *Am. J. Phys. (Am. Phys. Teacher)*, **7**, 357 (1939).

<sup>3</sup> See Appendix I.

said to make it obvious that a Coolidge tube should act as a rectifier also, for no electrons will be emitted from the anode unless it should become very hot. The anode, however, often does become hot, as is to be seen shortly. Nevertheless, Coolidge tubes in many cases are operated directly from a high-voltage transformer and are depended upon to rectify their own current.

**7. Fundamentals of X-ray Tube Construction.** A few more details remain to be added to complete the rudimentary idea of the construction

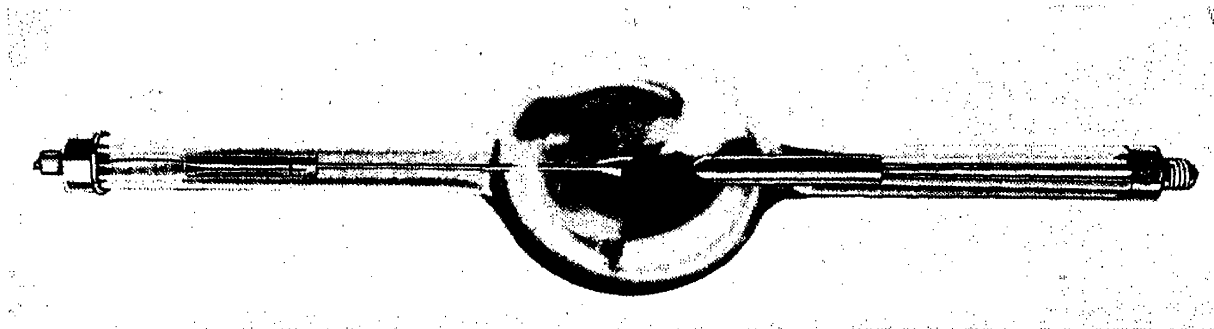


FIG. 2-4.—Coolidge x-ray tube, "universal" type. (Courtesy of General Electric X-ray Corporation.)

and operation of an x-ray tube. Since a vacuum is required within the tube, its walls must be gastight. The walls of the tube must likewise serve as mechanical support for the electrodes; and since a high voltage is applied between the electrodes, the tube walls must serve as a good high-voltage insulator. Hence glass is very commonly chosen as the material for the tube envelope. If the tube is to operate at 200,000 volts, for example, the glass envelope must have a length of the order

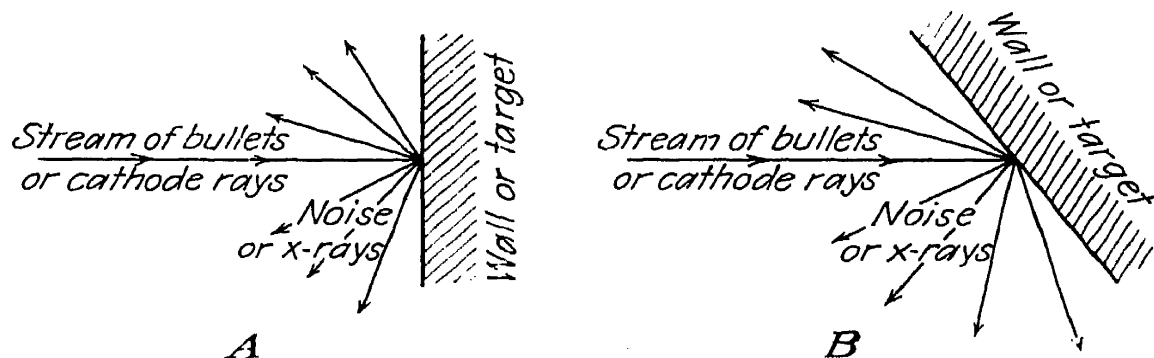


FIG. 2-5.—To explain generation of x-rays.

of 2 or 3 ft. to prevent sparking over the outside. This length can be reduced by immersing the tube in transformer oil, which also may serve to cool the tube. Cooling will be discussed in the next section.

It has been emphasized that the x-rays are generated at the spot where the cathode rays strike the target, much as sound would radiate from a spot on a wall being hit by machine-gun bullets. If it is desired to throw most of the radiation off to one side of the stream of bullets (or cathode rays), the bullets, or rays, might be directed against the wall

or target at a 45-degree angle as indicated in Fig. 2-5B. Likewise, the targets of many x-ray tubes are cut off at an angle when it is desired to distribute the radiation predominantly on one side of the tube. See Figs. 2-1 to 2-4, for example.

On the other hand, tubes used in diffraction work, to be discussed later, commonly are provided with anodes in which the face bombarded by the cathode rays is perpendicular to them, as in Fig. 2-5A. Consequently, the x-rays are radiated as strongly out one side of the tube as the other. This permits one to surround the tube with several "cameras," each of which will receive an equal amount of radiation, as is desired.

**8. Heat Dissipation.** The energy represented by the cathode-ray beam that strikes the tube target is ordinarily sufficient to generate very considerable heat at the focal spot where it strikes. This heat is generated because, unfortunately, only a small fraction of the cathode-ray energy is converted into x-rays. The generation of x-rays at the focal spot is a very inefficient process in which most of the cathode-ray energy is merely wasted in heating the target.

An equation for the efficiency of an x-ray tube was formulated by Beatty<sup>1</sup> in 1913; recent investigations by Kirkpatrick and others indicate that it is essentially correct. It is

$$\text{Efficiency} = \frac{\text{x-ray energy}}{\text{cathode-ray energy}} = 1.4 \times 10^{-9} ZV \quad (2-5)$$

where  $Z$  is the atomic number of the metal composing the target and  $V$  is the electric potential drop applied to the tube, in volts. For a tube with a tungsten ( $Z = 74$ ) target operating at 100 kv, this gives an efficiency of 1 per cent. Hence in this case, which is quite typical, 99 per cent of the electrical power supplied to the x-ray tube is dissipated in the form of heat generated at the focal spot of the target.

If the anode of this tube is a block of tungsten weighing  $\frac{1}{4}$  pound and if the tube is being operated so that a current of 5 ma. passes through it in the form of cathode rays, it is easy to calculate that the anode will soon get hot.

Assuming an operating potential difference of 100 kv., the power expended is 500 watts, which will heat up the anode at a rate of about 30°C. per second. Unless some way is found to get rid of the heat, the anode will have an average temperature of about  $60 \times 30$ , or 1800°C. after only 1 min. of operation. This means that the anode will be white-hot.

Many x-ray tubes are built and used that have for their anode a block of tungsten of about this mass, supported on a long, slender rod.

<sup>1</sup>R. T. Beatty, *Proc. Roy. Soc. (London) A*, **89**, 314 (1913); P. Kirkpatrick and L. Wiedmann, *Phys. Rev.*, **67**, 321 (1945); see also W. Rump, *Z. Physik*, **43**, 2 (1927).

in the center of a highly evacuated tube so that there is only negligible loss of heat from the anode by convection or conduction. Such a tube is shown in Fig. 2-4, this type sometimes being called the "universal" type. The target does not melt in these tubes (if their rating is not exceeded); for the melting point of tungsten is  $3370^{\circ}\text{C}.$ , and before it reaches that temperature it gets rid of its heat quite rapidly by radiation. The well-known Stefan-Boltzmann law of radiation states that heat is

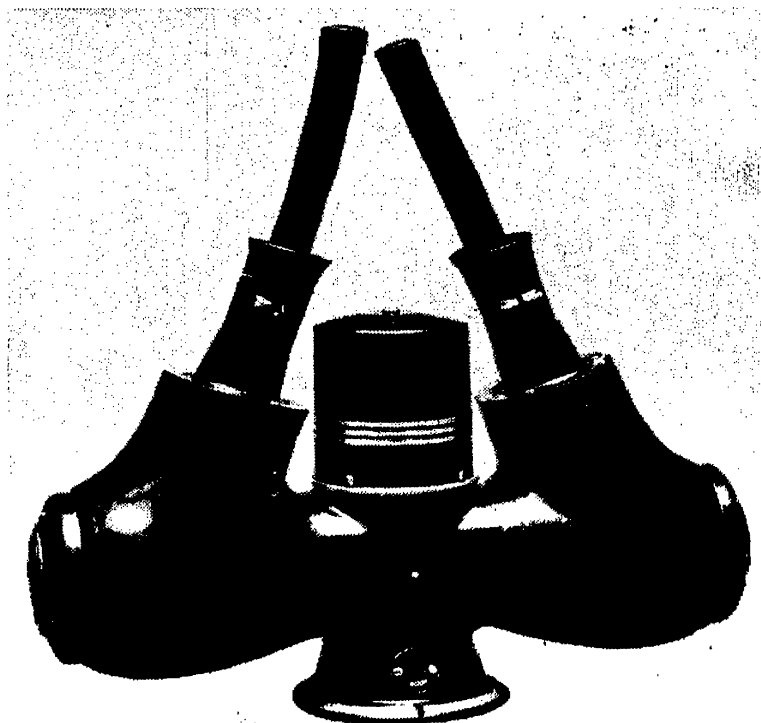


FIG. 2-6.—Oil-immersed, shockproof tube. (Courtesy of General Electric X-ray Corporation.)

radiated at a rate  $aT^4$ , where  $a$  is a constant and  $T$  is the absolute temperature. Hence, when these high temperatures are reached, the anode radiates its heat at a rate which rapidly increases until it equals the rate at which it is being supplied. Nevertheless, x-ray tubes constructed in this manner cannot be continuously operated at inputs much above 1,000 watts (for example, 10 ma. at 100 kv. or 5 ma. at 200 kv.) without danger of melting the anode or parts of it. Such tubes will not rectify an a.c. supply when the anode attains the temperature at which thermionic emission becomes appreciable; if this is attempted, electrons bombard the delicate cathode filament, quickly destroying it.

In many cases the tubes are so constructed that water or oil can be circulated in the interior of the anode, which is hollow, so as to cool it. In others, the anode is mounted on a metal rod designed to conduct the heat out to a series of metal fins, which lose the heat to the air by convection (Fig. 2-7). In others, the anode is constructed in the form of a circular metal disk mounted on a central bearing so that it can be rotated

rapidly, and the cathode rays are directed so that they strike it at small focal spot near the periphery. This does not help to get the heat out of the anode, but it does help to distribute the heat throughout the anode instead of localizing it all at the small focal spot. By rotating

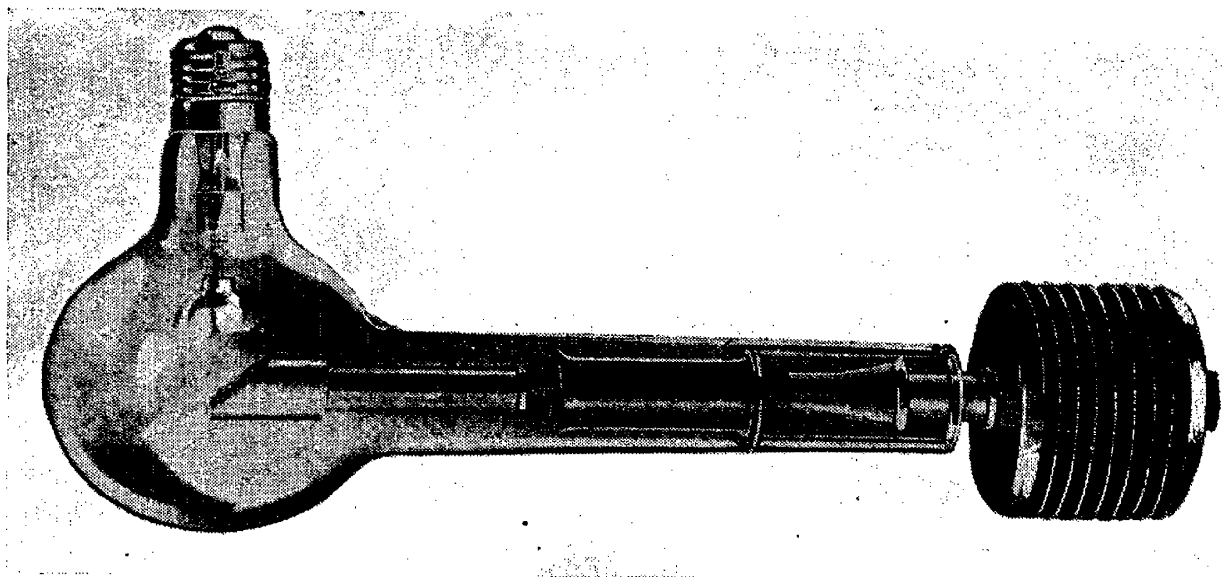


FIG. 2-7.—Dental tube with fins for air cooling. (Courtesy of General Electric X-ray Corporation.)

the anode, the metal surface at the focal spot is rapidly moved out of the spot and replaced by other cooler metal before it has time to melt, which it would do if it remained in the spot, even for a small fraction of a second.

**9. Focal-spot Size.** When the object is merely to produce x-ray without any particular need for their being produced at one very small

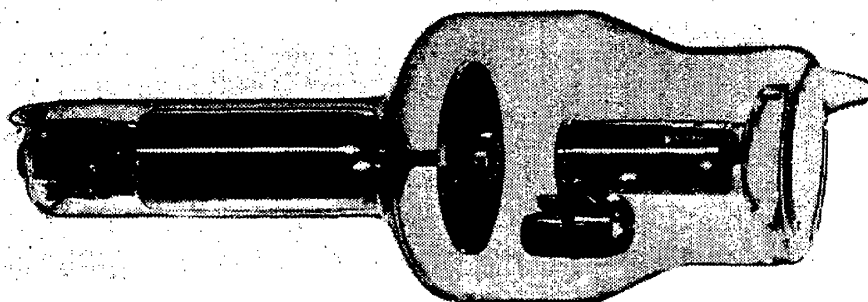


FIG. 2-8.—Modern rotating anode tube. (Courtesy of Machlett Laboratories.)

spot, the cathode rays are often poorly focused and permitted to strike the anode over a wide area, which may in some cases be as large as a penny or a nickel. An example is the case of x-ray tubes intended for therapeutic work, killing tumors, etc.

One of the most common uses for x-rays is for radiography. x-rays are passed through an object, such as one's hand, and allow

to fall on a photographic film placed behind it, one can obtain an x-ray picture, called a "shadowgraph," an "exograph," or a "radiograph" of the object, which will reveal internal details of the object, such as the bone structure.

The quality and usefulness of the radiograph depends largely upon the size of the source of x-rays, that is, upon the size of the focal spot on the target of the x-ray tube. The case is similar to that of visible light when one wishes to obtain a clear shadow of some object. The source of light should be small if a clear shadow is desired.

In radiography, and in other types of work to be discussed later, it is a great advantage to have a source of x-rays that approaches the ideal of a "point source." This can be achieved in a Coolidge tube by winding the filament in a perfectly formed conical spiral and setting it in perfect alignment at just the correct depth in the focal cup that surrounds it. The focal cup must have the proper diameter in relation to the cathode-target distance, and all the other factors just mentioned must be adjusted so that the electrostatic field set up by the high voltage between the anode and cathode (especially near the cathode) will direct the cathode rays so that they converge to a small spot on the anode.

In a gas tube, the circular aluminum cathode rounded at the edges and provided with a concave spherical surface of radius of curvature about half the cathode-target distance, likewise focuses the cathode rays upon a small spot on the target. The quantitative theory of focusing electron beams is a subject known as "electron optics."<sup>1</sup>

It is quite possible to be too successful in achieving a small focal spot, however. If the spot has an area as small as 1 mm.<sup>2</sup> the concentration of, say, one or two kilowatts of power on such a small spot might melt the metal there, even though the anode were adequately cooled by a generous flow of cold water inside it. This would occur simply because the thermal conductivity of even copper or silver is not great enough to carry heat away from such a small spot rapidly enough to prevent it from rising to the melting point under such a concentrated generation of heat. Consequently, the design of x-ray tubes is usually a compromise between a focal spot small enough to be satisfactory as a point source and large enough to permit operation of the tube at the desired power without rapid deterioration or pitting of the target at the focal spot.

Two common methods will be described that are used in practice to reduce the focal-spot size and still keep the power input (and hence

<sup>1</sup> See, for example, E. Brüche and O. Scherzer, "Geometrische Elektronenoptik," Julius Springer, Berlin, 1934; *Z. tech. Physik*, **17**, 584, (1936); I. G. Maloff and D. W. Epstein, "Electron Optics in Television," McGraw-Hill Book Company, Inc., New York, 1938; F. Gray, *Bell System Tech. J.* **18**, 1 (1939).



x-ray intensity) large. In one, the anode is rotated, as already mentioned. The commercial production of rotating anode tubes was achieved only after several difficult technical problems had been overcome. In some cases, only the rotor of the driving (induction) motor is placed inside the tube; in others, the whole motor is inside the glass walls. It must be well balanced, and it must rotate the target at high speed (commonly 3,600 revolutions per minute). It must withstand the heat from the target when the latter becomes red-hot from cathode-ray bombardment. The problem of lubricating the high-speed bearings in a high vacuum was overcome by the use of barium as a lubricant.

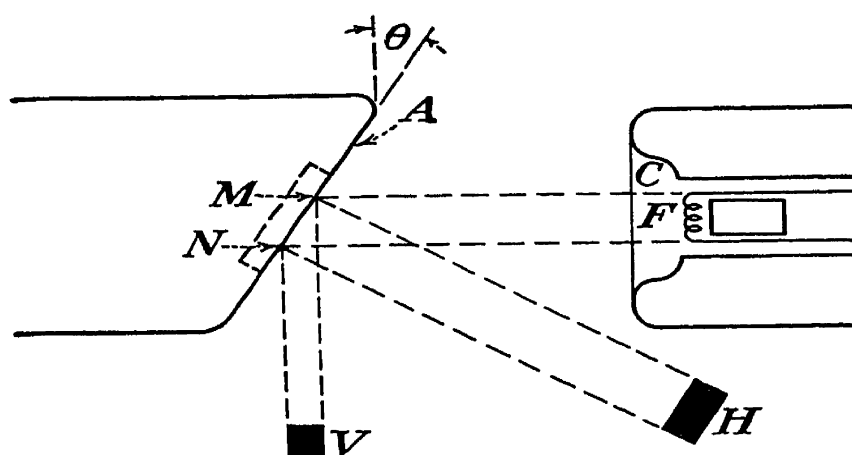


FIG. 2-9.—The principle of line-focus tubes.

A second common method of reducing the focal-spot size makes use of a trick in which the *apparent* size of the spot is reduced without reducing the actual size. The anode face *A* (Fig. 2-9) is a flat surface that usually is perpendicular to the cathode-ray beam in the case of diffraction tubes or inclined at an angle  $\theta$  of perhaps  $20^\circ$  in radiographic tubes. The cathode cup *C* is oval rather than circular in shape, and the filament *F* within it is in the form of a long, narrow, cylindrical coil rather than the usual cone. The axis of the cylinder lies parallel to the length of the oval focusing cup and in the plane of the angle. The cathode-ray beam then has the form of a ribbon that strikes the anode and produces a focal spot having a long narrow shape, approaching a rectangle, of length *MN*. This focal spot has the form and size represented at *H* when viewed normally; when viewed from a direction at right angles to the cathode-ray beam in the plane of the "ribbon," it has the shape of a small square as represented at *V*. Thus the apparent size of the focal spot is reduced, while the actual area of the anode that must absorb the heat is kept sufficiently large to allow a reasonable tube life. This type of focus is sometimes called a *Benson focus*.

<sup>1</sup> Z. J. Atlee, J. T. Wilson and J. C. Filmer, *J. Applied Phys.*, **11**, 611 (1940)

Goetze focus.<sup>1</sup> In most types of work, this apparent reduction in focal-spot size is just as satisfactory as though the focal-spot size were really reduced.

**10. Other Details.** Many other details of x-ray tube construction remain to be discussed, such as choice of metal for the target, use of Lindemann and beryllium windows, multisection tubes for very high voltages, and differences between radiographic tubes, diffraction tubes, and therapeutic tubes. These details cannot be discussed intelligently until more is learned about the nature of x-rays. They will be therefore discussed in Chap. 7 and at appropriate places throughout the book.

### QUESTIONS AND PROBLEMS

1. What is an ion? A free electron? In addition to regulation of the high-voltage supply, how are the tube current and tube voltage controlled in (a) a gas tube? (b) A Coolidge tube?

2. If an x-ray tube filament emits 1 ma. at 2000°K., what current will it emit at 2100°K.? At 2200°K.? (K. stands for "Kelvin"; the absolute temperature in degrees Kelvin is the centigrade temperature plus 273.16°.) Neglect the  $AT^2$  factor in equation (2-2); consider only the  $e^{-\frac{b}{T}}$  factor, and assume  $b = 50,000$ .

*Ans.*  $3\frac{1}{3}$  ma. at 2100°K.; 10 ma. at 2200°K.

3. A typical modern incandescent lamp has an efficiency of about 15 lumens/watt. 1 lumen = 0.0015 watt in the form of light. If a typical x-ray tube be regarded as one having a tungsten target and operating at 100 kv. and 10 ma., and requiring 20 watts to heat the cathode filament, how does the efficiency of an x-ray tube compare with that of an incandescent lamp?

*Ans.* The x-ray tube is about one-third as efficient as the lamp.

<sup>1</sup> U.S. patent 1,174,044 (1916). Optical workers familiar with Lambert's cosine law of optics will be interested in knowing that x-rays do not obey this law. The x-ray intensity in direction  $MV$  is nearly as great as in direction  $MH$  (Fig. 2-9).

## CHAPTER 3

### THE CONTINUOUS X-RAY SPECTRUM

**1. The Nature of X-rays.** The previous chapter has made it clear that x-rays must be some form of radiation which spreads out from the focal spot of the tube. By allowing the rays to pass through a small hole in a lead shield at a distance of 2 ft. from the tube and then striking a photographic film enclosed in a paper envelope at a distance of 4 ft. from the target, it is easy to show that they travel in straight lines. It will be found that, if the film is now moved to a distance of 8 ft. from the target, it must be exposed four times as long as before to become equally black when developed. Careful measurement shows that the familiar inverse-square law for intensity is accurately obeyed. That is, the intensity of the rays decreases as they spread out from the target, the intensity at any point being inversely proportional to the square of its distance from the focal spot.

Later, experiments will be described that can scarcely be explained unless one thinks of x-rays as consisting of waves. There are other experiments that are equally difficult to explain unless one thinks of x-rays as consisting of particles. This dilemma is not restricted to x-rays, however. It is encountered, for example, in the study of ordinary light, which likewise has a dual nature. Therefore it is probably better for one to begin the study of x-rays by first thinking of them as consisting of minute bundles or packets of waves.

These packets are technically known as *photons* or *quanta*. These waves are of an electromagnetic nature. That is, they consist of an electric and a magnetic vibration of enormously high frequency that travel in a straight line through space at a speed of  $3 \times 10^{10}$  cm./sec. or 186,000 miles/sec. The electric and magnetic vibrations are always present together, each being associated with the other and perpendicular to the other. The vibrations are transverse, which means that the vibrations are perpendicular to the line of travel of the waves. Thus a beam of x-rays traveling straight up consists of packets of waves in which the electric vibrations are horizontal and the magnetic vibrations are also horizontal, but at right angles to their associated electric vibrations.

The foregoing statements, however, apply equally well to ordinary light or infrared or ultraviolet radiation or radio waves. All the various types of radiation make up what is known as the *electromagnetic*

*spectrum*, and they are all of the same general nature and should be regarded as members of the same family.

The difference between the members of the family is chiefly a matter of the frequency of the waves or vibrations or of the energy of the wave packets, or photons. Thus, if the waves have a frequency of  $3 \times 10^{18}$  vibrations/sec., the packets will each have an energy of about  $2 \times 10^{-8}$  erg, and a group of them would be called x-rays. On the other hand, if the frequency were only one-thousandth as great,  $3 \times 10^{15}$  per second, the packets would each have only one-thousandth of the energy, or  $2 \times 10^{-11}$  erg, and such photons would make up ultraviolet radiation. Again, a frequency of  $5 \times 10^{14}$  per second and a quantum energy of  $3 \times 10^{-12}$  erg describe the waves or photons composing ordinary visible light, the only member of the family that affects the human eye. One cannot see x-rays or any of the other types of electromagnetic radiation. A frequency of  $10^{14}$  per second and a photon energy of  $7 \times 10^{-13}$  erg would be typical for infrared radiation and a frequency of  $10^6$  cycles/sec. corresponding to a photon of  $7 \times 10^{-21}$  erg energy is characteristic of a radio wave. It will be noticed that the energy given for a radio wave packet is 100 million times smaller than for any of the others. This may account for the fact that, in the case of radio waves, the wave characteristics predominate, and they seldom if ever behave as packets, or photons. However, all of the other members of this family have a distinct dual nature, behaving in some ways like waves and in others like particles.

**2. X-rays as Waves.** The preceding section has emphasized the dual nature of electromagnetic radiation in general and x-rays in particular. The wavelike characteristics seem to be more obvious. Indeed, at the beginning of this century it was universally believed that light and other electromagnetic radiation was purely a wave motion, because the particlelike phenomena of radiation were so obscure as to have escaped notice.

Let us then first consider the wavelike nature of x-rays. The mathematical analysis of Fourier has proved that *any* wave can be compounded by adding together simple sine waves of the correct amplitude, phase, and frequency. Conversely, any wave can be mathematically treated as a sum of sine waves, or as a "Fourier series."

A simple sine wave is represented in Fig. 3-1 as it appears at a given instant. It is characterized by a definite wave length, which is the distance between any two adjacent crests, and is commonly represented by the letter  $\lambda$ , as indicated. This wave train is to be regarded as moving toward the right in the figure, with a uniform velocity  $v$ . The frequency  $\nu$ , of the wave, is the number of crests that pass by a fixed position  $PP$  in unit time, or in 1 sec., say. It is obvious that in 1 sec. the wave will move forward a distance  $v$  (because  $v$  is so defined), and

likewise that  $\nu$  wave crests will have passed  $PP$  in 1 sec., by definition. Hence since the wave length (distance between crests) is  $\lambda$ , it follows that

$$v = \nu \lambda \quad (3-1)$$

This is one of the fundamental equations of wave motion, and enables one to compute easily any one of the three terms  $v$ ,  $\nu$ , or  $\lambda$  if the other two are known. In Sec. 1 it was stated that x-rays (and other electromagnetic waves) travel through space in a straight line at a velocity of  $3 \times 10^{10}$  cm./sec. Since this velocity is so universal

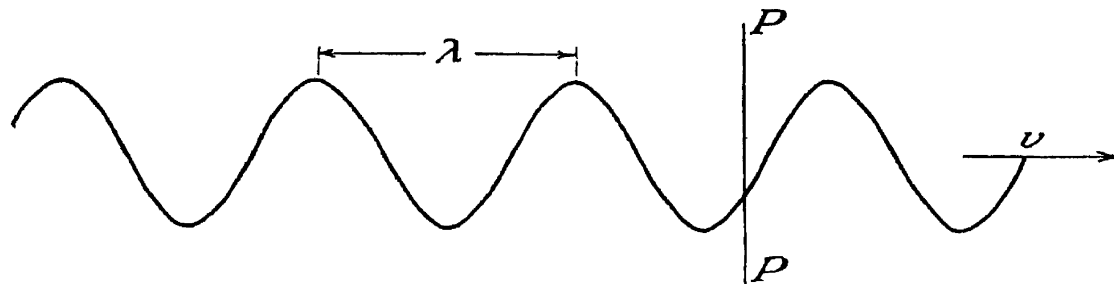


FIG. 3-1.—A sine wave moving with velocity  $v$  past a stationary position  $PP$ .

for all types of electromagnetic radiation, it is one of the fundamental physical constants<sup>1</sup> and is commonly represented by the letter  $c$ .

When one is dealing with x-rays, then, one may write  $v = c$ . Then (3-1) becomes

$$c = \nu \lambda \quad (3-2)$$

which is a very useful equation in dealing with any electromagnetic radiation. The latest estimate by Birge<sup>2</sup> of the exact value of  $c$  is  $c = (2.99776 \pm 0.00004) \times 10^{10}$  cm./sec., so the error is less than one-tenth of 1 per cent when one writes  $c = 3 \times 10^{10}$  cm./sec. This enables one to compute the wave lengths associated with the various types of radiation mentioned in the preceding section.

In Sec. 1 it was stated that electromagnetic radiation having a frequency of  $3 \times 10^{18}$  per second represents a typical x-ray. From equation (3-2) one has  $\lambda = c/\nu$ , so that a typical wave length for x-rays is  $3 \times 10^{10}/3 \times 10^{18} = 10^{-8}$  cm. Since such short wave lengths are continually encountered in dealing with x-rays, ultraviolet, and ordinary light, it is convenient to adopt an arbitrary small unit of length in which to express them. The unit that has been adopted is known as the "angstrom" (commonly abbreviated Å.), and it is defined as  $10^{-8}$  cm. Hence the wave length that has just been computed as typical for x-rays is 1 Å. Actually, x-rays in general have wave lengths varying over the range from 0.02 to 10 Å. These limits are not sharp and are not definite. Of course, 1 Å. is merely a "typical" value and is not to be taken as implying narrow limits for the wave lengths of x-rays.

<sup>1</sup> See Appendix I.

<sup>2</sup> R. T. Birge, *Rev. Modern Phys.*, **13**, 234 (1941).

The electromagnetic spectrum may be roughly divided on the basis of wave length, then, somewhat as follows:

TABLE 3-1

X-rays.....	0.02 to	10 A.
Ultraviolet.....	10. to	4,000 A.
Visible light.....	4,000. to	7,000 A.
Infrared.....	7,000. to	1,000,000 A. (0.1 mm.)
Radio waves.....	0.1 mm. to	3 or 4 kilometers

One may gain a better idea of the spread of these various general types of radiation by an analogy with sound waves, which are propagated by means of mechanical vibration, usually through the air. In music, one note (for example, high C) is said to be one "octave" above another note (for example, middle C) if it has twice the frequency (or half the wave length) of the second one. Thus middle C has a frequency of 256 vibrations/sec., and high C has just twice that frequency, or 512 vibrations/sec. A standard piano has a range of just over 7 octaves, so that its highest note has a frequency more than  $2^7$ , or 128 times that of the lowest. On the basis of octaves as in music, then, x-rays spread over about 9 octaves, ultraviolet about 9 octaves, infrared 7 or 8 octaves, and radio waves about 25 octaves. In contrast to these wide spreads, it will be noticed that visible light has a spread of slightly less than 1 octave.

The evidence upon which the idea is founded that x-rays have the characteristics of waves is the same as the evidence indicating that the other types of electromagnetic vibration have wavelike characteristics. X-rays, like visible light, ultraviolet, and the other types, show interference, diffraction, and polarization phenomena, which will be described in later chapters. Such phenomena are difficult to explain upon any basis other than that of a wave motion.

Before closing this brief discussion of x-rays regarded as waves, it should be mentioned that radioactive elements, such as radium, emit an electromagnetic radiation called gamma rays ( $\gamma$ -rays). These rays are physically the same as very short-wave-length x-rays, the only difference being that they are produced by the disintegration process of radioactive material instead of by an x-ray tube. Thus x-rays and gamma rays are both short-wave-length electromagnetic radiation, just as the noise of a waterfall and the music from a violin are both sound, the distinction being merely one of source rather than in fundamental nature. Gamma rays have a wave-length range covering several octaves in the vicinity of 0.02 to 0.001 A.

The cosmic rays should also be mentioned. At the surface of the earth there are found a few atomic fragments (such as positrons and mesotrons) moving with enormous energies that could be generated

electrically only by potentials of hundreds of millions or even billions of volts. Most of these fragments are probably "secondary" in the sense that they have been wrenched loose from the atoms composing the atmosphere by the "primary" cosmic rays which bombard the atmosphere from above and originate somewhere in outer space. Compared with the number of atoms per cubic meter of air, these cosmic-ray particles are so rare that the number per cubic meter at any instant is practically infinitesimal. Nevertheless, though rare, such high-energy particles colliding with the atoms in the air probably generate an associated electromagnetic radiation of correspondingly high energy. If so, this radiation is mixed in with the secondary, and perhaps also in the primary, radiation. It is a very high energy electromagnetic radiation of very low intensity, having a wavelength of the order of  $10^{-5}$  or  $10^{-6}$  Å. The term "energy radiation" refers to the energy of the photons described in Sec. 1. In the next section will be explained how one can determine the wavelength of a radiation if the "energy" is known. Cosmic rays have been mentioned here, along with gamma rays, so that the full extent of the electromagnetic spectrum may be visualized from the wave-mechanics viewpoint and the relation of x-rays to these other types of radiation better understood.

Table 3-1 may be supplemented, then, as follows:

TABLE 3-2

Gamma rays.....	0.001 to 0.02 Å.
Possible cosmic-ray component.....	$10^{-6}$ to $10^{-3}$ Å.

**3. X-rays as Particles.** This phase of the nature of x-rays was introduced by digressing briefly to discuss a few fundamental properties of infrared rays mentioned in the preceding section. Infrared radiation is the familiar "radiant heat" felt when a hot flatiron is held within a few inches of one's cheek. These rays can be spread out into a spectrum by passing them through a rock-salt or fluorite prism, just as ordinary white light can be spread out into a rainbowlike spectrum by passing through a glass prism. The intensity of the rays in any part of the spectrum can be measured in arbitrary units by placing a thermocouple in that part of the spectrum and reading the deflection of a galvanometer connected to it.

If the radiation from an ordinary flatiron is thus analyzed by means of a fluorite or rock-salt prism, mirrors, thermocouple, etc. (the ensemble is called an infrared spectrometer), it is found that the energy distribution of the radiation is represented by a curve of the type shown in Fig. 3-2 published in 1900 by Lummer and Pringsheim.<sup>1</sup> These curves

<sup>1</sup> O. Lummer and E. Pringsheim, *Verhandl deutsch physik. Ges.*, 1, 23, 215 (1900); *Ann. Physik*, 6, 192 (1901).

vary with the nature of the surface of the emitter. For example, a flatiron covered with soot will give a slightly different curve from a chromium-plated one at the same temperature. Consequently, for standardization, such curves are ordinarily obtained from a black body, which consists of a chamber provided with a small hole to the exterior. If the temperature of the chamber is  $500^{\circ}$ , then the radiation emerging to the exterior through the small peephole is defined as  $500^{\circ}$  black-body radiation.

The curve in Fig. 3-2 marked "998" was obtained from such a black body at a temperature of  $998^{\circ}\text{K}$ ., which is  $724.84^{\circ}\text{C}$ . The abscissas of the graph represent the wave length of the infrared radiation in microns (commonly abbreviated by  $\mu$ ;  $1\mu = 10^{-3}\text{mm.} = 10^4\text{A.}$ ). The ordinates represent the relative intensity of the radiation, which is determined by merely reading the thermopile galvanometer. Thus one sees that, at  $725^{\circ}\text{C}$ ., the most intense rays have a wave length of about  $3\mu$  or  $30,000\text{A.}$ , and the intensity falls off at both longer and shorter wave lengths than this.

As the temperature of the black body is raised, Fig. 3-2 shows how the radiation becomes more intense at all wave lengths but always reaches a maximum value at some wave length (such as  $1\frac{1}{2}\mu$  for the  $1646^{\circ}$  curve) with diminishing intensity at both longer and shorter wave lengths.

The shape of these experimental black-body radiation curves is quite different from that predicted by the classical theories of radiation, which were based on the assumption that all types of electromagnetic radiation consist simply of waves. Attempts to explain the discrepancy between theory and experiment were quite fruitless until 1900, when Planck proposed a revolutionary modification in the theory.<sup>1</sup>

His modification consisted in introducing the postulate that the

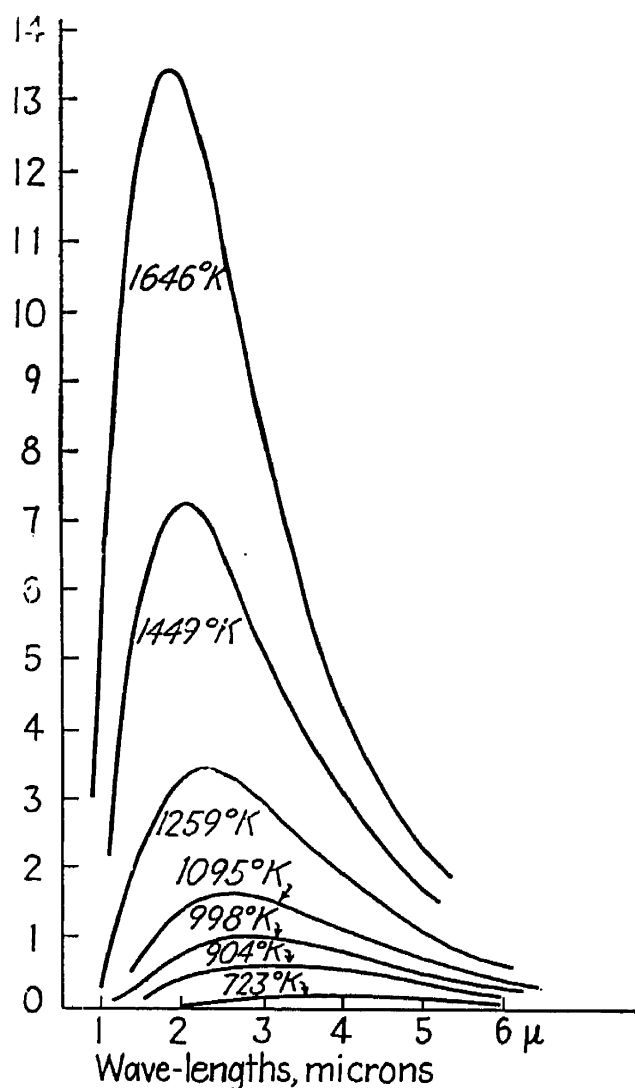


FIG. 3-2.—Black-body radiation curves showing infrared energy distribution. (Lummer and Pringsheim.)

<sup>1</sup> Max Planck, *Ann. Physik*, **1**, 719 (1900), **4**, 553 (1901).



energy is radiated, not continuously as must be the case for pure waves but in small packets, which he called "quanta." This revolutionary change marked the birth of the modern quantum theory of radiation and atomic energy. In order to make the theory fit the experimental data Planck found it necessary to postulate that the energy contained in these minute quanta radiated from a black body was proportional to the frequency of the radiation, or, as he wrote it,

$$E = h\nu \quad (3-3)$$

where  $E$  is the energy of each quantum,  $\nu$  is the frequency of the radiation as defined in Secs. 1 and 2, and  $h$  is the proportionality constant now known as "Planck's  $h$ " or "Planck's constant." The value assigned to  $h$  by Planck in 1900 was  $6.55 \times 10^{-27}$  erg-sec., based on the infrared data available to him at that time. The value indicated by the latest data<sup>1</sup> is  $6.624 \times 10^{-27}$  erg-sec. Incidentally, the best experimental method now known for determining Planck's constant is one using x-rays, as will be explained later. The unit "erg-seconds" follows from ordinary dimensional analysis. In equation (3-3),  $E$  is energy, measured in the standard c.g.s. unit of energy, the erg; and  $\nu$  is frequency measured in cycles per second, which has the dimensions of 1/sec. or sec.<sup>-1</sup>. Hence  $h = E/\nu = \text{ergs/sec.}^{-1} = \text{erg-sec.}$

This fundamental postulate of Planck was soon found to have wide application in fields of physics other than that of the infrared. One of its most important successes was in accounting for the previously unexplained phenomena of the photoelectric effect. The photoelectric effect is ordinarily thought of as the phenomenon occurring in a photoelectric cell when light falls on a sensitive surface like cesium and ejects electrons from it, thus permitting one to use photocells for a wide variety of practical applications. However, x-rays have a photoelectric action which is more pronounced than that of visible light, because their frequency  $\nu$  (and hence energy  $h\nu$ ) is much greater. Some knowledge of the fundamentals of the photoelectric effect is therefore helpful in understanding such things as the action of lead intensifying screens on an x-ray film.

One of the most important uses for Planck's equation (3-3) in the study of x-rays, however, is its application to their generation, because it is the basis of the relation between the electric potential applied to the x-ray tube and the wave lengths of the x-rays generated.

Let us suppose that a potential difference of 150 kv. is imposed between the electrodes of an x-ray tube. This is a potential difference of 500 electrostatic units, for 1 e.s.u. = 300 volts. It will be remembered that potential difference  $V$  between two points is defined as the work

<sup>1</sup> R. T. Birge, *Rev. Modern Phys.*, 13, 236 (1941).

required to carry unit positive charge from one point to the other. Therefore the work required to carry any charge  $q$  from one point to the other is  $qV$ . The charge on an electron is a fundamental physical constant<sup>1</sup> and is therefore commonly represented by the letter  $e$ . Birge's latest<sup>1</sup> estimate for  $e$  is  $4.8021 \times 10^{-10}$  e.s.u. Consequently the work  $qV$  required to carry an electron from the anode to the cathode in the above example, where  $q = e$  and  $V = 500$  e.s.u., is  $4.8 \times 10^{-10} \times 500$  or  $24 \times 10^{-8}$  erg. Conversely, an electron emitted from the cathode and proceeding to the anode under the action of the electrostatic field between the electrodes will acquire  $24 \times 10^{-8}$  erg of kinetic energy by the time it strikes the anode. Incidentally, it is usually more convenient to speak of the energy of such electrons in terms of "electron volts." Thus, in this example, one commonly would express the electron energy as being 150,000 electron volts, rather than  $24 \times 10^{-8}$  erg.<sup>2</sup>

The probability that any particular electron striking the anode will happen to strike one of the atoms composing the anode in just the proper manner to transform all its kinetic energy into a single photon or quantum of x-ray energy is very small, but it is possible and does happen occasionally. When this occurs, the energy of the photon will of course be equal to the energy of the electron; therefore, applying (3-3),

$$Vc = h\nu_0 \quad (3-4)$$

or  $500 \times 4.8 \times 10^{-10} = 6.624 \times 10^{-27} \nu_0$  so that  $\nu_0$  (the highest x-ray frequency generated at 150 kv.) is easily computed as  $3.62 \times 10^{19}$  cycles/sec. Applying (3-2),  $\lambda_0 = c/\nu_0$ , or

$$\lambda_0 = \frac{3 \times 10^{10}}{3.62 \times 10^{19}} = 0.083 \times 10^{-8} \text{ cm.} = 0.083 \text{ A.}$$

Actually, this coincides exactly with experimental observation, which shows that the maximum x-ray frequency generated varies strictly in proportion to the tube voltage, as indicated by (3-4). If a tube is operated at 150 kv., it is found that the highest energy (that is, the shortest wave-length) x-rays generated have a wave length of 0.083 A. This is called the "short-wave-length limit" or the "Duane-Hunt<sup>3</sup> limit." Most of the rays are found to have wave lengths longer than this, as is to be expected, since most of the electrons in the cathode-ray beam will strike the atoms in the target in such a way as to convert only part (or none) of their energy into x-ray photons, so that the rays will therefore consist of waves of lower frequency or longer wave length by equations (3-3) and (3-2).

This example illustrates the best-known direct experimental method of

<sup>1</sup> R. T. Birge *Am. J. Physics*, **13**, 63 (1945).

<sup>2</sup> See Appendix I.

<sup>3</sup> W. Duane and F. L. Hunt, *Phys. Rev.*, **6**, 166 (1915).

determining Planck's constant (if  $e$  is known) or  $h/e$  if  $e$  is assumed to be known no more accurately than  $h$ . From (3-4), one has  $h/e = V/\nu$ . Hence an x-ray tube may be operated at a carefully measured potential  $V$ , and the highest frequency  $\nu_0$  of the x-rays generated may be observed. This limiting frequency is found by measuring the wave length of the shortest waves present at the Duane-Hunt limit and applying  $\nu_0 = c/\lambda$ .  $c$  is supposedly known more accurately than either  $h$  or  $e$ . Dividing by  $\nu_0$  then gives a direct experimental value<sup>1</sup> of  $h/e$  or of  $h$  if  $e$  is assumed known accurately. The method of measuring the wave length  $\lambda$  will be described later.

The most conclusive proof that x-rays behave in certain respects as particles is afforded by observation of their photoelectric action when they strike some object. Suppose that an x-ray tube is operated at 100 kv. and that the x-rays from this tube strike a metal plate near by. The x-rays eject electrons photoelectrically from the plate. If it is placed in a vacuum, the energy of the photoelectrons from it can be measured by a device known as a magnetic spectrograph.<sup>2</sup> The significant fact about such an experiment is that the maximum energy observed for the fastest photoelectrons is always equal to the energy of the cathode rays in the x-ray tube, whether the distance between the x-ray tube and the metal plate is 1 or 3 ft. In the present example, the fastest photoelectrons will have an energy of 100,000 electron volts because the x-ray tube is operating at 100 kv.

If one thinks of the x-rays as being pure *waves*, Sir W. H. Bragg has suggested<sup>3</sup> an analogous phenomenon:

Suppose we drop a plank into the sea from a given height, say 100 feet; there is a splash and waves spread away over the surface of the water. They pass by boats and ships without any effect, and then after travelling thousands of miles they find a ship on which their effect is disastrous: a plank is torn out of the ship's side and hurled, ninety feet into the air. . . . This is a fair parallel to an explanation of the photoelectric effect on the simple wave theory.

On the other hand, if one thinks of the x-rays as being particles, or photons, the explanation of the experiment is quite simple. A cathode ray electron in the x-ray tube strikes the target  $T$  in such a manner as to transform all its 100,000 electron volts of energy into an x-ray photon which therefore likewise possesses an energy of 100,000 electron volts.

<sup>1</sup> A recent determination by W. K. H. Panofsky, A. E. S. Green, and J. W. N. DuMond, *Phys. Rev.*, **62**, 214 (1942), indicates that  $h/e = 1.3786 \times 10^{-17}$  erg-sec e.s.u.; P. Ohlin, *Nature*, **152**, 329 (1943), has found  $h/e = 1.3787 \times 10^{-17}$ .

<sup>2</sup> See, for example, H. Robinson, *Proc. Roy. Soc. (London) A*, **104**, 455 (1923) *Phil. Mag.*, **50**, 241 (1925).

<sup>3</sup> W. H. Bragg, "The Universe of Light," George Bell & Sons, Ltd., London, 1931; quoted by permission.

The photon travels to the metal plate and encounters an electron there, to which it imparts this energy.

**4. The Continuous X-ray Spectrum—Experimental.** In the preceding section, the method was outlined by which the data are obtained for infrared energy distribution curves such as those shown in Fig. 3-2. In the case of x-rays, it is not possible to obtain such curves by making use of a rock-salt prism, for x-rays are refracted to such a slight extent by a prism (of any material) that this method is impractical. However, it is possible to obtain the x-ray spectrum of polychromatic rays (that is, x-rays composed of many wave lengths, like white light) by diffraction methods analogous to the production of a colored visible spectrum when white light is passed through a finely ruled diffraction grating. The

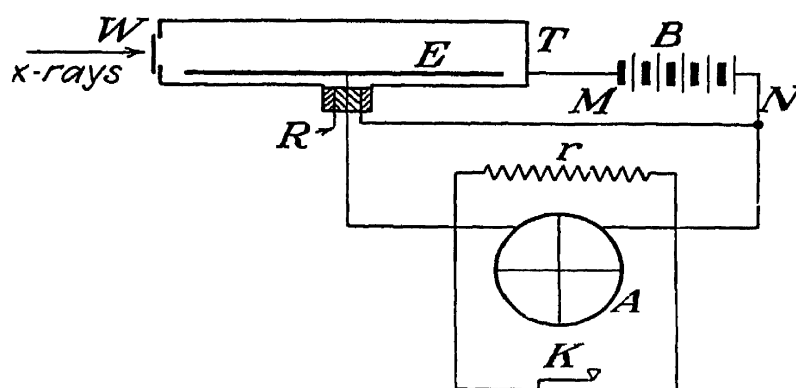


FIG. 3-3.—Ionization chamber and connections. (After Richtmyer and Kennard, "Introduction to Modern Physics," 3d ed.)

instrument for this purpose, called an "x-ray spectrometer," is described in Chap. 16.

In the case of infrared radiation, the intensity in various parts of the spectrum can be measured by a thermocouple or thermopile. This can also be accomplished with visible light and the near ultraviolet by means of a photocell. However, the energy of an x-ray beam is contained in a much smaller number of much more energetic photons than is the case with the energy in a beam of light or infrared rays. This different character of x-rays makes photocells or thermocouples very inefficient instruments for detecting or measuring the intensity of x-rays.

The best-known device for giving a continuous indication of the intensity of an x-ray beam is the ionization chamber. Figure 3-3 is a schematic diagram of one of these reduced to its simplest form.  $T$  is a metal tube a few inches in diameter and 6 or 8 in. to 1 yard or more in length. At one end it is provided with a "window"  $W$ , consisting of a hole covered with a thin sheet of aluminum foil, mica, or cellophane, although cellophane sometimes deteriorates from the action of the x-rays. The metal electrode  $E$ , usually a rod, is mounted parallel to the axis of the tube  $T$ , but displaced far enough from this axis so that the direct x-ray beam entering the window along the axis will not strike  $E$  at any point.

It is important that  $E$  be supported and insulated from  $T$  by a good insulator such as amber or quartz. A wire leading from  $E$  is connected to an electrometer  $A$ , the other quadrants of the electrometer being connected in series with a battery  $B$  to the tube  $T$ .  $B$  should have an electromotive force of 100 volts or more. If it is important that  $T$  be grounded, this may be done provided that the electrometer and the wire connecting it to  $E$  and the discharge key  $K$  are very well insulated. If the circuit is grounded at  $N$  rather than  $M$ , the danger of errors due to insulation leakage is reduced, but then the chamber itself is charged, in which case it may be constructed as a wire cage inside of, but insulated from, a grounded metal cylinder or case.

If the chamber is to be used to measure intensity directly, this may be done by shunting the electrometer with a high resistance  $r$  (say 1,000 megohms), so that the electrometer deflection measures the ionization current. If the intensity is very low or if it is desired to measure quantity of radiation (intensity times time), then  $r$  is omitted so that the electrometer deflection measures the electric charge conducted from  $E$  to  $T$  in a measured time by the ion current in the chamber. This charge may be removed at any time by closing the well-insulated key  $K$ . The electrical leakage through the insulating collar where the lead to  $E$  enters the tube  $T$  may be reduced by incorporating in it a guard ring  $R$  connected to the opposite side of the electrometer, as shown. Modern practice often substitutes a vacuum tube amplifier for the electrometer.

The x-rays that are to be measured for intensity are restricted to a beam of approximately parallel rays by passing them through collimating holes in parallel sheets of lead, for example. The beam must be narrow enough so that no part of it will strike the electrode  $E$  or the interior of the tube  $T$ .

The photoelectric action of the rays will eject electrons from some of the atoms composing the gas in the chamber. As will be described later, some of the x-rays will be scattered, and in the process high-energy "recoil" electrons are produced. These high-energy photoelectrons and recoil electrons tear through the gas, colliding with hundreds of atoms and knocking electrons out of them so that hundreds of electrons and ions are formed. All these will immediately be collected by the charge electrode  $E$  and the tube  $T$ , the ions going to the one and the electrons to the other, depending upon the polarity of the battery. Together with the migration of the electrons and ions collected will constitute an ionic current that will flow through the external electric circuit and cause the electrometer  $E$  to deflect. If the x-ray beam is intense, a large number of photons per second pass through the chamber and a large electrometer deflection (or rate of deflection, if  $r$  is omitted) results.

If the x-ray intensity is reduced 50 per cent, so is the electrometer deflection if a shunting resistance  $r$  is used; otherwise, its rate of deflection is reduced by half.

The gas in the chamber is usually at atmospheric pressure and may be dry air, although some gas of high molecular weight, like argon, methyl bromide, or methyl iodide, is often used. The use of such heavy gases increases the ionization rate, and hence the sensitivity, by a factor of 10 or more, compared with air. Additional details regarding ionization chambers and other means of detecting and measuring x-rays will be reserved for Chap. 8.

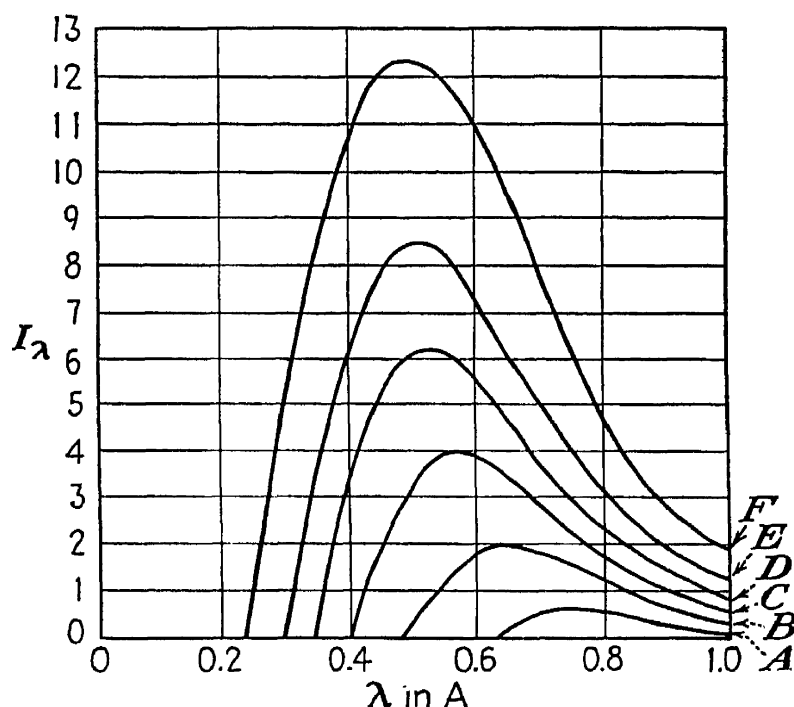


FIG. 3-4.—Intensity curves for continuous x-ray spectrum at various voltages, from tube with tungsten target. A, 20 kv. B, 25 kv. C, 30 kv. D, 35 kv. E, 40 kv. F, 50 kv. (By Ulrey; courtesy of *Physical Review*.)

By using an ionization chamber in place of a thermocouple or photocell to measure intensity, it is possible to obtain curves for the spectral distribution of x-rays like those shown in Fig. 3-2 for infrared rays. Such a set of curves for x-rays from a Coolidge tube with a tungsten target are shown in Fig. 3-4, obtained by Ulrey<sup>1</sup> in 1918. In this figure, the abscissas represent wave lengths in angstroms, and the ordinates represent intensities, which were obtained by taking readings from an ionization chamber 75 cm. long filled with ethyl bromide. The various curves were obtained by operating the x-ray tube (which had a tungsten target) at the different voltages indicated beneath the figure.

It will be noted that, as the voltage is increased, (1) the intensity of the radiation increases at all wave lengths (the curves get higher, and the area under them increases); (2) the wave length at which the maxi-

<sup>1</sup> C. T. Ulrey, *Phys. Rev.*, **11**, 401 (1918).

imum intensity occurs decreases (the peaks shift to the left); and the minimum wave length present grows shorter (the left end of curve intersects the  $\lambda$  axis at a point that moves to the left with increasing voltage). The third statement regarding the minimum wave length  $\lambda_0$  present has been discussed in Sec. 3 [see the paragraph containing equation (3-4)].

To elaborate on the first statement, Ulrey found that the area under these curves increased proportionally to the square of the x-ray tube voltage. This means that, over the ordinary voltage range used in x-ray work, the total intensity of the continuous x-ray radiation generated in the tube, considering all wave lengths, increases with the square of the voltage, other things such as the tube current remaining constant. That is,

$$I_{\text{continuous}} = kV^2 \quad (3-5)$$

The term "continuous radiation" is used to designate the type of x-ray generated by the impact of the cathode-ray electrons directly, and is the only type of x-ray radiation discussed in this chapter. There are other x-rays generated *indirectly* by these electron impacts (to be discussed in the next chapter), and in order to distinguish the two types, the term "continuous radiation" is applied to the type thus discussed.

To elaborate on the second statement regarding Ulrey's curves, the wave length of the most intense rays decreases as the tube voltage is increased, Ulrey concluded that

$$\lambda_m V^{1/2} = \text{constant} \quad (3-6)$$

over the range studied, where  $\lambda_m$  is the wave length at the peak of the curve, corresponding to the maximum intensity occurring at any voltage  $V$ . Ulrey's curves in Fig. 3-5, upon which this conclusion was based, were uncorrected for such effects as second-order diffraction in the spectrometer, incomplete absorption in the ionization chamber, absorption by the x-ray tube wall, the atmosphere and the ionization-chamber window, variation in the so-called "reflecting power" of the crystal in the spectrometer, and, finally, absorption of the x-rays in the target itself, since most of them are generated at a small but finite distance beneath the surface of the target. Pike<sup>1</sup> has replotted Ulrey's curves after making all the above corrections except the first and last.

After making some of these corrections, Dauvillier<sup>2</sup> concluded that equation (3-6) is incorrect, and he suggested instead that the variation of  $\lambda_m$  with voltage is the same as the variation of  $\lambda_0$  with voltage,  $\lambda_0$  being

<sup>1</sup> E. W. Pike, *J. Applied Phys.*, **12**, 206 (1941).

<sup>2</sup> A. Dauvillier, *Ann. phys.*, **13**, 49 (1920).

the wave length at the Duane-Hunt short-wave limit where Ulrey's curves intersect the  $\lambda$  axis. That is, Dauvillier suggested the relation

$$\lambda_m = k\lambda_0 \quad (3-7)$$

where  $k$  is a constant. Subsequent work by Kulenkampff<sup>1</sup> tended to confirm this, but still later work by Kirkpatrick<sup>2</sup> led him to propose the relation

$$\lambda_m = k + k'\lambda_0 \quad (3-8)$$

where  $k$  and  $k'$  are two different constants. Kirkpatrick's corrections did not include absorption in the tube target, so the relation governing  $\lambda_m$  is still in some doubt.

There is no such doubt about  $\lambda_0$ , however. From (3-2) and (3-4),

$$\lambda_0 V = \frac{hc}{e} \quad (3-9)$$

in which  $hc/e$  is, of course, a constant, and this has been experimentally verified with very high accuracy. In this equation, it must be remembered that  $\lambda_0$  is in centimeters (not angstrom units) and  $V$  is in e.s.u. (not volts; 1 e.s.u. of potential = 300 volts).

In the paper by Kulenkampff mentioned in connection with equation (3-7), he determined that the family of curves in Fig. 3-5 can be represented quite accurately by the empirical equation

$$I_\lambda = CZ \frac{1}{\lambda^2} \left( \frac{1}{\lambda_0} - \frac{1}{\lambda} \right) + BZ^2 \frac{1}{\lambda^2} \quad (3-10)$$

where  $B$  and  $C$  are constants and  $Z$  is the atomic number of the target element.  $B$  is so small that the second term is ordinarily neglected in comparison with the first.

The matter of correcting ionization-chamber readings to obtain the true intensity is quite complex, but the problem is comparable to a similar one encountered in other physical measurements that may be more familiar. The only fundamental and absolute way of measuring and expressing the intensity of any radiation such as light, sound, x-rays, or radio waves is to measure the energy flow per second through unit area of an imaginary plane perpendicular to its direction of travel. When so measured, light intensity, sound intensity, x-ray intensity, etc., will all be expressed in terms of ergs/cm.<sup>2</sup>/sec., and not in such arbitrary units as foot-candles, decibels, roentgens per second (see Chap. 8), etc., which are measured by such instruments as photocells, sound meters,

<sup>1</sup> H. Kulenkampff, *Ann. Physik*, **69**, 548 (1922).

<sup>2</sup> P. Kirkpatrick, *Phys. Rev.*, **22**, 37 (1923).



and ionization chambers. Thus a photocell and meter such as photographers use to judge camera exposures may read 17 in a beam of red light and 17 in another beam of green light, even though the red light beam is really twice as intense measured in absolute units, ergs/cm.<sup>2</sup>/sec. The same is true of ionization chambers when used to measure x-ray intensity. They ordinarily give a higher reading when measuring the intensity of a long-wave-length x-ray beam than they do when placed in a short-wave-length beam of the same absolute intensity, and the relative readings will change or even reverse when one gas like air is replaced by another like methyl iodide in the chamber. Ionization chambers can therefore be used to compare x-ray intensities at different wave lengths only after corrections for several factors have been carefully made.

The experimental studies of Ulrey, Dauvillier, Kulenkampff, and Kirkpatrick mentioned above all indicated also that the total intensity of the continuous radiation is proportional to the atomic number  $Z$  of the target material, so that equation (3-5) may be generalized to

$$I_{\text{continuous}} = KZV^2 \quad (3-11)$$

where  $K$  is a constant. This result might have been anticipated from the relation for x-ray tube efficiency evolved from the experiments of Beatty and Rump mentioned in Chap. 2 [equation (2-5)]. The proportionality between  $I_{\text{continuous}}$  and  $Z$  has not been established as one of strict accuracy, but it is a very good approximation. The  $V^2$  relationship is quite accurate, although it has not been verified with the extreme accuracy of equation (3-9).

In practical work such as radiographing a casting or treating a tumor, there are three primary points to be kept in mind as one concludes this section (Sec. 4). (1) *An increase in the voltage used increases the x-ray intensity in a square-law relationship* (tripling the voltage increases the intensity ninefold). (2) *An increase in the voltage used makes the rays more penetrating by decreasing their wave length.* (3) *For a given voltage, the x-ray intensity at all wave lengths is directly proportional to the tube current.*

The second point brings up the question of the relation between the wave length of the x-rays and their ability to penetrate matter. This will be discussed in detail in Chap. 5. For the present, it will merely be stated that short-wave-length x-rays are able to penetrate matter much more effectively than long-wave-length x-rays. High-voltage short-wave-length x-rays are commonly called "hard" x-rays. Low-voltage long-wave-length x-rays are commonly called "soft" x-rays. If they are quite soft (wave length of 2 Å. or more), they are sometimes called "grenz rays." "Grenz" comes from a Greek word meaning

“border” and suggests that the grenz rays are on the border between x-rays and ultraviolet rays.

X-rays of the type discussed thus far, which have the spectral distribution graphically represented in Fig. 3-4, are called the continuous radiation because their wave lengths vary continuously over a wide spectral range in a way similar to the continuous spread of the wave lengths present in white light from an incandescent lamp. It is this continuous x-ray radiation which is used in most radiographic work (hunting flaws in castings, broken bones, etc.), therapeutic work (killing tumors, etc.), and other work outside of the field of x-ray diffraction (to be discussed later), and it is useful in certain types of diffraction work.

**5. The Continuous X-ray Spectrum—Theoretical.** A brief outline of theories of the origin of the continuous x-ray spectrum may help to guide practical workers into fruitful types of work and prevent waste of effort. According to the early classical theory, one may visualize the cathode-ray stream bombarding the x-ray tube target as analogous to a hail of machine-gun bullets fired into a room packed full of baseballs. According to this analogy, the bullets represent the cathode-ray electrons and the baseballs represent the atoms composing the target; if it is a tungsten target, they will be tungsten atoms. The bullets will immediately encounter the baseballs, which may be imagined to be constructed each with a central core harder for the bullets to penetrate than the outer portion. A few of the bullets will happen to strike the first ball they hit in such a way as to be stopped at once by the central core. Most of the bullets will pass through the outer portions of the first two or three balls they strike, without encountering a core, and may therefore penetrate to a depth of several layers of balls before they are finally stopped. In any case, the bullets are stopped in a short distance; and since they had a high initial velocity, their quick stop subjected them to a high deceleration, or negative acceleration.

According to the electrical theories of classical physics, an electron, supposed to be a negatively charged particle, will indeed generate an electromagnetic wave, or at least a pulse (as distinguished from a continuous train of waves), when subjected to such an acceleration, either positive or negative. As already mentioned in Sec. 1, such waves are transverse, associated, mutually perpendicular, electric, and magnetic vibrations. According to the bullet-baseball analogy, the accelerations of the bullets (electrons) will take place predominantly in the direction of their initial line of travel, although glancing blows will cause them to ricochet to some extent among the baseballs, thus introducing smaller accelerations in directions perpendicular to the line of travel of the bullets.

In Fig. 3-5, an electron supposedly travels along the line  $AO$  with velocity  $v$  until it strikes the atoms of the target. Thereupon it experiences an acceleration  $a$  in the opposite direction represented by the vector  $a$  at  $O$  (which may be thought of as the point at which the electron encounters an atom). Assuming that the continuous x-ray radiation is

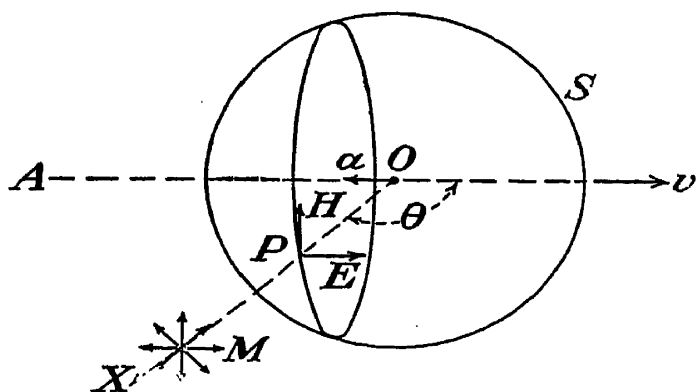


FIG. 3-5.—To illustrate Thomson's classical theory of continuous x-ray generation.

generated by a process of the sort described in the preceding paragraph, J. J. Thomson<sup>1</sup> worked out the theory on the basis of classical physics and showed that it predicts an electromagnetic pulse radiating from  $O$ . It radiates in all directions with velocity  $c$ , and so at an instant  $r/c$  sec. after the pulse started from  $O$  its position will be represented by the sphere  $S$  of radius  $r$  with center at  $O$ , being the velocity of light. In the arbitrary direction  $OPX$  making an angle  $\theta$  with the direction of the vector  $a$ , the electric vibration at  $P$ , where  $OPX$  pierces  $S$ , is represented by the electric vector  $E$ .  $E$  is perpendicular to  $OX$  and lies in the plane  $AOX$ . The associated magnetic vibration is represented by the magnetic vector  $H$ .  $H$  is perpendicular to the plane  $AOX$ . If  $a$  is in the direction shown,  $E$  and  $H$  have the directions indicated by the arrow heads in the figure. Calculations based upon the classical<sup>2</sup> theory lead to the result

$$E = H = \frac{ae}{rc^2} \frac{\sin \theta}{(1 - \beta \cos \theta)^3} \quad (3-12)$$

where  $E$  is in c.g.s. e.s.u. of electric field intensity,  $H$  is in oersteds (formerly called gauss),  $a$  is the acceleration in centimeters per second per second,  $e$  the electronic charge in e.s.u.,  $r$  is the distance  $OP$  in centimeters,  $c$  is the velocity of light in centimeters per second, and  $\beta = v/c$ ,  $v$  being the velocity of the electron when it struck the atom. Together, the vectors  $E$  and  $H$  move along the line of travel  $OX$  with velocity  $c$ , the magnitudes decreasing inversely in proportion to their distance  $r$  from  $O$ . They represent the part of the electromagnetic pulse generated at which is radiated in the arbitrary direction  $OX$ .

The well known classical expression for the energy per cubic centimeter of the space through which such an electromagnetic vibration

<sup>1</sup> J. J. Thomson, *Phil. Mag.*, **45**, 172 (1898).

<sup>2</sup> The  $(1 - \beta \cos \theta)^3$  term is a correction term that enters from the application of the special theory of relativity. The simple classical equation is one in which the term equals 1 and so does not appear.

passing is

$$\text{Energy/cm.}^3 = \frac{E^2}{8\pi} + \frac{H^2}{8\pi} = (\text{in empty space}) \frac{E^2}{4\pi} \quad (3-13)$$

This quantity multiplied by  $c$  gives the energy passing per second through 1 cm.<sup>2</sup> of an imaginary plane perpendicular to the direction of motion of the radiation, which of course is the intensity  $I$ . Hence the intensity at the point  $P$  in Fig. 3-5 is given by

$$I = \frac{a^2 e^2}{4\pi r^2 c^3} \frac{\sin^2 \theta}{(1 - \beta \cos \theta)^6} \quad (3-14)$$

each letter having the same significance as in (3-12);  $I$  will be given in ergs/cm.<sup>2</sup>/sec.

This theory obviously oversimplifies the picture, for the electron is pictured as being stopped by uniform negative acceleration in the direction of its original velocity, rather than by repeated accelerations of various magnitudes in various directions. To check the theory, experiment can be made to approach these idealized assumptions by using extremely thin metal foil as the x-ray tube target. In this case, most of the electrons pass right through, but a few experience accelerations in the foil of the type assumed in the theory.

Various workers<sup>1</sup> have performed such thin-target experiments in order to check the theory. It has been found that the x-ray intensity from thin targets varies with voltage and direction in a way which is only roughly represented by (3-14). For a more accurate expression, see equation (3-23).

This classical theory of the generation of the continuous x-radiation predicts that the continuous rays generated in an extremely thin target will be completely polarized in the plane of the cathode rays and the x-ray in question. This follows from the fact that the vector  $\mathbf{E}$  is in the plane  $AOX$  in Fig. 3-5, whereas in the case of ordinary unpolarized x-rays (or light or other electromagnetic radiation) the electric vibration represented by the vector  $\mathbf{E}$  is found to occur in all directions perpendicular to the ray, as represented at  $M$ , each different vector  $\mathbf{E}$  being associated with a magnetic vibration perpendicular to that  $\mathbf{E}$  and to the ray. Thus the magnetic vibrations  $\mathbf{H}$  are also found in all directions perpendicular to the ray in unpolarized radiation. The prediction that thin-target x-rays are completely polarized as shown in Fig. 3-5 is in fair agreement with the results of thin-target experiments, which have revealed the x-rays to be highly, but not 100 per cent, polarized in the

<sup>1</sup> H. Kulenkampff, *Ann. Physik*, **87**, 597 (1928); *Physik. Z.*, **30**, 513 (1929). W. W. Nicholas, *Bur. Standards J. Research*, **2**, 837 (1929). K. Böhm, *Ann. Physik*, **33**, 315 (1938). R. Honerjäger, *Ann. Physik*, **38**, 33 (1940). K. Harworth and P. Kirkpatrick, *Physik. Rev.*, **62**, 334 (1942).

plane predicted. The definition of "per cent polarization" and method of measuring it for x-rays are discussed later in this section.

The predictions of the classical theory are therefore only in approximate qualitative agreement with experiment, both as regards angular intensity distribution, variation of intensity in a given direction with voltage, and per cent polarization. A glaring defect of the classical theory is that it predicts that any accelerated electron must radiate electromagnetic waves as long as it is accelerated. This implies that every atom should radiate such waves all the time, because atoms consist of a positively charged nucleus surrounded by swarms of electrons supposedly revolving about the nucleus as the planets revolve about the sun and hence continuously subject to enormous centripetal acceleration. Some of the evidence for this statement will be described in Chapter 4. Ordinary atoms do not constantly radiate energy, of course, and so it is difficult to explain why merely accelerating an electron should generate radiation.

When one calculates the wave lengths of the radiation on the basis of the classical theory outlined above, the resulting equations predict that they will cover a continuous range extending both above and below the Duane-Hunt short-wave limit. Of course, this is in direct conflict with the data represented by Fig. 3-4.

In spite of these shortcomings, the angular intensity distribution of the continuous x-rays from a thin target can be predicted with considerable accuracy by the classical theory. Equation (3-14) gives the intensity of the radiation to be expected at the point  $P$  (Fig. 3-5) at any given instant due to the acceleration  $a$  of an electron at  $O$  at an instant  $r/c$  sec. earlier. To calculate the integrated intensity to be expected due to the entire stopping process of the electron, during which its velocity drops from  $v = \beta c$  to  $v = 0$ , it is necessary to integrate expression (3-13) over the corresponding time interval. Calling the integrated intensity  $\bar{I}$ , one has

$$\bar{I} = \int_{t_1}^{t_2} I dt \quad (3-15)$$

where  $t_1$  is the value of  $t$  at the start of the deceleration when  $v = \beta c$  and  $t_2$  is the value of  $t$  at the end of the deceleration when  $v = 0$ . Sommerfeld<sup>1</sup> was the first to carry through this integration, and he obtained the result

$$\bar{I} = \frac{|a|e^2}{16\pi r^2 c^2} \frac{\sin^2 \theta}{\cos \theta} \left[ \frac{1}{(1 - \beta \cos \theta)^4} - 1 \right] \quad (3-16)$$

where  $|a|$  is the absolute value of the acceleration (assumed to be constant during the stopping process).

<sup>1</sup> A. Sommerfeld, *Physik. Z.*, **10**, 969 (1919).

When this expression is plotted in polar coordinates as a function of  $\theta$ , one obtains theoretical energy distribution curves of the type shown in Fig. 3-6. The corresponding experimental thin-target energy distribution curve obtained by Honerjäger<sup>1</sup> from a thin target for a value of  $\beta$  of about  $\frac{1}{3}$  is shown in Fig. 3-7. It will be noted that the maximum of the  $\beta = \frac{1}{3}$  curve in Fig. 3-6 occurs at about  $70^\circ$ , whereas the maximum of the experimental curve occurs at about  $55^\circ$ ; therefore, the data fit the theory only in an approximate and qualitative way.

With the advent of the quantum theory, efforts have been made to apply it to the continuous x-ray spectrum, and among these the work of Kramers<sup>2</sup> may be mentioned as one of the more successful efforts to patch up the classical theory by introducing some of the concepts of the quantum theory. This was done by making use of a postulate advanced by Niels Bohr in 1918, called the "correspondence

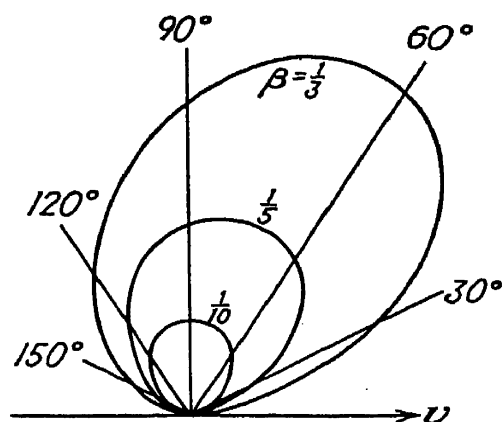


FIG. 3-6.—Theoretical angular energy-distribution curves for continuous radiation from a thin target at three different voltages. (After Compton and Allison; courtesy of D. Van Nostrand Company, Inc.)

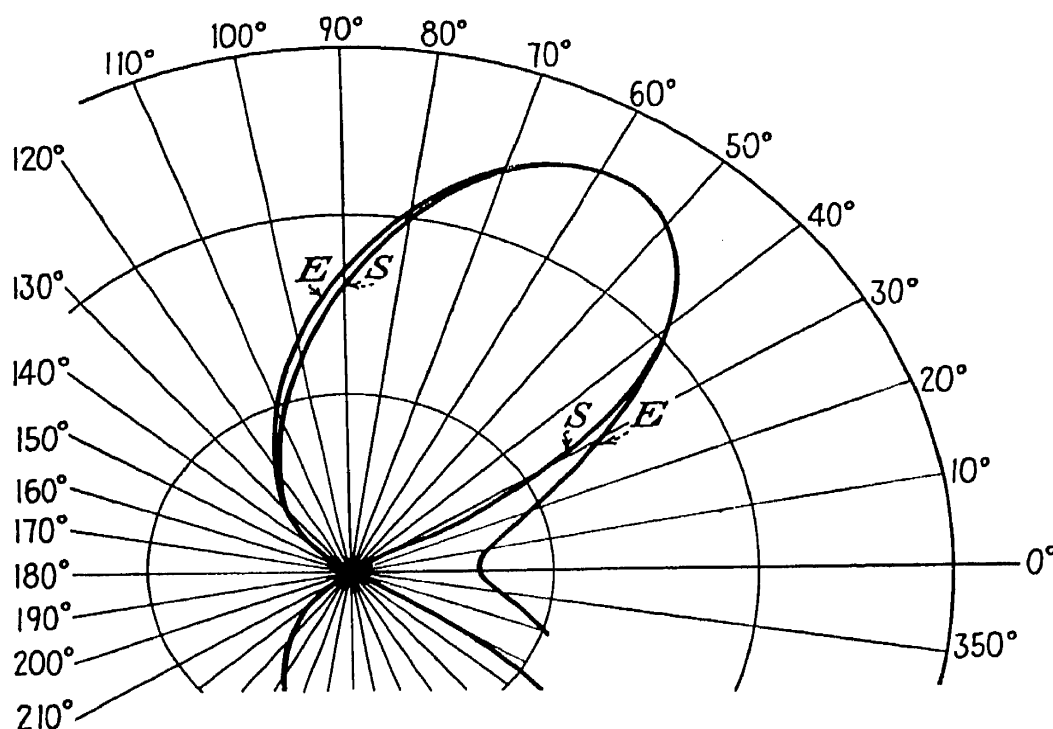


FIG. 3-7.—Angular x-ray energy-distribution curves for a thin target. *E*, experimental curve for rays at short wave-length limit only, from aluminum foil target about 200A . thick, at 34 kv., obtained by Honerjäger. *S*, the corresponding theoretical curve for a target of infinitesimal thickness, calculated by Scherzer.

principle." It states that under certain conditions of high quantum energy (as in the case of x-rays) the frequency of the electromagnetic radi-

<sup>1</sup> R. Honerjäger, *Ann. Physik*, **38**, 33 (1940).

<sup>2</sup> H. A. Kramers, *Phil. Mag.*, **46**, 836 (1923).

ation generated by oscillating or accelerated electrons may be calculated on the basis of classical electrodynamics, as already outlined, and then quantum theory may be applied to calculate the intensities. Such a hybrid "classical-quantum" treatment is never very satisfactory, but Kramers was able, on such a basis, to arrive at an expression for the efficiency of x-ray generation that agrees within experimental error with the Bethe equation (2-5). His theory also indicated that if the intensity of continuous x-radiation in any given direction from a thin target is plotted as a function of the frequency the result should be merely a straight horizontal line terminating at  $\nu = \nu_0$ , the Duane-Hunt limit. The height of the horizontal line of course depends upon the angle for which it is plotted (see Figs. 3-6 and 3-7). That is, for a given

$$I_\nu = \text{constant} \quad (\nu < \nu_0) \quad (3)$$

This being the case, one might suppose at first thought that a horizontal

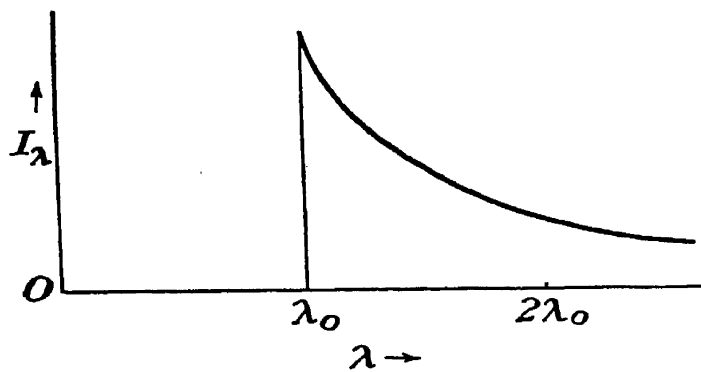


FIG. 3-8.—Typical energy-distribution curve for the continuous radiation from a thin target. (Compton and Allison; courtesy of D. Van Nostrand Company, Inc.)

straight line would also represent the intensity when plotted as a function of wave length. Consideration of the meaning of energy of this type (for example, Figs. 3-2 and 3-4) will show that this is not true, however.

When the intensity  $I_\lambda$  is plotted as a function of the wave length, the ordinate of the curve at any value of  $\lambda$ , such as  $\lambda_1$ , represents the average intensity of the radiation present in the wave-length

range  $d\lambda$  lying between  $\lambda_1$  and  $\lambda_1 + d\lambda$ . Hence the energy in this range is  $I_\lambda d\lambda$ . In the same way, if  $I$  is plotted as a function of the frequency, the energy in a frequency range  $d\nu$  is  $I_\nu d\nu$ . Two such curves are then equivalent only if  $I_\nu d\nu = -I_\lambda d\lambda$ , the negative sign entering because a positive value of  $d\lambda$  corresponds to a negative value of  $d\nu$ . From the relation  $\nu = c/\lambda$  one has  $d\nu/d\lambda = -c/\lambda^2$ . Hence

$$I_\lambda = -I_\nu \frac{d\nu}{d\lambda} = \frac{c}{\lambda^2} I_\nu.$$

Therefore the relation (3-17) is equivalent to the relation

$$I_\lambda = \frac{c}{\lambda^2} (\text{constant}) = \frac{b}{\lambda^2} \quad (\lambda > \lambda_0)$$

where  $b$  is a constant. This relation is represented graphically in Fig. 3-8; with proper choice of the value of  $b$ , it fits the experimental data fairly well and may be contrasted with Fig. 3-4 for a thick target.

The empirical equation (3-10) is not in the form given by Kulenkampff but is derived from the form

$$I_\nu = C'Z(\nu_0 - \nu) + B'Z^2 \quad (3-19)$$

given by him, by making use of the relation

$$I_\lambda = \frac{c}{\lambda^2} I_\nu \quad (3-20)$$

In the paper by Kramers, just discussed, he derived theoretically the equation (for a massive target)

$$I_\nu = s \frac{8\pi}{3l} \frac{e^2 h}{mc^3} Z(\nu_0 - \nu) = 5 \times 10^{-50} s Z(\nu_0 - \nu) \quad (3-21)$$

which transforms to

$$I_\lambda = 45 \times 10^{-30} s Z \frac{1}{\lambda^2} \left( \frac{1}{\lambda_0} - \frac{1}{\lambda} \right) \quad (3-22)$$

where  $s$  is the number of electrons striking the target (of atomic number  $Z$ ) per second,  $l$  is a constant having a value of approximately 6,  $h$  is Planck's constant, and  $e$  and  $m$  are the charge (in e.s.u.) and mass of an electron. It will be noted that (3-21) checks (3-19) when  $B'$  is neglected, as usual.

Sommerfeld<sup>1</sup> initiated the work of applying quantum mechanics to the theory of the continuous x-ray spectrum as generated in thin targets. He arrived at approximate expressions for the intensity and polarization of the rays by considering the interaction between the cathode rays and the "pure coulomb field"<sup>2</sup> of the nuclei of the atoms that retard them. These expressions agree well with the experimental data for thin targets.

More recent developments have been added to the theoretical groundwork of Sommerfeld by Scherzer,<sup>3</sup> Sauter,<sup>4</sup> Elwert,<sup>5</sup> and Weinstock,<sup>6</sup> and the agreement between experimental<sup>7</sup> and theoretical thin-target angular energy distribution curves is now very good. This progress is due to refinement of the experimental technique as well as to refinement of the theory. Reliable experimental data have been secured from targets only 100 or 200 Å. thick.<sup>7</sup> Scherzer's equation<sup>3</sup> correspond-

<sup>1</sup> A. Sommerfeld, *Ann. Physik*, **11**, 257 (1931); *Proc. Natl. Acad. Sci.*, **15**, 393 (1929).

<sup>2</sup> That is, an inverse-square-law repulsion is substituted for Thomson's assumption that the electrons are subject to a constant negative acceleration.

<sup>3</sup> O. Scherzer, *Ann. Physik*, **13**, 137 (1932).

<sup>4</sup> F. Sauter, *Ann. Physik*, **18**, 486 (1933).

<sup>5</sup> G. Elwert, *Ann. Physik*, **34**, 178 (1939).

<sup>6</sup> R. Weinstock, *Phys. Rev.*, **61**, 584 (1942), **64**, 276 (1943); see most recent paper by P. Kirkpatrick and L. Wiedmann, *Phys. Rev.*, **67**, 321 (1945).

<sup>7</sup> See footnote 1, p. 37.



ing to the classical equation (3-16) is

$$\bar{I}_\theta = \frac{\alpha^4 Z^4 e^2 h^2 c}{(E - E_0)^2 (e^{\frac{2\pi\alpha Z}{\beta}} - 1)} \sin^2 \theta \left[ \frac{2(1 - \beta^2)^{\frac{3}{2}}}{(1 - \beta \cos \theta)^4} + \frac{(1 - \sqrt{1 - \beta^2})(1 - 2\sqrt{1 - \beta^2})}{(1 - \beta \cos \theta)^3} \right] \quad (3-17)$$

where  $e$  in the denominator is Napierian log base,  $e$  in numerator is electronic charge in e.s.u.,  $\alpha = 2\pi e^2/hc$ ,  $\beta = v/c$  as before,  $E_0 = m_0 c^2$  being the rest mass of an electron (see Sec. 4-3),  $E = \frac{E_0}{\sqrt{1 - \beta^2}}$ ,  $Z$  is the atomic number of the element composing the tube target.

Curve  $S$  in Fig. 3-7 is a plot of this equation, which may be compared with curve  $E$  in the same figure, obtained by Honerjäger<sup>1</sup> for the short-wave-length limit portion of the continuous radiation at 34 kv. from an aluminum target 200 or 300 Å. thick. The largest discrepancy is at  $\theta = 0$ , but this discrepancy appears to approach zero as the thickness of the target approaches zero.

Using modern quantum mechanics, Sommerfeld<sup>2</sup> derived an expression for the percent polarization to be expected in the x-rays generated in a thin target of a light material like aluminum bombarded with high-voltage cathode rays (say at least 30 kv.). He found that the polarization should vary with the wave length. At the short-wave limit the polarization should be complete (100 per cent) with the electric vector in the plane of the x-ray beam and cathode-ray beam, just as predicted by classical theory. For the longer waves, however, the polarization should be less complete. For example, the waves having a wavelength twice that at the short-wave limit should be only 57 per cent polarized. These results check reasonably well with the experimental data for thin targets.<sup>3</sup>

So far as the continuous x-rays radiated from an ordinary x-ray tube with a massive target (as opposed to thin foil) are concerned, Barkla was the first accurately to measure their polarization experimentally. His results have been verified by various other investigators. Figure 3-9 illustrates the essentials of his experimental arrangement.

X-rays generated at the x-ray tube target  $T$  pass through a hole in a lead shield, and most of them pass on through the scattering block of some light material like carbon. Part of them, however, are scattered

<sup>1</sup> R. Honerjäger, *Ann. Physik*, **38**, 33 (1940).

<sup>2</sup> A. Sommerfeld, *Ann. Physik*, **11**, 257 (1931); see also P. Kirkpatrick and E. Biehl, *Wiedemann, Phys. Rev.*, **67**, 321 (1945).

<sup>3</sup> B. F. Boardman, *Phys. Rev.*, **60**, 163 (1941); D. S. Piston, *Phys. Rev.*, **43**, 1 (1936).

<sup>4</sup> C. G. Barkla, *Phil. Trans. Roy. Soc. London*, **204**, 467 (1905).

in  $S$ , and it is found that more of these reach the ionization chamber  $B$  than the chamber  $A$ . When the tube is rotated  $90^\circ$  so that the cathode and target are at  $C'$  and  $T'$ , then more rays scattered from  $S$  reach  $A$  than  $B$ . In each case, the intensity  $I_\perp$  of the rays scattered perpendicular to the plane  $CTS$  (or  $C'T'S$ ) exceeds the intensity  $I_\parallel$  of the rays scattered parallel to this plane, which is the plane of the electric vector if the rays were 100 per cent polarized (see Fig. 3-5). The per cent polarization  $P$  is defined as

$$P = \frac{I_\perp - I_\parallel}{I_\perp + I_\parallel} \quad (3-24)$$

and the various experimenters find that for the rays near the short-wave limit (which are generated practically at the surface of the target, whereas the longer waves are mostly generated several atomic layers beneath the surface)  $P$  has values ranging from 10 to 90 per cent. For massive targets,  $P$  decreases as the tube voltage increases and as one includes more of the longer waves farther from the short-wave limit.

This section outlining theories of the continuous x-ray radiation will be closed by emphasizing two points. (1) All the theories of the continuous x-ray spectrum are able to arrive at quantitative mathematical expressions which fit some of the experimental data accurately enough so that there is no room for doubt that the continuous spectrum is generated by the cathode-ray electrons themselves during their sudden stop as they interact with the target atoms. (2) This continuous x-ray radiation becomes harder (more penetrating, shorter wave length) and more intense with increasing tube voltage and more intense (but not harder) with increasing tube current.

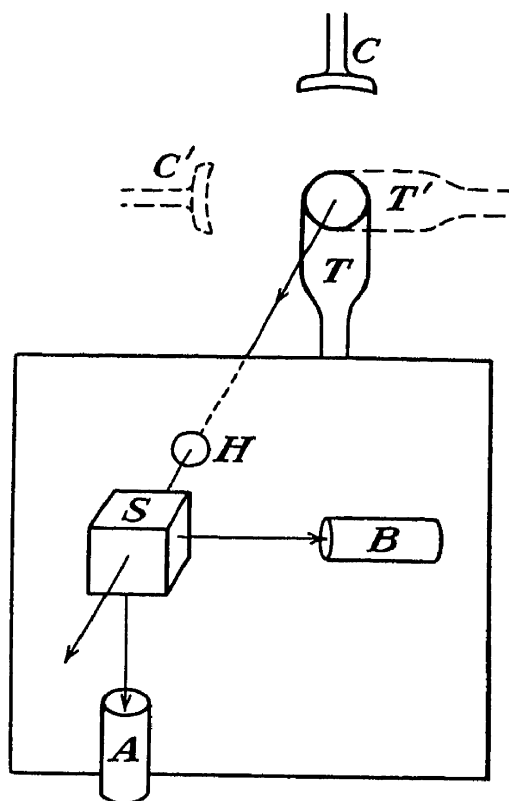


FIG. 3-9.—Barkla's experimental arrangement for measuring the degree of polarization of x-rays. (Adapted from *Compton and Allison*; courtesy of D. Van Nostrand Company, Inc.)

### QUESTIONS AND PROBLEMS

1. What are x-rays? Grenz rays? Gamma rays? What is a photon? Is the photoelectric effect more pronounced in the case of x-rays than it is with ordinary light? Why, or why not? What are hard x-rays? What instrument is commonly used to measure the intensity of an x-ray beam? Planck postulated the existence of energy quanta in order to explain the character of what kind of radiation?

2. If the wave length of a monochromatic x-ray beam is  $0.1 \text{ \AA}$ ., what is its frequency? How much energy does each photon in this beam have?

Ans.  $3 \times 10^{19}$  per second;  $19.9 \times 10^{-8}$  erg.

3. If this beam strikes an object, it will eject electrons from its surface. The maximum energy possessed by the fastest of these photoelectrons will be how many electron volts? *Ans.* 124,000 electron volts

4. If a Coolidge tube is operated at 200 kv., the hardest x-rays generated have what wave length? From Fig. 3-5, what voltage should be impressed upon the tube if it is desired that the *most intense* rays should have a wave length of about 0.6 Å.? *Ans.* 0.062 Å.; 27½ kv

5. How will the total x-ray energy emitted in the continuous radiation from a tube operating at 36 kv. with a lead target compare with that from a tube operating at 18 kv. with a columbium target, the tube current being 10 ma. in both cases? *Ans.* the same question if the tube current is 10 ma. in the columbium tube but only 1 ma. in the lead tube. *Ans.* 8 times; 4 times

6. Are the x-rays from an ordinary x-ray tube polarized to a measurable extent? In what plane? What is meant by the statement that they are 10 per cent polarized?

7. If an extremely thin target is used in an x-ray tube, will the most intense x-rays radiate from the side of the target next to the cathode or from the other side?

8. If the intensity  $I_\lambda$  over a given range of wave lengths were constant in an x-ray beam, how would the intensity  $I_\nu$  vary over the corresponding frequency range?

*Ans.*  $I_\nu = A/\nu$

9. If a given tube operating at a given voltage and current and placed 2 ft. from the photographic film gives a satisfactory radiograph of a certain object in 10 sec., what will be the time required if the tube-to-film distance is increased to 4 ft. to improve detail and reduce distortion? If increased to 6 ft.? If the tube current was originally 5 ma., one might make the radiographs at 4 ft. and 6 ft. without increasing the time by increasing the tube current to what value in each case?

*Ans.* 40 sec.; 90 sec.; 20 ma.; 45 ma

## CHAPTER 4

### CHARACTERISTIC X-RAY SPECTRA

**1. Experimental Introduction.** In the same paper<sup>1</sup> in which Ulrey published the continuous x-ray distribution curves reproduced in Fig. 3-4, he also published the curve shown in Fig. 4-1. This curve was obtained by the same technique used in obtaining Fig. 3-4, except that the x-ray tube had a molybdenum target instead of a tungsten target. The tube was operated at 35 kv. when the curve of Fig. 4-1 was obtained, and it may therefore be compared with curve *D* in Fig. 3-4. Except for the

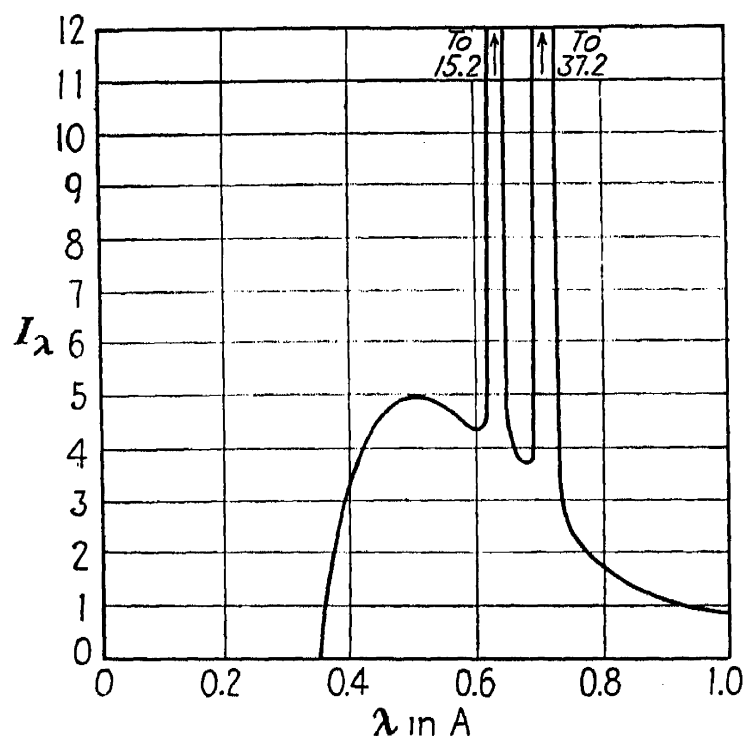


FIG. 4-1.—Intensity curve for x-rays radiated from tube with molybdenum target, operated at 35 kv. (By Ulrey; courtesy of *Physical Review*.)

two spectacular narrow peaks at about 0.71 and 0.63 Å., Fig. 4-1 practically duplicates curve *D* in Fig. 3-4. It shows a somewhat decreased intensity at all wave lengths, as would be expected from equation (3-11), since *Z* is only 42 for molybdenum as compared with 74 for tungsten.

Since the only difference between the techniques is that the curves of Fig. 3-4 were obtained with a tungsten target and those of Fig. 4-1 with a molybdenum target, the two strong narrow peaks evidently are related in some way to the target material. The absence of such peaks in any of the spectra in Fig. 3-4 becomes less surprising when it is stated that such peaks do occur in the tungsten x-ray spectrum provided that

<sup>1</sup> C. T. Ulrey, *Phys. Rev.*, **11**, 401 (1918).

the tube is operated at a voltage above 70 kv. However, the tungsten peaks obtained at these higher voltages occur at wave lengths of about 0.21 and 0.18 Å. instead of 0.71 and 0.63 Å., as with molybdenum. Furthermore, if the molybdenum tube is operated below 20 kv., its peaks disappear just as the tungsten peaks disappear below 70 kv.

These peaks are analogous to the bright-line optical spectra produced by such sources as hot sodium vapor or mercury vapor; and since they are characteristic of the target material, they are called *characteristic spectra*. If the target is a compound, for example silicon carbide, characteristic spectra of all the component elements (silicon and carbon in this case) will be excited. If high-voltage cathode rays can be made to bombard a liquid, like mercury, or a gas, like krypton, their characteristic spectrum is likewise excited.

These spectra were first discovered in 1909 by C. G. Barkla,<sup>1</sup> who found that, in addition to the strong maxima shown in Fig. 4-1, there are also other characteristic maxima for each element at a region in the spectrum not shown in Fig. 4-1, and having a considerably greater wave-length. Since these two groups of maxima are found for all elements except the very lightest elements, each group is called a "series." In 1911 the long-wave-length series (not shown in Fig. 4-1) was first called the "L series" by Barkla,<sup>2</sup> and the short-wave-length series shown in Fig. 4-1 was called the "K series," also known today as the "K radiation" or the "K lines" by analogy with the "lines" in optical spectra. Barkla discovered these series of x-ray spectra and named them before the discovery of x-ray diffraction, and therefore before any such thing as an x-ray spectrometer existed. He achieved this by making use of the fact that "hard" rays (short wave length) are absorbed in aluminum to a lesser extent than "soft" rays (long wave length).

After the discovery of x-ray diffraction in 1912, Moseley was able to use an x-ray spectrometer to study these spectra, and he soon discovered a mathematical relation between their wave lengths and the atomic number of the chemical element of which the x-ray tube target was composed. It is

$$\nu^{\frac{1}{2}} = K(Z - \sigma) \quad (4-1)$$

Here  $K$  and  $\sigma$  are two constants, the same for the K series for all elements, or, by introducing different values for these constants, the equation may be made to fit the L series for all elements that have an L series.  $Z$  is the atomic number of the target element, and  $\nu$  the frequency of one of the (or L) lines. Moseley called the more intense longer wave-length peak in Fig. 4-1 (at 0.71 Å.) the K alpha, or  $K_{\alpha}$ , line and the less intense

<sup>1</sup> C. G. Barkla, *Proc. Cambridge Phil. Soc.*, May, 1909.

<sup>2</sup> C. G. Barkla, *Phil. Mag.*, **22**, 396 (1911).

<sup>3</sup> H. G. J. Moseley, *Phil. Mag.*, **26**, 1024 (1913), **27**, 703 (1914).

shorter wave-length peak (at 0.63 Å.) the K beta, or  $K_\beta$ , line.<sup>1</sup> He also designated the various L lines by Greek letters as  $L_\alpha$ ,  $L_\beta$ , etc. He published tables from which a few figures are listed in Table 4-1. A modern table of characteristic x-ray spectra will be found in Appendix. III.

TABLE 4-1.—CHARACTERISTIC X-RAY SPECTRA  
(Moseley, 1914)

Element composing x-ray tube target	Atomic number	Wave lengths, Å.				
		$K_\alpha$ line	$K_\beta$ line	$L_\alpha$ line	$L_\beta$	$L_\gamma$
Iron.....	26	1.946	1.765			
Cobalt.....	27	1.798	1.629			
Nickel.....	28	1.662	1.506			
Copper.....	29	1.549	1.402			
Zinc.....	30	1.445	1.306			
Molybdenum.....	42	0.721	.....	5.423	5.187	
Ruthenium.....	44	0.638	.....	4.861	4.660	
Rhodium.....	45	.....	.....	4.622		
Palladium.....	46	0.584	.....	4.385	4.168	3.928
Silver.....	47	0.560	.....	4.170		
Tin.....	50	.....	.....	3.619		

The L lines for elements of lower atomic number than molybdenum were too soft for measurement, and the K lines for elements of higher atomic number than silver were too hard for measurement with the technique then available. Nevertheless, it is clear from these data that the wave lengths of the K series and the L series of x-ray spectra decrease systematically with increasing atomic number, as represented by equation (4-1). This is called *Moseley's law*. This relation enabled Moseley to determine for the first time the correct order in which the elements should be arranged in the periodic table. Their general order was, of course, known before 1914, but there were several doubtful cases, such as cobalt and nickel, or tellurium and iodine, which have atomic weights indicating that iodine should precede tellurium and that nickel should precede cobalt in the table.<sup>2</sup> Such cases were cleared up by Moseley's study of these characteristic x-ray spectra.

Moseley's work was cut short when he was killed in the First World War; but others, notably Manne Siegbahn, continued it, and at present the wave lengths of the K series have been accurately measured for all

<sup>1</sup> Actually, both of these "lines" are doublets, so close together that Moseley's spectrometer did not resolve them. For example, the  $K_\alpha$  "line" really consists of a  $K_{\alpha_1}$  line at 0.707Å. and a  $K_{\alpha_2}$  line at 0.712Å. for molybdenum. The origin of these lines will be explained in detail in Sec. 3.

<sup>2</sup> For bibliography on development of Mendelyceev's periodic table, see F. A. Paneth, *Nature*, **149**, 565 (1942).

elements (except missing or rare ones) from sodium (11) to uranium (92) and for the L series from iron (26) to uranium. It has been found that the L radiation in reality consists of three separate series of lines now known as the  $L_I$ ,  $L_{II}$ , and  $L_{III}$  series. These three allied series require slightly different minimum potentials to excite them,  $L_{III}$  being the easiest and  $L_I$  hardest to excite. Furthermore, two additional characteristic series (really series groups, like the L series) of x-ray spectra have been discovered far out in the long-wave-length region and named the M series and the N series, respectively. This M "series" radiation is a multiple series, like the L radiation. It consists of five separate closely allied series, commonly designated as  $M_I$ ,  $M_{II}$ ,  $M_{III}$ ,  $M_{IV}$ ,  $M_V$ . The N "series" is likewise a series group. The wave lengths of the M series have been measured for most elements from dysprosium (66) to uranium, but the N series has been measured for only a few of the heaviest elements like thorium and uranium. Indeed, it is theoretically impossible for lighter elements like zinc to produce any N radiation or for still lighter elements like aluminum to produce any M or N radiation, as will be explained in the next section. The wave lengths of characteristic x-ray spectra as determined by Siegbahn and his associates are listed in the Appendix.

As already mentioned, the K radiation appears only when the voltage applied to the x-ray tube exceeds a definite value, which has been given as 20 kv. for a molybdenum target and 70 kv. for tungsten.<sup>1</sup> The same behavior is shown by the softer L, M, and N radiations, except that their minimum excitation potentials are lower. For example, the L radiation appears when the tube voltage reaches 2.51 kv. for molybdenum and 12.1 kv. for tungsten. These minimum excitation potentials for various characteristic spectra of the different elements are tabulated in Appendix IV.

If one represents the minimum excitation potential for a given radiation for a given element (for example, for the K radiation of molybdenum) by  $V_0$  (20 kv. in this case), then there is an empirical relation which has been evolved experimentally, connecting the intensity of the characteristic spectra and the tube voltage  $V$ . It is

$$I = C(V - V_0)^n \quad (1)$$

where  $C$  and  $n$  are constants. Various experimenters<sup>2</sup> studying

<sup>1</sup> Characteristic x-ray spectra can be excited by bombarding some of the lighter metals with protons or deuterons, but only at potentials of the order of a few volts. See, for example, M. S. Livingston, F. Genevieve, and E. J. Konopinski, *Rev.*, **51**, 835 (1937); J. M. Cork, *Phys. Rev.*, **59**, 957 (1941).

<sup>2</sup> D. L. Webster and H. Clark, *Proc. Natl. Acad. Sci.*, **3**, 181 (1917); A. Jönsson, *Z. Physik.*, **36**, 426 (1926); S. K. Allison, *Phys. Rev.*, **32**, 1 (1928).

different spectral series of various elements have found values for  $n$  such as 1.5, 1.7, 1.8, and 2. It appears that 1.7 might be taken as a reasonably accurate value for  $n$ . Thus, for general purposes, one may use the approximate relation

$$I = C(V - V_0)^{1.7} \quad (4-3)$$

to represent the variation of the intensity of characteristic spectra with voltage up to  $V = 4V_0$ . At voltages above  $4V_0$ , the intensity is usually found to be less than that predicted by (4-3). In contrast to the continuous radiation, the characteristic radiation exhibits no polarization effects.<sup>1</sup>

**2. Fundamental Theory of Characteristic X-ray Spectra.** Chapter 3 presented the evidence that the continuous radiation is generated by the cathode-ray electrons striking the target. Moseley's law makes it obvious that the characteristic x-ray radiation is generated by some process closely related to the chemical properties of the element composing the target, and hence to the structure of these atoms. Modern atomic theory accounts for characteristic x-ray spectra very satisfactorily. However, the experimental evidence obtained from characteristic x-ray spectra and Moseley's law played an essential role in formulating the theory that accounts for such a wide variety of physical phenomena, including characteristic x-ray spectra.

In 1911, Rutherford<sup>2</sup> concluded from his studies on the scattering of alpha and beta particles (from radioactive sources) by matter that the atom probably had a structure consisting of "a positive central charge  $Ne$ , surrounded by a compensating charge of  $N$  electrons."  $e$  is the electronic charge, which in 1911 was estimated to be  $4.56 \times 10^{-10}$  e.s.u. In 1913, van den Broek<sup>3</sup> suggested that Rutherford's  $N$  is the "atomic number," that is, the number of the corresponding element in Mendeleev's periodic table (Appendix VII).

In the same year, Bohr<sup>4</sup> proposed that Rutherford's atom be thought of as a "system consisting of a positively charged nucleus of very small dimensions and electrons describing closed orbits around it." He then pointed out the "inadequacy of the classical electrodynamics to account for the properties of atoms from such an atom-model" because it would predict that the radiation of the revolving electrons would rapidly waste away their energy (as discussed in Sec. 3-5, page 38) and hence cause the orbits to collapse about the nucleus.

<sup>1</sup> J. A. Bearden, *Proc. Natl. Acad. Sci.*, **4**, 539 (1928); E. O. Wollan, *Proc. Natl. Acad. Sci.*, **4**, 864 (1928).

<sup>2</sup> E. Rutherford, *Phil. Mag.*, **21**, 669 (1911).

<sup>3</sup> A. van den Broek, *Physik. Z.*, **14**, 32 (1913).

<sup>4</sup> N. Bohr, *Phil. Mag.*, **26**, 1 (1913).



He made the observation that,

... before and after the energy characteristic of a typical atomic system is radiated, the system settles down in a stable state of equilibrium. Now an essential point in Planck's theory of radiation is that the energy radiation from an atomic system does not take place in the continuous way assumed in ordinary electrodynamics, but that it, on the contrary, takes place in distinct separated emissions, the amount of energy radiated out from an atomic system of frequency  $\nu$  in a single emission being equal to  $\tau h\nu$  where  $\tau$  is an entire (integer) number, and  $h$  is a universal constant.<sup>1</sup>

Bohr then set down two postulates, which, together with the idea of electronic orbits around a central positive nucleus, form the basis of modern atomic theory. The first postulate was that the orbits are ordinarily stable and no radiation is emitted in spite of the centripetal acceleration. The second was that, when energy is radiated, it is during a process in which one of the orbital electrons jumps from one stable orbit to another, simultaneously emitting monochromatic radiation "for which the relation between the frequency and the amount of energy emitted is the one given by Planck's theory." That is,

$$A_1 - A_2 = h\nu$$

where  $A_1$  and  $A_2$  are the energies of the atomic system in the initial and final stationary states. These various "energy levels" of the orbital electrons are fundamental in modern atomic theory.

At the time Bohr was formulating these fundamental ideas, Moseley published his data revealing the relationship between characteristic x-ray spectra and atomic number. Kossel,<sup>3</sup> studying Moseley's work, was the first to notice that the frequencies of the  $K_\beta$ ,  $K_\alpha$ , and  $L_\alpha$  lines for a wide variety of elements were related, to a very good degree of accuracy, by the equation

$$\nu_{K\beta} - \nu_{K\alpha} = \nu_{L\alpha}$$

The similarity between the forms of equations (4-4) and (4-5) suggested to Kossel that Bohr's theory might account for the characteristic x-ray spectra if the orbital electrons were arranged in "rings," one on the other. J. J. Thomson<sup>4</sup> and Bohr<sup>5</sup> had previously made suggestions along these same lines, but Kossel put them on a more quantitatively specific basis. The term "rings," however, suggests that the elec-

<sup>1</sup> M. Planck, *Ann. Physik*, **31**, 758 (1910).

<sup>2</sup> H. G. J. Moseley, *Phil. Mag.*, **26**, 1024 (1913), **27**, 703 (1914).

<sup>3</sup> W. Kossel, *Verhandl. deut. physik. Ges.*, **14**, 953 (1914), **18**, 339, and 396 (*Physik. Z.*, **18**, 240 (1917); *Z. Physik*, **1**, 119 (1920), **2**, 470 (1920).

<sup>4</sup> J. J. Thomson, *Phil. Mag.*, **23**, 456 (1912)

<sup>5</sup> N. Bohr, *Phil. Mag.*, **26**, 498 (1913).

orbits all lie in one plane, whereas later developments suggested that they do not; therefore, the modern term is electronic "shells," rather than "rings." Kossel suggested that the K radiation resulted from the removal of an electron from the innermost ring (now known as the K shell), the  $K_\alpha$  line being the radiation emitted when an electron falls from the next ring (now known as the L shell) to the first ring (K shell), and the  $K_\beta$  line being the radiation emitted by an electron falling from ring 3 (M shell) to ring 1 (K shell). He also suggested that the L radiation results from the removal of an electron from ring 2 (the L shell) and is emitted by electrons falling from rings 3, 4, etc. (the M, N, etc., shells) into the vacant space in ring 2 (the L shell). The designation of these rings or shells as K, L, M, etc., beginning with the innermost one, is due to Barkla,<sup>1</sup> who independently arrived at ideas similar to Kossel's. Thus Barkla's K, L, M, N nomenclature proposed in 1911<sup>2</sup> is used today to name the atomic electron shells between which occur the electronic transitions that generate the characteristic x-ray spectra. Note that the removal of an electron is the first step, so that the radiation process occurs in ions, not atoms.

This theory of the origin of characteristic x-ray spectra has endured through all the years since 1915 and is accepted today as fundamentally correct, although a vast amount of detail has been added to this early framework. The reasons for its acceptance may now be set forth.

1. It explained the existence of the minimum excitation potentials. The fact that none of the K lines appear for molybdenum below 20 kv. or for tungsten below 70 kv.<sup>3</sup> is now accounted for because the "K electrons" in the innermost shell of the atom are firmly bound to the nucleus, the binding energy being such that the cathode rays striking the target atoms are unable to wrench one of these K electrons loose unless they have acquired a certain definite energy, that is, unless the x-ray tube voltage is at least a certain definite minimum value. Once this minimum excitation potential is reached, the cathode-ray electrons bombard the target atoms with an energy sufficient to enable a few of them, which happen to hit just right, to wrench a K electron out of some of the atoms. Once this is done, electrons from the L, M, and other outer shells, if present, will fall into the vacant spaces thus created in the K shells, and in so doing the  $K_\alpha$ ,  $K_\beta$ , and other K lines are radiated, all as observed experimentally.

<sup>1</sup> C. G. Barkla, *Nature*, **95**, 7 (1915).

<sup>2</sup> *Phil. Mag.*, **22**, 396 (1911).

<sup>3</sup> These minimum excitation potentials had been discovered by the time Kossel proposed his explanation. See R. Whiddington, *Proc. Roy. Soc. (London) A*, **85**, 323 (1911); R. T. Beatty, *Proc. Roy. Soc. (London) A*, **87**, 511 (1912); W. H. Bragg, *Phil. Mag.*, **29**, 407 (1915).



“quantum number.” Hence, when an electron drops from one stable orbit to another, the energy represented by this transition is

$$A_1 - A_2 = \frac{2\pi^2 m e^4}{h^2} \left( \frac{1}{\tau_2^2} - \frac{1}{\tau_1^2} \right) \quad (4-9)$$

Since this energy is radiated in the form of a photon of energy

$$E = h\nu = A_1 - A_2,$$

equation (4-9) may be divided by  $h$  to obtain  $\nu$ ,

$$\nu = \frac{2\pi^2 m e^4}{h^3} \left( \frac{1}{\tau_2^2} - \frac{1}{\tau_1^2} \right) \quad (4-10)$$

The constant  $2\pi^2 m e^4 / h^3$  has a value of about  $33 \times 10^{14}$  per second. This formula was found to predict values for the frequencies of the atomic spectral lines of hydrogen that agreed well with the experimental values. For example, if one sets  $\tau_1 = 2$  and  $\tau_2 = 1$ , (4-10) gives

$$\nu = \frac{3}{4} \times 33 \times 10^{14} = 24.75 \times 10^{14} \text{ per second,}$$

and  $\lambda = \frac{c}{\nu} = \frac{3 \times 10^{10}}{24.75 \times 10^{14}} = 1,213 \times 10^{-8} \text{ cm.} = 1,213 \text{ \AA.}$ , as compared with the strong line experimentally observed at 1,216 Å. The substitution of  $\tau_1 = 3$  and  $\tau_2 = 1$  in (4-10) gives  $\nu = \frac{8}{9} \times 33 \times 10^{14}$  or  $\lambda = 1,025 \text{ \AA.}$ , as compared with the experimentally observed line at 1,026 Å.

By 1915 the idea of electronic rings or shells was well established, and it was natural to suppose that these quantum numbers  $\tau$  of Bohr's might be associated in some way with the shells. Of course, hydrogen, with only one electron, could hardly have K, L, and M shells in the sense suggested by Kossel, but a more complex atom like molybdenum might have electronic transitions fundamentally similar to those worked out for hydrogen by Bohr if suitable modification were made to allow for the added complexity. By 1915, Bohr<sup>1</sup> had shown that his hydrogen formulas could be made to predict the atomic spectra of elements of low atomic weight like helium and lithium with reasonable accuracy by introducing the factor  $Z^2$  where  $Z$  is the atomic number. By that time, it had become customary to represent the quantum number by  $n$  rather than  $\tau$  so that, for light elements, Bohr's formula became

$$\nu = Z^2 \frac{2\pi^2 m e^4}{h^3} \left( \frac{1}{\tau_2^2} - \frac{1}{\tau_1^2} \right) \left( \frac{M}{M + m} \right) \quad (4-11)$$

The factor  $\frac{M}{M + m}$  is a small correction factor that will be neglected

<sup>1</sup> N. Bohr, *Phil. Mag.*, **30**, 394 (1915).

ion like molybdenum  $K_{\alpha}$ , but the same tube filled with fine lead will not. The reason is that practically all rays ordinarily used in diffraction work will be absorbed by the lead, but this is not true of  $K_{\alpha}$ . A thinner sample should be used for absorbent materials than for comparatively transparent materials like aluminum.

powdered material loaded into glass tubes, however, it is more convenient and practical to compensate for the absorption of the more absorbent materials by diluting them with some filler like cornstarch, so that a standard-sized glass tube can be used for all samples. To determine the proportion of filler to use, one should first estimate the average atomic number of the sample, if its composition is known. For example, if a sample is known to be bismuth subnitrate ( $\text{BiONO}_2 \cdot \text{H}_2\text{O}$ ) a com-

in subsequent equations.  $M$  is the mass of the nucleus and  $m$  the mass of an electron. Since  $M$  is large compared with  $m$ , the factor very nearly equals 1.

This equation can be extended to more complex atoms by reasoning as follows: In a complex atom like molybdenum, for example, containing 42 orbital electrons, the electrons in the inner shells close to the nucleus (which has a positive charge of 42 electronic units) will not be bound by it 42 times as strongly as they are in hydrogen, but this attractive electrostatic binding to the nucleus will be reduced by the "screening" effect of the 30 or 40 electrons in the outer shells. The effect of the outer electrons is to cause the inner electrons to behave as though the nuclear charge were only, say,  $39\frac{1}{2}$  or  $40\frac{1}{2}$ , or some such value. Hence the formula must be modified by substituting  $Z - \sigma$  for  $Z$ , where  $\sigma$  is a quantity called the "screening constant." Thus one has

$$\nu = \frac{2\pi^2 me^4}{h^3} (Z - \sigma)^2 \left( \frac{1}{n_2^2} - \frac{1}{n_1^2} \right) \quad (4-12)$$

If one now assumes that  $n = 1$  corresponds to electrons in the innermost, or K, shell, and  $n = 2$  corresponds to electrons in the next shell (the L shell), etc., then Kossel's suggestion that the  $K_\alpha$  line is emitted by an electron falling from the L shell to a vacant space in the K shell indicates that, for the  $K_\alpha$  line,  $n_1 = 2$  and  $n_2 = 1$ , from which

$$\nu = \frac{2\pi^2 me^4}{h^3} (Z - \sigma)^2 \frac{3}{4} \quad (4-13)$$

from which  $\nu^{\frac{1}{2}} = K(Z - \sigma)$ , which is Moseley's law (4-1). Thus the theory explains Moseley's law in a quantitative as well as a qualitative way. The value of  $K$  predicted by (4-13) is about  $25 \times 10^{14}$ , which agrees within about 1 per cent with the value of  $K$  experimentally determined for the  $K_\alpha$  line in Moseley's empirical equation. Experiment indicates a value of  $\sigma$  for the  $K_\alpha$  line of about 1.13, which seems a reasonable value for the screening constant introduced into the theory. Similar agreement between theory and the experimental frequencies of the  $K_\beta$  lines results when one sets  $n_1 = 3$  and  $n_2 = 1$ . Likewise, the  $L_\alpha$  lines fit the theory when one sets  $n_1 = 3$  and  $n_2 = 2$ .

Although the theory thus far discussed was all developed before 1916, it is still generally accepted as fundamentally correct to picture the  $K_\alpha$  radiation as being generated in the x-ray tube when the cathode-ray electrons (the tube voltage being high enough) knock a K electron out of the target atoms, whereupon an L electron falls into the vacancy thus created in the K shell, simultaneously emitting an x-ray photon. Likewise the  $K_\beta$  radiation is generated by an M electron falling into a K-shell

vacancy, and the  $L_\alpha$  radiation is generated by an M electron falling into an L-shell vacancy.

**3. Modern Developments.** Modern atomic theory has advanced far beyond the fundamental groundwork outlined in the preceding section. One of the most far-reaching changes in scientific ideas of atomic structure and the mechanism of characteristic x-ray spectra has transpired because of new evidence which has shown that in many ways electrons behave, not as particles, as they were regarded in 1915, but as bundles of waves. Today it is known that cathode rays and electrons have dual wave-and-particle characteristics similar to those of photons and x-rays.

This must not be taken as indicating that electrons and photons or cathode rays and x-rays are alike, however. To point out a few fundamental differences, x-rays and photons always have a velocity  $c$  in free space, whereas electrons and cathode rays may have any speed less than  $c$ . Electrons are charged particles affected and deflected by electric and magnetic fields, whereas photons and x-rays are not so deflected. Electrons combine with other elementary particles such as neutrons and protons to make matter; but photons and radiation in general, including x-rays, are a form of energy, and energy is, of course, quite different from matter.

The idea that some sort of wave motion is associated with moving particles, such as electrons, was originated by Louis de Broglie in 1924. In order to understand how he arrived at such an idea, one must be familiar with two of the fundamental equations of special relativity. These two equations are indispensable, also, if one is to calculate such simple quantities as the mass or the energy of an electron or other particle moving at a velocity high enough to be an appreciable fraction of the velocity of light. The cathode rays in an x-ray tube are an excellent instance of such particles. The two equations were derived by Einstein<sup>1</sup> in 1907 from the theoretical groundwork of the theory of special relativity that he began in 1905. The equations are

$$m = m_0 \frac{1}{\sqrt{1 - \frac{v^2}{c^2}}} \quad (4-14)$$

and

$$E = mc^2 \quad (4-15)$$

Equation (4-14) indicates that a body or particle having a mass  $m_0$  when at rest (with respect to an observer) will have a mass  $m$ , greater than  $m_0$ , when the particle is moving with velocity  $v$  relative to the observer. This mass  $m$  is given by the equation, in which  $c$  is the velocity of light. The increase in mass is negligible for velocities as low as that

<sup>1</sup> A. Einstein, *Ann. Physik*, **23**, 371 (1907).

of a rifle bullet. For example, a rifle bullet that has a mass of 1 gram as it is loaded into the gun will have a mass of 1.00000000000055 g. as it leaves the gun if its muzzle velocity is 1,000 m./sec. However, the increase in mass is not negligible if one considers an electron having a velocity half that of light. Such an electron has a mass of  $10.13 \times 10^{-28}$  g. instead of the  $9 \times 10^{-28}$  g. given in the tables.

The second equation (4-15) states that any body or particle having a mass  $m$  is equivalent to an amount of energy  $E$  given by the equation, where  $c$  is again the velocity of light. The direct transformation of matter into energy, and vice versa, has been achieved experimentally on a microscopic scale, as, for example, in the phenomenon of "pair formation," to be discussed in the next chapter. It is believed that a large-scale transformation of this sort is continually in progress in the sun and stars and that it is the source of the enormous energy radiated by them. The "atomic bomb" developed in World War II converts only a small fraction of 1 per cent of its mass into energy when it explodes. Probably an ounce or so of matter is transformed into energy in the explosion; yet this is sufficient to destroy a city. For a discussion of the "fission" process which releases this energy, see Sec. 8-4.

Returning to equation (4-15),  $E$  is in ergs,  $m$  in grams, and  $c$  in centimeters per second. Hence 1 g. of matter is equivalent to  $9 \times 10^{20}$  ergs, or 3,000 hp. continuously for over 1 year. This equation may be brought closer home by showing that it is the general equation from which the familiar equation for kinetic energy

$$E_k = \frac{1}{2}mv^2 \quad (4-16)$$

is derived as an approximation when  $v$  is small compared with  $c$ .

Substituting (4-14) in (4-15), one has

$$E = m_0 c^2 \frac{1}{\sqrt{1 - \frac{v^2}{c^2}}} = m_0 c^2 \left(1 - \frac{v^2}{c^2}\right)^{-\frac{1}{2}} \quad (4-17)$$

Applying the binomial theorem of elementary algebra,

$$(1 - x)^{-n} = 1 + nx + \frac{n(n+1)x^2}{2!} + \dots \quad (4-18)$$

one has

$$E = m_0 c^2 \left(1 + \frac{1}{2} \frac{v^2}{c^2} + \frac{3}{8} \frac{v^4}{c^4} + \dots\right) \quad (4-19)$$

or

$$E = m_0 c^2 + \frac{1}{2} m_0 v^2 + \frac{3}{8} m_0 \frac{v^4}{c^2} + \dots \quad (4-20)$$

When  $v$  is small compared with  $c$ , the third and higher terms may be



dropped [this is more obvious in (4-19) than in (4-20), perhaps], leaving

$$E = m_0 c^2 + \frac{1}{2} m_0 v^2 \quad (4-21)$$

Equation (4-21) indicates that, when a body or particle of mass  $m_0$  is at rest ( $v = 0$ ), it is equivalent to an energy  $E = m_0 c^2$ . When it is given a velocity  $v$ , however, it has the additional energy  $\frac{1}{2} m_0 v^2$  that is the familiar kinetic energy  $E_k$ , or energy due to the motion at ordinary speeds.

One other consequence of relativity that should be kept in mind for reference later is the postulate that no material particle may have a velocity exceeding  $c$ , nor may any energy be transmitted (by waves, for example) at a velocity exceeding  $c$ .

To return to the idea of the association of a wave with any moving particle, originated by Louis de Broglie,<sup>1</sup> in 1924, he noted that a moving body of "rest mass"  $m_0$  moving with regard to a given observer with velocity  $v$  less than  $c$  must contain an internal energy equal to  $m_0 c^2$ .

Moreover, the quantum relation ( $E = h\nu$  or  $\nu = E/h$ ) suggests the ascription of this internal energy to a periodical phenomenon whose frequency is  $\nu_0 = \frac{1}{h} m_0 c^2$ .

For the fixed observer, the whole energy is  $\frac{m_0 c^2}{\sqrt{1 - \frac{v^2}{c^2}}}$  and the corresponding

frequency is

$$\nu = \frac{1}{h} \frac{m_0 c^2}{\sqrt{1 - \frac{v^2}{c^2}}} \quad (4-22)$$

Let us suppose, that, at time 0, the moving body coincides in space with a wave whose frequency  $\nu$  has the value given above, and which spreads<sup>2</sup> with velocity  $c^2/v$ . This wave, however, cannot carry energy, according to Einstein's ideas. We are then inclined to admit that any moving body may be accompanied by a wave and that it is impossible to disjoin motion of body and propagation of wave.

These waves suggested in a somewhat vague way by de Broglie have become known as "de Broglie waves" or, as he called them, "phase waves." Since he assigned them a velocity of  $c^2/v$  ( $v$  being the velocity of the associated particle) and a frequency given by (4-22), it is easy to calculate the wave length of his phase waves from the equation of wave motion  $v' = \nu\lambda$  [(3-1)] or  $\lambda = v'/\nu$ , in which one sets  $v' = c^2/v$  and

<sup>1</sup> L. de Broglie, *Phil. Mag.*, **47**, 446 (1924); see also *Ann. phys.*, **3**, 22 (1925).

<sup>2</sup> A velocity  $c^2/v$  assigned to the wave exceeds  $c$ . Hence the statement that it cannot carry energy (see second paragraph above).

as in (4-22), thus obtaining

$$\lambda = \frac{c^2}{v} \frac{h \sqrt{1 - \frac{v^2}{c^2}}}{m_0 c^2} = \frac{h}{m_0 v} \sqrt{1 - \frac{v^2}{c^2}} \quad (4-23)$$

or, substituting (4-14) in (4-23),

$$\lambda = \frac{h}{mv} \quad (4-24)$$

The idea of phase waves associated with a moving body or particle was suggested tentatively by de Broglie. He wrote somewhat apologetically, "Many of these ideas may be criticized and perhaps reformed," but he pointed out that "this idea gives a physical interpretation of Bohr's analytical stability conditions." This last point is the one which indicated that there might be some fundamental truth underlying the idea of phase waves.

To make this point clear, let us return to Bohr's expression (4-7) or (4-8) for the energy of a hydrogen atom when the orbital electron is in one of its "allowed" stable orbits. These allowed orbits, characterized by an arbitrary quantum number  $\tau$  and obviously related in an intimate way with Planck's quantum relation  $E = h\nu$ , had never been explained in a way that had any obvious physical interpretation. These stable, allowed atomic states were called "quantized" states, and it was easy to show<sup>1</sup> on the basis of classical physics that they might be explained by assuming a series of allowed circular orbits of radius  $r$  for the electron, related to the mass  $m$  and orbital velocity  $v$  of the electron by the equation  $rmv = \tau \frac{h}{2\pi}$ . In fact, this relation was valid independently of the value of the nuclear charge and hence was valid for any "hydrogenlike" atom as long as the electronic orbits were assumed circular. Since the quantum number  $\tau$  was later commonly designated by  $n$ , this condition for stability of the electronic orbits becomes

$$rmv = n \frac{h}{2\pi} \quad (4-25)$$

The quantity  $rmv$  represents the angular momentum of the electron in its allowed orbit, for angular momentum is defined as moment of inertia times angular velocity,

$$\text{or} \quad mr^2 \frac{v}{r} = mvr \quad (4-26)$$

Hence (4-25) indicates that the angular momentum of the electrons in any simple hydrogenlike atom may take on only integral multiples of the value  $h/2\pi$ . This mathematical rule of the Bohr theory had no

<sup>1</sup> N. Bohr, *Phil. Mag.*, **26**, 1 (1913).

obvious physical interpretation; it was impossible to see why the angular momentum of the electrons might be restricted to such values.

If one now regards the orbital electron moving with linear momentum  $mv$  as associated with a de Broglie wave having a wave length given by (4-24), then (4-25) may be rearranged thus,

$$n \frac{h}{mv} = 2\pi r$$

so that the condition for orbital stability becomes, by (4-24),

$$n\lambda = 2\pi r \quad (4-27)$$

This equation has an obvious physical interpretation. It indicates that the quantized states or allowed orbits of simple hydrogenlike atoms are those in which the circumference of the orbit is an integral number of de Broglie wave lengths. If this idea represents some general atomic principle, then one might suppose that in more complex atoms the K shell ( $n = 1$ ) contains electrons whose de Broglie wave length is equal to the circumference of their orbit; the L shell ( $n = 2$ ) contains electrons whose de Broglie wave length is half the circumference of their orbit, etc.

Such simplification of the atom in order to obtain a clearer mental picture is misleading, however, for even before de Broglie's proposal of phase waves, it was known that there were various subsidiary energy states for the L electrons ( $n = 2$ ), M electrons ( $n = 3$ ), etc., which involved a second quantum number, called the "azimuthal quantum number"  $k$  by Sommerfeld. Modern developments have shown, however, that the angular momentum of the electrons is most closely associated with a quantum number commonly designated by the letter  $l$  which is different from any of those used in the early Bohr theory, being equal to  $k - 1$  where  $k$  is the now obsolete quantum number mentioned above.

Nevertheless, as de Broglie pointed out, his phase waves offered a possible physical interpretation of Bohr's analytical stability conditions. This alone was sufficient to raise his idea above the status of mere speculation. Three years later the physical reality of the phase waves was established beyond question by the experiments of Davisson and Germer,<sup>1</sup> who succeeded in diffracting a beam of electrons by a crystal of nickel; the diffraction maxima had the exact positions to be expected for a wave length  $\lambda = h/mv$  given by (4-24). Electron diffraction was also discovered by Thomson,<sup>2</sup> working independently in England. The subject of electron diffraction will be discussed in Chap. 24.

Meanwhile Schrödinger had begun a mathematical treatment of

<sup>1</sup> C. J. Davisson and L. H. Germer, *Phys. Rev.*, **30**, 705 (1927).

<sup>2</sup> G. P. Thomson, *Proc. Roy. Soc. (London) A*, **117**, 600 (1927).

atomic structure in which the orbital electrons were regarded as de Broglie waves instead of particles. This analysis led him to the so-called "Schrödinger wave equation," which may be expressed in ordinary Cartesian coordinates as

$$\frac{\partial^2 \psi}{\partial x^2} + \frac{\partial^2 \psi}{\partial y^2} + \frac{\partial^2 \psi}{\partial z^2} + \frac{8\pi^2 m}{h^2} (W - U) = 0 \quad (4-28)$$

in which  $m$  is the mass of the associated particle,  $W$  its total energy, and  $U$  its potential energy expressed as a function of its position,  $x, y, z$ , and  $\psi$  is the amplitude of the de Broglie wave. By using this equation, which represents the electrons as waves, Schrödinger was able to calculate the quantized energy levels of atoms and arrive at values that agreed with experiment in greater detail than was possible in the case of the early Bohr theory. This new method of Schrödinger<sup>1</sup> became known as "wave mechanics."

An approach to the problem of atomic mechanics from a different direction by Heisenberg<sup>2</sup> in 1925 had been developed by the cooperation of Born and Jordan<sup>3</sup> into a mathematical method of calculating atomic energy levels that became known as "matrix mechanics." This method and Schrödinger's wave mechanics led to the same results, and both methods have since been developed into an entire new mathematical theory of the atom now known as "quantum mechanics."

So far as an understanding of characteristic x-ray spectra is concerned, quantum mechanics has developed three new features of special importance. (1) A complete calculation or explanation of the various allowed energy levels of an atom involves several new subsidiary quantum numbers in addition to the principal quantum number  $\tau$  or  $n$  appearing in the early Bohr theory. (2) It has been found that there is a simple rule which may be applied to the various quantum numbers which accounts for the way that K, L, and M shells build up as they do as one goes through the periodic table. This rule was first enunciated by Pauli<sup>4</sup> and is known as the "Pauli exclusion principle." (3) It has been found that when atoms radiate (or absorb radiation) the orbital electrons are not permitted to jump from any allowed energy level to any other, but only from certain particular allowed levels to certain others. That is, certain transitions are "forbidden" by simple rules applied to the various quantum numbers. These rules are called the "selection rules." Some of the selection rules had been established from early quantum theory by applying the correspondence principle (page 39).

<sup>1</sup> E. Schrödinger, *Ann. Physik*, **79**, 361, 489, 734 (1926); *Phys. Rev.*, **28**, 1049 (1926).

<sup>2</sup> W. Heisenberg, *Z. Physik*, **33**, 879 (1925).

<sup>3</sup> M. Born, W. Heisenberg, and P. Jordan, *Z. Physik*, **35**, 557 (1926).

<sup>4</sup> W. Pauli, Jr., *Z. Physik*, **31**, 765 (1925).

1. Let us first consider the various quantum numbers appearing in the new quantum mechanics. An electron in an atom is characterized by the "principal" quantum number  $n$ , already discussed in reference to the early Bohr theory. It appears in the principal mathematical factor for the binding energy of the electron in the atom. For electrons in the K shell,  $n = 1$ ; for those in the L shell,  $n = 2$ , etc. Sommerfeld's azimuthal quantum number  $k$  could have integral values from 1 to  $n$ . Quantum mechanics has shown that this second number should logically have values from 0 to  $n - 1$  rather than from 1 to  $n$ , and so  $k$  has been supplanted by  $l$ , which equals  $k - 1$ , and  $l$  may have any integral value from 0 to  $n - 1$ . The magnitude of the vector  $l$  representing the angular momentum of the electron in its orbit is related to  $l$  by the equation

$$|l| = \frac{h}{2\pi} \sqrt{l(l+1)} \quad (4-29)$$

Quantum mechanics has shown that every electron has an inherent angular momentum of its own, presumably owing to the fact that it is spinning like a top about some axis passing through it.<sup>1</sup> This "spin angular momentum" vector  $s$  has a magnitude

$$|s| = \frac{h}{2\pi} \sqrt{s(s+1)} \quad (4-30)$$

where  $s$  is the "spin quantum number."  $s$  always equals  $\frac{1}{2}$ . The orbital angular momentum  $l$  and the spin angular momentum  $s$  are both vectors, and (4-29) and (4-30) merely give their magnitudes. There is an interaction between these two vectors, as might be expected, since angular momentum of an electric charge is equivalent to magnetic moment. One vector precesses about the other, and this is called the "inner precession" of the atom. The two momentum vectors (spin and orbital) are added vectorially to obtain the vector  $j$  representing this inner precession whose magnitude is given by

$$|j| = \frac{h}{2\pi} \sqrt{j(j+1)} \quad (4-31)$$

where  $j$  is the "inner" quantum number.  $j$  has the possible values  $l - \frac{1}{2}$  or  $l + \frac{1}{2}$ , except that, when  $l = 0$ , then  $j$  cannot equal  $l - \frac{1}{2}$ , which would give it a negative value.

2. The next topic is the Pauli exclusion principle. This principle cannot be applied unless the directional degeneration of the atom is considered removed by some external directional agency, such as, for example, a magnetic field. The idea of a "distinguished direction"

<sup>1</sup> J. J. Thomson, *Phil. Mag.*, **27**, 1 (1939), has suggested that the frequency of this spin is given by (4-22), being  $1.2 \times 10^{20}$  per second for an electron at rest.

in the atom introduces three more quantum numbers,  $m_l$ ,  $m_s$ , and  $m$ , which represent the allowed values of the projection of the vectors  $l$ ,  $s$ , and  $m$  on the distinguished direction (for example, on an impressed magnetic field vector  $H$ ).  $m_l$  may have any integral value from  $-l$  to  $+l$ , including zero.  $m_s$  may have only two possible values,  $-\frac{1}{2}$  and  $+\frac{1}{2}$ .  $m$  may have any half integral value from  $-j$  to  $+j$ . These seven commonly used quantum numbers are summarized in Table 4-2.

Before proceeding to discuss the Pauli principle and its relation to the Mendelyev periodic table, a word should be said about the addition of the orbital and spin angular momentum vectors  $l$  and  $s$  to obtain the inner precession vector  $j$ . These vectors not only interact with each other for a given electron, but there is an interaction between these

TABLE 4-2.—QUANTUM NUMBERS

Symbol	Name	Significance	Allowed values
$n$	Principal or total	Principal binding energy	1, 2, 3, . . . etc.
$l$	Reduced azimuthal	Orbital angular momentum	0 and integral values up to $n - 1$
$s$	Spin	Spin angular momentum	$\frac{1}{2}$
$j$	Inner	Inner precession	$l - \frac{1}{2}$ or $l + \frac{1}{2}$ except that $j$ may not be negative
$m_l$	Magnetic azimuthal	Projection of $l$	$-l, -l + 1, \dots, +l$
$m_s$	Magnetic spin	Projection of $s$	$-\frac{1}{2}$ or $+\frac{1}{2}$
$m$	Magnetic	Projection of $j$	$-j, -j + 1, \dots, +j$

vectors for different electrons in the same atom. There are two different ways in which the vectors may be added. In the first, the orbital momentum vectors  $l_1, l_2$ , etc., for the various electrons in the atom are added to give a combined orbital angular momentum vector  $L$ . Likewise, the spin vectors  $s_1, s_2$ , etc., for the various electrons are added to give a combined  $S$ . Then the vectors  $L$  and  $S$  are added to give a total inner momentum vector  $J$  for the atom, neglecting the nucleus. This type of coupling between the spin and orbital moments of different electrons in the atom is called "Russell-Saunders" coupling, and it is approximated in the lighter atoms like helium and lithium. In the heavier elements like tungsten or uranium, the tendency is for the coupling to approach the so-called " $jj$  type," in which the  $l_1$  and  $s_1$  vectors are added to obtain  $j_1$  for the first electron, and the  $l_2$  and  $s_2$  vectors are added to obtain  $j_2$  for the second electron, etc., and then the various  $j$  vectors are added to obtain the total inner momentum vector  $J$ . In intermediate atoms, the coupling is of an intermediate type.

In 1925, Pauli stated<sup>1</sup> the principle now known as the Pauli exclusion

<sup>1</sup> W. Pauli, Jr., *Z. Physik*, **31**, 765 (1925).

principle governing the electrons in an atom. He wrote,

There can never be two or more equivalent electrons in the atom, for which, in a strong field, the values of all the quantum numbers  $n, l, j, m$  (or what is the same thing,  $n, l, m_l, m_s$ ) agree. If an electron is present in the atom for which these quantum numbers (in an external field) have certain values, then this level is filled.

The second set of numbers given by Pauli ( $n, l, m_l, m_s$ ) is customarily used in applying his principle.

This principle explains how the various electronic shells fill up as one progresses through the periodic table of the elements. The simplest element, hydrogen, has only one electron. It has the lowest possible principal quantum number ( $n = 1$ ) and the lowest possible value of  $l$  ( $l = 0$ ). Since  $l$  is zero,  $m_l$  is also zero. When the nuclear charge is increased from 1 to 2 and a second electron is added to form a helium atom, this second electron may also have  $n = 1$ ,  $l = 0$ , and  $m_l = 0$  because  $m_s$  can be varied. If the first electron had  $m_s = \frac{1}{2}$ , the second can have  $m_s = -\frac{1}{2}$ . When the third electron is added to make lithium, however, there are no more possible values for  $m_s$ .  $m_l$  cannot be changed as long as  $l$  remains zero, and  $l$  cannot be changed so long as  $n$  remains 1; hence  $n$  must be 2 for the third electron in lithium. That is, the K shell ( $n = 1$ ) can contain only two electrons, and helium has a full and complete K shell. With lithium, the L shell is started. There can be only eight electrons in this shell, corresponding to the possibilities listed in Table 4-3. Therefore element of atomic number 10 (neon) has a full and complete L shell. With atomic number 11 (sodium), the M shell is started. Thus the shells build up as one progresses through the periodic table.

TABLE 4-3.—QUANTUM NUMBERS OF THE EIGHT ELECTRONS IN A COMPLETE L SHELL

$n$	$l$	$m_l$	$m_s$	
2	0	0	$\frac{1}{2}$	s electrons*
2	0	0	$-\frac{1}{2}$	
2	1	-1	$\frac{1}{2}$	p electrons*
2	1	-1	$-\frac{1}{2}$	
2	1	0	$\frac{1}{2}$	
2	1	0	$-\frac{1}{2}$	
2	1	1	$\frac{1}{2}$	
2	1	1	$-\frac{1}{2}$	

\* See Sec. 4.

In general, there are  $2n^2$  electrons in a complete shell where  $n$  is the principal quantum number. Thus the M shell ( $n = 3$ ) will have 18 electrons when it is full. This simple filling up of the allowed electronic

states is not without its irregularities, however. For example, when one reaches  $n = 3$ ,  $l = 1$  and all six possible values of  $m_l$  have been used (this is the case for argon), one might expect that the next electron added would have  $n = 3$  and  $l = 2$ . Instead<sup>1</sup> it has  $n = 4$  and  $l = 0$  (potassium). That is, the N shell begins to fill up before the M shell is full. Likewise, the O shell begins to fill before the N shell is complete. The tendency for an inner shell like the N shell to postpone filling up until the O and even the P shell is partly filled results in a series of elements of successive atomic numbers having chemical properties all very

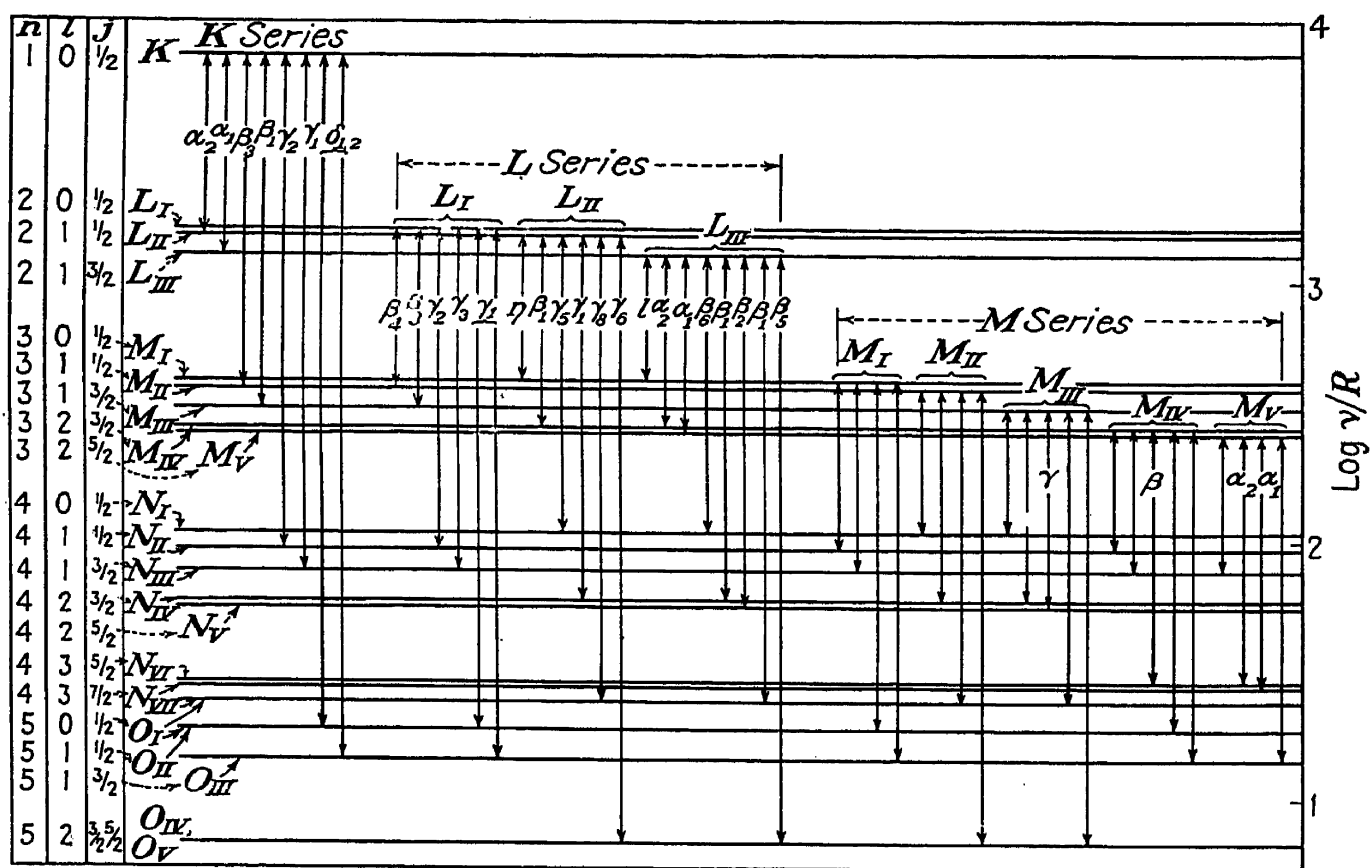


FIG. 4-2.—Atomic-energy-level diagram showing origin of characteristic x-ray spectra. (After Richtmyer and Kennard.)

much alike, as in the case of the rare earths (lanthanum, 57, to lutecium, 71). This is true because the chemical properties of an element are largely determined by the outermost electrons.

3. Modern quantum mechanics has evolved atomic energy-level diagrams much more detailed and complete than those which could be deduced from the early Bohr theory. Nevertheless, the essential features remain as they were in 1915. The  $K_\alpha$  radiation is still ascribed to electronic transitions between the L and K shells, the  $K_\beta$  lines to transitions between the M and K shells, the  $L_\alpha$  lines to transitions between the M and L shells, etc.

<sup>1</sup>See Table VIII, Appendix.



Figure 4-2 is a modern atomic-energy-level diagram<sup>1</sup> based on quantum mechanics. It is seen that the vertical distances in this diagram are marked  $\log \nu/R$ . The explanation of this follows from equation (4-12), where the frequency of an x-ray line is expressed as a difference between two terms that might be called  $\nu_1$  and  $\nu_2$ , thus:

$$\nu = \frac{2\pi^2 me^4}{h^3 n_2^2} (Z - \sigma)^2 - \frac{2\pi^2 me^4}{h^3 n_1^2} (Z - \sigma)^2 = \nu_2 - \nu_1 \quad (4)$$

If both sides of this equation were multiplied by  $h$ , it would represent radiation as an energy difference

$$h\nu = h\nu_2 - h\nu_1 \quad (4)$$

in ergs.  $\nu_1$  and  $\nu_2$  do not represent real frequencies that can be measured. Although  $\lambda$  is the quantity measured in experimental work, theoretical physicists find it convenient to deal with the reciprocal of the wavelength,  $1/\lambda = \nu/c$ , called the "wave number" (number of waves per centimeter), because  $\nu/c$  may be calculated easily by subtracting terms of the form

$$\frac{2\pi^2 me^4}{ch^3} \frac{(Z - \sigma)^2}{n_x^2} = \frac{\nu_x}{c} = R \frac{(Z - \sigma)^2}{n_x^2} \quad (4)$$

from each other. This is obvious from equation (4-32), so far as the first form given is concerned. In the second form,  $\nu_x$  represents  $\nu_2$  as used in (4-32) and (4-33). The constant  $2\pi^2 me^4/ch^3$  thus appears frequently and is commonly called the "Rydberg constant"<sup>2</sup> and designated by  $R$ , as in the third form.  $\nu_x$  is to be thought of as a quantity defined by (4-34), which has the dimensions of a frequency, but no experimental reality as such.

Thus energy levels expressed in terms of  $\nu_x/R$  are convenient for calculation, and this is the reason for plotting them in this manner. When they are so plotted, the subscript  $x$  is dropped, but one must keep in mind that the levels themselves do not represent frequencies. Only the vertical arrows, connecting one level with another, which represent an emission or absorption transition characterized by a frequency in the usual sense.

Since the energy difference between K and L electrons is large compared with that between L and M electrons, this in turn being compared with that between M and N electrons, it is necessary to use a logarithmic scale to represent the various levels in the same diagram.

Since all the various lines in the characteristic spectrum represent differences in energies, the absolute value of these energies is arbitrary.

<sup>1</sup> From F. K. Richtmyer and E. H. Kennard, "Introduction to Modern Physics," 3d ed., McGraw-Hill Book Company, Inc., New York, 1942.

<sup>2</sup> See Appendix I.

in the sense that  $50 - 20$  gives the same result as  $150 - 120$ . The zero point chosen for the atomic energy levels in such a diagram as Fig. 4-2 is arbitrarily taken as that of an atom in which the outermost, most loosely bound electron of the atom has been removed. The energy involved in doing this (called the "ionization potential") is practically negligible compared with the energies represented in most x-ray energy-level diagrams; thus, it is ordinarily convenient to think of zero energy in x-ray energy-level diagrams as representing a normal atom. For example, the ionization potential of molybdenum is 7.35 volts, whereas the energy represented by the  $L_{\alpha_1}$  line is about 2,290 electron volts.<sup>1</sup> Therefore, it alters the picture only slightly to regard this line as representing a jump from about 2,780 to 490 electron volts (on the basis of zero energy representing a normal atom) instead of from 2,772.65 to 482.65 electron volts in accordance with the usual convention.

Energy is required to remove an electron from an atom, and this energy is recovered when the electron falls back in. It is this type of energy that is represented in Fig. 4-2. The zero of energy is represented by a horizontal line at or near the bottom of the diagram. The top horizontal line, marked K, represents the "K level," and its ordinate (which is seen in the diagram to have a  $\nu/R$  logarithm of about 4 or a  $\nu/R$  value of about 10,000) is the logarithm of the energy (not in ergs) required to remove a K electron from the atom (that is, to remove an electron from the K shell to a point outside the atom). Then the  $K_{\alpha_1}$  line is emitted by electrons falling from the level marked  $L_{III}$  in the diagram into the vacancy thus created in the K level. Thus the emission of the various spectral lines is represented in the diagram by upward-pointing arrows connecting lower levels with upper ones. The  $K_{\alpha_1}$  line of molybdenum, for example, having a wave length of 0.708 Å. represents a photon energy of about 17,350 electron volts. The conversion of angstroms to electron volts or the reverse is accomplished by the relation  $E = hc/\lambda$ , which may be converted into the handy form

$$\text{Energy in electron volts} = \frac{12,400}{\text{wave-length in angstrom units}} \quad (4-35)$$

The splitting of the L level into three sublevels, commonly called  $L_I$ ,  $L_{II}$ , and  $L_{III}$ , and of the M level into  $M_I$ ,  $M_{II}$ ,  $M_{III}$ ,  $M_{IV}$ , and  $M_V$ , etc., is shown in Fig. 4-2. The origin of the  $L_I$ ,  $L_{II}$ ,  $L_{III}$ ,  $M_I$ ,  $M_{II}$ , etc., series (mentioned on page 48) is now clear from the diagram. It will be seen that the  $L_I$  series of spectral lines originates from electronic transitions which have the  $L_I$  level as their final state. Similar statements may be made regarding the relation of the  $L_{II}$  series to the  $L_{II}$  level, the  $M_I$  series to the  $M_I$  level, etc.

<sup>1</sup> See p. 27 regarding the convention of measuring energies in electron-volts.

The notation along the left margin of the diagram indicates that the splitting of the main levels into sublevels corresponds to the various values given for the quantum numbers  $l$  and  $j$ , already discussed, which are restricted to the allowed values listed in Table 4-2. The value of  $n$ , the principal quantum number, distinguishes between the various main shells, K, L, M, etc. It will be noticed that there is less difference between the  $N_{VII}$  level and the  $O_I$  level, for example, than there is between  $N_I$  and  $N_{IV}$ , so that, for high values of  $n$ , its role is no longer so superior to that of  $l$  in determining the energy.

The diagram also illustrates the "selection rules" that govern the characteristic x-ray spectra. These selection rules are

$$\left. \begin{aligned} \Delta n &\neq 0 \\ \Delta l &= \pm 1 \\ \Delta j &= \pm 1 \text{ or } 0 \end{aligned} \right\} \quad (4-36)$$

These equations mean "the change in  $n$  cannot be zero" (that is,  $n$  must change), " $l$  must increase or decrease by 1," and " $j$  must either remain unchanged or else increase or decrease by 1." Exceptions to these rules are found, but such forbidden lines are rare; they are also weak compared with ordinary prominent allowed lines conforming to the selection rules.

The diagram in Fig. 4-2 is obviously representative of some fairly heavy element like one of the rare earths. Simpler atoms, like iron, for example, have a diagram in which no levels beyond  $N_I$  appear. For carbon, only the K,  $L_I$ , and  $L_{II}$  levels are filled; for uranium, the diagram should show P and Q levels.<sup>1</sup>

The notation  $K_{\alpha_1}$ ,  $K_{\alpha_2}$ ,  $K_{\beta_1}$ ,  $K_{\beta_2}$ ,  $L_{\alpha_1}$ , etc., used to designate the more important characteristic x-ray lines is by now quite familiar. However, the complete notation including subscripts such as  $\alpha_1$ ,  $\alpha_2$ ,  $\beta_1$ ,  $\beta_2$ ,  $\beta_3$ ,  $\gamma_1$ ,  $\gamma_2$ ,  $\eta$ , etc., used to designate all the lines has been built up somewhat arbitrarily, and consequently there is considerable variation among writers in the designation of some of the less prominent lines, such as  $L_{\gamma_8}$ . A much more certain way to designate such a line is to use such notation as  $L_{II} - N_{VI}$ , which indicates that the line is the one resulting from an electronic transition from the  $N_{VI}$  to the  $L_{II}$  level. However, the more prominent lines such as  $K_{\alpha_1}$ ,  $K_{\alpha_2}$ ,  $L_{\alpha_1}$ ,  $L_{\alpha_2}$ ,  $K_{\beta_1}$ , etc., are universally recognized unambiguously by all workers in x-rays.

Something has already been said regarding the intensities of characteristic spectra on pages 48 and 49, where the empirical equation (4-3), which governs the various series, was set forth. It should also be mentioned that simple rules have been found to govern the approximate relative intensities of some of the more important lines such as

<sup>1</sup> Appendix, Table VIII.

$K_{\alpha_1}$ ,  $K_{\alpha_2}$ ,  $K_{\beta_1}$ ,  $K_{\beta_2}$ ,  $L_{\alpha_1}$ ,  $L_{\alpha_2}$ , etc. In 1924 Burger and Dorgelo<sup>1</sup> deduced such rules, now commonly called the "sum rules." In the case of lines that terminate on a single undivided level, like the K level in Fig. 4-2, the sum rules indicate that the relative intensities of lines such as  $K_{\alpha_1}$  and  $K_{\alpha_2}$  which form a "narrow doublet" (that is, of which the frequencies are close together) are given simply by the relative "weights" of the initial states  $L_{III}$  and  $L_{II}$ , respectively. The weight of a level is

$$\text{Weight} = 2j + 1 \quad (4-37)$$

where  $j$  is the inner quantum number of the level. Thus the weights of the  $L_{III}$  and  $L_{II}$  levels, for which  $j = \frac{3}{2}$  and  $\frac{1}{2}$ , respectively, are 4 and 2, so that the  $K_{\alpha_1}$  line should be twice as intense as the  $K_{\alpha_2}$  line. Experimentally, this has been found to be true. Likewise,  $K_{\beta_1}$  is about twice as intense as  $K_{\beta_2}$ . In cases where both the initial and final levels from which a line originates are multiple, as in the case of the L and M levels from which the  $L_{\alpha_1}$  and  $L_{\alpha_2}$  lines originate, then the application of the sum rules becomes more complex; an explanation of it here is too lengthy to be warranted. However, for the  $L_{\alpha_1}$  and  $L_{\alpha_2}$  lines just mentioned, the rules predict that the former will be nine times as intense as the latter, which agrees with experimental observation. There are several known cases, however, in which the sum rules predict relative line intensities not in agreement with experiment.

In addition to the ordinary spectral lines thus far described as composing the characteristic x-ray spectra, there are found faint subsidiary lines called x-ray "satellites." These faint lines are found close to the more intense "diagram" lines shown in Fig. 4-2. They are generated by electronic transitions between the quantized energy levels of *doubly* ionized atoms or, in rare cases, triply ionized atoms. Ordinary x-ray lines shown in Fig. 4-2 are due to transitions between the various levels of a *singly* ionized atom, as stated on page 51. The  $K_{\alpha}$  lines are due to a transition of the type K — L, and one of the satellites of these lines might be KL — LL, where KL indicates one electron missing from the K shell and one from the L shell and LL indicates two electrons missing from the L shell. The energy of the KL — LL transition is slightly greater than the ordinary K — L transition, and hence the satellites are of slightly shorter wave length than the parent line. The character, occurrence, and number of these satellites depend upon the atomic number of the target element. For a discussion and bibliography on x-ray satellites, the reader is referred to an article by Hirsh.<sup>2</sup>

Many details of the theory of characteristic x-ray spectra have not been mentioned because space will not permit. Some of the rudiments

<sup>1</sup> H. C. Burger and H. B. Dorgelo, *Z. Physik*, **23**, 258 (1924).

<sup>2</sup> F. R. Hirsh, Jr., *Rev. Modern Phys.*, **14**, 45 (1942).

of quantum mechanics have been discussed because they are essential to an understanding of the energy-level diagram in Fig. 4-2. Once this diagram is fully understood, one will have sufficient knowledge of characteristic x-ray spectra to engage in most types of industrial x-ray work. The excitation potentials discussed on pages 46, 48, and 51 are represented in the diagram by the ordinates of the levels on which a group of upward-pointing arrows terminate. Thus it may be seen why the  $L_{III}$  series is excited at a slightly lower voltage than the  $L_I$  series, for example. The diagram also explains absorption edges, which will be discussed in the next chapter.

**4. Relation to Optical Spectra.** Optical spectra are represented by energy-level diagrams very similar to Fig. 4-2. As stated on page 66, the zero of energy in these diagrams is usually the ionization potential, which is 5.12 volts for sodium and 10.38 volts for mercury, as typical examples. Most optical spectra involve energies less than the ionization potential; and if it is to be taken as the zero energy line at the top of the diagram instead of the bottom, the energies increase downward instead of upward, and emission is represented by arrows pointing downward. Atomic optical spectra are generated by electronic transitions between the allowed energy levels of the outermost electrons of the atom, as contrasted to the inner levels involved in x-ray spectra.

The optical notation using an alphabet of the form  $s, p, d, f, g, h$ , etc., to represent the values 0, 1, 2, 3, etc., of the reduced azimuthal quantum number  $l$  is frequently borrowed in discussing the electronic structures of the atomic (K, L, M, etc.) shells. The electronic structure of the K shell is thus abbreviated as  $1s^1$  in the case of hydrogen, for example, the 1 indicating that  $n = 1$  (K shell), the  $s$  indicating that  $l = 0$ , and the superscript 1 indicating that only one electron is present in this level. Thus the helium configuration is  $1s^2$ , lithium  $1s^2 2s^1$ , and potassium  $1s^2 2s^2 2p^6 3s^2 3p^6 4s^1$ , etc. (see Table 4-3). This last example indicates that for potassium there are two electrons in the  $1s$  (K) level, two in the  $2s$  ( $L_I$ ) level, six in the  $2p$  ( $L_{II}$  and  $L_{III}$ ) level, two in the  $3s$  ( $M_I$ ) level, six in the  $3p$  ( $M_{II}$  and  $M_{III}$ ) level, and one in the  $4s$  ( $N_I$ ) level (see Fig. 4-2 and Appendix VIII).

Notation such as  $L_{III} - M_V$  to represent x-ray lines follows a convention similar to optical notation of the type  $3^2S_{\frac{1}{2}} - 3^2P_{\frac{3}{2}}$  representing an optical line. In both cases, the notation of the final level is given first, followed by that of the initial level.

### QUESTIONS AND PROBLEMS

1. The  $K_{\alpha_2}$  line of one element has a wave length of 0.190 Å.; the  $K_{\alpha_2}$  line of a second element has a wave length of 0.196 Å. Which of the two has the higher atomic number?

2. The  $L_{\alpha_1}$  line of praseodymium (59) has a wave length of 2.458 Å.; the  $L_{\alpha_1}$  line of neodymium (60) has a wave length of 2.365 Å.; the  $L_{\alpha_1}$  line of samarium (62) has a wave length of 2.195 Å.; the  $L_{\alpha_1}$  line of europium (63) has a wave length of 2.116 Å. Even though element 61 (illinium) is very rare, its  $L_{\alpha_1}$  line will have what wave length, within  $\frac{1}{100}$  Å.?

*Ans.* 2.28 Å.

3. A molybdenum tube is operating at 5 ma. and 30 kv. At a point 1 m. from the target, the  $K_{\alpha_1}$  line has an intensity  $I$ . What will be the approximate intensity of the  $K_{\alpha_2}$  line at this point? If the voltage is raised to 40 kv., what will be the intensity of the  $K_{\alpha_1}$  line at this point, the current still being 5 ma.? If the tube current is now increased to 10 ma., what will be the intensity of the  $K_{\alpha_1}$  line at this point?

*Ans.*  $\frac{1}{2}I$ ;  $3\frac{1}{4}I$ ;  $6\frac{1}{2}I$ .

4. From Fig. 4-2, which series has the higher excitation potential, the  $M_I$  or the  $M_{IV}$ ? Which line will have a longer wave length,  $L_I - M_{II}$  or  $L_I - M_{III}$ ?

5. A beam of 50-kv. cathode rays will have associated with it de Broglie waves having a wave length of how many angstrom units?

*Ans.* 0.055 Å.

6. What is the Pauli exclusion principle? What sort of rules are the selection rules? The sum rules? What is the combination principle (sometimes called the "Ritz" combination principle)?

7. Using equation (4-35), calculate the energy in electron volts contained in a photon of molybdenum  $K_{\beta}$  radiation (wave length 0.63 Å.). Your answer will be less than the K excitation potential of molybdenum (20 kv.). The difference between this 20-kv. figure and your answer represents what?

## CHAPTER 5

### ABSORPTION AND SCATTERING; SECONDARY X-RAYS

**1. Introductory Discussion.** The general law governing the absorption of radiation as it passes through matter was first formulated in 1729 by Bouguer and rediscovered later in the eighteenth century by J. H. Lambert. In optics, it is commonly called Lambert's law of absorption (not to be confused with Lambert's cosine law, page 19). The same law is as valid for x-rays as it is in optics.

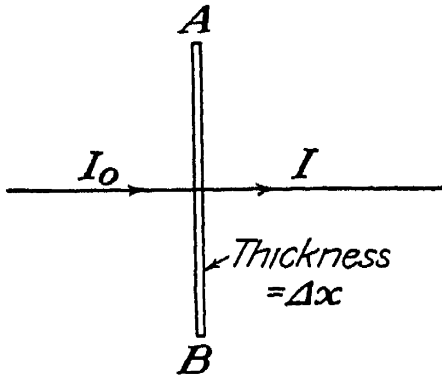


FIG. 5-1.—Absorption in a thin layer.

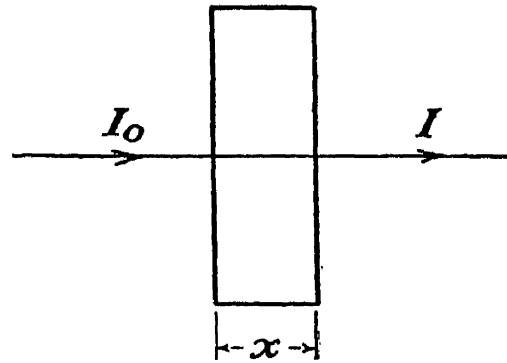


FIG. 5-2.—Absorption in a thick layer.

The basic principle from which the law is derived is that the fraction of the radiation absorbed in passing through a *thin* layer of matter is proportional to the thickness of the layer and a factor called the “absorption coefficient,” which depends upon the nature of the absorbing matter and the wave length of the radiation. Expressed mathematically, where  $I_0$  is the intensity of the radiation incident upon a thin layer  $AB$  (Fig. 5-1) of the absorbing medium and  $I$  is the intensity of the radiation that passes through, one has

$$\frac{I_0 - I}{I_0} = \frac{\Delta I}{I_0} = -\mu_l \Delta x \quad (5-1)$$

$\Delta x$  being the thickness of the layer and  $\mu_l$  the linear absorption coefficient for the particular material and wave length concerned. The negative sign arises because  $\Delta I$  is a mathematical symbol for the “increase” in intensity  $I$  of the radiation as it passes through the layer. Since the intensity decreases,  $\Delta I$  is negative. Theoretically, (5-1) holds accurately only when  $\Delta x$  becomes infinitesimal; it therefore becomes

$$\frac{dI}{I} = -\mu_l dx \quad (5-2)$$

since in this limiting case  $I_0$  may be replaced by  $I$  in the denominator. To apply this to a practical case, where the absorber will have a finite thickness  $x$  (Fig. 5-2), one integrates (5-2), obtaining

$$\log I = -\mu_l x + C \quad (5-3)$$

To evaluate the constant of integration  $C$ , one notes that, when  $x = 0$ ,  $C = \log I_0$  because in this case  $I = I_0$ . Hence,

$$\log I - \log I_0 = \log \frac{I}{I_0} = -\mu_l x \quad (5-4)$$

These are natural logarithms; hence, (5-4) indicates that

$$I = I_0 e^{-\mu_l x} \quad (5-5)$$

This is Lambert's law.

If the beam of radiation has a cross section of 1 cm.<sup>2</sup>, it is seen from (5-1) that  $\mu_l$  represents the fraction of the energy absorbed per cubic centimeter of the absorber traversed. Practically, one is more often interested in the absorption per gram or pound of the absorber than in the absorption per cubic centimeter or cubic inch. Hence, that absorption coefficient most commonly measured and used in x-ray work is  $\mu_l/\rho$ , where  $\rho$  is the density of the absorbing material. This quantity is called the "mass absorption coefficient"  $\mu$  (Appendix V).

$$\mu = \frac{\mu_l}{\rho} \quad (5-6)$$

Lambert's law, as applied to x-rays, is usually written

$$I = I_0 e^{-\mu x \rho} \quad (5-7)$$

A striking characteristic of the absorption of x-rays is that it is independent of the physical or chemical state of the absorbing material. Thus a beam of x-rays passing from the ceiling to the floor of a chamber filled with hydrogen and oxygen may be 10 per cent absorbed, or 90 per cent of it will reach the floor. If a spark explodes the hydrogen and oxygen, filling the chamber with steam, 90 per cent of the x-rays will still reach the floor. Then, if the chamber is chilled so that the steam condenses into a thin layer of water or ice on the floor, 90 per cent of the x-rays will still reach the floor. This is not true for light or ultraviolet or infrared radiation, and it explains why the mass absorption coefficient of x-rays is commonly used, whereas the linear absorption coefficient  $\mu_l$  is ordinarily used in optics.

All that has been said about absorption thus far is true only if "monochromatic" x-rays (rays of one wave length) are used. The rays from an x-ray tube are not monochromatic, of course. When such hetero-



geneous rays strike an object, the soft rays will be absorbed much more strongly than the hard rays because the absorption coefficient in general increases with the wave length.

The variation of the absorption coefficient with the wave length is not represented by a continuous function, however. The discovery that the absorption curve as a function of wave length contains discontinuities known as "absorption edges" was made by M. de Broglie<sup>1</sup> in 1916. Figure 5-3 is a typical curve showing the manner in which the mass absorption coefficient of lead varies with the wave length of the x-rays. Such curves are obtained with the aid of an x-ray spectrometer, which will be described in a later chapter. In this instrument, the wave length is selected and varied by diffraction with a crystal, and the intensity is measured with an ionization chamber.

Examination of Fig. 5-3 shows that, beginning at short wave lengths around 0.1 Å., the absorption of the lead increases with wave length quite rapidly until the wave length 0.138 is reached. At this point, the absorption coefficient drops suddenly to a much lower value and then begins to increase again. This discontinuity at 0.138 Å. is called the "K absorption edge." The explanation of the discontinuity is quite simple. Wave lengths below 0.138 Å. are associated with x-ray photons that have sufficient energy  $\left(E = h\nu = h \frac{c}{\lambda}\right)$  to eject electrons from the

K shell of the lead atoms. In the energy-level diagram of Fig. 4-2, they have energy exceeding that represented by the highest line, the K level. Consequently, many of these x-ray photons while passing through the lead proceed to eject electrons photoelectrically from the K shell of the lead atoms. Such photons simply vanish and consequently fail to emerge on the far side of the lead. Hence the absorption coefficient for such rays (say, those having a wave length of 0.130 Å.) is much higher than the coefficient for rays having a wave length just above that of the K edge (say, those having  $\lambda = 0.145$  Å.). The latter rays

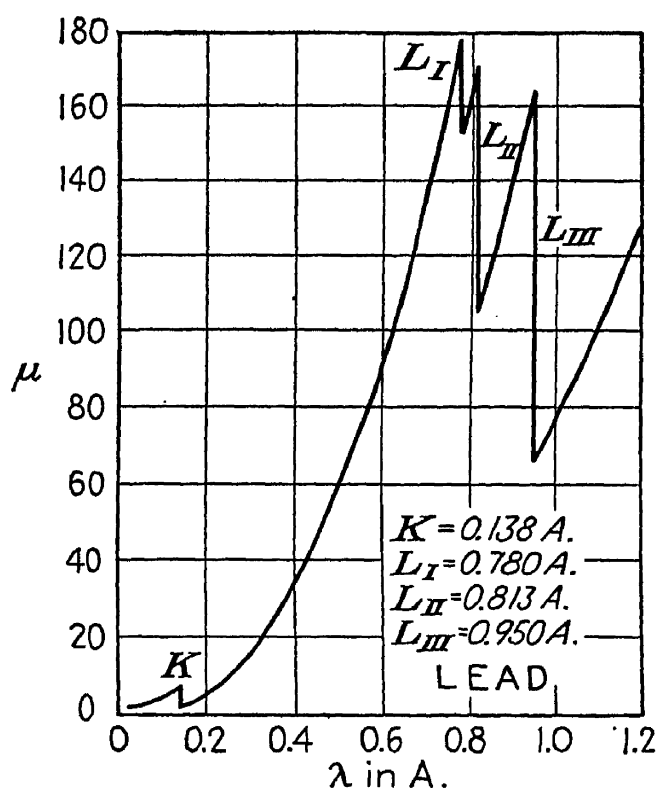


FIG. 5-3.—Mass absorption coefficient of lead as a function of the wave length. (F. K. Richtmyer.)

<sup>1</sup> M. de Broglie, *J. phys.*, **5**, 161, 227 (1916); *Compt. rend.*, **163**, 87, 352 (1916).

consist of photons whose energy is slightly less than that required to eject the K electrons from the lead atoms; and, being unable to expend themselves in this manner, they pass on and emerge on the far side of the lead.

At this point it is worth digressing briefly to mention a peculiarity of x-ray photography that is due to the phenomenon of the K absorption edge. When x-ray spectra are recorded photographically, it is often found that the film after development exhibits two lines of demarcation

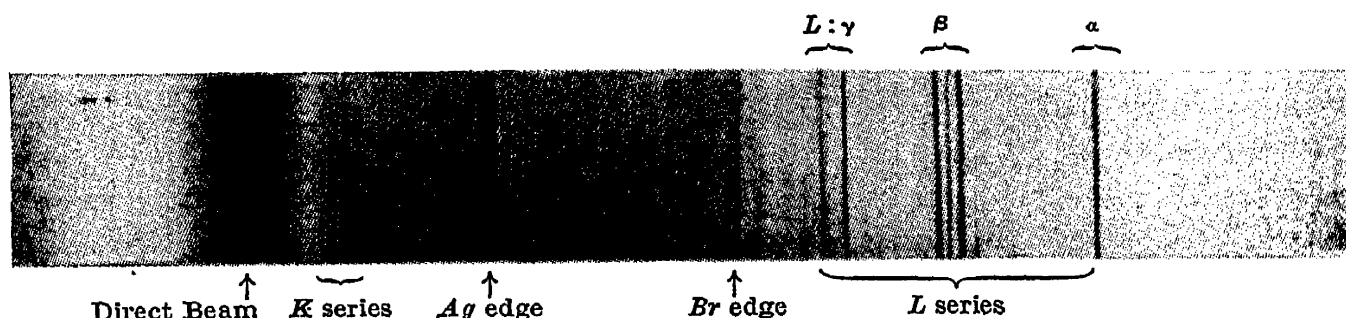


FIG. 5-4.—Spectrum of the continuous and characteristic x-radiation from tungsten, showing effect of K edges of silver and bromine in the photographic emulsion. (*M. de Broglie.*)

which appear to divide a less sensitive portion of the film (where the photographic image is faint) from a more sensitive portion (where the photographic image is stronger). This may be seen in Fig. 5-4 obtained by *M. de Broglie*. These lines occur at the points in the spectrum where the wave lengths equal the K absorption limit of silver (0.485 Å.) and the K limit of bromine (0.918 Å.). The photographic emulsion consists chiefly of silver bromide, and the x-rays on the short-wave-length side of each of these K edges are absorbed more strongly by it (and hence cause more blackening) than those on the long-wave-length side. This is a good illustration of the fact that the absorption of x-rays by any substance is determined only by the chemical elements it contains, not by their state of chemical combination.

To return to Fig. 5-3 and the discussion of the absorption edges<sup>1</sup> of a typical material such as lead, one notes that, as  $\lambda$  increases beyond the K edge, the absorption coefficient rises rapidly and continuously until three more absorption edges, called the "L edges,"  $L_I$ ,  $L_{II}$ , and  $L_{III}$ , are reached at 0.780, 0.813, and 0.950 Å., respectively. The energy-level diagram of Fig. 4-2 makes it clear why three L edges should be expected, and these L discontinuities in the absorption curve may be explained in a manner analogous to that in which the K edge was explained. That is, x-rays with longer wave length than one of the L edges are associated with photons of energy insufficient to eject electrons photoelectrically from the corresponding L level, while rays of shorter wave length (photons of higher energy) have enough energy to expend themselves in this manner, and they do so. Experimental investigation in the long-wave-

<sup>1</sup> The wave lengths of the K edges are tabulated in Appendix VI.

length region reveals five M edges for the heavy elements whose atoms are complex enough to have the M levels filled. Thus the number of absorption edges observed is in exact accord with atomic theory and the Pauli principle.

The probability that an x-ray photon encountering an atom will photoelectrically eject any particular electron in that atom increases very rapidly with the tightness of binding of the electron. If the photon has energy exceeding  $h\nu_K$  (the energy required to eject an electron from the K shell), it is probable that it will eject one of the K electrons or else pass by the atom without exercising any photoelectric action at all. If the photon has energy less than  $h\nu_K$  but exceeding  $h\nu_L$ , it is probable that it will eject one of the L electrons, if it ejects any at all. For a detailed quantum-mechanical treatment of photoelectric x-ray absorption, the reader is referred to an article by Hall.<sup>1</sup>

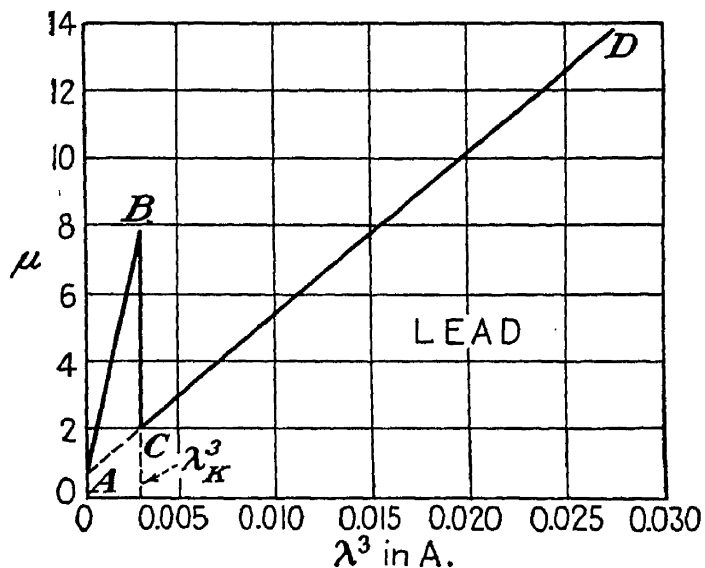


FIG. 5-5.—Mass absorption coefficient of lead as a function of the cube of the wave length. (From Richtmyer and Kennard.)

If an absorption curve like that in Fig. 5-3 is plotted on a graph in which the abscissas are  $\lambda^3$  instead of  $\lambda$ , the curve becomes very nearly a straight line, except at the absorption edges, as shown in Fig. 5-5.<sup>2</sup> The K-edge discontinuity occurs at  $BC$ . On each side of this, the graph consists of straight lines  $AB$  and  $CD$ , which appear to have a common intercept on the  $\mu$  axis. The mathematical equation for such a straight line is

$$y = mx + b \quad (5-8)$$

where  $m$  is the slope and  $b$  is the  $y$  intercept. Applying this equation to Fig. 5-5,

$$\mu = C_1\lambda^3 + \sigma \quad (5-9)$$

for the portion  $AB$  and

$$\mu = C_2\lambda^3 + \sigma \quad (5-10)$$

for the portion  $CD$ . The term  $\sigma$  is commonly called the “mass scattering

<sup>1</sup> H. Hall, *Rev. Modern Phys.*, **8**, 358 (1936).

<sup>2</sup> Figures 5-3 and 5-5 are taken from papers by F. K. Richtmyer. See, for example, *Phys. Rev.*, **18**, 13 (1921), **27**, 1 (1925). The latter article contains several plots like Fig. 5-5 for Mo, Ag, Sn, W, and Au, as well as Pb. There is some doubt about the exact value of the exponent; W. Wrede, for example, *Ann. Physik*, **36**, 681 (1939) deduces 3.2.

coefficient," and equations (5-9) and (5-10) may be interpreted as indicating that the observed absorption  $\mu$  of a beam of x-rays passing through an absorber is caused primarily by the "photoelectric" or "fluorescent" or "true" absorption  $C\lambda^3$ , but partly by the "modified" and "unmodified" scattering  $\sigma$  of the x-rays as they pass through the absorber.

All these new terms require some elaboration. Suppose a narrow beam of parallel x-rays having intensity  $I_0$  strikes perpendicularly upon the surface of a metal plate. An ionization chamber placed behind the plate in a position to catch the beam after it has passed through the plate will measure the intensity  $I$  of the beam as it emerges. Suppose, further, that this "primary" beam is monochromatic, consisting entirely of rays of the single wave length  $\lambda_0$ , or of photons all having the same energy  $h \frac{c}{\lambda_0}$ . If the rays are hard [say,  $\lambda_0 = 0.1$  A., so that the photons have an energy of 124,000 electron volts, from equation (4-35)] and the plate is thin (for example, lead foil 0.005 in. thick), most of the primary rays (photons) will pass completely through it, being neither absorbed nor scattered. A few of the photons will expend their energy, however, in photoelectrically ejecting electrons from the K shell of some of the lead atoms. These photons disappear and are said to be "truly" absorbed. It is these which account for the  $C\lambda^3$  term (often represented by the symbol  $\tau$ ) in equations (5-9) and (5-10). Since only 87,600 electron volts is required to eject K electrons from lead, such electrons, if ejected by 124,000-electron-volt photons, will have a kinetic energy of 36,400 electron volts when they leave the atom. Such high-speed electrons are sometimes called "secondary beta rays" or "beta particles" by analogy with the high-speed electrons emanating from radioactive material. Perhaps 1 per cent of these electrons, striking other lead atoms, will generate a continuous x-ray radiation, just as in an x-ray tube with a lead target operating at 36.4 kv., but, just as in the tube, 99 per cent or so of these photoelectrons will dissipate their energy by ionizing a large number of atoms, the energy being converted to heat eventually. A very few of them may also eject L electrons from lead atoms. The comparatively large number of vacancies created in the K shells by the primary 124,000-electron-volt photons will be filled by electrons from the outer shells falling in, so that the characteristic x-ray spectrum of lead will be excited. One may suppose that each K vacancy will eventually be filled<sup>1</sup> and hence that the characteristic radiation thus generated should be roughly a hundred times as intense as the continuous radiation just mentioned. These newly generated x-rays are called *secondary x-rays* or "fluorescence x-radiation." It may now be

<sup>1</sup> See Sec. 2 regarding this point.

seen why this absorption process just described is called "fluorescent" or "photoelectric" absorption. It is also called "true" absorption to distinguish it from the scattering process, which will be described next.

In addition to the fraction of the primary x-rays that are truly absorbed, as just described, some of the primary rays will emerge from the sheet of lead foil traveling in directions different from the one they had when they entered. Hence they will not enter the ionization chamber, and this will make it appear as though they, too, were absorbed. This "scattering" of the primary x-rays is represented by the term  $\sigma$  in equations (5-9) and (5-10). The scattered x-rays that emerge from the lead are found to consist partly of rays having the same wave length (0.1 A.) as the primary beam and partly of rays having a wave length somewhat greater than this. The former type are called the "unmodified" rays and are said to have been scattered "coherently," whereas the latter type are called the "modified" rays and are said to have been scattered "incoherently." This incoherent scattering is often called "Compton scattering" because A. H. Compton was the first to measure it accurately and work out the theory of its cause. It is the coherently scattered rays that play the leading role in the phenomena of x-ray diffraction, by means of which scientists have been able to learn so much about the arrangement of atoms in solids, the arrangement of atoms in molecules, and even the distribution of the electrons in the atoms. X-ray diffraction also yields much information about the size and orientation of the "grains" in metals and other solids and about strains that may be present. Discussion of these matters will be reserved for later chapters.

Both the unmodified and modified scattering are represented by the term  $\sigma$  in equations (5-9) and (5-10). The form of these equations suggests that  $\sigma$  is independent of the wave length, but this is not the case. The scattering  $\sigma$  increases with wave length, but not as rapidly as the true absorption  $\tau$ , or  $C\lambda^3$ . The question of the variation of  $\sigma$  with  $\lambda$  and the atomic number  $Z$  of the scatterer was investigated from the standpoint of classical physics by Thomson,<sup>1</sup> who deduced the relation

$$\sigma = \frac{8\pi n e^4}{3m^2 \rho c^4} \quad (5-11)$$

where  $n$  is the number of electrons per cubic centimeter of the scattering material,  $\rho$  is its density,  $e$  and  $m$  are electronic charge (in e.s.u.) and mass, and  $c$  is the velocity of light. One notes that  $n/\rho$  in this expression represents the number of electrons per gram of the scatterer. The equa-

<sup>1</sup> See, for example, J. J. Thomson and G. P. Thomson, "Conduction of Electricity through Gases," 3d ed., vol. 2, p. 258, Cambridge University Press, London 1933.

tion indicates that  $\sigma$  should be proportional to this and that there should be no dependence upon the wave length of the x-rays.

Actually, this is found to be true experimentally if the scattering material is a very light element like lithium or beryllium and if the wave length of the incident x-rays is 0.2 A. or more. If the incident x-rays are harder than this, most of the scattering is incoherent (see Sec. 4) and there is a considerable difference between the wave length of the incident and the scattered x-rays. Under these conditions,  $\sigma$  is less for all scattering materials than that predicted by (5-11), becoming much less as  $\lambda$  decreases further below 0.2 A. There is a modern wave-mechanical formula that fits this case very well [see equation (5-36)].

In case the scattering material is an element heavier than beryllium, such as carbon, oxygen, aluminum, and up to about  $Z = 20$  (calcium),  $\sigma$  is nearly proportional to  $Z\lambda$ , when  $\lambda > 0.1$  A., and  $\sigma$  has the value predicted by (5-11) only when  $\lambda =$  about 0.2 A.

For heavy scattering elements like iron, copper, tin, tungsten, gold, and lead,  $\sigma$  is proportional to  $Z^m\lambda^n$  when  $\lambda > 0.2$  A., where  $1 < m < 2$  and  $1 < n < 3$ , and  $\sigma$  has the value predicted by (5-11) only when  $\lambda =$  about 0.2 A.

The increase of  $\sigma$  with  $\lambda$  and  $Z$  above 0.2 A. for medium and heavy scatterers is supposedly due to the fact that the distance between electrons becomes small compared with the x-ray wave length under these conditions, resulting in constructive interference.<sup>1</sup>

The intensity of the scattered rays also varies with the angle  $\phi$  between their lines of travel and that of the primaries (small values of  $\phi$  indicating rays scattered forward with the primaries). Thomson's classical theory indicates that the intensity of the scattered ray should vary proportionally to  $1 + \cos^2 \phi$ , the relation being<sup>1</sup>

$$\frac{I_a}{I_0} = \frac{Ze^4}{2r^2m^2c^4} (1 + \cos^2 \phi) \quad (5-12)$$

where  $I_a$  is the intensity of the rays scattered per atom, of atomic number  $Z$ , at distance  $r$  (in centimeters),  $I_0$  being the intensity of the primary rays. In the case of heavy atoms like lead, gold, etc., in which some of the electrons are close together compared with the wave length of the x-rays,  $Z$  in this equation should be replaced by  $Z^2$ . Equation (5-11) for  $\sigma$  is obtained by integrating (5-12) over a sphere, including all values of  $\phi$ . Experiment shows that, for rays of wave length greater than 0.2 A., the  $1 + \cos^2 \phi$  relation is approximately true, unless  $\phi$  is small (say, less than  $30^\circ$ ). For these small angles, there is again constructive interference, so that the observed intensity exceeds the predicted. For hard rays ( $\lambda < 0.2$  A.) the observed intensity of the scattered rays is less

<sup>1</sup> See pp. 332-333.

at all angles than that predicted by (5-12). In this case, the Klein-Nishina formula [see equation (5-37)] must be used.

Both the true absorption  $\tau$ , or  $C\lambda^3$ , and the scattering  $\sigma$  [equations (5-9) and (5-10)] increase with the atomic number  $Z$  of the absorber-scatterer. Bragg and Pierce<sup>1</sup> first suggested that the absorption  $\tau$  varied as the fourth power of  $Z$ , and Richtmyer and Warburton<sup>2</sup> confirmed this experimentally, although some workers have found other exponents for  $Z$  ranging from 2.95 to 4.3. To incorporate this factor in equations (5-9) and (5-10), they should be appropriately modified. These equations give the value of the mass absorption coefficient  $\mu$  in terms of the true absorption  $\tau$ , or  $C\lambda^3$ , and the mass scattering coefficient  $\sigma$ . On the other hand, workers in this field commonly give their results in terms of "atomic absorption coefficients"  $\mu_a$  and atomic scattering coefficients  $\sigma_a$  because the constants  $C$  are supposedly the same for all elements when so expressed. If the absorption or scattering per gram is  $\mu$  or  $\sigma$ , the absorption or scattering per atom will be given by dividing these quantities by the number of atoms per gram, or  $N_0/A$  where  $N_0$  is Avogadro's number and  $A$  is the atomic weight of the absorber. Thus, if

$$\mu_a = \frac{\mu A}{N_0} \quad C_a = \frac{CA}{N_0} \quad \sigma_a = \frac{\sigma A}{N_0} \quad (5-13)$$

equations (5-9) and (5-10) become

$$\mu_a = C_{a1}Z^4\lambda^3 + \sigma_a(Z, \lambda) \quad (5-14)$$

and

$$\mu_a = C_{a2}Z^4\lambda^3 + \sigma_a(Z, \lambda) \quad (5-15)$$

Equation (5-14) applies to the case  $\lambda < \lambda_K$  and (5-15) to the case

$$\lambda_K < \lambda < \lambda_L.$$

Here  $C_{a1}$  has a value around  $2\frac{1}{2} \times 10^{-26}$  and  $C_{a2}$  a value around  $10^{-27}$  when  $\lambda$  is expressed in angstrom units.<sup>3</sup> The symbol  $\sigma_a(Z, \lambda)$  indicates that  $\sigma_a$  is a function of  $Z$  and  $\lambda$ , as already discussed.

In addition to true absorption and scattering, there is a third process by which x-rays dissipate their energy in traversing matter, provided that the rays are generated at potentials of about 1 million volts or more. Such extremely hard x-rays and gamma rays produce a phenomenon within an absorber known as "pair formation." This process was discovered by Anderson and Neddermeyer<sup>4</sup> shortly after Anderson discovered<sup>5</sup> the existence of positive electrons, which he called "positrons."

<sup>1</sup> W. H. Bragg and S. E. Pierce, *Phil. Mag.*, **28**, 626 (1914).

<sup>2</sup> F. K. Richtmyer and F. W. Warburton, *Phys. Rev.*, **22**, 539 (1923).

<sup>3</sup> For the case  $\lambda < \lambda_K$ , see recent articles by W. Wrede, *Ann. J. Physik*, **36**, 681 (1939), and J. A. Victoreen, *J. Applied Phys.*, **14**, 95 (1943).

<sup>4</sup> C. D. Anderson and S. H. Neddermeyer, *Phys. Rev.*, **43**, 1034 (1933).

<sup>5</sup> C. D. Anderson, *Science*, **76**, 238 (1932); *Phys. Rev.*, **43**, 491 (1933).

Positrons were discovered when cloud-chamber photographs revealed that they are occasionally created by cosmic rays passing through matter. Anderson and Neddermeyer then found that positrons may also be created by gamma rays or x-rays generated at potentials above 1 million volts, as they pass through matter.

It is now believed that each positron thus created appears simultaneously with an ordinary negative electron. The present view is that, in order to create such a "pair," a very energetic photon must interact with the extremely strong electrostatic field present in the immediate vicinity of an atomic nucleus, the photon vanishing under these circumstances and its energy  $h\nu$  appearing in the form of an electron of mass  $m$  and a positron of equal mass  $m$ , both of them usually having a high velocity (kinetic energy). According to Einstein's equation (4-15), these two electrons (positive and negative) having a rest mass of  $m_0$  each or  $2m_0$  combined might be created from energy  $E$  equal to  $2m_0c^2$ ; therefore, a photon would have to have at least this much energy to create them. Upon setting

$$h\nu = 2m_0c^2 = Ve \quad (5-16)$$

and solving for  $V$ , the result is  $1.02 \times 10^6$  volts, and the experimental observation that this process occurs only for rays generated above 1 million volts is thus checked. When the energy is  $1\frac{1}{2}$  million electron volts, for example, the surplus  $\frac{1}{2}$  million electron volts appears as kinetic energy of the positron and electron.

The electron dissipates its energy by ionizing atoms in its path in the usual way. The positron does likewise, but it is such a short-lived particle that it has only about a 90 per cent chance of continuing to exist until it stops moving. It vanishes or is "annihilated" either while it is still tearing through the absorber on its rapid flight or within a millionth of a second after it stops at the end of this flight. After it stops (that is, slows down to mere thermal velocity), it will combine with any electron close to it, and the two will vanish simultaneously, generating two new photons with energy  $h\nu_1 + h\nu_2$  equal to the  $2mc^2$  energy to which the annihilated particles were equivalent. If the positron is annihilated in flight, sometimes only one photon is generated, but even in flight the generation of two photons is more common.

The pair-formation process does not dissipate enough x-ray energy to become relatively important in the measurement of x-ray absorption until extremely high voltages are attained. At 5 million volts it becomes as important as the scattering in lead; in fact, it increases so rapidly that x-rays having energy greater than 5 million volts are actually inferior to 3-million-volt x-rays in their power to penetrate lead.<sup>1</sup> In

<sup>1</sup> This fact, predicted by theory, was experimentally verified by G. D. Adams and



carbon this does not occur until the potential reaches 25 or 30 million volts.

On the other hand, scattering dissipates more x-ray energy than is absorbed (by true photoelectric means) in lead only when the potential exceeds 500 kv. In carbon, scattering dissipates more energy than that which is truly absorbed when the tube voltage at which the primaries are generated exceeds about 25 kv.

Thus the relative importance of the three phenomena (true absorption, scattering, and pair formation) in dissipating the energy of an x-ray beam passing through an absorber depends upon the atomic number of the absorbing material and the hardness of the primary rays.

In closing this general discussion, it should be emphasized that the secondary x-ray radiation generated within the absorber itself is very feeble compared with the primary, for three reasons. (1) Only a small part of the energy of the absorbed primaries is reradiated in the form of x-rays. (2) The secondaries spread in all directions, so that their intensity in any one direction is small. (3) Those secondaries generated deep within the absorber will themselves be absorbed.

**2. The Auger Effect.** In 1925, P. Auger<sup>1</sup> was experimenting with hard x-rays passing through a 95 per cent hydrogen-5 per cent argon mixture in a Wilson cloud chamber. He observed short cloud tracks originating at the same points as many of the long tracks due to the photoelectrons. This led him to conclude that the  $K_{\alpha}$  photon generated when an L electron drops into a K-shell vacancy frequently acts photoelectrically on another (L or M, probably) electron in the same atom, ejecting it. These electrons ejected with comparatively low energy are called "Auger electrons," and the phenomenon is called the "Auger effect." The Auger electrons cause the short tracks observed by Auger in his cloud chamber. Elements of low atomic number display the Auger effect much more prominently than those of high atomic number.

The Auger electrons and the photoelectrons dissipate their energy by ionizing several hundred atoms that they encounter before coming to rest. These ions are formed by merely knocking the outermost electrons from the atoms. Photoelectrons ejected from atoms on or near the surface of the absorbing plate often escape from the metal. Such "beta particles" constitute a secondary radiation distinct from the secondary x-ray radiation.<sup>2</sup>

---

R. K. Clark, using Kerst's 20-million-volt betatron (see p. 150); see A. R. Wildhagen, *Sci. American*, **168**, 207 (1943).

<sup>1</sup> P. Auger, *Compt. rend.*, **180**, 65 (1925); *J. phys.*, **6**, 205 (1925).

<sup>2</sup> For information about the energy spectrum of such secondaries, see H. Robinson, *Proc. Roy. Soc. (London) A*, **104**, 55 (1923); *Phil. Mag.*, **50**, 241 (1925).

**3. The Structure of the Absorption Edges.** In Sec. 1, the absorption edges were represented as in Fig. 5-3, indicating that they were sharp mathematical discontinuities in the absorption curve. Actually, if the absorption is measured in the immediate vicinity of an edge, a spectrometer with high resolving power being used, the edge is found to be not mathematically sharp. Furthermore, the absorption curve immediately on the short-wave-length side of the edge exhibits a few maxima and minima, as in Fig. 5-6 obtained from a copper absorber by Beeman and Friedman,<sup>1</sup> and this irregularity is called the “structure” associated with the absorption edge.

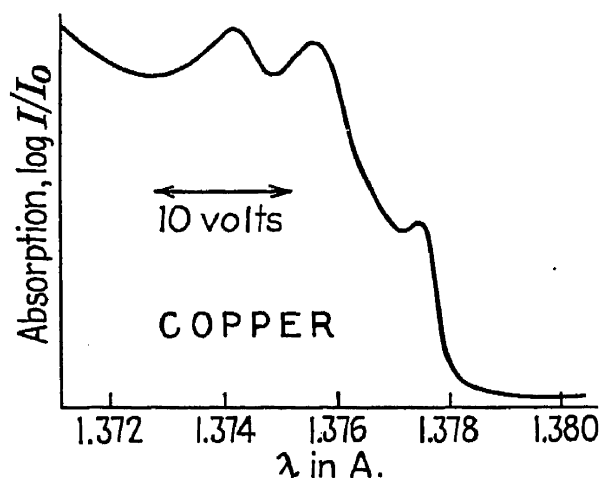


FIG. 5-6.—The structure of the K edge of copper. (Beeman and Friedman; courtesy of *Physical Review*.)

These peaks occur at a wave length corresponding to a photon energy just slightly greater than that required to remove an electron from the K shell. Hence, when such a photon is absorbed, the ejected K electron does not come tearing out of the atom with some 20 or 30 kv. of energy but barely is able to emerge, and that is all. In such a case, the photoelectron is comparable to the ordinary “free” electrons or “conduction” electrons in the metal. Just as in the case of the free

electrons, then, there are a few definite energy bands into which it must fit itself. If the x-ray photon that encounters the atom has exactly enough energy to push a K electron out with just the right energy to fit into these allowed bands, it is more likely to be absorbed than if it has a little more or a little less energy so that its absorption would release the K electron with an energy not fitting into these allowed bands. This is the explanation of the small peaks seen in Fig. 5-6.

The idea that the free electrons in a metal must have energies which permit them to fit into certain allowed energy-level bands has evolved as a result of the theoretical work of several investigators. First, Pauli<sup>2</sup> accounted for some of the paramagnetic properties of the alkalis by a quantum-mechanical treatment based on the assumption that the free electrons move unrestrained through the metal and obey the Fermi statistics. Then Sommerfeld<sup>3</sup> developed the theory of metals more completely on the basis of the Fermi statistics and succeeded in accounting for many of the thermal and electrical properties of metals. Later,

<sup>1</sup> W. W. Beeman and H. Friedman, *Phys. Rev.*, **56**, 392 (1939).

<sup>2</sup> W. Pauli, *Z. Physik*, **41**, 81 (1927).

<sup>3</sup> A. Sommerfeld, W. V. Houston, and C. Eckart, *Z. Physik*, **47**, 1, 33, 38, 43 (1928).

Bloch<sup>1</sup> made the assumption that the free electrons do not move simply as free particles within the metal but are constrained in a force field which has the same periodicity as the atomic lattice structure of the metal crystals (see page 536). He showed that this led to the conclusion, from quantum-mechanical calculations, that the free electrons must be limited in allowed energies to certain bands. These band energies have been specifically calculated in the case of some of the common metals,<sup>2</sup> and Beeman and Friedman<sup>3</sup> have shown that the observed structure of the K edge of several metals may be explained satisfactorily on this basis.

**4. Modified and Unmodified Scattering and the Compton Effect.** Sections 2 and 3 have dealt with certain details of the true absorption of x-rays. A few details remain to be considered regarding the scattering of x-rays, which is a phenomenon closely associated with absorption, so far as its experimental manifestations are concerned, as mentioned in Sec. 1.

The first thorough investigation and measurement of the wave lengths of x-rays scattered from light elements, using an x-ray spectrometer, was made by A. H. Compton<sup>4</sup> in 1922–1923. Light elements were investigated because earlier workers<sup>5</sup> had found not only that secondary x-rays were radiated from the heavy elements, as explained on page 76, but that some unexplained radiation of considerable hardness, not very inferior to that of the primaries, was also radiated from light elements traversed by an intense primary beam. Fairly hard secondaries from the heavy elements were explained by the theory that the primaries merely excited the characteristic K radiation of the heavy material, as outlined in Sec. 1. However, the characteristic K radiation from an element like carbon is so soft that it would be almost entirely absorbed by even 1 in. of air. Therefore, the above-mentioned fairly hard rays from the light elements were not understood in 1922. The unmodified scattered rays were accounted for by the classical theories of scattering. These unexplained rays were definitely softer than the primaries, and yet they were far too hard to be true characteristic secondaries. It is now known that these rays are scattered rays of a different type called “modified” or “incoherently scattered rays” resulting from a process known as “Compton scattering.”

<sup>1</sup> F. Bloch, *Z. Physik*, **52**, 555 (1928).

<sup>2</sup> R. de L. Kronig and W. G. Penney, *Proc. Roy. Soc. (London) A*, **130**, 499 (1931); H. Krutter, *Phys. Rev.*, **48**, 664 (1935); J. C. Slater, *Phys. Rev.*, **49**, 537 (1936).

<sup>3</sup> W. W. Beeman and H. Friedman, *Phys. Rev.*, **56**, 392 (1939).

<sup>4</sup> A. H. Compton, *Phys. Rev.*, **21**, 715, **22**, 409 (1923).

<sup>5</sup> See, for example, C. A. Sadler and P. Mesham, *Phil. Mag.*, **24**, 138 (1912); J. Laub, *Ann. Physik*, **46**, 785 (1915); J. A. Gray, *J. Franklin Inst.*, **190**, 633 (1920); A. H. Compton, *Phys. Rev.*, **18**, 96 (1921); J. A. Crowther, *Phil. Mag.*, **42**, 719 (1921).

Compton observed that more than half the scattered rays, in the case of carbon, were of the modified type, the rest having a wave length identical with that of the primaries. His most significant discovery, however, was that the wave length  $\lambda$  of the modified rays increases (gets farther away from the wave length  $\lambda_0$  of the primaries) as the angle

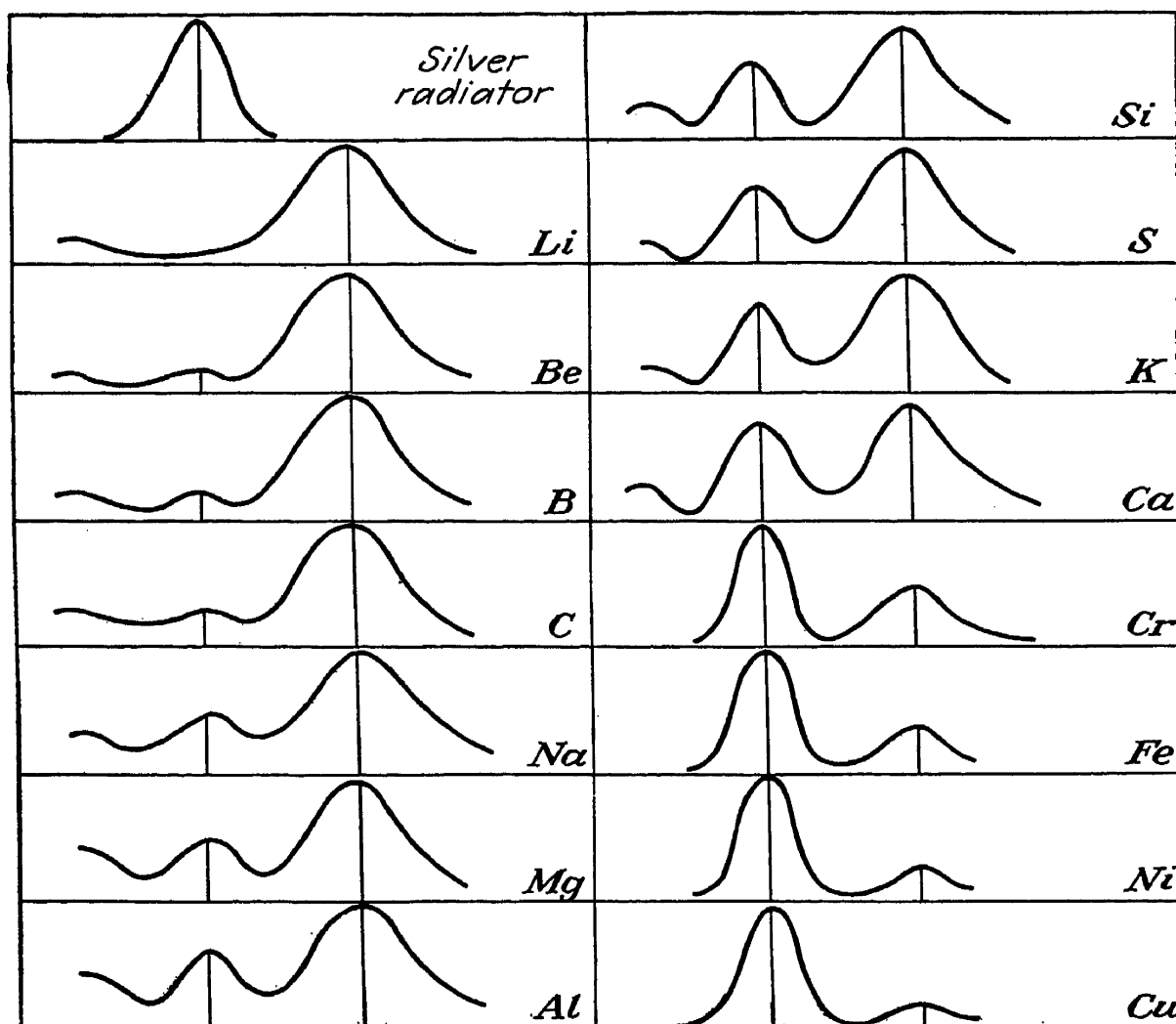


FIG. 5-7.—Showing relative intensities of coherent and incoherent scattering from various materials for silver K radiation. (After Woo, Compton, and Allison; courtesy of D. Van Nostrand Company, Inc.)

$\phi$  between the primary beam and the scattered beam increases, the relationship being

$$\lambda - \lambda_0 = \frac{h}{mc} (1 - \cos \phi) = 0.02427(1 - \cos \phi) \quad (5-17)$$

the latter expression holding when  $\lambda - \lambda_0$  is in angstrom units, the former when it is in centimeters.  $h$  is Planck's constant,  $m$  the mass of an electron, and  $c$  the velocity of light. This phenomenon is known as the "Compton effect," and its significance lies in the fact that the wave length of the modified rays increases with angle in a way which can be explained

most simply by the quantum theory.<sup>1</sup> Therefore its discovery was important evidence in favor of the quantum theory and the quantum nature of x-rays, as well as a basis for the explanation of incoherent x-ray scattering.

Figure 5-7 shows a series of curves obtained by Woo<sup>2</sup> at a scattering angle ( $\phi$ ) of  $120^\circ$ . Note the increasing prominence of Compton scattering, compared with the coherent scattering, as the atomic number decreases. The relative prominence of the modified and unmodified scattering also depends upon the wave length of the primary radiation, as will be explained on page 88. Figure 5-8 (by Compton)<sup>3</sup> shows the change of wave length of the modified line in the spectrum of the scattered rays as compared with the unmodified line for increasing scattering angles when carbon (graphite) is the scattering element.

Equation (5-17) for the wave length  $\lambda$  of the incoherently scattered rays was first derived by Compton. The derivation resembles the calculations for the collision of two smooth elastic balls of different mass. According to this analogy, one ball is a primary x-ray photon, which collides with the other stationary ball, which is an electron in the scattering material.

To return to Einstein's equation (4-15) relating mass to energy, it may be written

$$m = \frac{E}{c^2} \quad (5-18)$$

If  $E$  is regarded as representing the energy  $h\nu$  of a photon, then (5-18) gives its mass  $m$ . Its velocity in free space is  $c$ , of course. Hence, its momentum  $p$  (= mass  $\times$  velocity) is

$$p = \frac{E}{c^2} c = \frac{E}{c} = \frac{h\nu}{c} = \frac{h}{\lambda} \quad (5-19)$$

On page 56 [equations (4-16) to (4-21)], it was pointed out that the

<sup>1</sup> For the difficult classical treatment, see C. V. Raman, *Indian J. Phys.*, **3**, 357 (1928).

<sup>2</sup> See also Y. H. Woo, *Proc. Natl. Acad. Sci.*, **11**, 123 (1925).

<sup>3</sup> A. H. Compton, *Phys. Rev.*, **22**, 409 (1923).

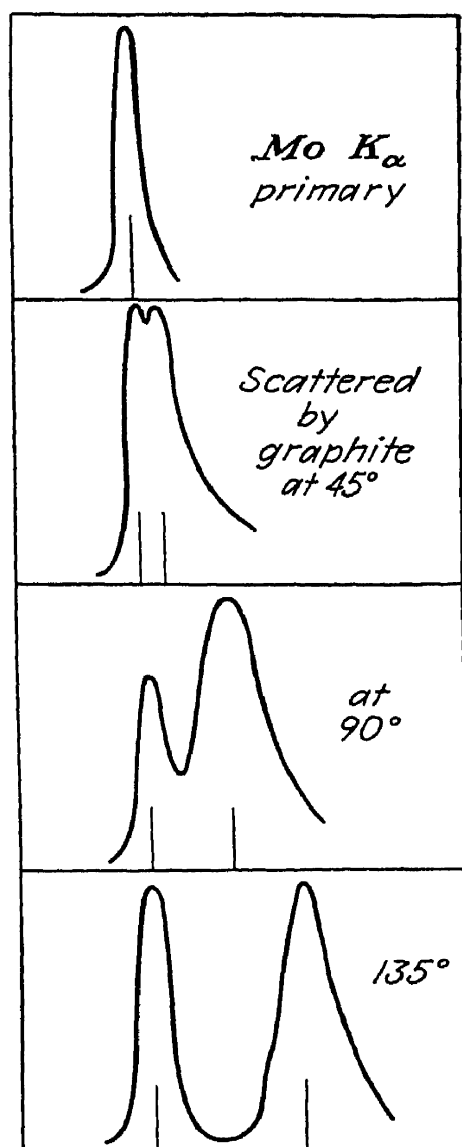


FIG. 5-8.—Coherent and incoherent scattering of molybdenum K radiation from graphite at various angles. (Compton; courtesy of *Physical Review*.)

ordinary expression  $\frac{1}{2}mv^2$  for kinetic energy is only an approximation for the true expression  $mc^2 - m_0c^2$  where  $m = \frac{m_0}{\sqrt{1 - \frac{v^2}{c^2}}}$  [equation (4-14)].

When a particle having a rest mass  $m_0$  is moving with a velocity  $v$  comparable with  $c$ , its kinetic energy is  $c^2(m - m_0)$  and its momentum is  $mv$  where  $m$  is given by (4-14).

Referring now to Fig. 5-9, a primary x-ray photon enters from the left with energy  $h\nu_0$  and momentum  $h/\lambda_0$  where  $\nu_0$  and  $\lambda_0$  are the frequency

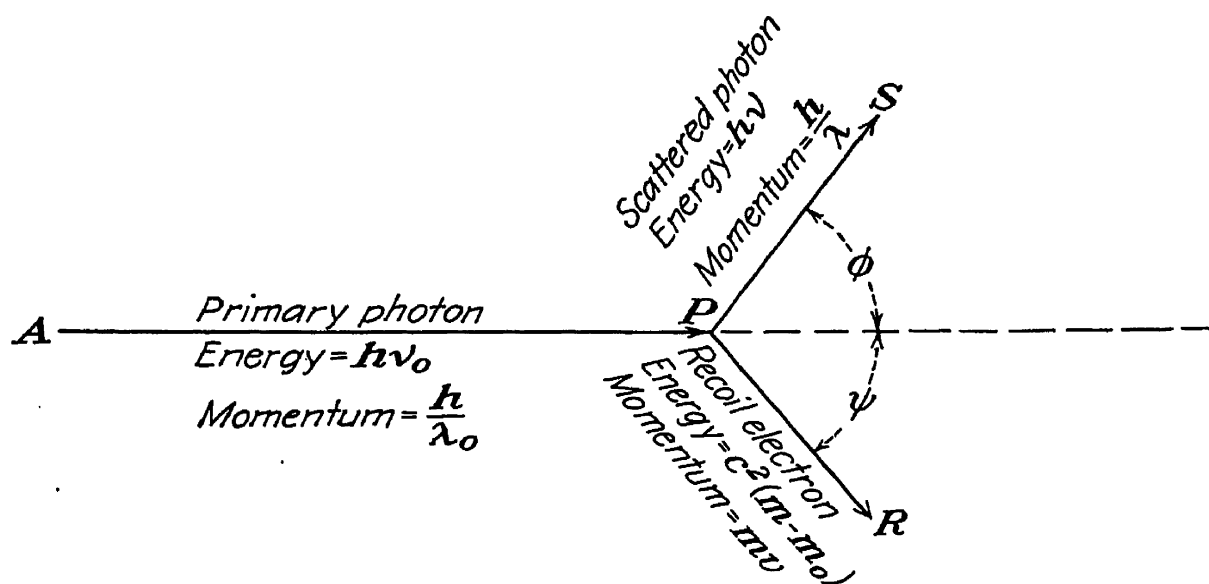


FIG. 5-9.—Illustrating the theory of Compton scattering.

and wave length of the primary x-ray beam. It strikes an electron at rest<sup>1</sup> at  $P$  and bounces off in the direction  $PS$ , making an angle  $\phi$  with the direction of the primary x-ray beam. This impact causes the electron to recoil in the direction  $PR$ , making an angle  $\psi$  with the direction of the primary x-ray beam. If the frequency and wave length of the scattered x-rays in the direction  $PS$  are  $\nu$  and  $\lambda$ , then the energy and momentum of the photon after the collision are  $h\nu$  and  $h/\lambda$ . The electron, recoiling with velocity  $v$ , has energy  $c^2(m - m_0)$  and momentum  $mv$ .

According to the principle of conservation of energy one has

$$h\nu_0 = h\nu + c^2(m - m_0) \quad (5-20)$$

<sup>1</sup> Although the thermal velocities of the electrons in matter at ordinary temperatures greatly exceed that of a rifle bullet, they are still so low as to be negligible compared with the velocities involved in this calculation. The theory has been worked out for the case in which the electronic motion is not neglected by Jauncey, DuMond, and others [see, for example, J. W. M. DuMond, *Rev. Modern Phys.*, **5**, 1 (1933)]. When this is considered, it leads to the conclusion that the spectrum of scattered monochromatic radiation in any given direction is not a monochromatic, sharp line but a broad, "fuzzy" line whose width increases with  $\phi$ , as observed. The agreement between this theory and experiment reveals important information regarding the motion of the electrons in the atoms as suggested by the Bohr theory.

The principle of conservation of momentum indicates that in the horizontal direction in Fig. 5-9

$$\frac{h}{\lambda_0} = \frac{h}{\lambda} \cos \phi + mv \cos \psi \quad (5-21)$$

and in the vertical direction

$$0 = \frac{h}{\lambda} \sin \phi + mv \sin \psi \quad (5-22)$$

These three equations, containing the four unknowns  $\lambda$ ,  $v$ ,  $\phi$ , and  $\psi$ , enable one to eliminate  $v$  and  $\psi$  and solve for  $\lambda$  in terms of the scattering angle  $\phi$ , as is desired. This may be done by introducing the new variables

$$x = \frac{h}{mc\lambda} = \frac{h\nu}{mc^2} \quad \text{and} \quad y = \frac{h}{mc\lambda_0} = \frac{h\nu_0}{mc^2} \quad (5-23)$$

and rearranging the equations. Equations (5-20) to (5-22) then become

$$y - x = 1 - \frac{m_0}{m} \quad (5-24)$$

$$y - x \cos \phi = \frac{v}{c} \cos \psi \quad (5-25)$$

$$\text{and} \quad x \sin \phi = -\frac{v}{c} \sin \psi \quad (5-26)$$

Squaring these,

$$x^2 + y^2 - 2xy = 1 + \left(\frac{m_0}{m}\right)^2 - 2\frac{m_0}{m} \quad (5-27)$$

$$x^2 \cos^2 \phi + y^2 - 2xy \cos \phi = \frac{v^2}{c^2} \cos^2 \psi \quad (5-28)$$

$$x^2 \sin^2 \phi = \frac{v^2}{c^2} \sin^2 \psi \quad (5-29)$$

Adding (5-28) and (5-29),

$$x^2 + y^2 - 2xy \cos \phi = \frac{v^2}{c^2} \quad (5-30)$$

Subtracting (5-27) from this,

$$2xy(1 - \cos \phi) = 2\frac{m_0}{m} - \left(\frac{m_0}{m}\right)^2 - \left(1 - \frac{v^2}{c^2}\right) \quad (5-31)$$

From (4-14),

$$1 - \frac{v^2}{c^2} = \left(\frac{m_0}{m}\right)^2 \quad (5-32)$$

so that (5-31) becomes

$$2xy(1 - \cos \phi) = 2\frac{m_0}{m} \left(1 - \frac{m_0}{m}\right) \quad (5-33)$$

or, from (5-24),

$$xy(1 - \cos \phi) = \frac{m_0}{m} (y - x) \quad (5-34)$$

$$\text{or} \quad 1 - \cos \phi = \frac{m_0}{m} \left( \frac{1}{x} - \frac{1}{y} \right) = \frac{m_0 c}{h} (\lambda - \lambda_0) \quad (5-35)$$

yielding

$$\lambda - \lambda_0 = \frac{h}{m_0 c} (1 - \cos \phi) \quad (5-17)$$

Schrödinger<sup>1</sup> has derived this same equation by applying modern wave mechanics. Note that it indicates that x-rays scattered incoherently at right angles to the primary beam ( $\phi = 90^\circ$ ) will always have a wave length 0.02427 Å. greater than that of the primaries, regardless of the nature of the scattering material or the hardness of the primaries.

The accurate agreement of equation (5-17) with the observed wave lengths of the x-rays scattered at various angles  $\phi$  indicates that the scattering of x-rays is a process in which the photons may be imagined as literally bouncing off of the electrons in the scattering material. Absorption, on the other hand, is a process in which the photon encounters an electron (preferably one of the inner orbital electrons) and instantly vanishes, the electron acquiring its energy  $h\nu$ . Experiments indicate<sup>2</sup> that the photon has no preference among the electrons so far as scattering is concerned; it is just as likely to bounce off a K electron as a valence electron or a free electron, except for the fact that one type of electron may be more numerous than the other in the scattering material.

This theory accounts for the difference between coherent and incoherent scattering, as follows: If the photon bounces off a firmly bound electron, like the inner electrons of a heavy atom like lead, the recoil of the electron is not vigorous enough to shake it loose from the atom and it is unable to acquire kinetic energy from the photon. Hence the photon emerges with the same energy  $h\nu$  (and hence the same wave length) as it had originally, and the scattering is coherent. If the x-ray photon bounces off a free electron or a valence electron or even a K electron of a light element like lithium or magnesium, the electron, being very loosely bound, recoils, as suggested in the derivation of formula (5-17), and the scattering is incoherent. This accounts for the fact that gamma rays (which have such high energy photons that they will shake loose even a firmly bound electron when they bounce from it) are scattered almost entirely incoherently,<sup>3</sup> whereas ordinary light (which has such low energy photons that they cannot dislodge even a valence electron) is scattered coherently.

<sup>1</sup> E. Schrödinger, *Ann. Physik*, **82**, 257 (1927).

<sup>2</sup> F. Kirchner, *Ann. Physik.*, **83**, 969 (1927).

<sup>3</sup> A. H. Compton, *Phil. Mag.*, **41**, 760 (1921).



The intensity of the x-rays scattered from free electrons (hence for modified scattering) is given by an equation derived by Klein and Nishina,<sup>1</sup> using modern quantum mechanics. It is therefore commonly called the "Klein-Nishina formula." In the case of very hard x-rays and gamma rays, the scattering is practically all incoherent, and the formula is therefore widely used for calculating the scattering of such rays. It is

$$\sigma = \frac{2\pi n e^4}{m^2 c^4 \rho} \left\{ \frac{1+Q}{Q^2} \left[ \frac{2(1+Q)}{1+2Q} - \frac{1}{Q} \log_e (1+2Q) \right] + \frac{1}{2Q} \log_e (1+2Q) - \frac{1+3Q}{(1+2Q)^2} \right\} \quad (5-36)$$

This equation corresponds to Thomson's classical equation (5-11) and yields approximately the same value of  $\sigma$  when  $Q$  is small.

Equation (5-11) was obtained by integrating the relation (5-12). In a similar way, (5-36) is obtained by integrating the relation

$$\frac{I_a}{I_0} = \frac{Z e^4}{2 r^2 m^2 c^4} \frac{1 + \cos^2 \phi}{(1 + Q \text{ vers } \phi)^3} \left[ 1 + \frac{Q^2 \text{ vers}^2 \phi}{(1 + \cos^2 \phi)(1 + Q \text{ vers } \phi)} \right] \quad (5-37)$$

which is the Klein-Nishina directional formula corresponding to Thomson's classical relation (5-12). In these equations,  $I_0$  is the intensity of the primary beam,  $I_a$  the beam scattered incoherently per atom at an angle  $\phi$  with the primary beam, and  $Q = h\nu/mc^2$  where  $\nu$  is the frequency of the primary ray and  $m$  the mass of an electron at rest. The expression  $\text{vers } \phi$  means  $1 - \cos \phi$ .  $Z$ ,  $n$ , and  $\rho$  have the same meanings as in (5-11) and (5-12).

Equation (5-36) reduces to a simpler relation when  $Q$  is large, corresponding to very hard rays ( $\frac{1}{2}$  million volts or more). For this case,

$$\sigma = \frac{\pi n e^4}{m^2 c^4 \rho} \frac{1}{Q} \left( \log_e 2Q + \frac{1}{2} \right) \quad (5-38)$$

and this relation indicates that, for very hard rays,  $\sigma$  is nearly proportional to the wave length. All these Klein-Nishina relationships are in close agreement with experiment.

From equations (5-20) to (5-22) the following equation for the direction of recoil of the electrons involved in inelastic scattering may be derived,

$$\cot \psi = -(1 + \delta) \tan \frac{1}{2} \phi \quad (5-39)$$

and the kinetic energy of such "recoil electrons" may be shown to be

$$E = \frac{2}{\lambda_0} \frac{hc \delta \cos^2 \psi}{(1 + \delta)^2 - \delta^2 \cos^2 \psi} \quad (5-40)$$

<sup>1</sup> O. Klein and Y. Nishina, *Z. Physik*, **52**, 853 (1929).

where, in both equations,  $\psi$  and  $\phi$  are the angles indicated in Fig. 5-9 and  $\delta = h/mc\lambda_0$ ,  $\lambda_0$  being the wave length of the primary rays and  $m$  the rest mass of an electron. Consideration of Fig. 5-9 will make it clear that  $\psi$  must be less than  $90^\circ$ , so that the recoil electrons must have a forward direction. In all such equations, standard units are used, so that one must remember to convert angstrom units to centimeters, etc., to get the answer in ergs.

The recoil electrons from Compton scattering may be observed if the scattering medium is a gas in a cloud chamber. Figure 5-10 is a photograph obtained<sup>1</sup> by C. T. R. Wilson, inventor of the cloud chamber. The chamber contained air at a pressure of 50 cm. of mercury, after the expansion, traversed by a 3-mm. beam of hard x-rays entering at the right in the figure. The recoil electron tracks may be distinguished from the photoelectron tracks, for the former are much shorter. They may be distinguished from Auger electron tracks, for these, although short, always originate at the same point as a long photoelectron track. The recoil tracks frequently look like a comma, with the tail pointing toward the x-ray tube; they are sometimes called "fish tracks," a name suggested by Wilson. It is seen that the long photoelectron tracks usually end in a white dot due to the greatly increased ionizing power of the photoelectron when it slows down to a comparatively slow speed just before stopping. The recoil electrons do not have much more speed than this to start with, and so they make only a short track, which is the tail of the comma, before ending in a ball of intense ionization, which is the head of the comma.

**5. Polarization Effects.** It has already been mentioned in Chap. 3, (page 42) that the continuous radiation from an x-ray tube is partly polarized. Barkla<sup>2</sup> first demonstrated experimentally in 1906 that x-rays scattered at right angles to the primary beam by a light material like carbon are highly polarized with their electric vector (x-rays being thought of as waves, for a change) perpendicular to the plane determined by the primary and scattered ray. More modern experiments by Compton and Hagenow<sup>3</sup> indicate that when  $\frac{1}{4}$  A. rays are scattered by infinitesimally thin sheets of light material like paper, aluminum, or sulfur, the polarization is 100 per cent complete.

Barkla's experiments, on the other hand, indicated that the secondary rays from a heavy absorber like a thick iron plate are not polarized at all. In the light of modern knowledge, it is known that such rays are not scattered rays but fluorescent characteristic iron rays generated in the

<sup>1</sup> C. T. R. Wilson, *Proc. Roy. Soc. (London)*, **104**, 1 (1923).

<sup>2</sup> C. G. Barkla, *Proc. Roy. Soc. (London) A*, **77**, 247 (1906).

<sup>3</sup> A. H. Compton and C. F. Hagenow, *J. Optical Soc. Am. and Rev. Sci. Instruments*, **8**, 487 (1924).

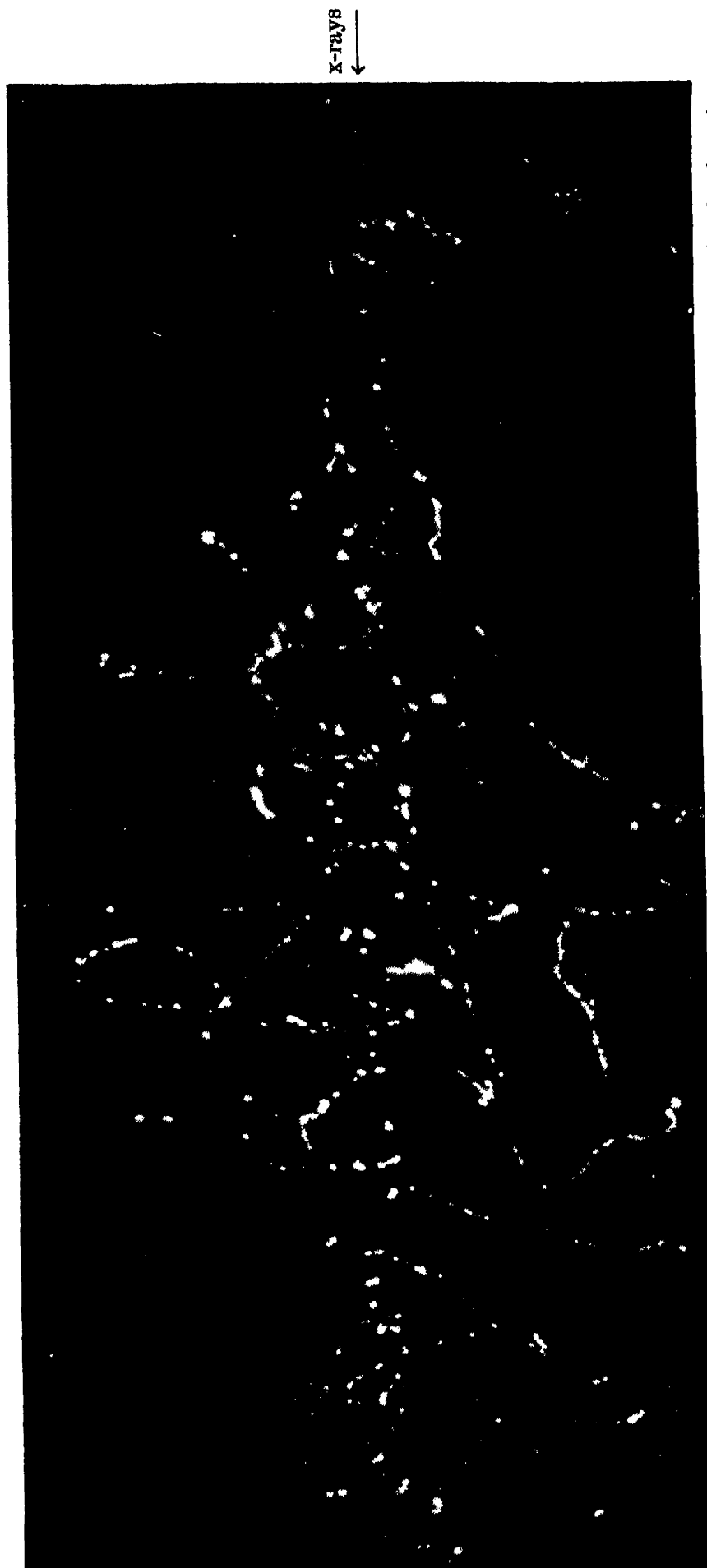


FIG. 5-10.—Cloud-chamber photograph by C. T. R. Wilson, showing (a) the long ion tracks made by the photoelectrons, (b) the short ion tracks made by the Auger electrons, which always originate at the starting point of one of the long tracks, and (c) the short isolated comma-shaped tracks made by the recoil electrons. (*Courtesy of The Royal Society.*)

iron, which indeed Barkla assumed, in 1906. This indicates that such rays are entirely unpolarized, although it has been found<sup>1</sup> that if the primary rays are themselves polarized they tend to eject the photoelectrons in the absorber in a direction lying in or near the plane of polarization of the primaries. Even in this case, the fluorescent secondaries are not found to be, or expected to be, polarized. It has also been found<sup>2</sup> that polarized primary rays scattered in a gas tend to produce recoil electrons which have a direction lying in or near to a plane containing the ray but perpendicular to the plane of polarization.

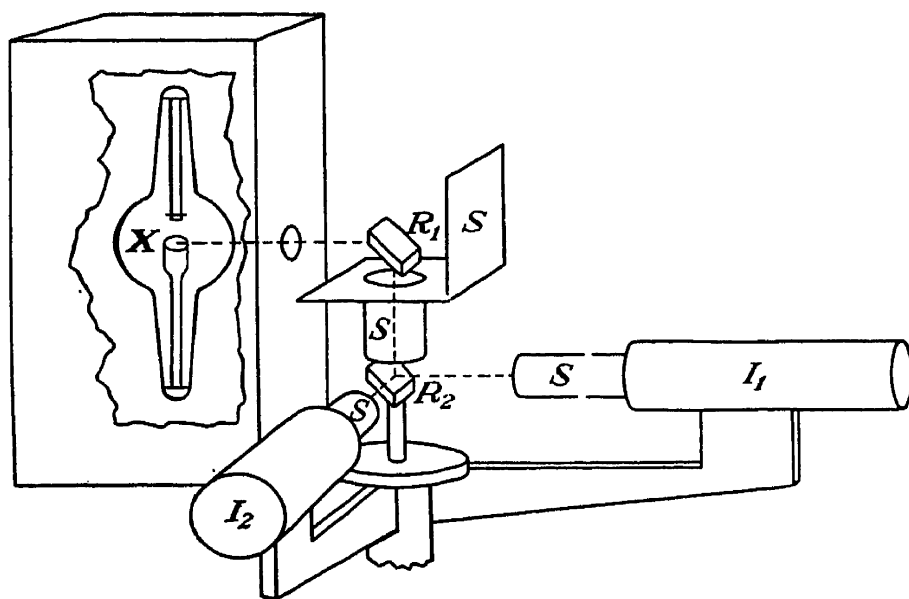


FIG. 5-11.—Apparatus for measurement of the degree of polarization of scattered x-rays. (Compton and Hagenow; courtesy of American Institute of Physics.)

Figure 5-11 shows the experimental arrangement used by Compton and Hagenow, who found that the ionization produced in chamber  $I_2$  was small compared with that in  $I_1$ . This is explained by classical scattering theory by pointing out that the primary beam  $XR_1$  consists of electromagnetic vibrations in a plane perpendicular to  $XR_1$  which set the electrons in  $R_1$  into forced vibrations in this plane. Only those electrons which happen to vibrate horizontally (parallel to  $R_2I_2$ ) in  $R_1$  are able to radiate a new wave in the direction  $R_1R_2$ . Hence the scattered secondary ray  $R_1R_2$  will be polarized in the plane  $R_1R_2I_2$ . It in turn will set up vibrations of the electrons in  $R_2$  in the direction  $R_2I_2$ . These will be unable to radiate a scattered tertiary ray in this direction ( $R_2I_2$ ) because electromagnetic vibrations are transverse, but they will radiate a tertiary ray in the direction  $R_2I_1$ . The parts marked  $S$  in the figure are x-ray screens, probably made of sheet lead.

It is not clear how polarization is to be explained when the rays are regarded as consisting of photons. One may imagine the photons as

<sup>1</sup> See, for example, P. Kirkpatrick, *Phys. Rev.*, **38**, 1938 (1931).

<sup>2</sup> F. Kirchner, *Phys. Z.*, **27**, 385, 799 (1926); *Ann. Physik*, **81**, 113 (1926).

elastic disks, the plane of the disk always containing its line of motion. Then, in Fig. 5-11, such disks bouncing off spherical electrons in  $R_1$  would bounce in the direction  $R_1R_2$  only if they were horizontal beforehand; the others would bounce in other directions. After bouncing from  $R_1$ , the photon disks would lie in the plane  $R_1R_2I_2$  as they traveled along  $R_1R_2$ . Upon reaching  $R_2$ , they would be unable to bounce in the direction  $R_2I_2$  but would bounce in the direction  $R_2I_1$ , at the same time producing recoil electrons in  $R_2$ . Most of these would obviously have a motion in the plane  $R_1R_2I_1$ , as observed by Kirchner. On the other hand, such a disk type of photon might act photoelectrically upon an electron that it encountered, imparting its  $h\nu$  energy to the electron in such a way that the electron would move off in a line lying in or near the plane of the disk, as observed by Kirkpatrick. Although the structure of photons is a matter of mere speculation at present, there is an advantage in regarding them as disks in the present case because it helps one to fix in mind the relationships between the directions of the various scattered rays and the corresponding planes of polarization and also the predominating directions of the recoil and photoelectrons. Modern quantum mechanics is able to arrive at equations which indicate that x-rays scattered coherently from bound electrons should be polarized just as predicted by classical theory.

To summarize, scattered x-rays, both coherent and incoherent, are polarized; fluorescent secondaries are not.

**6. Dual Nature of Both Matter and Radiation.** For a discussion of the manner in which modern quantum mechanics harmonizes the divergent wave-versus-particle aspects of matter and radiation into a unified theory, the reader is referred to articles by Darrow<sup>1</sup> and by Margenau and Wightman.

It may be well to summarize here the four fundamental equations that link the particle aspect to the wave aspect, regardless of whether one is discussing electrons (a constituent of matter) or photons (a constituent of radiation, which is a form of energy). They are

$$\left. \begin{aligned} E &= h\nu \\ p &= \frac{h}{\lambda} \\ E &= mc^2 \\ p &= mv \end{aligned} \right\} \quad (5-41)$$

$c$  seems to be the fundamental item with photons; they always have velocity  $c$  in empty space, but their mass varies with their energy,

<sup>1</sup> K. K. Darrow, *Rev. Modern Phys.*, **6**, 23 (1934); H. Margenau and A. Wightman, *Am. J. Phys.*, **12**, 119 (1944).

frequency, and wave length. Both the photon and its associated electromagnetic wave move with the same velocity  $c$ . The photon is uncharged.

$e$  and  $m_0$  seem to be the fundamental items with electrons; they always have mass  $m_0$  at rest, but their velocity varies with their energy, frequency, and wave length. The phase wave associated with the electron has a velocity  $c^2/v$  inversely proportional to the electron's velocity  $v$ . The electron has a charge  $e$ .

### QUESTIONS AND PROBLEMS

1. Explain the existence of absorption edges. Why are there three L edges but only one K edge? What is meant by pair formation? For pair formation to occur, the tube generating the x-rays must be operated at at least what voltage? Why?

2. What is the Auger effect? Does it increase or decrease the fluorescent secondary x-radiation? Is it more pronounced in heavy absorbers or light ones?

3. What is meant by the structure of an absorption edge? In what way is it connected with the allowed electronic energy-level bands in a metal? Should you expect the absorption edges of a nonmetal, like arsenic, to show more or less structure than those of a metal, like copper?

4. Compared with coherent scattering, is Compton scattering more prominent in light materials or heavy ones? Why? Compared with coherent scattering, is Compton scattering more prominent for hard x-rays or soft ones? Why? Distinguish between the "absorption" of x-rays and the "true absorption" of x-rays.

5. What is a recoil electron? How may such electrons be observed in a gas? When so observed, how may they be distinguished from photoelectrons and Auger electrons? What are secondary beta rays? In an ionization chamber, are most of the electrons collected by the positive electrode photoelectrons, recoil electrons, and Auger electrons, or do they belong in some other classification?

6. A beam of fairly hard x-rays is directed downward upon a small block of carbon. Rays scattered from this block are intercepted by a second carbon block 6 in. east of the first one. Some of these are scattered a second time by the second block. Will these doubly scattered rays be most intense (a) north and south of the second block or (b) above and below it? Why?

7. Does there appear to be any hope of harmonizing the wave and particle aspects of radiation and so escaping from the wave-versus-particle dilemma? What modern developments tend to harmonize the two aspects?

8. For x-rays having a wave length of  $\frac{1}{8}$  A., the mass absorption coefficient of iron is approximately  $\frac{3}{8}$ . If  $\frac{1}{8}$ -A. x-rays strike a steel plate 1 cm. thick, what fraction of the rays will emerge undeflected on the opposite side, assuming the density of the steel is 8 g./cc.? Answer the same question for a 2-cm. plate. A 3-cm. plate.

*Ans.* 5 per cent; 0.25 per cent; 0.0123 per cent.

9. The mass of an atom of unit atomic weight is  $1.66 \times 10^{-24}$  g. The atomic weight of iron is 55.84. How many atoms of iron in a gram of iron? The atomic number of iron is 26. How many electrons in a gram of iron? Calculate the mass scattering coefficient of iron, using Thomson's classical formula. From this answer, calculate the atomic scattering coefficient of iron.

*Ans.*  $28.1 \times 10^{22}$  electrons; 0.186;  $1.73 \times 10^{-23}$ .

10. If one wishes to estimate the atomic absorption coefficient of iron for 0.2-A. x-rays, should formula (5-14) or (5-15) be used? Make the estimate, using the value of  $\sigma_a$  from Prob. 9. From this result, estimate the mass absorption coefficient of iron for 0.2-A. x-rays. *Ans.*  $\mu_a = (9.12 + 1.73) \times 10^{-23} = 10.85 \times 10^{-23}$ ;  $\mu = 1.17$ .

11. A beam of gamma rays contains considerable radiation of 0.02-Å. wave length. This beam, traveling north, encounters a small block of aluminum. Directly east or west of this block (or above it or below it), one will find some scattered radiation of what wave length?

*Ans.* 0.04427 Å.

12. Calculate the mass scattering coefficient of aluminum for 0.02-Å. x-rays, using formula (5-38). Assume the atomic weight of aluminum is 27; its atomic number is 13.

*Ans.*  $\sigma = 0.103$ .

13. If an intense beam of 0.13-Å. x-rays strikes a piece of lead foil, there will be considerable radiation in the vicinity having what wave lengths (see Appendix)?

*Ans.* 0.165, 0.170, 0.146, and 0.141 Å.; also 0.13 Å. itself.

## CHAPTER 6

### REFRACTION OF X-RAYS AND THEIR DIFFRACTION BY RULED GRATINGS

**1. The Practical Absence of Reflection, Refraction, and Dispersion Phenomena with X-rays.** Everybody is familiar with the reflection of light by a mirror and with the refraction of light. Ordinary eyeglasses or optical lenses of any sort depend upon refraction for their function. The dispersion of white light into a varicolored spectrum is likewise familiar in the rainbow. It is well known that in such a spectrum, formed by a glass prism, for example, the blue light is "bent," or refracted more than the red light.

These familiar phenomena are equally prominent with infrared and ultraviolet radiation, except that for the sake of transparency, other media such as rock salt or quartz may have to be used instead of glass. It is therefore surprising to learn that, for ordinary practical purposes, x-rays are not reflected, refracted, or dispersed.

Röntgen naturally expected to detect these familiar phenomena in the rays that he had discovered, and his surprise must have been considerable when he failed to do so. He was unable to detect any deviation of x-rays by prisms of various materials or any difference between the behavior of the rays at a rough surface and a polished surface of any material. He then tried passing the rays through powdered rock salt, silver powder, and zinc dust<sup>1</sup> and found that the beam after emerging in each case had exactly the same intensity and degree of parallelism as if it had traversed an equal mass of solid salt, silver, or zinc. He reasoned that even slight refraction or reflection at the surfaces of the thousands of powder particles should make the emergent beam quite diffuse but that, since the emerging beam was not diffuse, both reflection and refraction at the surfaces of the particles must be negligible or absent entirely. If there is no refraction, there can be no dispersion.

It was not until about 25 years later that x-rays were first reflected<sup>2</sup> from a polished mirrorlike surface in a specular manner like light. The reason for this is that reflection does not occur at all unless the incident and reflected rays graze the surface at an angle of only a fraction of a degree.

<sup>1</sup> W. C. Röntgen, *Ann. Physik*, **64**, 1 (1898).

<sup>2</sup> A. H. Compton, *Phil. Mag.*, **45**, 1121 (1923).



**2. Refraction and Dispersion of X-rays.** It was not until 1919 that any experimental evidence appeared to indicate that the index of refraction of x-rays ever differs even slightly from 1, that is, that x-rays are refracted slightly. This evidence was the result of refined experiments<sup>1</sup> by Stenström in x-ray diffraction, which was itself not discovered until 1912. Stenström's data showed a slight discrepancy, which might be explained on the basis of an index of refraction of x-rays slightly less than 1.

In optics, the empirical formula for the index of refraction  $\mu$  is the well-known Sellmeier formula dating from about 1870.

$$\mu^2 = 1 + \frac{D_1\lambda^2}{\lambda^2 - \lambda_1^2} + \frac{D_2\lambda^2}{\lambda^2 - \lambda_2^2} + \dots \quad (6-1)$$

where  $D_1$ ,  $D_2$ , etc., are constants,  $\lambda$  is the wave length of the light, and  $\lambda_1$ ,  $\lambda_2$ , etc., are the wave lengths of the light that would be radiated by the various natural or resonant vibration frequencies of the "oscillators" (electrons) supposed to be elastically embedded in the refracting medium. A theoretical explanation of this empirical formula was deduced by Lorentz and Drude on the basis of classical physics, thus giving some insight into the mechanism of refraction and dispersion and the meaning of the constants  $D_1$ ,  $D_2$ , etc. In this theory, Sellmeier's equation appears in the form<sup>2</sup>

$$\mu^2 = 1 + \frac{e^2}{\pi m} \left( \frac{N_1}{\nu_1^2 - \nu^2} + \frac{N_2}{\nu_2^2 - \nu^2} + \dots \right) \quad (6-2)$$

where  $e$  and  $m$  are the charge (in c.s.u.) and mass of an electron;  $N_1$ ,  $N_2$ , etc., are the number of the various types of electrons per cubic centimeter of the refracting medium, classified according to their natural frequencies  $\nu_1$ ,  $\nu_2$ , etc.; and  $\nu$  is the frequency of the refracted light. On the basis of this classical theory, one should expect that, in the case of x-rays,  $\nu$  would be so much higher than it is for light that the various electronic resonant frequencies  $\nu_1$ ,  $\nu_2$ , etc., might be very small compared with  $\nu$ . In this case, equation (6-2) can be approximated by neglecting the  $\nu_1$ ,  $\nu_2$ , etc., terms, and then  $N_1 + N_2 +$ , etc., may be replaced simply by  $N$ , the total number of electrons per cubic centimeter. Equation (6-2) then becomes

$$\mu^2 = 1 - \frac{Ne^2}{\pi m \nu^2} \quad (6-3)$$

<sup>1</sup> W. Stenström, dissertation, Lund (1919); see p. 329.

<sup>2</sup> See, for example, H. A. Lorentz, "The Theory of Electrons," p. 149, Columbia University Press, New York, 1909, or R. A. Houstoun, "Treatise on Light," 7th ed., p. 463, Longmans, Green and Company, New York, 1938.

Applying the binomial theorem,

$$\mu = 1 - \frac{Ne^2}{2\pi m\nu^2} - \frac{1}{8} \left( \frac{Ne^2}{2\pi m\nu^2} \right)^2 - \dots \quad (6-4)$$

To gain some idea of the value of  $Ne^2/2\pi m\nu^2$ , let us assume that the x-rays are the  $K_\alpha$  radiation from molybdenum passing through aluminum. Then, since the number of atoms per gram of any element is Avogadro's number  $N_0$  divided by its atomic weight  $A$ , the number of atoms per cubic centimeter will be this quantity multiplied by the density  $\rho$ . The number of electrons is equal to the number of atoms multiplied by the atomic number  $Z$ , and therefore

$$N = \frac{N_0 \rho Z}{A} \quad (6-5)$$

which is  $7.83 \times 10^{23}$  for aluminum. For  $\text{MoK}_\alpha$ ,  $\lambda = 0.71$  A. and  $\nu = c/\lambda = 4.2 \times 10^{18}$  per second, and hence  $Ne^2/2\pi m\nu^2 = 1.67 \times 10^{-6}$ . Therefore it is obvious that this quantity is small enough in all practical cases so that its square and higher powers may be neglected compared with itself, and thus (6-4) may be written

$$\mu = 1 - \frac{Ne^2}{2\pi m\nu^2} = 1 - \frac{Ne^2\lambda^2}{2\pi mc^2} = 1 - \delta \quad (6-6)$$

where

$$\delta = \frac{Ne^2}{2\pi m\nu^2} = \frac{Ne^2\lambda^2}{2\pi mc^2} \quad (6-7)$$

Thus it is seen that classical dispersion theory leads one to expect that the index of refraction of x-rays should be *less* than 1 by a quantity  $\delta$  of the order of  $10^{-6}$ .

The index of refraction  $\mu$  of a substance for a particular type of radiation is commonly defined as the ratio of the velocity  $c$  of the radiation in vacuum to its velocity  $v$  in the substance. Hence an index less than 1 for x-rays might imply a velocity  $v$  of the x-rays in the medium greater than  $c$ , thus violating the relativity principle mentioned on pages 56 and 57. This inference is false, however, because the velocity  $v$  with which one is concerned in this definition of  $\mu$  is the so-called "wave velocity" or "phase velocity" of the waves in the medium, whereas the *energy* of the x-rays is actually transmitted through the medium at a lower velocity  $u$ , called the "group velocity." This is given by

$$u = v - \lambda_m \frac{dv}{d\lambda_m} \quad (6-8)$$

where  $\lambda_m$  is the wave length of the x-rays in the medium. It may be

shown that  $u$  does not exceed  $c$ , so that there is no violation of relativity principles.<sup>1</sup>

Some reflection experiments by A. H. Compton in 1922, to be described in the next section, Stenström's results, and the above theory—all indicated that x-rays might have an index of refraction around  $1 - 10^{-6}$ , or 0.999999; therefore in 1924 Larsson, Siegbahn, and Waller<sup>2</sup> were led to attempt once more to detect and measure experimentally the deviation of x-rays by refraction in a prism. Many earlier experimenters, beginning with Röntgen, had obtained only negative results from such experiments. By directing the incident beam at a polished surface of the prism at a grazing angle of about  $1^\circ$  or less, so that the expected deviation would be a maximum, Larsson, Siegbahn, and Waller succeeded in demonstrating beyond doubt that a measurable refraction at the surface existed, in a direction indicating an index of refraction slightly less than 1.

By further refinement of technique, Davis and Slack<sup>3</sup> were able to set an aluminum prism at the more conventional position of minimum deviation, as in optics, and measure  $\delta$  with an accuracy of the order of a few per cent. Using molybdenum  $K_\alpha$  radiation, they determined experimentally that  $\delta = 1.68 \times 10^{-6}$ , which compares satisfactorily with the value  $1.67 \times 10^{-6}$  calculated on page 98. Good agreement with the classical theory was also obtained when copper  $K_\alpha$  radiation was used, for which they determined an experimental value of  $\delta$  of  $8.4 \times 10^{-6}$ . As an example of the degree of refinement possible with modern technique, Bearden<sup>4</sup> has determined  $\delta$  for copper  $K_\beta$  rays in diamond to five significant figures:  $\delta = 9.2244 \times 10^{-6}$ .

Instead of trying to measure the index of refraction directly with a prism, there are other experimental methods devised by various workers that also yield accurate values of  $\mu$ . One of these is based upon measurement of the critical angle of total reflection, to be discussed in the next section. Other methods depend upon diffraction of x-rays in crystals. The basic law of diffraction, known as Bragg's law, predicts the angles at which x-ray beams will be diffracted in a crystal in terms of other known or measurable quantities. When observation fails to check exactly with the law, the discrepancy may be ascribed to refraction, if the measurements are sufficiently refined and accurate. From the magnitude of the discrepancy, the value of  $\mu$  may be calculated, but not with very great accuracy because the discrepancy is so small. This was the first method to yield a value of  $\mu$  other than 1, used by Stenström,

<sup>1</sup> See, for example, F. A. Jenkins and H. E. White, "Fundamentals of Physical Optics," p. 300, McGraw-Hill Book Company, Inc., New York, 1937.

<sup>2</sup> A. Larsson, M. Siegbahn, and T. Waller, *Naturwissenschaften*, **12**, 1212 (1924); *Phys. Rev.*, **25**, 235 (1925).

<sup>3</sup> B. Davis and C. M. Slack, *Phys. Rev.*, **27**, 18 (1926).

<sup>4</sup> J. A. Bearden, *Phys. Rev.*, **54**, 698 (1938).

as already mentioned. By cutting and polishing the crystal so that the incident ray grazes its surface and the diffracted ray does not, or vice versa, a dissymmetry is produced that may be measured and used<sup>1</sup> to calculate  $\mu$ .

All methods yield values of  $\mu$  that agree fairly well with equation (6-7) deduced from the early classical theory, unless the wave length of the x-rays used happens to be close to an absorption edge. From equation (6-7),

$$\frac{\delta}{\lambda^2} = \frac{Ne^2}{2\pi mc^2} \quad (6-9)$$

indicating that, for any given material,  $\delta/\lambda^2$  should remain constant. Experimental values of  $\delta$  have been obtained with sufficient accuracy in the vicinity of absorption edges in some cases (for example, on both sides of  $\lambda = 3.064$  Å., the K edge for calcium, using a calcite prism) to show that  $\delta/\lambda^2$  varies rather rapidly in the immediate vicinity of such edges. This is not surprising; for equations (6-7) and (6-9) were based on the assumption that  $\nu$  was much greater than any natural electronic frequencies  $\nu_1, \nu_2$ , etc., and this is apparently not true at an absorption edge. X-rays display a behavior in the vicinity of these edges, so far as refraction is concerned, somewhat analogous to anomalous dispersion in optics. This phenomenon need not cause concern in ordinary practical x-ray work, however, for  $\delta$  never exceeds  $10^{-4}$  or thereabouts, even at the edge.

Theoretical values of  $\mu$  near such edges have been calculated on the basis of modern quantum mechanics,<sup>2</sup> and the results are in close agreement with the experimental data.<sup>3</sup>

**3. Reflection of X-rays and Their Diffraction by Ruled Gratings.** By 1922, the theory discussed on page 98 and Stenström's results indicated a refractive index for x-rays slightly less than 1. If  $\mu$  is less than 1, Snell's law of refraction

$$\mu = \frac{\sin i}{\sin r} \quad (6-10)$$

indicates that  $r > i$ , so that a ray entering a dense medium from a rare one will be bent away from the normal rather than toward it. Hence total reflection will occur for values of  $i$  that make  $r$  exceed  $90^\circ$  rather than for values of  $r$  that make  $i$  exceed  $90^\circ$ , as in the case of light in glass. Therefore total reflection should occur for rays striking sufficiently obliquely from without, rather than from within the denser medium.

<sup>1</sup> See C. C. Hatley and B. Davis, *Phys. Rev.*, **23**, 290 (1924); R. von Nardroff, *Phys. Rev.*, **24**, 486 (1924).

<sup>2</sup> See, for example, H. Hönl, *Z. Physik*, **84**, 1 (1933).

<sup>3</sup> See, for example, R. M. Whitmer and G. A. Lindsay, *Phys. Rev.*, **54**, 988 (1938).

Referring to Fig. 6-1, let  $AB$  represent the polished surface of a solid (or clean surface of a liquid) with x-rays incident upon it from without (that is, from above) in the direction  $IP$ , striking it at  $P$ , and being refracted in the direction  $PR$ .  $NP$  is the normal to the surface at  $P$ . Then total reflection should be expected to occur when the angle of incidence  $i$  is large enough (or the angle of grazing incidence  $\theta_i$  is small

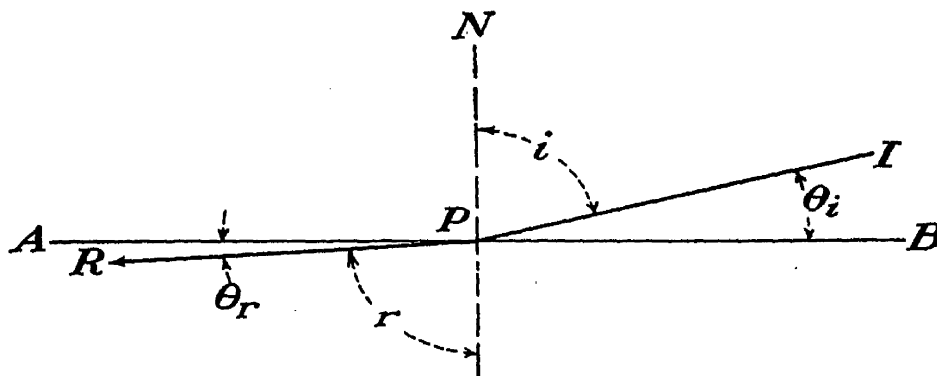


FIG. 6-1.—To illustrate calculation of the critical angle of total reflection for x-rays.

enough) for  $r$  to exceed  $90^\circ$ , as calculated from (6-10). The critical grazing angle  $\theta_c$  at which total reflection should begin is then given by

$$\cos \theta_c = \sin i_c = \mu \sin r = \mu \sin 90^\circ = \mu = 1 - \delta \quad (6-11)$$

or

$$\delta = 1 - \cos \theta_c \quad (6-12)$$

One of the standard trigonometric relations is  $1 - \cos 2x = 2 \sin^2 x$ ; therefore,

$$1 - \cos \theta_c = 2 \sin^2 \frac{1}{2}\theta_c = \delta \quad (6-13)$$

Since  $\delta$  is of the order of  $10^{-5}$  or  $10^{-6}$  as mentioned in the preceding section,  $\sin^2 \frac{1}{2}\theta_c$  is of this order, and thus  $\sin \frac{1}{2}\theta_c$  is of the order  $10^{-3}$ . For such small angles, the sine may be replaced by the angle if the latter is measured in radians, and (6-13) becomes

$$\delta = 2(\frac{1}{2}\theta_c)^2 = \frac{1}{2}\theta_c^2 \quad (6-14)$$

or

$$\theta_c = \sqrt{2\delta} \quad (6-15)$$

With these things in mind, an attempt was made in 1922 by A. H. Compton<sup>1</sup> to reflect a fine beam of x-rays, of very slight divergence, from the polished surface of a piece of crown glass into an ionization chamber. The attempt was successful; when  $\theta_i$  was less than 10 min. of arc, a strong reflected beam was found in the direction predicted by the ordinary laws of specular reflection of light. The reflection does not drop from 90 per cent to zero instantly at the critical angle; the cutoff is sharp, but not mathematically discontinuous. By measuring  $\theta_c$  as accurately as possible and applying (6-14), Compton computed that, for  $\lambda = 1.279 \text{ \AA}$  (a tungsten L line),  $\delta = 4.2 \times 10^{-6}$  for glass and  $21.5 \times 10^{-6}$  for :

<sup>1</sup> A. H. Compton, *Phil. Mag.*, **45**, 1121 (1923).

silver mirror, as compared with  $5.2 \times 10^{-6}$  and  $19.8 \times 10^{-6}$  predicted by (6-7).

These results encouraged Larsson, Siegbahn, and Waller to make their successful attempt to observe the refraction of x-rays directly soon afterward, as mentioned in the preceding section. In the case of highly absorbing materials like lead, when soft rays are used, the simple theory already outlined must be modified,<sup>1</sup> for in this case no critical angle  $\theta_c$  is observable.

Having demonstrated that x-rays could be reflected, Compton and Doan<sup>2</sup> soon attempted to diffract them by reflection from a ruled grating of speculum metal, as in the case of light. At that time, x-ray diffraction

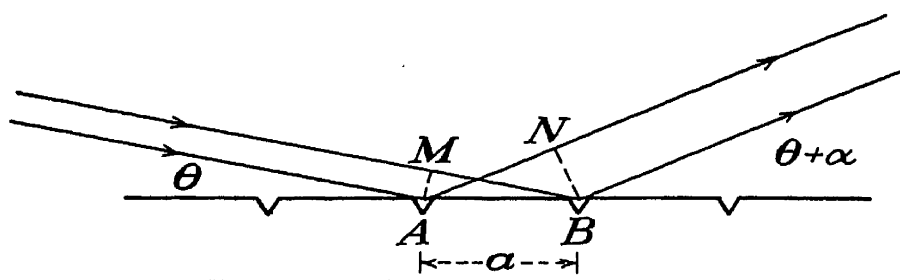


FIG. 6-2.—Diffraction of x-rays by a grating.

by crystals was an old story, but x-ray diffraction by a ruled transmission grating had not been achieved (nor has it yet), and x-ray diffraction by a ruled reflection grating had not been seriously considered because x-ray reflection had never been achieved.

Compton and Doan directed the x-rays at the grating surface at a small grazing angle  $\theta$  (Fig. 6-2) so that they would be reflected. The attempt resulted in the successful photographing of x-ray grating spectra. The equation governing diffraction from a grating at grazing incidence is derived by noting the difference in the distances traveled by the rays, which are coherently scattered at adjacent grooves ruled on the grating. The grooves or lines on a diffraction grating are ruled parallel and equidistant, and there are several hundred of them per inch.

From Fig. 6-2 it is obvious that the incident rays travel equal distances before reaching  $MA$ , a plane perpendicular to the rays at groove  $A$ . It is also obvious that the scattered rays travel equal distances after they pass the plane  $NB$ , perpendicular to the rays at the groove  $B$ . Between these two planes, the ray scattered at  $B$  travels a distance  $MB$ ; meanwhile, the ray scattered at  $A$  travels a distance  $AN$ . If the difference in these paths is exactly 1 (or 0 or 2 or 3) or, in general,  $n$  wave lengths, where  $n$  is an integer, then the waves beyond  $NB$  will be in

<sup>1</sup> See, for example, P. Drude, "Theory of Optics" (translated by Mann and Millikan), p. 295 and Chap. IV, p. 358, Longmans, Green and Company, New York, 1925.

<sup>2</sup> A. H. Compton and R. L. Doan, *Proc. Natl. Acad. Sci.*, 11, 598 (1925).

phase (that is, "in step"), and constructive interference will occur for all the rays from all the grooves. There will be only certain values of the angle  $\theta + \alpha$  for which it will be true that  $MB - AN = n\lambda$ . At other angles,  $MB - AN$  will not be an integral number of wave lengths. If it is  $1.1\lambda$ , for example, then the waves scattered from grooves spaced  $5a$  apart ( $a$  is the "grating spacing," or "grating constant," Fig. 6-2) will have a path difference of  $5\frac{1}{2}\lambda$  and this will result in complete destructive interference.

For the grating to diffract x-rays,  $\theta$  must be less than the critical angle  $\theta_c$  [Equation (6-15)] and  $\alpha$  must not exceed two or three times  $\theta_c$ . In general, this will not be true unless the grating is ruled somewhat more coarsely (lines farther apart) than is usual for optical reflection gratings.

The whole phenomenon just discussed is called "x-ray diffraction." It is obvious that x-ray diffraction is much easier to understand if the x-rays are regarded as composed of waves rather than particles. It will be remembered that x-rays were first defined as a form of radiation consisting of bundles of waves, or photons. X-ray diffraction also occurs (in fact, it was first discovered) in crystals, and it will be discussed in much greater detail in later chapters in connection with this phase of the subject.

From Fig. 6-2, one must have, for constructive interference,

$$MB - AN = n\lambda = a[\cos \theta - \cos (\theta + \alpha)] \quad (6-16)$$

which is frequently written in the trigonometrically equivalent form

$$n\lambda = 2a \left( \sin \frac{2\theta + \alpha}{2} \sin \frac{\alpha}{2} \right) \quad (6-17)$$

or sometimes in the approximate form

$$n\lambda = a(\alpha\theta + \frac{1}{2}\alpha^2) \quad (6-18)$$

in which  $\theta$  and  $\alpha$  must be expressed in radians. The integer  $n$  is the "order" of the diffracted spectrum; if  $n = 1$ , it is the first order, for example. In this particular case, negative orders, or negative values of  $n$  are possible, there being corresponding negative values of  $\alpha$ .

Refinement in technique in recent years has resulted in x-ray grating spectra of such high quality that  $\lambda$  can be calculated from (6-16) or (6-17) with an accuracy of five significant figures. For example, Bearden<sup>1</sup> has determined the wave length of the copper  $K_{\alpha_1}$  line from grating measurements to be 1.5406 Å, and Bäcklin<sup>2</sup> has found the  $K_{\alpha_{1,2}}$  line of aluminum to have a wave length of 8.3395 Å. For determining the absolute value of the wave length of x-rays (as distinguished from determining one wave length in terms of another), the ruled grating is now

<sup>1</sup> J. A. Bearden, *Phys. Rev.*, **48**, 385 (1935); see also footnote 1 on page 104.

<sup>2</sup> E. Bäcklin, *Z. Physik*, **93**, 450 (1935).

superior to the older method using a crystal. By combining the two methods, it is possible to deduce accurate values of two of the fundamental physical constants,<sup>1</sup> namely, Avogadro's number  $N_0$  and the electronic charge  $e$ . The value of  $e$  thus deduced is  $4.8024 \times 10^{-10}$  e.s.u. When this was first computed accurately, the accepted value of  $e$ , based on Millikan's oil-drop method, was  $4.774 \times 10^{-10}$  e.s.u. The discrepancy was quite disturbing to physicists. The resulting thorough search for the source of the trouble led to the discovery of an error in the value of the viscosity of air that Millikan used. After this was corrected, Millikan's oil-drop value of  $e$  agreed with the x-ray grating value within the limits of experimental error.<sup>2</sup>

### QUESTIONS AND PROBLEMS

1. A fine beam of parallel x-rays strikes an equilateral ( $60^\circ$ ) glass prism parallel to its base, so that the angle of incidence is  $30^\circ$ . After traversing the prism, it travels 10 ft. and strikes a fluorescent screen perpendicularly, producing a spot of light. How far will this spot of light move when the prism is removed, assuming that  $\delta = 10^{-5}$ ?

*Ans.* 0.00126 in.

2. Compute  $\delta$  for the case of nickel  $K_\alpha$  radiation ( $\lambda = 1.66$  A.) in chromium ( $Z = 24$ ,  $A = 52$ ,  $\rho = 7.1$ ), Avogadro's number being  $6 \times 10^{23}$  atoms/g.-atom.

*Ans.*  $\delta = 2.4 \times 10^{-5}$ .

3. If one attempts to compute  $\delta$  for the case of manganese  $K_\alpha$  radiation ( $\lambda = 2.10$  A.) in chromium, there might be considerable doubt about the accuracy of the result, unless the solution were obtained by quantum-mechanical methods. Why? (See Appendix VI.)

4. If one wishes to measure the wave lengths of the nickel  $K_\alpha$  lines by using a reflection grating ruled on chromium, the incident rays must strike the grating at an angle no greater than how many degrees or minutes?

*Ans.*  $24'$ .

5. In view of the result in the preceding problem, the angle of diffraction ( $\alpha$  in Fig. 6-2) should not exceed about  $1^\circ$ . If it is desired to observe both first and second orders in the spectrum, the grating used must not have more than about how many lines per centimeter?

*Ans.* 8,000.

<sup>1</sup> J. A. Bearden, *J. Applied Phys.*, **12**, 395 (1941).

<sup>2</sup> See p. 338.



## CHAPTER 7

### X-RAY GENERATING EQUIPMENT

**1. Types of X-ray Tubes.** Some of the fundamentals of the construction and operation of various types of x-ray tubes were discussed in Chap. 2. Since x-ray tubes are used for a wide variety of purposes, there is a wide variety of tube types. The following outline lists the more important variations:<sup>1</sup>

#### 1

- a. Gas tubes, versus
- b. Coolidge-type (hot-cathode) tubes, versus
- c. Tubes in which the cathode is an "electron gun"; see, for example, the Lilienfeld tube (Sec. 4e), versus
- d. Field emission tubes (see page 296).

#### 2

- a. Demountable tubes that can be taken apart to change targets, etc., and consequently are connected to a vacuum pumping system so that they can be exhausted during use, versus
- b. Sealed-off tubes.

#### 3

- a. Tubes in which the target gets white-hot and dissipates its heat by radiation, versus
- b. Tubes in which the target or both cathode and target are cooled by external convection fins, versus
- c. Tubes in which the target or cathode and target are cooled by water or oil circulated through them, versus
- d. Tubes in which the target is cooled by water, which boils inside it and condenses in an external metal bulb.

#### 4

- a. Rotating anode tubes,<sup>2</sup> versus
- b. Tubes with a fixed target.

#### 5

- a. Glass tubes, versus
- b. Metal tubes provided with windows for the x-ray beam; the cathode is insulated by a glass or porcelain insulator.

<sup>1</sup> See V. Hicks, *J. Applied Phys.*, **12**, 364 (1941); W. D. Coolidge and E. E. Charlton, *Gen. Elec. Rev.*, **48**, 36 (November, 1945); Z. J. Atlee, *Electronics*, **18**, 136 (November, 1945).

<sup>2</sup> Now made for power up to 10 kw. or more; see, for example, J. Beck, *Physik. Z.*, **40**, 474 (1939); J. W. M. DuMond and J. P. Youtz, *Rev. Sci. Instruments*, **8**, 291 (1937).

## 6

- a. Low-voltage tubes that generate such soft rays that special windows are required to let them out, such windows being of special paper-thin glass (Lindemann glass) or aluminum foil or beryllium,<sup>1</sup> versus
- b. Tubes generating hard x-rays, which escape from the tube without needing any special windows.

## 7

- a. "Shockproof" tubes, semipermanently mounted in a close-fitting container, which may contain oil, provided with a window for the x-ray beam, and usually supplied with electric power through high-voltage insulated cables with a grounded exterior metal sheath (these are called "shockproof cables"); these tubes afford complete protection against high-voltage electrical shock, and sometimes against x-rays escaping in other directions than through the window, versus
- b. Tubes not so protected.

## 8

Tubes having targets of

- a. Tungsten
- b. Tantalum
- c. Molybdenum
- d. Copper
- e. Nickel
- f. Cobalt
- g. Iron
- h. Chromium
- i. Other less common materials.

## 9

- a. Tubes built in several alternating sections of metal and insulating material, called "multisection tubes,"<sup>2</sup> to distribute extremely high voltages uniformly along the length of the tube, versus
- b. Ordinary single-section tubes.

## 10

- a. Very high voltage tubes having a thin target at one end so that the useful x-ray beam penetrates the target and emerges from the anode end of the tube<sup>3</sup> in the direction of travel of the cathode rays, versus
- b. Ordinary tubes from which the useful rays emerge laterally, (a) some with square-cut targets, (b) some with targets cut obliquely, versus
- c. Tubes having a target provided with a conical cavity at the focal spot, the useful x-ray beam traveling opposite to the direction of motion of the cathode

<sup>1</sup> See G. E. Clausen and J. W. Skehan, *Metals & Alloys*, April, 1942; also R. R. Machlett, *J. Applied Phys.*, **13**, 398 (1942); also H. Brackney and Z. J. Atlee, *Rev. Sci. Instruments*, **14**, 59 (1943).

<sup>2</sup> See, for example, E. E. Charlton and W. F. Westendorp, *Gen. Elec. Rev.*, **44**, 654 (1941) (1-million-volt tube); *Electronics*, **17**, 128 (December, 1944) (2-million-volt tube); R. R. Machlett, *Electronic Ind.*, **3**, 79 (November, 1944).

<sup>3</sup> The European "oxtail" tube, designed to generate x-rays inside tanks and pressure vessels that are to be inspected, also has the target at the end of a long projection. See J. E. de Graaf, *J. Inst. Elec. Eng.*, **84**, 545 (1939).

rays, passing through the center of the cathode filament, which is wound in circular (not spiral) form, and emerging from the cathode end of the tube.

### 11

- a. Tubes with two or more separate cathode filaments, so that, by using one or the other, focal spots of various sizes may be obtained in the same tube
- b. Benson or Goetze focus tubes; see page 18 and Fig. 2-9; also U.S. patent 1,174,044 (1916)
- c. Tubes with conventional spiral cathode filaments, and
- d. Tubes with ring-type cathode filaments (see 10c, on page 106).

### 12

- a. Therapeutic tubes designed for high voltage and moderate power in which large focal spots are no disadvantage
- b. Tubes for industrial radiography, in which high voltage and moderate or high power are required but are compromised by necessity for a small focal spot
- c. Medical radiographic (diagnostic) tubes requiring lower voltage and fine focal spot and perhaps special right-angle shapes, etc., as in dental tubes
- d. X-ray diffraction tubes<sup>1</sup>
- e. Tubes for microradiography, and
- f. Other special-purpose tubes.

### 13

- a. Tubes for x-ray snapshots,<sup>2</sup> which are designed for tube currents of several thousand amperes (not milliamperes!) at 300 kv. for about 1 microsecond only (Fig. 7-1) (these tubes operate by "field emission" from a cold cathode), versus
- b. Ordinary tubes for continuous operation.

### 14

- a. Tubes with a control grid<sup>3</sup> to suppress the tube current except during the short time when the sine wave of the a.c. voltage is near its crest, thus increasing the tube efficiency, versus
- b. Ordinary diode-type tubes.

### 15

- a. Tubes designed to operate with the anode grounded, and
- b. Tubes designed to operate mid-grounded, that is, with the anode aboveground potential and cathode belowground potential, at least on the useful half cycle, if alternating current is used.

<sup>1</sup> See, for example, J. E. de Graaf and W. J. Oosterkamp, *J. Sci. Instruments*, **15**, 293 (1938).

<sup>2</sup> See, for example, M. Steenbeck, *Wiss. Veröffent. Siemens-Werken*, **17**, 363 (1938); E. A. W. Müller, *Arch. tech. Messen*, **102**, T157½ (December, 1939); K. H. Kingdon and H. E. Tanis, Jr., *Phys. Rev.*, **53**, 128 (1938); W. J. Oosterkamp, *Philips Tech. Rev.*, **5**, 22 (January, 1940); C. M. Slack and L. F. Ehrke, *J. Applied Phys.*, **12**, 165 (1941), **15**, 628 (1944); C. M. Slack, E. R. Thilo, and C. T. Zavallas, *Electronic Ind.*, **3**, 104 (November, 1944).

<sup>3</sup> See, for example, A. Eisenstein, *Rev. Sci. Instruments*, **13**, 208 (1942).

## 16

Other variations, such as hooded anodes to reduce electronic bombardment of the glass envelope.

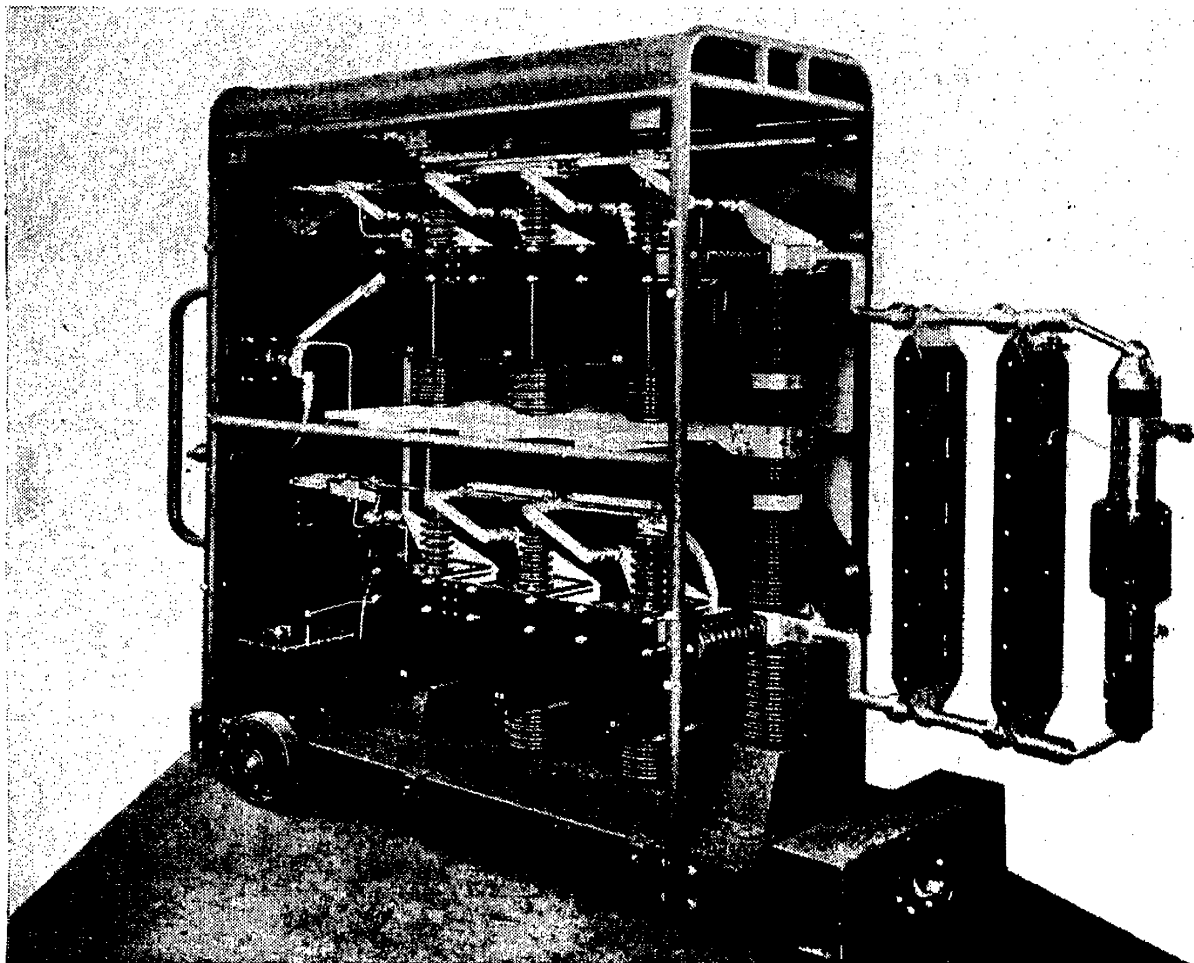


FIG. 7-1.—Marx-type surge generator and 300-kv. field-emission x-ray tube for instantaneous radiography. (Courtesy of Westinghouse X-ray Division.)

The variations just outlined are interdependent, so that the various possible combinations are very numerous indeed. For example, there are shockproof glass tubes, shockproof metal tubes, nonshockproof glass tubes, nonshockproof metal tubes, etc. Detailed discussion of some of these types will be reserved for other chapters.

One of the best places to find excellent illustrated descriptions of the more common tube types is in the catalogues of the various x-ray tube manufacturers. In the United States, a few of the more prominent tube manufacturers in alphabetical order are:

General Electric X-ray Corporation, Chicago, Ill.  
Machlett Laboratories, Inc., Springdale, Conn.  
North American Philips Co., Inc., New York, N.Y.  
Westinghouse Electric & Mfg. Co., X-ray Division, Baltimore, Md.

Others may be found in MacRae's Blue Book or Thomas's Register of American Manufacturers. Outside the United States, two of the most

prominent tube manufacturers are the N. V. Philips Gloeilampenfabrieken, Eindhoven, Netherlands and the Siemens-Werke, Germany.

**2. Diffraction Tubes—Demountable.** In most x-ray work, it is the continuous radiation that is of chief interest. X-ray diffraction work is an exception in that the characteristic radiation of the tube target is usually of paramount interest. Hence tubes for such work are often demountable so that targets of one metal or another may be inserted as desired. Demountable tubes for diffraction work are usually homemade rather than factory-built. Descriptions of such tubes are frequently found in such periodicals as the *Review of Scientific Instruments* and the *Journal of Scientific Instruments*, the latter a British publication. Since 1920, most volumes of either of these magazines contain descriptions of at least one such tube.<sup>1</sup>

For many years, one of the most widely used types of demountable diffraction tube was the Hadding type.<sup>2</sup> This is a gas tube with steel body, electrically grounded, surrounded in turn by a metal jacket, water being circulated between the two. The target is also kept at ground potential and is water cooled. It is quickly and easily fitted into the tube by means of a tapered greased joint (which should be greased only on the outer portion by low-vapor-pressure grease like Apiezon L). The focal spot is only about 1 cm. from the aluminum-foil window for the x-rays. In mounting such windows, which should be about 0.01 mm. thick, orange shellac is suitable as an adhesive and may be brushed very thinly over the foil to seal microscopic holes in it. The aluminum cathode is insulated from the steel body of the tube with a porcelain insulator. The cathode is water-cooled, but only a very small stream of water is required for it, say a few drops per minute. Since it is at high (negative) voltage, the water leads to it should contain a section of fine glass tubing to minimize electrical leakage through the water. The porcelain insulator may be sealed to the steel tube body and to the cathode by some wax such as Picein.

A tube of this type is operated at from 10 to 40 kv., depending upon the target used, and will carry up to 30 ma. easily. Such power concentrated on a target so close to a thin window produces a very intense x-ray beam at the window. After a tube of this type is operated a few hundred hours, the x-ray intensity begins to fall off gradually until it finally drops to only a few per cent of its original value. Since the tube voltage and current remain normal, this effect is puzzling until the cause

<sup>1</sup> See, for example, F. G. Chesley, *Rev. Sci. Instruments*, **14**, 3 (1943).

<sup>2</sup> Described and illustrated by A. Hadding, *Z. Physik*, **5**, 369 (1920); also by M. Siegbahn, "The Spectroscopy of X-rays," translated by G. A. Lindsay, p. 35, Oxford University Press, New York, 1925. Another popular tube of this type is the Shearer tube. See, for example, W. H. Bragg and W. L. Bragg, "The Crystalline State," p. 308, George Bell & Sons, Ltd., London, 1933.

is learned. Upon opening the tube, it will be found that the aluminum cathode has developed a small pit in its center. This destroys its focusing action. The cathode may be mounted in a lathe and the pit removed with emery cloth in a few minutes. Upon reassembling, the x-ray output will be found as intense as ever.

A modern demountable gas-type diffraction tube of a somewhat different kind is illustrated in Fig. 2-2. Such metal gas tubes are practically indestructible, so long as the water supply is maintained. With any water- or oil-cooled tube, the power supply should be provided with a shutoff relay to operate upon failure of the water or oil supply. Such relays should depend, not upon pressure, but upon flow. Relays that operate when the pressure drops do not protect against clogged passages, which is one of the commonest causes of cooling failure.

Gas tubes are often preferred for diffraction work for six reasons. (1) A demountable tube is frequently disassembled to change targets. Such treatment may knock a delicate filament out of alignment or damage it. (2) Very ordinary care in vacuum technique is sufficient to secure a pressure of  $10^{-4}$  mm. of mercury, which is low enough to operate a gas tube; if a leak develops and the pressure rises, no harm is done. Greater care is required to obtain a pressure of  $10^{-5}$  or  $10^{-6}$  mm. of mercury for hot-cathode operation; if even a small leak develops so that the pressure increases to, say,  $10^{-4}$  mm., positive-ion bombardment of the filament quickly destroys it. (3) Greater care in cathode design and construction is required to obtain a good focal spot with a hot cathode than with a cold one. With the latter, it is necessary only to make the radius of curvature of the concave surface a little less than half the distance from cathode to target and to avoid sharp edges. (4) The hot cathode, being at high voltage, requires insulated storage batteries and rheostat or a highly insulated filament transformer to energize it, whereas gas tubes require only a simple leak valve for their control. (5) Tungsten tends to evaporate from a hot tungsten cathode and condense on the target slowly. If this occurs, the characteristic spectrum of the target (copper, for example) has superimposed upon it the characteristic spectrum of tungsten, which is undesirable in diffraction work. (6) If the tube is being used with a vacuum spectrograph so that the tube and spectrograph are all at the same pressure, the "window" being omitted, then the visible light from the glowing cathode filament may be reflected from the target surface into the spectrograph and fog the film or plate. Gas tubes can be made self-rectifying, as already mentioned, so that the inherently self-rectifying hot-cathode tubes no longer offer that advantage.

The leak valve required to control a gas tube may be very simple. Wyckoff and Lagsdin<sup>1</sup> have found that a screw clamp on a rubber tube

<sup>1</sup> R. W. G. Wyckoff and J. B. Lagsdin, *Rev. Sci. Instruments*, **7**, 35 (1936).

will serve. With this arrangement, some have reported improved performance if a small wire is inserted in the tube before the clamp is applied.

**3. Diffraction Tubes—Sealed Off.** A more elegant solution to the diffraction-tube problem is to buy several factory-built sealed-off diffraction tubes, each with a different target, such as molybdenum, copper, cobalt, etc., and change tubes for different problems instead of changing targets. For copper, nickel, cobalt, iron, and chromium, it is recommended that the recently developed beryllium window tubes be selected. With molybdenum, this is not so important; in this case, Lindemann glass windows are nearly as good, as may be seen from Table 7-1.

TABLE 7-1.\*—PER CENT TRANSMISSION OF THE  $K_{\alpha}$  RADIATION OF VARIOUS ELEMENTS BY X-RAY TUBE WINDOWS

Target element	Window material	
	Lindemann glass	Beryllium
Cr (24).....	5	62
Fe (26).....	15	74
Co (27).....	22	80
Ni (28).....	30	82
Cu (29).....	40	85
Mo (42).....	88	95

\* Compiled from data published by the General Electric Company, by permission.

The use of factory-built sealed-off tubes overcomes most of the six advantages listed for gas tubes in the preceding section and overcomes the two important disadvantages of demountable tubes, (1) the necessity of having a vacuum system and (2) the lack of flexibility (because the tube is attached to the vacuum system). Factory-built sealed-off tubes, properly used, will not suffer from burned-out or misaligned filaments even after thousands of hours of use. The vacuum stays good; the tungsten deposition has been reduced to a point where it is of no consequence in ordinary routine work;<sup>1</sup> and such tubes may be used in a self-rectifying circuit.

The cathode in such tubes is sometimes of the "hemispherical type" (see Fig. 7-2C), although the present trend is toward a line-focus or Benson-type cathode (Fig. 2-9) with target cut off square.

**4. X-ray Tubes—General.** *a. Cathode.* Most x-ray tubes except diffraction tubes are useful chiefly for the continuous x-ray spectrum they produce. Their metal parts must withstand high temperatures in a vacuum without melting, warping, evaporating, or releasing much

<sup>1</sup> For details, see *J. Sci. Instruments*, **22**, 67 (1945).

absorbed gas. Sealed-off hot-cathode tubes usually have their cathode focusing cups made of molybdenum or tantalum.

The older type of universal cathode (Fig. 7-2A) was surrounded by a flat circular shield *S*. This has but little to do with the focusing but screens the glass support from possible ion bombardment. The newer type of universal cathode is represented in Fig. 7-2B. The hemispherical type shown in Fig. 7-2C is used when a very fine focal spot is desired. It is ordinarily placed closer to the target *T* than the universal type. Both types produce a circular focal spot. The present trend in

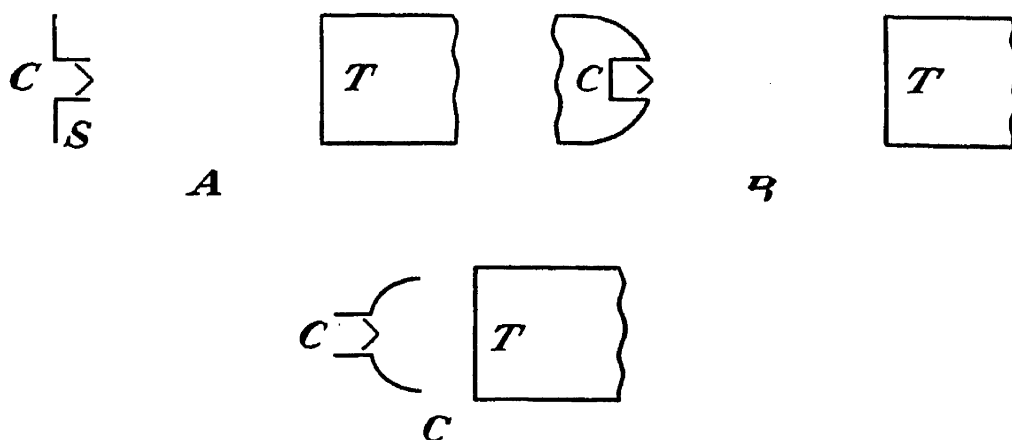


FIG. 7-2.—Various types of hot cathodes with spiral filaments. A, universal cathode, older type. B, universal cathode, newer type. C, hemispherical cathode.

tubes for most purposes seems to be toward the Benson-Goetze type of focus<sup>1</sup> (Fig. 2-9).

The filament is made of tungsten wire, the most rugged and durable metal for this purpose. Most x-ray tube filaments operate at about 6 volts and require 3 or 4 amp. to maintain an emitting temperature. The high-voltage electrostatic field exerts enough mechanical force on the filament to distort or destroy it if it does not have considerable mechanical strength when hot. By using an oxide-coated or a thoriated filament, the required heating power might be reduced from around 20 watts to perhaps 2 or 3 watts, but this would reduce the life of the costly tube seriously and would be false economy.

*b. Target.* The target is usually made of solid tungsten in the form of a block or a thick disk. Sometimes a tungsten button is set into a block of copper (Fig. 2-9). Tungsten is usually chosen because it offers the best combination of desirable properties, such as high melting point, high atomic number, and high thermal conductivity. Other metals are occasionally used. For example, the 600-kv. therapeutic tube at Harper Hospital, Detroit, Mich., has a lead target. Its comparatively large focal spot makes a high-melting-point target unnecessary.

<sup>1</sup> For details regarding the focusing of electrons upon a suitable focal spot, a Benson-Goetze focus being used, see N. C. Beese, *Rev. Sci. Instruments*, **8**, 258 (1937).



Lead was chosen because its high atomic number (82) makes it about 10 per cent more efficient than tungsten as an x-ray emitter [see equations (2-5) and (3-11)].

c. *Windows for Hard Rays.* In some medical diagnostic tubes, the glass envelope is ground down thin opposite the target, to serve as a window for the x-rays, even though they are fairly hard, being generated at 50 to 90 kv.

d. *Shockproof Tubes.* "Shockproof" tubes are tubes which are enclosed in a protective cover. Such covers are sometimes made of lead-impregnated porcelain or lead-impregnated plastic material; the central portion, which contains the window for escape of the x-rays, is often made of metal. The cover may be difficult or easy to remove, depending on whether or not it contains oil and on the design. Some Philips and Siemens tubes are built with the central metal portion of the protective cover sealed to the glass, the cover not being intended to be removed. On the other hand, a General Electric XP tube will slip out of its cover easily.

These covers serve several purposes. (1) By surrounding the tube with a grounded conducting cover, they make it impossible for the user to be electrocuted by the high voltage, which is supplied through shockproof cables. (2) By the use of lead in the cover, the intensity of the x-rays radiating in other directions than through the window is reduced, sometimes enough to afford very good protection to the operator from x-rays, and sometimes not. (3) They often serve to redistribute the electrostatic field about the glass tube inside in such a way that the tube can withstand a higher voltage with the cover on than off. This redistribution of the field frequently makes it unnecessary to have the glass tube swell out into a large bulb in the center, as with most unprotected tubes. This has the advantage of enabling one to work close up to the focal spot with diffraction cameras, etc., where the rays are intense (inverse-square law). The purpose of the bulb in unprotected tube is to reduce electronic bombardment of the glass and consequent charging up of the glass, which is likely to puncture it or to disturb the focusing of the cathode rays. (4) Shockproof covers sometimes serve as containers of transformer oil or cooling oil, which cools the whole tube and at the same time improves the insulation so that the length of the tube for a given high voltage may be considerably less than that required for an unprotected tube capable of withstanding the same voltage.

e. *The Oxtail Tube and the Lilienfeld Tube.* In the European oxtail tube<sup>1</sup> the cathode-ray beam is focused so that it passes down a metal tube several inches long to the target at the far end (Fig. 7-3). The focusing is accomplished and controlled in part by a "magnetic lens,"

<sup>1</sup> Footnote 3, p. 106.

“focusing coil.” This is a wire coil wound around the tube body, its axis coinciding with the tube axis. A steady direct current through such a coil serves to focus the cathode rays much as an ordinary lens focuses light rays. A coil used in this way is called a magnetic “electron lens.”

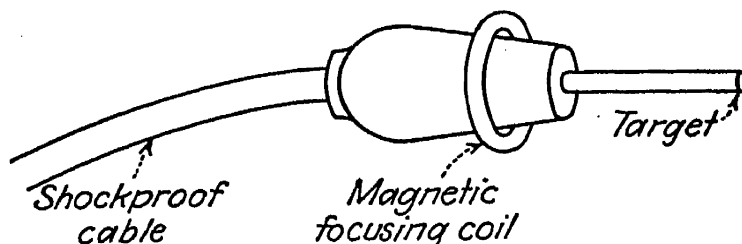


FIG. 7-3.—European oxtail tube.

A tube of this type necessarily operates with the anode (target) grounded. The high negative potential is supplied to the cathode through a shockproof cable, as shown in Fig. 7-3. Besides the added complexity of the magnetic focusing, there is the disadvantage that the x-ray intensity attainable with this type of tube compares unfavorably with that produced by a conventional tube. This may explain why this type of tube has never been used widely in the United States.

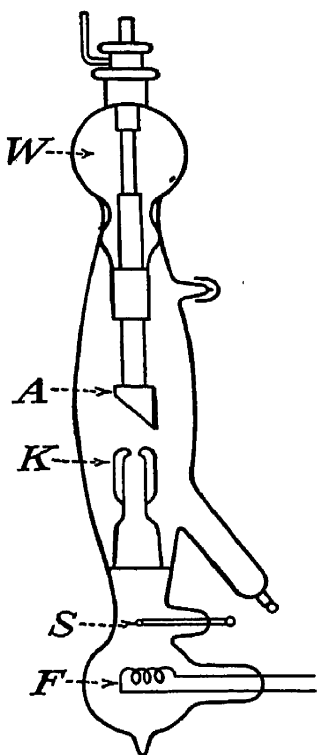


FIG. 7-4.—Lilienfeld tube, formerly popular in Europe.

The Lilienfeld tube was formerly popular in Europe. An early model of this type is represented in Fig. 7-4. Instead of a simple cathode, the tube was provided with an “electron gun,” somewhat similar to those used in cathode-ray oscillograph tubes. The hot filament *F* served as the electron source, and the electrons were given a preliminary acceleration by the auxiliary electrode *S* before emerging through the hole in the cathode *K*. The gun focuses the electron beam electrostatically.

An experimental gun-type tube has been described recently by McCue.<sup>1</sup> The chief advantages of a gun-type tube are (1) electrical control of the focal-spot size; (2) reduction of target contamination by evaporation; (3) ability to operate at low voltages such as 5 kv. At such low voltages, space charge often limits the electron current to a very low value in Coolidge-type tubes. On the other hand, the Coolidge type is simpler, and the auxiliary electric circuits needed for an electron gun are eliminated.

*f. Stray Radiation.* Tests have shown that, even in well-designed tubes, only about 80 per cent of the x-rays are generated in the focal

<sup>1</sup> J. J. G. McCue, *Rev. Sci. Instruments*, **14**, 339 (1943).

spot. The other 20 per cent or so originate from the sides and back of the target and other portions outside the focal spot. This "stray radiation" is probably generated by electrons that have hit the focal spot and have been scattered there and by secondary electrons that the primaries knock out of the target within the focal spot. These scattered and secondary electrons fly out of the focal spot and rain down upon other parts of the anode, generating x-rays that are softer than those generated at the focal spot.

*g. Tube Rating and Tube Life.* X-ray tubes are usually rated, first, for maximum voltage. This depends upon the tube length, insulation, shape, type of protecting case (if any), whether immersed in oil or not, and similar factors. If a tube rated at 100 kv. is used at 200 kv., it will probably flash over, puncture, or go "gassy" or the filament will collapse from electrostatic forces. Similar failure is to be expected if a tube rated at 100 kv. when immersed in oil is operated at 100 kv. not immersed. The abbreviation "kv.p." or "kv.c." (kilovolts peak or kilovolts crest) is frequently used in rating a tube. This serves to remind the user that this rating is not to be confused with the "kilovolts" supplied by the secondary of a high-voltage transformer. The voltage of an a.c. source ordinarily varies in a sinusoidal way with time, and the value assigned to it is ordinarily the r.m.s. (root mean square) value. Thus, when one says that his house is supplied with 110 volts a.c., he means that an incandescent lamp on the circuit glows just as brightly as it would if supplied with 110 volts d.c. Nevertheless, the a.c. voltage supplied to the lamp varies from  $-156$  to  $+156$ , and it is this maximum voltage which is considered in the voltage rating of an x-ray tube. Hence a 70-kv. (r.m.s.) transformer will supply all the voltage which a 100 kv.p. x-ray tube is intended to withstand. However, transformers built for x-ray service are usually rated in terms of maximum voltage rather than r.m.s. voltage as is usual for other transformers. When the x-ray tube is supplied with a steady source of high-voltage direct current, there is no distinction between kilovolts and kilovolts peak.

X-ray tubes are next rated for maximum continuous power input. This depends upon the provision for cooling the target. For example, a tube may have a continuous rating of 5 ma. at 200 kv. or 10 ma. at 100 kv., either figure representing a power input of 1 kw. if the high voltage is continuous direct current. This cannot be carried to extremes, however. For example, if one attempted to operate such a tube at 5 kv. with a tube current of 200 ma., he would only melt the filament because it was not designed to emit such a large electron current, even though the tube power rating would not be violated. In fact, one is likely to find it impossible to attain a tube current of even 1 or 2 ma. when the tube voltage is reduced to only 10 or 15 kv. Such low voltages permit a

"space charge" (page 121) to build up so that the tube current is limited to 1 ma. or less, even though the filament heating current is increased until the filament melts. A tube designed to be cooled from an external water or oil supply will quickly fail if operated at its rated capacity with the water or oil cut off.

Most tubes may have their power rating considerably exceeded for a short time. For example, one particular tube rated at 100 kv.p., 6 ma. continuous, may be operated at 100 kv.p., 10 ma. for 50 sec., or 100 kv.p., 15 ma. for 20 sec. or 100 kv.p., 20 ma. for  $2\frac{1}{4}$  sec., or 50 kv.p., 40 ma. for  $2\frac{1}{4}$  sec., etc. During the

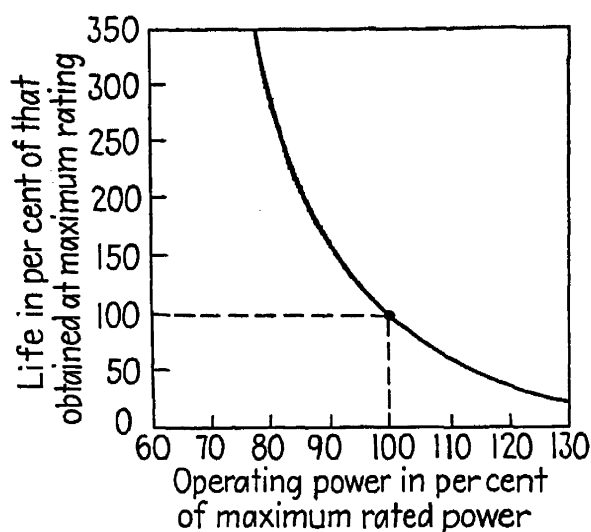


FIG. 7-5.—X-ray tube life as a function of power used in its operation.

overload the target heats up because it is absorbing energy faster than it can get rid of it, but the excess energy is stored as heat in the target. If the time is short enough so that the temperature does not reach the danger point, no harm is done. Such overloads cannot be applied safely one after the other, of course, unless the tube is shut off between times long enough to cool to a temperature that will be a safe starting point for the next overload, which must not produce a dangerous final temperature.

Some tubes have their maximum power rating based, not upon the rate at which the target can be cooled, but upon the rate at which the target metal can conduct the heat away from the focal spot and distribute it through the whole mass of the target. Rotating anode tubes are in this class. If such a tube is rated at 10 kw., it is likely to be ruined by a power input of 20 kw., even if only for a second.

The power rating also depends upon the type of circuit in which the tube is to be used. For example, one particular typical tube is rated at 220 kv.p., 20 ma., when used in a circuit provided with rectifiers but no smoothing condensers. Nevertheless, the rating of this tube is only 200 kv., 18 ma. when used in a constant-potential direct-current (c.p.d.c.) circuit. This is because the average voltage is only a fraction of the peak voltage in pulsating d.c. operation, but in c.p.d.c. operation the average voltage is practically identical with the peak voltage. This will be discussed further in Sec. 11e.

The life of a well-made tube used at its full power rating is usually a matter of several thousand hours. This can be reduced to almost nothing by overloading the tube, even 50 per cent, as indicated in Fig. 7-5. It can be increased manyfold by operating the tube below its rated power, as indicated.

If the tube is required to rectify its own current, either wholly or partly, that is, if it is subjected in service to a high inverse voltage making the anode negative and cathode positive, the tube life is noticeably reduced. If the high-voltage circuit includes rectifiers so that the tube is subjected to a pulsating d.c. voltage only, tube life is as long under those conditions as any. If the tube is supplied with a steady high-voltage c.p.d.c. approximating that from a high-voltage battery, tube life is shorter than with pulsating d.c. This point is further discussed on page 135.

Tubes that are operated conservatively so that their voltage or power ratings are never exceeded usually are eventually retired from service because of excessive pitting, checking, or cracking of the target at the focal spot. The rapid and extreme changes in temperature at this spot cause the metal to crack and chip or to melt locally so that eventually a bad pit results.<sup>1</sup> The x-rays generated in the pit are absorbed by the surrounding target metal instead of radiating outside as desired, and the loss of efficiency eventually becomes serious enough for the tube to be discarded. If the tube is not retired for this reason, the cathode filament will eventually fail, like the filament in an incandescent lamp.

*h. Million-volt Tubes.* The recently developed million-volt General Electric tube is located within the high-voltage transformer that energizes it, the tube axis coinciding with the transformer axis. The tube rectifies its own current. It is built in 12 sections, glass tubing alternating with Fernico rings. Fernico is an alloy having a coefficient of expansion near that of glass. By connecting each ring to taps from the transformer secondary winding, each section is required to withstand just one-twelfth the total potential drop. In tubes built in one section, the potential drop is ordinarily nonuniform along the tube length, and this makes such tubes impractical for potentials as high as 1 million volts. The inside walls of the glass sections are sandblasted further to equalize the voltage gradient in each section. The tube is permanently evacuated and sealed off.

Both tube and transformer are enclosed within a steel tank containing Freon ( $\text{CCl}_2\text{F}_2$ ) under a pressure of 50 or 60 lb./in<sup>2</sup>. This vapor mixed with air is superior to air alone as an insulator. The target is grounded and is made of a tungsten disk set in copper. The disk is thin enough so that part of the useful x-rays escape laterally in the usual way but the rest pass through and escape in the direction of travel of the cathode rays. The 2-million-volt x-ray tubes recently developed by General Electric and by Machlett (Fig. 7-6) follow this same general design.<sup>2</sup>

<sup>1</sup> See F. R. Abbott, *J. Applied Phys.*, **13**, 384 (1942).

<sup>2</sup> See *J. Applied Phys.*, **16**, 314 (1945).

The use of Freon under pressure in a tank to serve as insulation for potentials running to millions of volts was demonstrated in the Wisconsin electrostatic generator in 1937.<sup>1</sup> Such generators have been used with multisection x-ray tubes to produce x-rays at potentials up to 2 million



FIG. 7-6.—Two-million-volt multisection x-ray tube. (Courtesy of Machlett Laboratories.)

volts<sup>2</sup> by Van Atta and Northrup, who found that at 2 million volts the radiation is three times as intense (at a given tube current) and four times as penetrating as at 1 million volts.

**5. Cathode-ray Tubes.** If the cathode rays in an evacuated tube are directed against a very thin place in the tube wall, they can be made

<sup>1</sup> C. M. Hudson, L. E. Hoisington, and L. E. Royt, *Phys. Rev.*, **52**, 664 (1937); D. B. Parkinson, R. G. Herb, E. J. Bernet, and J. L. McKibben, *Phys. Rev.*, **53**, 642 (1938).

<sup>2</sup> L. C. Van Atta and D. L. Northrup, *Am. J. Roentgenology Radium Therapy*, **41**, 633 (1939).

to penetrate it and escape into the air outside. Their energy is rapidly dissipated in ionizing the atoms composing the air. Even 200-kv. cathode rays travel only a few inches. An early low-voltage cathode-ray tube of this type was built by Lenard<sup>1</sup> in 1894. It must necessarily have produced x-rays when he operated it, but they escaped his notice.

Tubes of this type are manufactured by General Electric,<sup>2</sup> having a window of nickel foil supported against atmospheric pressure by a metal honeycomb grid, and by Westinghouse,<sup>3</sup> having a window of paper-thin glass in the form of a reentrant spherical bulb, which permits it to withstand the pressure. Such tubes are sometimes called "Lenard ray tubes."

Many of the electrons that penetrate these windows suffer elastic or inelastic collisions in doing so and consequently emerge in all directions at all speeds from the maximum down. In addition, a swarm of secondary electrons, mostly of low energy, are knocked out of the window and are present on both sides of it.

Cathode rays in the open air can perform spectacular feats, such as causing calcite crystals to glow brilliantly after a short exposure. It is amusing to hand someone a large calcite crystal that appears to be red-hot but is actually stone-cold. Little practical use has been found for cathode rays at voltages up to several hundred kilovolts. They can produce vitamin D from ergosterol,<sup>4</sup> but this can be done very much more efficiently and cheaply with ordinary ultraviolet radiation. Recently, cathode rays have been projected into the open air in this manner at  $1\frac{1}{4}$  million volts,<sup>5</sup> and Kerst's betatron is capable of projecting a 20-million-volt cathode-ray beam into the air. These supervoltage cathode-ray beams appear to have promising possibilities in therapeutic work, which will be discussed in Chap. 11.

**6. High-voltage Rectifier Tubes—Kenotrons—Valves.** The rectifying action of Coolidge-type x-ray tubes has already been explained in Sec. 2-5. If a high-voltage diode (a diode is a two-electrode vacuum tube) is built primarily to serve as a rectifier rather than as an x-ray generator, then it is commonly called a "kenotron." Kenotron is a trade name that, strictly speaking, is applicable only to high-voltage rectifier tubes made by the General Electric Company, but like other popular trade names it has come into general use for any such tube. Tubes of this type are also often called "valve tubes," probably by

<sup>1</sup> P. Lenard, *Ann. Physik Chem.*, **51**, 225 (1894).

<sup>2</sup> W. D. Coolidge, *J. Franklin Inst.*, **202**, 693 (1926).

<sup>3</sup> C. M. Slack, *J. Optical Soc. Am.*, **18**, 123 (1929).

<sup>4</sup> R. M. Hoffman and F. Daniels, *J. Biol. Chem.*, **115**, 119 (1936).

<sup>5</sup> J. G. Trump, R. J. Van de Graaff and R. W. Cloud, *Am. J. Roentgenology Radium Therapy*, **43**, 728 (1940).

analogy with a check valve, which allows water or other fluid to flow in one direction through it, but not in the other.

Kenotrons are widely used in the electric circuits that are provided to supply the high voltage for x-ray tubes. High-voltage rectifier tubes have had a history generally parallel to that of the x-ray tube. In the days of gas-filled x-ray tubes, there were gas-filled high-voltage rectifier tubes, but these have been supplanted by the hot-cathode type, much as gas x-ray tubes have been supplanted by Coolidge-type tubes.

The outer glass envelope of a kenotron is much like that of an unprotected (nonschockproof) x-ray tube designed for the same voltage. The

cathode is decidedly different, however. It is not intended to focus the electrons it emits but only to emit them, and it is intended to emit them in much greater profusion than an x-ray tube filament. Consequently, the cathode consists of a large rugged tungsten filament that usually requires about 150 watts merely to keep it hot enough to emit; 12 amp. at 12 volts is a common requirement. The electrodes are usually constructed according to one of two general plans, represented

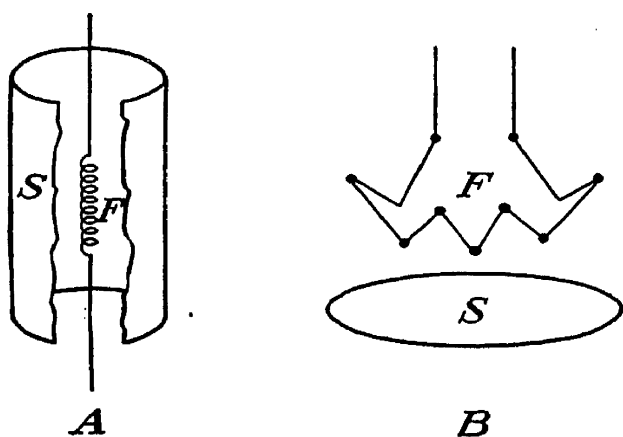


FIG. 7-7.—The two common arrangements of the electrodes in kenotrons. (After Terrill and Ulrey; courtesy of D. Van Nostrand Company, Inc.)

schematically in Fig. 7-7 A and B. In arrangement A, the cathode filament *F* is surrounded by the anode *S* in the form of a hollow cylinder of some high-melting-point sheet metal like tantalum or molybdenum. In arrangement B, the filament *F* is supported in a circular zigzag arrangement above or below the anode, which is merely a flat circular disk of high-melting-point sheet metal. In general, type A is used when the inverse voltage applied to the kenotron does not exceed 100 kv. or so, and type B is used for the higher voltages, but exceptions to this are numerous.

The anode is intended merely to collect the electrons emitted by the cathode and is therefore sometimes called the “collector.” The filament should be big enough and hot enough to emit several hundred milliamperes, but such a current does not ordinarily flow. When the voltage is inverse, that is, when filament is positive and collector negative, no current flows, even though this inverse voltage may be 100 or 200 kv. When the voltage is in the forward direction (filament negative and collector positive), electrons travel from filament to collector and a current flows.

In an x-ray tube, the space current is said to be “emission limited,”



while in a kenotron the current is "space charge limited," as in most radio vacuum tubes. The emission of a kenotron filament is so great that the current is limited by the external circuit, perhaps by an x-ray tube or by the back voltage built up in a condenser, for example. Nevertheless, in order to make any current flow through a kenotron, some voltage is necessary. Suppose the collector is 1 volt positive with respect to the filament. Then if the filament is big enough and hot enough to emit 500 ma. according to equation (2-2), will 500 ma. flow? The answer is no. The reason is that the cloud of electrons on their way from filament to collector carries such a large negative charge, called a "space charge," that the electrons behind them at the surface of the filament are shielded from the positive charge on the collector. Hence the emission is greatly reduced and is said to be space charge limited, although in high-voltage x-ray supply circuits the real limitation on the current flow is in the external circuit, as mentioned above.

In rectifying high-voltage alternating current, during the forward portion of the cycle when the current flows through the kenotron, the transformer may be supplying an e.m.f. of perhaps 200 kv., which is balanced by a potential drop of 198 kv. across the x-ray tube and 2 kv. in the kenotron. Or if a high-voltage condenser is being charged, the current through the kenotron may be quite large at first while the condenser is nearly uncharged; but as the condenser rapidly charges, its back voltage quickly checks the current. In this case, the forward potential drop across the kenotron may reach a high value momentarily during the first part of the charging quarter cycle, but the average drop in the forward direction (while current is flowing) for a complete cycle will not exceed a few kilovolts if the circuit is properly designed and operated.

In view of the possibility of momentary forward potential drops of several kilovolts across kenotrons, it is possible for them to generate soft x-rays under certain conditions. It is therefore strongly advisable to check this by placing small wrapped-up x-ray films in their vicinity as suggested in Chap. 10. If x-rays are detected, it may be possible to eliminate them by increasing the filament heating current. If the full rated heating current is reached and x-rays are still being generated, then the kenotrons should be surrounded with  $\frac{1}{16}$ -in. sheet lead to protect those in the vicinity. The lead must not be close enough for the high voltage to spark across to it or set up a corona discharge; but, aside from this limitation, it should be as close to the tubes as practical so as to economize on the lead required and at the same time afford adequate protection. The life of a kenotron is greatly reduced and excessive and dangerous x-rays are generated if the filament current is so low that the tube operates emission limited continuously.

One manufacturer gives the following data for a particular type and

size of kenotron: If the tube current is never to exceed 30 ma., then 11.8 amp. of filament heating current at 12.0 volts is sufficient. By increasing this to 16.0 volts and 14.0 amp., the kenotron will carry a full ampere, not continuously, but during the early stages of charging a condenser, for example, probably without generating x-rays enough to require protection with lead. The kenotron tube life will be much shorter with its filament as hot as this than if it could be operated at the lower temperatures, for example with a filament heating drop of 12 volts. The collector should not become red-hot in service. If it does, the tube is probably operating emission limited.

Kenotrons are rated, first, for maximum inverse voltage. A 200 kv.p. kenotron will safely withstand a maximum (not r.m.s.) voltage of 200 kv. when the filament is positive and collector negative, without passing any appreciable current. High-voltage kenotrons are longer and larger than those for lower voltages. They are rated next for the maximum electron current they will safely carry in the forward direction. The filaments are usually heated from a transformer, and the volts and amperes required for this are stated in the usual r.m.s. values. Transformers for heating kenotron filaments must be of a special type and will be discussed in the next section.

**7. Filament Transformers.** The filaments of Coolidge-type x-ray tubes and cathode-ray tubes (see Sec. 5) usually require 3 or 4 amp. at about 6 volts to heat them, and kenotron filaments usually require 12 to 15 amp. at 12 to 16 volts. At first thought, a transformer to supply these requirements seems very simple and ordinary. However, in most cases, the x-ray tube, cathode-ray tube, or kenotron will be placed in a high-voltage circuit arranged in such a way that the filament will be at a high potential above or below ground. Consequently, if an ordinary transformer were used to heat it, the high voltage would jump across from its secondary to its primary, which is of course connected to an ordinary commercial power line at ground potential.

Therefore the primary and secondary windings of such a transformer must be insulated from each other to withstand 100 or 200 kv. or whatever the maximum filament potential may be in the particular circuit used. Such transformers are manufactured commercially, usually with the windings immersed in transformer oil contained in a closed metal case, with the filament leads brought out through a high-voltage insulator bushing.

Filament transformers are one item of equipment that can often be built more cheaply in an ordinary shop by unskilled workmen than they can be bought factory-made. A common homemade type is shown in Fig. 7-8. The primary *P* has a core *C* built up of strips of transformer (silicon) steel, 29 gauge, 2 or 3 in. wide, and 8 or 10 ft. long. The core

will be an inch or so thick when completed. Wrapped around the core and insulated from it (for 220 volts) is the primary winding *W*, of copper wire, about 16 or 18 gauge. The secondary *S* is a ring interlocked with the primary ring. It consists of a few (20 to 50) turns of heavy (5 to 8 gauge) copper wire. The two rings should be of equal inside diameter, and the radius of each should be larger than the minimum air gap that the high voltage will jump, figured for, say, 2-in. spheres. When completed, the two rings are supported at right angles to each other with maximum clearance between rings by fastening them with tape or cord to a wooden support made of well-seasoned shellacked wood free from nails or screws (see Fig. 7-26).

It is not difficult to design such a transformer in a few hours with the aid of a 25-page pamphlet by Herbert B. Brooks, entitled "Information for the Amateur Designer of Transformers for 25 to 60 Cycle Circuits" available from the Superintendent of Documents, Washington, D.C. Such a transformer should cost about \$50 for material and labor, whereas factory-built oil-immersed ones usually cost from \$200 up.

In the case of x-ray tubes and cathode-ray tubes, the filament heating current is controlled by a rheostat in series with the primary of the transformer, plus any voltage regulator that may be incorporated to compensate for fluctuations in the line voltage. With kenotrons, the transformer should be designed exactly to meet the filament requirements, so that the primary may be connected directly to the power line and the secondary directly to the filament without any rheostats. After such a transformer is built, it may be found that the primary requires 230 volts, for example, instead of the 220 it was intended to use, in order to supply the kenotron filaments with the correct voltage and current. This small discrepancy may be corrected by energizing the primary of the filament transformer from properly chosen taps of the autotransformer, which is nearly always used for regulating the main transformer primary voltage (see Sec. 12).

An unsatisfactory alternative to the filament transformer is the insulated storage battery. X-ray tubes may have their filaments heated by a storage battery and rheostat, both mounted on a special highly insulated pedestal, the rheostat being controlled by means of a long glass or Bakelite rod. If the tube is operated only in the daytime, the battery or batteries may be charged during the night. Kenotron filaments require so much power that battery heating is impractical.

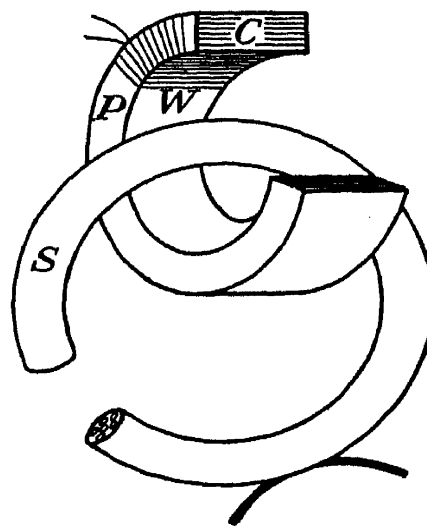


FIG. 7-8.—Showing construction of simple home-made filament transformer.

**8. Mechanical Rectifiers.** As an alternative to the high-voltage vacuum-tube rectifiers discussed in Sec. 6, there is the mechanical high-voltage rectifier. In Fig. 7-9, suppose the sine wave represents the alternating high voltage between the terminals of the secondary of a step-up transformer. If this is to be used to operate an x-ray tube, it might be connected directly to the tube, thus required to rectify its own current. In this case, the tube would generate x-rays only during the intervals *PQ*, *RS*, *TU*, etc., and remain idle during the intervals *QR*, *ST*, etc. Furthermore, during the intervals *PA*, *BQ*, *RE*, *FS*, *TI*, *JU*, etc., the average voltage applied to the tube would be low so that the principal product during these intervals would be heat in the target, rather than x-rays. X-rays would be generated chiefly during the intervals *AB*, *EF*, *IJ*, etc.

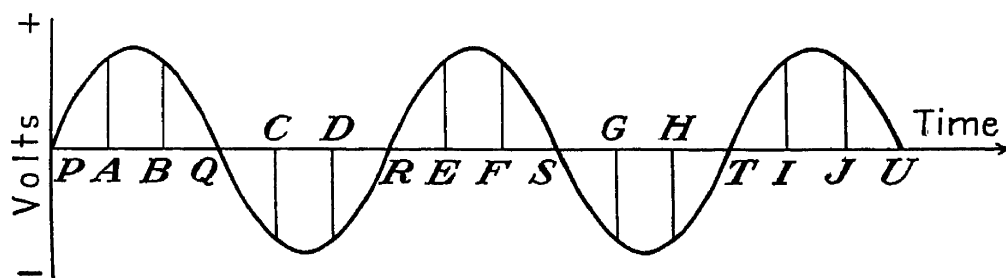


FIG. 7-9.—Illustrating mechanical rectification of high voltage.

Next, suppose that an ordinary reversing switch is placed in the high-voltage line between transformer and tube. One may imagine such a switch left open from *P* to *A*, closed at *A* so as to make the cathode negative, and left closed to *B*; opened from *B* to *C*, closed in the reverse direction at *C* (but since the transformer voltage has meanwhile reversed, too, the cathode will again be negative), and left closed to *D*; opened from *D* to *E*, closed in the first direction from *E* to *F*, opened from *F* to *G*, closed in the reverse direction from *G* to *H*, etc. Such a procedure would cause the x-ray tube to generate x-rays efficiently during the intervals *AB*, *CD*, *EF*, *GH*, *IJ*, etc., and to spend the remaining time cooling off, and at no time would it be subjected to an inverse voltage.

If a switch is to be manipulated 240 times each second, it is obvious that the usual hand-thrown knife switch must be modified to some form such as a commutator and brush arrangement. Furthermore, if the switch is to be operated in synchronism with the alternations of the (60-cycle, say) power supply, it must be driven by a synchronous electric motor energized from the same a.c. supply. In addition, if the switch is connecting and disconnecting circuits in which the potentials are many kilovolts, the various poles and switch arms or segments must be well insulated and adequately separated from each other and from the driving motor, and they should be free of edges, corners, and points, to reduce corona loss. Such a rotary mechanical full-wave high-voltage rectifier

for x-ray circuits is commonly called a "Snook rectifier" because the first one was supposedly built by C. S. Snook in 1908.

Such rectifiers are driven at 1,800 r.p.m. or 30 r.p.s. (revolutions per second) for 60-cycle alternating current, and they have four arms or disks that come into close proximity (say  $\frac{1}{8}$  in.) at their periphery with eight stationary metal shoes. The high voltage used jumps these small gaps almost as easily as if actual contact were made, as in a commutator and brush arrangement, although the gaps do introduce a high-frequency ripple which is superimposed upon the 120-cycle pulsating direct current supplied to the tube.

Although Snook rectifiers are noisy ozone producers with moving parts and are not well adapted to circuits using condensers to smooth out the pulses, they are rugged, dependable, and comparatively inexpensive. They are used fairly widely in radiographic and therapeutic work without condensers as full-wave rectifiers furnishing pulsating direct current. Mechanical rectifiers are seldom used in x-ray circuits including smoothing condensers (see Sec. 11e), because in such cases the timing of the rectifier must be carefully adjusted to avoid destructive surges. When this is accomplished for a given load, then an increase or decrease in the load usually results in surges again. Hence such an arrangement is not recommended except where a Snook rectifier is already available and the work will not require wide variations of tube current and voltage.

**9. Main Transformers.** Modern practice is to use high-voltage transformers as the high-voltage supply for x-ray tubes, perhaps with auxiliary equipment such as rectifiers and condensers to rectify and smooth the tube voltage. Early workers used induction coils supplied with direct current through an interrupter, but such equipment is now obsolete. Some precision work, such as the determination of  $h/e$  from the Duane-Hunt limit, for example, may warrant the use of such remarkable devices as a 50,000-volt storage battery to supply an x-ray tube, but at least 99 per cent of the world's x-ray tubes are energized from transformers today. The Van de Graaff generator<sup>1</sup> may offer the transformer some future competition, but as yet it is only a threat.

Most x-ray transformers are single-phase iron-core transformers with the windings immersed in oil in a metal tank for insulation. In the United States, 60 cycles is the most common frequency, but higher frequencies such as 500 or 2,000 cycles/sec. are often used, the primary being supplied with these higher frequencies from a motor generator set. The use of higher frequencies permits the use of smaller (hence cheaper) high-voltage condensers for filtering out the a.c. ripple.

The center of the high-voltage secondary winding is usually grounded to the transformer tank or case so that, if it is a 200 kv. transformer, the

<sup>1</sup> J. G. Trump and R. J. Van de Graaff, *J. Applied Phys.*, **8**, 602 (1937).

secondary leads can be brought outside the tank through two insulator bushings, each designed for 100 kv. An end-grounded transformer, in which one end of the secondary is grounded to the tank and the other brought out through an insulator bushing designed for the full transformer voltage, is much less common and more expensive. If end grounding is necessary, it is possible to use a mid-grounded transformer

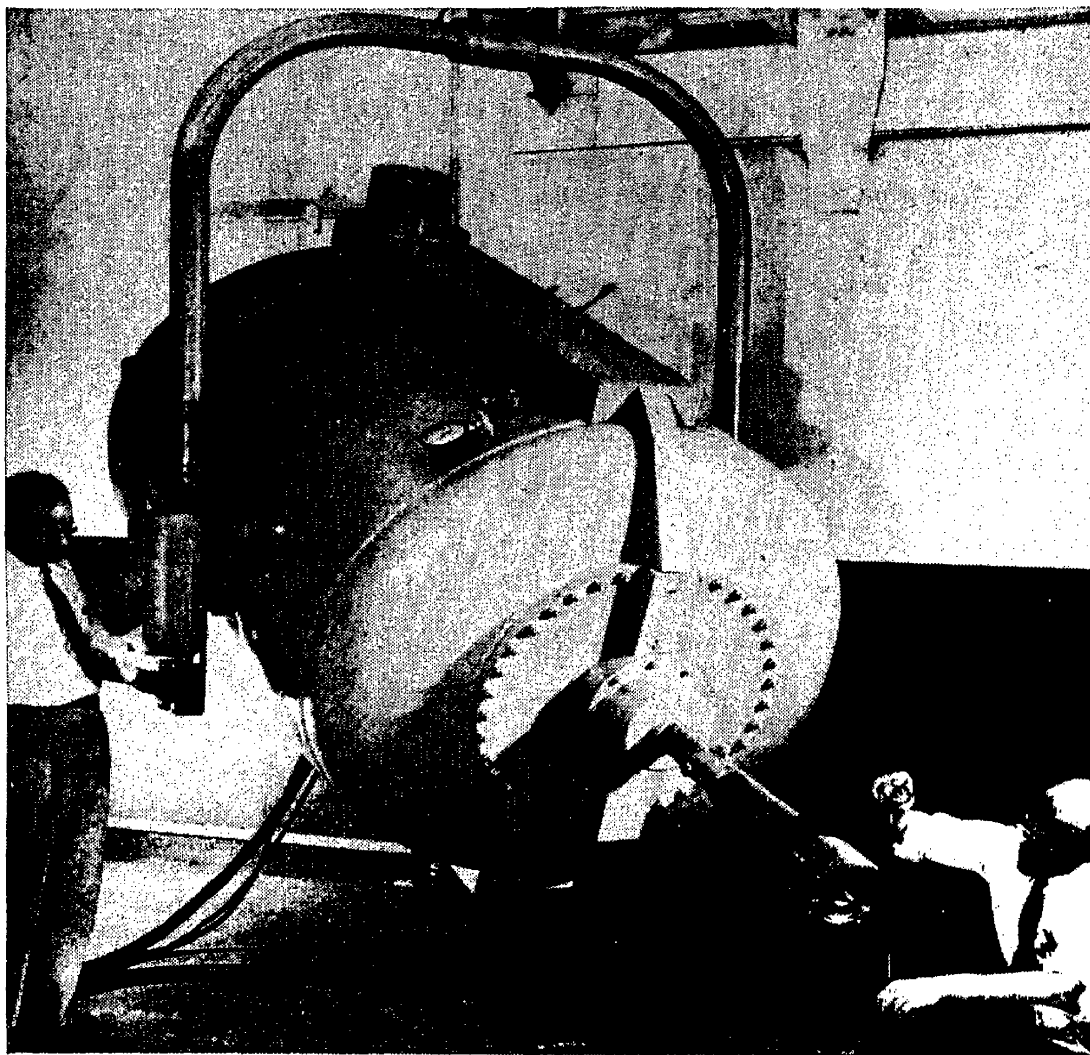


FIG. 7-10.—General Electric 2-million-volt x-ray unit. (Courtesy of General Electric X-ray Corporation.)

and set it on an insulated table, supplying the primary winding with 110 or 220 volts a.c. obtained from a “cascading transformer,” or “insulating transformer.” A cascading transformer is usually a 1 to 1 transformer in which the primary and secondary windings are insulated from each other for high voltages, as in a filament transformer.

X-ray transformers are usually rated primarily for the peak kilovolts (not r.m.s. volts—see Sec. 4g) they are designed to supply. There is ordinarily little if any difference between one designed to supply 5 ma. and one designed to supply 25 ma., for example, because the finest wire that it is practical to use in the secondary winding (No. 40) has a safe current-carrying capacity of some 250 ma.

In such equipment as the new million-volt and 2-million-volt General Electric designs (see Fig. 7-10), the conventional arrangement is not used.<sup>1</sup> The million-volt unit uses an end-grounded air-core transformer, insulated in a tank containing Freon ( $\text{CCl}_2\text{F}_2$ ) under pressure, and the secondary winding, which is built to enclose the x-ray tube, is provided with 11 intermediate taps for distributing the voltage evenly along the multisection tube (see Sec. 4*h*). The transformer is built so as to resonate at a frequency of 180 cycles and is provided with primary voltage of this frequency from a motor generator set. The high-voltage end of the secondary is provided with an auxiliary winding to heat the x-ray tube filament, the current being regulated by a variable reactor controlled by means of a long glass rod rotated by a small filament-control motor. The newer 2-million-volt model follows the same general design.

A few of the larger manufacturers of x-ray transformers and associated control equipment in the United States, in alphabetical order, are

General Electric X-ray Corp., Chicago, Ill.

Kelley-Koett Mfg. Co., Inc., Covington, Ky.

North American Philips Co., Inc., New York, N.Y.

Picker X-ray Corp., New York, N.Y.

Westinghouse Electric & Mfg. Co., X-ray Division, Baltimore, Md.

Others may be found in MacRae's Blue Book or Thomas's Register of American Manufacturers.

**10. Shockproof Cables.** Shockproof tubes have already been discussed in Sec. 4*d*. There is no advantage in making a tube shockproof if exposed wires carrying high voltage are to be attached to it. In some cases, the x-ray tube and the main transformer are both enclosed in one metal container so that only low-voltage wiring is needed outside the container. This results in a heavier, bulkier, less flexible unit than a shockproof x-ray tube alone.

For voltages up to 250 kv., it is common practice to transmit the high voltage to a shockproof x-ray tube through shockproof cables. These are cables having an outer flexible metal sheath that is grounded. The high-voltage wire passes through the center and is insulated from the metal sheath by some material such as rubber or oil-impregnated varnished cambric. The metal sheath is usually made of stranded woven wire braid. The diameter of such cables is surprisingly small. It does not exceed  $1\frac{3}{4}$  in., even for a 220-kv. tube. Of course, such tubes are nearly always operated mid-grounded, so that the cable insulation is required to withstand only half the tube voltage. The cables are ordinarily several feet long, and with a length as great as this their

<sup>1</sup> E. E. Charlton and W. F. Westendorp, *Gen. Elec. Rev.*, **44**, 654 (1941) (1-million-volt unit); *Electronics*, **17**, 128 (December, 1944) (2-million-volt unit) *Science News Letter*, Oct. 14, 1944, p. 243, Oct. 21, 1944, p. 263.

flexibility is quite satisfactory. Occasionally they fail electrically in service but one manufacturer claims that in severe industrial work the need for replacement averages less than 2 per cent per year.

Such cables, consisting of two conductors separated by a dielectric, introduce an appreciable capacitive load on the high-voltage power supply. This may decrease the power factor slightly and so impose a somewhat higher thermal load on the transformer, but Rogers<sup>1</sup> has found that in such cases the x-ray output is increased more than enough

to offset this. The capacitive effect of the cables on the x-ray output rarely exceeds a few per cent and often increases it. The effect depends upon the cable length, the voltage, the current, and the type of high-voltage circuit used.

### 11. A Few Common Circuits.

In high-voltage circuits, brass tubing having a diameter large enough to prevent corona loss is the usual

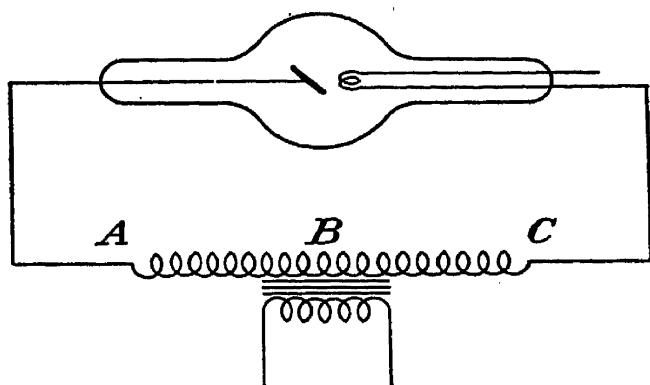


FIG. 7-11.—Self-rectification.

conductor playing the role of wire in low-voltage circuits.

*a. Self-rectifying Circuit.* The simplest circuit is one in which the secondary of the transformer is connected directly to the x-ray tube, as shown in Fig. 7-11. In the case of diffraction tubes, such a circuit is usually end-grounded at A, the anode end. In other cases, the circuit is usually mid-grounded (at B). The tube rectifies its own current.

The advantages of the circuit are its simplicity, compactness, and low cost. There are four disadvantages. First, the full voltage for which the tube is designed cannot be usefully realized. If this voltage is 140 kv., for example, then the e.m.f. developed in the transformer secondary will be applied to the tube on the inverse portion of the cycle, when no current is flowing, and this must not exceed 140 kv. During the useful portion of the cycle, then, when current flows through the circuit, the internal impedance of the transformer secondary subtracts itself from the e.m.f., leaving perhaps only 130 or 135 kv. as the maximum realized at the tube. Second, the tube is idle half the time, during the inverse half of each cycle. This is characteristic of any circuit that gives only half-wave rectification. In order to maintain an average direct current through the tube of 5 ma., the average during the forward half of the cycle must be 10 ma. This, combined with the effects of high inverse voltage, accounts for the third disadvantage, which is a reduction of the length of the life of the tube as compared with that realized with various other circuits. Fourth, during the forward portion

<sup>1</sup> T. H. Rogers, *Radiology*, **32**, 202 (1939).



of the cycle, the average voltage on the tube is only  $2/\pi$ , or 63.6 per cent of the maximum reached during the forward half cycle, this maximum in turn being necessarily less than the rated tube voltage. Thus the average useful voltage is only a little over half the rated tube voltage. Consequently, the x-ray production is inefficient [see equation (3-11)].

*b. Primary Rectification.* In 1930, Kearsley<sup>1</sup> described a circuit that is rather widely used today. It alleviates to some extent the first, third, and fourth disadvantages of the self-rectifying circuit mentioned in Sec. 11a.

This circuit is shown in Fig. 7-12. *R* is a tube rectifier of the Tungar<sup>2</sup> or Rectigon<sup>2</sup> type. This type of tube is designed to rectify much larger currents than a kenotron (Sec. 6) at a much lower voltage. Instead of a high vacuum, it contains argon at a pressure of about  $\frac{1}{15}$  atm. The cathode is a rugged tungsten filament, as in a kenotron, but the anode is usually made of graphite. The argon positive ions neutralize most of the space charge discussed in Sec. 6, permitting the passage of a heavy current with only small loss. A Tungar or Rectigon tube will withstand an inverse voltage of only a few hundred volts; a higher voltage causes the argon to break down, and an arc discharge in the wrong direction results. This limitation is no handicap when the tube is used in a 110- or 220-volt circuit as shown in Fig. 7-12. A slight voltage (say 10 or 20 volts) is also required to start the current in the normal direction because it is really carried through the tube in the form of an arc discharge. A typical tube has the following characteristics: filament heating voltage, 2.2; filament heating current, 18 amp.; maximum tube current (in forward direction), 6 amp.; maximum voltage drop in forward direction, 90; maximum inverse voltage, 375; over-all length of tube,  $6\frac{3}{4}$  in.

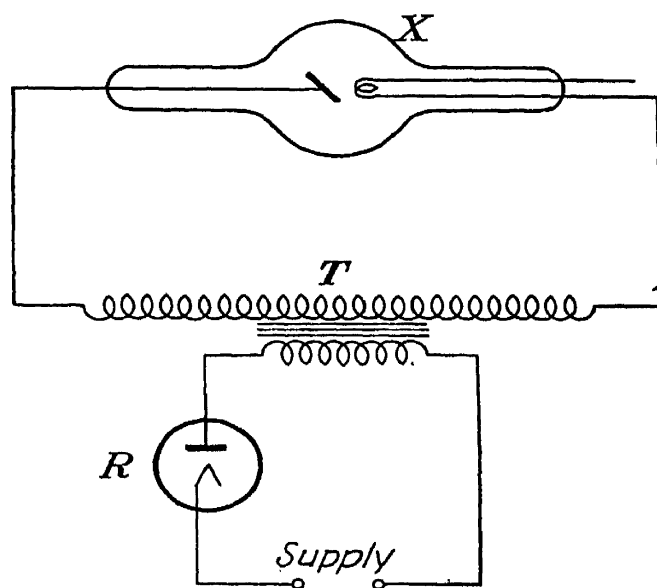


FIG. 7-12.—Primary rectification.  
(Kearsley.)

In Fig. 7-12, it is necessary to connect the rectifier *R* and the x-ray tube *X* so that the current flows in both on the same half wave; that is, the anodes of both tubes must have the same polarity at the same instant. Kearsley gives the following figures regarding the operation

<sup>1</sup> W. K. Kearsley, *Gen. Elec. Rev.*, **33**, 572 (1930).

<sup>2</sup> Tungar is a trade name used by the General Electric Company, and Rectigon is a trade name used by Westinghouse Electric & Mfg. Co.

of the x-ray tube in this circuit, as compared with the simple circuit of Fig. 7-11:

Without the rectifier (Fig. 7-11), in order to obtain a useful tube voltage of 85 kv. at an average tube current of 30 ma., the tube had to withstand an inverse voltage of 92 kv., whereas with the rectifier (Fig. 7-12) the inverse voltage was only 87.5 kv. at 30 ma. Or whereas the circuit of Fig. 7-11 would produce a tube current of only 30 ma. without dropping below a useful voltage of 85 kv. forward and 92 inverse, the circuit of Fig. 7-12 produced a tube current of 80 ma. at 85 kv. useful and 91 inverse.

Oscillograph tracings of the primary voltage and current and secondary current, obtained by Kearsley, are shown in Fig. 7-13. Although

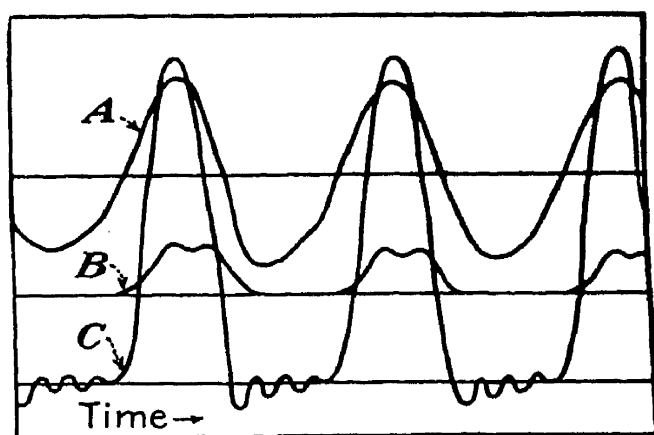


FIG. 7-13.—Oscillogram from Kearsley circuit (Fig. 7-12). A, primary voltage, 240 v. B, primary current, 50 amp. C, secondary current, 80 ma.

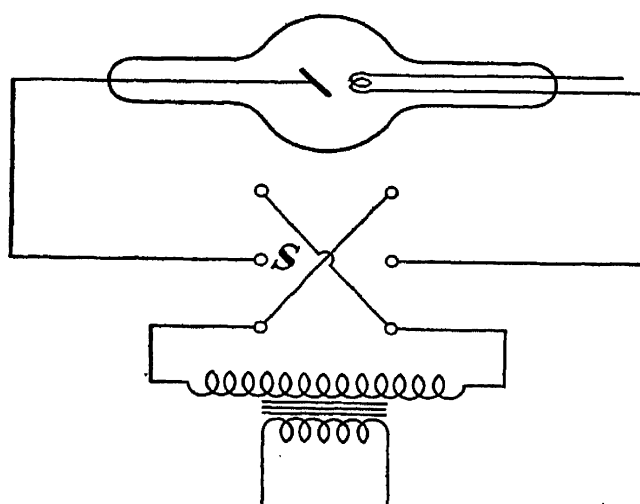


FIG. 7-14.—The principle of the mechanical rectifier.

this circuit reduces the difference between inverse and useful voltage, increases tube life, and brings the average forward voltage nearer to the maximum forward voltage, as compared with the circuit of Fig. 7-11, it still leaves three things to be desired: (1) elimination of inverse voltage; (2) elimination of idle time on the inverse half cycle; (3) the average useful forward voltage should be closer to the maximum voltage for which the tube was designed so as to increase the efficiency.

This circuit may be operated either mid-grounded or end-grounded, but in the latter case the transformer must be designed for such service, or a cascading transformer must be provided (see Sec. 9).

*c. Mechanical Rectification.* The Snook-type rectifier has already been discussed in Sec. 8. It is mentioned again here because it is a practical alternative to the various tube circuits to be discussed in this section. The essentials of the Snook circuit are shown in Fig. 7-14, where *S* is a synchronous high-speed high-voltage reversing switch. It should be kept in mind that it is a full-wave rectifier, eliminating all

inverse voltage and using the most efficient part of each half cycle. The average useful voltage is a large fraction of the maximum voltage, although the tube is idle more than half the time.

*d. The Villard Circuit.* The Villard circuit is the first "voltage-doubling" circuit that has been mentioned. A voltage-doubling cir-

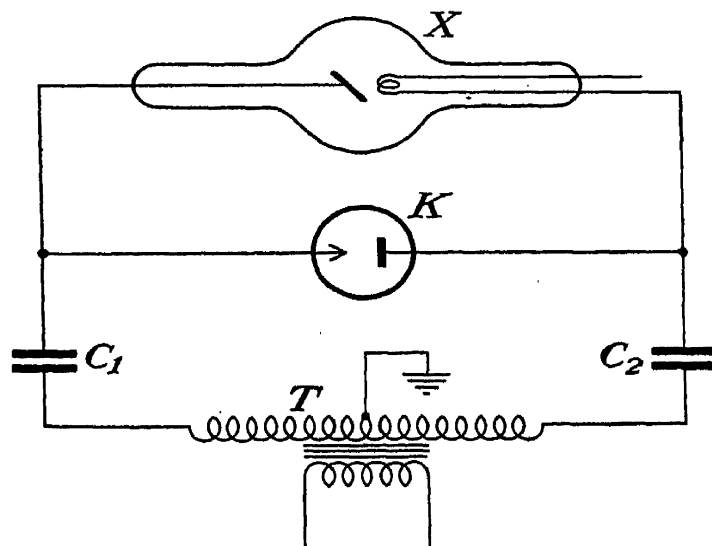


FIG. 7-15.—Villard circuit with one valve.

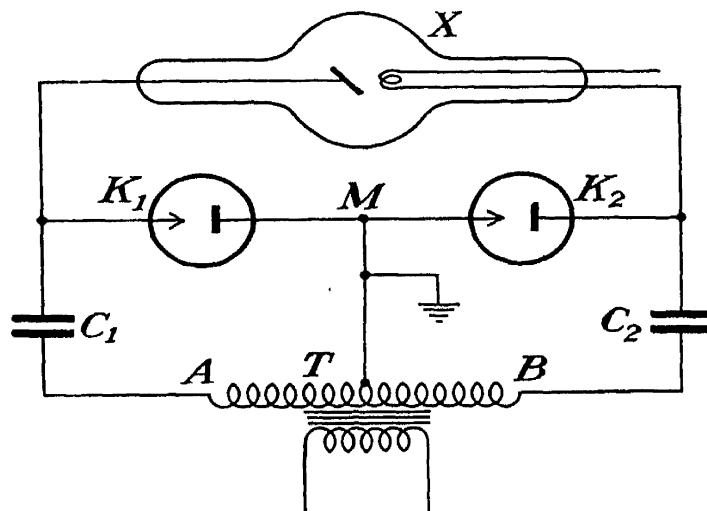


FIG. 7-16.—Villard circuit with two valves.

cuit is one in which the voltage applied to the x-ray tube has a peak value approximately twice the maximum supplied by the transformer. Although the Villard circuit is very old, being first devised in 1901,<sup>1</sup> it is still one of the most popular. It is shown in its simplest form in Fig. 7-15.

In practice, the single kenotron  $K$  is often replaced by two smaller ones, as shown in Fig. 7-16, in which case the wire between them is connected to the mid-grounded transformer case, as shown. Although the circuit of Fig. 7-16 is slightly more complex than that of Fig. 7-15, its action is easier to follow, and therefore it will be discussed first.

<sup>1</sup> P. Villard, *J. Phys.*, **3**, 28 (1901).

Assume that  $T$  is a 100 kv.p. transformer. At the start of the a.c. cycle, points  $A$  and  $B$  are at the same potential. One quarter cycle later,  $A$  has a potential of  $-50$  kv. and  $B$  a potential of  $+50$  kv. with respect to ground. The electrons that flowed onto the lower plate of condenser  $C_1$  caused an equal number to flow off the upper plate by repulsion, and these flowed through the valve  $K_1$ . The electrons that flowed off the lower plate of condenser  $C_2$  caused an equal number to flow onto the upper plate, and these were supplied through the valve  $K_2$ . The potential of the upper plates of  $C_1$  and  $C_2$  is approximately zero at the end of this first quarter cycle because the current has been flowing forward through the valves; under these circumstances they have low resistance, and both are connected to ground. The potential of the lower plates is of course  $-50$  kv. for  $C_1$  and  $+50$  kv. for  $C_2$ . During this first quarter cycle, the potential on the x-ray tube has remained approximately zero (actually, it may reach 2 or 3 kv. inverse, owing to the drop in the kenotrons).

During the second quarter cycle, the lower plates of both condensers return to ground potential; but the upper plate of  $C_1$  is unable to regain its lost electrons, and the upper plate of  $C_2$  is unable to get rid of its surplus through the valves. Hence the end of the first half cycle finds the potential of the  $C_1$  upper plate  $+50$  kv. and that of the  $C_2$  upper plate  $-50$  kv.; a small part of the charge has leaked off through the x-ray tube, so that the true values are perhaps  $+48$  and  $-48$  kv.

During the third quarter cycle, the potential of the lower plate of  $C_1$  rises to  $+50$  kv., and that of the lower plate of  $C_2$  drops to  $-50$  kv. Since the valves remain closed to inverse currents, the potential of the upper plate of  $C_1$  rises to approximately  $+100$  kv. (actually, perhaps  $+92$  kv. owing to leakage through the x-ray tube), and that of the upper plate of  $C_2$  drops to approximately  $-100$  kv. At this instant, the potential drop across the x-ray tube is therefore nearly 200 kv., or approximately twice the full transformer voltage.

During the fourth quarter cycle, the potentials of the lower condenser plates return to zero. At the same time the potential of the top plate of  $C_1$  drops to perhaps  $+44$  kv., and that of the top plate of  $C_2$  rises to perhaps  $-44$  kv.

During the first quarter of the next cycle (and all succeeding cycles) the potential of the lower plate of  $C_1$  drops, and that of the upper plate drops with it, but no current will flow through the valve until the potential of the upper plate drops to zero or below, when the lower plate potential will be, say,  $-42$  or  $-43$  kv. A similar statement applies to  $C_2$ . During the remaining small part of the first quarter cycle, the condensers are recharged to a potential difference of 50 kv. each.

From this detailed account, it is seen that the x-ray tube voltage and

current and the condenser-charging current will be functions of time somewhat as represented in Fig. 7-17. It will be noted that the x-ray tube experiences one voltage pulse per cycle.

This circuit thus accomplishes several desirable objectives. (1) Very high tube voltages can be obtained with a transformer of moderately high voltage because of the voltage-doubling feature. This reduces transformer cost, perhaps nearly enough to pay for the valves or the condensers. (2) The tube is idle only about a quarter of the time. (3) The tube is subjected to practically no inverse voltage, and thus long tube life is realized. The average forward voltage is not very high, however, being only about half the peak; more heat and less x-rays are therefore generated in the tube than in an ideal circuit.

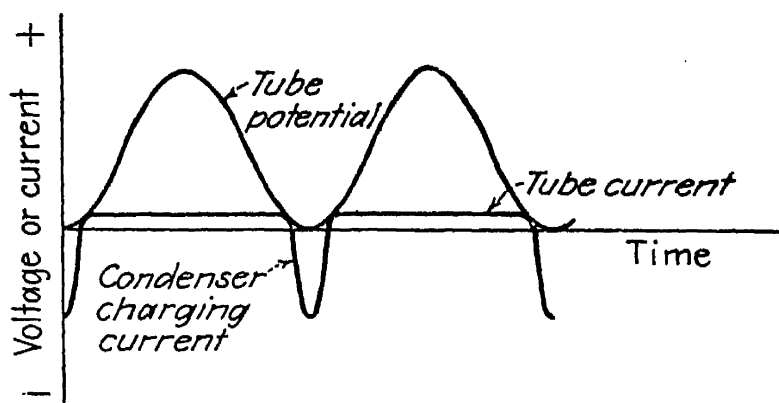


FIG. 7-17.—Wave forms for the Villard circuit. (After Sarsfield; courtesy of Chapman & Hall, Ltd., London.)

In the circuit of Fig. 7-16, each condenser and each kenotron must withstand the full transformer voltage, and the x-ray tube must withstand twice this voltage. In the circuit of Fig. 7-15, the kenotron must withstand twice the full transformer voltage.

This circuit has been analyzed in detail because it is one of the more difficult ones to understand and because it is frequently used. The detailed analysis of the other circuits to be mentioned may be worked out by using the above analysis of the Villard circuit as an example.

*c. The Greinacher Circuit.* This circuit is shown in Fig. 7-18 and is sometimes called the "La Tour circuit." Several of these circuits may be arranged with the condensers in series to build up a very high voltage. The Greinacher circuit is also a voltage-doubling circuit. It is the first circuit yet mentioned that furnishes high voltage approaching c.p.d.c. as distinguished from pulsating direct current. The transformer must be of the end-grounded type, however (or else set on an insulating stand and its primary fed through a cascading transformer); hence no large saving in transformer cost results from the voltage-doubling feature. Two kenotrons are required and two condensers. The latter need with-

stand only the transformer voltage, but the former must take the full doubled x-ray tube voltage.

The curves representing the approximate variation of the tube voltage and current, condenser voltage and current, and transformer voltage as a function of time are shown in Fig. 7-19. It will be noted that the tube cathode voltage is boosted to maximum negative value once each cycle and the tube anode voltage is boosted to maximum positive voltage once each cycle; but these boosts occur on alternate half cycles so that the tube voltage as a whole is boosted twice per cycle, as in a full-wave rectifier. The rate at which the tube voltage dies down between boosts is directly proportional to the x-ray tube current and inversely proportional to the capacity of the condensers. The time permitted for this dying down of the tube voltage (and hence the amount

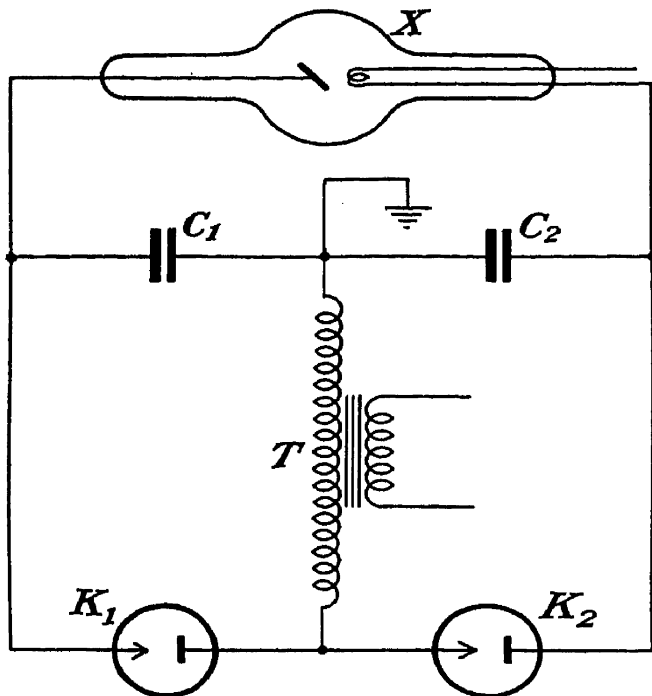


FIG. 7-18.—Greinacher circuit.

of the tube voltage ripple) may be reduced by using a higher frequency, for example from a motor generator set. This circuit, used at a high frequency (say 500 or 1,000 cycles) with high-capacity condensers is a good source of c.p.d.c. for any ordinary type of x-ray work.

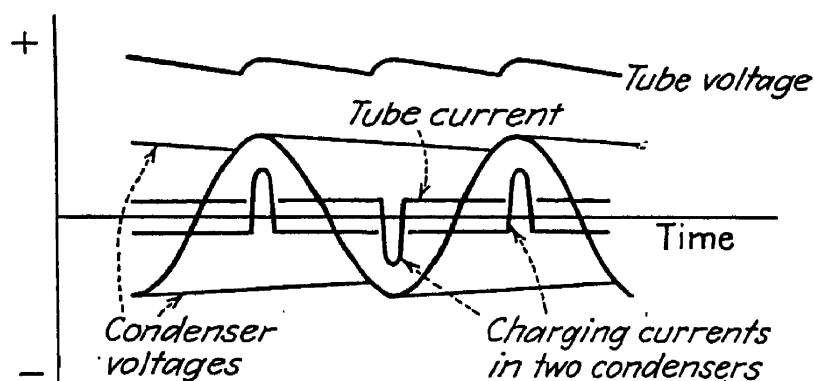


FIG. 7-19.—Wave forms for the Greinacher circuit. (After Sarsfield; courtesy of Chapman & Hall, Ltd., London.)

To figure the amount of the ripple, the following method is reasonably accurate: Suppose the condensers  $C_1$  and  $C_2$  (Fig. 7-18) each have a capacity of  $\frac{1}{2}$  microfarad ( $\mu f$ ) and that  $T$  is a 100-kv.p. transformer, the x-ray tube  $X$  operating at 200 kv. and drawing 6 ma. When one of the condensers is fully charged, its charge will be

$$Q = CV = 0.5 \times 10^{-6} \times 10^5 = 0.05 \text{ coulomb,}$$

if the forward potential drop in the kenotrons during the charging of the condensers is neglected. If the equipment is energized from a 60-cycle power line, both condensers will experience a discharge current of 6 ma. for  $\frac{1}{120}$  sec. before one of them is recharged. This current for this time is a quantity of electricity  $q = It = 0.006 \times \frac{1}{120} = 5 \times 10^{-5}$  coulomb. The fraction of its total charge lost by each condenser is then  $q/Q = 5 \times 10^{-5} \div 0.05 = 0.001 = 0.1$  per cent. This means that the voltage of each condenser will drop 0.1 per cent during a half cycle, after which one of them is recharged. Then they both die down 0.1 per cent during the next half cycle, after which the other is recharged. Hence the x-ray tube voltage will have a 120-cycle 0.1 per cent ripple under these conditions, or it will vary between 200,000 and 199,800 volts 120 times per second. For ordinary purposes, this is c.p.d.c. If the tube current is increased to 12 ma., then the tube voltage will drop to 199,600 volts 120 times per second, but this is still only a  $\frac{1}{2}$  per cent ripple.

Perhaps  $\frac{1}{2}$   $\mu$ f is a rather high capacity for 100-kv. condensers, which are rather bulky and expensive. The example just given shows that, for a given tube current, the alternatives to high-capacity condensers are to increase the frequency or else tolerate a larger ripple. The usual method of increasing the frequency is to use a motor generator set, but a considerable amount of condenser capacity can be bought for the price of a motor generator set. If the power-line voltage is subject to large fluctuations, there is another reason for desiring a motor generator set, however, namely, to provide voltage stabilization (see Sec. 15).

The Greinacher circuit overcomes all but one of the shortcomings mentioned in part *a*. It makes full use of the maximum tube voltage rating; the tube is never idle during any part of the operating cycle; and the average operating voltage is almost identical with the maximum so that the x-ray tube operates very efficiently (produces more x-rays and less heat). In regard to the last point, a Greinacher circuit operating at 200 kv. and 5 ma. will produce about the same result in radiographic work as the circuits shown in Figs. 7-11, 7-12, 7-14, 7-15, and 7-16 operating at 200 kv.p. and from 8 to 14 ma.

Surprisingly, however, x-ray tube life is often shorter when the tube is used on steady direct current of this type than when it is used on pulsating direct current as in a Villard circuit or with a Snook rectifier. Tube manufacturers often specify two ratings for their tubes, for example 220 kv.p., 20 ma., in rectified circuits like those shown in Figs. 7-14 and 7-15, but only 200 kv., 18 ma., for c.p.d.c. This is partly a matter of heat dissipation. A Villard circuit operating at 200 kv.p., 20 ma., is really supplying only about 2,000 watts to the tube because the average voltage is only about 100 kv., whereas a c.p.d.c. circuit operating at

200 kv., 20 ma., is supplying 4,000 watts to the tube. Nevertheless, there are definite indications that the periodic "rest" a tube enjoys on pulsating direct current helps to prevent it from breaking down by relieving the tension at such short intervals that discharges and puncturing surges do not have time to develop.

f. *The Gratz Four-valve Full-wave Circuit.* The straightforward way to obtain full-wave rectification with kenotrons is to use a Gratz circuit,

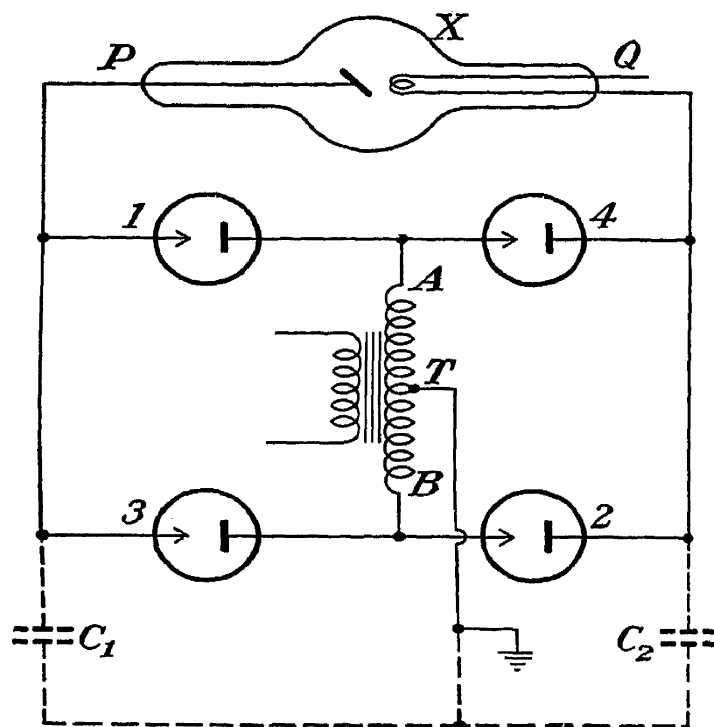


FIG. 7-20.—Gratz four-valve full-wave circuit.

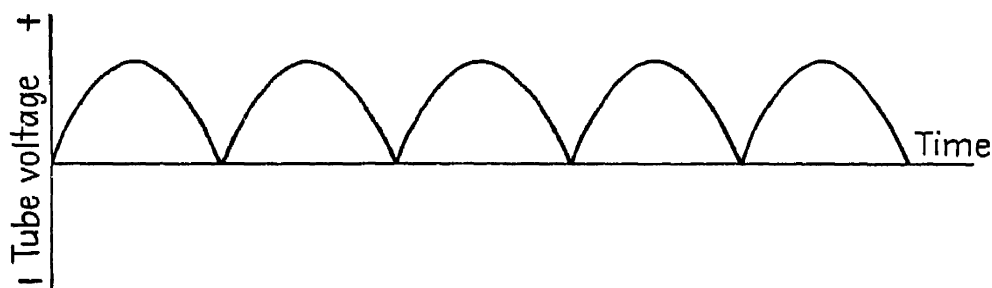


FIG. 7-21.—Full-wave rectification.

which is shown in Fig. 7-20 (the dotted lines are disregarded for the time being). The functioning of this circuit is obvious. When  $A$  is  $+$  and  $B$  is  $-$ , current flows through valves 1 and 2, making  $P$   $+$  and  $Q$   $-$ . On the alternate half cycle when  $A$  is  $-$  and  $B$  is  $+$ , current flows through valves 3 and 4, so that  $P$  is still  $+$  and  $Q$  is still  $-$ . The x-ray tube voltage then has the form indicated in Fig. 7-21.

By providing two condensers, each good for half the tube voltage (Fig. 7-20, dotted lines), or one condenser, good for full tube voltage, and shunting it (or them) across the tube, the pulses of Fig. 7-21, which occur twice per cycle, may be smoothed out so as to obtain c.p.d.c.



The circuit requires four kenotrons (and hence four kenotron filament transformers), and each kenotron must be able to withstand a back voltage equal to the full x-ray tube voltage. The mid-grounded transformer must generate full tube voltage, since this is not a voltage-doubling circuit. These facts account for the popularity of the Greinacher circuit.

*g. Two-tube Full-wave End-grounded Circuit.* A circuit that is well adapted for x-ray diffraction and especially for electron diffraction work (see Chap. 24) is shown in Fig. 7-22. Such work usually does not

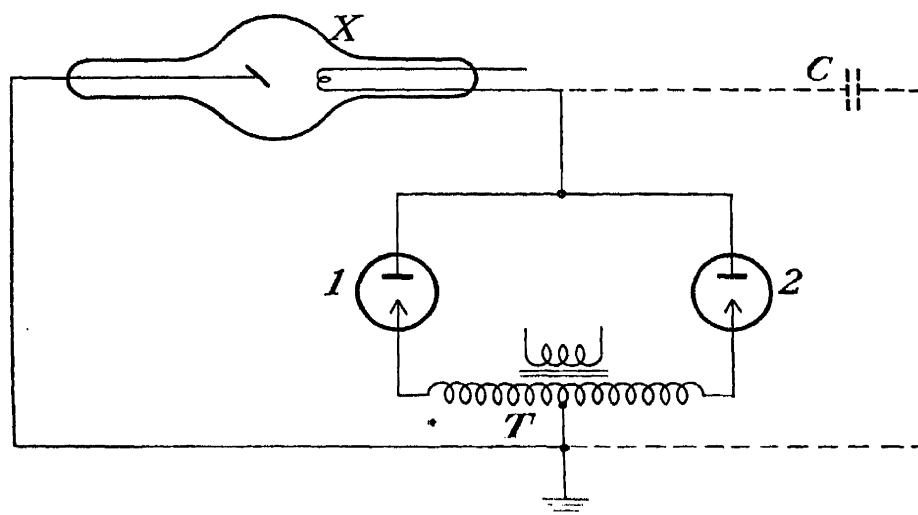


FIG. 7-22.—Full-wave rectification with only two valves.

require potentials above about 50 kv., and it is usually desired that the voltage be end-grounded at the positive end so that all the apparatus except the cathode will be at ground potential.

The potential supplied to the x-ray tube (or electron gun of the electron diffraction apparatus) is only half the transformer voltage; this might therefore be called a “voltage-halving” circuit. However, this disadvantage is not serious when only 50 kv. is desired, for used x-ray transformers designed for 100 kv. are fairly plentiful and cheap. The full-wave rectifying action of the kenotrons is easily followed from Fig. 7-22; it will be noted that current flows through first one half of the transformer secondary and then through the other half. The kenotrons must each withstand the full transformer voltage (twice the tube voltage), but the filament transformers for energizing the kenotron filaments need withstand only half the transformer voltage.

For electron diffraction work, which demands c.p.d.c., a smoothing condenser  $C$  (Fig. 7-22) is necessary. Since such equipment usually draws only a fraction of a milliamper, the condenser need not have very high capacity. Moderate capacity is nevertheless required, for such work demands nearly complete elimination of the ripple, which should amount to only 0.01 per cent or less.

For x-ray diffraction work, the condenser  $C$  is helpful but not necessary. Since the x-ray tube in diffraction work is sometimes operated continuously for scores or hundreds of hours at a time, the life of the kenotrons is a factor to be seriously considered. For this reason, a circuit of the type shown in Fig. 7-11 or 7-12 is commonly used for such work, since no kenotrons are required.

*h. Other Circuits.* The most popular circuits have been mentioned. There are many other circuits that have been used in x-ray work, but they are less common and will not be described here.<sup>1</sup> To mention an example, high voltages are sometimes built up by arranging the condenser portions of several Greinacher circuits in series. Such a circuit is called a "Dessauer circuit."

Special circuits are used for special purposes. For example, a high-voltage high-capacity condenser is slowly charged and then instantaneously discharged through a field-emission x-ray tube to obtain x-ray snapshots of bullets penetrating barriers, etc.<sup>2</sup>

**12. Voltage and Current Control.** Whatever high voltage circuit is used, some provision must be made for controlling the high voltage applied to the tube and also the low-voltage current that heats its filament. The former is usually accomplished by using both an autotransformer  $A$  and a rheostat  $R$  in the main transformer primary circuit, as shown in Fig. 7-23. Here,  $L$  is the single-phase power line (usually 220 volts, sometimes 110 volts). For three-phase circuits, the reader is referred to the books by Sarsfield and by Terrill and Ulrey.<sup>1</sup> In Fig. 7-23,  $P$  is the connection to the primary of the main transformer,  $S$  is the main line switch, and  $X$  is the x-ray on-off switch, which turns on or off the high voltage to the x-ray tube without affecting any of the auxiliary circuits to tube filament, kenotron filaments, mechanical rectifier motor, etc.

An autotransformer is an iron-core transformer that has only one winding, this winding being provided with numerous taps. The figure shows 13 taps, numbered from 0 to 12. The connection of one terminal may be shifted to any tap selected by means of the multiple switch  $M$ . If the main supply voltage is 220 and if it is connected to taps 0 and 10 as shown, the voltages appearing between tap 0 and taps 1 to 12 might be, for example, 40, 60, 80, 100, 120, 140, 160, 180, 200, 220, 240, and 260, respectively.

By using both rheostat and autotransformer, a continuous control

<sup>1</sup> See, for example, L. G. H. Sarsfield, "Electrical Engineering in Radiology," Chapman & Hall, Ltd., London, 1936; or H. M. Terrill and C. T. Ulrey, "X-ray Technology," D. Van Nostrand Company, Inc., New York, 1930.

<sup>2</sup> See footnote 2, p. 107; also, p. 296.

of the main transformer voltage up to the maximum rating is provided. Care must be exercised in applying the high voltage to an x-ray tube, especially if it is to exceed, say, two-thirds the maximum tube rating. If, while the switch  $X$  is open, one sets the controls in such a position that the full rated voltage will be applied to the tube when the switch is closed and then closes the switch, the resulting surge is likely to injure or puncture the tube or damage some other part of the equipment. If no automatic device for applying the load gradually is provided in the circuit, one must be careful to keep the rheostat control  $N$  on tap 1 when the switch  $X$  is open. Then, after the switch is closed, the rheostat

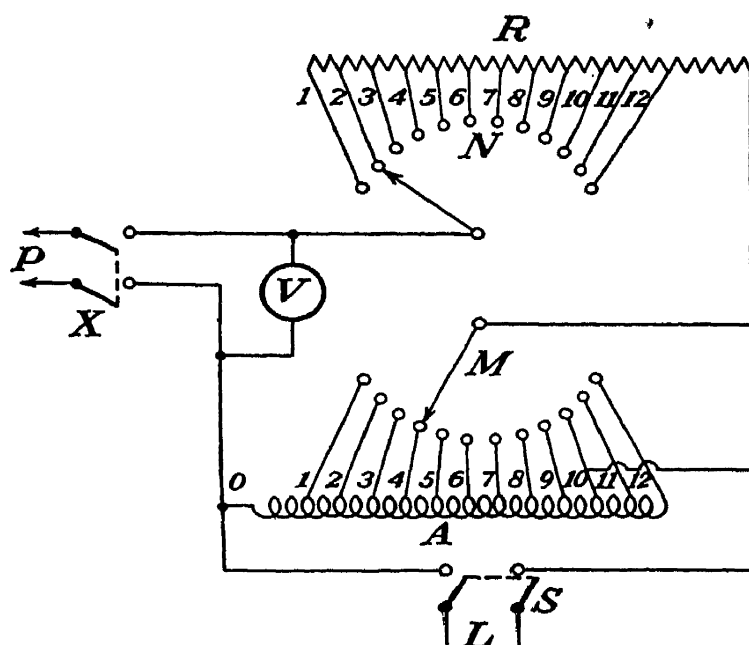


FIG. 7-23.—The usual means of controlling the high voltage.

control  $N$  may be shifted to the desired setting by a movement slow enough to require a second or two. For the same reason, one must avoid shifting the multiple switch  $M$  while the equipment is operating at or near its rated voltage, for shifting from one autotransformer tap to the next involves an off-and-on operation, just as though switch  $S$  were opened and closed again at full load. If it is desirable to shift  $M$  with the load on, this should be done only while the rheostat control  $N$  is set on tap 1 or 2.

The x-ray tube-filament heating current is controlled by putting a rheostat or a variable inductance in series with the primary of its filament transformer.

The voltmeter  $V$  in Fig. 7-23 indicates the primary voltage supplied to the main transformer when the switch  $X$  is closed and the voltage supplied by the autotransformer when  $X$  is open. The former value is a rough indication of the high voltage being supplied to the x-ray tube. Thus, if the main transformer steps up the voltage approximately a thousand times, one may deduce that the tube voltage is roughly 180 kv. if

$V$  reads 180 volts when  $X$  is closed. This is only a rough indication, for the following reasons: First, the magnetization curve for iron is not linear; therefore, it is ordinarily true that, if 30 volts is stepped up to 30 kv. (at no load) by the transformer, then 230 volts will be stepped up in a different ratio (at no load), say to 210 kv. In addition to this, there is variation with load. For example, 180 volts on the primary may produce 180 kv. on the secondary at no load, but only 170 kv. at full load.

**13. Meters.** Two meters are practically essential for satisfactory work with x-ray equipment. One of these is the voltmeter  $V$  just mentioned in the preceding paragraph. Although the relation between the reading of this voltmeter and the high voltage supplied to the tube is not linear, and it varies with the load in addition, one can plot a curve showing the kilovolts peak supplied to the tube as a function of the voltmeter reading, the tube current being, say, 10 ma. throughout. A family of such curves for several different tube currents is desirable.

The other essential meter is a milliammeter to read the x-ray tube current. In many instances, this meter must be placed in the high-tension circuit at a point that is at a high potential with respect to ground and so cannot be placed on the instrument panel. Since it must therefore be viewed from a distance in such cases, it should have a large dial. There are some exceptions. For example, in the two-valve Villard circuit of Fig. 7-16, the milliammeter may be placed in the high-voltage circuit at  $M$ , where it is grounded, and hence can be mounted on the control panel.

The milliammeter used in such service should be as rugged and dependable as is obtainable, and it is essential to protect it from high-frequency ripples and surges. Milliammeters manufactured for x-ray service are usually provided with condensers, chokes, gaps, etc., inside the case to protect against surges and ripples, and special construction may be employed to minimize the electrostatic forces acting on the needle. This electrostatic effect arises because the meter is at high voltage (in most installations); a serious error from this cause is most likely to occur when the equipment is c.p.d.c.

When an error in the milliammeter reading is likely to be especially serious, as in therapeutic work, it is a good idea to use two meters in series, so that if a surge damages one the other will presumably be undamaged or else damaged to a different degree; in either case the two meters will thereafter disagree, thus revealing the damage. The meter should be checked against a standard meter from time to time, a battery and rheostat being used. The standard meter should be used only for this purpose, never in the high-voltage circuit.

If an ordinary milliammeter (not designed for x-ray usage) is to be

employed in experimental work, for example in an x-ray diffraction outfit, it should be protected against surges and ripples by some scheme like that of Fig. 7-24. Each side of the movement should be connected to the case by a condenser  $C_1$ ,  $C_2$  of a few microfarads capacity. The two condensers in series thus shunt the movement. Further protection is provided by the resistors  $R_1$  and  $R_2$  of about 5,000 ohms each and the neon lamp  $N$ . When the meter can be used at ground potential, as in a two-valve Villard circuit, its case should be well grounded.

Other auxiliary meters of much less importance may be included in the equipment. For example, an ammeter may be included to read the x-ray tube-filament heating current. With mechanical rectifiers, a meter may be used to show whether the synchronous driving motor has

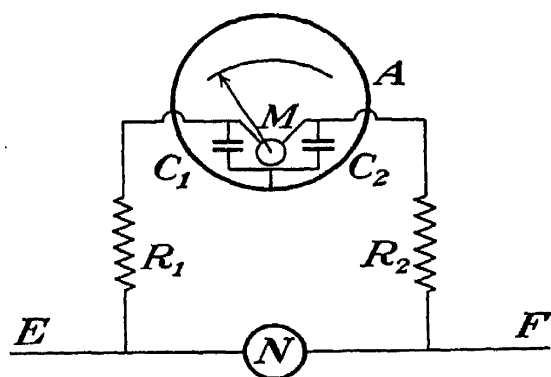


FIG. 7-24.—One method of protecting a milliammeter from high-voltage surges. (After Sarsfield; courtesy of Chapman & Hall, Ltd., London.)

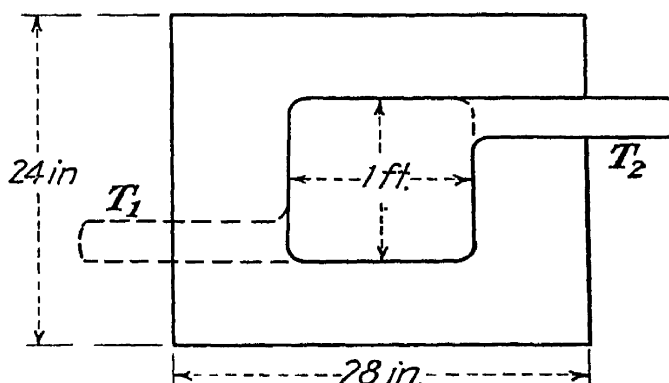


FIG. 7-25.—Construction of a high-voltage filtering condenser.

fallen into the correct synchronism so that the cathode will be negative and anode positive or whether it has fallen into the opposite, wrong synchronism.

**14. High-voltage Condensers.** In Sec. 11, several circuits were described that include high-voltage condensers. Such condensers may be purchased from x-ray equipment manufacturers, such as General Electric, Kelley-Koett, Picker, or Westinghouse, or from condenser manufacturers, such as Aerovox Corporation, New Bedford, Mass., or Cornell-Dubilier Corporation, South Plainfield, N.J., with d.c. ratings up to about 0.3  $\mu\text{f}$  at 100 kv.

In the case of circuits for x-ray diffraction or electron diffraction work, where the d.c. voltages required do not exceed 50 kv., it may be found that a homemade condenser is more suitable. For example, if a 60-cycle supply is to be used, it may be decided that a condenser with a capacity as high as 0.1  $\mu\text{f}$  is desirable. This may be built by stacking up two piles of glass plates alternating with thin sheet metal. The glass may be ordinary plate glass  $\frac{1}{4}$  in. thick and about 24 by 28 in. The metal used between should be soft and corrosion resistant, such as

copper, a thickness of 0.005 to 0.010 in. being suitable. Alternate sheets of metal should have their connecting lugs  $T_1$  and  $T_2$  placed at opposite sides of the pile as indicated in Fig. 7-25, where one sheet is outlined by dotted lines and the next one above or below it is outlined by solid lines. The overlapping portions are 1 ft. square, as indicated.

The familiar formula for the capacitance of such a condenser is

$$C = \frac{N\epsilon A}{4\pi d} \quad (7-1)$$

where  $N$  is one less than the number of metal plates in the condenser,  $\epsilon$  is the dielectric constant of the glass,  $A$  is the area of the overlap of the metal plates (in square centimeters), and  $d$  is the thickness of the glass plates (in centimeters). Equation (7-1) gives the capacitance in c.g.s.e.s.u. of capacity. The capacitance in microfarads is given by

$$C = \frac{N\epsilon A}{36 \times 10^5 \pi d} \quad (7-2)$$

If the capacitance is to be 0.1  $\mu$ f, one has

$$N = \frac{3.6 \times 10^5 \times 3.14 \times 0.63}{6 \times 900} = 132 \text{ approximately}$$

assuming that  $\epsilon = 6$ . A stack of 132 glass plates of this size is so heavy that the weight will crack the bottom ones. Therefore the condenser should be built in two stacks of 66 glass plates, each supported on a sturdy, flat insulating platform and covered with a wood cover, free of nails, screws, or other metal, to keep out the dust.

**15. Voltage Stabilization.** The power required to energize x-ray equipment is usually drawn from a commercial power line, although mobile equipment intended for field work may depend upon an electric generator driven by a gasoline engine. In some cases, the voltage of a commercial power line fluctuates slowly, and only a few per cent at most; in other cases, the fluctuation is rapid and amounts to several per cent. In the latter instance, some provision for voltage stabilization in the x-ray equipment is necessary for satisfactory work. For some types of precision work it is necessary even with a comparatively stable power line. In Sec. 2-5 it was stated that the electron emission from a Coolidge-tube filament (which controls the x-ray intensity) varies very rapidly with the filament heating current, the stabilization of this heating current being therefore most important. Next to this, the most important need is to stabilize the voltage impressed across the primary of the main transformer; for the secondary voltage varies with the primary voltage, and the secondary voltage determines the quality or hardness

of the x-rays. Stabilization of the quality of the x-rays is placed second to stabilization of their intensity because the latter may vary 10 per cent when the power-line voltage varies 1 per cent, whereas the tube voltage will vary only about 1 per cent for a 1 per cent line-voltage variation. In electron diffraction work, a 1 per cent variation in the voltage accelerating the electrons is more objectionable than a 10 per cent variation in the beam intensity; in this case, therefore, stabilization of the main transformer voltage is the primary consideration.<sup>1</sup>

One common method of stabilizing the voltage is to energize the equipment from a motor generator set, the motor being of the synchronous type. In most of the larger commercial power networks, the a.c. frequency is quite constant, so that a synchronous motor will run at constant speed regardless of any ordinary fluctuation of the line voltage. When such a motor drives an a.c. generator, a steady voltage is therefore generated. Of course the voltage at the generator terminals will decrease as the load imposed by the x-ray equipment itself increases, but this is not objectionable so long as the power rating of the motor generator set is not exceeded. The motor generator set is intended to prevent variations during an exposure when the controls are not being changed; and if its output is used exclusively to energize the x-ray equipment, it will accomplish this purpose. That is, it will stabilize both the x-ray tube-filament heating current and the high voltage supplied to the tube.

An important feature of a motor generator set is that it may be used to change the frequency, also. For example, the 60-cycle frequency of the power line may be converted to a 600-cycle frequency, if desired. This would enable one to use high-voltage smoothing condensers having a capacity only one-tenth that required to achieve the same per cent voltage ripple at 60 cycles.

A motor generator set may thus accomplish three purposes: (1) stabilization of the tube voltage; (2) stabilization of the tube current; (3) change of frequency to permit smaller, cheaper smoothing condensers.

The first two purposes (but not the third) may be accomplished by using one of the "constant-voltage transformers" developed in recent years. This device has no moving parts and hence requires no attention or maintenance, whereas a motor generator set does require occasional attention. One type of constant-voltage transformer manufactured by the Sola Electric Co., Chicago, Ill., has the characteristics listed in Table 7-2. The Sola catalogue describes the operating principle of these transformers, which are available at ratings up to 10 kilovolt-amperes. One model suitable for stabilizing the voltage supply to most x-ray outfits is

<sup>1</sup> See S. H. Bauer, J. M. Hastings, and D. P. MacMillan, *Rev. Sci. Instruments*, **14**, 30 (1943).

rated at 5 kva., 190 to 250 volts primary, 230 volts secondary, size  $35\frac{1}{2} \times 21\frac{7}{8} \times 9\frac{3}{8}$  in., shipping weight 570 lb.

TABLE 7-2.—CHARACTERISTICS OF 500-VOLT-AMPERE CONSTANT-VOLTAGE TRANSFORMER AT FULL LOAD

Input volts	Input amperes	Output volts	Per cent efficiency
95	6.33	114.5	84.5
100	6.10	115.0	84.0
105	5.80	115.4	84.5
110	5.63	115.4	84.0
115	5.40	115.7	84.0
120	5.22	115.7	84.0
125	5.04	115.4	84.0

If a high degree of stabilization is unnecessary or if the power line available happens to be exceptionally stable, one may need no stabilizing device. If the x-ray circuit is one that supplies pulsating direct current to the tube (not c.p.d.c.), the tube current (only) may be stabilized by means of a magnetic-relay type of stabilizer manufactured for this purpose. One common type is known as the "Kearsley stabilizer."

The trend at present is to equip new installations with a filament current stabilizer, which operates without moving parts. These stabilizers contain inductances and capacitors and operate on a principle similar to that of the constant-voltage transformers already mentioned.

**16. Voltage-measuring Equipment.** The simplest and commonest way of obtaining an approximate indication of the peak tube voltage for plotting the calibration curve mentioned in Sec. 13 is by means of an adjustable sphere gap. One of these may be seen in Fig. 7-26.

The gap should be provided with a resistance in series with it that is capable of withstanding the full voltage and absorbing the energy when the gap breaks down. This resistor should have a value in ohms about five or ten times the volts being measured. It is good practice to divide this resistance into two equal parts and put each half on opposite sides of the gap. Thus if one is measuring a voltage of the order of 100 kv., a  $\frac{1}{2}$ -megohm high-voltage resistor should be provided on each side of the gap. The spheres for such a voltage should be about 5 in. or more in diameter, and each sphere should be supported from the side opposite the gap, at a distance at least twice its diameter from earthed bodies or supporting framework.

The breakdown voltage of such a gap varies with the diameter of the spheres and the distance between them, and the voltage for a particular diameter and gap length may be found from tables<sup>1</sup> for the case of air

<sup>1</sup> See A.I.E.E. "Standard Number 4" or L. W. Chubb and C. Fortescue, *Trans.*



at standard temperature (25°C.) and pressure (76 cm. of mercury). The breakdown voltage at other pressures and temperatures may be calculated, it being known that it varies directly as the pressure and inversely as the absolute temperature for ordinary room temperatures and pres-

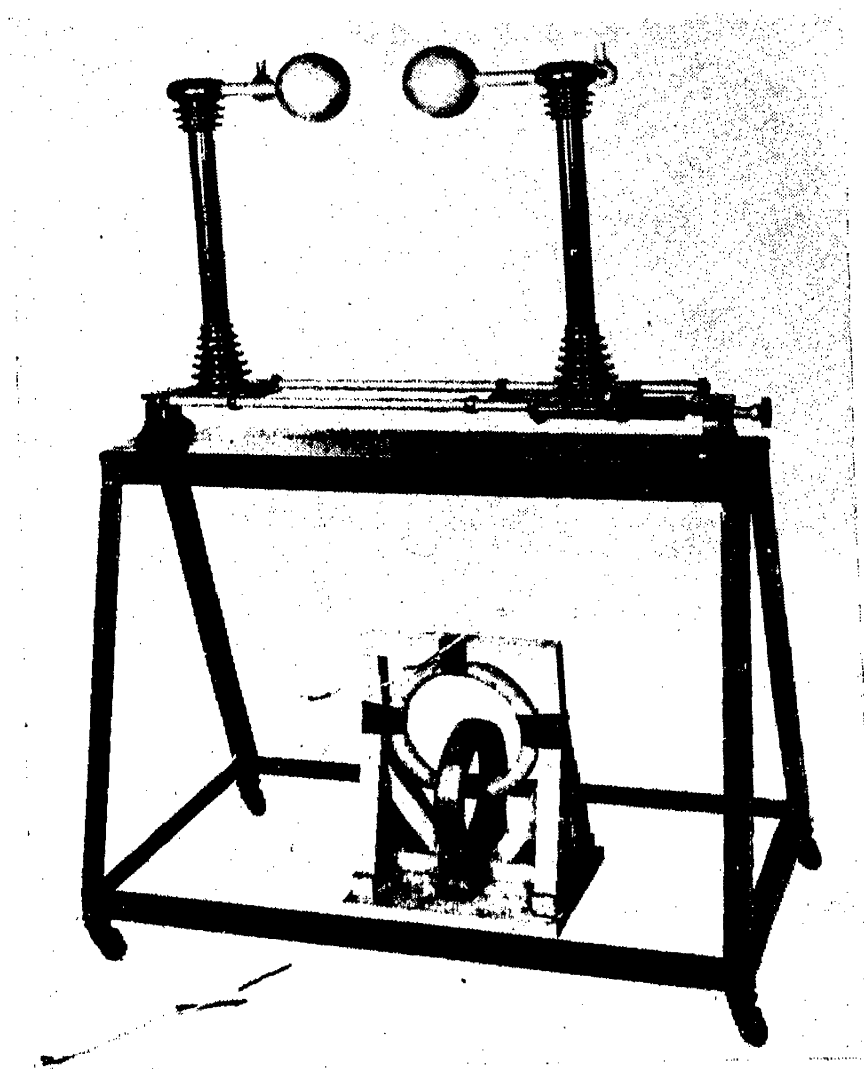


FIG. 7-26.—Calibrated 5-in. sphere gap for measuring potentials up to 220 kv. Underneath it is seen a filament transformer of the type described in Sec. 7.

ures. The humidity has only a very slight effect upon the breakdown voltage.

A ripple on the main voltage wave (in the case of alternating current or pulsating direct current) will cause the gap to indicate a higher voltage than is actually effective in producing x-rays in the tube. If there is doubt about the presence of such a condition, a cathode-ray oscillograph record of the wave form should be obtained. When an x-ray tube

---

*A.I.E.E.*, **32**, 739 (1913). For small spheres, up to 25 cm., see "Handbook of Chemistry and Physics," C. D. Hodgman, editor, Chemical Rubber Publishing Company, Cleveland, O. There is doubt about these tables above 500 kv.; see J. E. Henderson, W. H. Goss, and J. E. Rose, *Rev. Sci. Instruments*, **6**, 63 (1935).

rectifies its own current, a sphere gap will indicate the peak inverse voltage rather than the peak useful voltage, of course.

For a continuous indication of the high voltage, probably the best instrument yet devised is the Kirkpatrick type of generating voltmeter.<sup>1</sup> The instrument as originally built has been improved for use with c.p.d.c. by Herb and coworkers<sup>2</sup> and for pulsating voltages of the type common in x-ray work by Kirkpatrick.<sup>3</sup> Trump, Safford, and Van de

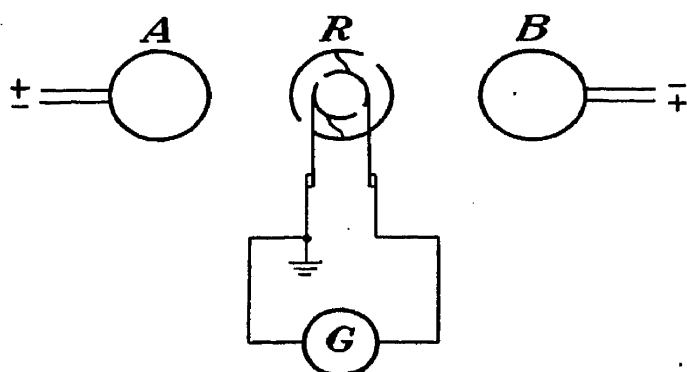


FIG. 7-27.—Illustrating the operating principle of the generating electrostatic voltmeter. (After Kirkpatrick and Miyake; courtesy of the American Institute of Physics.)

Graaff<sup>4</sup> have also developed this type of meter, in a form that requires no amplification or mechanical commutation. Henderson, Goss, and Rose have checked the A.I.E.E. sphere-gap voltage tables with a generating voltmeter and found some discrepancy above 500 kv.<sup>5</sup>

The operating principle of the instrument can be explained with the help of Fig. 7-27. *A* and *B* are two electrodes connected to the terminals between which the potential difference *V* is to be measured. *R* is a rotating sheet-metal cylinder split in half longitudinally and rotated at constant speed by a synchronous motor about an axis through the center perpendicular to the paper. The alternating electrostatic charges thus induced on the two sectors of *R* are rectified by the commutator shown and flow through the galvanometer *G*, which is grounded, as pulsating direct current.

If *C* is the capacity of the condenser formed by either sector of *R* and the sphere *A* or *B* adjacent to it when the plane of the split is vertical and if *R* rotates at *n* r.p.s., then the current *I* through the galvanometer is given by

$$I = 2CVn \quad (7-3)$$

all units being in the same system. If practical units are used, *I* will be in amperes if *C* is in farads, *V* in volts, and *n* in r.p.s. Since *C* and *n* are constants, *I* is proportional to *V*.

<sup>1</sup> P. Kirkpatrick and I. Miyake, *Rev. Sci. Instruments*, **3**, 1, 430 (1932); R. Gunn, *Phys. Rev.*, **40**, 307 (1932); U.S. patent 1,919,215.

<sup>2</sup> D. B. Parkinson, R. G. Herb, E. J. Bernet, and J. L. McKibben, *Phys. Rev.*, **53**, 648 (1938).

<sup>3</sup> P. Kirkpatrick, *Rev. Sci. Instruments*, **5**, 33 (1934); see also H. A. Thomas, *Rev. Sci. Instruments*, **8**, 448 (1937).

<sup>4</sup> J. G. Trump, F. J. Safford, and R. J. Van de Graaff, *Rev. Sci. Instruments*, **11**, 54 (1940).

<sup>5</sup> Footnote, 1, p. 144.

Because of this linear characteristic, the instrument can be calibrated by noting the galvanometer deflection for one known value of  $V$ , such as 100 kv. One way of fixing such a calibration point is convenient if an x-ray ionization spectrometer (page 334) is available. It is aimed at an x-ray tube and set for 0.124 Å., the wave length obtained from equation (4-35), for 100 kv. The generating voltmeter is connected to read the high voltage on the x-ray tube. As this is gradually increased, the first indication of a current from the spectrometer ionization chamber (page 29) will occur just as the high voltage reaches 100 kv. owing to the Duane-Hunt limit relationship (page 27). If the generating voltmeter reading is 17.3 when this occurs, for example, then a subsequent reading of 34.6 indicates that the high voltage is 200 kv., and similarly for other readings.

In the absence of a spectrometer, one may obtain a calibration point from a high-voltage transformer if the number of turns on its secondary is known. If one winds 10 turns of wire around the core and the secondary has 10,000 turns, then the secondary peak voltage will be 97,600 volts, for example, when the peak voltage from the 10 turns is 97.6 volts, provided that the transformer is operated at no load.

Another way to obtain the needed calibration point is to construct a wire-wound resistor having a resistance of several megohms and capable of withstanding a high voltage. Then one merely applies Ohm's law. Thus, if the resistor has a resistance of 5 megohms, a current of 20 ma. through it indicates that the high voltage applied to it is exactly 100 kv.<sup>1</sup>

If only a rough calibration is required, this may be accomplished by establishing the calibration point with a sphere gap, correcting for temperature and barometric pressure, and averaging 10 or more gap readings.

**17. Arrangement of Equipment.** The usual arrangement in fixed x-ray installations is to place the high-voltage electrical equipment in one room, the x-ray tube and its supporting stand or crane in an adjacent room, which may be lined with lead for protection, and the control panel and meters in a third room (see, for example, Fig. 7-28). A typical million-volt installation for industrial radiography is described and illustrated in a recent article in *Automotive Industries*<sup>2</sup> (see also Fig. 12-39). The cost, including the special building, is given as \$100,000. For photographs and description of the treatment room and high-voltage room for 1,200,000-volt cancer therapy, the reader is referred to an article in *Nature*.<sup>3</sup> Medical diagnostic installations are well illustrated in the catalogues of the x-ray equipment manufacturers, as well as portable medical units and mobile industrial units. In the case of

<sup>1</sup> See, for example, H. Clark, *Rev. Sci. Instruments*, **1**, 615 (1930).

<sup>2</sup> *Automotive Ind.*, Dec. 15, 1942, p. 46.

<sup>3</sup> *Nature*, **138**, 1106 (1936).

diffraction equipment, the electrical equipment is usually contained in a cabinet, on top of which is placed the tube and the diffraction cameras surrounding it (see Fig. 18-6). This type of equipment is also illustrated and described in the catalogues.

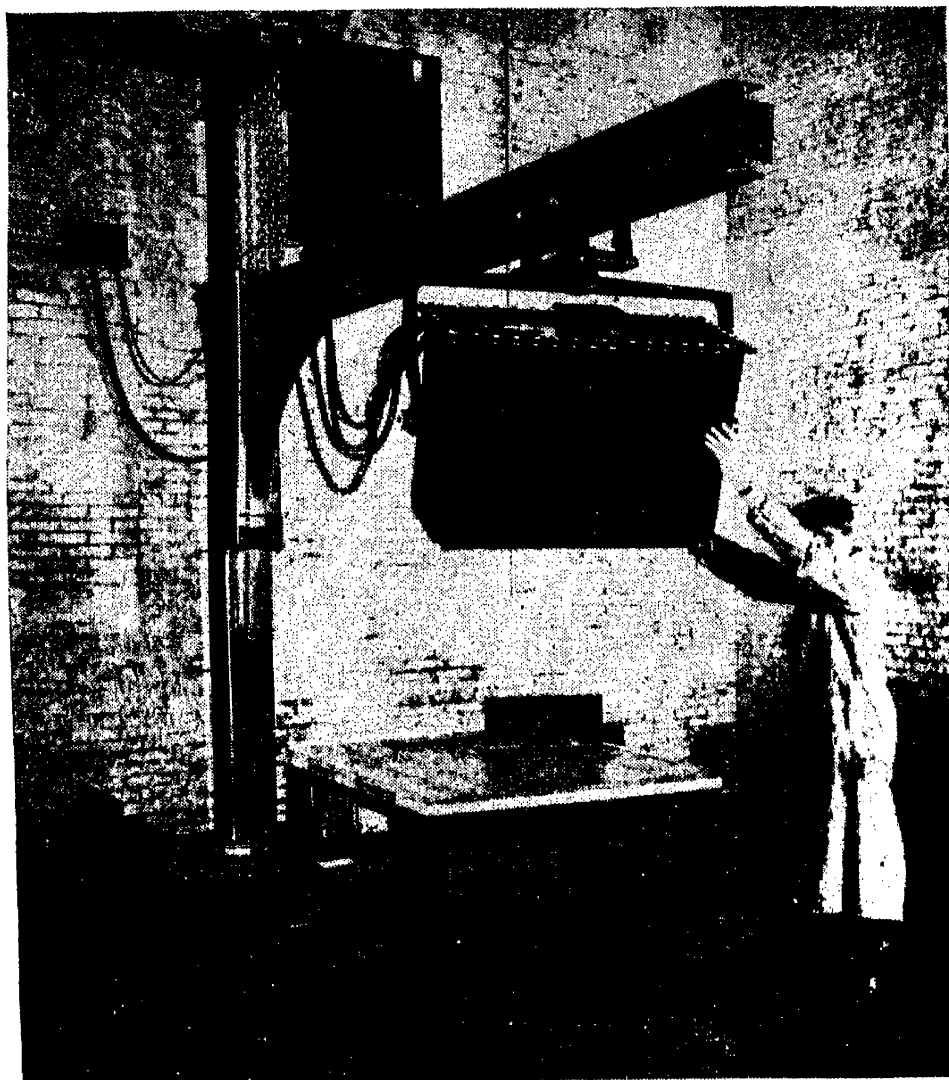


FIG. 7-28.—A fixed installation for industrial radiography. This is a 250-kv. unit with the main transformer and all high voltage circuits enclosed within the shockproof tubehead. The control panel and primary regulating circuits are contained in another unit located in the adjoining room. No third room for high-voltage equipment is required. (*Courtesy of General Electric X-ray Corporation.*)

Small portable diagnostic equipment is built that may be carried in one or two cases by hand. Such equipment is used in rural districts or can be carried from room to room in a hospital.

Between the fixed-installation and portable equipment, there is "mobile" equipment. This may be mounted in an automobile trailer or motor truck<sup>1</sup> with a gasoline-engine-driven generator to supply electric

<sup>1</sup> Such a unit for radiographic inspection of wooden electric-power-line poles is illustrated and described by M. Zucker, *Elec. World*, **113** (Mar. 23, 1940); also *A.S.T.M. Bull.*, October, 1940, p. 19.

power, or it may be mounted on a rubber-tired motorless truck, which can be pushed about in a factory where electric power is available at various points.<sup>1</sup>

**18. The Van de Graaff Generator.** For the generation of x-rays at potentials ranging from 1 million up to 2 or 3 million volts, the Van de Graaff generator deserves serious consideration, although the betatron, to be described in the next section may soon supersede other types of x-ray generators in this range. The Van de Graaff generator was first described in 1933 in an article by Van de Graaff, Compton, and Van Atta.<sup>2</sup> It consists of a highly insulated electrode, shaped so as to minimize corona loss, and a fast-moving nonconducting belt, which conveys a continuous supply of electrostatic charges to the electrode. The belt is usually made of rubber-impregnated fabric and runs on two pulleys, one grounded and the other located in the high-voltage insulated electrode but insulated (for several thousand volts) from it. A comb of needle points close to the grounded motor-driven pulley is charged to some 20 or 40 kv. positive or negative direct current by a small x-ray transformer and kenotron set. These needles spray electrostatic charges on the belt, which moves past them rapidly. The charges are carried to the insulated pulley in the high-voltage electrode, which thus becomes more highly charged than the electrode itself. When this pulley acquires a potential of several thousand volts with respect to the electrode, additional charges brought up by the belt are automatically transferred to the electrode by a comb of corona needle points placed near the pulley where the belt is arriving. Another comb placed at the opposite side of the pulley sprays the departing belt with charges of the opposite sign, which it carries back to the grounded drive pulley. Thus the insulated electrode soon builds up a potential limited by the insulation or by corona loss.

These two limitations recede somewhat if the generator is enclosed in a tank containing compressed air or Freon ( $\text{CCl}_2\text{F}_2$ ) or both, as Herb and coworkers have done.<sup>3</sup> In Huntington Memorial Hospital, Boston, Mass., Trump and Van de Graaff<sup>4</sup> have constructed for therapeutic work a million-volt x-ray installation that uses a Van de Graaff generator to supply the high voltage. This installation has a capacity of 3 ma.

<sup>1</sup> Illustrated in catalogues of x-ray equipment manufacturers. A darkroom is included in a special unit built by T. Triplett, illustrated in *Electronic Ind.*, **2**, 45 (January, 1943).

<sup>2</sup> R. J. Van de Graaff, K. T. Compton, and L. C. Van Atta, *Phys. Rev.*, **43**, 149 (1933).

<sup>3</sup> R. G. Herb, D. B. Parkinson, D. W. Kerst, E. J. Bernet, and J. L. McKibben, *Rev. Sci. Instruments*, **6**, 261 (1935); *Phys. Rev.*, **51**, 75 (1937), **53**, 642 (1938).

<sup>4</sup> J. G. Trump and R. J. Van de Graaff, *J. Applied Phys.*, **8**, 602 (1937). See also *Phys. Rev.*, **55**, 1160 (1939).

at 1 million volts, but in actual treatments only 1 or  $1\frac{1}{2}$  ma. is ordinarily used. A 2-million-volt installation has been built by Van Atta and Northrup,<sup>1</sup> and sealed-off tubes for such equipment are now manufactured<sup>2</sup> (see Fig. 7-5).

A potential of  $\frac{1}{2}$  million volts may be obtained with quite a small generator of this type. Trump, Merrill, and Safford<sup>3</sup> built such a model delivering 200 microamperes at this voltage, the cost being only about \$325. A model similar to this has been placed on the market by the Central Scientific Company, Chicago, Ill.

**19. The Betatron, or Electron Induction Accelerator.** The betatron, developed quite recently by Kerst,<sup>4</sup> is so new that only a few experimental models have been built. Nevertheless, it has already produced 20-million-volt x-rays with an intensity comparable with that of the x-rays generated by an ordinary x-ray tube operating at, say, 100 kv. and 10 ma.; it is thus not hard to foresee that it is likely to be widely used in x-ray work eventually. For many years the trend in certain types of therapeutic work has been to higher and higher voltages; therefore the betatron may be used in this field, perhaps in sizes generating x-rays of many millions of electron volts energy ( $h\nu$ ) or perhaps for cathode-ray therapy (see final paragraphs of Chap. 11). A 130-ton 100-million-volt model is now in operation.<sup>5</sup> For other uses, Kerst's 2-million-volt betatron having dimensions of roughly 10 by 10 by 20 in. and an output equivalent to that from a gram of radium is quite impressive, for this is smaller and lighter than an ordinary 140-kv. x-ray outfit. A 4-kw. 600-cycle generator is also required for this size of betatron, but this need not be moved with it if the betatron is used for radiographic or therapeutic work. The compactness of this 2-million-volt x-ray generator is more impressive, perhaps, than the  $3\frac{1}{2}$ -ton model, which produces 20-million-volt x-rays. A small, light, mobile 2-million-volt betatron should find wide application in industrial radiography.

The betatron produces x-rays by hurling high-speed electrons against

<sup>1</sup> L. C. Van Atta and D. L. Northrup, *Am. J. Roentgenology Radium Therapy*, **41**, 633 (1939).

<sup>2</sup> R. R. Machlett, *Electronic Ind.*, **3**, 79 (November, 1944).

<sup>3</sup> J. G. Trump, F. H. Merrill, and F. J. Safford, *Rev. Sci. Instruments*, **9**, 398 (1938).

<sup>4</sup> D. W. Kerst, *Phys. Rev.*, **60**, 47 (1941); D. W. Kerst and R. Serber, *Phys. Rev.*, **60**, 53 (1941); D. W. Kerst, *Am. J. Phys.*, **10**, 219 (1942); A. R. Wildhagen, *Sci. American*, **168**, 207 (1943); D. W. Kerst, *Rev. Sci. Instruments*, **13**, 387 (1942); D. W. Kerst, Radionics Section (vol. 1) of *Radio News*, **30**, 6 (September, 1943); *Science News Letter*, **43**, 200 (1943); J. H. Bartlett, *Phys. Rev.*, **64**, 185 (1943); D. Iwanenko and I. Pomeranchuk, *Phys. Rev.*, **65**, 343 (1944); *Gen Elec. Rev.*, **46**, 58 (1943); T. J. Wang, *Electronics*, **18**, 128 (June, 1945); D. W. Kerst, *Ind. Radiography*, **3**, 36 (summer, 1944); W. F. Westendorp, *J. Applied Phys.*, **16**, 657 (1945).

<sup>5</sup> W. F. Westendorp and E. E. Charlton, *J. Applied Phys.*, **16**, 581 (1945).

a target, just as in an x-ray tube. The novel feature is that it uses a principle which makes it possible to bombard the target with electrons having an energy of, say, 10 million electron volts, *without* its being necessary to have a potential difference of 10 million volts between electrodes. In fact, no high voltage whatever is used. The electrons are accelerated in a vacuum tube by a moving magnetic field just as the free electrons in the wire used for the secondary winding of a transformer are impelled to move through the wire by the alternating magnetic field created in the transformer core by the primary alternating current. That is, the electrons are accelerated by the electric field associated with a time-varying magnetic field. The free electrons in the wire of a transformer secondary winding are unable to attain high speeds because of their continual collisions with the atoms composing the wire. If these

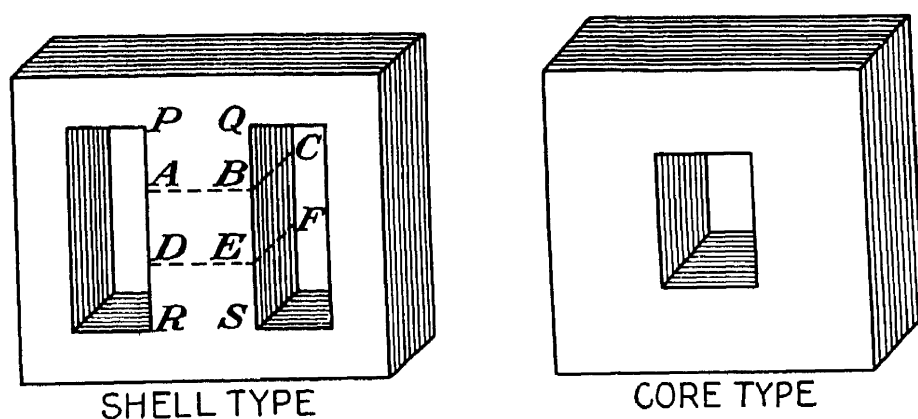


FIG. 7-29.—The two common types of transformer cores—to help illustrate the construction of a betatron.

electrons were in a vacuum, however, there would be no collisions to impede their progress, and they could speed up to enormous velocities. This possibility is realized in Kerst's betatron.

Since the betatron is closely akin to a transformer, let us digress briefly to review the essentials of the construction of a transformer, especially the core. There are two common types, shown in Fig. 7-29. The one on the left is called the "shell type" (disregard the dotted lines). The other is called the "core type." The filament transformers in Figs. 7-8 and 7-26 are of the latter type. The cores are built of laminated iron to reduce eddy-current loss. One might take a shell-type core, as shown at the left in Fig. 7-29, and cut a piece out by sawing along the dotted lines *ABC* and *DEF*. Then, instead of winding the primary winding around the post *PQRS* as usual, half of it might be wound about the lower portion *DEFRS* and the other half about the upper portion *ABCPQ*. The secondary winding is a strange departure. It consists of a highly evacuated glass tube shaped like an inflated automobile-tire inner tube or a doughnut. This evacuated glass doughnut surrounds the central leg of the core (just as the usual secondary winding surrounds

it) at the gap  $ABCDEF$ . The inner walls of the doughnut are covered with a thin film of evaporated metal to keep them from charging up and producing disturbing electrostatic fields.

The core should be designed to give a high voltage per turn, say 25 volts, as contrasted with the usual fraction of a volt per turn in ordinary small transformers. This means that the core should have as large a cross section as practical, and the frequency used should be higher than the usual 60 cycles. Furthermore, the post  $PQRS$  must be circular, not square. Finally, the pole faces  $ABC$  and  $DEF$  must not be cut off flat as thus far imagined but must be tapered so that the gap is shortest in the center and gets longer as one goes toward the edge of the circular gap. This tends to concentrate the magnetic flux in the center portion of the gap. That is, if  $H$  is the magnetic field strength at a point in the gap at a distance  $r$  from the axis of the post  $PQRS$ , then  $H$  decreases as  $r$  increases. Of course,  $H$  also varies with time in a sinusoidal manner, as indicated in Fig. 7-30, as in any transformer. It is well known that electrons moving in a vacuum, perpendicular to a constant, uniform magnetic field will pursue a circular course, the plane of the circle being perpendicular to the field, and its radius  $R$  is given by

$$R = \frac{mvc}{He} \quad (7-4)$$

where  $R$  is in centimeters,  $m$  and  $c$  have their usual significance,  $H$  is in oersteds,  $v$  is the velocity of the moving electron in cm./sec., and  $e$  is in e.s.u. If  $e$  is in e.m.u., then the  $c$  is omitted from the equation.

The electrons are injected into the doughnut tube by means of an electron gun (see Sec. 4e), which directs them at a low voltage (a few hundred volts) tangentially into the evacuated tube. If the taper of the gap faces or pole pieces has been chosen so that  $0 < n < 1$  between the inner and outer edges of the doughnut,  $n$  being defined by

$$H = k \frac{1}{r^n} \quad (7-5)$$

( $k$  being a constant and  $r$  having been defined in the preceding paragraph), then there will be a stable circular orbit into which the electrons will tend to gather. The radius  $r_0$  of this stable orbit is given by

$$r_0 = \sqrt{\frac{\phi_0}{2\pi H_0}} \quad (7-6)$$

where  $\phi_0$  is the flux within the orbit and  $H_0$  is the field strength at the stable orbit,<sup>1</sup> that is, at  $r_0$ .

<sup>1</sup> D. W. Kerst and R. Serber, *Phys. Rev.*, **60**, 53 (1941). See also J. H. Bartlett, *Phys. Rev.*, **64**, 185 (1943).



Electrons that happen to start from the gun in orbits not coinciding with this stable orbit will be gathered into it after making numerous trips around the doughnut. That is, they will be focused into a beam. This is true not only in a radial sense, for electrons whose orbits have a larger or smaller radius than  $r_0$ , but also for electrons whose orbits lie above or below the plane of the stable orbit, that is, for electrons which, except for the focusing action, would wander up toward the plane  $ABC$  or down toward the plane  $DEF$

(Fig. 7-29) instead of staying in the mid-plane. For this axial focusing action to be as effective as the radial focusing action,  $n$  in equation (7-5) must be at least  $\frac{1}{2}$ . Hence the pole pieces are constructed in practice so that  $n$  lies between  $\frac{1}{2}$  and 1. In Kerst's 2-million-volt model,  $n = \frac{2}{3}$ ; in the 20-million-volt model,  $n = \frac{3}{4}$ . Equations (7-4) to (7-6) are all valid even when the electrons at-

tain a velocity approaching  $c$ , so that their mass increases several fold; otherwise, these high relativistic energies could not be achieved. Iwanenko and Pomeranchuk calculated that electromagnetic radiation from the cathode rays fixes 500 million volts as the maximum attainable by a betatron.<sup>1</sup>

Once the electrons are focused into a beam, they continue to accelerate because of the time variation of the magnetic field. If a swarm of electrons are injected at an instant  $A$  early in the cycle (Fig. 7-30), they will circulate faster and faster around the doughnut owing to the increase in the field during the interval between instant  $A$  and instant  $C$ . In the 2-million-volt model, small, pressed, powdered-iron disks at the center of each pole piece were used and became magnetically saturated slightly before the maximum field strength was attained at  $C$ . When this occurs,  $H_0$  increases faster than  $\phi_0$  in equation (7-6), and so  $r_0$  decreases. This action caused the circular electron beam to contract slightly at the last moment just as the electrons attained their highest velocity, and hence they struck the target, which was a piece of thin tungsten. During their journey from gun to target, the electrons traveled around the doughnut many thousands of times—about 60 miles, Kerst calculated.

In the 20-million-volt model, the target was mounted at the outer edge of the doughnut instead of the inner edge, and provision was made

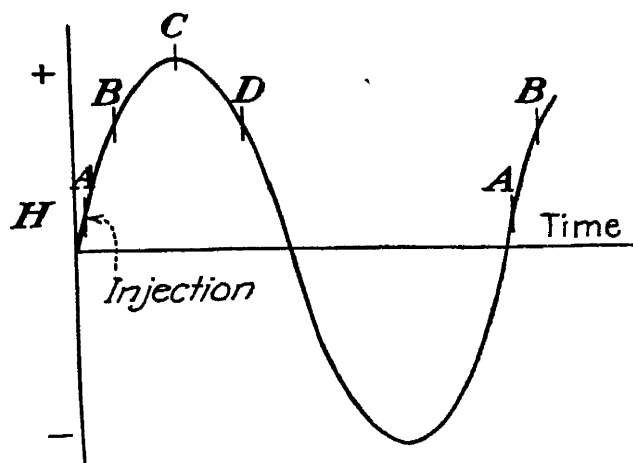


FIG. 7-30.—Showing the timing of events in Kerst's betatron.

<sup>1</sup> D. Iwanenko and I. Pomeranchuk, *Phys. Rev.*, **65**, 343 (1944).

to expand the beam to hit it instead of contracting it, as in the 2-million-volt model. This is an advantage because it places the target (which is the x-ray source) out at the edge of the instrument instead of in near the middle. At this enormous voltage (20 million volts), the efficiency of x-ray production becomes very high,<sup>1</sup> as predicted by Beatty's equation (2-5). Kerst's observations indicate that 65 per cent of the cathode-ray energy is transformed into x-ray energy. In the 20-million-volt model, the alternating current had a frequency of 180 cycles/sec., the power required being about 26 kw. In the 2-million-volt model, the frequency was 600 cycles/sec., the power required being about 4 kw. Others had conceived the general principle of the betatron<sup>2</sup> before Kerst, but they had not worked out the theory of the injection and focusing well enough to construct a successful model.

There should be no confusion between the betatron and the well-known cyclotron<sup>3</sup> used for accelerating protons, deuterons, and alpha particles by whirling them in a spiral path between the poles of an electromagnet. The principles of the two instruments are essentially different. A cyclotron uses a radio-frequency alternating-high-voltage electrostatic field synchronized with the frequency of the ions in their spiral orbits, as the accelerating means. The magnet furnishes a steady magnetic field whose strength is practically the same at the center as it is at the outermost part of the spiral orbit of the particles. The betatron uses a laminated transformer core—it is not really a magnet at all. This is magnetized in an alternating manner at audio frequency, the field being stronger in the center than at the edges.

A cyclotron cannot accelerate electrons to a high energy because their small mass (compared with that of protons) makes it impossible for them to have a kinetic energy of the order of millions of electron volts without their velocity becoming a large fraction of  $c$ . When this happens, their mass increases by a factor of 2 or more. This greatly reduces their frequency of revolution in their spiral orbit in a cyclotron, this frequency being

$$f = \frac{He}{2\pi mc} \quad (e \text{ in e.s.u.}) \quad (7-7)$$

and so they get hopelessly out of synchronism with the alternating electrostatic field. In contrast, a 20-million-volt proton has a mass only 2 per cent greater than one at rest.

<sup>1</sup> For a brief discussion of x-ray yield at high voltages from the quantum-mechanical viewpoint, with bibliography, see H. Dänzer, *Ann. Physik*, **43**, 182 (1943).

<sup>2</sup> G. Breit and M. A. Tuve, "Carnegie Institution Year Book (1927-1928)," No. 27, p. 209; R. Wideröe, *Arch. Elektrotech.*, **21**, 400 (1928); E. T. S. Walton, *Proc. Cambridge Phil. Soc.*, **25**, 469 (1929); W. W. Jassinsky, *Arch. Elektrotech.*, **30**, 500 (1936).

<sup>3</sup> For a discussion of both, see J. D. Cockroft, *J. Sci. Instruments*, **21**, 189 (1944).

One other point should be mentioned in contrasting the betatron with a cyclotron. The magnetic field  $H$  required to curve the orbit of a singly charged particle like an electron, proton, or deuteron having charge  $e$  (in e.s.u.) and mass  $m$  so that the radius of curvature is  $r$  is given by

$$Hr = \frac{mc}{e} v = c \sqrt{\frac{mV}{150e}} \quad (7-8)$$

where  $v$  is the velocity of the particle in centimeters per second and  $V$  is its energy in electron volts. The final expression assumes that the kinetic energy is  $\frac{1}{2}mv^2$  and so is only a rough approximation at high energies, especially for an electron. Nevertheless, it shows that, for a given energy  $V$ , both  $H$  and  $r$  vary inversely in approximate proportion to the square root of the specific charge  $e/m$  of the particle. Since  $m$  is about 1,850 times as great for a proton as for an electron, the magnetic field required in a betatron is much less both in magnitude ( $H$ ) and extent ( $\pi r^2$ ). For example, a magnet producing some 5,000 oersteds over a 12-cm. circle is sufficient to control 5-million-volt electrons, but 5-million-volt deuterons or alpha particles require some 17,000 oersteds over an 80-cm. circle, uniform within 1 or 2 per cent. This calls for a 50-ton magnet as compared with a fraction of a ton for the equivalent betatron. In closing, it may be repeated that Livingston, Genevese, and Konopinski have succeeded in exciting characteristic x-ray spectra (not continuous spectra) by proton bombardment, using a cyclotron.<sup>1</sup>

### QUESTIONS AND PROBLEMS

1. What is a shockproof x-ray tube? A shockproof cable? A Hadding tube intended for what type of work? A Shearer tube? In what type of x-ray circuit is a rectigon or tungar tube used? What is a kenotron? A Lenard ray tube? An autotransformer? An electron gun?

2. Draw the wiring diagram for two different high voltage circuits that will supply c.p.d.c.

3. Name a type of x-ray tube that may be operated at a power input exceeding its continuous rating for a short time. Name a type of tube that must not be so operated. Is it advisable to exceed the maximum voltage rating of an x-ray tube for short intervals? How may the life of an x-ray tube or kenotron be extended?

4. Dichlorodifluoromethane ( $\text{CCl}_2\text{F}_2$ ) finds what use in x-ray equipment? Answer the same question for beryllium. Lead might be considered a metal suitable for use as the target material in an x-ray tube intended for what purpose? Why? Answer the same question for molybdenum.

5. Why should a kenotron not be operated emission limited? What is a cascading transformer? A 200-kv. Greinacher circuit requires a main transformer with what voltage rating? This transformer must be different from the usual x-ray transformer in what respect? Why does this increase its cost?

<sup>1</sup> Footnote 1, p. 48.

6. By what means have the highest voltage x-rays been generated, "voltage" here meaning electron volts of photon energy? What is the wave length of the hardest x-rays produced at 20 million volts? *Ans.* 0.00062 Å.

7. Describe the operating principle of a generating electrostatic voltmeter. How does the breakdown voltage of a sphere gap vary with the barometric pressure? With the temperature? With the humidity? Why is an ordinary milliammeter unsuitable for measuring x-ray tube currents? When should one avoid changing the setting of the autotransformer control in x-ray equipment? Why? What is a Snook rectifier? What are its advantages and disadvantages?

8. In the circuit of Fig. 7-22, if 50 kv. c.p.d.c. is to be generated from a 60-cycle source, what capacity condenser will be required to obtain a 1 per cent ripple when the current used is 2 ma.? If the condenser is built as shown in Fig. 7-25, about how many  $\frac{1}{4}$ -in. glass plates will be required? *Ans.*  $\frac{1}{30}$   $\mu$ f; 44 plates.

9. How does a 20-million-volt betatron compare with a 20-million-volt cyclotron in size and mass? Why? What is the essential feature distinguishing x-ray tube or kenotron filament transformers from most other transformers? Van de Graaff generators have been used to generate x-rays in what voltage range, roughly?

10. What is a constant-voltage transformer? What advantage does it have over a motor generator set for stabilizing voltage and current in x-ray equipment? What advantage does the motor generator set have over the constant-voltage transformer for this purpose?

11. For the radiography of lead 5 in. thick, should you recommend a 2-million-volt betatron or a 20-million-volt betatron? (Refer to page 80.)

## CHAPTER 8

### RUDIMENTS OF RADIOACTIVITY

**1. Introduction.** The use of radium as a valuable supplement to x-rays is gaining favor in industrial radiography. Radium is commonly used along with x-rays in therapeutic work, and its use in this field is older than that of x-rays. Artificial, or induced, radioactivity has recently become a new method of approach in research in biological chemistry, and it may serve as a supplementary aid in x-ray therapy. Therefore it seems worth while to discuss the rudiments of radioactivity so that the handling and use of radioactive material as a valuable supplementary agent in radiology and industrial radiography (see Chaps. 11 and 12) may be understood and appreciated.

In addition to this, it will be realized that the knowledge of atomic structure gained in Chap. 4 was limited entirely to the outer electronic swarm which surrounds the nucleus. Some knowledge of the nucleus itself will be found helpful in later chapters on x-ray diffraction and its applications.

**2. Natural Radioactivity.** Present knowledge indicates that the nucleus of an atom consists of two kinds of particles, protons and neutrons. There is some doubt as to whether or not these particles are truly fundamental and indivisible, but this need not concern us here. That is, one need not ponder such questions as whether a proton may or may not really be a particle formed by the coalescence of a neutron and a positron (defined in Chap. 5), or whether a neutron may or may not be formed by the union of a proton and an electron, or whether the nucleus may not also contain other particles such as the meson<sup>1</sup> (also known as "mesotron," "barytron," "Yukawa particle," or "heavy electron") or the neutrino.<sup>2</sup> It may be stated in passing that the meson is a particle carrying a charge equal to that of the electron, sometimes positive and sometimes negative, the mass being some 180 times that of an electron; mesons have been observed in cosmic-ray experiments. The neutrino is a hypothetical uncharged particle of mass very small compared with that of a proton or neutron. It has not yet been directly observed experimentally, but there are theoretical grounds for suspecting that such a particle exists. To return to the main theme, the proton is a particle

<sup>1</sup> See, for example, W. Heitler, *Nature*, **148**, 680 (1941).

<sup>2</sup> See, for example, J. S. Allen, *Phys. Rev.*, **61**, 692 (1942); E. J. Konopinski *Rev. Modern Phys.*, **15**, 209 (1943).

carrying a positive charge exactly neutralizing the negative charge of an electron, but its mass is 1,837 times that of an electron. The neutron is an uncharged particle having the same mass as a proton.

Of the atoms in ordinary hydrogen, 99.98 per cent have merely a proton for their nucleus. The other 0.02 per cent have a nucleus called a deuteron (or deutron), a particle formed by the union of one proton and one neutron. Since both types of hydrogen atom have a nuclear charge of 1 (that is, a positive charge equal in magnitude to the negative charge of one electron), they both have one orbital electron. The orbital electrons determine the chemical properties. Therefore these varieties of the same element, called "isotopes," are practically identical in their chemical behavior. The symbol  ${}_1\text{H}^1$  designates the ordinary hydrogen atom or its nucleus, the proton, of "mass number" 1 (mass of the nucleus, the mass of a proton or neutron being called unity) and atomic number 1 (charge of the nucleus, the charge of a proton being called unity). Likewise,  ${}_1\text{H}^2$  designates "deuterium," the heavy rare isotope of hydrogen with mass number 2, atomic number 1.

Next in the periodic table comes  ${}_2\text{He}^4$  (helium), with nucleus consisting of two protons and two neutrons, mass number 4, atomic number 2, so that the neutral atom has two orbital (K) electrons. When these electrons are detached, the extremely stable nucleus that is left is called an "alpha particle." These particles are commonly projected at high energy from many unstable radioactive nuclei when they "disintegrate"—for example, when radium disintegrates into radon. Streams of these particles are called "alpha rays." Among every 100,000 or so ordinary atoms of helium, there is found one atom of the rare isotope  ${}_2\text{He}^3$  having a mass number 3 (two protons, one neutron).

Continuing to list the ordinary *stable* isotopes in the same manner, one has  ${}_3\text{Li}^6$  (7.5 per cent) and  ${}_3\text{Li}^7$  (92.5 per cent). This mixture results in an "average mass number" (atomic weight) of 6.94.

Then follow  ${}_4\text{Be}^9$  (100 per cent);  ${}_5\text{B}^{10}$  (18.4 per cent) and  ${}_5\text{B}^{11}$  (81.6 per cent);  ${}_6\text{C}^{12}$  (98.9 per cent) and  ${}_6\text{C}^{13}$  (1.1 per cent);  ${}_7\text{N}^{14}$  (99.62 per cent) and  ${}_7\text{N}^{15}$  (0.38 per cent);  ${}_8\text{O}^{16}$  (99.76 per cent),  ${}_8\text{O}^{17}$  (0.04 per cent), and  ${}_8\text{O}^{18}$  (0.20 per cent);  ${}_9\text{F}^{19}$  (100 per cent);  ${}_{10}\text{Ne}^{20}$  (90.00 per cent),  ${}_{10}\text{Ne}^{21}$  (0.27 per cent), and  ${}_{10}\text{Ne}^{22}$  (9.73 per cent);  ${}_{11}\text{Na}^{23}$  (100 per cent);  ${}_{12}\text{Mg}^{24}$  (77.4 per cent),  ${}_{12}\text{Mg}^{25}$  (11.5 per cent), and  ${}_{12}\text{Mg}^{26}$  (11.1 per cent);  ${}_{13}\text{Al}^{27}$  (100 per cent);  ${}_{14}\text{Si}^{28}$  (89.6 per cent),  ${}_{14}\text{Si}^{29}$  (6.2 per cent) and  ${}_{14}\text{Si}^{30}$  (4.2 per cent);  ${}_{15}\text{P}^{31}$  (100 per cent);  ${}_{16}\text{S}^{32}$  (95.0 per cent),  ${}_{16}\text{S}^{33}$  (0.74 per cent),  ${}_{16}\text{S}^{34}$  (4.2 per cent), and  ${}_{16}\text{S}^{36}$  (0.016 per cent); etc.

Chemists arbitrarily set the atomic weight of oxygen as exactly 16 before all the facts indicated by the above symbols had been discovered. In view of the foregoing data on oxygen, the logical value of the atomic weight of oxygen should be 99.76 per cent of 16 plus 0.04 per cent of

17 plus 0.20 per cent of 18, or 16.004, which indeed is the atomic weight of oxygen on the "physical scale" of atomic weights.<sup>1</sup> This introduces a discrepancy of 1 part in 4,000 between mass number and ordinary chemical-scale atomic weight in the case of a pure element (only one stable isotope) like sodium (mass number 23, chemical-scale atomic weight 22.997). However, if one considers a case like that of hydrogen, the discrepancy is much greater than this; 99.98 per cent of 1 plus 0.02 per cent of 2 equals 1.0002, whereas the atomic weight of hydrogen is 1.0078, a discrepancy of about 8 parts in 1,000. This discrepancy is due to the packing energy, or binding energy.

To make this clear, consider the case of helium, which is almost entirely  ${}^4_2\text{He}$ , so that it should have an atomic weight of exactly 4 on the physical scale or 3.999 on the chemical scale. Actually, it has an atomic weight of 4.003 on the chemical scale or 4.004 on the physical scale, and this discrepancy is due to the packing energy. An atom of  ${}^4_2\text{He}$  consists of two neutrons, two protons, and two orbital electrons. An atom of  ${}^{16}_8\text{O}$  consists of eight neutrons, eight protons, and eight orbital electrons. Yet the mass of the latter is only 3.996 times that of the former. The reason for this is that much energy would be required to dissect the atoms in a gram of oxygen and re-form the parts into the resulting 1.001 g. of helium. If this could be done, the energy used would be converted into mass, appearing as the extra milligram according to the relation (4-15)  $E = mc^2$ . In fact, this enables one to compute that the energy required for such a process, if it could be accomplished at all, would be  $9 \times 10^{17}$  ergs, or about 30,000 hp.-hr. Conversely, one could convert a little helium into oxygen, much energy would be generated. Still more energy would be generated by converting hydrogen to helium or oxygen, for its packing energy is greater, as has been pointed out. However, hydrogen is not so good as an instructive example because  ${}^1_1\text{H}$  contains no neutrons whereas all other elements do, and hence the reaction would not "come out even" with respect to the neutrons and protons as the  ${}^4_2\text{He} - {}^{16}_8\text{O}$  process would.

The stable isotopes up to sulfur have already been listed. For a complete list, the reader is referred to an article by Seaborg.<sup>2</sup> The heaviest stable isotope is  ${}^{209}_{83}\text{Bi}$ . All the elements heavier than this, up to and including the uranium isotope  ${}^{238}_{92}\text{U}$ , and some lighter ones, for example the thallium isotope  ${}^{207}_{81}\text{Tl}$ , are naturally unstable or radioactive. There are also two elements of comparatively low atomic number that are slightly radioactive, namely, potassium and rubidium. The radioactivity of potassium can be used to make a chemical analysis for it.<sup>3</sup>

<sup>1</sup> R. T. Birge, *Rev. Modern Phys.*, **13**, 234 (1941).

<sup>2</sup> G. T. Seaborg, *Rev. Modern Phys.*, **16**, 1 (1944).

<sup>3</sup> R. B. Barnes and D. J. Salley, *Ind. and Eng. Chem. (Anal. Ed.)*, **15**, 4 (1943).

The natural radioactivity of uranium was discovered by A. H. Becquerel in 1896. The phenomenon was studied intensively by Becquerel, Rutherford,<sup>1</sup> and others and was given added impetus in 1898 when Pierre and M. S. (Mme.) Curie and G. Bémont first obtained radium chloride. Radium, together with its disintegration products, is the most active and important of the naturally radioactive elements. Radium itself was not obtained until 1911 by Mme. Curie and A. Debierne. Until 1930, most of the world's radium was refined from pitchblende obtained in the Belgian Congo. The price in 1930 was about \$60,000 per gram. The discovery in 1930 of extensive rich deposits of pitchblende near Great Bear Lake in Canada<sup>2</sup> has greatly increased the supply and reduced the price, which is now less than \$25,000 per gram.

Such radioactive substances in general emit three types of "rays" historically designated as alpha, beta, and gamma ( $\alpha$ ,  $\beta$ , and  $\gamma$ ). The alpha rays are high-energy streams of alpha particles, now known to be identical with the nuclei of helium atoms. Beta rays are high-energy electrons, like cathode rays, except that they are ejected in all directions, whereas cathode rays ordinarily form a beam. Gamma rays have already been described as high-energy photons or electromagnetic radiation like x-rays.

Obviously, if an atom "disintegrates" radioactively by ejecting an alpha particle, its mass number will decrease by 4 and its atomic number will decrease by 2. An example is the most plentiful isotope of radium,  ${}_{88}\text{Ra}^{226}$ , which disintegrates by ejecting an alpha particle; that is,  ${}_{88}\text{Ra}^{226}$  divides into  ${}_{86}\text{Rn}^{222}$  (radon, also called "niton" or "radium emanation") and  ${}_{2}\text{He}^4$ . In this type of radioactive disintegration process, the mass of the products (helium and radon in this case) is slightly less than the mass of the parent material (radium in this case). The lost mass is converted into energy ( $mc^2$ ). This appears as the kinetic energy of the alpha particle, which comes tearing out with an energy of several million electron volts; in other types of disintegration it is a beta particle or a gamma-ray photon that is ejected. In many disintegrations, both alpha and gamma or beta and gamma radiations are produced. There are a few cases where feeble beta rays are found along with strong alpha rays, but they are probably generated in a secondary manner rather than in the initial disintegration.

If an atom disintegrates by ejecting a beta particle (electron), its

<sup>1</sup> E. Rutherford, J. Chadwick, and C. D. Ellis, "Radiations from Radioactive Substances," The Macmillan Company, New York, 1930. For additional details about natural radioactivity, see J. W. Mellor, "Comprehensive Treatise on Inorganic and Theoretical Chemistry," the volume on radium; also M. Curie, A. Debierne, A. S. Eve, H. Geiger, O. Hahn, S. C. Lind, St. Meyer, E. Rutherford, and E. Schweidler, *Rev. Modern Phys.*, 3, 427 (1931).

<sup>2</sup> C. Camsell, *J. Franklin Inst.*, 233, 545 (1942).



mass number remains unchanged and its atomic number will increase by 1. For example,  $_{82}\text{Pb}^{214}$ , an isotope of lead that is commonly called "radium B," disintegrates by ejecting a beta particle (and gamma rays), the product being an isotope of bismuth,  $_{83}\text{Bi}^{214}$  that is called "radium C."

There are long chains of such disintegration processes. For example, radium's most plentiful isotope,  $_{88}\text{Ra}^{226}$ , disintegrates by ejecting an alpha particle to radon gas,  $_{86}\text{Rn}^{222}$ , which in turn disintegrates by ejecting an alpha particle to  $_{84}\text{Po}^{218}$  (called "radium A"), which in turn disintegrates by ejecting an alpha particle to  $_{82}\text{Pb}^{214}$  (radium B), which in turn disintegrates by ejecting a beta particle to  $_{83}\text{Bi}^{214}$  (radium C), which in turn disintegrates by ejecting a beta particle to  $_{84}\text{Po}^{214}$  (called radium C'), which disintegrates by ejecting an alpha particle, etc., the process finally ending with a stable isotope<sup>1</sup> of lead,  $_{82}\text{Pb}^{206}$ .

Some of these disintegrations are accompanied by strong gamma radiation, and some are not. Surprisingly enough, radium emits practically no gamma rays when it disintegrates into radon. Radon, however, is a powerful emitter of gamma rays as it disintegrates into polonium 218, lead 214, etc., as outlined above, most of the gamma rays being generated in the last four disintegrations mentioned. There is also a wide variation in the instability of these various substances. For example, it requires some 1,700 years for a sample of radium to disintegrate to an extent that half of it will have changed into radon, but only 3.85 days is required for a sample of radon gas to disintegrate to this extent. A microgram of radon will be half gone after it lies for 3.85 days in a sealed tube; after 3.85 more days, it will be three-fourths gone; after 3.85 more days it will be seven-eighths gone, etc. Thus radon is said to have a "half life" of 3.8 days, and radium a half life of 1,700 years. Radium A, radium B, and radium C have half lives of only a few minutes; radium C', of about  $10^{-6}$  sec. From this, it is obvious that radon is much more unstable and therefore much more radioactive than an equal mass of radium. In fact, a gram of radon, if it could be obtained, would have an activity equal to that of several hundred pounds of radium; its container would be red-hot.

These disintegration rates are unchanged by pressure, temperature, state of chemical combination, etc. Thus a gram of radium in the form of radium chloride kept immersed in liquid air has the same half life as a gram of pure radium kept at  $500^{\circ}\text{C}$ . under a pressure of 1,000 lb./in. and both eject alpha particles at the same rate.

In industrial radiography and in most hospitals, radium or radium compounds are usually purchased or rented and used in a sealed capsule. There are comparatively few places where the necessary facilities and qualified experts are available for working with radium or its compounds outside of a sealed capsule. As already stated, pure radium emits prac-

<sup>1</sup> See Appendix, Table IX.

cally no gamma rays. However, a piece of pure radium or pure radium chloride or other radium compound does not remain pure when left alone. One gram of pure radium emits  $3.4 \times 10^{10}$  alpha particles each second. Hence  $3.4 \times 10^{10}$  radon atoms are produced each second within the gram of radium. Meanwhile the radon, which is a gas (the heaviest known, 111 times as dense as hydrogen), also continually disintegrates into a whole series of highly active products as already outlined, and it is these multiple disintegration processes which generate the gamma rays.

A piece of radium left in the open air thus slowly evolves radon gas. The quantity evolved is so slight that most of it remains absorbed in the radium. Hence the radium appears to emit gamma rays. If the radium is melted or is heated in a vacuum, the radon is driven out. After the radium cools off, it is then pure radium and will be found to emit practically no gamma rays for a while. However, if left standing a few days it soon saturates itself with a fresh supply of radon and hence emits gamma rays again.

Radon is considered one of the most deadly gases known. If one breathes air containing even a minute trace for any length of time, he saturates his body with it and thus subjects every portion of his body to alpha, beta, and gamma rays for years afterward, for the disintegration products of radon are solids, some with long half lives. If much has been breathed, the result is a slow and terrible death. Therefore radium is kept in sealed capsules during use. These capsules are usually made of silver for industrial work and have a wall thickness of about  $\frac{1}{2}$  mm. Obviously, a radium capsule should not be crushed, stepped on, or pinched with pliers, for this might cause a radon leak, with disastrous consequences.

If a gram of radium that has just been freed of radon is sealed in a capsule, it starts accumulating radon, which in turn disintegrates. Eventually, these two processes balance each other; the radon disintegrates within the capsule just as fast as it is evolved by the radium. A capsule containing 1 g. of radium that has reached this equilibrium condition regarding its radon content is said to contain 1 curie of radon, a unit established in 1910 by the Radiology Congress at Brussels. A capsule containing 100 milligrams of radium that has reached an equilibrium radon content is said to contain 100 millicuries of radon. At 0°C. and 76 cm. of mercury pressure, 1 curie of radon occupies 0.6 mm.<sup>3</sup>.

A capsule containing 1 g. of radon-free radium will acquire an activity of  $\frac{1}{2}$  curie in 3.85 days;  $\frac{3}{4}$  curie in 7.70 days; 99 $\frac{1}{2}$  per cent curie in 30 days, and 99.99 per cent curie in 50 days. At places where the capsules are opened, the ventilation must keep the radon content of the air below 10<sup>-11</sup> curie/liter for safety. That is, 1 part of radon in 10<sup>18</sup> (1 quintillion) parts of air by volume is on the borderline of safety for breathing pur-

poses.<sup>1</sup> A Geiger-Mueller counter (see Chap. 9) that will detect  $10^{-12}$  curie of radon was described recently by Brown, Elliott, and Evans.<sup>2</sup> The equation governing the accumulation of radon<sup>3</sup> in a capsule containing  $g$  g. of radium, initially radon-free, is

$$C = g(1 - e^{-\delta t}) \quad (8-1)$$

where  $C$  is the curies of radon present after  $t$  days,  $\delta$  is a constant equal to 0.180 when  $t$  is in days, and  $e$  is the Napierian log base.

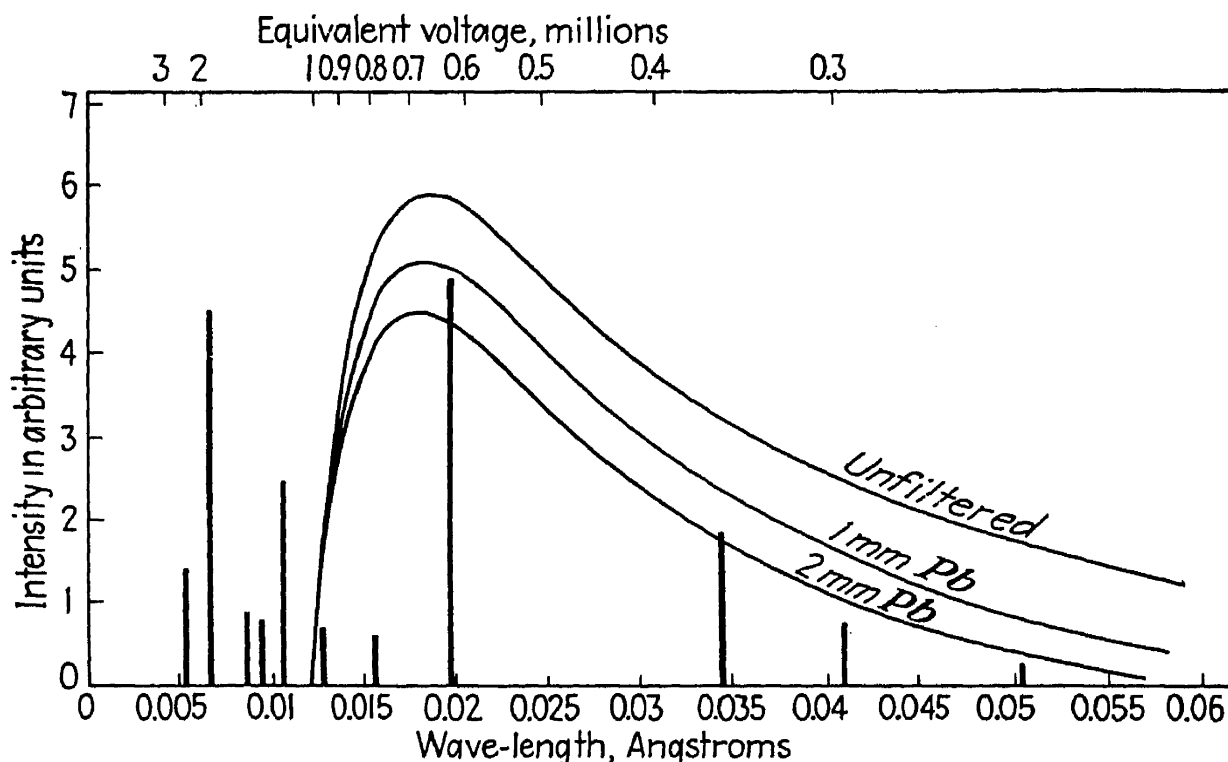


FIG. 8-1.—Comparing the spectral energy distribution of radium gamma rays and million-volt x-rays. (Eve and Grimmett; courtesy of "Nature," and Macmillan & Company, Ltd.)

The spectral energy distribution of the gamma rays from radium in equilibrium with its products, in the sense just explained, has been represented graphically by Eve and Grimmett.<sup>4</sup> Figure 8-1 is a graph that they prepared to compare the spectrum of million-volt x-rays with the spectrum of the gamma rays from radium. Since the latter is a line spectrum while the former is continuous, the gamma-ray spectrum is plotted as a series of vertical lines, the position of the line indicating its

<sup>1</sup> See *Nat. Bur. Standards Handbook H27*; also *Engineering*, **152**, 360 (1941).

<sup>2</sup> S. C. Brown, L. G. Elliott, and R. D. Evans, *Rev. Sci. Instruments*, **13**, 147 (1942).

<sup>3</sup> For radon collection and purification technique, see W. Duane, *Phys. Rev.*, **5**, 311 (1915); G. Failla, U.S. patent 1,553,794 (1925); R. Livingston, *Rev. Sci. Instruments* **4**, 15 (1933); P. A. Macdonald and M. S. Margolose, *Rev. Sci. Instruments*, **12**, 320 (1941).

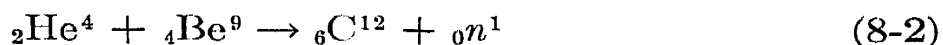
<sup>4</sup> A. S. Eve and L. G. Grimmett, *Nature*, **139**, 52 (1937).

wave length and the height indicating its relative intensity. This plot shows only the more prominent lines in the gamma-ray spectrum. For a more detailed description of this spectrum, the reader is referred to an article by Steadman,<sup>1</sup> who found one line with a wave length of only 0.00017 Å. The upper curve for the continuous x-ray spectrum at 1 million volts was computed from Kramers's formula (3-22). The lower curves for lead filters were calculated from the upper curve, the mass absorption coefficient of lead at these wave lengths being known. From the graph, it may be seen that 2-million-volt x-rays would probably be a better substitute for radium gamma rays than 1-million-volt x-rays are. Absorption coefficients of radium B + C gamma rays in aluminum, carbon, and lead have been determined by Roberts.<sup>2</sup>

The fact that gamma rays have a line spectrum naturally suggests that their origin might be explained on the basis of discrete nuclear energy levels, just as characteristic x-ray spectra are explained on the basis of the electronic energy levels of an ion. The existence of discrete nuclear excitation levels, corresponding to the K, L, etc., excitation levels for x-rays, has been experimentally confirmed. The prediction of nuclear energy levels by quantum mechanics cannot be very successful until the law of interaction between the nuclear particles (protons, neutrons, etc.) is known.<sup>3</sup> The generally accepted view is that the nucleus, after ejecting an alpha or beta particle, sometimes makes a readjustment immediately afterwards (as in the disintegration of  $_{82}\text{Pb}^{214}$ ) and sometimes does not (as in the disintegration of radium), this readjustment being the process that generates the gamma rays.

Details regarding the handling and use of radium will be found in Chaps. 11 and 12, and the precautions necessary for protection from the gamma rays are explained in Chap. 10.

In 1932, Chadwick<sup>4</sup> discovered that a piece of beryllium placed close to a piece of polonium emitted neutrons. The energetic alpha particles from the disintegrating polonium bombarded the beryllium, with the result that the following reaction took place,



which means that a nucleus of a helium atom, having charge of 2 and mass of 4 (that is, an alpha particle), collides with the nucleus of a beryllium atom, having charge of 4 and mass of 9, the two unite to form a new atomic nucleus having charge of 6 and mass of 12 (this must be carbon

<sup>1</sup> L. T. Steadman, *Phys. Rev.*, **36**, 460 (1930). See also J. E. Roberts, *Phil. Mag.* **36**, 264 (1945).

<sup>2</sup> J. E. Roberts, *Proc. Roy. Soc. (London) A*, **183**, 338 (1945).

<sup>3</sup> See, for example, K. M. Guggenheimer, *Proc. Roy. Soc. (London) A*, **181**, 169 (1942).

<sup>4</sup> J. Chadwick, *Proc. Roy. Soc. (London) A*, **136**, 692 (1932).

since the atomic number of carbon is 6), and a neutron (particle with no charge and mass of 1) is ejected. Equation (8-2) is often written in the more abbreviated form



Later it was discovered that a copious supply of neutrons could be obtained from beryllium by bombarding it with deuterons, for example from a cyclotron, the reaction being

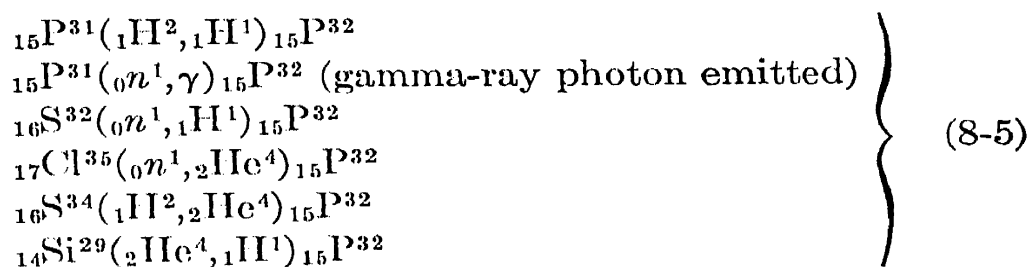


In both these processes, the neutrons are ejected at energies of several million electron volts. Such free neutrons are short-lived particles. A neutron soon encounters some atomic nucleus and coalesces with it, the result being a new nucleus that is usually unstable.

The commonest methods of obtaining neutrons have been described here so that a few remarks in Chap. 11 regarding neutron therapy will be more intelligible and also so that there will be no doubt as to the origin of the neutrons used in some of the reactions to be mentioned in the next section. Neutrons which have slowed down, nearly to thermal velocities, are called "resonance neutrons."

**3. Artificial Radioactivity, or Induced Radioactivity.** One of the first discoveries<sup>1</sup> made when the first cyclotrons were put into operation was that unstable radioactive isotopes of most of the elements could be produced by bombarding matter with neutrons or high-energy deuterons, alpha particles, or protons. Over 300 such radioactive isotopes have already been produced and listed in tables.<sup>2</sup> Most of them can be prepared by several different processes.

For example, the radioactive isotope of phosphorus,  ${}_{15}\text{P}^{32}$ , has been used in efforts to develop improved methods of radiation therapy. It disintegrates by ejecting beta particles, but no gamma rays. The energy of the beta particles is 1.69 million electron volts. Its half life is 14.3 days. It has been prepared in the following ways:



This is a typical example of an artificially radioactive isotope.

<sup>1</sup> J. D. Cockroft and E. T. S. Walton, *Proc. Roy. Soc. (London) A*, **137**, 229 (1932). See also Irène Curie and F. Joliot, *Compt. rend.*, **196**, 1885 (1933), **198**, 254, 559 (1934); *J. phys.*, **4**, 494 (1933), **5**, 153 (1934); J. D. Cockroft, C. W. Gilbert, and E. T. S. Walton, *Nature*, **133**, 328 (1934).

<sup>2</sup> G. T. Seaborg, *Rev. Modern Phys.*, **16**, 1 (1944). This article contains a bibliography of more recent work on induced radioactivity.

Practically all artificially radioactive isotopes decay by ejecting beta particles; but in a surprisingly large number of cases, perhaps 10 or 20 per cent, the beta rays are positive, consisting of positrons instead of electrons. Examples are  $C^{11}$ ,  $N^{13}$ ,  $O^{15}$ ,  $F^{17}$ ,  $Na^{22}$ , and  $Al^{26}$ . In beta-ray decay of natural radioactive substances, the emission of positrons is almost, but not quite, unknown. There is evidence that perhaps 1 per cent of the beta rays from some of them consist of positrons.<sup>1</sup> It has been found possible to manufacture  ${}_{84}Po^{210}$  (radium F) artificially; it decays by emitting an alpha particle, but since this isotope is also a naturally occurring radioactive material it is rather a poor exception to the general rule that artificially radioactive materials do not decay by alpha-particle emission. Several of these materials disintegrate by a process known as "K electron capture."  ${}_4Be^7$  is an example.<sup>2</sup> This atom has an unstable nucleus with a half life of 43 days. When it disintegrates, it captures one of its own K electrons, thus becoming an atom of  ${}_3Li^7$ , and gamma rays are emitted in the process, although this is not always the case.<sup>3</sup>

The alpha particles ejected by the disintegration of natural radioactive elements have discrete energy values constituting a "line" spectrum. The beta particles from both natural and artificial radioactive disintegration have a continuous energy spectrum, all energies being observed up to a definite maximum; a beta-ray line spectrum is superimposed upon this. The gamma rays from either artificial or natural disintegration have a line spectrum.

**4. Fission.** This discussion may be brought to a close by mentioning the process known as "fission," discovered<sup>4</sup> in 1939. This is a process in which the isotope  ${}_{92}U^{235}$ , upon capturing a neutron, becomes unstable in such a way that it splits into two large parts instead of merely ejecting an alpha or beta particle. The resulting fragments may be  ${}_{56}Ba$  and  ${}_{36}Kr$ , or  ${}_{57}La$  and  ${}_{35}Br$ , or  ${}_{55}Cs$  and  ${}_{37}Rb$ , or, at any rate, elements having atomic numbers around 56 and 36 and adding to 92.  $U^{235}$  can be excited so as to split in this way by the mere presence of neutrons that are "at rest," that is, neutrons of only thermal energy, called "thermal neutrons." Ordinary uranium contains less than 1 per cent  $U^{235}$ , and the problem of separating it from the principal isotope,  $U^{238}$ , appeared almost insuperable when it was first contemplated.

Taking the fission of  ${}_{92}U^{235}$  into  ${}_{56}Ba$  and  ${}_{36}Kr$  as an example, one

<sup>1</sup> J. Chadwick, P. M. S. Blackett, and G. P. S. Occhialini, *Proc. Roy. Soc. (London)* A, **144**, 235 (1934); D. Skobel'tzyn and E. Stepanowa, *Nature*, **133**, 565, 646 (1934).

<sup>2</sup> R. B. Roberts, N. P. Heydenburg, and G. L. Locher, *Phys. Rev.*, **53**, 1016 (1938).

<sup>3</sup> P. K. Weimer, J. D. Kurbatov, and M. L. Pool, *Phys. Rev.*, **66**, 209 (1944).

<sup>4</sup> See L. A. Turner, *Rev. Modern Phys.*, **12**, 1 (1940); also N. Bohr and J. A. Wheeler, *Phys. Rev.*, **56**, 426 (1939); for details regarding the atomic bomb, see H. D. Smyth, "Atomic Energy for Military Purposes," Princeton University Press, 1945.

notes that the atomic weights of barium and krypton are 137.4 and 83.7, respectively, adding to 221.1. This is considerably less than the mass 235 present in the original uranium isotope. The apparent discrepancy in mass number of about 14 (235 minus 221) may be slightly illusory if the products are radioactive isotopes of mass greater than 137 and 84; and then, too, several neutrons are liberated in the fission of each atom, so that the mass which actually vanishes is considerably less than 14; perhaps only 1 or 2, or even less than 1. Nevertheless, a significant fraction of the original 235 mass units is transformed into energy according to the  $mc^2$  relationship [equation (4-15)]. The liberation of several (fast) neutrons by each uranium atom undergoing fission makes the process cumulative, when conditions are adjusted so that the fast neutrons are retarded to thermal velocities before escaping from the sample. Hence, a terrific explosion can be produced.

Resonance neutrons from the fission of  $U^{235}$  may be used to change some of the plentiful isotope of uranium ( $U^{238}$ ) into  $U^{239}$ . This undergoes beta-type radioactive decay (half life 23 min.) into a new element "neptunium"  ${}_{93}\text{Np}^{239}$ , which in turn undergoes beta decay (half life 2.3 days) into another new element "plutonium"  ${}_{94}\text{Pu}^{239}$ , emitting gamma rays in the process. Plutonium also is capable of undergoing fission, and it appears that it is the essential ingredient of the atomic bombs first revealed in the bombing of Hiroshima and Nagasaki, Japan.

### QUESTIONS AND PROBLEMS

1. What is a proton? Neutron? Positron? Meson? Neutrino? Deuteron? Alpha particle? How many neutrons and how many protons are in an atom of ordinary stable sodium? What is mass number? What are thermal neutrons?

2. In radioactive decay, is the mass of the disintegration products the same as the mass of the original material, or is it greater or smaller? If these masses are accurately measured, how may one calculate the energy released in the process?

3. Is the rate of the disintegration or fragmentation process controllable in natural radioactivity? In artificial radioactivity? In nuclear fission? Is alpha-ray emission commonplace in artificial or natural radioactivity, or both? Answer the same question for K-electron capture.

4. A half gram of radon-free radium is combined with chlorine to form radium chloride, which is sealed in a capsule designated as capsule *A*. A week later, the capsule will contain how many millicuries of radon? On this day (Monday), the capsule is opened and the radon pumped out into another capsule, designated as capsule *B*, after which both *A* and *B* are sealed again, *A* containing the radium chloride and *B* the week's accumulation of radon. On the next day (Tuesday) which capsule will exhibit the greater gamma-ray activity? Answer the same question for the following Friday.

*Ans.* (part 1) 358 millicuries.

5. Would you describe the energy distribution of alpha rays as a continuous spectrum or a line spectrum? Beta rays? Gamma rays? Suggest a reason why any of these might have a line spectrum.

6. Some  $P^{32}$  might be produced by bombarding sand with what kind of projectile of high energy? What sort of particles are required to cause uranium to undergo fission? How may one obtain these particles?

## CHAPTER 9

### X-RAY DETECTION, MEASUREMENT, AND REGISTRATION

**1. Fluoroscopy.** Having discussed the generation of x-rays and gamma rays in the preceding chapters, we logically turn next to methods of detecting, measuring, and registering them. The oldest method in the case of x-rays is, of course, the one that enabled Röntgen to discover them—fluorescence. This method has little or no practical value in the case of gamma rays, but it was nevertheless an important method of investigation in early studies of radioactivity, the “scintillations” of a fluorescent screen being the historic way to detect alpha and beta rays and to estimate their intensity.

It was mentioned in Chap. 1 that Röntgen’s fluorescent screen depended upon the fluorescence of barium platinocyanide. Such a material is able to absorb photons of high energy, such as x-rays or ultraviolet rays, and emit part of this absorbed energy in the form of the lower energy photons that constitute ordinary light. A fluorescent solid inorganic material of this sort is called a “phosphor.” Phosphors can also fluoresce under the action of high-energy particles such as cathode rays and alpha and beta rays. Familiar examples are a cathode-ray oscillograph tube screen, or the screen of a television receiver, or the material that glows on the hands and numerals of many watches and clocks under the action of the radioactive material mixed with it. Fluorescence in ultraviolet radiation is familiar in fluorescent lamps, which have the inner walls of the glass coated with a phosphor.

The commercial use of phosphors really began with Röntgen’s discovery of x-rays in 1895. They are used for two different purposes in radiography. In both cases, they are coated upon the surface of a suitable backing, usually white cardboard; the resulting coated cardboard is called a “screen.” Depending upon which of the two purposes just mentioned is intended, such a fluorescent screen is called (1) a “fluoroscopic” screen or (2) an “intensifying” screen. Fluoroscopic screens are used in medical work to make visual observations of a patient and in industrial work for inspecting objects easily penetrated by x-rays, such as oranges and packaged foods, for fitting shoes in shoe stores, for detecting nails and ruptures in automobile tires, etc. Intensifying screens are used to increase the sensitivity (and sometimes the contrast) of photographic films or plates to x-rays. X-rays will act upon a photographic emulsion much as light does, but this effect can be greatly



increased by pressing an intensifying screen tightly against each face of the photographic film so as to form a "sandwich." Then, in addition to the direct action of the rays on the film, the fluorescence of the phosphor on the screens exposes the film to visible light, thus producing a given exposure in a much shorter time or a much heavier exposure in the same time.

Barium platinocyanide was widely used commercially for fluoroscopic screens until about 1910. It fluoresces with a brilliant green light. It went out of use because it is quite expensive and not stable, deteriorating under x-ray exposure. Next, artificial willemite was used commercially for fluoroscopic screens. This is zinc orthosilicate, although closely allied compounds are also sometimes called willemite. Willemite also fluoresces with a brilliant green light, but it has two defects. (1) It phosphoresces; that is, it glows a while after the x-rays are shut off, and displays "afterglow." (2) It fluoresces efficiently for soft x-rays, but not for hard ones. Hence, a physician attempting to examine a patient with a thick chest cannot see much with a willemite screen because only hard rays pass through to the screen.

In 1914, C. V. S. Patterson introduced cadmium tungstate for fluoroscopic screens, and until 1933 these "Patterson standard screens" were in practically world-wide use.<sup>1</sup> They fluoresce with a bluish-white light, have no afterglow, and are quite stable, so that a 20-year-old screen that has been well cared for is as good as new.

In 1933, Levy and West<sup>2</sup> developed a new type of zinc cadmium sulfide for fluoroscopic screens. Zinc sulfide had been known as a phosphor for years but was not used in fluoroscopy because of its phosphorescent afterglow. Levy and West discovered that this could be suppressed by the addition of a trace (1 part in 2 million, or less) of nickel. Screens of this material as now made glow ten times as brightly as the earlier cadmium tungstate screens, under the action of x-rays, their color being a brilliant yellow-green. They are known commercially in this country as Patterson "type B" screens.

To turn from fluoroscopic screens to intensifying screens, the phosphor used for these has been calcium tungstate ever since they have been used. An intensifying screen should fluoresce so as to produce light of the wave length to which photographic films are most sensitive, namely the blue-violet or near ultraviolet. Such photographically active radiation is said to be "actinic." Calcium tungstate has a strong actinic fluorescence. For general usage, calcium tungstate intensifying screens

<sup>1</sup> The Patterson Screen Division, E. I. duPont de Nemours & Company, Inc., Towanda, Pa.

<sup>2</sup> L. Levy and D. W. West, *J. Soc. Chem. Ind.*, **58**, 457 (*Chemistry & Industry*, 1939).

are still the best known. They have an intensifying factor of 10 or 15 for ordinary radiographic work. That is, the exposure required without the screens is 10 or 15 times as long as with them. Extremely heavy x-ray exposures will sometimes discolor and damage such screens. For this reason, part of the screen should not be left unprotected while radiographing thick pieces of steel, etc.

For soft rays, however, having an energy ( $h\nu$ ) around 40 kv., a new type of intensifying screen was developed in 1937 by Levy and West; it fluoresces a brilliant blue and is said to be six times as active as a calcium tungstate screen for these soft rays. These are known commercially as Patterson "Fluorazure" intensifying screens, and they are useful in certain types of diffraction work,<sup>1</sup> especially where it is not necessary to make quantitative comparisons of intensities. These screens are likewise made with a zinc sulfide phosphor, but a trace of silver is employed instead of the nickel used in the type B fluoroscopic screens. Gamertsfelder and Gingrich<sup>2</sup> report that for the molybdenum  $K_\alpha$  lines this type of screen has an intensifying factor which varies from 1 to 13, depending upon the x-ray intensity. For copper  $K_\alpha$ , they report intensifying factors from 1 to 4, concluding that "it appears impractical to use this screen when true intensity measurements are necessary."

The desirable features of a satisfactory fluoroscopic or intensifying screen are uniform brightness of fluorescence for the whole screen, freedom from graininess, freedom from afterglow, and as intense a fluorescence as possible when exposed to x-rays of moderate or low intensity. These features can be attained only by careful manufacture. The basic ingredient of the phosphor used (ordinarily a sulfide, tungstate, silicate, phosphate, or borate) must be freed of even slight traces of such elements as iron, cobalt, chromium, or vanadium (or their compounds). On the other hand, the addition of a trace of copper, nickel, manganese, or silver (usually a compound of one of these elements) may be essential for success. This trace of added material is called an "activator" or "phosphorogen." The material is then heated, sometimes with a volatile flux such as sodium chloride, to a temperature near its melting point to induce crystallization; otherwise it will not fluoresce. The prepared phosphor must then be coated very evenly upon its backing. All this helps explain the astonishing price of what looks like "just a piece of cardboard." A 14- by 17-in. type B fluoroscopic screen costs about \$90. Intensifying screens are usually sold in pairs, since they are used on both sides to make a film "sandwich." A pair of 14- by 17-in. calcium tungstate intensifying screens costs from \$30 to \$50. Such valuable screens deserve good care. They should not be left out

<sup>1</sup> See N. H. Kolkmeijer, C. J. Krom, and H. Kunst, *Nature*, **140**, 67 (1937).

<sup>2</sup> C. Gamertsfelder and N. S. Gingrich, *Rev. Sci. Instruments*, **9**, 154 (1938).

to gather dust, nor should they be placed where drops of water, developer, or fixer might splash on them. They should be freed of dust occasionally by wiping with soft flannel, which may be moistened with pure ethyl alcohol if the screen is dirty.

The light emitted by a phosphor usually covers a continuous broad band in the visible. The theory of the fluorescence of phosphors depends upon the electronic energy-level bands present in insulating or semi-conducting crystals.<sup>1</sup> In the case of zinc sulfide,<sup>2</sup> the process is supposedly somewhat as follows: An electron is excited from a lower, filled band to one of the upper, normally vacant bands. An electron from one of the activator atoms (the trace of copper or nickel, etc.) then falls into the vacancy thus left by the excited electron, which has meanwhile dropped into one of the levels existing only at grain boundaries, surfaces, etc. There it remains trapped (in a metastable state) until it is reexcited to the upper band again, from which it may be captured by one of the activator atoms that has lost an electron, as already mentioned. This last process represents an energy drop that supposedly emits the light photon.

Gaertner<sup>3</sup> has measured the efficiency of a Schering-Kahlbaum<sup>4</sup> cadmium tungstate fluoroscopic screen, using the continuous radiation from a tungsten target bombarded at 90 kv., a voltage commonly used in medical diagnostic work. His results indicated that only about one-half of 1 per cent of the energy of the x-rays absorbed by the screen reappeared in the form of light.

Ilford, Limited, London, England, has developed a photographic paper, called "Kryptoscreen x-ray paper." This paper is coated with a photographic emulsion, like the paper upon which ordinary photographs are printed, but it is intended to be used in place of a photographic film for certain types of x-ray work. Such x-ray papers have been manufactured by various companies for years, but this particular one is mentioned because it is made with a fluorescent pigment underneath the usual silver halide emulsion—a sort of self-contained intensifying screen. In addition, Ilford sells an intensifying screen called "Brytex intensifying leaf" and made specially for this paper, to press against the top of the emulsion on it. Like any intensifying screen, it must be pressed firmly into contact with the entire surface of the photographic emulsion; otherwise, only a blurred indistinct image will result upon development.

Ordinary intensifying screens are not very flexible. Bending the

<sup>1</sup> F. Seitz and R. P. Johnson, *J. Applied Phys.*, **8**, 84, 186, 246 (1937); cf. also Sec. 5-3.

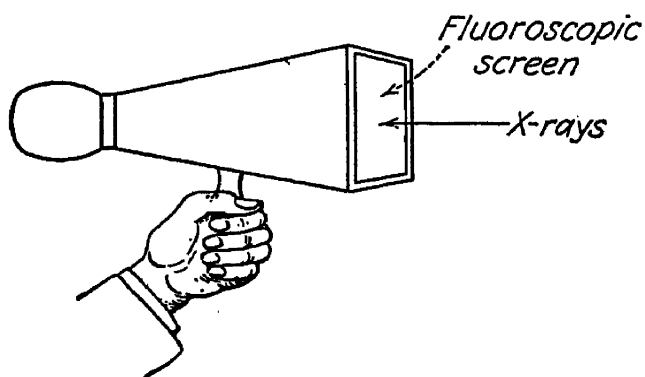
<sup>2</sup> R. P. Johnson, *Am. J. Phys.*, **8**, 143 (1940).

<sup>3</sup> O. Gaertner, *Z. tech. Physik*, **16**, 9 (1935).

<sup>4</sup> Schering-Kahlbaum A.G., Berlin, Germany.

sharply damages them. This lack of mechanical flexibility makes it impractical to curl them up to place them inside small cylindrical castings for industrial radiographic work,<sup>1</sup> in which it is often necessary to cut the film to special odd sizes to fit into corners, etc. Cutting up fluorescent intensifying screens is an expensive business, and this limits their use in such work.

When a fluoroscopic screen is incorporated into a device that enables one to view the screen effectively while it is fluorescing under the action of x-rays that have passed through something to be examined, the



SIMPLE FLUOROSCOPE

FIG. 9-1.

device is called a "fluoroscope."

In its simplest form, a fluoroscope may be merely a pyramidal box with a handle, with which one may view the screen behind a protective lead glass in a light room (Fig. 9-1). In its more complex forms, it may include a motor-driven conveyer belt to bring up and carry away the objects examined, a mechanism for rejecting the defective ones, a heavy lead-glass screen for partial protec-

tion of the operator from x-rays, a mirror so the screen may be viewed by reflected light for further protection, shutters, etc. In medical work it may include shutters and timing devices, rests to support and steady a standing patient, or an adjustable cot for him to lie on. It may also include a counterweighted mechanism permitting the screen to be moved to any desired position, automatically keeping the tube in alignment at the proper distance.

To be of much use, a fluoroscopic screen must be viewed in a dark or nearly dark room by a person whose eyes have had time to become adapted to the dark. Under the best conditions, a fluoroscope will reveal cavities in steel plates 1 in. thick if the cavities have a diameter of about 0.1 in. or more, 200-kv. x-rays being used. This performance is so much poorer than the photographic method (that is, radiography), that the latter is universally used in such work. For production-line inspection of light objects like canned foods, packaged foods, and citrus fruits and for such purposes as inspecting automobile tires, checking the fit of shoes, setting bone fractures, and observing heart action, fluoroscopy is widely used.

Care must be exercised to protect the operator of a fluoroscope from

<sup>1</sup> Eastman Kodak Co., Rochester, N.Y., manufactures calcium tungstate intensifying screens for industrial work that may be bent to a radius of 4 in. or, for added cost, to a radius of 2 in.

exposure to the x-rays. Protection is discussed in the next chapter. In continuous work, eye fatigue limits the operator to about 1 hr. at a time.

**2. X-ray Photography.** X-rays affect a photographic film much like ordinary light, and consequently x-ray photography has much in common with ordinary optical photography. The words "photography" and "photograph" are derived from the roots "photo" (light) and "graph" (write). When x-rays or gamma rays usurp the role of the light, the terms "radiography" and "radiograph" (radiation writing) are used, or occasionally the term "shadowgraph" is used synonymously with the noun "radiograph," but not as a verb like the verb "radiograph." If it is desired to exclude gamma rays from consideration and limit the term strictly to x-rays, the term "x-ograph" or "exograph" is sometimes used. None of these terms is applied to a photographically recorded x-ray diffraction pattern, however.

Although optical photography resembles x-ray photography in many respects, there are also numerous important differences. For one thing, there is nothing in x-ray photography corresponding to the lens of an optical camera. For another, the x-ray "cassette," which corresponds to a plateholder or film holder in an optical camera, need not have a slide that pulls out to expose the film because x-rays are so penetrating. This high penetration creates the problem of stopping or absorbing as much of them as possible in the film. In the case of hard x-rays, 99 per cent or more of the rays will pass right through the film. Only the small fraction that is absorbed has any effect in "exposing" the film. Hence x-ray film is usually made thicker than optical film, and it is usually coated with an emulsion on both sides. Such film is sometimes called "duplitized" film. Single-coated x-ray film is used in some types of diffraction work where extreme detail and contrast are desired and the rays are soft. Single-coated film or plates are also used in micro-radiography or other similar work with very soft x-rays.

Double-coated x-ray film is of two general types. One type is intended for use with fluorescent intensifying screens, although it may be used without screens. This is "ordinary" x-ray film, of the same general type that has been used for many years. The other general type is intended for use without any fluorescent intensifying screens, although lead foil is often used in contact with the film and acts as an intensifying screen. This intensifying action of lead foil is due, not to fluorescence, but to the high-speed photoelectrons that the x-rays eject from its surface and that help to expose the film. This type of film is known as "no-screen" or "nonscreen" film.

When used without screens, Gamertsfelder and Gingrich<sup>1</sup> have determined that nonscreen film is about  $2\frac{1}{2}$  times as fast as ordinary x-ray

<sup>1</sup> C. Gamertsfelder and N. S. Gingrich, *Rev. Sci. Instruments*, **9**, 154 (1938).

film used in the same way, when exposed to molybdenum  $K_{\alpha}$  radiation. Since this gain is constant, as contrasted with the variable gain that they observed (page 170) with fluorescent intensifying screens, the nonscreen type of film is widely used without screens in diffraction work, especially where relative intensities must be measured. When extreme sharpness and detail are more important than speed in the case of a particular

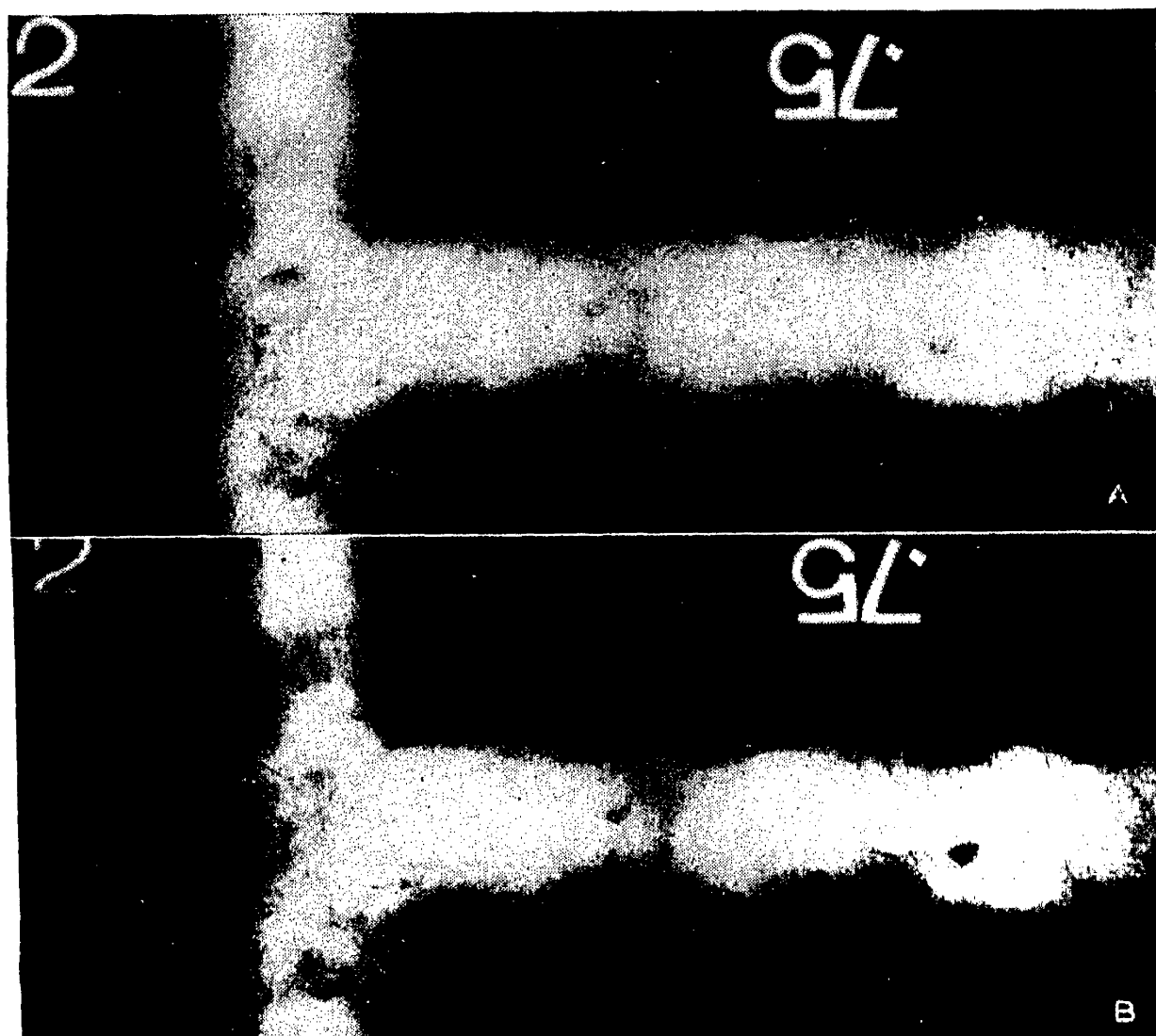


FIG. 9-2.—Comparing *A* (upper) ordinary nonscreen x-ray film with *B* (lower) fine-grained nonscreen film.

diffraction pattern, it is advisable to use the nonscreen film coated with an emulsion on only one side, like optical film.

The nonscreen type of film was first placed on the market by Agfa in 1936. At present, this type of film is available from other manufacturers as well and is made in grades having high speed with moderate contrast or moderate speed with fine grain and high contrast. Ordinary x-ray film, intended for use with fluorescent intensifying screens, is also made in several types so that one may choose a fine grain for detail and contrast by sacrificing some speed, or vice versa. The high speed x-ray films have a grain size that permits them to resolve some 20 to 40 lines

per millimeter (500 to 1,000 lines/in.). The fine-grained films will resolve some 60 to 100 lines/mm. (1,500 to 2,000 lines/in.).

Figure 9-2 compares the radiographs of a weld in  $\frac{3}{4}$ -in. steel plate obtained (1) using ordinary nonscreen film, like Agfa Non-screen or Eastman Industrial Type K, and (2) using a fine-grained nonscreen film, like Eastman Industrial Type M or Agfa Superay B, for example. It will be seen that the fine-grained film is "harder" or more "contrasty" than the film of ordinary grain size. The fine-grained film requires an exposure about ten times as long as that needed when ordinary nonscreen film is used.

For very hard radiation, such as million-volt x-rays or gamma rays, the nonscreen type of film is to be recommended. If the exposure is inconveniently long, the film may be sandwiched between lead-foil intensifying screens. The film should be of the moderate-speed fine-grained high-contrast type, unless it is necessary to show very thick and thin sections as clearly as possible in the same radiograph. Ordinary film and fluorescent screens are to be avoided in this type of work, for the fluorescent screens have little or no intensifying action with such hard rays and under these conditions usually produce coarse graininess in the radiograph.

The nonscreen type of film is not widely used in medical work because it is not as sensitive as ordinary film sandwiched between fluorescent intensifying screens. Lead-foil intensifying screens are avoided in medical work because they would absorb a large fraction of the comparatively soft rays used for diagnostic purposes. The use of nonscreen film or lead screens would lengthen exposures, increasing the chance of movement of the patient or organs such as lungs, heart, etc., during the exposure. If many radiographs are to be taken, a long exposure for each one might result in an unduly high and perhaps harmful x-ray dose to the patient.

In addition to x-ray film, there are also manufactured x-ray "papers." These are similar to the photographic papers on which ordinary photographs are printed. The chief advantage of x-ray paper over film is that it is cheaper. For this reason it is sometimes used in routine radiography of large groups of persons, for example to detect diseases of the chest in their early stages in school children. The disadvantages of paper are its inferior sensitivity and latitude, the impossibility of using an intensifying screen behind it, and the difficulty of making duplicates from an original. The first two disadvantages have been at least partly overcome in the new Kryptoscreen x-ray paper mentioned in the preceding section.

For microradiography, where the photographic image is subsequently enlarged, sometimes as much as 300 diameters, it is necessary to use a

TABLE 9-1.—X-RAY FILMS

Agfa Ansco	Buck	duPont	Eastman
Industrial Film for Use with Fluorescent Intensifying Screens			
Industrial	.....	504	F
Industrial Nonscreen Film—Fast, Wide Latitude, Medium Grain			
Non-screen	.....	.....	K
Industrial Nonscreen Film—Medium Speed, Contrasty, Fine Grain			
Superay A	.....	506	A
Industrial Nonscreen Film—Slow, High Contrast, Very Fine Grain			
Superay B	.....	.....	M
Medical Film for Fluorescent Intensifying Screens—Medium Speed			
.....	Standard	502	.....
Medical Film for Fluorescent Intensifying Screens—Fast			
High Speed	Fast	508	Blue Brand
Medical Nonscreen Film			
Non-screen	.....	.....	No-screen
Medical Film for Photoroentgen Work*			
“Fluorapid”(35 mm.)	.....	507	Super NX
X-ray Diffraction			
Non-screen	.....	.....	No-screen
Microradiography up to 20 Diameters			
Superay B	.....	.....	M
Microradiography from 20 to 30 Diameters			
“Minipan”	.....	Fine-grained positive motion-picture film or process film or plates	
Microradiography from 30 to 200 Diameters			
.....	.....	.....	Spectrographic 548-O

\* See p. 222.



grainless type of photographic emulsion such as the Lippmann emulsion. This type of film, which is extremely slow, was formerly available only from the Gevaert Company of Antwerp, Belgium, but plates and film with a sufficiently fine grain are now made by Eastman. They are called "type 548-O" spectrographic film or plates and have a resolving power of 2 microns, or 500 lines per millimeter. These are also very slow compared with ordinary x-ray film.

When x-ray spectra are recorded photographically, a peculiar effect is produced because of the K absorption edges of silver and bromine. The reason for this was explained on page 74, and the phenomenon was illustrated in a photograph by M. de Broglie (Fig. 5-4).

The principal x-ray film manufacturers in the United States, in alphabetical order, are

Agfa Ansco General Aniline and Film Corp., Binghamton, N.Y.  
 Buck X-Ograph Co., St. Louis, Mo.  
 duPont Film Mfg. Corp., New York, N.Y.  
 Eastman Kodak Co., Rochester, N.Y.

X-ray film as supplied by the manufacturer is wrapped so that each film is enveloped in a piece of black paper folded at one edge so as to cover both faces. If it is desired to use the film in a cassette provided with intensifying screens (either fluorescent or metallic), the film must of course be removed from this wrapper before inserting it in the cassette, unless it is desired deliberately to prevent any intensifying action and make a true nonscreen exposure.

To turn to the quantitative study of the effect of x-rays on photographic films or plates, it is found that the relationships are somewhat different from those for ordinary light. The usual method of determining the blackening of a photographic film is to measure the percentage of ordinary white light that will pass through it. If a narrow beam of parallel light rays is directed perpendicularly against a certain spot on the film and only 5 per cent of the light emerges on the other side, the film is said to have an "opacity" of 20 at that spot because only one-twentieth of the light is transmitted. The common logarithm of the opacity (1.301 in this case) is called the "density" of the blackening at the spot in question. The density resulting when a film is developed depends upon the "exposure" to which it was previously subjected. The exposure, in turn, is a quantity  $E$  which is proportional to the intensity  $I$  of the radiation which struck the film and the time  $t$  for which this intensity was maintained. That is,

$$E = kIt \quad (9-1)$$

where  $k$  is a constant and  $I$  is also constant during the time  $t$ . Thus, an

exposure to x-rays from a tube operating at 150 kv. and 10 ma. for 3 min. at a distance of 4 ft. is six times as great as an exposure at 150 kv. and 5 ma. for 1 min. at 4 ft. If the voltage is raised to 180 kv., so as to change the wave lengths of the radiation and increase the intensity, then the exposures at this higher voltage must all be multiplied by a constant that may be determined experimentally, in order to compare them with the 150-kv. exposures and to predict the density that they will produce in the

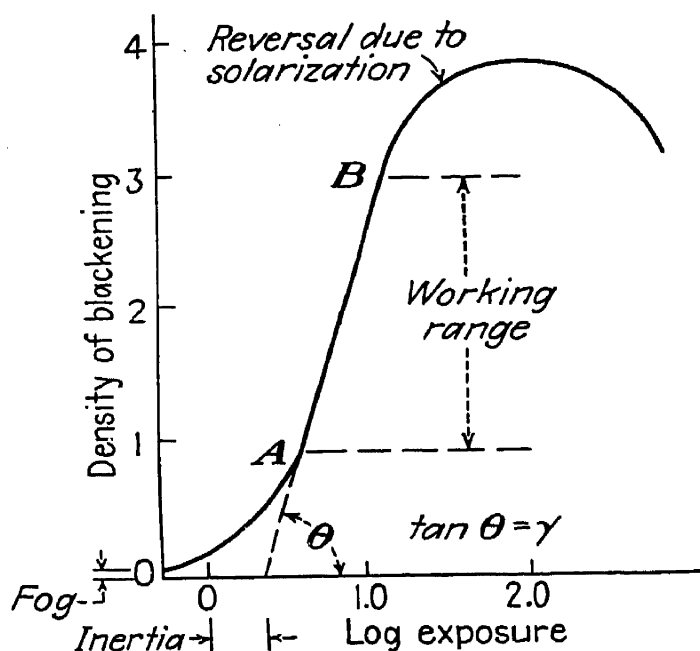


FIG. 9-3.—Typical *H* and *D* curve for visible light.

photographic film. If  $I$  varies during the time of the exposure then  $E$  is given by

$$E = k \int_0^t I dt \quad (9-2)$$

The usual method of expressing the relation between the exposure and the density is to plot a curve in which the logarithm of the exposure is the abscissa and the resulting density after development is the ordinate. This method was first used by F. Hurter and V. C. Driffeld, and hence such curves are called "*H* and *D* curves" or "characteristic curves" for a given film with a given type of radiation. Figure 9-3 shows a typical *H* and *D* curve for film exposed to ordinary light. The film has a small density even if developed without any exposure, and this represents a minimum unavoidable "fog." The initial part of the curve up to the point *A* is called the "toe" of the curve. From *A* to *B* the curve is straight or nearly so; and in this range, called the "working range of densities," from about 1 to 3, the density increases uniformly with increasing exposure. If the straight line *AB* is projected back to the horizontal axis, the intercept is called the "inertia." The inertia is sometimes regarded as an indication of the film speed, "fast" films having small

inertia and "slow" films much inertia. The speed of a film is more practically defined as the reciprocal of the exposure required to produce the density desired, for example the average density of a photograph. The slope of  $AB$  (that is,  $\tan \theta$  in Fig. 9-3) is called the "gamma" of the film. If the film has high gamma, it is said to be "hard" or "contrasty." If the gamma is low, the film is "soft." Beyond  $B$  the curve rounds off to a maximum beyond which the density actually decreases with exposure. This occurs only for exposures perhaps a million times or more greater than those ordinarily used. This phenomenon is called "solarization," and it is one type of photographic "reversal." Solarization with x-rays has been studied and compared with solarization by visible light by May.<sup>1</sup>

The exposure was defined as a quantity proportional to the intensity of the radiation times the time it strikes the film. This naturally brings up the question as to whether an exposure to a certain intensity for 100 sec. will have the same effect as an exposure to a hundred times that intensity for 1 sec. There is a law of photography, known as the "Bunsen-Roscoe reciprocity law," which states that it will produce the same density. Actually, this law fails if carried to extremes with ordinary light. In the case of x-rays, Bell<sup>2</sup> has determined that the law holds over an intensity ratio of 100:1 and with fair accuracy over a ratio of 1,000:1. However, x-ray exposures vary from 1 microsec. in x-ray snapshots of bullets in flight (page 296) to 100 hr. or more in some x-ray diffraction work, and thus the ratio of intensities actually used in practice is roughly 500 billion, although for any given application the ratio seldom exceeds 1,000. The question of an intermittency effect also arises. If a film is exposed for 1 sec. each minute for 1 hr., is the resulting density the same as for a steady exposure for 1 min. at the same intensity? If not, there is said to be an "intermittency effect." Bell could detect no such effect for x-rays.

To return to the  $H$  and  $D$  curve, Fig. 9-3 is a typical curve for ordinary light. Figure 9-4 compares a typical  $H$  and  $D$  curve for x-rays with one for light. This figure is due to Charlesby.<sup>3</sup> It will be noticed that the characteristic curve has a much longer toe for x-rays than for light. The difference between the effect of x-rays and the effect of light upon a photographic emulsion, for slight exposures, may be made clearer by plotting density  $D$  against exposure  $E$ , as in Fig. 9-5, rather than against  $\log E$  as in an  $H$  and  $D$  plot. It is seen that, with x-rays, density is proportional to exposure from zero up to densities of 1 or more. According to Bel

<sup>1</sup> A. May, *J. Optical Soc. Am.*, **33**, 81 (1943).

<sup>2</sup> G. E. Bell, *Brit. J. Radiol.*, **9**, 578 (1936).

<sup>3</sup> A. Charlesby, *Proc. Phys. Soc. (London)*, **52**, 657 (1940); see also H. E. Seeman *A.S.T.M. Bull.*, 17, May, 1945; also E. A. Owen and I. G. Edmunds, *Phil. Mag* **36**, 54 (1945).

the density does not vary linearly with  $\log E$  (as in the case of light) until a value of 3 or more is reached for  $D$  with double-emulsion film (or until  $D = 2$  with single-emulsion film). Inasmuch as a film density of 3 is

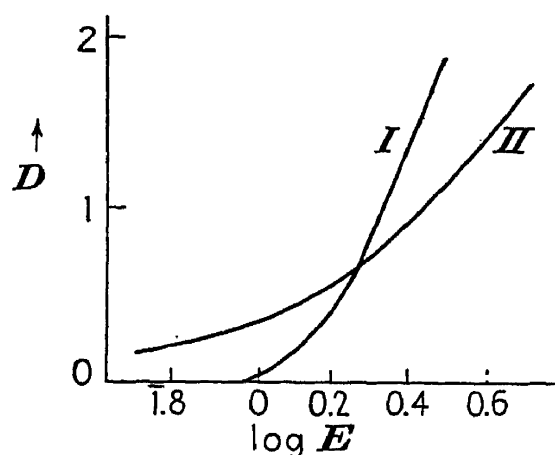


FIG. 9-4.—Typical  $H$  and  $D$  curves for (I) light and (II) x-rays compared. (Charlesby; Courtesy of The Physical Society, London.)

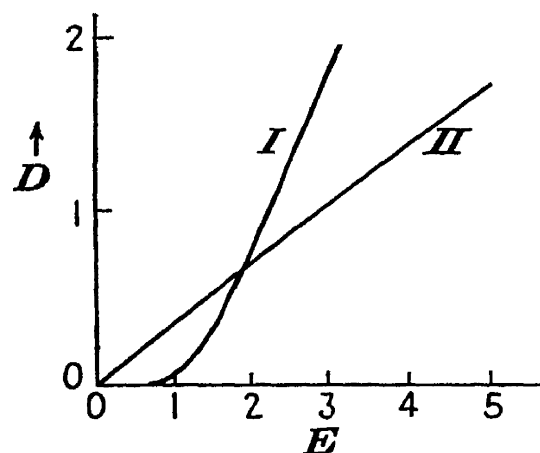


FIG. 9-5.—Typical density-versus-exposure curves for (I) light, and (II) x-rays compared. (Charlesby; courtesy of The Physical Society, London.)

quite dark, the behavior in the region  $D = 4$ , where  $D$  increases linearly with  $\log E$ , has but little practical interest. As may be seen in Fig. 9-3, reversal occurs after  $D$  reaches 4 or 5.

These curves show that the x-ray photographer is faced with a simpler situation than a photographer using ordinary light. With

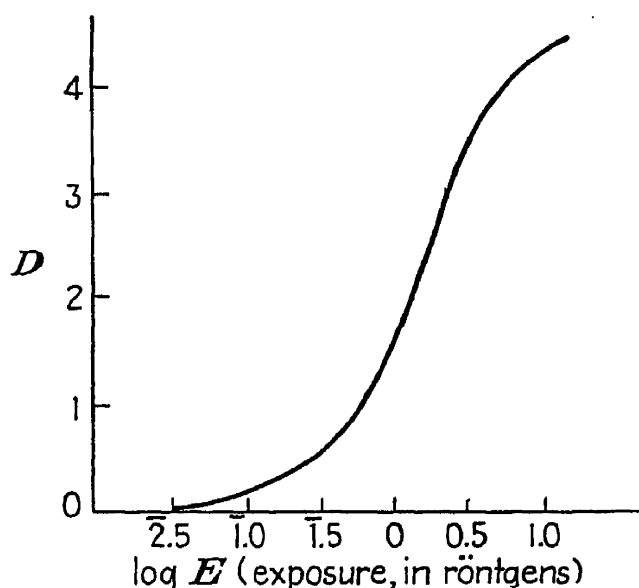


FIG. 9-6.—Typical  $H$  and  $D$  curve for x-rays. (Bell.)

fit the  $H$  and  $D$  curve for any other wave length by merely multiplying all the  $E$  values by a constant.

Figure 9-6 is a typical  $H$  and  $D$  curve obtained by Bell for single-emulsion film with x-rays. The abscissas represent the logarithm of the

x-rays, when the exposure is doubled (by doubling the time, doubling the tube current, or reducing the distance 29 per cent), the film density will be doubled, for light and medium exposures at any rate, when a non-screen technique is used. The shape of the  $H$  and  $D$  curve for x-rays is independent of the wave length, except for extremely soft rays having a wave length of 10  $\text{\AA}$ . or more. Rays as soft as this will not penetrate even a few inches of air and are rarely used in ordinary work. For ordinary x-rays, one can make the  $H$  and  $D$  curve obtained at any wave length

x-ray exposure measured in roentgens, a unit that will be defined in the next section.

On the basis of the quantum theory, Silberstein and Trivelli<sup>1</sup> have derived a theoretical equation for the  $H$  and  $D$  curves for x-rays. It is

$$K = N(1 - e^{-n\alpha\epsilon}) \quad (9-3)$$

where  $K$  is the number of photographic "grains" in the photographic emulsion, out of a total number  $N$ , that are rendered developable by an incident quantity of radiation consisting of  $n$  photons per unit area;  $\alpha$  is the cross-sectional area of each grain; and  $\epsilon$  is the probability of a grain becoming developable when struck by a photon. This equation fits x-ray  $H$  and  $D$  curves quite well but is unsatisfactory for ordinary light, supposedly because one x-ray photon usually suffices to render a grain developable, this being untrue for light. Bell's curve of Fig. 9-6 fits the empirical equation

$$D = 4.41(1 - e^{-0.479E}) \quad (9-4)$$

which obviously agrees with (9-3).

With duplitized x-ray film, average densities of  $1\frac{1}{2}$  to  $2\frac{1}{2}$  are best for radiographic work, and the film should be viewed against a brilliantly illuminated translucent screen in order to bring out detail as clearly as possible. Underexposure is a greater handicap than overexposure to the person trying to interpret the radiograph.

Metallic intensifying screens usually consist of sheets of lead foil pressed firmly against the front and back surfaces of the x-ray film which is duplitized and usually of the nonscreen type. The front screen nearest to the x-ray tube, is usually about 0.005 to 0.010 in. thick. The back screen is usually thicker, 0.010 in. or more. The x-rays must pass through the front screen in order to reach the film, and the soft secondary and scattered rays are absorbed to a considerable extent by 0.005 in. of lead. Hence the front screen tends to filter out the undesirable secondaries and pass only the desired primaries, which are much harder. Therefore the front screen serves as both an intensifying screen and a filter.

Seemann<sup>2</sup> has suggested that part of this filtering action may be due to the screen intensifying the primaries more than it does the secondary and scattered rays, as well as to the accepted explanation that the lead absorbs more of the secondaries and scattered rays than it does of the primaries. He determined that the intensifying factor for double screen is about 3.9 at 160 kv. and increases to about 4.4 at 200 kv., the front screen having a greater intensifying action than the rear one. The intensifying factor reaches a maximum somewhere in this region, how-

<sup>1</sup> L. Silberstein and A. P. H. Trivelli, *Phil. Mag.*, **9**, 787 (1930).

<sup>2</sup> H. E. Seemann, *J. Applied Phys.*, **8**, 836 (1937).

ever, for it is only about 2 or less for million-volt x-rays and is still less for gamma rays. Seemann also investigated the use of other metals but concluded that lead offers the best combination of properties. In ordinary radiography, as distinguished from microradiography, the definition achieved in a radiograph is as good with lead screens as without screens. This is not true of fluorescent intensifying screens.

As already mentioned, the intensifying action of lead foil in contact with the sensitive emulsion of an x-ray film is due to the photoelectrons and Compton recoil electrons that the x-rays eject from the surface of

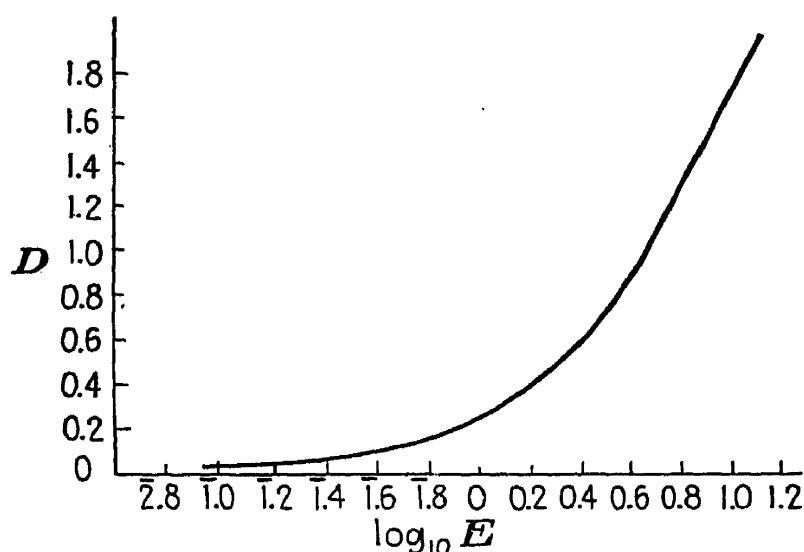


FIG. 9-7.— $H$  and  $D$  curve for high-voltage electrons or cathode rays. (Baker, Ramberg, and Hillier; courtesy of American Institute of Physics.)

the foil (see Chap. 5). Such electrons have but slight penetrating power in work at ordinary voltages, and therefore the lead screens should be kept clean; even a dirty thumbprint will absorb some of the photoelectrons and be noticeable in the radiograph. As with any intensifying screen, the foil must be in intimate contact with the film if results are to be satisfactory; if it is not, only a blurred image results. Since the Compton recoil electrons have a forward direction (page 90), the front screen has a stronger intensifying action than the rear one.

When metallic intensifying screens are used, more than half the effect on the film is due to the photoelectrons and recoil electrons from the screens; therefore, it is well to know the character of the  $H$  and  $D$  curves for high-voltage electrons. Such curves have been obtained for electrons between 40 and 212 kv. by Baker, Ramberg, and Hillier,<sup>1</sup> using lantern-slide plates. They found that the shape of the curve (Fig. 9-7) is independent of the voltage over this range, although the sensitivity ( $D/E$ ) reaches a maximum at 100 kv., falling off at both higher and lower voltages. When one considers that the continuous radiation from an x-ray tube operating at 200 kv. might be expected to produce a plentiful

<sup>1</sup> R. F. Baker, E. G. Ramberg, and J. Hillier, *J. Applied Phys.*, **13**, 450 (1942).

supply of photoelectrons from lead foil, most of them having an energy of the order of 100 electron kilovolts, the 100-kv. maximum for  $D/E$  observed by Baker, Ramberg and Hillier harmonizes with the observations of Seemann mentioned on page 181.

By comparing Fig. 9-7 with Fig. 9-4, it will be seen that the  $H$  and  $D$  curve for electrons is more like the one for light than the one for x-rays. Therefore one must expect an x-ray film sandwiched between metal screens to have an exposure characteristic for x-rays resembling that of a film for light.

In order to secure good photographic results with x-rays, it is of course necessary to observe all the precautions in the darkroom that must be observed in ordinary optical photography. Film should not be used after its expiration date. A suitable developer must be used; it should be fresh, its temperature should be correct—which usually means heating in winter and cooling in summer—and the time of development must likewise be correct. The developer must be agitated during use, especially in the case of tray development. Similar considerations apply to fixing. Fixing solution should not be stored mixed; the hypo solution and the hardener should be mixed just before the fixer is to be used. Careful washing and drying are also important.

Two difficulties arise in an x-ray darkroom that are not usually encountered in a darkroom used for optical photography. (1) The prevalence of double-emulsion (duplitized) films greatly increases the chance of scratching, which can be prevented only by great care in handling. (2) X-ray film sizes<sup>1</sup> are frequently much larger than optical films. A 14- by 17-in. film is rare in optical work but commonplace in x-ray work. A technique in handling that is quite satisfactory for film of small size is unsuitable for large, thick, heavy films. If one attempts to manipulate such a film in a horizontal position with one hand, as in loading into or unloading from the cassette, the film is almost certain to be slightly crinkled or kinked at the place where it is grasped. Such mechanical strain causes blemishes to appear after development that look like regions of underexposure. When the humidity is low, static discharges can be generated by pulling a film out of its black paper cover rapidly, and these leave ragged blemishes on the film after development.

Satisfactory developers often used in x-ray work are monomelic hydroquinone and metol-hydroquinone. Greenwood<sup>2</sup> states that the latter type should have a bromide content of one-half of 1 per cent or less and a sulfite-carbonate ratio of 3:2. He recommends a ratio for the metol-hydroquinone developing agents of 1:4. This type of developer keeps well. Detailed formulas will be found in any good list

<sup>1</sup> For tables of x-ray film sizes, see *J. Optical Soc. Am.*, **34**, 626, 628 (1944).

<sup>2</sup> W. H. Greenwood, *Brit. J. Phot.*, **86**, 757 (1939).

common developers. X-ray developers prepared in forms requiring very little subsequent mixing for use are sold by x-ray equipment manufacturers. The fixer should be acid and, according to Greenwood, should contain not over 40 per cent thiosulfate. The use of a "short-stop" (dilute acetic acid bath) between developer and fixer prolongs fixer life. The familiar series of Wratten safelight filters for various types of film includes a "series 6B" intended especially for use with x-ray film.

If the negatives developed per day average 100 or more, it is most economical to use tank development and fixing. After exposure, each negative is clipped at each of its four corners to a film hanger. The hanger and film are then suspended in a tank containing 5 gallons or more of developer, each hanger being fitted with projections that permit the top of it to lie on the edges of the tank. Such hangers and tanks are available from x-ray equipment manufacturers or photographic-supply or x-ray film concerns. After sufficient time in the developer, the hanger and film are dipped in water for a rinse and then hung in the fixing tank for fixing. After this, they are transferred to a washing tank where plenty of fresh, clean water is circulating. After 15 to 30 min. of washing, they are transferred to a drying rack, where a fan speeds the drying. Finally, the films are removed from the hangers.

If the negatives developed per day average less than 100, it is much more economical so far as consumption of developer and fixer are concerned to use tray development. The films should be turned over frequently while in the tray to prevent bubbles from spotting them. The trays must be rocked to agitate the developer and keep the film from adhering to the bottom. After developing and fixing, the negatives are clipped in hangers for washing and drying. For films of odd size that will not fit the hangers, film clips may be used, one at the top and another at the bottom, to keep the film from curling.

Development time depends upon the type of developer, its freshness, and its temperature and upon the type of film and its exposure. In industrial work on a large scale, these factors are usually chosen so as to keep the development time under 4 min. Fixing time should be about twice "clearing time," which is the time required for the film to become clear after it is immersed in the fixer. Films should not be left in the fixer much longer than the proper time. Washing should last 15 to 30 min. Films are damaged if neglected and left washing for several hours.

Positive prints may be made from the film negative in the usual way, but for greatest detail it is best to view the original film as a transparency<sup>1</sup> by means of a good illuminated translucent screen or film viewer, prefer-

<sup>1</sup> For the technique of duplicating radiographic films, see S. D. Herbein and J. F. McKenna, Jr., *Ind. Radiography*, 4, 28 (summer, 1945).



ably one using fluorescent lamps, for these furnish a bright, distributed light of the desired color without much heat. Correct exposure is greatly to be desired, of course; but if an error is made, it is better to have a slight overexposure than an underexposure. With duplitized films, the best detail is obtained at densities greater than those commonly regarded as most satisfactory in optical photography. Densities as high as 3 are occasionally used in radiography, although the most satisfactory average is probably about 2. For very dense negatives, an auxiliary high-intensity viewer is very helpful. One viewer of this type on the market uses an incandescent "Photoflood" lamp in a fan-ventilated case with a  $\frac{1}{8}$ -in. thick piece of Corning "Aklo" heat-absorbing glass. A rheostat in series with the lamp permits regulation of the intensity. The Kelley-Koett model uses a water cell to absorb the radiant heat. General Electric provides 11 fluorescent lamps for brilliant illumination.

In radiography with hard x-rays, say at 140 kv. or higher, it is not uncommon to use two films instead of one. For a nonscreen exposure, two films are loaded into the cassette. With lead screens, a "double-decker" sandwich is used consisting of foil-film-foil-film-foil. If any doubt arises as to whether some faint mark on the film is a stain, scratch, or blemish on the film or whether it really represents a defect in the object radiographed, then a comparison of the two films will settle the question. It is sometimes advantageous for two different persons to be able to keep "originals" in their files. Two films are sometimes used in gamma-ray radiography to save time. The exposure time required for a given radiograph with radium may be 8 hr. with duplitized non-screen film. By using two films and viewing them doubly after development, the required time may be reduced to 4 or 5 hr. The use of two double-emulsion films increases the "fog" (density for zero exposure) undesirably, and it is difficult to keep two negatives exactly superimposed while viewing them.

In diffraction work it is often essential to compare the intensities of the x-rays in different parts of the pattern. When the pattern is registered photographically, this requirement makes it necessary to avoid the use of fluorescent intensifying screens. The negative having been developed, the next step is to compare the film density in the various rings, lines, or spots in question by means of a "microphotometer," or "densitometer." One of these instruments is simply a device for focusing a fine beam of light of constant intensity perpendicularly upon the spot on the film where the density is to be determined; it must include a means of measuring the intensity of the beam transmitted through the film. This measurement may be indicated by a moving needle or light beam; or in instruments of the recording type a graph is automatically drawn showing film transparency as a function of distance along the film in a chosen direction. The transparency, which is the

quantity measured by such an instrument, is the ratio of the intensity of the transmitted beam to that of the incident beam. The reciprocal of this is the opacity, and the logarithm of the opacity is the density. When this is less than 2, it is a good indication of the x-ray intensity, as may be seen from the straight-line relationship in Fig. 9-5. The use of microphotometers will be discussed in greater detail in Sec. 19-5. Instruments of this type may be constructed fairly simply by rebuilding a microscope, for example as described by Spiegel-Adolf and Peckham;<sup>1</sup> or they may be purchased from manufacturers of scientific apparatus.

Cassettes are of various types. In medical work and in some types of industrial radiography, a rigid aluminum cassette is used, which includes the desired intensifying screens and lead backing. For example, in radiographing a casting it may be desirable to have the x-rays first pass through the casting, then a piece of lead foil to filter out scattered rays and secondaries, then a fluorescent intensifying screen, then the film and a rear fluorescent screen, backed by lead to protect the film from the rear. The lid at the rear is provided with spring fasteners, which ensure that the intensifying screens will be pressed firmly and uniformly against the film.

For nonscreen work, cheap cardboard film holders made by Eastman are quite satisfactory. They are provided with lead backing and may be bent to some extent to fit the contour of the object being radiographed.

Flexible cardboard cassettes for industrial use are manufactured by Saint John X-ray Service, Inc., Long Island City, N.Y. They permit some mechanical flexibility and the use of screens, either fluorescent or metal,<sup>2</sup> at the same time. Fluorescent screens made for use where they are to be bent are sold by Eastman.

In diffraction work, the chief requirements of the cassette are that it protect the film from light, keep it flat against its (usually cylindrical or plane) back plate, and permit the x-rays to strike the film without first passing through any more material than is necessary to keep out the light, except when a filter is used. The use of special filters in diffraction work (such as zirconium for molybdenum radiation) will be discussed in Sec. 18-2. In cassettes for diffraction work, a rigid metal plate, flat or cylindrical as desired, serves to back the film and protect it from stray radiation from the rear and to hold the film in the desired shape and position. A frame around the edge of the film pressing against its front surface serves to hold it flat against the back plate. The surface of the film to be exposed to the x-rays is covered with a sheet of thin black paper or Bakelite having a uniform texture. Paper may

<sup>1</sup> M. Spiegel-Adolf and R. H. Peckham, *Ind. & Eng. Chem., Anal. Ed.*, **12**, 182 (1940).

<sup>2</sup> For details, see J. Delisa, *Steel*, **116**, 110 (Apr. 30, 1945).

be in the form of an envelope completely enclosing the film; if so, the flaps must be behind the film so that its front surface is covered by only one layer of paper.

**3. The Ionization Chamber.** The construction of an ionization chamber for measuring x-ray intensity has already been outlined in Chap. 3 in connection with its use in an x-ray spectrometer. The modern tendency is to use Geiger counters in such work because of their greater sensitivity. Ionization chambers are widely used for measuring x-ray intensity in therapeutic work, and for this reason they will be discussed primarily from the viewpoint of the medical worker.

In therapeutic work, where the object is to apply an x-ray dose sufficient to destroy diseased tissue but not enough to destroy the surrounding healthy tissue, it is obvious that some standard method of measuring the dose must be devised. The essential quantity to be measured is the quantity of x-ray energy absorbed by the patient or some particular region of his body during a treatment, and this quantity is proportional to both the x-ray intensity and the time during which it is maintained, like the "exposure" of a photographic film.

The ionization produced in a gas by x-rays passing through it is the best physical or chemical effect yet found upon which to base the measurement of x-ray dosage. Since the effective atomic number of air is of the same order as that of soft animal tissues, air has been selected as the standard gas for the ionization chamber in medical work. Heavy gases like methyl iodide give greater sensitivity and are used in x-ray spectroscopy for this reason.

Eisl<sup>1</sup> has investigated the energy dissipation of cathode rays passing through air and has found that the energy which such high-speed electrons lose each time they form an ion pair (that is, an ion and the electron wrenched from it in forming it) is about 32 electron volts regardless of whether the high-speed electron has an initial energy of 10 electron kilovolts or 60 electron kilovolts. For example, he found that an electron having an initial energy of 9.4 electron kilovolts formed 294 ion pairs before it stopped, so that on the average it lost 32 electron volts each time it formed such a pair; on the other hand, an electron having an initial energy of 57.5 electron kilovolts formed 1,800 ion pairs before it stopped, so that its average energy loss per pair formed was also 32 electron volts.<sup>2</sup> The x-rays absorbed in a gas dissipate their energy by producing both Compton recoil electrons and photoelectrons. In either case, these high-energy electrons in turn dissipate their energy by forming ion pairs, losing 33 electron volts for each pair. It follows that the number of ions formed

<sup>1</sup> A. Eisl, *Ann. Physik*, **3**, 277 (1929).

<sup>2</sup> More recent work by L. H. Gray, *Proc. Roy. Soc. (London) A*, **156**, 578 (1936), indicates a value of 33 electron volts per ion pair.

per milligram of gas per second is an accurate measure of the x-ray energy absorbed per milligram per second.

Since these ions can be collected and the ion current measured, as outlined in Chap. 3, such a measurement of the ionization per gram of air in an ionization chamber filled with air is a good indication of the x-ray energy, or "dose," absorbed per gram of animal tissue per second if both the tissue and the chamber are subject to the same x-ray intensity for the same time.

The Fifth International Congress of Radiology in 1937 adopted the following official definition of the unit dose: "The roentgen<sup>1</sup> shall be that quantity of x- or gamma radiation such that the associated corpuscular emission per 0.001293 gram of air produces, in air, ions carrying 1 e.s.u. of quantity of electricity of either sign." This is a slight modification of the earlier official definition adopted in 1928. 0.001293 gram is the mass of 1 cm.<sup>3</sup> of dry air at 0°C. and 76 cm. of mercury pressure. The roentgen is also called an "r. unit," and a dose of 100 roentgens is commonly written 100 r. The roentgen is a measure of quantity of radiation absorbed rather than a time rate, and the dosage rate in roentgens per minute or per second is therefore the quantity that is related to x-ray intensity.

To gain some idea of the size of this unit, it may be stated that a tube with a tungsten target, operating at 100 kv. and 10 ma., will generate x-rays giving a dosage rate of about 25 r./min. at a distance of 1 yd. from the target. At 1 million volts and 3 ma. the figure is roughly 100 r./min. The dosage rate 1 meter away from 1 g. of radium in equilibrium with its disintegration products is about  $\frac{1}{75}$  r./min. As stated in Chap. 3, the absolute unit of x-ray intensity, as for the intensity of any other type of radiation, is energy per unit area per unit time, or ergs/cm.<sup>2</sup>/sec. The next thing to be considered, then, is the relation between the roentgen per second and the erg/cm.<sup>2</sup>/sec.

An x-ray beam passes through 1 cm.<sup>3</sup> of air in an ionization chamber. A little of the beam is absorbed, the energy being transferred to a few high-energy photoelectrons. A little more of it undergoes Compton scattering, producing a few recoil electrons of high energy. The rest of the x-ray beam passes on through. Each photoelectron and each recoil electron in turn tears through the air, dissipating its energy by wrenching electrons loose from several hundred atoms, producing ion pairs, each one of which subtracts 33 electron volts of energy from the high-energy photoelectron or recoil electron. Each ion pair thus formed consists of a positive ion and an electron. The electrons are all collected by the positive electrode and the positive ions by the negative electrode of the chamber.

<sup>1</sup> Anglicized spelling of the German name Röntgen.

The total x-ray energy absorbed in the cubic centimeter of air then equals 33 electron volts multiplied by the number of electrons collected at the positive electrode (or positive ions at the negative electrode). After enough electrons have been collected to equal one electrostatic unit of charge, the cubic centimeter of air has had an x-ray "dose" of 1 r. If  $e$  represents the charge of one electron, measured in e.s.u., then the number of electrons collected from the cubic centimeter of air during its 1-r. dose is  $1/e$ , and each one represents 33 electron volts of x-ray energy absorbed or scattered. Therefore the x-ray energy absorbed by the cubic centimeter of air during its 1-r. dose is  $33/e$  electron volts. Now 1 electron volt =  $e/300$  ergs. Therefore  $33/e$  electron volts equals 0.11 erg, which is the energy absorbed by the 0.001293 g. (1 cm.<sup>3</sup>) of air during its 1-r. dose, or 85 ergs would be absorbed by 1 g. of air during a 1-r. dose. If  $D'$  is the dosage rate in roentgens per second, the energy is absorbed by 1 g. of air at a rate  $85D'$  ergs/sec.

The absorption of x-rays of ordinary wave length by a cubic centimeter of air is so slight that equation (5-1) may be applied, rather than (5-7). If  $I$  is the intensity of the x-ray beam in ergs/cm.<sup>2</sup>/sec. [ $I_0$  in equation (5-1)] and  $\mu_a$  is the mass absorption coefficient of air, then the energy absorbed per gram of air per second is  $\mu_a I$ . Therefore,

$$D' = \frac{1}{85} \mu_a I \text{ r./sec.} \quad (9-5)$$

$$\text{or} \quad D = \frac{1}{85} \mu_a I t \text{ r.} \quad (9-6)$$

where  $D$  is the dose in roentgens and  $I$  is the corresponding x-ray energy flux in ergs per square centimeter during the period of irradiation.

These equations show that dosage in roentgens per second is proportional to the product of the x-ray intensity and the mass absorption coefficient of air,  $\mu_a$ . Since  $\mu_a$  is much greater for x-rays

having a wave length of 1 Å. than it is for 0.1-Å. rays, for example, a much greater x-ray intensity is required to give a 500-r. dose at 0.1 Å. than at 1 Å. This relation is represented<sup>1</sup> graphically in Fig. 9-8. At 1 Å., 1 r./sec. corresponds to only 27 ergs/cm.<sup>2</sup>/sec., but at 0.1 Å. it corresponds to over 3,000 ergs/cm.<sup>2</sup>/sec.

So much for the definition of the unit dose. Next, how is it to be

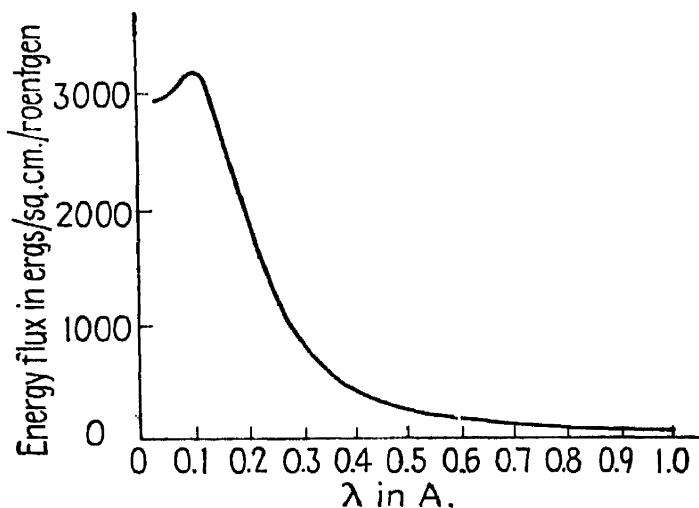


FIG. 9-8.—Relation between x-ray intensity and dosage rate at various wave lengths. (Courtesy of W. V. Mayneord, "Nature," and Macmillan & Company, Ltd.)

<sup>1</sup> From W. V. Mayneord, *Nature*, **145**, 973 (1940); *Brit. J. Radiol.*, **13**, 235 (1940), 17, 359 (1944).

measured? In order to measure it accurately in such a way that the results obtained by different workers using different equipment will agree, various precautions are necessary. First, the secondary electrons must be fully utilized. This means that the voltage between the chamber electrodes must be high enough so that all the ions are collected before they recombine and the chamber must be large enough so that the high-speed electrons run their full course and stop before they strike any part of the chamber. The first point can be checked by observing whether or not a small (say 10 per cent) change in the voltage applied to the chamber electrodes produces an appreciable change in the ion current. For example, if the voltage is increased from 150 to 165 volts and the ion current changes from  $3.000 \times 10^{-9}$  to  $3.001 \times 10^{-9}$  amp., then the ion current is properly "saturated." If, on the other hand, the ion current should change from  $3.000 \times 10^{-9}$  to  $3.020 \times 10^{-9}$  amp., this would indicate that a considerably higher voltage should be used in order to obtain saturation. The required voltage increases with the distance between plates and the air pressure in the chamber. A good minimum figure for general practice, with air, is 100 volts/cm. of electrode separation at 1 atm. pressure. For very hard rays like gamma rays from radium, it is necessary to use an electrode separation of 30 or 40 cm. and an air pressure of 10 atm., and under these conditions 25,000 volts or more must be applied between the electrodes for work with a "standard" chamber.

In medical practice, standard chambers are employed chiefly to calibrate small portable "air-wall" chambers, which are used to measure the dose in the actual treatment.

The second precaution to be observed in measuring the dose requires that the wall effect of the chamber must be avoided. This means that the chamber and the space between its electrodes must be large enough so that the photoelectrons and recoil electrons from the chamber window where the rays enter will all be absorbed before they reach the region of the chamber from which the ions are being collected for measurement. Throughout this region, that is, the primary beam must be in a state of electronic equilibrium if accurate measurements are desired. This means that the recoil electrons and photoelectrons which escape from the region must be exactly compensated by electrons which enter it from the surrounding space. This is true only when the region is surrounded by an envelope (preferably of air) having a thickness in all directions at least equal to the maximum range of the secondary electrons in those directions.

Figure 9-9 shows the general arrangement and dimensions of the standard ionization chamber used by Taylor and Singer<sup>1</sup> to measure the

<sup>1</sup>L. S. Taylor and G. Singer, *Bur. Standards J. Research*, **24**, 247 (1940), **16**, 165 (1936), **5**, 507 (1930).

ionization produced by gamma rays from radium. Their results indicated a dosage rate of 8.16 r./hr./mg. of radium at 1 cm. distance.

An ionization chamber to be practical for use in medical work must be small, light, and portable. Small metal chambers are impractical because of the wall effect, already mentioned. It has been found, however, that small closed chambers about the size of a thimble, with walls of organic material, such as Bakelite or Lucite, having a density of about 1 g./cm.<sup>3</sup> and an effective atomic number approximately equal to that for air (about 7.2), will give readings proportional to those from a standard chamber over a range of wave lengths from tubes operating between 50 and 250 kv. Such a chamber is called an air-wall chamber (also a "thimble" chamber

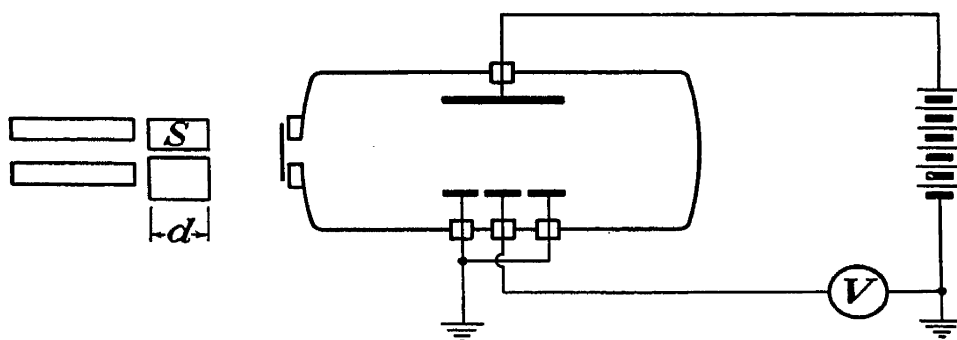


FIG. 9-9.—Standard ionization chamber. Plate length, 75 cm. Plate separation, 40 cm. Tank length, 8 ft; diameter, 2½ ft. Air pressure, 10 atm. Aluminum window 1 mm. thick, 6 cm. diameter. Hole through lead block *S* has length *d* = 6 in. *V* is vacuum-tube galvanometer. (Taylor and Singer; by permission of U.S. Bureau of Standards.)

because of its size) because its wall takes the place of the air used in a standard chamber to absorb the photo- and recoil electrons from outside the measuring region. The inner surface of the chamber is coated with colloidal carbon (Aquadag) to render it conducting like a metal chamber. For rays harder than 250 kv., the chamber walls must be thickened so that they are equivalent to the air needed to avoid wall effects. For million-volt x-rays, these organic (plastic) walls must be about 2 mm. thick. For gamma rays from radium, they must be about 4 mm. thick. For soft x-rays, such as those generated below 50 kv., the thinnest practical plastic walls absorb a significant fraction of the x-rays before they ever penetrate to the interior. This causes the chamber to indicate a dose smaller than that actually received. This error is further increased because the photoelectrons ejected from the organic walls of the chamber at these low photon energies have very slight penetrating power. Consequently, the photoelectrons entering the chamber when used for x-rays under 50 kv. come primarily from the carbon (Aquadag) lining, which has an atomic number of 6 as compared with 7 for the nitrogen and 8 for the oxygen in the air. Hence, for such soft rays, these thimble chambers are no longer "air-wall" chambers.

This type of chamber, including the auxiliary electrical equipment necessary to obtain the dose indication in roentgens, is manufactured in a small, convenient, portable unit by the Victoreen Instrument Company, Cleveland, Ohio.<sup>1</sup> Figure 9-10 shows the essential parts of this "r-meter." The tube containing the ionization chamber 14 and highly insulated condenser 13 can be removed easily from its socket, where it makes contact at 12 with the auxiliary electrical equipment. With the tube in its socket, the central electrode in the chamber 14 is charged,

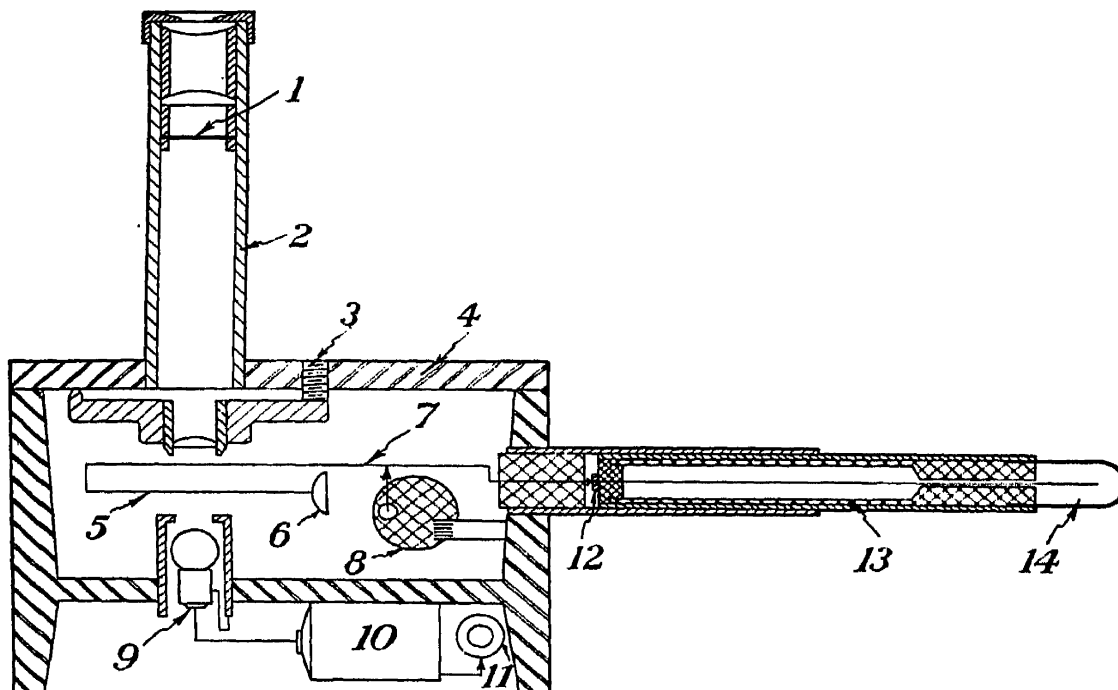


FIG. 9-10.—Victoreen r-meter. (1) Scale to read deflection of string. (2) Microscope. (3) Focus adjustment. (4) Lead case. (5) Platinum string. (6) Quartz loop. (7) Switch. (8) Amber charging disk. (9) Lamp. (10) Batteries. (11) Lamp switch. (12) Contact. (13) Amber condenser. (14) Thimble ionization-chamber tube. (Courtesy of Victoreen Instrument Company.)

along with the condenser 13, to which it is directly connected. This is done by rotating a knob until the string electrometer, as viewed through the eye-piece above its scale, 1, indicates zero, corresponding to a predetermined voltage on the condenser 13.

The tube 13, 14 is then removed and placed so that the chamber 14 will be exposed at the place where the dosage is to be measured. If the dosage rate is also to be measured, the exact time for which it is exposed must be observed. The ion current through the chamber is supplied by the condenser, which is thus partly discharged during the exposure. Afterward, the tube is reinserted in its socket, and the reduction in condenser voltage will cause the electrometer to read differently from what it read before. The new indication is read on the scale, which is calibrated in roentgens. The calibration is performed at the factory against a

<sup>1</sup> See O. Glasser and J. Victoreen, *Radiology*, **29**, 341 (1937).



standard ionization chamber. The instrument is supplied with tubes having different condenser capacities so that a suitable electrometer deflection may be obtained for any ordinary dose.

The principal objection to this instrument, for ordinary work, is its high cost, which amounts to about \$500. A cheaper model known as the "Minometer" is made for measuring the dose received by an x-ray technician during a day's work. For safety, this should not exceed 1 r./week or  $\frac{1}{2}$  r./day. The detachable tube in the Minometer is provided with a clip like a fountain pen so that the technician may carry it in his pocket. With this tube, full-scale deflection of the electrometer represents 0.1 r. A larger one giving a full-scale reading of 0.01 r. is also available. The Minometer costs less than \$100.

The Victoreen Instrument Company has also recently introduced a new instrument that indicates the ionization current by means of a vacuum-tube current amplifier. This instrument indicates roentgens per minute rather than roentgens. It will read as low as 0.0001 r./min. accurately. Its cost is about \$500. An instrument of this general type has been described by Krebs and Kersten.<sup>1</sup> Another has been developed by Zucker, Stoker, and Sampson,<sup>2</sup> and still another is sold by the Geophysical Instrument Company, Arlington, Va.

For other types of portable medical dosimeters of the ionization-chamber type, the reader is referred to an article by Mayneord.<sup>3</sup> The type of ionization chamber used in x-ray spectroscopy was described briefly in Chap. 3. Additional details on this type of chamber will be reserved for Sec. 16-3.

**4. The Geiger-Mueller Counter.** In 1908, Rutherford and Geiger<sup>4</sup> built an ingenious device for counting alpha particles from radioactive materials. It consisted of a small wire stretched along the axis of a metal tube filled with gas at a pressure less than atmospheric. A potential difference was impressed between wire and cylinder, the wire being positive. The potential difference was large enough so that the presence of even one charged atomic particle, like an alpha particle, would initiate a cumulative ionization process<sup>5</sup> and the particle would reveal its presence by causing an electric pulse. In 1928 and 1929 Geiger and Müller<sup>6</sup> improved the "Geiger counter" by devising an improved method of quenching it so that it could count large numbers of particles in a short time.

<sup>1</sup> R. P. Krebs and H. Kersten, *Rev. Sci. Instruments*, **13**, 332 (1942).

<sup>2</sup> M. Zucker, R. Stoker, and L. H. Sampson, *Elec. World*, **118**, 54 (Oct. 3, 1942).

<sup>3</sup> W. V. Mayneord, *J. Sci. Instruments*, **13**, 245 (1936).

<sup>4</sup> E. Rutherford and H. Geiger, *Proc. Roy. Soc. (London) A*, **81**, 141 (1908).

<sup>5</sup> See p. 7.

<sup>6</sup> H. Geiger and W. Müller, *Physik. Z.*, **29**, 839 (1928), **30**, 489 (1929).

The "Geiger-Mueller counters" are usually constructed at present in a glass envelope and are widely used for studies of natural and artificial radioactivity, cosmic rays, and research in nuclear physics. Their use for detecting and measuring the intensity of x-rays is also growing rapidly, especially in x-ray spectroscopy and diffraction work. Their enormous amplification makes them the most sensitive device known for detecting and measuring the intensity of very weak x-rays. Eisenstein and Gingrich<sup>1</sup> have compared the Geiger-Mueller counter with the secondary electron multiplier (to be described in the next section) and with photographic film in respect to their relative speed in recording x-ray spectra. They found the Geiger-Mueller counter five to ten times as fast as the

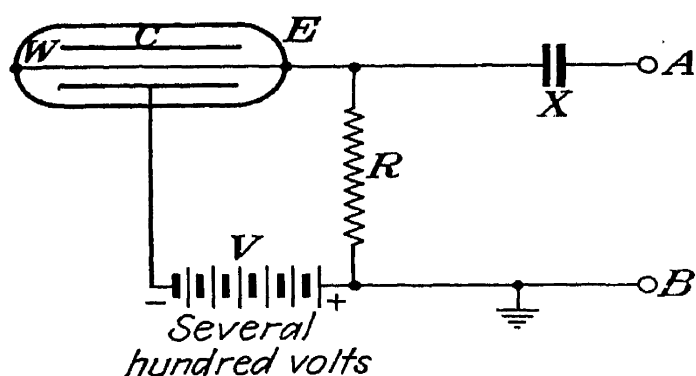


FIG. 9-11.—Geiger-Mueller counter tube and electrical connections.

secondary-electron multiplier and twenty times as fast as photography for this purpose.

Figure 9-11 shows the essential parts of a counter tube with connections. *E* is the glass tube envelope, which contains gas (usually an argon-oxygen or argon-hydrogen mixture) at a pressure of a few centimeters of mercury. *C* is a metal cylinder open at both

ends. *W* is a tungsten wire stretched along the axis of the cylinder. If an x-ray photon passing through the tube produces a photoelectron or recoil electron inside the cylinder, it initiates a cumulative ionization process; the gas then becomes conducting, and within a few microseconds an electric pulse of several hundred volts is produced across *AB*. The magnitude of this pulse as a function of the gas mixture used, etc., has been investigated by Miller.<sup>2</sup> Some provision is necessary, then, to "quench" the discharge by momentarily removing the tube voltage so that the tube will be ready to count the next particle. If the form and material of the electrodes, the voltage *V*, and the type of gas and its pressure are correctly<sup>3</sup> selected, then the provision for quenching becomes simple or unnecessary. Davey, Smith, and Harding<sup>4</sup> recommend a krypton-ether mixture for maximum sensitivity.

Geiger-Mueller counters, including various types of tubes and auxiliary electrical equipment, are available in the United States from Herbach and Rademan, Inc., Philadelphia, Pa. Their "GLB-20" tube for x-rays

<sup>1</sup> A. Eisenstein and N. S. Gingrich, *Rev. Sci. Instruments*, **12**, 582 (1941).

<sup>2</sup> C. W. Miller, *Rev. Sci. Instruments*, **14**, 68 (1943).

<sup>3</sup> In this connection, see H. M. Sullivan, *Rev. Sci. Instruments*, **11**, 356 (1940).

<sup>4</sup> W. P. Davey, F. R. Smith, and S. W. Harding, *Rev. Sci. Instruments*, **15**, 37 (1944).

contains 94 per cent argon and 6 per cent oxygen at 9 cm. of mercury pressure. The cylinder *C* is of copper, 3 cm. in length and 1 cm. in diameter. The wire *W* is 3-mil tungsten. The left end of the glass envelope in Fig. 9-11 is provided with a glass window only 0.0005 in. thick so that soft x-rays may enter.

The counter circuit shown in Fig. 9-11 is usually connected to a vacuum-tube amplifier; this amplifies the pulses so that they will operate a mechanical counter, which registers them. If the x-rays are so weak that only three or four or less recoil electrons or photoelectrons are produced in the counter tube per second, then the mechanical counter counts them directly. If the x-rays become more intense, however, the Geiger-Mueller tube counts the pulses much faster than the mechanical counter can respond to them. In this case, it is necessary to introduce an electric scaling circuit. A "scale of 32" circuit is one that must receive 32 pulses from the Geiger-Mueller counter before it imparts one to the mechanical counter. Thus the Geiger-Mueller counter may be averaging 96 pulses/sec., and the mechanical counter will register 3 pulses/sec. The scaling circuit may be adjustable so that, by merely turning a knob, one can make it work at 1, 2, 4, 8, 16, or 32 to 1 as desired, for a wide range of intensities.

For additional details regarding the theory and operation of Geiger-Mueller counters, the reader is referred to articles by Locher and Le Galley, Weisz, Montgomery and Montgomery, and Brown, Elliott, and Evans.<sup>1</sup>

**5. The Secondary-electron Multiplier.** The secondary-electron multiplier is a vacuum tube containing a series of electrodes (usually 10 or 12). It is designed to make use of the fact that when an electron having a kinetic energy of about 100 electron volts or more strikes a metal surface its impact knocks several electrons (called "secondary electrons") loose from the metal at the point of impact. If it is assumed that such a bombarding electron produces, say, 10 secondary electrons upon impact, on the average, it is easy to see that a few repetitions of the process will produce enormous amplification.

The electrodes are connected so that each one is about 200 or 300 volts positive with respect to the previous one, the twelfth thus being some 2,200 or 3,300 volts positive with respect to the first. Then if an x-ray photon ejects an electron photoelectrically from the first electrode, it strikes the second and releases 10 secondaries, which strike the third, releasing 100, which strike the fourth, releasing 1,000, etc., until finally the twelfth electrode gathers in about  $10^{10}$  electrons. Therefore even a

<sup>1</sup> G. L. Locher and D. P. Le Galley, *Phys. Rev.*, **46**, 1047 (1934); *Rev. Sci. Instruments*, **6**, 279 (1935). P. Weisz, *Electronics*, **14**, 18 (December 1941). C. G. Montgomery and D. D. Montgomery, *J. Franklin Inst.*, **231**, 447 (1941). S. C. Brown, L. G. Elliott, and R. D. Evans, *Rev. Sci. Instruments*, **13**, 147 (1942).

weak beam of x-rays incident on the first electrode will produce a current to the last one that is large enough to operate a vacuum-tube amplifier; and if the output of the amplifier is read by a meter its indication is a measure of the x-ray intensity.

A secondary-electron tube for this purpose has been constructed by Allen,<sup>1</sup> who used 12 nickel electrodes, each coated thinly (to increase the secondary yield) by evaporating beryllium onto its surface. The potential difference between successive electrodes was 300 volts, and the first one upon which the x-rays were directed had a thin sheet of tantalum spot-welded to it that served as the photoelectric surface. The beryllium is an efficient emitter of secondary electrons, after it has been "sensitized." This is done by applying a high voltage of high frequency from a small Tesla coil to the high-potential end of the tube for an hour after it has been highly evacuated and sealed off. A thin window was provided in the tube to admit the x-rays so that they could strike the tantalum.

As already mentioned, experiments by Eisenstein and Gingrich<sup>2</sup> indicate that a Geiger-Mueller counter is more sensitive than the electron multiplier for measuring the intensity of weak x-rays. For additional details regarding the theory and construction of electron-multiplier tubes, the reader is referred to papers by Zworykin, Morton, and Malter and Pierce.<sup>3</sup>

**6. Other Methods.** Although a photocell is very insensitive to x-rays, it does respond well enough to use for measuring fairly high x-ray intensities. Mackenzie<sup>4</sup> states that a Weston Photronic (barrier-layer type) cell gives a current of 1 microamp. when exposed to an x-ray beam giving a dosage rate of 300 r./min., so that a galvanometer with a sensitivity of  $10^{-8}$  or  $10^{-9}$  amp./mm. will read ordinary therapeutic intensities satisfactorily. Mackenzie states that for voltages between 40 and 120 kv. and for intensities from 20 to 300 r./min. the readings obtained with the photocell agree with readings from an ionization chamber. Of course, the photocell must be covered with black paper or some other screen that will admit the x-rays but exclude the light. Scharf and Weinbaum<sup>5</sup> found that copper oxide cells are stable in measuring x-ray intensities but that selenium cells of this type fatigue under x-rays.

In the early days of x-ray therapy, chemical methods were rather widely used for measuring dosage. One of the most popular types of chemical dosimeter consisted of a barium platinocyanide disk about  $\frac{1}{2}$  cm.

<sup>1</sup> J. S. Allen, *Rev. Sci. Instruments*, **12**, 484 (1941).

<sup>2</sup> A. Eisenstein and N. S. Gingrich, *Rev. Sci. Instruments*, **12**, 582 (1941).

<sup>3</sup> V. K. Zworykin, G. A. Morton, and L. Malter, *Proc. I.R.E.*, **24**, 351 (1936); J. R. Pierce, *Bell Labs. Record*, **16**, 305 (1938).

<sup>4</sup> K. Mackenzie, *Nature*, **142**, 116 (1938).

<sup>5</sup> K. Scharf and O. Weinbaum, *Z. Physik*, **80**, 465 (1933).

in diameter, called a "pastille." Initially a bright green color, it changes first to a pale yellow and finally to a deep orange color as the dose increases. The pastille was placed at a specified distance from the target, and by comparing its color with a standard color chart the dose could be estimated. Other chemical methods used depended upon the liberation of iodine from a 2 per cent solution of iodoform in chloroform, the precipitation of calomel from a mixture of mercuric chloride and ammonium oxalate solutions, etc. For more details on the history of x-ray dosimeters, the reader is referred to an article by Glasser.<sup>1</sup>

### QUESTIONS AND PROBLEMS

1. Distinguish between a fluoroscopic screen and a fluorescent intensifying screen. Between a fluorescent intensifying screen and a metallic intensifying screen. Explain the action of the last two. What is the active material in most fluorescent intensifying screens?

2. Distinguish between no-screen, or nonscreen, film and ordinary x-ray film. Which is more commonly used in medical diagnostic work? Why? In what type of industrial radiographic work is the ordinary type of film required?

3. What is an *H* and *D* curve? Distinguish between hard and soft film. Fast and slow film. Should a coarse- or a fine-grained film be used if it is desired to reveal very small flaws? Does fine grain tend to make a film hard or soft? Fast or slow? What are the principal differences between optical photographic film and x-ray film?

4. If an irregular-shaped casting is to be radiographed in such a way that flaws in the thick parts and in the thin parts can both be seen in a single radiograph, should a hard or soft film be used? Should hard or soft x-rays be used?

5. What is meant by the statement that the density of a spot on a photographic film is 2? How is film density measured? If the exposure time were reduced 50 per cent, would this density of 2 be reduced to about 1, in the case of nonscreen film and x-rays, used without screens? In the case of optical film and light? In the case of x-ray film used with screens? In diffraction work, why are screens ordinarily not used? If they are used, what type is well suited for this work?

6. What is a roentgen? Why does its definition call for the use of air in the chamber? In measuring dosage, what is meant by the statement that the secondary electrons must be fully utilized? What is the wall effect, and why and how is it to be avoided? What is an air-wall chamber?

7. The mass absorption coefficient of air for the x-rays used in a certain therapeutic treatment is 0.15. If 200 r. was the dose administered, how many ergs of x-ray energy actually flowed into each square centimeter of the skin of the patient?

*Ans.* 113,333 ergs.

8. How does the work of Fisl and Gray justify the use of the roentgen as a unit for measuring dosage in x-ray and radium therapy?

9. What is the most sensitive device known for detecting x-rays in a short time? Describe briefly how it is constructed and how it operates.

<sup>1</sup> O. Glasser, *Radiology*, **37**, 221 (1941).

## CHAPTER 10

### PROTECTION

**1. Protection from High Voltage.** Most modern factory-built x-ray equipment is of shockproof construction, that is, all parts of the high-voltage circuit are enclosed within grounded metal cabinets, tanks, cables, shields, and guards. Such equipment is well named. In ordinary usage, it is truly shockproof. Practically the only danger of electric shock from such equipment is during repair or maintenance work. If the door of a cabinet containing high-voltage equipment is unlocked in order to inspect or repair some part inside, if a shockproof cable is disconnected, or if a shockproof tube is removed from its protecting case, it is possible for the person doing such work to be electrocuted if someone else turns on the power. In order to prevent such accidents, it is necessary to follow only one rule. Whenever any adjustments or repairs are to be made upon any part of the electrical equipment, the first move always must be for the person authorizing or undertaking such work to open the main switch, lock it open, and firmly affix a large red tag warning that men are working on the equipment and that the switch must not be closed. When the work is completed or a test is to be made, the repairman himself must be the one to close the switch. To help enforce this rule, it is advisable to keep the key to the door to the high-voltage room or cabinet locked up inside the main switch cover so that it cannot be obtained until the switch is opened.

In the case of equipment that has exposed high-voltage leads or other parts, other precautions are necessary. There should be conspicuous high-voltage warning signs. A red lamp should glow whenever the high voltage is on. The exposed parts may be only an x-ray tube, not of the shockproof type, and the leads to it. It may not be necessary for the operator to be in the same room with these parts while the equipment is operating. In this case, it is helpful to include a door switch in the primary circuit so that the opening of the door to this room shuts off the power. A person should not be left unattended around high-voltage equipment until he has had time to familiarize himself with it, even though he may not operate it. If the equipment includes a Snook rectifier, he will soon become familiar with the noise it makes when the high voltage is on. If the equipment operates silently, it may be advisable to introduce one sharp projection on the exposed high-voltage conductor so that it will

make an audible corona hiss when the high voltage is on. The technicians will soon learn the sound of this hiss and know that it is a warning of sudden death.

**2. Human Tolerance to X-rays and Gamma Rays.** If a person works day after day near an x-ray tube or a quantity of radium, his whole body will of course be exposed to x-rays or gamma rays of dangerous intensity unless the x-ray or gamma-ray source is adequately shielded. In such a case of exposure, the person will sooner or later experience a loss of vitality and frequent headaches. If the exposure continues, the probable consequences in progression are sterility, lowered blood count, anemia, leukemia, and death. X-ray or gamma-ray injury is insidious in that its symptoms and effects usually appear days, weeks, or even months after the injury occurred.

An x-ray worker may be adequately protected against general exposure and yet subject his hands or some other body part to a dangerous exposure while working with a fluoroscope or while handling radium, for example. In the case of the hands, this first causes a reddening of the skin, called "erythema," somewhat as in the case of sunburn. Next, there is an embrittlement and cracking of the fingernails, and the skin becomes thick and leathery. Such x-ray burns are painful, especially if exposed to heat or cold, and cuts and scratches near the burn heal poorly or not at all. In severe cases, warty growths appear, which may become ulcerated and infected and may eventually degenerate into cancer. These local burns are also insidious, for they develop days, weeks, or months after the injury actually occurred.

Some of the early x-ray workers suffered from x-ray burns and general exposure to x-rays because the danger of such injury was not realized until too late. These pioneers were true martyrs of science. Today, however, such injury is inexcusable; it indicates only ignorance or carelessness, or both. The danger is fully understood, and the means of protection and tests of its effectiveness are well known. Of course, it may be necessary to subject a cancer patient to x-ray or gamma-ray injury in order to save his life, but aside from these cases nobody need suffer such injuries.

It has been determined as a result of careful study of a large number of cases that an x-ray or gamma-ray exposure of about 1 r./week can be tolerated indefinitely by the human body without any ill effects. Reference to Bell's *H* and *D* curve for x-rays (Fig. 9-6) shows that a single emulsion x-ray film (which is less sensitive than the usual double-emulsion x-ray film) will have a density greater than 1 upon development after an exposure of 1 r. (in reading the horizontal scale, remember that  $\log 1 = 0$ ). This suggests a simple test for general bodily exposure to x-rays. The x-ray technician may take a fresh dental-type x-ray film (not a compara

tively slow film like Agfa Superay B or Eastman Industrial Type M) and dental holder, tape a paper clip to the front side of it, then place it in his pocket with the clip side away from his body. After carrying it thus during working hours for 1 week or 10 days, the film is developed and fixed. If there is no visible darkening of the film and no trace of an image of the paper clip, the general body exposure to x-rays is definitely safe, although it might be true that the exposure of the hands during some particular operation was dangerous. If there is only a slight darkening of the film and a faint image of the paper clip, the x-ray exposure is somewhere near the safe borderline. If the film is quite dark, a dangerous condition is indicated. Of course, if there is serious doubt as to the adequacy of the protection, one should not carry film for a week before finding out. In such a case, the film should be developed after a half hour or an hour of work; if it shows no darkening, then a second film can be carried for a day. If this shows no darkening, then a third film can be carried for the week or 10-day test.

If a small portable ionization chamber or dosimeter (such as the Minometer described in Chap. 9) is available, it is a simple matter to check the exposure of an individual by having him carry the 0.1-r. chamber in his pocket for half a working day. His exposure should not exceed 0.1 r. in this time. If a 0.01-r. chamber is available, readings may be taken with it at various locations around the x-ray equipment while it is operating. The chamber may be laid at the test location for 5 min. and then read. If the reading is 0.003 r., then a person working steadily at this location is receiving  $10^{-5}$  r./sec., which is the maximum considered safe.

The revised recommendations of the International X-ray and Radium Protection Commission<sup>1</sup> contain the following:

The evidence at present available appears to suggest that under satisfactory working conditions, a person in normal health can tolerate exposure to x-rays or radium gamma rays to an extent of about 0.2 international roentgen (r) per day, or 1 r. per week. On the basis of continuous irradiation during a working day of seven hours, this figure corresponds to a tolerance dosage rate of  $10^{-5}$  r. per second.

In addition to the reference just given, the interested reader may consult the *U.S. National Bureau of Standards Handbook 20* (X-ray Protection) and *N.B.S. Handbook 23* (Radium Protection).<sup>2</sup> The American Standards Association is now printing a standard "Safety Code for the Industrial Use of X-rays."

There is some disagreement about the  $10^{-5}$  r./sec. figure. Some

<sup>1</sup> *Radiology*, **30**, 511 (1938). Recently the tendency has been to set the tolerance limit at 0.1 r. per day; see, for example, *Ind. Radiography*, **4**, 35 (fall, 1945).

<sup>2</sup> Obtainable from the Superintendent of Documents, Government Printing Office, Washington, D.C. *Handbook 23* is reprinted in *Radiology*, **31**, 481 (1938).



geneticists argue that the normal mutations occurring in the chromosomes of animals and plants may be caused by the cosmic rays, for it is known that x-rays produce abnormal mutations in both plants and animals. If this be true, they argue that an x-ray exposure of  $10^{-5}$  r./sec., being  $10^4$  times the cosmic-ray exposure, which is only some  $10^{-9}$  r./sec., will cause genetic defects in the second generation. The international figure of  $10^{-5}$  r./sec. is based only on the effect on the individual exposed, and not upon possible genetic effects in his children. These geneticists suggest  $10^{-6}$  r./sec. as a limit.

The foregoing discussion has been concerned with long-continued exposure of the whole body to weak x-rays; let us next discuss brief exposures of a part of the body to intense x-rays. Medical workers sometimes speak of a "threshold erythematous dose" or a "threshold skin dose." This is defined as the amount of radiation that will produce a visible skin reaction (reddening) in 80 per cent of the patients receiving the exposure within 4 weeks after the treatment and no reaction in the remaining 20 per cent. The number of roentgens in an erythematous dose increases with the hardness of the x-rays. Duffy, Arneson, and Voke<sup>1</sup> concluded that this unit is equivalent to 525 r. over a local area at one sitting or to two doses of 400 r. each administered 24 hr. apart. This value has been verified by Quimby and MacComb,<sup>2</sup> who add that the doses should be delivered at a rate of 40 to 60 r./min. In their experiments, the tube operated at 200 kv.p., a  $\frac{1}{2}$ -mm. copper filter was used, the target-skin distance was 50 cm, and the irradiated area was  $10 \times 10$  cm.

Thus there is a wide discrepancy between the dose considered harmless when administered rapidly and only once to a small area of the body for a short time and one administered slowly but constantly to the whole body—500 r. in 10 min. in one case, and 1 r. in a week in the other. The body recovers fairly rapidly from a localized threshold erythematous dose. A person not working with x-rays or radium could probably have his right hand subjected to such a dose once a year for a lifetime without ill effects, but if this were attempted each week, or even each month, the results might be very serious. In the treatment of cancer, a dose of 300 r. daily for 20 days, administered to an area of the body 15 cm. square, is considered "heavy irradiation." If some portion of the intestinal tract or the parotid gland is included in the treated area, such heavy doses usually cause the patient to suffer "irradiation sickness" with nausea and vomiting unless certain precautions are taken to prevent it.<sup>3</sup>

**3. X-ray Protection.** The preceding section sets forth the requirements that must be met in providing adequate protection of workers

<sup>1</sup> J. J. Duffy, A. N. Arneson, and E. L. Voke, *Radiology*, **23**, 486 (1934).

<sup>2</sup> E. H. Quimby and W. S. MacComb, *Radiology*, **29**, 305 (1937).

<sup>3</sup> See, for example, C. L. Martin and W. H. Moursund, *Radiology*, **30**, 277 (1938).

against x-rays and gamma rays. This section should suggest how adequate protection may be achieved.

In radiographing a tooth, a small dental diagnostic tube should be used. Being a small low-voltage tube, this is usually enclosed in a shock-proof rayproof shield at the factory, and only a narrow beam of comparatively soft rays emerges for a second or two during an exposure. A dentist making a dozen such exposures a day need only stand behind the tube and keep his hands out of the beam to be safe.

In radiographing the chest, a larger, more powerful tube is required. It is placed farther from the patient, and the exposure is usually longer. Such tubes are often enclosed in a shield, which may be designed to reduce the radiation to  $10^{-5}$  r./sec. in directions other than that of the useful beam, although the mere presence of a shockproof case is no guarantee of its being rayproof in the above sense. Even with a rayproof case, there will be plenty of scattered and secondary rays from objects struck by the primary beam. Therefore a person who spends his day making 50 or 100 chest pictures must protect himself by standing behind a lead shield at least 1 mm. thick or lead glass<sup>1</sup> of the equivalent thickness. One typical sample of lead glass  $\frac{7}{32}$  in. thick is equivalent to  $1\frac{1}{2}$  mm. of lead in absorbing 100-kv. x-rays. There may be a few cases where the patient must be held with the hands during an exposure. In such cases, lead rubber gloves and apron are necessary, but they should not be depended upon for protection except on rare occasions. Such gloves and apron should have a protective value of at least  $\frac{1}{8}$  mm. of lead, both back and front, including fingers and wrist. If the tube is of the nonenclosed type, it should be operated in the usual lead-glass bowl, and the operator should stand in a lead-lined booth during exposures. The control stand should be in this booth. At least a 1-mm. aluminum filter should be used at the tube to cut out the very soft rays, which in any case are too soft to reach the photographic film.

Medical fluoroscopic equipment may consist of the x-ray tube supported in a lead-lined container and a fluoroscopic screen mounted in a frame and covered with a lead-glass plate. This is supported so as to be movable in all directions in its own plane. A thin wood or Bakelite partition between the tube and the patient serves to steady the patient. Between this and the tube, lead shutters may be provided. The lead glass should be thick enough to be equivalent to the lead thickness listed for the voltage used in Table 10-1. Lead rubber gloves and apron should be worn by the operator. A 1-mm. aluminum filter should be used at the tube. The fluoroscopic exposures should be as brief as practical and intermittent rather than steady. In setting bone fractures and removing

<sup>1</sup> For information regarding the absorption of x-rays by such glasses, see G. Singer *Radiology*, **27**, 44 (1936).

foreign objects under the fluoroscope, the protection of the hands by lead rubber gloves is essential, and the exposure should be kept as short as possible.

In therapeutic work where very soft rays are used to treat skin conditions like eczema or warts, the same sort of protection as that already outlined for diagnostic radiography is ample. This type of work is called "superficial therapy."

In deep therapy with high-voltage x-rays, the x-ray tube or tubes should be located in a treatment room having concrete walls of sufficient thickness for protection of those outside. In place of concrete, a lining of sheet lead of sufficient thickness may be used. Nobody but the patient should be in the treatment room while the equipment is operating; the patient may be observed through a thick lead-glass window, and a telephone may be provided for communication.

TABLE 10-1.—RECOMMENDED MINIMUM THICKNESSES OF PROTECTIVE LEAD LINING FOR X-RAY ROOMS

Peak x-ray-tube kilovolts	Minimum lead thickness, mm.	Weight, lb./ft. <sup>2</sup>
75	1	2.4
100	1.5	3.5
125	2	4.7
150	2.5	5.9
175	3	7.1
200	4	9.5
225	5	12
250	6	14
300	9	21
350	12	28
400	15	35
500	22	52
600	35	82
1,000	84*	196

\* Calculated by extrapolation from lower voltages.

Fixed installations for industrial radiography are similar to deep therapy installations, so far as protection is concerned. With these, the tube should be located in a lead-lined room or a room with thick concrete walls, and nobody should be in the room while the equipment is operating. The control panel should be outside this room, of course. Lead-glass windows may be provided, if desired. In order to be equivalent to the walls, such glass may consist of several sheets, with a total thickness of 1 in. or more. The doors must be kept closed during operation, and

the doors must be as opaque to the rays as the walls are. Leakage through cracks must be prevented.

The thickness of the lead lining in these rayproof rooms depends upon the voltages used on the tube inside. The International Commission on X-ray and Radium Protection recommends<sup>1</sup> the thicknesses listed in Table 10-1. This table is based upon the assumption that the average dosage rate of the x-rays striking the inner walls of the x-ray room is 3 r./min., or 0.05 r./sec. Under these conditions, the lead thicknesses recommended will reduce the dosage so that the rays penetrating the lead will be reduced to a dosage rate of  $10^{-5}$  r./sec., the maximum considered safe for continuous exposure of the whole body.

TABLE 10-2.—COST OF PROTECTIVE LEAD LINING FOR X-RAY ROOMS

Peak x-ray-tube kilovolts	Cost per square ft, lead only	Cost installed	Covered with lath and plaster
100	\$0.35	\$0.85	\$1.20
200	0.95	1.45	1.80
300	2.10	2.70	3.05
400	3.50	4.10	4.50
500	5.20	6.00	6.50
600	8.00	9.00	9.50

TABLE 10-3.—COMPARATIVE DATA ON LEAD AND CONCRETE BARRIERS FOR X-RAY PROTECTION

Kv.p.	Recom- mended lead, mm.	Equivalent concrete, in. Density = 2.4 g./cm. <sup>3</sup>	Thickness concrete ÷ thickness lead	Mass concrete ÷ mass lead	Cost of concrete per sq. ft.	
					Wall	Floor
100	1.5	4 $\frac{3}{4}$	80	16.5	\$0.63	\$0.38
200	4	8 $\frac{1}{2}$	55	11.8	0.72	0.47
300	9	9 $\frac{1}{2}$	26.7	5.6	0.77	0.52
400	15	10 $\frac{1}{4}$	17.3	3.5	0.79	0.54
1,000	84*	30*	9.1*	1.9*	2.00*	1.50*

\* These figures are based on Prob. 9; they are not necessarily recommended by Taylor.

Taylor<sup>2</sup> has estimated the cost of the lead plus fastening it to furring on a terra-cotta wall, as listed in Table 10-2. It is seen that at the higher voltages the cost of lining even a small room with lead becomes high. For example, a cubical room 10 by 10 by 10 ft. containing a 600-kv. x-ray tube would require \$4,800 worth of lead, to say nothing of installing it. The same room would require only about \$600 worth of lead for a 200-kv.

<sup>1</sup> *Radiology*, **30**, 511 (1938).

<sup>2</sup> L. S. Taylor, *J. Applied Phys.*, **10**, 598 (1939).

installation. The result is that for equipment from about 400 kv. up, concrete walls are usually installed for protection, rather than lead. Data on concrete construction are given in Table 10-3. Concerns now exist<sup>1</sup> that specialize in the manufacture and installation of lead partitions and other devices for x-ray or gamma-ray protection.

In a typical million-volt installation for industrial radiography, a special building was constructed<sup>2</sup> 30 by 45 ft. and 25 ft. high. The concrete walls are 18 in. thick up to a height of 14 ft., the top portion being 12 in. thick. Building and equipment together cost about \$100,000. The million-volt tube is provided with some lateral shielding; and since it is some 15 ft. from the walls, the average dosage rate at the inside surface of the wall is doubtless less than the 3 r./min. figure upon which Table 10-3 is based. Eighteen inches of concrete is probably sufficient for the installation mentioned.

In the case of mobile equipment for industrial radiography, where the equipment is mounted on a rubber-tired chassis and moved to the work, it is usual to locate the control panel in a lead-lined booth, also on the chassis, in which the operator stands while the tube is turned on. A heavy metal cone limits the primary rays chiefly to the neighborhood of the work, and others who may be working in the vicinity should keep a good distance away (say 100 ft. or more) and thus let the inverse-square law protect them from secondaries and scattered rays.

With x-ray diffraction equipment, the voltages used rarely exceed 50 kv.; hence the tube itself can be made rayproof, or it can be enclosed in a small lead chamber having a few small ports. The diffraction cameras are placed immediately in front of these ports and are provided with collars, which intercept the scattered and secondary rays. If only two cameras are being used with a tube shield having four ports, for example, the two unused ports should be covered with lead at least 1 mm. thick.

The rays issuing from one of these ports when uncovered may be used for microradiography. Although they are soft rays, they are quite intense, and it is important to keep hands, arms, etc., out of the beam. The equipment should be placed behind a lead barrier when used in this way, or, at any rate, some positive provision should be made to screen it effectively from persons in the vicinity.

In industrial fluoroscopy of oranges, candy, corn flakes, etc., it is imperative that the x-ray dosage be kept down to the  $10^{-5}$  r./sec. level at every point in the vicinity; for the operators of such equipment sit right against it for several hours every day, and it operates continuously. No dependence should be placed on gloves or aprons. Careful checks at

<sup>1</sup> For example, Bar-Ray Products, Inc., Brooklyn, N.Y. Also, Ray Proof Corporation, New York, N.Y.

<sup>2</sup> *Automotive Ind.*, Dec. 15, 1942, p. 46.

all the points likely to be reached by x-rays, especially around the operator's position and at places where he may put his hands, should be checked with an accurate x-ray dosimeter while the tube is on before the equipment is placed in service. No dosage rate above  $10^{-5}$  r./sec. should be tolerated anywhere around the equipment. To keep down the thickness of the lead glass through which the fluoroscopic screen is viewed, in order to obtain better vision, the screen may be viewed by reflection in a mirror so that the primary rays will not strike the glass. The oranges, candy, etc., should be brought up and carried away by a conveyer, and the defective ones should be rejected mechanically when the operator pushes a lever or a button.

Kenotrons or high-voltage rectifier tubes often radiate some x-rays. A check should be made by placing dental films at several places in their vicinity and developing them after a week of service. If the films are darkened, an increase in the filament heating current or voltage (not exceeding the rated maxima) may eliminate the rays. If not, a lead screen 1 mm. thick should be installed, as described on page 121.

The test with dental film carried in the pocket for a week is one that all x-ray workers should make occasionally for their own safety. An undue drop in a worker's blood count should bar him from further x-ray work for several months at least.

**4. Protection from Ozone and Oxides of Nitrogen.** There is usually some corona discharge around most high-voltage equipment. This generates some ozone and some oxides of nitrogen. In addition to this, the x-rays themselves generate small quantities of these gases from the air, as may be readily understood from their ionizing action.

Ozone in considerable concentration is toxic, as are also some of the oxides of nitrogen. There is a difference of opinion regarding the amount that is harmful. Some say that concentrations of 20 parts of ozone per million parts of air breathed for 2 hr. may be fatal. Others say that 50 parts of ozone per million parts of air may be breathed for  $\frac{1}{2}$  hr. without any ill effects. At any rate, 1 part of ozone in a million parts of air is readily noticed by its characteristic odor, and there is thus no danger of breathing these gases in injurious quantities without being aware of it.

Ventilation should be provided that will keep the concentration of these gases down to the point where the air is pleasant to breathe, but a slight odor of ozone is no cause for alarm.

**5. Gamma-ray Protection.** The gamma rays from radium are commonly used in therapeutic work, much as x-rays are used. Likewise, gamma rays are very useful in certain types of industrial radiography. Workers in either of these fields must be careful to protect themselves and others from the gamma rays, just as with x-rays.

The problem of protection from radium, radon, and gamma rays can

be fully understood only when the details of the preparation and use of radium, radon, and radium capsules are kept in mind. These details have been given in Chap. 8. It will be assumed here that the radium is to be obtained and used only in sealed capsules, which are never to be opened, crushed, stepped on, handled with pliers, etc. Such treatment is likely to cause a radon leak, and, as stated in Chap. 8, a few parts of radon in 1 quintillion parts of air is dangerous to breathe. The great majority of workers never have occasion to open a radium capsule.

The gamma-ray emission from a radium capsule which has reached radon equilibrium is such that at a point 1 cm. away the dosage rate is 8.16 r./hr./mg. of radium (or millicurie of radon).<sup>1</sup> Hence, at a distance of 1 meter from a capsule containing 100 mg. of radium (in equilibrium), the dosage rate is  $2.27 \times 10^{-5}$  r./sec., or about 3 times the maximum safe continuous body exposure rate of  $10^{-5}$  r./sec. specified in Sec. 2. At a distance of 2 meters from the capsule, the dosage rate is one-fourth of this, or  $0.57 \times 10^{-5}$  r./sec. Hence one can spend 8 hr. every working day sitting only 6 ft. from a 100-mg. radium capsule and suffer no ill effects, according to the International X-ray and Radium Protection Commission.

Some qualified workers who have worked for many years with large quantities of radium, both in and out of capsules, have set a somewhat lower safe continual body dosage rate than the International Commission's 1 r./week figure. Failla,<sup>2</sup> for example, suggested 0.6 r./month as a safe figure. On this basis, one should work steadily every day no closer than about 4 meters or about 13 ft. from an unprotected 100-mg. capsule. At any rate, the inverse-square law affords effective protection from radium. One could spend a lifetime only 30 ft. or so from a gram of radium sealed in a capsule without any additional protection, and the indications are that no adverse effect on his health would be noticed.

Most injuries from radium are of the local-burn variety. Even 1 mg. of radium held in the hand will soon cause a serious burn, and if one is handling radium at all the quantity involved is usually many milligrams. Those whose work involves only the use of sealed capsules have no excuse for suffering radium burns. The danger is well known, and the necessary precautions to avoid injury in handling radium capsules are quite simple.

Radium may be rented or purchased for use in industrial radiography. Convenient amounts for such work range from 100 to 500 mg. It is shipped in a radium "safe." This is a wooden cube about 9 in. on an edge, in which is embedded a lead sphere about 5 in. in diameter. At the center of this otherwise solid sphere, there is a cavity about 1 in. in diameter. Some safes are bisected horizontally and hinged at one side so

<sup>1</sup> L. S. Taylor and G. Singer, *Natl. Bur. Standards J. Research*, **24**, 247 (1940).

<sup>2</sup> G. Failla, *Radiology*, **19**, **12** (1932).

that when the latch is released the upper half of the safe may be laid back, this "lid" containing one lead hemisphere and the other hemisphere being in the lower half of the safe. Other safes open by withdrawing a massive lead plug from a hole in the top. This exposes an aluminum or steel container about the size of a walnut. A piece of fishing line about 1 yd. long is attached to the top of this. When the safe is closed, the fishing line extends outside, where it may be reached with the safe closed. Inside the small container is the silver radium capsule, which contains the radium and radon. When the safe is closed, with the radium inside it, the hand cannot be brought closer to the radium than about 4 in. and is then shielded by 2 in. of lead. The hand is then exposed to the same gamma-ray intensity as it would be if held 1 ft. from the radium without any safe. This should make it clear that such a "safe" is rather a joke. For safety, do not rely on the safe; rely on the inverse-square law.

When it is not in use, keep the radium in the safe, keep the safe closed, and put it where people will not ordinarily come within 15 ft. of it. To avoid fogging, undeveloped photographic and x-ray film must be stored 20 ft. or more from the safe. A handy fixture to hold the radium when it is in use can be made by pushing the stem of a small glass funnel partly through the hole of a large rubber stopper, so that the latter will act as a base to hold the funnel upright. After the castings or other objects to be radiographed have been arranged in place and the film holders placed behind them, a barricade (ladder, tables, chairs, for example) should be erected around the setup and warning signs displayed. Then the funnel and stopper may be placed at the point where the radium is to be located. A meter stick or yard stick provided with a  $\frac{1}{4}$ -in. hole about 1 in. from one end is a convenient device for handling the radium container.

When all else is ready, approach the radium safe and tie a piece of string to one of the fishing lines dangling from it, so as to increase its length to about 4 or 5 ft. Put the loose end of the string through the hole in the meter stick and pull it through until it can be grasped underneath the hand that holds the stick at the opposite end, like a fishing hole. Then open the safe and remove the radium with the stick just as a fish is removed from the water with a fishing pole and line. Carry it, with the stick held out horizontally, to the glass funnel. Lower the radium into the funnel, and then move away to a minimum distance of 10 ft. or more, depending upon the amount of radium used. After the exposure, the radium is returned to the safe by the fishing-pole method, and the safe is closed, before anything else is done. If the safe is located in a different room from the radiographic setup, one will expose himself less by carrying the radium from the safe several hundred feet to the glass funnel on a meter stick and string than if he carries the safe this distance with the radium in it.



If one spends 10 min. each working day carrying 1 g. of radium at the end of a meter stick, he will receive a gamma-ray dose of about  $\frac{1}{8}$  r. each day, or  $\frac{3}{4}$  r. for a 6-day week, which is within the accepted safety limit. Ordinarily, the operation should require 1 min. or less, rather than 10 (5 each way), and the radium used is likely to be only a fraction of a gram. The above procedure is outlined merely as an example. Obviously, it can be modified to suit the particular application at hand if the basic principles of protection are observed.

Radium precautions may be summarized thus: (1) When not actually carrying or handling the radium, keep it at least 15 or 20 ft. from people, in its safe. (2) When handling it (in capsules), do so with a meter stick or yard stick as described above, or use long forceps. (3) When handling it or carrying it, make the operation as brief as possible by planning your movements ahead of time.

Radium should be removed from its capsule only by persons who have been fully instructed in the technique by an expert in this work, who is familiar with the handling of radon, which is much more dangerous than its parent radium.<sup>1</sup> Such work requires special facilities.

The test of keeping dental film in the pocket for 10 days should be carried out occasionally by all radium workers as a check on the general bodily exposure they are receiving. Any undue drop in the blood count makes it imperative that the person concerned stop working with radium for several months, at least.

### QUESTIONS AND PROBLEMS

1. Outline the precautions to be observed in avoiding electric shock from shock-proof x-ray equipment. Suggest additional safeguards for equipment that is not shockproof.

2. What is the maximum weekly x-ray dose considered safe for a normal person? Answer the same question for gamma rays. What are the early symptoms of excessive exposure to x-rays or gamma rays?

3. Would 500 r. administered only to your elbow in 10 min. be likely to result in the loss of your arm? What is irradiation sickness?

4. If one stands behind a lead shield 8 ft. square and 1 ft. thick, why may he still be dangerously injured by a 200-kv. x-ray machine operating in front of this shield?

5. Should x-rays from kenotrons be considered as a possible danger? Which is more dangerous, a little ozone or a little radon in the air?

6. Why is it dangerous to step on a radium capsule? Would it be dangerous to keep radium in a radium safe under your desk? Would it be dangerous to work all day only 20 ft. from a 200-mg. radium capsule lying on a table?

7. Outline a practical and safe method of handling radium containers while radiographing heavy castings.

8. If one is experiencing a dangerous x-ray or gamma-ray exposure, how can this be detected by a dental film and holder? By a Minometer or similar device? By blood count, if the exposure is continued?

<sup>1</sup> See pp. 161 and 162.

9. According to Jaeger and Trost,<sup>1</sup> 115 mm. of lead or 105 cm. of concrete is required to reduce million-volt x-rays having a dosage rate of 75 r./min. to the  $10^{-6}$  r./sec. tolerance limit. If the dosage rate on the lead or concrete wall were only 3 r./min., as assumed by the International X-ray and Radium Protection Commission, instead of 75 r./min., what thickness of lead and concrete would be required to shield against million-volt x-rays, according to this data? [See equation (5-5).]

Ans. 83.5 mm. of lead; 76.2 cm. (30 in.) of concrete.

<sup>1</sup> R. Jaeger and A. Trost, *Elektrotech. Z.*, 61, 1025 (1940).

## CHAPTER 11

### X-RAYS IN THE MEDICAL FIELD (RADIOLOGY)

**1. Introduction.** X-rays were put to practical use in medical work almost as soon as they were discovered. Röntgen himself was the first to obtain a radiograph of the bones in the hand. The applications of x-rays and gamma rays in medical work are often regarded as the subject matter of a distinct science, called "radiology." Broadly speaking, the word "radiology" means merely the science of x-rays and gamma rays, but the term is ordinarily applied to the medical aspects and uses of these rays.

Radiology in this sense is usually regarded as consisting of two general divisions. The first of these includes the use of radiography and fluoroscopy to detect and study bone fractures, dental cavities, local infections, foreign objects in the body, such as bullets and safety pins, and diseased conditions such as tuberculosis and cancer, or merely to obtain helpful information in planning an operation or determining whether one is necessary, etc. This type of work may be called diagnostic radiology.<sup>1</sup> The second division includes the use of x-rays and gamma rays to kill or arrest the spread of malignant or benign tumors and to cure skin diseases such as eczema. This division may be called therapeutic radiology or x-ray and radium therapy. Therapy applied to deep-seated tumors is called "deep therapy"; therapy applied to the skin is called "superficial therapy."

**2. Diagnostic Radiology.** Some of the various types of x-ray tubes for diagnostic work were described and illustrated in Chaps. 2 and 7. There was some discussion of diagnostic fluoroscopy in Sec. 9-1, and precautions to be taken to avoid injury in such work were outlined in Chap. 10.

Dental equipment and some of the portable and mobile equipment intended to be moved from room to room in a hospital usually operates at a maximum tube potential of around 50 to 75 kv. The larger fixed installations for radiography of the chest, stomach, etc., usually operate at potentials up to 90 kv.; for fluoroscopic examination of the chest, potentials up to 110 kv. or thereabouts are sometimes used.

During the exposure, movement of the part of the body being radiographed will blur the radiograph. To reduce the probability of move-

<sup>1</sup> See, for example, G. W. Files, "Medical Radiographic Technic," Charles C. Thomas, Publisher, Springfield, Ill., 1944.

ment, the exposure time in such work is kept short, so as to approximate a radiographic "snapshot." In the case of radiography of the hands, arms, legs, and feet, the part can be rested on the cassette and weighted down with partly filled small sandbags laid near but not on the cassette. In dental work, a headrest can be used; in other work, bands can be used to "immobilize" the part. In thin parts like the hands, toes, teeth, etc., enough radiation is available from an ordinary tube to obtain a satisfactory exposure in a second or two without using any intensifying screens. In such work, two films are sometimes used so that any faint or doubtful marking in the image appearing on one film may be confirmed (or discounted as a film blemish, abrasion, etc.) by referring to the other one. In radiographing thicker parts of the body, fluorescent intensifying screens are usually used to keep the exposure time short.

A 4-mm. focal spot 4 ft. from the film will give just as clear and detailed a radiograph as a 2-mm. spot 2 ft. from the film, and at the same time less distortion due to divergence of the rays will be experienced. Since the distance is twice as great, four times as much tube current will be required in the former case as in the latter if the exposure time and the tube potential are to remain the same. However, the short-time current rating of a tube with a 4-mm. focal spot should be four times that of a tube with a 2-mm. spot; therefore, one should be able to use four times the current in the former case for a few seconds. The idea of using a tube with a large focal spot operated at heavy currents at large distances from the cassette cannot be carried to extremes without the equipment becoming bulky, awkward, and expensive. Therefore, one should compromise between these conflicting factors in making a selection. The tube support should be rigid; tube vibration blurs the radiograph.

Some typical exposure data for diagnostic radiographs, a tube with a Benson-Goetze type of focus being used, are as follows:

For the hand, with an effective focal spot 2 mm. square, 30 in. from the film, 40 kv.p., 15 millamp., 5 sec., no intensifying screens. With a spot 4 mm. square, 36 in., 32 kv.p., 100 ma., 3 sec., without screens.

For the skull, anterior-posterior or posterior-anterior position, with spot 2 mm. square 30 in. from the film, 82 kv.p., 15 ma., 5 sec., using fluorescent intensifying screens and a Bucky grid (page 216).

For the chest, posterior-anterior, with spot 4 mm. square, 72 in. from the film, 75 kv.p., 100 ma., 0.1 sec., using fluorescent intensifying screens.

Exposure time and voltage are of course considerably less for a small child or an infant than for an adult. It should be remembered that the time will drop off exponentially as the size of the body is reduced, according to Lambert's law [equation (5-5)].

If higher voltages, such as 200 kv., were used for medical radiography, these harder x-rays would result in a "flat" picture lacking in contrast.

For successful radiography, it is essential that the object which is to be seen absorb a reasonable fraction of the rays. For example, suppose a radiograph of the stomach is required. At 80 kv., perhaps 85 per cent of the rays passing through the body near the stomach may be absorbed and scattered, but 88 per cent of the rays passing through the body and stomach may be absorbed and scattered before emerging. This 3 per cent difference is what determines the success or failure of the radiograph in revealing the desired information. If 200 kv. were used, perhaps only 60 per cent of the rays passing near the stomach and 61 per cent of those passing through it would be absorbed. Hence the differential would be reduced to one-third its former value, and the radiograph would show a disappointing lack of contrast. If only 40 kv. were used, then perhaps 99 per cent of the rays passing near the stomach would be absorbed as compared with perhaps 99.1 per cent of those passing through it. This heavy absorption would make the exposure time too long to be practical, although the differential (0.9 per cent transmitted through, 1 per cent transmitted near the stomach) would be enough to yield the desired information if it were not fogged out by the scattered and secondary rays from the 99 per cent that was absorbed.

Tables giving approximate time, voltage, tube current, and other data for various parts of the body with various techniques will be found in the recent book by Files<sup>1</sup>, and some of the x-ray tube catalogues.

In medical fluoroscopic work, somewhat higher voltages are common than in medical radiography. The fluoroscope enables the physician to observe heart and lung action, to watch the broken bones while he is setting a fracture, and to preview any radiograph he intends to take, by mounting the fluoroscopic screen and a cassette interchangeably in the same carriage, or it may help him remove a swallowed safety pin, etc. The patient should be exposed only for a few intervals of a few seconds each. The operator and physician should have their eyes well adapted to the dark beforehand. Other details have been discussed on pages 172 and 202.

It is common practice to protect the patient from the very soft rays in diagnostic (either fluoroscopic or radiographic) work by using a "filter" consisting of a sheet of aluminum  $\frac{1}{2}$  to 1 mm. thick placed near the tube so that the harder primary rays pass through it on their way from the target to the patient but the softer ones are absorbed by the filter instead of the patient. Further protection may be afforded the patient by using a cone or similar device (Fig. 11-9) to limit the rays to the part of the body being radiographed.

In all types of radiographic work, it is essential to place the cassette

<sup>1</sup> Footnote 1, p. 211.

as close to the object being radiographed as is practical. The longitudinal axis of the cassette should be perpendicular to the axis of the x-ray tube to take advantage of the more uniform intensity of the rays in the transverse plane of the tube. The central ray of the primary beam should strike the center of the film perpendicularly immediately after it traverses the object, except when such an arrangement is impractical, as it may be in certain cases. The cassettes used in medical work are usually made of aluminum so that they are rugged and rigid, yet light. The hinged back is heavy enough to protect the film against secondaries and scattered rays

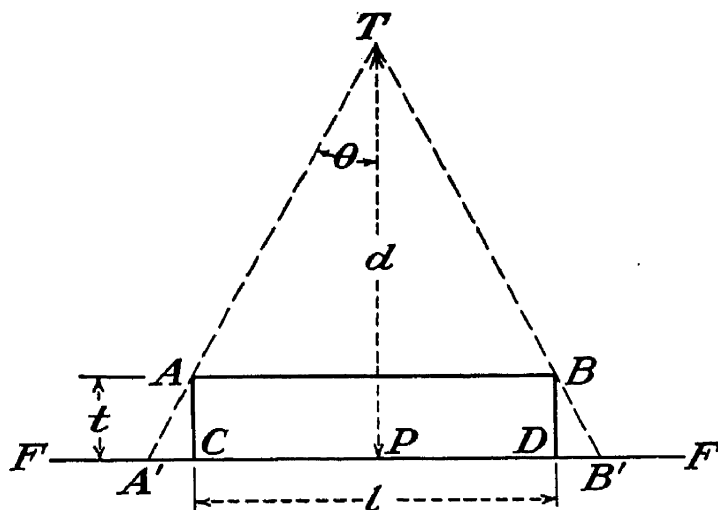


FIG. 11-1.—Diagram illustrating radiographic distortion.

from the rear. When the back is closed it is held with spring clips so as to exert a uniform pressure on any intensifying screens that may be used.

In Fig. 11-1, assume a point source of x-rays at  $T$ , which is a distance  $d$  from the film  $FF$  in contact with the object  $ABCD$  being radiographed. The thickness  $AC$  of  $ABCD$  is  $t$ , and the length  $CD$  is  $l$ .

From the diagram it is obvious that the shadows of the points  $A$  and  $B$  will fall at points  $A'$  and  $B'$  on the film. The distances  $A'C$  and  $DB'$  may be taken as a measure of the distortion of the radiograph due to the nonparallelism of the rays. If  $t$  is small compared to  $d$  (as it must be, for good radiography), then one has the approximate relation  $\tan \theta = l/2d$ , and for the distortion  $A'C$  the approximate relation

$$\text{Distortion} = t \tan \theta = \theta l = \frac{lt}{2d} \quad (11-1)$$

In Fig. 11-2,  $AB$  represents a circular spot source of x-rays of diameter  $AB = s$ . As before, the object of thickness  $t$  that is being radiographed lies on the film, and  $d$  is the distance  $AA'$  from focal spot to film. A particle  $P$  at the top surface of the object will then cast a shadow  $B'A'$

on the film, this shadow being a spot of diameter  $B'A'$  equal to  $t\phi$  where  $\phi$  is the angle  $APB$  or  $A'PB'$  in radians. If  $d$  is large compared with  $t$  (as it must be for good radiography), then  $\phi$  is approximately equal to  $s/d$ . Hence one has for the diameter of the spot  $B'A'$ , which may appropriately be called the "blurring," the approximate relation

$$\text{Blurring} = \phi t = \frac{st}{d} \quad (11-2)$$

The reciprocal of this,  $d/st$ , is commonly called the "definition."

Every effort should be made to minimize the two quantities (11-1) and (11-2) if clear, undistorted radiographs are desired. It is clear that the tube-to-film distance  $d$  must be increased as the size of

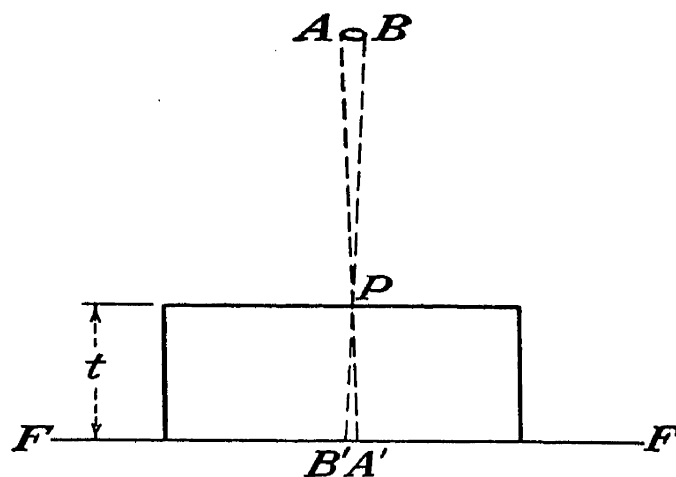


FIG. 11-2.—Diagram showing factors controlling radiographic definition.

the radiograph,  $l$ , or the thickness of the object,  $t$ , or the diameter of the focal spot,  $s$ , increases, unless one is willing to sacrifice definition and tolerate distortion for the sake of speed, which varies inversely as  $d^2$ . This applies equally well to either medical or industrial radiography.

Equation (11-1) gives the distortion in the same units in which  $l$ ,  $t$ , and  $d$  are measured. For example, if a patient's chest is 9 in. thick and is radiographed on 14- by 17-in. film with the tube focal spot 4 mm. ( $\frac{1}{8}$  in.) square 72 in. from the film, the maximum distortion at the top and bottom edges of the radiograph will be  $\frac{lt}{2d} = \frac{17 \times 9}{2 \times 72} = \frac{17}{16}$ , or slightly over 1 in.

Likewise, (11-2) gives the blurring in the same units in which  $s$ ,  $t$ , and  $d$  are measured. In the above example, the blurring will be

$$\frac{st}{d} = \frac{\frac{1}{8} \times 9}{72} = \frac{1}{48}$$

or slightly over 0.02 in. Since the photographic grain size when fluorescent intensifying screens are used is usually about 0.02 in. in any case, this much blurring can be tolerated.

In industrial radiography, the film can to some extent be protected from fogging by the comparatively soft secondary and scattered rays by enclosing the film in sheet lead and by using "blocking material." In medical radiography, the primary rays are too soft to permit enclosing the film in lead foil except in radiography of the ribs, spinal column, etc., and the use of blocking materials is inconvenient, if not impractical, for reasons that will appear when their use in industrial radiography is dis-

cussed in the next chapter. The cassette should protect the film from back scatter by lead backing or other strongly absorbent backing.

The problem of protecting the film from fogging by secondary and scattered rays from the body of the patient, the filter, and surrounding objects has been solved for certain types of work by the invention and use of the "Potter-Bucky grid," also sometimes called a "Potter-Bucky diaphragm" and sometimes merely a "Bucky." Since secondary rays radiate in all directions from the point of origin and scattered rays likewise radiate in all directions from the point where the scattering occurs, it follows that only a small portion will travel in the same direction as the original primaries. Therefore, assuming that the primaries strike the film perpendicularly, as they ordinarily do, most of the secondaries and the scattered rays will strike the film at angles ranging from 0 to 85° and from 95 to 180°, let us say, and comparatively few of them will strike at angles between 85 and 95°. It therefore occurred to G. Bucky that most of these unwanted rays could be intercepted by constructing a gridwork of lead ribbons and placing it immediately in front of the cassette. Suppose a 14- by 17-in. film is to be used. Then 112 lead ribbons, each  $\frac{1}{2}$  in. wide and 17 in. long could be placed in front of the cassette, each ribbon being stretched straight and parallel to the length of the film, the planes of the ribbons being perpendicular to the film, and the distance between the parallel ribbons being  $\frac{1}{8}$  in. so that the 112 ribbons would cover the full 14-in. width of the film. It is obvious that rays lying in or near the plane of the ribbons may now strike the film, but other rays will be intercepted by the ribbons.

If the x-ray tube is located at a great distance from the film, the primary rays from it will be nearly parallel at the film and will pass between the ribbons, but most of the scattered and secondary rays will be intercepted by them. In order to keep the ribbons in place, 111 strips of wood or plastic (like Bakelite), each 17 by  $\frac{1}{2}$  by  $\frac{1}{8}$  in. may be inserted between the lead ribbons and the whole assembly glued together and supported in a framework. The wood, being comparatively transparent to the x-rays, does not interfere seriously. If the tube is to be used 25 in. from the film, it is better to align the lead ribbons to conform to the radii of a 50-in. cylinder with its axis parallel to the strips, the grid itself being kept flat, however. With such a "focused" grid, the primary rays will lie in the plane of the lead ribbons at the edges of the film as well as at the center, even though the rays diverge. The grid can be thus focused by using wood strips slightly thicker at one side than at the other.

Obviously, such a grid lying stationary on the film will leave a series of 112 white lines running lengthwise of the radiograph after development. It occurred to H. E. Potter that this difficulty could be eliminated by making the grid wider than the film (say 17 by 18 in. for a 14- by 17-



in. film) and providing a slow, steady movement of the grid crosswise to the film during the exposure. This improvement resulted in the device coming into wide use in medical radiography. As actually constructed, the lead ribbons and wood strips are usually about  $\frac{3}{8}$  in. wide and 18 in. long, the wood strips being about  $\frac{1}{8}$  in. thick. The motion is often provided by a steel spring, the speed being controlled by a plunger that forces oil through an orifice having a size that can be adjusted. The motion must begin before the x-ray exposure starts and end after the exposure is complete, in order to avoid grid lines appearing in the radiograph. If the exposure is only  $\frac{1}{10}$  sec., for example, the grid usually moves such a short distance during this time that grid lines appear in the radiograph.

The wood absorbs some of the primaries and the lead ribbons obstruct some of them, and this means that exposures with the grid must be two or three times as long as without it. Hence the grid is not ordinarily used in radiography of the chest, for two reasons. (1) Chest exposures must be short in order to minimize blurring due to heart and lung action,  $\frac{1}{10}$  sec. or less being the usual exposure. This is so short that the grid motion is arrested and the grid lines appear. (2) The use of the grid necessitates an increase in the exposure time required to obtain the desired film density, thus increasing the blurring due to heart and lung action. Another disadvantage of the grid is that it necessarily increases the distance between the object and the film, which is always a serious objection. Hence for thin parts of the body such as hands, ankles, etc., where there are not many scattered or secondary rays set up, the Bucky is rarely used.

Nevertheless, the Bucky does eliminate 80 or 90 per cent of the fogging due to secondaries and scattered rays, and so is frequently used in radiography of the spine (see Fig. 11-3), pelvis, sternum, ribs, kidney, urinary bladder, gall bladder, stomach, colon, fetus, mastoid, sinus, jaw, shoulder, and head (lateral). It is occasionally used for radiography of the head (anterior-posterior or posterior-anterior) and extremities such as the knee, etc.

Some parts of the body such as the intestine, bronchial tubes, gall bladder, and kidney are comparatively transparent to x-rays and are embedded deep in surrounding body structures at least as opaque as they are. In order to obtain a satisfactory radiograph of such organs, it is often necessary artificially to increase their density. In the case of the gastrointestinal tract, this may be accomplished by feeding the patient barium sulfate. For radiography of the gall bladder, the patient may be fed sodium tetraiodophenolphthalein. In the case of the bronchi, an iodized oil such as Lipiodol may be injected. For the kidneys, sodium iodide solution may be introduced through a catheter. A colloidal suspension of thorium hydroxide has also been used for uterus, cervix,

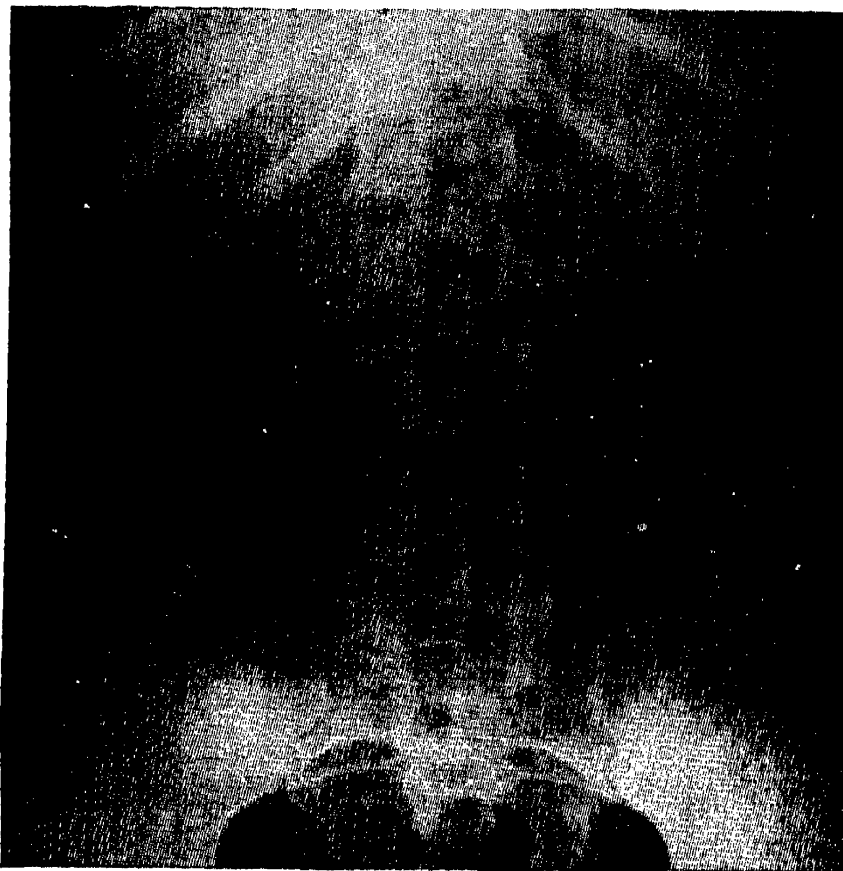


FIG. 11-3A.—Anterior-posterior radiograph of the spine, taken without the Potter-Bucky diaphragm. (After Files; courtesy of Charles C. Thomas, Publisher.)

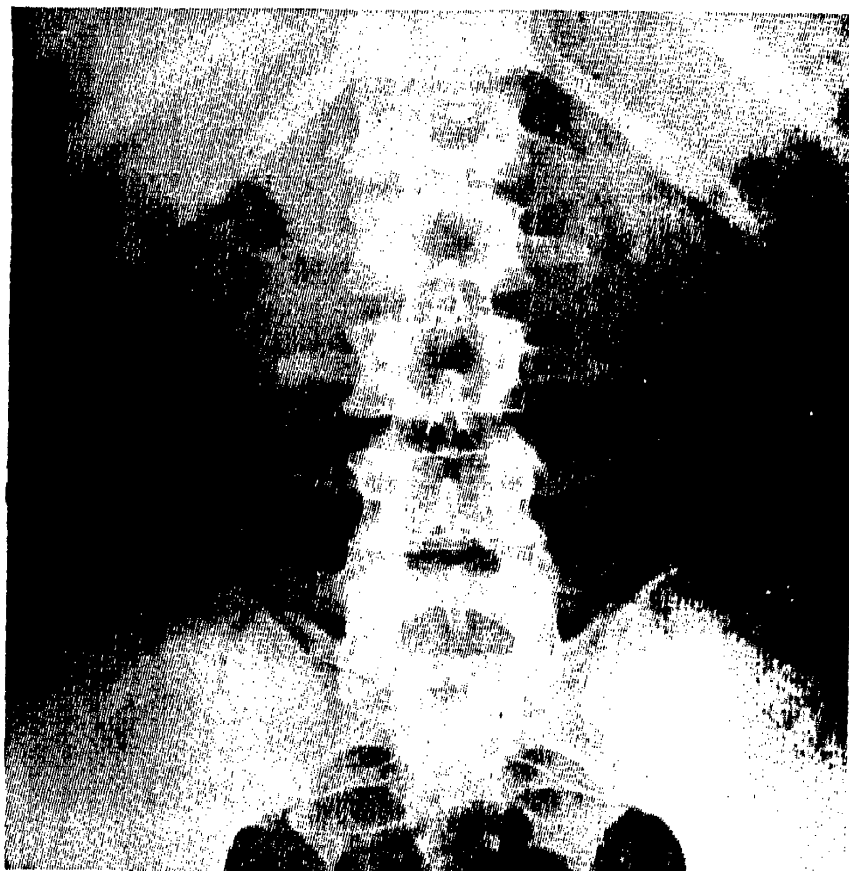


FIG. 11-3B.—Anterior-posterior radiograph of the spine, taken with the Potter-Bucky diaphragm. (After Files; courtesy of Charles C. Thomas, Publisher.)

fistulas, and sinus tracts, and thorium dioxide for spleen, liver, arteries, veins, and lymphatics. These materials are called "diagnostic opaques."

In a simple radiograph of the type thus far discussed, it frequently happens that a lesion, tumor, foreign object, or other abnormality appears. Examination of the radiograph readily reveals its location,<sup>1</sup> in two dimensions; for example, it may be determined that it lies between the third and fourth ribs, 3 in. to the right of their juncture with the sternum. The other dimension may be difficult or impossible to determine from the original radiograph; that is, there may be no way of telling

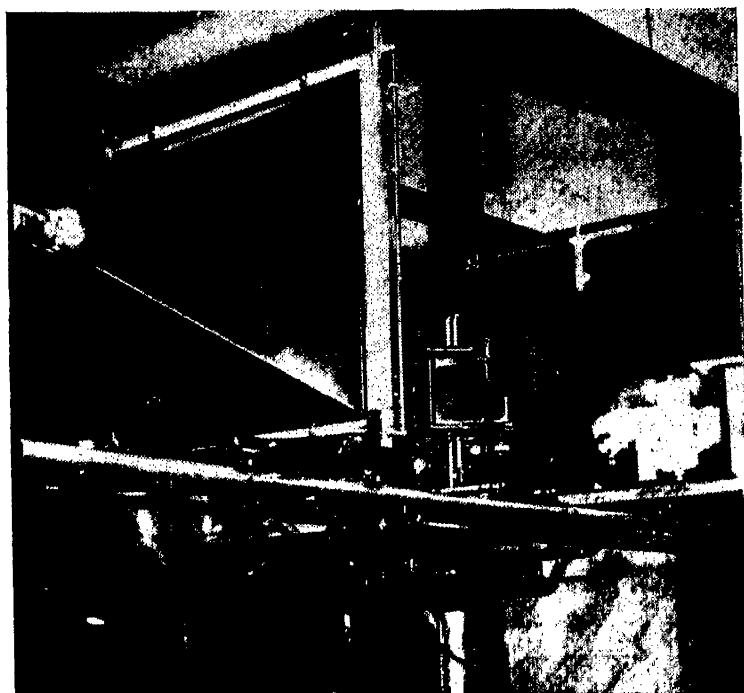


FIG. 11-4.—Stereoscope for viewing stereoscopic radiographs on film.

whether the point in question lies 1 in. behind the skin or 3 in. unless additional radiographs are secured.

Perhaps a radiograph taken laterally will provide the answer, but in some cases this is unsatisfactory or impractical. In such an event, one may resort to stereoscopic radiography. This is accomplished by taking two radiographs and moving the x-ray tube 3 or 4 in. (roughly the distance between a person's two eyes) between the two exposures. If an exaggerated effect is desired, the tube may be moved farther. The resulting radiographs are viewed in a stereoscope of the type shown in Fig. 11-4. Such a stereoscopic view usually conveys a fairly accurate impression of the relative positions of the various details seen, in three dimensions. When a Bucky is used in stereoscopic work, it is much more satisfactory to move the x-ray tube parallel to the lead strips between exposures, the

<sup>1</sup> Lead oxide ointment on the skin may be helpful in certain radiographs of the extremities. For illustration, see *Life*, Jan. 24, 1944, p. 8.

target being kept on the axis of its cylindrical focus, rather than to move the tube perpendicular to the strips and thus get the target away from the axial position for which the grid is designed.

As an elaboration upon the simple stereoradiograph, apparatus has been constructed in some medical centers for taking "planigraphs," or, as the British call them, "tomographs." This is a radiograph taken while the tube is in motion in a direction parallel to the film; the film may also be in motion in its own plane but in the direction opposite to the tube motion. This may be accomplished by connecting the film (and Bucky carriage, if used) to one end of a lever and the tube carriage to the opposite end. The lever is provided with an intermediate pivot, the position of which can be adjusted along the lever, closer to the tube and farther from the film, or vice versa. There are numerous modifications and variations of this general idea, and this has given rise to a multiplicity of terms in this type of work. For example, there are "stratigraphs," "planigraphs," "planeographs," "tomographs," "differential radiographs," "laminagraphs," and "body-section radiographs," all supposedly different, yet all so much alike that even the specialists in this type of work are confused by the terminology.<sup>1</sup>

In a radiograph of this type, points in the body of the patient that lie in a plane parallel to the film and containing the pivot give a clear sharp image on the film, but points above or below this plane give an image that is blurred by the motion and thus obliterated. Hence, such a planigraph is a radiograph limited primarily to a particular known plane in the body. The exploration of the internal structure of a body in three dimensions by analysis of a series of planigraphs is known as "serioscopy." This subject is discussed in an article by Kaufman and Koster.<sup>2</sup> The series of planigraphs is taken for various planes in the body, of course, and an analysis permits one to locate any particular point of interest.

This same purpose may be achieved in other ways. For example, two pairs of scales may be mounted in parallel planes a known distance apart and radiographed along with the subject. By the relative position in the radiograph of the scale graduations and the point of interest, quantitative information regarding its position may be obtained, as outlined by Hummell and Hume.<sup>3</sup>

There have been some elaborations upon the process of planigraphy, or tomography, in which the tube and film are subject to complex spiral motion, but their application has been limited. The additional com-

<sup>1</sup> See, for example, S. Moore, *Radiology*, **33**, 605 (1939), or D. Wheeler and E. W. Spencer, *Radiology*, **34**, 499 (1940).

<sup>2</sup> J. Kaufman and H. Koster, *Radiology*, **34**, 626 (1940).

<sup>3</sup> A. D. Hummell and O. F. Hume, *Phys. Rev.*, **51**, 60 (1937).

plexity apparently is not justified by any marked superiority in the results.

There is another variation of simple radiography that is frequently employed to obtain a permanent record of the motions of the internal organs such as the lungs and especially the heart. This is called "kymography," and the record is a "kymograph." The usual method of obtaining a kymograph is to take a radiograph of the chest, but between the patient and the film is placed an opaque diaphragm, for example, 1-mm. sheet lead. This diaphragm contains a narrow slit as long as the width of the film, the width of the slit usually being of the order of 1 mm. During the exposure, the x-ray film is moved at uniform speed perpendicular to the slit. In some cases, the film is stationary, and the slit is moved perpendicular to itself. In this case, one obtains a "scanograph" rather than a kymograph. The film speed (or slit speed) is usually such that the width of the slit is traversed in the time required for an ordinary chest radiograph, say  $\frac{1}{20}$  sec. The exposure may be maintained for a second or two so that the motion will be some 20 or 40 slit widths. Thus a comparatively opaque organ like the heart will cast its shadow on the slit, and the length of the slit covered by the shadow will increase and decrease as the heart beats and as the film moves. The result is that the kymograph exhibits a saw-tooth outline which serves as a time record of the heartbeat for the particular part of the heart casting its shadow on the slit. For a slower motion, such as the stomach movement, which has about a 30-sec. period, the film speed chosen is slower, the x-ray tube power is reduced, and the exposure lasts a longer time, say 30 sec. so as to include a complete pulse.

Obviously, it is advantageous to obtain such a kymographic record of various parts of the organ simultaneously in a single exposure, and therefore a standard multiple-slit kymographic diaphragm, or grid, has been adopted that is ordinarily used in such work. It is provided with 20 or more parallel slits each 0.4 mm. wide and spaced 1.2 cm. apart. By choosing the film speed and exposure time so that each slit makes a 1-cm. record, overlapping of the records is avoided. For a detailed discussion, the reader is referred to an article by Schwartzschild<sup>1</sup> and for a reproduction of a kymograph of the heart to an article by Steinberg and Robb.<sup>2</sup>

Intensifying screens are used in certain types of medical diagnostic equipment in a manner resembling the use of fluoroscopic screens. A 14- by 17-in. screen is used as a fluoroscopic screen would be used to examine a patient's chest. The blue actinic light that it emits is photographed by an ordinary camera using optical photographic film having a size as small as 35-mm. motion-picture film or sometimes as large as 4 by 5

<sup>1</sup> M. Schwartzschild, *Radiology*, **33**, 90 (1939).

<sup>2</sup> I. Steinberg and G. P. Robb, *Radiology*, **33**, 293 (1939).

in. In the ordinary method of radiographing the chest, a 14- by 17-in. x-ray film is exposed, developed, and examined for diagnosis. The cost of this standard method prevents its use in routine radiography of school children, for example, to detect tuberculosis or other diseases in their early stages when treatment is most effective. To reduce the cost, one may use the cheaper x-ray papers (page 175) instead of film, or the indirect method just mentioned may be used.

In one installation of this type used in Germany, the fluorescent image is photographed with a miniature camera on 35-mm. film. After development, this photograph may be projected (and enlarged) at 10 to 15 times the film size for examination and diagnosis. The fluorescent screen used is a "Super-Astral," made by Schering-Kahlbaum, 30 by 40 cm., placed 150 cm. from the focal spot of the x-ray tube. The exposure is made at 50 to 57 kv., 500 to 600 ma., in 0.22 sec. The miniature camera is placed 1 meter from the screen and photographs the image at f.1.4. One person may be radiographed each minute. According to Steps,<sup>1</sup> it was planned to examine the entire German population in this manner.

The heavy power requirements of this method make the equipment rather expensive. A minimum tube current of about 400 ma. is needed. This technique is called "photoroentgenology," "indirect radiography," "photofluorography," or "x-ray screen image photography." It was first developed for practical use in Europe, but such equipment is now offered by American manufacturers of x-ray equipment. One of the earliest installations was in the German Hospital at Rio de Janeiro; the design of this equipment and the experience obtained while examining some 700,000 persons with it are described with good illustrations in articles by Bowers<sup>2</sup> and de Abreu.<sup>3</sup> Detailed recommendations regarding type of screens, film, camera lens, etc. are to be found in these two articles. De Abreu estimates that 1 million persons can be examined in this manner for \$112,000 as compared with \$900,000 for direct radiography. For a more recent discussion of this type of equipment, one may refer to an article by Hirsch.<sup>4</sup> A photoelectric device for timing<sup>5</sup> the exposure has been developed by Westinghouse. Millions of men have had their chests examined by indirect radiography upon their induction into the United States Army. The pictures obtained in most instances were 4 by 5 in.<sup>6</sup>

<sup>1</sup> H. Steps, *Phot. Ind.*, **36**, 1138 (1938).

<sup>2</sup> A. Bowers, *Radiology*, **33**, 357 (1939).

<sup>3</sup> M. de Abreu, *Radiology*, **33**, 363 (1939).

<sup>4</sup> I. S. Hirsch, *Am. J. Roentgenology Radium Therapy*, **43**, 45 (1940).

<sup>5</sup> *Aero Digest*, **48**, 112 (Jan. 1, 1945); H. D. Moreland, *Electronic Ind.*, **4**, 96 (January, 1945).

<sup>6</sup> J. Stafford, *Science News Letter*, **43**, 230 (Apr. 10, 1943).

A recent development that makes use of some of the features of planigraphy, stereoscopic radiography, and indirect radiography combined is due to Winnek.<sup>1</sup> In Winnek's apparatus, the arrangement is similar to that used in planigraphy, except that a fluorescent screen replaces the cassette. As the tube moves in one direction and the screen in the other (Fig. 11-5), the latter is photographed with a special moving camera as shown. In this camera the lens and film move in such a way that the

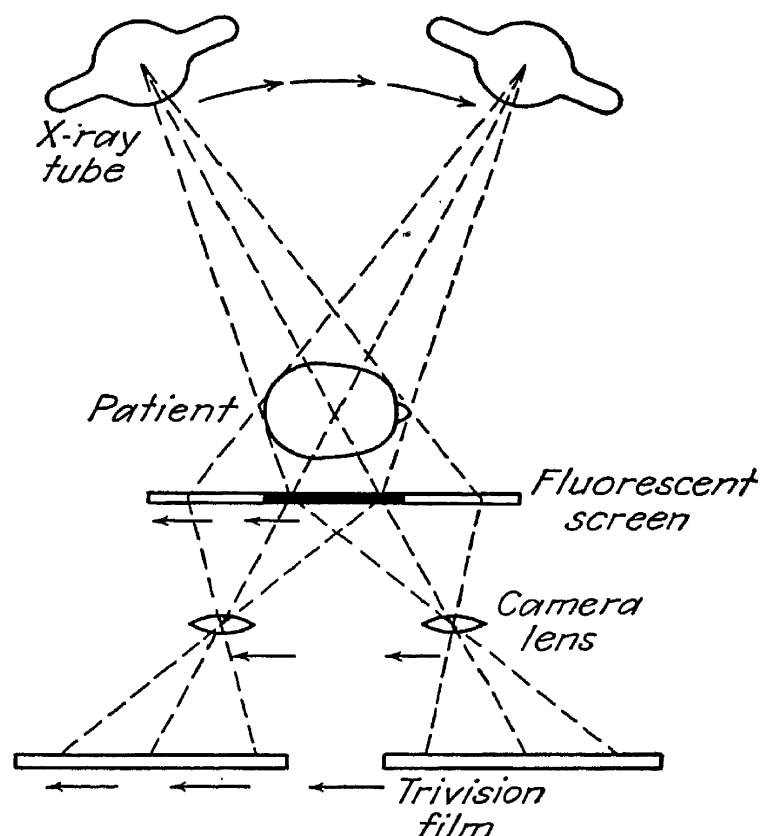


FIG. 11-5.—Winnek's stereoscopic radiographic apparatus. (Courtesy of *Popular Science Monthly*.)

image of each point of the moving fluorescent screen remains stationary on the film, but the obliquity of the rays that form the image constantly changes with the motion during the exposure.

A special corrugated film is used, embossed with parallel microscopic ridges, 200 to the inch. This is accomplished by means of a special embossing machine, which prepares ordinary film for use in this apparatus. The ridges are perpendicular to the plane of the diagram in Fig. 11-5. The early part of the exposure affects one side of the ridges, and the late part affects the other side. After the film is developed, a very realistic stereoscopic effect is obtained without the use of any stereoscope. By mounting the film behind a special measuring grid, viewing it at various angles in a plane perpendicular to the ridges, and counting the number of divisions across which some radiographic feature

<sup>1</sup> D. F. Winnek, *Popular Science*, **141**, 88 (September, 1942).

moves under these conditions, one may infer its depth. The stereoscopic realism of these corrugated-film photographs is very impressive.

There has been some success in obtaining motion pictures of x-ray fluoroscopic images. Such a process may be called "indirect cinematography," "indirect kineradiography," or "x-ray fluoroscopic cinematography." The chief difficulty in such work is to obtain a fluoroscopic image sufficiently brilliant to yield an adequate exposure of the motion-picture film. Reynolds<sup>1</sup> has obtained some very interesting radiographic motion pictures by this method. The x-ray tube is operated at 110 kv. and 60 ma., and the rays are filtered through the usual  $\frac{1}{2}$  mm. of aluminum. In order to protect the subject or patient from excessive x-ray exposure, the x-rays are cut off completely between exposures while the motion-picture film is moving up for the next frame. The 10- by 18-in. fluoroscopic screen is about 5 ft. from the 16-mm. motion-picture camera. No lead glass is used, as in conventional fluoroscopes. The motion-picture film in the camera and camera reels is protected from x-ray fogging by a lead shield 3 mm. thick. The total time the apparatus is operated for one patient is limited to 20 sec. to avoid danger of x-ray injury. Reynolds's article shows illustrations, both of his apparatus and some of his indirect cinemaradiographs. It is stated that his apparatus is now manufactured and sold, but the manufacturer is not identified.

There has also been some success in obtaining radiographic motion pictures directly on x-ray film by moving the film intermittently, as in optical cinematography. Such a process may be called "direct cinematography," "direct kineradiography," or "x-ray cinematography." Because of the brief time permitted for each exposure in motion-picture work, it is necessary to use quite intense x-rays. Such equipment has been constructed and used by van de Maele.<sup>2</sup> He reports that three different models were built, the last being the most practical. Each exposure or frame is 13 by 18 cm., and the entire apparatus is only 50 by 35 cm. In order to obtain sufficient exposure of the film in the brief time available, duplitized film pressed between fluorescent intensifying screens must be used. Between exposures, the screens must be separated so that the film can be moved up about 13 cm. for the next exposure, and then screens and film must be compressed again during the exposure. The apparatus is so constructed that the operator may observe what he is radiographing on a fluoroscopic screen. When the equipment is operated for the usual fraction of a minute, the patient is subjected to about one-fifth an erythema dose (see page 201) and some \$50 or \$60 worth of x-ray film is exposed. Thus, the equipment might be

<sup>1</sup> R. Reynolds, *Radiology*, **31**, 177 (1938).

<sup>2</sup> M. van de Maele, *Brit. J. Radiology*, **11**, 804 (1938).



useful as a means of advancing medical knowledge of heart action, etc., but it hardly could be used as a routine method of radiography. For a discussion of the uses of both indirect and direct cinemaradiography the reader may refer to an article by Barclay, Franklin, and Prichard.<sup>1</sup>

Reference has already been made (page 107 and Fig. 7-1) to the x-ray tubes developed for taking radiographs in 1 microsec. This method is ideal for "stopping" the motion of the heart, lungs, etc., and may very well find widespread use in hospitals and medical centers in the future. The main factor militating against this is the necessity for a large focal spot (1 cm. diameter, approximately) in this type of tube. This will make it impossible to obtain the fine definition or detail attainable by conventional methods (see Sec. 13-8).

The importance of good darkroom technique in securing good radiographs has already been emphasized in Chap. 9. It is also important to view the radiograph with a good illuminated translucent screen or viewer if its possibilities are to be realized to the fullest extent. Excellent illuminators are now offered by the x-ray equipment manufacturers using fluorescent lamps, thus achieving high brilliance without undue heating of the translucent glass. For very dense negatives, a high-intensity viewer (page 185) is needed. If a radiographic film must be viewed without an illuminator, it is best to stand in a comparatively dark room and hold the film up to a window so that it is silhouetted against a portion of the sky not near the sun. A cardboard frame should be used to intercept the light, which would otherwise pass by the edge of the film and tend to blind the observer.

The interpretation of medical radiographs should be entrusted to one who has had, not only thorough medical training, but also training and practice in this specialty under the guidance of a teacher who has learned to read medical radiographs through long experience.

**3. Therapeutic Radiology, or X-ray and Radium Therapy.** It did not require much time, after the discovery of x-rays in 1895 and the isolation of radium salts in 1898 by Mme. Curie, to learn that both x-rays and gamma rays have a destructive effect on living matter. The harmful effects of large doses of radiation upon the human body as a whole, as well as burns caused by localized heavy doses, have been described in Chap. 10.

One of the problems frequently encountered in medical work is the eliminating of abnormal and harmful growths from the body. The range from minor growths such as warts to the rampant major growth of cancer. There are two obvious possible procedures in eliminating :

<sup>1</sup> A. E. Barclay, K. J. Franklin, and M. M. L. Prichard, *Brit. J. Radiology*, **227** (1940); for industrial applications, see S. L. Fry, *Metal Ind.*, **67**, 2 and 25, July and 13, 1945.

abnormal growth—either to remove it surgically, or to destroy it in place. Surgical removal of certain types, for example uterine fibroid tumors, early skin cancers, etc., is quite practical and usually affords a permanent cure, but obviously it would be preferable to accomplish the cure by some more convenient and less hazardous method.

It is only natural, then, that medical men should attempt to destroy such growths by x-rays or gamma rays, for these will readily penetrate to any part of the body, and in sufficiently large doses they will kill any type of living matter. The possibilities of this line of attack were therefore investigated, and the encouraging fact was soon discovered that, in many cases, abnormal growths will succumb to a dose of x- or gamma radiation which can be tolerated by the surrounding healthy tissue, usually without fatal results and frequently without harmful results.

This encouraged the use of x-ray and radium therapy, especially in the case of tumors located deep in the body in or near some vital organ, where surgical removal is dangerous or impractical. It was found that in the case of "malignant" tumors (growths which tend to spread to other parts of the body), the chances of spreading could be reduced by combining surgery with radiation therapy. That is, irradiation of the tissues surrounding the site of the tumor makes it less likely that such growths will recur elsewhere after the tumor is removed surgically. In the case of advanced and incurable cancer, the pain and suffering can be partly relieved by radiation therapy.

It is obvious that the primary needs of a worker in therapeutic radiology are (1) a source of radiation and (2) a means of measuring the dose. It has already been explained in Chap. 9 that in therapeutic work the dosage is measured by an ionization chamber containing air because air has approximately the same mass absorption coefficient as the soft animal tissues and also because the biological effects of x-rays and gamma rays are caused directly by the ionization produced within the tissue by the photoelectrons, recoil electrons, and Auger electrons. If the radiation is so hard that most of it passes on through the tissue, the small fraction absorbed producing only slight ionization, then the dosage rate is less than when an equally intense beam of softer rays is used. For these reasons the roentgen has been chosen as appropriate for measuring dosage in therapeutic radiology. The definition of this unit was given and discussed in Chap. 9.

The so-called "x-ray survival curves" offer some concept of the destructive effects of these rays on living matter as the dose is varied. Such a curve is shown in Fig. 11-6. This type of curve is obtained by subjecting large numbers of *Drosophila* eggs to irradiation with x-rays ("Drosophila," as here used, is an abbreviation of the full technical name of the common fruit fly, *Drosophila melanogaster*). This fly is used

extensively by zoologists in breeding experiments to study the mechanism of heredity and by radiologists to study the biological effects of x-rays and gamma rays. To outline roughly the method of plotting the survival curve, one may imagine that a million fertile *Drosophila* eggs are spread on a piece of paper and irradiated with x-rays. A typical tube potential for such a test is 120 kv., with the rays filtered through  $\frac{1}{4}$  mm. of copper and 1 mm. of aluminum before striking the eggs.

A thimble chamber laid on the paper measures the dosage, there being no complicating back scatter because the paper is supported at its

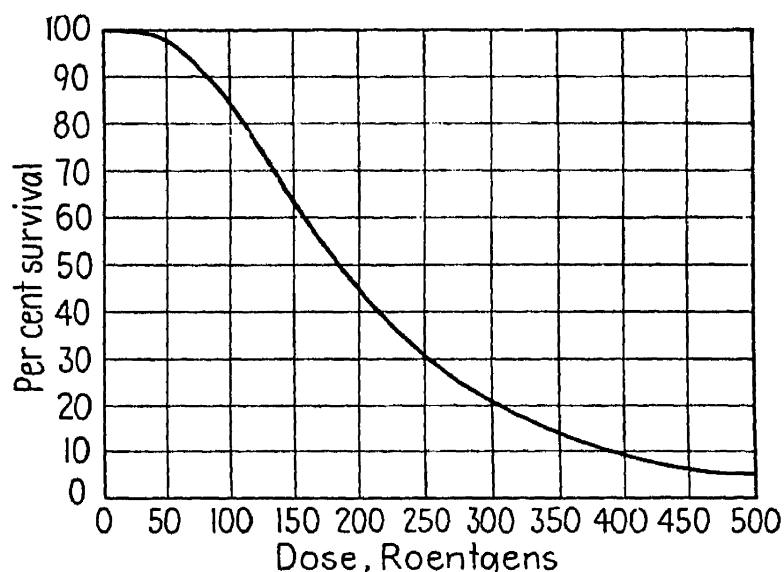


FIG. 11-6.--X-ray survival curve for eggs of the fruit fly *Drosophila melanogaster*. (After C. Packard, *Radiology*, **27**, 191 (1936), by permission.)

edges and the primary beam traverses several feet of empty air after it passes through the paper. After the dosimeter reads 1 r., 2,000 eggs are removed; after it reads 2 r., 2,000 more eggs are removed, etc., until after it reads 500 r. all the eggs have been removed. Then all the eggs are subjected to favorable hatching conditions. In the batch that received only a 1-r. dose, just as many will hatch as if no dose whatever had been given. In the batch that received 190 r., only half as many of the eggs hatch as if no dose had been given. From data of this type the curve is plotted.

Figure 11-7 shows a set of *Drosophila* survival curves obtained by Henshaw and Francis both for x-rays and for gamma rays. It is seen that the shape of the curves is the same for both types of radiation and that a change in the type of radium applicator used causes as much change in the results as a change from x-rays to gamma rays. In general, then, two x-ray beams (or an x-ray beam and a gamma-ray beam) having equal dosage rates at a point within the tissue have the same biologic effect at that point, irrespective of the wave length, so far as can be determined by means now available. Some organisms, like certain

bacteria, are very resistant to x-rays, some of them surviving doses of 70,000 r. Irradiation totaling a few hundred roentgens is sufficient to render certain spermatozoa incapable of fertilizing the ovum.<sup>1</sup>

There is a tendency for radiologists to refer to the dosage rate, in roentgens per minute, as the "intensity" of a beam of x-rays or gamma

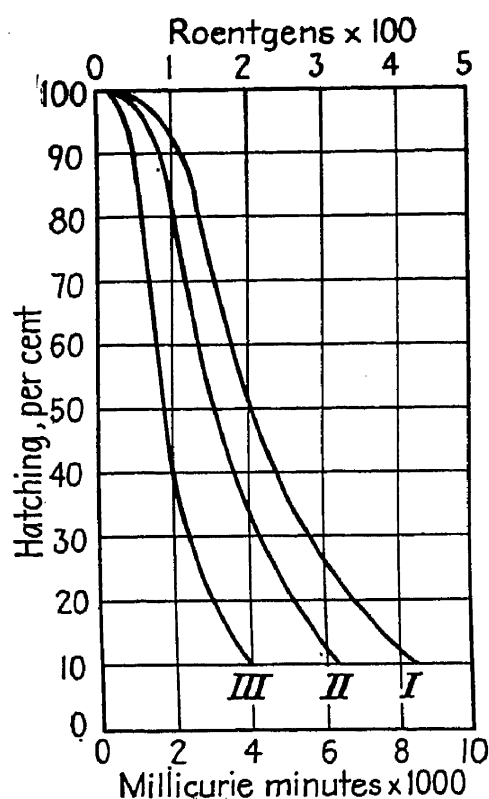


FIG. 11-7.—X-ray and gamma-ray survival curves for eggs of *Drosophila*. I, x-rays. II, radium (cylindrical applicator). III, radium (spherical applicator). (From S. P. Henshaw and D. S. Francis, *Radiology*, **27**, 569 (1936), by permission.)

rays. It must be remembered that this is not the intensity in the ordinary physical sense of ergs/cm.<sup>2</sup>/sec. but is only an arbitrary measure like a foot-candle or a decibel. If the tube potential, the tube distance, the filtration, and the subject (say a given area on the body of a certain patient) all remain the same, then the dosage rate is proportional to the intensity, which may be varied by altering the tube current. Otherwise, the two are not proportional.

The problem of accurately measuring the dosage actually administered to a selected point or points within the human body is quite complex. For a detailed discussion, the reader is referred to articles by Mayneord<sup>2</sup> and by Quimby.<sup>3</sup> One method of arriving at an estimate of the dose administered to a point at a given depth in the body is to experiment with a tank of water, since water has a density and mass absorption coefficient nearly the same as that of the soft animal tissues.

Figure 11-8, obtained by Mayneord, shows graphically how the dosage rate varies with the depth in the water along the axis of the beam sent perpendicularly into it, in the case of 200-kv. (constant-potential) x-rays filtered through 1.1 mm. of copper, the target being 50 cm. from the surface of the water. Mayneord states that the main features of these curves may be accounted for by use of the Klein-Nishina formulas (5-36) and (5-37). The "percentage depth dose" is the dose at a point at the depth indicated expressed as a percentage of the dose measured at the axis of the beam on the surface. The various curves are for various cross sections of the beam at the surface, the cross section in square centimeters

<sup>1</sup> See, for example, R. Rugh, *Proc. Am. Phil. Soc.*, **81**, 447 (1939); E. C. Amoroso and A. S. Parkes, *Nature*, **152**, 244 (1943).

<sup>2</sup> W. V. Mayneord, *Proc. Phys. Soc. (London)*, **54**, 405 (1942).

<sup>3</sup> E. H. Quimby, *J. Applied Phys.*, **13**, 678 (1942).

being indicated in the figure. The percentage depth dose depends chiefly on three factors, namely the hardness of the rays (the tube potential and filtration), the distance from target to water surface, and the area of cross

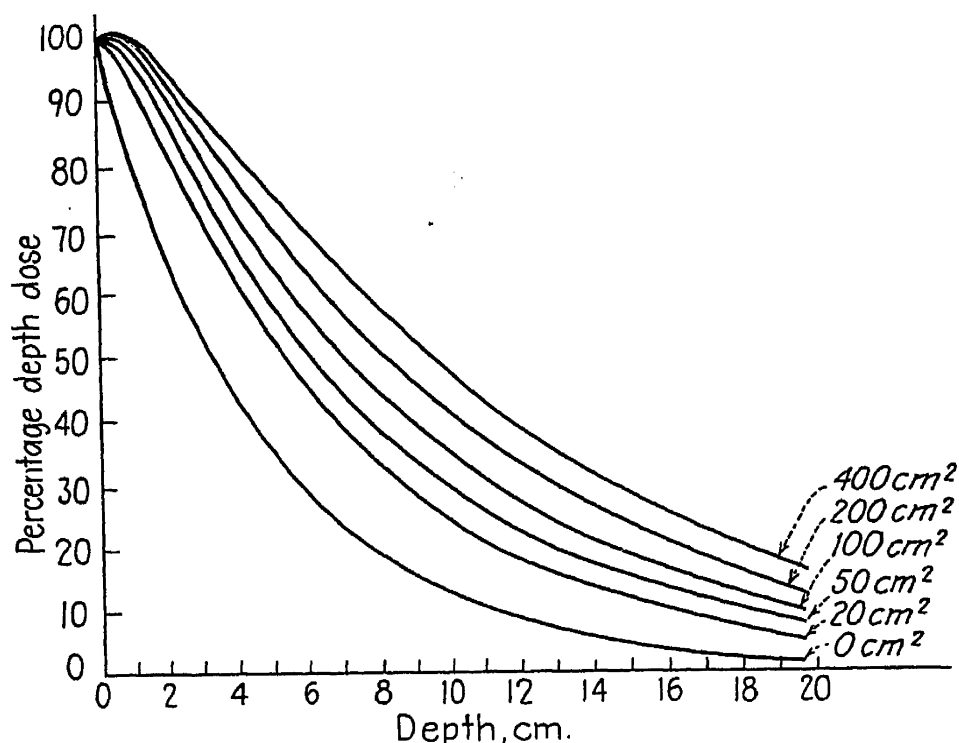


FIG. 11-8.—Dependence of dosage upon depth and area of the x-ray beam. (Courtesy of Prof. W. V. Mayneord and The Physical Society, London.)

section of the beam, which is the factor determining the volume of water from which scattered radiation is received by a point on the axis. The area of cross section is controlled by means of a "treatment cone" of the type illustrated in Fig. 11-9. The collar *C* intercepts the rays that would otherwise pass outside the cone, and it is usually lead-backed. The rest of the cone is usually made of steel. A square cross section is common, in which case the "cone" becomes a hollow pyramid.

Figure 11-10 shows the dosage administered at the points in any plane containing the axis *AB* of the beam, as determined by Mayneord. This particular graph was obtained with the target 50 cm. above the water, the tube operating at 200 kv. and the diameter of the circular beam at the surface of the water being 10 cm. The rays were filtered through 1.1 mm. of copper and 1 mm. of aluminum. The figures across the top of the diagram represent distances in centimeters from the beam axis, measured on the water surface. The depth in centimeters is indicated along the vertical axis. The curves are called "isodose curves" because they connect all the points in the plane where the dosage is the same. The cur

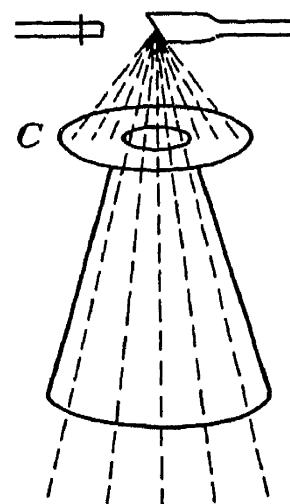


FIG. 11-9.—Treatment cone.

marked 30, for example, connects points for which the dose is 30 per cent of that on the beam axis at the surface, that is, for which the depth dose is 30 per cent.

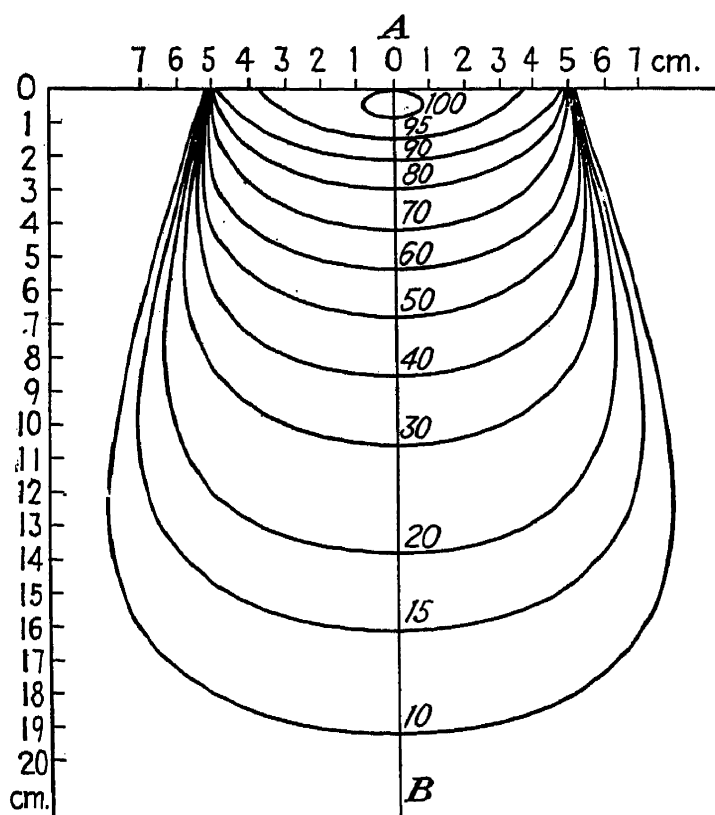


FIG. 11-10.—Isodose curves in water. (Courtesy of Prof. W. V. Mayneord and The Physical Society, London.)

A large number of graphs of this sort are required to represent the dosage at various points for various voltages, tube distances, filters, and beam sections. Nevertheless, to quote Mayneord,

Hundreds of these are plotted as transparencies so that they may be laid on cross sectional diagrams of the body and the dose administered at any point may be estimated for any conditions of irradiation or arrangement of converging beams which are proposed. Modern radiation therapy is increasingly dependent on such distribution diagrams.

The case of an inclined beam complicates matters further; and when two noncoplanar beams are used, depth-dose estimation is a complex problem.

The use of water for such dose surveys is being superseded to a certain extent in America by solid materials of specific gravity about 1. A popular material is one known in the building trade by the name "Pressd-wood." By its use a "phantom" can be built up from piled sheets of the material, of any size and shape desired, with the thimble chamber embedded at the point of interest. With such a phantom, measurements can

be made for any arrangement of any number of x-ray tubes at any voltage, beam section, and filtration desired.

Filters are nearly always inserted between the x-ray tube and the patient in deep therapy. In superficial therapy, for example in the treatment of warts, filters are often omitted because soft rays that will be absorbed by the skin and surface layers are desired. A typical treatment for warts, which effected a complete cure in many of the cases treated,<sup>1</sup> was accomplished with a total of 2.5 skin erythema dose of unfiltered 80-kv. radiation. Here, the erythema dose is regarded as 400 r., instead of the 525 r. mentioned in Chap. 10.

In deep therapy, filters are used to absorb most of the soft rays that would otherwise be absorbed mostly by the skin and surface layers of tissue of the patient, the idea being to transmit only the harder rays needed to penetrate to the point to be treated, deep in the body. The filter material used should have an atomic number high enough truly to absorb (not scatter) the softer components of the beam only. If the atomic number is too high, the desired hard rays are unduly weakened and an undesired secondary characteristic radiation of considerable intensity will be generated in the filter. Failla<sup>2</sup> states that "in practice, it has been found that aluminum is a satisfactory filter for x-rays produced at voltages up to 100 kv.p. Copper is ordinarily used for voltages in the neighborhood of 200 kv.p." To eliminate the copper characteristic secondary radiation, a sheet of aluminum is added to the filter on the side next the patient. The aluminum characteristic radiation is so soft that it is absorbed by a few inches of air. A composite filter of this sort must always be used with the denser material next to the tube. In figuring the filtration used, one should not neglect the inherent filtration of the x-ray tube itself, especially if it is an oil-immersed shockproof tube with thick windows or if it is a thin target tube so placed that the x-rays must penetrate the target to escape (for example, the General Electric million-volt tube).

Failla says that a filter of 0.5 mm. of copper and 0.5 mm. of aluminum is satisfactory for 200-kv. radiotherapy, although filters of 2 or 2.5 mm. of copper or equivalent composite filters are also used. He states that, in radium therapy, 2 mm. of brass, 1 mm. of lead, or 0.5 mm. of gold or platinum is needed to stop all the primary beta rays and that it is not advisable to push the filtration much beyond this point for this reduce the soft gamma-ray components effectively. The secondary beta ray (see page 76) emitted by the filter are sometimes absorbed in an organic (for example, Bakelite) filter several millimeters thick.

<sup>1</sup> W. C. Popp and J. W. Olds, *Radiology*, **31**, 218 (1938).

<sup>2</sup> G. Failla, "Biological Effects of Radiation," edited by B. M. Duggar, Chap. III, p. 104, McGraw-Hill Book Company, Inc., New York, 1936.

The filtration of x-ray beams in x-ray therapy above 200 kv. is discussed by Hayden, Corrigan, and Cassen.<sup>1</sup> They conclude that at these supervoltages (500 kv. and up) a filter adds a significantly large component of hard scattered radiation to the beam. The quality of the filtered beam depends upon the thickness of the filter, which may degrade it rather than improve it. They discovered that the quality of the filtered beam reaching the patient varies considerably with the position of the filter (near the tube or near the patient) and that improper choice of position and thickness may greatly reduce the depth dose. For the filtration of a parallel beam, they state that lead is more efficient than a larger thickness of lighter material of equivalent true absorption. Dresser<sup>2</sup> reports the routine use of  $3\frac{1}{2}$  mm. of lead plus 8 mm. of copper filtration for million-volt therapy.

The trend in deep therapy over a period of years has been toward higher and higher x-ray tube voltages, in order to increase the percentage depth dose. Million-volt therapy is no longer uncommon. For photographs and description of the treatment room and high-voltage room for 1,200,000-volt cancer therapy, the reader is referred to an article in *Nature*.<sup>3</sup> At these high voltages the depth dose becomes much less dependent upon the area of cross section of the beam or the size of the portal of entry. For example, with 200-kv. rays from a tube 70 cm. from the surface, using a  $\frac{1}{2}$ -mm. copper filter, the percentage depth doses at 10 cm. with 100-, 225-, and 400-cm.<sup>2</sup> portals of entry are 34, 42, and 45.5 per cent, respectively, whereas with 1,000-kv. rays at the same distance, with 3.5 mm. of lead and 8 mm. of copper filtration, the percentage depth doses at 10 cm. with these three portal areas are 49, 50.5, and 53 per cent, respectively, according to Dresser. Experiments with the 20-million-volt betatron, using a phantom, indicate that at a depth of  $2\frac{1}{2}$  in. a percentage depth dose considerably exceeding 100 per cent is attainable.<sup>4</sup> As an indication of the dosage rate administered at these high voltages, Trump and Cloud<sup>5</sup> determined that it is about 45 r./min. at the skin when a tube 70 cm. away is operated at 1,200 kv.,  $\frac{1}{2}$  ma., using a 10- by 10-cm. field and a filter of 2 mm. of lead + 5 mm. of copper + 2 mm. of aluminum. A comparison between such supervoltage x-rays and gamma rays from radium was made in Chap. 8. Two-million-volt x-rays approximate the quality of such gamma rays more closely than 1-million-volt rays.

Because of the small amount of radium available in the first two or

<sup>1</sup> H. S. Hayden, K. E. Corrigan, and B. Cassen, *Radiology*, **31**, 312, 319 (1938).

<sup>2</sup> R. Dresser, *J. Applied Phys.*, **12**, 331 (1941).

<sup>3</sup> *Nature*, **138**, 1106 (1936).

<sup>4</sup> A. R. Wildhagen, *Sci. American*, **168**, 207 (May, 1943).

<sup>5</sup> J. G. Trump and R. W. Cloud, *Am. J. Roentgenology Radium Therapy*, **44**, 615 (1940).



three decades after its discovery, its use was limited to local applications in capsules containing a small fraction of a gram. As time went on, the amount of radium in use gradually increased, most of it being refined from ores obtained in the Belgian Congo. As a result of the discovery in 1930 of pitchblende in Canada and the reduced price, some 120 g. of radium is now used (throughout the world) for "radium-beam therapy," known in Europe as "telecurietherapy" or "Radiumfernbestrahlung." The Canadian mines alone have an output of about 100 g. of radium per year.

Since the gamma rays from radium radiate in all directions and are extremely hard, yet not very intense, the problem of producing an intense beam of gamma rays is rather difficult. To restrict the radiation to one direction, the radium is enclosed in a cylindrical container open at one end only. In order to obtain reasonable intensity for therapeutic work at a distance of, say, 6 in., from 2 to 10 g. of radium is required. To restrict the gamma rays from this much radium to a tolerable intensity in directions other than that of the beam, the enclosing cylinder must have thick, dense walls. Such a cylinder for radium-beam therapy is usually called a "radium bomb." These bombs are usually made of lead (density 11.35 g./cm.<sup>3</sup>) and weigh 50 to 100 lb. In 1937 a tungsten-copper-nickel alloy having a density of about 16.4 g./cm.<sup>3</sup> was developed<sup>1</sup> that permits a reduction in the weight of the bomb.

With such a radium bomb 75 cm. from the surface of the water in a tank, a depth dose of 58 per cent at 10 cm. below the surface is achieved, a  $\frac{1}{2}$ -mm. platinum filter being used. However, even with several grams of radium, the intensity is so low that the usual practice is to use the radium only 5 to 10 cm. from the patient, according to Eve and Grimmett.<sup>2</sup> This reduces the percentage depth dose at a depth of 10 cm. in water to a value only about one-third that achieved by a 200-kv. x-ray tube at a distance of 75 cm., with a  $\frac{1}{2}$ -mm. copper filter. Taking the figure given by Taylor and Singer (see Chap. 9, page 191: 8.16 r./hr./mg. of radium at 1 cm.), it may be calculated that the skin dosage rate from 1 g. of radium at a distance of 10 cm. is only 1.36 r./min. Thus it is clear that the usual treatments for cancer, totaling hundreds or thousands of roentgens, consume much time by this method.

Radiologists sometimes use the concept of a "half-value layer" (HVL) as an indication of the hardness of the radiation being considered. Dresser gives  $10\frac{1}{2}$  mm. of copper or 4 mm. of lead as the HVL of million-volt x-rays after filtering through  $3\frac{1}{2}$  mm. of lead plus 8 mm. of copper. This means that a layer of copper  $10\frac{1}{2}$  mm. thick placed between the filter and a dosimeter will reduce the dosage rate indication by 50 per cent. The HVL found by Mayneord for the 200-kv. c.p.d.c. x-rays

<sup>1</sup> C. J. Smithells, *Nature*, **139**, 490 (1937).

<sup>2</sup> A. S. Eve and L. G. Grimmett, *Nature*, **139**, 52 (1937).

used for Figs. 11-7 and 11-9 was 1.5 mm. of copper. The gamma rays from radium have an HVL of about  $1\frac{1}{2}$  cm. of lead.

The local application of radium in capsules, tubes, needles, etc., in the treatment of cancer has been practiced since the beginning of the present century. This type of therapy is particularly adapted for intense localized radiation of a small area or region. Surface applications of radium in small amounts are used for skin lesions. For treatment of the body cavities, radium tubes are placed within them for intense local irradiation. This is called "intracavitary" application. The principle of local irradiation near the center of the neoplastic area is carried one step further in "interstitial" irradiation. In this case, radium salt in metal needles or radon in small metal containers called "seeds" are implanted in and around the tumor-bearing region. The use of radon seeds reduces the chances of losing radium, permits greater flexibility in size and shape of applicators, and its short half life minimizes the danger in case an applicator is lodged accidentally in the patient's body.

The present trend is to combine the localized radium treatments with more generalized irradiation by x-ray (or sometimes radium-beam) therapy. Lacassagne<sup>1</sup> summarizes the results of x-ray and radium therapy in cancers of the cervix at the Institute of Radium in Paris from 1919 to 1932. These were treated by means of tubes 22 by 3.15 mm. incorporating a 1-mm. platinum filter and tubes 22 by 4.15 mm. incorporating a 1.5-mm. platinum filter. The tubes contained about 22 mg. of radium. Three such tubes were usually placed in an applicator, which was inserted in the uterine cavity, making a total of about 67 mg. in the applicator. This application continues for 5 days (120 hr.), the treatment thus figuring about 8,000 mg.-hr. About 1924, the practice of combining this intracavitary radium therapy with x-ray therapy (and sometimes radium-beam therapy) was begun. Of the 79 cases treated, 59 (74 per cent) were cured completely. Generally speaking, cancer can usually be cured if treatment is administered by qualified experts while the disease is in its early stages.

To convey some idea of the dosage schedules commonly followed in x-ray therapeutic treatment for cancer, it may be stated that the total dose administered (as measured at the skin) usually totals several thousand roentgens, say 6,000 r. as a rough general figure, although values as low as 1,800 r. or as high as 10,000 r. are not rare. These total dosages are usually built up by a series of 5 to 30 treatments administered daily or perhaps four, five, or six times per week, in doses of around 200 to 700 r. Coutard<sup>2</sup> suggests the following schedules: (1) Cancer slightly

<sup>1</sup> A. Lacassagne, *Radiology*, **33**, 20 (1939).

<sup>2</sup> H. Coutard, *J. Applied Phys.*, **12**, 329 (1941).

differentiated—two series of 6 days separated by 14 days without treatment; daily doses 500 to 700 r.; doses of the series 3,000 to 3,500 r.; total doses 6,000 to 7,000 r.; duration 26 days. (2) Cancer moderately differentiated—three series of 3 days separated by 7 and 10 days without treatment; daily doses 800 r.; doses of the series 2,400 r.; total dose 7,200 r.; duration 26 days. (3) Cancer very differentiated—four series of 2 days separated by 9, 11, and 11 days without treatment; daily doses 800 to 1,000 r.; doses of the series 1,800 to 2,000 r.; total dose 7,600 to 8,000 r.; duration 39 days.

The “irradiation sickness” mentioned in Chap. 10 is often a problem in these treatments when some portion of the intestinal tract or parotid gland is irradiated. According to Martin and Moursund,<sup>1</sup> this may be forestalled or alleviated by a high carbohydrate diet and administration of 2,000 international units of vitamin B<sub>1</sub> daily.

It was recently reported by G. Failla that the effectiveness of x-ray therapy could be appreciably increased by injecting sterile water into the tumor immediately following irradiation.

Cancers are broadly classified as of two general types, carcinoma and sarcoma. Carcinoma is a malignant growth originating in epithelial tissue (skin, lining of body organs, etc.). Sarcoma is a malignant growth derived from nonepithelial tissue of mesodermal embryonic origin (muscles, bone, etc.).

Cancers have the same type of survival curve as in Fig. 11-6 for *Drosophila*. Figure 11-11 is a survival curve obtained by Wood<sup>2</sup> for a rat carcinoma known as *FRC*. Such a curve is obtained by cutting the tumor from the animal, cutting it in small pieces, and then irradiating these. At equal intervals of time, pieces are removed from the group being rayed. Finally, all the pieces are grafted on other animals. The percentage of grafts that “grow” depends upon the irradiation time, as indicated by the figure.

Some idea of the success obtained in x-ray therapeutic treatment of diseases other than cancer is conveyed by a summary of the results in the treatment of 5,438 patients with skin diseases by Thoroczkay.<sup>3</sup> With eczema, 34 per cent of the cases were cured; with neurodermite, 30 per cent; with dysidrosis, 32 per cent; with acne vulgaris, 25 per cent.

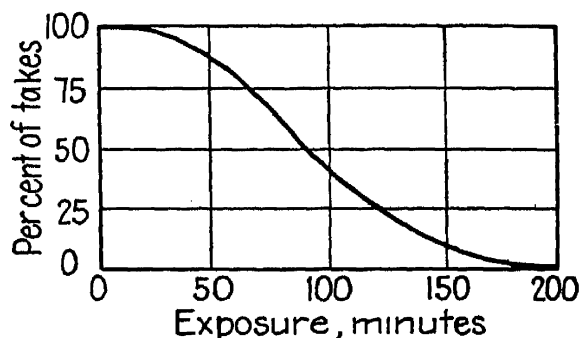


FIG. 11-11.—X-ray survival curve for *FRC* carcinoma in rats. (After Wood.)

<sup>1</sup> C. L. Martin and W. H. Moursund, *Radiology*, **30**, 277 (1930).

<sup>2</sup> F. C. Wood, *Radiology*, **5**, 199 (1925).

<sup>3</sup> N. v. Thoroczkay, *Radiology*, **26**, 381 (1936).

Plantar warts treated by Popp and Olds<sup>1</sup> were cured in 63 per cent of the cases.

About 10 years ago, therapy by means of radioactive material was given new impetus by the advent of the cyclotron (see Sec. 7-19) and the discovery that it could be used<sup>2</sup> to produce artificially unstable radioactive isotopes of most of the elements. Among these is the isotope of phosphorus having a mass number of 32 (see Chap. 8). It radiates ordinary negative electrons (beta-rays) when it disintegrates, but no gamma rays. The energy of the beta particles is 1.69 million electron volts. Its half life is 14.3 days.

Lawrence, Scott, Erf, and Tuttle<sup>3</sup> have found that phosphorus fed to human beings (in the form of compounds) tends to concentrate in the bone marrow; when fed to mice, it also concentrates in<sup>4</sup> the leukemic tissues. Because of its short radioactive half life, a radioactive phosphorus ( $P^{32}$ ) compound can be fed to a patient and will produce beta-ray ionization in the leukemic tissues for a few days and then gradually quit. Although such treatment has thus far failed to cure cases of acute lymphatic leukemia, such a plan of attack may be found useful in other ways by further research.<sup>5</sup>

The advent of the cyclotron has also permitted experiments on cases of human cancer with neutron therapy. Eight-million-volt deuterons and later 16-million-volt deuterons were directed against a beryllium target to produce the neutrons (see page 165). Some 50 or more cancer patients too advanced for successful treatment with x-rays or other known methods were treated. Preliminary results indicate that neutrons are perhaps as effective as x-rays in cancer therapy, but no marked superiority is apparent at this date.<sup>6</sup>

The possibilities of cathode-ray therapy now loom impressively on the scientific horizon. The foregoing discussion of x-ray and radium therapy brings out two points. (1) It is the *ionization* produced in the diseased tissue by the photoelectrons, recoil electrons, and Auger electrons that arrests its growth, directly or indirectly. (2) The x-rays

<sup>1</sup> W. C. Popp and J. W. Olds, *Radiology*, **31**, 218 (1938).

<sup>2</sup> J. D. Cockroft and E. T. S. Walton, *Proc. Roy. Soc. (London) A*, **137**, 229 (1932). For papers on the discovery of artificial radioactivity, see also Irène Curie and F. Joliot, *Compt. rend.*, **196**, 1885 (1933), **198**, 254, 559 (1934); *J. phys.*, **4**, 494 (1933), **5**, 153 (1934); J. D. Cockroft, C. W. Gilbert, and E. T. S. Walton, *Nature*, **133**, 328 (1934).

<sup>3</sup> J. H. Lawrence, K. G. Scott, and L. W. Tuttle, "New International Clinics," pp. 33ff, J. B. Lippincott Company, 1939.

<sup>4</sup> J. H. Lawrence, L. A. Erf, and L. W. Tuttle, *J. Applied Phys.*, **12**, 333 (1941).

<sup>5</sup> R. D. Evans and J. G. Hamilton, *J. Applied Phys.*, **12**, 260, 440 (1941); F. G. Spear, *J. Sci. Instruments*, **22**, 21 (1945).

<sup>6</sup> R. S. Stone and J. C. Larkin, *J. Applied Phys.*, **12**, 332 (1941); *Radiology*, **39**, 608 (1942).

that produce these high-energy electrons produce them not only in the diseased tissue, as desired, but also in the healthy tissue they encounter before and after they pass through the diseased tissue, thus injuring healthy tissue.

Trump, Van de Graaff, and Cloud<sup>1</sup> have projected the cathode rays from a Van de Graaff generator through a thin window into the open air, as described in Sec. 7-5, except that they used  $1\frac{1}{4}$  million volts. They projected the cathode rays into wood, lead, copper, aluminum, and water and measured the "dose" at various depths. The results indicated that such rays would produce considerably heavier ionization below the skin than in it, owing to the fact that high-speed electrons produce much greater ionization near the end of their path just before they stop than they do in the early part of their journey when their energy is much greater.

Kerst<sup>2</sup> has generated 20-million-volt cathode rays (and x-rays) with his betatron and points out that such cathode rays will pass halfway through the human body. This should make it possible to subject a deep-seated tumor to intense ionization while the overlying tissue will experience less irradiation (rather than more, as with x-rays) than the tumor. In addition, the tissue beyond or underneath the tumor will not be injured, as it is with x-rays, which cannot be made to stop at the tumor, like the cathode rays. A 100-million-volt betatron is now in operation.<sup>3</sup>

If supervoltage cathode rays are to be used in deep therapy, the x-rays generated at the window where they emerge from the betatron can be held to a minimum by making the window out of some light material like aluminum or beryllium and keeping it as thin as practical. If the window is regarded as an x-ray tube target, it will be seen from Figs. 3-7 and 3-8 that the x-rays radiated in the direction of travel of the cathode rays are of low intensity for very thin targets, although the intensity is high at angles of 20 or 30° to the electron beam. It is also an advantage that the x-rays radiate in all directions, while the high-energy cathode rays maintain a parallel beam. The high x-ray generating efficiency of 65 per cent that Kerst obtains with a tungsten target at 20 million volts can be reduced to 3 or 4 per cent by using a beryllium window, according to Beatty's equation (2-5). The most troublesome factor probably would be the secondary electrons knocked out of the window, but these would have a lower relative intensity at 20 million volts than at 200 kv., for example, and they might be kept from striking

<sup>1</sup> J. C. Trump, R. J. Van de Graaff and R. W. Cloud, *Am. J. Roentgenology Radium Therapy*, **43**, 728 (1940).

<sup>2</sup> D. W. Kerst, *Am. J. Phys.*, **10**, 219 (1942).

<sup>3</sup> *Science News Letter*, **43**, 200 (1943); *Gen. Elec. Rev.*, **46**, 58 (1943).

the patient by means of a local magnetic field perpendicular to the beam. This would deflect the primaries only slightly but would so deflect the slower secondaries that they would not reach the patient.

### QUESTIONS AND PROBLEMS

1. Distinguish between diagnostic and therapeutic radiology. Between superficial and deep therapy. Suggest a technique (focal-spot size, tube-to-film distance, tube voltage and current, time, type of film and screens) suitable for radiography of the chest. What kind of filter is ordinarily used?

2. Compute the maximum distortion in an 8- by 10-in. radiograph of the thigh if it is 6 in. thick, the tube-to-film distance being 36 in. *Ans.*  $\frac{5}{6}$  in.

3. Compute the blurring in the above problem if the focal spot is 2 mm. square. *Ans.*  $\frac{1}{2}$  in.

4. What is the purpose of the Potter-Bucky grid? How does it operate? When is it used? Why is it not always used?

5. Fluoroscopy is used chiefly for what types of medical work? Name a commonly used diagnostic opaque. How does one proceed in taking stereoscopic radiographs?

6. Distinguish between a planigraph and a kymograph. What is the chief advantage of indirect radiography? Suggest a method of obtaining a truly instantaneous radiograph of a moving object like the heart. Have x-ray motion pictures ever been obtained?

7. Have x-ray and radium therapy supplanted surgery in the treatment of cancer? Draw a rough graph showing the general shape of the x-ray survival curve for *Drosophila*. What does the curve mean? Is the curve essentially different for gamma rays? Are there some microorganisms that are considerably more radio-resistant than *Drosophila*?

8. Define percentage depth dose. Upon what three factors does it depend? What are isodose curves, and for what are they used? What is a phantom? Define skin erythema dose. Which side of a composite filter goes next to the tube? What is the purpose of a treatment cone?

9. What is telecurietherapy? In practice, does it yield a higher percentage depth dose than, say, 200-kv. x-ray therapy? Does the HVL as a criterion of hardness indicate much difference between x-rays and gamma rays? What is intracavitary radium therapy? Is it still generally practiced, or is it out of date? It is commonly supplemented by what other type of treatment?

10. Does x-ray or radium therapy ever really cure cancer? Does the treatment usually require a day, a week, or a month, and roughly what dosage is administered, in roentgens, over how large an area of the body? What other diseases besides cancer sometimes respond to x-ray therapy?

11. One might expect radioactive phosphorus treatments to afford some relief for what type of affliction? Why does cathode-ray therapy appear to be a promising field for research?

## CHAPTER 12

### INDUSTRIAL RADIOGRAPHY

**1. Developmental Radiography on a Moderate Scale.** The advantages of radiography as a means of inspecting the internal structure of every sort of object are self-evident. Any kind of localized flaw such as a cavity, inclusion, or crack that has a minimum dimension of the order of 1 per cent of the thickness of the object can be detected, unless the object is inaccessible or too thick for the rays to penetrate effectively. The outstanding features of radiographic inspection are the facts that it is nondestructive, that it reveals flaws hidden deeply in the interior, and that its indications are permanently recorded on x-ray film for future reference. The chief factor restraining the almost universal application of radiography to all sorts of inspection processes is its high cost.

Radiography cannot be recommended as a universal method that may be profitably employed in inspecting every kind of object. It is best suited for inspecting the first units of a new product, such as the first castings made of a new type or the first welds made by a new method or by a new welding operator. It is also useful in production-line inspection of objects where the failure of even one in a thousand would be disastrous.

The selection of the best radiographic equipment for the type of work that is to be undertaken must be a compromise between such factors as cost, capacity, flexibility, durability, and mobility. Let us assume that no routine radiography is contemplated on articles or parts in production, but rather that a wide variety of parts and articles are to be examined in order to find the best way of making a certain casting; the best method of making a particular weld; whether a few special parts are safe when their failure would be disastrous; etc. This may be called "developmental radiography" in order to distinguish it from production radiography, where hundreds or thousands of identical objects are to be radiographed. In the former, an endless variety of material to be radiographed may be expected. There may be parts made of metal, ceramics, plastics, rubber, or wood, weighing from a fraction of an ounce to a ton or more, with sections from  $\frac{1}{16}$  in. to several inches; welds of various types, castings, forgings, and complex assemblies. The average volume of work may be such that one man can ordinarily handle the entire operation including all the darkroom work, with extra help neces-

sary only at occasional rush periods. It will be assumed that the work can always be brought to the x-ray shop and that it will not be necessary to radiograph any large object such as a railroad bridge or hydroelectric penstock that cannot be moved.

For demands of this sort, probably a fixed 220- or 250-kv. x-ray installation in a lead-lined room, supplemented by about 200 mg. of radium, will be found sufficient. To be specific, we may assume that the equipment installed has a continuous rating of 10 ma. at 220 kv.p. and an effective or projected focal spot (see page 18) 5 mm. square. Presumably a suitable darkroom has been provided near by. A typical "fixed x-ray installation" is illustrated in Fig. 7-28. The tube support should be rigid; tube vibration blurs the radiograph.

Three types of film are in stock—an industrial screen film, an industrial nonscreen film of the high-speed wide-latitude ordinary-grain-size type, and an industrial nonscreen film of the fine-grained-size high-contrast (and consequently slow-speed) type, all three in two sizes, 8 by 10 and 14 by 17 in. Cassettes in both these sizes have been provided, some lined with lead foil and some provided with a pair of fluorescent intensifying screens. For some kinds of work, rigid, flat metal cassettes of the medical type are preferable. Flexible film holders with lead screens or fluorescent intensifying screens are available from St. John X-ray Service, Inc., Long Island City, N.Y. It will be supposed that there are also on hand numerous cardboard film holders of both sizes (8 by 10 and 14 by 17), lead-backed, such as those made by Eastman Kodak Co., Rochester, N.Y. A sizable box full of wood blocks of various shapes and sizes should also be provided. These blocks, timbers, wedges, and shims will be found indispensable in blocking up cassettes, castings, and other objects of all sizes and shapes in positions suitable for radiography.

**2. Technique Charts.** Everything being ready, the first job is brought in. A rolled-steel plate 1 by 4 by 10 in. has been electrically butt-welded to another along the 10-in. edge, and it is desired to know whether the technique used produces a weld of good quality.

This being the first job with new equipment, the operator may profitably consult the "technique charts," which the manufacturer ordinarily supplies with industrial radiographic equipment. Figures 12-1 and 12-2 are examples of such charts. They indicate the proper voltage to use on the tube with a given target-to-film distance, a given tube current and exposure time, and a given thickness of a certain kind of metal. If it is preferable to select the tube voltage and tube current, the chart will suggest the correct exposure time. Figure 12-1 is for a 36-in. target-to-film distance, for rolled steel, and for nonscreen film sandwiched between lead foil, and of course it is for a certain x-ray



apparatus. The chart for c.p.d.c. equipment would be different from that for half-wave equipment, for example. Figure 12-2 is like Fig. 12-1 except that it is for screen film sandwiched between fluorescent intensify-

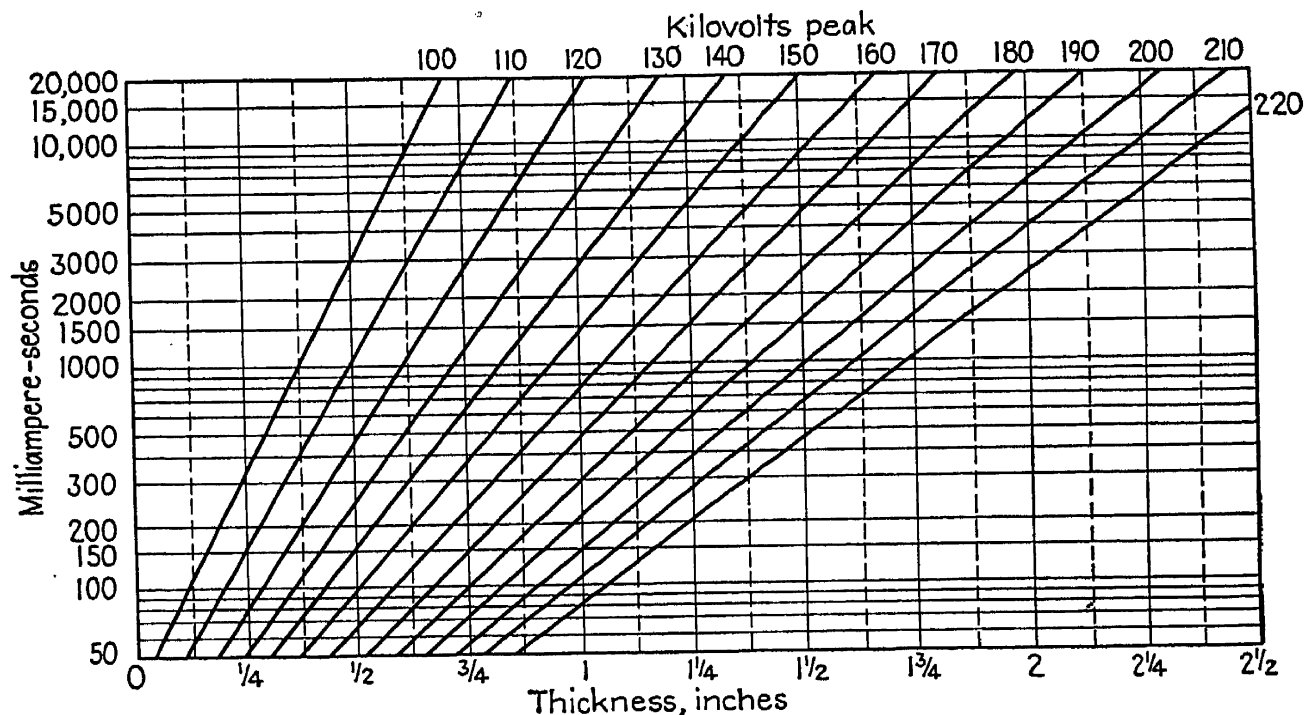


FIG. 12-1.—Technique chart for 220-kv. x-ray unit for radiography of steel plate, using industrial nonscreen film with 0.005 and 0.010 in. lead screens, 36 in. from tube target.

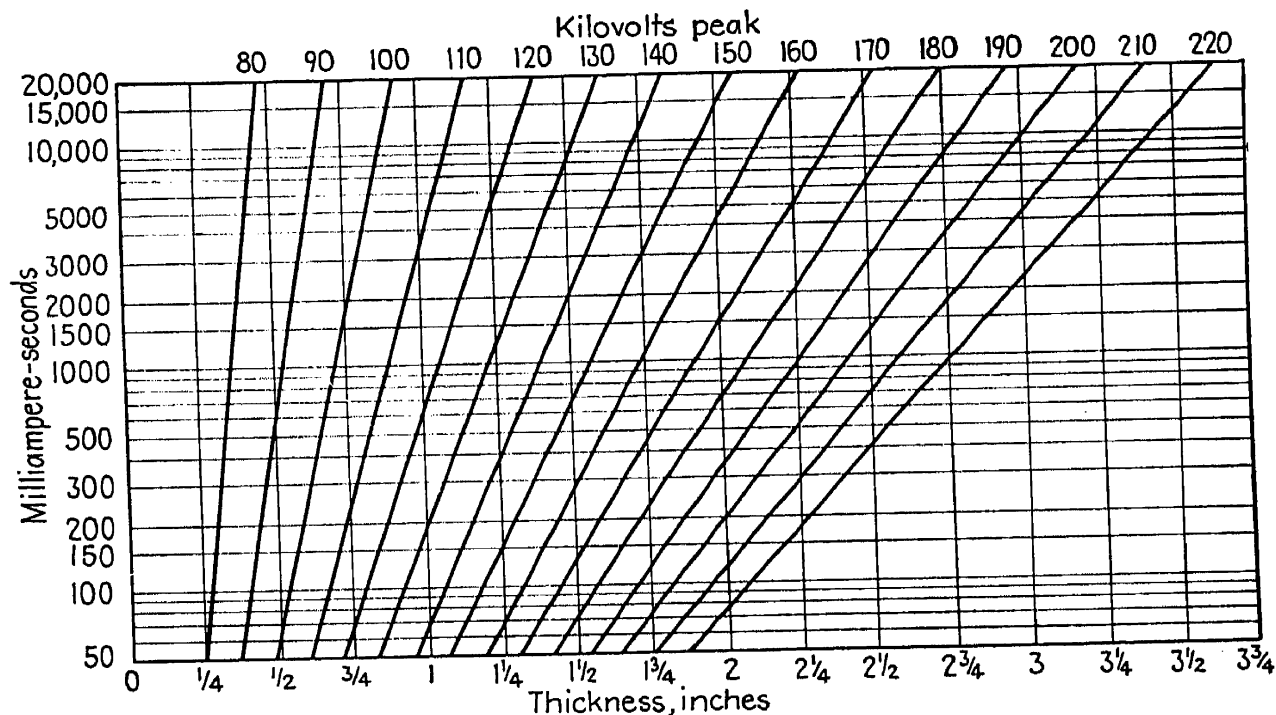


FIG. 12-2.—Technique chart for 220-kv. x-ray unit for radiography of steel plate, using industrial screen film with fluorescent intensifying screens, 36 in. from tube target.

ing screens. Figure 12-3 is a chart similar to Fig. 12-1, plotted for the General Electric million-volt equipment. This is not intended to be operated at reduced voltages such as 600 kv., for example, although it

tube current can be varied from zero to 3 ma. Consequently, the curves in Fig. 12-3 are for various target-to-film distances at 1 million volts, rather than for various voltages at a fixed distance.

It will be seen that these charts are a series of straight lines plotted on semilogarithmic graph paper, the ordinates representing milliampere-seconds on a logarithmic scale and the abscissas representing the thick-

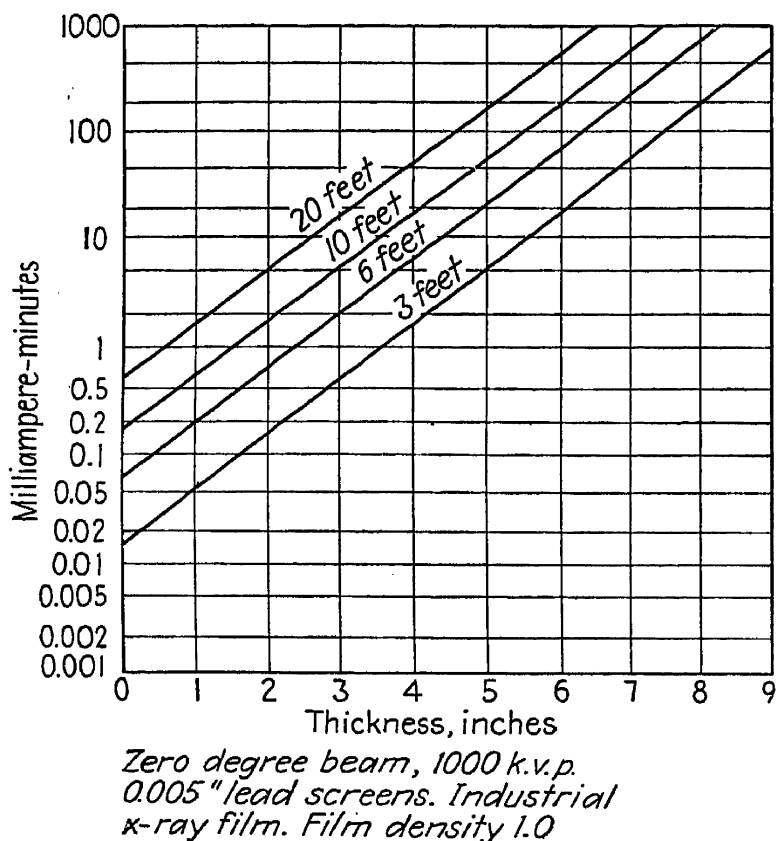


FIG. 12-3.—Technique chart for General Electric million-volt unit. (After Charlton and Westendorp.)

ness of the steel on a linear scale. This may be understood from equation (5-4), which may be written in the form

$$\log I_0 = \mu_l x + \log I \quad (12-1)$$

If  $t$  is the time of the exposure, one may add  $\log t$  to both sides of the equation, obtaining

$$\log I_0 + \log t = \mu_l x + \log I + \log t \quad (12-2)$$

or

$$\log I_0 t = \mu_l x + \log It \quad (12-3)$$

Since  $I_0$  is the intensity of the rays striking the steel plate and  $I$  is the intensity of those emerging to expose the film, it is clear that for a given type of film to be exposed to a given desired photographic density (Sec. 9-2),  $It$  will be a constant. Hence (12-3) becomes

$$\log I_0 t = \mu_l x + C \quad (12-4)$$

which is of the form

$$y = mx + b \quad (12-5)$$

the equation for a straight line, when  $\log I_0 t$  is plotted as ordinate and  $x$  is plotted as abscissa. For a given tube voltage and distance,  $I_0$  is proportional to the tube current, and so it is seen that the logarithm of the milliamperes-seconds plotted against the plate thickness should yield a straight line for a given tube voltage and distance. Since the slope of the curve is proportional to the linear absorption coefficient  $\mu$ , it follows that the curves should become steeper and steeper as the tube voltage is reduced. The intercept  $b = C = \log It$  of the curves on the vertical axis obviously represents the milliamperes-seconds that would be required to expose the film to the desired density with no specimen whatever present.

This intercept will therefore be greater for nonscreen film sandwiched between lead foil than for screen film sandwiched between fluorescent intensifying screens. These conclusions explain all the characteristics of the typical technique charts shown in Figs. 12-1 and 12-2 and also account for the differences between the two.

The charts in Figs. 12-1 and 12-2 have been plotted for a target-to-film distance  $d$  of 36 in. Upon calculating the distortion on this basis for the 10 by 8 by 1 welded plate, with equation (11-1), it is found that

$$\frac{h}{2d} = \frac{10 \times 1}{72} = \frac{1}{7} \text{ in. approximately, which is acceptable. The blurring [equation (11-2)] } \frac{st}{d} \text{ is } \frac{1}{5 \times 36}, \text{ or about 0.006 in., which only slightly}$$

exceeds the grain size of most x-ray film, although some of the fine-grained films are considerably finer than this (see page 175). If such a fine-grained film were to be used, the tube distance  $d$  should be increased in order to realize the benefit of the fine grain.

The next step is to decide upon some convenient exposure time, say 1 min. If the equipment is operated at its rated tube current of 10 ma., this will yield a product of 600 ma.-sec. Referring to Fig. 12-1, one sees that, for a thickness of 1 in. and an "exposure" of 600 ma.-sec., about 165 kv. should be used with nonscreen technique. If the weld has been built up so that a welt, or reinforcing bead,  $R$  (Fig. 12-8) extends  $\frac{1}{16}$  in. above the surface on both faces, the weld thickness is  $1\frac{1}{8}$  in. rather than 1 in. For this thickness, the chart suggests 175 kv.

It would be permissible to reduce the tube-to-film distance below 36 in. since this could be done without exceeding usual tolerances for distortion and blurring; but there would be no point in doing so, for the exposure time is already conveniently short and the voltage required is well below the maximum available. It would also be permissible to increase the tube-to-film distance from 36 to 72 in., for example, but there would be no

point in doing so unless extremely fine detail is demanded. Such fine detail could be seen only by examining the film with a magnifying glass, and with film of ordinary grain size the graininess makes magnification profitless. If such magnification is demanded, a fine-grained film should be used, it being remembered that such films are slower and hence require a longer exposure under the same conditions. If it should be decided to use a 72-in. distance, this has the effect of reducing the milliamperere-seconds from 600 to 150 because of the inverse-square law. Hence, if the exposure time is to remain 1 min., Fig. 12-1 indicates that 215 kv. should be used for the  $1\frac{1}{8}$ -in. weld with film of ordinary speed. If fine-grained (and hence slower) film is used, a longer exposure time will be required.

It may be asked why Fig. 12-1 was used rather than Fig. 12-2, that is, why nonscreen technique rather than screen technique? In indus-

TABLE 12-1

To increase contrast as in radiographing welds in flat plate	To increase latitude as in radiographing irregular castings	To improve definition	When maximum voltage available seems insufficient for thick dense objects	To radiograph thin objects
<ol style="list-style-type: none"> <li>1. Reduce tube voltage until fogging from scattered and secondary rays begins to appear</li> <li>2. Use long exposure time—1 min. or more</li> <li>3. Use fine-grained film of nonscreen type</li> </ol>	<ol style="list-style-type: none"> <li>1. Increase tube voltage</li> <li>2. Use short exposure time—a fraction of a minute</li> <li>3. Use fast film</li> </ol>	<ol style="list-style-type: none"> <li>1. Increase tube-to-film distance</li> <li>2. Keep film holder snug against object</li> <li>3. Use fine-grained film</li> </ol>	<ol style="list-style-type: none"> <li>1. Use maximum voltage</li> <li>2. Use fluorescent screens</li> <li>3. Use lead-foil filter in front of screens in cassette</li> <li>4. Use copper filter 1 mm. thick or less at tube</li> <li>5. Use blocking material</li> <li>6. Decrease tube-to-film distance without violating requirements for definition and distortion</li> </ol>	<ol style="list-style-type: none"> <li>1. Use voltage low enough so exposure time is at least 1 min. when usual tube current and target-to-film distance are employed</li> <li>2. Use nonscreen technique</li> <li>3. Use no filters</li> <li>4. Fine-grained film usually preferable</li> </ol>

trial radiography, a general working rule to follow may be stated thus: *When the maximum voltage available, used with the maximum rated tube current for about 100 sec. at the minimum desirable tube-to-film distance, yields an underexposed radiograph on fast (ordinary grain size) nonscreen film sandwiched between lead-foil intensifying screens, then, and only then, should one resort to screen film and fluorescent intensifying screens.* This practical working rule may be called the “screen rule” for future reference. Like most rules, it has exceptions. It obviously does not apply to radiographic “snapshots” of bullets piercing barriers, etc, for such

equipment operates for only 1 microsec. or so at a time; screen technique is used in this work. Also, in production radiography where, for example, 10,000 one-inch plates must be radiographed in one day, it may be desirable to violate the rule and sacrifice some detail in the radiographs by using screen technique in order to reduce the exposure time from 1 min. to 10 sec, perhaps. In gamma-ray radiography with radium, the nonscreen technique is preferable.

In addition to the technique chart, the general rules tabulated in Table 12-1 should serve as a guide in finding the proper technique.

To summarize, then, it has been decided to use nonscreen technique, with a target-to-film distance of 36 in., an exposure of 1 min. at 175 kv.p., 10 ma., as a first trial.

**3. Welds in Flat Plate, or Plate Having a Radius of Curvature Large Compared with the Thickness.** With steel of this thickness (1 in.), there is considerable scattering and secondary radiation, but 0.005-in. lead foil serves to protect the film from this satisfactorily. A 10- by 8- by 1-in. steel plate weighs only about 22 lb., and so it may be laid directly on top of a medical-type cassette without crushing it. In order to prevent it from scuffing the aluminum face of the cassette, this may be covered with photographic masking tape or something similar. When a film exactly as long as the specimen is used, detail at the extremities is usually missed. Hence the use of an 8 by 10 cassette and film is inadvisable. The use of a full 14 by 17 film is wasteful; it is therefore decided to cut a 4- by 14-in. strip from one end of such a film, and this is placed in one end of a lead-lined 14- by 17-in. cassette.

Before the cassette is taken into the x-ray room for the first exposure, it is advisable to "tune up" the equipment, much as a violinist tunes up before starting a performance. This is not ordinarily necessary before subsequent exposures unless there is to be a radical change in the tube voltage and current used. In tuning up, the door to the lead-lined x-ray room is closed and the x-ray voltage switched on. It is determined how the controls must be set so that the tube operates at 175 kv.p. and 10 ma. It may be found, for example, that the autotransformer control must be set on tap 8 and the rheostat control on tap 9 (Fig. 7-23) to accomplish this. Then the x-ray switch *X* is opened and the rheostat shifted to tap 1 (maximum resistance). This completes the tuning up.

The cassette is placed lid side down on a table in the x-ray room. This table should be sturdy, and should have its top covered with  $\frac{1}{8}$ -in. sheet lead to absorb scattered rays from beneath. The welded plate is then laid on the cassette so that the weld lies along the center of the 4- by 14-in. film inside, about 2 in. of unused film being left at each end. The jib crane or tube stand is then manipulated so as to bring the tube target 36 in. above the cassette in such a position that a plumb bob suspended from the

target would hang over the center of the weld. The axis of the x-ray tube should be horizontal. If the weld lies north and south, the x-ray tube axis should be east and west, for the ray distribution is more uniform in a plane bisecting the tube than in planes containing the tube axis. Identifying lead letters and penetrameters (see Sec. 7) are then laid on the steel plate near the weld so that they will register on the film. The date is useful information to have on a radiograph, for future reference.

The operator then leaves the room and closes the door. The exposure is made by closing the x-ray switch and moving the rheostat control from tap 1 to tap 9. After a minute, the x-ray switch is open and the control returned to tap 1. The film is then developed, fixed, washed, and viewed with a good illuminated translucent screen viewer. If the exposure appears to be too heavy or too light, a second exposure can be made with appropriate correction in the time or voltage.

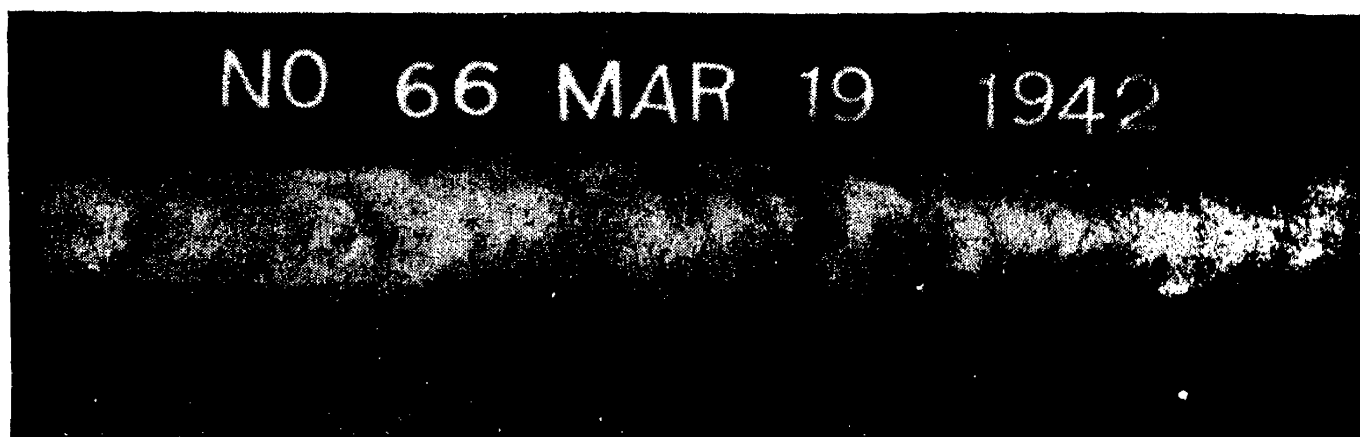


FIG. 12-4.—Porosity in butt weld in 1-in. steel plate.

Small air bubbles in the developer or fixer, rough handling, etc., will cause spots, streaks, scratches, etc. to appear on the film; in interpreting such films, one must be careful not to regard these as defects in the object. Doubt as to whether a particular mark is a film flaw or a real flaw can often be dispelled by viewing the film critically at a grazing angle, observing the light that is specularly reflected from the film surface. Film flaws are usually obvious under these conditions, whereas real flaws are not. If the doubt persists, a second radiograph should be taken. Sometimes two films are exposed as regular practice, as explained on page 185, so that retakes are not necessary.

Figure 12-4 shows the radiograph obtained as just described. This was an open double-V butt joint, arc-welded. The radiograph indicates considerable porosity in certain parts of the weld. Pores or slag inclusions are indicated in the film by small black dots. The slag or voids in the metal are of course more transparent to the x-rays than the metal is, and the x-rays which pass through such pores or slag are therefore absorbed in lesser proportion than those which encounter steel all the way through.

Thus the film is subjected to a heavier exposure behind the defects, and the defects appear as dark markings on a light background. Occasionally film flaws or poor darkroom technique will cause markings to appear on the film that are *lighter* than the background. Such markings rarely represent real defects in metal. When a print is made from the negative, this condition is reversed, of course, and flaws appear as light markings on a dark background.

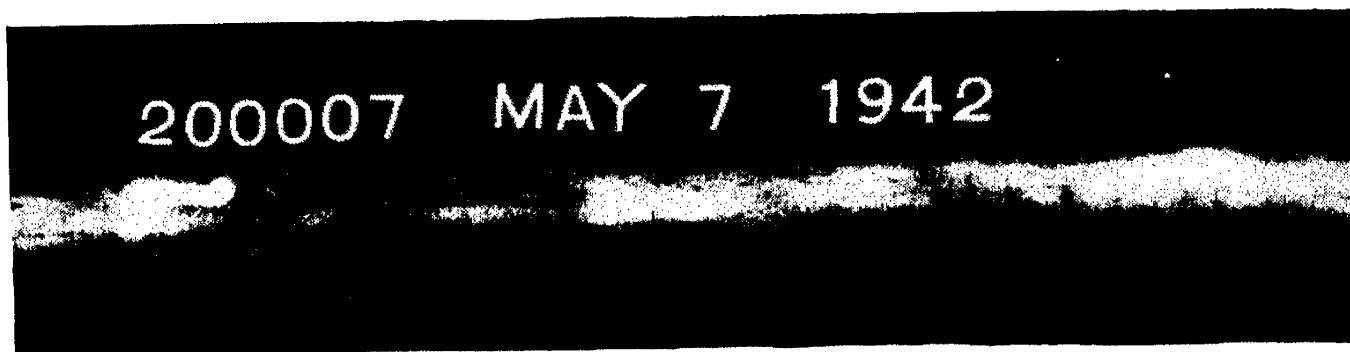


FIG. 12-5.—Slag inclusions in arc weld in steel plate.



FIG. 12-6.—Extreme case of lack of fusion and lack of penetration in arc weld.

Figure 12-5 is a radiograph of another weld of the same type as the first one, but having different defects. In this figure, the flaws are represented by dark spots drawn out into an elongated shape, whereas the spots in Figure 12-4 are nearly circular. This suggests that Fig. 12-5 represents slag inclusions, for gas bubbles or pores are naturally spherical, whereas slag tends to be drawn out into elongated inclusions as the welding progresses.

Figure 12-6 represents an extreme case of incomplete fusion and incomplete penetration. By penetration, one means the fusion of the parent metal at and beneath the face of the scarf, resulting in a union between parent metal and weld metal. In this radiograph the weld metal appears to have failed even to flow into the central portion  $BCC'B'$  (Fig. 12-8) of the weld, much less penetrate or fuse with the parent metal. The entire "free distance"  $BB'$  (Fig. 12-8) that separated the joint sections initially along the faces  $BC$  and  $B'C'$  appears to be practically void of metal.

Figure 12-7 shows the radiograph of a weld in which the metal has flowed in to fill the central part of the joint but in the right half of the figure has failed to unite completely with the parent metal along the faces  $BC$  and  $B'C'$  (Fig. 12-8). The two fine dark lines (indicated by arrows  $PP$ , Fig. 12-7) clearly reveal the edges  $B$  and  $B'$  of the two joint

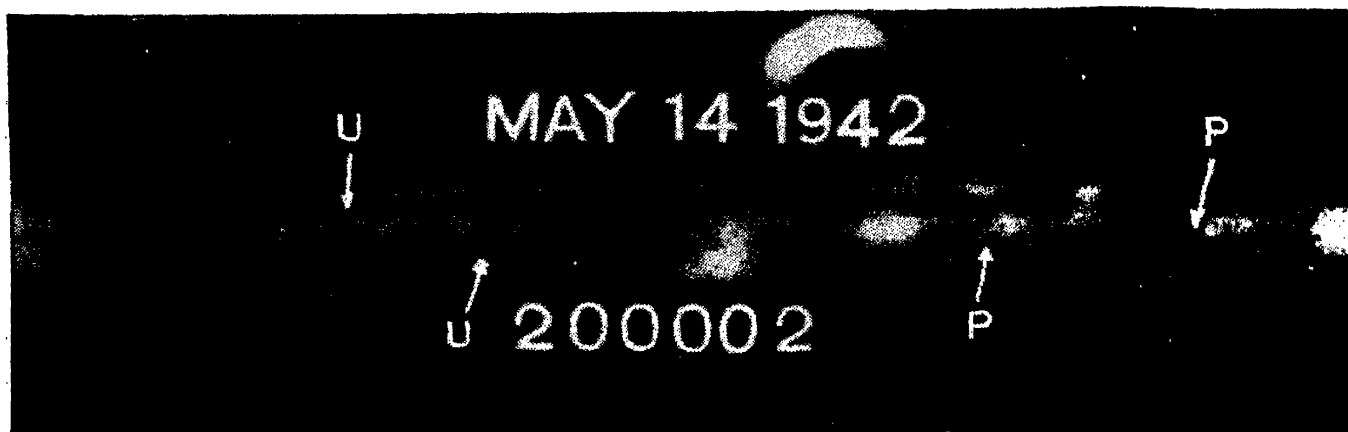


FIG. 12-7.—Undercutting in arc weld.

sections, which evidently were not “penetrated,” or melted, so that the weld metal could form a strong union.

Penetration has been achieved along the central portion (faces  $BC$  and  $B'C'$ ) of the weld in the left part of Fig. 12-7, but the dark streaks along each edge of the weld (arrows  $UU$ ) indicate that the weld metal

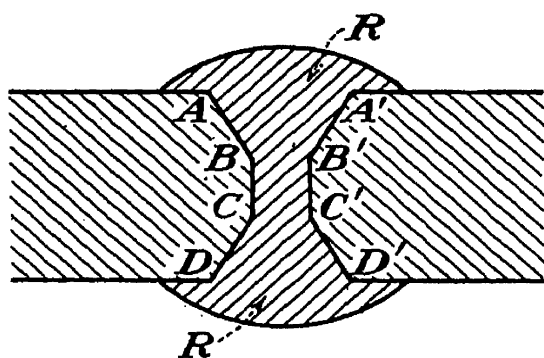


FIG. 12-8.—Cross section of butt weld.

failed to penetrate the scarf faces  $AB$ ,  $A'B'$ ,  $CD$ , and  $C'D'$ , especially near  $A$  and  $A'$  or  $D$  and  $D'$  or perhaps all four places (Fig. 12-8). Since the x-rays pass through parallel to the faces  $BC$  and  $B'C'$ , lack of penetration of these faces appears in the radiograph as a fine straight line; but incomplete penetration of the upper scarf faces near  $A$ ,  $A'$ ,  $D$ , or  $D'$  appears as a rather hazy streak because the rays are inclined to the faces.

This condition is commonly called “undercutting” and it weakens the weld just as seriously as when the penetration is incomplete at the faces  $BC$  or  $B'C'$ . An undercut is commonly defined as a depression melted out of the parent metal along the edge of a weld.

Figure 12-9 is a radiograph showing local lack of fusion of the metal at  $F$  and  $F'$ , but otherwise the weld is very good.

Figure 12-10 shows a combination of practically all the common defects in a weld. There are incomplete fusion and penetration, local undercutting, slag and porosity, and also what is known as a “crater crack.” A crater crack is a series of two or three fine cracks radiating



from one spot, caused by excessive local shrinkage. In Fig. 12-10, the crater crack is indicated by the arrow P.

Figure 12-11 is an example of a double crack in one weld where it crosses a second one. These cracks could not be seen on the surface of the weld at all, even after the radiograph revealed and located them so that the exact place to look for them was known.

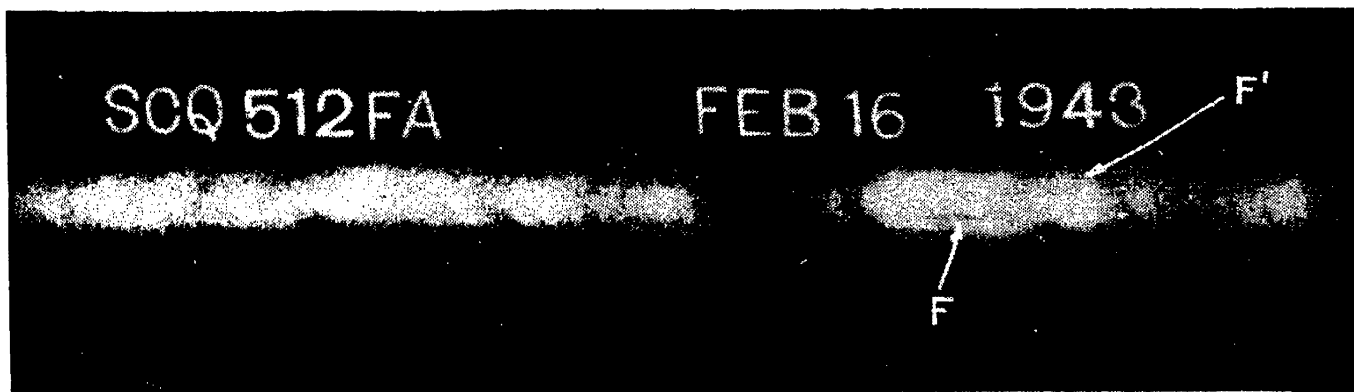


FIG. 12-9.—Localized incomplete fusion in arc weld.

Figure 12-12 is a radiograph of a good weld and also furnishes an example of one type of film flaw. The peculiar marks along the upper edge of the weld at the extreme right are caused by a static discharge set up when the film was withdrawn from the box on a dry day to be loaded into the cassette or perhaps when it was removed from the cassette. Figure 12-7 illustrates (immediately above the 1942) the type of film

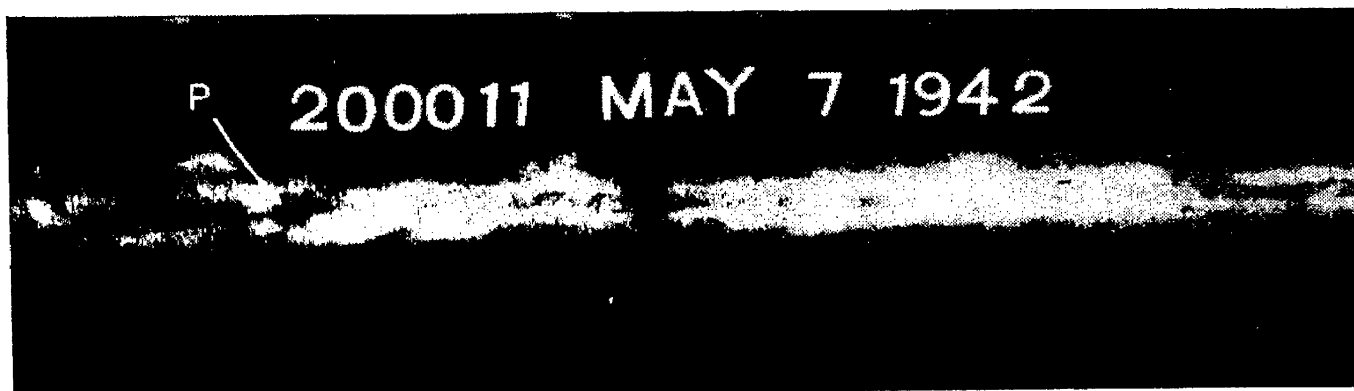


FIG. 12-10.—Showing various defects in the same arc weld.

flaw resulting from slight kinking of the film before development. The x-ray technician must learn to recognize such markings and to know what causes them so that he can take steps to prevent them and will not interpret them as defects in the object examined. The light marks along the top edge of Fig. 12-10 were caused by cutting the film with a pair of scissors, each mark resulting from a scissor stroke. Small air bubbles in the developer or fixer cause characteristic circular spots on the radiograph.

In general, scattered porosity or slag does not seriously weaken the

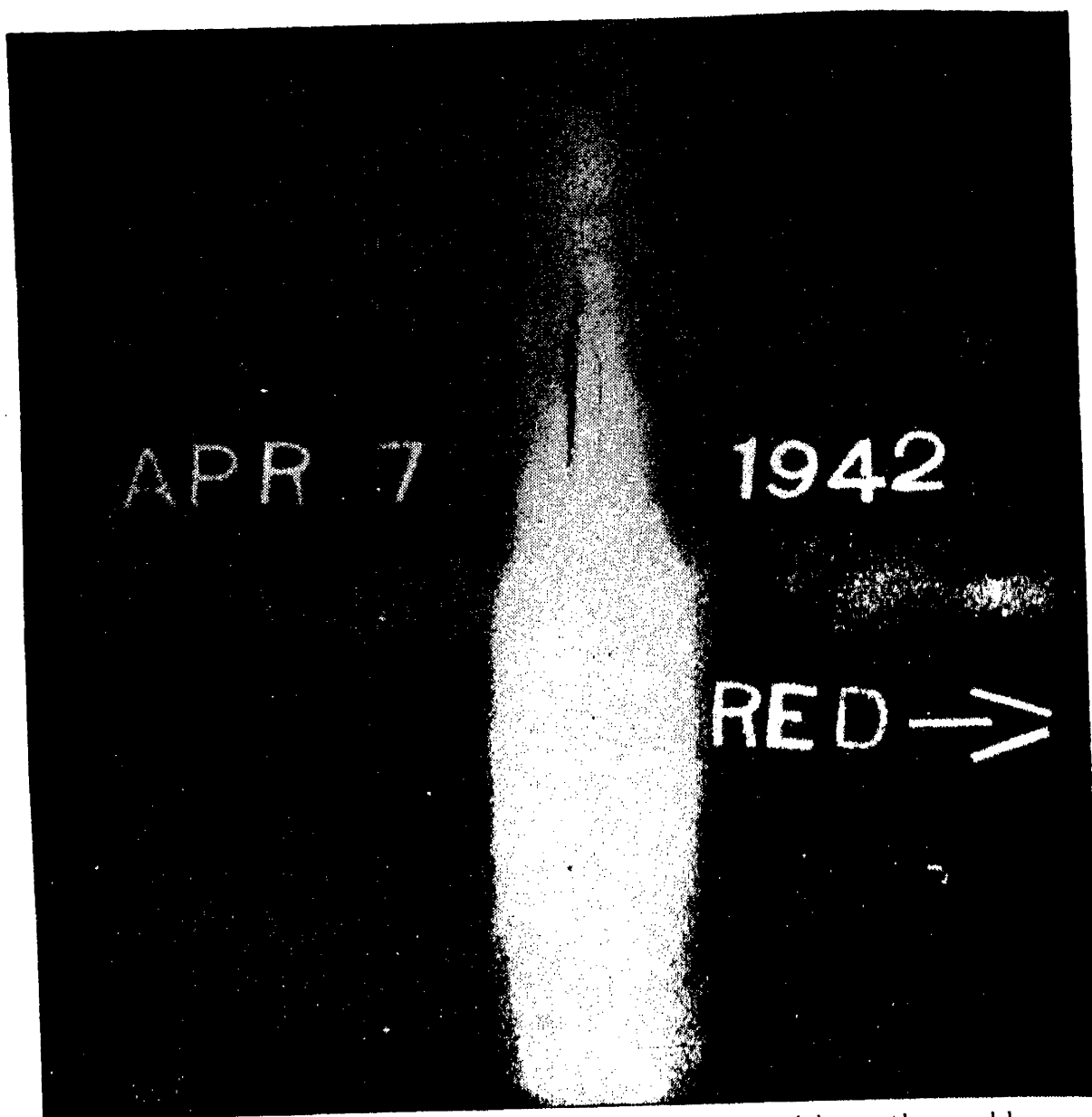


FIG. 12-11.—Cracks in a weld near its intersection with another weld.

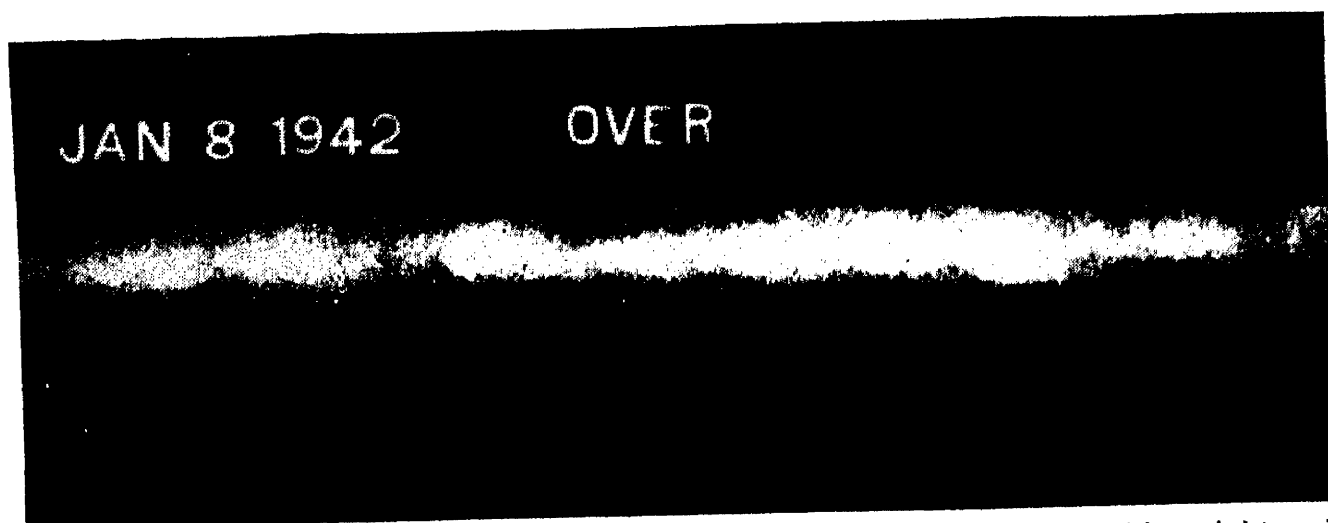


FIG. 12-12.—A good weld. Note dark fine lines along upper edge of weld at right end. These are caused by static electrical discharges generated when film is handled on days of very low humidity. They should not be mistaken for cracks in the weld.

metal. If the porosity or slag is concentrated in a particular region, that region is weak; or, as often occurs in welds, pores or slag will be found along a line, and this may result in a break along that line. Incomplete fusion, incomplete penetration, and undercutting seriously weaken a weld unless the condition is strictly local. An isolated small crater crack need not be regarded as cause for rejection of a weld, in the opinion of the author, although the official codes (see Sec. 7) declare that *any* crack makes a weld unacceptable. Most crater cracks are barely visible in a good radiograph and usually consist of three or four hairlike cracks radiating from a point for a distance of  $\frac{1}{8}$  in. or less. When the welded plate is more than 1 in. thick, most crater cracks probably escape radiographic detection. Several crater cracks indicate poor welding technique, and in such a case the weld should be rejected. A crack as extensive as the one shown in Fig. 12-11 greatly weakens a weld, of course.

It will often be found that flaws appearing in a radiograph are surface flaws which can be seen by merely comparing the radiograph with the surface of the object. In the case of a rough surface, it is sometimes advisable to have it ground or machined off smooth before taking the radiograph.

Nothing essentially new or different is involved in radiographing fillet welds. Often it is desirable to direct the rays at a  $45^\circ$  angle to the plate surface, but each particular job should be considered carefully and the best arrangement of tube and film holder decided upon in the light of what has already been said about butt welds. A sound knowledge of radiographic principles will indicate the best procedure to follow. The use of an equalizing wedge as illustrated in Fig. 12-13 is sometimes helpful.

Figure 12-14 is a radiograph of a fillet weld joining two steel forgings. The weld runs along the left edge of the rib from its top end to its center where it crosses over and runs along the right edge to the lower end. Incomplete fusion is evident in the former portion, and slag inclusion in the latter.

If 2-in. rather than 1-in. plate had been used in making a butt weld of the type shown in Figs. 12-4 to 12-10, one might again select 600 ma. sec. and 36 in. as suitable, since the distortion and blurring as calculated by equations (11-1) and (11-2) are about  $\frac{2}{7}$  and 0.011 in., respectively

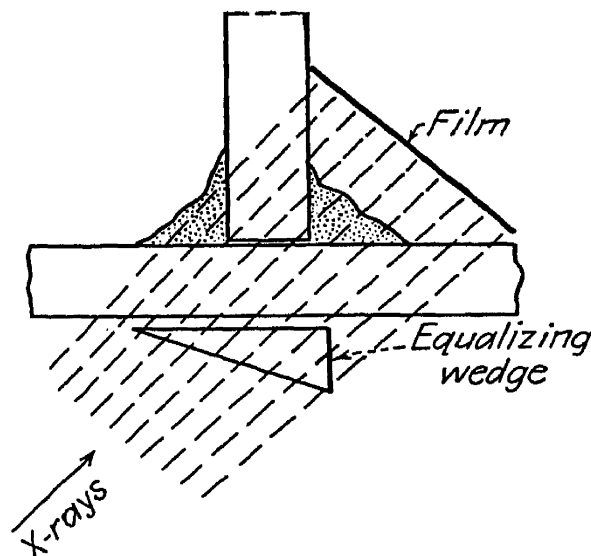


FIG. 12-13.—Radiography of a fillet weld.

In general, one should strive to reveal flaws having an extent of 1 or 2 per cent of the thickness of the object examined, which is 0.02 or 0.04 in. in the present case, a figure exceeding the calculated blurring by a margin sufficient to make success possible if other features of the

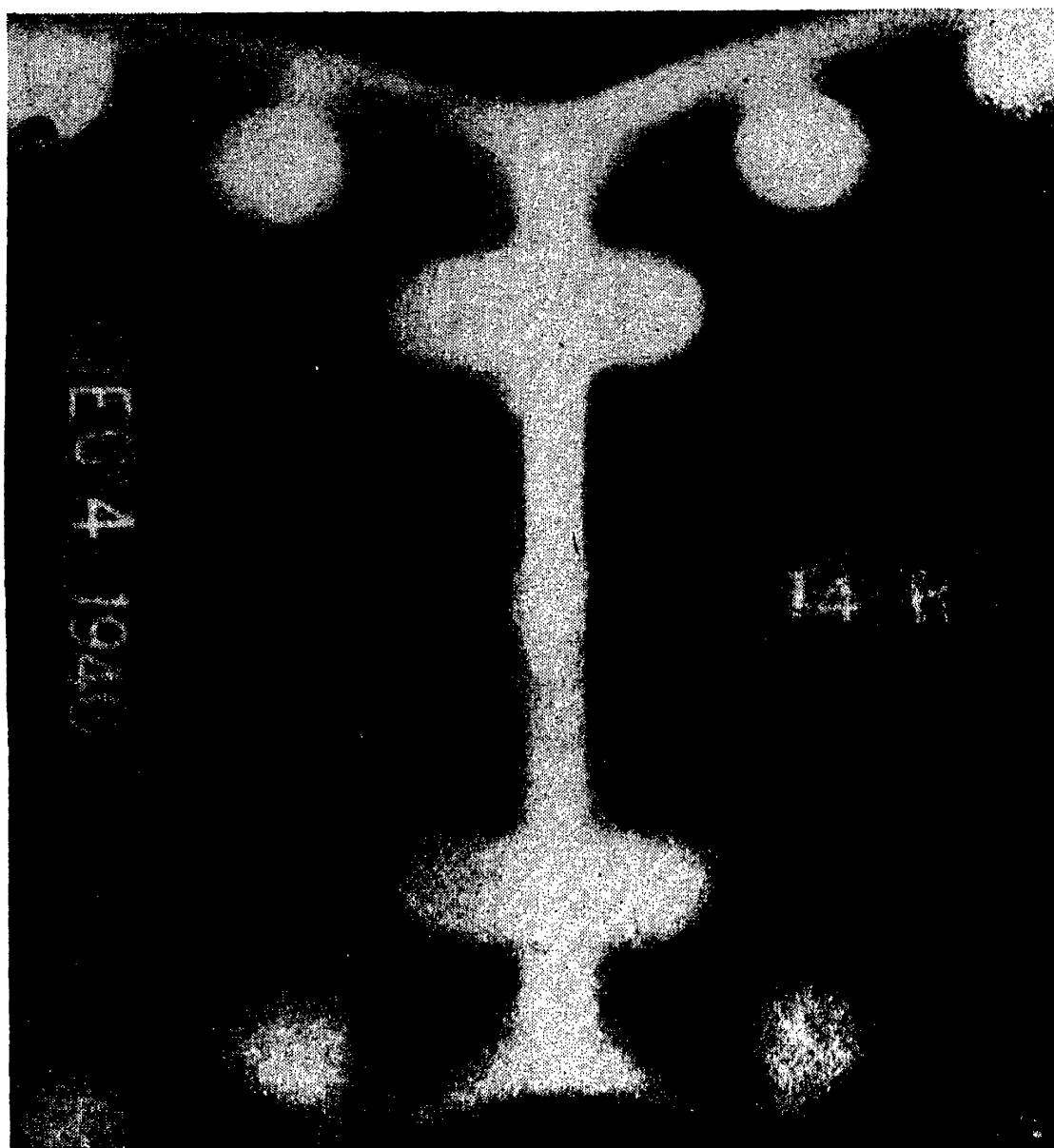


FIG. 12-14.—Fillet weld joining two forgings.

technique are sufficiently favorable. Reference to Fig. 12-1 shows that nonscreen technique is unsuitable at the above distance, current, and time, even though the highest tube voltage available were used. Therefore fluorescent intensifying screens are needed. Figure 12-2 indicates that about 182 kv.p. will be required for 2 in. or 197 kv.p. for  $2\frac{1}{4}$  in. if the weld extends  $\frac{1}{8}$  in. above the surface of the plate on both sides.

With plate as thick as this, it will be found that the secondaries and scattered rays from 220-kv. (or less) primaries will fog the film near the edge of the plate unless blocking material is used to prevent it. Hence

the procedure in radiographing the butt weld in 2-in. steel plate might be as follows: Adjust tube to horizontal position with focal spot 36 in. above the table. Retire from room, "tune up" for 197 kv.p. at 10 ma., and shut off the high voltage. Cover table top with large piece of boxboard (the material used in making shipping cartons). Use cassette having 0.005-in. lead foil to act as filter, and insert double fluorescent intensifying screens; then place industrial screen film between them, and close cassette. Lay cassette on boxboard cover. Lay steel plate on cassette carefully so as to avoid scuffing or other damage (on the assumption that plate is only 8 by 10 in.—if plate is 3 feet square, the procedure will be different, of course). Pour fine steel shot around edges of plate as indicated in Fig. 12-15. Lay identification markers and penetrameters on plate. Retire from room, and make 1-min. exposure. When markers, plate, and cassette are removed, the shot will lie on the boxboard. This may then be picked up and permitted to fold in the center, parallel to the corrugations of its inner layer, so as to form a convenient trough to convey the shot back to its container.

**4. Blocking Material.** The shot just mentioned is one type of so-called "blocking material" or "industrial opaque" used in industrial radiography to protect the x-ray film. Since the term "opaque" is used to designate materials such as barium sulfate used in medical work for a different purpose (page 219), it is desirable to avoid use of the term in a different sense here; the name "blocking material" thus eliminates confusion.

In Fig. 12-15, *P* represents a 2-in. plate lying on a cassette, and *S* is the shot piled against the edge of the plate as a blocking material. Since the plate *P* is so thick, the intensity of the primary x-rays striking the cassette at *A*, in the absence of the shot, will be hundreds of times their intensity at *B*. Consequently, the scattered and secondary rays from *A* and points near it have an intensity at *B* comparable with the primaries at *B*, without any blocking material. This causes fogging of the film for a considerable distance from the edge *E* of the plate.

When the shot *S* is used, however, the primaries at *A* are reduced in intensity to such a degree that scattered and secondary rays no longer fog the film to the left of *E*. The use of shot as a blocking material is discussed in detail in an article by Moriarty.<sup>1</sup> He states that 70-mesh shot is the best size (about 0.015 in. in diameter). Commercial steel

<sup>1</sup> C. D. Moriarty, *Gen. Elec. Rev.*, **42**, 109 (1939).

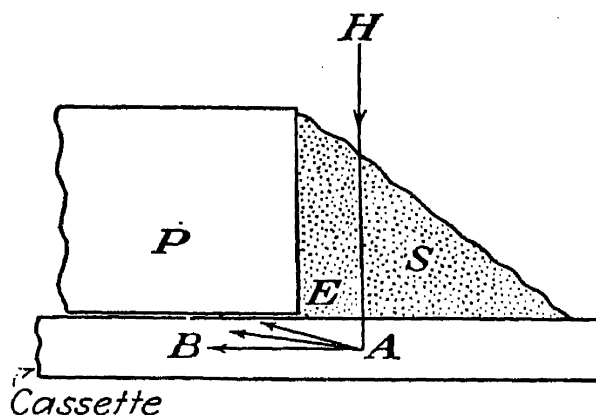


FIG. 12-15.—To explain the purpose of blocking material.

shot used in shot blasting operations is satisfactory, although Moriarty believes that copper shot is somewhat better for radiographing steel objects. For the radiography of thick aluminum and magnesium objects of cylindrical, spherical, or irregular shape, aluminum shot may sometimes be used to advantage.

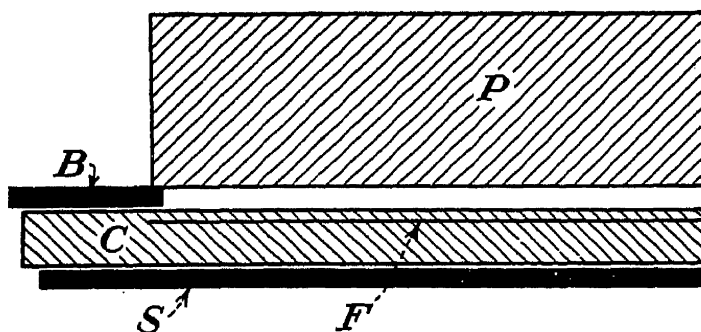


FIG. 12-16.—Lead strip *B* used as blocking material along edges of thick metal specimen *P*.

If it is required to radiograph a 2-in. steel plate 3 ft. square, for example, the procedure outlined above is not suitable. Such a heavy plate would crush a cassette and perhaps the table. It may be laid horizontally on sturdy horses or a special fixture that will support it with most of the underside exposed. There must be no possibility of

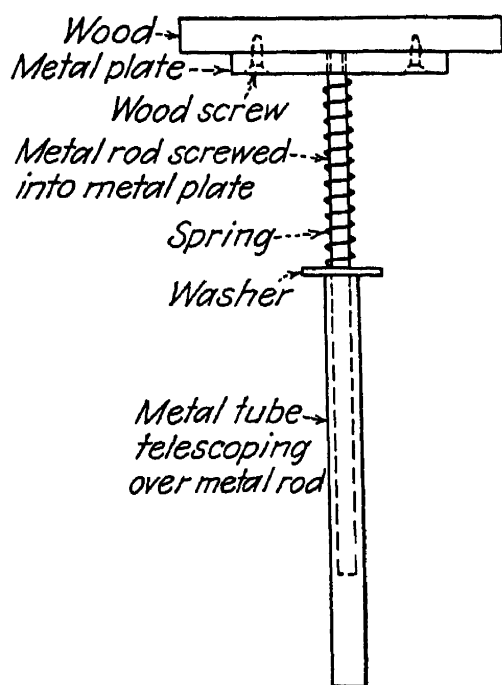


FIG. 12-17.—Spring support pedestal for cassettes.

the horses or the fixture slipping or collapsing and allowing the 750-lb. plate to fall on a man working underneath. A 14- by 17-in. cassette may be placed against the undersurface of the plate and blocked in position by means of some device such as the one shown in Fig. 12-17. The use of shot is inconvenient here; therefore, lead strips *B* about  $\frac{1}{8}$  by 2 by 25 in. may be tucked under the edge of the plate to protect the exposed edge of the cassette as shown in Fig. 12-16. Here *P* is the steel plate and *C* the cassette containing the film *F*. It will be found necessary to place a sheet of  $\frac{1}{8}$  in. lead *S* under the cassette to protect it from scattered rays coming up from the floor.

For a 1-in. by 3-ft. by 3-ft. plate, the lead backing in the cassette itself will furnish this protection, for the scattered rays are relatively less intense. Also, the lead strip *B* can be omitted, and nonscreen technique can be used. With a  $\frac{1}{4}$ -in. plate, the scattered and secondary rays are so feeble compared with 200-kv. primaries that the use of a lead

filter on the tube side of the film is unnecessary. Hence a lead-backed cardboard film holder may be used. In fact, for objects as thin as  $\frac{3}{16}$ -in. steel or  $\frac{3}{8}$ -in. aluminum, etc., a cardboard film holder *should* be used rather than a lead-lined cassette; the lead foil absorbs the primaries to an extent comparable with that due to the object, and thus better contrast and detail will be achieved with the cardboard holder. In determining the probable exposure time required from a technique chart like Fig. 12-1, it must be remembered that the omission of lead screens will increase the exposure time considerably because of their intensifying action. With 220-kv. equipment, it may be best to use a lead-lined cassette for  $\frac{3}{8}$ -in. and thicker steel plates and a cardboard film holder for  $\frac{1}{4}$ -in. and thinner steel plates. In this case, it may be found that a longer exposure is required to radiograph  $\frac{1}{4}$ -in. than  $\frac{3}{8}$ -in. plate because of the intensifying action of the lead.

The two most useful types of blocking material have already been mentioned, namely, metal shot and  $\frac{1}{8}$ -in. sheet lead. There are other types sometimes used in industrial radiography. For example, some x-ray equipment manufacturers sell a putty containing a compound of some absorbent element like barium. The object to be radiographed may be immersed in a liquid solution of some absorbent solute such as lead acetate. It is difficult to avoid voids and inhomogeneities in using putty. Liquid solutions have a comparatively low absorption coefficient and are obviously inconvenient except for special purposes.

TABLE 12-2

Voltage available, kv.p.	Blocking Material Helpful and Often Essential in Radiographing Cylinders, Spheres, and Irregular-shaped Objects Made of
140... ..	Magnesium and aluminum more than 1 in. thick; denser materials of equivalent thickness
200... ..	Steel more than $\frac{1}{2}$ in. thick; denser materials of equivalent thickness
220... ..	Steel more than 1 in. thick; denser materials of equivalent thickness
250... ..	Steel more than $1\frac{1}{2}$ in. thick; denser materials of equivalent thickness
400... ..	Steel more than 2 in. thick; denser materials of equivalent thickness
1,000... ..	Brass, bronze, and copper more than 3 in. thick; denser materials of equivalent thickness
Radium... ..	Blocking material unnecessary

An example of the practical use of liquid blocking is the process devised by Woods and Hight<sup>1</sup> for inspecting internal screw threads at Bell Aircraft Corp., Buffalo, N.Y., with the same degree of microscopic precision ordinarily attained in inspecting external threads only. In this process, the part is immersed in a blocking liquid consisting of high-grade pure white lead thinned to the desired density with a volatile toluol thinner. It is then radiographed on a special fine-grained film with lead

<sup>1</sup> R. C. Woods and E. K. Hight, *Aero Digest*, May, 1941, p. 199.

screens and soft x-rays. The resulting radiograph shows the internal threads so accurately that they can be measured microscopically by the methods used for external-thread inspection.

A blocking material should be used around the edge of a flat plate whenever the screen rule (page 244) calls for a screen technique. Blocking should also be used for any object which has such a shape that the film holder cannot be made to conform to it, in the cases listed in Table 12-2.

A steel pipe 2 ft. in diameter with 1-in. walls is not regarded as a cylindrical or irregular-shaped object in interpreting Table 12-2. Such a pipe can be radiographed by using a flexible film holder and curving it to conform to the inner surface of the pipe, which should be radiographed a section at a time with the x-ray tube located outside, the pipe wall being regarded as a 1-in. plate. An extreme example of this type of work is the radiographic inspection of every inch of the 75 miles of welds in the penstocks at Boulder Dam. Some of this work was done with mobile x-ray equipment inside the penstock and film holders on the outside. Some was done with fixed x-ray equipment outside and the film holders inside. The diameters of this pipe varied from  $8\frac{1}{2}$  to 30 ft., with wall thicknesses up to 3 in.<sup>1</sup> In work of this type where there are no edges or holes in the object, blocking material is unnecessary.

A steel pipe three inches in outside diameter with 1-in. walls is regarded as a cylinder in Table 12-2, however, for the only practical way to radiograph it is to lay it on a flat film holder and pass the rays clear through it. Two-inch steel plate requires screen technique with 220-kv. equipment; the use of shot will prevent most of the edge fogging.

**5. Filtration.** The quality of the radiograph can often be improved by the use of filters, which were discussed from the medical standpoint on page 231. A 1-mm. copper filter next to the tube will remove the softer rays, which are the ones most scattered by the object. Thus the fogging of the film by scattered radiation is reduced. With million-volt equipment, lead filters are sometimes used next to the tube instead of copper. The filtration introduced by lead screens in the cassette was discussed on page 181. These cassette filters reduce film fogging by absorption of both the secondary and the incoherently scattered rays from the object being radiographed.

**6. The Industrial Grid.** When thick objects, for example, welds in 4-in. steel plate, are to be radiographed, the use of million-volt equipment or radium is best. Sometimes the volume of the work is so great or the available time so limited that the use of radium is ruled out. If 300-kv. or 400-kv. x-ray equipment is all that is available, the results obtainable with it on work of this thickness (4 in.) are usually disappointing, as are

<sup>1</sup> *Gen. Elec. Rev.*, **37**, 40 (1934).



results on 3-in. plate using 200- or 220-kv. equipment. The reason, of course, is excessive scattering and secondary radiation.

This can be reduced considerably in such cases by using an "industrial grid." This is a Potter-Bucky grid (see Sec. 11-2) built on a more rugged plan than the ones used for medical radiography. The lead ribbons are thicker, and the supporting framework and mechanism for moving the grid are designed for convenient and dependable service in a boiler factory or foundry rather than a hospital. As explained in Chap. 11, the exposure time is considerably increased when such a grid is used, which is unfortunate, for the type of work where a grid is most needed is work where the exposure time is already excessive. Such grids are sold by the x-ray equipment manufacturers.

**7. Welds in Tubes or Cylindrical Objects.** To resume the discussion of radiographic examples, it may be supposed that the next job brought in for examination is an experimental weld in one of the journals of a crankshaft. The journal is  $2\frac{1}{2}$  in. in outside diameter and hollow, the wall thickness being about  $\frac{1}{2}$  in. Rays that pass diametrically through the center of the journal will penetrate only 1 in. of steel, but those passing on either side of the center will penetrate a greater thickness. With the 220-kv. equipment available, the screen rule calls for non-screen technique, but Table 12-2 calls for the use of blocking material. The average thickness of the steel to be penetrated may be regarded as about  $1\frac{1}{2}$  in. Figure 12-1 indicates that 210 kv.p., 10 ma., for 1 min. is suitable for this thickness. However, where there is considerable variation in thickness to be examined in a single radiograph, it is advantageous to reduce the contrast or increase the "latitude" by using a high voltage for a short time rather than a lower voltage for a longer time. Hence it may be decided to make a trial exposure at 220 kv., the highest voltage available, 10 ma., 50 sec., the tube-to-film distance being 36 in.

The table is covered with boxboard, and the equipment tuned up for 220 kv., 10 ma. Then a lead-lined cassette loaded with nonscreen film is laid on the boxboard. If the crankcase is too heavy for the cassette, the major part of its weight may be supported by wood blocks on each side of the cassette. The welded journal is placed as close to the cassette as possible. Since the identifying figures and letters will be buried under the shot, they should be bound together by pressing them against the adhesive side of a piece of masking tape, for example, so that they may be more easily retrieved after the exposure. After laying the marker on the cassette, steel shot is poured around the journal until its lower half is buried, after which the exposure is made.

Figure 12-18 shows the resulting radiograph. The elliptical black line indicates incomplete penetration at and near the inner surface of the

hollow journal. The two black dots are due to oilholes drilled in the journal. If the first radiograph obtained of such a weld reveals no defects, it is advisable to confirm this by taking a second radiograph in which the journal is rotated  $90^\circ$  from its first position.

Welded vessels, cylinders, or tubes having an inside diameter between about 6 in. and 2 ft. and a wall thickness between 1 and 5 in. are most conveniently radiographed with radium. The technique will be described in sec. 17, as well as the advantages of gamma-ray radiography in certain types of work.

**8. Radiographic Standards.** About 12 years ago the A.S.M.E. Boiler Construction Code was revised<sup>1</sup> in such a way as to recognize that

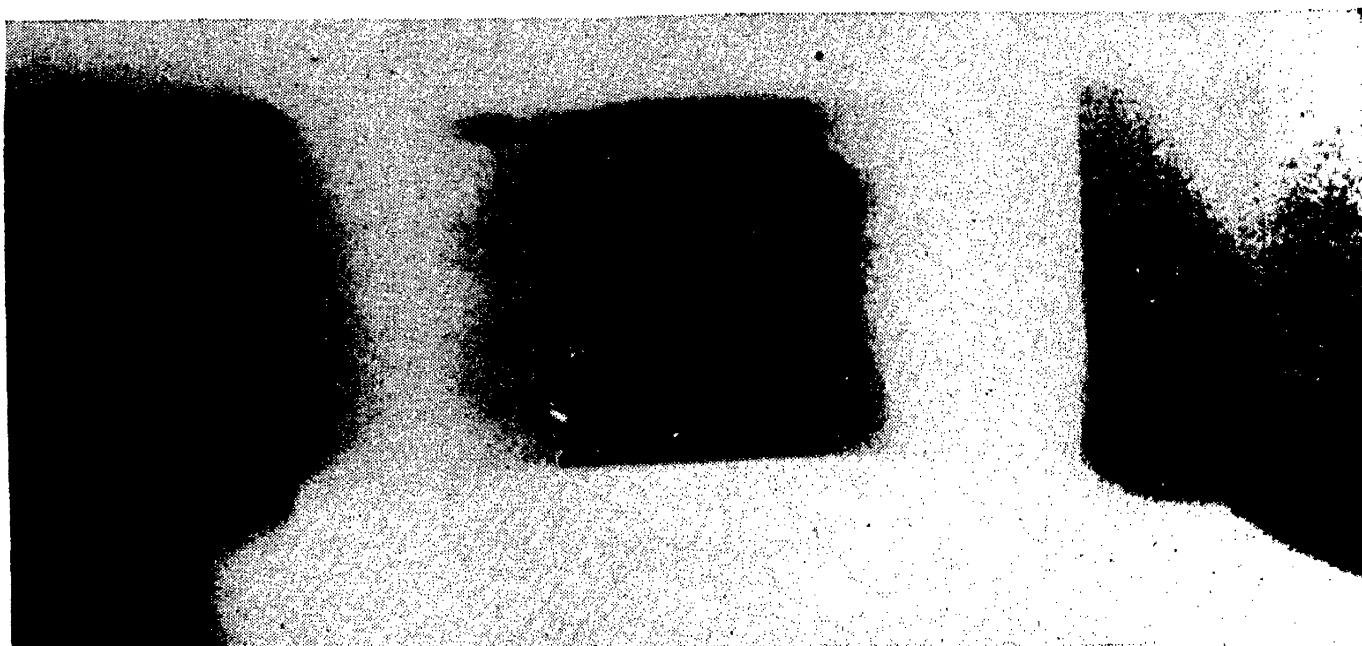


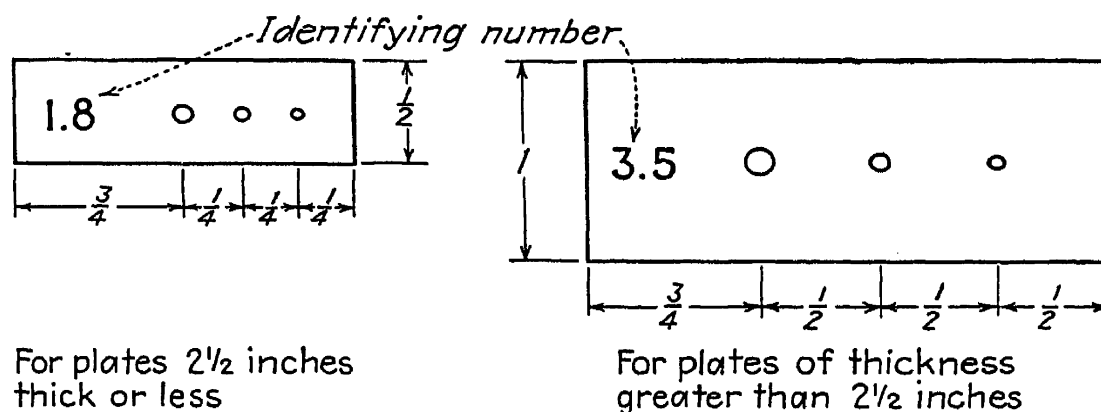
FIG. 12-18.—Butt weld in a hollow shaft, showing incomplete fusion.

radiography is the best means known for determining the quality of welds in pressure vessels. More recent revisions<sup>2</sup> read, "All longitudinal and circumferential welded joints of the structure shall be examined throughout their entire length by the x-ray or the gamma ray method of radiography." The code goes on to specify that penetrameters shall be used in taking these radiographs. For thicknesses of  $2\frac{1}{2}$  in. or less, the penetrameter is to be a  $1\frac{1}{2}$ - by  $\frac{1}{2}$ -in. plate of material substantially the same as that of the plate under examination, the thickness of the penetrameter being not more than 2 per cent of the thickness of the plate (Fig. 12-19). The three holes shown are to have the diameters specified in the figure. The identifying number shown in the figure consists of lead figures cemented on with some adhesive like Duco household cement; it represents, to two significant figures, the minimum thickness of plate for which the penetrameter may be used. The penetrameters are to be

<sup>1</sup> *Mech. Eng.*, **55**, 267 (1933).

<sup>2</sup> *Mech. Eng.*, **62**, 333 (1940).

placed on the side of the plate nearest the source of radiation. The smallest hole must be distinguishable on the radiograph, and the images of the identifying numbers must also appear clearly. Two penetrameters



*Diameters of holes (left to right) to be 2, 3 and 4 times the thickness of the penetrameter, but not less than  $\frac{1}{16}$  inch*

FIG. 12-19.—Dimensions of A.S.M.E. penetrameters (1940).

are to be used for each exposure, one at each end of the exposed length, parallel and adjacent to the weld seam with the small holes at the outer ends. Figure 12-20 shows how one of these penetrameters appears in a radiograph of a weld in  $\frac{3}{4}$ -in. plate.

The United States Army Ordnance Specification AXS-476 for welds calls for similar penetrameters except that the holes are one, three, and four times the thickness of the penetrameter, but not less than  $\frac{1}{32}$  in.

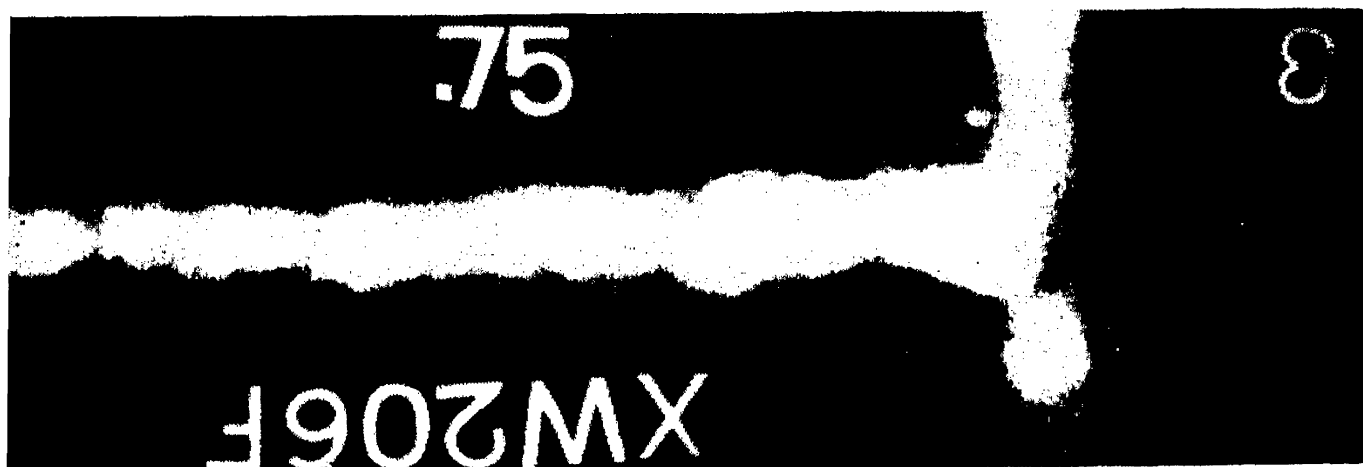


FIG. 12-20.—Appearance of penetrameter in a radiograph.

Obviously, the object of both these codes or specifications is to ensure that defects having a minimum extent equal to 2 per cent or more of the plate thickness shall be visible in the radiograph, whether this minimum extent is in a direction perpendicular to the plane of the plate, or in this plane. When the smallest hole in the appropriate Army Ordnance penetrameter can be seen in the radiograph it is said that the “sensitivity” of the radiograph is 2 per cent.

TABLE 12-3.\*—DIMENSIONS OF U.S. ARMY ORDNANCE PENETRAMETERS

Specimen thickness, in.	Identifying number	Penetrameter thickness in.	Hole diameters, in.		
			Large	Medium	Small
$\frac{1}{4}$	.25	0.005	0.03(69)	0.03(69)	0.03(69)
$\frac{3}{8}$	.38	0.008	0.03(69)	0.03(69)	0.03(69)
$\frac{1}{2}$	.50	0.010	0.04(60)	0.03(69)	0.03(69)
$\frac{5}{8}$	.63	0.013	0.05(56)	0.04(60)	0.03(69)
$\frac{3}{4}$	.75	0.015	0.06(53)	0.05(56)	0.03(69)
$\frac{7}{8}$	.88	0.018	0.07(50)	0.05(56)	0.03(69)
1	1.0	0.020	0.08(46)	0.06(53)	0.03(69)
$1\frac{1}{8}$	1.1	0.023	0.09(43)	0.07(50)	0.03(69)
$1\frac{1}{4}$	1.3	0.025	0.10(39)	0.08(46)	0.03(69)
$1\frac{3}{8}$	1.4	0.028	0.11(35)	0.08(46)	0.03(69)
$1\frac{1}{2}$	1.5	0.030	0.12(31)	0.09(43)	0.03(69)
$1\frac{5}{8}$	1.6	0.033	0.13(30)	0.10(39)	0.03(69)
$1\frac{3}{4}$	1.8	0.035	0.14(28)	0.10(39)	0.04(60)
$1\frac{7}{8}$	1.9	0.038	0.15(25)	0.11(35)	0.04(60)
2	2.0	0.040	0.16(21)	0.12(31)	0.04(60)

\* Numbers in parentheses are equivalent Brown and Sharpe gauge drill sizes.

The A.S.M.E. code goes on to specify<sup>1</sup> that

. . . Identification markers whose images will appear on the film shall be placed adjacent to the weld and their location accurately and permanently stamped near the weld on the outside surface of the drum or shell, so that a defect appearing on the radiograph may be accurately located in the actual weld.

This matter of identification is very important in any type of radiograph. If it is objectionable to stamp on figures or letters with steel stamps, they may be painted or stenciled on or, if permanence is unnecessary, may be marked on with a china-marking pencil.

When the object must stand vertically while being radiographed, the lead letters and figures cannot be laid on a vertical surface, of course. In such a case, they may be held in place with scotch tape. With steel objects, a small magnet may be used for this purpose.

The A.S.M.E. code specifies the minimum distances between the radiation source and the back (film) side of the plate as follows:

Plate Thickness, In.	Distance, In.
Up to 1.....	14
1 to 2.....	21
2 to 3.....	28
3 to 4.....	36
4 to 4 $\frac{1}{2}$ .....	38

<sup>1</sup> *Mech. Eng.*, 55, 267 (1933).

The code also states that the film shall be as close as practicable to the back surface of the weld (the side opposite the radiation source), not exceeding 1 in. if possible. These requirements are of course intended to limit the blurring and distortion (pages 214 and 215). The following requirements are quoted:

1. Welds in which the radiographs show elongated slag inclusions or cavities shall be unacceptable if the length of any such imperfection is greater than  $\frac{1}{3}T$  where  $T$  is the thickness of the weld. If the lengths of such imperfections are less than  $\frac{1}{3}T$  and are separated from each other by at least  $6L$  of acceptable weld metal, where  $L$  is the length of the longest imperfection, the weld shall be judged acceptable if the sum of the lengths of such imperfections is not more than  $T$  in a weld length of  $12T$ .

2. Welds in which the radiographs show any type of crack or zones of incomplete fusion shall be unacceptable.

3. Welds in which the radiographs show porosity shall be judged as acceptable or unacceptable by comparison with the standard set of radiographs, reproductions of which may be obtained by purchase from the Boiler Code Committee.

A few interesting excerpts from the Army Ordnance specifications may be quoted.

The following are rejectable defects:

1. Porosity 2. Slag inclusions 3. Imperfect fusion 4. Incomplete penetration 5. Undercuts 6. Cracks 7. Lack of prescribed fit. . . . When the undesirable fusion condition is in the penetration zone, it is referred to as improper penetration. The radiographic image is a more or less straight line. . . . All cracks are rejectable. Various types of cracks are . . . longitudinal, transverse, crate cracks, and plate cracks.

The A.S.M.E. code and the Army Ordnance specifications are two of the best known examples of the "radiographic standards" that have been established to guarantee the quality of radiographic inspection. Without such standards, a few careless radiographic technicians could soon discredit the method in the eyes of those who depend upon it, for it is only too easy unconcernedly to "shoot a radiograph" that reveals no defects in a dangerously defective part. As a result of the advent of million-volt equipment, greatly improved x-ray film, and the steady improvement of radiographic equipment of ordinary voltage, there has been a trend toward stricter radiographic standards. At present, most operators are striving for 1 per cent sensitivity, even in thicknesses up to 8 in. of steel, and the requirement of 2 per cent sensitivity is practically universal.

9. Iron and Steel Castings. The radiography of an iron or steel casting differs in no essential way from the radiography of a vessel or device welded together from rolled plates, girders, etc. In the latter

instance, the rolled shapes are usually assumed to be free of flaws, and attention is centered on the welds. In a casting, flaws are suspected everywhere and are especially searched for at points where the casting will be subjected to the greatest stresses in service, where a break would be disastrous, even though the stress may not be high, where there is a sudden change in section, and where previous experience has revealed flaws.

The flaws found in castings differ from the flaws found in welds. Among the common internal flaws occurring in ferrous castings are "blowholes," shrinkage cavities, or "draws," "pipes," cracks, "cold shuts," and inclusions (of slag, sand, etc.). Blowholes are cavities due to entrapped gases and usually appear in the radiograph as circular or elliptical spots. Shrinkage cavities, or draws, have a rough interior surface with projecting dendrites and appear in the radiograph as a flaw of irregular outline, usually with a ragged edge. A pipe is a series of draws extending in a line, this condition being due to shrinkage. A crack appears as a ragged line in the radiograph when the rays are in the plane of the crack. When the rays are inclined at a large angle to this plane, the crack may not show at all, or it may appear as a slightly darkened irregular stripe, scarcely noticeable. A cold shut is an imperfection caused by metal entering the mold through different sprues, cooling, and failing to unite on meeting. This appears as a smooth line in the radiograph when the rays are in the plane of the cold shut, but may escape notice when the rays are inclined at a large angle to this plane. An inclusion usually appears as an irregular, but not ragged-edged, spot in the radiograph.

The usual role of radiographic inspection in producing castings is to examine critically the first ones made, to discover the type and location of the flaws. This information then usually enables the foundryman to change the casting technique by altering the gating, relocating chills, changing pouring temperatures, etc., in such a way as to eliminate the flaws or at any rate to minimize them or to cause them to appear in a part of the casting where they are less objectionable. Having discovered an acceptable casting technique, the casting can then be put into production. There are cases, for example in the aircraft industry, where the use of more metal than that actually needed is not permitted. In such cases, the assurance that 999 out of 1,000 castings made in a certain way will be sound may not be enough. It may be imperative that that thousandth unsound casting be detected and rejected. This may be done by incorporating radiographic inspection as one of the steps in the production process.

With large castings of irregular shape, there are sometimes corners and awkward locations where it is impossible to place a standard-sized

cassette or film holder in order to take the desired radiograph. In such cases one may improvise by cutting the film to the required size and shape and wrapping it in black paper held in place with scotch tape or paper clips. Small films of this type can be pressed between pieces of stiff cardboard faced with lead foil and held with paper clips. Such films are ordinarily placed at inside locations with the x-ray tube outside. In such situations, it is well to consider the possibility of suspending a

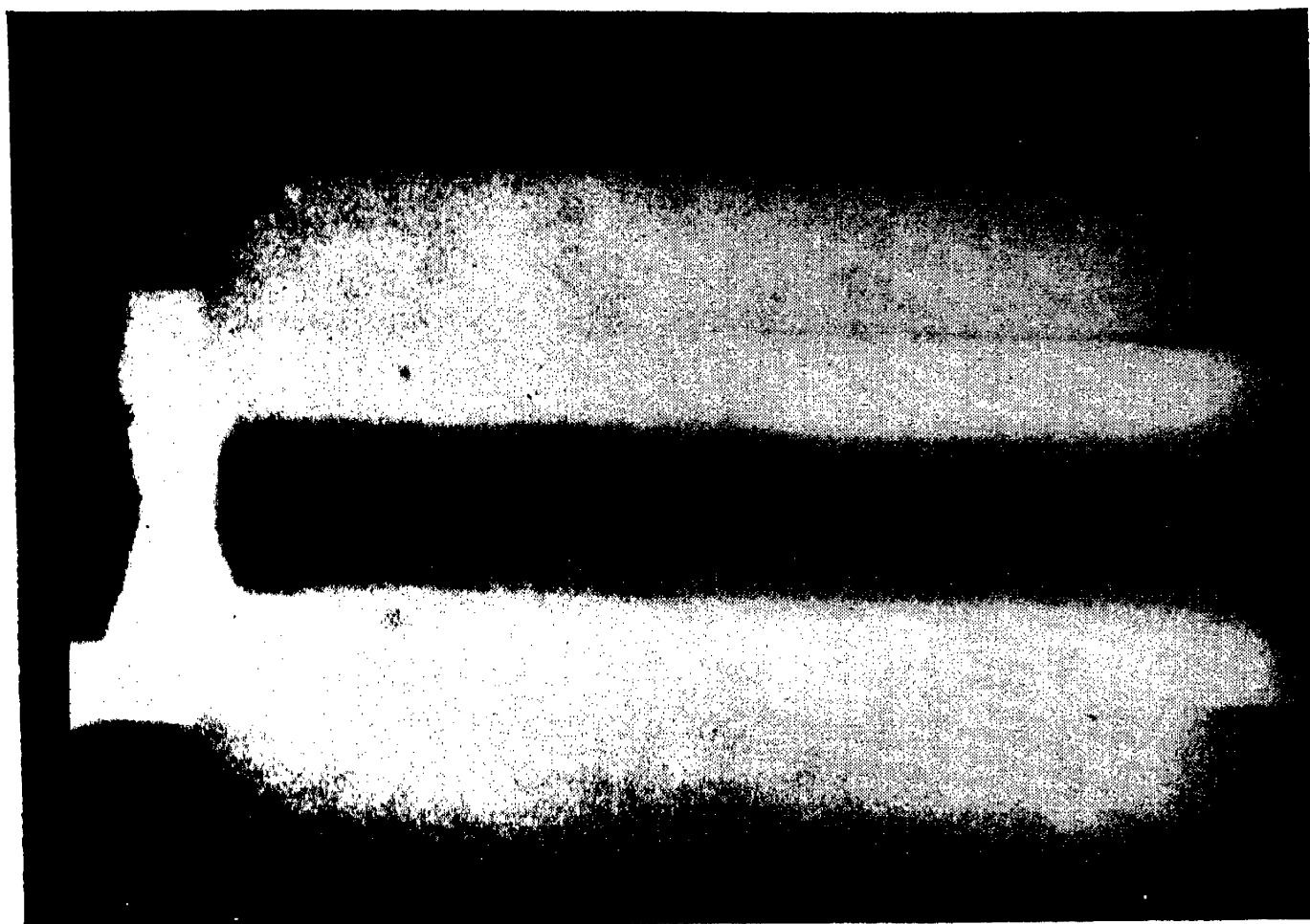


FIG. 12-21.—Porosity in steel casting for cylinder liner.

radium capsule inside and placing the film outside in a standard-sized film holder or cassette. The exact location of flaws in a complex casting, once they have been detected, may sometimes be most easily determined by means of stereoscopic radiography, as outlined on page 219.

Figure 12-21 is a radiograph of a hollow cylindrical steel casting to be used for a cylinder liner in an engine, after machining. Porous areas near the left end of the casting consisting of numerous small blowholes are seen. The walls of the casting were about  $\frac{3}{8}$  in. thick. It was laid on a lead-lined cassette containing nonscreen film and half buried in shot. Note the flange on the left end. This would permit shot to sift under the casting at this end. To prevent this, a rolled aluminum strip was laid under the casting, the thickness of the aluminum being equal to

the distance the flange projects radially beyond the outer surface of the casting. To prevent shot from sifting inside the casting, a piece of thin cardboard or an old magazine several inches longer than the casting

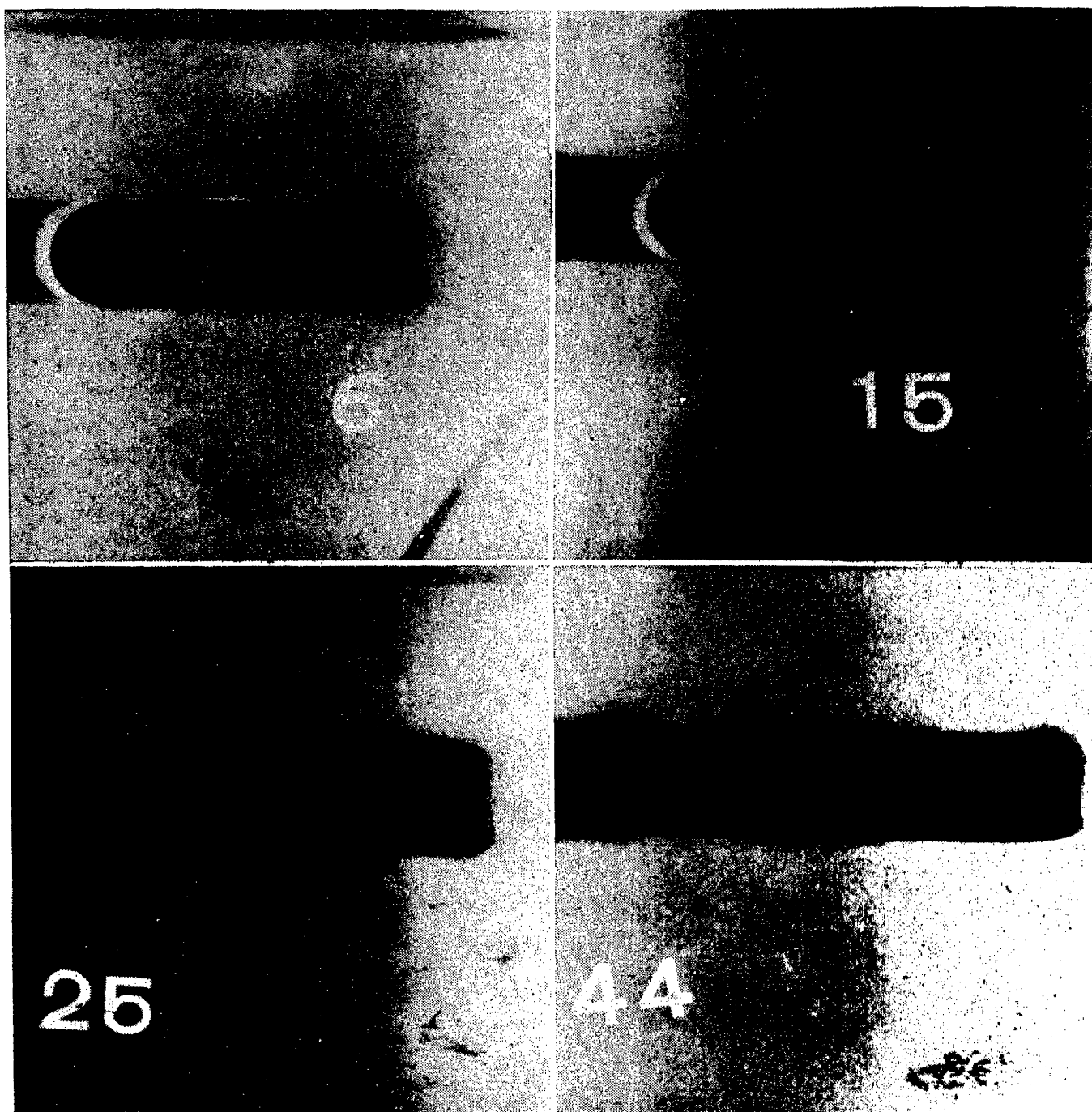


FIG. 12-22.—Shrinkage cavities in cast-iron valve sleeves.

may be rolled up and inserted inside and then allowed to spring out against the inner walls. Such simple tricks as this take very little time yet noticeably improve the quality of the radiograph.

Figure 12-22 is a radiographic print of four cast-iron valve sleeves for a sleeve-valve type of internal-combustion engine. All four show shrinkage cavities, or draws, quite prominently.

Figure 12-23 is a radiograph of a section of a heavy cast-steel door



about  $1\frac{1}{2}$  in. thick, with lugs, bosses, and a flange near the edge. The heavy lugs represent a sudden and extreme change in section; and, as often happens in such cases, cracks result. Strange as it may seem, neither the bad crack nor the fine ones parallel to it could be seen on the surface of the casting, even after the radiograph showed exactly where

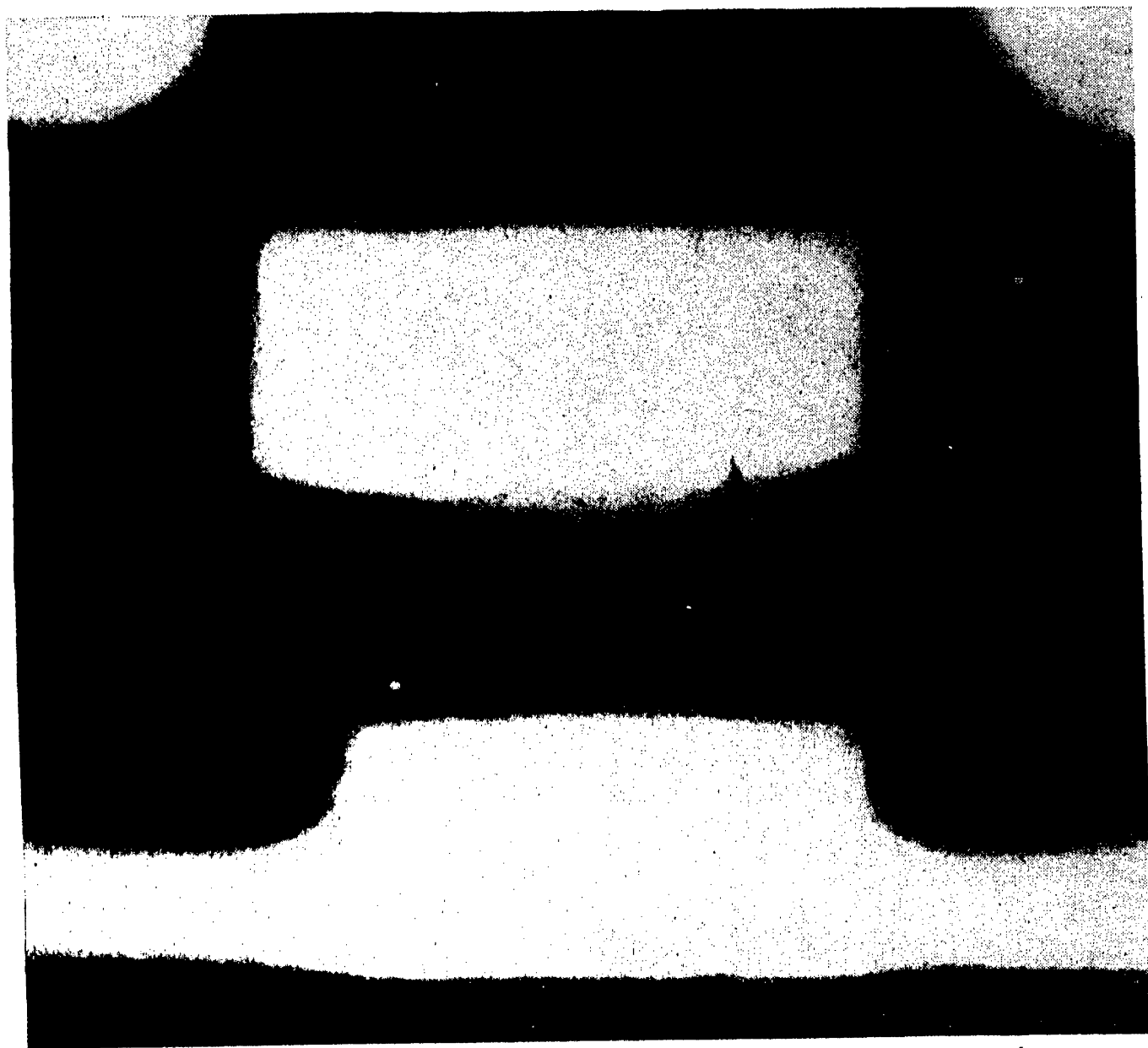


FIG. 12-23.—Cracks in steel casting located near abrupt change in section.

one should look for them. A few blowholes are also seen. This radiograph was taken with screen technique, a lead-lined cassette being used. A  $\frac{3}{16}$ -in. lead strip was tucked under the edge of the door as blocking material. Note that an exposure light enough to reveal detail in the door proper is too light to reveal anything in the heavy lugs, which project about 2 in. above its surface.

The remedy for this situation is to use extremely hard radiation. Figure 12-24 is a radiograph of another heavy cast-steel door, with

thicknesses varying from about  $\frac{3}{4}$  in. in some spots to about  $2\frac{1}{2}$  in. in others. Since this is a copy of the original film, rather than a print, cavities appear as dark spots on a light background. Cavities are to be seen in two regions, both circled in the figure. The remarkable feature is that one region is in one of the thickest parts of the casting, and the other in one of the thinnest parts; yet both appeared clearly in

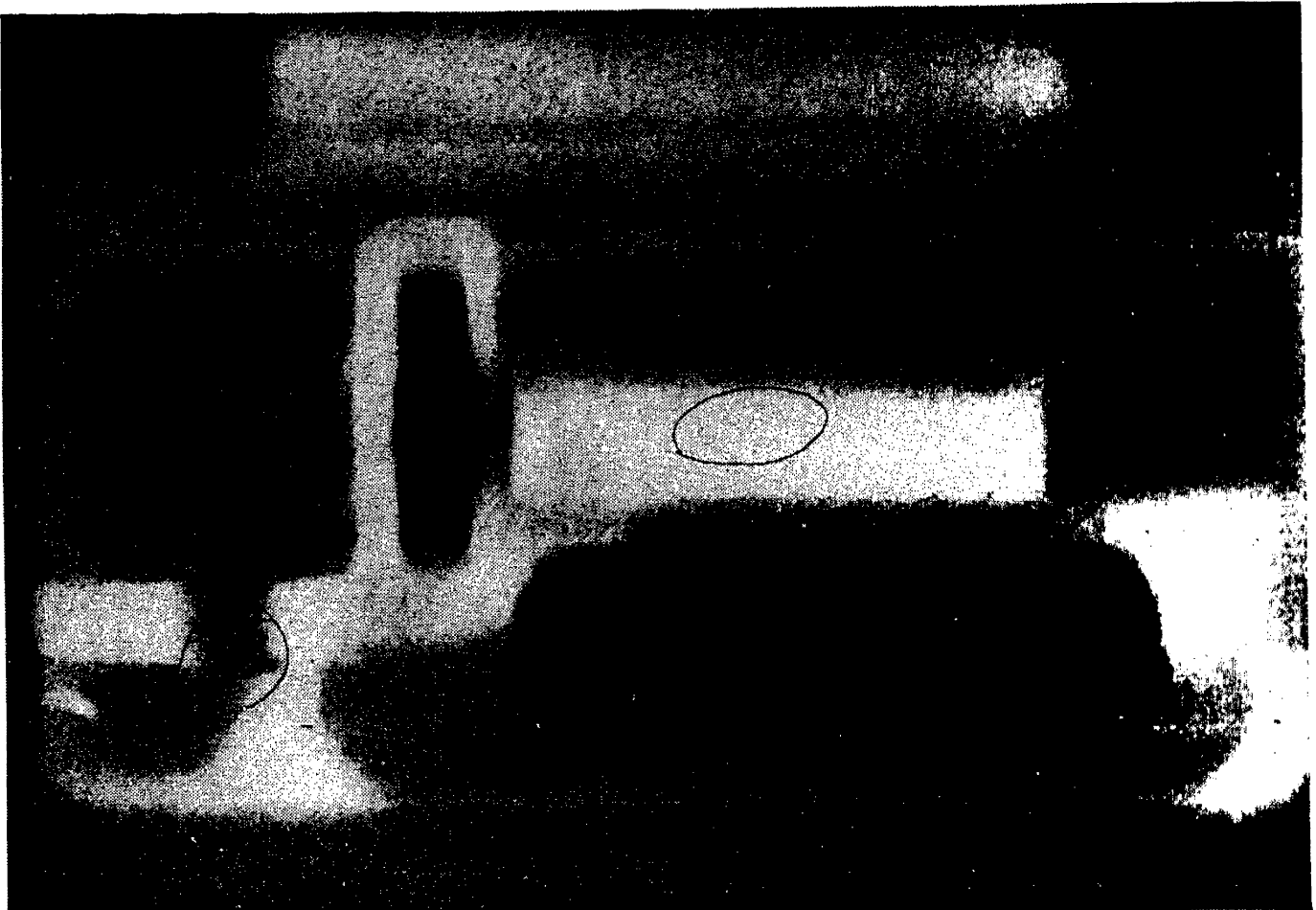


FIG. 12-24.—Gamma-ray radiograph of heavy steel-door casting.

the same radiograph on the first attempt. This could be achieved only with radium or supervoltage x-rays. With x-rays generated at ordinary voltage, a long exposure would be required to reveal one region and a short exposure to reveal the other.

**10. Forgings.** In general, steel forgings are quite free of gross macroscopic flaws of the types just mentioned in the discussion of castings. Engineers usually rely on this fact so confidently that they regard the radiography of forgings as a waste of time, effort, and money. After having radiographed many forgings and discovering only a few serious flaws,<sup>1</sup> the author feels that there is considerable justification for this view. Figure 12-25 is a typical radiograph of a forging—it reveals no

<sup>1</sup> Some large forgings contain flaws due to cavities which were present in the original ingot.

defects. It is evident that this forging has a shape complex enough so that, if it were a casting, one could be fairly certain that a radiograph would reveal at least a few scattered cavities or similar minor defects.

One of the commoner types of flaw in a forging occurs when a ridge of metal folds over and is hammered down flush with the surface so that it appears smooth or perhaps reveals only a faint line. This condition is usually called a "lap" or sometimes a "fold." The metal at the lap usually does not knit together as homogeneously as if the lap were

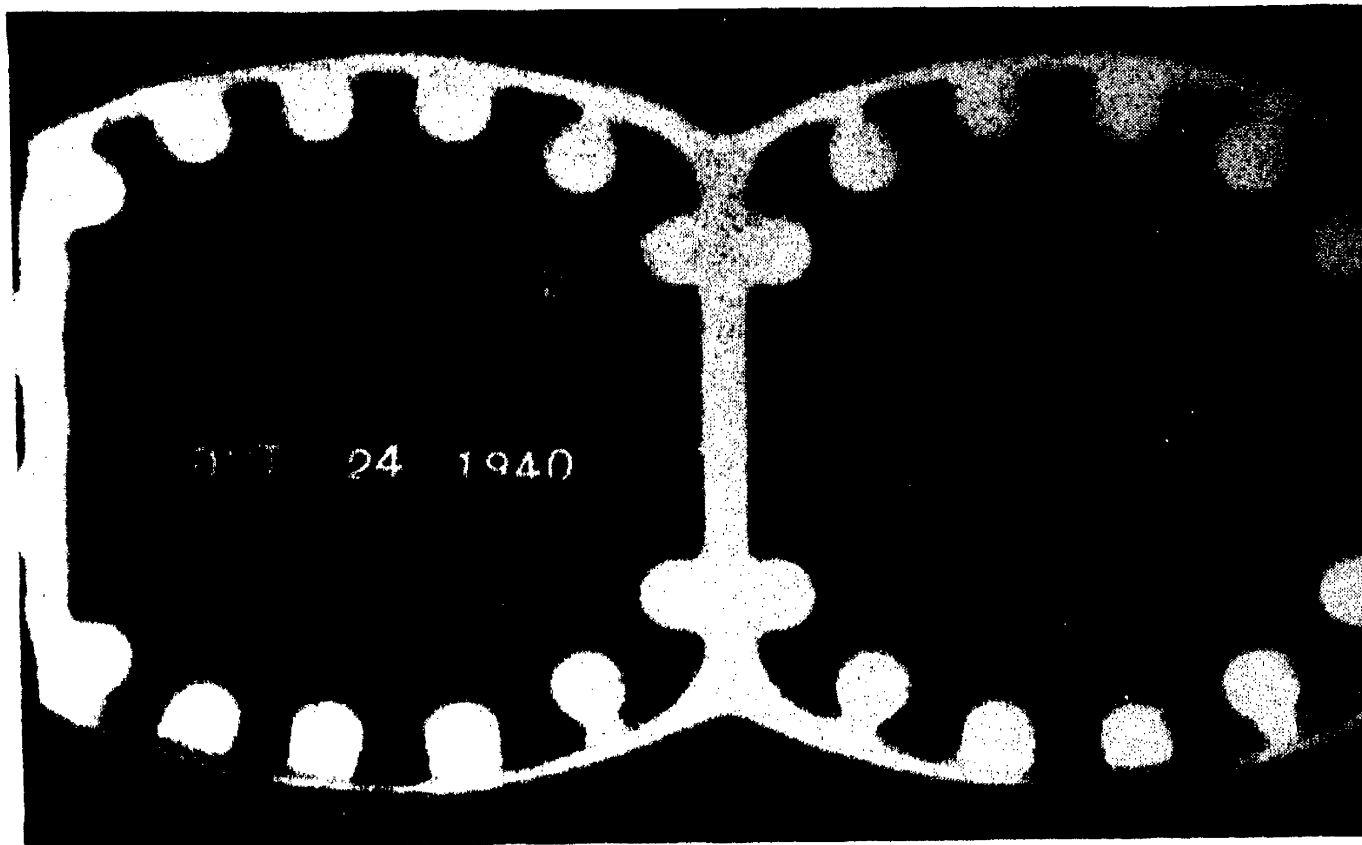


FIG. 12-25.—Radiograph of steel forging.

absent, and so a condition somewhat analogous to a cold shut in a casting may exist. However, it is difficult or impossible to detect such laps in a radiograph if the metal has been thoroughly mashed together so as to make intimate contact over the whole surface of the lap, even though the interpenetration, or knitting together, of the metal at this surface may be superficial or lacking entirely. If the x-rays traverse the forging in the plane of the lap (or the casting in the plane of the cold shut), the chances of observing it are much better than if the rays are inclined to this plane; but this type of flaw, like a fine crack, may easily escape detection.

**11. Bonding.** The above discussion of cold shuts, fine cracks, and laps suggests the analogous problem of determining the quality of bonding by radiographic methods. In the manufacture of such articles and

steel-backed bearings of bronze, babbitt, silver, etc., the surface of the steel backing is prepared by making it very smooth and very clean. Likewise, the soft bearing metal or alloy is given a smooth, clean back surface. Then the two are soldered together using a flux and a solder that usually melts at a temperature near the melting point of the bearing metal. If properly made, the bearing metal will be bonded to its steel backing so tenaciously that any effort to remove it will result only in

tearing it in shreds; the bond is as strong as or stronger than the bearing alloy itself. However, if some step in the manufacturing process is improperly executed, the bond may be poor and the bearing metal under severe operating conditions may be pulled loose from its backing in spots. A nondestructive test for this condition is much sought after, but the radiographic methods so far devised are of little value in this problem.

If the faces of two equal-sized steel blocks are machined and polished flat and then pressed together firmly by a C clamp, a radiograph will show them as a single block, even though there is no bond whatever between them.

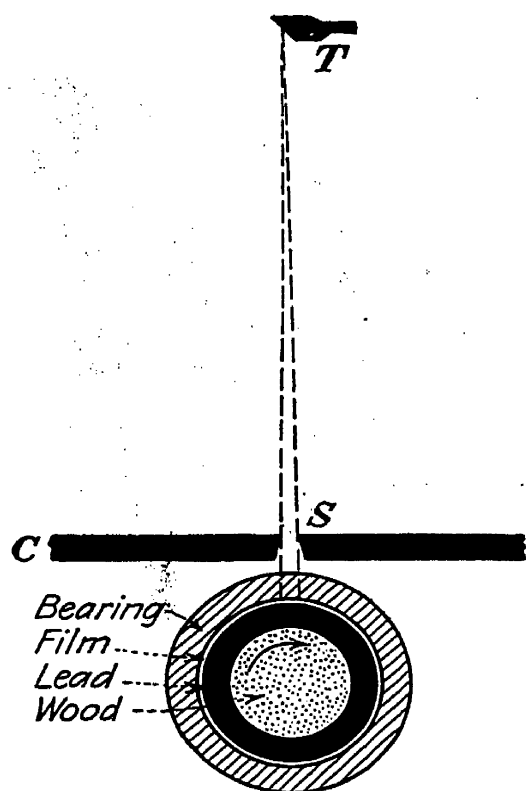


FIG. 12-26.—Arrangement for radiographing plain bearings.

arrangement of the type indicated in Fig. 12-26. A nonscreen x-ray film is wrapped securely once around a lead-sheathed wood roll, or mandrel. The film may then be covered with black paper for protection. The diameter of the roll, or mandrel, must be such that the bearings to be radiographed will slip over the paper-covered film tightly enough so that they will not wobble or slip when the roll revolves slowly. A lead cover *C* is provided with a slit *S* parallel to the axis of the roll. The whole equipment may be located in a darkroom to prevent fogging of the film by light, or it may be enclosed in a lighttight lead cabinet.<sup>1</sup>

With the x-ray tube target *T* in the position shown, the exposure is made while the roll is slowly rotated at a constant speed. The greater the distance *TS* and the narrower the slit, the finer will be the detail shown in the radiograph but the longer the exposure time becomes. The best compromise depends upon the thickness, diameter, and material

<sup>1</sup> This type of equipment is illustrated in *Gen. Elec. Rev.*, 45, 54 (1942).

of the bearings, the size of the focal spot, the tube current and voltage, and the size of the smallest pores that the radiograph is required to reveal; this compromise can best be determined by trial.

Although the radiography of bearings is a special problem, it is as a typical example of the radiography of small, hollow cylindrical objects with at least one open end.

**13. Aluminum and Magnesium.** The radiography of aluminum castings differs from the radiography of ferrous castings (Sec. 8) only in minor respects. The lower absorption coefficient of aluminum and magnesium makes it possible to obtain radiographs of castings of these metals at ordinary voltages such as 200 kv. or less that are comparable with radiographs of ferrous castings obtained by using radium or million-volt equipment. The use of blocking material is rarely required in either of these instances.



FIG. 12-27.—Distributed pin-point porosity in cast aluminum.

The defects commonly encountered are similar to those in ferrous castings. In general, gas cavities and shrinkage cavities are more common and more widely distributed in aluminum castings than in ferrous castings. Widespread distributed porosity and large local draws and pipes are frequently present, for aluminum shrinks while solidifying more than cast iron or steel. Gas is more easily trapped in an aluminum casting than in a ferrous casting. Aluminum is one of the metals that develops a scum on its surface while it is molten, such a scum being called "dross." Dross is occasionally poured into the mold, in spite of efforts to avoid this, and is therefore sometimes revealed by radiographs, usually scattered through the casting in small pieces.

Figure 12-27 is a radiograph of a cast-aluminum plate after machining down to a thickness of  $\frac{1}{8}$  in. It is seen that there are hundreds of small cavities distributed throughout the metal, especially at the right end, which was next to the gate. This type of radiograph is helpful in studying the effects of variables in the casting technique, such as pouring temperature, metal composition, gating, and use of chills. To show such fine flaws, a fine-grained contrasty film should be used, without screens of any kind. An exposure of  $\frac{1}{2}$  min. at 100 kv.p., 5 ma., was used in taking Fig. 12-27, the tube-to-film distance being 6 ft. The condition illustrated in Fig. 12-27 is often called "pin-point porosity."

It is sometimes caused by the agglomeration of absorbed gas, sometimes by shrinkage, and sometimes by both. Aluminum contains considerable absorbed gas. When the metal melts, the gas sometimes agglomerates in small bubbles somewhat as it does in water heated to 80°C., for

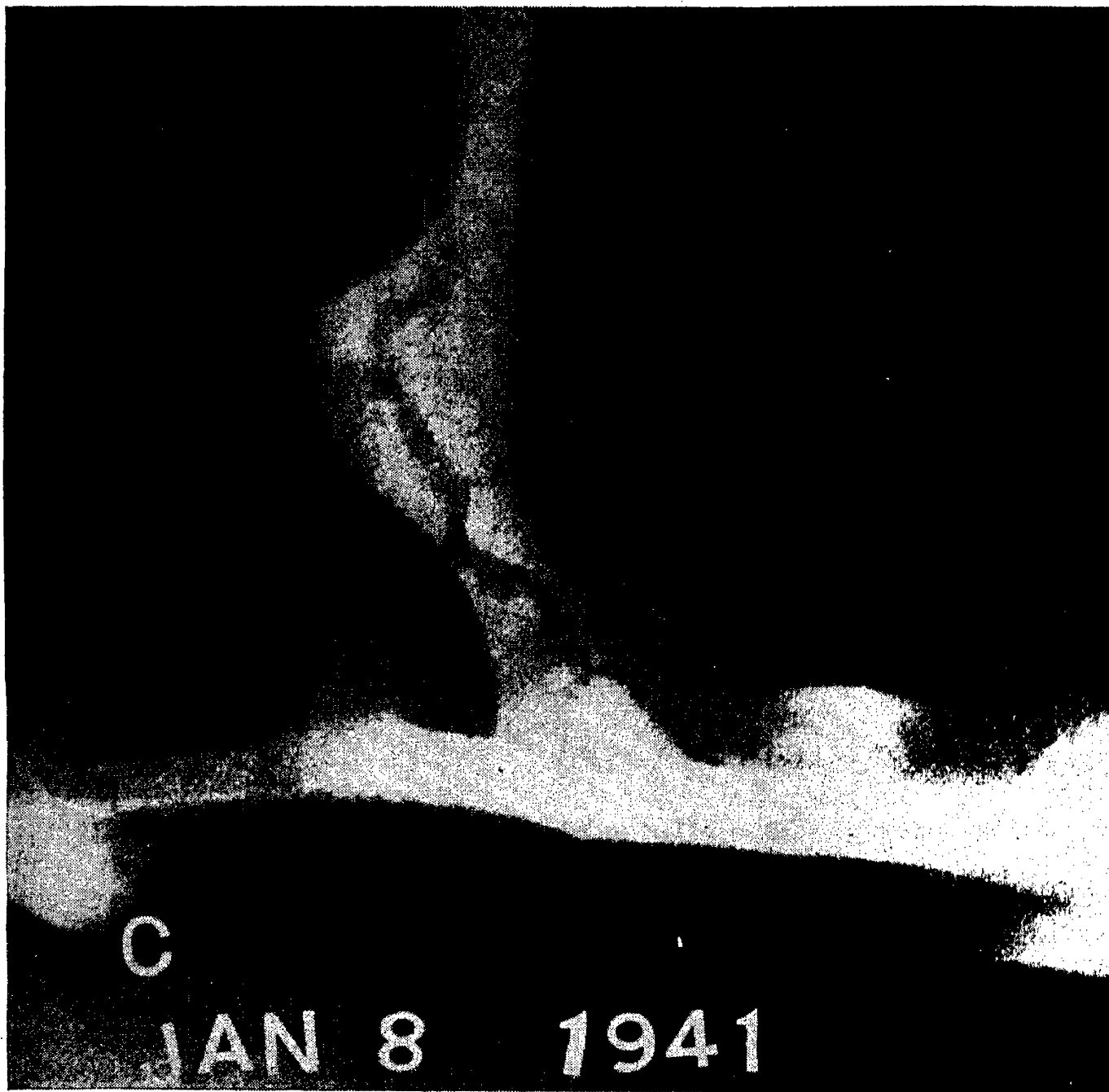


FIG. 12-28.—“Wormhole” or pipe in an aluminum casting.

example. When the metal freezes, these small bubbles sometimes remain scattered through it. Under certain conditions, the metal shrinks in such a way as to produce hundreds of small cavities fairly uniformly distributed, rather than a localized draw in the part of the metal that freezes last. The pin-point porosity near the right end of Fig. 12-27 is primarily due to shrinkage. This was determined by sectioning, etching, and examining the cavities with a microscope. The dendritic structure

of the cavities is characteristic of shrinkage and indicates that it is the primary cause.

Figure 12-28 shows a radiograph revealing a wormhole or pipe 5 to 6 in. long in an aluminum casting. These nearly always have one opening at the surface of the metal, and careful visual examination of the surface usually reveals their presence. However, when one of these orifices is seen on the surface, the opening is usually less than  $\frac{1}{16}$  in. in diameter, and it is usually not possible to tell whether the wormhole has a length of  $\frac{1}{2}$  or 6 in. or which direction it takes from the opening. Sometimes a fine wire can be pushed 2 in. into such a hole, but radiography will reveal that it has a length of 5 in., for example, and whether or not it penetrates into a vital part of the casting.

The radiograph in Fig. 12-28 was taken by laying the casting on a cardboard film holder and using nonscreen film. The thickness penetrated by the x-rays probably varied from  $\frac{1}{4}$  to 2 in., the average thickness being perhaps  $\frac{1}{2}$  in. Stereoradiography (page 219) is helpful in locating flaws in a casting of this sort.

Most of the castings brought to a radiographic technician for examination have an irregular shape, wide variation in thickness, and few if any flat external surfaces against which one can lay a flat cassette. Consequently, the problem of the radiographer frequently is to increase latitude, that is, to reduce the contrast, rather than increase it (see Fig. 12-1). Only occasionally are the time and money available to take several radiographs, some heavily exposed to show detail in the thick sections, some lightly exposed to show detail in the thin sections, some moderately exposed to show detail in the average sections. However, one may take a radiograph, of the type shown in Fig. 12-29, and rotate the casting 90° and take a second exposure; in this way, flaws appearing in both views can be accurately located, and flaws not revealed in one view are practically certain to appear in the other.

To obtain the low contrast or wide latitude needed for typical castings of this sort, one should use nonscreen film and keep the exposure low and the voltage high. Radiographing aluminum castings at 200 kv. is much like radiographing ferrous castings at a million volts; blocking material is rarely needed.

This wide-latitude technique permits some of the fine detail such as pin-point porosity to escape notice, but a surprising amount can nevertheless be seen. Figure 12-29, for example, is a radiograph of a cast-aluminum crankshaft having bearing journals more than 4 in. in diameter, the radiograph being taken by laying the casting on a lined cassette, without blocking, and exposing at 200 kv.p., 5 ma., 5 sec. This radiograph reveals a few shrinkage cavities, some including cross in the lower right portion of the connecting-rod journal, and a

spread pin-point porosity throughout, even though the thickness penetrated by the rays varies from 1 to 5 in.

When a thin flat slab is to be radiographed, as in Fig. 12-27, to show fine detail as clearly as possible, one then increases the contrast by using

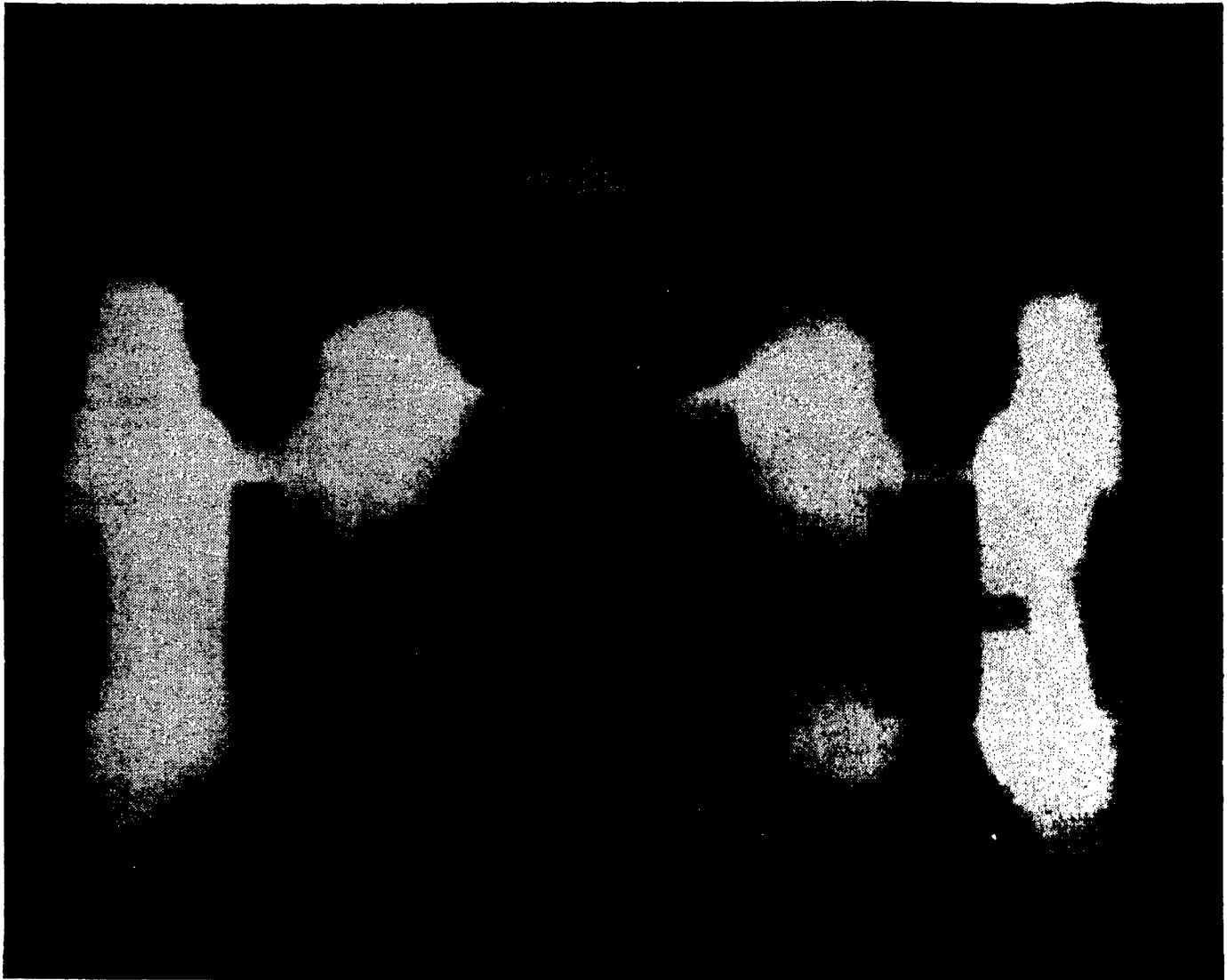


FIG. 12-29.—Porosity and shrinkage in an aluminum casting of irregular contour.

an entirely different technique. Figure 12-30 is a similar radiograph showing the difference between rolled- (4), extruded- (5), and cast- (66) aluminum plate. The latter shows considerable porosity, whereas the rolled plate shows none at all. The extruded aluminum shows an intermediate degree of porosity. This radiograph was taken with a cardboard film holder (no lead foil), an extra-fine-grained nonscreen film, at 120 kv., 5 ma., 30 sec., the tube-to-film distance being over 6 ft. so as to obtain the effect of a true "point source" of the x-rays.

X-ray motion pictures of the molten metal being poured into the mold have been found helpful for small aluminum castings. See page 225, and footnote reference to S. L. Fry.

**14. Spot Welds.** The spot welding of aluminum sheets is a process



widely used in aircraft construction. The quality of spot welds depends upon electrode size, shape, temperature,<sup>1</sup> and cleanliness, the current used and its duration, the pressure applied, the thickness and composition

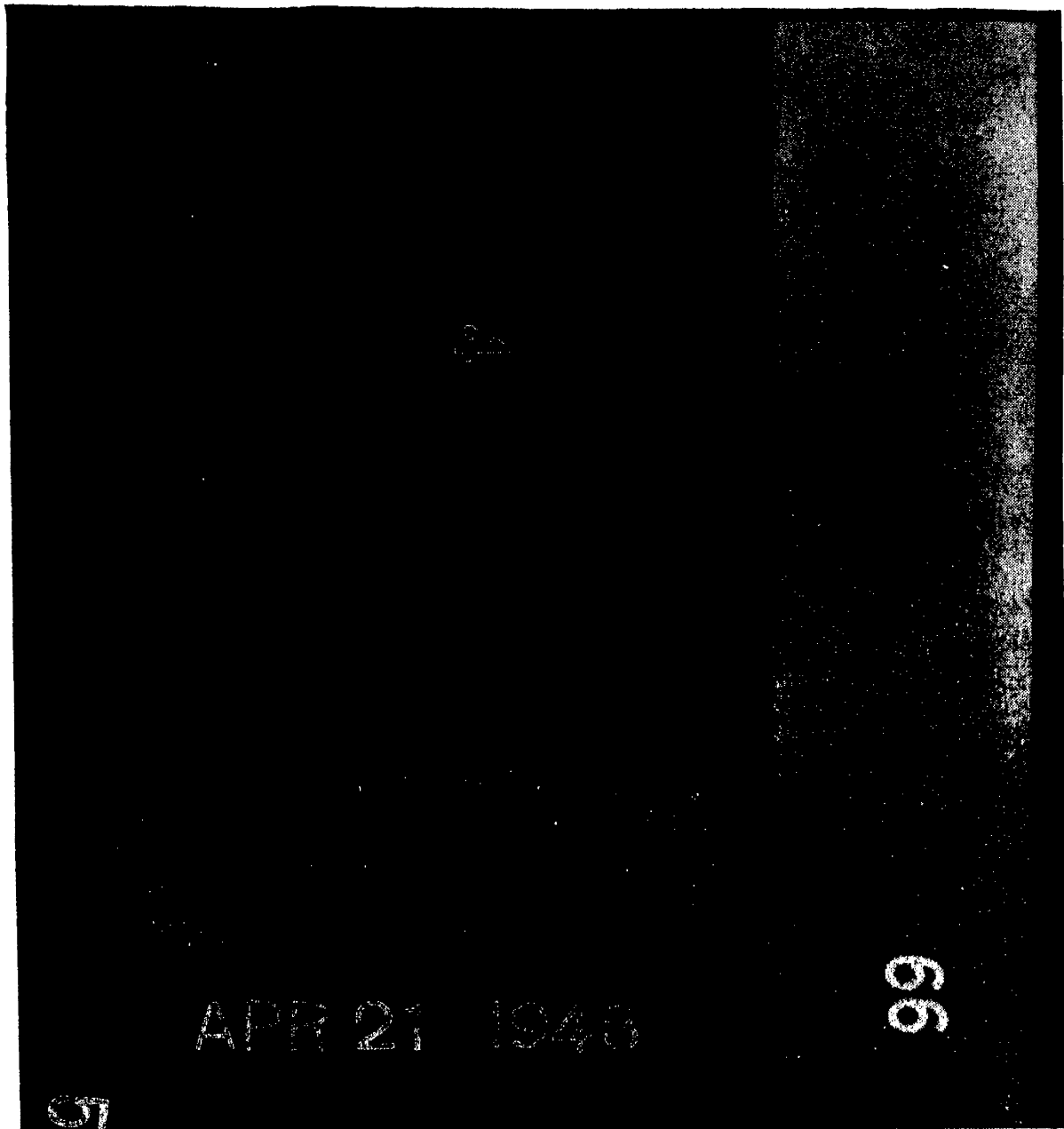


FIG. 12-30.—Rolled aluminum (4), free of porosity; extruded aluminum (5), slightly porous; cast aluminum (66), moderately porous.

of the sheets, etc. Some information about the quality of spot welds and how it is related to the aforementioned factors has been obtained by radiographic methods, and several well-illustrated articles describing the details have been published.<sup>2</sup> Figure 12-31 is a radiograph of two

<sup>1</sup> See, for example, F. M. Reek, *Aero Digest*, **41**, 164 (October, 1942).

<sup>2</sup> D. W. Smith and F. Keller, *J. Am. Welding Soc.*, **21**, 573 (supplement) (1942); R. Taylor, *Aero Digest*, **43**, 263 (July, 1943); R. C. Woods and V. C. Cetrone, *Iron Age*, **151**, 52 (Mar. 25, 1943); G. W. Scott, L. G. Sutton, and J. H. Widmyer, *Welding J.*, **23**, supplement, p. 560-S, November, 1944.

experimental welds of this type, with  $\frac{1}{8}$ -in. sheets. It was taken with a tube having a focal spot 1 mm. in diameter, at a distance of 42 in., 50 kv.p., 5 ma., 12 sec., with a paper cassette and a fine-grained nonscreen film. The small size of the welds makes it advisable to use a very fine-grained film and enlarge the radiograph several diameters, somewhat as

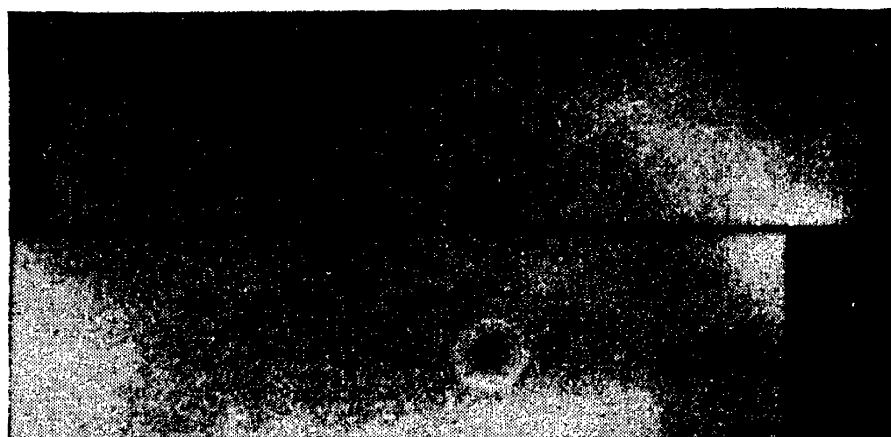


FIG. 12-31.—Spot welds in aluminum sheet.

described in Sec. 13-3. Woods and Cetrone<sup>1</sup> recommend the use of 12-kv. continuous radiation for this work. In attempting to use such a low voltage with ordinary radiographic x-ray tubes, one is likely to encounter difficulty due to space-charge limitation of the tube current (page 115), and with shockproof tubes the inherent filtration of the tube

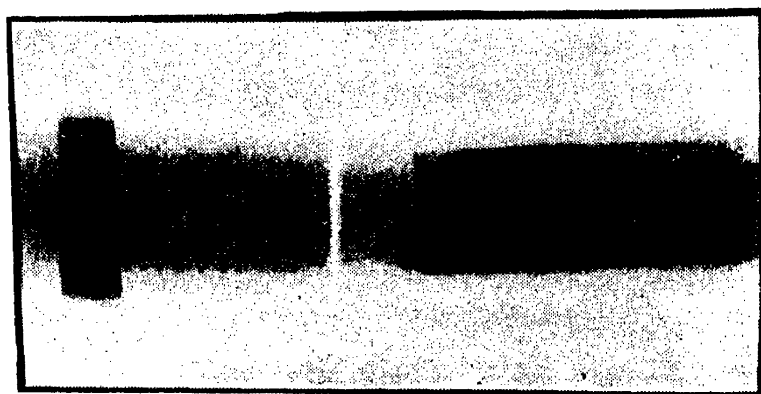


FIG. 12-32.—Spot weld in stainless steel sheet.

(page 231) may defeat the purpose of the very soft radiation by absorbing most of it. This may partly account for the greater success attained by the use of tubes with thin windows designed for diffraction work, as reported by various workers in microradiography (page 287). The lower radiograph in Fig. 12-31 shows small cracks radiating from the center of the weld “nugget,” as it is called by Smith and Keller.

Spot welding is a common means of fabricating structures from sheet steel. Figure 12-32 is a radiographic print of a spot weld joining two pieces of  $\frac{1}{8}$ -in. sheet steel. It was obtained at 80 kv., 5 ma., in 5 min.,

<sup>1</sup>See footnote 2 on page 273.

with a fine-grained nonscreen film with no screens, placed 26 in. from the target.

**15. Die Castings.** By using the die-casting process, many intricately shaped parts are cast with surfaces so smooth and dimensions so accurate that little or no machining is required. These are made from various alloys, among which the zinc-base alloys have been widely used. A good example of the complex shapes made by die casting zinc is the

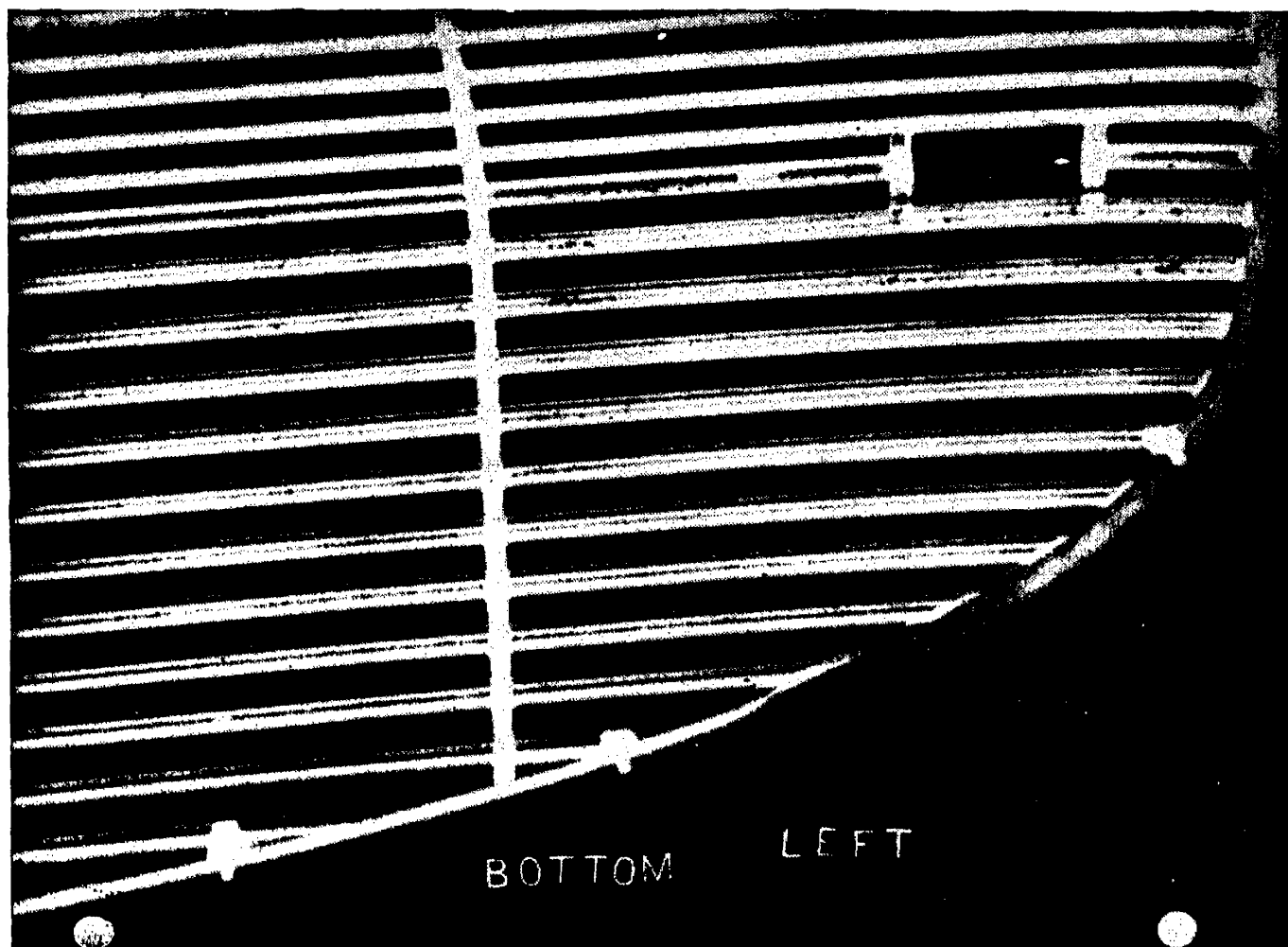


FIG. 12-33.—Porosity in early experimental zinc die-cast radiator grille.

casting for an automobile radiator grille. Figure 12-33 shows a radiograph of one of the first castings made for a particular model of grille. Note the clusters of trapped air bubbles in certain sections of the casting. Porosity due to entrapped gas is probably the most common type of flaw in zinc die castings. It is easy to detect and locate such porous areas by radiography. Once this is done, a die-casting expert can deduce what changes to make in the casting technique to correct the trouble. A change in the gating of the grille of Fig. 12-33 eliminated the porosity before production was started. Zinc has a fairly high linear absorption coefficient; but as a rule zinc die castings have thin sections so that they can be radiographed at ordinary voltages, such as 200 kv. or less.

In radiographing small die castings or any small objects, for that matter, such as door handles or vacuum tubes, it is often desirable to radiograph the objects in one position and then rotate them  $90^\circ$  so as to obtain both a "plan" and "profile" view. If six such objects are to be radiographed, for example, they may be laid on the upper 5 by 8 half of an 8- by 10-in. film holder, the lower half being covered with a sheet of  $\frac{3}{16}$ - or  $\frac{1}{4}$ -in. lead. After the radiograph is made, the lead can be placed over the upper half and the parts transferred to the lower half, where they are laid down rotated  $90^\circ$ . The film holder (or the

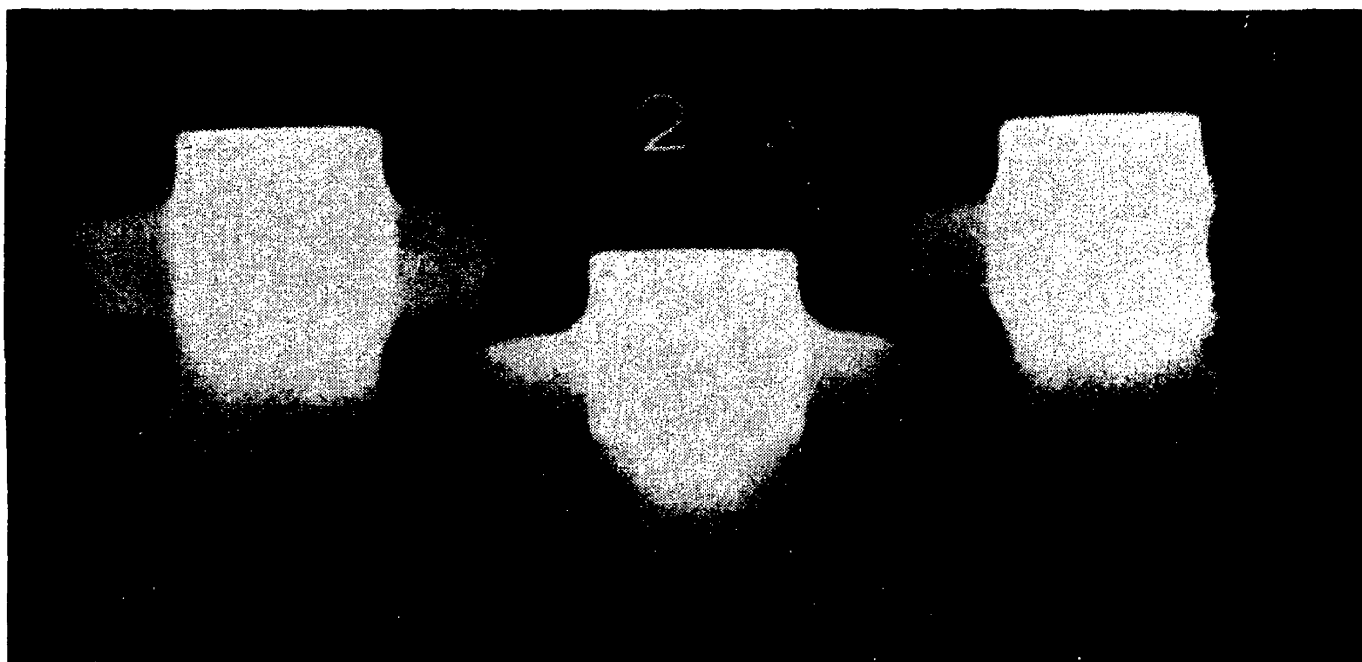


FIG. 12-34.—Porosity in cast copper welding electrodes.

x-ray tube) should be moved between exposures so that the target is directly over the object in both exposures.

**16. Bronze, Brass, and Copper Castings.** These castings are often thick and massive; and since the linear absorption coefficient of the metals and alloys is high, it is often necessary to use radium or super-voltage x-rays to obtain satisfactory radiographs. Large shrinkage cavities are common. Figure 12-34 shows radiographs of three cast copper welding electrodes  $\frac{5}{8}$  in. thick. These radiographs were taken with nonscreen film using lead screens, target-to-film distance 30 in., 200 kv.p., 4 ma., and 45 sec. The right-hand lug of electrode 3 is seen to be so porous that it will break off easily. To make objects like this stand up on the cassette for radiography, they may be leaned against wood blocks.

Bronze, brass, and copper castings should be radiographed if they are to be subjected to high stresses unless a liberal allowance has been made for porosity and shrinkage cavities.

**17. Concealed Assemblies.** There are numerous articles which are welded or sealed together in such a way that subsequent visual inspection of the finished assembly is impossible. Examples are radio vacuum tubes, pressure gauges, rubber tires and fan belts, and exhaust mufflers. In some cases, radio vacuum tubes are being subjected to production-

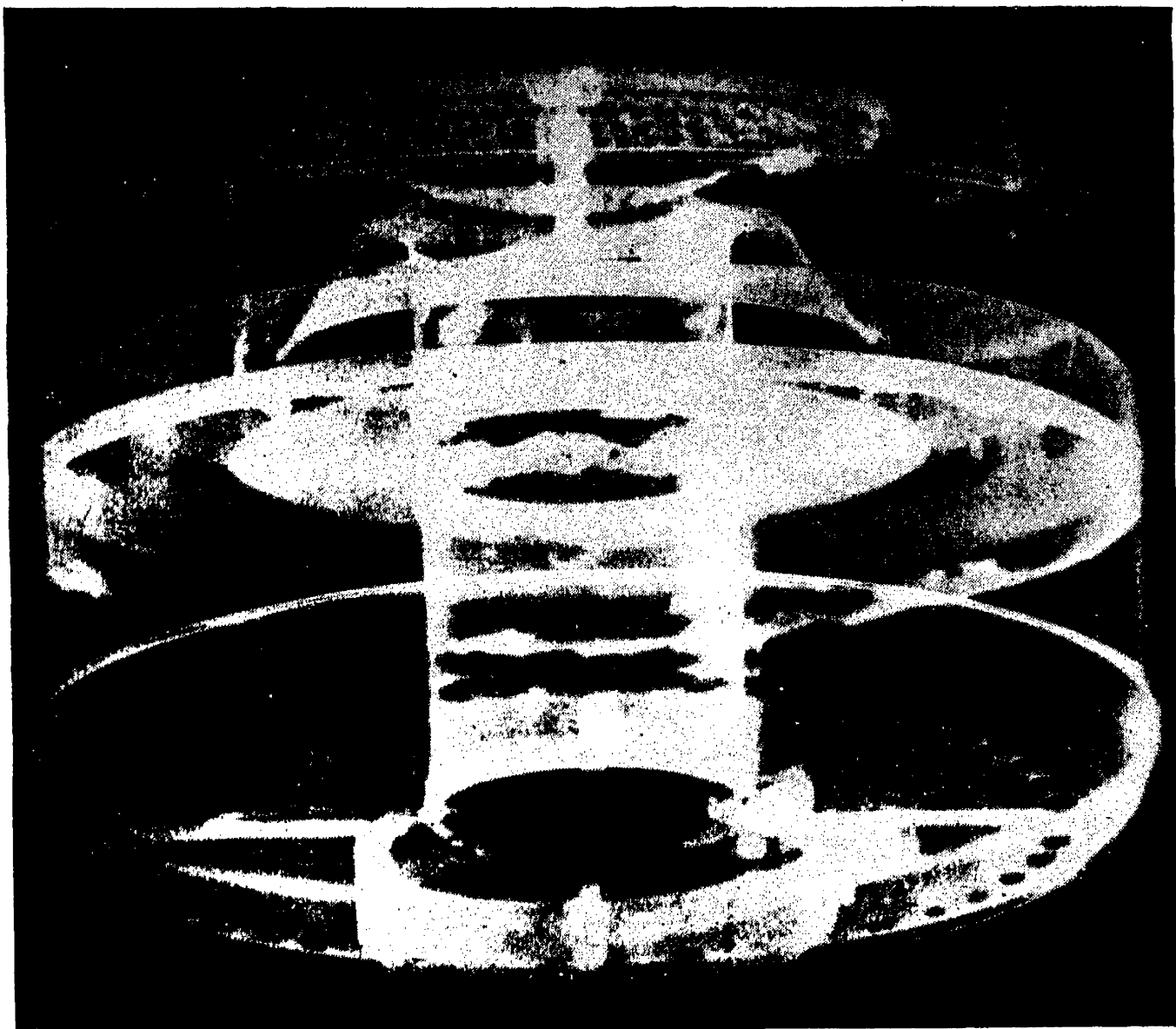


FIG. 12-35.—Radiograph of welded intake silencer—air cleaner.

line inspection by radiographic or fluoroscopic methods to check the alignment and spacing of the elements.

Figure 12-35 is a radiograph of a welded intake silencer—air cleaner for automotive use. These units are welded together in such a way that their internal assembly cannot be determined except by radiography without destroying the article. In expensive radio power tubes it may be advisable to inspect each one fluoroscopically or radiographically. Before and after making sound tests or air-flow resistance tests of a welded exhaust muffler or an intake silencer, for example, it is well to check the internal parts for alignment radiographically.

Figure 12-36 is a radiograph of a heavy-duty rubber belt reinforced with small steel cables instead of the usual cotton cord. By taking such radiographs periodically during the course of a life test of the belt, the manner in which the wear and tear deteriorates the cables and finally causes them to fail can be readily determined.

**18. Gamma-ray Radiography.** Figure 8-1 indicates that the gamma rays from radium are somewhat harder than million-volt x-rays. The intensity of the x-rays at a given distance from the target of a million-volt x-ray tube as ordinarily operated is equal to the intensity of the gamma rays from several pounds of radium. This means that a piece of steel 5 in. thick can be radiographed with gamma rays from radium in

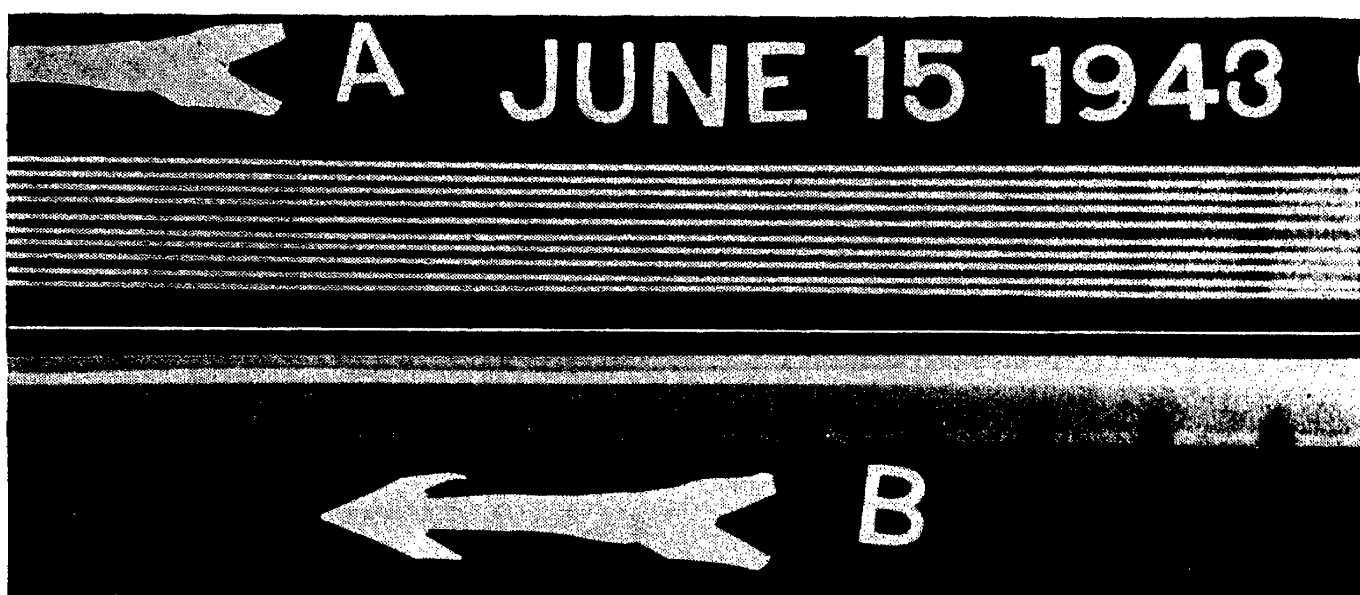


FIG. 12-36.—Radiograph of wire-reinforced rubber belt.

2 or 3 days, whereas it could be radiographed with million-volt x-rays in a few minutes. With material of more ordinary thickness, such as steel  $\frac{1}{2}$  in. thick, the time required for radiography with radium drops to 3 or 4 hr., but such material can be radiographed with better sensitivity by using x-rays from ordinary 140- or 200-kv. equipment in about a minute.

Nevertheless, in many cases there is a great advantage in the use of radium for industrial radiography. If the need for radiographing castings or other objects too thick for 220-kv. equipment arises only infrequently, it would be uneconomical to build a suitable room and buy a million-volt x-ray outfit for about \$100,000 that would be needed only for a few minutes every month or two, for 100 mg. of radium to radiograph the castings, etc. can be rented at a cost of about \$7 per day or \$25 per month. If, on the other hand, it is necessary to radiograph 300,000 six-inch-thick castings, million-volt x-ray equipment should be used.

The small portable radium container (page 208) offers obvious radio-

graphic advantages for projects such as the inspection of welded joints in the Moffat tunnel.<sup>1</sup> There are also many cases where the piece to be radiographed is hollow. Examples are pressure vessels 1 ft. or less in inside diameter, large high-pressure pipe, valves and fittings and cannon. Such pieces can be radiographed with radium by suspending it inside on a fishing line and placing film holders around the outside. For solid cylinders or bars of large diameter, gamma rays or supervoltage x-rays are needed to give a satisfactory radiograph. Rays of 220 kv. and

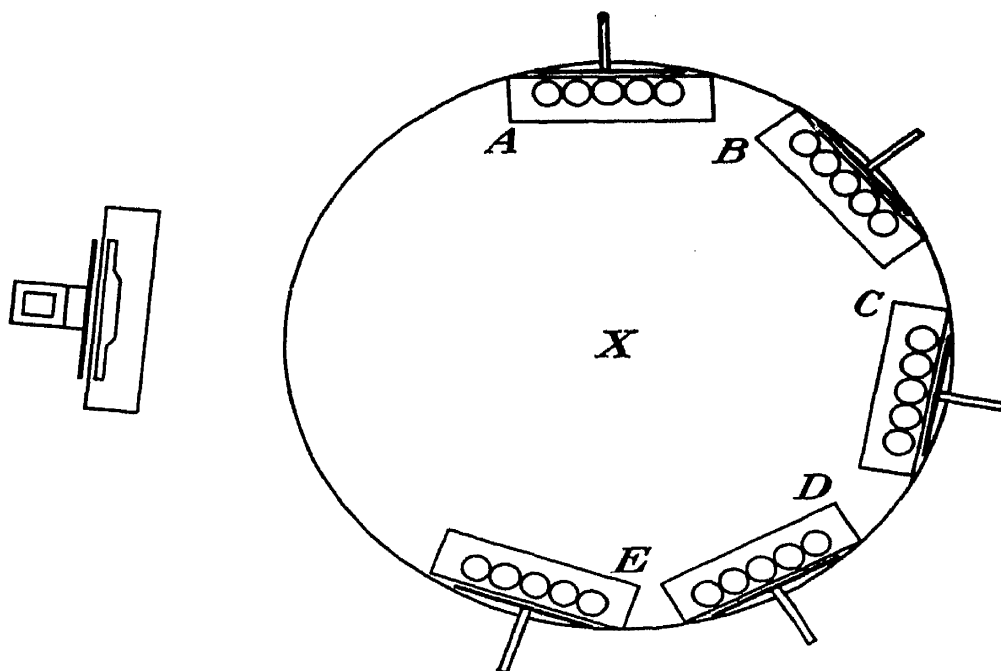


FIG. 12-37.—Plan of typical arrangement for gamma-ray radiography.

hard enough to give fairly good results with 3-in. steel plate, but not with 3-in.-diameter steel bars or solid cylinders. Reasonably good results can be obtained with 400-kv. equipment by burying a bar of the same diameter in shot, but this is unnecessary with radium or million-volt x-rays.

A technique suitable for gamma-ray radiography may be described by means of an example. Suppose a steel door casting like the one in Fig. 12-24 and 25 three-inch cast-steel bars 1 ft. long are brought in for radiography at 2 p.m. A room which will be unoccupied during the night and in which no undeveloped photographic films or plates are stored is selected. A cross is marked on the floor (Fig. 12-37, center) with a piece of chalk to fix the location of the radium. The distortion  $lt/2d$  [equation (11-1)] may be permitted to be as great as  $\frac{1}{2}$  in. and the blurring  $st/d$  as much as 0.01 in. [equation (11-2)] in order to minimize the exposure time, and this yields a value of about 36 in. for  $d$  for the steel bars. Hence a circle of 3 ft. radius is drawn on the floor with chalk and a piece of string, the cross being used as center. Five two-

<sup>1</sup> *Railway Age*, 117, 108 (1944).

fours *ABCDE*, about 18 in. long or longer, are laid flat on the floor around the 6-ft. circle as shown. Five of the steel bars are stood up side by side on each of the five two-by-fours. A 14- by 17-in. cardboard film holder loaded with nonscreen film is placed behind each group of bars. The tube side of each holder should be in contact with the bars on the side away from the center of the circle, the 17-in. edge lying on the floor. The holders may be propped against the bars with a stick of wood. Markers

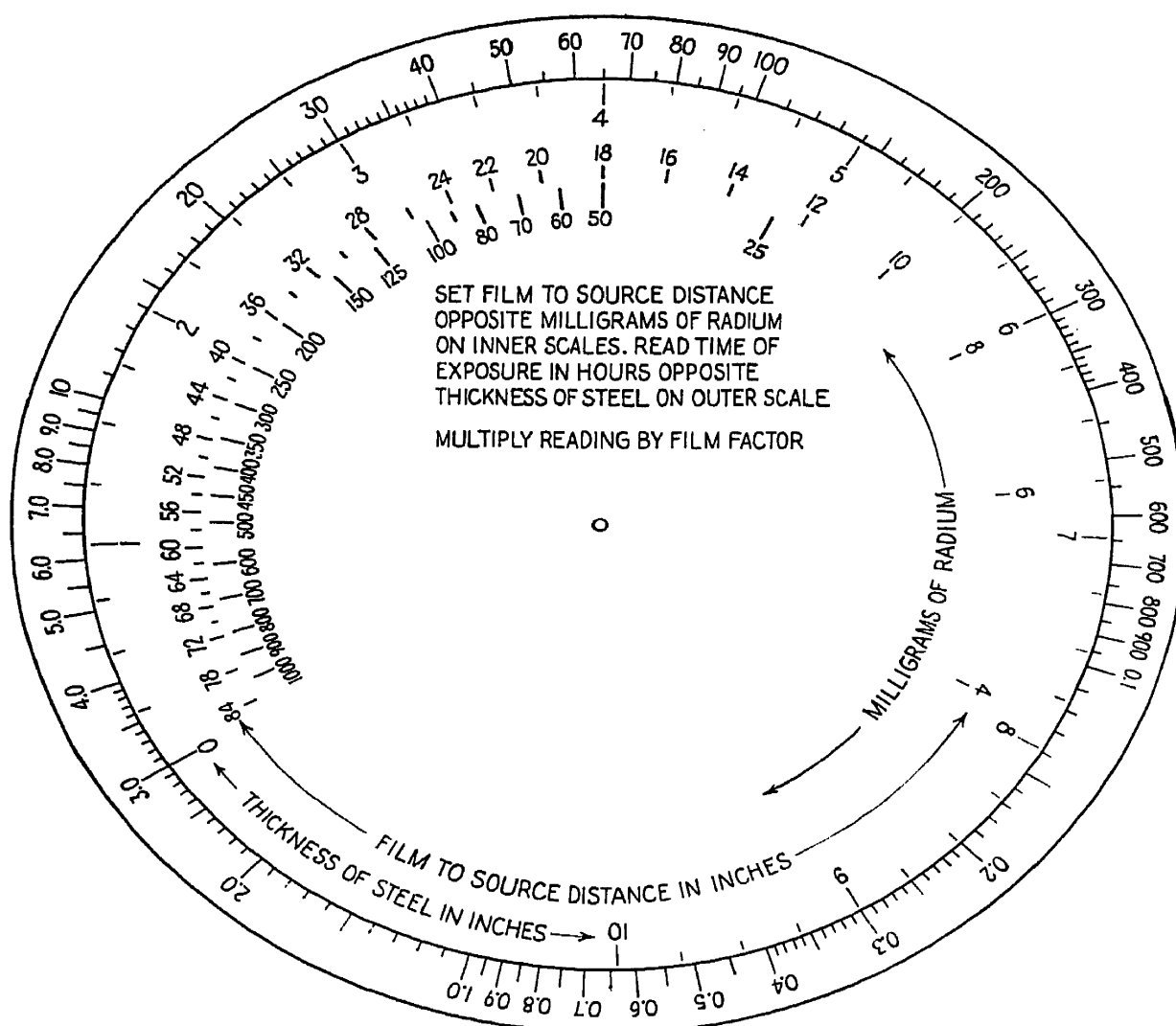


FIG. 12-38.—Circular slide rule for calculating radiographic exposure time, using radium. Designed by U. S. Naval Research Laboratories.

and penetrameters are attached to the bars with scotch tape on the side next the center of the circle. Without the two-by-fours, the lower end of the steel bars, resting on the floor, would be even with the bottom edge of the film, thus leaving no margin.

The door of Fig. 12-24 is about 1 by 1½ ft. and varies in thickness from ¾ to 2½ in., the average being about 1¾ in. The circular slide rule (Fig. 12-38) supplied to radium users by the radium supply companies may next be consulted.<sup>1</sup> If 200 mg. of radium is to be used, the film-to-source

<sup>1</sup> Such as Canadian Radium and Uranium Corp., New York, N.Y., or Radium Chemical Co., Inc., New York, N.Y.



distance for the bars (36 in.) is set opposite 200 (milligrams) on the two inner scales. Then opposite 3 (thickness of steel bars in inches), 30 (hours) is read on the two outer scales. This indicates that with ordinary x-ray film about 30 hr. of exposure will be required. Nonscreen film is about twice as fast (film factor = 0.5); the time will therefore be about 15 hr. Upon turning the dial so as to set  $1\frac{3}{4}$  (inches average thickness of the door) opposite 30 (hours) on the two outer scales, it is seen that 58 (inches) falls opposite 200 (milligrams) on the inner scales. This indicates that the film behind the door should be placed 58 in. from the cross on the floor in order to receive the same exposure through the door in front of it as that received by the films behind the bars. This will give a distortion of about  $\frac{1}{4}$  in. and a blurring of about 0.004 in. for the door, which is also set up on a two-by-four like the bars. Any handy heavy object can be placed behind the film and door for them to lean against in a nearly vertical position. The slide rule of Fig. 12-38, like the technique chart in Fig. 12-3, has its scales computed on the basis of Lambert's law (Sec. 5-1) and the inverse-square law.

Next, a glass funnel with rubber stopper (page 208) is stood at the cross on the floor. If the room cannot be locked for the night, warning signs should be posted on a barricade made of chairs, tables, or other convenient objects. When 5 P.M. quitting time arrives, the radium container is lowered into the funnel with fishing line and meter stick, as described on page 208. In the morning when work is resumed at 8 A.M., the radium container is removed to its safe and the films are developed. In this way, the 15-hr. exposure time is no handicap; the work is accomplished just as quickly as if the exposure time were 15 sec. A large amount of material can be placed around the radium container and radiographed overnight. If circumstances make it urgent, the exposure time may be reduced nearly 50 per cent by using two films, as explained on page 185.

Figure 12-24 is the radiograph of the door. It was discussed on page 266. Note the lines in the radiograph that have been made more evident by the dotted ink lines. These represent the edges of the paper flaps that enclosed the film in the film holder. This effect is due to photoelectrons ejected from the lead backing by the gamma rays. The electrons are absorbed to a greater degree by three layers of heavy paper than by two layers. Hence the lines of demarcation at the edges of the flaps appear clearly in the radiograph. As long as the person interpreting the radiograph understands this, no harm is done, but the usual practice is to sandwich the film in lead foil to prevent this effect.

**19. Supervoltage Radiography.** For the routine radiography of large numbers of heavy metal parts (steel thicknesses of 2 in. or more, aluminum thicknesses of 4 in. or more, etc.), million-volt equipment is

most suitable. For thicknesses above 4 or 5 in. of steel, 2-million-volt equipment is much faster and gives better sensitivity and definition than that attainable at 1 million volts. Million-volt radiography will reveal defects of 2 per cent or less of total thickness in steel objects for thicknesses between 2 and 6 in., roughly. A 2 million-volt unit will give 2 per cent sensitivity or better from about 4 to 8 in. of steel. The very hard rays, like gamma rays, permit wide latitude in the range of thickness that

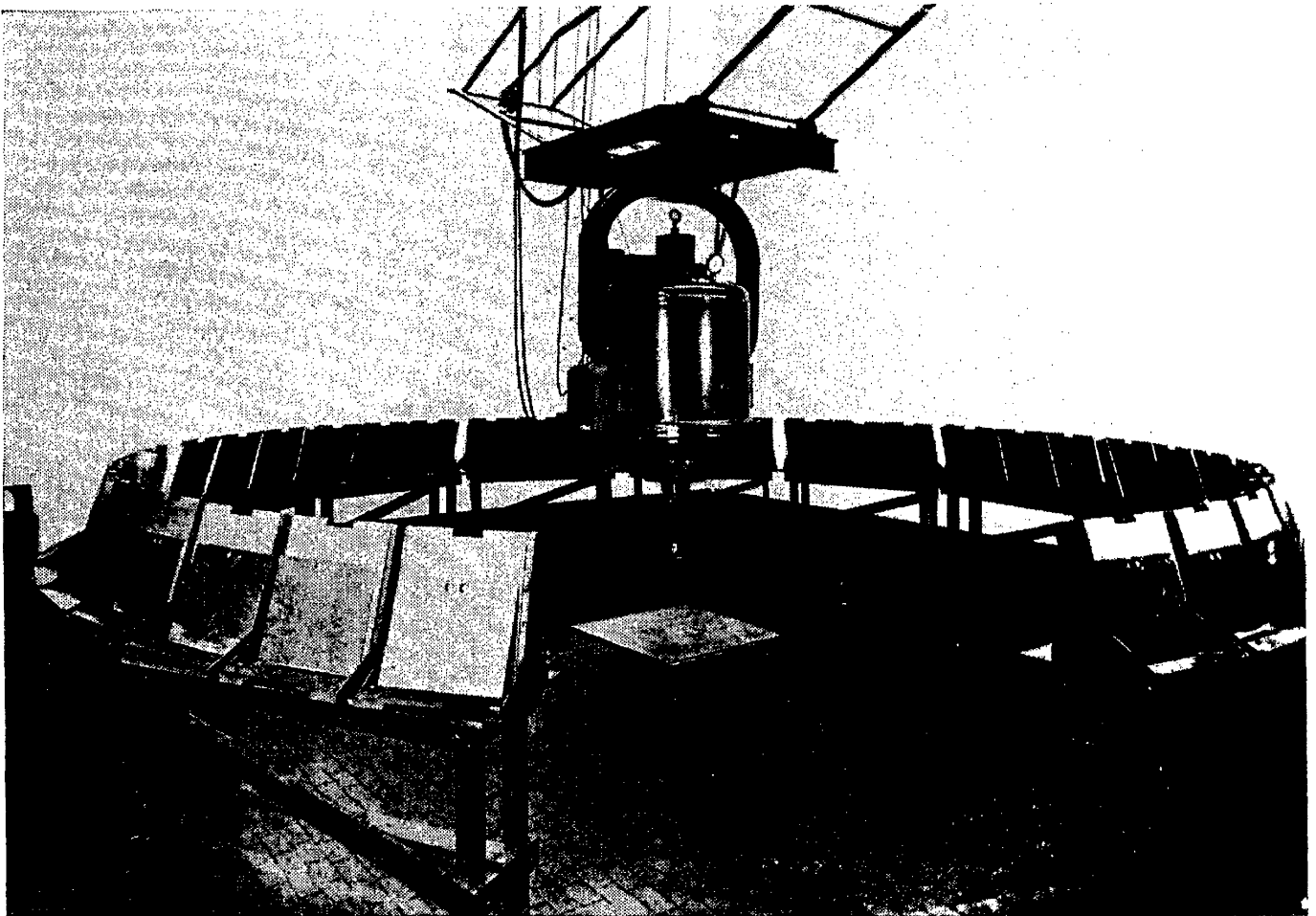


FIG. 12-39.—A General Electric million-volt industrial x-ray unit, as used to inspect turbo-supercharger parts. (Courtesy of General Electric X-ray Corporation.)

can be examined in a single radiograph, and the time-consuming blocking technique required at lower voltages is eliminated. In addition, the great intensity of the rays results in great radiographic speed and allows the tube to be placed 10 ft. or more from the work (see Figs. 12-3 and 12-39).<sup>1</sup> There is no need to sacrifice definition by placing the radiation source near the film to gain speed, as with radium.

Thus it follows that superior definition and sensitivity can be achieved in radiographing thick, dense objects. Since a large number of undistorted radiographs can be taken at one time, it is possible to radiograph about thirty to fifty times the volume of heavy objects per hour that can

<sup>1</sup> See E. E. Charlton and W. F. Westendorp, *Gen. Elec. Rev.*, **44**, 654 (1941).

be handled with 400-kv. equipment, provided that the additional man power is available to load cassettes, develop film, move the material in and out, arrange lead markers and penetrameters, and examine the finished radiographs. Other features of supervoltage radiography have been discussed under Gamma-ray Radiography and other headings in the earlier sections of this chapter and in earlier chapters.

**20. Production Radiography.** The need to inspect large numbers of parts of moderate or small thickness is the most common problem in production radiography. For such parts, supervoltage equipment is not needed, nor indeed is it desirable, for it will not yield the radiographic contrast that can be achieved at the lower voltages (see Table 12-1). Frequently the volume of work makes it practical to build complex installations where the parts to be radiographed are brought up and carried away by conveyers; the operation of carrying the parts into and out of a lead-lined room can be altered so that the parts are enveloped in a large lead-lined power-operated hood or cabinet during the exposure. An example of special equipment of this type for production radiography is the machine built by Triplet and Barton at the Lockheed Aircraft Plant, Burbank, Calif. Several of these machines are in use,<sup>1</sup> each capable of radiographing 5,000 small castings for aircraft use daily. Each machine will expose a thousand 14 by 17-in. negatives daily. In one of the General Motors Corporation divisions, trays of small parts are radiographed, and the negatives are developed, fixed, and then examined, while still wet, by the inspector before the parts are removed from the trays. On the basis of the inspection, the defective parts are rejected and the negatives discarded while still wet.

By using an ionization chamber, some simple types of x-ray inspection may be made completely automatic. This type of machine is described in Sec. 13-2.

### QUESTIONS AND PROBLEMS

1. For what type of inspection is radiography best suited? Distinguish between fixed and mobile radiographic equipment. Explain the use of a technique chart. With 200-kv.p. equipment, what technique should you try for a first exposure on a butt weld in  $\frac{3}{4}$ -in. plate? In  $1\frac{1}{2}$ -in. plate?

2. Explain the terms "porosity," "undercutting," "incomplete fusion," "crater crack," and "incomplete penetration." Point out examples of these defects in Figs. 12-4 to 12-15. Some of the more common film flaws are caused by what factors? How may such flaws be distinguished from actual flaws in the specimen?

3. What is blocking material? When should it be used? Why is it necessary? Describe two of the most practical types. What is an industrial grid, and when is it helpful?

<sup>1</sup> Illustrated in *Aero Digest*, **38**, 224 (May, 1941) and *Electronic Ind.*, **2**, 45 (January, 1943). See also *Iron Age*, **146**, 39 (Nov. 21, 1940); R. Taylor, *Aero Digest*, **45**, 88 (Apr. 1, 1944).

4. Are there any particular radiographic specifications which are at least semi-officially recognized as a criterion of sound welding? What is a penetrameter? What is it for? How may a radiograph be identified several months after it has been developed and filed away?

5. Define and distinguish between blowholes, draws, pipes, cold shuts, and dross. These flaws are common in what? Explain what these defects look like in a radiograph and how to distinguish between them in examining the film.

6. Are fine cracks, cold shuts in castings, laps in forgings, and poor bonding between flat surfaces always revealed by a good radiograph? What method is sometimes used to radiograph the bronze or babbitt in plain bearings to reveal fine pores? What flaws are common in aluminum castings but not in ferrous castings? What is meant by "wide-latitude technique"?

7. Is stereoradiography helpful in certain types of industrial work, as well as in medical work? Is it possible to distinguish between rolled, cast, and extruded aluminum radiographically? How does one obtain two or more radiographic views of the same object or group of objects on a single film?

8. In radiographing a flat plate for maximum detail, should one use a low-voltage long-time exposure or a high-voltage short-time exposure? Answer the same question if it is desired to detect flaws quickly in an irregular-shaped casting.

9. For what type of work should you recommend gamma ray radiography? Why is gamma-ray radiography preferable to million-volt radiography in examining certain types of hollow vessels and fittings? In examining only a few objects occasionally? Is the long exposure time with radium always a handicap? How does one estimate the exposure time and radium-to-film distance for a given object?

10. For what type of work should you recommend million-volt radiography? Can the General Electric million-volt equipment be operated readily at, say, 200 kv.? For what type of inspection would million-volt x-ray equipment be superior to radium?

11. Is it ever practical to radiograph, say, 25,000 parts per day in production in a single shop? Is it always necessary to file away the huge quantities of film used in production-line radiographic inspection?

## CHAPTER 13

### MISCELLANEOUS APPLICATIONS

**1. Industrial Fluoroscopy.** Compared with radiography, fluoroscopy has four disadvantages. (1) A fluoroscopic screen lacks the integrating power of a photographic film. The light emitted by the screen must be generated from the energy of the x-rays absorbed by the screen at that instant, whereas the energy needed to impress a latent image on photographic film can be stored up from the x-ray energy absorbed by the film and intensifying screens (if used) over a period of minutes. Hence, if the x-ray intensity is great enough to yield a good radiograph in 2 or 3 sec. or less, it is great enough to make a fluoroscopic screen glow so that it can be seen easily in a dark room; but if  $\frac{1}{4}$  min. or more is required to expose the x-ray film, the intensity is probably too low to be satisfactory for fluoroscopy. (2) A fluoroscopic screen lacks the contrast achieved by x-ray film. If a spot on the film is exposed to rays 2 per cent more intense than those striking the surrounding area, this spot is noticeably darker after the film is developed; with a fluoroscopic screen, such a spot escapes notice unless the x-ray intensity is nearly 10 per cent greater in the spot, that is, the screen lacks "contrast." (3) Fluoroscopic screens, being rather coarse-grained, also lack resolving power, which means that the spot just discussed is easily seen on a photographic film if it is  $\frac{1}{32}$  in. in diameter but might easily escape notice on the screen unless it is  $\frac{1}{8}$  in. or more in diameter. (4) Fluoroscopy leaves no record—there is only the memory of the person who looked at the screen.

Therefore fluoroscopy is limited to cases where a radiograph could be taken in a few seconds or less, and where the flaws could be detected in a radiograph at first glance. This being the case, why is fluoroscopy used at all? It is used because it also has important advantages, as well as disadvantages, compared with radiography. (1) Its speed. It is easy to examine an orange every second fluoroscopically and reject the bad ones, but it would be very difficult to radiograph them at this rate with a single machine and select the bad ones, which would have to be identified and rejected several minutes later after development of the film. (2) Its low cost. The expense of the film, developer, and fixer alone would make the radiography of oranges cost more than the oranges are worth; yet fluoroscopic examination of oranges on a large scale is commercially profitable. (3) Fluoroscopy is adapted to moving objects, such as those on a conveyer belt; radiography is not.

Some success has been achieved recently in the fluoroscopy of aluminum and magnesium sheet and plate in thicknesses of less than 1 in. by keeping it moving slowly so that the eye may more easily notice any small flaws. The troublesome reflections in the lead-glass protective screen are eliminated by surface treatment.<sup>1</sup> The fluoroscopic method is commonly used for inspecting packaged foods such as corn flakes, candy, etc., canned foods, vegetables in bulk, citrus fruits, meats, and oysters and clams. Foreign objects, bone slivers or broken shells, partly filled packages and cans, hollow hearts (in potatoes, etc.), and frost damage and crystallization (in citrus fruits) are detected in this manner. Fluoroscopy is also employed to examine automobile tires for ruptures of the fabric, sand blisters, nails, etc.; it is common in shoe stores for fitting shoes; it is used in the building trade to locate concealed wiring, pipes, timbers, braces, reinforcing rods, etc., in walls and floors. It is sometimes used by postal and immigration inspectors to examine packages suspected of containing bombs, smuggled goods, etc. It is also used to check the assembly of radio tubes, shell fuses, etc., and for inspecting small ammunition, wire and cable for breaks and centering in the insulation, golf balls, firebrick, arc carbons, etc.

Fluoroscopic screens were discussed in Sec. 9-1. Medical fluoroscopy was discussed in Sec. 11-1. The necessity of protection for the operator and methods of achieving it were discussed in Chap. 10. In the fluoroscopy of foodstuffs or of large numbers of manufactured articles in production, the tube and high-tension equipment should be enclosed in a grounded metal cabinet with lead lining of the thickness indicated in Chap. 10. About 100 kv. should be sufficient for this work. The fluoroscopic screen may be viewed in a mirror or in a double-mirror periscopic arrangement so as to remove the operator from the primary x-ray beam. A lead-glass window of sufficient thickness to absorb all scattered and secondary rays must be provided. Rejections and manipulations must be performed mechanically by pushing or turning levers or buttons, so that there is no possibility of the operator or others exposing their hands to x-rays or contacting a high-tension conductor. The material examined should be carried into and out of the fluoroscope by conveyer. Equipment of this type is manufactured complete, except for the conveyer, by the x-ray equipment manufacturers.

**2. Automatic Industrial Inspection with an Ionization Chamber.** Woods and Kenna report<sup>2</sup> that the soldered joint between the blade and handle of table knives is regularly subjected to x-ray inspection at

<sup>1</sup> See, for example, K. B. Blodgett, *Phys. Rev.*, **55**, 391 (1939), or C. H. Cartwright and A. F. Turner, *Phys. Rev.*, **55**, 595 (1939); also K. M. Greenland, *Am. Cinematographer*, **25**, 223 (1944).

<sup>2</sup> R. C. Woods and L. P. Kenna, *Electronics*, **14**, 29 (April, 1941).

Oneida, Ltd., Oneida, N.Y., at a rate of 1,400 per hour, by a machine which automatically rejects the defective ones. In this machine, an x-ray beam is directed through the soldered joint, after which it enters an ionization chamber (Sec. 9-3). If the joint is defective, the emergent beam (and hence the ionization current) is stronger than if the joint is sound. The ionization current is only about  $10^{-9}$  amp., but it is amplified and used to control a relay that mechanically rejects the defective knives. Hand grenade fuses have been automatically inspected by a similar method, except that the x-ray beam strikes a phosphor (Sec. 9-1) instead of an ionization chamber. The fluorescent light from the phosphor is measured by a type 931 photomultiplier tube and amplifier.<sup>1</sup>

Attempts to use this method for inspecting extruded forms and shapes have not achieved the sensitivity that is attained by radiography. The x-ray beam is directed through the extruded bar transversely, thence into an ionization chamber. When a cavity or similar flaw in the moving bar passes through the x-ray beam, the ionization current momentarily increases and, after amplification, may cause the flaw to be marked by a daub of paint at the point on the bar where the flaw is located. The flaws that can be detected in this manner are fairly gross; flaws such as a spherical cavity  $\frac{1}{50}$  in. in diameter in a bar 1 in. square will not be detected, although they would be revealed easily in a good radiograph. The thicknesses that can be inspected in this manner are also limited. Extruded aluminum shapes not thicker than  $\frac{1}{4}$  in. or plastic (for example, Lucite) shapes up to  $\frac{1}{2}$  in. in thickness should be suitable for this type of examination. General Electric X-ray Corp. has manufactured some equipment of this type. The Electronic Control Corp., Detroit, Mich., has also placed this type of equipment on the market.

**3. Microradiography and Grenz-ray Radiography.** Ordinary radiography corresponds to ordinary photography. It is only natural that an effort should be made to develop the radiographic equivalent of photomicrography. In photomicrography, the magnification is accomplished by passing the light through lenses after it leaves the object and before it reaches the photographic film or plate. If lenses were not available, a microscope might be built using concave and convex mirrors; but with x-rays neither lenses nor mirrors are of any use, as explained in Chap. 6. Hence the only solution is to make the radiograph at unmagnified actual size and then magnify the radiograph.

This immediately raises the question of photographic grain size and the practical limit attainable in photographic enlargement. Obviously, the original radiograph should be taken on a film or plate having the smallest grain size available if maximum enlargement is the primary

<sup>1</sup> See H. M. Smith, *Gen. Elec. Rev.*, **48**, 13 (March, 1945); for illustration, see *Science News Letter*, **44**, 259 (1943).

requirement. In the United States, the finest grain available is in the Eastman Type 548-O spectrographic film or plates, as mentioned on page 177. When magnified 200 diameters, the definition of the resulting enlargement is still good. However, as the grain size is reduced, so is the speed. Consequently, this film is extremely slow compared with ordinary x-ray film. Fine-grained positive 35-mm. motion-picture film has about three times the speed of 548-O, but the maximum permissible enlargement is only about 30 diameters. Process film or plates may also be used up to about 30 diameters. A step beyond this comes the fine-grained x-ray films like Agfa Suparay B or Eastman Industrial Type M. These may profitably be enlarged about 15 or 20 diameters, and they have a speed about 10 per cent of that of ordinary x-ray films.

Photomicrography has been found to be a valuable method of investigation in many fields, of which two of the best known are perhaps biology and metallography. In the former field, a microtomic section only a few thousandths of an inch thick is examined by transmitted light. In the latter, a carefully ground, polished, and etched surface is examined by reflected light. Owing to the very limited depth of focus of the microscope lenses, even the first of these two methods essentially limits the photomicrograph to two dimensions.

Two primary advantages of microradiography should be pointed out. The first is the removal of the two-dimensional limitation just mentioned. This is achieved by using a penetrating radiation (x-rays) so that the microradiograph will be a sort of superphotomicrograph revealing detail in three dimensions. A photomicrograph may be thought of as a picture 1 in. square of a flat surface  $\frac{1}{100}$  in. square. A microradiograph<sup>1</sup> may be thought of as a picture 1 in. square showing the details of the structure of a solid cube  $\frac{1}{100}$  in. on each edge. A microradiograph is obtained by passing x-rays through a slice of the material about  $\frac{1}{100}$  in. thick or less; if a thicker sample were used, the shadows of the various details to be seen would be superposed upon one another in such profusion that only confusion would result. The second primary advantage makes use of the x-ray absorption edges (Chap. 5). These make it possible to obtain effects in a microradiograph that cannot be duplicated in optical microscopy. In an alloy of copper and nickel, for example, one may take the microradiograph with monochromatic (characteristic) x-rays of a wave length just less than the K limit of nickel but longer than that of copper

<sup>1</sup> L. V. Chilton, *Rev. Sci. Instruments*, **21**, 33 (1944), contends that the terms "x-ray micrograph" and "x-ray micrography" are preferable to "microradiograph" and "microradiography"; E. L. Garvin, *J. Applied Phys.*, **15**, 455 (1944), concurs in this. See also S. E. Maddigan, *J. Applied Phys.*, **15**, 626 (1944). However, C. S. Barrett has applied the name "x-ray micrograph" to an entirely different type of enlarged x-ray image (see p. 482).



so that the nickel is clearly differentiated from the copper. Likewise the calcium compounds in the bone structure may be made to stand in a microradiograph of a microtomic slide.

The first problem, then, is to obtain a radiograph of a sheet or of material only a few thousandths of an inch thick, an extremely grained film being used. If hard x-rays were used, such as the continuous x-rays generated at 150 kv., more than 99 per cent would go through the sheet, so that even if it consisted of metallic powder suspended in gelatine the resulting radiograph would not show much contrast. This explains why the early efforts in this field favored the use of the continuous x-radiation generated at low voltages. These early efforts use x-rays generated at 5 or 10 kv. were limited because the rays were so soft that their absorption in the air made it necessary to use vacuum cameras and the samples had to be impractically thin. The "green" rays gave beautiful radiographs of insect's wings, flower petals, etc.,<sup>1</sup> but they were too soft for the thinnest practical metal samples.

In 1939, Dershem<sup>2</sup> pointed out that characteristic x-ray spectra might be superior to the continuous spectrum for this type of work. A monochromatic x-ray beam could be chosen in such a way that its wavelength would be just less than the K absorption edge of some chemical element in the object. For example, he used the K lines of scandium to radiograph the leg bones of a rat because the bones contained calcium which has its K absorption edge at 3.06 Å. and the  $K_{\alpha}$  lines of scandium have a wave length just below this, at 3.02 Å.

Instead of building a special tube with a scandium target, Dershem used a vacuum camera in which was placed a piece of scandium, and a K spectrum was excited<sup>3</sup> by irradiating it with rays from a tube operated at 40 kv. and 10 ma. A satisfactory radiograph was obtained in 40 minutes. For radiographing the wings of a grasshopper, he found scandium radiation too hard, magnesium  $K_{\alpha}$  radiation (9.86 Å.) too soft, sulfur  $K_{\alpha}$  radiation (5.36 Å.) correct.

In the same year, Clark published the first account of his experiments using the  $K_{\alpha}$  radiation from molybdenum and later from cobalt, copper and iron to radiograph thin metal specimens on fine-grained film with subsequent enlargement to 100 diameters or more. This work by Clark and his coworkers has opened up the new field known as "microradiography." The following table of linear absorption coefficients is

<sup>1</sup> See, for example, *Gen. Elec. Rev.*, **41**, 337 (1938).

<sup>2</sup> E. Dershem, *J. Optical Soc. Am.*, **29**, 41 (1939).

<sup>3</sup> Fluorescence x-radiation; see p. 76.

<sup>4</sup> G. L. Clark, *Photo Tech.*, December, 1939; G. L. Clark and W. M. Shafer, *Trans. Am. Soc. Metals*, **13**, 732 (1941); G. L. Clark and S. T. Gross, *Ind. Eng. Chem. Anal. Ed.*, **14**, 676 (1942).

one of their papers. It lists the x-ray absorption coefficient of the K radiation from copper, iron, and molybdenum in various commercially important metals.

TABLE 13-1.\*—LINEAR ABSORPTION COEFFICIENTS OF K RADIATION FROM COPPER, IRON, AND MOLYBDENUM IN VARIOUS METALS

Copper		Iron		Molybdenum	
Be	2.96	Be	5.64	Be	0.58
Mg	71.4	Mg	135.	Mg	7.53
Al	132.	Al	252.	Al	14.1
Si	144.	Si	266.	Si	15.2
S	182.	S	346.	S	19.8
Ag	228.	Fe	560.	Ti	109.
Zn	418.	Zn	785.	Mo	203.
Ni	427.	Ni	797.	Cr	221.
Cu	454.	Cu	868.	Sn	248.
Ti	958.	Ti	1,777.	Ag	289.
Cr	1,659.	Cr	2,460.	Fe	303.
Sn	1,798.	V	2,612.	Co	383.
Mn	2,124.	Sn	3,422.	Zn	421.
Fe	2,578.	Ag	4,253.	Ni	427.
Pb	2,609.	Pb	4,854.	Cu	455.
Co	3,186.	W	5,790.	Pb	1,537.
W	3,397.			W	2,007.

\* By G. L. Clark and S. T. Gross. Reprinted by permission of the American Chemical Society.

The table indicates that nickel might be differentiated from iron in a

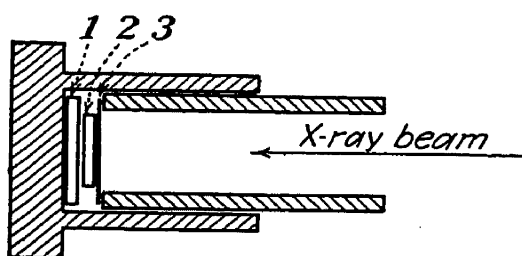


FIG. 13-1.—Microradiographic camera designed for insertion in collimating system of commercial x-ray diffraction equipment. 1, fine-grained film. 2, specimen. 3, black paper, or Wratten filter No. 87. (By G. L. Clark and S. T. Gross; reprinted by permission of The American Chemical Society.)

nickel steel by copper radiation, but not easily with iron or molybdenum radiation, whereas chromium and iron in stainless steel, for example, would be more easily differentiated with iron radiation than with copper or molybdenum. Clark<sup>1</sup> recommends 0.003 in. as a satisfactory thickness for steel samples, 0.005 in. for copper alloys, and up to 0.010 in. for magnesium. The sample may be reduced to the desired thickness by grinding (slowly enough to avoid overheating and change of structure), or etching, or both, and the specimen should be given a final polish with 2 (0) emery paper moistened with oil, Clark says.

A commercial diffraction tube (see Sec. 7-3) is suitable as a source of radiation. The target-to-film distance should be about 5 or 6 in., and exposure time varies from as low as a few minutes with magnesium to

<sup>1</sup> See, for example, S. T. Gross and G. L. Clark, *Iron Age*, **152**, 44 (July 22, 1943).

several hours for some of the more opaque metals and alloys. Figure 13-1 illustrates one type of camera used by Clark.<sup>1</sup> It is designed to fit in the collimating tube of an ordinary x-ray diffraction camera. The sample must be against the film or plate for good definition in the micro-radiograph. When glass plates are used, they are cut in pieces small enough to go in the camera, and a piece is wrapped in black paper,<sup>2</sup> which also encloses the sample in intimate contact with the emulsion.

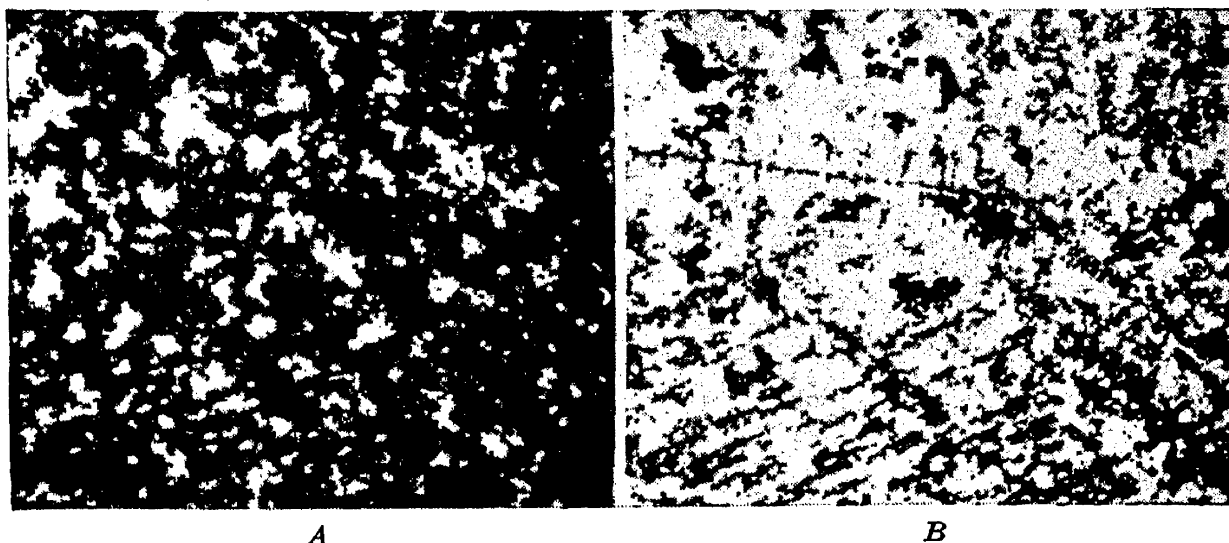


FIG. 13-2.—Microradiographs (negative prints) of one area of bronze 0.0035 in. thick. *A*, with characteristic molybdenum radiation. *B*, with characteristic copper radiation. Lead light in *A*. Lead and tin light in *B*. Magnification, 90 times. (By G. L. Clark and S. T. Gross; reproduced by permission of The American Chemical Society.)

Clark has published several microradiographs in the articles already referred to, which are noteworthy advances over comparable photomicrographs. Figure 13-2 is a reproduction of two of his microradiographs, which illustrate the value of this technique in the study of segregation in alloys. Note how the tin may be made to appear either light or dark at will by the proper choice of x-radiation.

The experiments of Woods and Cetrone<sup>3</sup> led them to recommend the use of 12-kv. continuous radiation for the microradiography of aluminum spot welds, etc. This might suggest that Clark and his coworkers had overemphasized the role of the characteristic radiation in the microradiography of metals and that the earlier techniques using low-voltage continuous radiation were, after all, almost as satisfactory. In a more recent article describing further work along this line, Maddigan<sup>4</sup> concludes that the selection of a suitable characteristic radiation for the detection of regions of secondary phases in alloys, etc., is desirable, as

<sup>1</sup> See also G. L. Clark and R. W. Eyler, *Rev. Sci. Instruments*, **14**, 277 (1943).

<sup>2</sup> Black paper is characterized by inhomogeneities that are sometimes troublesome. For this reason, a window of an opaque gelatine such as Wratten filter No. 87 may be preferable to black paper.

<sup>3</sup> R. C. Woods and V. C. Cetrone, *Iron Age*, **151** (12), 52 (Mar. 25, 1943).

<sup>4</sup> S. E. Maddigan, *J. Applied Phys.*, **15**, 43 (1944); see also D. M. McCutcheon, "A.S.T.M. Symposium on Radiography, 1943," p. 89.

found by Clark and his coworkers, but that due consideration should also be given to the continuous radiation.

As a general rule, based on consideration of equations (2-5), (3-10), and (4-3), Maddigan suggests that the tube voltage should be roughly three times the K excitation potential for its target, although individual cases will call for variations from this rule. He also recommends the usual metallographic procedure of mounting specimens in Bakelite moldings to finish one surface, followed by reverse mounting to finish the second surface, the final thickness usually being less than 0.005 in. for best results.

Microradiography is a new method of investigation that is still in its infancy, with a promising future.

**4. Radiography of Paintings and Documents.** Radiography has proved to be a valuable aid in the examination of paintings, checks, deeds, letters, and other documents. A good radiograph often reveals alterations and supplies information helpful in deciphering the nature of the original. In this way, paintings may sometimes be proved to be authentic or fraudulent, and fraudulent alterations of legal documents are sometimes revealed and frustrated. Infrared and ultraviolet photography are also used in a similar way.

An interesting example of radiography of this type is described in an article by Barrell,<sup>1</sup> in which he presents radiographic evidence from old paintings tending to show that William Shakespeare was the pen name of Edward De Vere, seventeenth Earl of Oxford and Lord Chamberlain of England, and that Willm Shakspeare of Stratford-on-Avon was a butcher's apprentice, malt dealer, moneylender, and land speculator who had no unusual literary ability.

In radiography of this type, soft rays are used. Grenz rays in a vacuum camera may be best to try first in radiographing paper documents<sup>2</sup>. With paintings, where a vacuum camera is impractical, the softest rays that will penetrate the air may be employed; for example, the K radiation from a chromium, iron, or copper target. It may be possible to find some chemical element that is abundant in the paint and then use characteristic radiation having a wave length slightly less than the K absorption limit of this element.

**5. Coloration of Glass and Crystals by X-rays.** Soon after the discovery of x-rays, it was noticed<sup>3</sup> that glass exposed to them slowly became colored brown. Glass x-ray tubes acquire a brown color that becomes darker with continued use. Some special glasses become purple, yellow, etc., depending upon their chemical composition. Holzknecht<sup>4</sup> noticed

<sup>1</sup> C. W. Barrell, *Sci. American*, **162**, 5, 264 (1940).

<sup>2</sup> H. S. Tasker and S. W. Towers have used secondary beta rays (p. 76) successfully in radiographing paper. See *Nature*, **156**, 50 (1945).

<sup>3</sup> P. Villard, *Compt. rend.*, **129**, 882 (July-December, 1899).

<sup>4</sup> G. Hotzknecht, *Verhandl. deut. physik. Ges.*, **4**, 25 (1902).

in 1902 that certain chemicals undergo similar coloration upon x-ray exposure. Investigation of this phenomenon has attracted the attention of various workers. Bayley,<sup>1</sup> for example, found that RbF, CaF<sub>2</sub>, CsCl, RbCl, KCl, NaCl, LiCl, AgCl, BaCl, BeCl, (CsBr, RbBr, KBr, KI, NaI, CdI, HgI, and K<sub>2</sub>SiO<sub>3</sub> were colored, whereas KF, NaF, LiF, NaBr, RbI, ZnCl<sub>2</sub>, and NH<sub>4</sub>Cl were not colored, in 5 hr. of intense exposure. Most of these colored materials lose their color or fade logarithmically when exposed to daylight.

Some glass colored by x-rays retains its color permanently. Reinhard and Schreiner<sup>2</sup> report that bismuth glass colors yellow with x-ray exposure and that the color can be removed only by heating the glass nearly to the melting point. The brown color of window glass colored by x-rays, however, fades logarithmically in a few hours, according to Kersten and Dwight.<sup>3</sup>

Kronhaus<sup>4</sup> reports that the x-ray coloration of semiconducting crystals of SiC, Sb<sub>2</sub>S, and PbS is accompanied by a change in their electrical resistances. Podasevskij<sup>5</sup> observed a 143 per cent increase in the tensile strength of rocksalt crystals upon coloration with x-rays. The oscillation rates of piezoelectric quartz crystals can be reduced as much as three kilocycles by irradiation when the frequency is several megacycles, according to C. Frondel.<sup>6</sup> Baking at 175°C. restores the original frequency. The fundamental nature of x-ray coloration is not well understood, although some quantitative measurements of the coloring rate have been made by Nurnberger and Livingston.<sup>7</sup>

**6. Effects of X-rays on Liquids.** When x-rays pass through water hydrogen is liberated, but this is not true for ice, according to Günther and Holzapfel.<sup>8</sup> When x-rays pass through a dilute solution of H<sub>2</sub>O<sub>2</sub>, it is slowly decomposed, according to den Hoed and Spiers.<sup>9</sup> This type of x-ray-induced chemical change, like the generation of ozone from oxygen by x-rays, is probably due to the photoelectric action of the rays.

A peculiar effect of x-rays on colloidal suspensions has been reported by Crowther, Leibmann, Lane, and Jones.<sup>10</sup> They have observed that

<sup>1</sup> P. L. Bayley, *Phys. Rev.*, **24**, 495 (1924).

<sup>2</sup> M. C. Reinhard and B. F. Schreiner, *J. Phys. Chem.*, **32**, 1886 (1928).

<sup>3</sup> H. Kersten and C. H. Dwight, *J. Chem. Phys.*, **1**, 627 (1933).

<sup>4</sup> A. Kronhaus, *J. Tech. Phys. (U.S.S.R.)*, **9**, 202 (1939); see also S. Shimizu, "Anniversary Volume to K. Honda, Sendai, Japan (1936)," pp. 113-128.

<sup>5</sup> M. Podasevskij, *Compt. rend. acad. sci. U.S.S.R.*, **3**, 71 (1935).

<sup>6</sup> *Science News Letter*, **47**, 242 (1945); also *Electronics*, **17**, 227, (December, 1944).

<sup>7</sup> C. E. Nurnberger and R. Livingston, *J. Phys. Chem.*, **41**, 691 (1937).

<sup>8</sup> P. Günther and L. Holzapfel, *Z. physik. Chem., Abt. B.*, **44**, 374 (1939).

<sup>9</sup> D. den Hoed and C. W. F. Spiers, *Z. physik. Chem., Abt. A.*, **6**, 412 (1935).

<sup>10</sup> J. A. Crowther, H. Leibmann, T. B. Lane, and R. Jones, *Phil. Mag.*, **24**, 65 (1937), **28**, 64 (1939).

the electrophoretic mobility of colloidal suspensions of gold, quartz, or carbon (Aquadag) undergoes a rhythmical variation when irradiated with x-rays. For example, one Aquadag suspension showed an increase of about 12 per cent in the mobility after a dose of about 25 r., then regained its original mobility after a dose of about 50 r., then showed a decrease of about 5 per cent after 75 r., back to normal at 100 r., followed by successive maxima and minima like the displacement of a pendulum from its mid-position. Similar effects were observed earlier with ferric hydroxide suspensions.<sup>1</sup> The explanation of this peculiar behavior is not known.

**7. Induced Mutation in Plants and Animals by X-rays and Gamma Rays.** Before 1927, plant and animal breeders trying to develop improved breeds or specialized strains could make only recombinations of the existing breeds, supplemented on rare occasions by mutational variations that occur naturally but infrequently. The geneticists were hampered in their studies of these mutations and of the genes in which they occur because of the extreme slowness of the natural rate of mutation. Biologists desired some method of control over the hereditary changes within the genes.

The only method now known was discovered in 1927, when Muller<sup>2</sup> published the results of his extensive experiments along this line. He worked with the zoologist's favorite subject (Chap. 11), the fruit fly *Drosophila melanogaster*. He stated that

It has been found quite conclusively that treatment of the sperm with relatively heavy doses of x-rays induces the occurrence of true "gene mutations" in a high proportion of the treated germ cells. . . . The mutants obtained in this way are stable in their inheritance, and most of them behave in the manner typical of the Mendelian chromosomal mutant genes found in organisms generally. . . . The effects of application of x-rays to *Drosophila melanogaster* are truly mutational and not to be confused with the well known effects of x-rays upon the distribution of the chromatin, expressed by non-disjunction, non-inherited cross-over modifications, etc.

To complement Muller's work in the animal kingdom, Stadler was independently working along the same lines in the plant world. He found that x-rays and gamma rays would induce mutations in barley<sup>3</sup> and maize.<sup>4</sup> He found that for barley, "heavy" irradiation (5 ma., 78 kv.p.,  $2\frac{3}{4}$  min., at 22.7 cm. distance, repeated once an hour for 12 exposures, or 5 ma., 54 kv.p.,  $5\frac{1}{2}$  min., at 22.7 cm., repeated once an hour for 12 exposures) was about six times as effective as "light" irradiation (same

<sup>1</sup> J. A. Crowther, H. Leibmann, and C. C. Mill, *Brit. J. Radiol.*, **9**, 631 (1936).

<sup>2</sup> H. J. Muller, *Science*, **66**, 84 (1927).

<sup>3</sup> L. J. Stadler, *Science*, **68**, 186 (1928).

<sup>4</sup> L. J. Stadler, *Proc. Natl. Acad. Sci.*, **14**, 69 (1928).

as heavy except that target-to-barley distance was 45.4 cm.). His results are summarized in Table 13-2. He found that if he soaked the

TABLE 13-2.\*—INDUCED MUTATIONS IN BARLEY

	Total head progenies examined	Number segregating mutant seedling characters
78 kv.:		
Heavy.....	210	6
Light.....	259	1
54 kv.:		
Heavy.....	494	6
Light.....	280	1
Total x-rayed.....	1,243	14
Radium treated.....	1,039	3
Untreated.....	1,341	0

\* From Stadler.

seeds for 7 hr. in a  $\frac{1}{8}$  mole solution of  $\text{Ba}(\text{NO}_3)_2$ ,  $\text{Pb}(\text{NO}_3)_2$ , or  $\text{UO}_2(\text{NO}_3)_2$  to increase their absorption coefficient for the x-rays the number of mutations was about doubled for a given x-ray dose.



FIG. 13-3.—Double paper-white narcissus (right) grown from x-rayed bulb. A few hundred r units suffice to produce effects of this sort. (Courtesy of Dr. C. P. Haskins.)

Subsequent investigations along these lines have been numerous and fruitful. For a summary and extensive bibliography up to 1936, the reader is referred to Chaps. XXVII, XXIX, XXX, XXXVI, XXXVIII, XXXIX, XL, XLI, XLII, and XLIII in the book by Duggar and others.

In general, these mutations may be induced in either plants or

<sup>1</sup> B. M. Duggar, "Biological Effects of Radiation," McGraw-Hill Book Company Inc., New York, 1936. See also L. R. Maxwell and S. B. Hendricks, *J. Applied Phys.*, **9**, 237 (1938); P. C. Koller, *Nature*, **155**, 778 (1945).

animals by rays ranging from grenz rays generated at 10 kv. or less up to x-rays generated at a million volts or more and by gamma rays. Figure 13-3 is an interesting example. A typical "dose" is one administered at 50 kv., 5 ma., without any filter at 30 cm., lasting from 10 min. to an hour or more. For *Drosophila*, the doses range from 2,000 to 4,000 r. For some plants, such as *Antirrhinum*, 400 r. is more effective than 3,000 r. For *Nicotiana tabacum* var. *purpurea*, mutations can be induced by irradiating the embryo-sac mother cells, the zygote, the mature pollen, the seeds, or the seedlings.

**8. Instantaneous Radiography.** Reference has already been made (page 107 and Fig. 7-1) to the x-ray tubes developed for taking radiographs of bullets penetrating wood planks, etc., the exposure requiring only about 1 microsec. This was accomplished by Slack and Ehrke in 1941 by charging condensers of about 0.02  $\mu$ f capacity to a voltage of 100 kv. The condensers were then discharged at the desired instant through the x-ray tube, the current being roughly 2,000 amp. The cathode is designed for "field emission."<sup>1</sup> The discharge is initiated by a third auxiliary electrode close to the cathode that first assumes the potential of the anode, being connected to the latter through a high resistance. When the discharge starts, this auxiliary electrode immediately assumes the potential of the cathode, because of the high resistance, and the main discharge occurs between anode and cathode.

Since 1941 (see Fig. 7-1), this technique has been developed to a point where a potential of 300 kv. has been attained by a Marx type of surge generator. A pulse from an induction coil breaks down a spark gap to initiate the discharge. Successful radiographs have been taken of bullets passing through gun barrels and striking armor plate. This greatly increases the possible fields of application of this technique. Hitherto, the method was limited to the radiography of comparatively transparent objects like wooden planks. Now it appears that it may be practical to obtain radiographs of fast-moving processes in the interior of objects almost as readily as such objects can be radiographed when no motion is involved. The chief drawback is likely to be the size of the focal spot in such an x-ray tube. Slack and Ehrke<sup>2</sup> used a spot about 2 cm. in diameter to absorb the enormous power (approaching 1 million horsepower); it is remarkable that energy can be absorbed at such a prodigious rate by a spot this small. According to latest informa-

<sup>1</sup> For a definition and explanation of the term "field emission," see any good book on conduction of electricity through gases or an elementary book on electronics, like D. G. Fink, "Engineering Electronics," (McGraw-Hill Book Company, Inc., New York, 1938).

<sup>2</sup> C. M. Slack and L. F. Ehrke, *J. Applied Phys.*, **12**, 165 (1941); C. M. Slack, E. R. Thilo, and C. T. Zavalles, *Electronic Ind.*, **3**, 104 (November, 1944).



tion, the focal-spot diameter has now been reduced to less than .001 in. The anode is a tungsten button.

**9. Measurement of Wall Thickness.** Moyer<sup>1</sup> has developed a method of measuring the wall thickness of hollow steel airplane propeller blades. This method is applicable to other industrial problems of similar nature. According to Moyer's technique, a 7- by 8½-in. strip of fine-grained nonscreen film in a cardboard holder is held against the inner surface of the blade wall by means of an air-filled bladder. The film, 90 in. away, is operated at 130 kv., the exposure being 1,350 m. The density of the film after exposure and development is measured with a microphotometer and compared with that of calibration films exposed through steel sheets or penetrameters of known thicknesses. In this way, the wall thickness can be determined with a maximum error of about 4 per cent without damaging the propeller blade.

By using a fluorescent screen and photomultiplier tube to measure the intensity of the transmitted beam, as explained in Sec. 2, x-ray fluorescence has been employed to measure the thickness of white-hot sheet steel moving at 20 miles/hr. through the rolls of a rolling mill.<sup>2</sup>

It is also possible, with a Geiger counter or similar device,<sup>3</sup> to measure accurately the thickness of a wall from one side only when the other side is inaccessible, by irradiating the wall with x-rays from radium and measuring the intensity of the radiation scattered by the walls. The device used for this work is called the "Permeability Meter."

**10. Duplicating Templates.** A recent important industrial application of x-ray fluorescence is a process for duplicating templates used in the lofting departments of factories. The original metal template is sprayed with Eastman Kodak fluorescent lacquer (Spec. 20,540). The dry surface is then scribed by the lofting man with the desired design. He may use a scribing tool, pencil, or pen and in the process a proper type of photographic film (Eastman matte transfer film) is adhered to the wood, glass, or metal surface to which the design is to be transferred, by means of a laminating machine, after which it is exposed for 15 min. or more. This film-covered surface is then pressed against the fluorescent-coated template and exposed 3 to 5 min. to x-rays. The tube is made to sweep the surfaces by traversing it laterally.

<sup>1</sup> H. P. Moyer, *Aviation*, March, 1944, p. 147.

<sup>2</sup> *Science News Letter*, Apr. 29, 1944, p. 275; *J. Applied Phys.*, **15**, 62 (1944); *Gen. Elec. Rev.*, **46**, 59 (1943).

<sup>3</sup> D. G. C. Hare, U.S. patent reissue 22, 531 (Aug. 22, 1944); *Electron. Eng.*, **101** (August, 1945); *Electronics*, **18**, 154 (August, 1945).

<sup>4</sup> This method was developed by P. G. Filmer and the General Motors Corp. Photographic Department, the Eastman Kodak Co., and the North American Aviation Lofting and Photographic Departments. See *Automotive and Aviation*, **86**, 45 (May 15, 1942).

surface may be curved to a radius of 10 or 15 ft., and the x-ray tube, mounted at the center of this circular arc, sweeps the surface by a slow rotation. The fluorescent lacquer fluoresces everywhere except where the surface has been scribed and exposes the film like any x-ray intensifying screen. The negative, still adhering to the surface, is then developed, after which it is ready to be cut and trimmed. A second transfer is required if a negative in mirrored image form is unsuitable, which is true for only about half of the templates.

### QUESTIONS AND PROBLEMS

1. What are the limitations of industrial fluoroscopy as compared with radiography? What are its advantages over radiography? Mention some common industrial applications of fluoroscopy.

2. How may an ionization chamber be used to accomplish automatic x-ray inspection and rejection in certain special cases?

3. In what way is microradiography an advance over photomicrography? How does one proceed to detect segregation in an alloy by microradiography? How does one select the best type of x-radiation to use for a particular job? What type of film or plates is required? Can you say anything about the exposure time required? If one desires to use scandium  $K_{\alpha}$  radiation in this type of work, is it necessary to have a special tube with a scandium target?

4. How may x-rays sometimes be of value in examining altered or otherwise doubtful paintings or documents? Can you make any suggestions regarding the technique?

5. Is an x-ray exposure of 15 min. likely to color ordinary glass appreciably? Do all glasses color in the same way upon prolonged exposure? Is the coloration always permanent? Are all alkali halides colored by prolonged x-ray exposure? Is there ever any other observable change in the physical properties of materials accompanying their coloration by x-rays?

6. Does the electrophoretic mobility of certain colloidal suspensions increase or decrease with the x-ray dosage? Would a dose of 25 r. be sufficient to produce a noticeable change, in some cases? How can templates be duplicated by means of x-rays? What is the "Penetron"?

7. If you wished to produce mutational effects upon plants by the x-irradiation of the seeds or bulbs, for example, suggest the tube voltage, current, distance, and time that you might use for a first attempt. Are the mutants obtained as a result of such treatment different in any essential way from the rarer mutants that occur naturally? Does the possibility of mutation induced by x-rays have any special importance to the biological sciences?

8. What type of equipment is required to radiograph high-speed phenomena like the piercing of armor plate by a bullet? Suggest some of the possibilities and limitations of this type of radiography.

## CHAPTER 14

### CRYSTALLOGRAPHY BEFORE THE DISCOVERY OF X-RAY DIFFRACTION

**1. Why Study Crystallography? Its Modern Ramifications and Practical Importance.** It has already been related in Sec. 6-3 how Compton and Doan for the first time,<sup>1</sup> in 1925, succeeded in diffracting x-rays by means of a ruled grating, at grazing incidence. Thirteen years earlier however, Friedrich, Knipping, and Laue had discovered<sup>2</sup> that a beam of x-rays could be made to yield a diffraction pattern by passing it through a crystal. Their first pattern was from a crystal of blue vitriol (copper sulfate). They attempted this because earlier experiments by Walter Pohl, Sommerfeld, and Koch<sup>3</sup> indicated that x-rays must have a wavelength of the order of 0.1 Å., whereas crystallographers like Bravais<sup>4</sup> had concluded as early as 1848 that the atoms of a crystal were arranged at the points of a geometrical space-lattice. From the geometry of the crystal, its molecular weight, density, and number of molecules per gram molecule, the distance between neighboring atoms in such a lattice was calculated to be of the order of 1 Å.<sup>5</sup> Laue, Sommerfeld, and others, in discussing a paper by P. P. Ewald on the transmission of light through a crystal, concluded that x-rays should exhibit interference effects when they encounter the atomic space-lattice which Bravais and others had assumed to exist in a crystal. Consequently, two of their coworkers, Friedrich and Knipping, undertook their successful experiments to observe the phenomenon.

Not only did this reveal a powerful new method for investigations into the nature of x-rays, but also it soon was recognized as a means of investigating the molecular and atomic structure of solids that is still superior to any other known method. By its aid, the arrangement of the atoms in such "simple" solids as copper or salt (sodium chloride) has been

<sup>1</sup> A. H. Compton and R. L. Doan, *Proc. Natl. Acad. Sci.*, **11**, 598 (1925).

<sup>2</sup> W. Friedrich, P. Knipping, and M. Laue, *Ann. Physik*, **41**, 971 (1913), reprint from an earlier publication in 1912.

<sup>3</sup> B. Walter and R. Pohl, *Ann. Physik*, **25**, 715 (1908), **29**, 331 (1908); A. Sommerfeld, *Ann. Physik*, **38**, 473 (1912); P. P. Koch, *Ann. Physik*, **38**, 507 (1912).

<sup>4</sup> A. Bravais, "Abhandlung über die Systeme von Regelmässig auf einer Ebene oder in Raum vertheilten Punkten," 1848. Translated by C. and E. Blasius. Appeared as No. 90 of Ostwald's "Klassiker der exakten Wissenschaften," Wilhelm Engelmann, Leipzig, 1897.

<sup>5</sup> See Sec. 10.

deduced so that their crystal structure is known as accurately as the structure of an egg crate or a wire fence might be known to an observer using a telescope 100 yd. away. In some extremely complex compounds such as rubber or some of the proteins, the structure has been deduced only in a qualitative or semiquantitative way. X-ray diffraction also has proved to be a powerful method in metallography (Chap. 20) for determining the "grain size" (crystal size), detecting preferential orientation (texture), revealing grain distortion (strain), and correlating these three factors with heat-treatment, cold work, drawing, rolling, etc. Thus it has contributed greatly to the understanding of the nature of the changes occurring to the crystals during such processes. The importance of these changes may be emphasized by pointing out that there is as much difference between the physical properties of steel before and after heat-treatment as there is between lead and tin, for example. The recent book by Barrett<sup>1</sup> treats many of the topics discussed in the later chapters of this book, and it should serve as a good reference work for the reader interested in these topics.

X-ray diffraction now serves as a convenient and practical method of chemical analysis (Chap. 19) superior to any other in certain cases. It can also be used as a method of measuring strain (Chap. 21). Its field of application extends to liquids and gases (Chap. 22) and to various other fields (Chap. 23).

**2. The Crystal Lattice and the Law of Rational Indices.** In 1690, C. Huygens made some measurements on calcite crystals and theorized that they were composed of some basic unit which built up the crystal by geometric repetition. In 1784, M. l'Abbé Haüy of the University of Paris published an "Essai d'une théorie sur la structure des cristaux," which marks the beginning of modern crystallography. Most of the early theory of crystals was based on the phenomenon of cleavage. The fact that common crystals like mica, calcite, and rocksalt can be split into pieces and that the pieces of any one such substance always have the same shape naturally suggests the idea of some minute fundamental building block characteristic of the particular substance. By building a structure composed of such identical cells arranged in rows and layers, and always with the same orientation, a crystal with "cleavage planes" like those observed in actual crystals should result.

Haüy suggested that three nonparallel faces of a crystal be selected and that their intersections define a set of geometrical axes suitable for use in describing the crystal. In Fig. 14-1, these axes are represented as  $OA$ ,  $OB$ , and  $OC$ , the three nonparallel planes being  $AOB$ ,  $AOC$ , and  $BOC$ . Haüy then chose a fourth face that cuts all three of

<sup>1</sup> C. S. Barrett, "Structure of Metals," McGraw-Hill Book Company, Inc., New York, 1943.

these axes, its plane being represented in Fig. 14-1 by  $ABC$ . Let  $OA = a'$ ,  $OB = b'$ , and  $OC = c'$ . Then as an example, it may be found that  $a' = 17.3$ ,  $b' = 25.7$ , and  $c' = 14.4$  mm., in., or lignes, it makes no difference; the angles in the figure will remain the same regardless of the units of length used. Since only relative lengths are significant, it simplifies matters somewhat to set  $b' = 1$  arbitrarily. In the above example, one then has  $a' = 17.3/25.7 = 0.673$ ;  $b' = 1$ , and  $c' = 14.4/25.7 = 0.561$ .

Haüy then found that all faces of actual crystals are always parallel to planes having intercepts  $a'/h'$ ,  $b'/k'$ , and  $c'/l'$  on the three axes, where  $h'$ ,  $k'$ , and  $l'$  are small integers. This is known as the "law of rational indices," one of the fundamental laws of crystallography. Subsequently, other workers pointed out that this law and other facts about crystallography could be explained by assuming that crystals are built up by elementary particles arranged at the points of a "space-lattice." Prominent

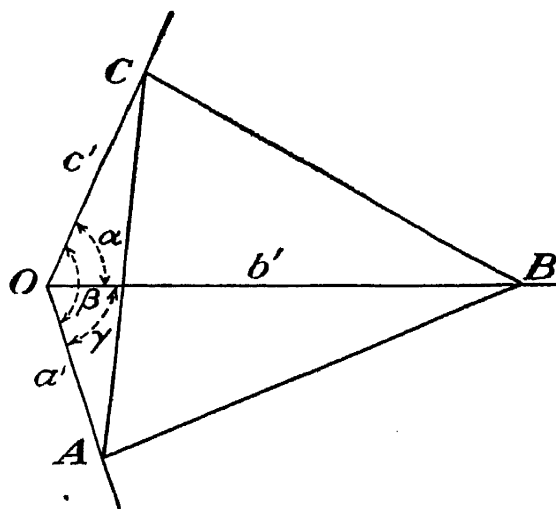


FIG. 14-1.—The crystallographic axes and the law of rational indices.

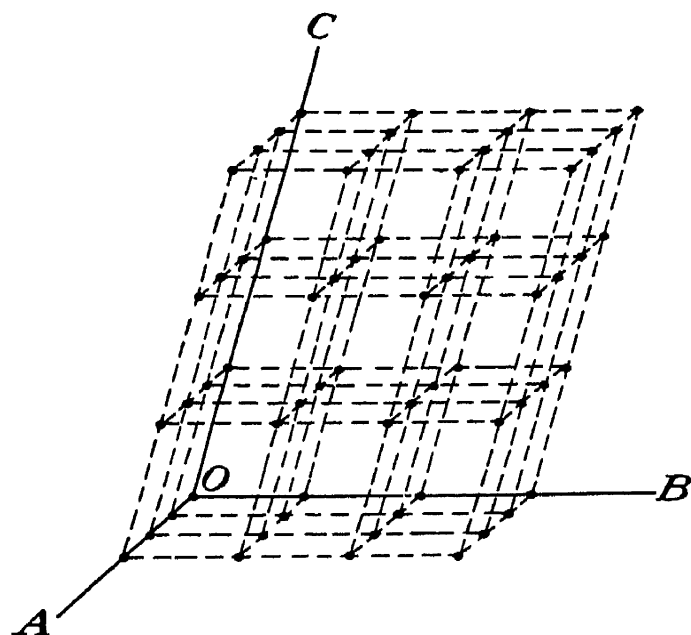


FIG. 14-2.—Point lattice (dots). Line lattice (dotted lines).

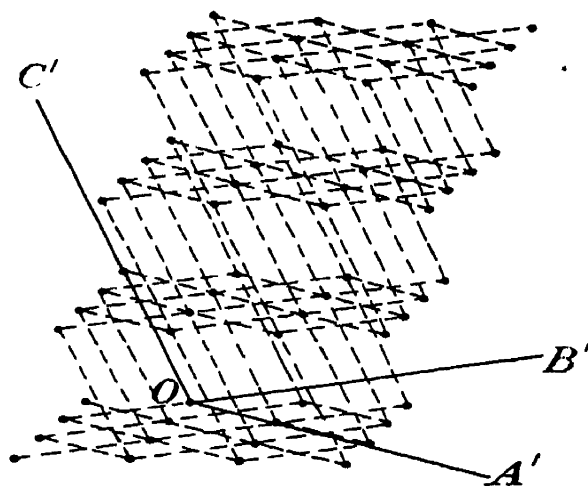


FIG. 14-3.—Same point lattice as in Fig. 14-2, but associated with a different line lattice.

among these workers about 1850 was Bravais. Figure 14-2 illustrates a point space-lattice. It is a geometrically arrayed set of points, represented in the figure by dots. The network of straight lines that connect the points of the point lattice constitute a line space-lattice,

constructed to conform to the axes  $OA$ ,  $OB$ , and  $OC$ . Both the line lattice and the point lattice may be imagined to extend indefinitely in all three directions. The point lattice of Fig. 14-2 is not necessarily associated with any particular line lattice. The same point lattice is shown in Fig. 14-3 associated with a different line lattice constructed on the axes  $OA'$ ,  $OB'$ , and  $OC'$ .

If one now imagines an atom or group of atoms placed at each point of such a point lattice, the composition and orientation of each group being identical with that of all the others, the resulting structure is called a "crystal lattice." By extending it indefinitely in all directions, a crystal is built up. These ideas regarding the structure of crystals were well established before the discovery of x-rays or x-ray diffraction.

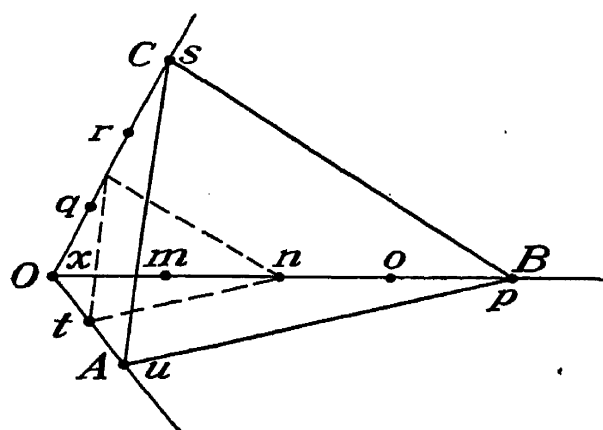


FIG. 14-4.—Lattice planes.

Reference to Fig. 14-4 shows how such a theory accounts for the law of rational indices. The crystal axes  $OA$ ,  $OB$ , and  $OC$  of Fig. 14-1 coincide with rows of identical atoms located at  $xtu$ ,  $xmnop$ , and  $xqrs$ . The planes  $OAB$ ,  $OAC$ , and  $OBC$  are seen to be planes of atoms, and the faces that naturally develop on the surface of crystals coincide with such atomic

planes. Likewise,  $ABC$  is a "rational" atomic plane containing the atoms or atomic groups located at  $p$ ,  $s$ , and  $u$  on the axes. In fact, the whole crystal may be thought of as being built up of a system of atomic planes parallel to  $ABC$  (see Fig. 14-5). The plane indicated by the dotted lines, including the atoms at  $t$  and  $n$ , is one of these. Other atomic planes parallel to  $ABC$ , but not shown in the figure, are one passing through  $m$ , one through  $q$ , one through  $r$ , one through  $o$ , one through atom  $x$  at the origin  $O$ , and several others between  $O$  and  $ABC$ , defined by atoms not shown in the figure because they do not lie on the axes  $OA$ ,  $OB$ , or  $OC$ . If a complete three-dimensional model of the lattice were examined, it would be found that there are 12 equally spaced parallel atomic planes between the origin and  $ABC$ , counting  $ABC$  itself. Similar planes parallel to  $ABC$  extending in both directions beyond these 12 would include all the atoms in the crystal, and these planes all contain the same number of atoms per unit area. The number 12 is obtained by multiplying 2 ( $A$  is 2 atoms from  $O$ ) by 4 ( $B$  is 4 atoms from  $O$ ) by 3 ( $C$  is 3 atoms from  $O$ ) and dividing by any common integral factor other than 1 (2 is a factor of both 2 and 4, among the numbers 2, 4, and 3). In general, the number  $N$  of such planes between a rational plane like  $ABC$  ("rational" because it intersects all three axes at a lattice point) and the

origin is given by

$$N = \frac{ABC}{rst} \quad (14-1)$$

where  $A$  is the number of lattice intervals from  $O$  to  $A$ ;  $B$  is the number of intervals from  $O$  to  $B$ ;  $C$  is the number of intervals from  $O$  to  $C$ ;  $r$  is the highest common integral factor of  $B$  and  $C$ ;  $s$  is the highest common integral factor of  $A$  and  $C$ ; and  $t$  is the highest common integral factor of  $A$  and  $B$ .

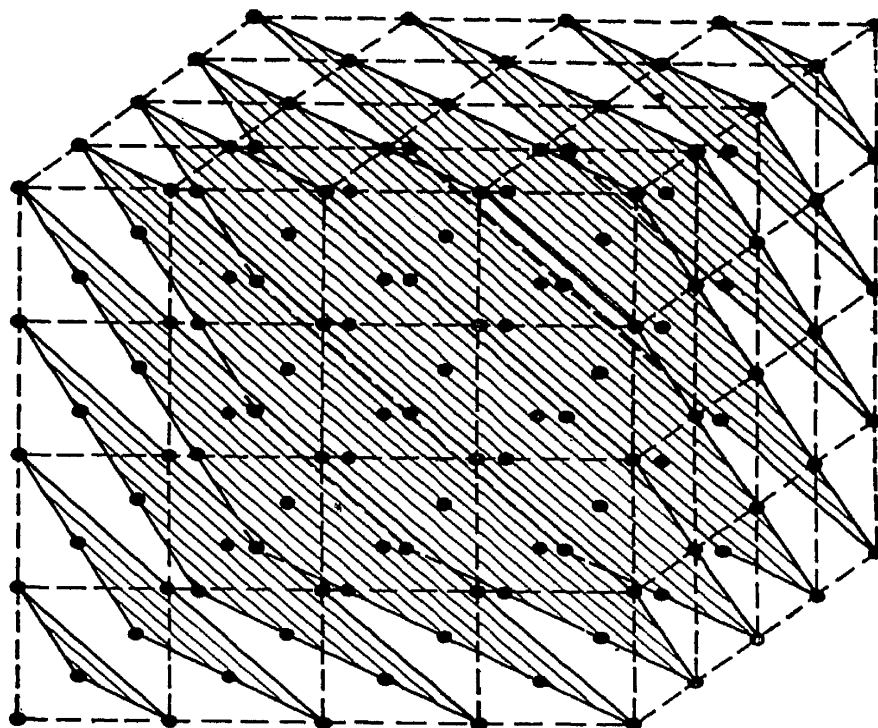


FIG. 14-5.—A space-lattice may be regarded as composed entirely of any single chosen set of rational planes—in this case, the (111) set.

In a similar way, a set of planes can be selected parallel to the rational plane through the points  $u$ ,  $n$ , and  $q$ , for example. If the intercepts of the plane  $ABC$  are  $a'$ ,  $b'$ , and  $c'$ , then the intercepts of the new plane through  $u$ ,  $n$ , and  $q$  will be  $a'$ ,  $b'/2$ , and  $c'/3$ , where  $a'$ ,  $b'$ , and  $c'$  are measured in angstroms, let us say. That is, the intercepts of any rational atomic plane (associated with an extended set of parallel atomic planes) will be given by  $a'/h'$ ,  $b'/k'$ , and  $c'/l'$ , where  $h'$ ,  $k'$ , and  $l'$  are small integers (1, 2, and 3 in this case). Hence, if the faces that naturally develop on a crystal coincide with rational planes of atoms in the crystal lattice, it is evident that they must be oriented in accordance with the law of rational indices.

**3. Miller Indices.** Thus far, all distances and intercepts have been thought of in terms of ordinary units of length, such as inches, angstrom units, or millimeters. In the discussion of rational atomic planes such as  $ABC$  in Fig. 14-4, it will often be more convenient to express the intercepts in terms of the number of lattice-point intervals along the axis. That is, if the distance between points  $x$  and  $t$ ,  $t$  and  $u$ , etc., is designated as  $a$  and

the distance between  $x$  and  $m$ ,  $m$  and  $n$ ,  $n$  and  $o$ , etc., is designated as  $b$ , and the distance between  $x$  and  $q$ ,  $q$  and  $r$ ,  $r$  and  $s$ , etc., is designated as  $c$ , then the intercepts of the plane  $ABC$  are  $2a$ ,  $4b$ , and  $3c$ , respectively. In general, of course,  $a$ ,  $b$ , and  $c$  are not equal. To abbreviate matters further, one may say that the intercepts of the plane  $ABC$  are 2, 4, and 3, it being understood that the  $A$  intercept is always given first, the  $B$  intercept second, and the  $C$  intercept last and that the  $A$  intercept is measured, not in centimeters, but in units of length equal to  $a$ , the  $B$  intercept in units of length equal to  $b$ , and the  $C$  intercept in units of length equal to  $c$ . Henceforth, whenever intercepts are mentioned or designated merely by a whole number, it is to be understood that the meaning is the one just given.

The need for some convenient and conventional way of designating the naturally occurring faces of a crystal and the atomic planes with which they are associated is obvious. The designation now universally used is the one evolved by the English crystallographer and mineralogist W. H. Miller (1801-1880). The planes are designated by three numbers, called "Miller indices." These numbers, or indices, are the lowest three integers having the same ratios as the reciprocals of the intercepts of the plane in question, the intercepts being expressed in the shorthand manner just described. For example, the reciprocals of the intercepts of the plane  $ABC$  in Fig. 14-4 are  $\frac{1}{2}$ ,  $\frac{1}{4}$ , and  $\frac{1}{3}$ . The lowest three integers having the same ratios as  $\frac{1}{2}$ ,  $\frac{1}{4}$ , and  $\frac{1}{3}$ , are 6, 3, and 4. Hence the Miller indices are 6, 3, and 4. They are customarily written in parentheses to designate a set of parallel planes, and the plane  $ABC$  is referred to as a (634) plane. The plane indicated by the dotted lines in Fig. 14-4 has intercepts 1, 2, and  $1\frac{1}{2}$ , the reciprocals being 1,  $\frac{1}{2}$ , and  $\frac{2}{3}$ , and hence it is also a (634) plane. As already mentioned, there are twelve (634) planes between  $ABC$  and  $O$ , counting the one through  $O$ .

The plane passing through  $u$ ,  $n$ , and  $q$  (Fig. 14-4) has intercepts 2, 2, and 1 and reciprocals  $\frac{1}{2}$ ,  $\frac{1}{2}$ , and 1 and hence is a (112) plane. The application of equation (14-1) to this plane shows that it is the second (112) plane from the origin, since  $N = 2$ . Equation (14-1) may be expressed in another form, which is often more convenient when Miller indices are used.

$$N = \frac{hkl}{efg} \quad (14-2)$$

where  $h$ ,  $k$ , and  $l$  are the Miller indices and  $e$ ,  $f$ , and  $g$  are the highest common integral factors of  $k$  and  $l$ ,  $h$  and  $l$ , and  $h$  and  $k$ , respectively.

The planes  $AOB$ ,  $AOC$ , and  $BOC$  in Fig. 14-4 each have intercepts on only one axis, and it is zero. How does one then determine their Miller indices? Since parallel lattice planes have the same Miller indices, let us determine the indices of a rational plane parallel to plane



$AOB$ , for example the plane through  $q$  parallel to  $AOB$ . Its intercepts are infinity, infinity, and 1, commonly written  $\infty$ ,  $\infty$ , and 1. The reciprocals of these are 0, 0, and 1; therefore,  $AOB$  is an (001) plane. Likewise,  $AOC$  is an (010) plane, and  $BOC$  is a (100) plane. In speaking of these, they are called "oh, oh, one," "oh, one, oh," and "one, oh, oh" planes.

When the intercept is negative, the reciprocal is also negative, and in this case the minus sign is written over the index, as  $(\bar{1}00)$ . However a  $(\bar{1}00)$  plane is parallel to a (100) plane, the two merely being on opposite sides of the origin, so that both belong to the same family. Hence the use of negative indices is not usually necessary in discussing simple crystals. In a cubic crystal, there is no particular distinction between a (100) plane and an (010) plane or an (001) plane or between (111),  $(\bar{1}\bar{1}1)$ ,  $(1\bar{1}\bar{1})$ , and  $(11\bar{1})$  (see Fig. 14-5); but in a tetragonal crystal (001 and  $00\bar{1}$ ) are different from (100),  $(\bar{1}00)$ , (010), and  $(0\bar{1}0)$  because  $c$  is different from  $a$  and  $b$ . The (100), (010), and (001) planes in a cubic crystal are said to constitute the  $\{100\}$  "form" (note the braces instead of parentheses).

**4. The Seven Crystal Systems and the 14 Holohedral Space-lattices.** In Bravais' work of 1848, he showed that there were 14 symmetrical ways of arranging a point lattice in space, which in turn might be classified under seven general systems of crystal symmetry. Two of these seven crystal systems, the hexagonal and the rhombohedral, are interrelated in such a way that modern writers often classify the together, there being then only six general systems. Referring to Fig. 14-6, the seven systems are as follows:

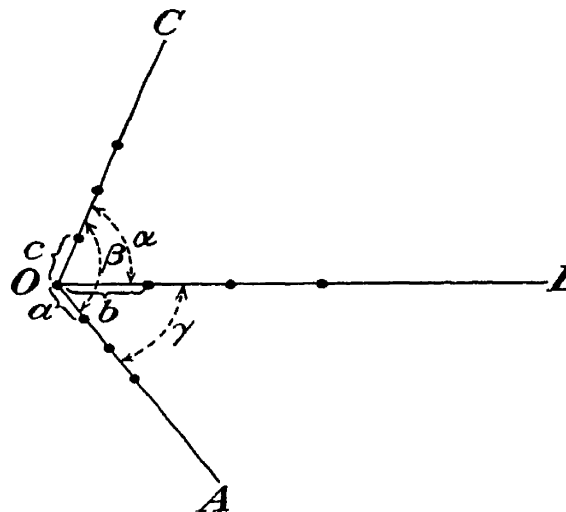


FIG. 14-6.—The lattice constants  $a$ ,  $b$ ,  $c$ ,  $\alpha$ ,  $\beta$ , and  $\gamma$ .

TABLE 14-1.—THE SEVEN SYSTEMS OF CRYSTAL SYMMETRY

1. Cubic or isometric system . . . . .	$a = b = c$	$\alpha = \beta = \gamma = 90^\circ$
2. Hexagonal system, hexagonal division . . . . .	$a = b \neq c$	$\alpha = \beta = 90^\circ \gamma = 120^\circ$
3. Hexagonal system, rhombohedral division (sometimes called the "rhombohedral" or "trigonal" system) . . . . .	$a = b = c$	$\alpha = \beta = \gamma \neq 90^\circ$
Since $\alpha = \beta = \gamma$ , all three are sometimes designated by the single letter $\omega$		
4. Tetragonal system . . . . .	$a = b \neq c$	$\alpha = \beta = \gamma = 90^\circ$
5. Orthorhombic or rhombic system . . . . .	$a \neq b \neq c$	$\alpha = \beta = \gamma = 90^\circ$
6. Monoclinic system . . . . .	$a \neq b \neq c$	$\alpha = \gamma = 90^\circ \neq \beta$
7. Triclinic system . . . . .	$a \neq b \neq c$	$\alpha \neq \beta \neq \gamma$

TABLE 14-2.—THE 14 SYMMETRICAL SPACE-LATTICES OF BRAVAIS

1. Face-centered cubic.

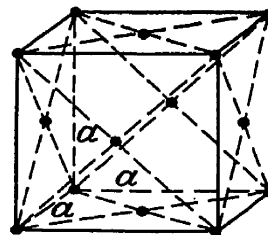
 $O_h^5$ 

FIG. 14-7.

2. Body-centered cubic.

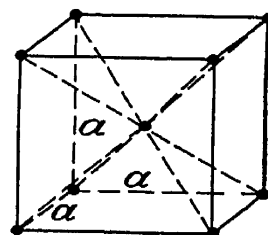
 $O_h^8$ 

FIG. 14-8.

3. Simple cubic.

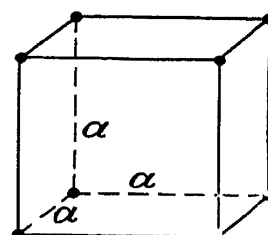
 $O_h^1$ 

FIG. 14-9.

4. Body-centered tetragonal.

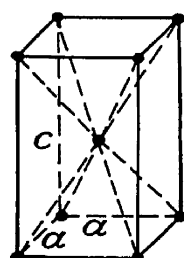
 $D_{4h}^{17}$ 

FIG. 14-10.

5. Tetragonal.

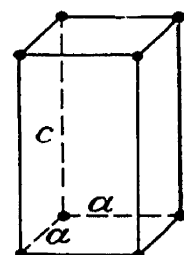
 $D_{4h}^1$ 

FIG. 14-11.

6. Rhombohedral.

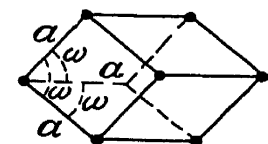
 $D_{3d}^5$ 

FIG. 14-12.

7. Hexagonal.

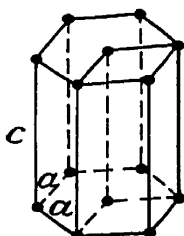
 $D_{6h}^1$ 

FIG. 14-13.

TABLE 14-2.—THE 14 SYMMETRICAL SPACE-LATTICES OF BRAVAIS.—(Continued)

8. Face-centered orthorhombic.

$$V_h^{23} \text{ or } D_{2h}^{23}$$



FIG. 14-14.

9. Body-centered orthorhombic.

$$V_h^{25} \text{ or } D_{2h}^{25}$$



FIG. 14-15.

10. Orthorhombic, one face centered.

$$V_h^{19} \text{ or } D_{2h}^{19}$$

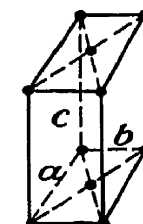


FIG. 14-16.

11. Simple orthorhombic.

$$V_h^1 \text{ or } D_{2h}^1$$

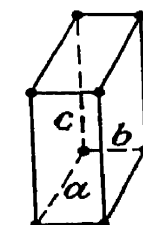


FIG. 14-17.

12. Monoclinic, one face centered.

$$C_{2h}^3$$

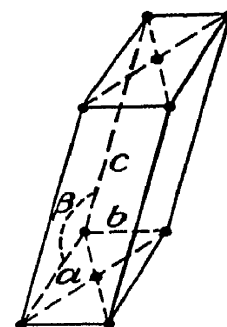


FIG. 14-18.

13. Simple monoclinic.

$$C_{2h}^1$$

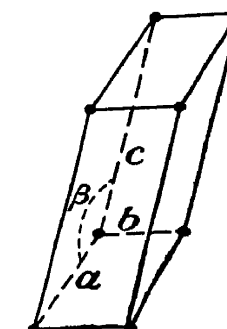


FIG. 14-19.

14. Triclinic.

$$C_i^1 \text{ or } S_2^1$$

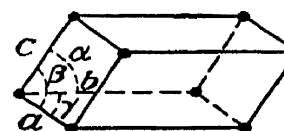


FIG. 14-20.

**5. The 32 Point Groups.** Subsequent work showed that these 14 lattices of Bravais were only the "holohedral" types of the seven crystal systems and that there are in reality 32 classes of crystal symmetry, called the 32 "point groups." A holohedral crystal is one having all the faces required by complete symmetry. A more elaborate classification is required in order to include the "hemihedral" crystals (crystals having half the similar parts of a crystal form instead of all, as a tetrahedron, which is hemihedral to an octahedron), the "tetartohedral" crystals (crystals having one-fourth the number of faces required for symmetry), the "hemimorphic" varieties (unsymmetrical in form as regards the two ends of an axis), and the "enantiomorphic" varieties (related to each other as a right-handed to a left-handed glove).

The 32 point groups are as follows:

TABLE 14-3.—THE 32 POINT GROUPS

	Schoenflies Symbol
1. Cubic system, holohedral class.....	$O_h$
2. Cubic system, enantiomorphic hemihedral class.....	$O$
3. Cubic system, hemimorphic hemihedral class.....	$T_d$
4. Cubic system, paramorphic hemihedral class.....	$T_h$
5. Cubic system, tetartohedral class.....	$T$
6. Hexagonal system, hexagonal division, holohedral class..	$D_{6h}$
7. Hexagonal system, hexagonal division, enantiomorphic hemihedral class.....	$D_6$
8. Hexagonal system, hexagonal division, hemimorphic hemihedral class.....	$C'_{6v}$
9. Hexagonal system, hexagonal division, paramorphic hemihedral class.....	$C'_{6h}$
10. Hexagonal system, hexagonal, division, tetartohedral class.....	$C'_6$
11. Hexagonal system, hexagonal division, trigonal holo- hedral class.....	$D_{3h}$
12. Hexagonal system, hexagonal division, trigonal para- morphic hemihedral class.....	$C'_{3h}$
13. Hexagonal system, rhombohedral division, holohedral class.....	$D_{3d}$
14. Hexagonal system, rhombohedral division, enantio- morphic hemihedral class.....	$D_3$
15. Hexagonal system, rhombohedral division, hemimorphic hemihedral class.....	$C'_{3v}$
16. Hexagonal system, rhombohedral division, hexagonal tetartohedral class of the second sort.....	$C'_{3i} = S_6$
17. Hexagonal system, rhombohedral division, tetartohedral class.....	$C'_3$
18. Tetragonal system, holohedral class.....	$D_{4h}$
19. Tetragonal system, enantiomorphic hemihedral class...	$D_4$
20. Tetragonal system, hemimorphic hemihedral class.....	$C'_{4v}$
21. Tetragonal system, paramorphic hemihedral class.....	$C'_{4h}$

TABLE 14-3.—THE 32 POINT GROUPS—(Continued)

	Schoenflies Symbol
22. Tetragonal system, hemihedral class of the second sort...	$V_d = D_{2d}$
23. Tetragonal system, tetartohedral class.....	$C_4$
24. Tetragonal system, tetartohedral class of the second sort.	$S_4$
25. Orthorhombic system, holohedral class.....	$V_h = D_{2h}$
26. Orthorhombic system, enantiomorphic hemihedral class.....	$V = D_2$
27. Orthorhombic system, hemimorphic hemihedral class...	$C_{2v}$
28. Monoclinic system, holohedral class.....	$C_{2h}$
29. Monoclinic system, hemimorphic hemihedral class.....	$C_2$
30. Monoclinic system, hemihedral class.....	$C_s$
31. Triclinic system, holohedral class.....	$C_i$
32. Triclinic system, hemihedral class.....	$C_1$

**6. Crystal Nomenclature and the Schoenflies Notation; the 230 Space Groups.** The names in the preceding table are those used by A. Schoenflies in 1891. Other authoritative crystallographers have unfortunately used different names. For example, point group 2 (cubic system, enantiomorphic hemihedral class, according to Schoenflies) was called the “cubic plagihedral” class by E. S. Dana, the “tesseral holoaxial” class by H. A. Miers, the “regular plagihedral hemihedral” class by Liebisch, and the “pentagonalicositetrahedral” class by P. Groth, these men being crystallographers or mineralogists of recognized authority about 1900.

The symbols  $O_h$ ,  $T$ ,  $C_{4v}$ ,  $D_{2h}$ , etc., in Tables 14-2 and 14-3 are the notation used by Schoenflies to identify and classify the various types of crystals. This notation was one of the earliest invented to represent the various crystal classes. The meanings of the symbols are as follows:

$C_1$  or  $C_4$ , etc., represents groups having a single rotation axis of onefold, fourfold, etc., symmetry.

$C_s$  represents groups having a single rotation axis of onefold symmetry and a plane of symmetry.

$C_i$  represents groups having a single rotation axis of onefold symmetry and a center of symmetry, or center of inversion.

$S_4$ ,  $S_6$ , etc., represents groups having a fourfold or sixfold, etc., axis of rotary reflection.

$C_{3i}$ , for example, represents groups having a single rotation axis of threefold symmetry and a center of inversion. Such groups also necessarily have a sixfold axis of rotary reflection. Hence  $C_{3i} = S_6$ .

$D_2$ ,  $D_4$ ,  $D_6$ , etc., represent groups having a twofold, fourfold, sixfold, etc., principal axis and 2, 4, 6, etc., twofold axes at right angles to the principal axis.

$V$  is a special symbol standing for *Viererguppe* (four group) and is identical with  $D_2$ . This is a special case because, with 3 twofold axes, the preference for one as the main axis no longer exists.

$T$  represents tetrahedral groups, which have 3 twofold and 4 threefold axes.

$O$  represents octahedral groups, which have 3 fourfold, 6 twofold, and 4 threefold axes.

Subscript  $h$  indicates a "horizontal" plane of symmetry, that is, one perpendicular to the principal axis. For example,  $C_2$  indicates a single axis of twofold symmetry, but  $C_{2h}$  indicates a plane of symmetry perpendicular to this axis in addition.

Subscript  $v$  indicates a "vertical" plane of symmetry, that is, one containing the principal axis.

Subscript  $d$  indicates a diagonal plane of symmetry.

Only significant planes of symmetry are indicated. For example,  $T_h$  does not mean that "vertical" planes of symmetry are absent; such planes necessarily arise through the cyclic operations of the three twofold and four threefold axes combined with the horizontal plane of symmetry.  $C_{1h}$  is a special case equivalent to  $C_s$  because a single plane of symmetry can be considered at will as parallel or perpendicular to an optional onefold axis of rotation.

The meanings of such terms as "threefold axis of symmetry," "center of inversion," "axis of rotary reflection," and "plane of symmetry" will be explained shortly, although they are well named and are therefore almost self-explanatory. It will be well first to carry on the business of classifying crystals to its final step.

Thus far, consideration has been given to ways of grouping only points into a symmetrical space-lattice. In an actual crystal, however, one is dealing, not with points, but with atoms and especially with groups of atoms that are identical with each other, but not necessarily oriented identically in space. When this is considered, the crystal classifications are no longer limited to the 32 possible point groups but expand to some 65 categories. Even this is not enough. It was found that in order to classify all the different crystals found in nature it would be necessary to postulate that the groups of atoms located at the lattice points may be of two different enantiomorphic types in a single crystal. "Enantiomorphic" has already been defined. One may easily visualize the possibility of, say, 10 atoms, such as 1 calcium, 1 magnesium, 2 silicons, and 6 oxygens, grouping themselves into a configuration of a certain shape or into one related to this shape as a left-handed glove is related to a right-handed glove; such configurations are enantiomorphic.

When the possibilities of enantiomorphic atomic groups, oriented in various systematic ways at the points of the 32 different kinds of possible symmetrical space-lattice are considered, it develops that there are 230 possible "space groups." It was found that all the crystals occurring in nature may be classified in these 230 possible groups.

Schoenflies expanded his notation to include all these by introducing superscripts. Thus, in the holohedral class of the orthorhombic system ( $V_h$  or  $D_{2h}$ ), there are 28 different possible space groups. Schoenflies

enumerated these one by one in a way that appeared logical to him. The first he called  $V_h^1$  or  $D_{2h}^1$ ; the second,  $V_h^2$  or  $D_{2h}^2$ , etc., up to  $V_h^{28}$  or  $D_{2h}^{28}$ . Thus  $D_{2h}^{14}$  or  $V_h^{14}$  represents the fourteenth variety (as classified by Schoenflies) of the group of crystals having three mutually perpendicular twofold axes and a plane of symmetry coinciding with two of them (which automatically establishes symmetry planes coinciding with each of the three pairs of axes).

Other crystallographers have been generally unwilling to accept this Schoenflies notation and use it, for there are certain valid objections to it. They have invented various "improved" and "less confusing" systems to supplant the Schoenflies notation, each much better and less confusing than the Schoenflies system, according to its inventor. However, the only system that nearly everybody understands is the Schoenflies system. For example, the space group designated as  $D_{4h}^{13}$  in the Schoenflies notation is designated 4Di-13 in the Wyckoff notation and  $P4/mbc$  or  $C4/mbc$ , according to the orientation, in the Mauguin notation.

If a straight line can be drawn through the center of a crystal in such a way that a  $180^\circ$  rotation of the crystal about this "axis" leaves it in a position indistinguishable from its initial one, it is a twofold axis of symmetry. If a  $120^\circ$  rotation does this, the axis is threefold; if  $90^\circ$  does it, it is fourfold; if  $60^\circ$  does it, it is sixfold. Of course, a  $360^\circ$  rotation must do it; therefore, any line through the center of any crystal is a onefold axis of that crystal.

If a plane can be found, passing through the center of a crystal, such that the part of the crystal on one side of the plane is a mirror image or reflection of the part on the other side, the plane is a plane of symmetry.

If, for every point in a crystal, there can be found an equivalent point such that a straight line joining them passes through the center of the crystal and is bisected by this center point, then this point is a center of symmetry, or a center of inversion.

If a plane can be found, passing through the center of a crystal, such that the part of the crystal on one side of the plane may be rotated about the axis perpendicular to the plane and then "reflected" to coincide with the part of the crystal on the other side of the plane, the plane is a plane of rotary reflection, and the axis perpendicular to it is an axis of rotary reflection. If the minimum rotation necessary is  $60^\circ$ , it is a sixfold axis; if  $90^\circ$ , it is a fourfold axis, etc.

These operations of rotation, reflection, inversion, and rotary reflection are called "symmetry operations." Reflection is equivalent to a  $180^\circ$  rotation of one-half of the crystal, plus an inversion. Symmetry operations such as inversion or reflection that convert an object into its enantiomorphic counterpart are called "operations of the second kind." Others are "operations of the first kind."

**7. The Unit Cell; the Hexagonal Close-packed Structure; Number of Units of Structure per Unit Cell.** Fortunately, the commonest and most plentiful crystals have a high degree of symmetry, such as cubic or hexagonal. That is, most crystals have a simple, easily visualized structure. In 1897, W. Barlow speculated that a likely arrangement for many simple substances such as the chemical elements would be one in which the atoms, which he visualized as balls, or spheres, would be packed together in a systematic but compact manner. He drew diagrams of two or three likely types of arrangement, or structure. One of the most obvious and natural of these is the arrangement known as the

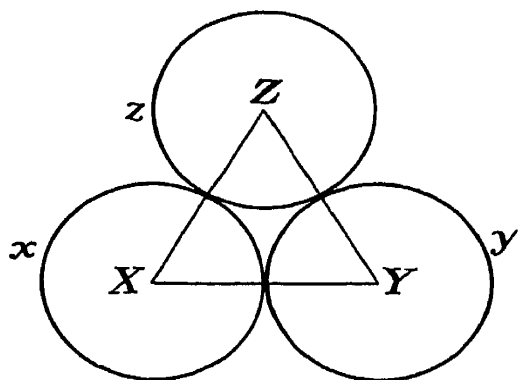


FIG. 14-21.—Three equal balls in contact.

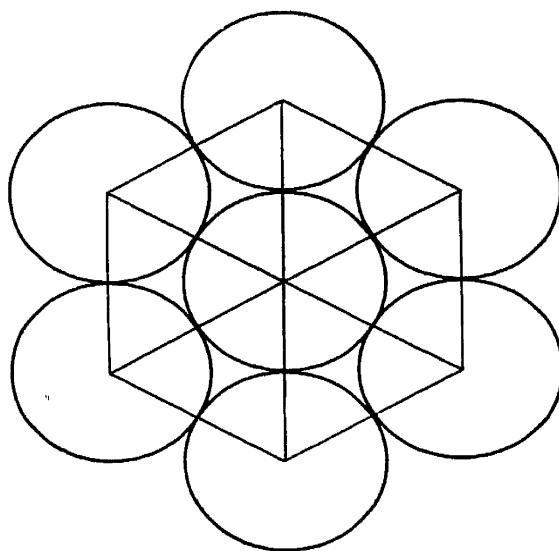


FIG. 14-22.—Hexagonal pattern formed by layer of equal balls.

“hexagonal close-packed” structure; another is the “face-centered cubic” structure.

In Fig. 14-21, three balls  $x$ ,  $y$ , and  $z$  touch each other. The balls are identical, each with a diameter of one arbitrary unit of length. Their centers define an equilateral triangle  $XYZ$ , of which the length of each side is 1, also. An extension of this leads immediately to a hexagonal pattern in two dimensions, as when seven balls are grouped on a table top (Fig. 14-22). One may imagine tennis balls laid in a flat-bottomed pan until they cover the bottom of it in a hexagonal pattern of this sort. As more balls are added, a second layer is begun, the balls in this layer naturally occupying the positions shown by the dotted circles in Fig. 14-23. When the third layer of balls is begun, there are two alternatives. The balls may be placed at the points indicated by the small circles in Fig. 14-23 (directly over the balls in the bottom layer) or at the points indicated by the black dots. In the former case, one may continue to build up a systematic structure by placing successive layers of balls at the circles, then the squares, continuing in a circle-square-circle sequence. The resulting arrangement is the hexagonal close-packed structure. If



one builds up layers in a circle-square-dot-circle-square-dot sequence, the resulting structure is face-centered cubic,<sup>1</sup> which will be discussed in

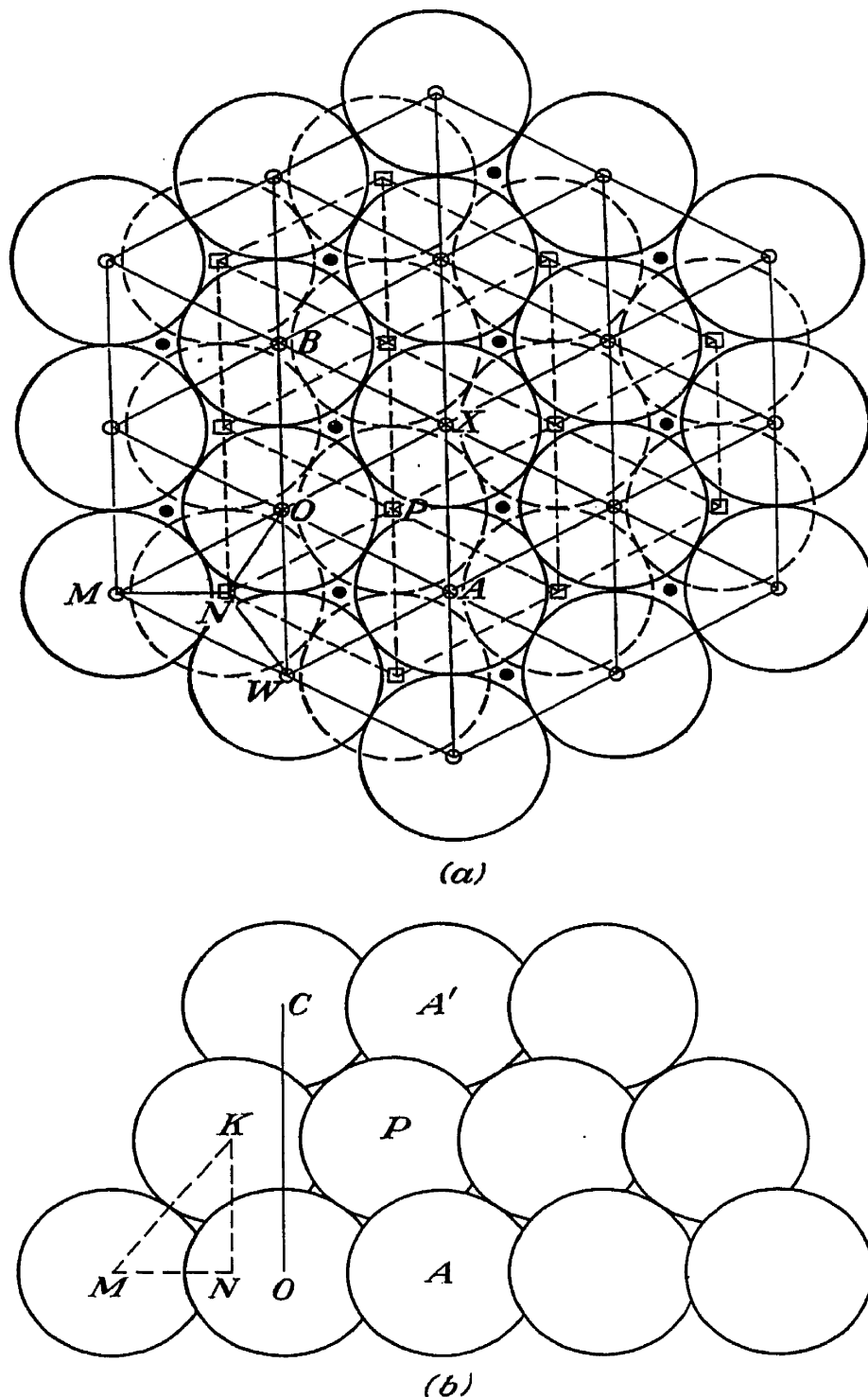


FIG. 14-23.—(a) Plan of two types of close packing of spheres: (1) hexagonal, and (2) face-centered cubic. (b) Hexagonal close packing in elevation.

Sec. 9. The lower part of Fig. 14-23 illustrates the hexagonal close-packed structure in elevation. The upper part (a) showing the structure in plan makes it clear that each ball is in contact with the surrounding

<sup>1</sup> Instructive models of these structures are readily constructed. See, for example, D. B. Langmuir and R. B. Nelson, *Rev. Sci. Instruments*, **11**, 295 (1940).

six balls in its own layer and also with three balls in the layer below and three in the layer above, or with twelve in all.

Examination of Fig. 14-23a indicates that

$$MN = WN = ON = \frac{1}{\sqrt{3}}$$

since  $MO = WO = MW = 1$ . It is seen that  $MN$  in the upper diagram (a) is identical with  $MN$  in the lower diagram (b), where, in the triangle  $MNK$ ,  $MK = 1$  and  $MN = 1/\sqrt{3}$ . Hence

$$NK = \sqrt{1 - \frac{1}{3}} = \sqrt{\frac{2}{3}} = 0.8165 = \text{distance between layers of balls.}$$

If  $O$  is chosen as origin and  $OA$ ,  $OB$ , and  $OC$  are chosen as the crystallographic axes, it is seen that  $OA = a = 1$ ,  $OB = b = 1$ , and

$$OC = c = 1.633,$$

where  $a$ ,  $b$ , and  $c$  have the meanings assigned to them in Sec. 3. On this basis, it is seen that the coordinates of  $P$ , a ball in the second layer, are  $\frac{2}{3}a$ ,  $\frac{1}{3}b$ ,  $\frac{1}{2}c$ , or, as it is usually expressed, simply  $\frac{2}{3}$ ,  $\frac{1}{3}$ ,  $\frac{1}{2}$ . On this basis, the "unit cell" of the "crystal lattice" for these balls is delineated by the points  $O$ ,  $A$ ,  $X$ , and  $B$  in the bottom layer of balls and the similar points  $C$ ,  $A'$ ,  $X'$ , and  $B'$  directly above them in the third layer. It is easy to compute that the volume of this unit cell is  $\sqrt{2}$  when  $a = b = 1$ , as has been assumed. When  $a \neq 1$ , the volume of the cell is  $\sqrt{2} a^3$ . The "axial ratio"  $c/a$ , which is an important factor in lattice calculations, is of course 1.633. In figuring axial ratios,  $b$  is conventionally taken as the basis of measurement, the axial ratios being  $C = c/b$  and  $A = a/b$ . When  $a = b$ , the ratio  $C$  is often written as  $c/a$ , as in the above case.

Thus far in the discussion, the origin of coordinates has been taken at the center of ball  $A$ . Obviously, the origin could have been taken at the center of any other ball without essentially altering the discussion. In this sense, any unit cell in the whole lattice may be said to have a ball at the point 0, 0, 0. In effect, this means that each unit cell has a ball located at, say, the bottom southwest corner. Likewise, every ball in the second layer is located at the point  $\frac{2}{3}$ ,  $\frac{1}{3}$ ,  $\frac{1}{2}$  in its cell. Each ball in the third layer is located at the top northeast (or northwest or southeast or southwest) corner of the first layer of unit cells, but each of these balls must be logically regarded as associated with the second layer of unit cells in the same way that the balls in the first layer were associated with the first layer of unit cells. That is, when thinking of unit cells, one should visualize each ball in the third layer as attached to the bottom southwest corner of a unit cell in the second layer of cells, directly above the corresponding ball and the corresponding cell in the first layer. The balls in the fourth layer of balls are related to the second layer of cells in the same way that the balls in the second layer of balls are related

to the first layer of cells. When considered in this way, it becomes evident that there are only two balls per unit cell,<sup>1</sup> their coordinates being 0, 0, 0 and  $\frac{2}{3}, \frac{1}{3}, \frac{1}{2}$ .

**8. Miller-Bravais Indices.** In the preceding discussion of the hexagonal close-packed arrangement of spheres, the geometry of the lattice was referred to the axes  $OA$ ,  $OB$ , and  $OC$  in Fig. 14-23, which were selected as convenient. However, the hexagonal symmetry of the structure offers no logical reason why the axes  $OA$  and  $OB$  should be preferred to the axes  $OB$  and  $OM$  or  $OM$  and  $OA$ . As Bragg puts it, "... to choose two (of these three) axes arbitrarily, and name the faces accordingly (as (100), (010), etc.) would disguise the hexagonal symmetry of the lattice." The hexagonal system of crystal structure is therefore logically referred to four axes ( $OA$ ,  $OB$ ,  $OM$ , and  $OC$ , Fig. 14-23) rather than three, as in all other crystal systems. This is not always done; that is, one will sometimes find references to the (100) or the (010), etc., planes in a hexagonal crystal, but one will also often find these planes designated as  $(10\bar{1}0)$ ;  $(01\bar{1}0)$ , etc. In this latter notation where four indices are given to identify planes in a hexagonal crystal the four numbers are called "Miller-Bravais indices." If the intercept of a crystal face or an atomic plane on the  $A$  and  $B$  axes of the crystal are  $a/h$  and  $a/k$  ( $a = b$ , of course), it can be shown that the intercept on the third ( $OM$ , Fig. 14-23) is  $-a/(h + k)$ . Hence, if the Miller indices of a plane in a hexagonal crystal are  $h$ ,  $k$ , and  $l$ , the Miller-Bravais indices will be  $h$ ,  $k$ ,  $-(h + k)$ , and  $l$ . The minus sign is commonly written above the index rather than in front of it. The six faces of hexagonal prism have the indices  $(10\bar{1}0)$ ,  $(01\bar{1}0)$ ,  $(\bar{1}100)$ ,  $(\bar{1}010)$ ,  $(0\bar{1}10)$ , and  $(1\bar{1}00)$ , as shown in Fig. 14-24.

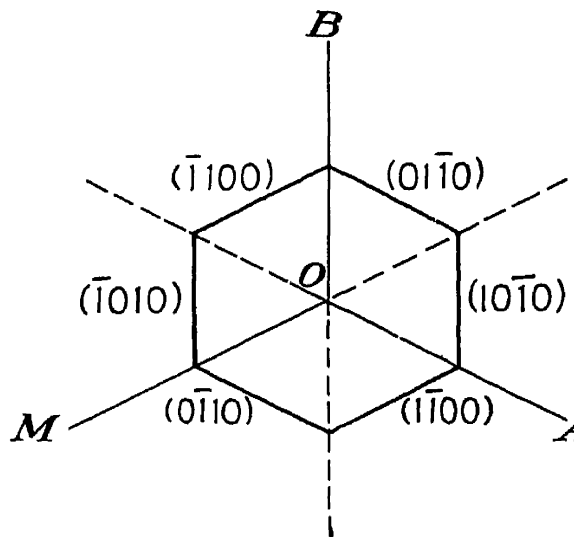


FIG. 14-24. Miller-Bravais indices of faces of a hexagonal prism.

**9. The Face-centered Cubic Structure.** In discussing Fig. 14-23 and the hexagonal close-packed structure, it was stated that a structure in which the layers of balls were built up in a circle-square-dot-circle-square-dot sequence is known as the face-centered cubic structure. Using the same approach as in Sec. 7, one might logically conclude that

<sup>1</sup> This fact is sometimes expressed by the statement that the lattice is "double primitive." A primitive lattice is one having only one translation-equivalent unit or group of units per unit cell. A triply primitive lattice has three groups per unit cell, a quadruply primitive lattice has four, etc.

this structure has a hexagonal lattice with a unit cell containing three balls at  $0, 0, 0$ ;  $\frac{2}{3}, \frac{1}{3}, \frac{1}{3}$ , and  $\frac{1}{3}, \frac{2}{3}, \frac{2}{3}$ ; and an axial ratio of  $3 \times 0.8165$ , or 2.45. However, this is not the fundamental unit cell for the structure; the choice of this cell as the fundamental one would disguise the fact that the structure has a higher type of symmetry than hexagonal,

namely, cubic. The analysis of crystal structure is beset with such pitfalls.

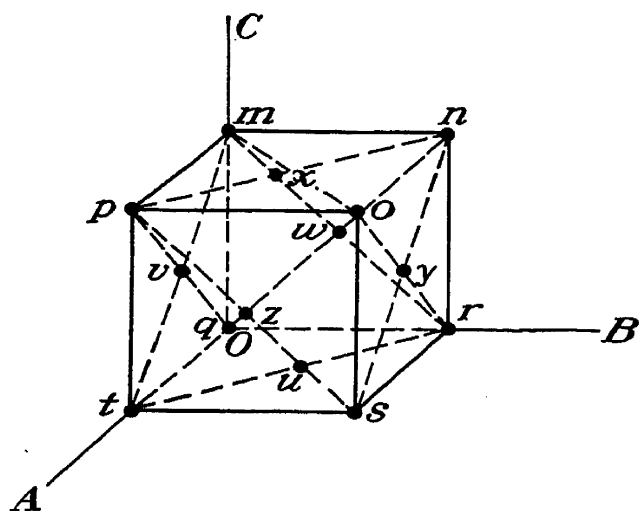


FIG. 14-25.—The face-centered cubic structure.

Examination of a pile of balls stacked in this manner will reveal that it is possible to select a set of three mutually perpendicular axes, each coinciding with a row of equally spaced balls, as shown in Fig. 14-25. Here the balls are represented as though they had been stacked up and then shrunk in size with their centers fixed in space.

This representation makes it easier to see the relative positions of the balls in a diagram. The hexagonally packed planes of balls now appear as  $(111)$ ,  $(\bar{1}11)$ ,  $(1\bar{1}1)$ , and  $(11\bar{1})$  planes, belonging to the  $\{111\}$  form.

From Fig. 14-25, it is obvious why this arrangement is called a face-centered cubic structure. There is a ball at each of the eight corners of the cube and one at the center of each of the six faces. The cube  $mnpqrst$  is the unit cell, and the balls  $q, u, v$ , and  $w$  may be regarded as belonging to it. Upon this basis,  $t$  and  $z$  belong to the cell in front of  $mnpqrst$ , and  $p$  to the one above it;  $r$  and  $y$  to the one at the right of  $mnpqrst$ , and  $n$  to the one above it;  $s$  to the one at the right front corner, and  $o$  to the one above it; and  $m$  and  $x$  to the cube above  $mnpqrst$ . Thus it is seen that there are four balls per unit cell, their coordinates being  $0, 0, 0$ ;  $\frac{1}{2}, \frac{1}{2}, 0$ ;  $\frac{1}{2}, 0, \frac{1}{2}$ ; and  $0, \frac{1}{2}, \frac{1}{2}$ . Also,

$$Ot = a = Or = b = a = Om = c = a;$$

and angle  $AOB = BOC = AOC = 90^\circ$ . The volume of the unit cell is obviously  $a^3$  and the axial ratio  $c/b = 1$ .

**10. The Lattice Constants.** The unit cell having been found and its relative dimensions known, the next step is to determine its absolute size. In the case of a triclinic lattice, it is desirable to know the values of  $a$ ,  $b$ , and  $c$  in angstrom units, let us say, and the values of  $\alpha$ ,  $\beta$ , and  $\gamma$  in degrees. These are called the "lattice constants." In the case of a perfect hexagonal close-packed lattice (Sec. 7) it is necessary merely to find the value of  $a$ , for it is already known that  $b = a$  and  $c = 1.633a$

and that  $\alpha = \beta = 90^\circ$  and  $\gamma = 120^\circ$ . Similarly, for the face-centered cubic lattice (Sec. 9), the value of  $a$  is all that one needs, for it is already known that  $b = c = a$  and  $\alpha = \beta = \gamma = 90^\circ$ . In such cases,  $a$  is called the lattice constant.

In 1897, Barlow<sup>1</sup> published an article in which he speculated that crystals of simple compounds like sodium chloride probably consisted of a symmetrical latticework of atoms arranged in some simple structure like the two just considered. He suggested that one arrangement might be a composite face-centered cubic structure in which unlike atoms alternated, forming two interlocked systems, each in itself being a simple face-centered cubic structure. In this case, the unit cell becomes a cube having sodium atoms (for example) at the cube corners and face centers and chlorine atoms (for example) at the center of each edge and at the cube center, or vice versa. In a structure of this sort, there would be four "molecules" (or at any rate four sodium and four chlorine atoms) per unit cell, the coordinates of the sodium atoms being  $000$ ;  $\frac{1}{2}\frac{1}{2}0$ ;  $\frac{1}{2}0\frac{1}{2}$ ;  $0\frac{1}{2}\frac{1}{2}$ , and the coordinates of the chlorine atoms  $\frac{1}{2}\frac{1}{2}\frac{1}{2}$ ;  $00\frac{1}{2}$ ;  $0\frac{1}{2}0$ ; and  $\frac{1}{2}00$ .

Upon such an assumption, one can calculate the lattice constant from chemical data. As an example, see page 337, where the value of  $a$  for rock salt is calculated to be 5.628 Å.

**11. Directions, Zone Axes, and Zones.** In a space-lattice, the coordinates of any particular lattice point  $P$  are usually expressed by merely counting points along the three principal axes  $A$ ,  $B$ , and  $C$ . Thus, if the coordinates of  $P$  are, respectively, the distance from the origin to the third lattice point out the  $A$  axis, the distance from the origin to the second lattice point out the  $B$  axis, and the distance from the origin to the fourth lattice point out the  $C$  axis, then the coordinates of  $P$  are usually said to be simply 3, 2, 4. This general idea has already been set forth in Sec. 3 in regard to the way of expressing the axial intercepts of planes.

A straight line from the origin through the lattice point  $P$  having coordinates  $u$ ,  $v$ ,  $w$  in the sense just described is commonly called the "[ $uvw$ ] direction." The square brackets are used to avoid confusion with the Miller indices of planes, which are always written in parentheses. Thus the  $[100]$  direction is simply the  $A$  axis; the  $[110]$  direction is a line  $OP$  lying in the  $AB$  plane and passing through the origin in a direction between that of the  $A$  axis and that of the  $B$  axis. If  $a$  happens to equal  $b$ , then angle  $AOP = POB = 45^\circ$ . The  $[111]$  direction in a cubic crystal makes equal angles with all three principal axes and is the cube diagonal.

The intersection of two crystal planes, like  $(100)$  and  $(110)$ , for example, is a line (or row) of atoms in the crystal lattice. Such a line,

<sup>1</sup> W. Barlow, *Proc. Roy. Dublin Soc.* (1897).

or row, is called a "zone axis," and each of these zone axes is designated by indices in square brackets, such as  $[uvw]$ , where  $[uvw]$  is the direction of the zone axis. The distinction between a direction and a zone axis is that the former is conceived as a geometrical line through the origin; the latter is conceived as a row of atoms not necessarily passing through the origin. The  $[uvw]$  zone axis is always parallel to the  $[u'v'w']$  direction if  $u = u'$ ,  $v = v'$ , and  $w = w'$ . Since  $(hkl)$  designates a family of parallel planes, the intersection of the  $(hkl)$  planes with the  $(h'k'l')$  planes is a family of parallel zone axes. The indices  $u, v, w$  of the zone axis  $[uvw]$  formed by the intersection of the  $(hkl)$  and  $(h'k'l')$  planes are given by

$$\left. \begin{aligned} u &= kl' - lk' \\ v &= lh' - hl' \\ w &= hk' - kh' \end{aligned} \right\} \quad (14-3)$$

All the lattice planes that pass through the zone axis  $[uvw]$  constitute a "zone," which is called the " $[uvw]$  zone."

The Miller indices  $h, k, l$  of a lattice plane determined by two intersecting zone axes  $[uvw]$  and  $[u'v'w']$  are given by

$$\left. \begin{aligned} h &= vw' - wv' \\ k &= wu' - uw' \\ l &= uv' - vu' \end{aligned} \right\} \quad (14-4)$$

The zone axes  $[100]$ ,  $[010]$ , and  $[001]$  are the  $A$ ,  $B$ , and  $C$  principal crystallographic axes, respectively.

**12. Lack of Confirmation.** The discussion in this chapter has made it clear that there was fairly substantial evidence in 1910 that (1) crystals are composed of atoms and groups of atoms arranged systematically with respect to the points of a three-dimensional space-lattice, (2) that such arrangements could be classified in 230 possible space groups, and (3) that the unit cell in these lattices had dimensions of the order of a few angstrom units or a few atomic diameters. Nevertheless, before the discovery of x-ray diffraction, there was a disconcerting lack of any *direct* evidence to confirm these conclusions. Many detailed questions remained unanswered, and exact quantitative measurements of the lattice constants were not obtainable.

### QUESTIONS AND PROBLEMS

1. How did the discovery of x-ray diffraction occur, and in what general fields has it proved to have practical importance?
2. Did the idea that crystals are built up by geometric repetition of a fundamental cell originate from x-ray diffraction studies? What are cleavage faces, and what does the law of rational indices say about them?
3. Distinguish between a point lattice and a crystal lattice. Can more than

one set of axes be chosen as a suitable reference frame for a given point lattice? How does the theory that a crystal has a structure resembling a geometrical point lattice account for the law of rational indices?

4. A plane has intercepts  $2a$ ,  $4b$ , and  $6c$ , respectively, on the  $A$ ,  $B$ , and  $C$  axes. What are its Miller indices? How many lattice planes parallel to it are to be found between it and the origin? How many (345) planes between the origin and the first rational (345) plane? *Ans.* (632); 12 planes; 60 planes.

5. Give the Miller indices of the planes belonging to the  $\{112\}$  form of a cubic crystal. Distinguish between a cubic and a tetragonal crystal. What is a body-centered cubic space lattice? What is the significance of the symbol  $O_h^9$  associated with it?

6. What is a holohedral crystal? A hemihedral crystal? A tetartohedral crystal? Define the terms hemimorphic and enantiomorphic. Why are there about seven times as many space groups as point groups? Name and distinguish between the seven crystal systems.

7. What is meant by the Schoenflies notation? Is it the only such system in use? What are symmetry operations of the first kind? What is a threefold axis of rotary reflection? A center of symmetry?

8. The unit cell of a crystal lattice has dimensions  $a$ ,  $b$ , and  $c$  parallel to the crystal axes  $A$ ,  $B$ , and  $C$ . By repeated translations of the cell through intervals of  $a$ ,  $b$ , or  $c$  parallel to the  $A$ ,  $B$ , or  $C$  axis, the crystal lattice can be built up indefinitely in all directions. For a given crystal lattice, is there always only one possible unit cell that can be chosen to meet these requirements? If not, what considerations govern the choice of "the" unit cell?

9. Describe the hexagonal close-packed structure in detail. Show that the volume of the unit cell is  $\sqrt{2} a^3$ .

10. In what crystal system are Miller-Bravais indices used? What are the Miller-Bravais indices corresponding to the following Miller indices: (100); (110); (111); (301); (211)? •

11. How many balls (or atoms) are there in the unit cell of the face-centered cubic structure? What are their coordinates? What is the order of magnitude of the distance between adjacent atoms in a crystal? How was this known in 1900?

12. What zone axis is formed by the intersection of the (123) and (111) planes of a cubic crystal? What lattice plane is determined by the [111] and [100] zone axes of a cubic lattice?

## CHAPTER 15

## LAWS OF X-RAY DIFFRACTION IN A CRYSTAL

**1. The Laue Equations.** When the possibility of x-ray diffraction in a crystal first occurred to Laue, x-rays were generally regarded as being short-wave-length electromagnetic waves, just as they are today, except that there was comparatively slight knowledge of their quantum characteristics. The equations that Laue derived for the diffraction of x-rays in a crystal were deduced by reasoning of the following sort:

In Fig. 15-1,  $pqrstuv$  represents a row of atoms parallel to the  $A$  axis in a crystal, the distance between successive atoms being  $a$ .  $H_1K_1$ ,

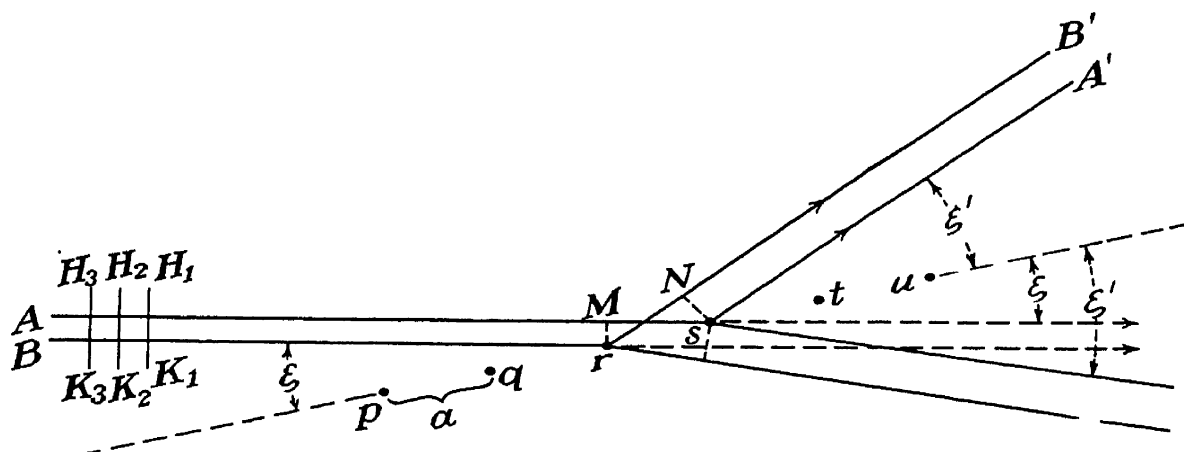


FIG. 15-1.—Diagram for derivation of the Laue equations.

$H_2K_2$ ,  $H_3K_3$ , etc., represent successive wave fronts of an x-ray beam from a distant source (so that  $H_1K_1$ , etc., may be regarded as plane wave fronts) approaching the row of atoms, the direction of travel being indicated by the rays  $As$  and  $Br$ . The x-rays are not necessarily monochromatic; but a finite part of their energy is transmitted by waves having a length  $\lambda$ , and the following discussion concerns only this part. Draw  $rM$  perpendicular to  $As$  and  $sN$  perpendicular to  $rB'$ . When a wave front reaches  $rM$ , it encounters atom  $r$ , which may coherently scatter some of the radiation in some new direction such as  $rB'$ . When the same wave front reaches  $s$ , additional coherent scattering may occur in the same direction  $sA'$ . These two scattered wavelets from  $r$  and  $s$  will be in phase with each other provided that  $Ms - rN = e\lambda$ , where  $e$  is an integer. If such constructive interference occurs between the rays  $rB'$  and  $sA'$  for some particular direction, the above argument can easily be extended to show that constructive interference in this direction



will occur for all the wavelets scattered from all the atoms  $pqrstu$ , etc., in the row, and a diffracted beam should be expected. The "order" of this beam is the integer  $e$ , which may have negative as well as positive values, including zero.

Up to this point, the argument has been similar to the one for a plane ruled grating [Fig. 6-2 and equation (6-16)]. However, since the present discussion is concerned with a row of particles, there is no need for the rays  $As$  and  $sA'$  (or  $Br$  and  $rB'$ ) and the row  $pqrstu$  to be coplanar, and in general they are not. For a given order (value of  $e$ ), the diffracted rays constitute a cone with  $pqrstu$  as axis, the generatrix making an angle  $\xi'$  with this axis. For other orders, there are other values of  $\xi'$ , and thus the diffracted rays make up a nest of coaxial cones with a common vertex.

Since  $Ms - rN = a \cos \xi - a \cos \xi'$ ,

$$a(\cos \xi - \cos \xi') = e\lambda \quad (15-1)$$

for the atomic rows parallel to the  $A$  axis. Likewise, if  $pqrstu$  is regarded as a row of atoms along the  $B$  axis, with interatomic spacing  $b$ , the angles being  $\eta$  and  $\eta'$  instead of  $\xi$  and  $\xi'$  and the order of diffraction being the integer  $f$ ,

$$b(\cos \eta - \cos \eta') = f\lambda \quad (15-2)$$

and, for the  $C$  axis,

$$c(\cos \zeta - \cos \zeta') = g\lambda \quad (15-3)$$

These are the *Laue equations*.

Suppose that  $Ms - rN$  (Fig. 15-1) differs from  $e\lambda$  by a small amount, say,  $Ms - rN = 1.1\lambda$ . Then the ray scattered from atom  $p$  will be exactly out of phase with the ray scattered from  $z$ , the tenth one down the row from  $p$ , and, by pairing off the rays from atoms  $10a$  apart, complete destructive interference can be demonstrated. This argument breaks down if the crystal is so small that there are only a few atoms in the row. For example, if  $Ms - rN = 1.01\lambda$ , one cannot prove destructive interference by pairing off atoms  $100a$  apart if there are only 30 atoms in the row. Hence the cones of diffracted rays should be sharply defined for crystals of ordinary size but blurred, fuzzy, or ill-defined for extremely minute crystals. That is, there is a loss of "resolving power" in the case of extremely minute crystals.

For a particular value of  $e$ , a particular value of  $f$ , and a particular value of  $g$ , there will be three cones of diffracted rays, one coaxial with each axis, the vertex of each being the origin of coordinates, for convenience. These three cones will intersect in general in six lines radiating from the origin. In these six directions the diffracted rays from two rows of atoms at a time, that is, from any single (100) plane, any single

(010) plane, or any single (001) plane, will be in phase, but there will be no constructive interference between rays from different planes in the family concerned. If the three cones happen to intersect in a single line, then all the atoms in the lattice will diffract rays in this direction at the same time; that is, there will be constructive interference, not only between rays from all the atoms in a plane, but between rays from all such planes in the family, or from all the atoms in the lattice. By changing the direction of the incident beam,  $\xi$ ,  $\eta$ , and  $\zeta$  (and hence  $\xi'$ ,  $\eta'$ , and  $\zeta'$ ) may be given such values that the cones do intersect in a common line, and a diffracted beam in this direction results. By reasoning in this way, Laue

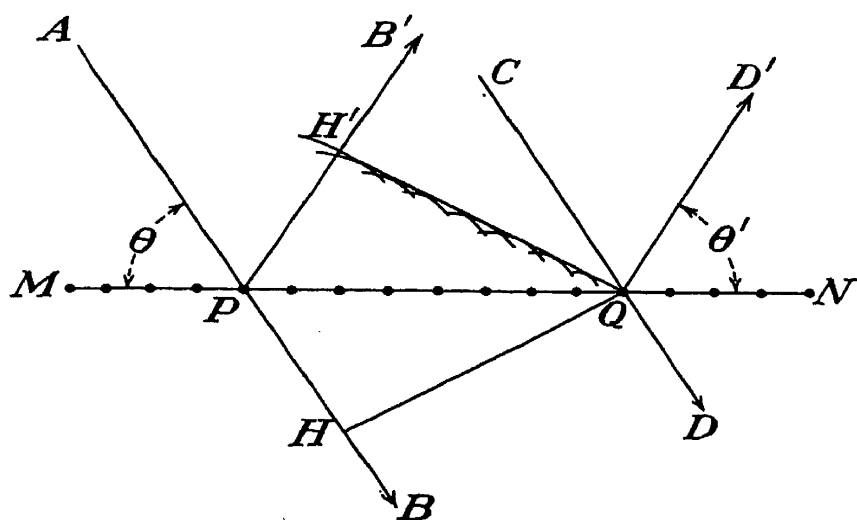


FIG. 15-2.—The coherent scattering of x-rays from a single atomic plane.

accounted for the diffracted beams observed photographically in the experiments of Friedrich and Knipping.

**2. Bragg's Law.** Many physicists turned their attention to x-ray diffraction after its discovery was announced by Laue. Among these, one of the foremost was W. H. Bragg. He soon proposed a simpler method of analysis that made the three-dimensional geometry involved easier to visualize.

In Fig. 15-2,  $MN$  represents a lattice plane viewed edgewise.  $HQ$  is a plane wave front in a beam of x-rays from a distant source, the rays traveling in the direction  $AB$  or  $CD$ . As in the preceding section, attention is centered on rays of a particular wave length  $\lambda$ . As the wave front  $HQ$  passes through the plane  $MN$ , the various scattering centers (atoms or groups of atoms) set up wavelets, which spread out spherically, and the usual Huygens construction establishes  $H'Q$  as the wave front of the beam diffracted in the direction  $PB'$  or  $QD'$  by the plane  $MN$ . In both this section and the preceding, it is understood that coherent scattering by the bound electrons in the atoms (see Chap. 5) is involved. Since this is identical with the Huygens construction for the wave front reflected from a plane surface, one has  $\theta' = \theta$ . If  $\theta'$  is slightly different

from  $\theta$ , the scattered wavelets may be shown to cancel each other by destructive interference, pairing off the ray from each atom against one located 5 or 12 or 23 intervals over, as the case may be, as explained in the preceding section.

Figure 15-3 is a two-dimensional diagram of a crystal, the polygon  $ABCDEFGG$  representing some of the faces that might naturally develop.  $M_1N_1$ ,  $M_2N_2$ ,  $M_3N_3$ , etc., represent a set of planes chosen at random, except that a fairly thickly "populated" set of planes with a correspondingly large interplanar distance is preferable to a thinly populated set with a correspondingly small separation.

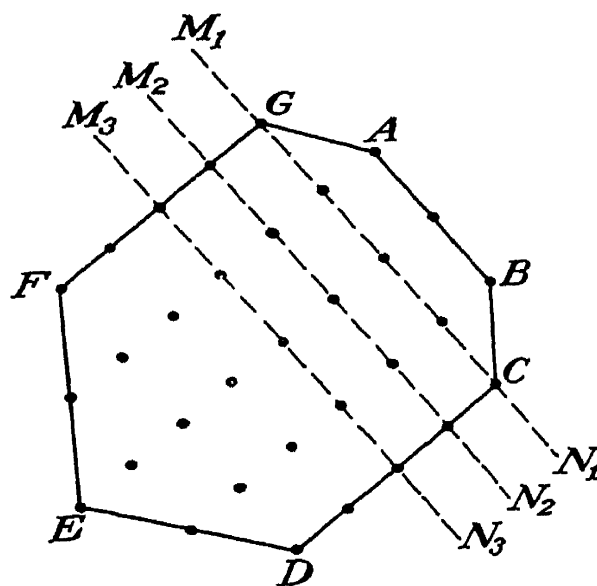


FIG. 15-3.—Showing relation between atomic planes and cleavage faces.

In Fig. 15-4,  $M_1N_1$ ,  $M_2N_2$ ,  $M_3N_3$ ,  $M_4N_4$ , etc., represent a set of planes such as the ones represented by the same letters in Fig. 15-3.  $A_1Z_1A_4Z_4$

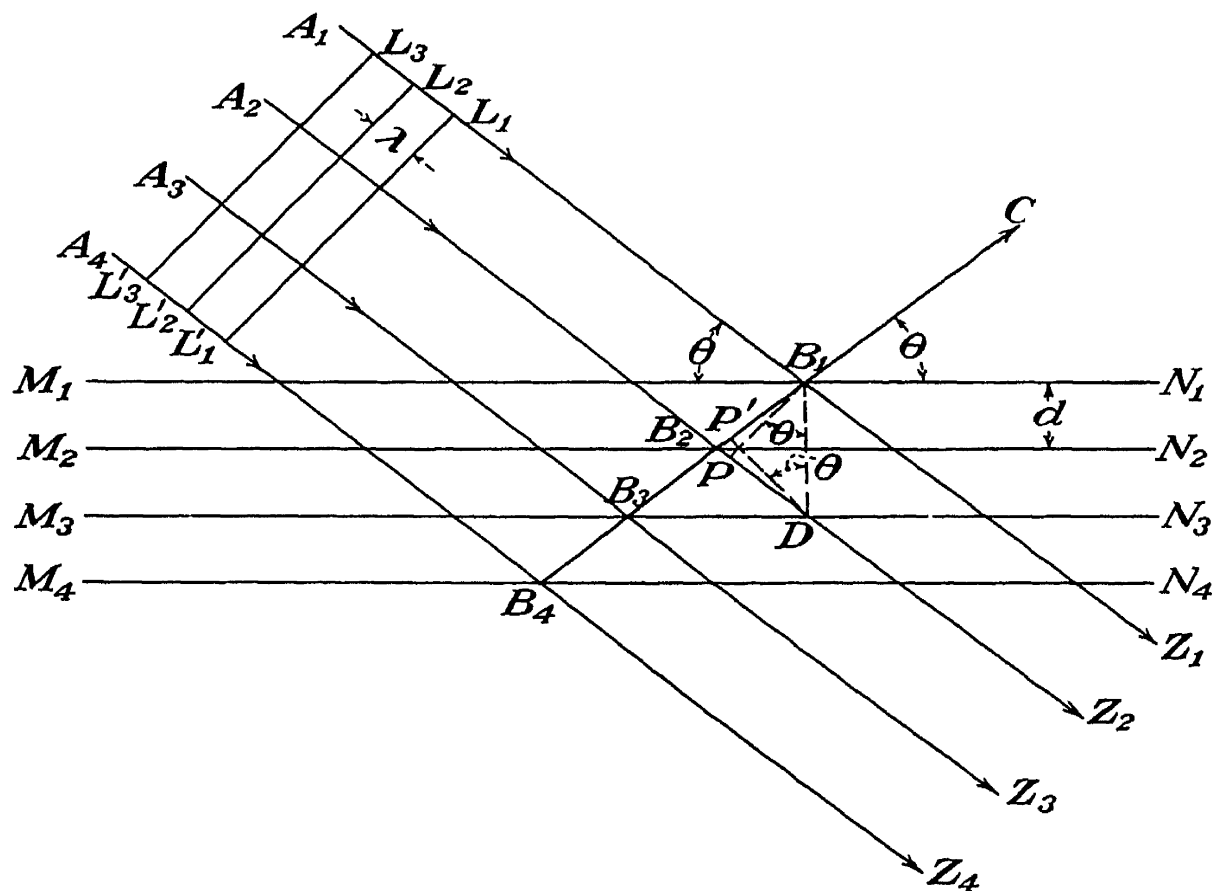


FIG. 15-4.—Diagram for the derivation of Bragg's law.

represents a beam of parallel x-rays from a distant source, successive plane wave fronts being indicated by  $L_1L'_1$ ,  $L_2L'_2$ ,  $L_3L'_3$ , etc., spaced one wave

length  $\lambda$  apart. It has already been shown from Fig. 15-2 that each plane, such as  $M_1N_1$ , tends to "reflect" the rays in the direction  $B_1C$  such that angle

$$A_1B_1M_1 = \theta = \text{angle } CB_1N_1.$$

When a wave front reaches the position  $B_1P$ , the portion of it at  $B_1$  is just on the point of initiating a scattered ray from  $B_1$  toward  $C$ . At the same instant, this wave front has reached  $P$  on the ray  $A_2Z_2$ , having already passed the point of intersection  $B_2$  with the plane  $M_2N_2$ . From this point  $B_2$ , the scattered ray in the direction  $B_2C$  will by now have reached  $P'$ , where  $B_2P' = B_2P$ . By geometry,  $P'$  is also the foot of the perpendicular dropped from  $D$  upon  $B_2C$ , and angle

$$PB_1D = \theta = \text{angle } P'DB_1.$$

Hence the wavelet scattered from  $B_2$  lags behind the one scattered from  $B_1$  by the wave front  $PB_1$ , the path difference being  $P'B_1$ . Since

$$B_1D = 2d,$$

the path difference  $P'B_1$  is  $2d \sin \theta$ . Similar reasoning shows that  $2d \sin \theta$  is also the path difference between the scattered radiation from  $B_2$  and  $B_3$  and from  $B_3$  and  $B_4$ . Therefore, if this path difference is an integral number of wave lengths  $n\lambda$ ,  $n$  being an integer, one should expect a diffracted beam in the direction  $B_1C$  if

$$n\lambda = 2d \sin \theta \quad (15-4)$$

The sort of reasoning used before will show that if the path difference is  $1.9\lambda$ , for example, then the scattered wavelet from each plane is destroyed by interference with the scattered wavelets from the plane  $10d$  beneath it. Equation (15-4) is *Bragg's law*.

**3. Relation between Bragg's Law and the Laue Equations.** In Sec. 1, it was concluded that a diffracted beam should be expected in a direction making angles  $\xi'$ ,  $\eta'$ , and  $\zeta'$  with the  $A$ ,  $B$ , and  $C$  axes of the crystal when the three Laue equations (15-1) to (15-3) are simultaneously satisfied. Under this condition, the  $A$ -axis rows are diffracting in the  $e$ th order, the  $B$ -axis rows in the  $f$ th order, and the  $C$ -axis rows in the  $g$ th order. Let us call this "condition I."

In Sec. 2, it was concluded that a diffracted beam might be expected in a direction coplanar with the incident beam and the normal to the  $(h_0k_0l_0)$  planes and departing from the crystal in a direction making a grazing angle  $\theta$  with these planes when Bragg's law is satisfied. This occurs for any given wave length  $\lambda$  only at certain discrete angles  $\theta$  for any given set of planes  $(h_0k_0l_0)$ . Let us call this "condition II."

It may be shown that condition I is equivalent to condition II or that

Laue's equations, when simultaneously satisfied for given directions of incident and exodent beams and a given  $\lambda$ , represent Bragg's law diffraction of the  $n$ th order from the  $(h_0k_0l_0)$  planes when

$$\begin{aligned} e &= nh_0 \\ f &= nk_0 \\ g &= nl_0 \end{aligned} \tag{15-5}$$

the same principal axes being used in both methods of analysis.

The Bragg viewpoint makes the mechanism of x-ray diffraction in a crystal much easier to visualize than does the Laue analysis, but for some purposes the Laue equations are most useful. Both predict the same result for the same set of given conditions, and the predictions are in accord with experimental observation, perfect agreement resulting when allowance is made for the slight refraction at the crystal surfaces (see Sec. 5).

**4. X-ray Diffraction upon the Basis of the Quantum Theory.** The equations of Laue and Bragg were derived by regarding x-rays as pure electromagnetic waves, and the accurate agreement between these equations and experimental observation was strong support for the view that x-rays consist purely of waves. However, the photoelectric properties of x-rays, the existence of K, L, M, etc., absorption edges, the Compton effect, the Auger effect, and other phenomena described in the earlier chapters—all visualize x-rays as consisting essentially of particles, or photons. These latter effects, as they were discovered and studied, kept building up more and more evidence against the theory that x-rays are purely and simply a wave motion. Consequently, it became desirable to try to explain x-ray diffraction on the basis of the quantum theory, which describes x-rays as consisting of energy packets (photons) that have waves associated with them. In 1923, Duane and Compton<sup>1</sup> succeeded in deriving Bragg's law from quantum postulates.

In order to understand the derivation, it will be helpful to recall that Bohr's equation (4-25) for the quantization of the orbits of hydrogenlike atoms indicated that the angular momentum of the orbital electrons may take on only integral multiples of the value  $h/2\pi$ . In 1915, Wilson and Sommerfeld<sup>2</sup> discovered that this quantum rule of Bohr was only a particular case of a more general rule which may be expressed in generalized coordinates, usually in terms of the variables  $q_1, q_2$ , etc., representing the positions of the particles in a system, and the "canonically conjugate"<sup>3</sup> variables  $p_1, p_2$ , etc., representing their momenta.

<sup>1</sup> W. Duane, *Proc. Natl. Acad. Sci.*, **9**, 159 (1923); A. H. Compton, *Proc. Natl. Acad. Sci.*, **9**, 359 (1923).

<sup>2</sup> W. Wilson, *Phil. Mag.*, **29**, 795 (1915), A. Sommerfeld, *Ann. Physik*, **51**, 1 (1916).

<sup>3</sup> If  $q_i$  represents a set of variables  $q_1 \dots q_n$  in generalized coordinates that define

This Wilson-Sommerfeld quantization rule is expressed by the relation

$$\oint p dq = nh \quad (15-6)$$

where  $n$  is an integer and  $h$  is Planck's constant. This integral is called an "action integral" and can be evaluated only for "conditionally periodic system," that is, for systems describable by coordinates, each of which goes through a cycle as time increases, independently of the others.

The symbol  $\oint$  indicates a definite integral taken over one cycle. This quantization rule was one of the main pillars of the "old" quantum theory; its limited application, restricted as it was to periodic systems, was one of the shortcomings of the old theory overcome by the more general theories of modern quantum mechanics.

The quantum derivation of Bragg's law or Laue's equations is based upon the Wilson-Sommerfeld quantization rule. In Fig. 15-5,  $OP$  represents the path of an x-ray photon in an x-ray beam incident upon a crystal lattice in the  $AB$  or  $(001)$  plane, the interplanar distances in the  $A$  and  $B$  directions being  $a$  and  $b$ . In this two-dimensional figure,  $q_1 = x$ . If the crystal

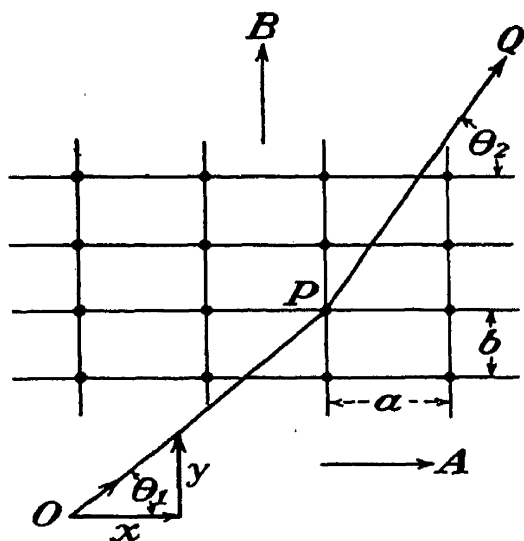


FIG. 15-5.—Illustrating x-ray diffraction on the basis of the quantum theory.

is supposed infinite in extent, the system repeats itself every time  $x$  increases by  $a$ ; that is, when  $x$  is replaced by  $x + a$ , the new system is indistinguishable from the old. Hence (15-6) becomes

$$\int_0^a p_x dx = n_a h = p_x a \quad (15-7)$$

whence

$$p_x = \frac{n_a h}{a} \quad (15-8)$$

Similarly,

$$p_y = \frac{n_b h}{b} \quad (15-9)$$

where  $n_a$  and  $n_b$  are integers and  $p_x$  and  $p_y$  are the  $x$  and  $y$  components of the momentum of the photon. These equations state that in this system the  $x$  component of the momentum of the photon must be an integral multiple ( $n_a$ ) of  $h/a$ ; hence, if it changes, it must change by an integral

the positions of the particles in the system in question and if  $p_i$  represents a second set of variables  $p_1 \dots p_n$ , called "generalized momenta" and defined as  $p_i = \partial L / \partial \dot{q}_i$ , then these variables are canonically conjugate if they satisfy Hamilton's equations  $\partial H / \partial p_i = \dot{q}_i$  and  $\partial H / \partial q_i = -\dot{p}_i$ . Here  $L$  is the Lagrangian function (kinetic minus potential energy),  $H$  is the Hamiltonian function, and  $\dot{q}_i = dq_i / dt$  and  $\dot{p}_i = dp_i / dt$ .

multiple  $\Delta n_a = n_x$  of  $h/a$ . That is,

$$\Delta p_x = n_x \frac{h}{a} \quad (15-10)$$

and similarly 
$$\Delta p_y = n_y \frac{h}{b} \quad (15-11)$$

In Secs. 5-4 and 5-6, it was shown that the momentum  $p$  of a photon is  $h/\lambda$  where  $\lambda$  is the wave length of the associated radiation. Hence the  $x$  component of the momentum of the photon before it collides with an electron in the atom  $P$  (Fig. 15-5) is  $h/\lambda \cos \theta_1$ . After the collision, which is elastic since the electron is supposed to be firmly bound and the scattering coherent, the  $x$  component of the momentum of the photon will be  $h/\lambda \cos \theta_2$ . Hence

$$\frac{h}{\lambda} (\cos \theta_1 - \cos \theta_2) = \Delta p_x = n_x \frac{h}{a} \quad (15-12)$$

and similarly

$$\frac{h}{\lambda} (\sin \theta_1 - \sin \theta_2) = \Delta p_y = n_y \frac{h}{b} \quad (15-13)$$

If the photon passes straight through without diffraction, then

$$\theta_1 = \theta_2 \quad \text{and} \quad n_x = 0 = n_y.$$

If  $n_x$  or  $n_y$  or both are not zero, the photon is diffracted. If  $n_x$  is zero but  $n_y$  is not,  $\cos \theta_1 = \cos \theta_2$  but  $\sin \theta_1 \neq \sin \theta_2$ ; hence  $\sin \theta_1 = -\sin \theta_2$ , and (15-13) becomes

$$n_y \lambda = 2b \sin \theta_1 \quad (15-14)$$

which is Bragg's law for reflection from the (010) planes. If  $n_y$  is zero but  $n_x$  is not,  $\sin \theta_1 = \sin \theta_2$  but  $\cos \theta_1 \neq \cos \theta_2$ ; hence

$$\cos \theta_1 = \sin (90^\circ - \theta_1) = -\cos \theta_2,$$

and (15-12) becomes

$$n_x \lambda = 2a \sin (90^\circ - \theta_1) \quad (15-15)$$

which is Bragg's law for reflection from the (100) planes. If neither  $n_x$  nor  $n_y$  equals zero, then (15-12) and (15-13) represent Bragg's law for reflection in some other set of crystal planes in the [001] zone, such as (110) or (210).

**5. Correction of Bragg's Law for Refraction.** It was stated in Chap. 6 that x-rays have an index of refraction  $\mu = 1 - \delta$  slightly less than 1. If the crystal planes from which the Bragg "reflection" occurs are parallel to the surface of the crystal (as when a cleavage face is used), the actual angle  $\theta_{\text{obs}}$  which experimentally yields maximum intensity in the diffracted beam for a given  $\lambda$  is slightly larger than the angle  $\theta_{\text{calc}}$

which one calculates by substituting the true value of  $\lambda$  and  $d$  in Bragg's equation  $n\lambda = 2d \sin \theta_{\text{calc}}$  and solving for  $\theta_{\text{calc}}$ . The difference can be shown to be (Fig. 15-6)

$$\theta_{\text{obs}} - \theta_{\text{calc}} = \delta \sec \theta_{\text{obs}} \operatorname{cosec} \theta_{\text{obs}} \quad (15-16)$$

This relation was first derived by Darwin.<sup>1</sup>

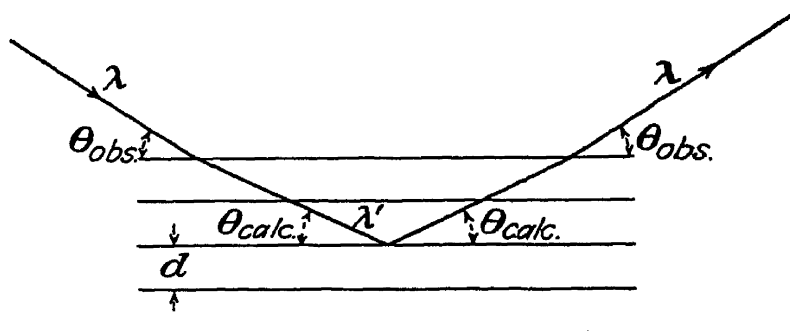


FIG. 15-6.—Diffraction corrected for refraction.

When the x-rays are diffracted by a set of planes parallel to the crystal surface, it may be shown that Bragg's law, corrected for refraction, becomes

$$n\lambda = 2d \left( 1 - \frac{\delta}{\sin^2 \theta} \right) \sin \theta \quad (15-17)$$

where  $\theta$  is the observed angle  $\theta_{\text{obs}}$  in Fig. 15-6. The derivation of this expression is based upon Snell's law  $\mu = \cos \theta_{\text{obs}} / \cos \theta_{\text{calc}}$  and the definition of the index of refraction  $\mu = c/c' = \lambda/\lambda'$  where the primes refer to velocity or wave length within the crystal. These relations are substituted into the equation  $n\lambda' = 2d \sin \theta_{\text{calc}}$ . After expanding by the binomial theorem, squares and higher powers of  $\delta$  are neglected in order to obtain (15-17). Since  $\delta$  is of the order  $10^{-5}$  or  $10^{-6}$ , equation (15-17) is only very slightly different from equation (15-4). Examination of either (15-16) or (15-17) shows that refraction will cause the greatest discrepancy from the simple form of Bragg's law when  $\theta$  is small, which corresponds to low orders of diffraction (small values of  $n$ ).

If one measures the angle  $\theta_5$  at which a beam of x-rays of wave length  $\lambda$  is diffracted in a high order, say  $n = 5$ , by a set of planes parallel to a crystal face, he may then calculate  $d$  from  $n$ ,  $\lambda$ , and  $\theta_5$  by the simple form of Bragg's law (15-4). If he then measures the angle  $\theta_1$  at which the beam (of wave length  $\lambda$ ) is diffracted by the same planes in the first order ( $n = 1$ ), he may again calculate  $d$  from  $n$ ,  $\lambda$ , and  $\theta_1$  by (15-4). When this is done accurately, the two values of  $d$  disagree slightly. However, if the two calculations are made with (15-17) instead of (15-4), the two values agree, thus proving the reality of the refractive correction.

<sup>1</sup> C. G. Darwin, *Phil. Mag.* **27**, 315 (1914).



The effect is very small, and thus careful measurements are required to estimate  $\delta$  and hence  $\mu$  by this method, as Stenström did (see page 97).

**6. Diffuse Scattering.** Lest this chapter leave the impression that there are no x-rays coherently scattered from a crystal at angles not satisfying Bragg's law, it should be stated that experiment and theory are in agreement that there are both coherent and incoherent "diffuse" scattering by a crystal at these "non Bragg" angles at room temperature. The coherent diffuse scattering is due to the thermal agitation of the atoms, and it would be theoretically zero between the Bragg maxima for a perfect crystal (page 366) at zero absolute temperature.

In Chap. 22, an equation (22-11) is given for the scattering, both coherent and incoherent, from a monatomic gas. Debye<sup>1</sup> has shown that the  $I_e f^2$  term representing the coherent part of the scattering in this formula should be replaced by  $I_e(f_0^2 - f^2)$  for a crystal, so that the total diffuse background scattering from a crystal is given by a similar equation,

$$I = I_e[(f_0^2 - f^2) + R(Z - \Sigma g_n^2)] \quad (15-18)$$

The terms before the  $+$  sign represent the diffuse coherent scattering, and those following the  $+$  sign represent the incoherent scattering. The meaning of the symbols in the equation is explained in Chap. 22 and in Secs. 16-9 and 16-14.

According to this equation, both the coherent and incoherent scattering between the Bragg maxima vary with the angle in a uniform monotonic fashion. Actually, weak maxima are sometimes observed superposed on this general background. These maxima are called "diffuse reflections." Whether they are due to coherent or incoherent scattering is a matter not yet definitely established (see pages 474-478).

### QUESTIONS AND PROBLEMS

1. What are the Laue equations, and what is their significance? What has the size of the crystal to do with its resolving power as a diffraction grating for x-rays?

2. What causes the angle  $\theta_0$  at which an x-ray beam is diffracted from a crystal plane to be so critical? That is, why does the intensity of the beam drop off to zero for angles only slightly greater or less than  $\theta_0$ ? What is Bragg's law? In general, if a beam of parallel monochromatic x-rays strikes a set of crystal planes ( $hkl$ ) at some fixed but arbitrary angle chosen at random, such as  $17^\circ$ , say, will there be any diffracted beam from these planes? If so, at what angle will it depart from the set of planes?

3. In general, the x-ray beam diffracted by a given set of crystal planes ( $hkl$ ) according to Bragg's law is called a Bragg "reflection." Can you suggest why? The second-order Bragg reflection from the (112) planes of a crystal, for example, is called the "(224) reflection," the designation being simply  $(nh, nk, nl)$ , where  $h, k, l$  are the Miller indices of the planes and  $n$  is the order of the Bragg reflection. If the

<sup>1</sup> P. Debye, *Ann. Physik*, **43**, 49 (1914).

Laue equations are applied to the case of the (246) Bragg reflection, what are the values of  $e$ ,  $f$ , and  $g$  in the three equations?

4. Bragg's law having been derived in the classical manner, what is the point of deriving it from quantum postulates?

5. If  $\delta = 5 \times 10^{-6}$  and  $\theta = 10^\circ$ , what is the percentage of error introduced in the value of  $\lambda$  or  $d$  when one uses the simple form of Bragg's law instead of (15-17)?

*Ans.* 0.017 per cent.

## CHAPTER 16

### THE BRAGG METHOD OF CRYSTAL ANALYSIS AND SOME PERTINENT PROPERTIES OF ACTUAL CRYSTALS

**1. The Mechanism of X-ray Diffraction.** In Chap. 15, Laue equations and Bragg's law were shown to be equivalent mathematical relationships governing the diffraction of a beam of parallel monochromatic x-rays when it passes through a geometrical three-dimensional lattice of scattering centers of the sort described in Chap. 14. If, now, these scattering centers are to be regarded as actual atoms, ions, or identical groups of atoms (sometimes molecules, sometimes not), the nature of the interaction of the x-rays and the atoms deserves more detailed discussion. Modern theory, confirmed by experiment, indicates that the diffracted beams discussed in the preceding chapter result from the *coherent* scattering of the rays by the electrons in the atoms. The scattering from the atomic nuclei is negligible in comparison. The incoherent scattering (see Chap. 5) is only a minor factor in ordinary x-ray diffraction phenomena.

**2. Classical Theory of X-ray Scattering—J. J. Thomson.** According to the classical theory of electromagnetic radiation (see pages 36 and 37), the intensity  $I$  of an electromagnetic wave is given by

$$I = \frac{cE^2}{4\pi} = \frac{cH^2}{4\pi} \quad (16-1)$$

where  $E$  is the amplitude of the electric vector in the wave or  $H$  is the amplitude of the magnetic vector,  $E$  and  $H$  being always numerically equal at any point. According to Thomson's calculations,<sup>1</sup> the electric amplitude  $E'_s$  of the wave at  $P$  (Fig. 16-1), scattered by an electron at  $A$  from a primary wave of amplitude  $E'_0$  traveling along the path  $AOB$ , is given by

$$E'_s = \frac{E'_0}{r} \frac{e^2}{mc^2} \quad (16-2)$$

where  $E'_s$  and  $E'_0$  are the magnitudes of the electric vectors in a direction perpendicular to the plane  $AOP$ ,  $r$  is the distance  $OP$ , and  $e$ ,  $m$ , and  $c$  are the electron charge, mass, and velocity of light, respectively.

<sup>1</sup> See, for example, J. J. Thomson and G. P. Thomson, "Conduction of Electricity through Gases," 3d ed., vol. 2, p. 258, Cambridge University Press, London, 1928. In Thomson's treatment,  $e$  is in e.m.u., whereas in the above discussion  $e$  is in e.s.u. Hence the extra factor  $c$ .

have their usual significance,  $e$  being in e.s.u. In general, the primary wave advancing along  $AO$  will not be polarized, and it will therefore have an electric vector  $E_0''$  in the plane  $AOP$  as well as the one already mentioned ( $E_0'$ ). Thomson's calculations show that the electric amplitude  $E_s''$  of the scattered wave at  $P$  due to the incident vector  $E_0''$  of the primary wave is

$$E_s'' = \frac{E_0''}{r} \frac{e^2}{mc^2} \cos \phi \quad (16-3)$$

where  $\phi$  is the angle between the primary and scattered rays, as indicated

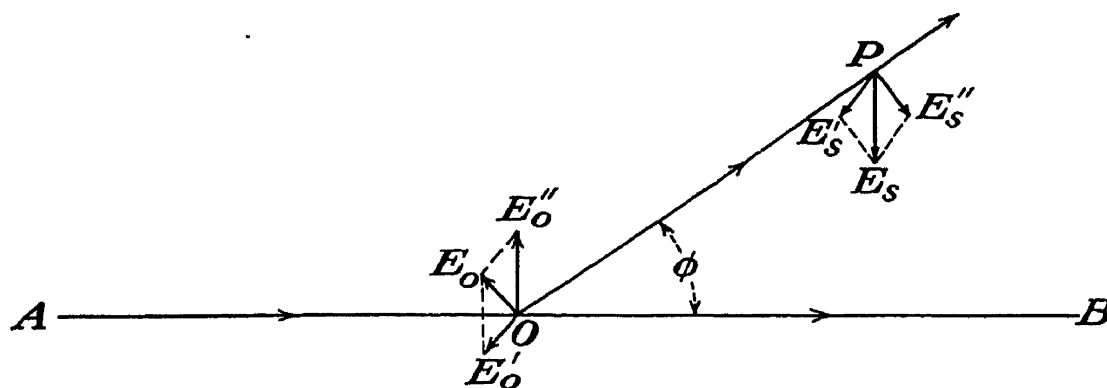


FIG. 16-1.—Classical picture of scattering of x-rays by an electron.

in Fig. 16-1. In an unpolarized wave,  $E_0' = E_0''$ , and the resultant vector  $E_0$  is given by

$$E_0^2 = E_0'^2 + E_0''^2 = 2E_0'^2 = 2E_0''^2 \quad (16-4)$$

or

$$\frac{1}{2}E_0^2 = E_0'^2 = E_0''^2 \quad (16-5)$$

Squaring and adding (16-2) and (16-3) and applying (16-5),

$$E_s^2 = E_s'^2 + E_s''^2 = \frac{E_0^2}{2r^2} \frac{e^4}{m^2c^4} (1 + \cos^2 \phi) \quad (16-6)$$

Application of (16-1) yields

$$I_e = I_0 \frac{e^4}{2r^2m^2c^4} (1 + \cos^2 \phi) \quad (16-7)$$

This is Thomson's equation for the intensity  $I_e$  of the rays scattered by a single electron when the intensity of the primary x-ray beam as it strikes the electron is  $I_0$ ,  $\phi$  is the angle between primary and scattered rays (Fig. 16-1), and  $r$  is the distance in centimeters from the electron to the point  $P$  at which  $I_e$  is measured. Note that none of these equations involve the wave length.

If one now supposes that an atom containing  $Z$  orbital electrons ( $Z$  = atomic number of the atom) is placed at the point  $O$  (Fig. 16-1), it seems reasonable to assume that the intensity  $I_a$  at  $P$  of the x-rays

scattered by the atom would be that scattered by a particle of charge  $Ze$  and mass (of the electrons only)  $Zm$ , in which case

$$I_a = I_0 \frac{(Ze)^4}{2r^2(Zm)^2c^4} (1 + \cos^2 \phi)$$

or 
$$I_a = I_0 \frac{Z^2e^4}{2r^2m^2c^4} (1 + \cos^2 \phi) \quad (16-8)$$

This equation agrees with experimental observation reasonably well in the case of the lighter elements. The massive nucleus of the atom scatters no appreciable fraction of the rays. If the electrons in the atom are separated by distances comparable with the wave length of the x-rays, then the electrons should scatter the rays more or less independently; in this case the intensity of the beam scattered by the electrons is simply  $Z$  times that scattered by one electron, or

$$I_a = I_0 \frac{Ze^4}{2r^2m^2c^4} (1 + \cos^2 \phi) \quad (16-9)$$

This equation agrees with experiment better than (16-8) in the case of the heavier elements. It is equation (5-12) already given in Chap. 4. Equation (16-9) is not accurate, however, for the wavelets scattered by the various electrons in the atom will not all be exactly in phase with one another when they reach  $P$ . The diameter of the heavier atoms is a considerable fraction of the wave length of the x-rays commonly used in diffraction work.

In the simple Bragg method of crystal analysis, equations (16-8) and (16-9) may be taken as a sufficiently accurate basis for calculating scattering intensities. In the more rigorous modern extensions of the Bragg method, the approximation is made much more accurate by introducing a corrective factor  $f$ , called the "atomic-structure factor," the use of which then supersedes equations (16-8) and (16-9).

**3. The Bragg X-ray Spectrometer.** Bragg describes his ionization spectrometer as "a siege gun to be brought into action when the lighter artillery fails." The lighter artillery here refers to the various simple photographic methods of crystal analysis such as the Laue method, the rotating-crystal method, and the powder method, to be discussed in Chaps. 17 and 18. The term "crystal analysis," as used here and in the title of this chapter, signifies the amassing and analyzing of sufficient data to reach the definite conclusion that a certain substance, such as potassium chlorate, for example, forms crystals which belong to a certain space group— $C_{2h}^2$  in the monoclinic system in this case—with known dimensions  $a$ ,  $b$ ,  $c$  for the unit cell—4.647, 5.585, and 7.085 Å. in this case—and known angles between the axes—in this case,  $\beta = 109^\circ 3'$ . Crystal analysis is quite essential so far as the advancement of know-

edge of the chemical and physical structure and properties of solids is concerned, but in the ordinary problems encountered in the average industrial laboratory, this type of analysis is not often demanded. Nevertheless, a general knowledge of its theory, methods, and possibilities is a very good groundwork on which to base a true understanding of the simpler and more important applications of x-ray diffraction in industrial work.

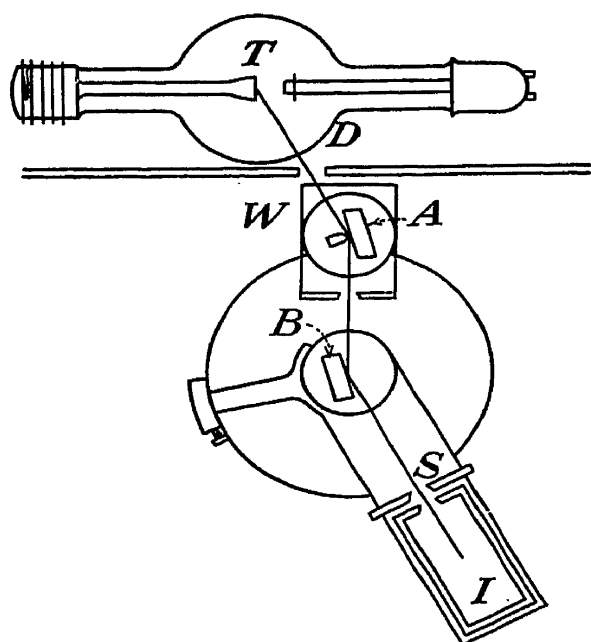


FIG. 16-2.—Double crystal x-ray spectrometer. (Courtesy of Sir W. L. Bragg, George Bell & Sons, Ltd., and The Macmillan Company.)

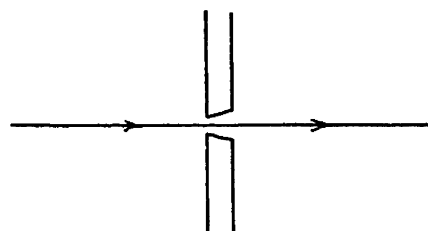


FIG. 16-3.—Tapered collimating slit, or pinhole.

crystal faces and is parallel to one of the more important zone axes of the crystal, usually one of the principal axes.

The crystal *A* is not always present. When it is present, the instrument is called a “double-crystal” x-ray spectrometer,<sup>1</sup> but if the rays from the tube are simply collimated into a parallel beam by slits and then allowed to fall on *B* directly the instrument is a simple Bragg spectrometer. The x-ray tube usually has a target of molybdenum, copper, or iron, for the  $K_{\alpha}$  lines of these elements have a convenient wave length for the work. The beveled slits, usually of lead, have the beveled edges facing away from the source, as shown in Fig. 16-3. Two adjustable slits about 2 in. apart and opened about 0.01 in. suffice for routine work. Behind these is a third, wider guard slit to intercept any rays scattered by the second slit. A fourth slit *S* (Fig. 16-2) guards the entrance to the ionization chamber *I*. For durability, steel or brass slits are sometimes used, and for precision work gold slits are not uncommon. In extreme cases, they are placed as much as 40 cm. apart and narrowed to 0.0025 cm. in the single-crystal instrument.

<sup>1</sup> A double-crystal x-ray spectrometer is described and illustrated by S. K. Allison, *Phys. Rev.*, **41**, 1 (1932); see also J. W. M. DuMond and D. Marlow, *Rev. Sci. Instruments*, **8**, 112 (1937).

Since monochromatic radiation is necessary to make the spectrometer useful, a close enough approach to this is obtained in the simple spectrometer by placing a filter over the ionization chamber slit  $S$  (Fig. 16-2). The filter must consist of a material having its  $K$  absorption edge at a wave length between the  $K_\alpha$  and  $K_\beta$  lines of the x-ray tube-target element. Thus a zirconium filter is used for molybdenum radiation. The filter is usually made of zirconium oxide or some other compound of zirconium with light elements, since the absorption edge is an atomic property not altered by chemical combination. W. P. Davey recommends 0.036 g. of zirconium atoms per square centimeter of filter in order to reduce the  $K_\beta$  and  $K_\gamma$  radiation to negligible intensity compared with the  $K_\alpha$  radiation transmitted. The filter is located at the ionization-chamber entrance because there it is able to filter out characteristic secondary rays from the crystal. A Ross filter (page 433) is sometimes used. The double-crystal spectrometer employs the crystal  $A$  and a lead wedge  $W$  as a "monochromator" in place of the filter and collimating slits just described. If, for example,  $A$  is a calcite crystal with a cleavage face next to the wedge  $W$ , then its table may be turned and the tube  $T$  and slit  $D$  so aligned that rays  $TA$  and  $AB$  are both inclined at  $6^\circ 42'$  to the crystal face. This angle is deduced by applying Bragg's law for first-order diffraction of molybdenum  $K_{\alpha_1}$  radiation from the cleavage planes of calcite, which have a grating spacing of 3.035 Å. With this setting, only the  $K_{\alpha_1}$  radiation will reach crystal  $B$ ; even the  $K_{\alpha_2}$  radiation so near by ( $K_{\alpha_1} = 0.707$ ;  $K_{\alpha_2} = 0.712$  Å.) will be excluded by the wedge  $W$  and crystal  $A$ . The efficiency of the diffraction process is so low (see Secs. 11 and 16) that the beam  $AB$  will be feeble compared with the beam  $DA$ . At first thought, this should make the double-crystal arrangement much slower and more difficult to work with than the simple spectrograph with collimating slits, but this handicap is more apparent than real. In order to secure high resolving power with either arrangement, the requirement is that a high reading for the ionization current in the chamber  $I$  be obtained at some definite value of the angle  $ABS$  (Fig. 16-2) but that this reading drop off to nearly zero when the angle  $ABS$  becomes very slightly more or less than the said definite value. This is accomplished in the simple spectrometer by making the collimating slits very narrow and far apart to obtain an extremely fine parallel beam. In the double-crystal arrangement, a monochromatic beam of parallel rays is obtained with fairly wide-open slits, for, by Bragg's law, all rays leaving crystal  $A$  will leave at the same angle and hence constitute a parallel monochromatic beam. This circumstance permits the double crystal spectrometer to compete with the simple spectrometer as regards sensitivity and speed combined with high resolution.

The monochromatic beam  $AB$  (Fig. 16-2) will be diffracted by the

crystal  $B$  that is being investigated, when its angular position is correct. The beam  $BS$  diffracted from this crystal may have its direction and intensity measured by means of the ionization chamber  $I$ , which swivels about the axis of the central table supporting  $B$ , much like the telescope of an optical spectroscope. This chamber is usually 15 cm. or so in length (see pages 29 and 187), and is connected to the electrometer or vacuum-tube amplifier. A Geiger-Müller counter may be substituted for the ionization chamber.<sup>1</sup>

To use a Bragg spectrometer to investigate the structure of the crystal  $B$  is analogous to using an optical grating spectrograph, with known light, to measure the grating spacing. Simple x-ray spectrometers are also used in the normal way like an optical instrument. In such work, with the simple spectrometer where crystal  $A$  is replaced by collimating slits, crystal  $B$  is a known crystal, such as calcite, and the spectrum of the x-radiation entering the collimator is investigated. This is the type of work that led Moseley to an understanding of characteristic x-ray spectra, as mentioned in Chap. 4. In this chapter, however, the chief concern is with the diffraction of known radiation by whatever crystal may be placed at  $B$  (Fig. 16-2) for analysis.

**4. Standard Crystals.** If the spectrometer is to be used to determine the structure of various crystals, then their grating spacings must be determined in terms of the spacings of some "known" standard crystal. In fact, it is only on some basis of this sort that it could be known that the wave length of the molybdenum  $K_{\alpha_1}$  radiation used is indeed 0.707 Å., unless one resorts to measurements with a ruled grating. This was "impossible" before 1926 and is unnecessary today.

Soon after the discovery of x-ray diffraction, this necessity for a standard crystal for x-ray spectroscopy became apparent. Moseley was the first to propose a standard value for the grating spacing of some "standard" crystal,<sup>2</sup> namely, rock salt. Analysis of x-ray diffraction patterns by Bragg, using both the Laue and the Bragg methods,<sup>3</sup> had proved that rock-salt crystals do indeed have a face-centered cubic lattice of the type postulated by the early crystallographers (Sec. 14-7). The unit cell, as described in Sec. 14-9, contains four atoms, or, more accurately, ions, of sodium and four of chlorine. The cell is a cube, and the distance  $d_{100}$  between adjacent (100) planes is half the length of the cube edge, or lattice constant  $a$ . That is,  $d_{100} = \frac{1}{2}a$ .

Rock-salt crystals naturally break into cubic fragments. The

<sup>1</sup> W. P. Davey, F. R. Smith, and S. W. Harding, *Rev. Sci. Instruments*, **15**, 37 (1944). Equipment of this type is manufactured by North American Philips Co., Inc., New York, N.Y.

<sup>2</sup> H. G. J. Moseley, *Phil. Mag.*, **26**, 1024 (1913).

<sup>3</sup> The Laue method of crystal analysis will be discussed in the next chapter. For the early analysis of rock salt by Bragg, using both methods, see W. L. Bragg, *Proc. Roy. Soc. (London) A*, **89**, 248 (1913).



naturally occurring "cleavage faces" of these crystals are the {100} form. The number of unit cells per cubic centimeter is of course the volume of a cubic centimeter (1) divided by the volume of the cell ( $a^3$ ), or  $1/a^3$ . Thus the number of Na and Cl atoms per cubic centimeter, which may be designated by  $q$ , is

$$q = \frac{8}{a^3} = \frac{1}{d_{100}^3} \quad (16-10)$$

From chemistry,<sup>1</sup> it is known that the molecular weight  $M$  of NaCl is  $23.00 + 35.46$  or  $58.46$ . Likewise, Avogadro's number  $N_0$ , the number of molecules per gram molecule, was taken by Moseley to be  $6.05 \times 10^{23}$ , that being the accepted value at the time. The number of Na and Cl atoms combined in  $58.46$  g. of rock salt is thus  $2N_0$ . Moseley took  $2.167$  g./cm.<sup>3</sup> as the density  $\rho$  of rock salt, and it follows that  $M$  g. has a volume of  $M/\rho$  cm.<sup>3</sup>. Therefore there are  $2N_0\rho/M$  atoms in  $1$  cm.<sup>3</sup> of rock salt. That is,

$$q = \frac{2N_0\rho}{M} = \frac{1}{d_{100}^3} \quad (16-11)$$

from which

$$d_{100} = \left( \frac{M}{2N_0\rho} \right)^{\frac{1}{3}} \quad (16-12)$$

Substituting the accepted values at that time into this equation, Moseley obtained  $d_{100} = 2.814 \times 10^{-8}$  cm. or  $2.814$  A., and  $a = 5.628$  A.

M. Siegbahn, the leading x-ray spectroscopist after Moseley's death adopted this value as the "standard" value of  $d$  upon which all other crystal lattice constants and x-ray wave-length determinations would be based. Upon this basis, the value of  $d_{100}$  for rock salt was arbitrarily defined as

$$d_{\text{rock salt}} = 2,814.00 \text{ X.U.} \quad (16-13)$$

Here, X.U. is an abbreviation for "x-unit," a new unit of length invented by Siegbahn, in terms of which he proposed that all x-ray wave length be expressed. If Moseley had known the true values of  $M$ ,  $N_0$ , and  $\rho$ , all of which must be determined experimentally,  $1$  X.U. would be exactly  $10^{-11}$  cm.; but since it was understood that unknown experimental errors were involved, the x-unit was defined as  $1/2,814$  of the rock salt (100) spacing, or approximately  $10^{-11}$  cm.

Siegbahn and others soon found that calcite crystals are much more nearly "perfect" than rock-salt crystals. That is, they have a less pronounced "mosaic" structure, to be discussed in Sec. 16, and consequently produce x-ray spectra practically free of the false lines sometimes obtained with rock salt. Calcite soon became the most common

<sup>1</sup> By reversing these calculations, atomic and molecular weights may be calculated and compared. See, for example, D. A. Hutchison, *J. Chem. Phys.*, **13**, 383 (1945)

used crystal in x-ray spectroscopy, although rock salt, gypsum, mica, sugar, quartz, and occasionally potassium ferrocyanide and carborundum were used for this purpose. By comparing the characteristic x-ray spectrum of some target with a rock-salt crystal and with a calcite crystal, it was then determined that the grating spacing  $d$  of the cleavage planes of calcite was 3,029.45 X.U. In the same way, the spacings for the other crystals were found to have the values listed in Table 16-1.

TABLE 16-1.—GRATING SPACINGS IN X-UNITS AT 18°C.

		X.U.
Rock salt.....	NaCl	2,814.00*
Calcite.....	CaCO <sub>3</sub>	3,029.45
Quartz.....	SiO <sub>2</sub>	4,246.02
Gypsum.....	CaSO <sub>4</sub> ·2H <sub>2</sub> O	7,584.70
Mica.....	.....	9,942.72

\* By definition.

For these crystals, the changes in  $d$  per degree centigrade, due to thermal expansion, were found to be, respectively, 0.11, 0.03, 0.04, 0.29, and 0.15 X.U.

As already mentioned on page 104, these values were accepted as being reasonably accurate and satisfactory until the technique of diffraction of x-rays by ruled gratings reached a high state of precision. When it became possible to compare the spectrum of a particular x-ray source as diffracted by a calcite crystal and by a ruled grating, it was found that the grating spacing of calcite was about 3.03560 Å., not 3.02945 Å.<sup>1</sup> This led to a reinvestigation of the possible sources of error in the values of  $M$ ,  $N_0$ , and  $\rho$  in equation (16-12). Among these,  $N_0$  was the most questionable, since it is not measured directly but calculated from the relation

$$N_0 = \frac{Sc}{10eE} \quad (16-14)$$

where  $S$  is the atomic weight of silver,  $E$  is the electrochemical equivalent (grams electrodeposited per coulomb) of silver,  $c$  is the velocity of light, and  $e$  is the electronic charge. Expressed in words, this relation says that the number of atoms per gram atom is equal to the charge carried by one gram atom ( $S/E$ , often called the "faraday") of univalent ions, divided by the charge carried by one such ion ( $e$ ). The 10 converts coulombs to abcoulombs (e.m.u.), and the  $c$  converts the e.m.u. to e.s.u., the units in which  $e$  is measured. It was finally concluded that the least accurately known quantity involved was the electronic charge  $e$ . If one

<sup>1</sup> See, for example, J. A. Bearden, *J. Applied Phys.*, **12**, 395 (1941); also, V. L. Bollman and J. W. M. DuMond, *Phys. Rev.*, **54**, 1005 (1938).

takes Bearden's 3.03560 A. value for  $d_{\text{calcite}}$ , then  $d_{\text{rock salt}}$  should be 2.81971 A. Upon inserting this and the best known values of  $M$ ,  $\rho$ ,  $S$ ,  $c$ , and  $E$  in (16-12) and (16-14),  $e$  was calculated to be  $4.8024 \times 10^{-10}$  e.s.u., as contrasted with the hitherto accepted value of  $4.774 \times 10^{-10}$  e.s.u. As stated on page 104, the discrepancy was finally traced to an incorrect value of the viscosity of air used in Millikan's oil-drop determination of  $e$ .

If one accepts Bearden's value for the grating spacing  $d$  of calcite, one then obtains the following "modern" values for  $d$ :

TABLE 16-2.—GRATING SPACINGS IN ANGSTROM UNITS AT 18°C.

		A.
Rock salt.....	NaCl	2.81971
Calcite.....	CaCO <sub>3</sub>	3.03560
Quartz.....	SiO <sub>2</sub>	4.25465
Gypsum.....	CaSO $\cdot$ 2H <sub>2</sub> O	7.6001
Mica.....	.....	9.9629

Some investigators prefer to define a "modern x-unit" *exactly* equal to  $10^{-11}$  cm. In terms of such a modern x-unit, the spacings become 2,819.71 X.U. for rock salt, 3,035.60 X.U. for calcite, etc. Other investigators object to the confusion caused by having x-units and modern x-units which are different, and insist that the modern values based on 3.03560 A. for calcite must be expressed in angstrom units.<sup>1</sup>

The wave lengths of the characteristic spectral lines, such as the K lines of molybdenum and copper, are listed in most tables in terms of the original Siegbahn x-unit. In the light of the above discrepancy, these wave-length tables will probably be revised eventually. For example the following values may be listed:

TABLE 16-3.—WAVE LENGTHS OF THE CHARACTERISTIC LINES OF MOLYBDENUM AND COPPER

		Old X.U.	A.
Molybdenum	K $\alpha_1$	707.831	0.709271
	K $\alpha_2$	712.105	0.713553
	K $\alpha$	709.26	0.71070
	K $\beta_1$	630.978	0.632261
Copper	K $\alpha_1$	1,537.395	1.540522
	K $\alpha_2$	1,541.232	1.544367
	K $\alpha$	1,538.7	1.5418
	K $\beta_1$	1,389.35	1.39218

\* W.M. = "weighted mean."

<sup>1</sup> H. Lipson and D. P. Riley, *Nature*, **151**, 250 (1943); M. Siegbahn, *Nature*, **151**, 502 (1943).

To obtain modern values of  $d$  or  $\lambda$  from old ones, multiply by<sup>1</sup> the conversion factor 1.00203.

### 5. Analysis of Rock Salt and Sylvine (KCl) by the Bragg Method.

At the outset, it should be recognized that the x-ray diffraction data alone are in general insufficient evidence from which to determine the lattice structure and establish the space group of a crystal. The geometrical shape of the crystal, its chemical composition, and the systematic relationships between the crystal structures of related compounds are all helpful and often indispensable factors to consider in determining the crystal structure by any of the x-ray methods.

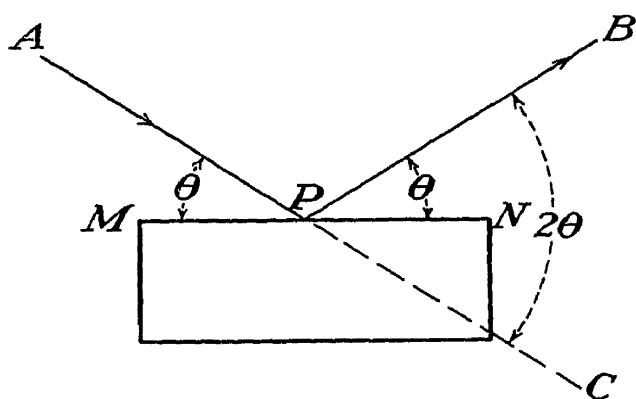


FIG. 16-4.—Diffraction by the cleavage planes of a single crystal.

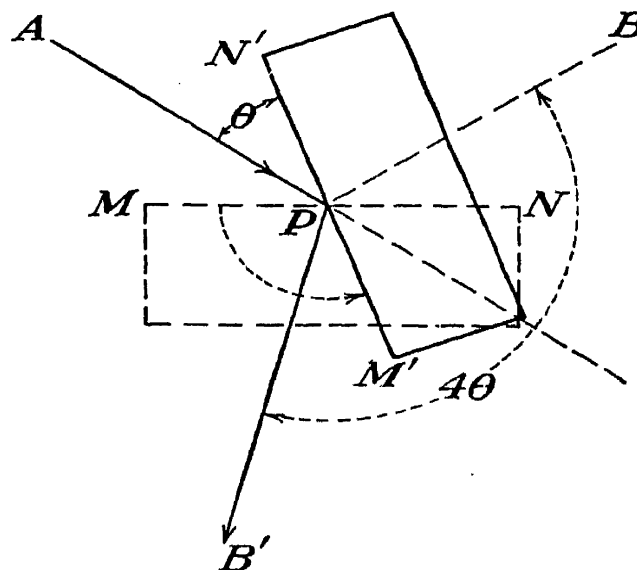


FIG. 16-5.—The two equivalent crystal positions of an x-ray spectrometer.

Placing a rock-salt crystal on the central table of the simple (single-crystal type) Bragg spectrometer, with one of its (100) cleavage faces containing the central vertical axis of the table, one may set the table so that the incident x-ray beam  $AP$  (Fig. 16-4) strikes the crystal face  $MN$  at a glancing angle  $\theta$  of 3 or 4°. The ionization chamber is then slowly moved around from an angle  $CPB$  (Fig. 16-4) of 5° or so, to 12 or 15°. If the planes of atoms parallel to the cleavage face happen to have a spacing  $d$  that satisfies Bragg's law for  $n = 1$  and for the particular wave length  $\lambda$  being used, at the grazing angle  $\theta$ , a maximum in the ionization current will result when the chamber reaches the angle  $CPB$  equal to  $2\theta$ . If not, no such maximum occurs, although a maximum may be found at some greater angle  $CPB$  because of diffraction from some other set of planes containing the zone axis parallel to the table spindle. The angle  $CPB$  at which any such maximum occurs is noted, as well as the maximum ion current; the ionization current at several slightly greater and slightly smaller angles is also noted. To determine the angle  $CPB$  more accurately, readings may be taken on the other side at  $B'$ , as indicated in Fig. 16-5. Then angle  $CPB$  may be taken as

<sup>1</sup> See *Nature*, **155**, 643 (1945) for latest developments; also R. T. Birge, *Amer. J. Physics*, **13**, 69 (1945).

half of the angle  $BPB'$ . In order to record all the diffraction maxima in this manner, it is necessary to repeat this procedure for values of  $\theta$  varying by small intervals (say  $\frac{1}{10}^\circ$ ) over the range from 3 or  $4^\circ$  up to 20 or  $25^\circ$ , by rotating the crystal table  $\frac{1}{10}^\circ$  after each set of readings.

This tedious process may be speeded up somewhat by various modifications. In the simplest arrangement, the ionization current is led directly to an electrometer, which therefore reads the accumulated

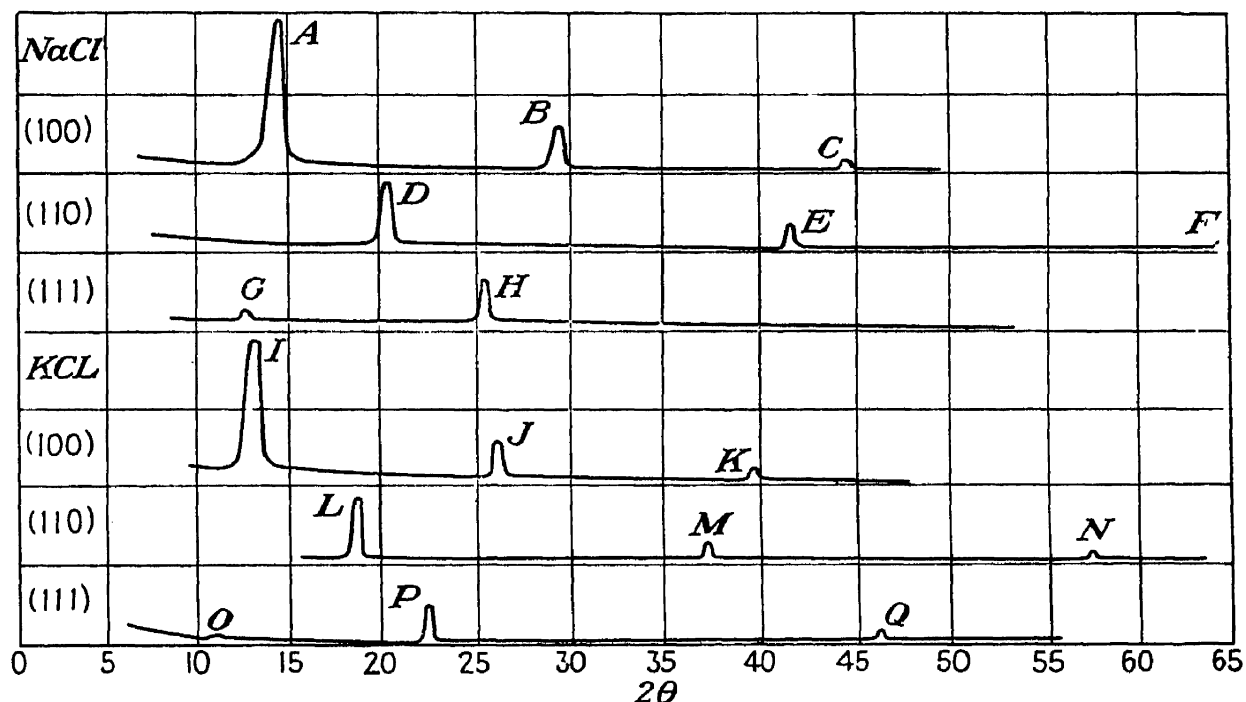


FIG. 16-6.—“Bragg reflections” from the (100), (110), and (111) faces of crystals of rock salt and sylvine. (Adapted from W. H. Bragg and W. L. Bragg, “*The Crystalline State*,” by permission of George Bell & Sons, Ltd., and The Macmillan Company.)

charge. Bragg originally operated his tube for an interval of 4 sec. and then read the electrometer, then discharged it, reset the chamber angle, turned the tube on for 4 sec. only, again read the electrometer, etc. By shunting the electrometer (or vacuum-tube voltmeter) with a high resistance (several megohms), the instrument then reads charging rate or current, so that the x-ray tube may be operated continuously. The electrometer or vacuum-tube-voltmeter deflections may be recorded by a light beam on a photographic film moving in synchronism with the chamber swivel so that a graph of intensity versus  $\theta$  is automatically plotted.

At any rate, one finally obtains a graph showing the intensity of the x-rays diffracted by the cleavage face planes (100) of the rock-salt crystal as a function of the glancing angle  $\theta$ . Then the crystal is sawed off and ground down in such a way as to obtain a (110) face. This new face must intersect a (100) cleavage face along a line parallel to a cube edge and the dihedral angle between the two faces must be  $45^\circ$ . The spectrum

record of maxima diffracted by the (110) planes is then obtained as before. Finally, a (111) face is obtained by grinding one perpendicular to a cube diagonal, and the diffraction maxima from this face are recorded. A sylvine crystal is also cubic. It is instructive to compare the spectra obtained from one with that obtained from rock salt; therefore, it will be supposed that the graphs mentioned above have been obtained for both crystals. If molybdenum  $K_\alpha$  radiation, filtered out with zirconium, were used, the resulting intensity versus angle curves would appear as represented in Fig. 16-6.

The peaks,  $A, B, C, D$ , etc., are superimposed upon a curve that is due to the diffuse scattering. The curves for the (100) and (110) faces of both rock salt and sylvine show three peaks,  $ABC, DEF, IJK$ , and  $LMN$ . If the values  $\theta_A, \theta_B, \theta_C$ , etc., of  $\theta$  at which the peaks  $A, B, C$ , etc., occur are substituted into Bragg's law written in the form

$$d = n\lambda/2 \sin \theta$$

on the assumption that  $\lambda$  is the 0.71-A. molybdenum  $K_\alpha$  doublet in each case, it will be found that they fit relationships of the following sort, within experimental error:

$$\left. \begin{aligned} {}_r d_{(100)} &= \frac{\lambda}{2 \sin \theta_A} = \frac{2\lambda}{2 \sin \theta_B} = \frac{3\lambda}{2 \sin \theta_C} \\ {}_r d_{(110)} &= \frac{\lambda}{2 \sin \theta_D} = \frac{2\lambda}{2 \sin \theta_E} = \frac{3\lambda}{2 \sin \theta_F} \\ {}_s d_{(100)} &= \frac{\lambda}{2 \sin \theta_I} = \frac{2\lambda}{2 \sin \theta_J} = \frac{3\lambda}{2 \sin \theta_K} \\ {}_s d_{(110)} &= \frac{\lambda}{2 \sin \theta_L} = \frac{2\lambda}{2 \sin \theta_M} = \frac{3\lambda}{2 \sin \theta_N} \end{aligned} \right\} \quad (16-15)$$

where the subscripts  $r$  and  $s$  refer to rock salt and sylvine. This indicates immediately, without much room for doubt, that each of the four groups of three peaks  $ABC, DEF, IJK$ , and  $LMN$  are the first-, second-, and third-order ( $n = 1, n = 2, n = 3$ ) diffraction maxima of the molybdenum  $K_\alpha$  doublet diffracted from the (110) and (100) planes.

Also, it is found that, within experimental error,

$$\left. \begin{aligned} {}_r d_{(100)} : {}_r d_{(110)} : {}_r d_{(111)} &= \frac{\lambda}{2 \sin \theta_A} : \frac{\lambda}{2 \sin \theta_D} : \frac{\lambda}{2 \sin \theta_H} = 1 : \frac{1}{\sqrt{2}} : \frac{1}{\sqrt{3}} \\ {}_s d_{(100)} : {}_s d_{(110)} : {}_s d_{(111)} &= \frac{\lambda}{2 \sin \theta_I} : \frac{\lambda}{2 \sin \theta_L} : \frac{\lambda}{2 \sin \theta_P} = 1 : \frac{1}{\sqrt{2}} : \frac{1}{\sqrt{3}} \end{aligned} \right\} \quad (16-16)$$

This indicates that there exist in these crystals atomic planes parallel to the (100), (110), and (111) faces having spacings respectively pro-

portional to  $1$ ,  $1/\sqrt{2}$ , and  $1/\sqrt{3}$ . This is what one might expect in a simple cubic type of lattice, as may be seen by considering Fig. 16-7. If the faces of the elementary cubes in this figure are (100) planes, then  $ABCD$  in (a) is a (110) plane and  $ABC$  in (b) is a (111) plane. If the cube edge [which is the distance between (100) planes] is supposed to have a length  $g$ , then the distance  $MO$  in (a), which is the distance between adjacent (110) planes, obviously has a length  $g/\sqrt{2}$  since it is half the distance  $OP$ , which has a length of  $\sqrt{2}g$  by the Pythagorean theorem. Likewise, adjacent (111) planes in (b) are  $ABC$ ,  $DEF$ , and planes parallel to them through  $O$  and  $P$ . Thus these planes divide the cube diagonal  $OP$  (which has a length of  $\sqrt{3}g$ ) into three equal parts, any one of which, such as  $OM$ , is therefore equal to  $g/\sqrt{3}$ .

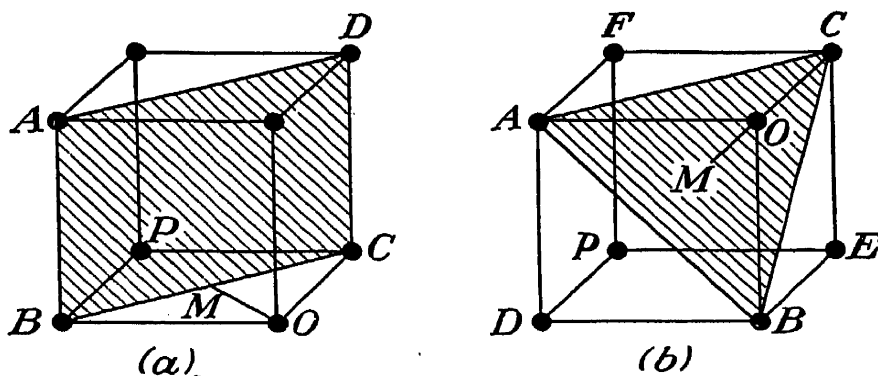


FIG. 16-7.—The (110) and (111) planes in a simple cubic lattice.

At this point, it begins to appear that the crystal lattices of rock salt and sylvine might be simple cubic arrays of atoms, as represented in Fig. 16-7. This is especially true of sylvine;  $Q$  turns out to be the second-order maximum corresponding to peak  $P$  if the latter is a first-order maximum, which it might be, for  $O$  is such a slight irregularity that its significance is doubtful. However, the (111) curve for rock salt (Fig. 16-6) fails to fit into this theory. (1) It shows no second-order peak corresponding to the first-order peak  $H$ , if indeed  $H$  is a first-order peak. (2)  $H$  itself is located at an angle  $\theta$  where a second-order peak would be expected if the small peak  $G$  is regarded as a first-order maximum.

Casting about for a likely cubic arrangement of the sodium and chlorine atoms that might account for all the observed maxima, one might consider a structure of the type proposed by Barlow (page 317) and shown in Fig. 16-8. In this figure, (a) represents the face-centered arrangement of atoms discussed in Sec. 14-9. It might be supposed that the sodium atoms could occupy the positions represented by the solid dots. A logical way to fit the chlorine atoms into such a structure would be to imagine them arrayed in the same way, as represented by the open circles  $A'B'C'D'E'F'G'H'$  in (b), and then shove the two lattices together so that they intermesh as shown in (c) and extended in (d).

In a structure of this sort, if the distance  $MN$  in Fig. 16-8*d* is called  $g$ , then the remarks already made regarding Fig. 16-7 are still valid, thus accounting for equations (16-15) and (16-16). Furthermore, the (100) and (110) planes are seen to consist of a 50-50 mixture of Na and Cl atoms, but the (111) planes consist entirely of Na or entirely of Cl atoms in alternation. Supposing that the chlorine atoms (atomic number 17) scatter the x-rays more effectively than the sodium atoms (atomic

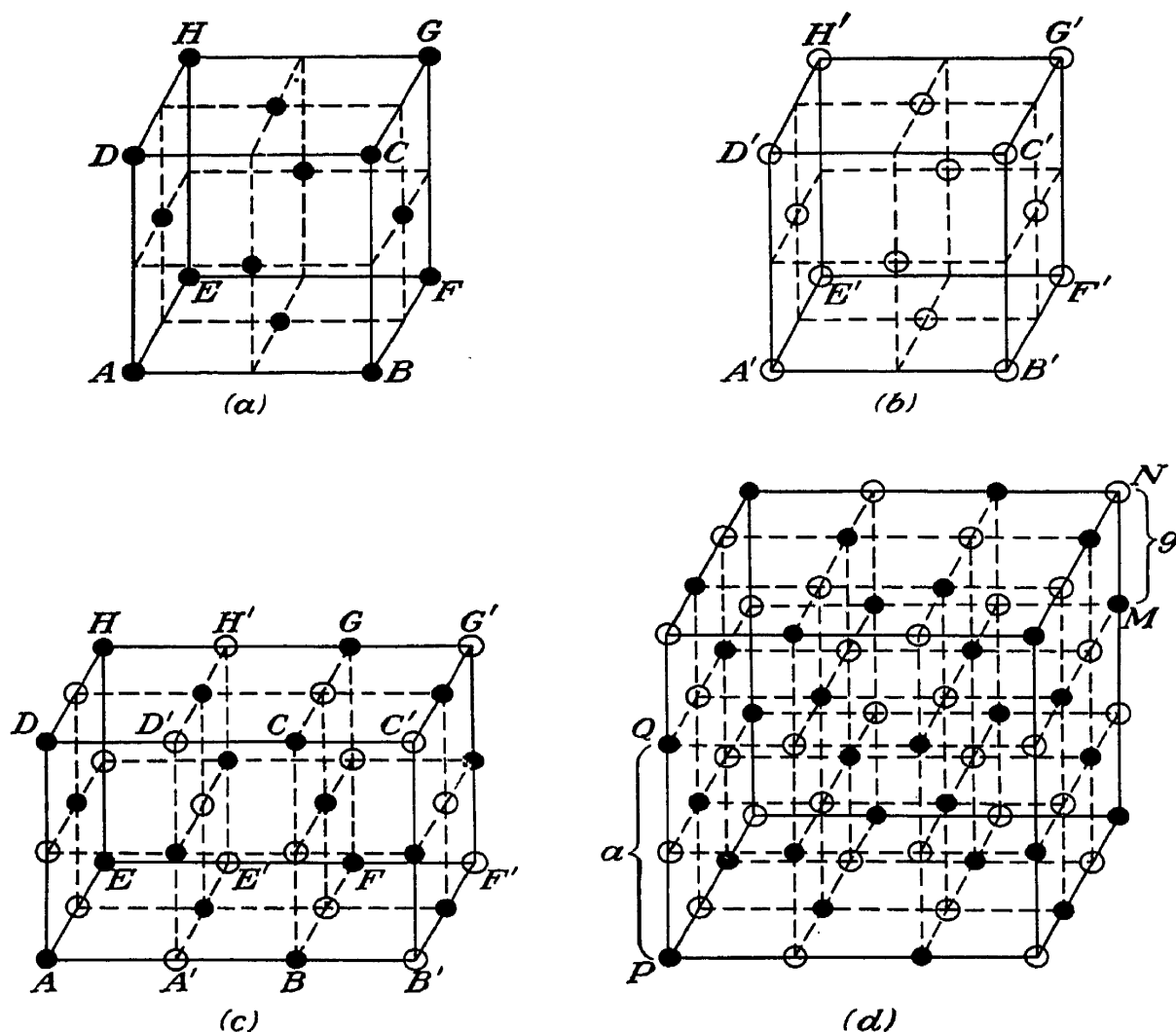


FIG. 16-8.—The interposition of two face-centered cubic lattices, as in rock salt.

number 11), the type of diffraction maxima to be expected may be deduced with the aid of Fig. 16-9. Here the solid lines in (a) and (b) represent the similar planes in the (100) and (110) families, and the alternating solid and dotted lines in (c) represent the unlike planes in the (111) family. If one supposes that the solid planes scatter x-rays twice as effectively as the dotted ones, it follows that the first-order Bragg diffraction maximum should correspond to a  $d$  value of  $2g/\sqrt{3}$  rather than  $g/\sqrt{3}$ . However, it will be relatively weak; for the wave crests returning from the solid planes will coincide with the wave troughs returning from the dotted planes, and the amplitude of the resultant



wave will be only the difference in the amplitudes of the two component waves, whereas the second-order maximum will be strong, because in this case the two sets of component waves add up. The third-order maximum, weak to begin with, will be further suppressed, so that it may not even be detected.

This is just what is observed in Fig. 16-6—a weak first-order peak  $G$ , a strong second-order peak  $H$ , and the third-order peak missing. Thus all the peaks for rock salt agree with the theoretical predictions from a structure of the type postulated in Fig. 16-8*d*. This being the case what does Fig. 16-6 indicate about sylvine structure? As noted on page 343, the position of peaks  $P$  and  $Q$  are those to be expected for a

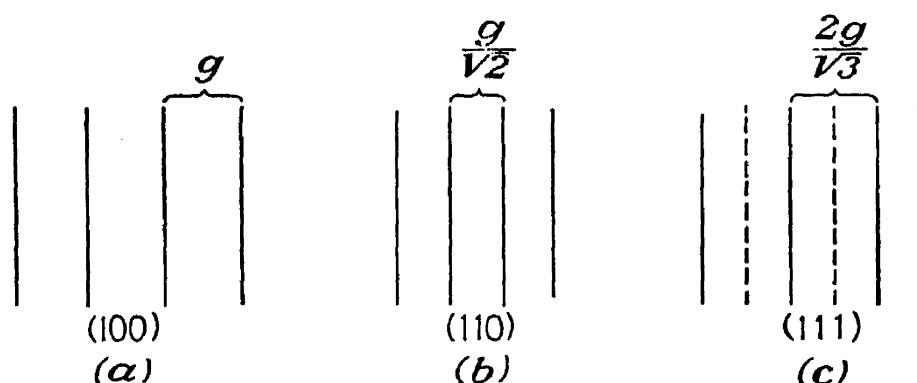


FIG. 16-9.—Adjacent atomic planes are alike in some sets; unlike in others.

simple structure as in Fig. 16-7. However, the structure of Fig. 16-8 degenerates to simple cubic, so far as x-ray diffraction is concerned, the circles and dots have equal scattering power for x-rays. The atom numbers of potassium and chlorine are 19 and 17, respectively, and the ionic character of the crystal discussed in the following paragraph results in a structure of  $K^+$  and  $Cl^-$  ions, each having 18 electrons and hence practically equal x-ray scattering power. The physical and chemical similarity of rock salt and sylvine, combined with the x-ray evidence therefore leads to the conclusion that sylvine has the same type of structure as rock salt.

The analysis thus shows that the unit cell of these two crystals is the cube of edge length  $a$  ( $a = 2g$ , Fig. 16-8*d*). The value for  $a$  for rock salt is calculated as explained in the preceding section. Thus, the  $d$  value in equations (16-15) and (16-16) being known,  $\lambda$  can be calculated, if it is not already known. The (100) spacing for rock salt that was assigned the standard value of 2,814 X.U. by Siegbahn is now seen to be identical with  $g$  in the present discussion, so that the lattice constant  $a$  for rock salt is evidently 5,628 X.U. Knowing  $\lambda$  and  $\theta$ , from equations of the type (16-15) one may readily calculate that the lattice constant for sylvine is 6,280 X.U. Both unit cells contain four atoms of Na (or K) and four atoms of Cl. As a matter of fact, these crystals are called

"ionic crystals" because the experimental evidence indicates that the valence electron ordinarily associated with each sodium (or potassium) atom departs from it and attaches itself to one of the chlorine atoms, so that the crystal thus consists of  $\text{Na}^+$  (or  $\text{K}^+$ ) and  $\text{Cl}^-$  ions. There are no  $\text{NaCl}$  (or  $\text{KCl}$ ) molecules in the crystal in the ordinary sense because each  $\text{Na}^+$  (or  $\text{K}^+$ ) is surrounded by six equidistant  $\text{Cl}^-$  neighbors, no one of which can be singled out and claimed to "belong" to it; the same is true regarding each  $\text{Cl}^-$  surrounded by its six  $\text{Na}^+$  (or  $\text{K}^+$ ) ions.

The coordinates of the Na (or K) ions in the unit cell are  $000$ ;  $\frac{1}{2}\frac{1}{2}0$ ;  $\frac{1}{2}0\frac{1}{2}$ ; and  $0\frac{1}{2}\frac{1}{2}$ . Those of the Cl ions are  $\frac{1}{2}\frac{1}{2}\frac{1}{2}$ ;  $00\frac{1}{2}$ ;  $0\frac{1}{2}0$ ; and  $\frac{1}{2}00$ . This structure is the fifth variety of symmetry (as classified by Schoenflies) of the group of crystals having holohedral cubic symmetry, and hence rock salt and sylvine both belong to the space group designated as  $O_h^5$ .

In the application of the simple Bragg method to the analysis of crystal structure, the precision required in determining the angles  $\theta$  at which the maxima occur is rarely if ever so great that one need consider the effects of the refraction of the rays as they enter and leave the crystal (Sec. 15-5). In precision x-ray spectroscopy, this correction should be made. The simple Bragg method of crystal analysis is seen to be rather a game of cut and try or trial and error. This characteristic is partly eliminated in the modern extensions of the method (see Sec. 11). These modern extensions are cumbersome, however, and for this reason one usually resorts to them only in the analysis of the more complex crystals. The crystal structures of all the more common chemical compounds have been tabulated by Wyckoff.<sup>1</sup> He gives the space group, unit cell, dimensions, arrangement of the atoms in the cell, and, in many instances, diagrams.

**6. Suppressed Reflections and the Reflections for the Seven Crystal Systems.** In the preceding section, it was seen that the first- and third-order Bragg diffraction maxima, commonly called Bragg "reflections," from the (111) planes were weakened in the case of rock salt and practically eliminated in the case of sylvine. The concept of the Bragg reflection is on no account to be confused with true x-ray reflection, which was discussed in Chap. 6. In terms of the notation usually employed to designate these reflections, (222) refers to the second-order reflection from the (111) planes, (330) to the third-order reflection from the (110) planes, etc. According to this convention, one thinks of the second-order reflection from the (100) planes, for example, as a first-order reflection from a fictitious set of (200) planes having half the interplanar spacing of the (100) planes. In the preceding section, one would say that the (222) reflections ( $H$  and  $P$ , Fig. 16-6) were present, but

<sup>1</sup> R. W. G. Wyckoff, "The Structure of Crystals," 2d ed., 1931, supplement, 1935, Reinhold Publishing Corporation, New York.

(111) and (333) were weakened or suppressed by destructive interference as explained from Fig. 16-9c. Suppression of certain Bragg reflections often results from a change in lattice type, as when a centered (that is, body-centered, face-centered, or end-centered) lattice is substituted for a simple lattice.<sup>1</sup>

This may be illustrated in a diagram by limiting the problem to two dimensions. In Fig. 16-10a, a simple rectangular two-dimensional lattice is shown. Here,  $MN$ ,  $PQ$ , and  $RS$  are three adjacent (12) lines (planes become lines in a two-dimensional lattice). Figure 16-10b represents the same lattice "centered." That is, the circles shown have been added at the centers of the rectangles formed by the dots of the original lattice. It will be noticed that this creates a new set of (12) lines represented by the dotted lines interspersed between the original solid (12) lines. In terms of Bragg reflections from these (12) lines, the odd orders will be completely suppressed if the dots and circles represent identical atoms or reduced in intensity if the dots have a different x-ray scattering power than the circles. In other words, the original (12), (36), etc., reflections will be suppressed.

For a simple cubic lattice there are no suppressions, and the Bragg reflections ( $hkl$ ) to be expected are given by the formula

$$d_{hkl}^{\text{cubic}} = \frac{a}{\sqrt{h^2 + k^2 + l^2}} \quad (16-)$$

where all possible sets of integral values of the indices  $h$ ,  $k$ , and  $l$  are inserted. These reflections include all the different orders of reflection for all possible sets of planes ( $hkl$ ) in a simple cubic lattice. The reflections correspond to a series of  $d$  values in the ratios  $\frac{1}{\sqrt{1}}, \frac{1}{\sqrt{2}}, \frac{1}{\sqrt{3}}, \dots, \frac{1}{\sqrt{5}}, \dots$ . Only reflections corresponding to  $\frac{1}{\sqrt{7}}, \frac{1}{\sqrt{15}}, \frac{1}{\sqrt{23}}, \frac{1}{\sqrt{31}}, \dots$  will be missing, not because of suppression, but because they do not exist.

<sup>1</sup> This topic is ably discussed under the title Space Group Extinction by M. Buerger, "X-ray Crystallography," John Wiley & Sons, Inc., New York, 1942. The term "suppression" has been used here to avoid possible confusion with the common use of the term "extinction," as in Sec. 15.

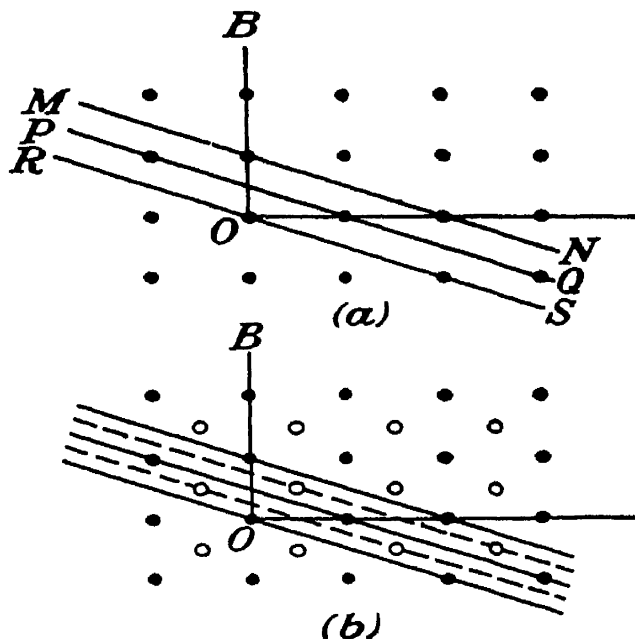


FIG. 16-10.—Showing how centered lattices suppress some Bragg reflections.

geometrically, since no integral values can be assigned to  $h$ ,  $k$ , and  $l$  that will make  $h^2 + k^2 + l^2$  equal 7, 15, 23, 31, etc. One may substitute the various  $d$  values given by (16-17) into the Bragg formula, always setting  $n = 1$ , and thus calculate for a given  $\lambda$  the various Bragg angles  $\theta$  at which the reflections will be found for a simple cubic lattice.

In the case of a face-centered (not necessarily cubic) lattice, the suppressions permit the appearance of only those Bragg reflections for which  $h$ ,  $k$ , and  $l$  are all even or all odd. Thus the reflections permitted in a face-centered cubic lattice correspond to a series of grating spacings in the proportions  $\frac{1}{\sqrt{3}}, \frac{1}{\sqrt{4}}, \frac{1}{\sqrt{8}}, \frac{1}{\sqrt{11}}$ , etc., since odd or even values for  $h$ ,  $k$ , and  $l$  will yield only such values as 3, 4, 8, 11, etc., for  $h^2 + k^2 + l^2$  in equation (16-17). Thus, face-centered lattices are said to yield reflections having "unmixed indices."

In the case of a body-centered (not necessarily cubic) lattice, only reflections for which  $h + k + l$  is even occur, the others, for which  $h + k + l$  is odd, being suppressed. Thus the reflections permitted in a body-centered cubic lattice correspond to spacings in the proportions  $\frac{1}{\sqrt{2}}, \frac{1}{\sqrt{4}}, \frac{1}{\sqrt{6}}, \frac{1}{\sqrt{8}}$ , etc.;  $\frac{1}{\sqrt{28}}$  is missing in this series.

In an end-centered prismatic (centered on its  $c$  end) lattice, only reflections for which  $h + k$  is even are permitted. If the lattice is centered on the  $a$  side,  $k + l$  must be even; if centered on the  $b$  side,  $h + l$  must be even.

A diamond has a cubic structure different from any of these; for this type of lattice, the reflections correspond to spacings in the proportions  $\frac{1}{\sqrt{3}}, \frac{1}{\sqrt{8}}, \frac{1}{\sqrt{11}}, \frac{1}{\sqrt{16}}, \frac{1}{\sqrt{19}}, \frac{1}{\sqrt{24}}, \frac{1}{\sqrt{27}}, \frac{1}{\sqrt{32}}$ , etc.

To determine which reflections are missing, it is necessary to know first which ones are to be expected in the case of a simple lattice with a primitive<sup>1</sup> cell. Starting with (16-17) for the cubic system, there are the following formulas giving the reflections from simple primitive holohedral lattices in the seven different crystal systems:

Cubic:

$$d_{hkl} = \frac{a}{\sqrt{h^2 + k^2 + l^2}} \quad (16-17)$$

Tetragonal:

$$d_{hkl} = \frac{1}{\sqrt{\frac{h^2}{a^2} + \frac{k^2}{a^2} + \frac{l^2}{c^2}}} \quad (16-18)$$

<sup>1</sup> Footnote 1, p. 315.

Orthorhombic:

$$d_{hkl} = \frac{1}{\sqrt{\frac{h^2}{a^2} + \frac{k^2}{b^2} + \frac{l^2}{c^2}}} \quad (16-19)$$

Hexagonal, hexagonal:

$$d_{hkl} = \frac{1}{\sqrt{\frac{4}{3a^2}(h^2 + hk + k^2) + \frac{l^2}{c^2}}} \quad (16-20)$$

Hexagonal, rhombohedral:

$$d_{hkl} = \frac{a \sqrt{1 + 2 \cos^3 \alpha - 3 \cos^2 \alpha}}{\sqrt{(h^2 + k^2 + l^2) \sin^2 \alpha + 2(hk + hl + kl)(\cos^2 \alpha - \cos \alpha)}} \quad (16-21)$$

Monoclinic:

$$d_{hkl} = \frac{1}{\sqrt{\frac{h^2}{a^2} + \frac{l^2}{c^2} - \frac{2hl}{ac} \cos \beta + \frac{k^2}{b^2} \sin^2 \beta}} \quad (16-22)$$

Triclinic:

$$d_{hkl} = \frac{1}{\sqrt{\begin{vmatrix} \frac{h}{a} \cos \gamma \cos \beta \\ \frac{h}{a} \frac{k}{b} 1 \cos \alpha \\ \frac{l}{c} \cos \alpha 1 \end{vmatrix} + \frac{k}{b} \begin{vmatrix} 1 \frac{h}{a} \cos \beta \\ \cos \gamma \frac{k}{b} \cos \alpha \\ \cos \beta \frac{l}{c} 1 \end{vmatrix} + \frac{l}{c} \begin{vmatrix} 1 \cos \gamma \frac{h}{a} \\ \cos \gamma 1 \frac{k}{b} \\ \cos \beta \cos \alpha \frac{l}{c} \end{vmatrix} + \begin{vmatrix} 1 \cos \gamma \cos \beta \\ \cos \gamma 1 \cos \alpha \\ \cos \beta \cos \alpha 1 \end{vmatrix}}}} \quad (16-23)$$

Having calculated and indexed the spacings to be expected from the assumed simple primitive cell, according to the appropriate equation above, one then compares this list with the list of spacings indicated by the observed reflections and thus determines which reflections are suppressed and, from this, whether the cell chosen is primitive, doubly or triply primitive, face-centered, body-centered, etc. From this type of analysis, supplemented by any other pertinent information that may be available, the space group may finally be determined. The suppressed reflections in the commonest cubic types of crystal may be represented in convenient diagrammatic form, as shown in Fig. 18-7.

**7. Parameters in the Unit-cell Configuration.** The atoms are by no means always situated at the corners, at the center, or at the face centers

of the unit cell. This situation is characteristic of only the simpler types of compounds, and even some of the elements<sup>1</sup> require the use of parameters to specify the coordinates of the atoms in the unit cell. In the simple compound  $\text{FeS}_2$ , for example, crystallization sometimes occurs

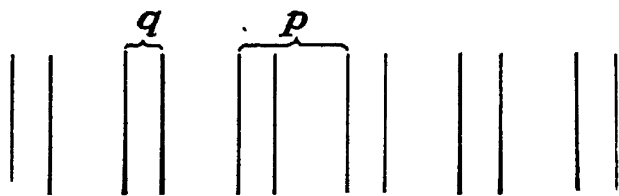


FIG. 16-11.—Illustrating complex arrangement of some sets of atomic planes.

in the orthorhombic form but more commonly in the cubic form called iron pyrites (fool's gold), the space group being  $T_h^6$  and the lattice constant  $a$ , 5.41 Å. In these crystals, the sulfur atoms have a face-centered cubic structure, but the iron atoms

are arranged differently in adjacent cubes so that these cubes are not unit cells. The arrangement requires the introduction of a "parameter"  $u$  to specify the positions of the sulfur atoms when the iron atoms are given their logical places in the unit cell.

In general, crystals having a structure requiring the use of parameters to locate the atoms in the unit cell will fail to yield any systematic series of reflections like  $ABC$ ,  $DEF$ ,  $IJK$ , and  $LMN$  in Fig. 16-6. Instead, the

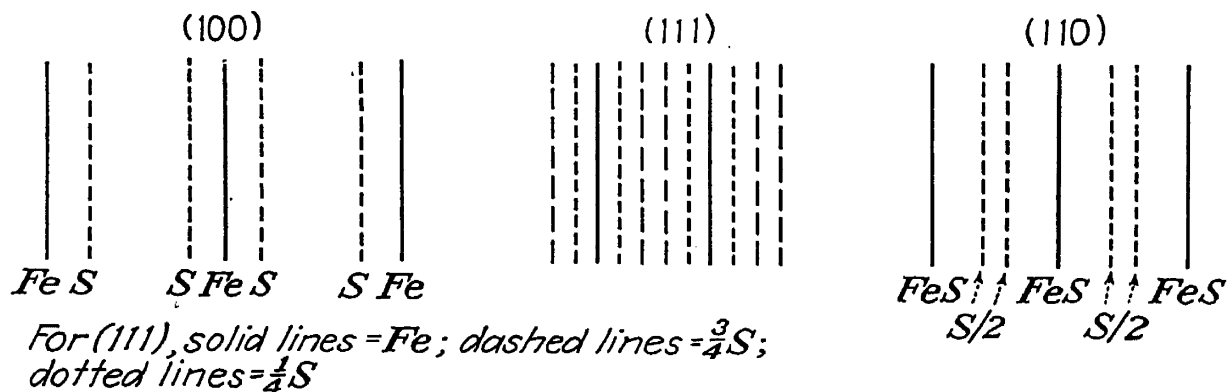


FIG. 16-12.—Spacings of principal atomic planes in pyrites, as deduced by Bragg. (Courtesy of Sir W. L. Bragg, George Bell & Sons, Ltd., and The Macmillan Company.)

reflections from all faces may show suppressed reflections like  $G$ ,  $O$ , etc., for all the principal sets of planes have a complex arrangement in which successive planes are spaced in a narrow-wide-narrow-wide sequence, as in Fig. 16-11. Although a diamond crystal has a cubic structure readily describable without the use of parameters, its (111) planes have a complex arrangement of this type, in which  $p = 4q$  (Fig. 16-11). The effect of this on the Bragg reflections can be readily deduced by imagining x-rays of wave length equal to  $p$  incident perpendicularly on these planes. Then the planes spaced  $p$  apart will "reflect" the waves in phase, but the planes spaced  $q = \frac{1}{4}p$  apart will reflect equally intense waves exactly out of phase with them, thus completely suppressing<sup>2</sup> the

<sup>1</sup> For example, antimony, arsenic, bismuth, gallium, iodine, selenium, and tellurium.

<sup>2</sup> A very weak (222) reflection is observable, the generally accepted reason being

(222), that is, the second-order (111), reflection. Similar reasoning leads to the conclusion that the first-, third-, and fourth-order reflections from this set of planes should be present, all of which agrees with observation.

To return to the discussion of iron pyrites, Fig. 16-12 represents the spacing of the principal sets of atomic planes (100), (110), and (111), as deduced by Bragg. Here, all the principal sets of planes are seen to have a complex arrangement, resulting in suppressed reflections from each set. The "unit-cell configuration," that is, the coordinates of the atoms in the unit cell of this crystal, may be given thus:

$$\text{Fe: } 000; \frac{1}{2}\frac{1}{2}0; \frac{1}{2}0\frac{1}{2}; 0\frac{1}{2}\frac{1}{2}$$

$$\text{S: } uuu; u + \frac{1}{2}, \frac{1}{2} - u, \bar{u}; \bar{u}, u + \frac{1}{2}, \frac{1}{2} - u; \frac{1}{2} - u, \bar{u}, u + \frac{1}{2}; \bar{u}\bar{u}\bar{u}; \frac{1}{2} - u, \\ u + \frac{1}{2}, u; u, \frac{1}{2} - u, u + \frac{1}{2}; u + \frac{1}{2}, u, \frac{1}{2} - u$$

where  $u$  is about 0.40. In some of the more complex compounds it is necessary to introduce a dozen or more of these parameters in order to specify the crystal structure.

**8. The Relationship between the Hexagonal and Rhombohedral Lattices.** Formulas (16-20) and (16-21) raise the question of the relation between hexagonal and rhombohedral lattices. It was stated in Chap. 14 that they are related, but the relationship was not explained. Figure 16-13 represents a hexagonal point lattice referred to a triply primitive rhombohedral line lattice. For such a unit cell, having unit axes  $A_1$ ,  $A_2$ , and  $A_3$ , all of the same length and same included angle  $\alpha = \beta = \gamma = \omega$ , only those reflections predicted by equation (16-21) for which  $h + k + l$  is divisible by 3 will occur, the others being suppressed. The crystals in the rhombohedral division of the hexagonal system are more conveniently described by referring them to a rhombohedral lattice in this manner. Those in the hexagonal division are more conveniently referred to hexagonal axes,  $a_1$ ,  $a_2$ , and  $c$  in Fig. 16-13, their reflections being given by equation (16-20).

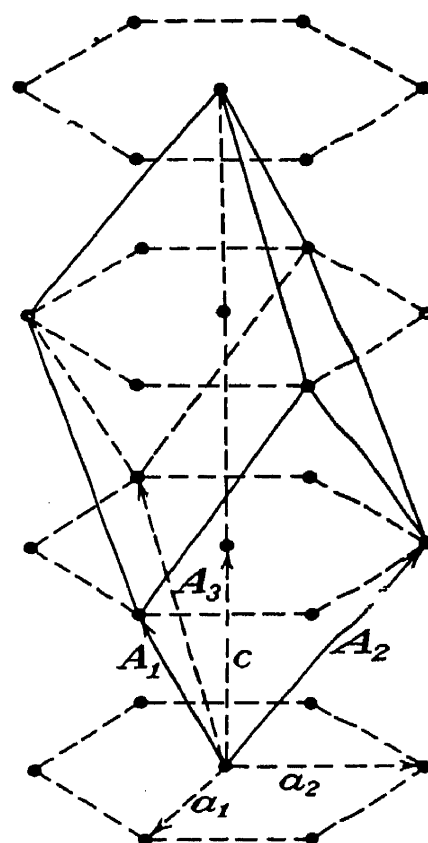


FIG. 16-13.—Relation between hexagonal and rhombohedral lattices. (Reprinted by permission from "X-ray Crystallography," by M. J. Buerger; published by John Wiley & Sons, Inc.)

that the four strong homopolar bonds between each atom and its four nearest neighbors distort the electron cloud around each atomic nucleus so that it acquires non-spherical symmetry.

**9. The Atomic-structure Factor.** Even in the simplest types of analysis by the Bragg method, as exemplified by rock salt and sylvine, it is evident that the intensities of the diffraction maxima are almost as important a factor to be considered as their angular position. When the diffraction maxima are recorded photographically, with a spectrograph instead of a Bragg type of ionization spectrometer, this kind of analysis calls for the use of a microphotometer to estimate the intensities of the lines on the film.

The preceding sections have shown how the distances between the atomic planes in crystals may be deduced by the simple Bragg method. Experiments along various lines, including x-ray diffraction, indicate

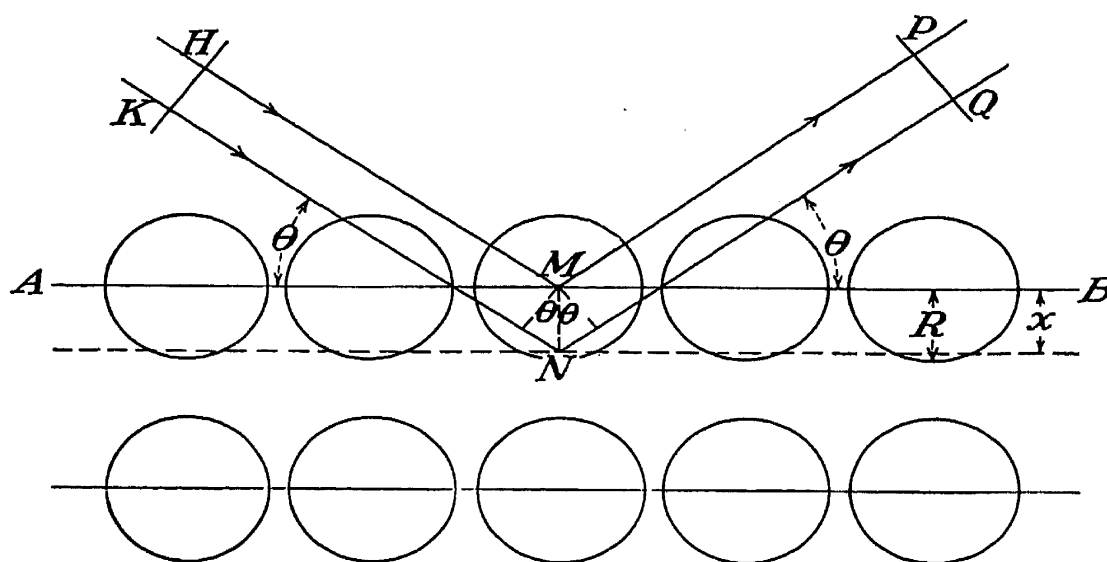


FIG. 16-14.—Showing interference between x-rays scattered by various electrons in an atomic plane.

that the diameter of the atoms in a crystal is of the same order of magnitude as these interplanar distances. Thus the analogy of stacked balls (page 312) is a reasonably accurate picture in this respect. This being the case, one may refer to Fig. 16-14 and to Fig. 15-4 for comparison and see that an accurate theory of x-ray diffraction must include a consideration of the interference effects between rays scattered from electrons near the center of the atoms in a lattice plane and rays scattered from electrons near the periphery of these same atoms, as mentioned in the last two paragraphs of Sec. 2.

If  $AB$  (Fig. 16-14) is a crystal lattice plane containing the centers of the atoms ordinarily described as lying "in" this plane, then the reasoning like that on page 324 it follows that rays such as  $NQ$  diffracted by electrons such as  $N$ , located a distance  $x$  below this plane, will lag behind rays such as  $MP$  diffracted by electrons such as  $M$  located in the plane, the path difference being  $2x \sin \theta$ . In the present discussion, we cannot argue, as before, that if this path difference is  $\frac{1}{10}\lambda$ , then rays scattered from a plane  $10x$  below plane  $AB$  will cause complete destruc-



tive interference, for there is no repetition of structure at intervals as there was before at intervals of  $d$ . This being the case, one is justified in adding the amplitudes of the wavelets of various phases scattered by the various electrons at the distance  $x$  above or below the grating lattice planes in question, for example, the (100) planes.

Suppose one now considers a single atom containing  $Z$  electrons.  $Z$  is its atomic number. If  $\delta$  is the phase difference between a wavelet scattered by an electron in the plane  $AB$  and a wavelet scattered by an electron a distance  $x$  below it, then the contribution  $E_x$  of the latter is the amplitude  $E_s$  of the former wavelets when the two are added. The amplitude of the resultant wave in phase with the former is<sup>1</sup>

$$E_x = E_s \cos \delta$$

The path difference between the two is  $2x \sin \theta$ , as already stated. If this is  $\lambda$ , the phase difference  $\delta$  is  $2\pi$ ; if it is  $\lambda/4$ ,  $\delta = \pi/2$ , etc.

$$\delta = \frac{2x \sin \theta}{\lambda} 2\pi = \frac{4\pi x}{\lambda} \sin \theta$$

Hence

$$E_x = E_s \cos \left( \frac{4\pi x}{\lambda} \sin \theta \right)$$

The probability that one of the electrons in the atom will be in the layer between the planes  $x = x_0$  and  $x = x_0 + dx$  is proportional to  $dx$ , but it also decreases as  $x_0$  increases, or one may say that it is proportional to an unknown function  $p(x_0)$ . Thus this probability is proportional to  $p(x) dx$  where  $x_0$  is now regarded as a variable. The contribution of the wavelets scattered by such electrons in the layer to the resultant amplitude will be

$$p(x) E_s \cos \left( \frac{4\pi x}{\lambda} \sin \theta \right) dx$$

To get the amplitude  $E_r$  of the resultant wave from the whole crystal of radius  $R$ , one must then integrate over the range from  $x = -R$  to  $x = +R$  for all  $Z$  electrons, obtaining

$$E_r = Z E_s \int_{-R}^{+R} p(x) \cos \left( \frac{4\pi x}{\lambda} \sin \theta \right) dx$$

In Sec. 2, Thomson's expression was given for the amplitude  $P$  of the wave coherently scattered by a free electron  $O$  from an incident primary ray  $AO$  polarized perpendicularly to the plane  $AOP$  and having amplitude  $E'_0$  at  $O$ . It was

$$E'_s = E'_0 \frac{e^2}{r m c^2}$$

<sup>1</sup> See, for example, F. A. Jenkins and H. E. White, "Fundamentals of Optics," p. 33, McGraw-Hill Book Company, Inc., New York, 1937.

where  $r = OP$ . When this was converted into intensities  $I$  (which are proportional to the square of amplitudes  $E$ ), the resulting expression was

$$I_e = I_0 \left( \frac{e^2}{rmc^2} \right)^2 \frac{1 + \cos^2 \phi}{2} \quad (16-7)$$

where the expression  $1 + \cos^2 \phi/2$  arose from the consideration of unpolarized instead of polarized rays. For this reason,  $1 + \cos^2 \phi/2$  is commonly called the "polarization factor" (P.F.). It is to be noted that  $\phi$  in Sec. 2 equals  $2\theta$  in the present discussion of Fig. 16-14, so that

$$\text{P.F.} = \frac{1 + \cos^2 2\theta}{2} \quad (16-27)$$

In mathematical treatments of x-ray diffraction, it has been customary to neglect the polarization factor when dealing with amplitudes  $E$  and then to insert it at the end of the calculation when one is ready to convert to intensities  $I$  by squaring. In the following discussion, this convention will be followed, but one should not lose sight of the fact that the equations expressed in terms of amplitude  $E$  apply, strictly speaking, only to polarized waves; yet one can convert them to equations in the experimentally measurable intensities  $I$  at any time by merely squaring and multiplying by the polarization factor. On this basis, equations (16-2), (16-3), and (16-6) become simply

$$E_s = \frac{E_0 e^2}{rmc^2} \quad (16-28)$$

The substitution of (16-28) in (16-26) yields

$$E_r = \frac{E_0 e^2}{rmc^2} f \quad (16-29)$$

where  $f$  is a quantity known as the "atomic-structure factor" or "atomic-scattering factor" given by

$$f = Z \int_{-R}^{+R} p(x) \cos \left( \frac{4\pi x}{\lambda} \sin \theta \right) dx = \frac{E_r}{E_s} \quad (16-30)$$

In words, the atomic-structure factor is the following ratio:

$$f = \frac{\text{amplitude at any point } P \text{ of the coherent (polarized) radiation scattered from an atom at rest}}{\text{amplitude at } P \text{ of the coherent (polarized) radiation scattered by a free electron}} \quad (16-31)$$

Here the denominator is taken conventionally as simply (16-28) because both Thomson's classical theory and modern wave mechanics yield this expression for small values of  $\theta$  or  $\phi$ .

This factor  $f$  is a function of  $\sin \theta/\lambda$ , and it approaches  $Z$  for small values of  $\theta$ , as may be seen from the typical  $f$  curves in Fig. 16-15. In general, it decreases rather rapidly as  $\theta$  increases, the fall being at a considerably slower rate for heavy atoms than for light ones, however. At small angles, the amplitude of the waves scattered by an atom is nearly proportional to its atomic number. The curves in Fig. 16-15 were computed by James and Brindley,<sup>1</sup> using wave mechanics. The upper curve is for a positive potassium ion and the lower for a negative chlorine ion, as in a sylvine crystal. Since the atomic numbers of K and Cl are 19 and 17, respectively, both these ions have 18 orbital electrons, so that both curves show the same  $f$  value of 18 for  $\theta = 0$ .

The words "at rest" were inserted in the definition of  $f$  because the wave-mechanical computation of  $f$  usually neglects the effects of the thermal vibration of the atom. The  $f$  as calculated and listed in tables is ordinarily for atoms at zero absolute temperature, that is, for atoms at rest. This  $f$  is therefore sometimes designated by  $f_0$ , the subscript serving to remind one that the temperature correction remains to be made before an accurate value of  $f$  is obtained. The  $f_0$  values for some of the commoner atoms and ions are listed in Table 16-4, as given

by James and Brindley. These were calculated from the theoretical work of Hartree, Pauling and Sherman, Thomas and Fermi, and others. At ordinary temperatures, the Bragg reflections are weakened slightly by the thermal vibrations of the atoms. According to Waller and James, the temperature correction for  $f$  for cubic crystals<sup>3</sup> like NaCl may be expressed as follows:

$$f = f_0 e^{-\frac{8\pi^2 \bar{u}^2 \sin^2 \theta}{\lambda^2}} \quad (16-32)$$

where  $e$  is the Napierian log base and  $\bar{u}^2$  is the mean square displacement of the atoms in a direction perpendicular to the reflecting planes such as  $AB$  in Fig. 16-14. At and above ordinary temperatures such as  $0^\circ\text{C}$ .,  $\bar{u}^2$  is nearly proportional to the absolute temperature. At ordinary tem

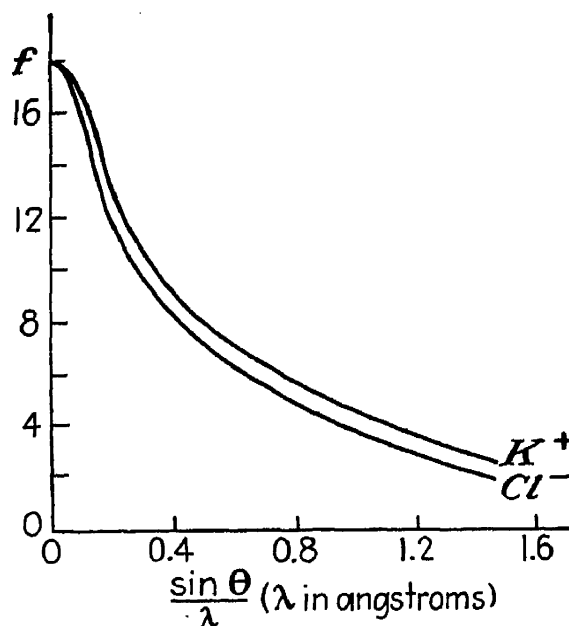


FIG. 16-15.—Atomic structure factors of  $\text{K}^+$  and  $\text{Cl}^-$  ions. (James and Brindley. Courtesy of The Royal Society.)

<sup>1</sup> R. W. James and G. W. Brindley, *Proc. Roy. Soc. (London) A*, **121**, 166 (1928) from wave functions computed by D. R. Hartree.

<sup>2</sup> I. Waller and R. W. James, *Proc. Roy. Soc., A*, **117**, 214 (1927).

<sup>3</sup> For the general case, see p. 365.

TABLE 16-4.\*—ATOMIC-STRUCTURE FACTORS AT ZERO ABSOLUTE TEMPERATURE

$\frac{\sin \theta}{\lambda}$	0	0.1	0.2	0.3	0.4	0.5	0.6	0.7	0.8	0.9	1.0	1.1
1H.....	1.0	0.81	0.48	0.25	0.13	0.07	0.04	0.03	0.02	0.01	0.00	0.00
2He.....	2.0	1.88	1.46	1.05	0.75	0.52	0.35	0.24	0.18	0.14	0.11	0.09
3Li <sup>+</sup> .....	2.0	1.96	1.8	1.5	1.3	1.0	0.8	0.6	0.5	0.4	0.3	0.3
3Li.....	3.0	2.2	1.8	1.5	1.3	1.0	0.8	0.6	0.5	0.4	0.3	0.3
4Be <sup>++</sup> ....	2.0	2.0	1.9	1.7	1.6	1.4	1.2	1.0	0.9	0.7	0.6	0.5
4Be.....	4.0	2.9	1.9	1.7	1.6	1.4	1.2	1.0	0.9	0.7	0.6	0.5
5B.....	5.0	3.5	2.4	1.9	1.7	1.5	1.4	1.2	1.2	1.0	0.9	0.7
6C.....	6.0	4.6	3.0	2.2	1.9	1.7	1.6	1.4	1.3	1.2	1.0	0.9
7N.....	7.0	5.8	4.2	3.0	2.3	1.9	1.65	1.55	1.5	1.4	1.3	1.15
8O.....	8.0	7.1	5.3	3.9	2.9	2.2	1.8	1.6	1.5	1.4	1.35	1.25
8O <sup>—</sup> .....	10.0	8.0	5.5	3.8	2.7	2.1	1.8	1.5	1.5	1.4	1.35	1.25
9F <sup>—</sup> .....	10.0	8.7	6.7	4.8	3.5	2.8	2.2	1.9	1.7	1.55	1.5	1.35
9F.....	9.0	7.8	6.2	4.45	3.35	2.65	2.15	1.9	1.7	1.6	1.5	1.35
10Ne.....	10.0	9.3	7.5	5.8	4.4	3.4	2.65	2.2	1.9	1.65	1.55	1.5
11Na <sup>+</sup> ....	10.0	9.5	8.2	6.7	5.25	4.05	3.2	2.65	2.25	1.95	1.75	1.6
11Na.....	11.0	9.65	8.2	6.7	5.25	4.05	3.2	2.65	2.25	1.95	1.75	1.6
12Mg <sup>++</sup> ...	10.0	9.75	8.6	7.25	6.05	4.8	3.85	3.15	2.55	2.2	2.0	1.8
12Mg.....	12.0	10.5	8.6	7.22	6.05	4.8	3.85	3.15	2.55	2.2	2.0	1.8
13Al <sup>+++</sup> ...	10.0	9.7	8.9	7.8	6.65	5.5	4.45	3.65	3.1	2.65	2.3	2.0
13Al.....	13.0	11.0	8.95	7.75	6.6	5.5	4.5	3.7	3.1	2.65	2.3	2.0
14Si <sup>++++</sup> ...	10.0	9.75	9.15	8.25	7.15	6.05	5.05	4.2	3.4	2.95	2.6	2.3
14Si.....	14.0	11.4	9.4	8.2	7.15	6.1	5.1	4.2	3.4	2.95	2.6	2.3
15P.....	15.0	12.4	10.0	8.45	7.45	6.5	5.65	4.8	4.05	3.4	3.0	2.6
16S.....	16.0	13.6	10.7	8.85	7.85	6.85	6.0	5.25	4.5	3.9	3.35	2.9
17Cl.....	17.0	14.6	11.3	9.25	8.05	7.25	6.5	5.75	5.05	4.4	3.85	3.35
17Cl <sup>—</sup> .....	18.0	15.2	11.5	9.3	8.05	7.25	6.5	5.75	5.05	4.4	3.85	3.35
18A.....	18.0	15.9	12.6	10.4	8.7	7.8	7.0	6.2	5.4	4.7	4.1	3.6
19K <sup>+</sup> .....	18.0	16.5	13.3	10.8	8.85	7.75	7.05	6.44	5.9	5.3	4.8	4.2
20Ca <sup>++</sup> ....	18.0	16.8	14.0	11.5	9.3	8.1	7.35	6.7	6.2	5.7	5.1	4.6
26Fe.....	26.0	23.1	19.1	15.6	13.4	11.7	10.2	8.9	7.9	7.1	6.4	5.8
29Cu.....	29.0	25.8	21.4	17.8	15.2	13.3	11.7	10.2	9.1	8.1	7.3	6.7
35Br.....	35.0	31.5	26.6	22.2	19.0	16.7	14.8	13.0	11.6	10.4	9.5	8.6
36Kr.....	36.0	33.0	28.0	24.2	21.2	18.9	16.7	14.4	12.3	10.6	9.2	8.3
37Rb <sup>+</sup> ....	36.0	33.6	28.7	24.6	21.4	18.9	16.7	14.6	12.8	11.2	9.9	8.9
47Ag.....	47.0	43.0	36.9	31.3	26.8	23.7	21.3	19.0	17.0	15.3	13.9	12.8
54Xe.....	54	50	43	37	32	28	25	23	20	18	17	15
80Hg.....	80	75	66	58	50	45	41	36	33	30	28	26
55Cs.....	55.0	50.7	43.8	37.6	32.4	28.7	25.8	23.2	20.8	18.8	17.0	15.6
$\frac{\sin \theta}{\lambda} =$	1.2	1.3	1.4	1.5	1.6	1.7	1.8	1.9	2.0			
55Cs.....	14.5	13.2	12.3	11.3	10.4	9.6	9.2	8.6	8.1			

\* R. W. James and G. W. Brindley, *Z. Krist.*, **78**, 470 (1931); *Phil. Mag.*, **12**, 81 (1931).

peratures one may regard  $f$  and  $f_0$  as practically identical in crystal analysis.

In Table 16-4 the structure factors for cesium ( $Z = 55$ ) are given for values of  $\sin \theta/\lambda$  up to 2.0,  $\lambda$  being in angstrom units in all cases. The atomic-structure factors for the heavier elements above  $Z = 55$  may be calculated quite accurately by multiplying the  $f_0$  values for cesium by  $Z/55$ .

**10. The Crystal-structure Factor.** The preceding section was concerned with the amplitude of the x-ray wave coherently scattered by a single atom in terms of the scattering from a single electron. The concept of the atomic-structure factor there developed can be carried one step further so as to apply, not to a single atom, but to all the atoms in the unit cell of the crystal. One thus arrives at a "crystal-structure factor"  $F$ , which is closely related to the experimentally measurable intensities of the diffracted x-ray beams. This factor  $F$  plays an essential role in the Bragg analysis of complex crystals. It is defined as the following ratio:

$$F = \frac{\text{amplitude of the coherent (polarized) radiation diffracted in a particular Bragg reflection } (nh, nk, nl) \text{ by all the atoms in the unit cell, measured at a distance } r \text{ from the cell}}{\text{amplitude of the coherent (polarized) radiation scattered by a free electron, measured at a distance } r \text{ from the electron}} \quad (16-33)$$

This factor may be expressed mathematically by the relation

$$F = \sum_j f_j e^{2\pi ni(hx_j + ky_j + lz_j)} \quad (16-34)$$

where  $f_j$  is the atomic structure of the  $j$ th atom in the unit cell,  $i = \sqrt{-1}$ , and  $n$  is the order of the Bragg reflection  $(nh, nk, nl)$  from the planes  $(hkl)$  of a crystal having a unit cell in which the atoms are located in the usual manner (for example, 000;  $\frac{1}{2}\frac{1}{2}0$ ;  $\frac{1}{2}0\frac{1}{2}$ , and  $0\frac{1}{2}\frac{1}{2}$  for the Na ions in NaCl) by coordinates  $x_j, y_j, z_j$  expressed as fractional parts of the cell dimensions  $a, b$  and  $c$ . The derivation of (16-34) is necessarily rather involved<sup>1</sup> because it entails the addition of the amplitudes of the wavelets scattered by each of the  $j$  atoms in the unit cell, each having fractional coordinates specified only in a generalized way as  $x_j, y_j, z_j$ . In adding these amplitudes, the phase differences of the wavelets must be considered, and for this reason the general expression is complex; that is, it

<sup>1</sup> Equation (16-34) is derived as equation 5.34 (page 353) in the book "X-rays in Theory and Practice" by A. H. Compton and S. K. Allison, 2d ed., D. Van Nostrand Company, Inc., New York, 1935. See also the discussion following equation 6.103 on page 445.

is partly imaginary.<sup>1</sup> However, the imaginary parts of  $F$  cancel out for all crystals having a center of symmetry, and this includes nearly all of them. In the rather rare cases where  $F$  is complex, the intensities  $I$  of the diffracted beams calculated from the  $F$  values will be real, nevertheless.

The following examples of the application of (16-34) to a few simple crystal types should allay any doubts regarding the usefulness of the equation, which appears rather cumbersome at first glance.

1. What are the crystal-structure factors for the (100), (111), (200), and (220) Bragg reflections from a rock-salt crystal?

Let  $f_{\text{Na}}$  = atomic-structure factor of  $\text{Na}^+$  and  $f_{\text{Cl}}$  = atomic-structure factor of  $\text{Cl}^-$ .

In the unit cell of rock salt, the coordinates of the Na atoms are 000;  $\frac{1}{2}\frac{1}{2}0$ ;  $\frac{1}{2}0\frac{1}{2}$ ;  $0\frac{1}{2}\frac{1}{2}$ ; while those of the Cl atoms are  $\frac{1}{2}\frac{1}{2}\frac{1}{2}$ ;  $00\frac{1}{2}$ ;  $0\frac{1}{2}0$ ;  $\frac{1}{2}00$ . That is, for atom 1 ( $j = 1$ ),  $x = 0$ ,  $y = 0$ , and  $z = 0$ ; for atom 2 ( $j = 2$ ),  $x = \frac{1}{2}$ ,  $y = \frac{1}{2}$ , and  $z = 0$ ; for atom 8 ( $j = 8$ ),  $x = \frac{1}{2}$ ,  $y = 0$ , and  $z = 0$ . For the (100) reflection,  $h = 1$ ,  $k = 0$ , and  $l = 0$ , of course. In this case, (16-34) becomes

$$\begin{aligned} F(100) &= f_{\text{Na}}[e^{2\pi i(0+0+0)} + e^{2\pi i(\frac{1}{2}+0+0)} + e^{2\pi i(\frac{1}{2}+0+0)} + e^{2\pi i(0+0+0)}] \\ &\quad + f_{\text{Cl}}[e^{2\pi i(\frac{1}{2}+0+0)} + e^{2\pi i(0+0+0)} + e^{2\pi i(0+0+0)} + e^{2\pi i(\frac{1}{2}+0+0)}] \\ &= f_{\text{Na}}(1 + e^{\pi i} + e^{\pi i} + 1) + f_{\text{Cl}}(e^{\pi i} + 1 + 1 + e^{\pi i}) \\ &= f_{\text{Na}}(1 - 1 - 1 + 1) + f_{\text{Cl}}(-1 + 1 + 1 - 1) = 0 \end{aligned}$$

The fact that  $e^{\pi i} = -1$  follows from footnote 1, below. The zero value found for  $F(100)$  indicates that no (100) Bragg reflection is to be expected for rock salt, and this agrees with experiment. In a similar manner, one has

$$\begin{aligned} F(111) &= f_{\text{Na}}(1 + 1 + 1 + 1) + f_{\text{Cl}}(-1 - 1 - 1 - 1) = 4(f_{\text{Na}} - f_{\text{Cl}}) \\ F(200) &= f_{\text{Na}}(1 + 1 + 1 + 1) + f_{\text{Cl}}(1 + 1 + 1 + 1) = 4(f_{\text{Na}} + f_{\text{Cl}}) \\ F(220) &= f_{\text{Na}}(1 + 1 + 1 + 1) + f_{\text{Cl}}(1 + 1 + 1 + 1) = 4(f_{\text{Na}} + f_{\text{Cl}}) \end{aligned}$$

Thus one should expect no first-order reflection from the (100) planes and a weak first-order reflection from (111) but strong second-order reflections from (100) and (110) in rock salt. This agrees with experiment. This type of calculation applies to all crystals having the NaCl type of structure.

2. Derive the law of unmixed indices (Sec. 6) for chemical elements with a face-centered cubic structure.

<sup>1</sup> For those unfamiliar with the exponential representation of complex quantities, the following general mathematical relationships will be found helpful:

$$e^{iy} = \cos y + i \sin y \quad \text{and} \quad e^{-iy} = \cos y - i \sin y$$

The coordinates of the atoms for such crystals are  $000; \frac{1}{2}\frac{1}{2}0; \frac{1}{2}0\frac{1}{2}; 0\frac{1}{2}\frac{1}{2}$ . Hence

$$F = f[1 + e^{\pi ni(h+k)} + e^{\pi ni(h+l)} + e^{\pi ni(k+l)}]$$

This expression equals  $4f$  when  $h$ ,  $k$ , and  $l$  are all odd or all even, but it equals zero when  $h$ ,  $k$ , and  $l$  are mixed.

3. Show that the (200) and (222) reflections should be missing for a diamond.

The coordinates of the carbon atoms in the unit cell are  $000; \frac{1}{2}\frac{1}{2}0; \frac{1}{2}0\frac{1}{2}; 0\frac{1}{2}\frac{1}{2}; \frac{1}{4}\frac{1}{4}\frac{1}{4}; \frac{3}{4}\frac{3}{4}\frac{1}{4}; \frac{3}{4}\frac{1}{4}\frac{3}{4}; \frac{1}{4}\frac{3}{4}\frac{3}{4}$ .

$$\begin{aligned} F(200) &= f_c(e^0 + e^{2\pi i} + e^{2\pi i} + e^0 + e^{\pi i} + e^{3\pi i} + e^{3\pi i} + e^{\pi i}) \\ &= f_c(1 + 1 + 1 + 1 - 1 - 1 - 1 - 1) = 0 \\ F(222) &= f_c(e^0 + e^{4\pi i} + e^{4\pi i} + e^{4\pi i} + e^{3\pi i} + e^{7\pi i} + e^{7\pi i} + e^{7\pi i}) \\ &= f_c(1 + 1 + 1 + 1 - 1 - 1 - 1 - 1) = 0 \end{aligned}$$

4. Calculate  $F(135)$  for ZnS.

In the unit cell of this crystal, the coordinates of the zinc atoms are  $000; 0\frac{1}{2}\frac{1}{2}; \frac{1}{2}0\frac{1}{2}; \frac{1}{2}\frac{1}{2}0$ , while those of the sulfur atoms are  $\frac{1}{4}\frac{1}{4}\frac{1}{4}; \frac{1}{4}\frac{3}{4}\frac{3}{4}; \frac{3}{4}\frac{1}{4}\frac{3}{4}; \frac{3}{4}\frac{3}{4}\frac{1}{4}$ .

$$\begin{aligned} F(135) &= f_{zn}(e^0 + e^{8\pi i} + e^{6\pi i} + e^{4\pi i}) + f_s(e^{\frac{9}{2}\pi i} + e^{\frac{25}{2}\pi i} + e^{\frac{21}{2}\pi i} + e^{\frac{17}{2}\pi i}) \\ &= 4f_{zn} + f_s(\cos \frac{9}{2}\pi + \cos \frac{25}{2}\pi + \cos \frac{21}{2}\pi + \cos \frac{17}{2}\pi) \\ &\quad + if_s(\sin \frac{9}{2}\pi + \sin \frac{25}{2}\pi + \sin \frac{21}{2}\pi + \sin \frac{17}{2}\pi) \\ &= 4f_{zn} + 0 + 4if_s = 4(f_{zn} + if_s) \end{aligned}$$

In this case,  $f_{zn}$  and  $if_s$  should be regarded as two vectors at right angles to each other, so that the parentheses represent the vector sum. By the Pythagorean theorem, this is

$$F(135) = 4 \sqrt{f_{zn}^2 + f_s^2}$$

**11. Integrated Reflections, or Coefficients of Reflection.** The two preceding sections have described two of the three links in the theoretical chain enabling one to calculate the intensities of the x-ray beams diffracted by a crystal having any assumed or known type of structure. The first two links are the factors  $f$  and  $F$ . The final link is the relationship between  $F$  and the actual intensities  $I$ . The examples in the preceding section have shown that, for many ordinary purposes, a knowledge of  $F$  alone is sufficient, without recourse to the relationships to be considered in this section.

The energy in an x-ray beam diffracted from a crystal may be measured experimentally by comparing it with the energy in the primary beam, by means of a Bragg double-crystal spectrometer of the type shown in Fig. 16-2. If  $E$  is the total amount of energy "reflected" from the crystal  $B$  (Fig. 16-2) when it is slowly rotated through the correct angle  $\theta_0$  to diffract the  $n$ th-order beam into the ionization chamber

from its  $(hkl)$  face (as measured by the total charge in coulombs that passes through the chamber during this process), if  $\omega$  is the angular velocity of this slow steady rotation of the crystal in radians per second, and if  $I$  is the energy per second entering the ionization chamber when it is lined up so as to receive the direct beam from crystal  $A$  with crystal  $B$  removed (as measured by the ionization current in amperes or in coulombs per second), then the integrated reflection  $R$  is given by

$$R = \frac{E\omega}{I} \quad (16-35)$$

This quantity  $R$ , called the "integrated reflection" by Bragg and the "coefficient of reflection" by Compton, is an experimentally measurable quantity proportional to the intensity of the diffracted x-ray beam for which it is measured. That is, if the integrated reflection  $R(200)$  for the second-order beam from the  $(100)$  face of a crystal is  $16 \times 10^{-6}$ , whereas the integrated reflection  $R(333)$  for the third-order beam from the  $(111)$  face of the crystal is only  $8 \times 10^{-6}$ , then the former beam is twice as intense as the latter. Since  $R$  always applies to a particular Bragg reflection  $(hkl)$ , it is usually written  $R(hkl)$ .

It has already been stated that the amplitude of the x-ray wavelet coherently scattered by an electron is proportional to  $e^2/mc^2$  and that this must be multiplied by  $F$  to get the amplitude of the scattered wavelet from a unit cell. The amplitude of the wave scattered per unit volume of the crystal should then be closely related to the quantity  $Ne^2F(hkl)/mc^2$ , where  $N$  is the number of unit cells per cubic centimeter. Squaring this and multiplying by the polarization factor (16-27) should give an expression proportional to the intensity, as already mentioned, and therefore proportional to the integrated reflection  $R$ , as just defined. Thus one should expect  $R$  to be proportional to  $\left(\frac{Ne^2F(hkl)}{mc^2}\right)^2 \frac{1 + \cos^2 2\theta}{2}$  for any given wave length  $\lambda$  of the primary x-rays. The complete mathematical analysis involves a consideration of the mosaic structure of the crystal (Sec. 16) and extinction effects (Sec. 15). Out of it, there emerges<sup>1</sup> an additional factor  $\lambda^3/\sin 2\theta$ . Thus  $R(hkl)$  is proportional to a quantity  $Q$  given by

$$Q = \left(\frac{Ne^2F(hkl)}{mc^2}\right)^2 \lambda^3 \frac{1}{\sin 2\theta} \frac{1 + \cos^2 2\theta}{2} \quad (16-36)$$

For a minute crystal, so small that its absorption can be neglected,

<sup>1</sup> See, for example, pp. 405-414 in the book "X-rays in Theory and Practice," by A. H. Compton and S. K. Allison, 2d ed., D. Van Nostrand Company, Inc., New York, 1935.



bathed in radiation of intensity  $I$ , one has simply

$$R = QV \quad (16-37)$$

where  $V$  is the volume of the crystal. When absorption must be considered, as in the Bragg reflection from the face of a large crystal,

$$R = \frac{Q}{2\mu_l} \quad (16-38)$$

where  $\mu_l$  is the linear absorption coefficient of the rays in the crystal. The relation for a powder consisting of fine crystalline grains is given on page 414. Conversely, measurements of the intensities of the diffracted beams from a crystal permit one to calculate the various  $F(hkl)$  for its unit cell.

## 12. The Representation of the Crystal Structure as a Fourier Series.

The use of Fourier series as an analytical method of deriving the crystal structure from the experimental diffraction data was first suggested in 1915 by W. H. Bragg,<sup>1</sup> but it was not until 1929 that a Fourier method of sufficient simplicity to be of much practical value in crystal analysis was proposed by W. L. Bragg.<sup>2</sup> In this method, the values of  $F(hkl)$  are experimentally determined for the reflected diffraction maxima from all the planes in a given zone. If the  $A$  axis of the crystal is chosen as a zone axis, all the various  $F(0kl)$  are measured. A double Fourier series is then formed in which these values are the coefficients and the coordinates  $y$  and  $z$  are the variables. The value of the series at any point  $y_1z_1$  represents the "electron density" at that point, as projected on the (100) face of the crystal. The series may be expressed as

$$\rho(y,z) = \frac{1}{A} \sum_{-\infty}^{\infty} \sum_{-\infty}^{\infty} F(0kl) e^{-2\pi i \left[ \frac{ky}{b} + \frac{lz}{c} + \eta(0kl) \right]} \quad (16-39)$$

$A$  being the area on the (100) face outlined by the  $b$  and  $c$  unit axes and  $\eta$  a phase constant that is a function of  $k$  and  $l$ .  $A = bc \sin \alpha$ . The summation symbols apply to  $k$  and  $l$ . The density  $\rho$  is calculated usually for 200 or 300 evenly distributed points, and then points of equal density are joined by lines like contour lines on a map. In the case of a crystal as complex as diopside  $[\text{CaMg}(\text{SiO}_3)_2]$ , the series has about 40 terms. Electrical devices have been built to reduce the labor of summing these series.<sup>3</sup> The x-ray data determine the amplitudes of all the terms in the series, but not the phase constants  $\eta$ , which must be

<sup>1</sup> W. H. Bragg, *Trans. Roy. Soc. (London) A*, **215**, 253 (1915).

<sup>2</sup> W. L. Bragg, *Proc. Roy. Soc. (London) A*, **123**, 537 (1929).

<sup>3</sup> See, for example, D. Macewan and C. A. Beevers, *J. Sci. Instruments*, **19**, 15 (1942).

known also in order to evaluate the series for  $\rho$ . This difficulty is surmounted in the case of crystals having a center of symmetry (as most of them do) by taking it as the origin of coordinates. This simplifies the equations by eliminating the imaginary part of the complex  $F$  given by (16-34). In this case,  $\eta(0kl) = 0$ ,  $\rho(y,z) = \rho(\bar{y},\bar{z})$ , and

$$e^{-2\pi i\left(\frac{ky}{b} + \frac{lz}{c}\right)} = \cos 2\pi \left(\frac{ky}{b} + \frac{lz}{c}\right)$$

by footnote 1, page 358.

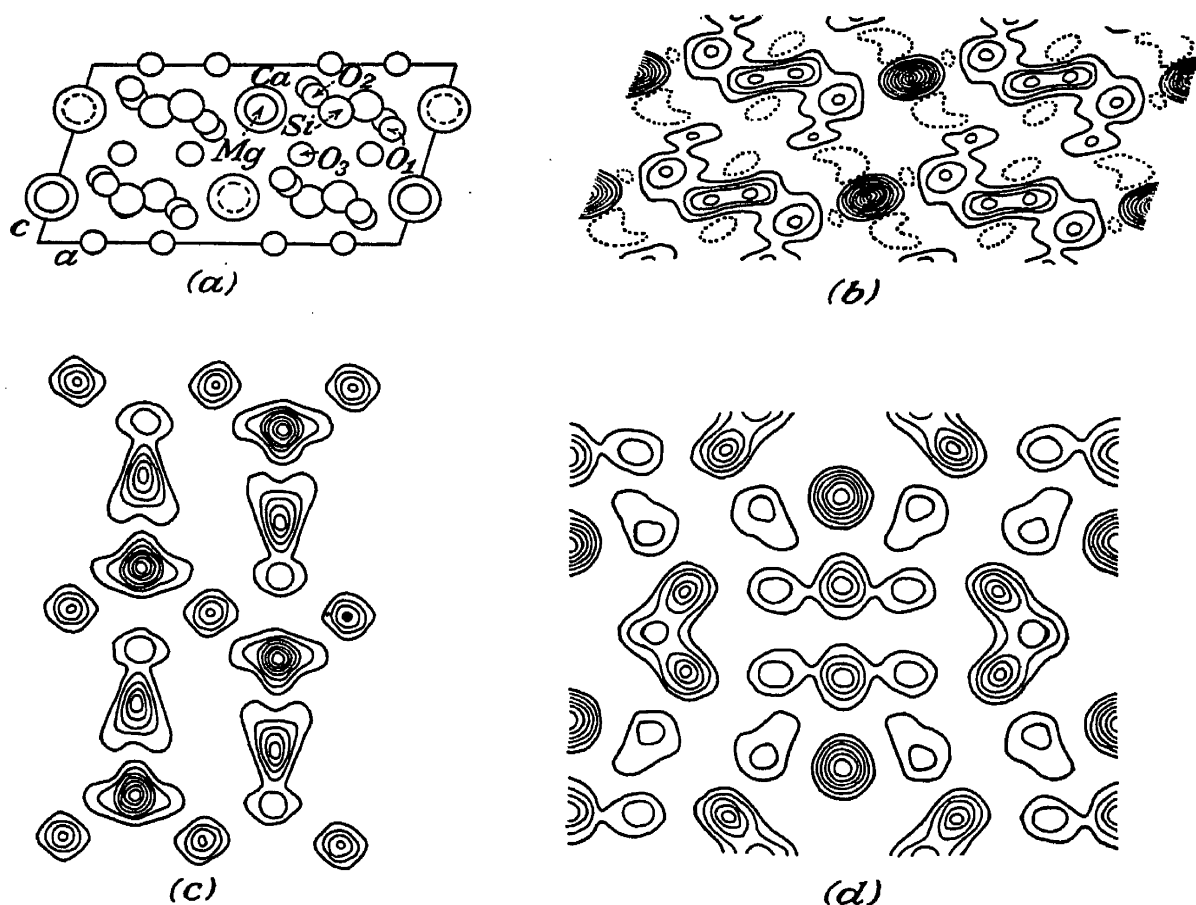


FIG. 16-16.—Electronic density contour maps for (b) (010), (c) (100), and (d) (001) planes of a diopside crystal. The conventional representation (a) may be compared with (b). (Courtesy of Sir W. L. Bragg, George Bell & Sons, Ltd., and The Macmillan Company.)

Figure 16-16a shows the usual projection drawing of the diopside structure on the (010) plane, *b* is a Fourier contour-line projection of this same structure on the (010) face, *c* shows the Fourier projection on the (100) face, and *d* is for the (001) face. All these were worked out by W. L. Bragg.<sup>1</sup> These maps may be regarded as representing the electron density in one plane, expressed in such units as electrons per square angstrom unit.

In some types of work, it may not be necessary to carry out a complete analysis of the crystal structure in order to obtain the information

<sup>1</sup> W. L. Bragg, *Z. Krist.*, **70**, 475 (1929)—in English.

desired. Instead, it may suffice to determine only the radial distribution of atoms surrounding any given atom. This is the general method of approach in analyzing the structure of liquids from their x-ray diffraction patterns (see Chap. 22). When one is aiming at this more easily attained goal, Warren and Gingrich<sup>1</sup> have shown that the phase constants  $\eta$  of the terms in the Fourier series (16-39) need not be known. Patterson,<sup>2</sup> in turn, has pointed out that the series

$$D(u,v) = \sum_{h,k=-\infty}^{\infty} \sum_{l=-\infty}^{\infty} F^2(hkl) e^{2\pi i \left( \frac{hu}{a} + \frac{kv}{b} + \frac{lw}{c} \right)} \quad (16-40)$$

yields a maximum value for  $D(u,v)$  whenever two points of maximum electron density  $\rho(x,y)$  in the (001) plane are located at points  $x_1, y_1$  and  $x_2, y_2$  such that  $u = x_2 - x_1$  and  $v = y_2 - y_1$ . Thus maxima of  $D(u,v)$  correspond to distances  $(u^2 + v^2)^{\frac{1}{2}}$  between electron-density maxima in the (001) plane. This type of series can be evaluated directly from the integrated reflections, use being made of relations such as (16-36) to (16-38). In applying the Patterson method to complex organic compounds, the graphical construction suggested by Robertson<sup>3</sup> may be helpful.

### 13. Bragg's "X-ray Microscope."

After working out the Fourier method outlined in the preceding section, Bragg showed that it is possible to sum the components of the series by an optical device<sup>4</sup> rather than mathematically. A couple of dozen lantern slides bearing alternating light and dark bands with a direction and spacing corresponding to the various components of the series were projected successively onto photographic paper, the time of each exposure being proportional to the amplitude of the component that it represented. After development, the resulting "x-ray micrograph" is the nearest approach man has yet made to a picture of the ultimate structure of matter. The atoms appear in their lattice as one might expect to see them if he had a microscope capable of useful magnification of the order of 100 million diam-

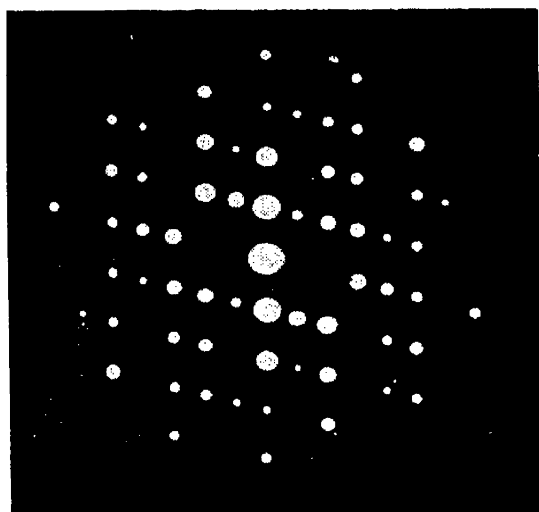


FIG. 16-17a.—Perforations in brass plate used in Bragg's x-ray microscope to project an "x-ray micrograph" of the atoms in the (010) plane of diopside. (W. L. Bragg; courtesy of "Nature" and Macmillan & Company, Ltd.)

<sup>1</sup> B. E. Warren and N. S. Gingrich, *Phys. Rev.*, **46**, 368 (1934).

<sup>2</sup> A. L. Patterson, *Phys. Rev.*, **46**, 372 (1934).  $D(u,v)$  has been used here instead of Patterson's  $A(u,v)$  to avoid confusion with the  $A$  in equation (16-39).

<sup>3</sup> J. M. Robertson, *Nature*, **152**, 412 (1943).

<sup>4</sup> W. L. Bragg, *Z. Krist.*, **70**, 475 (1929)—in English.

eters. Thus Bragg's x-ray microscope is an instrument resembling a projection lantern. It permits one to carry out some of the steps in the Fourier method optically. In this way, one may obtain some truly remarkable pictures of the atomic architecture of many solids.

Recently, Bragg has devised a simplification of this technique,<sup>1</sup> in which a perforated brass plate is inserted between two long-focal-length lenses. A point source of monochromatic light at the focus of one lens forms an image of the atomic structure at the focus of the other lens.

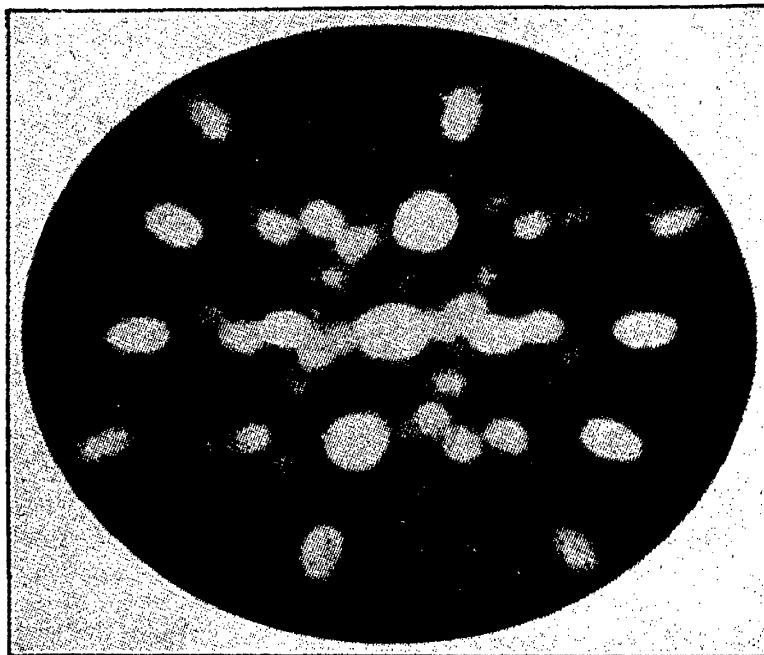


FIG. 16-17b.—X-ray micrograph of the atoms in the (010) plane of diopside. Magnification is about 100 million diameters. (W. L. Bragg; courtesy of "Nature" and Macmillan & Company, Ltd.)

In Fig. 16-17a, each hole in the perforated brass plate represents by its position one ( $h0l$ ) reflection, the area of the hole being proportional to  $F(h0l)$  for that reflection. Figure 16-17b is a photograph by Bragg obtained by means of this technique, showing the (010) projection of the diopside structure.

**14. Effect of Temperature on the Diffraction Pattern.** Thermal expansion causes the distance  $d$  between lattice planes to increase with temperature. In fact, this is the fundamental phenomenon that causes a foot rule to be more than a foot long when it gets hot. In accordance with Bragg's law, then, the diffraction maxima move toward a smaller angular position  $\theta$  as the crystal warms up. This effect explains why the crystal temperature must be controlled in precision spectroscopy.

In accordance with the kinetic theory, the atoms of a solid vibrate

<sup>1</sup> W. L. Bragg, *Nature*, **143**, 678 (1939), **154**, 69 (1944). See also M. L. Huggins, *J. Chem. Phys.*, **12**, 520 (1944); *Nature*, **155**, 18 (1945); A. D. Booth, *Trans. Faraday Soc.*, **41**, 434 (1945).

about their fixed equilibrium positions. The vibration of each atom not independent of that of its neighbors, however. Instead, they behave as if elastically coupled, so that the motions of a row of atoms resemble series of elastic waves in the crystal. In a qualitative way, it can be seen that this should cause the diffraction maxima from a crystal to become fainter and less distinct as the temperature of the crystal rises. For the motion, averaged over a period of time, smears the atoms out into a larger volume than their rest volume, like the blurred photograph of a fluttering flag.

In 1914, Debye<sup>1</sup> made quantitative calculations of the effects of the thermal waves. In terms of modern terminology, he found that they cause the value of the atomic-structure factor  $f_0$  at zero absolute temperature to decrease in accordance with the relation

$$f = f_0 e^{-\frac{M}{2}}$$

where

$$M = \frac{6h^2}{mk\Theta} \left( \frac{\phi(x)}{x} + \frac{1}{4} \right) \frac{\sin^2 \theta}{\lambda^2} \quad (16-4)$$

Here  $\Theta$  is the characteristic temperature<sup>2</sup> of the crystal,  $T$  is the absolute temperature of the crystal,  $x = \Theta/T$ ,  $h$  is Planck's constant,  $m$  is the mass of one of the atoms in the lattice,  $k$  is the Boltzmann gas constant  $= 1.38 \times 10^{-16}$  erg/deg., and  $\phi(x)$  is a function of  $x$  evaluated by Debye,<sup>3</sup> varying from 1 to 0 as  $x$  varies from 1 to  $\infty$ . This calculation by Debye was repeated by Waller<sup>4</sup> in 1925, who found the relation now recognized as correct, because of its agreement with experiment:

$$f = f_0 e^{-M} \quad (16-5)$$

A simplification for the case of simple cubic crystals has already been mentioned [equation (16-32)].

**15. Primary and Secondary Extinction.** If a monochromatic beam of x-rays strikes a crystal at an angle such that Bragg's law is not satisfied for any important set of planes, no diffracted beams will be present. In this circumstance, the mass absorption coefficient  $\mu$  or the linear absorption coefficient  $\mu_L$  of the beam in the crystal is about what one would calculate from an ordinary table of absorption coefficients, if the composition of the crystal and the wave length of the x-rays are known. However, when the crystal is oriented in the beam so that Bragg's law

<sup>1</sup> P. Debye, *Ann. Physik*, **43**, 49 (1914).

<sup>2</sup> See F. K. Richtmyer and E. H. Kennard, "Introduction to Modern Physics," 3d ed., p. 452, McGraw-Hill Book Company, Inc., New York, 1942.

<sup>3</sup> For tables, see R. W. James and G. W. Brindley, *Phil Mag.*, **12**, 81 (1931).

<sup>4</sup> I. Waller, Uppsala dissertation, 1925; *Z. Physik*, **17**, 398 (1923).

satisfied for a prominent set of planes such as the (100) planes, for example, a diffracted beam will be present. Under these conditions, the intensity of the primary beam entering the crystal diminishes with its depth of penetration owing to two effects. (1) Ordinary absorption. (2) The part of the beam that is diffracted at each succeeding (100) plane is subtracted from the primary beam. This second effect is called "primary extinction." As a result of it, the ordinary linear absorption coefficient  $\mu_l$  must be added to a second quantity called the "primary extinction coefficient"  $\mu_e$ , which may be as much as seventy times  $\mu_l$ . When one recalls that these "coefficients" are exponents in the intensity equations such as (5-5) and (5-7), it will be realized that this is a tremendous increase. For this reason, the diffraction is limited more to the surface layers of the crystal than one might suppose, judging merely from the fact that x-rays have great power to penetrate matter. It has been calculated that, when molybdenum  $K_\alpha$  rays are diffracted in the first order from the face of a good calcite crystal, the primary beam drops to half its incident intensity after penetrating to a depth of only about  $5 \times 10^{-5}$  cm.

Compton and Allison give<sup>1</sup> a formula for calculating the extinction coefficient  $\mu_e$ . It is

$$\mu_e = \frac{4\pi\delta F(hkl)}{Y\lambda \sin \theta_0} \quad (16-43)$$

where  $\delta$  is 1 minus the index of refraction of the rays used, in the crystal used;  $F(hkl)$  is the crystal-structure factor for the reflection concerned at the wave length  $\lambda$  used;  $Y$  is the number of electrons in a unit cell of the crystal; and  $\theta_0$  is the Bragg angle at which the diffraction occurs.

Secondary extinction is concerned with the mosaic blocks to be discussed in the next section. When some of these blocks near the surface of the crystal have exactly the right orientation to diffract the primary x-ray beam, they will screen the deeper blocks from the incident rays. This effect is called "secondary extinction."

When extinction is considered, it may introduce some changes into equations of the type of (16-37) and (16-38). These two equations, as they stand, are for "ideally imperfect crystals," that is, for crystals having very small mosaic blocks. Most actual crystals have a mosaic structure approximating this.

**16. The Mosaic Structure of Crystals.** Thus far in the discussion, crystals have been regarded as "perfect" in the sense that the lattice has been considered as a perfect geometrical structure of absolutely parallel, exactly equidistant planes of scattering centers. Actual crystals are not perfect in this sense. The investigation of the degree of imper-

<sup>1</sup> See p. 393 in the book cited in footnote 1, p. 357.

fection of various real crystals and the comparison of the perfection of crystals of one kind (for example, calcite) with that of crystals of another kind (for example, rock salt) were undertaken by various workers beginning about 1914.

One of the most successful plans of attack on this problem has been to measure the integrated reflections  $R(hkl)$  for various crystals experimentally, with a double-crystal spectrometer, and then compare them with the corresponding values of  $R$  calculated on the assumption that the crystals are perfect. Such calculations<sup>1</sup> are based on the theory developed by Darwin<sup>2</sup> and, later, Ewald.<sup>3</sup> Compton and Allison have derived the following simplified formula<sup>4</sup> for  $R(hkl)$ :

$$R(hkl) = \frac{8F(hkl)\delta(1 + \cos 2\theta_0)}{3Y \sin 2\theta_0} \quad (16-44)$$

where the symbols have the same meanings as in equation (16-43). Note that  $F(hkl)$  enters linearly for a perfect crystal, rather than quadratically, as in (16-37) and (16-38). For first-order diffraction of molybdenum  $K_{\alpha_1}$  by the cleavage planes of calcite, Compton and Allison suggest  $F = 51.6$ ,  $\delta = 1.82 \times 10^{-6}$ ,  $Y = 100$ , and  $\theta_0 = 6^\circ 42'$ . Thus equations of the type of (16-44) yield  $R$  values of  $2.2 \times 10^{-5}$  and  $2.13 \times 10^{-5}$ , respectively, for molybdenum  $K_{\alpha_1}$  in rock salt and calcite, whereas, experimentally,  $R$ , as defined by (16-35) is about  $4 \times 10^{-4}$  for rock salt and  $2 \times 10^{-5}$  for calcite.<sup>1</sup>

Darwin's theory also indicates that if a rock-salt crystal were perfect a truly monochromatic beam of parallel x-rays of wave length about 0.6 Å., striking a cleavage face of the crystal at the correct angle, should produce a first-order diffracted beam with a maximum angle of about 3 sec. of arc between the most divergent rays in it. Experimentally it has been found that the width varies from 87 sec. to several minutes for silver  $K_{\alpha}$  radiation (558 X.U.) for different rock-salt crystals, 5 min being a representative value for a good crystal.

To summarize: (1)  $R$  is observed to exceed its theoretical value (2) the excess is much greater for rock salt than for calcite; (3) the divergences of beams diffracted from single crystals exceed the theoretical values. These three facts may be explained on the grounds that single crystals actually have an imperfect structure, as suggested by Darwin in 1914.

<sup>1</sup> See, for example, S. K. Allison, *Phys. Rev.*, **41**, 1 (1932).

<sup>2</sup> C. G. Darwin, *Phil. Mag.*, **27**, 325, 675 (1914).

<sup>3</sup> See p. P. Ewald, *Physik Z.*, **26**, 29 (1925).

<sup>4</sup> See p. 397 in the book cited in footnote 1, page 357.

<sup>5</sup> See, for example, P. Kirkpatrick and P. A. Ross, *Phys. Rev.*, **43**, 596 (1933).

The modern theory visualizes a real crystal as being built up of a large number of microscopic or submicroscopic fragments or blocks, all having almost, but not quite, the same orientation. These fragments may be thought of as irregular in shape but in general roughly resembling a cube. The order of magnitude of the cube edge is about  $10^{-5}$  cm. These ideas are ordinarily designated as the theory of the "mosaic" structure of crystals. Zwicky has done considerable work<sup>1</sup> on the physical properties of solids, as influenced by their mosaic structure. It is not very difficult to see, in a qualitative way, how a mosaic structure can account for the three facts mentioned in the preceding paragraph.

If the blocks are regarded as having a nearly perfect lattice structure, then each one will "reflect" practically 100 per cent of a parallel primary monochromatic x-ray beam striking it at exactly the correct angle  $\theta_0$  satisfying Bragg's law. Such a primary beam will therefore penetrate an actual crystal, selecting perhaps 1,000 blocks that have exactly the right orientation to reflect it. If the crystal is rotated a few seconds of arc, the 1,000 blocks all take on the wrong orientation but about 1,000 others then have the right one. This makes the total beam diffracted from a crystal rocked slightly to either side of  $\theta_0$  carry more energy than if the crystal were perfect. A perfect crystal would consist of only one mosaic block, and primary extinction would limit the diffraction to a thin surface layer, effective at only exactly the right angle. One would also expect greater divergence of the rays in the diffracted beam from a mosaic structure than from a perfect crystal. The greater discrepancy between theory (of perfect crystals) and experiment for rock salt than for calcite indicates that rock-salt crystals are more imperfect than calcite crystals. That is, the rock-salt mosaic blocks have a greater variety of orientations and are probably smaller and more numerous than those in calcite, on the average. Calcite has about the same dispersive power as rock salt; but, in general, the degree of imperfection in rock-salt crystals is such that the resolution of an x-ray spectrometer or spectrograph with a rock-salt crystal is no better in the higher order spectra ( $n$  greater than 1) than it is in the first order, because of the decrease in the sharpness of the lines as  $n$  increases. Good calcite crystals being more easily obtained, they are preferred for high-accuracy spectrographic work. A freshly cleft crystal surface is more perfect than the same surface after polishing. Polishing apparently cracks up the surface layers of the crystal into more fragments than were originally present. This manifests itself experimentally by a considerable increase in the measured value of  $R$ .

**17. Twinning.** Twinning is a phenomenon that sometimes causes one to misinterpret the true structure of a crystal. Certain crystals

<sup>1</sup> See, for example, F. Zwicky, *Rev. Modern Phys.*, **6**, 193 (1934).



such as aragonite and quartz frequently develop in a normal manner for part of their length, and then at a certain plane the orientation of the lattice changes discontinuously so that on opposite sides of the plane the crystal axes are not parallel. Quartz has enantiomorphic (right- and left-handed) varieties. One common type of twinning in quartz involves an end-to-end junction of two right-handed individuals, each being rotated  $180^\circ$  about its threefold ( $C$ ) axis with respect to the other, the common axis being called the "twinning axis" in this case. In "Brazilian" twinning, right- and left-handed individuals unite along a plane of reflection (the twinning plane) parallel to the  $C$  axis; there are other, less common types. Aragonite is an orthorhombic crystalline form of  $\text{CaCO}_3$  that is very prone to twinning<sup>1</sup> across the (110) plane. Twinning is also very common in some metallic crystals, such as zinc.

It is not always easy to detect a twinned crystal if its untwinned form is unknown, for many twinned crystals look like a single crystal of higher symmetry. This has led to erroneous determinations of the structure of some substances.

### QUESTIONS AND PROBLEMS

1. A beam of soft x-rays passes through some hydrogen gas under high pressure. Will most of the scattering of the rays occur at the protons or at the electrons? If the amplitude of the electric vector in the primary beam  $AO$  at a point  $O$  is  $E_0$ , what is the corresponding x-ray intensity  $I_0$  at that point? What are the direction and magnitude of the accompanying magnetic vector at that point? If a point  $P$  is selected a distance  $r$  cm. from  $O$ , what is the amplitude at  $P$  of the x-rays coherently scattered by an electron at  $O$ , assuming an unpolarized primary beam? Answer the same question if the primary beam is polarized with its magnetic vector in the plane  $AOP$ . Does modern wave mechanics give a different answer to this last question than classical physics? What is the polarization factor, and how does it arise?

2. By what argument does classical physics conclude that coherently scattered rays from an atom might have an intensity proportional to the atomic number  $Z$  of the atom? That this intensity might, on the other hand, be proportional to  $Z^2$ ? Does x-ray diffraction result primarily from interference between coherently or incoherently scattered rays?

3. Describe a Bragg spectrometer. How is it modified to make a double-crystal spectrometer? Is the high resolution of the latter instrument achieved only by a serious sacrifice of sensitivity and speed, as compared with the simple Bragg instrument? Explain your answer. In using a Bragg spectrometer in the Bragg method of crystal analysis, does one obtain and study x-ray spectra, in the usual sense of the word?

4. What are the two crystals most commonly used in x-ray spectroscopy? Which is ordinarily used in the Bragg method of crystal analysis, as applied to copper sulfate, for example, or is either used? What is an x-unit? Why might one wish to multiply all the wave lengths in a table of characteristic x-ray spectra by 1.00203? How does this figure arise? How are absolute (not relative) values of x-ray wave lengths calculated in the first place?

<sup>1</sup> W. L. Bragg, *Proc. Roy. Soc. (London) A*, **105**, 37 (1924).

5. A certain crystal is composed of a compound of two chemical elements  $A$  and  $B$ . If the Bragg reflections from a particular face of this crystal occur at a series of angles  $\theta$  corresponding to  $d$  values proportional to  $1, \frac{1}{2}, \frac{1}{3}$ , etc., when  $n$  is set equal to 1, and if the intensities of these reflections decrease in a uniform manner with increasing  $\theta$ , should you conclude that the individual planes in this set are populated by (1)  $A$  atoms alone, (2)  $B$  atoms alone, or (3) both  $A$  and  $B$  atoms in each plane? Explain your answer.

6. Why is a (111) reflection found for NaCl but not KCl? Explain from Fig. 16-11 why there is no (222) reflection from a diamond crystal. In a crystal composed of only one chemical element, how can one distinguish between simple lattices, body-centered lattices, end-centered lattices, etc.? What are suppressed reflections? Some crystallographers refer to these by what term? How does one know where to expect reflections from a simple orthorhombic lattice, for example?

7. What are parameters in the unit-cell configuration? What is the unit-cell configuration of rock salt? Why is the use of parameters often necessary? The letter  $\omega$  is frequently used to designate the angle between rhombohedral axes. Why? Explain how a hexagonal point lattice can be referred to rhombohedral axes.

8. What is the atomic-structure factor? Why does the coherent x-ray scattering from an atom decrease with angle faster than that from an electron, on the basis of classical physics? The atomic number of mercury is 80. Without consulting tables, what is its atomic-structure factor for a very small scattering angle? Does the atomic-structure factor increase or decrease with temperature? Why?

9. What is the crystal-structure factor? Why is it often written  $F(hkl)$  rather than simply  $F$ ? If the atomic-structure factor of tungsten is  $f_W$  and if it crystallizes with a body-centered cubic structure having unit-cell configuration  $000; \frac{1}{2}\frac{1}{2}\frac{1}{2}$ , calculate its crystal-structure factor for the (110), (111), and (112) reflections.

10. For a body-centered cubic structure of a single element, show that all  $(hkl)$  reflections will be suppressed for which  $k + k + l$  is odd.

11. What is meant by integrated reflection, or coefficient of reflection  $R(hkl)$ ? Why is its calculated value less than its experimental value in some cases? Is  $R(hkl)$  proportional to the structure factor or the square of the structure factor for an actual mosaic crystal? For a perfect crystal?

12. Describe Bragg's x-ray microscope. What is the order of magnitude of the magnification attainable with it? Explain in a general way how contour maps like those in Fig. 16-16 are obtained. What do the lines in these maps represent?

13. What is the evidence for the existence of a mosaic structure of crystals? What is the order of magnitude of the size of the mosaic blocks? About how deeply into a calcite crystal does a primary molybdenum  $K\alpha$  x-ray beam penetrate when the crystal is oriented correctly for first-order diffraction at the cleavage face? Why is the penetration so slight? What is primary extinction? Secondary extinction?

14. In general, how much leeway is there in the angular setting  $\theta$  of an actual crystal for diffraction to occur, assuming that the correct value of  $\theta$  to satisfy Bragg's law is  $\theta_0$ ? When the primary beam is incident at the proper angle  $\theta_0$ , what is the order of magnitude of the divergence of the most divergent rays in the diffracted beam? Why is there any divergence whatever?

15. What is meant by twinning? Is there only one kind? Why may it be difficult to recognize twinning when one sees it? If one fails to recognize it, will he nevertheless arrive at a correct determination of the crystal structure by x-ray methods applicable to single crystals?

## CHAPTER 17

### THE LAUE METHOD, THE ROTATION METHOD, AND OTHER METHODS FOR A SINGLE CRYSTAL

**1. Introduction.** It is not expected that the average reader of this book will have need for carrying through the analysis of a particular crystal by the Bragg method, the Laue method, or the rotating-crystal method. Most practical applications of x-ray diffraction are limited to the powder method, for most actual solids consist of myriads of microscopic crystals. The main reason for studying crystal analysis in the sense used thus far is to acquire a fair understanding of the mechanism of x-ray diffraction, methods of calculating lattice constants and measuring x-ray wave-lengths, the significance of the intensities of the diffracted beams, the meaning and value of the concept of a "structure factor," the meaning of extinction, and a knowledge of the mosaic structure of crystals. A study of the Laue and rotation methods will introduce additional useful ideas, such as the concept of the reciprocal lattice. Then, too, single crystal methods are demanded in such industrial problems as the proper orientation of diamonds in dies, the orientation of artificial sapphires in jeweled pivot bearings, and the cutting of quartz crystal sections for piezoelectric oscillators in radio work. Therefore a general knowledge of these methods is most helpful, even in routine industrial work.

So far as the actual analysis of crystals is concerned, it should again be mentioned that optical, chemical, and other physical data are helpful and often necessary to help one to choose between two or three tentative possible structures, any one of which would produce the observed diffraction pattern.

**2. The Laue Method of Crystal Analysis.** Although this is the oldest method of crystal analysis by x-rays, it is still used today by some of the foremost crystal analysts, such as Wyckoff.<sup>1</sup> It was developed by Laue soon after his discovery of x-ray diffraction in 1912. The method uses continuous (heterogeneous) x-rays such as are radiated from a tungsten tube operating at a potential slightly less than the 69.3-kv. K excitation potential for tungsten. These rays are collimated into a fine beam of nearly parallel rays by collinear pinholes in three consecutive lead diaphragms *A*, *B*, and *C*, as indicated in Fig. 17-1. For ordinary work,

<sup>1</sup> Footnote, p. 346.

*A* and *B* are both about 0.025 in. in diameter and 2 in. apart. When extreme accuracy is more important than speed, holes as small as 0.005 in. may be used. When speed is the paramount requirement, 0.040-in. holes may be used. The third pinhole *C* is large enough so that all the direct rays transmitted by the first two, *A* and *B*, will pass through it yet small enough so that rays scattered or diffracted at a small angle by the lead edges of pinhole *B* will be intercepted by *C*. Often *B* and *C*

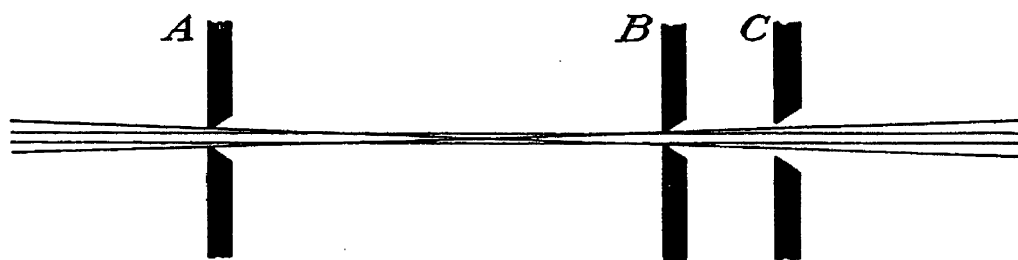


FIG. 17-1.—Slit or pinhole system for collimating x-rays.

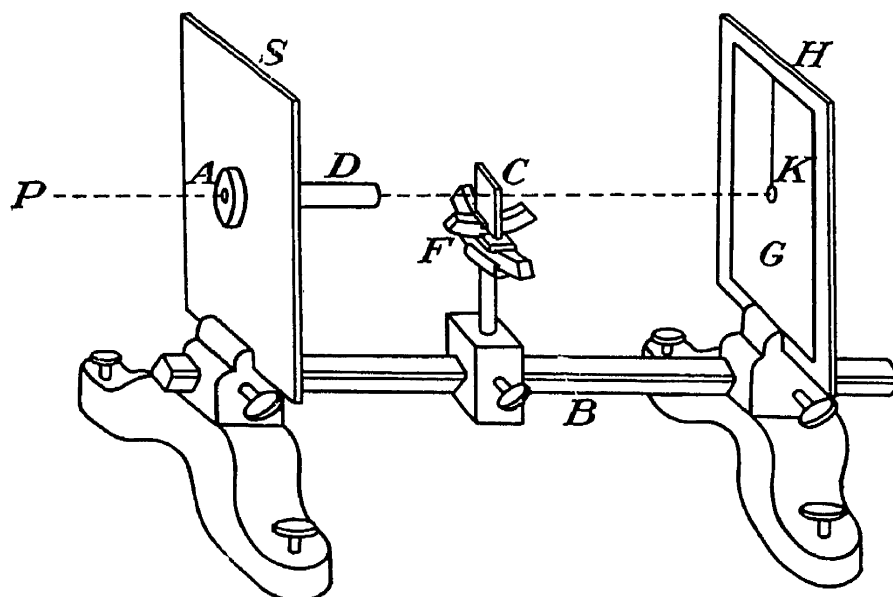


FIG. 17-2.—Laue camera.

are constructed and regarded as a single unit, called a “guarded pinhole” or “pinhole assembly.”

Figure 17-2 illustrates a simple type of “Laue camera.” The framework, or bench, *B* supports a screen *S*, which is placed as close as possible to the x-ray tube in such a position that the focal spot is located at a point *P* on the straight line *PACK*. *D* is the collimating pinhole assembly of Fig. 17-1. The first pinhole is represented by *A* in both figures. Two or three interchangeable pinhole assemblies with different hole sizes are ordinarily provided. *F* is a holder so constructed that it may be adjusted to support the thin single crystal *C* as close to *D* as practical and in the desired orientation. This is conveniently accomplished by mounting the crystal, or crystal section, by means of a drop of paraffin or balsam on two adjustable “goniometer arcs” perpendicular to each

other. One of these permits a limited adjustment of the crystal by rotation about an east-west axis, say, and the other about a north-south axis. These arcs may be seen in Fig. 17-2. Most of the heterogeneous primary x-ray beam traverses the crystal without being absorbed, scattered, or diffracted. Then it travels usually either 4 or 5 cm. to the small lead block or cup  $K$  at the center of the x-ray film protected by the black paper  $G$ , the film being supported perpendicularly to  $PACK$  by the holder  $H$ . The cup  $K$  absorbs the primary beam, which would otherwise cause a splotch on the film due to scattering and halation. This cup  $K$  should be moved aside for a few seconds at the end of the exposure, which may last 5 min. to several hours, in order to mark the primary beam position on the plate.

The chief resemblance between Bragg reflection and ordinary reflection is that the angle of incidence equals the angle of reflection as with light striking a mirror. In the present case, rays from about 0.2 to 2 Å. are present; therefore, for practically all the important sets of planes in the crystal and for all values of the angle  $\theta$  except very small ones, this mirrorlike reflection should occur, the diffracted rays being monochromatic radiation selected from the continuous primary beam.

Suppose that an important zone axis in the crystal, like  $[100]$ , for example, is parallel to the primary beam. Then the planes in that zone, such as  $(001)$ ,  $(010)$ ,  $(011)$ ,  $(012)$ , are all parallel to the beam and can reflect no rays, since  $\theta = 0$ . However, there will be other zone axes, perhaps  $[311]$ ,  $[512]$ , etc., two, three, four, six, or eight of which will be inclined at some specific angle, such as  $17^\circ 29'$ , to the  $[100]$  axis and hence to the primary beam. As an example, in Fig. 17-3, the primary beam may be regarded as originating at the focal spot  $X$ , passing through the collimating pinholes  $H_1H_2H_3$ , after which it passes through the hexagonal crystal  $I'J'K'L'M'N'I''J''K''L''M''N''$  in a direction parallel to  $[001]$ , or the  $C$  axis  $OC$ . After emerging from the crystal, the primary beam continues to the flat film  $DEFG$ , which it strikes perpendicularly at  $C$ . In this case, one notes the six zone axes  $I'OL''$   $[011]$ ,  $N'OK''$   $[111]$ ,  $M'OJ''$   $[101]$ ,  $L'OI''$   $[0\bar{1}1]$ ,  $K'ON''$   $[\bar{1}11]$ , and  $J'OM''$   $[\bar{1}01]$ , all equally inclined to the  $C$  axis  $[001]$ . Concentrating attention on one of these zone axes for the moment, namely,  $I'OL''$   $[011]$ , one notes several prominent planes belonging to its zone, such as  $I'J'L''M''$   $(1\bar{1}01)$ ,  $N'I'K''L''$   $(0\bar{1}11)$ ,  $JNK''M''$   $(1\bar{2}12)$ , and  $I'L'L''I''$   $(10\bar{1}0)$ . Considering the first-mentioned plane in this zone, namely,  $I'J'L''M''$   $(1\bar{1}01)$ , one next erects its gnomon, or gnomonic line,  $OP$ . This is simply the perpendicular to the plane at the origin  $O$ . Since all the planes in this zone contain the zone axis  $OL''Q$ , all their gnomons will be perpendicular to  $OQ$ . Therefore all the gnomons for this zone (or any zone) lie in a plane through  $O$  perpendicular to the zone axis. Since planes intersect each other in

straight lines, it follows that the gnomons for each zone will intersect the plane of projection  $DEFG$  in a series of points such as  $P$ , and these gnomonic points will lie on straight lines in the plane of projection.

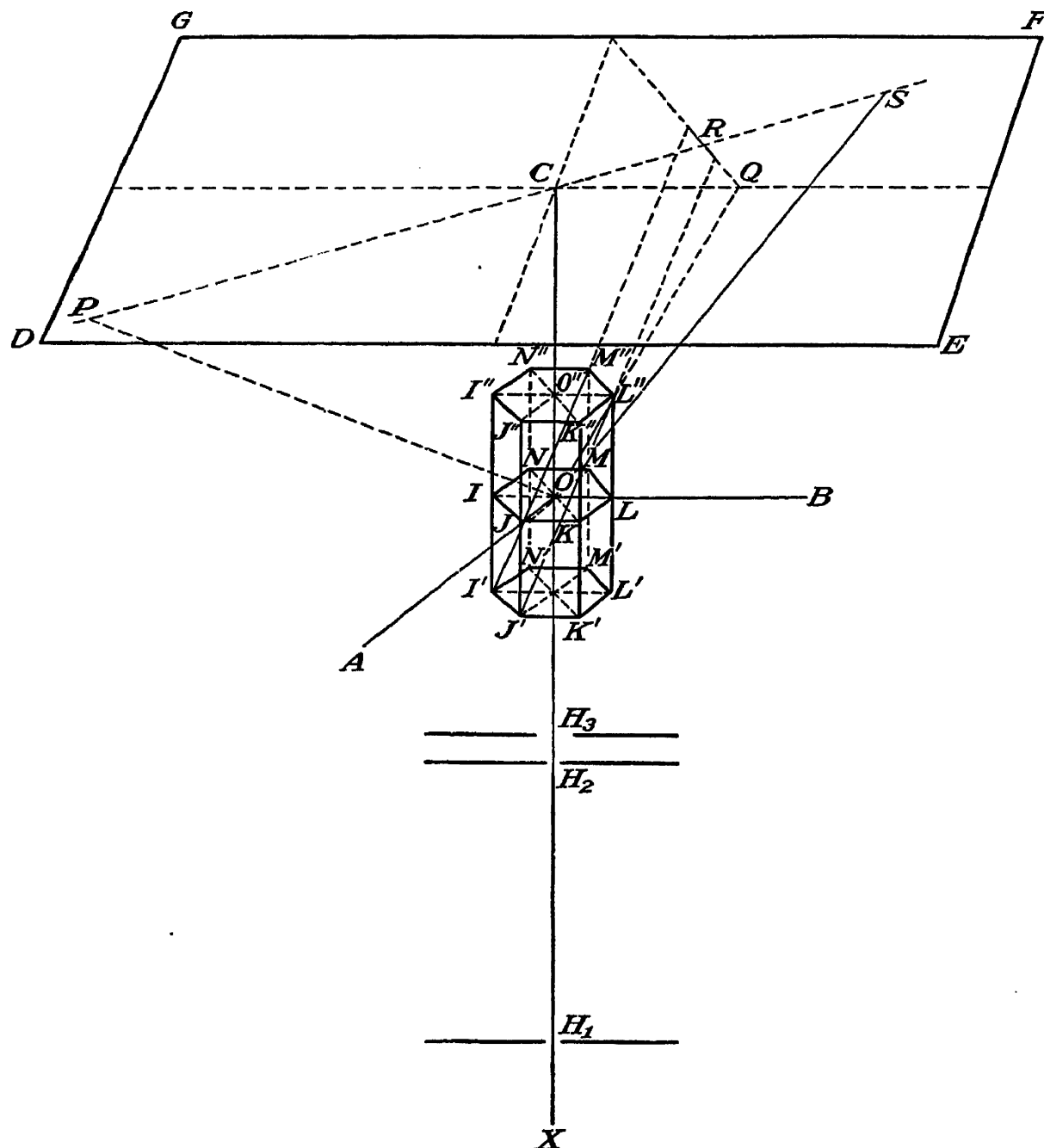


FIG. 17-3.—Illustrating analysis of Laue patterns by gnomonic projection.

If, as thus far supposed, an important zone axis coincides with the primary beam, the resulting diffraction pattern on the film will be symmetrical. Otherwise, the pattern will appear asymmetrical or distorted. In the former case, the symmetry of the pattern will depend upon the symmetry of the crystal. If it is hexagonal, as in Fig. 17-3, angle  $AOB$  will be  $120^\circ$  but angles  $AOC$  and  $BOC$  will be  $90^\circ$ , the unit of length  $OO''$  along  $OC$  will be different from those ( $OJ$  and  $OL$ ) along  $OA$  or  $OB$ , but

the latter two will be equal. The distance  $OC$  from crystal to film or plane of projection is usually set at either 4 or 5 cm.; let us assume 5 cm. in the present example.

The  $(1\bar{1}01)$  plane  $I'J'L''M''$  in Fig. 17-3 may be extended to the plane  $DEFG$ ,  $RQ$  being the intersecting line. If the spacing of these  $(1\bar{1}01)$  planes is  $d$ , there will be some x-rays in the heterogeneous primary beam having a wave length  $\lambda$  of the proper value to satisfy Bragg's law and some of these will be diffracted in the direction  $OS$ , forming a "Laue spot"  $S$  on the plate  $DEFG$ . The gnomonic line  $OP$  for these planes intersects the plane of the plate or the plane of projection at the point  $P$ . The equation of an arbitrary plane, such as  $I'J'L''M''$  referred to the crystallographic axes  $OA$ ,  $OB$ , and  $OC$ , is

$$\frac{x}{A} + \frac{y}{B} + \frac{z}{C} = 1 \quad (17-1)$$

from analytic geometry, where  $A$ ,  $B$ , and  $C$  are the intercepts of the plane on the three axes and  $x$ ,  $y$ , and  $z$  are the coordinates of any point in the plane,  $x$  being measured along  $OA$ ,  $y$  along  $OB$ , and  $z$  along  $OC$  and the units of length being  $a$ ,  $b$ , and  $c$ , which may be unequal. If the Miller indices of the plane in question ( $I'J'L''M''$  in this case) are  $(hkl)$ , then by definition

$$A = \frac{g}{h}, \quad B = \frac{g}{k}, \quad C = \frac{g}{l} \quad (17-2)$$

where  $g$  is a constant. For example, if  $A = 1$ ,  $B = \frac{3}{2}$ , and  $C = \frac{1}{2}$ , then  $h = 3$ ,  $k = 2$ , and  $l = 6$ ; in this case,  $g = 3$ . Hence the equation of the plane becomes

$$hx + ky + lz - g = 0 \quad (17-3)$$

The equations of the gnomonic line to such a plane are, from analytic geometry,

$$\frac{x}{h} = \frac{y}{k} = \frac{z}{l} \quad (17-4)$$

The equation of the plane of projection is of course  $z = D$ , where  $D = OC$  in the figure, usually 5 cm. The coordinates of the point  $P$ , where the gnomon strikes the plane of projection, are then given by

$$\frac{x}{h} = \frac{y}{k} = \frac{D}{l} \quad (17-5)$$

where  $x$  and  $y$  are still measured in units of  $a$  and  $b$ . Changing to centimeters,

$$x = h \frac{Da}{cl} \quad y = k \frac{Db}{cl} \quad z = D \quad (17-6)$$

Suppose, for a moment, that  $l = 1$  and that  $h$  and  $k$  have a series of (integral, of course) values from perhaps  $-5$  to  $+5$ . It is then seen that the points  $P$  from all these various sets of planes [such as  $(\bar{5}31)$ ,  $(401)$ ,  $(001)$ ,  $(301)$ ,  $(521)$ ] will form a two-dimensional lattice of points in the plane  $DEFG$ , because equations (17-6) show that the coordinates—

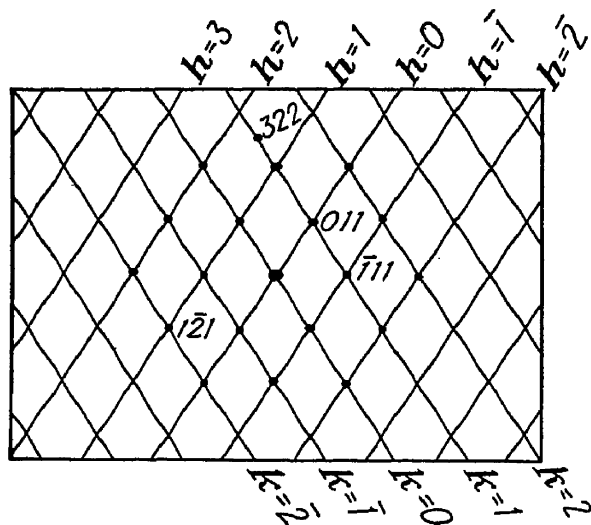


FIG. 17-4.—Gnomonic projection of Laue pattern of a hexagonal crystal. (R. W. G. Wyckoff, "The Structure of Crystals," 1931; courtesy of Reinhold Publishing Corporation.)

both  $x$  and  $y$ —of these points  $P$  will be  $-5Da/c$ ,  $-4Da/c$ ,  $-3Da/c$ ,  $-2Da/c$ ,  $-Da/c$ ,  $0$ ,  $Da/c$ ,  $2Da/c$ ,  $3Da/c$ ,  $4Da/c$ ,  $5Da/c$ , etc.,  $b$  being substituted for  $a$  for the  $y$  coordinates. However, if  $l = 2$ , then the coordinates of the gnomonic point  $P$  for a plane like  $(432)$  will be  $x = 2Da/c$ ,  $y = \frac{3}{2}Db/c$ . This array of gnomonic points is called a "gnomonic projection." Figure 17-4 illustrates the coordinate system that would be used to identify the points appearing in a gnomonic projection of the Laue pattern of a hexagonal or rhombohedral crystal on a plane perpendicular to the  $C$  axis, as just assumed.

The identification of the sets of planes corresponding to the various Laue spots is seen to be a rather simple straightforward process, once the gnomonic projection is complete. Since the  $(\bar{h}kl)$  planes are parallel to the  $(hkl)$  planes, the Laue pattern always has a center of symmetry, whether the crystal has or not. This fact is known as "Friedel's law." Consequently  $T_d$  and all the  $O$  groups of cubic crystals yield patterns exhibiting  $O_h$  symmetry. Likewise cubic groups  $T$  and  $T_h$  yield a pattern having  $T_h$  symmetry. In the hexagonal system, all the  $D$  groups in the hexagonal division and  $C_{6v}$  yield patterns with  $D_{6h}$  symmetry, while the other  $C$  groups yield  $C_{6h}$  patterns. In the rhombohedral division, all  $D$  groups and  $C_{3v}$  yield  $D_{3d}$  patterns, the other  $C$  groups yielding  $C_{3i}$  patterns. In the tetragonal system,  $V_d$ ,  $C_{4v}$ ,  $D_4$  and  $D_{4h}$  yield patterns characteristic of  $D_{4h}$ , while  $S_4$ ,  $C_4$ , and  $C_{4h}$  yield  $C_{4h}$  patterns. All orthorhombic crystals yield patterns characteristic of  $V_h$  groups; all monoclinic,  $C_{2h}$ ; all triclinic,  $C_i$ . A serious shortcoming of the Laue method is that the intensities of the spots depend not only upon the structure of the crystal but also upon other extraneous factors hard to evaluate, such as the intensity at various wave lengths in the continuous x-ray spectrum, superposition of first-, second-, and third-order diffraction spots, and variation of photographic effect at wave lengths above and below the K absorption edges of silver and bromine (see page 74).



The gnomonic projection may be laid out from the Laue pattern by using a specially calibrated rule, often called a "Wyckoff scale," after R. W. G. Wyckoff. The basis of this method may be understood from Fig. 17-3. Since angle  $COR = \theta = \text{angle } ROS$  and therefore angle  $COS = 2\theta$ , it is seen that  $CS = D \tan 2\theta$  and  $CP = D \tan COP$  or  $D \tan (90^\circ - \theta)$ , where  $D = OC$ . Hence, if  $CS$  and  $D$  are known,  $CP$  may be immediately calculated. Since  $SCP$  is a straight line, one may

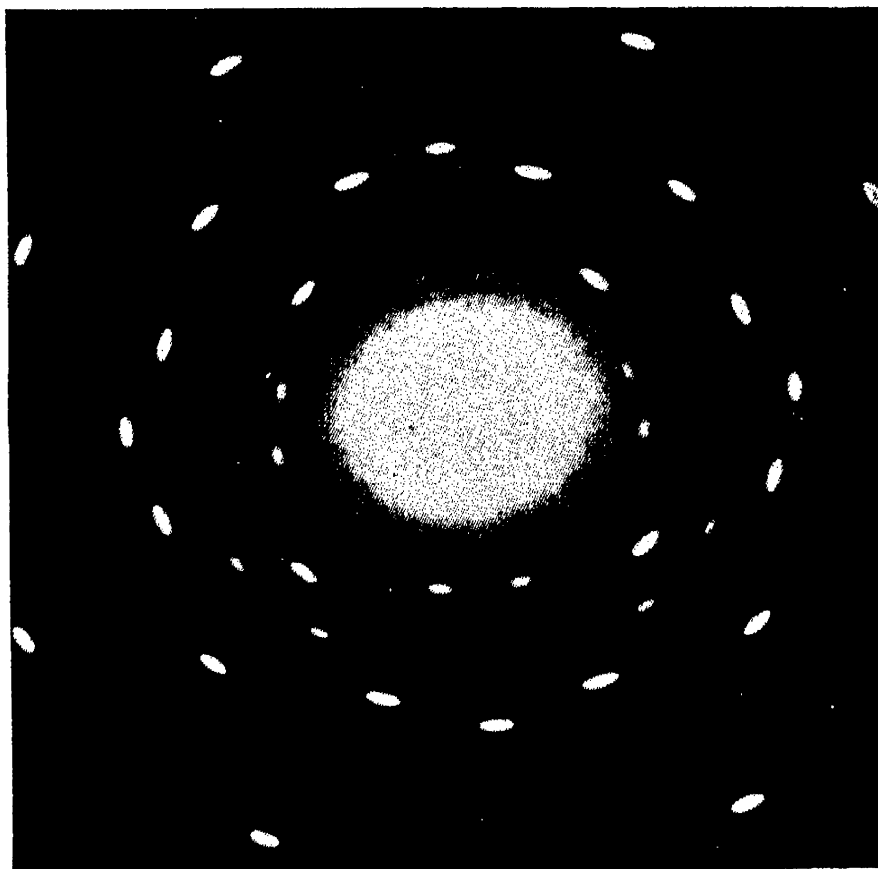


FIG. 17-5a.—Laue pattern of magnesium oxide crystal. (R. W. G. Wyckoff, "The Structure of Crystals," 1931; courtesy of Reinhold Publishing Corporation.)

pivot a rule at  $C$  by means of a thumbtack and lay off scales on the rule on each side of this pivot such that a Laue spot appearing at 5.2 divisions on one scale corresponds to a gnomonic point which may be marked on a piece of paper at 5.2 divisions on the other scale<sup>1</sup> on the opposite side of  $C$ . A reproduction of the Laue photograph may be tacked on top of a large piece of paper on a drawing board in order to lay out the gnomonic projection by this method. A Laue photograph of a cubic crystal of magnesium oxide obtained by Wyckoff is shown in Fig. 17-5a, the incident beam being perpendicular to a cube face. Figure 17-5b shows the reduced-size reproduction of the pattern in the small central circle, surrounded by its gnomonic projection on a plane perpendicular

<sup>1</sup> Wyckoff gives a table for calibrating such a rule on page 131 of his book, "The Structure of Crystals," 2d ed., Reinhold Publishing Corporation, New York, 1931.

to the  $C$  axis, as laid out by Wyckoff. Laue analyses are sometimes carried out by means of a different type of projection, called the "stereographic projection," but the gnomonic projection is more commonly and successfully used in most cases.

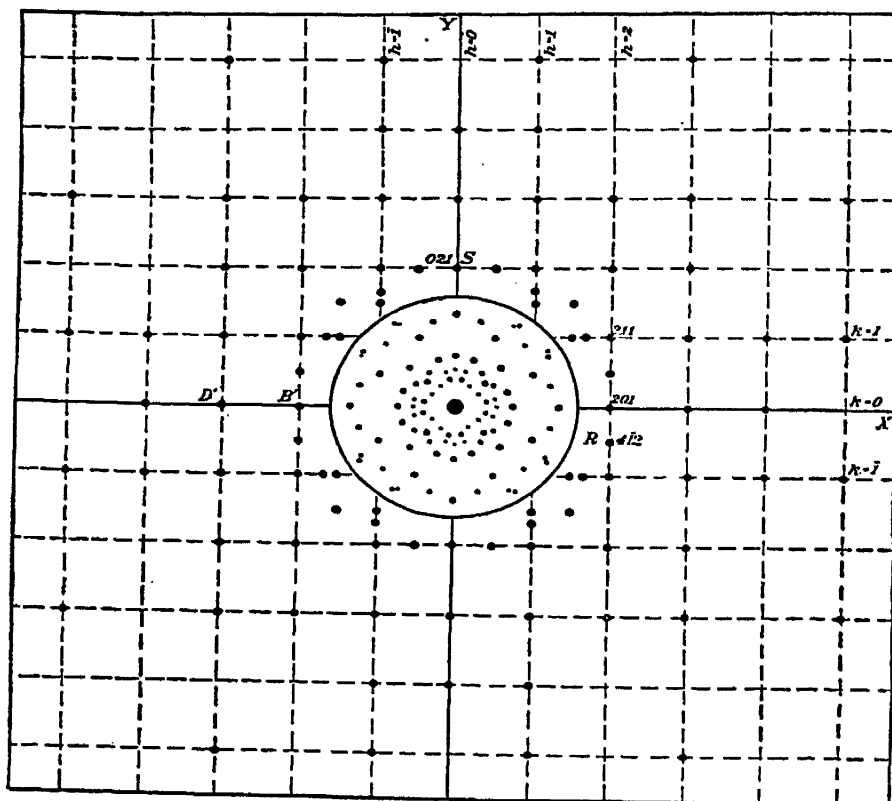


FIG. 17-5b. <sup>2</sup>Gnomonic projection of pattern in Fig. 17-5a. (R. W. G. Wyckoff, "The Structure of Crystals," 1931; courtesy of Reinhold Publishing Corporation.)

**3. The Rotating-crystal Method of Crystal Analysis.** This method has been used in the crystal analysis of more different substances than any other method. The first rotation-type x-ray pattern published was obtained in 1913 by M. de Broglie,<sup>1</sup> but he used it to study the x-ray spectrum of the platinum anticathode rather than the structure of the (rock-salt) crystal. In 1919, Seemann<sup>2</sup> used rotation diagrams to study crystal structure, but the development of a formal method of crystal analysis from rotation patterns was not accomplished until the work of Rinne and Schiebold<sup>3</sup> and Polanyi<sup>4</sup> in 1921.

The experimental procedure followed in obtaining a rotation pattern differs from that for the Laue pattern in the following particulars: (1) Monochromatic x-rays are used rather than polychromatic. (2)

<sup>1</sup> M. de Broglie, *Compt. rend.*, **158**, 177 (1914), Fig. 1.

<sup>2</sup> H. Seemann, *Physik Z.*, **20**, 55, 169 (1919).

<sup>3</sup> F. Rinne and E. Schiebold, *Abhandl. math.-phys. Klasse sächs. Akad. Wiss.*, **38**, 3 (1921).

<sup>4</sup> M. Polanyi, *Naturwissenschaften*, **9**, 337 (1921). See also *Z. Physik*, **7**, 149 (1921); M. Polanyi and K. Weissenberg, *Z. Physik*, **9**, 123 (1922), **10**, 44 (1922).

Although pinholes are usual, short vertical slits are sometimes used for collimation. (3) The crystal specimen is ordinarily only a fraction of a millimeter in diameter, whereas larger crystals or cut and ground sections are preferred in the Laue method. (4) The pattern is usually recorded on a photographic film supported by a holder that retains the film on the inner surface of a cylinder having a vertical axis through the center of the crystal, which is of course in line with the pinholes. As in the Laue method, a flat plate behind the crystal and perpendicular to the primary

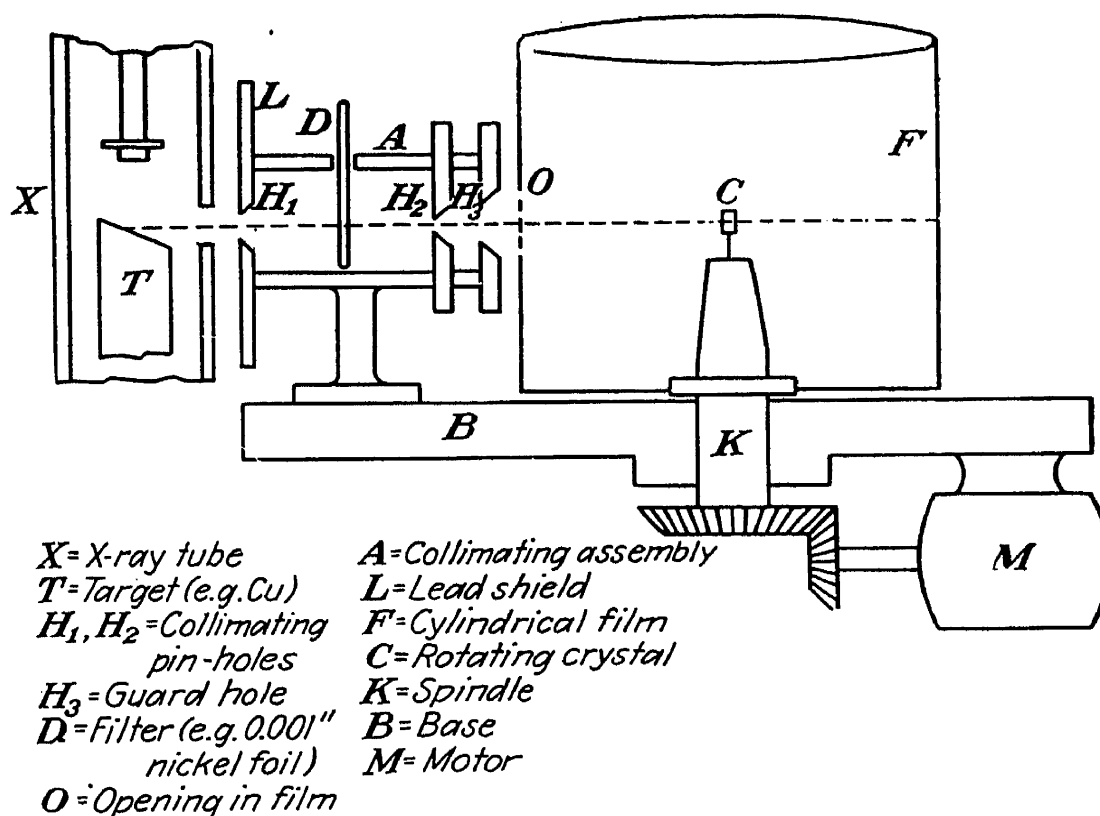


FIG. 17-6.—Diagram of rotation camera. (Adapted from "X-ray Crystallography," by M. J. Buerger, 1942; courtesy of John Wiley & Sons, Inc.)

beam is sometimes used, although the cylindrical film is preferable for most work. (5) The crystal is rotated at a uniform angular velocity, about the vertical axis through its center; alternatively, it may be given an oscillatory rotation about this axis, the angle of the oscillation usually being fixed at about 5, 10, or 15° and the angular velocity of the oscillation being constant between reversals. In the Laue method, the crystal does not move. (6) It is desirable to have an important zone axis of the crystal coinciding with the axis of its rotation, rather than with the axis of the beam, as in the Laue method.

Figure 17-6 is a schematic diagram of a "rotation camera," showing the essential parts. The filter *D* should be 0.001-in. nickel foil if the target *T* is copper; a zirconium oxide filter is usual with molybdenum radiation. However, if no filter is used, the pattern obtained from the  $K_{\alpha}$  and  $K_{\beta}$  radiation combined is not too confusing to analyze, for the

beta and alpha spots appear in separate layer lines except for the equatorial layer, where they are superposed. The nature of these layer lines will be explained later. If the crystal is to be oscillated rather than

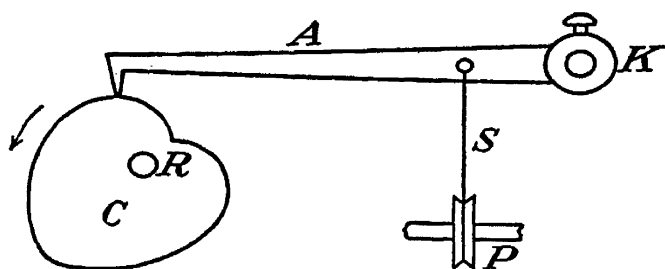


FIG. 17-7.—Heart-shaped cam for oscillating specimen. *A*, arm. *C*, heart-shaped cam having radius proportional to angular displacement. *K*, spindle supporting crystal or specimen. *R*, camshaft, motor-driven at low speed. *S*, string passing over pulley *P* to counterweight.

rotated, the spindle *K* (Figs. 17-6 and 17-7) is driven by a cam and lever arrangement as represented in Fig. 17-7.

The crystal used should be a small one of good quality, dimensions of about 0.1 to 0.5 mm. being preferable. The use of a large crystal makes it difficult to interpret the intensities of the observed diffraction spots, for these become sensitive to the shape of the crystal when the irradiated

portion is defined by the pinholes or slits. It is preferable to use a crystal small enough so that it is completely bathed in the primary beam passing through the holes or slits.

The crystal is often mounted on goniometer arcs, which are even more helpful in the rotation method than in the Laue method. After mounting it so that the desired zone axis is roughly parallel to the

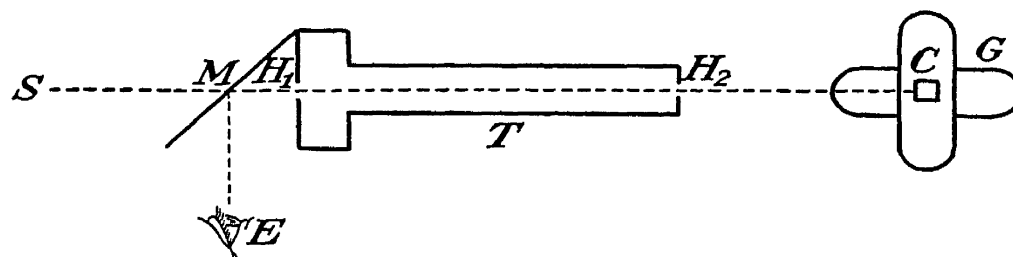


FIG. 17-8.—Device for aligning zone axis of rotating crystal. *S*, source of light. *E*, eye. *C*, crystal. *T*, collimating tube of rotation camera. *G*, goniometer arcs. *H*<sub>1</sub>, *H*<sub>2</sub>, collimating pinholes or slits. *M*, Microscope cover glass affixed to *T* at 45° angle. (From W. P. Davey, "Study of Crystal Structure and Its Applications," McGraw-Hill Book Company, Inc., 1934.)

(vertical) spindle axis, the final accurate adjustment is made with the arcs. The adjustment may be made optically if the crystal has well-developed zonal faces. Sometimes a crystal that has no such faces can be made to reveal them optically by etching it slightly chemically. For example, a tungsten crystal will develop microscopic "facets," which flash up brilliantly after it has been placed in a boiling 3 per cent aqueous solution of hydrogen peroxide for a minute or two. If no optical goniometer is available, one may use the method suggested by Davey<sup>1</sup> and

<sup>1</sup> W. P. Davey, "A Study of Crystal Structure and Its Applications," McGraw-Hill Book Company, Inc., New York, 1934.

illustrated in Fig. 17-8. When a crystal face is perpendicular to the line of the pinholes, the light beam from  $S$  passes through  $H_1H_2$ , strikes  $M$  and is reflected back through  $H_1H_2$  to  $M$  and thence into eye  $E$ . When the given zone axis is aligned with the spindle axis, a faint flash will be observed for each of the corresponding zone faces as the spindle is slowly rotated. If no optical faces exist, a series of x-ray patterns may be obtained by changing various crystal orientations and the desired orientation deduced from these.

In Fig. 17-9, suppose  $CC'$  is the desired zone axis of the crystal, which has been made to coincide with the spindle axis. The symbols  $q, r, s, t$  represent lattice points along this axis, where  $qr = rs = st = c$ , say, in case the zone axis is the  $C$  axis.  $Ar$  and  $Bs$  are primary x-rays from the collimating slits. It is clear that a diffracted beam in the direction  $rD$  or  $sE$  is to be expected if  $sP = g\lambda$ , where  $rP$  is a line perpendicular to  $CC'$  and  $g$  is an integer. If angle  $EsX = \text{angle } Prs = \phi$ , a diffracted beam is to be expected in the direction inclined at  $90^\circ - \phi$  with the axis where

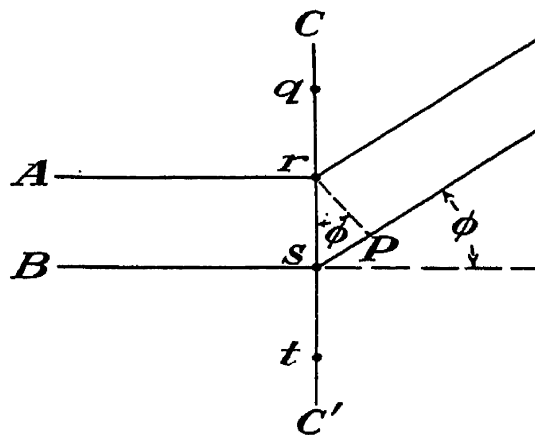


FIG. 17-9.—To explain existence of lines in a rotation pattern

$$g\lambda = c \sin \phi \quad \text{or} \quad \lambda = c \sin \phi \quad (g = 1)$$

whenever the rotation brings the other zone axes into a favorable position, which occurs ordinarily several times per revolution. It will be noted that (17-7) is the form of one of the Laue equations (15-3) when  $\zeta = 90^\circ$ ;  $\zeta$  equals minus angle  $CsE$  in the figure, the rotation causing the two Laue equations to be satisfied only at certain discrete positions. Setting  $g = 0$  in (17-7), one sees that a series of diffracted beam flashes will flash out in various directions in the (horizontal) plane through the crystal center perpendicular to its (vertical) rotation axis. Regarded from the Bragg diffraction viewpoint as “reflections” from various planes, it is clear that these planes responsible for the equidistant ( $g = 0$ ) spots must all contain the zone axis chosen as the rotation axis. If this is the  $C$  axis, for example, these planes belong to the  $[001]$  family and their Miller indices will be  $(hk0)$  where  $h$  and  $k$  are given various integral values. In a similar way, the diffracted beams for  $g \neq 0$  in (17-7) can be regarded as Bragg reflections from the various  $(hk1)$  planes. Thus, when cylindrical film is used, as in Fig. 17-10b, layers of diffraction spots will appear on the film where the various cones of diffracted beams intersect, corresponding to  $l = \dots -3, -2, -1, 0, +1, +2, +3 \dots$  in

the film. These layers of spots are evident in Fig. 17-11A, obtained by Buerger. They are called "layer lines." Their vertical separation (the radius of the film cylinder being known) yields the identity period ( $c$ , in the case of the  $C$  axis) of the lattice along the chosen zone axis of rotation, from equation (17-7). If flat film is used, as represented in Fig. 17-10a, these layer lines become hyperbolas except for the equatorial one, which is straight, as in Fig. 17-11B.

Thus far, complete rotation of the crystal with uniform angular velocity has been assumed. Suppose, instead, that the crystal is oscil-

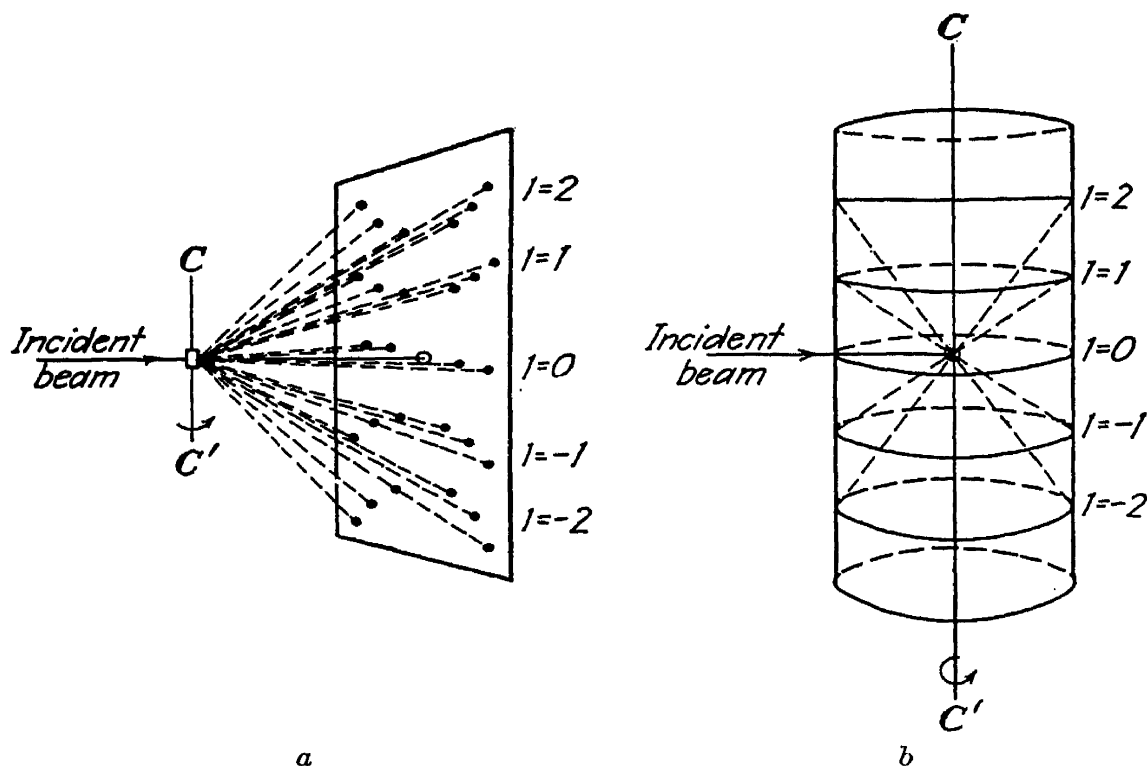


FIG. 17-10.—Diagram of rotation cameras. *a*, flat cassette arrangement. *b*, cylindrical cassette arrangement.

lated by means of a heart-shaped cam for a few degrees on either side of the position where its  $A$  axis coincides with the primary beam. As before, it will be assumed that the rotation axis is the  $C$  axis and that the crystal belongs to a system which has the  $A$  and  $C$  axes perpendicular. In this case, most of the diffracted spots will be Bragg reflections from planes parallel to the  $A$  axis, that is, planes for which the Miller index  $h$  is zero. Then the spots on the zero layer line will be reflections from  $(0\bar{3}0)$ ,  $(0\bar{2}0)$ ,  $(0\bar{1}0)$ ,  $(000)$  or primary beam,  $(010)$ ,  $(020)$ ,  $(030)$ , etc. The spots on the first layer line will be due to the reflections  $(1\bar{3}0)$ ,  $(1\bar{2}0)$ ,  $(1\bar{1}0)$ ,  $(100)$ ,  $(110)$ ,  $(120)$ ,  $(130)$ , etc. Since spots such as  $(\bar{2}20)$ ,  $(\bar{1}20)$ ,  $(020)$ ,  $(120)$ ,  $(220)$ , etc., will be in a vertical column in such a pattern, there will be vertical "row lines" as well as the horizontal layer lines, as seen in Fig. 17-11. In a case like this, the interpretation of the pattern and deduction of the crystal structure from two or three such patterns

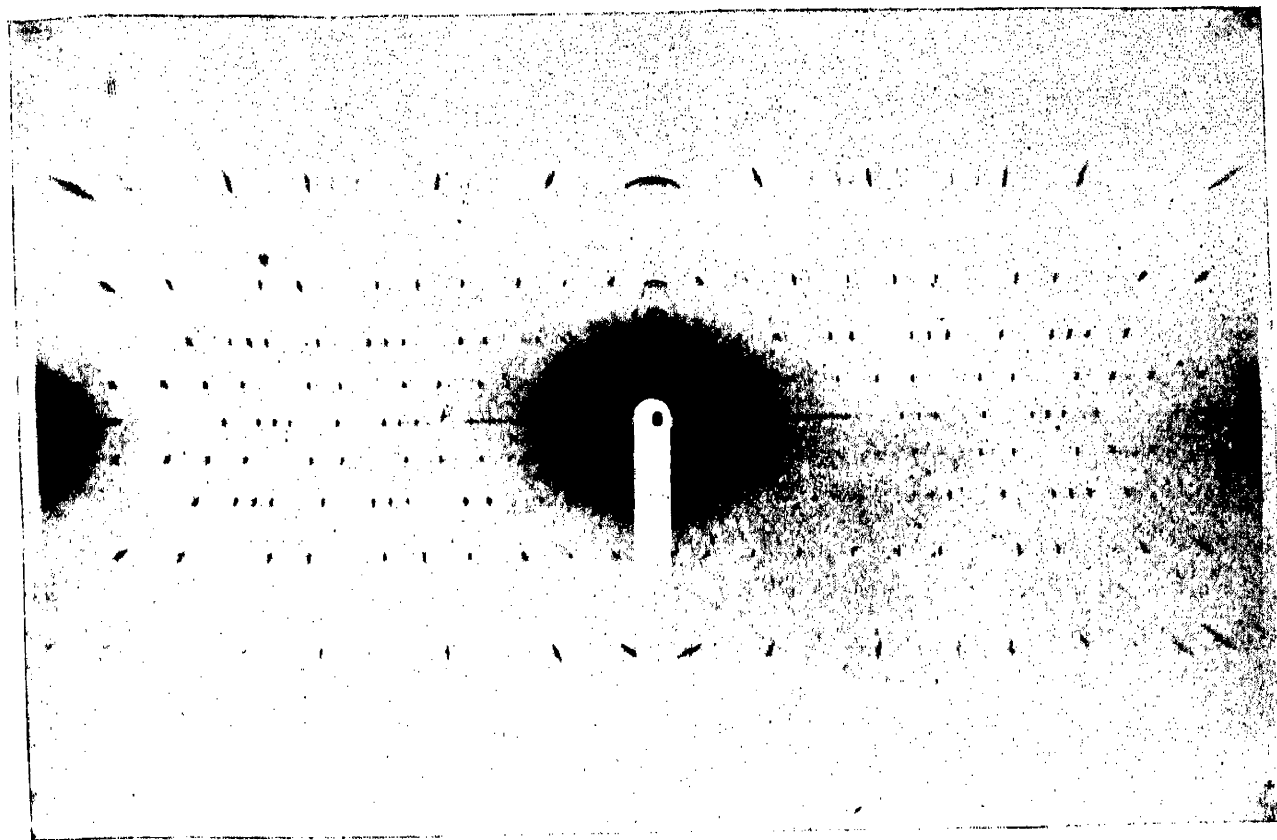


FIG. 17-11A.—Rotating crystal photograph taken with cylindrical camera. ( $\text{NaSbO}_3 \cdot 3\text{H}_2\text{O}$ , tetragonal; C-axis rotation;  $\text{CuK}\alpha$  radiation from gas x-ray tube, filtered through nickel foil.) Reprinted, by permission, from "X-ray Crystallography" by M. J. Buerger, 1942; published by John Wiley & Sons, Inc.)

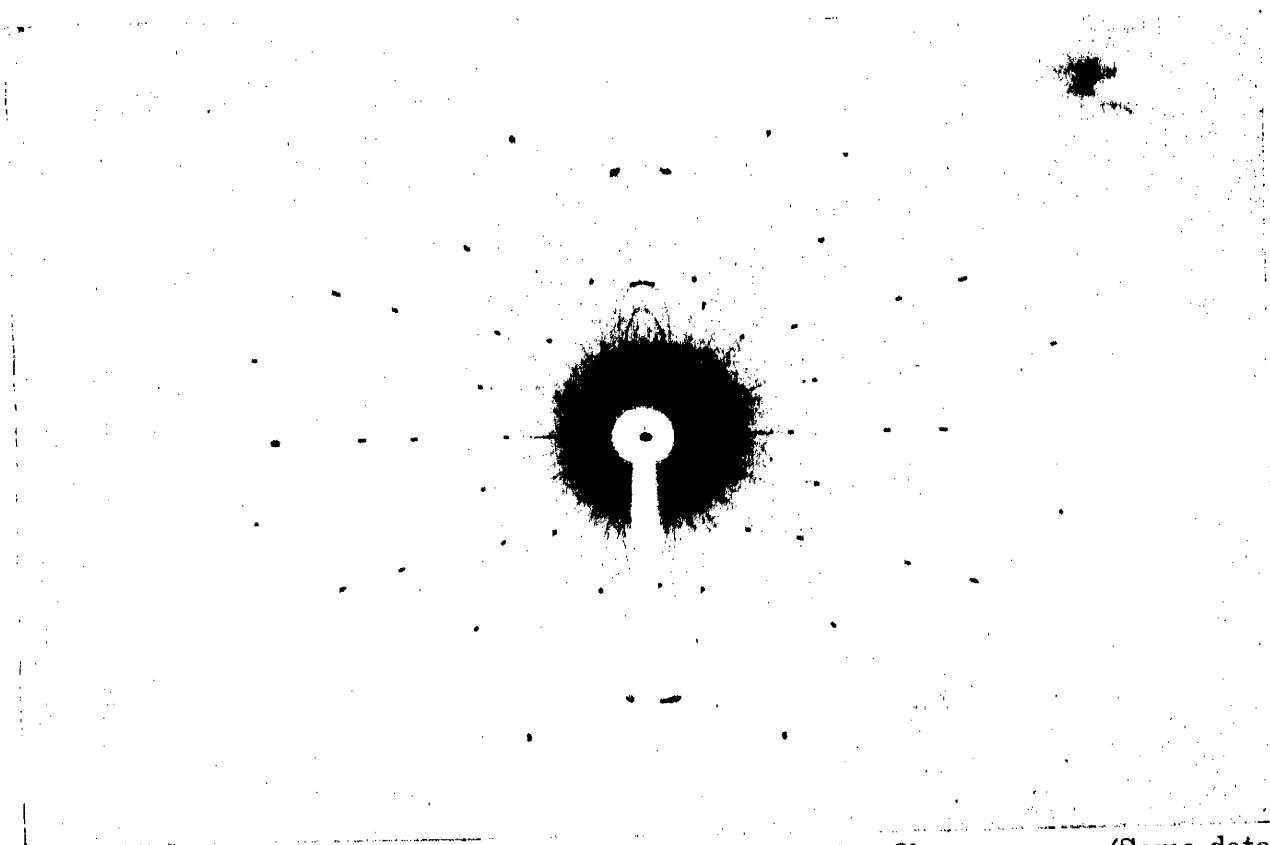


FIG. 17-11B.—Rotating crystal photograph taken with flat-film camera. (Same data as in Fig. 17-11A; also same acknowledgment.)

for different axes are fairly straightforward. For full-rotation patterns from an unknown complex crystal, the analysis becomes rather involved so that occasionally errors occur in the interpretation.

**4. Ewald's Reciprocal Lattice.** To aid in the interpretation of complex rotation patterns, one may resort to a helpful geometrical concept first suggested by Ewald,<sup>1</sup> known as the "reciprocal lattice." This concept is also useful in crystal analysis by other methods, notably the Fourier series representation (Sec. 16-12). It is most helpful in the

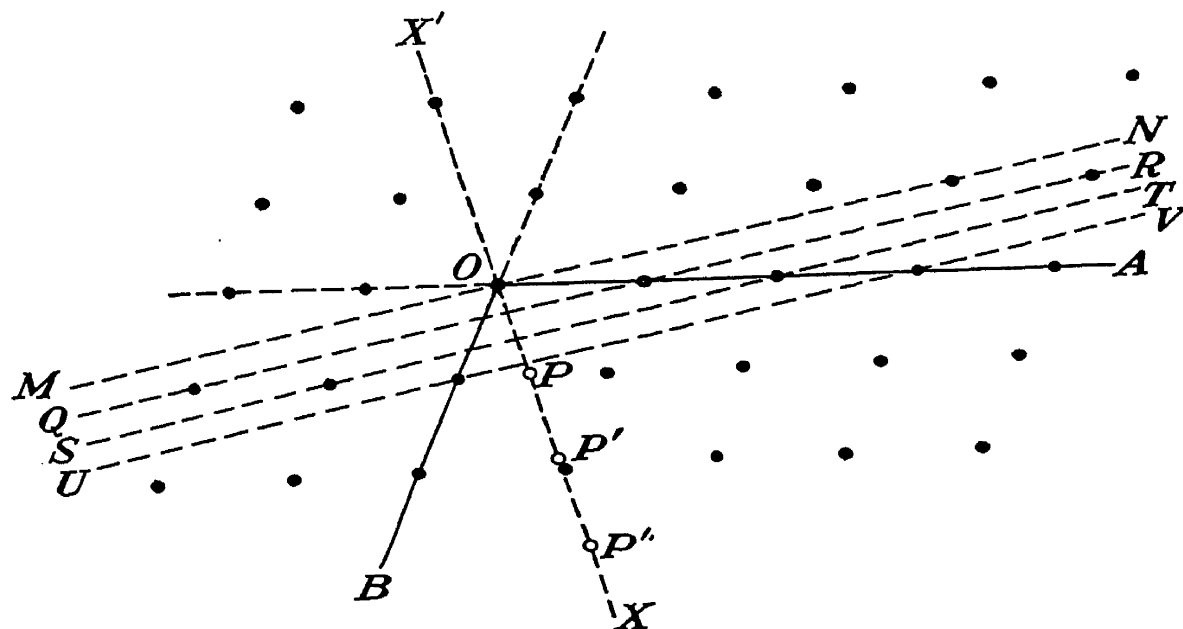


FIG. 17-12.—Illustrating construction of a reciprocal lattice.

case of crystals having a low order of symmetry, especially nonorthogonal crystals, that is, crystals for which one or more of the angles  $\alpha$ ,  $\beta$ ,  $\gamma$  is not  $90^\circ$ —hexagonal, rhombohedral, monoclinic, and triclinic. A good account of the interpretation of rotation patterns, making use of reciprocal lattice theory, has been given by Bernal.<sup>2</sup> The study of x-ray diffraction continually makes use of the concept of Bragg reflections from sets of planes inclined at various angles to one another in three dimensions. The difficulty of visualizing such a system of planes is simplified somewhat by considering their normals instead, since these uniquely determine the orientation of the corresponding planes yet have only one dimension rather than two.

The reciprocal lattice is one built up according to arbitrary mathematical conventions from any given space-lattice. Select any set of planes in a space-lattice, having indices  $(hkl)$ . In Fig. 17-12, for example, where  $OA$  and  $OB$  have been taken as the  $A$  and  $B$  axes, consider the  $(130)$  planes  $MN$ ,  $QR$ ,  $ST$ ,  $UV$ , etc. In this figure,  $UV$  is the nearest rational  $(130)$  plane to the origin, because its  $A$  and  $B$  intercepts are

<sup>1</sup> P. P. Ewald, *Z. Krist.*, **56**, 129 (1921).

<sup>2</sup> J. D. Bernal, *Proc. Roy. Soc. (London) A*, **113**, 117 (1927).



the integers 3 and 1, respectively. According to equation (14-1) or (14-2), there are three planes between it and the origin  $O$ , namely,  $MN$ ,  $QR$ , and  $ST$ . In constructing the reciprocal lattice, the key plane in such a set is always the one nearest the origin, namely,  $QR$  in the example. Its distance from the origin is, of course, the interplanar distance  $d_{hkl}$  (except for complex spacings, as in Fig. 16-11) for the set of planes in question, or  $d_{130}$  in this case. To be definite, suppose that  $d_{hkl} = 1.25$  Å. The line  $OX$  from the origin perpendicular to the set of planes is drawn next, toward the planes in question. If the  $(\bar{1}30)$  planes were under consideration, the line would be drawn in the opposite direction,  $OX'$ . Next, an arbitrary constant  $G$  is selected; in the example, it may be supposed that  $G = 0.842$  so as to have a definite value in mind. The reciprocal feature of the new lattice enters in the next step. The reciprocal  $\rho$  for the set of planes  $(hkl)$ , or  $(130)$  in this case, is defined as  $G^2/d_{hkl}$  or  $0.71/1.25 = 0.568$ . One then marks off this reciprocal distance  $\rho$  from  $O$  along the line  $OX$ , thus arriving at the point  $P$  in the figure, where  $OP = 0.568$  (in., say).  $P$  is then a point in the new reciprocal lattice. It represents the  $(hkl)$  planes, or the  $(130)$  planes in this case. Since these points in the reciprocal lattice are to be associated with the spots in the diffraction pattern,  $P$  may be thought of as associated with the first-order diffraction from this set of planes. In analyzing diffraction patterns, one usually thinks of the second-order diffraction maxima from a set of planes with spacing  $d$  as though they were first-order reflections from a "doubled" set of fictitious planes having spacing  $\frac{1}{2}d$ . In the present example, the second-order reflections may be regarded as due to a set of "(260)" planes, the third-order reflections as due to a set of "(390)" planes, etc. The reciprocals for these imaginary planes are of course  $2\rho$ ,  $3\rho$ , etc., and the lattice points that represent them are  $P'$ ,  $P''$ , etc., in Fig. 17-12, where  $OP = PP' = P'P''$ , etc. In the case of planes with complex spacing, as in Fig. 16-12, one assigns multiple values to  $d$ , such as  $d = p$  and  $d = q$ . The reciprocals  $\rho$  for the set then correspond to  $G^2/d$ ,  $2G^2/d$ ,  $3G^2/d$ , etc.

One sees that the reciprocal lattice is an "artificial" one in which each family of planes in the real lattice is represented by a group of points, according to an arbitrary reciprocal vector relationship, for  $\rho$  has all the characteristics of a reciprocal vector. Of course, Fig. 17-12 is only a two-dimensional diagram, which arbitrarily limits the discussion to the  $[001]$  zone. When all zones are considered, the reciprocal lattice is a three-dimensional array of points, resembling the original lattice in this respect. That is, the point  $P$  in Fig. 17-12 is only one of a geometrical array of such reciprocal lattice points, represented in Fig. 17-13 by small circles. This may be seen by drawing the normal  $OB'$  to the  $(010)$  planes  $OAC$  and the normal  $OA'$  to the  $(100)$  planes  $OBC$ . These

lines  $OA'$ ,  $OB'$ , and  $OC'$ , which is normal to the paper at  $O$ , are the axes of the reciprocal lattice. Marking off the appropriate  $\rho$ ,  $2\rho$ ,  $3\rho$ , etc., intervals along these axes, one constructs the system of reciprocal lattice points as shown. These rows of points correspond to  $h = 0$ ,

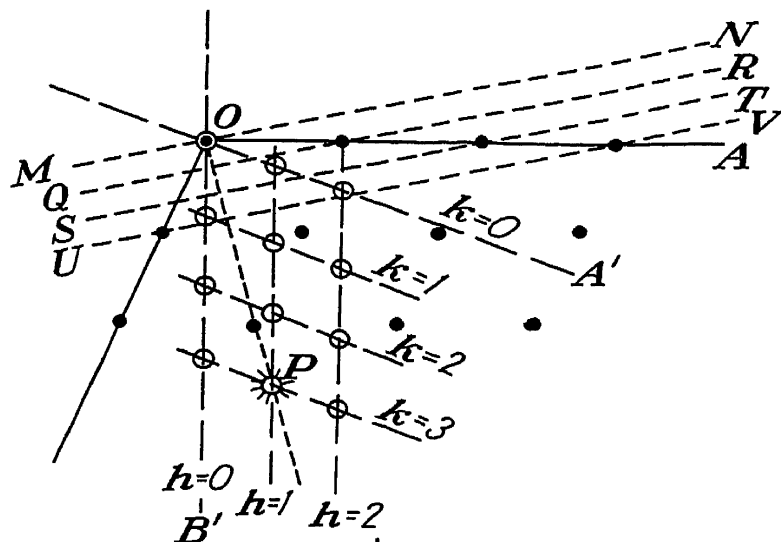


FIG. 17-13.—Illustrating structure of a reciprocal lattice.

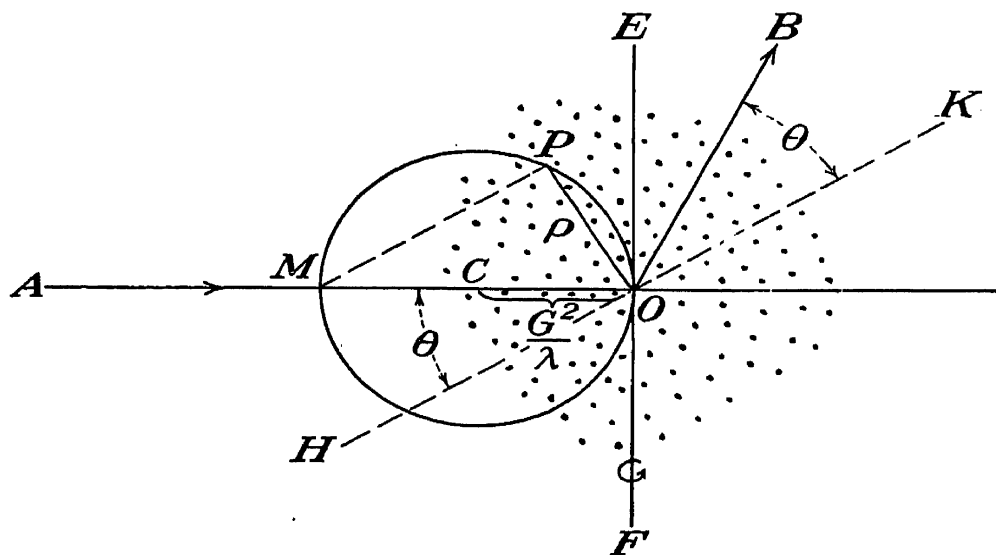


FIG. 17-14.—The Ewald sphere of reflection.

1, 2, etc., and  $k = 0, 1, 2, 3$ , etc., as shown. If the diagram is drawn to scale, it will be found that the point  $P$  corresponds to  $h = 1$  and  $k = 3$  as shown, which is as it should be, since it represents (130). If one now visualizes this construction extended to three dimensions, he will have a concept of the regular geometric character of the reciprocal lattice and its resemblance to an actual lattice.

The reciprocal lattice having been constructed, its points will be an assemblage surrounding the origin  $O$ , as represented by the numerous dots in Fig. 17-14. One of these points is  $P$ , which was located by moving out a distance  $\rho = OP$  from the origin  $O$ , in a direction perpendicular to a set of planes parallel to  $HK$  in the original lattice. Suppose that a

beam of x-rays of wave length  $\lambda$  is incident upon these planes  $HK$  in the direction  $AO$ , at an angle  $AOH = \theta$ . A diffracted beam is to be expected in the direction  $OB$  (where angle  $BOK = \theta$ ) if and only if

$$\lambda = 2d \sin \theta \quad (17-8)$$

supposing  $n = 1$ , tentatively. Since  $\rho = G^2/d$  by definition, the Bragg condition (17-8) becomes

$$\sin \theta = \frac{\lambda}{2d} = \frac{\lambda \rho}{2G^2} \quad (17-9)$$

From this, the above condition can be rephrased as follows: A diffracted beam (from planes  $HK$ , Fig. 17-14) is to be expected if and only if  $P$  lies on the sphere  $OMP$  in the figure. This sphere was arbitrarily drawn

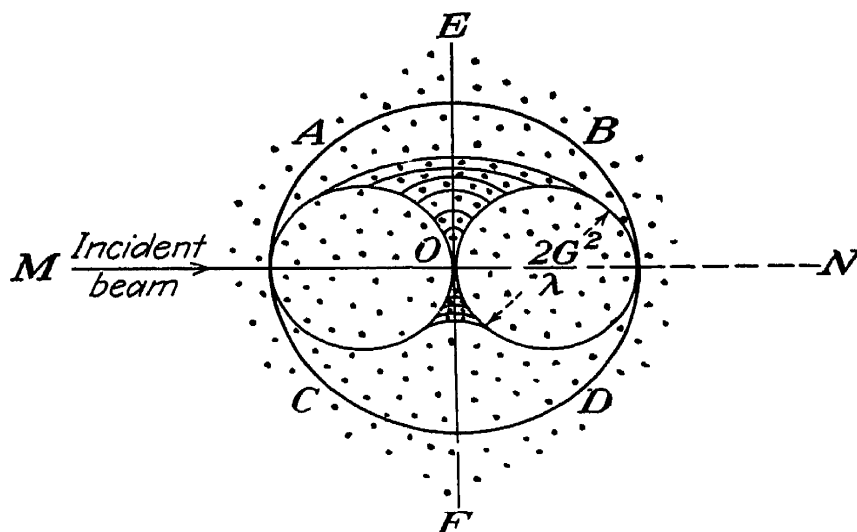


FIG. 17-15.—The limiting sphere.

through the origin  $O$ , with its center  $C$  on the incident ray  $AO$ , at a distance  $CO$  from  $O$  equal to  $G^2/\lambda$ , which is the radius of the sphere. This sphere is called the “Ewald sphere” or “sphere of reflection” because reciprocal lattice points such as  $P$  will “reflect” the primary beam only when they lie on its surface. The mathematics of the reciprocal lattice is considerably simplified by choosing  $G$  equal to the square root of the wave length so that the radius of the sphere of reflection equals 1. The sphere intersects the incident x-ray beam at  $M$ . If  $P$  lies on this sphere of reflection, then angle  $MPO = 90^\circ$ , being inscribed in a semicircle. Since angle  $POH = 90^\circ$ ,  $MP$  is parallel to  $HO$  and angle  $PMO = \theta$ . Hence, in the triangle  $MPO$ ,  $\sin \theta = \rho\lambda/2G^2$ , so that Bragg’s condition [(17-8) and (17-9)] holds provided that  $P$  is on the sphere.

If one now supposes the crystal mounted on its spindle in a rotation camera and rotated about an axis  $EF$  perpendicular to the primary beam  $AO$ , it follows that the sphere of reflection will sweep about this axis generating a torus in the reciprocal lattice space, as indicated in

Fig. 17-15. Since for every set of planes  $(hkl)$  there is a corresponding set  $(\bar{h}\bar{k}\bar{l})$  on the opposite side of  $O$ , it follows that the points of the reciprocal lattice will occur in pairs on opposite sides of and equidistant from  $O$ . Any given pair of points will in general pass through the surface of the reflecting sphere four times (each point passes in and then out of the sphere) for each of its revolutions about the torus, that is, for each revolution of the crystal. Hence each set of planes  $(hkl)$  will in general produce four diffraction spots on the film. The higher order spots  $P'$ ,  $P''$ , etc. (Fig. 17-12) already mentioned, corresponding to higher order ( $n = 2, 3$ , etc.) diffraction, frequently lie so far from  $O$  that they are entirely missed by the sphere of reflection in its journey around the torus. It is clear from Fig. 17-15 that some reciprocal lattice points near the top and bottom of the sphere  $ABCD$  of radius  $2G^2/\lambda$ , but within it, will fail to produce diffracted beams when the crystal is rotated about the axis  $EF$ ; but if a rotation axis such as  $MN$  or one perpendicular to the plane of the diagram were selected, most of these points would be made to diffract. It is also seen that reciprocal lattice points outside the sphere  $ABCD$  can never diffract; the sphere  $ABCD$  is therefore called the "limiting sphere." The points outside the limiting sphere represent sets of planes for which  $n\lambda > 2d$  so that  $\sin \theta$  would be greater than 1, in Bragg's law.

Supposing that a flat film is used in obtaining the rotation diagram, as indicated in Fig. 17-10a, let the crystal-to-film distance be represented by  $D$ . From the mathematics of the reciprocal lattice, Bernal has prepared charts, for  $D = 10$  cm., which make it easier to identify the spots in a rotation diagram. Ten centimeters is greater than the usual crystal-to-film distance, but the diffraction pattern may be enlarged to the size corresponding to this distance; then, by placing one of Bernal's charts (on translucent paper)<sup>1</sup> over it, the problem of identifying the spots is simplified. Bernal has prepared such charts for both flat and cylindrical film. Even with their help, the identification of the reflections is a process in which errors may arise. One of the most important sources of error is the difficulty of determining the cylindrical coordinate<sup>2</sup> angle  $\omega$  of the reciprocal lattice points responsible for the observed reflections. This difficulty may be minimized by taking one or more oscillation photographs in which the crystal is oscillated through a limited angle about a known position, using the heart-shaped cam arrangement already described.

When the crystal has been rotated about each of its crystallographic axes so as to deduce the identity periods of the lattice along the axes

<sup>1</sup> Printed on tracing paper in *Proc. Roy. Soc. (London) A*, **113**, 130, 132, 156 (1927).

<sup>2</sup> For mathematical convenience, cylindrical coordinates  $\xi$ ,  $\zeta$ , and  $\omega$  are usually employed to locate the reciprocal lattice points.

from the separation of the layer lines, the unit cell is ordinarily determined, or at any rate *some* unit cell is determined. In some cases that of calcite, the cell thus determined may be doubly primitive another cell may be preferable because it is truly primitive or has advantages. Determination of the unit cell is usually simpler and than determination of the space group. After identifying all the important reflections, it is then possible to determine which class reflections are suppressed, as explained in Sec. 16-6. If it turns out that  $h$ ,  $k$ , and  $l$  are all odd or all even for all reflections, for example, it follows that the lattice is face-centered. From considerations of this kind the space group may be determined eventually.

**5. Moving-film Methods for a Single Crystal.** In the discussion of the rotating-crystal method, it has been brought out that the identification of a diffraction spot on a photographic film or plate involves determination of three coordinates (represented by the three coordinates of a reciprocal lattice point) from the position of a spot on a two-dimensional film. In order to lessen the difficulty of identifying the reflections various moving-film methods have been devised with the idea of making the position of each spot on the film represent all three cylindrical coordinates of the corresponding reciprocal lattice point.

For a discussion of the moving-film methods, the reader is referred to the book by M. J. Buerger entitled "X-ray Crystallography." Among such methods may be mentioned the "normal-beam Weissenberg method," the "equiinclination Weissenberg method," the "Schiebold method," and the "de Jong and Buerger method."

### QUESTIONS AND PROBLEMS

1. What metal is usual in the x-ray tube target for Laue patterns? How does the voltage used compare with the usual 30 to 40 kv. common in other diffraction work? What is a guarded pinhole? In taking a Laue photograph, what is the choice of the crystal-to-film distance? What are goniometer arcs?

2. A Laue spot  $S$  (Fig. 17-3) is located 1.5 cm. from the central spot  $C$ . What is the distance  $CP$  from  $C$  to the corresponding gnomonic point  $P$ , if the crystal-to-film distance  $D$  is 5 cm.?  
Ans. 34.13 cm.

3. Why is the symmetry of the Laue pattern often higher than that of the crystal from which it was obtained? From the symmetry of the Laue pattern alone how can one distinguish between crystals with a  $V_d$  space group and those with a  $C_4$  space group?

4. In Fig. 17-4, mark the spot where the  $(\bar{5}32)$  gnomonic point would appear if it were present. Is it usual to have an important zone axis parallel or perpendicular to the primary beam in taking a Laue pattern? A rotation pattern? In what does the technique of photographing a rotation pattern differ from that for a Laue pattern?

5. If the distance between the zero-order and the first-order layer lines is 0.1 cm., what is the distance between the zero-order and the second-order layer lines?

<sup>1</sup> John Wiley & Sons, Inc., New York, 1942.

cylindrical-film (Fig. 17-10*b*) rotation pattern is 1.5 cm., what is the identity period of the lattice along the rotation axis if the film radius is 5 cm. and a copper target is used ( $\lambda = 1.54$  A.)? *Ans.* 5.365 A.

6. When  $G$  is taken equal to  $\sqrt{\lambda}$ , as is usual in constructing the reciprocal lattice, Bragg's law reduces to what simple equation, in terms of  $\rho$ ? What is the diameter of the sphere of reflection, in this case? Of the limiting sphere? Explain why four spots are to be expected (unless suppressed) in the full-rotation pattern for any given order of diffraction from the ( $hkl$ ) planes.

7. What is the purpose of taking oscillation patterns to supplement rotation patterns? What are row lines in such patterns? Explain how one would lay out the profile of the cam used in taking oscillation patterns.

8. An orthorhombic crystal has lattice constants  $a$ ,  $b$ , and  $c$ . If molybdenum  $K_\alpha$  radiation ( $\lambda = 0.71$  A.) is used, give the coordinates (with respect to the crystallographic axes) of the reciprocal lattice points for the  $\{100\}$  form. What is the purpose of devising moving-film methods of crystal analysis?

## CHAPTER 18

### THE HULL-DEBYE-SCHERRER POWDER METHOD

**1. Introduction.** The methods of crystal analysis thus far described have presupposed the availability of a single crystal reasonably free from twinning or distortion. It is true that the rotation method requires only a small crystal, but even so this limitation is a severe restriction to one who is interested in the ultimate structure of wood, rubber, brass, steel, and other solids of commercial importance. The question of the structure of liquids and gases also remains untouched, so far as any of the techniques thus far discussed are concerned. Nevertheless, some familiarity with such concepts as the structure factor, the reciprocal lattice, and the possibilities of Fourier analysis are most helpful in the study of the powder method and its applications.

The powder method was first used successfully about 1916. Debye and Scherrer<sup>1</sup> in Germany and Hull<sup>2</sup> in the United States, working independently of each other, obtained x-ray diffraction patterns from aggregates of microscopic crystals, that is, from "powders," at about this time. This new method made it possible to deduce the crystal structure of metals and other solids of commercial importance. He soon deduced the crystal structure of iron, aluminum, silicon, magnesium, sodium, lithium, nickel, graphite, etc. Incidentally, x-ray diffraction shows that graphite, lampblack, and diamond, the three common allotropic forms of carbon, differ in crystal structure, as might be expected.<sup>3</sup> For the person interested in the practical applications of x-rays, the powder method is far more than a method of crystal analysis, like the Bragg method, the Laue method, or the rotation method. Since the sample may be in its ordinary natural polycrystalline condition, the x-ray pattern is able to reveal information regarding three characteristics of the solid that have as much practical importance as the structure of the individual crystals that compose it. These three important characteristics are (1) the average size of the crystals, commonly called the "grain size"; (2) the absence or presence of any tendency for crystals to orient themselves in a preferred manner (the absence

<sup>1</sup> P. Debye and P. Scherrer, *Nachr. kgl. Ges. Wiss. Göttingen* (1915-1916); *Phys. Z.*, **17**, 277 (1916), **18**, 291 (1917).

<sup>2</sup> A. W. Hull, *Phys. Rev.*, **9**, 84, 564 (1917), **10**, 661 (1917).

<sup>3</sup> For a comparison of graphite with various lampblacks, see J. Biscoe and E. Warren, *J. Applied Phys.*, **13**, 364 (1942).

this condition is "random orientation," its presence "preferred orientation"; both degree and direction of the preferred orientation, sometimes called the "texture," may be deduced from powder patterns); (3) actual bending, twisting, or similar mechanical distortion of the crystals, commonly called "grain distortion" or strain.

**2. Powder Cameras.** Essentially, a camera for recording the Hull-Debye-Scherrer type of x-ray diffraction pattern need consist only of (1) a collimating tube provided with collinear pinholes (or, in some

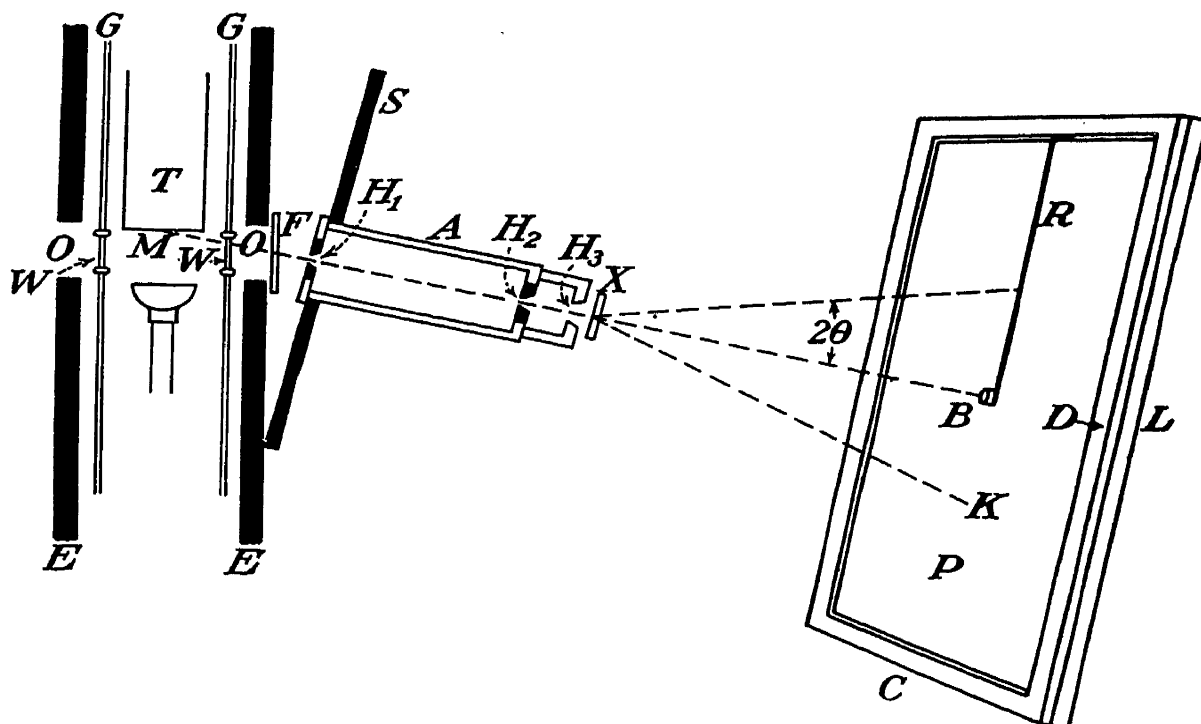


FIG. 18-1.—Flat cassette powder camera.

cases, slits), as in a Laue camera; (2) a filter to separate the  $K_{\alpha}$  from the  $K_{\beta}$  lines, eliminating the latter, since monochromatic radiation is used; (3) a support for the specimen, which may be stationary, although rotation is often desirable and sometimes necessary; (4) a cassette or lighttight holder for the photographic film. Figure 18-1 illustrates the simplest type of powder camera. It may be called a flat-film transmission type of powder camera, for the patterns obtained with it are one type of transmission pattern. In the figure, *A* is the collimating pinhole assembly, *X* is the specimen, and *C* is the cassette. The sketch is drawn in elevation, with the cassette represented in perspective but the other parts in section. The x-ray tube with its target *T*, envelope *G*, and Lindemann or beryllium windows *W* should be enclosed in a chamber, the walls *E* of which are usually made of lead, bronze, or steel, thick enough to afford protection to persons working near by (see Chap. 10). This chamber may be omitted if the tube is rayproof (page 202). The tube and its chamber are usually placed upright in the center of a table with the high-voltage supply underneath. The chamber is provided



with two or more openings  $\frac{1}{2}$  in. or less in diameter, in line with the tube windows, spaced equally around the circumference, one for each camera. Two windows at opposite ends of the elongated focal spot (page 18) is a popular arrangement. The chamber and tube should both be as slender as practical to minimize the distance  $MO$  because of the inverse-square law of decreasing intensity.  $M$  is the focal spot, and  $O$  is one of the openings.

The cameras arranged about the tube are inclined slightly, say 5 to 15°, above or below the horizontal, as indicated in Fig. 18-1 viewed as drawn or inverted. The pinholes  $H_1$  and  $H_2$  are usually about 2 to 2½ in. apart and 0.005 to 0.040 in. in diameter, depending upon whether speed or fine detail in the pattern is more urgent, 0.025 in. being an average size. Pinhole  $H_3$  is a guard for  $H_2$ , as explained for the Laue camera (Fig. 17-1).  $S$  is a lead shield 2 or 3 in. in diameter and about  $\frac{1}{8}$  in. thick, intended to intercept all the rays which pass through  $O$  except those which enter the pinhole  $H_1$ . If only a small filter  $F$  is available, it may be inserted between the window  $W$  and the first pinhole  $H$ , as shown in the figure. If a large filter can be obtained, it is preferable to place it in front of and near the film so that it will absorb secondary rays from the sample. As explained in Chap. 5, the filter should be of zirconium,<sup>1</sup> nickel, iron, or manganese, respectively, for tube targets of molybdenum, copper, cobalt, or iron. A piece of nickel foil 0.001 in. thick or nickel oxide of equivalent absorption is suitable as a filter for copper radiation; iron or soft steel foil or iron oxide is suitable as a filter for cobalt radiation. Manganese being brittle, a compound with light elements such as oxygen may be preferable as a filter for iron radiation. A hundredth of a gram of manganese atoms per square centimeter of filter should be sufficient. When the precision of measurement of the intensities is specially important, a "balanced filter" or "Ross filter" is sometimes used.<sup>2</sup> This will be described in Sec. 19-5. Molybdenum, copper, and cobalt are probably the most valuable target metals for all-round commercial work with powder cameras. For more extensive work or for special applications, chromium and nickel, plus tungsten for Laue patterns, are useful. A demountable tube with a variety of targets or, more conveniently, a series of sealed-off tubes will serve.

In Fig. 18-1,  $X$  represents the sample, which, for the moment, may be

<sup>1</sup> See p. 335. Sheets of zirconium oxide with dimensions of several inches are available from the Patterson Screen Division, E. I. du Pont de Nemours & Co. Inc., Towanda, Pa.

<sup>2</sup> J. C. Clark and R. H. Esling, *Rev. Sci. Instruments*, **13**, 383 (1942) suggest that a wide variety of x-ray filters may be prepared by vacuum distillation of metals onto a cellophane backing.

regarded as a piece of steel etched down to a thickness of about 0.001 in. It should be supported close to or against the pinhole  $H_3$ . The cassette  $C$  may consist of a flat plate  $L$ , next to which the film envelope  $P$ , usually of black paper, is pressed and held flat by the frame  $D$ . A thin sheet of Bakelite sometimes serves as a light shield, instead of black paper. The small lead button or cup  $B$  is supported by the rod or wire  $R$  in a position where it will intercept the main undiffracted part of the transmitted primary beam. A fast nonscreen type of film, preferably having an emulsion on one side only, is desirable for most diffraction work, as mentioned in Sec. 9-2. The minimum potentials at which the characteristic K radiation is excited are 20.0 kv. for molybdenum, 8.86 kv. for copper, 7.71 kv. for cobalt, and 7.10 kv. for iron; it is necessary to operate the tube above these potentials, of course. Thirty to forty kilovolts is a common operating potential for monochromatic x-ray diffraction work. A beryllium window helps to reduce exposure time, especially with copper, nickel, cobalt, iron, and chromium targets, as mentioned on page 111. Compared with a Laue camera, a simple flat-film powder transmission camera uses filtered characteristic radiation rather than the continuous radiation from a tungsten target; the polycrystalline sample requires no provision for alignment of the crystal axes, as in a Laue camera, but provision may be made for rotating the specimen.

A camera having a flat cassette, as represented in Fig. 18-1, is suited for recording rays diffracted at Bragg angles ( $\theta$ ) up to only about  $20^\circ$  or so. Since a wider range than this for  $\theta$  is frequently required, the cassette often takes the form of a cylinder, as in the rotation method, except that the length of the cylinder is much less. That is, the film used in a cylindrical cassette for powder work has the shape of a collar or hoop rather than that of a stovepipe, as in the rotation method. After the film is exposed, it is straightened, the resulting strip being some ten times as long as its width. Figure 18-2A shows a plan of the arrangement of this type of camera,  $C$  being the collimator and  $FFFF$  the cylindrical film coaxial with the specimen  $S$ , which may or may not be rotated about its axis perpendicular to the plane of the diagram during the exposure. A fluorescent window about  $\frac{1}{2}$  in. in diameter at  $O$  facilitates alignment of the specimen in the x-ray beam. Figure 18-2B shows one common type of cylindrical powder camera.  $C$  is the collimator with its two slits and guard slit, which direct a thin horizontal ribbon of rays on the sample  $S$ . This may be a thin-walled glass capillary filled with the sample powder; it may be rotated about its own axis by a small motor. The filter and film are bent to conform to the cylindrical holder  $P$ , the central image being formed on the film near  $O$ . In order to compare two different patterns on the same film, the "septum"  $D$  serves to separate the two

patterns from the sample tube when one end of it is filled with one powder, the other end with another. Several of these cameras, sometimes 10 or more, may be arranged radially around a central x-ray tube with its axis vertical, so as to obtain a number of patterns simultaneously.

In either of the types of camera in Fig. 18-2, distances  $OP$  along the film from the central spot  $O$  are proportional to  $2\theta$ , whereas with the flat cassette, as in Fig. 18-1, the comparable distance  $BK$  is proportional

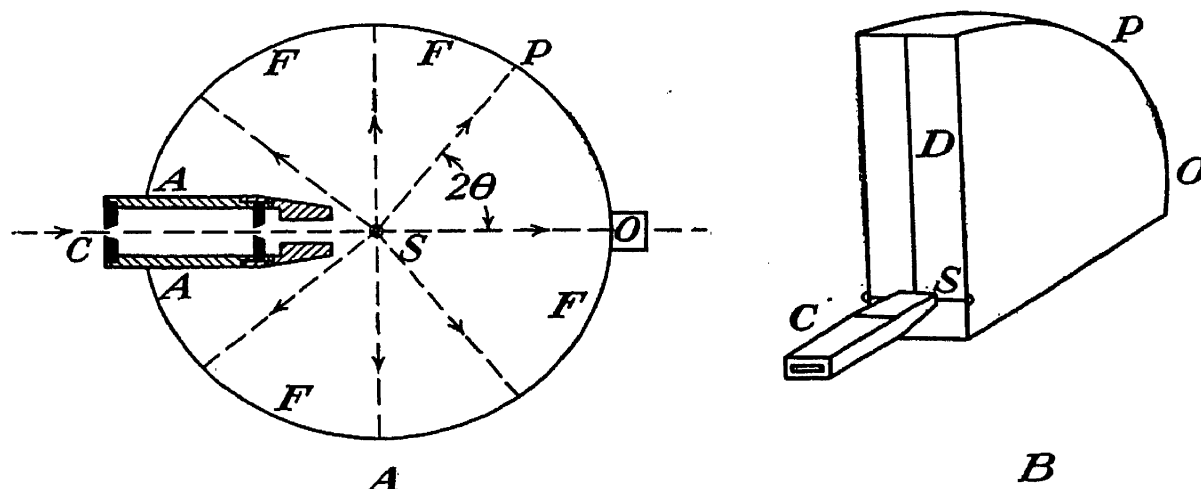


FIG. 18-2.—Two forms of cylindrical powder camera.

to  $\tan 2\theta$ . In cameras of the type shown in Fig. 18-2, slits up to  $\frac{3}{4}$  in. long by some 0.020 in. wide sometimes replace the pinholes in the collimator, the length of the slits being parallel to the axis of the specimen and cylindrical film. The specimen is usually prepared in a cylindrical shape and mounted with its axis coincident with that of the film and parallel with and in line with the collimating slits, when slits are used. Such a specimen might be a fine wire, or a thin-walled glass capillary containing the powder to be examined, or powder stuck to a hair stretched taut, etc. Provision should be made to rotate the sample about its own axis by motor drive, if desired. In order not to obstruct the rays diffracted back near the collimating tube, the latter is often tapered as shown, so that rays from  $S$  may reach the film near  $AA$ .

Finally, among simple powder cameras, there is the back-reflection type represented in Fig. 18-3. Here the primary beam from the collimating tube and pinholes  $C$  passes through a hole  $H$  in the flat cassette  $K$  and strikes the sample  $S$ , which may or may not be rotated slowly about an eccentric axis such as  $MN$ , parallel to  $SA$  (the axis of the pinholes) during the exposure so as to sweep the primary beam over a large number of crystals, thus reducing ring spottiness. This may be called "scanning." The only diffracted rays which strike the film are those which are diffracted at a Bragg angle  $\theta$  between about  $75^\circ$  and  $90^\circ$ . If the pinhole  $Q$  is so located that the points  $R$  and  $Q$  and the ring  $XY$  lie on a sphere, then one may dispense with the first pinhole  $P$ . This

permits one to obtain any chosen ring such as  $XY$  with a reduced exposure time by using the Seemann-Bohlin focusing principle, which will be explained on page 397.  $P$  is sometimes omitted even when the focusing condition is only approximately satisfied. It is always desirable to

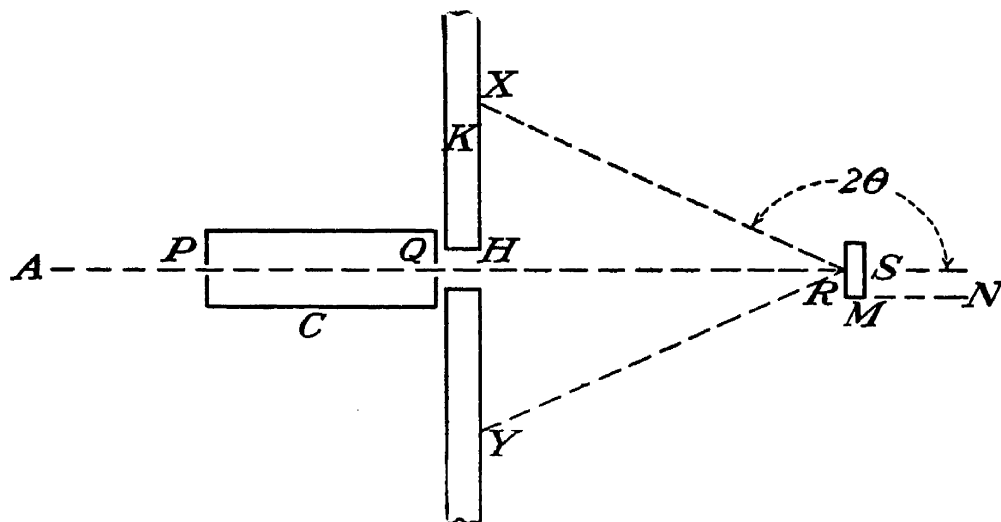


FIG. 18-3.—Back-reflection camera.

know the distance from film to specimen in any of these simple types of powder camera with an accuracy as good as that measurable by an ordinary scale—say to the nearest sixty-fourth of an inch. However, the type of work for which the back-reflection camera is adapted sometimes calls for this distance to be known and reproduced in successive

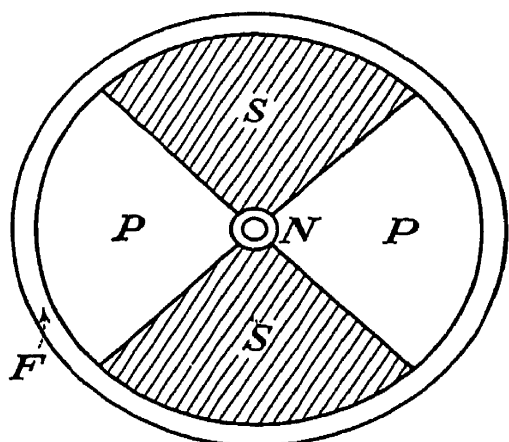


FIG. 18-4.—Cassette with sectors for multiple exposure.

exposures within a tolerance of only about a thousandth of an inch. This requires a good solid camera frame and some precise means of gauging the distance. In addition, the cassette must be provided with positive means for keeping the film flat. Figure 18-4 shows the usual appearance of a back-reflection cassette, as viewed from the specimen. The film, protected by sheet plastic  $P$ , is held down at its periphery by the frame  $F$ . At the hole cut in the center of the film for the passage of the primary beam, the film is held down by a nut  $N$ . The metal sectors  $SS$  protect a considerable area of the film from exposure and at the same time may serve to exert a slight pressure so as to keep the film flat. After an exposure is made on the areas  $PP$ , the sectors  $SS$  may be moved so as to protect these areas; the area formerly protected is then available for taking a comparison pattern with a different specimen, as may be seen in Fig. 21-9. The cassette may be rotated slowly about the axis of the primary beam during the exposure, further to reduce ring spottiness (see next section).

In addition to these widely used simple types, there are numerous special types of powder camera. Among these, one of the more popular is the Seemann-Bohlin<sup>1</sup> camera. Its chief advantage over the commoner types already described is its speed. As already mentioned, the exposures with ordinary cameras usually run from 1 hr. upward for metal samples, although patterns of the lighter metals and their compounds are sometimes obtainable in a few minutes. With a Seemann-Bohlin camera, the exposure time, even with a sample of a heavy metal such as copper, is usually only a few minutes.

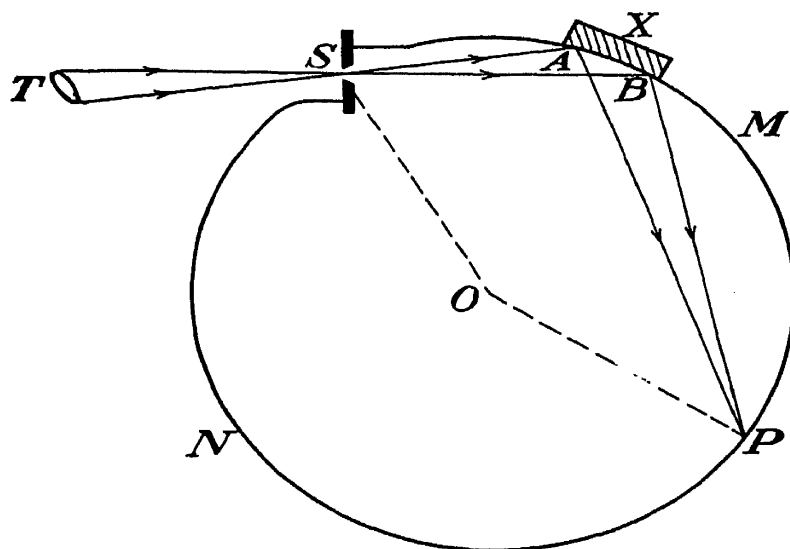


FIG. 18-5.—Seemann-Bohlin focusing camera.

The principle of the camera is illustrated by the diagram in Fig. 18-5. The inside of the camera is cylindrical, a section being represented by the circle. The depth is ordinarily only about one-tenth the diameter, the camera being much shallower than the rotation camera described in Chap. 17. The sample *X* must have a cylindrical concave diffracting surface *AB* to conform with the curvature of the camera, this requirement being the camera's greatest disadvantage. In the case of a powder, it can be glued to a heavy paper, which then lies against the camera wall, cornstarch or gum tragacanth powder being used as a binder. Metal foil or thin sheet can be bent to the proper curvature; but, in the case of a massive block of metal, machining is necessary to obtain the required shape. This machining leaves the surface in a different crystalline condition from its original one; but if the structure of the interior of the metal is the thing to be investigated, the surface layers can be etched away with acid. The etch must be deep if it is to remove the effects of cold working on the surface completely. The x-ray film is made to conform with the cylindrical surface *MPN*. The camera has only one slit *S*, which should be quite narrow, say 0.005 in. or so, and is usually only about  $\frac{1}{4}$  in. long, its length being perpendicular to the plane of the diagram.

<sup>1</sup> H. Seemann, *Ann. Physik*, **59**, 455 (1919); H. Bohlin, *Ann. Physik*, **61**, 421 (1920).

This slit is placed as close to the focal spot  $T$  of the x-ray tube as practical, a large focal spot being satisfactory for this camera. Characteristic radiation is used, and a filter may be inserted in the beam between  $T$  and  $S$  to remove the  $K_\beta$  radiation. The monochromatic rays from  $S$  bathe the surface  $AB$  of the specimen.

Suppose some of the crystals at  $A$  are so oriented as to diffract some of the primary rays  $SA$  in the direction  $AP$ . Then some of the crystals at  $B$  will have the same orientation with respect to the primary rays  $SB$ , and hence they will diffract rays  $BP$  in such a direction that angle  $SAP = \text{angle } SBP$ . Since angles of equal size are inscribed in equal arcs, it follows that the rays  $AP$  and  $BP$  will intersect at the same point  $P$  where they strike the x-ray film on the circle  $SMPN$ . That is, there is a "focusing" action causing the diffracted rays from all parts of the rather extensive sample  $X$  to produce sharp diffraction lines at certain locations such as  $P$  on the film. This focusing effect accounts for the speed of the camera. It can be shown that the Bragg angle  $\theta$  at which the rays are diffracted is one-fourth the angle  $SOP$  subtended by the diffraction line  $P$  and the slit  $S$ . If the circumferential distance  $SABMP$  is  $L$  and the radius  $OP$  of the camera is  $R$ , then  $L/R$  gives the angle  $SOP$  in radians, of course.

The general fogging of the film due to scattered and secondary radiation can be greatly reduced, according to Bozorth and Haworth, by using a bent-crystal focusing monochromator.<sup>1</sup> This consists of a rock-salt crystal plastically bent so as to focus the diffracted x-rays upon the slit of the Seemann-Bohlin camera. Various attempts have been made to avoid the limitations imposed by the requirement of a cylindrical surface while retaining the speed advantage of the Seemann-Bohlin principle. Among these, a design by Stephen and Barnes<sup>2</sup> is typical. One of the most outstanding devices for reducing exposure time or gaining speed in x-ray diffraction work of various types is the Soller<sup>3</sup> slit. This is a multiple slit built up by spacing flat pieces of lead foil parallel to each other and a fraction of a millimeter apart. Soller originally applied this type of slit to a Bragg spectrometer, but it has also been applied to various types of diffraction camera. It permits one to use a broad x-ray beam in cameras and spectrographs properly designed for them, without corresponding loss of resolving power. The slits used by Soller were 20.6 cm. long, the length of a Soller slit corresponding to the distance between slits in an ordinary

<sup>1</sup> R. M. Bozorth and F. E. Haworth, *Phys. Rev.*, **53**, 538 (1938); see also C. S. Smith, *Rev. Sci. Instruments*, **12**, 312 (1941); P. Kirkpatrick, *Rev. Sci. Instruments*, **12**, 552 (1941).

<sup>2</sup> R. A. Stephen and R. J. Barnes, *Nature*, **136**, 793 (1935).

<sup>3</sup> W. Soller, *Phys. Rev.*, **24**, 158 (1924).

collimator. The distance between adjacent lead-foil sheets, corresponding to the width of standard slits, was 1.24 mm. The lead foil was 0.0 mm. thick. With such slits on a Bragg spectrometer, the molybdenum  $K_{\alpha_1}$ - $K_{\alpha_2}$  doublet was readily resolved and the wave length ratio of the  $K_{\alpha_2}$  to the  $K_{\alpha_1}$  line was measured as 1.00604 as compared with the accepted value of 1.00605.

In the United States, the four principal manufacturers of x-ray diffraction equipment, chiefly for taking powder patterns, are

General Electric X-ray Corp., Chicago, Ill.

Hayes Scientific Appliances, Urbana, Ill.

North American Philips Co., Inc., New York, N.Y.

Pickering X-ray Corp., New York, N.Y.

These commercial x-ray diffraction units (Fig. 18-6) consist of a cabinet housing the electrical equipment. The top of the cabinet is flat, serving as a table top. In the center of this is located the x-ray tube, which is shockproof and rayproof in some models and provided with a shockproof and rayproof housing in others. Surrounding the tube, there are two or four tracks on which the diffraction cameras can be mounted. Since line focus tubes (page 18) are used, two of these tracks are much more favored than the other two, when four are present. One manufacturer provides a portable model in addition, whereas another provides for quick removal of the tube from the cabinet for remote operation by a shockproof cable.

For precision work, numerous refinements are incorporated into the construction of powder cameras.<sup>1</sup> For example, Donnay and Fankuchen<sup>2</sup> describe a pentaerythritol crystal monochromator that may be readily attached to the factory-built units just mentioned. Two types of cylindrical



FIG. 18-6.—Factory-built x-ray diffraction unit. (Courtesy of Pickering X Corporation.)

<sup>1</sup> See, for example, M. J. Buerger, *J. Applied Phys.*, **16**, 501 (1945).

<sup>2</sup> D. H. Donnay and I. Fankuchen, *Rev. Sci. Instruments*, **15**, 128 (1944).

powder camera (Fig. 18-2A) that have been evolved by W. L. Bragg and his coworkers after 20 years of intensive development have been described by Bradley, Lipson, and Petch.<sup>1</sup> One of these is designed to be evacuated so as to eliminate the absorption of soft x-rays by the air. If chromium  $K_{\alpha}$  radiation is used, 75 per cent of the rays are absorbed by the air in the camera alone, unless it is evacuated. A cylindrical powder camera for work where the sample may be heated to 1000°C. (1832°F.) has been described by Hume-Rothery and Reynolds.<sup>2</sup>

**3. "Transmission" and "Back-reflection" Patterns.** Hull-Debye-Scherrer patterns obtained with the simple type of powder camera shown in Fig. 18-1 are often called transmission patterns because the primary beam passes (is "transmitted") through the sample and both the primary and the diffracted rays emerge on the opposite side. For illustration, suppose that the sample is made up of a large number of small face-centered cubic crystals, as, for example, in a piece of copper foil. As already explained in Chap. 16, the interplanar distances of the various sets of planes for a cubic crystal are given by

$$d_{(hkl)} = \frac{a}{\sqrt{h^2 + k^2 + l^2}} \quad (16-17)$$

but, for a face-centered lattice,  $h$ ,  $k$  and  $l$  must all be even or all odd, so far as the Bragg reflections are concerned, because of the suppressions. Therefore, in order of decreasing values of  $d$ , the Bragg reflections to be expected are: (111),  $d = a/\sqrt{3}$ ; (200),  $d = a/\sqrt{4}$ ; (220),  $d = a/\sqrt{8}$ ; (311),  $d = a/\sqrt{11}$ ; (222),  $d = a/\sqrt{12}$ ; (400),  $d = a/\sqrt{16}$ ; (331),  $d = a/\sqrt{19}$ ; (420),  $d = a/\sqrt{20}$ ; (422),  $d = a/\sqrt{24}$ ; (511) and (333),  $d = a/\sqrt{27}$ ; (440),  $d = a/\sqrt{32}$ , etc. Here, the designation (222) for a Bragg reflection, for example, refers to the second-order reflections from the {111} form, that is, from the (111), ( $\bar{1}\bar{1}1$ ), ( $\bar{1}1\bar{1}$ ), and ( $1\bar{1}\bar{1}$ ) sets of planes. The accepted way of stating this is to say that there are four "cooperating planes" or "equivalent planes" contributing to the (222) reflection in a powder sample.

To help visualize the sequence of reflections to be expected, a diagram of the type shown in Fig. 18-7 is convenient. Distances from the left edge of the diagram to any of the various vertical lines are equal to the square roots of the various integers given in the top row. The vertical lines in the second row, marked "simple cube," represent the various Bragg reflections to be expected from a simple cubic lattice, as explained on page 347. The third row, marked "body-centered cube," has all

<sup>1</sup> A. J. Bradley, H. Lipson, and N. J. Petch, *J. Sci. Instruments*, **18**, 216 (1941); **22**, 57 (1945).

<sup>2</sup> W. Hume-Rothery and P. W. Reynolds, *Proc. Roy. Soc. (London) A*, **167**, 25 (1938).



the reflections deleted for which  $h + k + l$  is odd, because they are suppressed. The fourth row, marked "face-centered cube," has all reflections deleted except those for which  $h$ ,  $k$  and  $l$  are all even or else all odd. The fifth row shows the reflections characteristic of a diamond type of cubic lattice (see page 359).

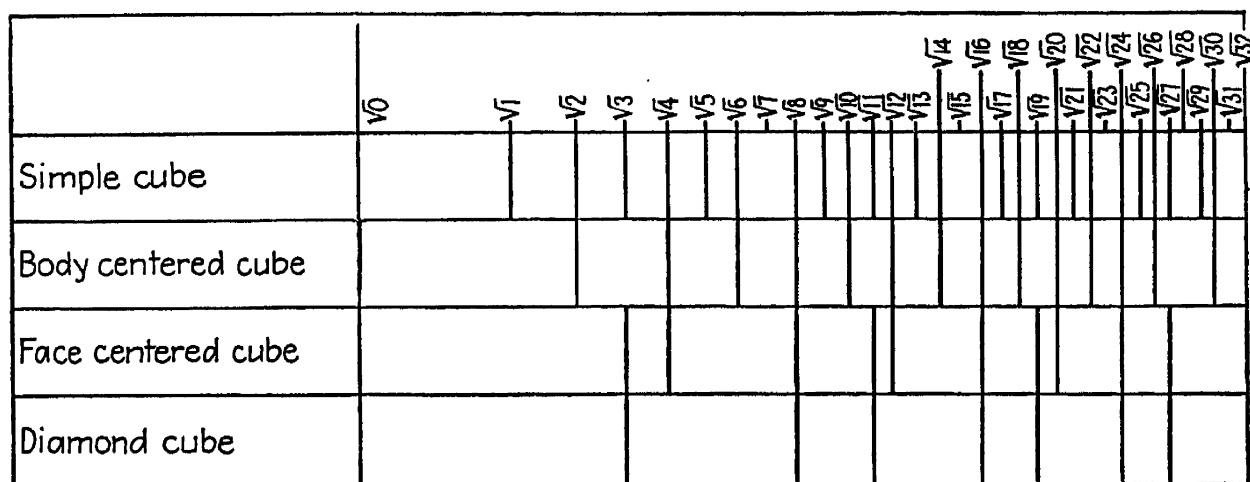


FIG. 18-7.—Line sequences in cubic powder patterns

Combining (16-17) with Bragg's law,

$$\sin \theta = \frac{\lambda}{2} \frac{\sqrt{h^2 + k^2 + l^2}}{a} \quad (18-1)$$

where  $h$ ,  $k$ , and  $l$  are the indices of the Bragg reflections. Since the abscissas in Fig. 18-7 represent the values of the radical for the four simplest types of cubic lattice, the sequence of the vertical lines in the figure corresponds with the lines or rings to be expected in the diagram as  $\theta$  corresponds to  $\sin \theta$ . Thus, face-centered cubic crystals in a powder sample should be expected to diffract the rays in the primary monochromatic beam so that the diffracted rays will diverge from it by certain discrete angles, these angles forming a sequence which may be described as "a pair followed by a single ring (or line), thrice in succession." This is obvious from the fourth row in Fig. 18-7. It is also obvious that a body-centered cubic powder sample should yield a regular series of 13 lines or rings, followed by a break, whereas a simple cubic sample should yield a regular series of six lines or rings, followed by a break. A diamond cubic powder sample is seen to yield a pattern consisting of a single line or ring followed by a series of pairs.

Figure 18-8 illustrates the manner in which the primary beam  $HS$  passes through the powder sample  $S$ , consisting of, say, 100,000 or more tiny crystals, and continues to the film, which it strikes at  $O$ . Assuming that the crystals are face-centered cubic, it seems probable that a few hundred of them would happen to have the proper orientation for the

(111) reflection to occur. The probability of any one crystal having the correct orientation obviously should be proportional to the number of "cooperating planes" involved. That is, a crystal is four-thirds as likely to be oriented for the (111) reflection as it is for the (200) reflection because there are four sets of planes in the  $\{111\}$  form but only three

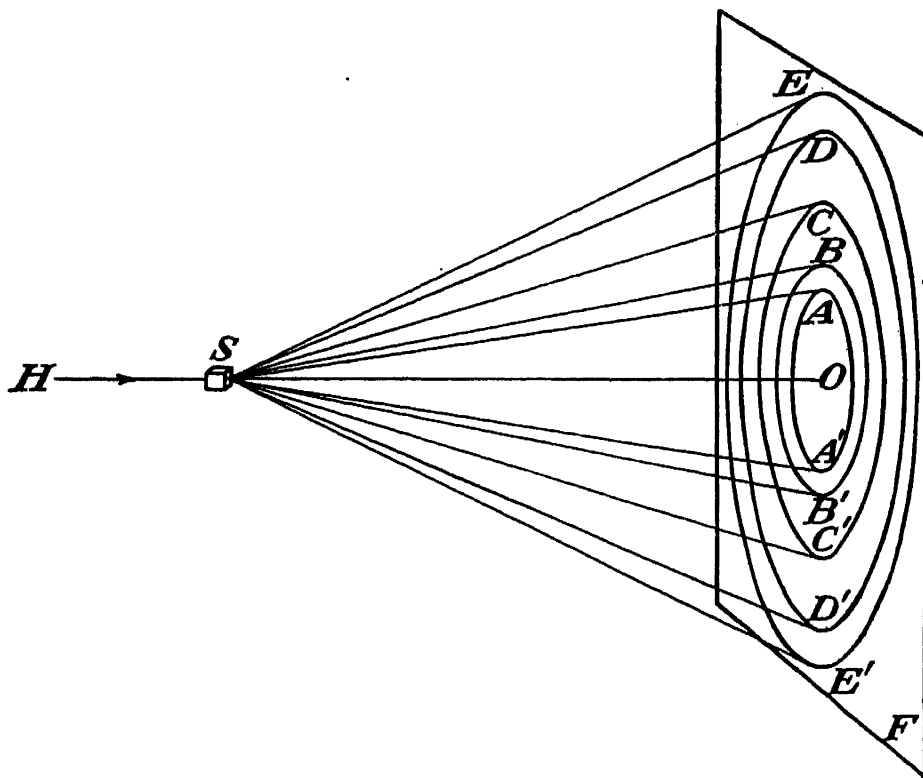


FIG. 18-8.—Formation of a transmission pattern.

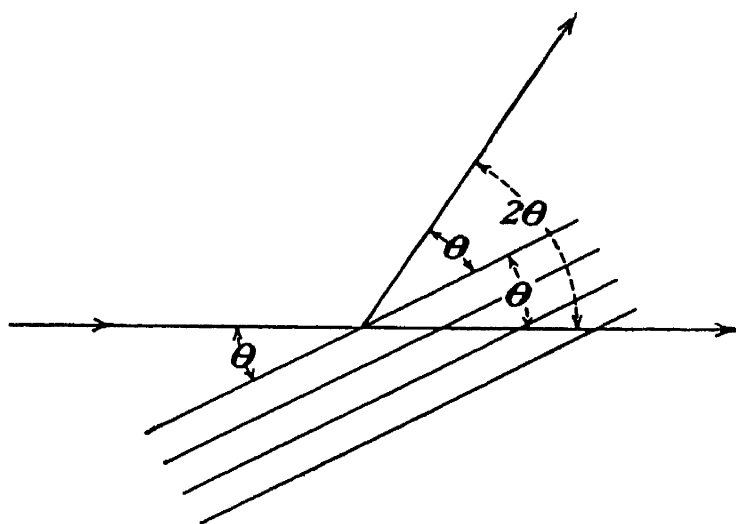


FIG. 18-9.—The Bragg angle  $\theta$  is only half of the angle of diffraction.

sets in the  $\{100\}$  form. Each crystal properly oriented for a (111) reflection will produce a diffracted ray that will deviate from the beam  $SO$  (Fig. 18-8) by an angle  $2\theta$  (see Fig. 18-9) given by equation (18-1) when the radical is  $\sqrt{3}$ . The chances are that some of these few hundred crystals will diffract their beams up, some down, some to the right, some

to the left, and so on to every possible direction lying in the surface of the cone  $SAA'$  in Fig. 18-8. This cone of rays obviously will cause a ring  $AA'$  on the flat film  $F$ , on the assumption that a simple flat-film transmission camera is used. Likewise, by chance, a few hundred other crystals will be so oriented as to yield the (200) reflection, diffracting a cone  $SBB'$  of rays, diverging from  $SO$  by an angle  $2\theta$  given by (18-1) when the radical is  $\sqrt{4}$ . Thus the pattern on the film will consist of a series of concentric rings in the sequence "a pair ( $AA'$  and  $BB'$ ) followed by a single ring ( $CC'$ ), then another pair ( $DD'$  and  $EE'$ ) followed by a single ring, etc.," which may be off the edge of the film  $F$ , in the case of a flat cassette.

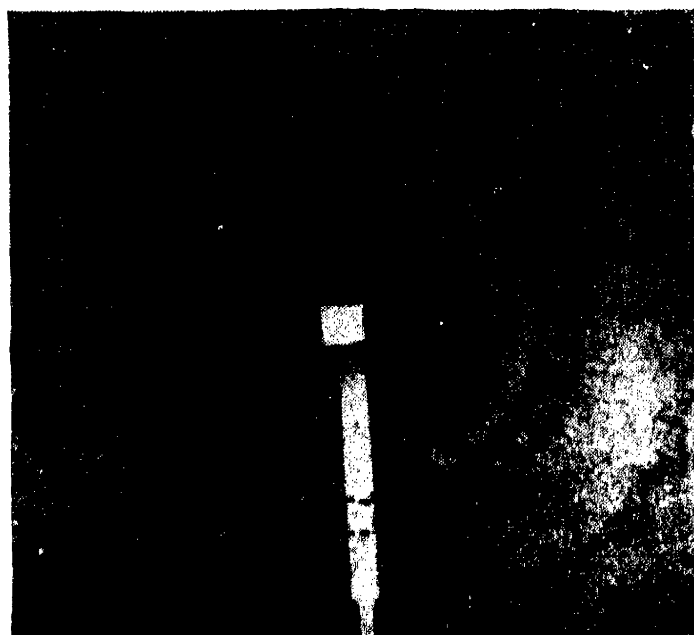


FIG. 18-10.—Transmission pattern of sheet copper.

Figure 18-10 shows a diffraction pattern obtained in this manner from a piece of sheet copper. The several hundred individual diffraction spots composing each ring are evident. Each spot represents a ray from one of the crystals in the sample which happened to have the right orientation to yield a Bragg reflection having indices corresponding to the particular ring in which it lies. The pair of rings  $DD'$  and  $EE'$  (Fig. 18-8) are to be seen in the four corners of Fig. 18-10. The shadow of the block  $B$  and rod  $R$  in Fig. 18-1 are also seen in Fig. 18-10. In order to ensure that some of the diffracted rays do not miss the film as they obviously did in Fig. 18-10, one may use the cylindrical type of camera described in the preceding section and represented diagrammatically in Fig. 18-11. The primary beam  $TS$  passes through the hole  $H$  in the cylindrical hoop of film, striking the specimen  $S$  at the center of the hoop. The coaxial cones of diffracted rays strike the film at  $AA'$ ,  $BB'$ ,  $CC'$ , etc., producing arcs that will have sharp curvature near  $O$ , as at  $AA'$ , but lessened curva-

ture at  $BB'$ ,  $CC'$ , etc. These arcs become straight lines at  $DD'$  when the Bragg angle  $\theta$  is  $45^\circ$ . For diffraction angles greater than this, the so-called "back-reflection" pattern is formed on the rear half of the hoop by cones of rays such as  $SEE'$ ,  $SFF'$ , etc. Here again, the pattern will consist of arcs with their curvature becoming more pronounced as the hole  $H$  is approached.

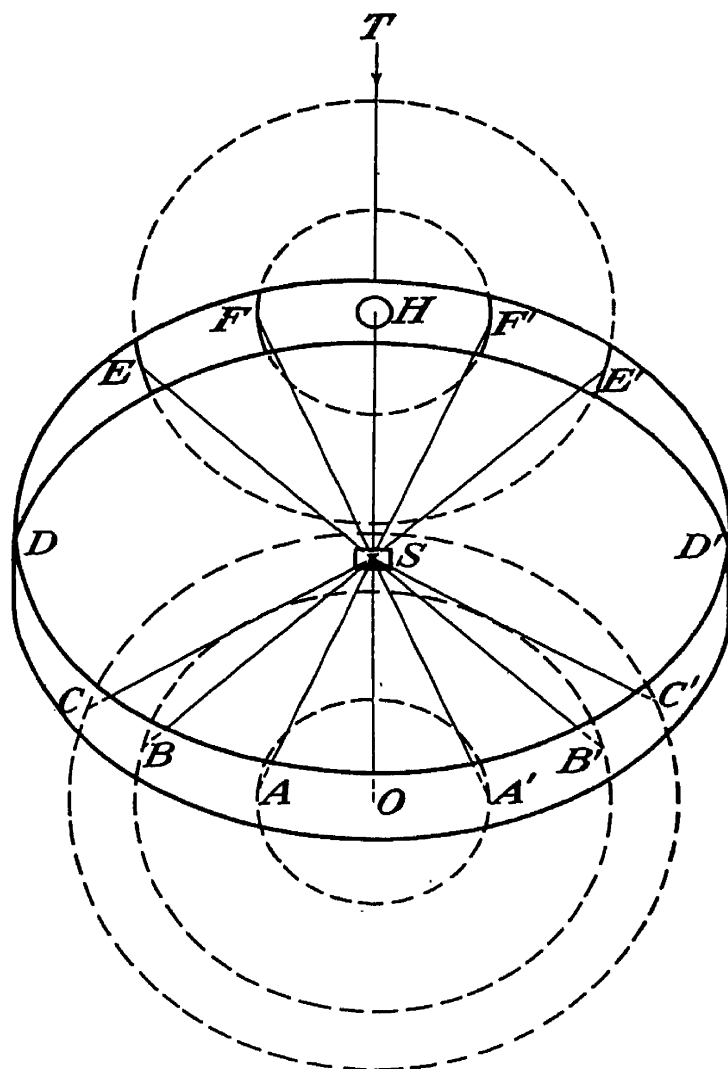


FIG. 18-11.—Formation of a powder pattern in a cylindrical camera.

When the transmission pattern is of paramount interest, the two ends of the film strip should be near  $F$  and  $F'$  (Fig. 18-11). For back-reflection studies, they should be near  $A$  and  $A'$ . For greatest accuracy in determining the Bragg angle  $\theta$  corresponding to a "line" such as the arc at  $C$ , both ends of the film are placed at  $D$  (or  $D'$ ), this procedure being known as the "Straumanis technique."<sup>1</sup> When the film is straightened,  $H$  is located midway between arcs  $F$  and  $F'$  (or  $E$  and  $E'$ ), and  $O$  is located midway between  $A$  and  $A'$ , or  $B$  and  $B'$ , etc. Then since angle  $OSH = \pi$  radians, it follows that an angle like  $OSC$  is  $\frac{1}{4}\pi$  radians if distance  $OC$  is one-fourth of distance  $ODH$ , for example. Thus the angle measure-

<sup>1</sup> M. Straumanis and A. Ievins, *Naturwissenschaften*, **23**, 833 (1935).

ment becomes independent of camera diameter, and errors due to film shrinkage are eliminated.

If the strip of film is placed with its ends at  $F$  and  $F'$  in the camera, it will look like Fig. 18-12 (a powder pattern of lead) when it is laid out flat. It will be noticed that the arcs of rings in this pattern do not show the individual diffraction spots like the rings in Fig. 18-10. The reason for this is that the crystals are finer, so that the portion of the sample penetrated by the primary beam had, say, 5 million crystals in it instead of 100 thousand, as before. Consequently there are, say, fifty times as many spots as before, and they are so small and so closely spaced that they are no longer distinguishable on (resolved by) the x-ray film. In some types of work, it is desirable to obtain continuous rather than spotty rings, even though the sample may be fairly coarse grained. By rotating the sample continuously during the exposure, a greater propor-



FIG. 18-12.—Powder pattern of lead, taken with a cylindrical camera. The letters  $F'$ ,  $O$ ,  $F$  indicate the corresponding positions in Fig. 18-11.

tion of the crystals can be brought into the proper orientation to diffract so that continuous rings are obtained from coarser samples than is possible without rotation. The rear half of the film hoop  $DEFHF'E'D'$  in Fig. 18-11 is the back-reflection pattern of lead.

**4. Preparation and Mounting of the Specimen.** If it is desired to obtain a powder pattern of a material for the purpose of determining its chemical composition or in order to investigate its crystal structure, then it should be reduced to a fine powder. If it is a material that can be ground up in a mortar, then this should be done. If it is a metal, fine filings may be obtained, by using light pressure on a fine, clean file. The powder or filings should be sieved through a 200-mesh (per inch) screen or cloth. Having obtained the powder, one may mix it with Canada balsam to produce a thick paste, which is coated onto a human hair; this is then mounted taut in a line perpendicular to the primary beam. This type of specimen is suitable for soft rays like iron  $K_{\alpha}$  radiation, provided that the powder is not hygroscopic. For this type of sample, a camera having a vertical axis is preferable, so that one may suspend the hair and hang a small weight on it to keep it taut and vertical. A motor-driven suspension capable of rotating the hair about its own axis should be provided.<sup>1</sup> If the axis of the camera is not vertical,

<sup>1</sup> See, for example, A. J. Bradley, H. Lipson, and N. J. Petch, *J. Sci. Instruments*, **18**, 216 (1941); **22**, 57 (1945).

a glass tube or rod drawn down to a diameter of about 0.01 in. may be substituted for the hair; if molybdenum  $K_{\alpha}$  radiation (which is hard enough to penetrate thin glass) is to be used, one may prepare a more durable specimen, better adapted to hygroscopic material, by loading the powder into a thin-walled glass tube having an inside diameter of about  $\frac{1}{4}$  mm. Pyrex glass or any easily worked lead-free glass is suitable for drawing into such tubes. Glass tubes are well adapted for producing two patterns (an unknown and a standard for comparison) on a single film, by using a camera with a septum (Fig. 18-2B). For this purpose, a tiny piece of cotton is pushed into the center of the tube with a "ram-rod" of Nichrome wire. Then the standard powder (usually NaCl) is worked into one end of the tube, a very little at a time, and shaken down by tapping with a pencil, for example. After filling, the end of the tube may be sealed with a tiny piece of wax (which should be kept out of the x-ray beam during the exposure), a miniature soldering iron or similar device being used. The other end of the tube may be filled in the same way with the unknown powder. If this is hygroscopic, it should be loaded into the tube from a cup or mortar heated to about 100°C., after which the tube should be sealed quickly. The tube should be accurately centered in the beam and rotated during the exposure by a small motor. With a simple flat-cassette powder camera, the powder may be enclosed between two sheets of Cellophane cemented to opposite faces of a  $\frac{1}{4}$ -in. brass washer, which is mounted concentric with and next to the final pinhole. This sacrifices the advantages of rotation, however.

As one might infer from the above remarks, glass, hair, and Canada balsam yield very faint, ill-defined x-ray diffraction patterns. Glass has an amorphous structure that is sometimes described as a "super-cooled liquid." Hair is mostly cellulose, an organic material with a complex, not highly regular, structure consisting of atoms of low atomic number (carbon, hydrogen, and oxygen). Canada balsam is an organic liquid. Other materials sometimes used as fillers, binders, or containers because of their faint, ill-defined patterns are cornstarch, tragacanth, and Cellophane. Powdered tragacanth is one of the best fillers from the standpoint of the faintness of its diffraction pattern, but cornstarch is suitable for most work. Some workers prefer to make a paste by adding a little Canada balsam or thin shellac to the sample powder. The paste is then extruded from a hypodermic needle by means of a wire plunger, after which it is mounted like a glass tube specimen. Others prefer to mold the paste into a wedge, which is mounted so that the primary beam grazes its edge. Such wedges should be oscillated about their edge as an axis; extruded specimens may be rotated.

A  $\frac{1}{2}$ -mm.-inside-diameter thin-walled glass tube full of fine aluminum filings will yield a satisfactory powder pattern by using a hard primary

radiation like molybdenum  $K_{\alpha}$ , but the same tube filled with fine lead filings will not. The reason is that practically all rays ordinarily used in diffraction work will be absorbed by the lead, but this is not true of aluminum. A thinner sample should be used for absorbent materials like lead than for comparatively transparent materials like aluminum. With powdered material loaded into glass tubes, however, it is more convenient and practical to compensate for the absorption of the more opaque materials by diluting them with some filler like cornstarch, so that a standard-sized glass tube can be used for all samples. To determine the proportion of filler to use, one should first estimate the average atomic number of the sample, if its composition is known. For example, if the sample is known to be bismuth subnitrate ( $\text{BiONO}_3 \cdot \text{H}_2\text{O}$ ), a compound of one atom of bismuth (atomic number 83), one of nitrogen (7), five of oxygen (8), and two of hydrogen (1), then the average atomic number is one-ninth of  $83 + 7 + 40 + 2$ , or about 15. In general, there should be no dilution if this number is less than 10, about a 50-50 dilution by volume for values from 10 to 15, a 2 parts filler to 1 part sample dilution from 15 to 20, a 3 to 1 dilution from 20 to 25, a 5 to 1 dilution from 25 to 30, a 7 to 1 dilution from 35 to 70, and about a 10 to 1 dilution for an average atomic number greater than 70. These figures are condensed from those given by W. P. Davey. Dilutions greater than 10 to 1 are inadvisable because the number of crystals of the sample exposed to the beam becomes too small to give continuous rings in the pattern. If the sample is one being subjected to chemical analysis by diffraction methods, its average atomic number may not be known, even approximately. In this case, one may have to make a rough guess based on the density; or, better, three or four patterns may be taken with different dilutions of the sample, and the best one selected.

If the problem is one of determining the grain size, orientation, or internal strains, then the sample must not be powdered, bent, heated, or treated in any way that will alter any of the factors to be determined. In preparing a transmission specimen of a piece of steel or other metal, for example, a sheet a few thousandths of an inch thick and  $\frac{1}{4}$  in. square or larger is usually desired unless the sample is a piece of wire or similar object not capable of reduction to sheet form. In the early stages of preparation, sawing, machining, grinding, etc., is permissible if done carefully so as to avoid any bending, or heating above about  $200^{\circ}\text{C}$ . After the thickness is reduced to  $\frac{1}{16}$  in., slow filing by hand will reduce it to about  $\frac{1}{32}$  in. If it is too hard to file, a surface grinder may be used, a thousandth of an inch or so being taken off at a time, the work being done so slowly that the piece never becomes too hot to lay the finger on it. After  $\frac{1}{32}$  in. thickness is reached, the final reduction in thickness should be achieved by chemical etching. Strong acids (sulfuric, hydrochloric, or

nitric) are most useful for this purpose. Sometimes the use of boiling concentrated nitric acid or aqua regia may be necessary. When the thickness reaches about a hundredth of an inch, care is necessary to see that the sample is not devoured entirely by the acid. It should be dipped in the acid for a second or two and then dipped in water, the process being repeated until the desired thickness is attained.

Hull<sup>1</sup> has derived the formula for the optimum thickness of such a sheet for transmission patterns, in terms of its linear absorption coefficient  $\mu$  for the x-rays used. In Fig. 18-13,  $I_0$  is the intensity of the primary

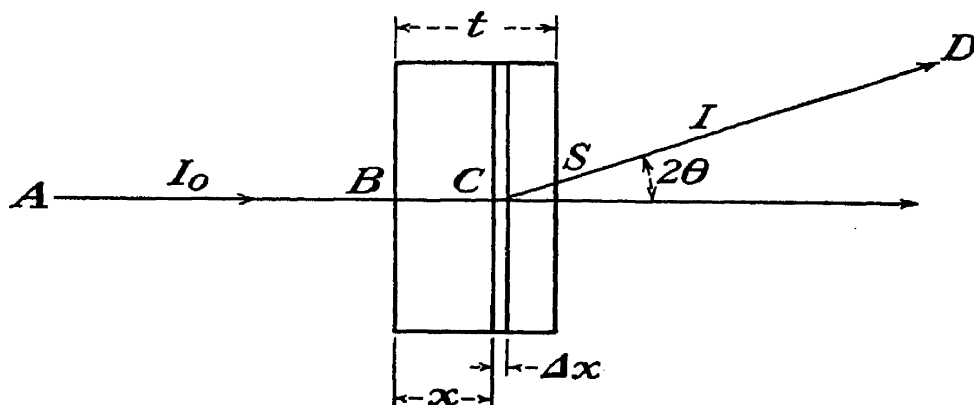


FIG. 18-13.—For calculation of the optimum specimen thickness.

x-ray beam  $AB$  that strikes the sample of thickness  $t$  cm. After penetrating to  $C$ , its intensity is

$$I_C = I_0 e^{-\mu x} \quad (5-5)$$

by Lambert's law (Chap. 5). The initial intensity  $I_D$  of the diffracted beam  $CD$  produced in the layer of thickness  $\Delta x$  will be proportional to  $I_C$  and to  $\Delta x$ , or

$$I_D = k I_C \Delta x = k I_0 e^{-\mu x} \Delta x$$

This diffracted beam must penetrate a thickness  $CS$  of the sample before emerging. If  $2\theta$  is small,  $CS = t - x$ , approximately. Therefore the intensity  $\Delta I$  of the emergent beam diffracted by the layer  $\Delta x$  is

$$\Delta I = I_D e^{-\mu(t-x)} = k I_0 e^{-\mu t} \Delta x$$

The intensity  $I$  of the emergent diffracted ray for the whole sample is the sum of the  $\Delta I$  components for all the  $\Delta x$  layers in the sample, or

$$I = k I_0 e^{-\mu t} \int_0^t dx = k I_0 t e^{-\mu t}$$

This will be a maximum when

$$\frac{dI}{dt} = k I_0 (e^{-\mu t} - \mu t e^{-\mu t}) = k I_0 e^{-\mu t} (1 - \mu t) = 0$$

or when

$$t = \frac{1}{\mu} \quad (18-2)$$

<sup>1</sup> A. W. Hull, *Phys. Rev.*, **10**, 669 (1917); for a rigorous modern treatment, see A. Taylor, *Phil. Mag.*, **35**, 632 (1944).



For molybdenum  $K_\alpha$  radiation and a steel sample, the mass absorption coefficient is 38.5 and the density of steel is about 7.8 g./cm.<sup>3</sup>, so that  $\mu$  is about 300. This gives  $t = \frac{1}{300}$  cm. or about  $\frac{1}{750}$  in. For a cylindrical sample, like a steel wire, the diameter should be slightly greater, say 0.002 in. Application of (18-2) to aluminum for molybdenum  $K_\alpha$  gives  $t = \frac{1}{14}$  cm., or  $\frac{1}{35}$  in. As a matter of practice, a thickness somewhat less than  $\frac{1}{32}$  in. is advisable for aluminum in order to obtain sharp lines with molybdenum radiation, but one will experience difficulty in obtaining patterns of aluminum foil less than a thousandth of an inch thick unless softer radiation is used. One may stack pieces of foil to increase the thickness; but if crystal orientation is one of the features being investigated, it is essential to keep each layer of foil in its proper orientation in the stack. More details regarding the preparation of samples will be given at appropriate places in later chapters, as in back-reflection work.

**5. Exposure Time.** The use of collimating pinholes or slits, soft radiation, and filters and the wastage of all except the small fraction of the primary beam that is diffracted—all combine to make the exposures in x-ray diffraction work much longer, as a rule, than in radiographic work. In the Laue method, the use of a single crystal and continuous radiation permit a pattern to be obtained in a few minutes, for each set of planes continuously diffracts a fair fraction of the primary rays of the proper wave length. In the rotating- or oscillating-crystal method, the use of monochromatic rays and rotation results in each set of planes having the proper orientation to diffract only for a very small fraction of the time, so that the exposure time is usually a matter of hours rather than minutes. In the powder method, the exposures are also long because the specimen consists of a large number of crystals, only a small fraction of which have the correct orientation in the primary beam to diffract the monochromatic rays at any instant. Fillers, binders, containers, or a hair support further reduce the efficiency of the diffraction process with the powder method.

By using large pinholes, say 0.04 in. in diameter, within an inch or two of the focal spot of a powerful water-cooled tube having a beryllium window, dispensing with the filter, and using a fast film and a light, highly crystalline transmission sample like sodium chloride, one can obtain a powder pattern in 5 min. or so. One may mount a Geiger counter behind a slit on a swivel, like the ionization chamber of Fig. 16-2, and swing the slit and counter around the loop  $OABCDE$  in Fig. 18-11, thus surveying the pattern in perhaps 1 hr.,<sup>1</sup> as illustrated in Fig. 18-14. In routine work, where the intensity of only one reflection

<sup>1</sup> See, for example, W. P. Davey, F. R. Smith, and S. W. Harding, *Rev. Sci. Instruments*, **15**, 37 (1944).

may be of interest, as in analyzing a series of samples chemically for the presence of a known constituent, one may take readings with a Geiger counter in this way almost as fast as the samples can be mounted in the apparatus.<sup>1</sup> However, in average work, with fine pinholes, using photographic recording, the exposures generally run from 1 to 50 hr., the average being perhaps around 5 hr.



FIG. 18-14.—X-ray diffraction unit for powder samples, with Geiger counter registration of the diffraction pattern. (Courtesy of North American Philips Co., Inc.)

**6. Crystal Analysis by the Powder Method.** As a first step, one obtains as clear and complete a powder pattern as possible from a pure, well-pulverized, and preferably rotating sample of the material in question. Fine pinholes should be used; usually, for a first attempt, copper radiation with a nickel filter is advisable. Everything possible should be done to protect the film from scattered rays from objects other than the sample. As already noted, a Hull-Debye-Scherrer pattern consists of a series of rings or arcs, each subtending a different double Bragg angle  $2\theta$  at the sample. From the series of rings or arcs, one thus calculates a corresponding series of  $\theta$  values and, knowing  $\lambda$  and setting  $n = 1$ , the  $d$  values of the corresponding Bragg reflections. Then by a cut-and-try, or trial-and-error, process, one assumes various tentative but likely structures and unit-cell sizes for the material and

<sup>1</sup> Available from North American Philips Co., Inc., New York, N.Y.

calculates the reflections to be expected from each one. The correct guess will yield a series of calculated reflections that will correspond exactly, in order of decreasing  $d$  spacing, with the observed  $d$  values, missing none. Furthermore, one should be able to show a qualitative correlation between the intensities of the observed reflections and the relative intensities of the various lines that might be expected from the assumed structure.

When the structure is cubic, tetragonal, hexagonal, or rhombohedral, the guessing game is usually not so very difficult, after some experience; but for triclinic, monoclinic, and orthorhombic crystals, where there are from three to six variables (length of unit cell, axial ratios, and angles between axes) to choose, the pattern has a much larger number of lines to fit, and finding a fit by trial and error becomes impractical unless there is additional information to guide one.

The application of the powder method to the analysis of a material with a simple structure may be illustrated by studying the case of fluorite ( $\text{CaF}_2$ ) as an example. Figure 18-15 shows a transmission pattern of a fluorite powder sample taken with a camera of the type shown in Fig. 18-2B, the radius of the camera being  $3\frac{3}{8}$  in. Copper  $K_\alpha$  radiation was used. A glance at the pattern immediately brings to mind the bottom row of Fig. 18-7, the diamond cubic pattern, "a single line followed by a series of pairs." Measuring the distances from the undiffracted image  $P$  to the various arcs and calling these distances in inches  $x_1, x_2, x_3$ , etc., one has  $x_1 = 1.65$ ,  $x_2 = 2.75$ ,  $x_3 = 3.26$ ,  $x_4 = 4.02$ ,  $x_5 = 4.45$ ,  $x_6 = 5.13$ , and  $x_7 = 5.54$ . Just from visual inspection of the pattern, one might describe the intensities of these reflections, respectively, as strong, very strong, strong, medium, medium, strong, and weak.<sup>1</sup> Since the angle between the primary and the diffracted ray is  $2\theta$ , it is obtained in radians by dividing the above  $x$  values by 3.375, the radius of the camera. One thus obtains the following series of values for  $2\theta$ : 0.489, 0.816, 0.965, 1.19, 1.32, 1.52, 1.64. Thus the  $\theta$  values in radians are 0.2445, 0.408, 0.4825, 0.595, 0.66, 0.76, and 0.82, or, in degrees,  $14^\circ$ ,  $23^\circ 20'$ .

<sup>1</sup> For more accurate methods of measuring intensities, see Sec. 19-5.

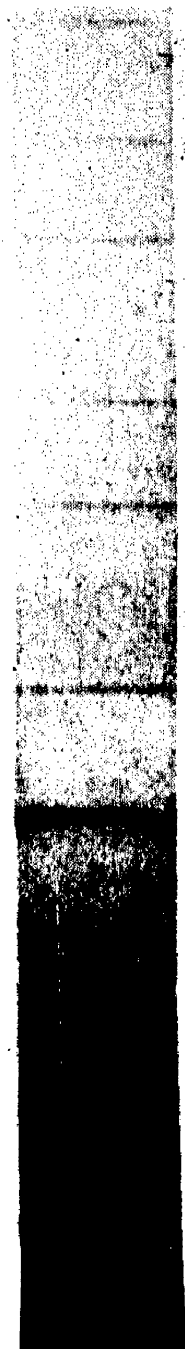


Fig. 18-15. Cylindrical camera pattern of fluorite using copper  $K_\alpha$  radiation collimated by slits.

27°40', 34°6', 37°50', 43°30', and 47°. The sines of these angles are, respectively, 0.242, 0.396, 0.464, 0.561, 0.613, 0.690, and 0.731; and the values of  $2 \sin \theta$  are 0.484, 0.792, 0.928, 1.122, 1.226, 1.38, and 1.462. Applying Bragg's law, one has

$$d = \frac{\lambda}{2 \sin \theta} = \frac{1.54}{0.484},$$

etc., so that the following  $d$  values are obtained: 3.18, 1.95, 1.66, 1.37, 1.26, 1.117, and 1.052 Å.

As already noted, the pattern strongly resembles that of a diamond, which is known to have, for the carbon atoms, the unit-cell configuration  $000; \frac{1}{2}\frac{1}{2}0; \frac{1}{2}0\frac{1}{2}; 0\frac{1}{2}\frac{1}{2}; \frac{1}{4}\frac{1}{4}\frac{1}{4}; \frac{3}{4}\frac{3}{4}\frac{1}{4}; \frac{3}{4}\frac{1}{4}\frac{3}{4}; \frac{1}{4}\frac{3}{4}\frac{3}{4}$ , there being 8 atoms per unit cell.<sup>1</sup> The chemical formula of fluorite ( $\text{CaF}_2$ ) suggests 3, 6, 9, 12, etc., atoms per unit cell, that is, 1Ca atom and 2F atoms, or 2Ca and 4F, etc. Studying the diamond configuration, one notes that the 4 atoms  $000; \frac{1}{2}\frac{1}{2}0; \frac{1}{2}0\frac{1}{2};$  and  $0\frac{1}{2}\frac{1}{2}$  have a face-centered cubic arrangement and, the other 4 have arrangements  $\frac{1}{4}\frac{1}{4}\frac{1}{4}; \frac{3}{4}\frac{3}{4}\frac{1}{4}; \frac{3}{4}\frac{1}{4}\frac{3}{4};$  and  $\frac{1}{4}\frac{3}{4}\frac{3}{4}$  occupying internal positions in the cube that might be described as "northeast and southwest downstairs" and "northwest and southeast upstairs." This leaves 4 "vacant spaces" in the cell that one could describe as "northwest and southeast downstairs" and "northeast and southwest upstairs." Granting that the  $\text{CaF}_2$  structure resembles the diamond structure, which has 8 filled spaces and 4 vacant ones in its cell, what is a reasonable way to fit 3, 6, 9, or 12 atoms systematically into such a cell? A reasonable guess is, naturally, to fit the Ca atoms into the face-centered outer framework of the cell at  $000; \frac{1}{2}\frac{1}{2}0; \frac{1}{2}0\frac{1}{2};$  and  $0\frac{1}{2}\frac{1}{2}$ , and fit the F atoms into the 4 internal occupied diamond-cell positions  $\frac{1}{4}\frac{1}{4}\frac{1}{4}; \frac{3}{4}\frac{3}{4}\frac{1}{4}; \frac{3}{4}\frac{1}{4}\frac{3}{4};$  and  $\frac{1}{4}\frac{3}{4}\frac{3}{4}$  plus the 4 vacant spaces just mentioned, namely,  $\frac{3}{4}\frac{3}{4}\frac{3}{4}; \frac{1}{4}\frac{1}{4}\frac{1}{4}; \frac{1}{4}\frac{1}{4}\frac{3}{4};$  and  $\frac{3}{4}\frac{1}{4}\frac{1}{4}$ . This gives 4Ca atoms and 8F atoms per cell, the structure being cubic and strongly resembling diamond.

Upon having made a "scientific guess" as to the type of structure, the next step is to see whether this tentative hypothetical structure would give the observed pattern. Since the pattern so strongly resembles the diamond pattern, one might suppose that the seven lines in the pattern are, as in diamond, due to the reflections in the bottom row of Fig. 18-7, namely, (111), (220), (311), (400), (331), (422), and a combination of (333) and (511). Calculating the structure factors for these, one has, from

$$F(hkl) = \sum_j f_j e^{2\pi i(hx_j + ky_j + lz_j)} \quad (16-34)$$

the results listed in Table 18-1.

<sup>1</sup> For further details, see, for example, G. D. Preston, *Nature*, **155**, 69 (1945); K. Lonsdale, *Nature*, **155**, 144 (1945); also Appendix XI.

TABLE 18-1

$F(111) = 4f_{Ca}$	$F(100) = 0$	$F(321) = 0$
$F(220) = 4f_{Ca} + 8f_F$	$F(110) = 0$	$F(322) = 0$
$F(311) = 4f_{Ca}$	$F(200) = 0$	$F(330) = 0$
$F(400) = 4f_{Ca} + 8f_F$	$F(210) = 0$	$F(420) = 0$
$F(331) = 4f_{Ca}$	$F(211) = 0$	$F(421) = 0$
$F(422) = 4f_{Ca} + 8f_F$	$F(300) = 0$	$F(332) = 0$
$F(333) = 4f_{Ca}$	$F(310) = 0$	$F(430) = 0$
$F(511) = 4f_{Ca}$	$F(222) = 0$	$F(431) = 0$
	$F(320) = 0$	

The number of cooperating planes for the reflections to be expected (those in column 1) are 4 for (111), 6 for (220), 12 for (311), 3 for (400), 12 for (331), 12 for (422), 4 for (333), and 12 for (511). On the assumption that the crystal is an ionic one, the number of orbital electrons in the  $Ca^{++}$  ion is 18 and in the  $F^-$  ion is 10. From Table 18-1 it is seen that,

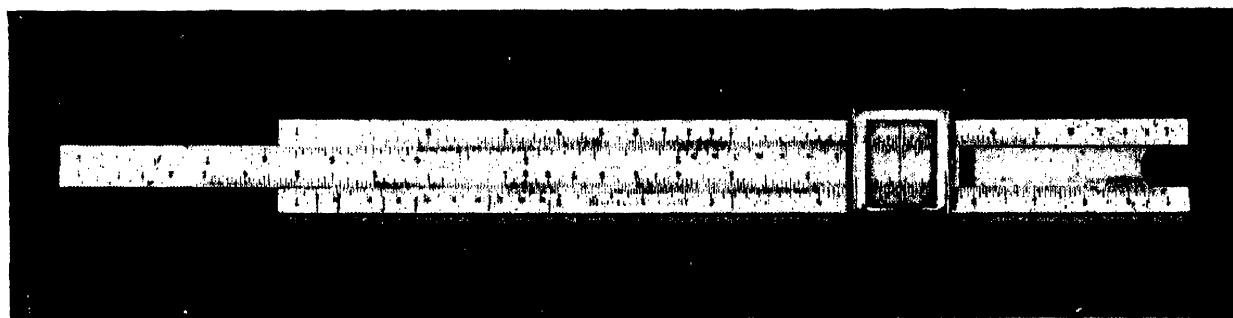


FIG. 18-16.—Illustrating use of slide rule to check analysis of materials with cubic crystal structure.

as in diamond, one should expect the first 7 reflections to correspond to a series of  $d$  values inversely proportional to  $\sqrt{3}$ ,  $\sqrt{8}$ ,  $\sqrt{11}$ ,  $\sqrt{16}$ ,  $\sqrt{19}$ ,  $\sqrt{24}$ , and  $\sqrt{27}$  from equation (16-17) if the tentatively chosen structure is the true structure. This can be quickly verified with a slide rule by pulling out the slide, reversing it, and replacing it so that the figures on the slide are upside down. This makes the lower (formerly upper) scale on the slide read values inversely proportional to the square root of the values on the lower main scale. One now marks the observed  $d$  values on the lower main scale (3.18, 1.95, 1.66, etc.) with a pencil, as shown in Fig. 18-16. When the slide is moved so that 3 on its lower scale coincides with 3.18 on the main scale, then it will be found immediately that the other pencil marks correspond to 8, 11, 16, 19, 24, and 27 on the slide scale. This immediately proves that the observed reflections all occur at exactly the same angles  $\theta$  as one would expect for the assigned structure, with none missing and no extra ones left over.

Next, to check the intensities qualitatively, one may prepare a table such as 18-2. In the second column,  $\sin \theta/\lambda$  is tabulated where  $\lambda$  is in angstrom units (1.54 Å. for copper  $K_\alpha$ ). From this, the atomic-structure factor for  $Ca^{++}$  (third column) can be estimated from Table 16-4 (pag

TABLE 18-2

Reflection	$\frac{\sin \theta}{\lambda}$	$f_{\text{Ca}^{++}}$	$f_{\text{F}^-}$	$F$	$p$	$U$	$F^2 p U$	Observed intensity
(111)	0.16	15	7.5	60	4	3.64	52,500	Strong
(220)	0.26	12.5	5.6	95	6	1.87	101,000	Very strong
(311)	0.30	11.5	4.8	46	12	1.43	36,400	Strong
(400)	0.36	10.3	4.0	73	3	1.02	16,300	Medium
(331)	0.40	9.3	3.5	37	12	0.865	14,200	Medium
(422)	0.45	8.7	3.1	60	12	0.72	31,000	Strong
(333) } (511) }	0.47	8.5	3.0	34	16	0.68	13,630	Weak

356), and likewise the atomic-structure factor for  $\text{F}^-$  (fourth column). The crystal-structure factor  $F$  (column 5) is then calculated from columns 3 and 4 and Table 18-1. The number of cooperating planes are listed in the sixth column. At this point, it is helpful to review Sec. 16-11, where it was stated that  $R = QV$  for a minute crystal and  $R = Q/2\mu_l$  for Bragg reflections from a large crystal. Theoretical calculations for a powder sample yield the relation<sup>1</sup>

$$P = Qp \frac{\cos \theta}{2} V \quad (18-3)$$

where  $Q$  is given by (16-36),  $p$  is the number of cooperating planes,  $V$  is the volume of the sample irradiated by the primary beam of intensity  $I_0$ , and  $P$  is the ratio of the power of the diffracted rays in one of the cones of rays (such as  $SCC'$  in Fig. 18-8) to  $I_0$ . That is,  $P$  represents the relative intensity of any given arc or ring in a cylindrical-camera powder pattern. For a flat-film camera, an inverse-square-law correction enters, obviously. Since  $Q$  contains the factor  $F^2 \left( \frac{1 + \cos^2 2\theta}{\sin 2\theta} \right)$  and (18-3) contains a  $p \cos \theta$  factor, it follows from (18-3) that  $P$  should be proportional to  $F^2 p U$  where  $U = \cos \theta (1 + \cos^2 2\theta) / \sin 2\theta$ . This is the factor tabulated in column 7 of Table 18-2.  $F^2 p U$  is tabulated in column 8, which then represents the relative intensities that should be expected from the type of structure proposed for  $\text{CaF}_2$ . The last column represents the observed intensities as casually read off from Fig. 18-15. The qualitative correlation is evident.

Thus it is seen that the structure guessed for  $\text{CaF}_2$  fully accounts for the observed positions of all the lines in Fig. 18-15 with none missing or left over. Furthermore, the intensities of the lines correspond to

<sup>1</sup> For the effect of absorption, see, for example, A. Taylor, *Phil. Mag.*, **35**, 215 (1944); *Proc. Phys. Soc.*, **57**, 108 (1945); B. E. Warren, *J. Applied Phys.*, **16**, 614 (1945).

the intensities to be expected from the proposed structure. This is fairly conclusive evidence that the guessed structure is the true structure. Microscopic examination of the individual fluorite powder particles will show that they are cubical in shape like NaCl particles, and this fact harmonizes with the hypothesis of a cubic lattice. The lattice constant  $a$  is obviously given by  $3.18 \sqrt{3}$  or  $1.95 \sqrt{8}$  or  $1.66 \sqrt{11}$  or  $1.37 \sqrt{16}$  or  $1.26 \sqrt{19}$  or  $1.117 \sqrt{24}$  or  $1.052 \sqrt{27}$ . Averaging these values, one obtains 5.46 Å. as the value of  $a$ . To restate the unit-cell configuration it is as follows: Ca—000;  $0\frac{1}{2}\frac{1}{2}$ ;  $\frac{1}{2}0\frac{1}{2}$ ;  $\frac{1}{2}\frac{1}{2}0$ . F— $\frac{1}{4}\frac{1}{4}\frac{1}{4}$ ;  $\frac{1}{4}\frac{1}{4}\frac{3}{4}$ ;  $\frac{3}{4}\frac{1}{4}\frac{1}{4}$ ;  $\frac{3}{4}\frac{1}{4}\frac{3}{4}$ ;  $\frac{1}{4}\frac{3}{4}\frac{1}{4}$ ;  $\frac{1}{4}\frac{3}{4}\frac{3}{4}$ ;  $\frac{3}{4}\frac{3}{4}\frac{1}{4}$ ;  $\frac{3}{4}\frac{3}{4}\frac{3}{4}$ . This structure is the fifth Schoenflies type of holohedral cubic lattices, and hence its space group is designated as  $O_h^5$ .

As a further check on the structure, one should calculate the density of fluorite and compare it with the observed value. The atomic weight of calcium is 40.08; of fluorine, 19.00. The mass of an atom of unit atomic weight is  $1.66 \times 10^{-24}$  g. Therefore the mass of the unit cell (4 atoms of Ca + 8 atoms of F) is  $(4 \times 40.08 + 8 \times 19) \times 1.66 \times 10^{-24}$  g and its volume is  $a^3$  or  $(5.46 \times 10^{-8})^3$  cm.<sup>3</sup> This gives a calculated density of 3.185 g./cm.<sup>3</sup> as compared with the accepted experimental value of 3.180. Since all these calculations from the proposed structure dovetail nicely with experimental results, one is now justified in saying that this is the true structure of the fluorite crystal. Obviously, the labor involved in this type of analysis is multiplied by the number of wrong guesses made regarding the structure before the right one is tested, and also the difficulty of the analysis becomes considerably greater for structures of lower symmetry such as hexagonal, rhombohedral, etc. For a discussion of precise evaluation of lattice constants by the powder method, the reader may consult an article by Taylor and Sinclair.<sup>1</sup>

**7. Hull-Davey Charts.** To simplify the labor in the analysis of tetragonal, hexagonal, and rhombohedral crystals, Hull and Davey have prepared a series of charts<sup>2</sup> that play a role in the analysis of the crystals corresponding to the role of the inverted slide rule in the fluorite example just given. One of the Hull-Davey charts is shown in Fig. 18-17, for a face-centered tetragonal lattice. Its use can be simply illustrated by an example. If one calculates the  $d$  values in angstrom units from a powder pattern of the element indium, the values are found to be as follows: 2.72, 2.46, 2.29, 1.68, 1.62, 1.462, 1.395, 1.35, 1.144, 1.088, 1.055, 1.040, 1.025, 0.980, 0.948, 0.905, 0.888, etc. On the theory that this element may have a face-centered tetragonal structure, lay a strip of paper along the scale seen at the bottom of Fig. 18-1

<sup>1</sup> A. Taylor and H. Sinclair, *Proc. Phys. Soc.*, **57**, 126 (1945); see also J. B. Nels and D. P. Riley, *Proc. Phys. Soc.*, **57**, 160 (1945).

<sup>2</sup> A. W. Hull and W. P. Davey, *Phys. Rev.*, **17**, 549 (1921).

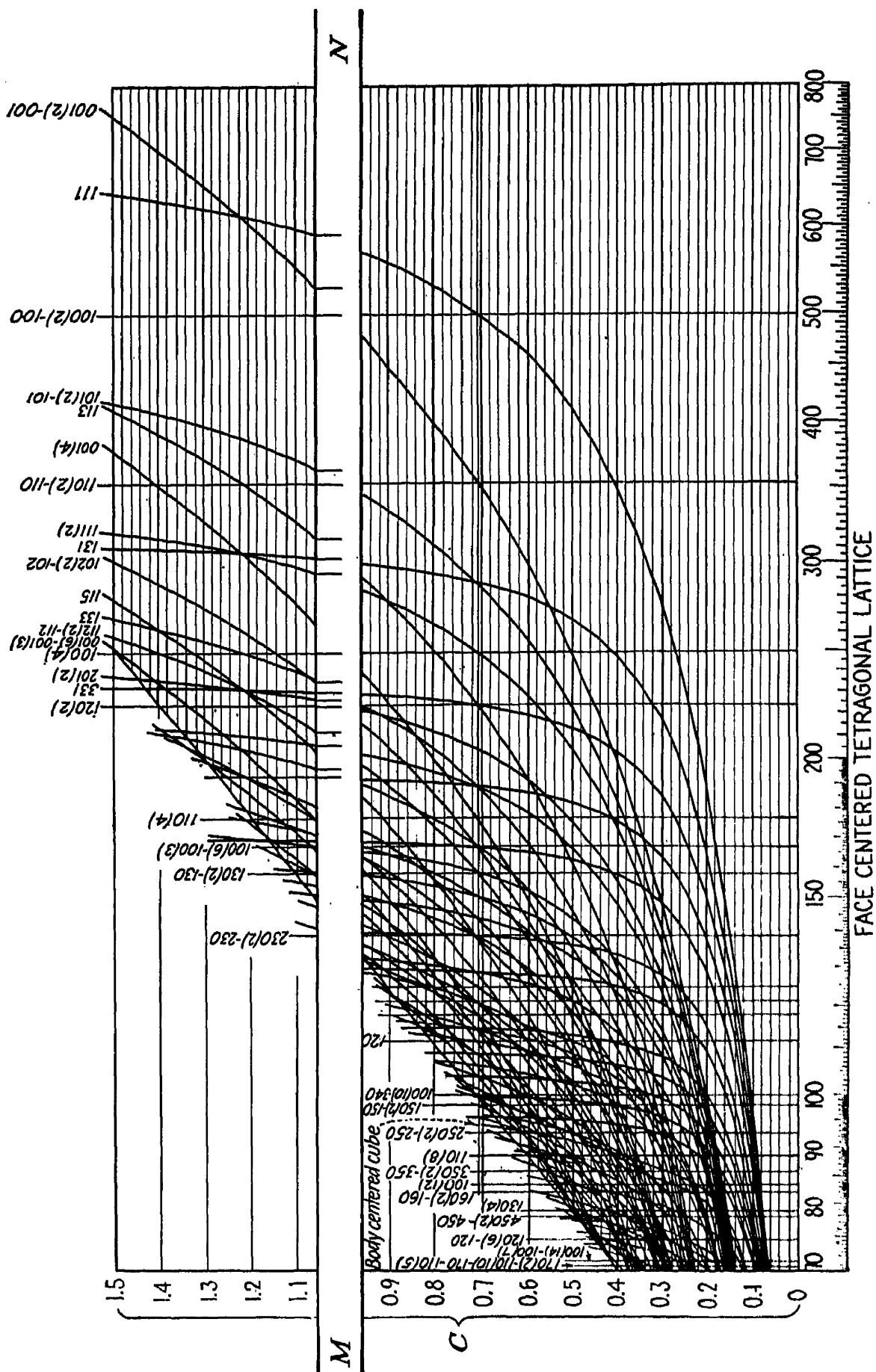


FIG. 18-17.—Illustrating use of Hull-Davey chart to check analysis of materials with tetragonal, hexagonal, or rhombohedral structure. (Courtesy of *Physical Review*.)



Immediately below 2.72 on the scale, make a mark at the edge of the paper. Without moving the paper, make similar marks below 2.46, 2.29, 1.68, etc., just as they were made on the slide rule in Fig. 18-16. When all the marks have been made, the marked strip of paper will look like the one designated *MN* in the figure. Keep this strip in a horizontal position and shift it about the chart, keeping the right-hand mark (the one for the largest observed spacing, 2.72) in coincidence with the prominent curves at the right side of the graph. When the strip is placed in the position *MN* shown in the figure, all the marks on the strip match the various curves, as is seen. The edge of the strip of paper is seen to intersect the ordinate scale at 1.08 when this coincidence occurs. This indicates that the indium pattern is the same as one to be expected from a face-centered tetragonal lattice of axial ratio  $c/b = 1.08$ . Since  $a = b$  in tetragonal lattices, it follows that

$$\frac{c}{a} = 1.08,$$

also.

For reasons already mentioned, such charts are impractical for triclinic, monoclinic, and orthorhombic crystals. Bjurström<sup>1</sup> has evolved a graphical method helpful in the analysis of orthorhombic crystals by the powder method. Unless specific clues are forthcoming from other sources, the powder method becomes impractical when completely unknown materials having a triclinic or monoclinic structure are encountered.

**8. Summary of Crystal-analysis Results.** By the various methods outlined in this chapter and the two preceding it, the crystal structure of nearly all the elements, many of the simpler inorganic compounds, alloys, and minerals, and a few organic compounds have been deduced. One will find the crystal system, space group, and lattice constants of most of these tabulated<sup>2</sup> in recent editions of the "Handbook of Chemistry and Physics."<sup>3</sup> Unit-cell configurations, illustrated in many cases by diagrams, have been tabulated by Wyckoff in his books.<sup>4</sup>

In general, most of these structures are illustrated by a few fundamental "types." For example, some 21 elements have a face-centered cubic structure or may take on this structure under certain conditions. Elements or compounds that crystallize with different structures under different conditions are said to be "allotropic," "polymorphic," or "pleomorphic," and these different structures are called "allotropic

<sup>1</sup> T. Bjurström, *Z. Physik*, **69**, 346 (1931).

<sup>2</sup> See Appendix X.

<sup>3</sup> C. D. Hodgman, editor, Chemical Rubber Publishing Co., Cleveland, Ohio.

<sup>4</sup> R. W. G. Wyckoff, "The Structure of Crystals," 2d ed., 1931, and supplement to the 2d ed., 1934, Reinhold Publishing Corporation, New York; see Appendix XI.

forms." For example, black or red phosphorus is orthorhombic, whereas white or yellow phosphorus is cubic, both existing at room temperature. Other elements or compounds crystallize with different structures at different temperatures and are also said to be pleomorphic. For example, "alpha" iron is body-centered cubic at room temperature and retains this structure above the Curie point ( $770^{\circ}\text{C}.$ ), where its magnetic properties change and it becomes known as "beta" iron. However, at  $800^{\circ}\text{C}.$ , it becomes face-centered cubic and is then called "gamma" iron; from  $1425^{\circ}\text{C}.$  up to the melting point ( $1535^{\circ}\text{C}.$ ), it reverts to the body-centered cubic structure and is called "delta" iron. Some 14 elements have or may assume a body-centered cubic structure, while some 15 are or may be hexagonal close-packed. A few have the diamond cubic structure, a few have the rhombohedral structure typified by arsenic, and a few others have the hexagonal structure typified by selenium. Some 65 compounds have been analyzed and found to have a structure like NaCl, for example, KBr, KCN, MnSe, NiO, etc.; some 20 have a structure like  $\text{CaF}_2$ , for example,  $\text{CeO}_2$ ,  $\text{Li}_2\text{O}$ ,  $\text{Mg}_2\text{Sn}$ ,  $\text{SrCl}_2$ , etc.

### QUESTIONS AND PROBLEMS

1. What advantages has the powder method over other methods of crystal analysis? Powder patterns reveal information about what three important physical characteristics of a crystalline solid, in addition to its crystal structure?

2. Describe four different types of powder camera using ordinary double-pinhole or double-slit collimators. What types of filters are employed in them, and where are they mounted?

3. Describe the Seemann-Bohlin camera, and explain the principle upon which it operates. What is a Soller slit?

4. Distinguish between a transmission pattern and a back-reflection pattern. Why do the diffracted rays from a powder sample generate a series of coaxial cones? Are such cones of rays found in the Laue or rotation methods?

5. Outline the procedure for preparing a sample for crystal or chemical analysis by the powder method. How does the procedure differ when the object is to study the grain size, orientation, or distortion?

6. Using molybdenum  $K_{\alpha}$  radiation ( $\lambda = 0.71 \text{ \AA}.$ ) a powder pattern is obtained with a simple flat-film camera, as in Fig. 18-1 or 18-8. The sample-to-film distance is  $2\frac{1}{2}$  in. The four most prominent rings in the resulting pattern have diameters of 1.69, 2.00, 3.00, and 3.68 in., respectively. What are the corresponding  $d$  spacings in the sample?

*Ans.* 2.18, 1.88, 1.33, and 1.136  $\text{\AA}.$

7. With cobalt  $K_{\alpha}$  radiation ( $\lambda = 1.785 \text{ \AA}.$ ), a back-reflection pattern is obtained from a steel sample with a camera of the type represented in Figs. 18-3 and 18-4. The sample-to-film distance is  $2\frac{1}{2}$  in. The most prominent ring in the pattern has a diameter of 1.65 in. What is the corresponding  $d$  spacing in the sample?

*Ans.* 0.904  $\text{\AA}.$

8. Since alpha iron is body-centered cubic and has a lattice constant  $a = 2.861 \text{ \AA}.$ , what are the indices of the reflection in the preceding problem? *Ans.* (310).

9. The next lower reflection (220), if it appeared at all in the pattern in the preceding problem, would have what ring diameter? *Ans.*  $7\frac{1}{4}$  in.

10. The next higher reflection (222) does not appear. Why not? Is iron pleomorphic? What is the commonest crystal structure among the chemical elements?

11. The mass absorption coefficient of copper for molybdenum  $K_\alpha$  radiation (0.71 Å.) is 51. For copper  $K_\alpha$  radiation (1.54 Å.), it is also 51. Account for the fact that the harder radiation is absorbed by copper just as strongly as the softer. If the density of copper is 8.94 g./cm.<sup>3</sup>, what is the optimum thickness for a sheet-copper sample in taking a transmission pattern with a copper or molybdenum target?

*Ans.* About 0.0007 in.

12. A chemical element with a cubic structure gives the following  $d$  values in angstrom units, as read from its powder pattern: 2.35; 2.03; 1.439; 1.227; 1.173; 1.019; 0.935; 0.910. By marking a slide rule with a pencil and referring to Fig. 18-7, determine whether it is simple cubic, body-centered, face-centered, or diamond-type cubic. What is its lattice constant  $a$ ?

13. If the density of this element is 19.32 g./cm.<sup>3</sup>, compute its atomic weight from the data of Prob. 12.

*Ans.* 197.

14. If the 2.72, 2.46, 2.29, 1.68, 1.62, etc., values for  $d$  given in Sec. 7 correspond to the (111), (002), (200), (202), (220), etc., reflections as indicated in Fig. 18-17, compute the lattice constants  $a$  and  $c$  for indium.

*Ans.*  $a = 4.58$  Å.;  $c = 4.95$  Å.

What is its unit-cell configuration?

*Ans.* 000;  $\frac{1}{2}\frac{1}{2}0$ ;  $\frac{1}{2}0\frac{1}{2}$ ;  $0\frac{1}{2}\frac{1}{2}$ .

15. If the atomic-structure factor for indium is 44.9 when  $\sin \theta/\lambda = 0.1$ , 38.6 when  $\sin \theta/\lambda = 0.2$ , and 32.8 when  $\sin \theta/\lambda = 0.3$ ,  $\lambda$  being in angstrom units, compute the relative intensities of the first five lines in the powder pattern with molybdenum radiation.

*Ans.*

Reflection	$\frac{\sin \theta}{\lambda}$	$f_{\text{In}}$	$F'$	$p$	$U$	$F^2 p U$
(111)	0.184	39.6	158.4	4	7.35	740,000
(002)	0.203	38.6	154.4	1	6.55	156,000
(200)	0.218	37.6	150.4	2	6.1	278,000
(202)	0.298	32.8	131.2	4	4.37	302,000
(220)	0.309	32.8	131.2	2	4.1	142,000

## CHAPTER 19

### CHEMICAL ANALYSIS BY X-RAY DIFFRACTION

**1. Introduction.** The phenomenon of x-ray diffraction by crystals may be applied to the chemical analysis of materials in two general ways. The first employs an x-ray spectrograph in a manner analogous to that in which optical spectrographs are used for the same purpose. This might be called "chemical analysis by x-ray spectroscopy." The second consists in simply mounting the unknown as a transmission sample in a powder camera like those described in the preceding chapter and obtaining its powder pattern, with the use of known radiation, such as molybdenum  $K_{\alpha}$ . The largest dozen or so  $d$  values calculated from the pattern are then compared with a table of known  $d$  values for various known compounds; and if the unknown happens to contain a fair percentage of one or more of the compounds listed in the table, at least a semiquantitative analysis is possible. This might be called the "Hanawalt method," because Hanawalt and his coworkers prepared the first extensive tables of  $d$  values to be published, thus making the method practical.

As in optical spectrographic analysis, the chief field of application of x-ray spectrographic analysis is the determination of the amount of various elements (not compounds) that may be present in small percentages in the (metallic) sample.

Chemical analysis by the Hanawalt method has rapidly gained widespread use since the publication of the first Hanawalt tables in 1938. Its field of application does not coincide with that of other common methods of chemical analysis but rather supplements and overlaps them. It is useful for the determination of the amount of various compounds (or elements, if present in uncombined form) that may be present in fairly large percentages in the sample. For example, one may determine that a certain powder is a 70-30 mixture of  $\text{CaSO}_4 \cdot 2\text{H}_2\text{O}$  and  $\text{Na}_2\text{SiO}_3$ . A very small sample—a few milligrams—will suffice. Since the method is nondestructive, the sample is preserved intact after it has been analyzed. The method is practical for any substance which exists or can be made to exist (for example, by freezing with liquid air) as a crystalline solid and for which the powder pattern is already known. The method is of doubtful value when the sample is a mixture of more than three or four major constituents. That is, it would be difficult to analyze a mixture that contains 10 different com-

pounds, each comprising 10 per cent of the sample, especially if several of them are not listed in the tables.

**2. Chemical Analysis by X-ray Spectroscopy.** X-ray spectroscopy is the technical application of the x-ray spectrometer, or spectrograph, to the analysis of any beam of x-rays, so as to determine its intensity distribution curve as a function of the wave length. After Moseley's death, Siegbahn became the foremost x-ray spectroscopist. These two workers turned their attention chiefly to the accurate tabulation of characteristic x-ray spectra, absorption edges, and excitation potentials and to the theory of their origin as outlined in Chaps. 4 and 5. Siegbahn has published a book<sup>1</sup> describing the apparatus and technique and tabulating all the more prominent characteristic x-ray spectra in x-units, which he invented. In recent years, the most notable change in x-ray spectroscopy has been the advent of the bent-crystal spectrograph. By bending a crystal, it is possible to obtain a focusing action upon the diffracted rays, as already mentioned in connection with the Seemann-Bohlin camera.<sup>2</sup> This permits one to build a spectrograph that has considerably more speed than the ordinary double-crystal spectrograph, but usually with some sacrifice of resolving power.<sup>3</sup>

Chemical analysis by x-ray spectroscopy has never become popular because the technique is more difficult than that of optical spectrographic analysis. X-ray spectroscopy as a method of chemical analysis was brought to the attention of chemists by Coster and Hevesy<sup>4</sup> in 1922, when they discovered hafnium in zirconium ores by this method. For quantitative analysis, the method is beset with some difficulties, such as fluctuation of line intensities due to the absorption edges of the internal standards or other materials present in the sample, selective volatilization of the various constituents present, etc. However, optical spectrographic analysis presents similar difficulties. In either the optical or the x-ray method, such difficulties can be overcome by suitable modification of the procedure.

Following the discovery of hafnium, various investigators became interested in x-ray spectroscopy as a method of chemical analysis, and articles on the subject were published by Coster, Günther and Stranski, Stintzing, Hevesy, and Glocker.<sup>5</sup>

<sup>1</sup> M. Siegbahn, "Spectroscopy of X-rays," translated by G. A. Lindsay, Oxford University Press, New York, 1925.

<sup>2</sup> Footnote 1, p. 398.

<sup>3</sup> See, for example, H. Karlsson and M. Siegbahn, *Z. Physik*, **88**, 76 (1934); S. T. Stephenson, *Rev. Sci. Instruments*, **10**, 45 (1939); H. Jupnik, *Rev. Sci. Instruments*, **10**, 32 (1939); E. Ingelstam, *Rev. Sci. Instruments*, **11**, 160 (1940); B. B. Watson, *Rev. Sci. Instruments* **8**, 480 (1937).

<sup>4</sup> D. Coster and G. v. Hevesy, *Nature*, **111**, 79 (1923); *Chem. News*, **127**, 65 (1923).

<sup>5</sup> D. Coster, *Z. Elektrochem*, **29**, 344 (1923); P. Günther and I. N. Stranski, *Z.*

Laby, Eddy, and Turner<sup>1</sup> applied this method to the analysis of commercial samples of zinc, iron, tin, and alloys of tin-cadmium, lead-bismuth, tin-zinc, and zinc-copper-tin. Special x-ray tubes were used, and special precautions were necessary to avoid the generation of x-rays from stray cathode-ray bombardment of metal other than that being analyzed.

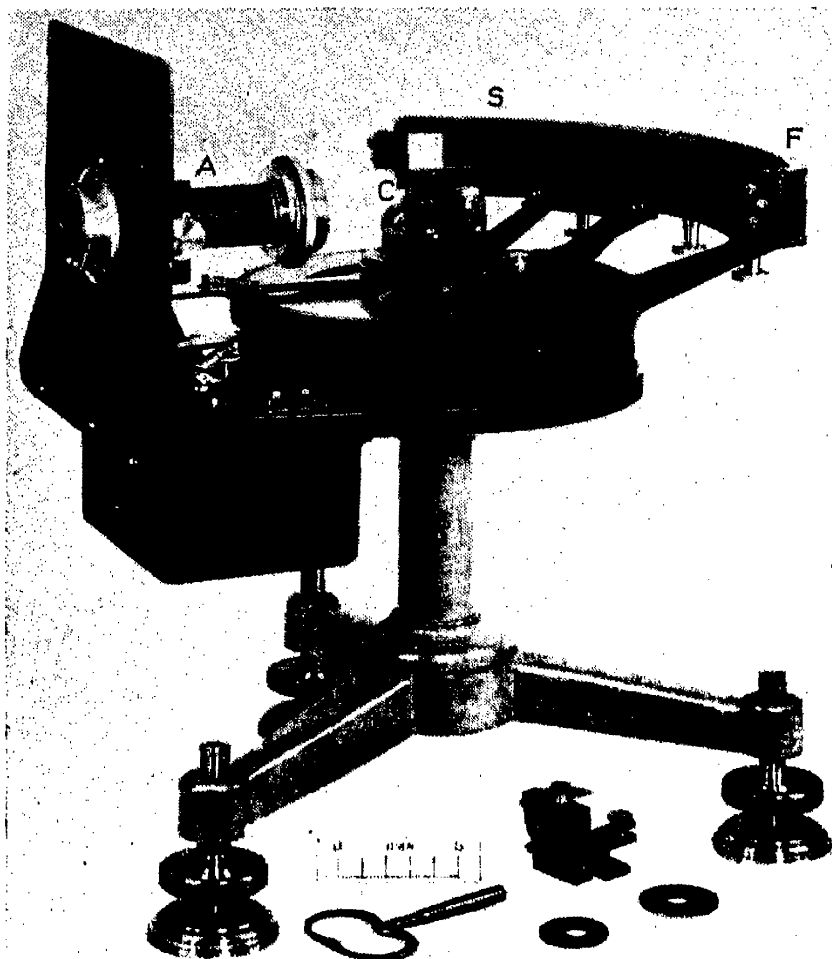


FIG. 19-1.—Professor Laby's x-ray spectrograph. (Courtesy of Adam Hilger, Ltd., London, England, manufacturers of the instrument.)

Figure 19-1 shows the x-ray spectrograph that was designed for this work by Laby. In order to reduce fogging of the film by scattered and secondary radiation, the film is protected by a curved lead screen geared to swing in front of it with twice the angular velocity of the central crystal. An opening in this lead screen permits the rays "reflected" from the crystal face to reach the film. A is the collimating slit assembly,

*physik Chem.*, **118**, 257 (1925); H. Stintzing, *Physik Z.*, **27**, 844 (1926); G. v. Hevesy, "Chemical Analysis by X-rays and Its Applications," McGraw-Hill Book Company, Inc., New York, 1932; R. Glocker, "Materialprüfung mit Röntgenstrahlen," pp. 113-132, 2d ed., Verlag Julius Springer, Berlin, 1936.

<sup>1</sup> T. H. Laby, C. E. Eddy, and A. H. Turner, *Proc. Roy. Soc. (London) A*, **124**, 249 (1929), **127**, 20 (1930), **135**, 637 (1932); *Trans. Faraday Soc.*, **26**, 497 (1930).

$C$  the crystal turntable,  $F$  the cylindrical film holder, and  $S$  the swiveling lead shield. Figure 19-2 shows the copper  $K_\alpha$  lines at the left, as photographed in the x-ray spectrum from a zinc sample containing only 0.0007 per cent copper.

Below atomic number 22, the K lines become so soft ( $2\frac{1}{2}$  Å.) that they are almost completely absorbed by a few inches of air, making it necessary to work with a vacuum spectrograph.<sup>1</sup> Above atomic number 75, the K excitation potential exceeds the 80 kv.p. for which the tube of Laby, Eddy, and Turner was designed, and the K wave lengths become too short for accurate measurement; however, the L lines might be used to analyze for elements up through uranium. A technique that requires the machining of a new target from the sample metal or alloy is too elaborate to be very practical except for special cases. Other variations in the technique are to (1) expose the sample to the high-voltage cathode rays from a Lenard ray tube (Sec. 7-5) to excite its characteristic x-ray spectrum; (2) place the unknown inside the tube, not on, but near, the target, so as to make it emit secondary x-rays by fluorescence from the primary rays; (3) excite secondary x-rays from the unknown by placing it outside the tube (these are so feeble that the exposure time becomes impractically long); (4) use the unknown as an absorber and detect its absorption edges by x-ray spectroscopy.<sup>2</sup>



FIG. 19-2.—Copper  $K_\alpha$  lines in the spectrum of a zinc alloy containing only 0.0007 per cent copper. (Laby, Eddy, and Turner; courtesy of the Royal Society.)

X-ray spectroscopy is the best method known for analyzing a substance for the presence of undiscovered elements, for Moseley's law (page 47) predicts accurately the wave length of the K and L lines of such elements, even though nobody ever had a sample for experimentation. The simplicity of x-ray spectra as contrasted with the complex optical spectrum of elements such as iron is also an important advantage. Elements that have already been discovered by means of x-ray spectroscopy include illinium (61), hafnium (72), masurium (43), and rhenium (75).

**3. The Hanawalt Method.** Up to the year 1938, the great wealth of data that had been amassed by crystal analysts was listed in the tables in the form of lattice constants or unit-cell configurations. This was very well indeed, unless one happened to be interested in identifying

<sup>1</sup> See, for example, C. M. Olson and W. C. Pierce, *Rev. Sci. Instruments*, **8**, 147 (1937).

<sup>2</sup> For a variation of this method, see H. A. Liebhafsky and F. H. Winslow, *Gen. Elec. Rev.*, **48**, 36 (April, 1945).

some unknown material from which he had obtained an x-ray diffract pattern. In this case, if he suspected that the unknown might be  $\text{Cr}_2\text{O}_3$  for example, he would naturally want to compare the  $d$  values and intensities of the various reflections in the pattern of the unknown with those in the pattern of  $\text{Cr}_2\text{O}_3$ . But these data were not in the table although obviously they were the foundation upon which all the other superstructure of statistics had been laboriously erected.

This ironic situation was remedied in 1938 when Hanawalt, Rinn, and Frevel published<sup>1</sup> the table that was so badly needed, listing the  $d$  values and their intensities for all the more prominent reflections in powder patterns of 1,000 common chemical substances. In this table when one looks up  $\text{Cr}_2\text{O}_3$ , for example, he finds that the  $d$  values and their relative intensities (in parentheses) are given as follows: 3.62 (45 per cent); 2.67 (70 per cent); 2.47 (70 per cent); 2.17 (30 per cent); 2.03 (4 per cent); 1.81 (45 per cent); 1.67 (100 per cent); 1.58 (6 per cent); 1.465 (30 per cent); 1.432 (45 per cent); 1.294 (16 per cent); 1.236 (6 per cent); 1.172 (5 per cent), etc. The intensity of the strongest reflection in the pattern (1.67) is also given an absolute value of 50 for comparison with the intensities of the stronger reflections for the other substances, for example, 150 for the strongest reflection in the  $\text{NaCl}$  pattern at 2.81 Å. As with most tables, this one is based on

$$d_{(100)\text{rock salt}} = 2.814 \text{ Å.},$$

rather than 2.820 Å. If it turns out that the powder pattern of the unknown yields these same spacings with corresponding intensities, the analysis is quickly completed—the unknown is mostly or entirely  $\text{Cr}_2\text{O}_3$ . For simple identification work of this sort, any type of transmission powder pattern will serve. For example, the flat-plate powder pattern in Fig. 19-3 is readily identified as the pattern of Al by computing the  $d$  values roughly and comparing them with those listed for  $\text{Al}_2\text{O}_3$  in the table.

Four questions immediately arise, however. (1) How does one proceed when he has no suspicion that the unknown might be  $\text{Cr}_2\text{O}_3$ ? that is, suppose there is no information at all to guide one, except the pattern? (2) Among the thousands of chemical compounds, is it possible that the x-ray patterns of some might be almost identical with the pattern of some other substance? (3) What is the procedure when the unknown is a mixture of two or three substances? (4) Is the method quantitative or only qualitative? These points will be considered in order.

Regarding the first point, it is obvious that a person having a pattern

<sup>1</sup> J. D. Hanawalt, H. W. Rinn, and L. K. Frevel, *Ind. and Eng. Chem., Anal.*, **10**, 457 (1938); see also **16**, 209 (1944); see also Appendix X.



of an unknown, with no other evidence giving a clue to its identity, would desire a table listing the substances which have specified  $d$  values rather than the  $d$  values for a specified substance. His problem is similar to that of determining the identity of the party having telephone number Chestnut 43587 from a metropolitan telephone directory. If it is likely that analyses by x-ray diffraction are to be undertaken frequently, the advisable procedure is to prepare an index book of the type suggested in the Hanawalt-Rinn-Frevel article. This enables one to find quickly the

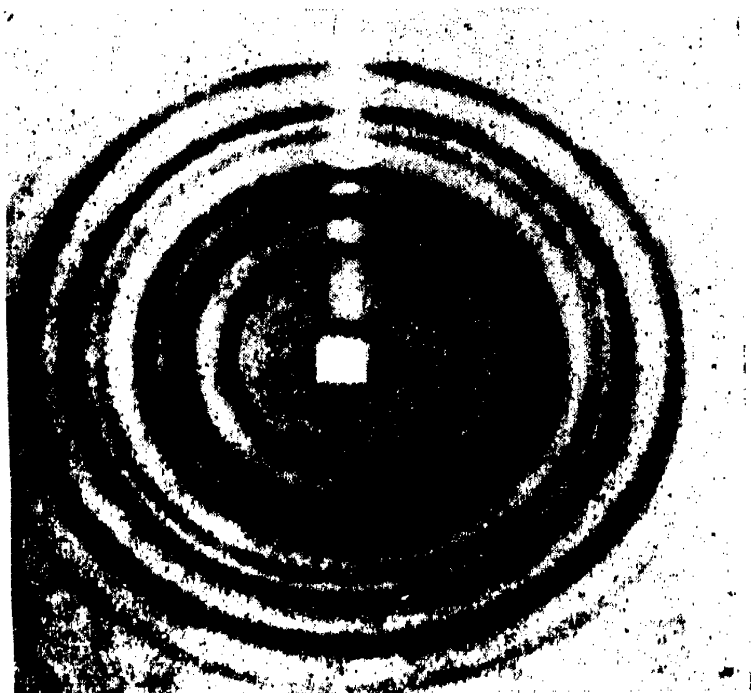


FIG. 19-3.—Flat cassette powder pattern of  $\text{Al}_2\text{O}_3$ .

compound having a powder pattern in which the three most intense reflections, in order of decreasing intensity, are  $d_1$ ,  $d_2$ , and  $d_3$ . For example, if the strongest line corresponds to  $d_1 = 2.68$  Å., the second strongest to  $d_2 = 2.45$  Å., and the third strongest to  $d_3 = 1.66$  Å., one merely turns to the section of the book designated as major group 2.70-2.65 because  $d_1$  falls in this range. Next, in this section of the book, one looks under subgroup 2.50-2.45 because  $d_2$  falls in this range. There, one immediately finds the compound  $\text{Ag}_3\text{PO}_4$  listed, with its third strongest line listed as  $d_3 = 1.66$  Å., thus checking the  $d_3$  value given above. The tables were not published in this form, for this type of table occupies several hundred pages in contrast to the 40 pages required for the table as published. The reversed form of the table is so much bulkier because of the numerous unoccupied subgroups. For example, no compounds are listed for which  $d_1$  lies between 3.30 and 3.40 Å. and  $d_2$  lies between 2.80 and 2.85 Å.; yet space must be provided in the table for such a compound, in case one should exist. Since the

labor involved in preparing an index book is considerable, it may be deemed preferable to purchase its equivalent in card-index form, as offered for sale by the A.S.T.M., Philadelphia, Pa. The A.S.T.M. index is also brought up to date from time to time and now contains over 2,000 compounds.

Figure 19-4 shows an index book opened for inspection. The major group is listed at the top of the pages as "group 3.40-3.30." There are 77 of the major groups, as suggested by Hanawalt-Rinn-Frevel,

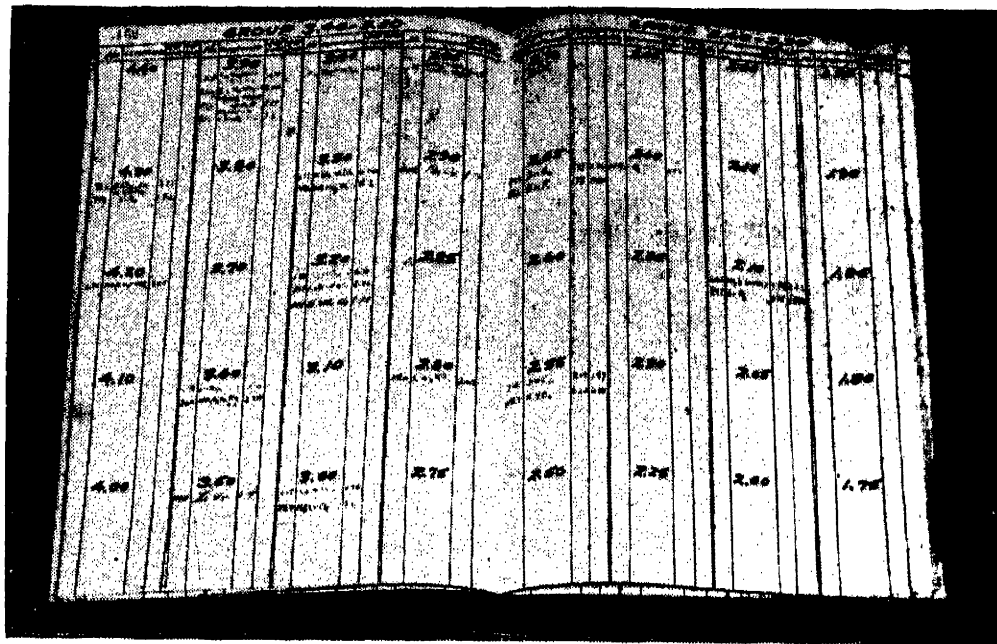


FIG. 19-4.—Index book for chemical analysis by the Hanawalt method.

each occupying five pages in the book shown in the figure. Each major group is in turn divided into 77 subgroups, 40 of which are seen in the figure, the other 37 being on other pages. Of the 40 shown, 23 are seen to be unoccupied; 8 list 1 compound, 7 list 2 compounds, 1 lists 3, and 1 lists 4. Of the  $77^2 = 5,929$  subgroups in the book, only 27 contain more than 3 compounds out of the 1,000 listed in the original publication. One of these is seen to be the 3.90–3.80 Å. subgroup in the figure, which lists  $C_1H_4(OH)COONH_4$ ,  $C_2H_5NH_3Cl$ ,  $MgCl_2 \cdot NH_4Cl \cdot 6H_2O$ , and telluric nitrate. These are readily distinguished by the fact that  $d_3$  differs widely among them, being 10.9, 3.00, 2.73, and 7.3 Å., respectively, for the 4 compounds. This is typical. The  $d_3$  values are listed in the column immediately following the name of the compound in the table. For a few compounds,  $d_1$ ,  $d_2$ , and  $d_3$  are nearly the same. (One of these rare cases is seen in the figure in the 2.65–2.60 Å. subgroup, which lists  $SnO_2$  and  $ZnF_2$ . For  $SnO_2$ ,  $d_1 = 3.34$ ,  $d_2 = 2.64$ , and  $d_3 = 1.75$ ; for  $ZnF_2$ ,  $d_1 = 3.33$ ,  $d_2 = 2.60$ , and  $d_3 = 1.75$  Å. In cases like this, the fourth most intense line has its spacing  $d_4$  listed after the entry of the compound in the book. For  $SnO_2$ ,  $d_4 = 2.36$  Å., whereas, for  $ZnF_2$ ,  $d_4 = 1.405$  Å.

Thus references to the fourth line should dispel any doubt in such cases. These facts answer the second question proposed on page 424.

At the end of each major group in the index book, there is listed a "supplementary group index" for that group. One of these is illustrated for the major group 2.95-2.90 in the lower part of Fig. 19-5. It is helpful in cases where there may be some doubt as to the relative intensities of the three strongest lines, so that one may be uncertain which is  $d_2$  and which is  $d_3$ , for example. This occurs chiefly in the analysis of mixtures. When the intensities of two lines for a given compound have equal intensities, the established rule is to give preference to the larger  $d$  value. For example, the three strongest lines for  $\text{SnO}_2$  correspond to  $d = 0.34$  A. (100 per cent),  $d = 2.64$  A. (63 per cent), and  $d = 1.75$  A. (63 per cent). In this case,  $d_2 = 2.64$  and  $d_3 = 1.75$  simply because 2.64 is greater than 1.75, the relative intensities being equal (both 63 per cent).

Regarding the third point, the procedure with mixtures is explained in detail by Hanawalt, Rinn, and Frevel. They give the following example. Suppose the pattern of the unknown mixture yields the  $d$  values and corresponding relative intensities listed in Table 19-1. Turning to group 2.95-2.90 (shown in condensed form in the upper part of

TABLE 19-1\*

Unknown			
$d$	$I_x$	$d$	$I_x$
4.65	12	1.82	8
3.79	25	1.75	60
3.28	60	1.71	4
2.93	100	1.63	2
2.67	40	1.58	20
2.52	100	1.54	3
2.32	100	1.50	30
2.18	30	1.465	3
2.07	4	1.430	12
1.97	12	1.406	20
1.86	20	1.372	20

\* Courtesy of J. D. Hanawalt and the American Chemical Society.

Fig. 19-5), one notes no compound in subgroup 2.55-2.50 that has a third line agreeing with any of those in the unknown. The same is true for subgroup 2.35-2.30. However, in subgroup 3.30-3.20,  $\text{NaClO}_3$  has a third line at 1.76, as compared with the 1.75 line listed for the unknown. This indicates that one of the components of the mixture

## Group 2.95-2.90.

Compound	3rd line	4th line	Compound	3rd line	4th line	Compound	3rd line	4th line	Compound	3rd line	4th line
20.00-15.00			4.40-4.30			2.80-2.75			1.90-1.85		
15.00-12.00			4.30-4.20			Sn	2.01	2.05	1.85-1.80		
12.00-10.00			NaIO <sub>3</sub>	3.19	1.66	CaC <sub>2</sub> II	1.95	2.09	NaN <sub>3</sub>	2.42	2.18
10.00-9.00			4.20-4.10			2.75-2.70	4.09	3.88	1.80-1.75		
9.00-8.50			4.10-4.00			2.70-2.65			In <sub>2</sub> O <sub>3</sub>	1.52	2.52
8.50-8.00			Pb <sub>3</sub> (PO <sub>4</sub> ) <sub>2</sub>	3.61	3.31	2.65-2.60			1.75-1.70		
8.00-7.50			4.00-3.90			2.60-2.55			1.70-1.65		
7.50-7.00			3.90-3.80			NaHCO <sub>3</sub>	3.48	3.04	CsCl	4.11	2.05
7.00-6.50			3.80-3.70			2.55-2.50			1.65-1.60		
P <sub>2</sub> S <sub>5</sub>	4.90	4.05	CdCO <sub>3</sub>	1.83	2.46	Th	1.79	1.52	1.60-1.55		
6.50-6.00			3.70-3.60			2.50-2.45			1.55-1.50		
HgSO <sub>4</sub> ·2HgO	5.5	3.33	Ba(ClO <sub>4</sub> ) <sub>2</sub> ·3H <sub>2</sub> O	2.14	1.92	K <sub>2</sub> C <sub>2</sub> O <sub>4</sub>	2.32	2.62	1.50-1.45		
6.00-5.75			3.60-3.50			2.45-2.40			1.45-1.40		
5.75-5.50			3.50-3.40			2.40-2.35			1.40-1.35		
5.50-5.25			3.40-3.30			2.35-2.30			1.35-1.30		
Na <sub>2</sub> S <sub>2</sub> O <sub>3</sub> ·5H <sub>2</sub> O	2.84	2.76	C <sub>16</sub> H <sub>8</sub> O <sub>2</sub> N <sub>2</sub> (SO <sub>3</sub> K) <sub>2</sub>	3.00	2.22	2.30-2.25			1.30-1.25		
5.25-5.00			3.30-3.20			2.25-2.20			1.25-1.20		
5.00-4.90			NaClO <sub>3</sub>	1.76	2.68	2.20-2.15			1.20-1.15		
4.90-4.80			3.20-3.10			Na <sub>2</sub> B <sub>4</sub> O <sub>7</sub> ·5H <sub>2</sub> O	4.40	3.44	1.15-1.10		
4.80-4.70			3.10-3.00			2.15-2.10			1.10-1.05		
4.70-4.60			3.00-2.95			2.10-2.05			1.05-1.00		
4.60-4.50			2.95-2.90			2.05-2.00			1.00-.90		
4.50-4.40			2.90-2.85			2.00-1.95			.90-.80		
			2.85-2.80			1.95-1.90			.80-		
(C <sub>6</sub> H <sub>4</sub> CO <sub>2</sub> ) <sub>2</sub> BONa	3.45	2.18									

## Supplementary Group Index 2.95-2.90.

Compound	1st line	2nd line	3rd line	Compound	2nd line	1st line	3rd line	Compound	3rd line	1st line	2nd line
P <sub>2</sub> S <sub>5</sub>	2.90	6.7	4.90	Mg <sub>3</sub> (PO <sub>4</sub> ) <sub>2</sub> ·8H <sub>2</sub> O	2.94	6.7	2.69	C <sub>6</sub> H <sub>4</sub> (CO) <sub>2</sub> NK	2.90	14.5	6.4
HgSO <sub>4</sub> ·2HgO	2.92	6.2	5.5	MnCl <sub>2</sub> ·H <sub>2</sub> O	2.93	5.7	2.55	Bi(C <sub>2</sub> H <sub>3</sub> O <sub>2</sub> ) <sub>3</sub>	2.90	13.5	3.35
Na <sub>2</sub> S <sub>2</sub> O <sub>3</sub> ·5H <sub>2</sub> O	2.93	5.4	2.84	BaCl <sub>2</sub> ·2H <sub>2</sub> O	2.91	4.48	2.54	AgC <sub>2</sub> H <sub>3</sub> O <sub>2</sub>	2.91	10.0	3.04
(C <sub>6</sub> H <sub>4</sub> CO <sub>2</sub> ) <sub>2</sub> BONa	2.94	4.40	3.45	Mg(NO <sub>3</sub> ) <sub>2</sub> ·6H <sub>2</sub> O	2.93	4.42	3.29	Ba(CN) <sub>2</sub>	2.94	9.4	3.37
NaIO <sub>3</sub>	2.93	4.25	3.19	MgSO <sub>4</sub> ·6H <sub>2</sub> O	2.92	4.40	4.04	SnCl <sub>4</sub> ·5H <sub>2</sub> O	2.94	6.2	5.3
Pb <sub>3</sub> (PO <sub>4</sub> ) <sub>2</sub>	2.91	4.03	3.61	KH <sub>2</sub> PO <sub>4</sub>	2.90	3.72	1.95	CoCl <sub>2</sub> ·6H <sub>2</sub> O	2.94	5.6	4.85
CdCO <sub>3</sub>	2.94	3.77	1.83	α-ZnS	2.91	3.29	1.76	CuOH·CuPO <sub>4</sub>	2.91	4.81	2.63
Ba(ClO <sub>4</sub> ) <sub>2</sub> ·3H <sub>2</sub> O	2.90	3.05	2.14	PbO	2.93	3.06	2.72	MgNH <sub>4</sub> PO <sub>4</sub> ·6H <sub>2</sub> O	2.93	4.28	2.69
C <sub>16</sub> H <sub>8</sub> O <sub>2</sub> N <sub>2</sub> (SO <sub>3</sub> K) <sub>2</sub>	2.90	3.35	3.00	CaC <sub>2</sub> III	2.92	2.86	2.05	HgCl <sub>2</sub> ·3HgO	2.92	3.95	2.70
NaClO <sub>3</sub>	2.94	3.28	1.76	Hg <sub>2</sub> PO <sub>4</sub>	2.94	2.60	3.09	PbHASO <sub>4</sub>	2.93	3.39	3.17
Sp	2.91	2.79	2.01					K <sub>2</sub> S <sub>2</sub> O <sub>7</sub>	2.90	3.23	3.07
CaC <sub>2</sub> II	2.93	2.79	1.95					Ag <sub>2</sub> CrO <sub>4</sub>	2.92	3.14	3.02
Na <sub>2</sub> CrO <sub>4</sub>	2.91	2.73	4.09					K <sub>2</sub> SeO <sub>3</sub>	2.94	3.08	4.35
NaHCO <sub>3</sub>	2.94	2.58	3.49					(NH <sub>4</sub> )HC <sub>2</sub> O <sub>4</sub> ·H <sub>2</sub> O	2.90	3.00	6.2
Th	2.92	2.53	1.79					Li <sub>2</sub> CO <sub>3</sub>	2.91	2.80	4.16
K <sub>2</sub> C <sub>2</sub> O <sub>4</sub>	2.92	2.46	2.32					Na <sub>2</sub> SiO <sub>3</sub> ·9H <sub>2</sub> O	2.92	2.79	3.83
Na <sub>2</sub> B <sub>4</sub> O <sub>7</sub> ·5H <sub>2</sub> O	2.94	2.19	4.40								
NaN <sub>3</sub>	2.91	1.82	2.42								

FIG. 19-5.—(Davey) Sample page from imaginary classification book. (Courtesy of American Institute of Physics.)

may be  $\text{NaClO}_3$ . To confirm this, one consults the Hanawalt-Rinn-Frevel tables as published and finds listed for  $\text{NaClO}_3$  the spacings given in Table 19-2. The correspondence leaves no doubt that one component of the mixture is  $\text{NaClO}_3$ .

TABLE 19-2\*

$\text{NaClO}_3$							
$d$	$I$	$d$	$I$	$d$	$I$	$d$	$I$
4.65	20	2.32	1	1.83	7	1.51	11
3.79	33	2.18	33	1.76	67	1.47	3
3.28	67	2.07	7	1.64	1	1.434	13
2.94	100	1.98	13	1.59	11	1.404	1
2.68	40	1.89	1	1.55	3	1.341	1

\* Courtesy of J. D. Hanawalt and the American Chemical Society.

The strongest line in the unknown not accounted for is at 2.52 Å., and the 2.32 line is very strong in the unknown but very weak for  $\text{NaClO}_3$ . Hence one turns to major group 2.55–2.50, subgroup 2.35–2.30, and finds  $\text{CuO}$  listed with a third line at 1.86. This indicates that one of the

TABLE 19-3\*

$\text{CuO}$			
$d$	$I$	$d$	$I$
2.51	100	1.50	15
2.31	100	1.408	20
1.85	20	1.370	20
1.70	8	1.298	5
1.57	8	1.258	10

\* Courtesy of J. D. Hanawalt and the American Chemical Society.

components of the mixture may be  $\text{CuO}$ . To confirm this, one consults the original tables and finds listed for  $\text{CuO}$  the spacings given in Table 19-3. These two compounds together account for all the spacings listed in Table 19-1, and so the mixture is found to consist primarily of  $\text{NaClO}_3$  and  $\text{CuO}$ . When some of the more intense lines are superposed (same  $d$  values), the procedure is slightly more complex and is described by Hanawalt, Rinn, and Frevel.

Regarding the fourth question on page 424, the method is probably best described as semiquantitative. In mixtures, one must consider

the possibility of differences in the absolute intensity of the lines in various patterns, due to (1) different exposure times, tube voltages, or currents; (2) different sample thickness or dilution; and (3) different structure factor. To help allow for (3), Hanawalt, Rinn, and Frevel have listed the absolute intensities, as well as the relative intensities of the three strongest lines in their patterns. For example, the absolute intensities of the three strongest reflections for nickelous tartrate are given as 8, 4, and 3, whereas those for NiO are given as 125, 75, and 75. Therefore, in a mixture of these two compounds, if the strongest line of nickelous tartrate were just about as intense as the strongest line of NiO, one would conclude that the mixture was roughly 15 parts nickelous tartrate, say, to 1 part NiO.

Returning to the  $\text{NaClO}_3$ -CuO example, however, the strongest lines of these two compounds are rated 75-50-50 and 62.5-62.5-12.5, respectively, for absolute intensity. In the pattern of the unknown (Table 19-1), the strongest  $\text{NaClO}_3$  line (2.94 Å.) and the strongest CuO line (2.51 Å.) were both rated 100 per cent for relative intensity. From this, one may safely conclude that the mixture is roughly in 50-50 proportions. At any rate, it is not 90 per cent  $\text{NaClO}_3$  and 10 per cent CuO, or vice versa. One can make fairly accurate quantitative analyses by preparing a series of known samples (such as 65 per cent  $\text{NaClO}_3$  + 35 per cent CuO, 60 per cent  $\text{NaClO}_3$  + 40 per cent CuO, etc.) and comparing their patterns with that of the unknown. When a perfect match is obtained, then the compositions of the known and unknown are nearly the same.

Hanawalt has pointed out that the chief limitation of the method is that, among the common inorganic substances, some have weak patterns like that from a liquid; it is commonly said that they are "amorphous." As a general rule, most compounds must be present in sufficient abundance to constitute about 5 per cent of the sample by weight before they reveal their presence in the pattern. In a few cases, 1 or 2 per cent can be detected, as with a highly crystalline material mixed with ninety-nine times its weight of some material with a weak pattern. On the other hand, amorphous materials like flour may not reveal themselves even at 50 per cent. On the positive side, the presence of the pattern of AgCl, for example, proves that it is present, although there may also be a little or much amorphous material mixed with it or in solid solution in it (see Sec. 5). On the negative side, however, if the strongest line of a certain compound is absent, one can only say that the compound probably constitutes less than 10 per cent of the sample (although it may be absent entirely, of course) if he knows from previous experience that that compound has a strong, clear pattern in low concentrations. If a definite lower limit is important to establish, then again the best

plan is to prepare a series of known samples and see at what concentration the strongest line of the compound in question finally vanishes.

This method is most valuable as an accessory method in the usual chemical laboratory or when used in coordination with optical spectrographic analysis and microscopic examination. It is simple, rapid, and inexpensive.

**4. A.S.T.M. Recommended Practice for the Hanawalt Method.** The tentative draft of the A.S.T.M.<sup>1</sup> "Recommended Practice" for the Hanawalt method raises the following points: The method may miss amorphous phases and solid solutions. The sample should be ground in an agate mortar to pass 200-mesh silk bolting cloth. If it is not brittle enough to grind, one may use filings. Load sample in glass (for example, Pyrex) tube 0.4 to 0.6 mm. inside diameter with walls less than 0.1 mm. thick. For long-wave-length radiation, mix with 10 per cent powdered gum tragacanth or collodion, and extrude in 0.5-mm. cylinder or mount on hair with Zapon lacquer. Exercise care with flakes and long fragments (metal filings, graphite, clays, mica, etc.) because of the possibility of preferential orientation causing false relative intensities (see next chapter); rotate the sample in such cases. For ionization chamber or Geiger-Mueller counter, use a flat sheet specimen and Soller slits (page 398). For high-atomic-weight material, dilute with flour, cornstarch, or gum tragacanth. For molybdenum radiation, operate at about 42 kv.p., and use  $\text{ZrO}_2$  filter.

Have slits wide enough to let primary rays bathe the complete specimen. Use guarded second slit. Place filter between specimen and film, not touching film. Use cylindrical film, its axis being the axis of the specimen and the film radius being between 5 and 20 cm. Use small film radius for soft radiation such as copper.<sup>2</sup> If film radius is 5.73 cm., then 1 mm. on film equals  $1^\circ$  for the angle  $2\theta$  (Fig. 18-9). Use nonscreen x-ray film without screens. Develop by time-and-temperature technique—not by removing film from developer when it "looks good" under the safelight. If intensifying screen is used, place it behind film in close contact. Clean Fluorazure screens are best. Instead of measuring from the central beam spot to the various lines or arcs on the film, it is better to obtain lines on both sides of the central beam, measure between corresponding lines, and divide by 4 to obtain  $\theta$ . Film expansion

<sup>1</sup> A.S.T.M. Standards, 1942, part 1, p. 1537.

<sup>2</sup> In this connection, Hanawalt, Rinn, and Frevel obtained the patterns for their tables using molybdenum radiation and cameras with an 8-in. radius. They state that "molybdenum radiation and a large camera radius makes possible the rapid measurement of the position of the lines on a scale, whereas use of a small precision camera and a comparator is not only tedious but also makes the measurement of weak lines very difficult."

troubles are lessened by recording a standard pattern such as that of NaCl on the same film. When there is extreme variation in line intensity, make a short exposure for the strong lines and a long one for faint lines.

For semiquantitative work, match lines against a calibrated film strip (see next section). Direct comparison with pattern of prepared known is necessary if one desires to approximate quantitative analysis.

For speeding up analyses, Seemann-Bohlin cameras may be used, or sheet specimens with Soller slits; also Geiger-Mueller counters, or ionization chambers equipped with Ross filters (see next section). Single slits should be no more than  $\frac{1}{2}$  mm. in width, and each slit of a Soller system should be not over  $\frac{1}{2}$  mm. in width.

**5. Additional Information Regarding the Hanawalt Method.** Hanawalt, Rinn, and Frevel recommend that the intensities of the lines in the pattern be measured by comparing them with a calibrated intensity scale. Such a scale can be prepared readily, by using a strip of the same x-ray film used in the diffraction cameras. A small section near one end of the strip is exposed to the same filtered radiation used by the camera for a time  $t$  just long enough to give noticeable darkening after development. Then the adjacent section can be exposed to the same radiation for  $2t$ , the next section for  $3t$ , the next for  $4t$ , etc.,<sup>1</sup> until at the opposite end of the film strip it will be practically opaque after development. According to Charlesby's curves (Fig. 9-5), this should yield nearly equal steps of increasing film density. Whether this is true or not, however, one may classify the lines of a diffraction pattern for intensity by comparing them with such a scale and deciding whether a given line has a density closer to step 8 or step 9, for example. This method of measuring intensities is simple, fast, and sufficiently accurate. Independent observers are found to obtain almost identical readings from such a scale.

When the highest possible accuracy of film-density measurement is desired, the use of a microphotometer is to be recommended.<sup>2</sup> Such instruments range from simple densitometers to the more complex recording microphotometers. They all measure the percentage of a narrow beam of light of constant intensity that is transmitted by any given small area of the test film. The reciprocal of this is the opacity, and the common logarithm of the opacity is the density, which is nearly proportional to exposure, for x-rays. The literature describing micro-

<sup>1</sup> A calibrated rotating sector disk for this purpose is described by J. M. Robertson, *J. Sci. Instruments*, **20**, 175 (1943), Fig. 5.

<sup>2</sup> For details of its application to chemical analysis by x-ray diffraction, see S. T. Gross and D. E. Martin, *Ind. and Eng. Chem., Anal. Ed.*, **16**, 95 (1944); also J. C. M. Brentano, *J. Optical Soc. Am.*, **35**, 382 (1945).



photometers and densitometers for x-ray diffraction work is extensive.<sup>1</sup> A recording microphotometer record obtained by Ballard, Oshry, and Schrenk is shown in Fig. 19-6.

When accuracy of intensity measurement is of paramount interest, it is often best to avoid photographic methods and use an ionization chamber or Geiger-Mueller counter. In diffraction work, the accuracy

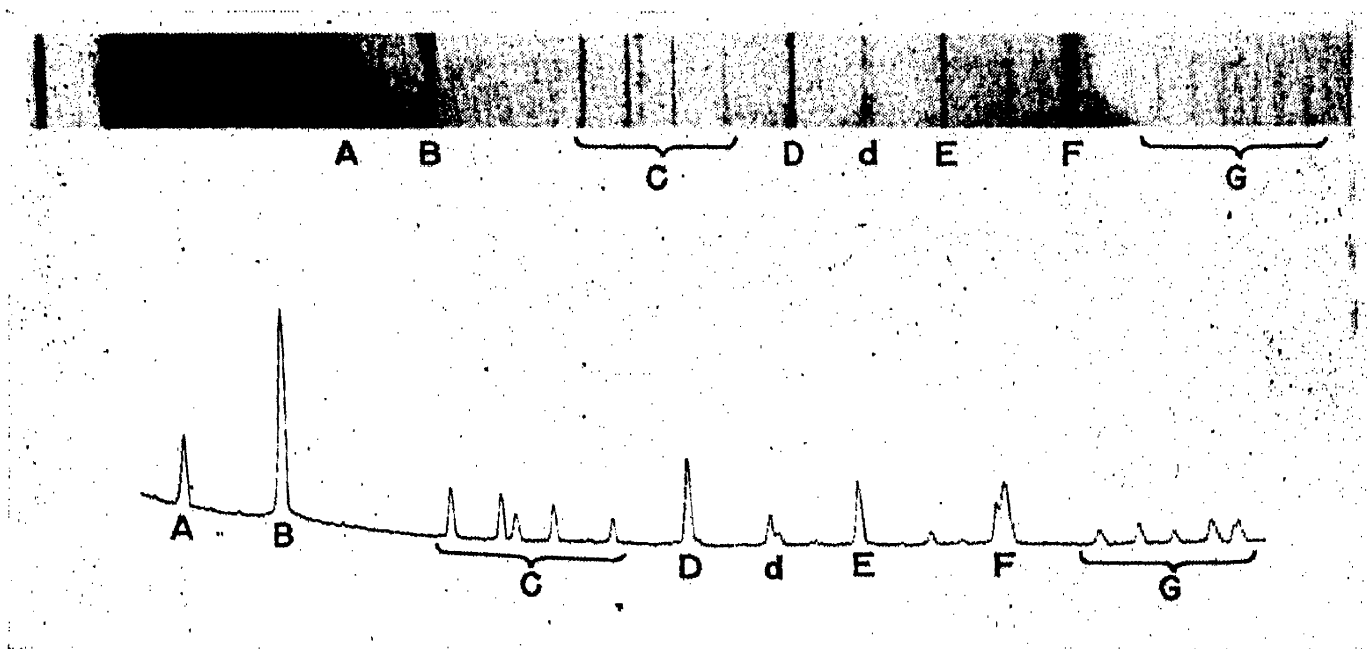


FIG. 19-6.—Powder pattern of quartz (above), and the microphotometer tracing of the pattern (below). (J. W. Ballard, H. I. Oshry, and H. H. Schrenk; courtesy of U.S. Bureau of Mines.)

of these devices for recording intensities can be considerably enhanced by making use of a device known as the "Ross filter"<sup>2</sup> or "balanced filter." This is in reality two filters, usually mounted in a turret so that either one or the other can be quickly inserted into the x-ray beam as it enters the ionization chamber or Geiger-Mueller counter. For molybdenum radiation, a common combination is zirconium and strontium, having their K absorption edges at 614 and 767 X.U., respectively. It is important to adjust the thicknesses of the two filters so that, above 767 and below 614 X.U., both absorb nearly the same proportion of the

<sup>1</sup> See, for example, J. W. Ballard, H. I. Oshry and H. H. Schrenk, *U.S. Bur. Mines, Bull.* RI 3638; J. M. Robertson, *J. Sci. Instruments*, **18**, 126 (1941); A. H. Jay, *J. Sci. Instruments*, **18**, 128 (1941); M. Spiegel-Adolf and R. H. Peckham, *Ind. and Eng. Chem., Anal. Ed.*, **12**, 182 (1940); E. E. Berkley and O. C. Woodyard, *Ind. and Eng. Chem., Anal. Ed.*, **30**, 451 (1938); H. R. Ronnebeck, *J. Sci. Instruments*, **20**, 154 (1943); J. Brentano, A. Baxter, and F. W. Cotton, *Phil. Mag.*, **17**, 370 (1934); J. C. M. Brentano, *Rev. Sci. Instrument*, **16**, 309 (1945).

<sup>2</sup> P. A. Ross, *Phys. Rev.*, **28**, 425 (1926); *J. Optical Soc. Am. and Rev. Sci. Instruments*, **16**, 433 (1928); for detailed discussion, P. Kirkpatrick, *Rev. Sci. Instruments*, **10**, 186 (1939), **15**, 223 (1944).

x-ray beam. Between 614 and 767 X.U., however, the strontium filter absorbs nearly all the radiation, and the zirconium filter absorbs very little. Consequently, the difference in the two readings obtained from the chamber or counter with one and then the other filter is due almost entirely to x-rays in this limited range of wave lengths. This device therefore eliminates most of the spurious readings from secondary and incoherently scattered radiation.

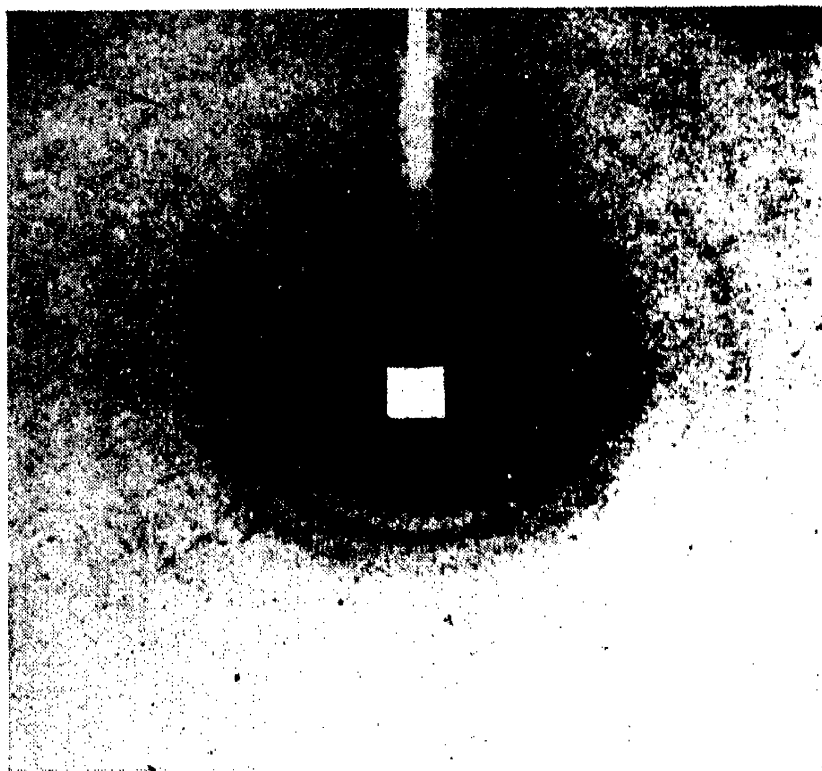


FIG. 19-7.—Pattern of mixture containing one hard, coarse-grained constituent. (Sample not rotated.)

Sometimes a sample is encountered in which one of the components is a hard, coarse-grained material like quartz or carborundum. Such a material may be so hard that an hour or more of vigorous grinding in an agate mortar will fail to reduce the grain size below about a thousandth of an inch. Figure 19-7 is a transmission pattern obtained from a stationary powdered sample using a flat cassette. Although the sample was ground in an agate mortar and passed through a 300-mesh screen, it will be noticed that the pattern consists of numerous rings on which are superposed numerous spots due to some coarse-grained constituent. When the specimen is rotated, the rings remain but the spots disappear. One should be careful not to overlook spots of this sort in the pattern, for they sometimes reveal the presence of some constituent that may be quite significant. As will be seen in the next chapter, crystals that are as small as a thousandth of an inch in diameter and that readily pass through a 300-mesh screen yield spotty patterns. If their concentration

is small, their spotty pattern may wash out entirely when the sample is rotated. The pattern from a stationary sample like Fig. 19-7 will reveal them, although such a spotty pattern is of little help in identifying the material in question. Helpful sampling, mixing, and grinding techniques in the preparation of samples for quantitative analysis by the Hanawalt method have been described by Ballard, Oshry, and Schrenk.<sup>1</sup>

Finally, the possibility of the sample containing amorphous materials or solid solutions must be considered. Because of their amorphous structure, flour, ground glass, or similar materials may be present in the sample in considerable abundance without being detected. An amorphous solid is one that has little or no tendency to crystallize. Sometimes, as in colloids, crystals are present, but they are so small (less than 100 Å. in diameter, say) that their resolving power as a diffraction grating for x-rays is greatly impaired, and the resulting x-ray pattern is indistinct and poorly defined (page 321). This will be considered further in the next chapter.

In the case of alloys, one often encounters samples in the form of a solid solution. For binary alloys (two metals, *A* and *B*), a solid solution is a structure in which the atoms of *B* are irregularly scattered through the lattice of the *A* crystals, or vice versa. In fact, the elements involved need not necessarily be metals. Carbon forms a solid solution in gamma iron, for example. Sometimes the *A* atoms retain their normal positions in the lattice, and the *B* atoms squeeze between them irregularly. This structure is an interstitial solid solution, for example, carbon in gamma iron. More often, however, for small percentages of *B* (usually less than 30 per cent), the *A* atoms are displaced from their normal positions in the crystal lattice and replaced irregularly by *B* atoms. This is a substitutional solid solution, for example, cadmium in silver. In either type of solid solution, the x-ray pattern will be the pattern of *A*, slightly distorted; the pattern of *B* will not appear unless it is also mixed in the sample in pure crystalline form.

When more *B* metal is added and the *B* atoms become sufficiently plentiful in a substitutional solid solution, as in a 50–50 ratio, the atoms usually begin to distribute themselves *regularly* through the *A* lattice, like the chlorine atoms in the cesium lattice in CsCl. Such intermetallic compounds are not ionic, like CsCl, or molecular, like organic compounds, the electrical forces between atoms being of a different character because of the presence of the free electron cloud, characteristic of metals. A new x-ray pattern different from that of either *A* or *B* will result, due to the presence of this type of “geometrical compound,” like CuZn. Such an intermetallic compound forms crystals

<sup>1</sup> J. W. Ballard, H. I. Oshry, and H. H. Schrenk, *J. Opt. Soc. Am.*, **33**, 667 (1943).

that mix in with the solid-solution type of crystals already present, and its presence is revealed by the appearance of numerous new lines in the x-ray pattern, interspersed between the original lines due to the solid solution. An intermetallic compound has a lattice structure characterized by a tendency for the *B* atoms to take up positions with a maximum distance between themselves. This type of intermetallic-compound lattice structure is called a "superlattice." The structures and their patterns will be discussed more fully in Chap. 23.

### QUESTIONS AND PROBLEMS

1. Distinguish between chemical analysis by x-ray spectroscopy and chemical analysis by the Hanawalt method. If a certain mineral is suspected of containing

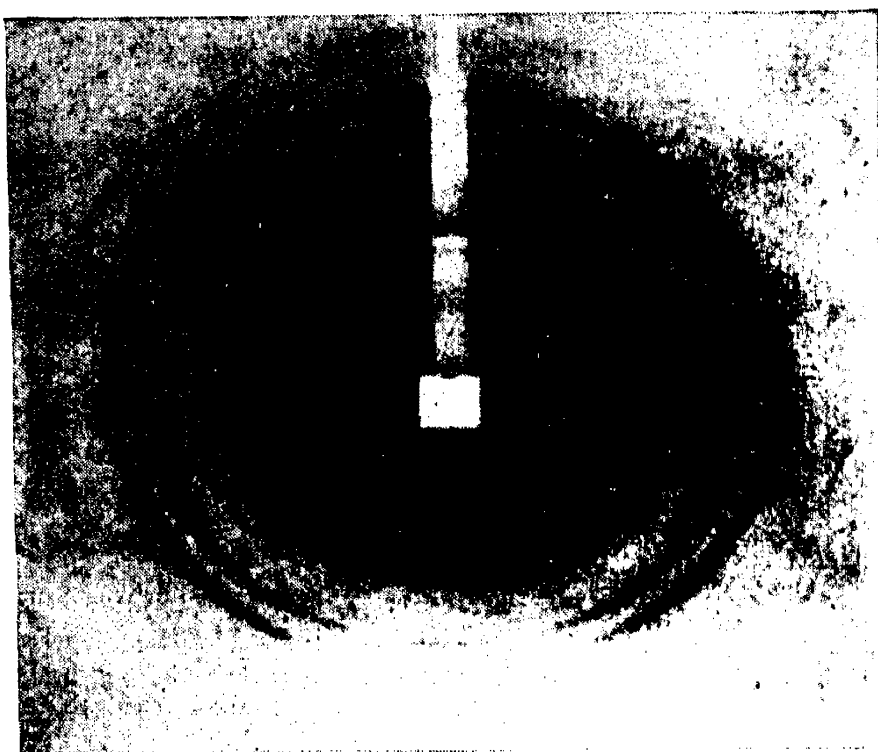


FIG. 19-8.

a small amount of the undiscovered element No. 87, how might one verify or disprove this? Is it possible to detect the presence of a thousandth of 1 per cent of antimony in a copper bar by x-ray methods? If so, how?

2. Since hundreds of elements and compounds had been subjected to crystal analysis by the powder method before 1938, why did the Hanawalt method remain nonexistent until that time? Most of the older methods of chemical analysis would have difficulty distinguishing between (a) a 50-50 mixture of calcium bromide and potassium phosphate, and (b) a 50-50 mixture of calcium phosphate and potassium bromide. How could one distinguish between (a) and (b), using x-rays?

3. What is a bent-crystal spectrograph? What is its chief advantage over ordinary x-ray spectrographs? What is a Ross filter? Explain how it works. What is a superlattice?

4. Figure 19-3 was taken with a sample-to-film distance of  $2\frac{1}{16}$  in., by using molybdenum  $K_{\alpha}$  radiation. Calculate the *d* spacings represented by the various rings, and estimate their intensities as very strong, strong, medium, etc. Compare your results with the following values for  $Al_2O_3$  from the Hanawalt-Rinn-Prevel table: 3.47

(50 per cent), 2.55 (75 per cent), 2.37 (30 per cent), 2.08 (100 per cent), 1.74 (50 per cent), 1.59 (100 per cent), 1.54 (5 per cent), 1.50 (5 per cent), 1.402 (40 per cent), 1.370 (50 per cent), 1.233 (20 per cent), 1.186 (10 per cent).

5. Figures 19-8 and 19-9 were also taken with molybdenum  $K_{\alpha}$  radiation at 2.1 and 2.0 in. distances respectively. From the following Hanawalt data, make a qualitative analysis of the two samples:  $\text{Fe}_3\text{O}_4$ —4.85 (6 per cent), 2.97 (28 per cent), 2.53 (100 per cent), 2.42 (11 per cent), 2.10 (32 per cent), 1.71 (16 per cent), 1.61 (64 per cent), 1.483 (80 per cent), 1.326 (6 per cent), 1.279 (20 per cent), 1.210 (5 per cent), 1.121 (10 per cent), 1.092 (32 per cent); Ag—2.36 (100 per cent), 2.04 (53 per

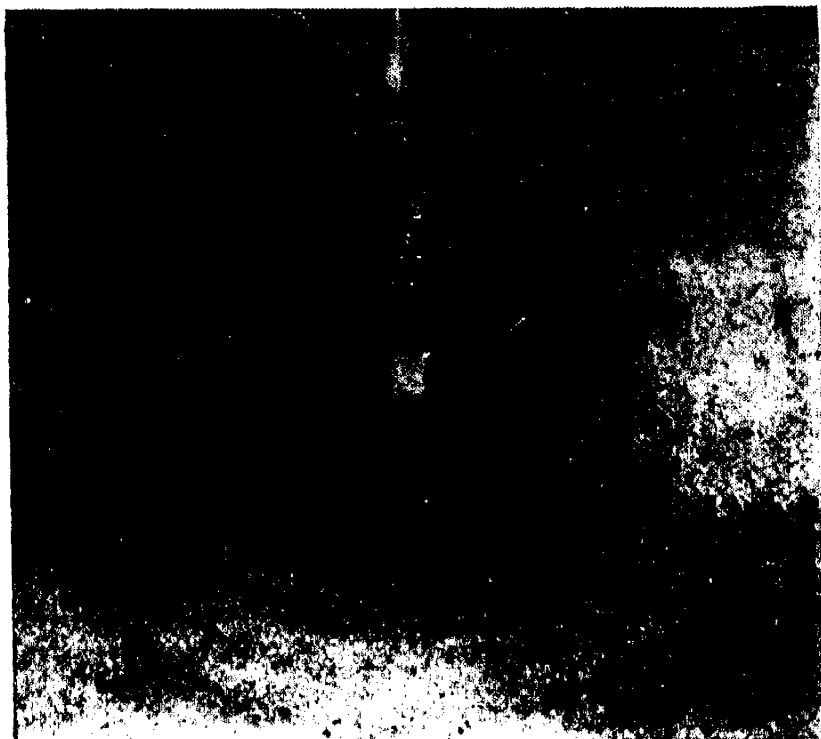


FIG. 19-9.

cent), 1.445 (27 per cent), 1.232 (53 per cent), 1.179 (5 per cent), 1.022 (1 per cent), 0.938 (8 per cent);  $\text{AgCl}$ —3.20 (40 per cent), 2.77 (100 per cent), 1.96 (75 per cent), 1.67 (20 per cent), 1.60 (25 per cent), 1.385 (9 per cent), 1.270 (6 per cent), 1.240 (20 per cent), 1.131 (13 per cent).

6. Explain how to prepare an index book from the Hanawalt-Rinn-Prevel tables. If a sample yields a powder pattern in which no line appears corresponding to  $d = 2.88$  Å. (the strongest reflection for  $\text{K}_2\text{SO}_4$ ), is it necessarily true that no  $\text{K}_2\text{SO}_4$  is present? How can one establish its maximum concentration, roughly?

7. In searching for traces of an abrasive such as  $\text{SiO}_2$ , why might it be better to use a stationary sample rather than a rotating one? Would the presence of ground glass in the sample be readily revealed in the pattern? How does one estimate the intensities of the lines in a powder pattern with a calibrated film strip?

8. If the sample is an 80 per cent Ag–20 per cent Cd alloy, will the Cd reflections appear in the pattern? What is a solid solution? Describe the structure of a substitutional solid solution. How does it differ from a superlattice?

9. Quartz is a hexagonal crystal with lattice constants  $a = 4.903$  Å. and  $c = 5.393$  Å. The Hanawalt-Rinn-Prevel tables list the following four  $d$  values for strong quartz reflections: 4.25 Å. (25 per cent); 3.35 Å. (100 per cent); 2.45 Å. (15 per cent); 1.82 Å. (25 per cent). Determine the Miller-Bravais indices of these four reflections. HINT: See page 349.

## CHAPTER 20

### GRAIN SIZE AND PREFERENTIAL ORIENTATION

**1. Introductory Discussion of Grain Size.** Most solids are composed of tiny crystals, often called “grains,” especially in referring to metals. In general, grains are of irregular shape. Even in a single small piece of

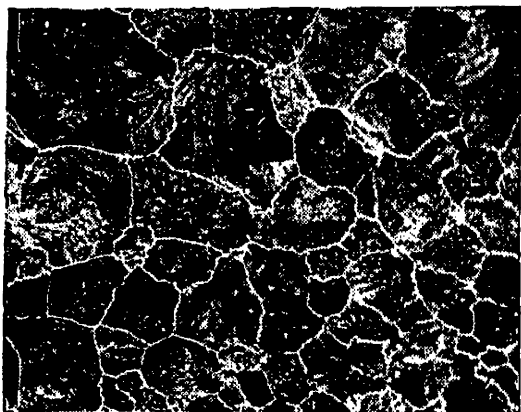


FIG. 20-1.—Photomicrograph of steel magnified 100 times.

metal there may be considerable variation in the size of neighboring grains. In estimating their average size, however, it is convenient to idealize and regard them as cubical or spherical. On a cubical basis, the edge length of a cube of average volume is called the “grain size.” The physical properties of metals and other solids are closely related to the grain size. Two pieces of metal of identical chemical composition will differ in their physical properties

if their grain sizes differ. Consequently, grain size is one of the features commonly measured by metallographers.

The usual method of measuring it consists in examining or photographing a carefully polished and suitably etched section of the metal with a microscope. Figure 20-1 shows such a photomicrograph of a steel sample. Usually, the magnified image is projected onto a screen on which a 79.8-mm. (50-cm.<sup>2</sup>) circle has been inscribed. One then counts the number of grains completely within the circle, plus half the number of those partly within and partly outside it. The result of this count may be designated by  $X$ . If the image projected on the screen is magnified  $M$  diameters, then the circle on the screen represents  $5,000/M^2$  mm.<sup>2</sup> of the etched surface of the specimen. Since there are  $X$  grains in  $5,000/M^2$  mm.<sup>2</sup>, there are  $XM^2/5,000$  grains in 1 mm.<sup>2</sup> If the (ideally cubical) grains have a cube edge length  $\sigma$ , then  $\sigma^2$  is the average area per grain in the section, and the number in 1 mm.<sup>2</sup> is  $1/\sigma^2$ , where  $\sigma$  is measured in millimeters. Equating these two expressions,

$$\frac{1}{\sigma^2} = \frac{XM^2}{5,000}$$

or

$$\sigma = \frac{1}{M} \sqrt{\frac{5,000}{X}} \quad (20-1)$$

Except for a "blind spot" between  $10^{-2}$  and  $2 \times 10^{-4}$  mm., the grain size of any crystalline solid can be determined by means of Hull-Debye-

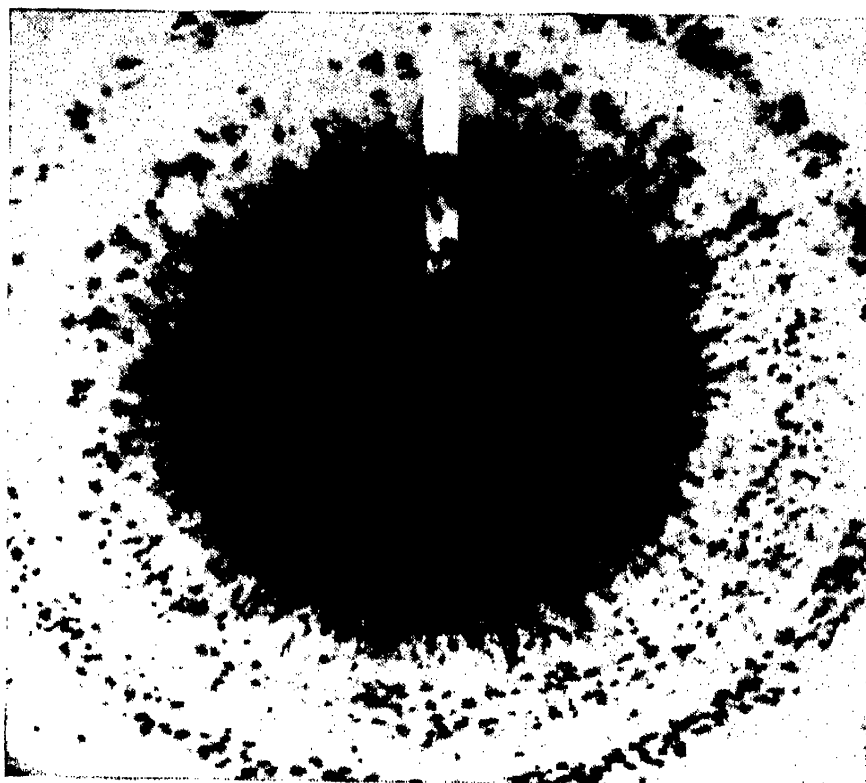


FIG. 20-2.—Transmission pattern of sheet steel.

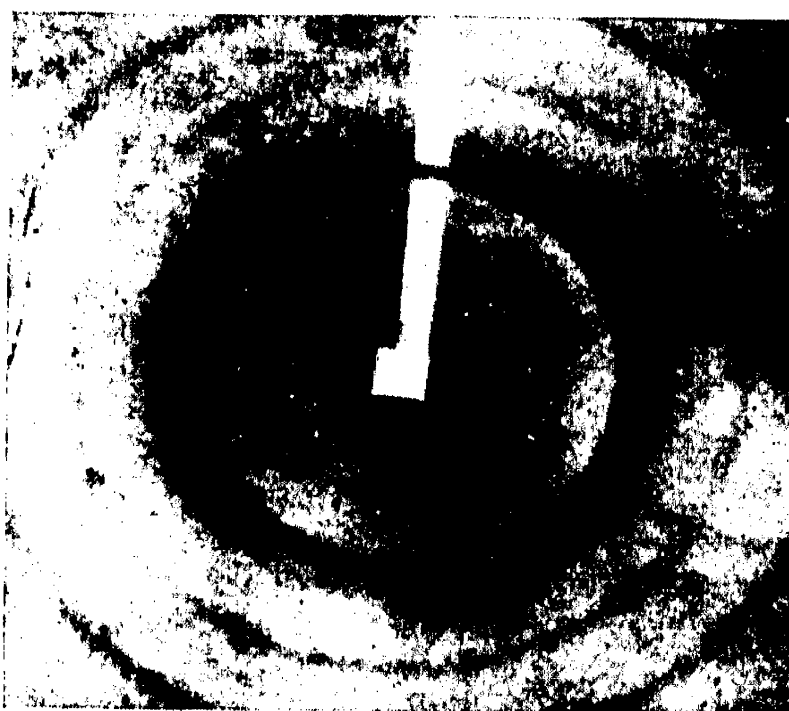


FIG. 20-3.—Transmission pattern of magnet steel.

Scherrer patterns. When the grain size is greater than  $10^{-2}$  mm., it may be estimated with considerable accuracy by counting the number of diffraction spots in an inner, intense ring of the transmission pattern.

As explained on page 405, a crystal structure as coarse as this yields a spotty ring pattern. For reference, this type of pattern is illustrated again in Fig. 20-2, which is from a sheet-steel sample. When the grain size is slightly less than  $10^{-2}$  mm., the powder pattern is characterized by continuous sharp rings, as in Fig. 18-12 or 20-3, the latter being from a bar of steel for making permanent magnets. As the grain size becomes smaller than this, the character of the powder pattern remains the same (sharp rings) until the grain size reaches about  $2 \times 10^{-4}$  mm. Thus, between  $10^{-2}$  and  $2 \times 10^{-4}$  mm.—a size range of about 25 to 1—the x-ray powder pattern is insensitive to grain size. When a sample yields a sharp ring pattern, one can only say that its grain size lies within this range.

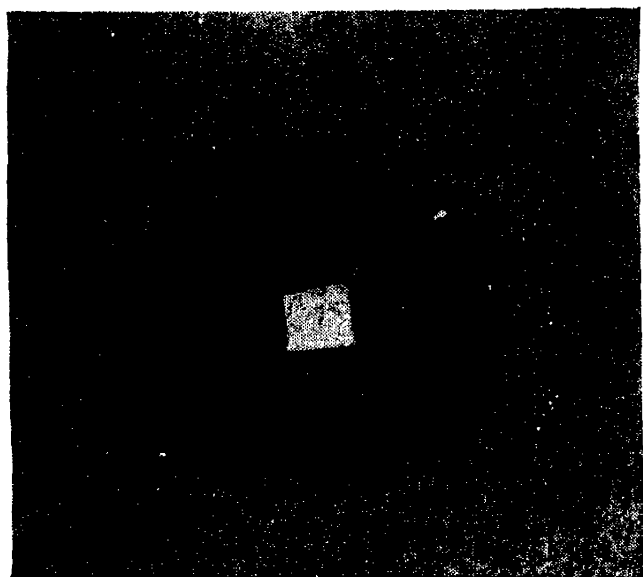


FIG. 20-4.—Pattern of colloidal adhesive cement.

When the grain size becomes smaller than  $2 \times 10^{-4}$  mm., however, the rings in the pattern begin to lose their sharpness and show signs of broadening and “fuzziness” because such small crystals lack the necessary resolving power to produce sharp rings, as already mentioned on pages 321 and 435. Crystals small enough to show perceptible broadening of the rings in the powder pattern may be obtained in metals by cold working. In colloidal suspensions, the grain size is exceedingly small—of the order of  $10^{-5}$  to  $10^{-6}$  mm.—

and these show a very obviously fuzzy ring pattern, as in Fig. 20-4.

**2. Estimation and Comparison of Grain Size above  $10^{-2}$  Mm.** If a cubic centimeter of steel, for example, could be dissected, it might be found to contain a billion crystals or grains. If they are regarded as tiny cubes, all of the same size, it follows that they are a hundredth of a millimeter on an edge, and on the basis of such an idealized picture one would say that the grain size of this steel is a hundredth of a millimeter. In order to discover the various factors that relate the grain size of a polycrystalline material to the character of its x-ray powder pattern, it will be instructive to carry through a rough calculation of the grain size of a sample that is just on the border line between giving a spotty ring pattern like Fig. 20-2 and a continuous ring pattern like Fig. 20-3.

For a commonly used primary beam, such as the molybdenum  $K_{\alpha}$  doublet, say, one may use the weighted average wave length of the two lines to calculate the value  $\theta_0$  of the Bragg angle that should yield a



diffracted beam from a given set of planes ( $hkl$ ) in a crystal, knowing their interplanar distance  $d$ . For ordinary commercial metals like annealed aluminum, iron, copper, or brass, the "width" of the diffraction maxima for the lower order Bragg reflections is<sup>1</sup> of the order of 0.01 radian, or  $\frac{1}{2}^\circ$ . This spread in the grazing angle of exodence  $\theta$  is due to such factors as mosaic structure, finite slit width, the use of a doublet as primary radiation, and the variation of the  $d$  spacings from point to point in the sample due to localized strains. The  $K_{\alpha 1}$  and  $K_{\alpha 2}$  components of the  $K_{\alpha}$  doublets ordinarily used for the primary beam are not usually resolved in the lower order reflections. For typical doublets (for example, 0.707 and 0.712 Å. for Mo and 1.543 and 1.537 Å. for Cu), the separation in the lower orders amounts to less than  $\frac{1}{2}^\circ$ . From a crystal properly oriented in the primary beam then, there is a variation in the grazing angle of exodence of  $\pm \Delta\theta$ , where  $\Delta\theta$  is about  $\frac{1}{4}^\circ$ , when the grazing angle of incidence has its correct value,  $\theta_0$ . Conversely, a diffracted beam strong enough to register on the x-ray film should emerge from a crystal or grain in a metal, even if its orientation is such as to make the grazing angle of incidence  $\theta$  larger or smaller by about  $\Delta\theta$  than the value  $\theta_0$  required by Bragg's law.

This being the case, what is the probability that a steel grain having a fixed orientation which is entirely a matter of haphazard chance will be so oriented that its (110) planes, say [excluding the (1 $\bar{1}$ 0), (011), (01 $\bar{1}$ ), (101), and (10 $\bar{1}$ ) planes, in this case], will diffract in the first order an incident beam of parallel x-rays belonging to a typical  $K_{\alpha}$  doublet? The lattice constant,  $a$  of iron is 2.86 Å., and so the (110) spacing is  $2.86/\sqrt{2}$ , or 2.02 Å. Taking 2 Å. as a representative value for  $d$ , then [copper (111) = 2.08 Å.; aluminum (111) = 2.33 Å.; etc.], and 1 Å. as a representative value for  $\lambda$

(molybdenum  $K_{\alpha}$  = 0.71 Å.; copper  $K_{\alpha}$  = 1.54 Å.),

one finds from Bragg's law that, for first-order diffraction,

$$\sin \theta_1 = \frac{\lambda}{2d} = \frac{1}{4}.$$

If  $\sin \theta_1$  is approximately  $\frac{1}{4}$ , then  $\cos \theta_1$  is approximately 1. To return to the question posed at the start of the paragraph, it follows that the grain must have its (110) planes inclined at an angle of  $(\sin^{-1} \frac{1}{4}) \pm \Delta\theta$  to the primary beam, but it may have any azimuth about the beam.

A man suspended by a rope (which represents the primary x-ray beam in this analogy) in the dark at the center of a large hollow sphere of radius  $r$  fires a pistol at random. The bullet will hit the surface

<sup>1</sup> See, for example, A. R. Stokes, K. J. Pascoe, and H. Lipson, *Nature*, **151**, 137 (1943), and C. S. Smith and E. E. Stickley, *Phys. Rev.*, **64**, 191 (1943).

of the sphere somewhere, this surface having an area  $4\pi r^2$ . The path of the bullet represents the normal to the planes ( $hkl$ ) in question, and it therefore determines their orientation in space. If the bullet's path is inclined at an angle  $90^\circ - \theta_1 \pm \Delta\theta$  to the rope, where  $\Delta\theta$  is small, it will strike the sphere somewhere in the annular zone having width  $2r \Delta\theta$  and circumference  $2\pi r \cos \theta_1$  and  $4\pi r^2 \cos \theta_1 \Delta\theta$ . Therefore the probability  $P$  of this happening is

$$P = \frac{4\pi r^2 \cos \theta_1 \Delta\theta}{4\pi r^2} = \cos \theta_1 \Delta\theta \quad (20-2)$$

where  $P$  is the probability of any one specific crystal having the proper orientation.  $P$  is also the fraction of the crystals in a large random group (say, a billion) that will have the proper orientation. Applying this to the present case, where  $\cos \theta_1 = 1$ ,

$$P = \Delta\theta \quad (20-3)$$

where  $\Delta\theta$  is in radians.

In the case of iron crystals, there are six sets of planes in the  $\{110\}$  form, any one of which would diffract if inclined at  $\theta_1 \pm \Delta\theta$  to the primary beam. That is, the innermost ring in the iron transmission pattern is formed by six "cooperating planes," as compared with four for the inner (111) ring of face-centered cubic metals like copper and aluminum. Taking five as an average number of cooperating planes, then, the chance of any plane in the form diffracting is  $5 \Delta\theta$ . Hence the probability of a crystal in a metal diffraction sample producing a diffraction spot in the innermost ring of its powder pattern is also about  $5 \Delta\theta$ , or there will be  $1/5\Delta\theta$  crystals in the irradiated part of the specimen for each crystal producing a spot. Therefore, if there are  $N$  diffraction spots in the innermost ring, there are about  $N/5\Delta\theta$  grains in the portion of the sample penetrated by the primary x-ray beam.

If the primary beam is 0.020 in. in diameter and the sample is 0.003 in. in thickness (taking representative values), this portion of the sample has a volume of about a millionth of a cubic inch and contains  $4N/5\Delta\theta$  grains. Therefore a cubic inch would contain  $\frac{N}{5\Delta\theta} \times 10^6$  grains, and the grain size  $\sigma$  in inches is thus given by

$$\sigma = 0.01 \sqrt[3]{\frac{5\Delta\theta}{N}} \quad (20-4)$$

In order to estimate the grain size for the case of a "border-line" pattern like Fig. 20-5 where the diffraction spots are just barely distinguishable, the value of  $N$  in such a pattern must be known roughly. Figure 20-5 was taken from a silver-alloy sample, using molybdenum  $K_\alpha$  radiation

and 0.020-in. pinholes. Silver has a face-centered cubic structure like aluminum, the  $d$  spacing of the inner (111) ring being 2.36 Å. as compared with 2.33 Å. for aluminum. Measurement of the width of the inner ring, combined with a knowledge of the specimen-to-film distance and collimator dimensions, permits a rough calculation of  $\Delta\theta$ , indicating that it is about  $\frac{1}{4}^\circ$ . It is to be remembered that  $\Delta\theta$  represents only half the angular width. By actual count, the number of spots visible in the inner ring of Fig. 20-5 is close to 500. Substituting this value for  $N$  and



FIG. 20-5.—Transmission pattern of electrodeposited silver.

0.0045 radian for  $\Delta\theta$  in equation (20-4), one obtains  $\sigma = 3.5 \times 10^{-4}$  in., or about  $9 \times 10^{-4}$  cm. or  $9 \times 10^{-3}$  mm. As a rough approximation, then, one concludes that if the rings are spotty the grain size exceeds  $10^{-2}$  mm.; if not, the grain size is less than  $10^{-2}$  mm. This calculation has been confirmed by the photomicrographic technique outlined in Sec. 1.

The term  $\Delta\theta$  has been retained in equation (20-4) because it varies with pinhole size, the x-ray source, filter, etc. If some arbitrary value such as 0.005 radian is inserted for making rough estimates, one has

$$\sigma_{\text{mm}} = \frac{0.075}{\sqrt[3]{N}} \quad (20-5)$$

The accuracy of this equation can be improved by reviewing its derivation and inserting the specific values for such items as pinhole diameter, sample thickness,  $d$  spacing, primary wave length, and number of

cooperating planes for the sample being examined and the technique being used.

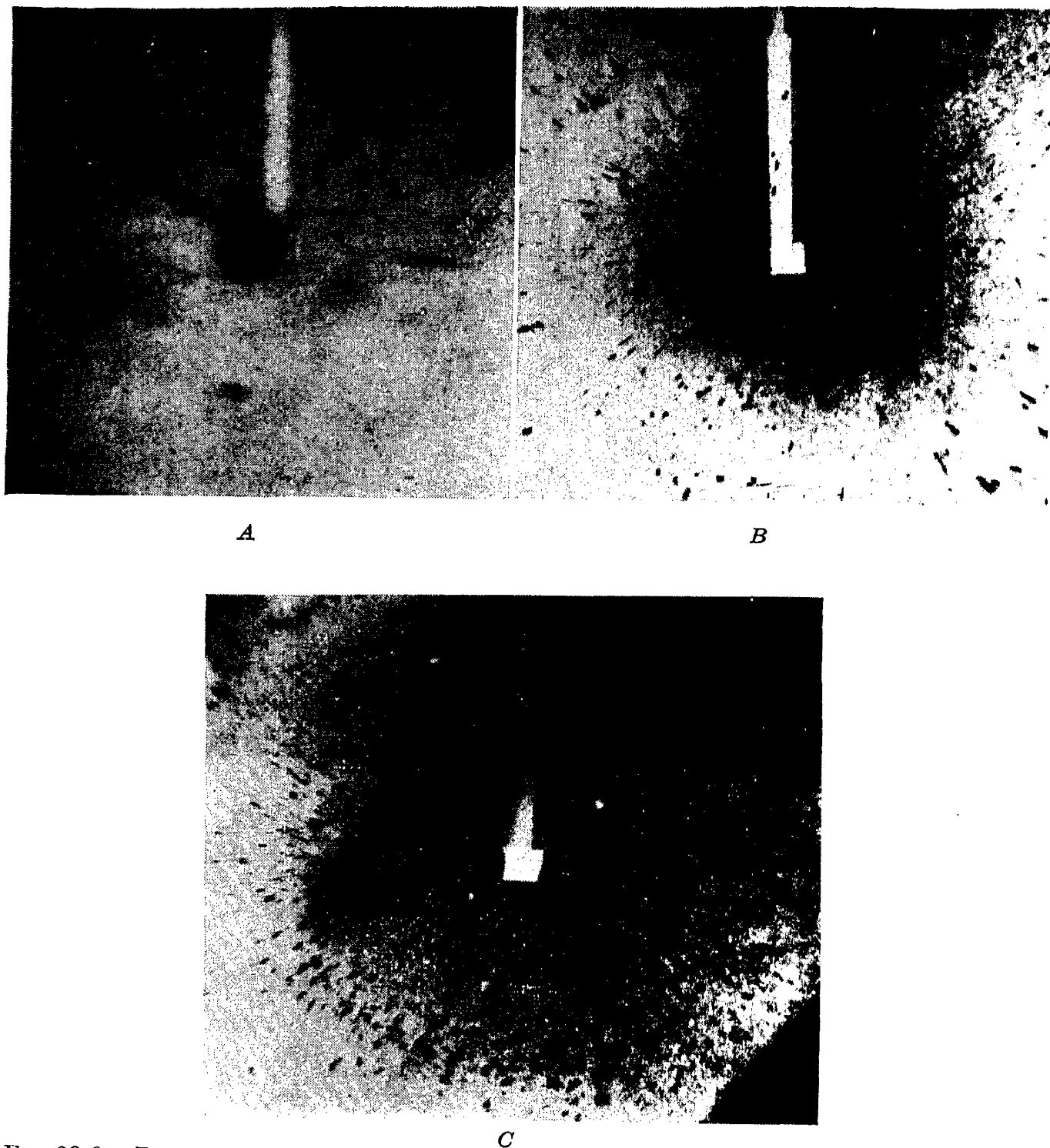


FIG. 20-6.—Patterns of copper specimens of various grain sizes. A, grain size about 1 mm. B, grain size about 0.2 mm. C, grain size about 0.05 mm.

As an example, one may estimate the grain size of the annealed sheet copper from which Fig. 18-10 was obtained. In one-quarter of the innermost ring, one may count about 70 diffraction spots, or about 280 for the whole ring. Hence  $\sigma$  in millimeters is about  $1/80$  mm.,

or 0.0125 mm. The chief reason for deriving equations (20-4) and (20-5) was to show the interrelation between the character of the powder pattern, the grain size of the sample, and the various other factors that

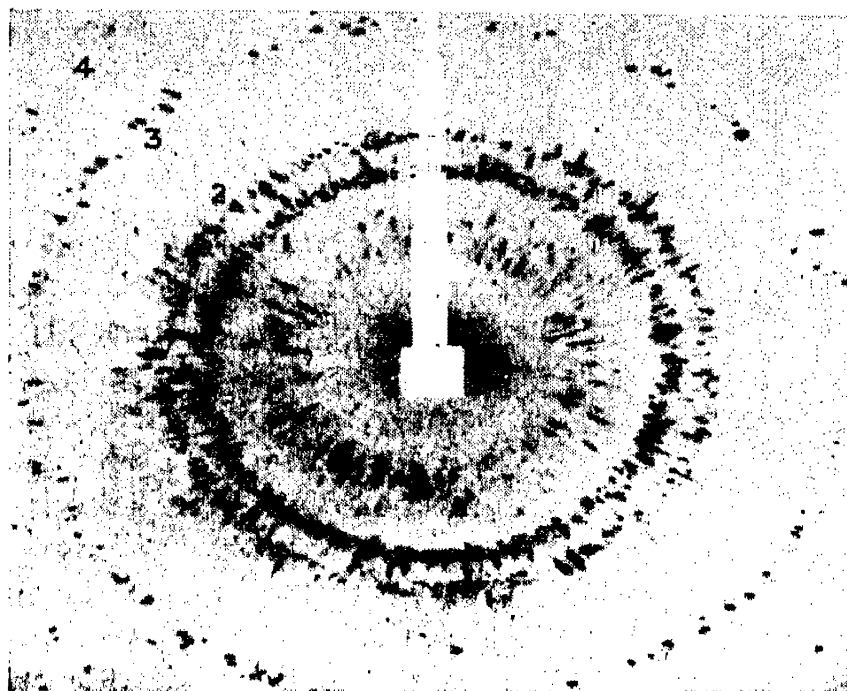
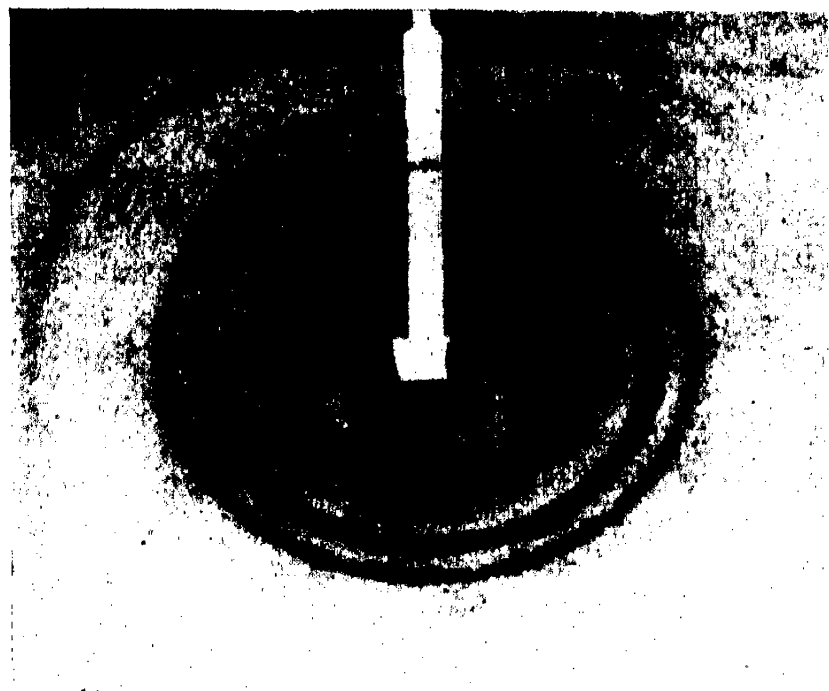
*D**E*

FIG. 20-6.—(Continued.) *D*, grain size about 0.03 mm. *E*, grain size about 0.003 mm.

must be considered. When there is a wide variation in grain size in a single small sample or when there is a strong preferential orientation (see Secs. 4 to 6), some of the assumptions upon which equation (20-4)

was derived are no longer valid. In practice, comparative estimates of grain size are usually all that are required, and absolute estimates from relationships like equation (20-5) are not to be emphasized unduly.

The ease with which comparative estimates of grain size can be made by mere inspection of the patterns is demonstrated by Fig. 20-6. This shows a series of copper patterns for samples ranging in size from about 1 mm. (sample *A*) to 0.003 mm. (sample *E*). When no rings are evident, as in *A* and *B*, the grain size exceeds 0.05 mm. Rings begin to evolve, as in *C*, when the grain size is about 0.05 mm.

**3. Estimation and Comparison of Grain Size below  $2 \times 10^{-4}$  Mm.** With a ruled optical grating, diffraction maxima that are close together,

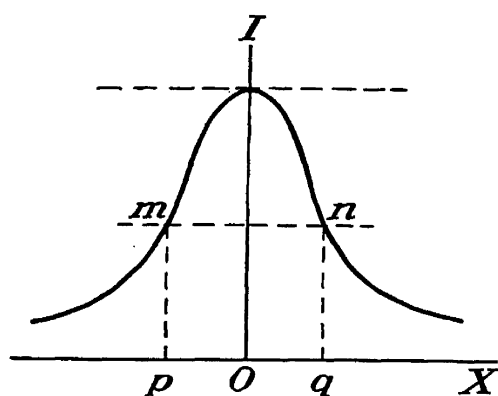


FIG. 20-7.—The “half-value width” ( $pq$ ) of a diffraction maximum.

like the sodium D lines, are readily distinguishable as separate maxima despite their proximity, as long as a well-made grating with a large number of ruled lines is used. When the number of lines in the grating is reduced to only 20 or 30, however, the spectral lines become broad and fuzzy, and close neighbors like the D lines merge into a single broad maximum; in technical language, there is a loss of resolving power. The same thing occurs in the case of x-rays when the grain size drops to about  $2 \times 10^{-4}$  mm. (see Sec. 1, and page 321).

Scherrer<sup>1</sup> first studied this phenomenon in a quantitative way, beginning about 1918. He derived a formula relating the breadth  $B$  of the diffraction maximum to the size of the crystals, that is, to the grain size  $\sigma$ . The formula was of the form

$$\sigma = \frac{K\lambda}{B \cos \theta} \quad (20-6)$$

where  $K$  is a constant roughly equal to 1,  $\lambda$  is the wave length, and  $\theta$  is the usual Bragg angle. The units for  $\sigma$  are the same as those for  $\lambda$ ; that is, if  $\lambda$  is in angstroms,  $\sigma$  is given in angstroms. The breadth of a diffraction line may be measured by means of an ionization chamber or by densitometry of a pattern that has been recorded photographically. This breadth  $B$  is ordinarily measured according to one of two conventions. In most cases, the so-called “half-value breadth” is measured. Figure 20-7 represents the ionization-chamber current plotted as a function of angular displacement on either side of the center of the diffraction maximum; or photographic density as measured by a densi-

<sup>1</sup> P. Scherrer, *Nachr. Ges. Wiss. Göttingen, Sitzber.*, July 26, 1918; contribution to the book “Kolloidchemie” by R. Zsigmondy, 3d ed., Otto Spamer, Leipzig, 1920.

tometer, plotted as distance along the film on either side of the maximum. In such a diagram, the intensity  $I_{\max}$  at the center of the peak drops to 50 per cent ( $\frac{1}{2}I_{\max}$ ) at two points on either side, such as  $m$  and  $n$ . The half-value breadth  $B$  of the line is then the angle in radians subtended at the diffraction sample by the line  $pq$ . That is, if the camera is cylindrical,<sup>1</sup> with radius  $r$ , then  $B = pq/r$ . Sometimes the breadth  $B$  is defined as that of a stripe of uniform intensity equal to the maximum,  $I_{\max}$ , and a total intensity equal to that of the actual line; that is,

$$B = \frac{\int I d\phi}{I_{\max}} \quad (20-7)$$

where  $\phi$  is the angle  $2\theta$  between the primary and diffracted rays. For precise work, the second definition of  $B$  given by (20-7) appears preferable.<sup>2</sup> For work of ordinary accuracy, the half-value breadth  $B$  is commonly employed.

Scherrer's formula has been subjected to further theoretical investigation, a paper by Laue<sup>3</sup> being the one that laid the groundwork of the theory accepted at present. Since Laue's paper, theoretical justification has been found for relaxing the restrictions that were formerly considered necessary. For example, Seljakow<sup>4</sup> has proved that the Scherrer formula is valid for noncubic crystals, as well as for cubic, and Patterson<sup>5</sup> has shown that the external form of the crystal need not be similar to that of the unit cell, as formerly supposed. When the half-value breadth is taken for  $B$ , the accepted value for  $K$  in (20-6) is 0.94, as calculated by Seljakow.

In using the formula (20-6) to calculate grain size from a pattern, there is some doubt whether  $B$  should be called "breadth" or "broadening," for  $B$  refers only to the *extra* breadth of the lines due to the grain size being less than  $2 \times 10^{-4}$  mm. When the grain size is of the order of  $10^{-5}$  or  $10^{-6}$  mm., as in colloids, so that the breadth of the lines or rings is at least five times that of the usual sharp lines, this point is not important; but when the grain size is of the order of  $10^{-4}$  mm., so that the line broadening is only just detectable, allowance must be made for the breadth of the line due to causes other than small particle size. This can be accomplished experimentally by photographing on the same film the pattern of a substance having a grain size known to be of the order of  $10^{-3}$  mm. For accurate work, a simple subtraction of the breadth of one of these reference lines from the observed breadth of one of the

<sup>1</sup> For Seemann-Bohlin cameras, divide by the diameter, not the radius.

<sup>2</sup> See, for example, F. W. Jones, *Proc. Roy. Soc. (London) A*, **166**, 16 (1938).

<sup>3</sup> M. von Laue, *Z. Krist.*, **64**, 115 (1926).

<sup>4</sup> N. Seljakow, *Z. Physik*, **31**, 439 (1924), errata, **33**, 648 (1925).

<sup>5</sup> A. L. Patterson, *Phys. Rev.*, **56**, 978 (1939).

lines of the unknown is not permissible. For a fair estimate, one may use the relation

$$B^2 = B_m^2 - B_0^2 \quad (20-8)$$

where  $B_m$  is the measured breadth and  $B_0$  the breadth of the "sharp" reference line. For accurate work, the details are too intricate to be set forth here; reference should be made to the article by Jones<sup>1</sup> already mentioned or to articles of a similar nature.<sup>2</sup> The factors determining the value of  $B_0$  have been discussed in Sec. 2.

It is important to know that line broadening in a powder pattern can be produced by factors other than small grain size; one should have evidence that the measured broadening is indeed due primarily to fine grain size before committing himself to any positive statements regarding grain-size values based on line broadening alone. The factor most likely to produce line broadening (that is, a value for  $B$ , as distinguished from  $B_0$ ), aside from ultrafine grain size, is grain distortion, which will be discussed in the next chapter. In a colloidal suspension of gold, there is scant possibility of grain distortion, and in such cases one may safely evaluate the grain size simply from line broadening. When the grain size drops to  $10^{-5}$  or  $10^{-6}$  mm., the rings or lines in the transmission pattern become greatly broadened, as in Fig. 20-4. Strains or grain distortion cannot produce such extreme broadening as this, obtained from a colloidal adhesive cement. Such broadening is characteristic of colloids, amorphous materials, and liquids (Chap. 22). The chances for confusion arise when there is comparatively slight line broadening in a pattern from a sample that might be characterized by either fine grains or internal strains, or both.

As an example, there have been various x-ray diffraction studies of the nature of the changes produced by cold work in metals. Wood has made extensive studies of this. Cold work of metals causes broadening of the diffraction lines. Assuming that this broadening is due entirely to fracture of the metal grains into smaller and smaller ones, Wood has found that cold work never reduces the grain size below certain characteristic values for various metals. For example, cold working never reduces the grain size of copper below  $0.7 \times 10^{-4}$  mm. Corresponding values for other metals, given by Wood,<sup>3</sup> are silver,  $0.8 \times 10^{-4}$  mm.; nickel,  $1.2 \times 10^{-4}$  mm.; aluminum,  $10^{-3}$  mm. (no appreciable line broadening); iron,  $3.2 \times 10^{-4}$  mm.; and molybdenum,  $2.2 \times 10^{-4}$  mm. From this, Wood suggests that "the crystallite must be regarded as a fundamental unit of the metallic grain," the sizes of these fundamental

<sup>1</sup> Footnote 2, p. 447.

<sup>2</sup> See, for example, G. H. Cameron and A. L. Patterson in the A.S.T.M. Symposium on Radiography and X-ray Diffraction (1937).

<sup>3</sup> W. A. Wood, *Proc. Phys. Soc. (London)*, **52**, 110 (1940).



crystallites<sup>1</sup> being  $0.7 \times 10^{-4}$  mm. for copper,  $0.8 \times 10^{-4}$  mm. for silver, etc.

This interpretation of line broadening due to cold work in metals is questioned by other investigators<sup>2</sup> on the grounds that it may be due to grain distortion. For theoretical purposes, a possible way of distinguishing between line broadening due to fine grains and broadening due to grain distortion is carefully to measure the variation of  $B$  with  $\theta$ . If the broadening is due to fine grain size only, then  $B$  should be proportional to  $\lambda \sec \theta$ , since

$$B = \frac{K}{\sigma} \lambda \sec \theta \quad (20-9)$$

from (20-6). On the other hand, if the broadening is due only to grain distortion or strain  $\epsilon$  that has been caused by the cold work, then the broadening  $B$  (proportional to  $d\phi$  in the following) is related to the Bragg angle  $\theta$  in a different way, as will now be shown. Recalling that strain  $\epsilon$  is defined as change of length ( $dd$ ) per unit length ( $d$ ), or  $dd/d$ , the Bragg equation is differentiated as follows, regarding  $d$  and  $\theta$  as variables:

$$\begin{aligned} \sin \theta &= \frac{\lambda}{2d} \\ \cos \theta d\theta &= -\frac{\lambda}{2} \frac{1}{d^2} dd = -\frac{\sin \theta}{d} dd \end{aligned}$$

or

$$B \propto d\phi = 2d\theta = -2 \frac{dd}{d} \frac{\sin \theta}{\cos \theta} = -2\epsilon \tan \theta \quad (20-10)$$

so that  $B$  should be proportional to  $\tan \theta$  and independent of  $\lambda$ . In experiments on tungsten and alpha brass, Smith and Stickley have found<sup>3</sup> that cold work produces a line broadening which varies with  $\theta$  in accordance with (20-10) rather than (20-9). From this, they conclude that the line broadening probably indicates that cold working sets up "microstresses" in the metal which are "supposed to be random in direction, magnitude, and sign, and uniform only over distances very small compared with the dimensions of the sample."

#### 4. Preferential Orientation with Respect to an Axis Only—Fibering

In the study of preferential orientation, crystal-lattice models of the face-centered and body-centered cubic structures are very helpful

<sup>1</sup>The word "crystallite" is used by some writers, especially Germans, in the same sense that the words "grain" and "crystal" are used in this book. Wood here uses it synonymously with "mosaic fragments" (Sec. 16-16). Owing to different usage by different writers, it is an ambiguous term.

<sup>2</sup>See, for example, R. S. Stokes, K. J. Pascoe, and H. Lipson, *Nature*, **151**, 137 (1943); also F. Niemann and S. T. Stephenson, *Phys. Rev.*, **62**, 330 (1942).

<sup>3</sup>C. S. Smith and E. E. Stickley, *Phys. Rev.*, **64**, 191 (1943).

The remainder of this chapter will be more intelligible if such models, made of wood balls and stiff wires, are handy for reference. A review of the discussion of Fig. 18-8 reveals that it was based on the assumption that the crystals in the sample *S* were oriented at random. The question to be considered now is the effect upon the powder pattern of "preferential orientation," that is, orientation that is not random.

In processes involving the plastic deformation of a metal, such as drawing a rod down to a wire, rolling a billet down to a sheet, or "deep drawing" a sheet to form a cup, the metal crystals cleave and glide or slip along certain crystallographic planes parallel to certain crystallographic axes in those planes. Such planes of slip are usually among the most densely populated sets, that is, sets of planes having more atoms per square angstrom unit than other crystallographic planes. In metals with a hexagonal structure, like zinc and magnesium, the densest planes are the basal (0001) planes. For such metals, plastic deformation causes the crystals to cleave into slices along these planes, followed by sliding or gliding of the slices along them. The gliding takes place along the {111} planes in face-centered cubic metals, and these are the densest planes in such metals. This gliding is confined to the  $[10\bar{1}0]$ ,  $[01\bar{1}0]$ , or  $[1\bar{1}00]$  directions in the hexagonal case and the  $[110]$ ,  $[011]$ , or  $[101]$  directions in the face-centered cubic case. In some of the body-centered cubic metals, like tungsten, {112} are the planes of slip, even though they are not the most densely populated.

These processes obviously will reduce the grain size by fragmentation; in addition, the special direction of the fragmentation and slip results in the fragments acquiring preferred orientations with respect to the drawing or rolling axis. In a few instances such a preferred orientation is desirable or beneficial. For example, Goss<sup>1</sup> has found that the electrical properties of silicon sheet steel for transformer laminæ are improved by allowing it to retain its preferential orientation.<sup>2</sup> Such steel has a considerably higher magnetic permeability in the direction of roll than in other directions. Snoek<sup>3</sup> has found that the resistance of nickel steel to corrosion improves when the orientation is preferential. In general, however, preferential orientation is objectionable because it weakens a metal and reduces its ability to withstand further deformation. The forming operations that cause preferential orientation are usually performed in several stages. Each forming step increases the preferential orientation, thus reducing the capacity of the metal to undergo additional forming steps. Therefore it is often necessary to anneal the metal between some of the stages to relieve the preferential orientation by

<sup>1</sup> N. P. Goss, *Trans. Am. Soc. Metals*, **23**, 511 (1935).

<sup>2</sup> R. M. Bozorth, *Trans. Am. Soc. Metals*, **23**, 1107 (1935).

<sup>3</sup> J. L. Snoek, *Z. Metallkunde*, **30**, 94 (1938).

permitting the grains to "recrystallize" before proceeding to the next stage. In most cases, annealing causes a recrystallization in which new crystals form of a size comparable with the size of those originally present, and these new crystals usually have a nearly random orientation. In some instances, however, a new and different preferential orientation results, called the "recrystallization orientation."

In wire drawing, the tendency is to align some crystallographic axis' (such as  $[111]$  and  $[100]$  in the face-centered cubic metals) with the axis of the wire. This may be the only effect, as with aluminum, where the crystals retain their original random orientation in the plane perpendicular to the wire. In such a case, the preferred orientation is sometimes called "fibering," and the wire axis is called the "fiber axis." In other cases, as with tungsten,<sup>1</sup> there may be a tendency, not only to align an axis ( $[110]$  in this case) with the wire, but also to align some other axis ( $[001]$  in this case) along the diameters of the wire, as shown in Fig. 20-8; this type of fibering is sometimes called "limited fibering." Limited fibering is characteristic of rolled sheet metal, because the preferential orientation not only aligns some crystallographic axis, such as  $[110]$ , with the rolling direction, but also aligns some set of planes, such as  $(001)$ , in the plane of the sheet, as shown schematically in Fig. 20-8.

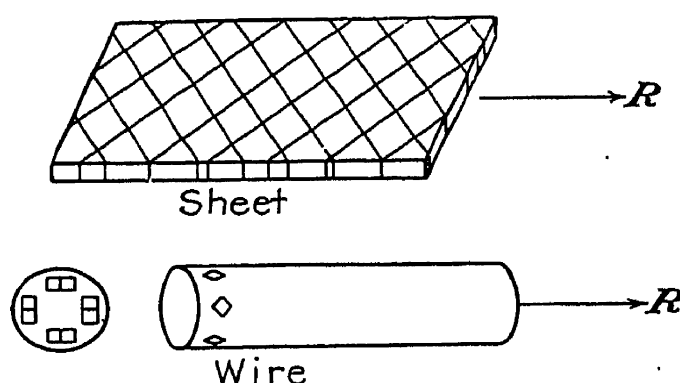


FIG. 20-8.—Preferential orientation assumed by crystals in rolled sheets and drawn wires of body-centered cubic metals like tungsten.

Suppose for a moment that the fibering in an aluminum wire is perfect, so that every grain has its  $[111]$  axis exactly parallel to the wire. Then one would expect that the powder pattern obtained with the x-ray beam passing perpendicularly through such a wire would bear a strong resemblance to the rotation patterns described in Chap. 17. In taking a rotation pattern, the x-ray beam passes through a single crystal, which is rotated steadily about one of its zone axes perpendicularly to the beam. In the wire, all the crystals have a particular zone axis perpendicular to the beam, and they have all possible orientations attainable by rotation about this axis. Therefore the resulting pattern should have the layer-line characteristics of a rotation pattern if the orientation, or fibering, is perfect, but the rings characteristic of random orientation should persist if the fibering is only partial. To approach the problem from the standpoint of the discussion (page 402) of Fig. 18-8, it is logical to expect that preferential orientations of the crystals in the sample  $S$

<sup>1</sup> See, for example, Z. Jeffries, *Trans. A.I.M.M.E.*, **70**, 303 (1924).

will disturb the random distribution of the rays in the cones  $SA A'$ , etc., resulting in rings that are not uniformly intense all the way around their circumference.

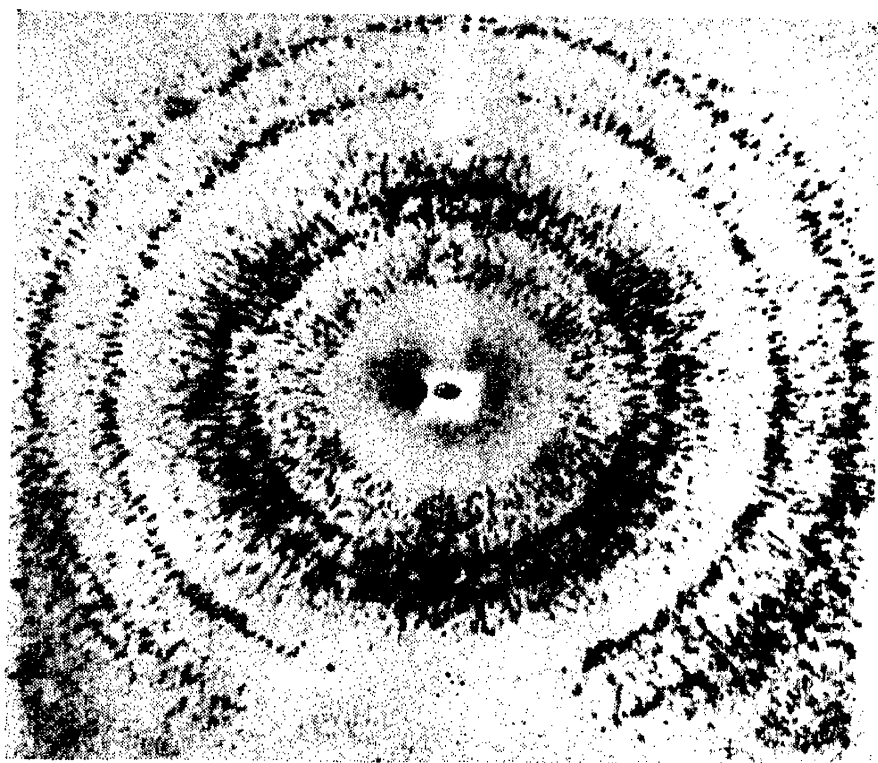


FIG. 20-9.—Transmission pattern of aluminum wire.

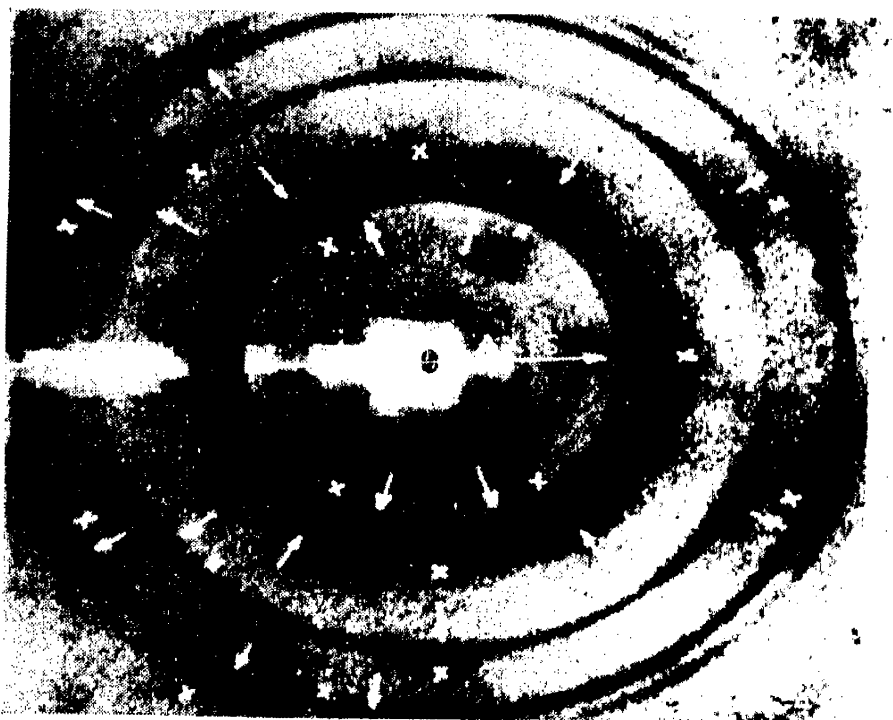


FIG. 20-10.—Pattern of same wire as in Fig. 20-9, after stretching beyond the elastic limit. Arrow marked *AXIS* indicates the axis of the wire.

Figure 20-9 is a pinhole Hull-Debye-Scherrer pattern of a piece of aluminum wire, and Fig. 20-10 is a similar pattern of the same wire after it has been stretched beyond its elastic limit. As suggested in the fore-

going discussion, the grain size has been greatly reduced by this plastic deformation, and the "lumpiness" of the rings indicates that the crystals have acquired a preferential orientation as a result of the stretching. Since aluminum is face-centered cubic, the fibering has supposedly aligned the [111] or [100] zone axes of the crystals with the wire axis.

A method of analyzing a pattern that shows fibering like figure 20-10 has been described by Glocker.<sup>1</sup> In Fig. 20-11,  $AS$  represents the primary x-ray beam striking the wire  $WS$  perpendicularly at  $S$ , the undiffracted beam then striking the film  $F$  at  $O$ . The diffracted ray  $SP$  strikes the

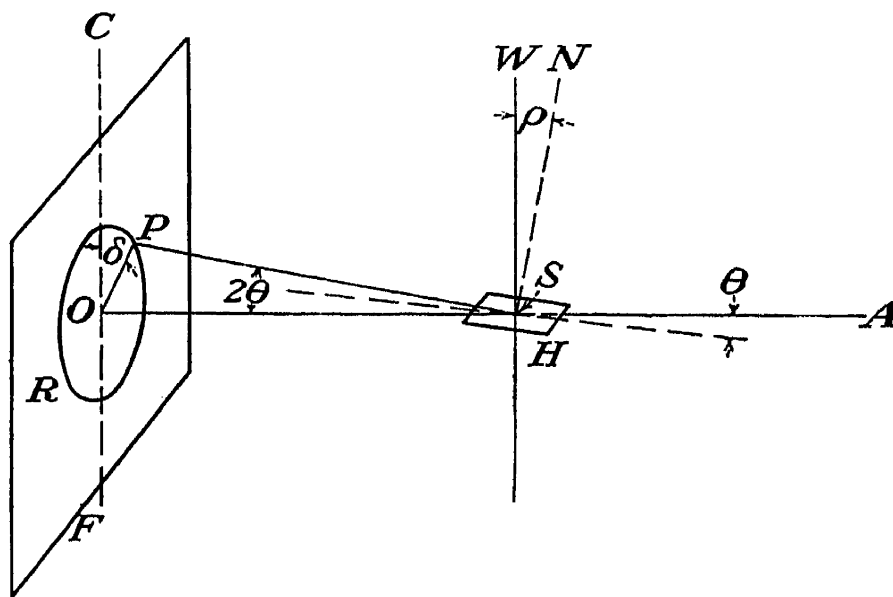


FIG. 20-11.—Showing the interrelated angles  $\delta$ ,  $\rho$ , and  $\theta$  involved in the analysis of fibering.

film at a point  $P$  on the circumference of one of the rings  $R$  in the resulting pattern like Fig. 20-10. Suppose, now, that  $P$  is one of the abnormally intense lumps (indicated by arrows and crosses in Fig. 20-10) on the ring  $R$  (Fig. 20-11).  $CO$  is a line drawn on the film parallel to the wire  $WS$ , marked "axis" in Fig. 20-10. From the analogy with the case of a single-crystal rotation pattern (see pages 387 to 388), such spots  $P$  will occur in groups of four, symmetrically located on opposite sides of  $CO$  and on opposite sides of a line on the film through  $O$  perpendicular to  $CO$ . This may be seen, also, by imagining the reflecting plane  $H$  to rotate about  $WS$ , maintaining its fixed inclination  $\rho$  to it ( $NS$  is the normal to plane  $H$ ). If  $\delta$  is the angle between  $OP$  and  $OC$  and  $\theta$  is the usual Bragg angle for the set of planes  $H$  from which ray  $SP$  is "reflected," Polanyi<sup>2</sup> has shown that  $\delta$  is given by

$$\cos \delta = \frac{\cos \rho}{\cos \theta} \quad (20-11)$$

<sup>1</sup> R. Glocker, "Materialprüfung mit Röntgenstrahlen," p. 327, 2d ed., Verlag, Julius Springer, Berlin, 1936.

<sup>2</sup> M. Polanyi, *Z. Physik*, **7**, 149 (1921).

Patterns like Fig. 20-10 are usually taken with fairly hard radiation—molybdenum  $K_\alpha$  in this case. Consequently  $\cos \theta$  is nearly 1, even for the outermost rings. In the present example,  $\cos \theta = 0.953$  for the outermost (222) ring. Therefore, to a good approximation, equation (20-11) becomes simply  $\rho = \delta$ . This being the case, one may readily calculate where the lumps in a pattern like Fig. 20-10 should appear if [111] is the fiber axis, for example. From the lattice geometry of cubic crystals, one finds the following expression for the inclination of the normal ( $SN$ , Fig. 20-11) for any set of planes ( $hkl$ ) to any zone axis [ $uvw$ ]:

$$\cos \rho = \frac{uh + vk + lw}{\sqrt{u^2 + v^2 + w^2} \sqrt{h^2 + k^2 + l^2}} \quad (20-12)$$

Using this equation, one readily calculates  $\rho$  for the (111), (100), (110), (311), etc., planes, assuming that [111] is the fiber axis, for example. For convenience, values of  $\rho$  from equation (20-12) have been listed in Table 20-1. Thus, for the innermost (111) ring in Fig. 20-10, six lumps

TABLE 20-1.—VALUES OF  $\rho$   
(In degrees)

Lattice plane	Fiber axis			
	[100]	[110]	[111]	[112]
(100)	0, 90	45, 90	55	35, 66
(110)	45, 90	0, 60, 90	35, 90	30, 55, 73, 90
(111)	55	35, 90	0, 71	19, 62, 90
(112)	35, 66	30, 55, 73, 90	19, 62, 90	0, 34, 48, 60, 71, 80
(310)	18, 72	27, 48, 63, 77	43, 69	25, 50, 59, 75, 83
(311)	25, 72	31, 65, 90	30, 59, 80	10, 42, 61, 76, 90

should appear at 0 and 71° from “axis” if [111] is the fiber axis. Similarly, for the second (200) ring, four lumps should appear at 55° from “axis,” etc. These predicted positions for the lumps have been indicated by the arrows in Fig. 20-10. On the other hand, if [100] is the fiber axis, reference to Table 20-1 shows that lumps should appear at the positions indicated by crosses in Fig. 20-10. Since strong maxima are actually observed where the arrows predict them and weaker maxima are also seen where the crosses predict them, one may conclude that perhaps two-thirds or three-fourths of the crystals in the wire tended to align their [111] axes parallel to the wire, whereas the remaining 25 or 35 per cent preferred [100] as a fiber axis. This is typical of face-centered cubic metal wires. As a rule, [110] is the fiber axis of body-centered cubic wires.

The positions for [111] fibering predicted for the maxima by the

arrows in Fig. 20-10 are represented by the black spots in Fig. 20-12, and the positions for [100] fibering are represented by the spots in Fig. 20-13 and by crosses in Fig. 20-10. The purpose of Figs. 20-12 and 20-13 is to show how these maxima lie on layer lines, as in Figs. 17-10 and 17-11 by the analogy already mentioned.

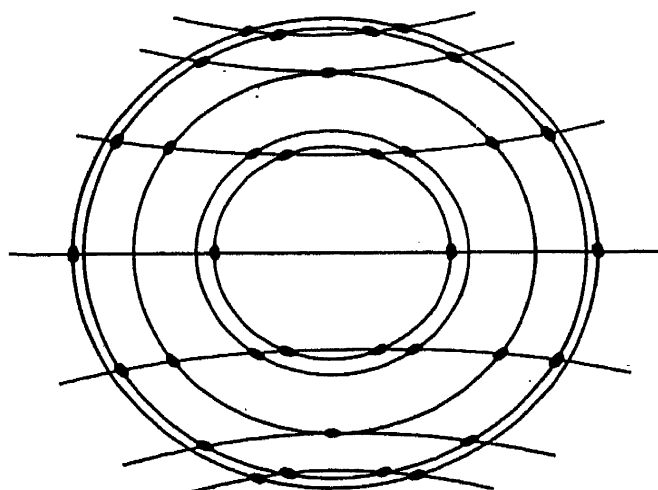


FIG. 20-12.—Fiber diagram for [111] fibering of face-centered cubic metals. Note the layer lines.

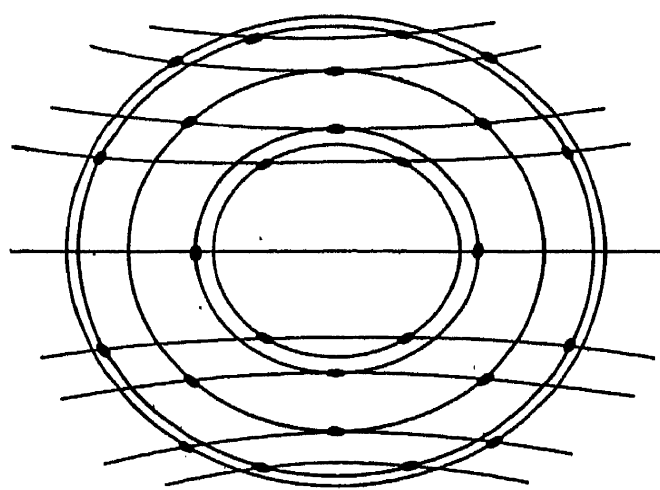


FIG. 20-13.—Fiber diagram for [100] fibering of face-centered cubic metals. Note the layer lines.

If the wire is inclined to the primary beam at an angle  $\beta$  less than  $90^\circ$  in Fig. 20-11, then the orientation maxima occur in groups of four as before, but they are crowded together in the half of the pattern toward which the wire leans and spread apart in the other half, so that there are two values for the angle  $\delta$ . One of these is given by the following equation, which replaces (20-11):

$$\cos \delta = \frac{\cos \rho - \cos \beta \sin \theta}{\sin \beta \cos \theta} \quad (20-13)$$

The other is found by substituting  $180^\circ - \beta$  for  $\beta$  in (20-13).

**5. Preferential Orientation with Respect to an Axis and a Surface—Limited Fibering.** Limited fibering, as distinguished from fibering, has already been described on page 451 and in Fig. 20-8. It is the type of preferential orientation commonly encountered in sheet metal subjected to rolling or deep drawing. As a rule, the direction of the preferred orientation resulting from cold work of sheet metal depends on the metal, whereas the degree or completeness of the preferred orientation depends on the number of passes, the size of the rolls, the per cent reduction, etc. Usually the body-centered cubic crystals in metals such as iron and tungsten tend to align themselves with their [110] axes (cube-face diagonals) parallel to the roll direction of the sheet and with their {100} faces lying in the plane of the surface.

Hanawalt has shown that the direction of preferential orientation in extruded magnesium alloys varies with the extruding temperature. At

a low temperature, the fiber axis is  $[210]$ , at a higher temperature,  $[110]$ .<sup>1</sup> Magnesium has a hexagonal close-packed structure, and rolling tends to cause the hexagonal axis ( $C$  axis) to take up a position perpendicular to the plane of the sheet.<sup>2</sup> The same is true of zinc,<sup>3</sup> which also has a hexagonal structure.

Upon turning to the face-centered cubic metals like copper, alpha brass, and aluminum, the situation is somewhat more complex. The nature of the preferred orientation produced by cold work in this case has been studied by Polanyi and Weissenberg,<sup>4</sup> Wever and Schmidt,<sup>5</sup> and others. Supplementing these general studies, there have been investigations of various face-centered cubic metals individually, such as aluminum<sup>6</sup> and copper.<sup>7</sup> Cold work tends to align the crystals of these metals with one of their  $[112]$  axes parallel to the direction of rolling or drawing and one of the planes of the  $\{110\}$  form parallel to the surface. There are two alternative orientations fulfilling this condition, as Cook and Richards<sup>7</sup> have pointed out. These are typified by the  $(110)$  plane (excluding the other  $\{110\}$  forms in this case) parallel to the surface and either the  $[\bar{1}12]$  axis or the  $[1\bar{1}2]$  axis parallel to the rolling direction. The methods by which these preferred orientations are determined from powder patterns are rather involved; the commonest method makes use of so-called "pole figures," which will be discussed later. Once the orientation has been deduced by such methods, however, its verification from the patterns obtained in ordinary routine work is fairly simple.

Figure 20-15 is a transmission pattern of a section cut from the corrugated wall of a brass bellows formed by deep drawing from sheet brass, the pattern of the original annealed sheet being shown in Fig. 20-14. It is at once evident that the grain size has been greatly reduced. The fact that the rings are not uniform in intensity all around their circumference immediately reveals preferential orientation of the crystals in a direction perpendicular to the primary x-ray beam, in this case, in the plane of the sheet. In Fig. 20-15 this nonuniformity is not very pronounced; in fact, it would be likely to escape the notice of a person examining it casually. As the preferential orientation in the sample becomes more pronounced, this nonuniformity becomes more pronounced

<sup>1</sup> A.S.T.M. Symposium on Radiography and X-ray Diffraction (1936), p. 321.

<sup>2</sup> D. E. Thomas, *J. Inst. Metals*, **67**, 173 (1941); L. Frommer, *J. Inst. Metals*, **67**, 361 (1941).

<sup>3</sup> M. L. Fuller and G. Edmunds, *T.A.I.M.M.E.*, **111**, 147 (1934).

<sup>4</sup> M. Polanyi, *Z. Physik*, **7**, 149 (1921); M. Polanyi and K. Weissenberg, *Z. Physik*, **9**, 123 (1922); **10**, 44 (1922).

<sup>5</sup> F. Wever and W. Schmidt, *Z. tech. Physik*, **8**, 398 (1927).

<sup>6</sup> W. G. Burgers and J. C. M. Basart, *Z. Physik*, **54**, 86 (1929); L. Frommer, *J. Inst. Metals*, **64**, 284 (1939).

<sup>7</sup> M. Cook and T. L. Richards, *J. Inst. Metals*, **66**, 1 (1940).



until the rings lose their identity as rings entirely and are replaced by (usually) four, six, or eight segments,<sup>1</sup> depending upon the metal, the

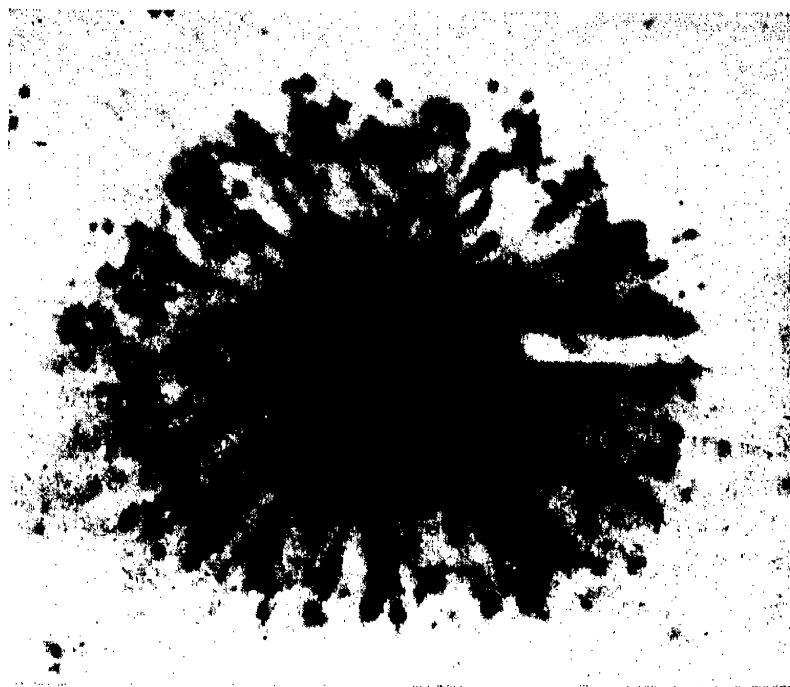


FIG. 20-14.—Pattern of annealed sheet brass.

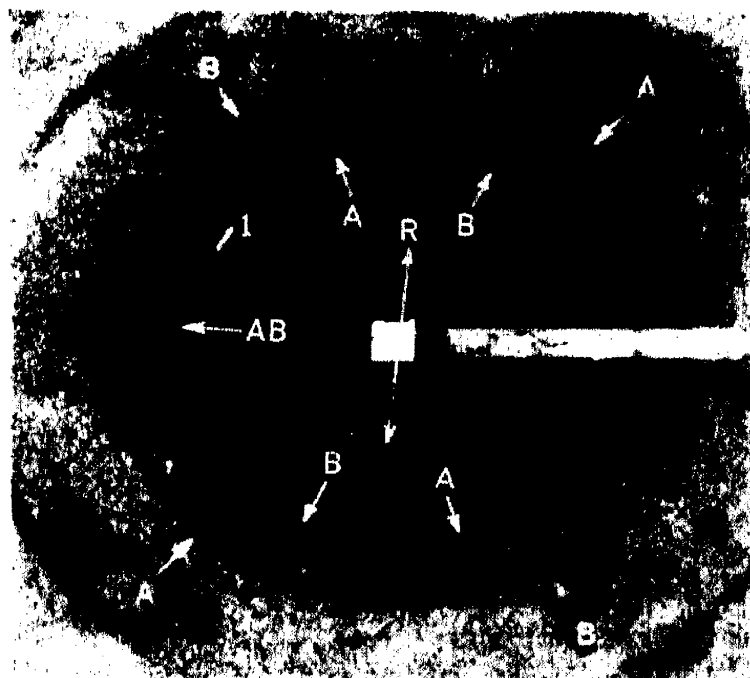


FIG. 20-15.—Pattern of same sheet brass as in Fig. 20-14, after deep drawing operation. The arrows indicate the nature of the cold work, and the relative directions of the axis of the work and of the primary x-ray beam. Although the degree of preferential

<sup>1</sup> An excellent series of illustrations for rolled aluminum is included in the article by L. Frommer, *J. Inst. Metals*, **64**, 284 (1939).

orientation seen in Fig. 20-15 is comparatively slight, it was enough to cause early fatigue failure by flexure of the bellows in service. By forming the bellows in four operations instead of three, this preferred orientation was practically eliminated and, with it, the fatigue failures.

Thus it is seen that a simple visual inspection of a diffraction pattern occasionally may be sufficient to discover and suggest a cure for some difficulty. As a method of detecting the internal damage due to fatigue stresses in metals, and hence as a warning of impending fatigue failure, x-ray diffraction has not proved successful, except in the rare cases where the pattern happens to be taken exactly at the point of failure shortly before it occurs.<sup>1</sup> In many instances where preferential orientation is an important factor, it is merely necessary to compare its severity in one sample with its severity in another or to compare the direction of the orientation in two samples. One can detect differences in either severity or direction of orientation by cursory examination of the non-uniformities of the rings.

When the question, "What is the orientation?" enters, however, as it does, in a few problems, the answer is not so readily evident. As an example, let us ask "What is the preferential orientation that caused the nonuniform rings in Fig. 20-15?" First, the material is brass. The innermost faint ring marked 1 in the figure is caused by the  $K_{\beta}$  radiation that evidently was present, probably owing to too thin a filter. If this is ignored, the pattern is seen to fit the "pair followed by a single ring" sequence (Fig. 18-7) characteristic of face-centered cubic materials. This indicates that the specimen is alpha brass, a solid solution of zinc in copper, characteristic of brass from zero up to about 38 per cent zinc. Therefore the innermost and strongest ring (neglecting 1) is the (111) ring, the next is (200), followed by the (220) ring considerably farther out. It might be presumed that deep drawing would produce the same sort of preferential orientation in the brass as rolling would, but this remains to be verified. Tentatively assuming that such is the case, however, what arrangement of ring nonuniformities is to be expected?

If the (110) planes tend to lie parallel to the surface and if the  $[1\bar{1}2]$  axis tends to be aligned with the "axis of roll" (whatever that may be, when one is forming a bellows!), then one is concerned with the most probable orientation of the planes of the {111} and {100} forms under these circumstances, since these planes diffract the two most prominent rings in Fig. 20-15. Reference to the model mentioned at the beginning of this section will show that Fig. 20-16A represents the desired relationships. The angles involved are angles such as  $\tan^{-1} 1/\sqrt{2}$ , etc., as may be deduced from the model. Table 20-2 will be found helpful

<sup>1</sup> See, for example, A. G. Barkow, *J. Applied Phys.*, **16**, 111 (1945) (aluminum); or R. G. Spenter, *Phys. Rev.*, **55**, 991 (1939) (malleable iron).

also in this type of work. Figure 20-16A is a diagram that represent the following facts: Looking along the primary x-ray beam, to which the (110) planes tend to become perpendicular, with the  $[1\bar{1}2]$  axis (that is, the direction of roll  $R$ ) vertical in the figure, the  $[\bar{1}11]$  axis is transverse to the direction of roll and the  $[001]$  axis is aligned  $54^\circ 44'$  counter

TABLE 20-2.—ANGLES BETWEEN CRYSTALLOGRAPHIC PLANES IN CUBIC CRYSTAL

( <i>HKL</i> )	( <i>hkl</i> )	Values of angles between ( <i>HKL</i> ) and ( <i>hkl</i> )					
100	100	0°	90°				
	110	45°	90°				
	111	54°44'					
	210	26°34'	63°26'	90°			
	211	35°16'	65°54'				
	221	48°11'	70°32'				
	311	25°14'	72°27'				
110	110	0°	60°	90°			
	111	35°16'	90°				
	210	18°26'	50°46'	71°34'			
	211	30° 1'	54°44'	73°13'	90°		
	221	19°28'	45°	76°22'	90°		
	311	31°27'	64°47'	90°			
111	111	0°	70°32'				
	210	39°14'	75° 2'				
	211	19°28'	61°52'	90°			
	221	15°48'	54°44'	78°54'			
	311	29°30'	58°30'	79°58'			
210	210	0°	36°52'	53° 8'	66°25'	78°28'	90°
	211	24° 6'	43° 5'	56°47'	79°29'	90°	
	221	26°34'	41°49'	53°24'	63°26'	72°39'	90°
	311	19°17'	47°36'	66° 8'	82°15'		
211	211	0°	33°33'	48°11'	60°	70°32'	80°24'
	221	17°43'	35°16'	47° 7'	65°54'	74°12'	82°12'
	311	19° 8'	42°24'	60°30'	75°45'	90°	
221	221	0°	27°16'	38°57'	63°37'	83°37'	90°
311	311	0°	35° 6'	50°29'	62°58'	84°47'	

\* R. M. Bozorth, *Phys. Rev.*, **26**, 390 (1925).

clockwise and the  $[\bar{1}1\bar{1}]$  axis  $70^\circ 32'$  clockwise with respect to it. In cubic crystal, the  $[hkl]$  axis is normal to the (*hkl*) planes, and so one would expect the (111) planes to congregate about a position causing them to diffract the primary rays to the left and right, as indicated by the line marked  $\bar{1}11$  in Fig. 20-16A. Therefore, in the pattern, as represented by Fig. 20-16C, one would expect abnormal intensities in the inner (111) ring at the points marked  $AB$ ,  $AB$ . Likewise, the  $\bar{1}1\bar{1}$  line in Fig. 20-16A would suggest abnormal intensities in the inner (111) ring at the two points marked  $A$ , and the 001 line in Fig. 20-16A predicts abnormal

intensities in the outer (200) ring at the two points marked *A* in Fig. 20-16*C*. Such preferential orientation must equally divide itself between  $[1\bar{1}2]$  alignment and  $[\bar{1}12]$  alignment, that is, between the alignment of

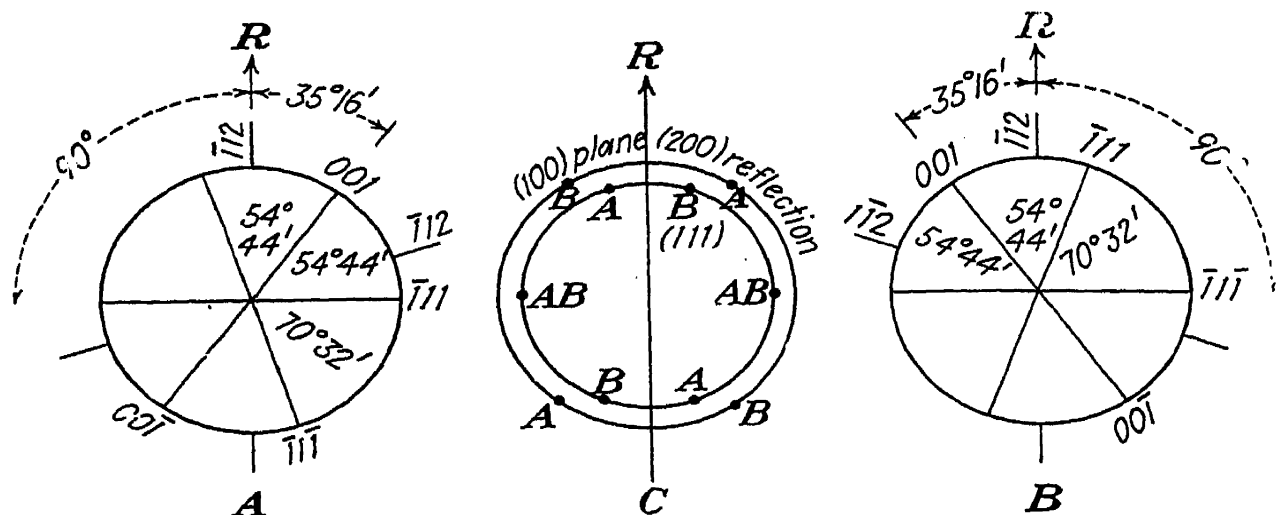


FIG. 20-16.—Diagrams for the study of preferential orientation in face-centered cubic sheet metal, such as alpha brass.

Fig. 20-16*A* and Fig. 20-16*B*, by probability, since both alignments are crystallographically equivalent. As before, Fig. 20-16*B* predicts abnormal intensities at the points marked *B* and *AB* in Fig. 20-16*C*.

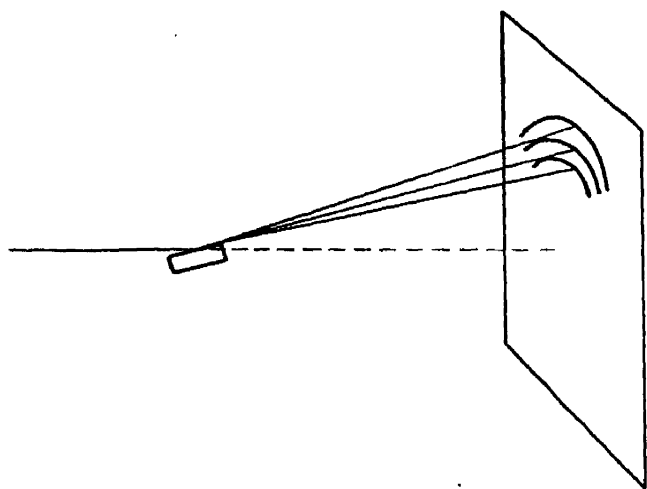


FIG. 20-17.—Method of obtaining pattern at grazing incidence.

Comparison of Fig. 20-16*C* with Fig. 20-15 shows that the observed abnormal intensities occur exactly as predicted, if *R* is taken as the rolling axis. Since the spots at *AB* are due to both alignments, whereas the other spots marked *A* and *B* are due to only one of the two, they should be twice as intense as the others. This appears to be the case, as far as one can judge by visual observation.

**6. Pole Figures.** The preceding section has made it evident that

the character and degree of the preferential orientation of the crystals in a solid is difficult to describe and represent clearly, because one is dealing with a large number of three-dimensional objects filling a three-dimensional space. In an effort to find some way of doing this, Wever<sup>1</sup> has devised an adaptation of the stereographic projections used in single-crystal studies by crystallographers. Wever's adaptation is called a "pole figure." To prepare a pole figure for the (111) plane in the case

<sup>1</sup>F. Wever, *Z. Physik*, **28**, 69 (1924); for more detail, see F. Wever, *Trans. A.I.M.M.E.*, **93**, 51 (1931).

of the drawn brass just discussed, it is necessary to take several transmission patterns at some 5 or 10 different angles between the beam and the metal surface. At small inclinations, only par normal transmission pattern is obtainable, as seen in Fig. 20-17 is, only the arcs forming the upper part of the usual rings in th will appear on the film.

In Fig. 20-18, the primary monochromatic x-ray beam  $X$  perpendicularly through the sheet specimen  $C$ , which has been down to suitable thickness, the primary beam then striking th

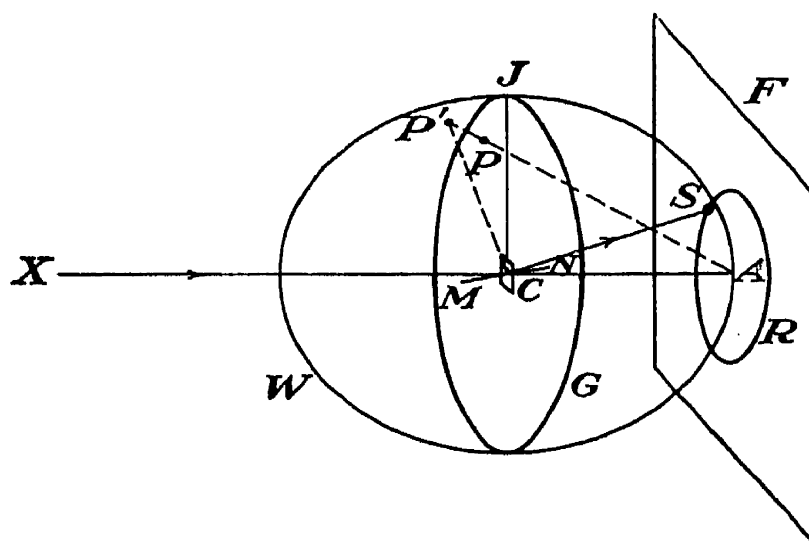


FIG. 20-18. Illustrating the construction of a pole figure.

perpendicularly at  $A$ . The sphere  $W$  of radius  $CA$  is drawn with center. The great circle  $G$  is drawn in the plane of the sheet specimen, the reference point  $J$  being on the line  $JC$ , the direction of rolling. If preferential orientation may be such that many of the (111) planes tend to congregate about a position  $MN$ , causing abnormal intensity of the (111) ring  $R$  at the spot  $S$  on the film  $F$ . Upon erecting the perpendicular  $CP'$  to the plane  $MN$ , it intersects the sphere at  $P'$ . When  $P'$  is viewed from an imaginary peephole at  $A$ , it appears to be at  $P$  on the plane of the great circle  $G$ . Such points  $P$  are plotted on a piece of paper representing this circular plane area  $JG$  to scale, for all spots  $S$  on the (111) ring.

Then the plane specimen  $C$  is rotated about the axis  $CJ$  through an angle of  $30^\circ$ , say, and a new pattern is photographed. The great circle  $G$  rotates about axis  $CJ$  with the specimen. The plotting is repeated on the same piece of paper. This is done for several such positions, and then for several more when the specimen (and  $G$ ) are rotated to four fixed positions about a transverse axis perpendicular to  $JC$  and  $XA$ . The resulting stereographically projected plot of points  $P$  in the plane of the great circle  $G$  is called a "pole figure" for the (111) planes because it was plotted from the abnormally intense spots on the (111) ring. If the abnormally intense spots on the (200) ring had been

instead, the resulting plot would be a pole figure for the (100) planes. The direction of roll  $CJ$  obviously will appear in the pole figure unless the specimen  $C$  is a sheet cut transversely out of a rolled plate, for example, when the direction of roll is perpendicular to the specimen and hence to the plane of the pole figure. In this case, the reference axis  $CJ$  may

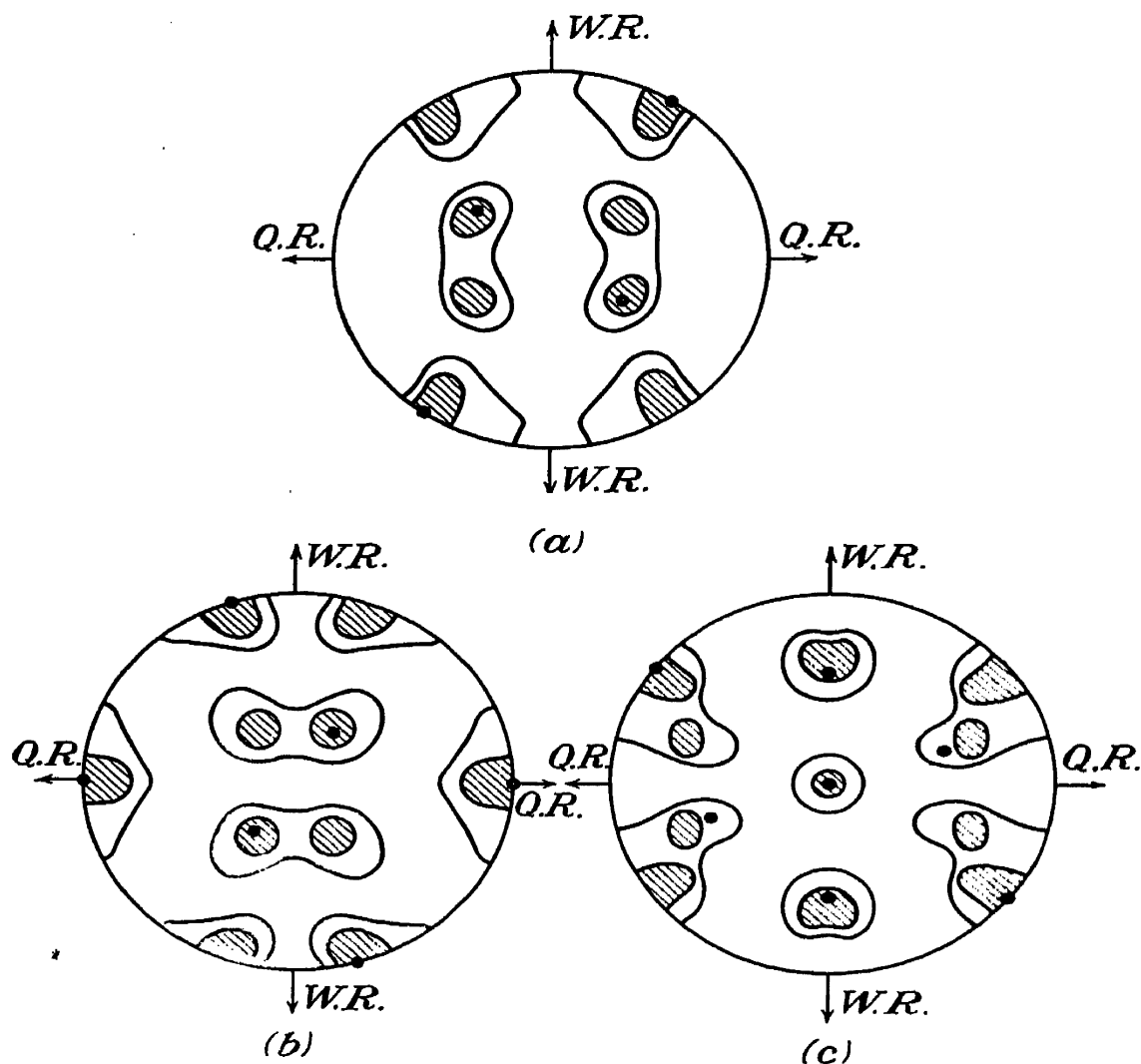


FIG. 20-19.—Pole figures showing the texture of rolled alpha brass. *a*, (100) planes; *b*, (111) planes; *c*, (110) planes. (Göler and Sachs.)

represent the normal to the original plate, and the other axis will represent the transverse direction (Fig. 20-20 is an example).<sup>1</sup>

Such pole figures are useful to those who wish to study preferential orientation in rolled or drawn metals in a quantitative way. They represent both the direction and the degree of orientation of the crystals quantitatively.<sup>2</sup> Figure 20-19 shows three pole figures in the plane of the sheet for rolled alpha brass, as plotted by Göler and Sachs.<sup>3</sup> The three

<sup>1</sup> For further details on plotting pole figures, see C. S. Barrett, *Trans. A.I.M.M.E.*, **124**, 29 (1937).

<sup>2</sup> B. F. Decker, *J. Applied Phys.*, **16**, 309 (1945).

<sup>3</sup> v. Göler and G. Sachs, *Z. Physik*, **56**, 477 (1929).

figures were plotted, respectively, from the (200), (111), and (220) rings in a series of patterns in which the central one (normal incidence) must have been very similar to Fig. 20-15. The small black dots in Fig. 20-19 mark the pole areas corresponding to the *A* orientation in Fig. 20-16, and the others correspond to the *B* orientation. The shaded areas show the most frequent locations of the poles on the stereographic plot. The surrounding clear borders show the less densely populated polar areas. Figure 20-20 is a pole figure plotted by Wever for the (011) plane of

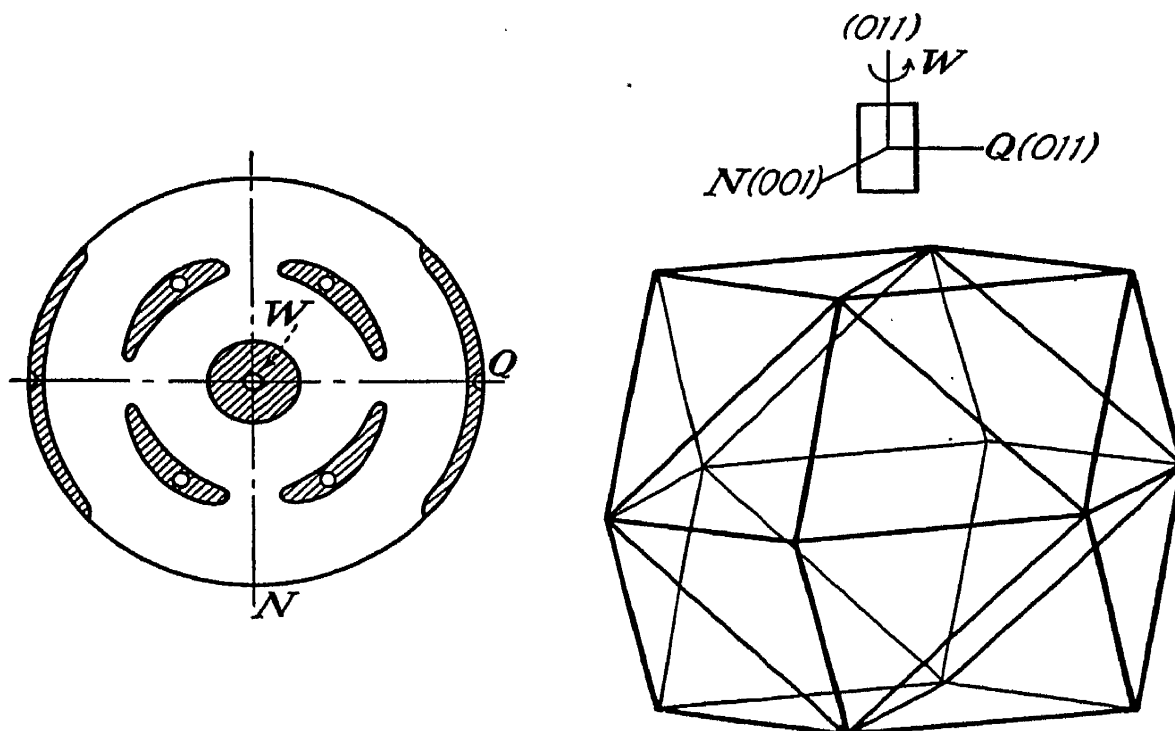


FIG. 20-20.—Pole figure (left) for the (011) planes of sheet steel, viewed along the direction of roll (Wever). Orientation of unit cubes is indicated at right. *W* is direction of roll; *N* is the normal to the sheet. *Q* is in the plane of the sheet, and perpendicular to *N* and *W*.

cold-rolled iron as viewed along the direction of roll, *W*, perpendicular to the diagram. The plane of the original rolled plate, also perpendicular to the diagram, intersects it along the horizontal line *Q*. The shaded areas along the right and left edges are the regions in which the  $[01\bar{1}]$  and  $[0\bar{1}1]$  poles *P* (Fig. 20-18) congregate. The area in the center is for  $[011]$ , of course, and the other four areas are for  $[110]$ ,  $[1\bar{1}0]$ ,  $[10\bar{1}]$ , and  $[101]$ .

**7. Preferential Orientation in the Direction of the Primary X-ray Beam.** The preceding sections may give the impression that preferred orientation always manifests itself in a powder pattern in the form of abnormally intense spots at certain definite positions around the circumference of certain diffraction rings. This is not true. When it is uniaxial and is in the direction of the primary x-ray beam, the preferential orientation manifests itself as a change in the relative intensities of the rings. This type is commonly encountered in the metallic coats deposited in

electroplating processes. As an example, one may consider the case of nickel electrodeposited on copper. Since nickel is face-centered cubic, its normal Hull-Debye-Scherrer transmission pattern consists of the (111), (200), (220), etc., rings, as indicated in Fig. 18-6. When one carries through a calculation of the type illustrated in Table 18-2 (page 414), the relative intensities of the (111) and (200) rings for nickel are found to be theoretically 128,300 and 72,000, respectively, or about 16 to 9. Such a calculation is of course based on the assumption that the orientation is random. When electrodeposited coats are of the order of a

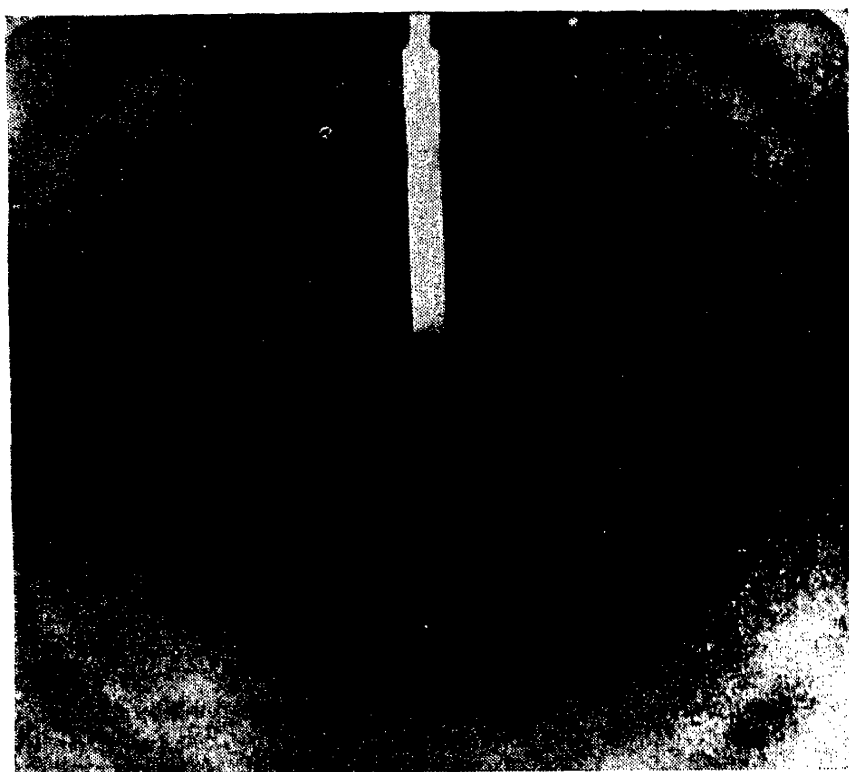


FIG. 20-21.—Electrodeposited nickel; random orientation. Inner (111) ring is noticeably heavier than (200) ring just outside it.

thousandth of an inch thick, an obvious way to examine them by x-ray diffraction is to strip the coat from the base metal and use the former as a transmission specimen. In the case of nickel electrodeposited on copper, this is readily accomplished by placing the nickel-plated sheet of copper in a strong KCN (potassium cyanide) solution for a few minutes.

Figure 20-21 shows the transmission pattern of such a stripped-off nickel coat. The broad, blurred rings are due to the use of large pin-holes, which were employed in this work to reduce the exposure time to about 5 min.; since a large number of samples were examined and the relative intensities of the (111) and (200) rings were the only feature of the pattern to be studied, clear, sharp rings were unnecessary. The nickel coat that gave the pattern in Fig. 20-21 was electroplated with a usual current density of 50 ma./cm.<sup>2</sup>. It is seen that the inner (111)



ring is stronger than the adjacent (200) ring. From casual examination, one might agree that (200) is about  $\frac{9}{16}$  as strong as (111), the theoretical ratio for random nickel.

Figure 20-22 shows the transmission pattern of another stripped-off nickel coat prepared under identical conditions except that the unusually low current density of 3 ma./cm.<sup>2</sup> was used in the plating process. To secure the same thickness of coat, the time for the plating was  $\frac{5.0}{3}$  as great as before. It is apparent that the (111) and (200) rings have nearly

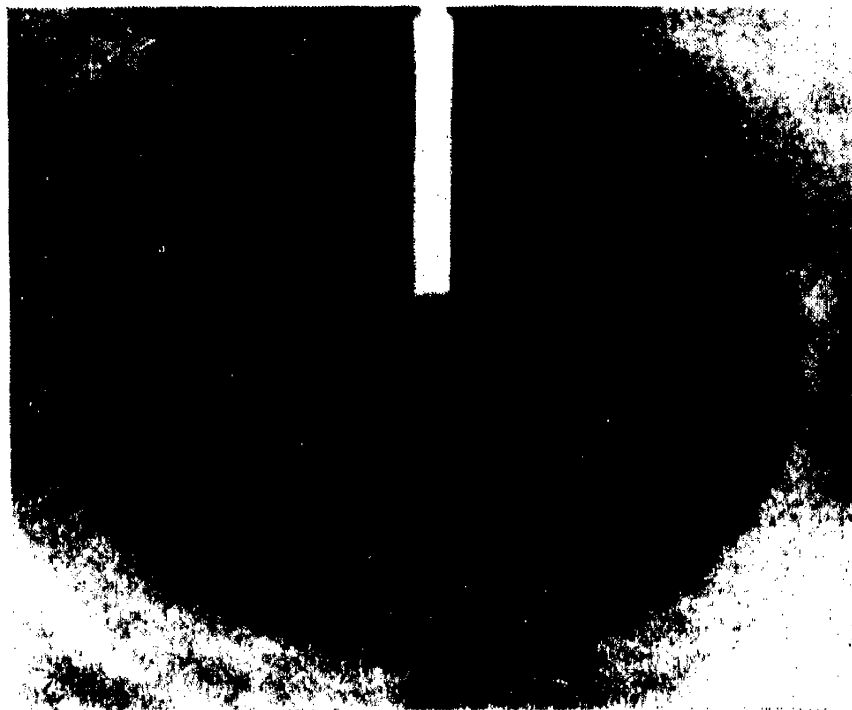


FIG. 20-22.- Electrodeposited nickel; preferential orientation (cube faces lie in the plane of the surface). The two rings (111) and (200) about equally intense.

equal intensity in this pattern. The explanation is that at such a low current density the nickel is deposited with a preferred orientation. The great difference in appearance of the two nickel-plated sheets makes it evident that there is some important difference in the structure of the two coats, and the x-ray patterns reveal what this difference is. Its nature would be very difficult to determine by any method other than x-ray or electron diffraction. Experiments of this type have been described by Wood.<sup>1</sup>

The fact that the (200) ring is abnormally strong for all azimuths (that is, uniformly strong all around its circumference) can be explained by supposing that the low-current-density nickel plate is deposited in the form of cubic crystals, a large fraction of which have one cube face in a position nearly parallel to the metal surface but the other four faces (the ones perpendicular to this one) oriented in random directions in the

<sup>1</sup> W. A. Wood, *Phil. Mag.*, **20**, 964 (1935).

plane of the metal surface. Presumably these other four faces are those which do most of the "reflecting" of the rays into the (200) ring, since they must lack just  $11.7^\circ$  of being perpendicular to the sheet in order to do so, by Bragg's law, for molybdenum  $K_\alpha$  radiation.

**8. Concluding Discussion.** This chapter has explained how grain size can be determined by x-ray diffraction unless it lies in the  $2 \times 10^{-4}$  to  $10^{-2}$  mm. blind spot. In practice, the region in which the x-ray method is superior to other methods of grain-size determination is in the lower ranges below  $10^{-4}$  mm., where the grains are too small to see microscopically; however, there are instances where the x-ray method is most helpful in determining grain size, even in the ordinary size range. The interdependence of the various factors such as (1) character of the x-ray pattern, (2) grain size, (3) grain distortion (strain), (4) crystal structure (amorphous or crystalline), (5) technique (back reflection or transmission, etc.), and (6) preferred orientation is now becoming evident. It is clear that one should be familiar with these interdependent relationships before undertaking to interpret diffraction patterns. Finally, the commercial importance of preferred orientation has been brought out, along with the fact that x-ray diffraction is the preeminent method, and practically the only method, of measuring and studying it.

### QUESTIONS AND PROBLEMS

1. What is grain size, and how is it usually measured? According to Wood, what is the smallest grain size attained in the commoner commercial metals by cold work? How can one measure the much finer grain sizes existing in colloidal suspensions, etc.? What is the blind spot in the x-ray method of grain-size measurement?

2. Make a rough estimate of the grain size of the steel sample giving the pattern in Fig. 20-2.

3. How should you tell by a glance at a transmission pattern whether the grain size of the sample was considerably above or below (a) 0.05 mm.; (b) 0.005 mm.; (c) 0.0002 mm.?

4. In estimating the grain size by actual counting of the diffraction spots in a pattern, what factors should be considered if an accurate estimate is desired? What is meant by the half-value breadth  $B$  of a diffraction line, as used in the Scherrer formula?

5. A transmission pattern of colloidal gold is obtained with molybdenum  $K_\alpha$  radiation. Gold is face-centered cubic with a lattice constant  $a = 4.07$  Å. After making all corrections, the breadth  $B$  as used in the Scherrer formula is 0.01 radian for the (111) ring. What is the grain size of the gold particles?

*Ans.*  $6\frac{1}{2} \times 10^{-6}$  mm.

6. Does the breadth  $B$  as ordinarily defined correspond to a spread  $\Delta\theta$  in the Bragg angle  $\theta$  or to a spread  $\Delta\phi$  in the angle of deflection  $\phi = 2\theta$ ? If the breadth of the (111) line from a sample of copper filings is 0.005 radian and if the breadth of the same line for some drawn copper is 0.01 radian, what is the value of  $B$  that should be used in the Scherrer formula for the drawn copper? *Ans.* 0.00866 radian.

7. Is there any way in which line broadening due to microstresses can be distinguished from line broadening due to ultrafine grain size? If so, how?

8. Does the direction of the preferential orientation caused by rolling depend primarily on (a) the metal being rolled or (b) the number of passes and per cent reduction? Does the degree or severity of the orientation depend primarily on (a) or (b)?

9. What feature or characteristic in an x-ray diffraction pattern usually reveals preferential orientation in the sample? Is it possible for preferential orientation to be quite pronounced without this feature appearing in the pattern? If so, what can be said about the direction of the orientation?

10. What differences should you expect to see in the x-ray pattern of sheet copper after one pass through the rolls and after two passes? What is a crystallite?

11. How could one measure the severity or degree of the preferential orientation in nickel plate by taking only one pattern of it? What is meant by recrystallization orientation?

12. What is a pole figure? With the aid of a wire and ball model, identify as many of the poles in Fig. 20-19 as you can. How should you expect the appearance of these figures to change with the severity or degree of the orientation?

13. What is meant by fibering? Limited fibering? Define the term "fiber axis." What is the usual fiber axis for body-centered cubic metals? For face-centered cubic metals in wires?

14. Draw a fiber diagram like Fig. 20-12 or 20-13 for a wire drawn from a body-centered cubic metal if  $[110]$  is the fiber axis, assuming random orientation in a plane perpendicular to the wire.

## CHAPTER 21

### THE MEASUREMENT OF STRESS AND STRAIN BY X-RAY DIFFRACTION; DIFFUSE REFLECTIONS

**1. Introduction.** On page 449 it was explained that grain distortion can cause line broadening and that this distortion is associated with strains, designated by the letter  $\epsilon$ , which may be introduced by such processes as cold work. Strains of this type have been called "microstrains" by some workers using x-ray diffraction methods. Microstrains may be defined as strains that vary widely and erratically in magnitude and direction between neighboring grains, or within the individual grains, in a crystalline solid. They occur when the elastic limit or yield point is exceeded, as in cold working. On the other hand, the strains resulting from the elastic distortion of a solid, such as a spring, when the elastic limit is not exceeded, may be called "macrostrains." Such distortion affects the crystals in such a way that the strains introduced vary from crystal to crystal and from point to point within each crystal in a systematic manner.

Interest in experimental methods of measuring the strains and stresses in all types of structural members, such as aircraft wing spars, pistons, cylinder blocks, bridge girders, steam boilers, and railroad rails, has been gathering momentum in recent years, as is indicated by numerous conferences and symposia on this subject.<sup>1</sup> Such strains are measured by wire strain gauges,<sup>1,2</sup> by photoelastic methods,<sup>1,3</sup> and by other methods.<sup>1</sup> The fact that x-ray diffraction is capable of measuring strains in the surface layers of any solid crystalline object having such a grain size (in the surface layers) that it will yield sharp rings or lines (about  $2 \times 10^{-4}$  to  $10^{-2}$  mm. grain size) was pointed out by Sachs and Weerts<sup>4</sup> in 1930.

In some respects, x-ray diffraction is inferior to the other methods; in others, superior. Its most important advantages, perhaps, are that (1) it can measure the strain without any necessity for comparing the strained specimen with a supposedly unstrained specimen and (2) it can

<sup>1</sup> See "Experimental Stress Analysis," Proceedings of the Society for Experimental Stress Analysis, vols. 1 and 2, Addison-Wesley Press, Cambridge, Mass., 1943-1944. For a bibliography of articles on stress measurement by x-rays, see H. R. Isenburger, *Welding J.*, **23**, supplement, p. 571-S, (November, 1944).

<sup>2</sup> See, for example, D. M. Nielsen, *Electronics*, December, 1943, p. 106.

<sup>3</sup> See, for example, *J. Applied Phys.*, **12**, 584-625 (1941).

<sup>4</sup> G. Sachs and J. Weerts, *Z. Physik*, **64**, 344 (1930).

measure the strain at a spot 1 mm. in diameter or less without any interpolation or extrapolation obtained from measurements outside that spot. Its disadvantages are that it is capable of measuring the macrostrain only when microstrains are not unduly severe and over the limited grain size range given above. In ferrous specimens, this limits one to material having a hardness below 40 Rockwell C, for example. The method is slow and requires an experienced operator and rather expensive equipment. It is useless for measuring rapidly changing strains, as in the parts of an engine while it is operating.

The strains introduced in a bar when it is stretched, compressed, bent, or twisted without exceeding the elastic limit are macrostrains, whereas quenching and cold work introduce both macrostrains and microstrains. A process like shot peening also introduces both macrostrains associated with the compressive stress set up in the surface layer, balanced by forces of tension underneath, and microstrains in the surface layer, which is stressed beyond the elastic limit by the peening. Bragg<sup>1</sup> has made instructive soap-bubble models illustrating the distortion of the grains by plastic deformation. As a result of the distortion, the grains are broken, compressed, stretched, bent, and twisted slightly, and the fragments slip along the cleavage planes.

Both macrostrains and microstrains cause variation in the interplanar  $d$  spacings in the crystals composing the solid. As a typical example, steel has a Young's modulus of the order of 30,000,000 lb./in.<sup>2</sup> and an elastic limit, or yield point, of the order of 30,000 lb./in.<sup>2</sup>, so that one should expect variations of the order of 1 part in 1,000 for any given  $d$  (say  $d_{110}$ ) in a sample subject to severe stresses, either macro- or micro-. The grain fracture resulting from plastic deformation soon reduces the grain size below  $10^{-2}$  mm., so that a continuous ring pattern is obtained. The variation in  $d$  spacing associated with the microstrain then causes a broadening of the lines that is difficult to distinguish from broadening due to ultrafine grain, as mentioned in the preceding chapter, and it will be independent of the direction of the x-ray beam in the sample. The broadening follows directly from the Bragg equation; slight variations of  $d$  correspond to slight variations in  $\theta$  for a given  $\lambda$  in a powder sample where all possible crystal orientations exist.

Returning to the discussion of ordinary macrostrain, one may consider the case of a steel bar 1 in. square and 1 ft. long. When a force of 20,000 lb. is applied to it, tending to stretch it, the bar becomes more than 1 ft. long and less than 1 in. square. This elongates the grains in a direction parallel to the bar and causes them to shrink in directions perpendicular to it. This elongation in one direction and shrinkage in another appears in the x-ray pattern as a slight shift in the lines or rings

<sup>1</sup> W. L. Bragg, *J. Sci. Instruments*, **19**, 148 (1942).

corresponding to the increase or decrease in the various crystal lattice spacings  $d$  and depending upon the direction of the primary and diffracted x-ray beams in the sample. This dependence of the line shift on the beam direction readily distinguishes such line shifts due to strain from the otherwise similar line shifts resulting from thermal expansion (which increases  $d$  uniformly in all directions) or from the shifts caused by change in composition, as when the copper lattice in alpha brass is expanded by the addition of more zinc in solid solution. The shifts from such composition change are also much larger than the shifts due to strains, limited as the latter are to about a 0.1 per cent change in  $d$ . The dependence upon direction enables one to compare the strains in 15 per cent zinc brass with the strains in 20 per cent zinc brass without any need for knowing the magnitude of the line shift in going from one brass to the other.

To summarize, then, ordinary macrostrains manifest themselves in the x-ray pattern as a line shift, whereas microstrains manifest themselves as a line broadening which may be difficult to distinguish from the similar broadening due to ultrafine grain. In spite of this possible ambiguity in some cases, x-ray diffraction yields more information on microstrain than any other known method. It is obvious that severe microstrain will subtract from the ability of a structural member to withstand the macrostresses for which it was designed. When a large casting is heat-treated to "relieve stress," the thermal stresses due to unequal rates of cooling in thick and thin portions (which are macrostresses) are relieved, but the relief of the microstresses in such an operation may be equally important.

**2. Why Back-reflection Technique Is Used for Strain Study and Measurement.** Both the slight line shift due to macrostrain and the slight line broadening due to microstrains are much easier to detect and measure in a back-reflection pattern than in a transmission pattern. In the first instance, the reason may be seen from the relation

$$d\theta = - \frac{dd}{d} \tan \theta \quad (21-1)$$

which was obtained in the derivation of equation (20-10). Equation (21-1) shows that the slight shift  $d\theta$  resulting from a strain  $dd/d$  varies as  $\tan \theta$ , the minus sign indicating merely that  $\theta$  decreases for positive strains (tensions) and increases for negative strains (compressions). Since  $\tan \theta$  becomes large as  $\theta$  approaches  $90^\circ$ , the line shift due to small changes in  $d$  becomes greater, and hence easier to detect and measure, when  $\theta$  approaches  $90^\circ$ . This occurs only in back-reflection patterns, of course.

The reason why a slight line broadening due to microstrains is easier

to detect by back reflection is also partly explainable from (21-1) where  $d\lambda/d$  is regarded as a continuous range of strain and  $d\theta$  the corresponding continuous range of  $\theta$  causing the broadening. Another reason appears upon differentiating Bragg's equation where  $d$  is regarded as a constant and  $\lambda$  as a variable.

$$\begin{aligned} d\lambda &= 2d \cos \theta \, d\theta \\ \frac{d\theta}{d\lambda} &= \frac{1}{2d} \sec \theta \end{aligned} \quad (21)$$

Equation (21-2) shows that a doublet, such as copper  $K_{\alpha_1}$ - $K_{\alpha_2}$  (1.47 and 1.543 Å.;  $d\lambda = 0.006$  Å.) will be resolved much more readily in Bragg reflection from any given set of planes with spacing  $d$  for large values of  $\theta$  than for small ones because the angular separation  $d\theta$  for a given wave-length separation  $d\lambda$  and interplanar spacing  $d$  varies as  $\sec \theta$ . With grains larger than  $2 \times 10^{-4}$  mm. and in the absence of microstrains the sharp lines in a powder pattern ordinarily have a breadth of order of  $\frac{1}{2}^\circ$ . Consequently, the  $K_\alpha$  doublet is not resolved in transmission patterns where  $\sec \theta$  is small and  $d\theta$  in (21-2) is less than  $\frac{1}{2}^\circ$  (it should be remembered that  $d\theta$  is in radians). When  $\theta$  becomes large enough so that  $\sec \theta$  equals 5 or 10 or more, however, as in a back-reflection pattern then  $d\theta$  becomes a degree or two and the  $K_{\alpha_1}$  and  $K_{\alpha_2}$  reflections are separated by an angle larger than the usual line breadth, that is, they are resolved. Why does this make it easier to detect slight line broadening? Obviously, if the usual line width is  $\frac{1}{2}^\circ$  in a doublet separated by  $1^\circ$ , the line appears double; but if this line breadth increases to  $1^\circ$  owing to microstrains or extremely fine grains, or both, the doublet merges into a single line in the pattern. Therefore doublet resolution in a back-reflection pattern may be conveniently used as a quick and easy index of the presence and magnitude of microstrains when the grain size is known to be above  $2 \times 10^{-4}$  mm. or as an index of grain size below  $2 \times 10^{-4}$  mm. when microstrains are absent. Figure 21-9 illustrates this point. A rate measurement of line broadening with a transmission camera or Seemann-Bohlin camera requires the use of a focusing monochromator.

**3. Choice of Radiation.** It has been seen that back reflection is the best technique for measuring strain, and the choice of the proper radiation now requires consideration. For back reflection,  $\sin \theta$  is nearly 1

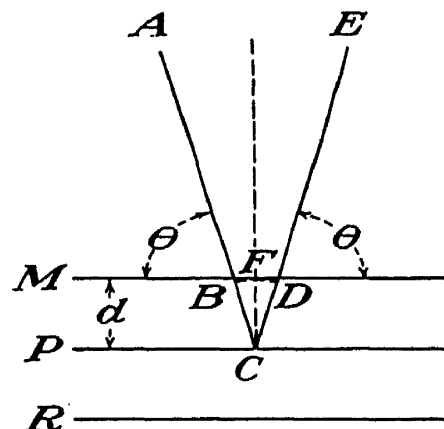


FIG. 21-1.—Showing the wave length should be slightly less than  $2d$  for back reflection work.

<sup>1</sup> Footnote 1, p. 398.

that Bragg's equation becomes  $n\lambda = 2d$  approximately. In Fig. 21-1, this means that  $n\lambda = BC + CD$  (exactly)  $= 2d$  or  $2CF$  (approximately). In accordance with usual practice in calculating Bragg reflections, fictitious planes permit one to set  $n = 1$ , and on this basis it is seen that the selection of the proper radiation involves a choice of  $\lambda$  slightly less than  $2d$ .

TABLE 21-1

ALUMINUM FACE-CENTERED CUBIC				COPPER FACE-CENTERED CUBIC			
Indices	$d$	$2d$	$I$ , per cent	Indices	$d$	$2d$	$I$ , per cent
(111)	2.33	4.66	100	(111)	2.08	4.16	100
(200)	2.02	4.04	40	(200)	1.81	3.62	53
(220)	1.43	2.86	30	(220)	1.277	2.554	33
(311)	1.219	2.438	30	(311)	1.089	2.178	33
(222)	1.168	2.336	7	(222)	1.043	2.086	9
(400)	1.011	2.022	2	(400)	0.905	1.810	3
(331)	0.928	1.856	4				
(420)	0.905	1.810	4				

IRON BODY-CENTERED CUBIC				ZINC HEXAGONAL			
Indices	$d$	$2d$	$I$ , per cent	Indices	$d$	$2d$	$I$ , per cent
(110)	2.01	4.02	100	(0002)	2.46	4.92	25
(200)	1.428	2.856	15	(10 $\bar{1}$ 0)	2.30	4.60	20
(211)	1.166	2.332	38	(10 $\bar{1}$ 1)	2.08	4.16	100
(220)	1.010	2.020	10	(10 $\bar{1}$ 2)	1.68	3.36	14
(310)	0.904	1.808	8	(10 $\bar{1}$ 3)	1.33	2.66	18
(222)	0.825	1.650	3	(11 $\bar{2}$ 0)	1.169	2.338	12
(321)	0.764	1.528	10	(11 $\bar{2}$ 2)	1.120	2.240	8
				(20 $\bar{2}$ 1)	1.040	2.080	2
				(20 $\bar{2}$ 2)	0.941	1.882	2
				(20 $\bar{2}$ 3)	0.905	1.810	2
				(10 $\bar{1}$ 5)			
				(11 $\bar{2}$ 4)			

For the sake of discussion, suppose that iron, aluminum, copper, and zinc and their alloys are regarded as the most important and the commonest materials in which one usually tries to measure stress. Table 21-1 lists the  $d$  values and corresponding intensities for the most prominent reflections from these metals, as given by the Hanawalt-Rinn-Frevel tables, together with the indices of the reflections. Table 21-2 lists the mean wave length of the  $K_{\alpha}$  doublet for the common target elements for diffraction work.



In the first place, it is evident from these tables that the most prominent reflections, like (111) for aluminum, have a value of  $2d$  which would make  $\lambda$  much too great (nearly 5 A.) for practical work. Even iron  $K_\alpha$  radiation (1.932 A.) is so soft that it is absorbed to a serious degree by the air in a large camera. Thus it is seen that, in general, back-reflection work requires a soft radiation. The radiation chosen should, however, be hard enough to eliminate the need for vacuum cameras for general industrial application. Iron  $K_\alpha$  is about the softest radiation suitable for ordinary cameras; in case of necessity, chromium  $K_\alpha$  can be used in small precision cameras, although with this radiation it is advisable to

TABLE 21-2

Target	Atomic number	Mean wave length of $K_\alpha$ doublet, A.
Cr	24	2.29
Fe	26	1.932
Co	27	1.785
Ni	28	1.655
Cu	29	1.54
Zn	30	1.435
Mo	42	0.71

find some means other than black paper to protect the film from the light. The 2.29-A. wave length of chromium  $K_\alpha$  radiation is seen to be slightly less than  $2d$  for the following reflections: Al (222); Fe (211); Zn (11 $\bar{2}$ 2). Its extreme softness is a handicap, however, as just explained. The 1.932-A. wave length of iron  $K_\alpha$  radiation is slightly less than  $2d$  for Al (400), Cu (222), Fe (220), and Zn (20 $\bar{2}$ 2), but the Al (400) and the Zn (20 $\bar{2}$ 2) reflections are quite faint. Iron radiation is also used sometimes for the (10 $\bar{1}$ 5) reflection from magnesium alloys. Considering the 1.785-A. cobalt  $K_\alpha$  radiation next, it is seen that this is suitable for the (331) and (420) aluminum, the (400) copper, the (310) iron, and the (20 $\bar{2}$ 3) zinc reflections. Since this radiation is hard enough to penetrate a thin piece of paper and a few inches of air, it is now clear why cobalt is the most widely used target material for strain measurement by back reflection. The 1.655-A. wave length of nickel  $K_\alpha$  radiation has just the wrong value to fit any of the  $2d$  values in Table 21-1, although it can be used for the  $2d = 1.688$  A. (331) reflection from cartridge brass, an alpha brass for which the lattice constant  $a = 3.675$  A. Nickel radiation might be used for the faint  $2d = 1.714$  A. (21 $\bar{3}$ 1) zinc reflection not listed in the Hannawalt-Rinn-Frevel table. The 1.54-A. copper  $K_\alpha$  radiation fits only the weak iron (222) reflection. Zinc  $K_\alpha$  at 1.435 A. is suitable for the iron (321) reflection, but the low melting point of zinc makes it a

poor target material. Beyond zinc, the elements are unsuitable for x-ray tube targets until one reaches zirconium (40), columbium (41), and molybdenum (42). The K radiations of these elements are all much less than  $2d$  for any reflection in Table 21-1.

Cobalt  $K_{\alpha}$  radiation is so soft that extinction and absorption of these rays in an iron or aluminum specimen, for example, will limit their penetration to a point at which the resulting back-reflection pattern will be characteristic of only the 0.002 or 0.003 in. of metal on the surface of the specimen. If a 0.003-in. aluminum foil is laid over a block of silver, for example, no trace of the (420) silver reflection will be found in the back-reflection pattern with cobalt radiation, although it can be seen faintly with 0.002-in. aluminum foil substituted for the 0.003. For this reason, the back-reflection pattern is quite sensitive to any surface operations such as shot blasting, filing, and grinding. In measuring stress by back reflection, it must be remembered that line broadening, line shift, and doublet resolution are characteristic of the strains in the surface layers of the metal only, to a depth of roughly 0.002 in.

#### 4. Asterism in Powder Transmission Patterns; Diffuse Reflections.

Section 2 has given the reasons for using back-reflection techniques to measure strain. Obviously, strains existing in the interior of a body, as distinguished from irrelevant surface strains due to shot blasting, etc., should be more accurately determinable from transmission patterns, if it were not for the unfortunate fact that transmission patterns give no quantitative information regarding strain. Numerous attempts<sup>1</sup> have been made to correlate the strains in a sample with the radial streaking, or "asterism," sometimes observed in transmission patterns. An example of asterism is seen in Fig. 21-2, a transmission pattern of a piece of cold-rolled steel, taken with unfiltered molybdenum radiation. This asterism is due to the continuous radiation, as may be seen by taking transmission patterns of a sample with and without a filter.

For many years, asterism was regarded as entirely explainable on the basis of Bragg's law, assuming slight bending or warping of the crystal lattice planes, associated with strain. Suppose, for example, that strains in a piece of steel have caused warping of a certain set of planes [say (110)] in some of the crystals, and that the maximum warping, or wrinkling, is such that in some places the normal to the planes is inclined at an angle  $\eta$  with the normal to the planes when the wrinkling is disregarded. Now consider the results to be expected when a primary beam

<sup>1</sup> See, for example, C. S. Barrett, *Metals & Alloys*, **5**, 154 (1934); N. P. Goss, *Trans. Am. Soc. Metals*, **24**, 977 (1936); C. S. Barrett, *Phys. Rev.*, **53**, 1021 (1938); G. L. Clark, "Applied X-rays," 3d ed., p. 512, McGraw-Hill Book Company, Inc., New York, 1940; W. H. Bragg and W. L. Bragg, "The Crystalline State," p. 202, George Bell & Sons, Ltd., London, 1933.

of unfiltered x-rays from a molybdenum target, for example, passes through a thin specimen of this steel. The characteristic  $K_\alpha$  rays will be diffracted from those (110) planes which have the proper inclination to the beam, and they will produce the usual strong innermost (110) ring in the transmission pattern. Since there is no filter, there will also be "white" x-rays (that is, continuous polychromatic radiation) in the primary beam. If the x-ray tube is operated at the usual 35 or 40 kv., the short-wave-length limit of this white radiation will be about  $\frac{1}{2}$  Å.,

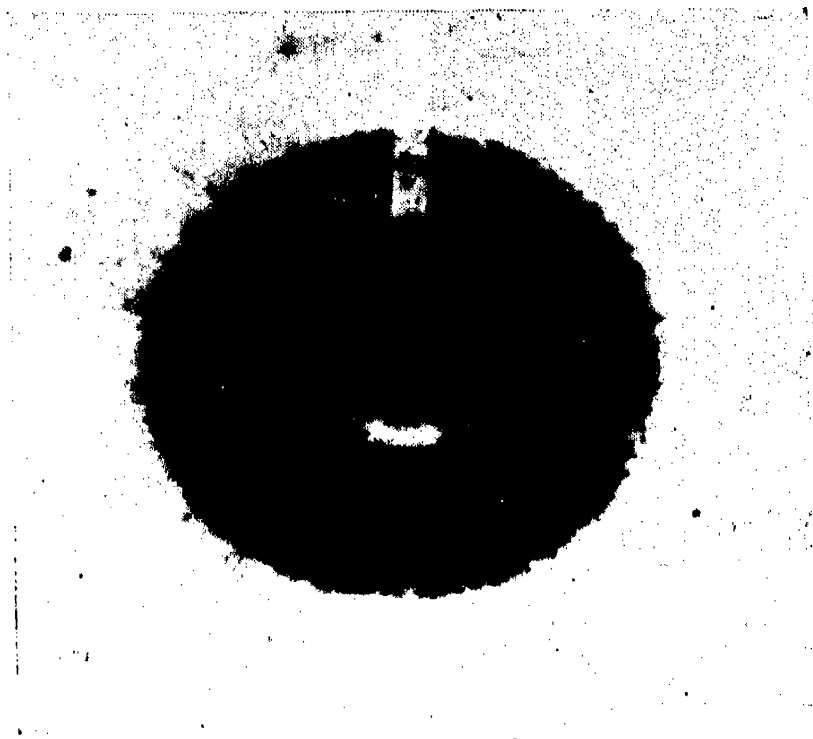


FIG. 21-2.—Pattern of sheet steel, showing asterism.

and the high intensities will be in the wave-length range around  $\frac{1}{2}$  Å. (Fig. 3-5), which is shorter than the 0.71 Å.  $K_\alpha$  radiation. Furthermore, the continuous range of wave lengths will permit the wrinkles in the (110) planes to diffract these rays much as a slightly wrinkled mirror reflects a light beam, because the variations in the Bragg angle, which range from  $\theta - \eta$  to  $\theta + \eta$ , still permit the wrinkled portions to select the appropriate wave length from the continuous range present in the beam, to fit the Bragg law for  $d_{110}$ . Since most of these rays are of shorter wave length than the  $K_\alpha$  rays, they will be "reflected" at a smaller Bragg angle  $\theta$ , so that they will strike the x-ray film at points inside of the innermost (110) ring.

Since white rays are reflected from slightly wrinkled planes much like light from a slightly wrinkled mirror, it is readily seen that the diffracted white rays will leave the sample in directions inclined to the undiffracted ray at angles from  $2\theta - 2\eta$  to  $2\theta + 2\eta$ . Since  $d_{110}$  for

steel is 2 Å. and  $\lambda$  varies from, say,  $\frac{3}{8}$  to  $\frac{5}{8}$  Å. for the strongest part of the continuous radiation, crystals having their (110) planes inclined to the primary beam at any angle  $\theta$  between  $5\frac{1}{2}^\circ$  and  $9^\circ$  ( $\sin^{-1} \frac{3}{8}$  and  $\sin^{-1} \frac{5}{8}$ ) will diffract these rays strongly. If the wrinkling is such that  $\eta$  has a maximum value of  $2^\circ$ , then a crystal with its (110) planes inclined at  $7^\circ$  to the primary beam will diffract white rays at angles ranging from  $10^\circ$  to  $18^\circ$  ( $2\theta - 2\eta$  to  $2\theta + 2\eta$ ) with the undiffracted beam, so far as wrinkling in the plane of incidence is concerned. The wrinkling perpendicular

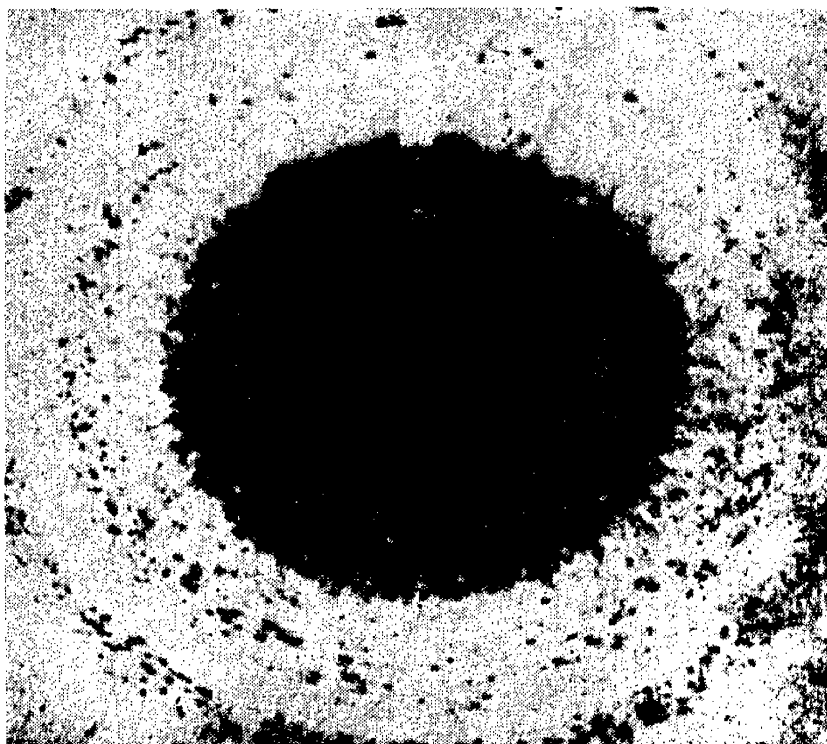


FIG. 21-3.—Pattern of same steel as in Fig. 21-2, using lower voltage and a filter. Note absence of asterism.

to the plane of incidence will cause a variation in the azimuth of the diffracted rays, the variation being  $2\eta \sin 2\theta$  or for small values of  $\theta$  simply  $4\eta\theta$  or about  $1^\circ$ , it being remembered that  $\theta$  must be in radians in making the approximation  $\sin 2\theta = 2\theta$ . Thus the wrinkling will cause the diffracted white rays to make spots on the film that are about eight times or in general  $1/\theta$  times ( $\theta$  in radians) as long in the radial direction as in the circumferential direction. That is, radial streaks, or asterism, of the type seen in Fig. 21-2 is a result to be expected from random warping of the grains, or from microstrain.

If this conclusion is tentatively accepted, it is clear that the asterism, being due to white radiation, should disappear almost entirely when a filter (for example, zirconium, with a molybdenum target) is used. Also, it should be accentuated by increasing the tube voltage. If the tube is operated at 75 instead of 45 kv., the white radiation may become so intense and so hard as to penetrate the filter and produce asterism in spite of it. To show the effect of the tube voltage, Figs. 21-2 and 21-3

were taken from the same piece of steel, using unfiltered molybdenum radiation, but the tube voltage was about 55 kv. in taking Fig. 21-2, as contrasted with the usual 35 kv. in taking Fig. 21-3. This change in tube voltage is seen to make the difference between the presence and absence of asterism. There are other complicating factors. One of them is the fact that asterism in a fine-grained pattern having continuous rings is not as conspicuous as asterism in a coarse-grained spotty ring pattern. Since microstrain is ordinarily induced by processes exceeding the elastic limit and reducing the grain size by fragmentation, the difficulty arises of comparing asterism in a coarse-grained spotty pattern with that in a fine-grained continuous ring pattern. Another complication is that asterism varies in an inexplicable way from substance to substance, being prominent for NaCl and KCl crystals but not for Iceland spar, mica, zinc blende, fluorite, or gypsum, according to Wadlund.<sup>1</sup> However, gypsum crystals show strong asterism in the Laue patterns obtained by Czochochalski;<sup>2</sup> the same is true of mica in Linnik's<sup>3</sup> patterns. These anomalies were increased when Preston,<sup>4</sup> studying aluminum alloys, observed that the asterism in his patterns increased and decreased with the temperature of the sample. After due study, he concluded that the asterism was "connected in some way with the temperature of the sample and is not to be ascribed to any mechanical strain or imperfection caused by changing the temperature."<sup>5</sup> Thus, asterism is now regarded only as a rough qualitative indication of the presence of some microstrain in the sample. Figure 20-6A is another pattern showing asterism in a coarse-grained copper sample, and Fig. 20-14 shows asterism in well-annealed brass, which disappeared as a result of deep drawing (Fig. 20-15)!

These radial streaks were observed in Laue patterns<sup>6</sup> as early as 1913. As a result of recent investigation of some of the anomalies mentioned in the preceding paragraph, asterism is now regarded as being associated to some extent with the phenomenon called "diffuse reflection" of x-rays. In general, diffuse reflections are any kind of x-ray diffraction maxima from crystals that are not governed by the Laue and Bragg equations (15-1) to (15-4). Since this discussion of asterism has brought up the general topic of diffuse reflections, it will be well to summarize the present knowledge of this phenomenon before continuing with the discussion of strain measurement.

<sup>1</sup> A. P. R. Wadlund, *Phys. Rev.*, **53**, 843 (1938).

<sup>2</sup> R. Glocker, "Materialprüfung mit Röntgenstrahlen," 2d ed., p. 297, Verlage von Julius Springer, Berlin, 1936.

<sup>3</sup> W. Linnik, *Nature*, **123**, 604 (1929).

<sup>4</sup> G. D. Preston, *Proc. Roy. Soc. (London) A*, **172**, 116 (1939).

<sup>5</sup> G. D. Preston, *Proc. Roy. Soc. (London) A*, **179**, 2 (1942).

<sup>6</sup> W. Friedrich, *Physik Z.*, **14**, 1082 (1913).

With single-crystal samples, diffuse reflections are observed even though the primary beam is practically free of any continuous radiation. The diffuse reflections give rise to spots on the film that are different from the regular Laue spots. The spots increase in intensity with the temperature of the crystal. Diffuse reflections are due to two causes, according to present theory: (1) incoherent (Compton) scattering in the crystal; (2) coherent scattering with due regard to the thermal agitation of the atoms, in the form of elastic waves,<sup>1</sup> increasing with the temperature (see page 329). Raman and Nilakantan<sup>2</sup> appear to believe that (1) predominates; Zachariasen,<sup>3</sup> who has modernized the earlier theories of Faxen and Waller,<sup>4</sup> appears to believe that (2) predominates. Other theoretical viewpoints have been presented by Bragg, Preston, Born, and Weigle and Smith.<sup>5</sup> The discussion of this topic reached a climax in a Royal Society meeting on Feb. 6, 1941, and fills the first 101 pages of volume 179 of the *Proceedings*. The article by Lonsdale and Smith<sup>6</sup> abounds with photographs.

**5. Microstrains and Line Broadening.** Experiments designed to correlate the severity of microstress with the degree of x-ray line broadening have been conducted by Niemann and Stephenson, Smith and Wood, Smith and Stickley, and Clark, Pish, and Seabury.<sup>7</sup> Niemann and Stephenson, working with alpha brass, have found that the breadth changes little with annealing until just before recrystallization, when it exhibits a comparatively sharp decrease. It appears doubtful that the rate of cold working affects the result.<sup>8</sup> There seems to be no close correlation with internal-friction measurements on the same samples.<sup>9</sup> Smith and Wood found that the sharply resolved doublet in the back-reflection pattern of mild steel dissolved into a single unresolved diffuse ring when the stress reached the yield point. Smith and Stickley, as

<sup>1</sup> See p. 365. A. J. Guinier, *Proc. Phys. Soc. (London)*, **57**, 323 (1945) has studied the relationship between these diffuse reflections and such practical matters as the age hardening of metals.

<sup>2</sup> C. V. Raman and P. Nilakantan, *Phys. Rev.*, **60**, 63 (1941); *Nature*, **150**, 366 (1943).

<sup>3</sup> W. H. Zachariasen, *Phys. Rev.*, **59**, 860 (1941); J. H. Hall, *Phys. Rev.*, **61**, 158 (1942).

<sup>4</sup> H. Faxen, *Z. Physik*, **17**, 266 (1923); I. Waller, *Z. Physik*, **17**, 398 (1923).

<sup>5</sup> W. H. Bragg, *Nature*, **148**, 112 (1941); G. D. Preston, *Nature*, **147**, 467 (1941); M. Born, *Nature*, **147**, 674 (1941); J. Weigle and C. S. Smith, *Phys. Rev.*, **61**, 23 (1942).

<sup>6</sup> K. Lonsdale and H. Smith, *Proc. Roy. Soc. (London) A*, **179**, 8 (1941).

<sup>7</sup> F. Niemann and S. T. Stephenson, *Phys. Rev.*, **62**, 330 (1942); S. L. Smith and W. A. Wood, *Proc. Roy. Soc. (London) A*, **179**, 450 (1942); C. S. Smith and E. E. Stickley, *Phys. Rev.*, **64**, 191 (1943); G. L. Clark, G. Pish, and R. Seabury, *J. Applied Phys.*, **14**, 284 (1943).

<sup>8</sup> See M. Petersen and C. W. Tucker, *Phys. Rev.*, **63**, 385 (1943).

<sup>9</sup> C. Zener, H. Clarke, and C. S. Smith, *Trans. A.I.M.M.E.*, **147**, 90 (1942).

already mentioned (page 449), found that the line broadening due to cold work in alpha brass and tungsten varied linearly with  $\tan \theta$  rather than  $\lambda \sec \theta$ , indicating that the broadening was due to microstresses caused by the cold work, rather than grain-size reduction by fracture. They used a Seemann-Bohlin type of camera with a focusing monochromator (page 398, and footnote 1, page 398). The dependence of the broadening upon direction in the case of brass was also noted, due to the preferential orientation. The absence of this effect in tungsten is explainable by the unique elastic isotropy of tungsten crystals. Clark Pish, and Seabury show a series of back-reflection patterns of an aluminum alloy subjected to simple tension stresses of 0, 5,000, 10,000, 15,000, 20,000, 22,500, and 25,000 lb./in.<sup>2</sup> and at fracture. Cobalt  $K_{\alpha}$  radiation was used, and the patterns show two rings, the inner probably being the (420) reflection and the outer the (331) reflection. Both rings are resolved into the  $K_{\alpha_1}$ - $K_{\alpha_2}$  doublet by the unstressed metal. Both rings show some spottiness, indicating the presence of some grains larger than the nominal  $10^{-2}$  mm. size at which such spots appear. The line broadening gradually increases so that it is difficult to distinguish the doublets at 15,000 lb./in.<sup>2</sup> tension. At 20,000 lb./in.<sup>2</sup> tension, the doublets are definitely unresolved. Beyond this, the spots already mentioned begin to dissolve, indicating the fracture of these larger grains. By the time the metal breaks, these spots have disappeared entirely. This series of patterns shows that microstrains become severe in this alloy when the macrostress reaches 20,000 lb./in.<sup>2</sup>, indicating that some plastic deformation evidently begins at about this stress. As it progresses, grain fracture takes place. It should be possible to study and measure microstress in the interior of a metal member by cutting a section from the interior, etching it down at least a hundredth of an inch, and taking a back-reflection pattern. Such a procedure should not seriously alter the microstrains, although it would of course greatly alter the macrostrains.

In order to correlate such patterns with the microstrains in a quantitative way, equation (21-1) may be rearranged thus:

$$\epsilon = \frac{dd}{d} = - \cot \theta d\theta \quad (21-3)$$

where  $\epsilon$  is the microstrain, or elongation per unit length, and  $d\theta$  is half the corresponding broadening  $d\phi$  where  $\phi = 2\theta$  is the angle between the primary beam (after passing through the sample) and the diffracted beam. That is, if the diffraction line were perfectly sharp or infinitesimally narrow for unstressed metal, then *AOPOD* might represent the diffraction line in Fig. 21-4. Then, when microstresses appear, the line broadens, as represented by *ABPCD* in the figure. In such a

idealized picture, equation (21-3) shows that the microstrain distribution curve for, say, a million grains in the sample is obtained by merely changing the labels and scales on the coordinates and reversing the curve, as shown in Fig. 21-5, since  $\cot \theta$  may be regarded as a constant (taken as 0.1 here) over the small range (of the order of a degree) considered. Since intensity  $I_0$  in Fig. 21-4 represents the background scattering, this point becomes zero on the ordinate scale in Fig. 21-5. The reversal of the curve is dictated by the minus sign in equation (21-3), which indicates that stretching the grains (positive stress) decreases  $\theta$  whereas compressing them (negative stress) increases  $\theta$ . In order to arrive

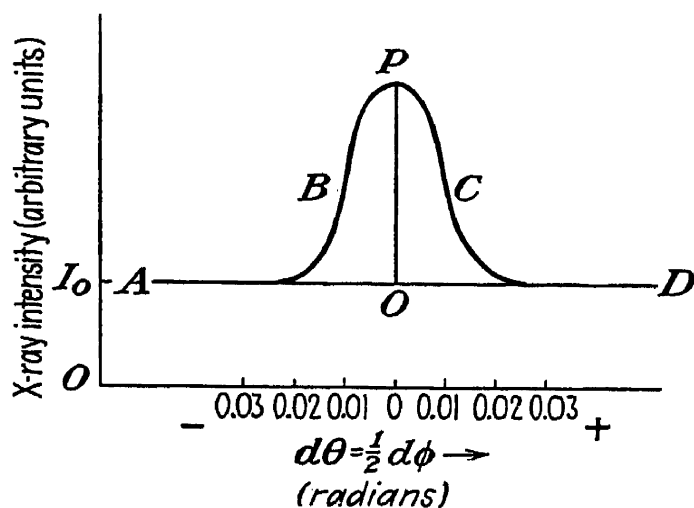


FIG. 21-4.

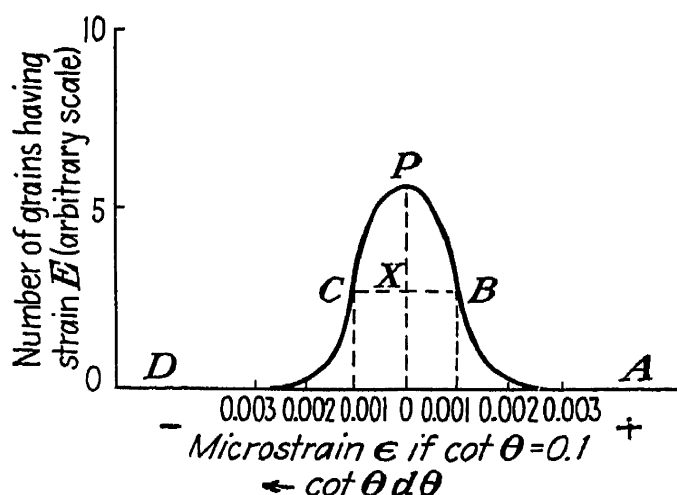


FIG. 21-5.

These two figures show the qualitative relation between line broadening and microstrain.

at some arbitrary figure or index,  $\bar{\epsilon}$ , to indicate the severity of the microstrain, one might take half of the half-value width  $CB$  of the peak<sup>1</sup> in Fig. 21-5. Note that this is only one-fourth of the half-value width as usually measured, in terms of  $\phi$  rather than  $\theta$ . In the figure as drawn, the index would be 0.001, that is, 0.1 per cent change in length per unit length. It is logical to take half of  $CB$  rather than all of it because  $XC$  represents negative strain  $\epsilon$  (compression) and  $XB$  represents positive strain  $\bar{\epsilon}$  (tension), so that the average  $\bar{\epsilon}$  is half their sum, not the whole sum.

The difficulty with this plan is that the diffraction line for the unstressed metal is not infinitesimally narrow. Methods to correct for this (1) when the  $K_\alpha$  doublet is resolved and (2) when the  $K_\alpha$  doublet is unresolved have been suggested by Niemann and Stephenson and Smith and Stickley,<sup>2</sup> respectively. For details, the reader is referred to their papers, but the correction methods will be outlined here. To consider

<sup>1</sup> In this connection, see A. R. Stokes and A. J. C. Wilson, *Proc. Phys. Soc.*, **56**, 174 (1944).

<sup>2</sup> F. Niemann and S. T. Stephenson, *Phys. Rev.*, **62**, 330 (1942); C. S. Smith and E. E. Stickley, *Phys. Rev.*, **64**, 191 (1943).



case (1) first, use is made of the fact that the  $K_{\alpha_1}$  line is twice as intense as  $K_{\alpha_2}$  (see page 68). The horizontal line  $AB$  drawn through the top  $T$  of the  $K_{\alpha_2}$  peak (Fig. 21-6) then cuts the  $K_{\alpha_1}$  peak at  $C$  and  $D$ , and hence  $CD$  or  $EF$  represents the half-value width without regard for the background intensity. This breadth  $B$  must be corrected for broadening due to the finite width of the collimator slit; this correction may or may not be negligible, depending upon circumstances. After making this

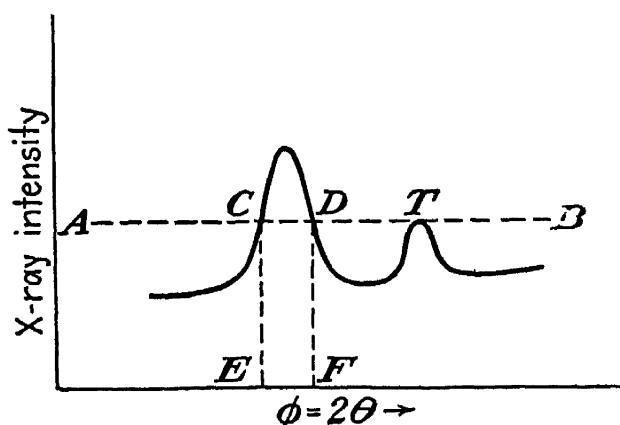


FIG. 21-6.—Niemann and Stephenson method of finding basic line breadth when  $K_{\alpha}$  doublet is resolved.

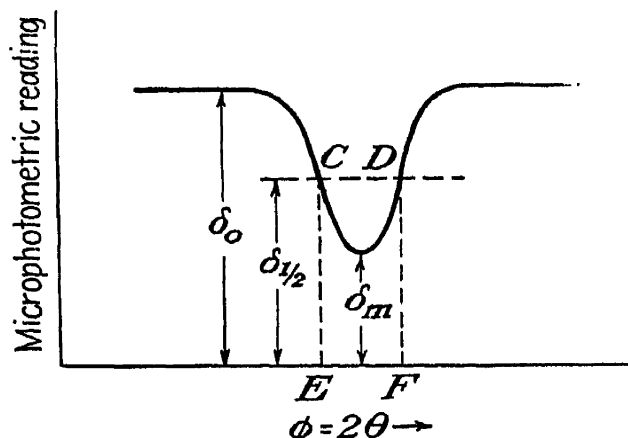


FIG. 21-7.—Smith and Stickley method of finding basic line breadth when  $K_{\alpha}$  doublet is not resolved.

correction, one may take  $CD/4 \cot \theta$  as the microstrain index. To consider case (2) next, Smith and Stickley measure  $\delta_0$  and  $\delta_m$  from the microphotometer record (Fig. 21-7) and define  $\delta_{\frac{1}{2}}$  as  $\delta_{\frac{1}{2}} = EC = \sqrt{\delta_0 \delta_m}$ . Then  $B_m$  is defined as  $EF$ , measured in radians. Then  $B$ , the breadth due to cold work (which is the quantity one wishes to evaluate), is found from the relation

$$B^2 = B_m^2 - B_{\alpha}^2 - B_{12}^2 - B_s^2 \quad (21-4)$$

where  $B_{\alpha}$  is the very slight (ordinarily negligible) correction due to the fact that even the  $K_{\alpha_1}$  line itself is not quite monochromatic,  $B_{12}$  is the correction due to the presence of the  $K_{\alpha_2}$  line in the unresolved doublet, and  $B_s$  is the correction for finite slit width. Smith and Stickley use the relation

$$B_{12} = \left( 2.45 \frac{\Delta \lambda}{\lambda} \tan \theta \right)^2 \quad (21-5)$$

to calculate  $B_{12}$ . Here  $\Delta \lambda$  is the 4-X.U. interval between the two lines of the doublet. If the angular slit width is  $\omega$ , they estimate that

$$B_s^2 = 0.45 \omega^2 \quad (21-6)$$

for their camera. One must remember that the angular breadth

$$\Delta \phi = 2 \Delta \theta$$

of a line is given by its linear width on the film divided by the camera

radius for ordinary cameras and by the camera diameter for Seemann-Bohlin type cameras.

C. S. Barrett<sup>1</sup> has recently discovered a method of "photographing" the microstress centers existing within the individual grains of metals of moderate or large grain size. A flat plate or sheet of the metal about 1 cm. square or larger is used. A piece of fine-grained film of the same size is laid flat against this specimen. Then one edge of the film is raised about 1 mm. and propped in this position, inclined a few degrees to the metal surface, and in contact along one edge.

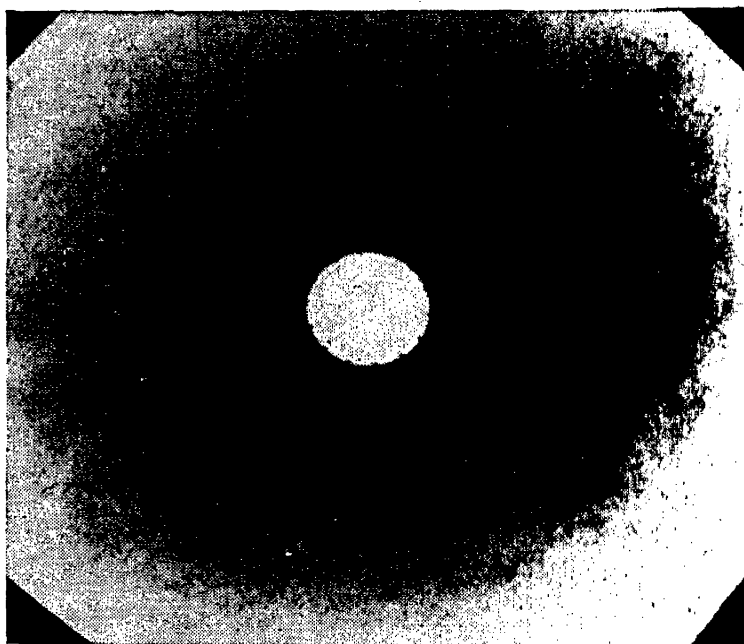


FIG. 21-8.—Back-reflection pattern of hard steel, taken with cobalt  $K_{\alpha}$  radiation. The ring is the (310) reflection. Note that it is broad and diffuse, characteristic of hard specimens.

A broad beam of parallel characteristic x-rays parallel to the sloping edges of the film is then made to strike obliquely upon the metal face. The diffracted beams from the individual grains cause gray spots on the film upon development.

Upon enlarging the image 50 or 100 diameters, the gray spots are found to have black dots and markings on them. These are supposedly due to the reduced secondary extinction resulting from mosaic fragmentation at local microstress centers in the individual grains (see Secs. 16-15 and 16-16).

**6. Surface Macrostrains and Line Shift—Introduction.** Section 1 included a general outline of this method. It has been used successfully by Frommer and Lloyd, for example,<sup>2</sup> to measure residual stresses in forged, machined, and drawn aluminum, due to quenching, cold work, etc.

Figure 21-8 shows the back-reflection pattern of a piece of tempered

<sup>1</sup> C. S. Barrett, *Metals Tech.*, **12**, *Tech. Pub.* 1865 (April, 1945).

<sup>2</sup> L. Frommer and E. H. Lloyd, *J. Inst. Metals*, **70**, 91 (1944).

alloy steel in which the microstresses are so severe and the grain size so small (a hard, brittle steel) that the back-reflection ring seen is too broad for accurate measurement of its diameter. Note that the  $K_{\alpha}$  doublet is unresolved. Figure 21-9, on the other hand, shows back-reflection patterns taken perpendicularly to the surface of a mild soft-steel bar. These patterns were taken with a cassette having sectors as in Fig. 18-4, except that the sectors were designed for taking four exposures on a single film rather than two. In Fig. 21-9A, sectors 1 and 3 show the patterns of a plain straight strip  $\frac{1}{8}$  in. thick. The Bragg reflection involved is  $\{310\}$ . Note that the (cobalt)  $K_{\alpha}$  doublet is resolved. In such patterns, the  $K_{\alpha_1}$  component only is used for measurement of radii.

After taking patterns 1 and 3 (Fig. 21-9A), the steel bar was bent through about  $10^\circ$  near its center, so that the elastic limit was exceeded at the bend. Sector 2 shows the pattern taken on the convex (tension) side of the bend. Sector 4 shows the pattern taken on the concave (compression) side. The loss of resolution reveals the grain fracture and micro-stress resulting from plastic deformation. However, the resolution is still sufficiently good to permit one to see and measure the increase in diameter of the rings in sector 2 as compared with 1 and 3; the same is true for the decrease in diameter in sector 4 compared with 2 and 3. An increase in diameter indicates expansion of the lattice normal to the surface and hence compressive stresses in the plane of the surface, the relation being given by equation (21-18). Thus it is seen that residual compression is found on the tension side of the bend and residual tension on the compression side, a well-known paradox.

After taking patterns 1 and 3 (Fig. 21-9B) from a straight mild-steel bar, the bar was shot peened. This strains the surface layer beyond the elastic limit and leaves it with a residual compressive stress in its own plane. Subsequently, patterns 2 and 4 (Fig. 21-9B) were taken, the primary beam being normal to the side of the bar in all four cases. The loss of resolution and increase in diameter are quite noticeable in this case. The magnitude of the latter indicates a compressive macrostress of 55,000 lb./in.<sup>2</sup>, according to equation (21-18).

In the discussion of Figs. 21-9A and 21-9B, the *change* in the strain accompanying some artificially applied change in the stress has been considered. By taking back-reflection patterns with the primary beam incident along suitably chosen oblique directions, however, it is possible to measure the magnitude of the stresses at any surface point without any need for comparing the reading with a doubtful zero reading based upon metal in which the stresses have supposedly been relieved. The x-ray method is unique in this respect. The unstrained zero reading is obtained by making use of the fact that the macrostress at a surface must be zero in the direction perpendicular to the surface. The pro-

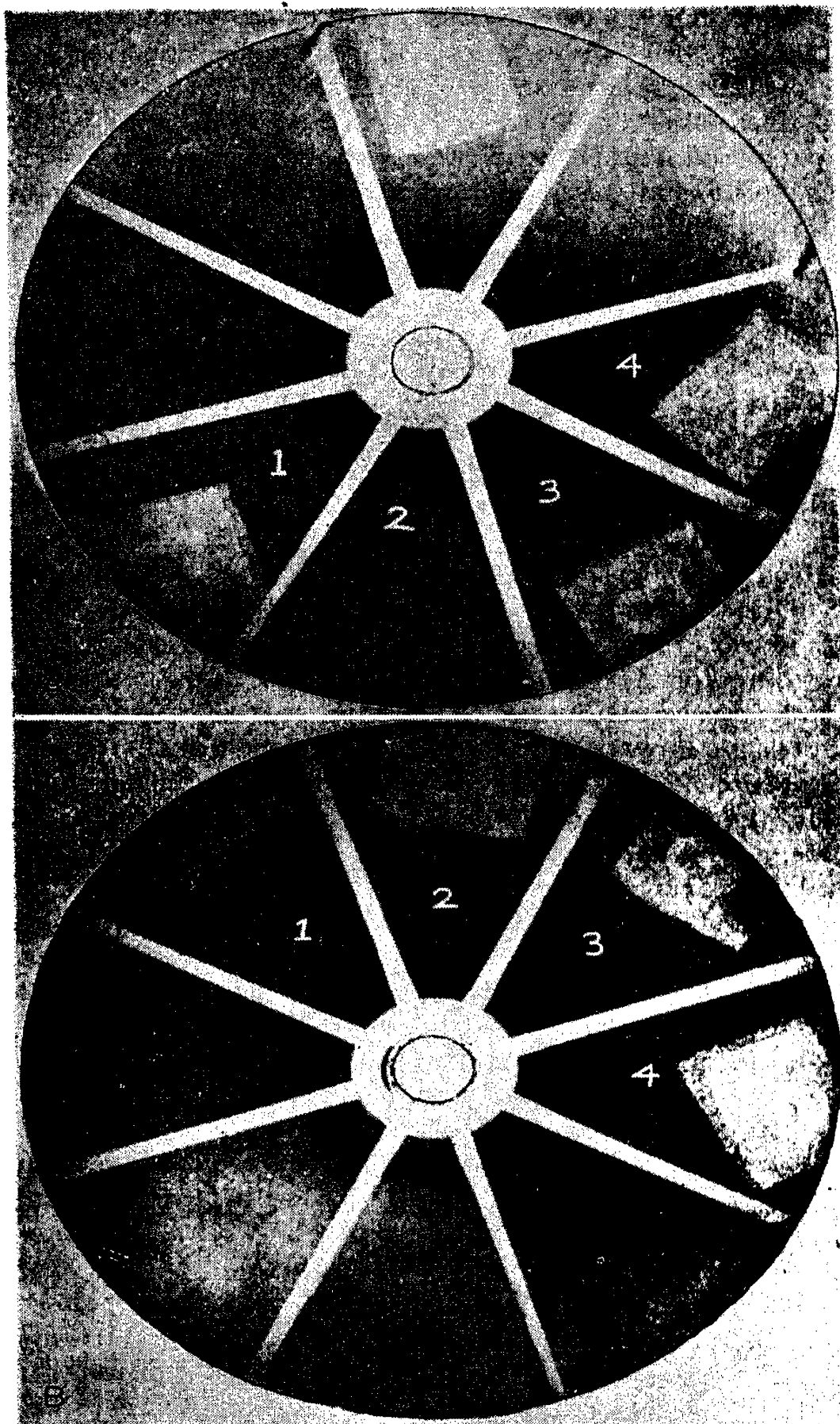


FIG. 21-9.—*A*, back-reflection patterns of mild steel (1) and (3), before bending. (2) convex side of bend. (4) concave side of bend. *B*, back-reflection patterns of mild steel bar, taken perpendicular to side. (1) and (3) before, (2) and (4) after shot peening.

cedure is to measure the difference between the strain in some arbitrary but known direction  $A$  at the surface point  $O$  and the strain in some other arbitrary direction  $B$  at the same point  $O$ . Then, it being known that the stress at  $O$  is zero along the normal to the surface, the magnitude of the stress in any specific direction in the plane of the surface can be computed. In practice,  $A$  may be the direction of the normal, and  $B$  a direction inclined at an angle between  $30$  and  $45^\circ$  to the normal. It is possible to get the measurements for the two directions  $A$  and  $B$  from a single diffraction pattern, so that one exposure can be made to yield the value of the surface stress in any one chosen direction in the surface at  $O$ . To determine the stresses in all directions at  $O$ , three or four exposures are ordinarily required.

A crystal, in general, has different elastic moduli in different directions, tungsten crystals being the only known exception. For a cubic crystal, the value of Young's modulus  $E$  in any arbitrary direction having direction cosines  $\gamma_1$ ,  $\gamma_2$ , and  $\gamma_3$  with respect to the crystallographic axes  $A$ ,  $B$ , and  $C$  is given by

$$\frac{1}{E} = A - B(\gamma_1^2\gamma_2^2 + \gamma_2^2\gamma_3^2 + \gamma_3^2\gamma_1^2) \quad (21-7)$$

where  $A$  and  $B$  are constants. However, a crystal that is only one of several billion cemented at random into a solid rigid mass, such as a bolt or a nut, is constrained to expand and contract, stretch and shrink in the isotropic manner characteristic of the metal, rather than as it would if it were a solitary crystal lying on a table top. At least, this is assumed in strain measurement by x-ray diffraction, and the fact that the x-ray method yields stress and strain values agreeing with those measured by other methods indicates that this assumption is safe.

The theory of macrostress measurement by line shift involves the use of appropriate "working equations," such as (21-26) and (21-28) which are derived in the next section. It is quite unsatisfactory merely to write down these equations and take them for granted, for their meaning and proper application cannot be adequately understood without some knowledge of the theory of elasticity on which they are based. For further details, the reader is referred to the various papers published on the subject as this method of strain measurement has developed.<sup>1</sup>

<sup>1</sup> G. Sachs and J. Weerts, *Z. Physik*, **64**, 344 (1930); A. E. van Arkel and W. G. Burgers, *Z. Metallkunde*, **23**, 149 (1931); F. Wever and H. Möller, *Naturwissenschaften*, **22**, 401 (1934); R. Glocker and E. Osswald, *Z. tech. Physik*, **16**, 237 (1935); F. Gisen, R. Glocker, and E. Osswald, *Z. tech. Physik*, **17**, 145 (1936); C. S. Barret and M. Gensamer, *Physics*, **7**, 1 (1936); R. Glocker, *Arch. tech. Messen*, **69**, T3 (March, 1937); D. E. Thomas, *J. Sci. Instruments*, **18**, 135 (1941); G. Kemnitz, *Z. Physik*, **23**, 77 (1942); L. Frommer and E. H. Lloyd, *J. Inst. Metals*, **70**, 91 (1944).

**7. Surface Stress and Line Shift—Theory.** For the reason just stated, a brief review of some of the basic mathematical groundwork of the theory of elasticity will be included at this point.<sup>1</sup> The following notation will be used:

- $\epsilon$  = linear strain
- $\epsilon_x$  = linear strain at origin in  $X$  direction, etc.
- $S$  = linear stress
- $S_x$  = linear stress at origin in  $X$  direction, etc.
- $T$  = shear stress
- $T_x$  = shear stress at origin across  $YZ$  plane, etc.
- $E$  = Young's modulus
- $\nu$  = Poisson's ratio
- $l_1$  = direction cosine of new  $X$  axis with respect to old  $X$  axis
- $m_1$  = direction cosine of new  $X$  axis with respect to old  $Y$  axis
- $n_1$  = direction cosine of new  $X$  axis with respect to old  $Z$  axis
- $l_2$  = direction cosine of new  $Y$  axis with respect to old  $X$  axis
- $m_2$  = direction cosine of new  $Y$  axis with respect to old  $Y$  axis
- $n_2$  = direction cosine of new  $Y$  axis with respect to old  $Z$  axis
- $l_3$  = direction cosine of new  $Z$  axis with respect to old  $X$  axis
- $m_3$  = direction cosine of new  $Z$  axis with respect to old  $Y$  axis
- $n_3$  = direction cosine of new  $Z$  axis with respect to old  $Z$  axis

In the case of pure tension, as when the ends of a 1-in.-square bar 1 ft. long are subjected to uniform longitudinal tension not exceeding the elastic limit, the bar stretches slightly, becoming more than 1 ft. long and less than 1 in. square. If the  $X$  axis is taken as the axis of the bar, the lateral contraction accompanying the stretch is given by

$$\epsilon_y = \epsilon_z = -\nu \frac{S_x}{E} \quad (21-8)$$

Poisson's ratio,  $\nu$ , is a constant having a value of about 0.3 for steel but closer to 0.25 for some other materials. To pass from this simple case to the more general one of several applied forces in various directions, the theory yields the following equations:

$$\left. \begin{aligned} \epsilon_x &= \frac{1}{E} [S_x - \nu(S_y + S_z)] \\ \epsilon_y &= \frac{1}{E} [S_y - \nu(S_x + S_z)] \\ \epsilon_z &= \frac{1}{E} [S_z - \nu(S_x + S_y)] \end{aligned} \right\} \quad (21-9)$$

<sup>1</sup> See, for example, S. Timoshenko, "Theory of Elasticity," McGraw-Hill Book Company, Inc., New York, 1934; John Prescott, "Applied Elasticity," Longmans, Green and Company, New York, 1924; A. E. H. Love, "Mathematical Theory of Elasticity," 3d ed., Cambridge University Press, London, 1920.

Elementary algebraic rearrangement changes these to the following form:

$$\left. \begin{aligned} E\epsilon_x &= S_x(1 + \nu) - \nu S \\ E\epsilon_y &= S_y(1 + \nu) - \nu S \\ E\epsilon_z &= S_z(1 + \nu) - \nu S \end{aligned} \right\} \quad (21-10)$$

where

$$S = S_x + S_y + S_z \quad (21-11)$$

Here the axes may be any orthogonal axes in an isotropic solid, the stresses being measured at the origin  $O$ . In general, shear stresses  $T_x$ ,  $T_y$ , and  $T_z$  will also be present at  $O$ .

If a new set of orthogonal coordinates  $OX'$ ,  $OY'$ , and  $OZ'$  are selected with the same origin  $O$  but a different orientation, then the linear stresses at  $O$  with respect to the new axes are given by

$$\left. \begin{aligned} S'_x &= l_1^2 S_x + m_1^2 S_y + n_1^2 S_z + 2m_1 n_1 T_x + 2n_1 l_1 T_y + 2l_1 m_1 T_z \\ S'_y &= l_2^2 S_x + m_2^2 S_y + n_2^2 S_z + 2m_2 n_2 T_x + 2n_2 l_2 T_y + 2l_2 m_2 T_z \\ S'_z &= l_3^2 S_x + m_3^2 S_y + n_3^2 S_z + 2m_3 n_3 T_x + 2n_3 l_3 T_y + 2l_3 m_3 T_z \end{aligned} \right\} \quad (21-12)$$

At any point  $O$  in an elastic isotropic solid, it is always possible to find a set of orthogonal Cartesian coordinates  $X$ ,  $Y$ ,  $Z$  defining three mutually perpendicular planes  $XOY$ ,  $YOZ$ , and  $XOZ$ , across which the shear stresses vanish. That is, the resultant stresses acting across these planes at  $O$  are perpendicular to the planes. The stresses and strains at  $O$  in the  $X$ ,  $Y$ , and  $Z$  directions are thus purely linear and are called the *principal* stresses and strains at this point.  $OX$ ,  $OY$ , and  $OZ$  are likewise called the *principal* axes. The stress at a point  $O$  is therefore completely defined if the directions of the principal axes and the magnitudes of the three principal stresses  $S_x$ ,  $S_y$ , and  $S_z$  are given.

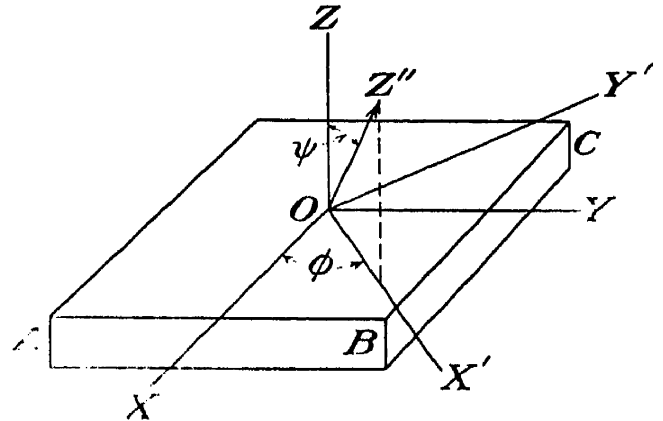


FIG. 21-10. Diagram to aid explanation of surface stress measurement by x-ray line shift.

To approach the problem of stress measurement by the shift of x-ray diffraction lines, suppose  $ABC$  in Fig. 21-10 is a solid,  $O$  being the point, within a few thousandths of an inch of its surface, at which measurements are to be made. Suppose that  $OX$ ,  $OY$ , and  $OZ$  are the *principal* axes through  $O$ .  $OZ$  will be normal to the surface, and  $S_z$  will be zero, but the directions of  $OX$  and  $OY$  may be unknown when experiments are begun. With a back-reflection x-ray camera, the spacing  $d'$  of some planes, such as  $\{310\}$ , is determined for the direction  $OZ''$  inclined at a known angle  $\psi$  to the normal and an unknown azimuth  $\phi$  to the principal axis  $OX$ . If there are no strains at  $O$ , this measured

value of  $d'$  will be the (310) spacing, say, for the unstrained material. If strains are present at  $O$ , the measured spacing will differ from the unstrained  $d$  value by an amount  $\Delta d$ . Then the strain at  $O$  in the direction  $OZ''$  is defined as  $\Delta d/d = \epsilon_{z''}$ . The unstrained  $d$  value is unknown, but the actual spacing  $d' = d + \Delta d$  can be measured for two or more different directions  $OZ''$ . How are these related to the principal stresses  $S_x$ ,  $S_y$ , and  $S_z$ ?

To answer this question, first use relations (21-12) to find the stress  $S'_x$  at  $O$  in the direction  $OX'$ , where  $OX'$ ,  $OY'$ , and  $OZ$  are new axes through  $O$  obtained from the original axes  $OX$ ,  $OY$ ,  $OZ$  by a rotation about  $OZ$  through the angle  $\phi$ . Since the original axes were principal axes,  $T_x$ ,  $T_y$ , and  $T_z$  are all zero. Substituting  $l_1 = \cos \phi$ ,  $m_1 = \sin \phi$ , and  $n_1 = 0$  in the first equation (21-12),

$$S'_x = S_x \cos^2 \phi + S_y \sin^2 \phi \quad (21-13)$$

Next, consider a third set of axes,  $OX''$ ,  $OY''$ ,  $OZ''$ , obtained by rotating  $OX'$ ,  $OY'$ ,  $OZ'$  about  $OY'$  through the angle  $\psi$ . To find the stresses at  $O$  along these new axes, one applies all three equations (21-12) to transform directly from the original principal axes  $OX$ ,  $OY$ ,  $OZ$  to the set  $OX''$  (not shown in Fig. 21-10),  $OY''$  (identical with  $OY'$ ),  $OZ''$ . Here one has  $T_x = T_y = T_z = 0$ .

$$\begin{array}{lll} l_1 = \cos \phi \sin \psi & m_1 = \sin \phi \cos \psi & n_1 = \sin \psi \\ l_2 = \sin \phi & m_2 = \cos \phi & n_2 = 0 \\ l_3 = \sin \psi \cos \phi & m_3 = \sin \psi \sin \phi & n_3 = \cos \psi \end{array}$$

so that

$$\left. \begin{array}{l} S''_x = S_x \cos^2 \phi \cos^2 \psi + S_y \sin^2 \phi \cos^2 \psi \\ S''_y = S_x \sin^2 \phi + S_y \cos^2 \phi \\ S''_z = S_x \sin^2 \psi \cos^2 \phi + S_y \sin^2 \psi \sin^2 \phi \end{array} \right\} \quad (21-14)$$

$$\text{from which} \quad S''_x + S''_y + S''_z = S = S_x + S_y \quad (21-15)$$

The last equation of the group (21-14), combined with (21-13), yields

$$S''_z = S'_x \sin^2 \psi \quad (21-16)$$

From the last equation of group (21-10), one has

$$E\epsilon_{z''} = S_{z''}(1 + \nu) - \nu S$$

Substituting (21-15) and (21-16) in this,

$$E\epsilon_{z''} = S'_x(1 + \nu) \sin^2 \psi - \nu(S_x + S_y) \quad (21-17)$$

This equation is the key to the question posed at the beginning of the paragraph. By measuring the *difference* between the values  $\epsilon''_z$  for two different  $OZ''$  directions corresponding to two different values of  $\psi$



and subtracting one from the other, the constant term  $\nu(S_x + S_y)$  is eliminated and the absolute value of the strain in the direction  $OX'$  can be found.

For the special case  $\psi = 0$ , equation (21-17) reduces to

$$E\epsilon_{z''} = -\nu(S_x + S_y) \quad (21-18)$$

This equation is the key relation for back-reflection work at normal incidence. When the specimen is stretched or bent, for example, the change of diameter of the back-reflection rings permits one to calculate  $\epsilon_{z''}$ , and hence  $S_x + S_y$ , from patterns such as those in Fig. 21-9. Such tactics yield no information about the *directions* of the principal stresses  $S_x$  and  $S_y$ , but these are often known from other considerations.

Figure 21-11 represents a back-reflection camera set up so that the primary beam  $WO$  passes through the film  $F$  at  $C$  and strikes the surface of the specimen at  $O$  at an angle  $\alpha$  (preferably about  $30^\circ$ ) with the normal  $ON$  to the surface. The diffracted rays  $OR_1$  and  $OR_2$  strike the film at  $R_1$  and  $R_2$ . The former is diffracted by a set of planes [(310) planes, for example]  $P_1$ , the latter by another set of planes [(310) planes, say],  $P_2$ , in different crystals with different orientations, perpendicular to  $OZ_1$  and  $OZ_2$ , respectively. Since these directions are different, the strains in the two sets of planes will be different, in general, so that the Bragg angle for  $OR_1$  will be not quite the same as the Bragg angle for  $OR_2$ . Hence the complementary angles  $\eta_1$  and  $\eta_2$  in the figure will in general be nearly, but not quite, equal.

It is seen that  $OZ''$  in Fig. 21-10 corresponds to  $OZ_1$  in Fig. 21-11 for planes  $P_1$  and to  $OZ_2$  for planes  $P_2$ . Neglecting the small difference between  $\eta_1$  and  $\eta_2$  and designating both by  $\eta$  where the angles themselves rather than the difference between them are involved, one has  $\psi = \alpha + \eta$  and  $\psi = \alpha - \eta$  for the two sets of planes  $P_1$  and  $P_2$ . Since  $\eta$  is the complement of the Bragg angle  $\theta$ , one has

$$\sin \theta = \cos \eta \text{ and } \cos \theta = \sin \eta \quad (21-19)$$

Applying (21-17) to the two sets of planes  $P_1$  and  $P_2$ , one has

$$E\epsilon_{z_1} = S'_x(1 + \nu) \sin^2 (\alpha - \eta) - \nu(S_x + S_y)$$

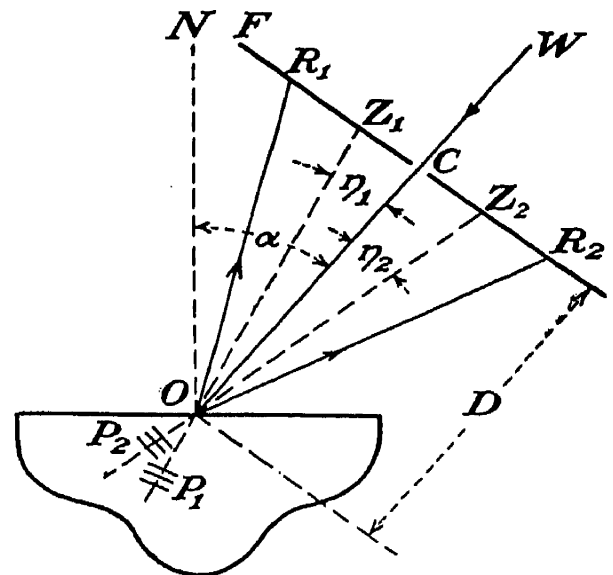


FIG. 21-11.—To illustrate stress measurement from a single camera position.

and

$$E\epsilon_{z_2} = S'_x(1 + \nu) \sin^2 (\alpha + \eta) - \nu(S_x + S_y)$$

Subtracting,

$$E(\epsilon_{z_2} - \epsilon_{z_1}) = S'_x(1 + \nu)[\sin^2 (\alpha + \eta) - \sin^2 (\alpha - \eta)] \quad (21-20)$$

As an exercise in trigonometry, it can be shown that the bracket reduces to  $4 \sin \alpha \cos \alpha \sin \eta \cos \eta$  so that

$$E(\epsilon_{z_2} - \epsilon_{z_1}) + 4S'_x(1 + \nu) \sin \alpha \cos \alpha \sin \eta \cos \eta \quad (21-21)$$

This difference in strain  $\epsilon_{z_2} - \epsilon_{z_1}$  manifests itself in the back-reflection pattern (Fig. 21-11) by making  $R_1C = r_1$  slightly different from  $R_2C = r_2$ . To return to the question posed on page 488, it is seen that the two strain values  $\epsilon_{z_1}$  and  $\epsilon_{z_2}$  involve two  $d$  increments  $\Delta d_1$  and  $\Delta d_2$  or two actual spacings  $d'_1$  and  $d'_2$ . Therefore we are now interested in the difference

$$\Delta d = d'_2 - d'_1,$$

which is related to the difference  $\epsilon_{z_2} - \epsilon_{z_1}$  as follows

$$\epsilon_{z_2} - \epsilon_{z_1} = \frac{\Delta d}{d} \quad (21-22)$$

Since  $\Delta d$  is so small compared with  $d$  that it can be regarded as an infinitesimal in differentiating Bragg's law with respect to  $d$ , as in equation (21-3), one has

$$\frac{dd}{d} = \epsilon_{z_2} - \epsilon_{z_1} = -\cot \theta d\theta \quad (21-23)$$

where  $d\theta$  is the difference between the Bragg angle  $\theta_2$  for planes  $P_2$  and the Bragg angle  $\theta_1$  for planes  $P_1$  in Fig. 21-11. That is,

$$d\theta = \theta_2 - \theta_1 = \eta_1 - \eta_2 = -d\eta.$$

In Fig. 21-11,  $R_1$  and  $R_2$  are on opposite sides of  $C$ . If they are imagined on the same side of  $C$ , as in Fig. 21-12, it is seen that

$$2d\eta = -2d\theta = \frac{R_2M}{R_2O} = \frac{R_1R_2 \cos 2\eta}{D} = \frac{R_1R_2}{D} \cos^2 2\eta = \frac{r_1 - r_2}{D} \cos^2 2\eta$$

where  $r_1 = R_1C$  and  $r_2 = R_2C$  in either figure so that

$$d\theta = \frac{r_2 - r_1}{2D} \cos^2 2\eta \quad (21-24)$$

Substituting (21-24) in (21-23),

$$\epsilon_{z_2} - \epsilon_{z_1} = \frac{r_1 - r_2}{2D} \frac{\cos \theta \cos^2 2\eta}{\sin \theta}$$

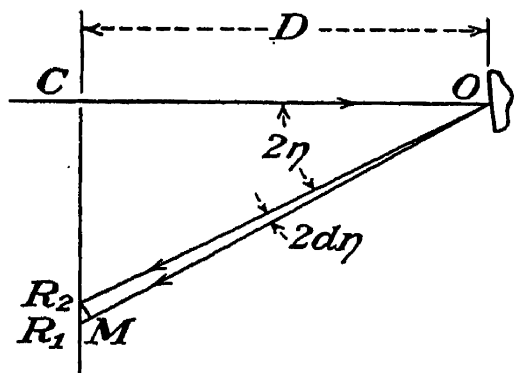


FIG. 21-12.—Showing relation between line shift, change in Bragg angle, distance  $D$ , and angle  $\eta$ .

or, from (21-19),

$$\epsilon_{z_2} - \epsilon_{z_1} = \frac{r_1 - r_2}{2D} \frac{\sin \eta \cos^2 2\eta}{\cos \eta} \quad (21-25)$$

Substituting (21-25) in (21-21),

$$E \frac{r_1 - r_2}{2D} = 2S'_x(1 + \nu) 2 \sin \alpha \cos \alpha \cos^2 \eta \sec^2 2\eta$$

$$\text{or} \quad r_1 - r_2 = 4D \frac{S'_x}{E} (1 + \nu) \sec^2 2\eta \cos^2 \eta \sin 2\alpha \quad (21-26)$$

This is the working equation adapted to one particular technique of surface stress measurement by x-ray line shift. For reference, it may be called "Thomas's technique A." Before discussing it, it will be well to derive the working equation adapted to Thomas's technique B, so that both equations will be available for comparison. In the B technique, two exposures are made at the same point  $O$  with different known camera inclinations  $\alpha_1$  and  $\alpha_2$  to the normal  $ON$  (Fig. 21-13). If  $\eta_1$  and  $\eta_2$  are small angles (of the order of  $5^\circ$ , as they usually are), the spacing computed from the ring diameter  $U_1U'_1$  may be taken as representative of the (310) (or whatever they may be) planes  $P_1$  normal to the primary beam  $W_1O$ , and the spacing computed from the ring diameter  $U_2U'_2$  as representative of the same set of planes  $P_2$  normal to the primary beam  $W_2O$ . Applying (21-17) to these planes,

$$E\epsilon_{z_2} = S'_x(1 + \nu) \sin^2 \alpha_2 - \nu(S_x + S_y)$$

and

$$E\epsilon_{z_1} = S'_x(1 + \nu) \sin^2 \alpha_1 - \nu(S_x + S_y)$$

Subtracting,

$$E(\epsilon_{z_2} - \epsilon_{z_1}) = S'_x(1 + \nu)(\sin^2 \alpha_2 - \sin^2 \alpha_1) \quad (21-27)$$

Substituting (21-25) in (21-27),

$$r_1 - r_2 = 2D \frac{S'_x}{E} (1 + \nu) \cot \eta \sec^2 2\eta (\sin^2 \alpha_2 - \sin^2 \alpha_1)$$

or, if  $u_1 = U_1U'_1 = \text{ring diameter} = 2r_1$  and  $u_2 = U_2U'_2 = 2r_2$ ,

$$u_1 - u_2 = 4D \frac{S'_x}{E} (1 + \nu) \cot \eta \sec^2 2\eta (\sin^2 \alpha_2 - \sin^2 \alpha_1) \quad (21-28)$$

These two working equations (21-26) and (21-28) are the ones used

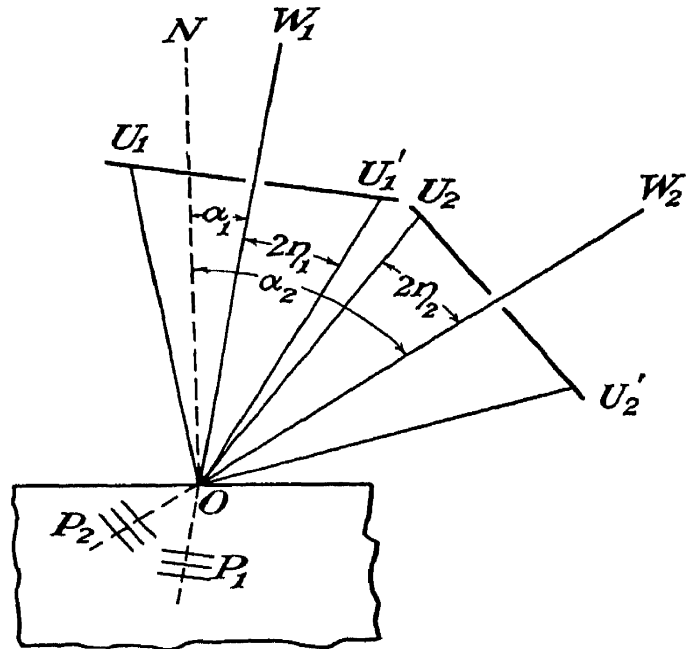


FIG. 21-13.—To illustrate stress measurement from different camera positions.

by Thomas.<sup>1</sup> They yield values for  $S'_x$  from measurements on patterns taken for different values of  $\psi$  in Fig. 21-10. Other workers have derived and used equations giving the principal stresses  $S_x$  and  $S_y$  from measurements on patterns taken for different values of  $\phi$ , rather than  $\psi$ . Among these, two equations of the same general character as (21-17) are often used,  $\phi$  being the variable instead of  $\psi$ . They are

$$E(\epsilon_{\phi=0} + \epsilon_{\phi=90}) = (S_x + S_y)[(1 + \nu) \sin^2 \psi - 2\nu] \quad (21-29)$$

and 
$$E(\epsilon_{\phi=0} - \epsilon_{\phi=90}) = (S_x - S_y)(1 + \nu) \sin^2 \psi \quad (21-30)$$

It will be noted that, for the special case  $\psi = 0$ , equation (21-29) reduces to equation (21-18),

$$E\epsilon_{\psi=0} = -(S_x + S_y)\nu \quad (21-18)$$

which was obtained on page 489. The symbols  $\epsilon_{\phi=0}$  and  $\epsilon_{\phi=90}$  of course represent the strain at  $O$  (Fig. 21-10) in a direction  $OZ''$  such that  $\phi = 0$  and in a second direction  $OZ''$  such that  $\phi = 90^\circ$ ,  $\psi$  being the same for both directions. The Thomas method is therefore by no means the only approach to the problem, but it is one of the simplest and most practical.

**8. Surface Stress and Line Shift—Experimental.** For simplicity, the surface stress at  $O$  in any arbitrary direction  $OX$  (Fig. 21-14) will henceforth be designated merely as  $S$  rather than  $S'_x$ , as in Sec. 7. This section

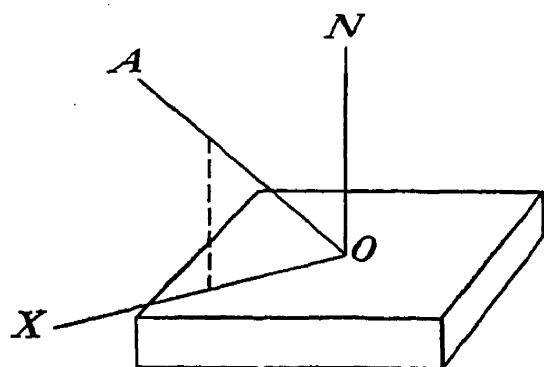


FIG. 21-14.—Simplification of Fig. 21-10.

has shown that  $S$  may be found from equation (21-26) by taking a single pattern with the primary x-ray beam along  $AO$  where  $A$  is in the plane  $XON$ ,  $NO$  being the normal at  $O$ . Some improvement in accuracy can usually be achieved by taking an additional pattern with the primary beam along  $NO$  and applying equation (21-28). In either of these equations,  $D$  must be in the same units as  $r_1$  and  $r_2$  or  $u_1$  and  $u_2$ . Then the stress

will be given in the same units as one chooses to use for Young's modulus  $E$ , usually given as pounds per square inch or dynes per square centimeter in the tables. Since Poisson's ratio enters into these equations added to 1, their accuracy is not seriously affected by uncertainty in the value of  $\nu$ , as between 0.25 and 0.3, for example.

In the case of the (310) back-reflection ring from iron, with cobalt  $K_\alpha$  radiation, calculation for the case of a specimen-to-film distance  $D$  of 5 cm. shows that the ring diameter should be about 34 mm. to give the accepted 2.861-Å. value for  $a$ . The effects of errors in the measurement of the ring diameter and in setting or measuring  $D$  are seen from Table

<sup>1</sup> D. E. Thomas, *J. Sci. Instruments*, **18**, 135 (1941).

21-3, which lists the calculated values of  $d_{(310)}$  for various values of the ring diameter and of  $D$ . Inspection of the table shows that a 1-mm error in the diameter causes a 0.0007-A. error in  $d_{(310)}$ , that is, a 0.07 per cent error. Likewise, a 1-mm. error in  $D$  causes a 0.0005-A. error in  $d_{(310)}$ , that is, a 0.05 per cent error. In view of the fact that a stress of 30,000 lb./in.<sup>2</sup> causes a strain of the order of 0.1 per cent in steel, it is clear that the ring diameter and  $D$  should both be determined with an accuracy of the order of 0.05 mm. or 0.002 in. if one wishes to estimate the stresses to the nearest thousand pounds per square inch. Obviously, this demands fairly sharp rings in the pattern.

TABLE 21-3

Ring diameter, mm.	$D = 49$ mm. $d_{(310)}$	$D = 50$ mm. $d_{(310)}$	$D = 51$ mm. $d_{(310)}$
33	0.9046 A.	0.9041 A.	0.9036 A.
34	0.9053 A.	0.9048 A.	0.9043 A.
35	0.9060 A.	0.9055 A.	0.9050 A.

The value of  $D$  may be determined by coating the surface of the sample with some "standard" material known to be stress-free. This material must be chosen so as to give a reference ring or rings on the film for direct comparison with the ring or rings from the sample. Standard coatings that have been used for this purpose include gold paint, gold leaf, silver paint,<sup>1</sup> and tungsten paint. These paints consist of the metal (gold, silver, tungsten, etc.) dust or filings in a binder, like shellac. Knowing the lattice constant  $a$  of the standard, the wave length, and the diameter of the standard ring on the film, one can calculate  $D$ .

Another way to measure  $D$  is to provide the collimator and cassette assembly with an accurate removable bullet-shaped template by means of which the distance  $D$  can be adjusted accurately to any predetermined value before the exposure. The template is then removed and the exposure made. This method dispenses with the standard paint or leaf. It has been described in detail by Thomas.<sup>2</sup>

If equation (21-26) is to be used and only one exposure taken, the camera inclination should be about 30° to the normal. In this case, the ring on the film is not quite circular, and the stress evaluation depends upon measurement of the slight difference between the radii on the lower and upper sides. Since the center of the ring comes in the hole in the film, it is impossible to measure these radii unless a special template

<sup>1</sup> L. Frommer and E. H. Lloyd (footnote, p. 485) use vacuum-annealed filings from pure cold-rolled silver, mixed with an adhesive and painted on to give a dry coat 0.004 in. thick.

<sup>2</sup> D. E. Thomas, *J. Sci. Instruments*, **18**, 135 (1941).

fitting accurately over the collimator tube is used to make reference marks on the film. Such a device is described by Thomas. If this is deemed objectionable, the only alternative is to take two patterns, one at  $30^\circ$  to the normal (preferably) and one at normal incidence. The difference in the ring diameters (not radii) between the two exposures is then determined, and equation (21-28) applied. In the former (single-exposure) method, it is not admissible to rotate the cassette about the collimator axis during the exposure, for this would wash out the very effect upon which the measurement depends. However, an oscillation or rocking through about  $15^\circ$  can be tolerated. According to Frommer and Lloyd,<sup>1</sup> rotation or oscillation of the cassette about the collimator axis is inadvisable if the sample is coarse-grained. Instead, they recommend oscillation of the specimen so that  $\alpha$  (Fig. 21-11 or 21-13) is given a slow periodic variation of 2 or  $3^\circ$  on either side of its desired value during the exposure. Scanning (page 395) at the same time also helps to smooth out the diffraction spots into continuous rings, the diameters or radii of which are more accurately measurable.

Thomas states that he obtains satisfactory patterns from steel in 5 min. with a front pinhole of 2 mm. diameter, using 20 ma. at 30 kv. with a cobalt target. It seems doubtful that such a large pinhole would yield rings whose diameter is measurable to 0.05 mm., however. Frommer and Lloyd<sup>1</sup> use a 0.35-mm. slit and an exposure of 1 or 2 hr. Unless one is studying the effects of shot-blasting, filing, etc., it is necessary to etch away about 0.01 in. of the surface to get rid of such effects before photographing the pattern. For aluminum, Frommer and Lloyd<sup>1</sup> suggest an etching solution, one part hydrofluoric acid, one hydrochloric acid, two nitric acid, and six water, by volume.

### QUESTIONS AND PROBLEMS

1. Distinguish between microstrain and macrostrain. Which has the same meaning as in the ordinary usage of the word "strain"? How does macrostrain reveal itself in an x-ray diffraction pattern? How does microstrain reveal itself? Is microstrain the only condition that could produce this effect upon the pattern? Does this ambiguity mean that x-ray diffraction is inferior to other methods of detecting and measuring microstress?

2. Can any information regarding stress be obtained from simple transmission patterns? What is asterism? What causes it? Is it more directly associated with the characteristic or the continuous radiation? Is there any relation between asterism and strain? What are diffuse reflections?

3. What type of x-ray diffraction pattern is best suited for the detection and measurement of microstress? Why? Answer the same questions for ordinary stress. If a Seemann-Bohlin camera is used, what type of primary radiation is to be recommended?

4. What type of primary radiation is best adapted for general use with back-reflection cameras for stress measurement? Why?

<sup>1</sup> L. Frommer and E. H. Lloyd, *J. Inst. Metals*, **70**, 91 (1944).

5. Can you suggest a reason why Wood did not observe any line broadening in cold-worked aluminum (presumably by transmission patterns), whereas broadening is fairly obvious in the back-reflection patterns of Clark, Pish, and Seabury, from aluminum stressed beyond the yield point?

6. Can macrostress in the interior portion of a metal block be measured by x-ray methods? Answer the same question for microstress. In making surface measurements of stress by x-ray diffraction, about how thick is the surface layer in which the stresses are being measured?

7. How can the stress be measured in a specimen without having an unstressed specimen for comparison? How can the stress be measured in a material like alpha brass for which the lattice constant is not accurately known? What is the minimum number of back-reflection patterns required to determine the stress at a given point on the surface in one direction only?

8. When the  $K_\alpha$  doublet is resolved in the back-reflection rings, describe a simple method of determining the half-value width of the line broadening. Does the half-value width refer to a peak in a curve for which  $\phi$  is the abscissa or for which  $\theta$  is the abscissa? If the corrected half-value width is 0.01 radian and if  $\theta = 85^\circ$ , what is the microstrain index?

9. Can the stress in the surface layer of any piece of steel be measured approximately by x-ray diffraction methods? If not, what are the limitations that render the method inapplicable in some cases?

10. Account for the elastic isotropy of a metal composed of anisotropic crystals. What are principal axes? Principal stresses?

11. A pencil line  $AP$  is drawn on a steel plate through a point  $P$ . Let  $NP$  be the normal to the plate at  $P$ . A back-reflection camera is so placed that its primary beam is in the plane  $NPA$ , inclined at  $30^\circ$  to  $NP$ , and strikes the metal at  $P$ . The distance from  $P$  to the plane of the x-ray film is 5.00 cm. Cobalt  $K_\alpha$  radiation is used. The radius of the (310) ring on the lower side is 16.72 mm.; on the upper side it is 16.82 mm. What is the stress at  $P$  in the direction  $PA$ ? Is it compression or tension? Assume Young's modulus = 30,000,000 lb./in.<sup>2</sup> and Poisson's ratio = 0.3.

*Ans.* 12,300 lb./in.<sup>2</sup> tension.

12. In the preceding problem, consider the diameter of the (310) ring as 33.54 mm. A second exposure is made at the same point at normal incidence, the diameter of the ring in this pattern being 33.72 mm., and  $D$  still being 5.00 cm. What value of the stress at  $P$  in direction  $PA$  does this indicate? *Ans.* 12,100 lb./in.<sup>2</sup> tension.

13. What is the purpose of the standard paints or foils sometimes used in stress measurement by x-ray diffraction? Name some of the materials used for this purpose. How can one get along without them? What can be done to improve the accuracy of stress measurement when the rings are spotty?

14. With cobalt  $K_\alpha$  radiation incident normally upon the face of a piece of mild sheet steel assumed stress-free, the (310) back-reflection ring is obtained on a film, as in Fig. 21-9A, sectors 1 and 3. Note that the ring is double. Is the inner component due to  $K_{\alpha_1}$  and the outer to  $K_{\alpha_2}$ , or vice versa? The specimen-to-film distance is 5 cm. The diameter of the  $K_{\alpha_1}$  ring is 3.40 cm. The sheet of steel is then wrapped around a cylindrical steel bar 4 in. in diameter and held in firm contact with it by wrapping with wire. A second normal-incidence pattern is then taken. The  $K_\alpha$  doublet is just barely resolved in the second pattern. What does this indicate about the sheet steel? The diameter of the  $K_{\alpha_1}$  ring in the second pattern is 3.33 cm. Does this indicate tension or compression in the plane of the outer surface of the sheet? From the nature of the problem, will this tension or compression be longitudinal or tangential or both? Calculate its value from equation (21-18) if Poisson's ratio is 0.3 and Young's modulus is 29,000,000 lb./in.<sup>2</sup>

*Ans.* About 43,000 lb./in.<sup>2</sup>

## CHAPTER 22

### X-RAY DIFFRACTION BY AMORPHOUS SOLIDS, LIQUIDS, AND GASES

**1. General Survey.** There has been a great deal of theoretical and experimental work in the field of x-ray diffraction by amorphous solids, liquids, and gases.<sup>1</sup> As mentioned in Sec. 15-6, the x-rays scattered from a monochromatic primary x-ray beam by a perfect crystal at  $0^\circ$  absolute temperature theoretically consist of very sharp and intense coherent scattering maxima at discrete angles satisfying Bragg's law, the maxima being superposed on a diffuse background of incoherently scattered radiation. As the temperature rises, this incoherent diffuse background is supplemented by a small amount of diffuse *coherent* scattering proportional to  $f_0^2 - f^2$  according to equation (15-18), the Bragg maxima becoming somewhat weaker and broader. This diffuse scattering sometimes displays secondary maxima called "diffuse reflections." Whether these are due primarily to the coherent or to the incoherent component is a matter of some dispute, as mentioned on page 478. One consistent feature of this diffuse background is that it falls off to nearly zero intensity as the scattering angle  $\phi$  approaches zero, for solids.

"Amorphous" solids, like glass or unstretched rubber, which have no extended orderly geometrical arrangement of their atoms, display the diffuse background just mentioned, but the Bragg maxima degenerate into one or two or sometimes three very broad, ill-defined maxima, which might be called "bands" or "diffuse rings."

The scattering from liquids is of the same general character as that from amorphous solids. In the case of monatomic liquids like mercury, the two or three broad maxima just mentioned are due entirely to interference effects between neighboring (monatomic) molecules. These molecules are separated by a distance that is fairly definite and fixed. The nearest neighbors surrounding any given molecule also maintain the second layer of molecules at a fairly constant distance from the chosen central molecule. These distances determine the positions of the broad coherent maxima.

<sup>1</sup> For more detailed accounts, see, for example, J. T. Randall, "The Diffraction of X-rays and Electrons by Amorphous Solids, Liquids, and Gases," John Wiley & Sons, Inc., New York, 1934; also A. H. Compton and S. K. Allison, "X-rays in Theory and Experiment," pp. 128-199, D. Van Nostrand Company, Inc., New York, 1935.



With liquids or amorphous solids composed of polyatomic molecules whose scattering power is concentrated chiefly near their centers, the diffraction patterns from  $\phi = 0$  out to and including the first (principal) maximum are likewise determined by interference effects between neighboring molecules. Beyond the principal maximum, however, the internal structure of the molecules is influential and generally preponderant.

With liquids or amorphous solids composed of polyatomic molecules whose scattering power is concentrated more toward the boundary of the molecule, even the principal maximum is strongly influenced by the internal structure of the molecule, except when the molecules are strongly anisotropic. With strongly anisotropic molecules, like the organic long-chain compounds, there is some evidence that in liquids the directions of the anisotropic axes (chain axes) are correlated over considerable groups of molecules, which supposedly have only a transient existence. This supposed formation of transient geometric molecular groups in liquids of this type has been called "cybotaxis" by Stewart.<sup>1</sup> As these long-chain molecules become longer (more  $\text{CH}_2$  links added with changing chemical composition), molecules like  $\text{C}_{29}\text{H}_{60}$  are able to form crystalline solids.

In the case of molecular gases, like oxygen or nitrogen, there is no longer any fairly definite distance between neighboring molecules, as in a liquid, but there is still a definite distance between the atoms in the molecule. The first fact results in a change in the character of the diffuse background scattering. Instead of falling off to a low value at small scattering angles, it now rises to a maximum as  $\phi$  approaches zero. The second fact causes the coherent part of the scattered radiation to still retain a maximum-and-minimum, or hump-and-valley, character, which, however, is usually fairly completely masked by the incoherent scattering. Nevertheless, it can be detected if the intensity versus angle distribution curve is properly analyzed.

Finally, in the case of monatomic gases like neon, argon, and helium, there is no longer any distance even approximately fixed, and both the coherent and the incoherent scattering are of a diffuse character, approaching maximum intensity at zero angle. Nevertheless, the shape of the scattering curve is still mathematically related to the radii of the electron shells in the atoms, and it is actually possible to deduce the radii of the electronic shells with considerable accuracy from the diffuse x-ray scattering curves.

**2. Experimental.** Amorphous solids are mounted in a diffraction camera and studied much like ordinary crystalline solids. If they are likely to have long molecular spacings, as in long-chain compounds like

<sup>1</sup> G. W. Stewart, *Rev. Modern Phys.*, **2**, 116 (1930).

paraffin, it is advisable to use a long-wave-length radiation such as iron  $K_{\alpha}$  so as to obtain a Bragg angle  $\theta$  that is large enough to measure accurately, in spite of the large values of  $d$  that may be encountered.

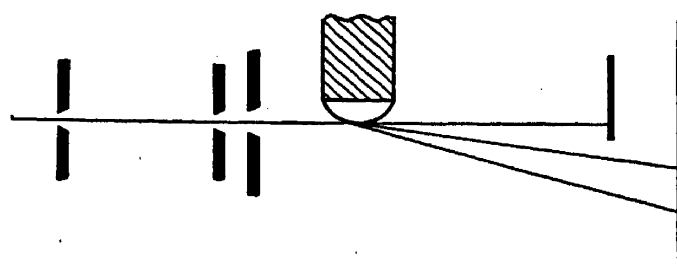


FIG. 22-1.—Method of obtaining pattern of a drop of liquid at grazing incidence.

Liquids may be placed in a small cell having thin walls of paraffined paper or glass. Cylindrical thin-walled glass cells are usually rotated during the exposure to avoid the effects of circumferential variation in the thickness of the glass walls. A drop of liquid may be suspended from the end of a glass rod and its

pattern obtained at grazing incidence, as shown in Fig. 22-1. Katzoff<sup>1</sup> has used a flowing liquid jet maintained by a circulating pump. He also recommends a crystal monochromator to reduce diffuse scattering and fogging.

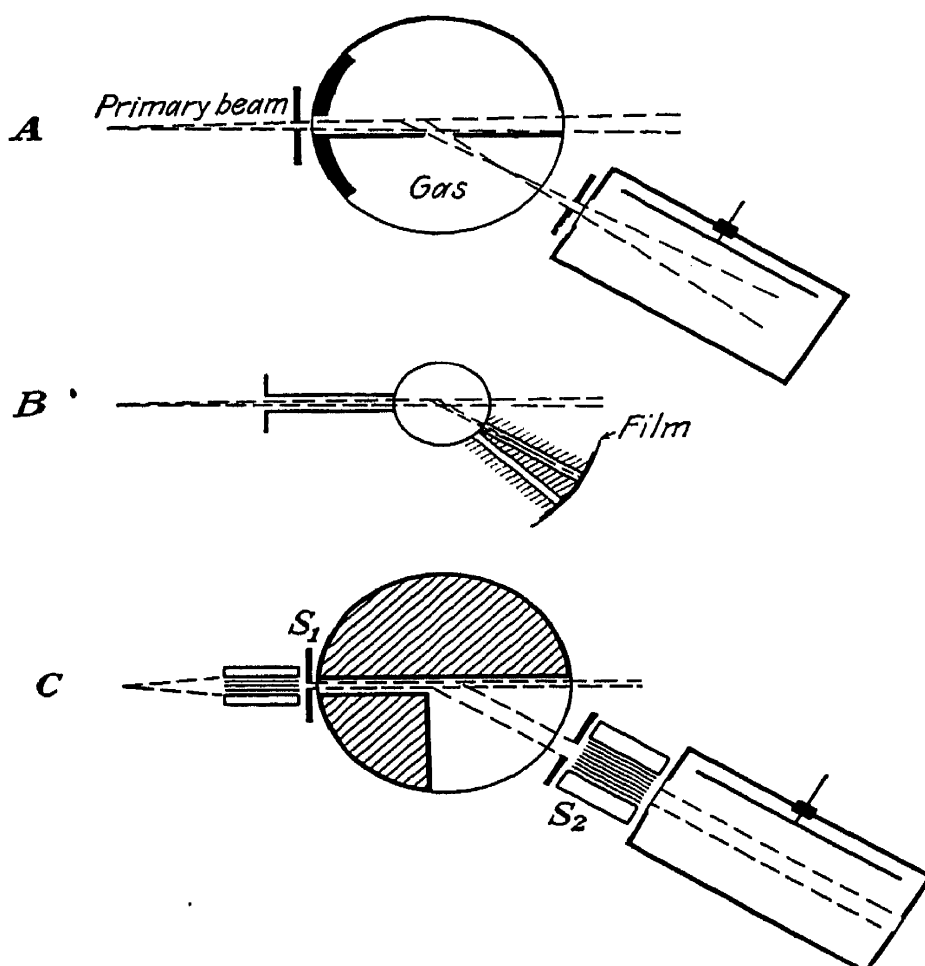


FIG. 22-2.—Apparatus used for measurement of x-ray scattering from gases. A, Barrett; B, Hertzog; C, Wollan. (Courtesy of *Review of Modern Physics*.)

With gases, a considerable modification of the diffraction camera is necessary for the x-ray beam to irradiate the much greater volume of the

<sup>1</sup> S. Katzoff, *J. Chem. Phys.*, **2**, 841 (1934).

sample required to scatter enough rays to make their intensity measurable. Figure 22-2 shows three types of gas x-ray diffraction apparatus. The first (A) was used by Barrett<sup>1</sup> to study x-ray scattering by monatomic gases; the second (B) was used by Herzog,<sup>2</sup> also for monatomic gases; the third (C), by Wollan.<sup>3</sup> Barrett and Wollan used molybdenum radiation in conjunction with a zirconium-strontium Ross type of filter, and Herzog used copper radiation and a nickel filter. The cylindrical gas chambers seen are some 5 or 6 in. in diameter and 4 or 5 in. in height, with metal walls strong enough to withstand gas pressures up to 200 lb./in.<sup>2</sup> The chamber must of course be provided with windows to permit the entry and exit of the x-rays. Wollan found that celluloid 0.7 mm. thick would give gastight windows 2 cm. high at this pressure. The heavy black lines in Barrett's gas chamber represent lead partitions. The shaded areas in Wollan's chamber represent solid blocks of sealing wax. It will be noted that Wollan used Soller slits. Barrett and Wollan used ionization chambers about 12 × 30 cm., filled with methyl bromide, and an electrode potential of 350 volts, whereas Herzog used photographic recording.

**3. The Scattering of X-rays by Monatomic Gases.** Space will permit only a bare outline here of the theoretical treatment of this subject.<sup>4</sup> On the basis of quantum mechanics, it was shown by Wentzel<sup>5</sup> in 1927 that the x-rays scattered by the various electrons in a single atom should consist of coherent and incoherent components. A year later, Raman<sup>6</sup> reached the same conclusion from his calculations based on classical theory.

As already stated [equation (16-7)], the intensity  $I_e$  at a distance  $r$  of the radiation coherently scattered by an electron from a primary beam of intensity  $I_0$  in a direction inclined at an angle  $\phi$  thereto is

$$I_e = \frac{e^4}{2r^2m^2c^4} (1 + \cos^2 \phi) \quad (22-1)$$

(On the basis of classical electromagnetic theory, the intensity  $I$  of the rays coherently and incoherently scattered by a group or cloud of  $Z$  electrons moving independently of each other about an atomic nucleus has been calculated by Raman<sup>6</sup> and Compton<sup>7</sup> as

$$I = I_e[Z^2g^2 + Z(1 - g^2)] \quad (22-2)$$

<sup>1</sup> C. S. Barrett, *Phys. Rev.*, **32**, 22 (1928).

<sup>2</sup> G. Herzog, *Z. Physik*, **69**, 207 (1931).

<sup>3</sup> E. O. Wollan, *Phys. Rev.*, **37**, 862 (1931).

<sup>4</sup> For a more detailed account, see, for example, A. H. Compton and S. K. Allison, "X-rays in Theory and Experiment," pp. 128-199, D. Van Nostrand Company, Inc., New York, 1935.

<sup>5</sup> G. Wentzel, *Z. Physik*, **43**, 1, 779 (1927).

<sup>6</sup> C. V. Raman, *Indian J. Physics*, **3**, 357 (1928).

<sup>7</sup> A. H. Compton, *Phys. Rev.*, **35**, 925 (1930).

where the term before the  $+$  sign represents the coherent scattering and the other term is the incoherent scattering,  $I_e$  is given by (22-1), and  $g$  is given by

$$g = \int_0^{\infty} u(a) \frac{\sin ka}{ka} da \quad (22-3)$$

$a$  being the distance from the nucleus to any arbitrary point in the cloud and  $u(a) da$  the probability that any particular electron will lie between  $a$  and  $a + da$ . From this it follows that

$$\int_0^{\infty} u(a) da = 1 \quad (22-4)$$

and

$$k = \frac{4\pi}{\lambda} \sin \frac{\phi}{2} \quad (22-5)$$

where  $\lambda$  is the wave length (measured in the same units in which  $a$  is measured) of the primary rays and  $\phi$  is the angle between the primary ray (beyond the cloud) and the scattered ray being measured. Here  $g$  is a quantity defined by (22-3) and called the "electronic-structure factor." It is related to the atomic-structure factor  $f$ , defined on page 354, by the equation

$$f = \sum_{n=1}^Z g_n \quad (22-6)$$

Or if  $U(a) da$  is the number of electrons between  $a$  and  $a + da$ , so that

$$\int_0^{\infty} U(a) da = Z \quad (22-7)$$

then

$$f = \int_0^{\infty} U(a) \frac{\sin ka}{ka} da \quad (22-8)$$

More rigorous derivation of the equation corresponding to (22-2) on the basis of quantum mechanics<sup>1</sup> indicates that a "recoil factor"  $R$  should be included, so that (22-2) becomes

$$I = I_e [Z^2 g^2 + RZ(1 - g^2)] \quad (22-9)$$

where

$$R = \left( 1 + \frac{h}{mc\lambda} \text{vers } \phi \right)^{-3} \quad (22-10)$$

$h$  being the Planck constant,  $m$  the mass of an electron, and  $c$  the velocity of light. This relation (22-9) is based on the assumption that there is no special grouping of electrons into K, L, M, etc., shells and that the

<sup>1</sup> G. Breit, *Phys. Rev.*, **27**, 362 (1926); P. A. M. Dirac, *Proc. Roy. Soc. (London) A*, **111**, 405 (1926).

electron cloud is spherically symmetrical. When the grouping into shells is considered, the relation found by quantum-mechanical analysis<sup>1</sup> is

$$I = I_e \left[ f^2 + R \left( Z - \sum_{n=1}^Z g_n^2 \right) \right] \quad (22-11)$$

where  $f$  is the atomic structure factor (22-8). Values of  $\Sigma g_n^2$  have been calculated and tabulated by Heisenberg<sup>2</sup> and are listed in Table 22-1. Equation (22-11) is also useful for calculating the diffuse scattering (between Bragg maxima) for a crystalline solid, except that in this case the coherent scattering is  $I_e(f_0^2 - f^2)$  instead<sup>3</sup> of  $I_e f^2$ , where  $f_0$  and  $f$  are related as in Sec. 16-14 [equation (16-42); see also Sec. 15-6, equation (15-18)].

TABLE 22-1.—INCOHERENT-SCATTERING FUNCTION  $\Sigma g^2$   
( $\theta = \frac{1}{2}\phi$ ;  $\lambda$  in angstrom units)

$\frac{\sin \theta}{\lambda}$	0	0.1	0.2	0.3	0.4	0.5	0.6	0.7	0.8	0.9	1.0	1.1
1H	1.0	0.66	0.23	0.06	0.02	0.0	0.0	0.0	0.0	0.0	0.0	0.0
2He	2.0	1.76	1.06	0.55	0.28	0.14	0.06	0.03	0.02	0.01	0.01	0.0
3Li <sup>+</sup>	2.0	1.9	1.6	1.1	0.8	0.5	0.2	0.1	0.1	0.05	0.0	0.0
3Li	3.0	1.9	1.6	1.1	0.8	0.5	0.2	0.1	0.1	0.05	0.0	0.0
4Be	4.0	2.2	1.9	1.6	1.2	0.9	0.6	0.3	0.2	0.2	0.1	0.0
6C	6.0	4.0	2.7	1.8	1.5	1.3	1.0	0.8	0.7	0.6	0.5	0.4
7N	7.0	5.2	3.3	1.9	1.7	1.4	1.2	1.0	0.9	0.9	0.8	0.6
8O	8.0	6.4	3.9	2.4	2.0	1.6	1.5	1.3	1.2	1.1	0.9	0.8
9F <sup>-</sup>	10.0	7.6	4.8	2.9	2.2	1.8	1.6	1.5	1.4	1.2	1.1	1.0
10Ne	10.0	8.3	5.6	3.8	2.7	2.1	1.8	1.6	1.5	1.3	1.2	1.1
11Na <sup>+</sup>	10.0	9.0	6.3	4.6	3.2	2.4	2.0	1.7	1.6	1.4	1.3	1.2
12Mg <sup>++</sup>	10.0	9.2	7.1	5.3	3.8	2.9	2.3	1.9	1.7	1.5	1.4	1.3
13Al	13.0	10.2	7.8	6.0	4.5	3.4	2.6	2.2	1.9	1.7	1.5	1.4
14Si	14.0	10.4	8.3	6.5	5.0	3.9	3.0	2.4	2.0	1.8	1.6	1.4
17Cl	17.0	13.1	9.7	7.8	6.5	5.4	4.4	3.6	3.0	2.5	2.2	2.0
17Cl <sup>-</sup>	18.0	13.4	9.8	7.8	6.5	5.4	4.4	3.6	3.0	2.5	2.2	2.0
18A	18.0	14.2	10.3	8.2	6.9	5.8	4.8	4.0	3.4	2.8	2.4	2.2
19K <sup>+</sup>	18.0	15.1	10.8	8.7	7.3	6.2	5.2	4.4	3.7	3.1	2.7	2.3
20Ca <sup>++</sup>	18.0	16.0	11.3	9.2	7.7	6.6	5.6	4.8	4.0	3.4	3.0	2.4
29Cu	29	24	18	14	12	10	9	7	6	6	5	4
36Kr	36	30	25	20	16	14	12	10	8	7	6	6
54Xe	54	48	40	33	27	23	20	17	15	13	12	10
80Hg	80	72	60	50	42	35	30	27	24	22	20	18

The error introduced by using the simpler equation (22-9) instead of the more rigorous (22-11) is small for atoms of low or high atomic

<sup>1</sup> G. Wentzel, *Z. Physik*, **43**, 781 (1927).

<sup>2</sup> W. Heisenberg, *Physik Z.*, **32**, 737 (1931); see also L. Bewilogua, *Physik. Z.*, **32**, 740 (1931).

<sup>3</sup> P. Debye, *Ann. Physik*, **43**, 49 (1914).

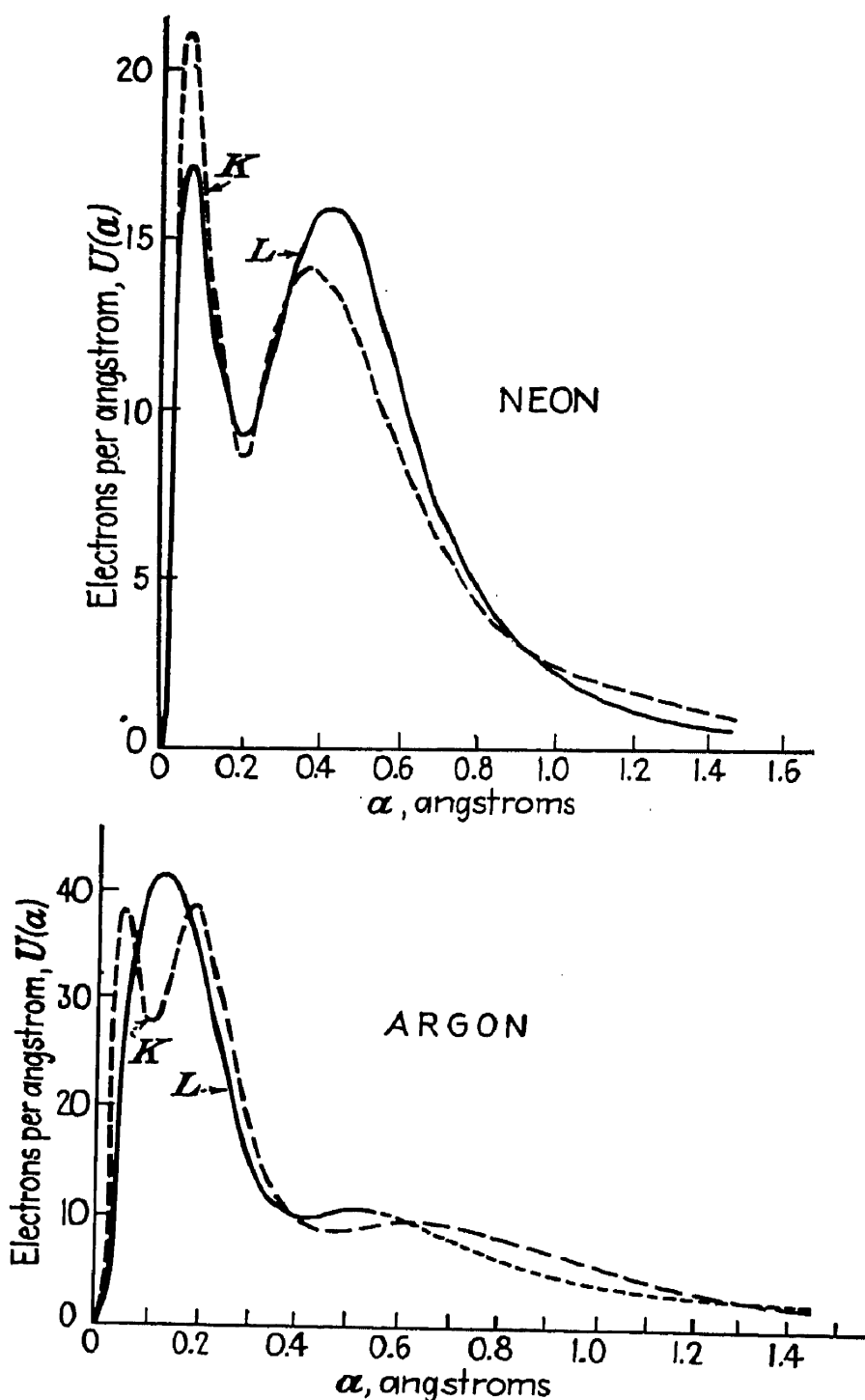


FIG. 22-3.—Radial electron distribution in neon (upper) and argon (lower). Solid line, experiment; broken line, Hartree theory. Note resolution of *K* and *L* shells in neon, and failure to achieve such resolution in argon. (After Wollan.)

number. The error is larger, but not too serious, for atoms of moderate atomic number like neon, according to Wollan.<sup>1</sup>

If one rewrites (22-9) in the form  $S = Zg^2 + R(1 - g^2)$  where  $S = I/ZI_e$ , one may then solve for  $g$ , obtaining

$$g = \sqrt{\frac{S - R}{Z - R}} \quad (22-12)$$

<sup>1</sup> E. O. Wollan, *Phys. Rev.*, **37**, 862; **38**, 15 (1931).

by means of which experimental values can be calculated for  $g$  from the measured values of  $S$  and known values of  $R$  and  $Z$ . Compton has shown that  $Zu(a)$ , the number of electrons per angstrom unit at any

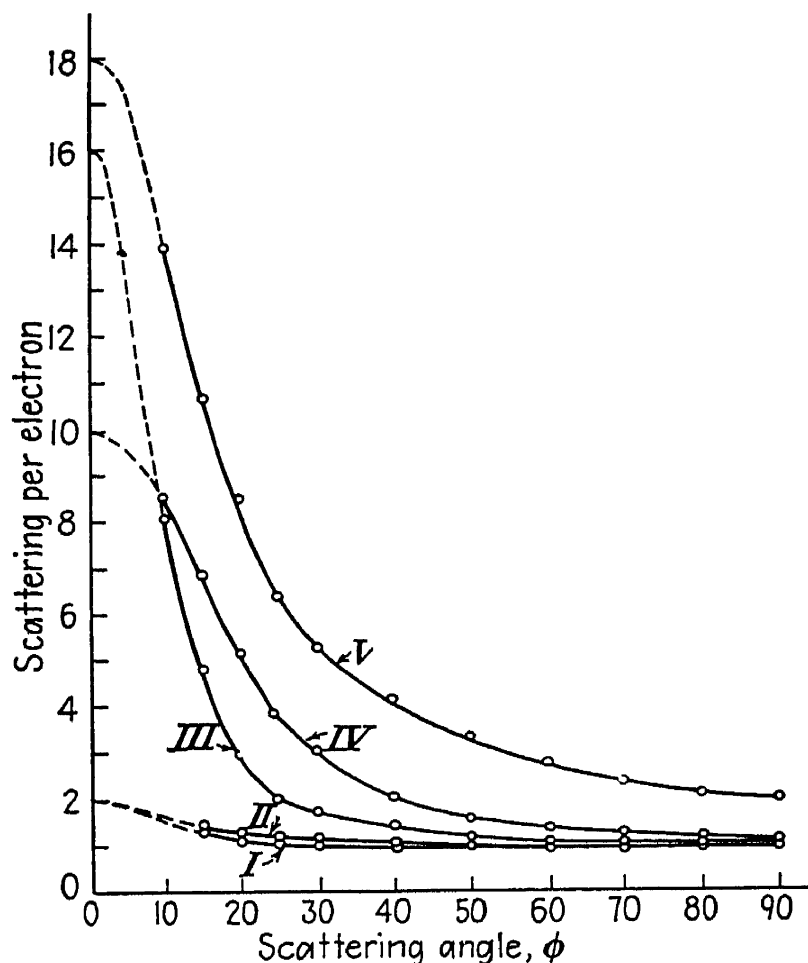


FIG. 22-4.—Intensity of x-rays scattered by gases. I, hydrogen. II, helium. III, oxygen. IV, neon. V, argon. (After Wollan; courtesy of *Review of Modern Physics*.)

distance  $a$  from the center of the atom, can be calculated from these experimental  $g$  values by the equation

$$Zu(a) = \frac{2ZA}{\pi} \int_0^{\infty} kg \sin(ak) dk \quad (22-13)$$

where  $k$  is defined by (22-5). This integral may be expressed as the sum of two integrals, the first with limits from 0 to  $a_1$  and the second with limits from  $a_1$  to  $\infty$ . The integration is then performed graphically by means of a planimeter, as described by Compton and Wollan.<sup>1</sup>

This theoretical analysis makes it possible to plot the radial electron distribution curves for monatomic gases such as helium, neon, and argon (Fig. 22-3) from x-ray scattering data of the type shown in Fig. 22-4, obtained by Wollan<sup>1</sup> with apparatus of the type represented diagrammatically in Fig. 22-2C. It is to be noted that the scattering intensity

<sup>1</sup> A. H. Compton, *Phys. Rev.*, **35**, 925 (1930); E. O. Wollan, *Rev. Modern Phys.*, **4**, 243 (1932).

approaches a maximum as the scattering angle  $\phi$  approaches zero, for gases. The fact that the K and L shells are separately resolved for neon but not for argon indicates a greater separation between these shells in the former gas than in the latter. Such calculations from x-ray and electron scattering curves (Chap. 24) have given more information on the dimensions and shape of actual atoms than any other experimental approach. The velocity distribution of the orbital electrons has also been calculated.<sup>2</sup>

Guided by these results, quantum-mechanical theories of the radial distribution of electrons in various atoms have been formulated by Thomas,<sup>3</sup> Fermi,<sup>4</sup> and Hartree<sup>5</sup> (dotted curves, Fig. 22-3) and account satisfactorily for the observed x-ray scattering curves. From these theories, James and Brindley<sup>6</sup> have calculated the table of atomic-structure factors given on page 356.

**4. The Scattering of X-rays by Polyatomic Gases.** The theory of x-ray scattering by polyatomic gases rests on the foundation laid in a paper by Debye<sup>7</sup> in 1915, in which he calculated that the coherent component of the rays scattered at an angle  $\phi$  from the primary beam by a molecule consisting of  $N$  groups of  $Z$  electrons each, separated by fixed distances, as measured at a distance  $r$ , should be

$$I_c = Z^2 I_e \sum_{m=0}^N \sum_{n=0}^N \frac{\sin x_{mn}}{x_{mn}} \quad (22-14)$$

where 
$$x_{mn} = \frac{4\pi}{\lambda} s_{mn} \sin \frac{1}{2} \phi \quad (22-15)$$

where  $I_e$  is given by (22-1) and  $s_{mn}$  is the distance (in the same units in which  $\lambda$  is measured) from the  $m$ th to the  $n$ th atom in the molecule. The summation is taken with respect to any one atom over all the other atoms, including the one singled out, and then the one singled out is in turn allowed to be each of the atoms in the molecule. This calculation was made before the concept of a structure factor had been introduced. In the modern version of the formula,  $Z^2$  is replaced by  $\sum_m \sum_n f_m f_n$ . The incoherent-scattering term must also be added, giving for the scattering  $I_m$  by a molecule

<sup>1</sup> E. O. Wollan, *Proc. Natl. Acad. Sci.*, **17**, 475 (1931); *Phys. Rev.*, **37**, 862, **38**, 15 (1931).

<sup>2</sup> W. E. Duncanson and C. A. Coulson, *Proc. Phys. Soc. (London)*, **57**, 190 (1945).

<sup>3</sup> L. H. Thomas, *Proc. Cambridge Phil. Soc.*, **23**, 542 (1927).

<sup>4</sup> E. Fermi, *Z. Physik*, **48**, 73 (1928).

<sup>5</sup> D. R. Hartree, *Proc. Cambridge Phil. Soc.*, **24**, 89, 111 (1928).

<sup>6</sup> R. W. James and G. W. Brindley, *Phil. Mag.*, **12**, 104 (1931).

<sup>7</sup> P. Debye, *Ann. Physik*, **46**, 809 (1915); *Physik Z.*, **31**, 419 (1930).



$$I_m = I_e \left[ \sum_{m=1}^N \sum_{n=1}^N f_m f_n \frac{\sin x_{mn}}{x_{mn}} + R \sum_{m=1}^N \left( Z_m - \sum_{j=1}^Z g_j^2 \right) \right] \quad (22-16)$$

where  $R$  and  $g$  are given by (22-10) and (22-3). This expression was obtained by Woo<sup>1</sup> by adding the coherent term due to Debye<sup>2</sup> to the incoherent term calculated by Bewilogua,<sup>3</sup> Jauncey,<sup>4</sup> and Woo.<sup>5</sup> In the case of diatomic molecules, (22-16) reduces to

$$I_2 = 2I_e \left[ f^2 \left( 1 + \frac{\sin x}{x} \right) + R(Z - \Sigma g^2) \right] \quad (22-17)$$

Here the kinship of the coherent-scattering term with Bragg's law can be seen by noting that the coherent scattering will be a maximum when  $\sin x/x$  is a maximum. If we let  $y = \sin x/x$ ,

$$\frac{dy}{dx} = \frac{1}{x} \cos x - \frac{\sin x}{x^2} = 0$$

for a maximum value of  $y$ . From this, one has  $\sin x = x \cos x$  or  $x = \tan x$ . It being remembered that  $x$  is in radians, the first value of  $x$  (other than zero) that satisfies this relation is  $x = 7.72$ . Hence one has, from (22-15),

$$\frac{4\pi}{\lambda} s_{mn} \sin \frac{1}{2} \phi = 7.72$$

or

$$\lambda = 0.814 \times 2s_{mn} \sin \frac{1}{2} \phi \quad (22-18)$$

Aside from the 0.814 factor, this is Bragg's law. This equation is generally known as "Keesom's equation" because he first derived it<sup>6</sup> for application to the problem of x-ray diffraction by liquids.

Comparing (22-17) with (22-11), one concludes that, for a monatomic gas, equation (22-11) indicates that both the coherent and incoherent scattering fall off from a maximum to smaller and smaller values with increasing  $\phi$ , as indicated by Fig. 22-4, but that, when the effect of neighboring atoms separated by a more or less fixed distance  $s_{mn}$  is introduced, this has the effect of making the coherent scattering a recurrent up-and-down function with maxima and minima, due to the introduction of the term  $1 + \frac{\sin x}{x}$ . This is the important feature of Debye's theory. Although this fluctuating character of the coherent

<sup>1</sup> Y. H. Woo, *Phys. Rev.*, **41**, 21 (1932).

<sup>2</sup> P. Debye, *Physik Z.*, **31**, 419 (1930); *Proc. Phys. Soc. (London)*, **42**, 340 (1930).

<sup>3</sup> L. Bewilogua, *Physik. Z.*, **32**, 740 (1931).

<sup>4</sup> G. E. M. Jauncey, *Phys. Rev.*, **38**, 194 (1931).

<sup>5</sup> Y. H. Woo, *Proc. Natl. Acad. Sci.*, **17**, 467 (1931).

<sup>6</sup> W. H. Keesom, *Physica*, **2**, 118 (1922), **5**, 125 (1924).

scattering is not strong enough to make itself apparent in curve III of Fig. 22-4, it will be noticed that this curve (being for a diatomic gas) does have a distinct dip when compared with curves IV and V. The "humps" introduced by Debye's term can be seen in the data from oxygen or nitrogen if the data are plotted in the form of a curve with  $X$  as ordinate and  $\sin \frac{1}{2}\phi/\lambda$  as abscissas, where

$$X = \frac{1}{f^2} \left[ \frac{I_2}{2I_e} - R(Z - \sum g^2) \right] \quad (22-19)$$

which, from (22-17) is seen to be Debye's  $1 + \frac{\sin x}{x}$  function. When one progresses one more step to the investigation of x-ray scattering by liquids, this "hill-and-valley" character of the coherent radiation

becomes evident in the scattering curves without any special plotting to bring it out.

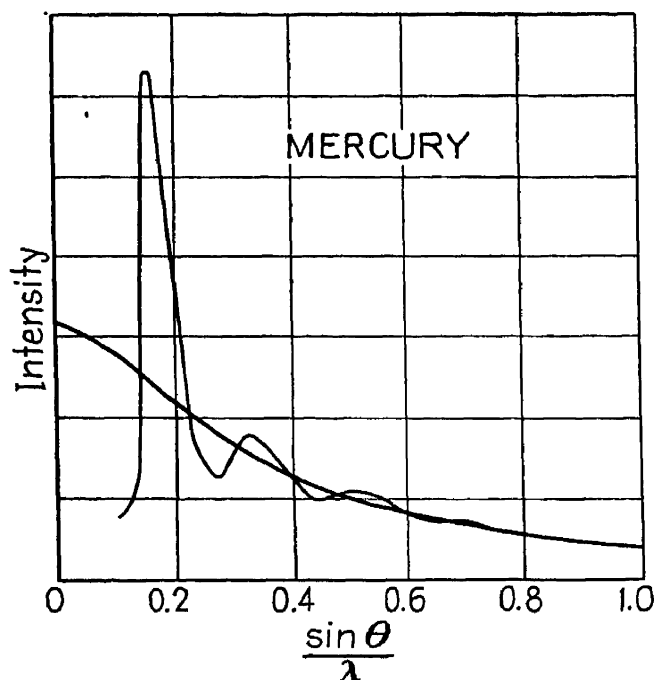


FIG. 22-5.—Scattering curve for mercury. (Gingrich; courtesy of Review of Modern Physics.)

By comparing the observed x-ray scattering curves for polyatomic gases with those predicted by (22-16) and (22-17), the interatomic distances  $s_{mn}$  for such cases as H—H in hydrogen<sup>1,2</sup> (1 A.), N—N in nitrogen<sup>1,2,3,6</sup> (1.09 A.), O—O in oxygen<sup>1,2,3,6</sup> (1.22 A.), O—O in carbon dioxide<sup>6</sup> (2.2 A.), and Cl—Cl in carbon tetrachloride<sup>4,5</sup> (3.11 A.) have been determined. Similar methods have shown that cis dichloroethylene<sup>7</sup> ( $C_2H_2Cl_2$ ) has the chlorine atoms and the hydrogen atoms at adjacent corners of a rectangle, whereas trans

dichloroethylene has them at the diagonally opposite corners. In several respects, electron diffraction has advantages over x-ray diffraction for the study of gases, as explained in Chap. 24.

## 5. The Diffraction of X-rays by Liquids and Amorphous Solids. As

<sup>1</sup> Y. H. Woo, *Proc. Natl. Acad. Sci.*, **17**, 467, 470 (1931).

<sup>2</sup> E. O. Wollan, *Proc. Natl. Acad. Sci.*, **17**, 475 (1931).

<sup>3</sup> C. S. Barrett, *Phys. Rev.*, **32**, 22 (1928); E. O. Wollan, *Phys. Rev.*, **35**, 1019 (1930).

<sup>4</sup> P. Debye, L. Bewilogua, and F. Ehrhardt, *Physik. Z.*, **30**, 84 (1929).

<sup>5</sup> L. Bewilogua, *Physik Z.*, **32**, 265 (1931).

<sup>6</sup> H. Gajewski, *Physik. Z.*, **33**, 122 (1932).

<sup>7</sup> P. Debye, *Physik Z.*, **31**, 419 (1930); *Proc. Phys. Soc. (London)*, **42**, 340 (1930).

already mentioned, the hill-and-valley character of the coherent scattering becomes apparent in the scattering curves for liquids, as may be seen in Fig. 22-5, which is a scattering curve for liquid mercury at room temperature, plotted by Gingrich<sup>1</sup> from the data of Debye and Menke.<sup>2</sup> Here the intensity of the scattered rays has been plotted simply as a function of  $\sin \theta/\lambda$  or  $\sin \frac{1}{2}\phi/\lambda$ . The incoherent part of the scattering is of the same character as that considered in Secs. 3 and 4 for gases. The tendency for the coherent scattering to drop off instead of increasing

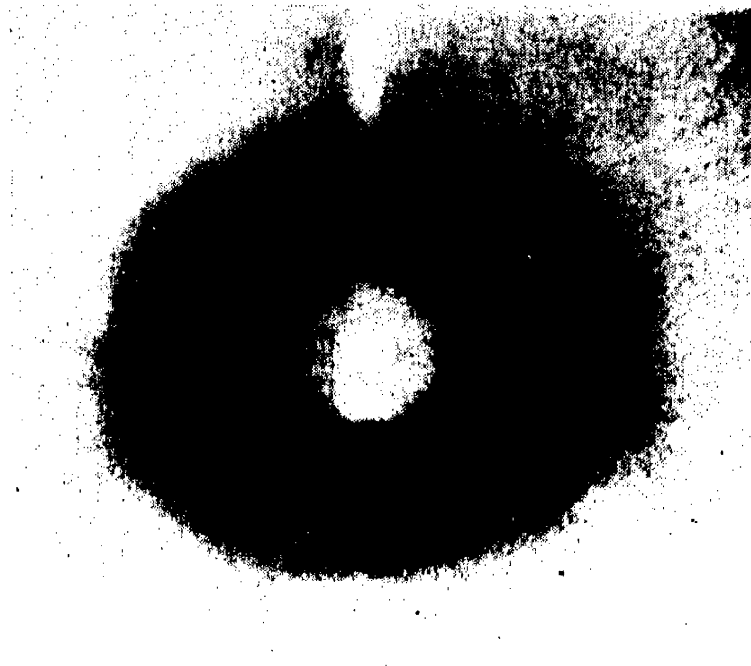


FIG. 22-6.—X-ray diffraction pattern of water.

as  $\phi$  approaches zero is seen by comparing Fig. 22-5 with Fig. 22-4. It is also seen in Fig. 22-6, a pattern of water at room temperature.

It was mentioned in Sec. 1 that for liquids and amorphous solids having monatomic molecules or polyatomic molecules whose scattering power is concentrated chiefly near the center the position of the principal diffraction peak in a curve like Fig. 22-5 is determined by interference effects between neighboring molecules. For brevity, such molecules are often called simply "spherical" molecules. For liquids and amorphous solids composed of such molecules, it has been found by Keesom and de Smedt<sup>3</sup> and by Katz<sup>4</sup> that the angular location  $\phi$  of the principal diffraction peak is given with acceptable accuracy by the Keesom equation

$$\lambda = 0.814 \times 2s \sin \frac{1}{2}\phi \quad (22-18)$$

<sup>1</sup> N. S. Gingrich, *Rev. Modern Phys.*, **15**, 109 (1943).

<sup>2</sup> P. Debye and H. Menke, *Physik Z.*, **31**, 797 (1930).

<sup>3</sup> W. Keesom and J. de Smedt, *Proc. Amsterdam*, **25**, 118 (1922), **26**, 112 (1923); *Physica*, **5**, 125 (1924).

<sup>4</sup> J. R. Katz, *Z. Physik*, **45**, 97 (1927).

where  $s_{mn}$ , or  $s$  for brevity, is the mean distance between any one molecule and its nearest neighbors. The preceding section showed how the Keesom equation is related to Debye's equation (22-14). When one is dealing with a liquid, the same theoretical reasoning is valid, except that one applies it, not to an array of atoms in a molecule, but to an array of molecules (they may be monatomic) which takes all possible orientations in space, as in a liquid. One may calculate  $s$  readily if close packing of spherical molecules is assumed, by the equation

$$s = 1.33 \sqrt[3]{\frac{M}{\rho}} \quad (22-20)$$

where  $M$  is the molecular weight and  $\rho$  the density of the liquid or solid. As mentioned in Sec. 1, equation (22-18) becomes inaccurate when the scattering power of the molecules is not centrally concentrated, and (22-20) likewise fails for nonspherical molecules.

A more general theory must be used to deduce from the shape of the x-ray scattering curve [ $I(\phi)$  versus  $\phi$ ], like Fig. 22-5, the distribution about any chosen molecule in a liquid of its neighboring molecules, as plotted by Gingrich for mercury in Fig. 22-7 from the scattering curve in Fig. 22-5. The general theory upon which such calculations are based has been developed by Zernike and Prins.<sup>1</sup> The following symbols are defined in their theory. The symbol  $\rho(r)$  designates the probability that, within the spherical volume element of radius  $r$  and thickness  $dr$  surrounding any one "chosen" molecule in the liquid, there will be found the center point of another molecule. Thus  $\rho(r)$  is the mean density of molecule centers if a molecule center is located at the origin  $r = 0$ , and the mean number of molecule centers between  $r$  and  $r + dr$  is  $4\pi r^2 \rho(r) dr$ . The average density of molecules throughout the liquid is arbitrarily taken as 1. Thus  $\rho(r) - 1 = \rho_0(r)$  is a function expressing the local departure from this average density in the vicinity of any chosen molecule. As in equation (22-5), let  $k = \frac{4\pi}{\lambda} \sin \frac{1}{2} \phi$ .  $I(k)$  is the intensity of the coherent component of the scattered radiation for various values of  $k$ .  $M$  is the molecular volume of the liquid in cubic angstrom units per molecule.  $P$  is the polarization factor  $\frac{1 + \cos^2 \phi}{2}$  given by (16-28).  $f(k)$  is the atomic-structure factor for a given value of  $k$ .  $C$  is a constant, and  $E(k) = I(k)/CPf^2(k)$ . In terms of these symbols, the theory of Zernike and Prins indicates that

$$\rho_0(r) = \frac{M}{2\pi^2} \int_0^\infty k^2 [E(k) - 1] \frac{\sin kr}{kr} dk \quad (22-21)$$

<sup>1</sup> F. Zernike and J. A. Prins, *Z. Physik*, **41**, 184 (1927), **56**, 617 (1929).

Space limitations make it impractical to set forth the details of application of this theory to various types of liquids. Instead, reader is referred to papers by Gingrich<sup>1</sup> for its application to the chemical elements in the liquid state, by Warren<sup>2</sup> for its application to long-chain liquids, and by Katzoff<sup>3</sup> for its application to water, heptane, decane, benzene, and cyclohexane and of course to the original papers of Zernike<sup>4</sup>.

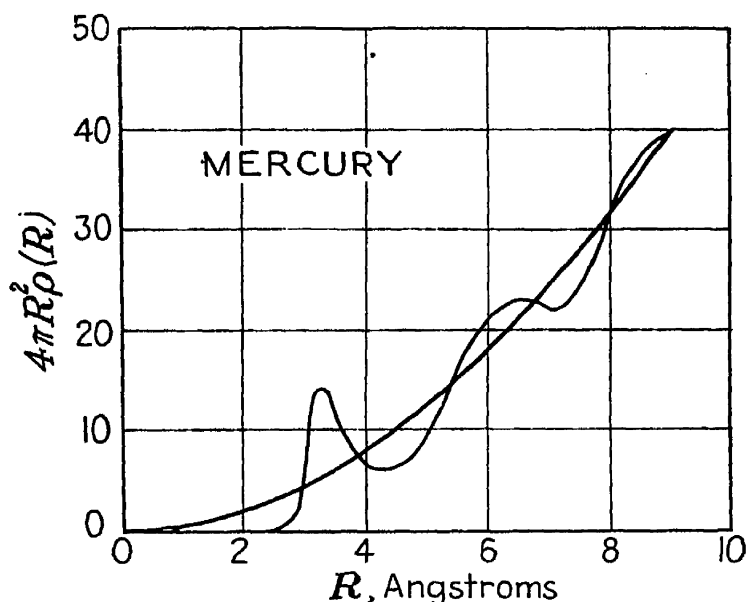


FIG. 22-7.—Radial distribution of neighboring atoms about any selected atom in mercury.  $R$  in the figure is equivalent to  $r$  in the text. (By N. S. Gingrich; courtesy of N. S. Gingrich, *Review of Modern Physics*)

and Prins already cited. Gingrich obtained Fig. 22-7 from Fig. 22-6 by the use of a harmonic analyzer and graphical integration with a planimeter.

Warren and Katzoff in the papers just cited conclude that in long-chain hydrocarbon liquids, about any one long molecule, the neighboring molecules are roughly parallel but that otherwise there is extensive disarrangement in the liquid. These normal hydrocarbon liquids yield scattering curves having a strong maximum at  $\phi = 8.83^\circ$

$$(\theta = 4.415^\circ),$$

as indicated in the series of curves for  $C_5H_{12}$  to  $C_{15}H_{32}$  shown in Fig. 22-8 obtained by Stewart,<sup>4</sup> who uses  $\theta$  as  $\phi$  or  $2\theta$  is used in this book. Katzoff was able to detect two fainter maxima for normal heptane at angles  $\phi$ ; as stated in Sec. 1, these are due to the internal structure of the molecule or intramolecular interference. They can be explained on the basis of a zigzag chain of carbon atoms where the C—C distance is

<sup>1</sup> N. S. Gingrich, *Rev. Modern Phys.*, **15**, 90 (1943).

<sup>2</sup> B. E. Warren, *Phys. Rev.*, **44**, 969 (1933).

<sup>3</sup> S. Katzoff, *J. Chem. Phys.*, **2**, 841 (1934).

<sup>4</sup> G. W. Stewart, *Phys. Rev.*, **31**, 174 (1928).

1.54 Å., according to Katzoff, on the basis of the Zernike-Prins theory. The main peak at  $\theta = 4.41^\circ$  is due to intermolecular interference and is characteristic of the closely packed parallel molecules. Application of

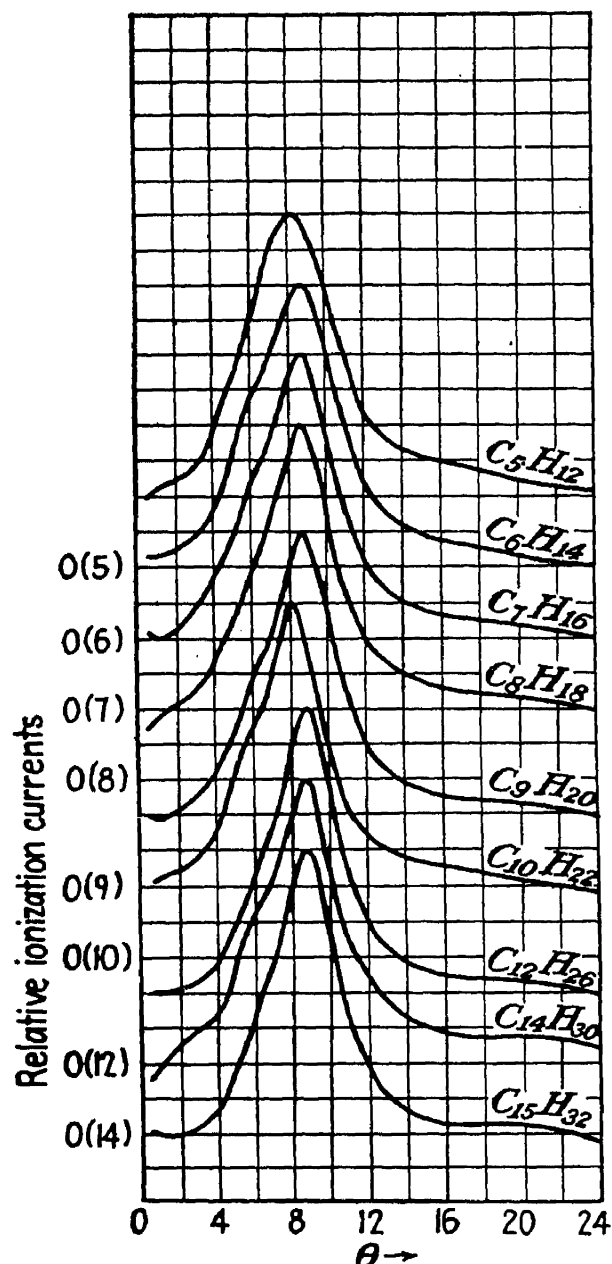


FIG. 22-8.—X-ray scattering curves for normal hydrocarbons, by G. W. Stewart.

The angle  $\theta$  indicated in these figures is equivalent to the angle  $\phi$ , or  $2\theta$ , as used in this book. (Courtesy of *Physical Review*.)

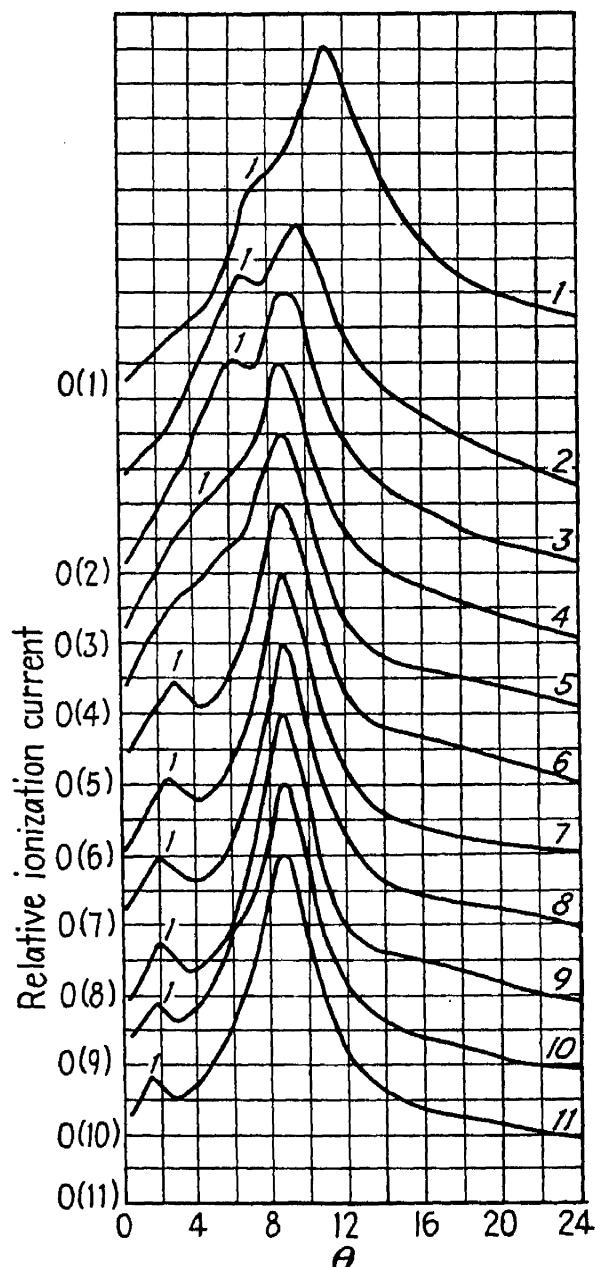


FIG. 22-9.—X-ray scattering curves for fatty acids containing 1 to 11 carbon atoms, by R. M. Morrow.

Keesom's equation to this maximum indicates that the lateral spacing  $s$  between molecules is about 5.7 Å.

The x-ray scattering curves for long-chain polar molecular liquids like the lower members of the fatty acid or normal alcohol series show an additional "inner" peak at a smaller angle  $\phi$  than that of the main  $9^\circ$  peak. This inner peak varies in its angular position systematically

with the number of carbon atoms in the molecule, as shown in Fig. 22-9 obtained by Morrow<sup>1</sup> for the fatty acids  $\text{CH}_2\text{O}_2$  to  $\text{C}_{11}\text{H}_{22}\text{O}_2$ . Warren has applied a sort of "negative Keesom equation" to this. If the polar  $\text{COOH}$  group is placed at the origin, the gap at the opposite end of the chain should cause a deficit of scattering matter at a distance roughly equal to the length of the zigzag chain, especially for the longer member

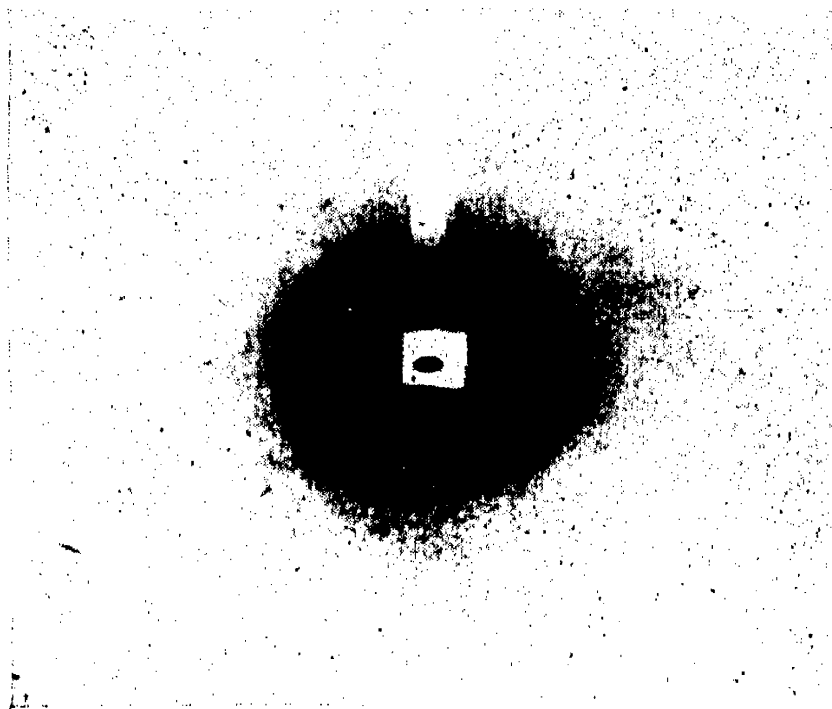


FIG. 22-10.—X-ray pattern of unstretched rubber.

of the series, so that a *minimum* value of  $\sin x/x$  results instead of maximum, as in deriving Keesom's equation. This occurs at  $x = 4.5$  radians; therefore the negative equation is

$$\lambda = \frac{2\pi}{4.5} \times 2s \sin \frac{1}{2} \phi \quad (22-2)$$

from which Warren calculates chain lengths agreeing with those calculated from the molecular weight and the density of the liquid. The curves of Stewart and Morrow in Figs. 22-8 and 22-9 were obtained using an ionization chamber to measure the intensity of the x-ray beam scattered at various angles by a sample in a thin-walled cylindrical glass cell rotated to eliminate wall-thickness variation effects.

The theory of x-ray diffraction in amorphous solids is practically identical with that applying to liquids. The similarity between the appearance of the patterns may be seen by comparing Fig. 22-10 for unstretched rubber, an amorphous solid, with Fig. 22-6 for water. For examples of the application of the Zernike-Prins theory to the determin-

<sup>1</sup> R. M. Morrow, *Phys. Rev.*, **31**, 10 (1928).

<sup>2</sup> B. E. Warren, *Phys. Rev.*, **44**, 969 (1933).

tion of the structure of such commercially important amorphous solids as rubber and glass, the reader is referred to papers by Warren, Biscoe,

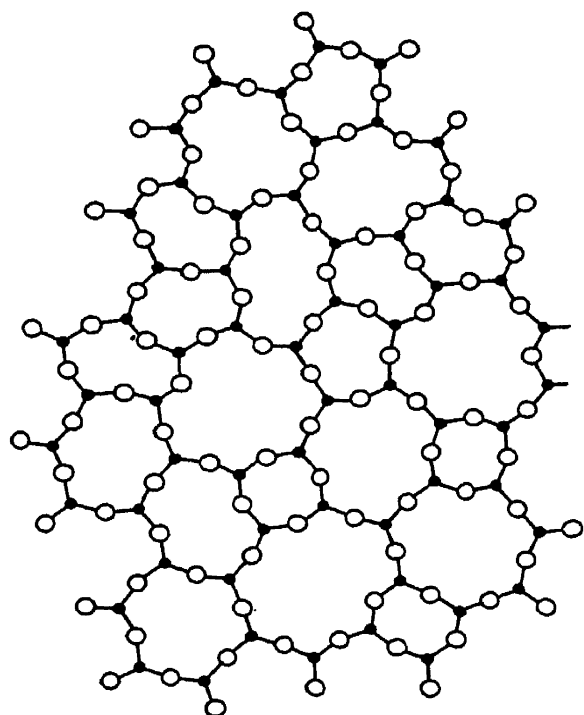


FIG. 22-11.—Two-dimensional representation of random network of  $\text{SiO}_4$  tetrahedra in glass. (By W. H. Zachariasen; courtesy of the American Chemical Society.)

Krutter, and Morningstar<sup>1</sup> and by Zachariasen<sup>2</sup> on glass and by Simard and Warren<sup>3</sup> on unstretched rubber. Figure 22-11 is a diagram by Zachariasen<sup>2</sup> representing the vitreous silica structure characteristic of glass, in two dimensions. In visualizing this structure in three dimensions one should remember that each Si atom (black dot) is tetrahedrally surrounded by four equally distant O atoms (white circles), instead of the three shown. Each O atom is shared between two such tetrahedral groups, as shown. The random nature of the network and the lack of regular geometric repetition are evident. The x-ray scattering curves calculated by Warren on the basis of such a structure, by the Zernike-Prins method, agree closely with those obtained experimentally from micropho-

tometer traces of the diffraction pattern. The pattern was photographed with a vacuum camera, using a rock-salt crystal monochromator.

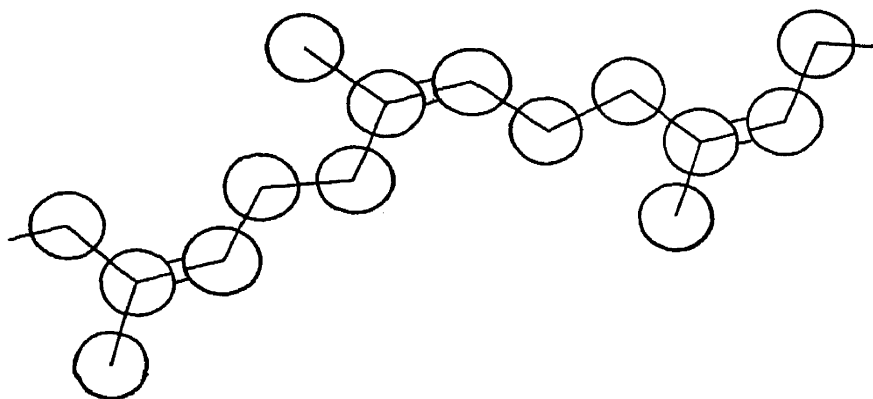


FIG. 22-12.—Molecular structure of rubber. (By G. L. Simard and B. E. Warren; courtesy of the American Chemical Society.)

Little information is to be obtained in this way from the pattern of unstretched rubber, although the scattering curves agree qualitatively

<sup>1</sup> B. E. Warren, *Phys. Rev.*, **45**, 657 (1934); B. E. Warren, H. Krutter, and O. Morningstar, *J. Am. Ceramic Soc.*, **19**, 202 (1936); B. E. Warren and J. Biscoe, *J. Am. Ceramic Soc.*, **21**, 49 (1938); B. E. Warren, *J. Applied Phys.*, **13**, 602 (1942).

<sup>2</sup> W. H. Zachariasen, *J. Am. Chem. Soc.*, **54**, 3841 (1932).

<sup>3</sup> G. L. Simard and B. E. Warren, *J. Am. Chem. Soc.*, **58**, 507 (1936). For patterns of stretched rubber, see Sec. 23-5.



with those to be expected from the generally accepted crooked long-chain structure of rubber, as represented in Fig. 22-12.

### QUESTIONS AND PROBLEMS

1. Is the shape of the scattering curve from a monatomic gas related to (a) the radii of the electronic shells in the atom, (b) the distance between the atoms in the molecule, or (c) the distance between neighboring molecules? Answer the same question for a polyatomic gas. For a monatomic liquid. For a polyatomic liquid. For an amorphous solid.

2. Is the angular location of the principal maximum in the x-ray scattering curve for a liquid related especially to (a), (b), or (c) in question 1? Answer the same question for the minor peaks.

3. What is implied by the term "cybotaxis"? How can the x-ray scattering curve of a gas be distinguished readily from that of a liquid? This difference is due to what physical characteristic of a liquid, not a characteristic of gases?

4. Why are Soller slits more commonly employed for x-ray diffraction work with gases than for solids or liquids? What are the chief modifications of x-ray diffraction technique in passing from solids to liquids and then to gases?

5. Does the intensity of the background scattering increase or decrease with scattering angle  $\phi$ , for gases? For liquids? For solids?

6. Compare the coherent diffuse scattering of x-rays from a crystalline solid with the coherent scattering from a monatomic gas, in terms of the atomic-structure factor.

7. What is the incoherent-scattering function, and how is it related to the electronic-structure factor? Does the former decrease with scattering angle more rapidly or less rapidly than the atomic-structure factor?

8. The x-ray scattering curve of carbon tetrachloride vapor exhibits maxima at  $\phi = 36, 65$ , and  $110^\circ$ . Neglecting the scattering from the carbon as compared with the four Cl atoms, which are supposedly at the four corners of a regular tetrahedron, what is the common Cl—Cl distance if copper  $K_\alpha$  radiation ( $\lambda = 1.54$  A.) is used?  
*Ans. 3.1 A.*

9. In Fig. 22-5 for mercury, the principal peak obviously occurs at about

$$\frac{\sin \theta}{\lambda} = 0.175.$$

Using Keesom's equation, calculate the distance between neighboring mercury atoms. How does your answer check with Fig. 22-7?

10. Assuming that  $R = 1$  in equation (22-11), compare the intensity of the coherent and incoherent components of the x-ray scattering from neon at  $\phi = 35^\circ$  if copper  $K_\alpha$  radiation is used.  
*Ans.  $I_{\text{coh}}$  = about 13 times  $I_{\text{incoh}}$ .*

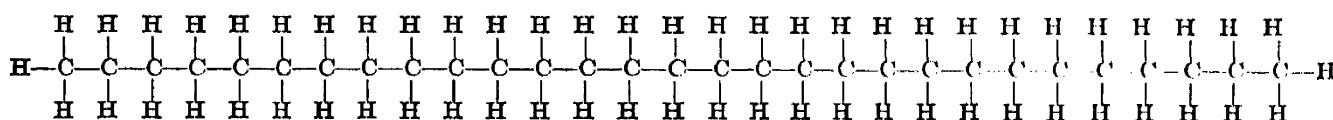
11. Name some commercially important amorphous solids. Describe the atomic arrangement in glass.

## CHAPTER 23

### ADDITIONAL APPLICATIONS OF X-RAY DIFFRACTION

The most important applications of x-ray diffraction have already been mentioned explicitly or suggested implicitly in the earlier chapters. The discussion here is intended to fill in the gaps. This accounts for the fact that the emphasis placed on the various topics in the following discussion is not in proportion to their commercial importance. For example, the sectioning of quartz crystals to make oscillator plates is emphasized more than the application of x-ray diffraction to problems in the textile industry because the former application involves techniques quite different from those previously discussed, whereas the latter does not.

**1. The Long-chain Compounds.** For continuity with the preceding chapter, the results of x-ray studies of the long-chain compounds will be summarized first. Müller has been one of the foremost investigators in this field. His determination of the structure of a single crystal of  $C_{29}H_{60}$  by the rotation method is an outstanding example of the contribution of x-ray diffraction to the advancement of organic chemistry. The organic chemist's structural formula for this compound is



If the molecules have a shape resembling this, one might expect some unusual characteristics in the x-ray reflections from a crystal composed of them. This indeed proved to be the case. One unusual feature was the prominence of the (0 0 60) and (0 0 62) reflections, which would not appear at all for most crystals, of course. By careful analysis of all the data obtained in the patterns, plus knowledge of the density and approximate molecular weight of the material, Müller was able to show<sup>1</sup> that the unit cell contains two pairs of molecules (that is, four), the two pairs lying end to end, the two molecules in each pair lying side by side, and the axes of all four being parallel. The carbon atoms in each molecular chain were shown to lie in a plane, but not in a straight line. Instead, they were arranged in a zigzag line, as indicated schematically in Fig. 23-1. The crystal was found to be orthorhombic with lattice

<sup>1</sup> A. Müller, *Proc. Roy. Soc. (London) A*, **120**, 437 (1928).

constants  $a = 7.45$  Å.,  $b = 4.97$  Å., and  $c = 77.2$  Å. The prominence of the 60th and 62d order (001) reflections already mentioned is then explained as due to a second-order interference reinforcement from the spacing  $s$  in Fig. 23-1. Thus this spacing  $s$  is found to be about 2.54 Å.,

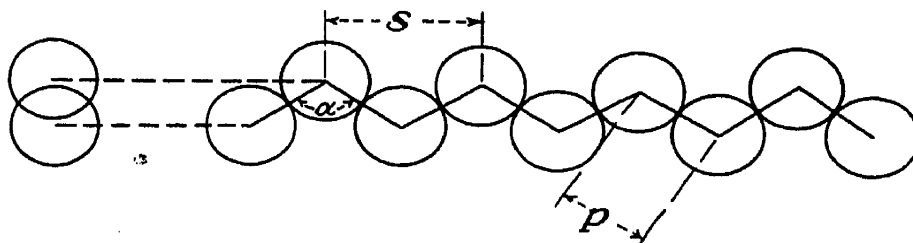


FIG. 23-1.—The zigzag structure of the long-chain hydrocarbons.

since  $c = 77.2$  Å. Some kinship with the diamond structure is now noticed, since the distance  $p$  of closest approach of the carbon atoms in diamond (lattice constant  $a = 3.56$  Å.) is the distance between the atom at 000 and the one at  $\frac{1}{4}\frac{1}{4}\frac{1}{4}$ , or  $3.56 \sqrt{\frac{3}{16}}$ , or 1.54 Å. If this value of  $p$  is taken in Fig. 23-1, then the angle  $\alpha$  is  $2 \sin^{-1} \frac{s}{2p}$ , which comes out

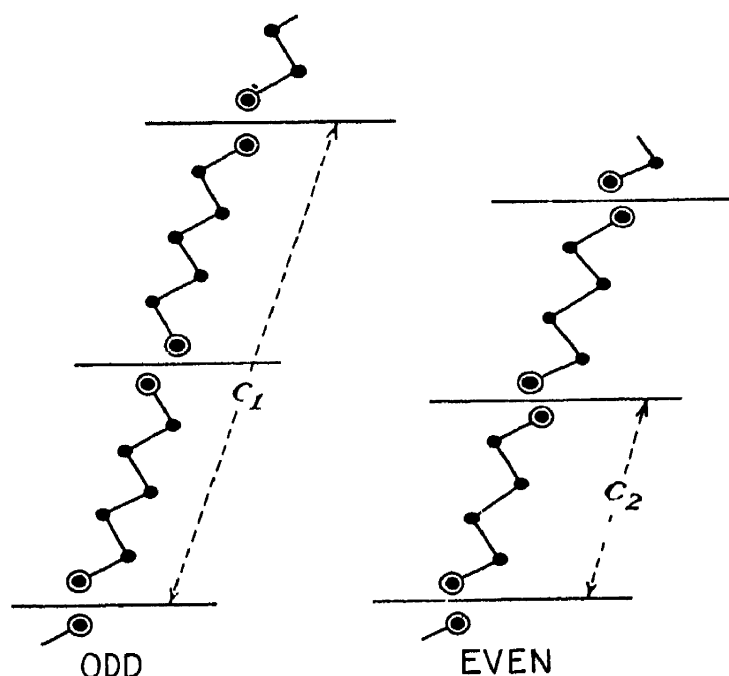


FIG. 23-2.—Diagram of long-chain compounds with odd and even numbers of carbon atoms. (By A. Müller; courtesy of The Royal Society.)

about  $110^\circ$ , agreeing closely with the  $109\frac{1}{2}^\circ$  angle ( $2 \cos^{-1} \sqrt{\frac{1}{3}}$ ) between the tetrahedral bonds joining the carbon atoms in the diamond lattice.

In a later paper, Müller<sup>1</sup> investigated other solid normal hydrocarbons and found that the length ( $c$  dimension) of the unit cell is only one molecule length in the even normal hydrocarbons like  $C_{20}H_{42}$  and  $C_{18}H_{38}$ , whereas it is two molecule lengths in the odd normal hydrocarbons like  $C_{19}H_{40}$ . The reason for this is evident from Müller's diagram repro-

<sup>1</sup> A. Müller, *Proc. Roy. Soc. (London) A*, **124**, 317 (1929).

duced in Fig. 23-2. It is evident that translation of one of the even molecules a distance  $c_2$  along its axis is sufficient to reproduce the lattice, whereas the distance of repetition  $c_1$  for the odd molecule is twice as great in proportion. This difference in structure accounts for the difference between the physical properties of the odd and even members of the normal paraffin series. Figure 23-3 is from a third paper,<sup>1</sup> in which it was found that the  $c$  spacing varies linearly with the number of carbon atoms for the various members of the series as shown, the two lines indicating two slightly different structures. In the  $A$  modification, the molecules are apparently perpendicular to the (001) planes, but in the  $B$  modification they may be inclined slightly, as indicated in Figs. 23-2 and 23-4. In fact, some of the compounds derived from the normal hydrocarbons, such as the solid fatty acids, crystallize with a monoclinic structure and are known to be so inclined.

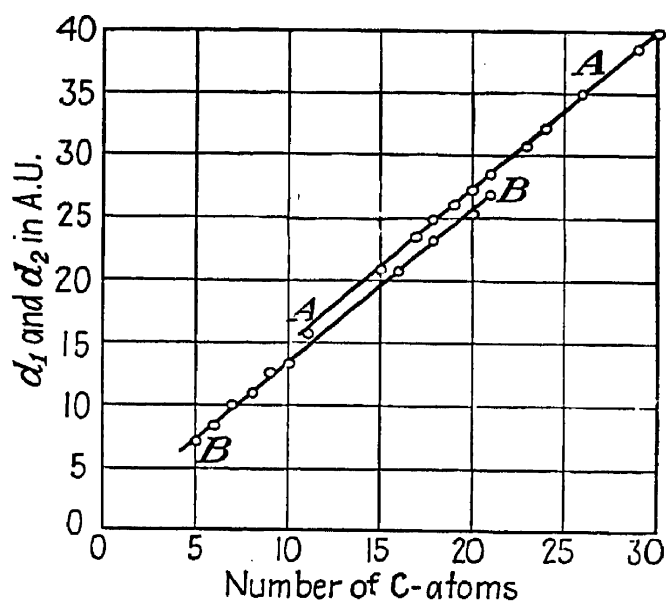


FIG. 23-3.—Plot for normal paraffin hydrocarbons showing the relationship of the two modifications. (By A. Müller; courtesy of The Royal Society.)

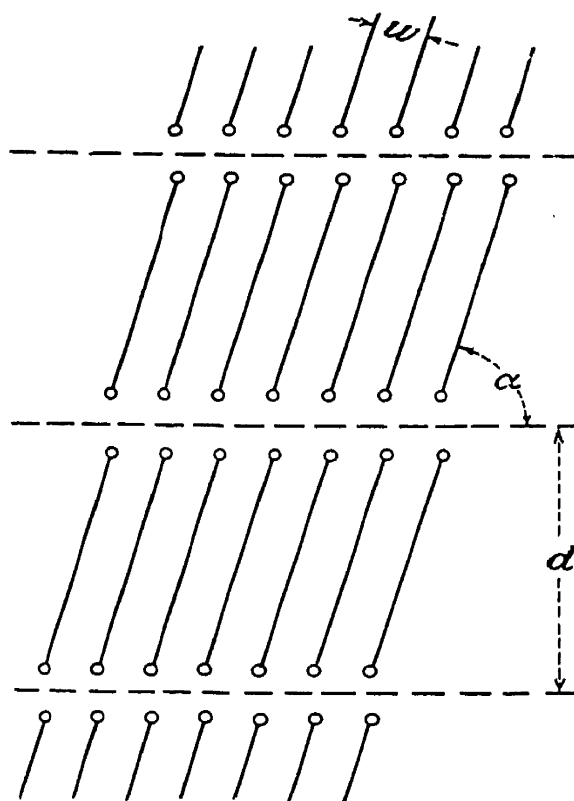


FIG. 23-4.—The crystal structure of some of the solid long-chain hydrocarbons. (After Müller; courtesy of The Royal Society.)

**2. The Contributions of X-ray Diffraction to Chemistry.** The application of x-ray diffraction to chemical analysis has been discussed in Chap. 19. Chapters 16 to 19 and 22 have outlined the methods by which the structure of matter in general and crystalline solids in particular may be deduced by x-ray diffraction. This type of information has been accumulated on such a large scale by so many workers that it has been possible to learn most of the rules nature follows in cementing the particles of the universe together. Of course, many of these rules

<sup>1</sup> A. Müller, *Proc. Roy. Soc., (London) A*, **127**, 417 (1930).

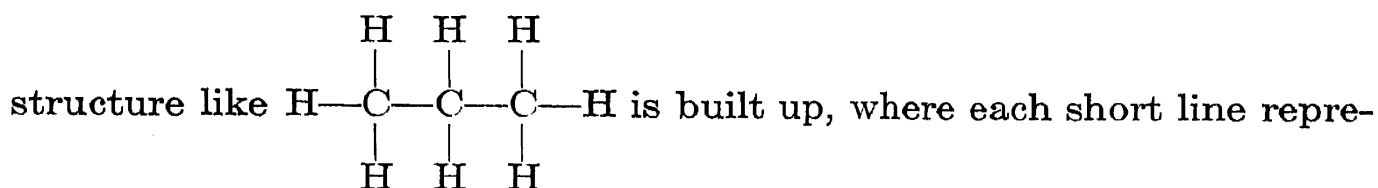
were discovered independently by chemists from experiments and theories not related to x-ray diffraction. Nevertheless, the quantitative data supplied by x-ray diffraction regarding the actual distances separating the atoms and molecules and their geometrical arrangement in various types of chemical compounds have constituted an important factor in the advances of chemistry in the past quarter century. As a result of this correlation, a borderline science known as "crystal chemistry" or "chemical crystallography" has come into existence. A few of its fundamental principles will be outlined here.<sup>1</sup>

It has already been mentioned in Sec. 18-8 that the chemical elements crystallize in a few general types of structure such as face-centered cubic and hexagonal close-packed. It has also been mentioned on page 346 that crystals like NaCl are "ionic," being composed of  $\text{Na}^+$  and  $\text{Cl}^-$  ions, the "binding" forces that hold the structure together being the electrostatic attraction between the oppositely charged ions. The structure is kept from collapsing by a repulsive force between the ions, which increases very abruptly when the ions approach each other to within a certain definite distance. Such an ionic crystal is said to be held together by *ionic bonds* or *heteropolar bonds*. As a consequence of this kind of binding, various types of ions pack into the structure as though they were spheres of a size depending upon their type. Thus "ionic radii" are assigned to various ions, such as  $\text{Na}^+$  (0.98 Å.),  $\text{K}^+$  (1.33 Å.),  $\text{NH}_4^+$  (1.43 Å.),  $\text{Mg}^{++}$  (0.78 Å.),  $\text{Ca}^{++}$  (1.06 Å.),  $\text{Zn}^{++}$  (0.83 Å.),  $\text{Fe}^{+++}$  (0.67 Å.),  $\text{Al}^{+++}$  (0.57 Å.),  $\text{Si}^{++++}$  (0.39 Å.),  $\text{F}^-$  (1.33 Å.),  $\text{Cl}^-$  (1.81 Å.),  $\text{Br}^-$  (1.95 Å.),  $\text{I}^-$  (2.20 Å.),  $\text{O}^{--}$  (1.32 Å.), and  $\text{S}^-$  (1.74 Å.). Therefore, in an ionic crystal, one should expect  $\text{Na}^+$  and  $\text{Cl}^-$  to be separated by a distance of about  $0.98 + 1.81$ , or 2.79 Å., as compared with the 2.81 observed for NaCl, etc. Owing to the non-spherical shape of polyatomic ions like  $\text{CO}_3^{--}$  and  $\text{SO}_4^{--}$ , the concept of ionic radii is not very helpful with them. In an ionic crystal like NaCl, the valence electron of each (neutral) sodium atom becomes attached to the electronic system of a chlorine atom, which would otherwise lack one electron to complete the stable (argon-type) configuration. Aside from this, however, there is no exchange of electrons. Roughly speaking, the atoms merely "come in contact"; they do not "merge."

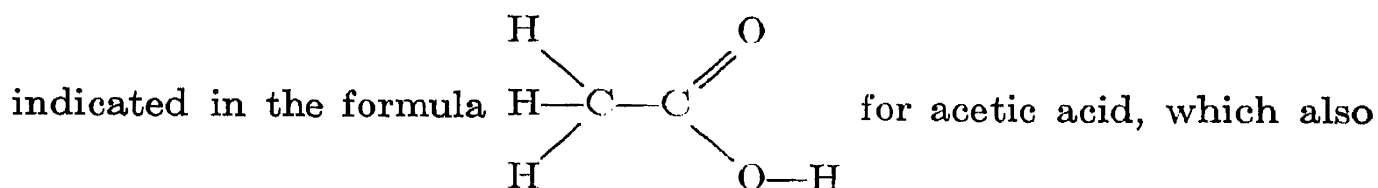
There is an exchange, or sharing, of electrons, however, when molecules like  $\text{H}_2$ ,  $\text{O}_2$ ,  $\text{N}_2$ ,  $\text{CO}_2$ , and  $\text{CCl}_4$  are formed. The electronic orbits interpenetrate, and the atoms are said to be united by a *covalent bond* or a *homopolar bond*. Since the atoms partly "merge," in a sense, the concept of atomic radii no longer applies but there are still definite

<sup>1</sup> For more detailed accounts, see W. H. Bragg and W. L. Bragg, "The Crystalline State," Chap. VII, George Bell & Sons, Ltd., London, 1933, or G. L. Clark, "Applied X-rays," 3rd ed., Chap. XVI, McGraw-Hill Book Company, Inc., New York, 1940; A. F. Wells, *Nature*, **155**, 350 (1945).

interatomic distances, which are found to be nearly the same in related compounds,<sup>1</sup> as has just been discussed for the long-chain hydrocarbons, fatty acids, normal alcohols, and diamond, for example. Different kinds of atoms form homopolar compounds in which they are linked together by a characteristic number of such bonds. Carbon, for example, characteristically links itself to other atoms by means of four such bonds, whereas hydrogen forms only one. Hence, in a long-chain compound, a



sents a homopolar bond. There can be double homopolar bonds, as



illustrates that oxygen characteristically forms two homopolar bonds. There can also be triple bonds, as in acetylene  $\text{H}-\text{C}\equiv\text{C}-\text{H}$ . These valence bonds are governed by the number of valence electrons in the atom, and their attractive force is exerted in certain specific directions about the atom, in contrast to electrostatic attraction. Since hydrogen has only one electron, and that a valence electron, its participation in homopolar linkage means that the entire electronic system participates. Therefore, hydrogen atoms lose their identity as such when they become part of a homopolar molecule, and x-ray diffraction patterns of such compounds yield no information about their location. In such a molecule as normal eicosane, only the straight zigzag character of the carbon atoms can be deduced.

X-ray diffraction has made it possible to establish the typical values of the interatomic distances involved in the formation of various types of homopolar compounds. This, in turn, helps one to make a "scientific guess" as to the possible and probable molecular and crystalline structures of a substance having a known chemical composition but an unknown structure. For example, the C—C distance in diamond<sup>2</sup> is 1.54 Å., and the atoms can be connected by  $109\frac{1}{2}^\circ$  zigzag lines. Likewise, the single-bond C—C distance for most aliphatic compounds has about this same value, and the C atoms in compounds such as cyclohexane as well as normal hexane tend to form a zigzag line; that is, the cyclo-

<sup>1</sup> See, for example, J. L. Kavanau, *J. Chem. Phys.*, **12**, 467 (1944).

<sup>2</sup> See, for example, D. P. Riley, *Nature*, **153**, 587 (1944).

hexane ring has a zigzag pucker, or wrinkle—it is not flat. On the other hand, the single-bond C—C distance in graphite is 1.42 Å., and the atoms form flat regular hexagons. This same C—C distance and flat hexagonal structure persist in aromatic compounds like benzene and hexamethylbenzene. Double bonding brings the C atoms closer together, the usual distance being about 1.35 Å., and only 1.2 Å. separates the triply bonded C atoms in acetylene. Incidentally, the demarcation between single and double bonds is not always sharp. There is said to be “resonance” between the bonds of some atoms,<sup>1</sup> which makes it impossible to say definitely that the bond is single or double.

In Sec. 1, the existence of  $C_{29}H_{60}$  crystals having a unit cell containing four molecules was mentioned. These molecules are certainly not ionic; on the other hand, all their covalent bonds are satisfied within themselves. This being the case, what holds the molecules together as a crystal? The answer is “van der Waals binding.” Van der Waals bonds are weak attractive forces that are exerted only between atoms or molecules practically in contact with each other. The inert gases (argon, neon, krypton, etc.) have no valence electrons and hence are subject only to van der Waals binding, which causes them to crystallize at extremely low temperatures only.

Finally, there are the metals and their alloys. The general description of these as an assemblage of positive ions, fixed in the case of solids, and permeated by a “gas” of free electrons was given in Chapter 2 (pages 10 to 12). The forces that hold the metallic ions in place and the metal together are called “metallic binding,” and the highly charged free-electron gas plays an essential role in this binding. Metallic binding, like ionic binding, does not limit the number of atoms that can be bound to another, nor are the bonds directional. However, metallic binding is exerted between identical or similar ions in metals and alloys, as contrasted with ionic binding between different, oppositely charged ions. The tendency of the metal ions to pack together like spheres is indicated by the large number that crystallize with face-centered cubic, hexagonal close-packed, and body-centered cubic structures, and the concept of atomic radii is again helpful. Typical radii are about 1.4 Å. for aluminum, gold, and silver and 1.25 Å. for iron and copper.

The three most important types of binding just described are ionic, homopolar, and metallic. Broadly speaking, the study of matter bound in these three different ways corresponds, respectively, to inorganic chemistry, organic chemistry, and metallurgy. The divisions between the three types of binding and between the three sciences are not sharp; that is, there are elements and compounds that are difficult to classify as definitely “metallic” or “nonmetallic” or definitely “organic” or

<sup>1</sup> See, for example, E. Warhurst, *Trans. Faraday Soc.*, **40**, 26 (1944).

"inorganic." Likewise, there are mixed covalent-ionic bonds and covalent-metallic bonds.

**3. Metals and Alloys.** Bragg has pointed out that the mode of crystallization of elements with metallic properties can be correlated in a general way with their positions in the periodic table (Appendix, Table VII) by dividing them into three groups, as follows:

A. ALKALI AND ALKALINE-EARTH ELEMENTS \*

3Li 4Be	11Na 12Mg	19K 20Ca	37Rb 38Sr	55Cs 56Ba
------------	--------------	-------------	--------------	--------------

B. TRANSITION ELEMENTS

21Sc 39Y 57La rare earths	22Ti 40Zr 72Hf	23V 41Nb 73Ta	24Cr 42Mo 74W	25Mn 43Mn 75Re	26Fe 44Ru 76Os	27Co 45Rh 77Ir	28Ni 46Pd 78Pt	29Cu 47Ag 79Au
------------------------------------	----------------------	---------------------	---------------------	----------------------	----------------------	----------------------	----------------------	----------------------

C. ELEMENTS OF B SUBPERIODS

30Zn 48Cd 80Hg	(13Al) 31Ga 49In 81Tl	(14Si) 32Ge 50Sn 82Pb	33As 51Sb 83Bi	34Se 52Te 84Po
----------------------	--------------------------------	--------------------------------	----------------------	----------------------

\* Adapted from W. H. Bragg and W. L. Bragg, "The Crystalline State," (1933), by permission of George Bell & Sons, Ltd., London, and the Macmillan Company, New York.

The elements in groups *A* and *B* tend to form typical metallic bonds and crystallize in one of the simple structures for packed spheres; the tendency toward homopolar binding, if present, is overcome by a stronger tendency toward metallic binding. In group *C*, however, the tendency toward homopolar binding is stronger, so that the atoms of these elements show a tendency to link themselves with certain of their neighbors more firmly than others. This tendency increases from left to right in the Mendelyev form of the periodic table until nonmetallic elements like the halogens, sulfur, and phosphorus are reached, in which the tendency toward metallic binding, if present, is overcome by a stronger tendency toward homopolar binding.

The structures of alloys have already been discussed briefly on pages 435 to 436. Figure 23-5 shows a series of x-ray diffraction patterns obtained by Westgren<sup>1</sup> for brasses (copper-zinc alloys) of various compositions. He used a series of three Seemann-Bohlin cameras constructed by his coworker G. Phragmen for their extensive studies of various alloys. For the low-order (small- $\theta$ ) Bragg reflections, a camera of 85 mm. radius was used. For the high-order reflections, a camera of 42 mm. radius was

<sup>1</sup> See, for example, A. F. Westgren, *Trans. A.I.M.M.E.*, **93**, 13 (1931).



used. For the intermediate range, an intermediate 48-mm. camera was used. The alloys were prepared by melting pure metals together in known proportions in small evacuated quartz or glass tubes; they were then reduced to powder by filing or crushing. The resulting microstrains would result in broad lines. To secure the desired strain-free equilibrium structure, the powder was heated in an evacuated glass tube to the

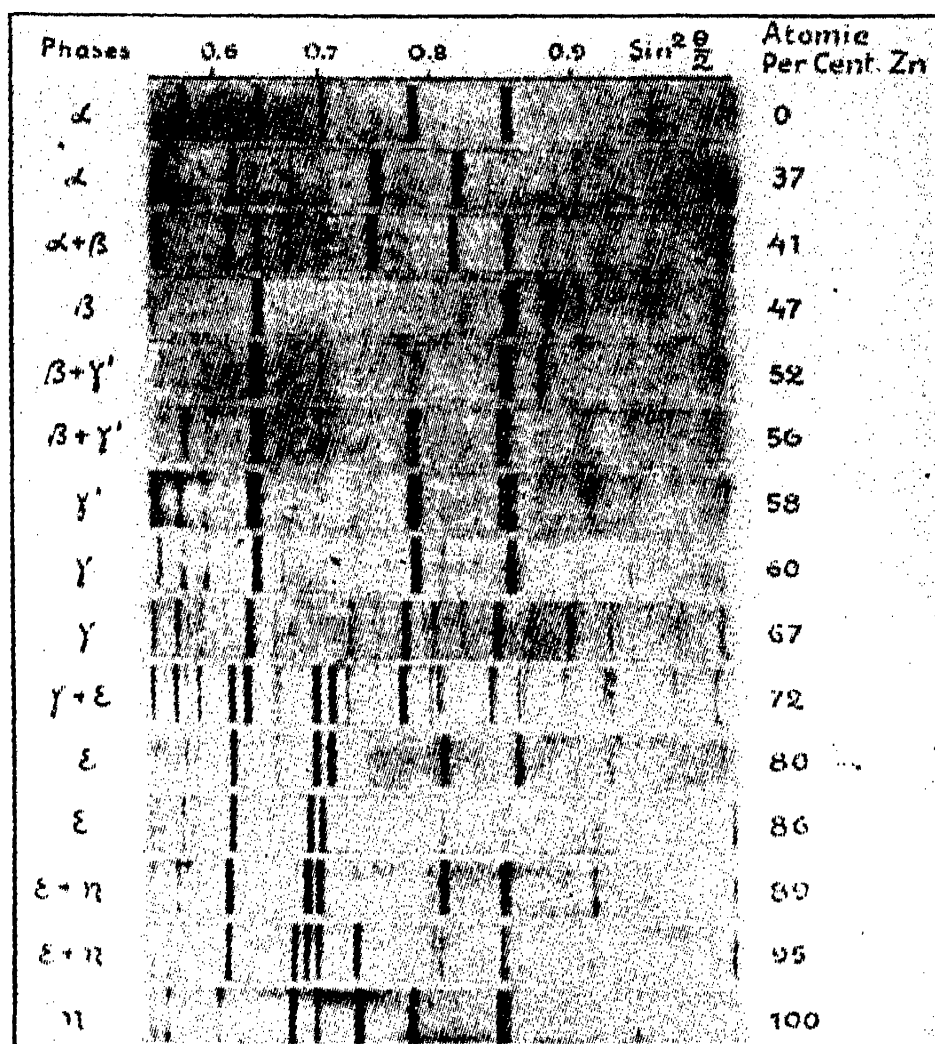


FIG. 23-5.—Powder patterns of copper-zinc alloys, taken with Phragmen type of Seemann-Bohlin camera, by A. F. Westgren. (Courtesy of the American Institute of Mining and Metallurgical Engineers.)

recrystallization temperature for a few minutes or longer until the equilibrium structure at that temperature was attained. To fix it, the hot glass tube was then quenched in water. This shattered it, and the powdered metal was quickly cooled in the water. The powder was then dried and stuck to a piece of paper with an adhesive like Canada balsam. This paper was pressed against the concave cylindrical surface of the camera to form the specimen. A comparison specimen of sodium chloride was also mounted so that its pattern would appear on the same film beside that of the alloy for accurate calibration of the spacings.

In Fig. 23-5, the top pattern is for pure copper. The second one

is for 63 per cent copper—37 per cent zinc alpha brass. It is seen that the lines in the pattern have merely shifted towards smaller values of  $\theta$ . Westgren uses  $\theta$  as  $\phi$  has been used in this book; it is twice the Bragg angle. This shift indicates that the face-centered cubic structure of the copper still persists, the cubes merely expanding in size as zinc atoms are substituted for copper atoms in the lattice. This has been called the “alpha structure” by Westgren; hence the name “alpha-brass.” At 41 per cent zinc, however, a new set of lines appears, as seen in the third pattern. This indicates that the brass is now a mixture of alpha-brass with a new type of material called “beta-brass.” At 47 per cent zinc (fourth pattern), the old alpha-brass lines have disappeared and only the new beta-brass lines are left, indicating that the sample is now pure beta-brass. Analysis of the pattern shows that this is a body-centered cubic structure in which the corner atoms are copper and the center atoms zinc, or vice versa. Or one could say that the structure consists of two simple cubic lattices centering each other, one of them holding mainly copper atoms, the other mainly zinc atoms. This is what is known as an “intermetallic compound,” with a composition corresponding to CuZn, since there are approximately equal numbers of Cu and Zn atoms arranged with a unit-cell configuration like CsCl (cesium chloride): Cs—000; Cl— $\frac{1}{2}\frac{1}{2}\frac{1}{2}$ . The unit cell of CuZn has a lattice constant  $a$  of 2.945 Å. Just as in CsCl, there is no “molecule of CuZn” formed. Furthermore, the description of the structure as “two lattices . . . , one holding *mainly* copper atoms, the other *mainly* zinc atoms” indicates an inexactness which is characteristic of these intermetallic compounds, for the relation of the two groups of ions to the free electron gas with which they are mutually saturated is a factor just as important as the relation between the two groups of ions. There is no such inexactness in an ionic compound like CsCl, where the opposite charges must be perfectly balanced throughout.

To return to Fig. 23-5, the fifth pattern for 52 per cent zinc shows the presence of a new set of lines due to another intermetallic compound that Westgren calls  $\gamma'$ . By the time 58 per cent zinc is reached, the structure is entirely  $\gamma'$ , the beta lines having vanished. This  $\gamma'$  structure is a slight modification of the next structure to appear, namely,  $\gamma$ , which is the equilibrium structure at 60 to 67 per cent zinc. The beta and gamma structures observed here for brass are of general interest, for numerous other alloys such as copper-aluminum, platinum-zinc, and silver-cadmium form the same structures. As already mentioned on page 436, they are called “superstructures” or “superlattices” in alloy systems.<sup>1</sup> The structure of this gamma type of superlattice has been

<sup>1</sup> For details, see F. C. Nix, *J. Applied Phys.*, **8**, 783 (1937).

analyzed from x-ray patterns by Bradley and Thewlis,<sup>1</sup> using gamma-brass. They found that it is a cubic structure with a lattice constant  $a = 8.9$  Å. The unit cell contains 20 Cu atoms and 32 Zn atoms, the formula of the intermetallic compound being  $\text{Cu}_5\text{Zn}_8$ . The space group is  $T_d^3$ . Figure 23-6(b) shows the structure of the unit cell as Bradley and Thewlis determined it. The interatomic distances are about 2.6 Å., which is about the value for copper or zinc. Gamma Ag-Zn ( $\text{Ag}_5\text{Zn}_8$ ) and gamma Au-Zn ( $\text{Au}_5\text{Zn}_8$ ) have a similar structure.

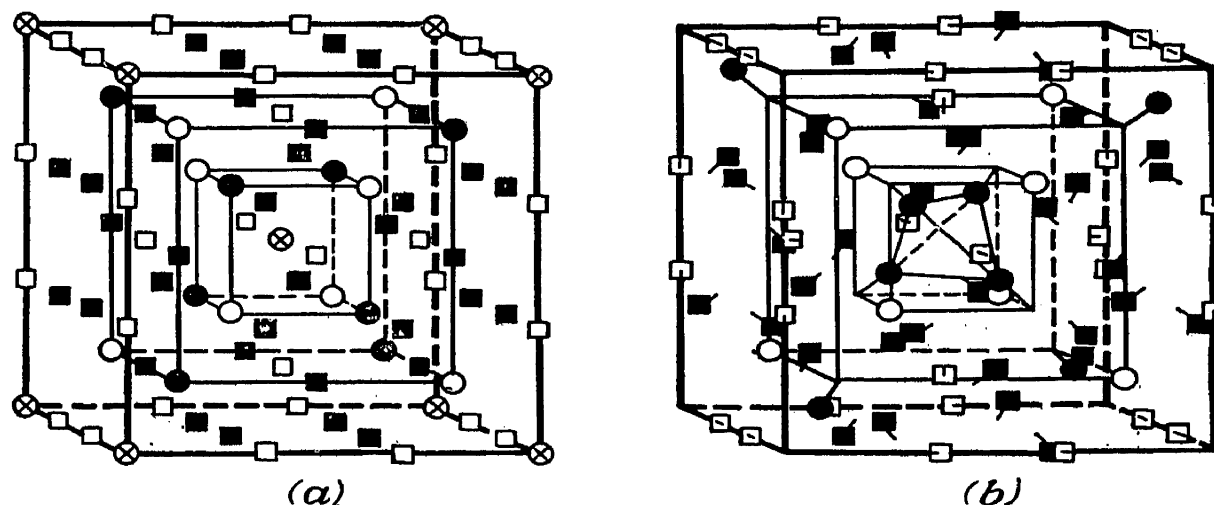


FIG. 23-6.—(a) The derivation of the structure of gamma brass from a simple cube-centered arrangement of atoms. (b) Structure of gamma brass. (By A. J. Bradley and J. Thewlis; courtesy of The Royal Society.)

Metallurgists refer to the various crystal forms existing in an alloy system as “phases,” and the transformations between the various phases are represented graphically as a function of temperature and composition in “phase diagrams.” These diagrams are of great importance in the heat-treatment of metals and alloys, including steels. The chief source of information for the plotting of phase diagrams consists of x-ray diffraction data.

In general, the term “phase” is associated with gross changes in crystal structure, whereas the term “superlattice” or “superstructure” refers to a highly ordered atomic arrangement in that phase. For example, the body-centered beta-brass structure already discussed is one of the phases of the copper-zinc alloy system. When the atoms are ordered so that all or nearly all of the cube corners are occupied by Cu and the cube centers by Zn, or vice versa, then one has a superlattice, or superstructure, this type of highly ordered beta brass being called  $\beta$  brass by some authors.<sup>2</sup> The  $\beta$  to  $\beta'$  transformation in brass is therefore not a change in phase, being merely a rearrangement of the atoms without a change in lattice type.

<sup>1</sup> A. J. Bradley and J. Thewlis, *Proc. Roy. Soc. (London) A*, **112**, 678 (1926).

<sup>2</sup> For example, F. W. Jones and C. Sykes, *Proc. Roy. Soc. (London) A*, **161**, 440 (1937).

In Fig. 23-5, it is seen that 72 per cent zinc–28 per cent copper is a mixture of gamma and epsilon brass, while 80 to 86 per cent zinc is epsilon brass, with a composition corresponding to  $\text{CuZn}_3$ . This epsilon brass has a hexagonal structure with  $a$  = about 2.75 Å. and  $c$  = about 4.29 Å., the axial ratio  $c/a = 1.56$  being nearly the ideal  $2\sqrt{\frac{2}{3}} = 1.63$  characteristic of close packing. In progressing toward pure zinc, this axial ratio gradually increases as the copper atoms disappear from the lattice until, for pure zinc, the hexagonal structure with a  $c/a$  ratio 1.86 is attained. This departure of zinc from close packing is attributable to its slight tendency toward homopolar binding, since it is one of the  $C$  group of elements listed on page 520. For zinc,  $a = 2.30$  and  $c = 4.92$  Å.

W. Hume-Rothery has discovered the law governing the formation of the 52-atom gamma structure just described. This gamma structure can be formed only when the ratio of the number of valence electrons to the number of atoms present is  $21/13$ . The valence is judged in this case from the group to which the element belongs in the periodic table, being 1 for Cu, Ag, Au; 2 for Zn, Cd; 3 for Al; 4 for Sn; and zero for Fe, Co, Pt, etc. Examples of gamma superstructure and the way in which Hume-Rothery's law applies to them follow:

Alloy	Atoms present, $A$	Total valence, $V$	$V/A$
$\text{Cu}_5\text{Zn}_8$	$5 + 8 = 13$	$5 + (8 \times 2) = 21$	$21/13$
$\text{Cu}_9\text{Al}_4$	$9 + 4 = 13$	$9 + (4 \times 3) = 21$	$21/13$
$\text{Cu}_{31}\text{Sn}_8$	$31 + 8 = 39$	$31 + (8 \times 4) = 63$	$21/13$
$\text{Fe}_5\text{Zn}_{21}$	$5 + 21 = 26$	$0 + (21 \times 2) = 42$	$21/13$
$\text{Pt}_5\text{Zn}_{21}$	$5 + 21 = 26$	$0 + (21 \times 2) = 42$	$21/13$

Similar laws apply to the body-centered cubic beta superstructure described above for beta brass.

Alloy	Atoms present, $A$	Total valence, $V$	$V/A$
AgCd	$1 + 1 = 2$	$1 + 2 = 3$	$3/2$
CuZn	$1 + 1 = 2$	$1 + 2 = 3$	$3/2$
$\text{Cu}_3\text{Al}$	$3 + 1 = 4$	$3 + 3 = 6$	$3/2$
$\text{Cu}_5\text{Sn}$	$5 + 1 = 6$	$5 + 4 = 9$	$3/2$
FeAl	$1 + 1 = 2$	$0 + 3 = 3$	$3/2$

In other alloys, a  $V/A$  ratio of  $3/2$  results in a complex cubic superstructure containing 20 atoms per unit cell, like beta manganese. Examples are as follows:

Alloy	Atoms present, $A$	Total valence, $V$	$V/A$
$\text{Ag}_3\text{Al}$	$3 + 1 = 4$	$3 + 3 = 6$	$3/2$
$\text{Cu}_5\text{Si}$	$5 + 1 = 6$	$5 + 4 = 9$	$3/2$
$\text{CoZn}_3$	$1 + 3 = 4$	$0 + 6 = 6$	$3/2$

The hexagonal epsilon superlattice illustrated by epsilon-brass is characterized by a  $V/A$  ratio of  $7/4$ .

The substitutional solid solutions such as alpha brass and the superstructures such as CuZn having been described, attention may now be turned to interstitial solid solutions and interstitial compounds. When carbon (up to 8 per cent of the atoms present) is dissolved in molten iron and cooled slowly to room temperature, the resulting material consists mostly of body-centered alpha iron with carbon atoms distributed more or less uniformly through the interstices between the iron atoms, in contrast to the case of alpha-brass, where the zinc atoms displace some of the copper atoms and occupy their regular positions in the lattice. This solution of carbon (up to 8 per cent) dissolved in alpha iron (page 418) is an example of an interstitial solid solution (page 435). It is the most important constituent of steel.

Metals in group  $B$  (transition elements, page 520) form compounds with nitrogen, carbon, boron, and hydrogen, which are metallic in character. Many of the simpler ones are so-called "interstitial compounds." An example is the commercially important tungsten carbide used for high-speed cutting tools. Metals in group  $A$  form nonmetallic compounds with these elements (for example, calcium carbide). Another example of an interstitial compound between nitrogen and a group  $B$  metal is  $\text{Fe}_4\text{N}$ . This compound is formed in the case-hardening process known as "nitriding" steel. The steel, at a temperature of 500 to  $540^\circ\text{C}$ ., is exposed to an atmosphere of ammonia for several hours. Some of the ammonia decomposes, and the nitrogen combines with the iron and also with alloying metals such as aluminum and chromium, if present in the steel. The resulting  $\text{Fe}_4\text{N}$  has a face-centered cubic structure with a lattice constant  $a$  of about 3.77 Å. The iron atoms occupy the usual positions in a face-centered cubic lattice, and the nitrogen atoms take up a systematic position within it, perhaps one at the center of most of the unit cells, for example. This elasticity in range of composition again distinguishes these metallic compounds from compounds of the ionic or molecular type. The presence of the nitrogen expands the lattice somewhat. For example, ordinary body-centered cubic alpha iron with two atoms per cell and a lattice constant  $a = 2.861$  Å. has an atomic volume of  $2.861^3/2$ , or 12 Å.<sup>3</sup>/atom, whereas the iron atoms in the face-centered cubic  $\text{Fe}_4\text{N}$  lattice with four atoms per cell

and  $a = 3.77$  Å. have an atomic volume of  $3.77^3/4$ , or  $13.3$  Å.<sup>3</sup>/atom. Figure 23-7 is a pattern of nitrided steel, the rings marked Fe being due to ordinary alpha iron and those marked N to  $\text{Fe}_4\text{N}$ , which is mixed with it in fairly large proportion.

Another important constituent of steel is the interstitial compound  $\text{Fe}_3\text{C}$  known as "cementite," having an orthorhombic structure with four atoms per cell and lattice constants  $a = 4.518$ ,  $b = 5.069$ , and  $c = 6.736$  Å. In general, steel is a complex mixture of various "aggre-

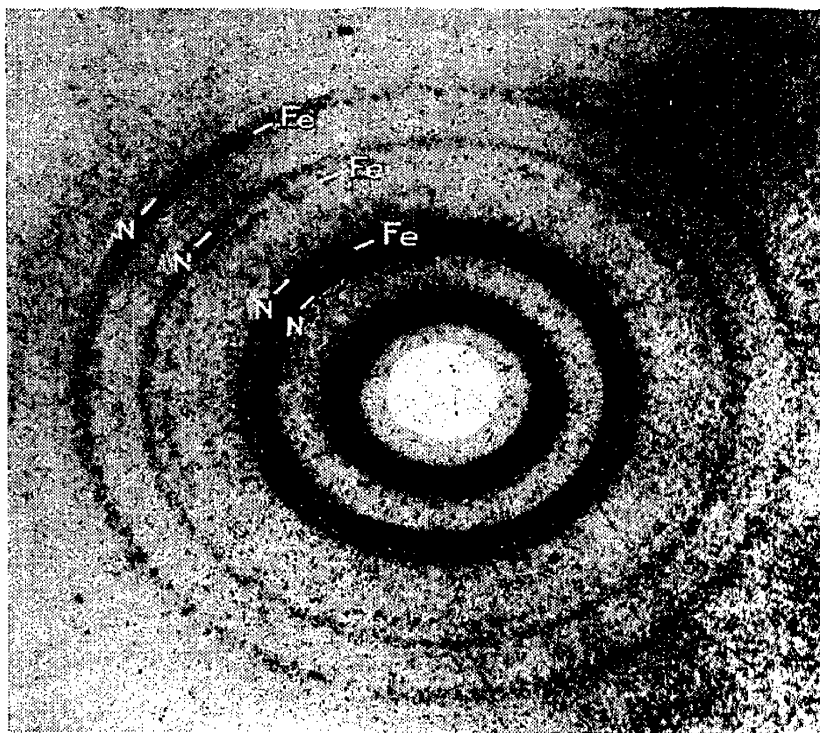


FIG. 23-7.—Pattern of nitrided steel. Rings marked "N" are due to  $\text{Fe}_4\text{N}$ .

gate constituents" that the metallurgists have named "ferrite," "austenite," "cementite," "martensite," "pearlite," "troostite," "sorbite," etc. Cementite is orthorhombic  $\text{Fe}_3\text{C}$ , as already stated. Austenite is a solid solution of carbon in (face-centered cubic) gamma iron<sup>1</sup> (for the meaning of the terms "alpha," "beta," "gamma," and "delta iron," see page 418). Ferrite is a solid solution of carbon in alpha or delta iron. Martensite is the product of the low-temperature transformation of austenite and is probably composed of ferrite. It often contains retained austenite. Pearlite is the lamellar aggregate of ferrite and carbide from direct transformation of austenite at temperatures above  $500^\circ\text{C}$ . For further details, the reader may consult an article by Vilella, Guellich, and Bain.<sup>2</sup> X-ray diffraction methods have been used to determine the amount of retained austenite in steel.<sup>3</sup>

<sup>1</sup> For details, see N. J. Petch, *Science Abstracts A-45*, No. 1340 (1942).

<sup>2</sup> J. R. Vilella, G. E. Guellich, and E. C. Bain, *Trans. Am. Soc. Metals*, **24**, 225 (1936).

<sup>3</sup> See F. S. Gardner, M. Cohen, and D. P. Anita, *Trans. A.I.M.M.E.*, **154**, 306 (1943).

Bragg<sup>1</sup> has proposed a theory of the strength of metals based on x-ray diffraction. It relates the elastic limit to the average size of the mosaic fragments, or "crystallites," resulting from grain fracture. It is indicated that the yield point of a metal can be calculated without making any assumptions about the way the glide is initiated or travels

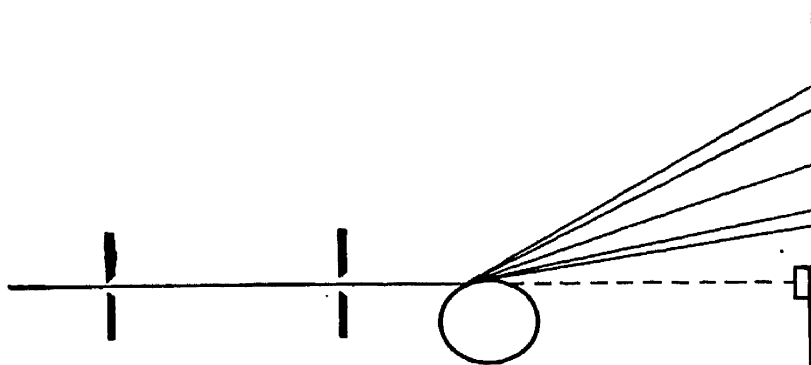


FIG. 23-8.—Method of obtaining powder pattern from surface of round object.

in a single crystal. It is known that the forces required to cleave a metal crystal are small, but further assumptions regarding them are unnecessary

The numerous applications of x-ray diffraction to a wide variety of metallurgical problems have been implicitly, if not explicitly, pointed out in earlier chapters. One type of transmission pattern that is very

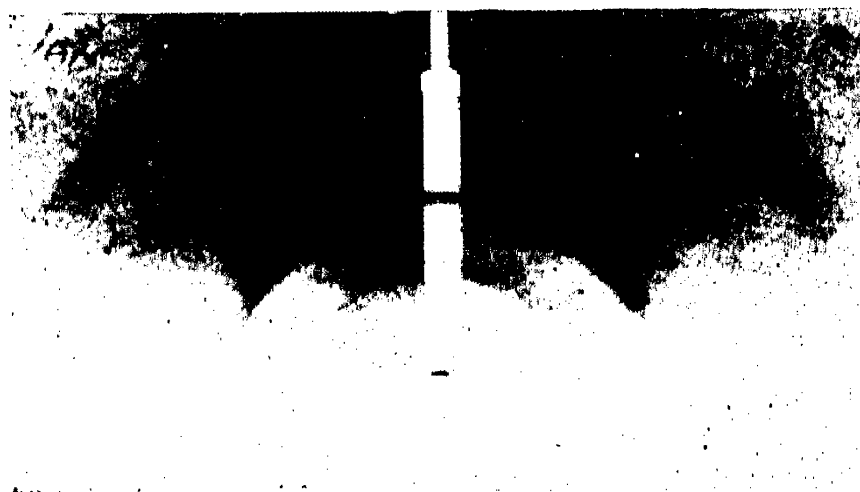


FIG. 23-9. Powder pattern of steel journal, obtained as in Fig. 23-8.

commonly employed in industrial work and that has not received its due attention in the discussion thus far is the grazing-incidence type of pattern. This is useful as a nondestructive method of studying the surface texture of any solid crystalline object such as a bearing journal for example, as illustrated schematically in Fig. 23-8. In this way, one can quickly and easily obtain information regarding grain size, orientation and chemical composition of the surface layer of such parts. Figure 23-9 is a pattern of a steel bearing journal obtained by this technique

<sup>1</sup> W. L. Bragg, *Nature*, **149**, 511 (1942).

The grain size appears to be about  $10^{-3}$  mm., and no preferential orientation is revealed in the radial planes.

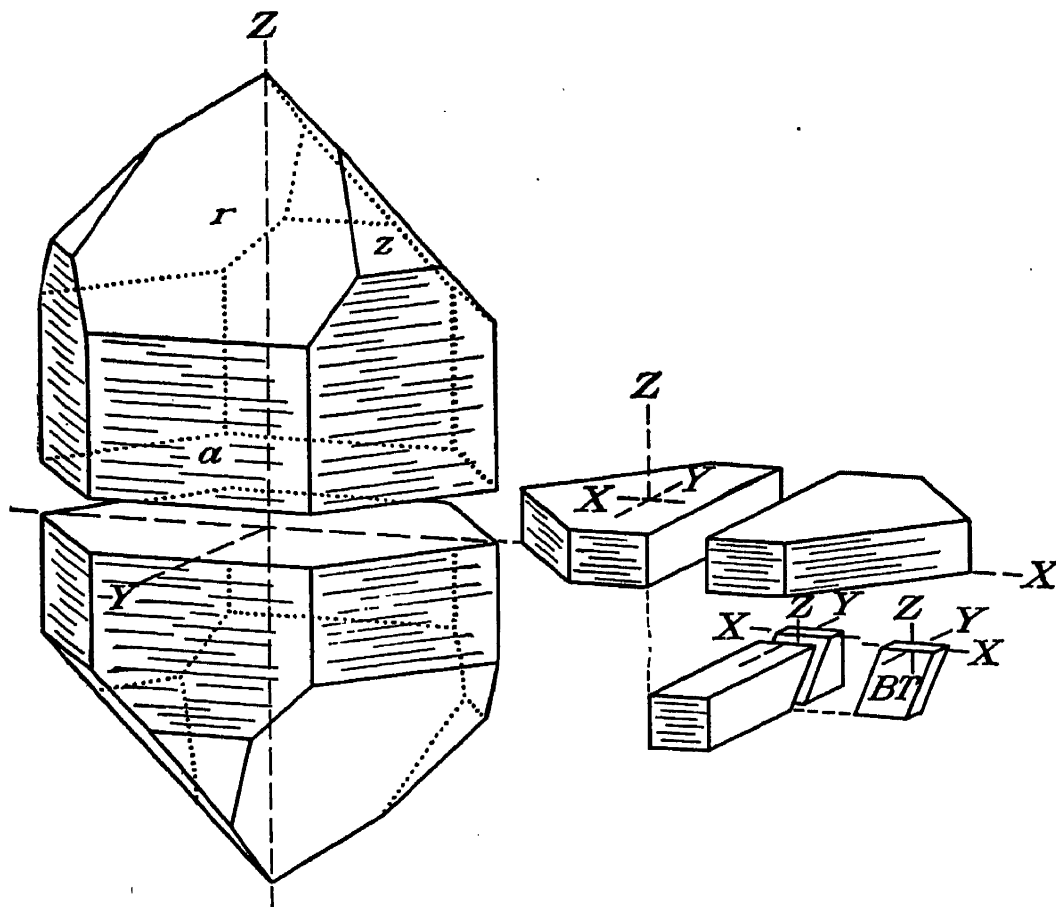


FIG. 23-10.—Z-section method of cutting piezoelectric quartz oscillator plates. (Reprinted by permission of *Electronic Industries*.)

#### 4. Orientation of Quartz Crystals in Cutting Piezoelectric Oscillator

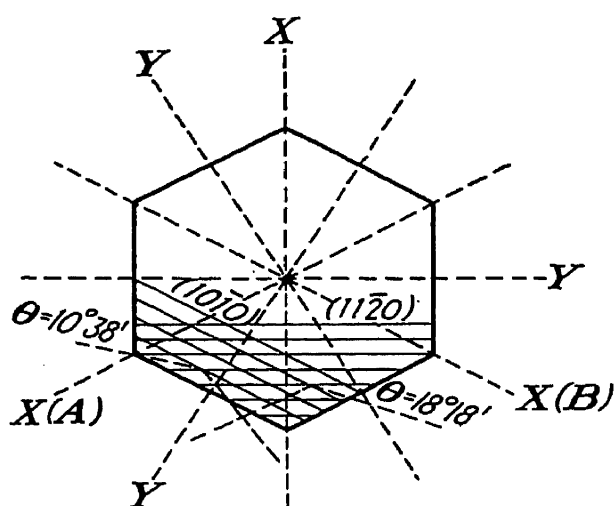


FIG. 23-11.—Transverse section of quartz crystal showing relation between A and B and X and Y axes. (R. Setty; reprinted by permission of *Electronic Industries*.)

**Plates.** The heavy demand for special electronic equipment resulting from the war has caused an unprecedented demand for quartz piezoelectric oscillator plates of various types. These are sawed out of quartz crystals, but the saw cuts must be made to coincide with certain crystallographic planes, such as (0001) and (1000). Since a large percentage of the crystalline quartz available as raw material for this purpose is unfaced or only partly faced (that is, the external surface does not consist of cleavage planes), the problem of orienting the crystal to make the desired saw cuts has assumed considerable commercial importance. This



problem is ideal for the application of x-ray diffraction. The Technical Staff of the U.S. Army Signal Corps has strongly recommended that x-ray diffraction equipment be purchased by any manufacturer planning to make such oscillator plates; in fact, such equipment is as essential as the saw or lapping machine.

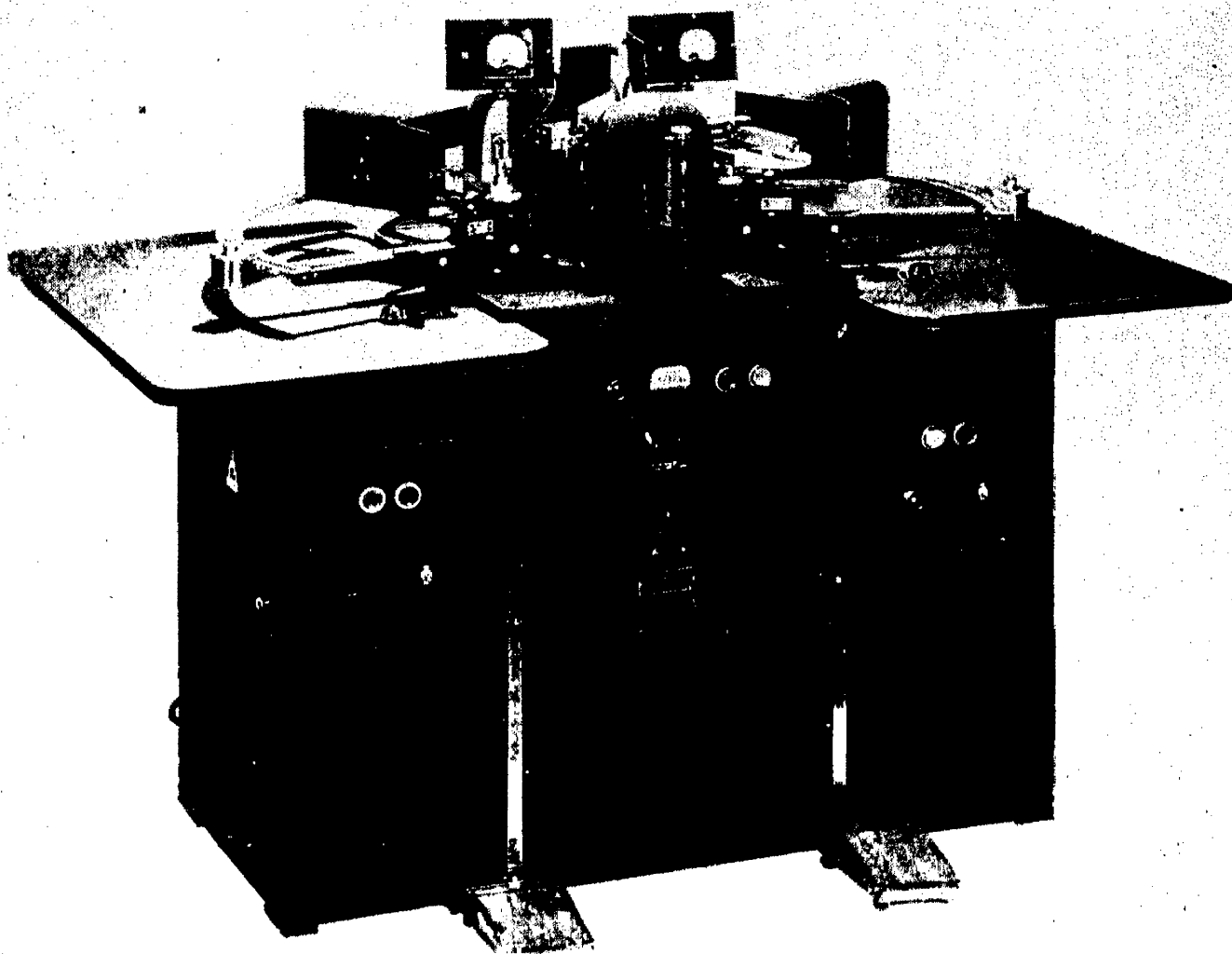


FIG. 23-12.—Geiger-Müller counter x-ray unit for crystal orientation. Left, goniometer. Right, natural-face orientation table. (Courtesy of North American Philips Co., Inc.)

Figure 23-10 is a diagram showing the “Z-section method” of cutting oscillator plates from a quartz crystal. The crystal is drawn with its external surface showing the various cleavage planes, but the actual quartz “boulders” to be cut may show none of these planes externally. It is seen that  $X$  and  $Z$  represent the  $A$  and  $C$  axes in the notation used in this book (Chap. 14).  $Y$  is not a crystallographic axis but the  $[\bar{1}20]$  zone axis. This is made clearer in Fig. 23-11, which represents a section perpendicular to the  $C$  or  $Z$  axis. The  $X$  axes, according to the piezoelectric notation, are seen to represent the  $A$  and  $B$  and the third unnamed axis corresponding to the third index in the Miller-Bravais notation. The  $Y$  axes, on the other hand, are the  $[210]$ ,  $[120]$ ,  $[\bar{2}10]$ ,

etc., zone axes. Since copper  $K_\alpha$  radiation is ordinarily used for this work, the Bragg angles  $\theta = 10^\circ 38'$  and  $\theta = 18^\circ 18'$  have been indicated for the  $(10\bar{1}0)$  and  $(11\bar{2}0)$  reflections, as shown. These values can readily be verified, since the lattice constants of quartz ( $a = 4.903$  A.,  $c = 5.393$  A.), the copper  $K_\alpha$  wave length (1.54 A.), and equation (16-20) are known.

Figure 23-12 illustrates the Philips equipment designed for this work. The copper  $K_\alpha$  radiation from the shielded tube in the center passes through collimating slits to either of two goniometers, each provided with a crystal turntable and swiveling Geiger counter, like a Bragg spectrometer. The pulses are amplified by vacuum-tube amplifiers and read on the meters shown. The angular position of both the crystal table and the ionization chambers is read on the scale, which need not extend more than about  $50$  or  $60^\circ$ , for the desired setting can never be more than  $15^\circ$  from a  $\{10\bar{1}0\}$  or  $\{11\bar{2}0\}$  plane, as seen in Fig. 23-11. The correct angular setting of the crystal corresponding to the desired Bragg reflection can be determined within 1 min. of arc and 1 min. of time from the maximum meter reading corresponding to a Bragg reflection.

In the  $Z$ -section method, a slab is cut out parallel to the  $(0001)$  planes, as shown in Fig. 23-10. The diagram shows a slab then cut into "Y-bars" by sawing parallel to  $(2\bar{1}\bar{1}0)$  planes. The Y-bar shown has again been cut into plates marked  $BT$ , apparently by sawing parallel to  $(0\bar{1}11)$  planes. There are two other common methods, namely, the "direct wafering method" and the "X-section method."<sup>1</sup>

**5. Rubber; Textiles; Plastics; Dusts.** The pattern of unstretched rubber has already been mentioned in Chap. 22. Figure 23-13 shows a series of patterns of various types of rubber, unstretched and stretched to various elongations, obtained by Gehman and Field.<sup>2</sup> Stretching of rubber to several hundred per cent elongation apparently causes the long-chain rubber molecules (Fig. 22-12) to straighten out and orient themselves nearly parallel to each other in the direction of stretch. The resulting structure has a crystalline character and yields an x-ray pattern resembling that of other crystalline solids.

Textile fibers have also been studied by x-ray diffraction. Cotton, wood, and rayon fibers consist mostly of cellulose. The crystal structure of cellulose has been investigated by x-ray diffraction methods by

<sup>1</sup> For further details, see W. L. Bond and E. J. Armstrong, *Bell System Tech. J.*, **22**, 293 (1943); *Electronic Ind.*, **2**, 58 (May, 1943); R. Setty, *Electronic Ind.*, **2**, 102 (December, 1943); *J. Sci. Instruments*, **20**, 80 (1943); S. X. Shore, *Commun. Mag.*, October–December, 1943, January, February, 1944.

<sup>2</sup> S. D. Gehman and J. E. Field, *J. Applied Phys.*, **10**, 564 (1939), **15**, 371 (1944).

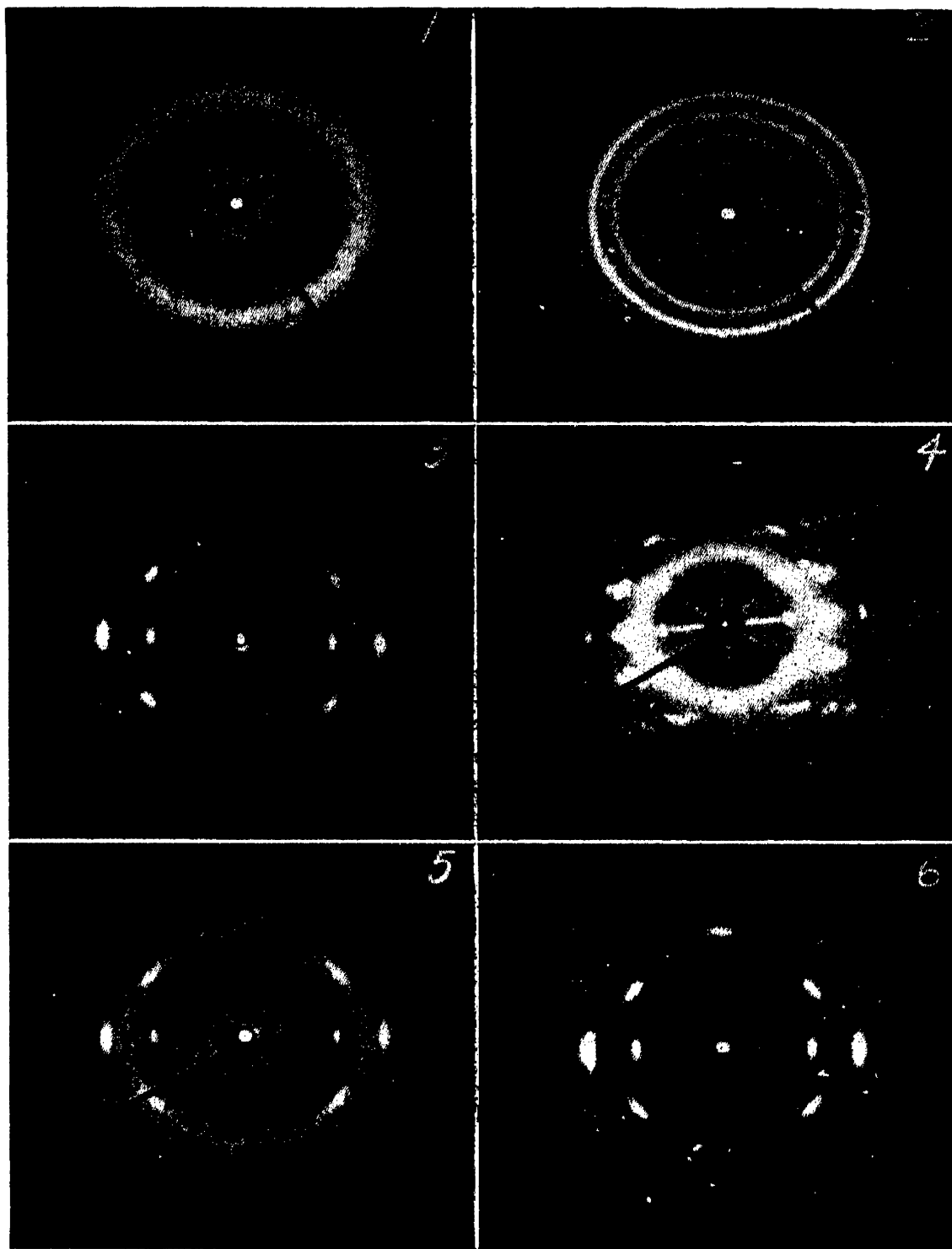


FIG. 23-13. X-ray patterns of: (1) unstretched rubber; (2) frozen rubber; (3) stretched rubber; (4) racked rubber, 2000 per cent elongation, film-specimen distance 3.4 cm.; (5) pale crepe rubber, 350 per cent elongation, room temperature; (6) pale crepe rubber, 350 per cent elongation, frozen. (By S. D. Gehman and J. E. Field; courtesy of the American Institute of Physics.)

Polanyi, Mark and Meyer, Gross and Clark, and others.<sup>1</sup> It is monoclinic, with lattice constants  $a = 8.35$  Å.,  $b = 10.3$  Å.,  $c = 7.95$  Å., and  $\beta = 84^\circ$ . The unit cell contains four  $C_6H_{10}O_5$  molecular units, which

<sup>1</sup> M. Polanyi, *Naturwissenschaften*, **9**, 228 (1921); H. Mark and K. H. Meyer, *Z. physik. Chem. B*, **2**, 115 (1928), **36**, 232 (1937); S. T. Gross and G. L. Clark, *Z. Krist.*, **99**, 357 (1938). For a full discussion, see E. Ott, "Cellulose and Cellulose

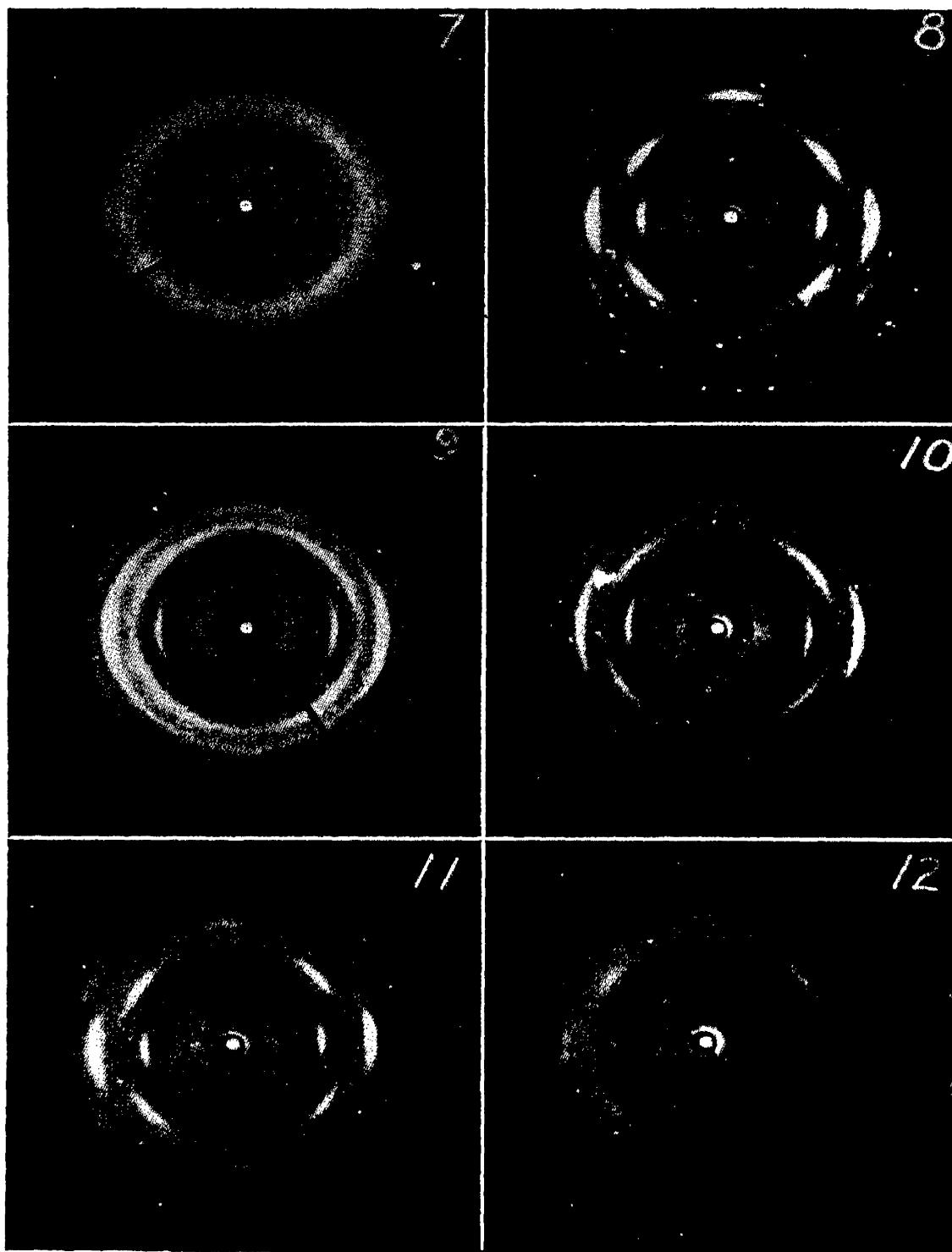


FIG. 23-13.—(Continued), (7) pale crepe rubber, 250 per cent elongation, room temperature; (8) pale crepe rubber, 250 per cent elongation, frozen; (9) pale crepe rubber, 30 per cent elongation, frozen; (10) milled, compounded rubber, 200 per cent elongation, frozen; (11) vulcanized rubber. Cure: 40 minutes at 260°F., 200 per cent elongation, frozen; (12) vulcanized rubber. Cure: 240 minutes at 260°F., 200 per cent elongation, frozen. (By S. D. Gehman and J. E. Field; courtesy of the American Institute of Physics.)

are linked together in chains having the structure shown in Fig. 23-14. Each of these hexagonal units is called a "cellobiose unit." The structure of Nylon and other synthetic fibers has been investigated by Fan-  
 Derivatives," vol. 5 of a series entitled "High Polymers," pp. 203-285 by W. A. Sisson, Interscience Publishers, Inc., New York, 1943.

kuchen and Mark,<sup>1</sup> who used miniature cameras so that x-ray patterns of a minute part of the fiber could be obtained.

The preferential orientation in natural<sup>2</sup> cellulose fibers (cotton, wood, flax, hemp, etc.,) and in synthetic<sup>3</sup> cellulose fibers (rayon, Cellophane, etc.,) has been studied by Sisson, using the method outlined in Sec. 20-4. Figure 23-15 is a pattern obtained from ordinary unmercerized cotton thread perpendicular to the primary x-ray beam. It shows evident preferential orientation, or fibering, as one would expect. The line AA shows the direction of the axis of the thread.

The structures of other textile fibers with a protein composition (wool, silk, etc.,) have also been studied by x-ray diffraction. They consist of polypeptide chains crystallizing in an orthorhombic or monoclinic lattice. The globular proteins composing egg albumin, hemoglobin, etc., have been studied by Wrinch<sup>4</sup> and others and found to have a hexagonal ring structure.

X-ray diffraction also is a useful tool in the study of plastics. A recent discussion of this topic by Astbury<sup>5</sup> will be helpful.

Many industrial operations are dusty. The effects of long-continued breathing of dust-laden air upon the health of the workmen depends considerably upon the nature of the dust. For example, crystalline quartz or silica dust breathed in large quantities over a long period of time may eventually cause a lung disease called "silicosis," especially if the dust particles are smaller than 0.01 mm. in size. On the other hand, other forms of the compound  $\text{SiO}_2$ , such as amorphous "silica gel," cristobalite, and even crystalline silica in sizes above 0.01 mm., are comparatively harmless. X-ray diffraction patterns of small dust samples collected from the air are therefore most useful as a means of detecting and preventing health hazards from dust.<sup>6</sup>

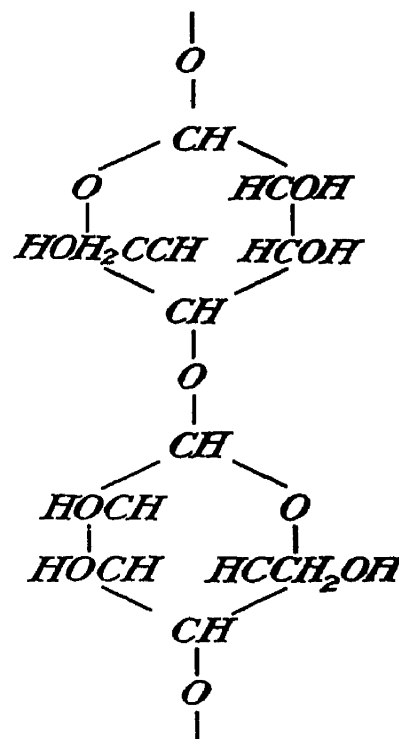


FIG. 23-14.—The structure of cellulose. (By G. L. Clark; "Applied X-rays," McGraw-Hill Book Company, Inc., 1940.)

<sup>1</sup> I. Fankuchen and H. Mark, *J. Applied Phys.*, **15**, 364 (1944).

<sup>2</sup> W. A. Sisson, *Ind. Eng. Chem.*, **27**, 51 (1935) (includes bibliography); see also *J. Applied Phys.*, **15**, 637 (1944).

<sup>3</sup> W. A. Sisson, *J. Phys. Chem.*, **44**, 513 (1940).

<sup>4</sup> D. M. Wrinch, *Proc. Roy. Soc. (London) A*, **160**, 59 (1937); *Phil. Mag.*, **31**, 177 (1941).

<sup>5</sup> W. T. Astbury, *Chemistry & Industry (London)*, (April 14, 1945); for a study of the structure of polythene, see C. W. Bunn and T. C. Alcock, *Trans. Faraday Soc.*, **41**, 317 (1945).

<sup>6</sup> See, for example, J. W. Ballard, H. I. Oshry, and H. H. Schrenk, *U.S. Bur. Mines, Bull.* RI 3520 (June, 1940); see also L. H. Berkelhamer, *J. Ind. Hyg. Toxicol.*, **23**, 163 (1941).

**6. Conclusion.** By searching the technical literature, a long list of problems and substances that have been studied with helpful results by x-ray diffraction methods could be set down here. However, such a list is not very instructive. Instead, the aim in this book has been to show *how* x-ray methods are applied to various typical problems and let the reader judge from these the nature of the numerous other applications and whether or not x-ray methods might be applicable to his own problems.

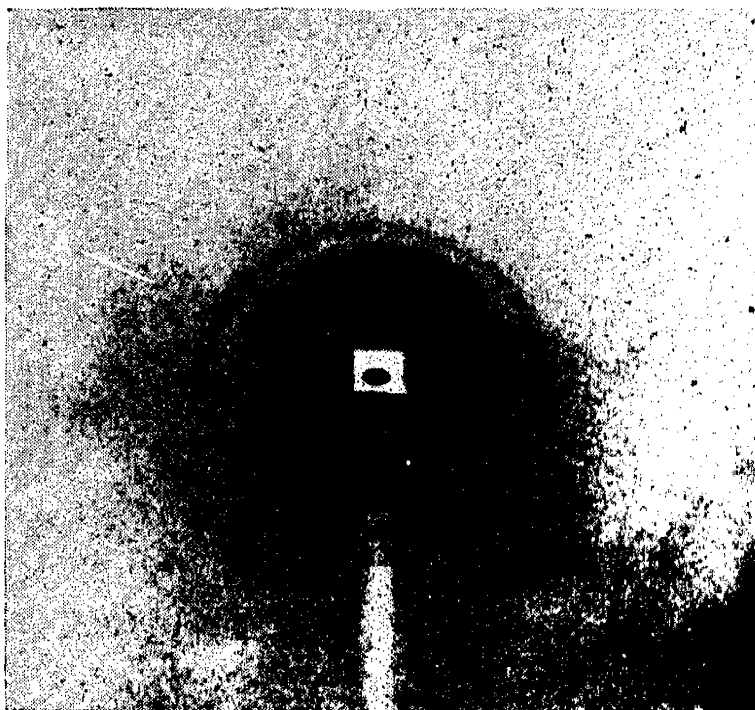


FIG. 23-15.—Pattern of unmercerized cotton thread parallel to line AA.

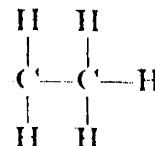
### QUESTIONS AND PROBLEMS

1. Is the molecular structure of the aliphatic organic compounds more closely related to the crystal structure of diamond or graphite? Answer the same question for the aromatic compounds. Give reasons for your answers. Account for the presence of an angle of  $109\frac{1}{2}^\circ$  in a zigzag carbon chain.

2. Account for the difference in physical properties between the odd- and the even-numbered normal hydrocarbons, fatty acids, etc. The fact that the graph in Fig. 23-3 consists of straight lines proves what? What is the significance of the presence of *two* lines in this graph?

3. Without consulting a table, predict the distance between K and Br atoms in a KBr crystal. Between Mg and O atoms in MgO. Between  $\text{NH}_4$  and Cl in  $\text{NH}_4\text{Cl}$ . These compounds illustrate what kind of binding? Give three examples of van der Waals binding. What kind of binding should you say holds the atoms together in a molecule of water? What kind of binding should you suppose holds the water molecules together in a snowflake crystal?

4. Without consulting tables, which molecule is longer, ethane



or acetylene  $\text{H}-\text{C}\equiv\text{C}-\text{H}$ ? Which molecule is larger, methane  $\begin{array}{c} \text{H} \\ | \\ \text{H}-\text{C}-\text{H} \\ | \\ \text{H} \end{array}$  or

acetylene? Explain how you arrived at your answers. Could you determine the distances between the hydrogen atoms in a methane molecule by x-ray diffraction? Explain your answer.

5. How many single homopolar bonds are usually associated with a carbon atom? An oxygen atom? A hydrogen atom? What is meant by a double bond? A triple bond? Resonance between bonds?

6. What distinguishes metallic binding from the other kinds of binding? Why did Phragmen use three different sizes of camera? What kind of cameras were they? Why did Westgren heat his powdered alloys to the recrystallization temperature and then quench them?

7. Give examples of a substitutional solid solution. An interstitial solid solution. An intermetallic compound. What distinguishes such compounds from ordinary chemical compounds like water, for example? A 44 per cent zinc, 56 per cent copper brass that has reached its equilibrium state of crystallization has what sort of crystal structure?

8. Describe briefly the alpha, beta, gamma, and epsilon brass structures. Which of these are superstructures? What other alloys form a beta superlattice? A gamma superlattice? What are the laws governing the formation of these two types of compound? Whose name is associated with the law, in one case?

9. How should you describe the crystal structure of a 90 per cent zinc, 10 per cent copper alloy? How does it differ from that of a 95 per cent zinc, 5 per cent copper alloy? How will the x-ray diffraction pattern of these two alloys differ?

10. What does nitriding do to the surface layer of a piece of steel? How is the x-ray diffraction pattern of the surface layer affected? How should you obtain such a pattern without damaging the surface?

11. From the lattice constants of quartz,  $a = 4.9 \text{ \AA}$ . and  $c = 5.4 \text{ \AA}$ ., compute the  $d$  values for the  $(10\bar{1}0)$  and  $(11\bar{2}0)$  planes. From these and the 1.54- $\text{\AA}$ . wave length of copper  $K_\alpha$  radiation, verify the values of the Bragg angles given in Fig. 23-11.

12. In order to pick up the  $(11\bar{2}0)$  reflection, the Geiger counter slits should be set at what angle with respect to the collimator axis? Suppose such a setting has been made and the setting that gives maximum meter reading found, for a slab cut perpendicular to the  $Z$  or  $C$  axis, the slab lying flat on the crystal table. At what angle with the counter slit axis should you draw a pencil line marking the direction of the desired saw cut along the  $(11\bar{2}0)$  planes?

13. Why does unstretched rubber give an amorphous type of x-ray pattern and stretched rubber a crystalline type? Do any of the patterns in Fig. 23-13 reveal preferential orientation? If so, which ones?

14. What type of information might x-ray diffraction studies of textiles reveal? Which chapter in this book do you think would be most helpful to someone confronted with a problem involving toxic dusts in the air?

## CHAPTER 24

### ELECTRON DIFFRACTION AND ITS APPLICATIONS

**1. Principal Differences between X-ray Diffraction and Electron Diffraction.** It was mentioned in Sec. 4-3 that a homogeneous beam of electrons has associated with it a train of de Broglie "phase waves" and that Davisson and Germer and Thomson discovered that these waves and their associated electrons could be diffracted by a crystal. Since this discovery in 1927, the theory and applications of electron diffraction have evolved along lines which are quite similar to those which have been outlined for x-ray diffraction in Chaps. 15 to 23. The practical potentialities of electron diffraction do not appear to be greatly inferior to those of x-ray diffraction, and the two phenomena are quite similar. This similarity makes it relatively easy for a person with a reasonable knowledge of x-ray diffraction to acquire equal familiarity with electron diffraction methods. This fact may justify the inclusion of a chapter on electron diffraction<sup>1</sup> in a book on x-rays.

Although the similarities of x-ray and electron diffraction are striking, they should not obscure the fact that there are also important differences. To one with a good knowledge of x-ray diffraction, the similarities may be less important than the differences of which the principal ones will therefore be outlined here.

*a.* X-rays penetrating matter are scattered, both coherently and incoherently, by the *electrons* in the atoms composing the matter. Interference between the coherently scattered rays results in the phenomena of x-ray diffraction. The phase waves associated with a homogeneous beam of electrons (electrons moving in the same direction at the same velocity) are diffracted by the periodic space variation of the electric potential caused by the atomic lattice structure within a crystal. The nuclei, as well as the electrons, of these atoms play a role in producing this space variation of the electric field, and their influence is therefore not greatly inferior to that of the electrons, as it is in x-ray diffraction.

<sup>1</sup> For a much more complete discussion, see G. P. Thomson and W. Cochran, "Theory and Practice of Electron Diffraction," Macmillan & Company, Ltd., London, 1939; also symposium, *Trans. Faraday Soc.*, **31**, 1049-1135 (1935); R. Beeching, "Electron Diffraction," Methuen & Co., Ltd., London, 1936; C. F. Meyer, "The Diffraction of Light, X-rays, and Material Particles," University of Chicago Press, 1934.



These periodic potential variations within a crystal have been discussed in an article, with bibliography, by Slater<sup>1</sup> (see also page 83).

b. As a result of the difference just mentioned, the quantity, customarily designated by  $E$ , which plays a role in electron diffraction equivalent to that of the atomic-structure factor  $f$  in x-ray diffraction is not identical with  $f$ . Instead, Mott<sup>2</sup> has shown that  $E$  is related to  $f$  by the equation

$$E = \frac{1}{16\pi^2} \frac{Z - f}{(\sin \theta/\lambda)^2} \quad (24-1)$$

where  $Z$  is the atomic number of the atom,  $\theta$  is the Bragg angle or half the scattering angle  $\phi$ , and  $\lambda$  is the wave length of the phase waves.

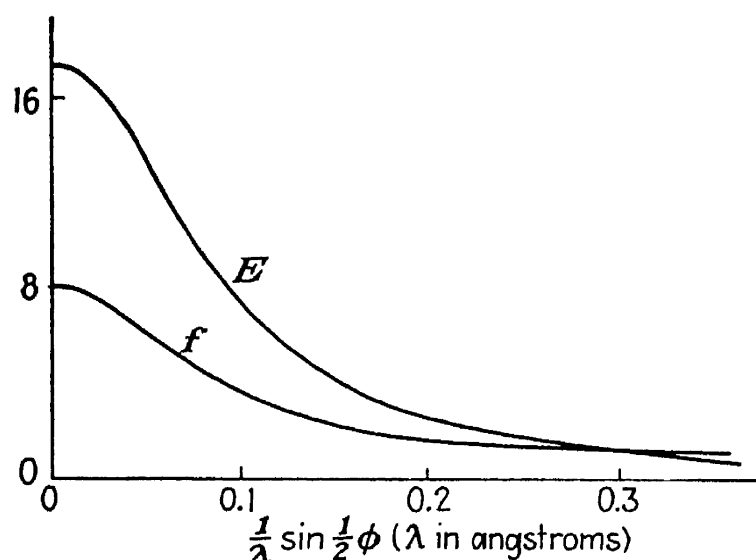


FIG. 24-1.—The function  $E$ , analogous to atomic structure factor  $f$ , in electron diffraction, for oxygen. (By N. F. Mott; courtesy of The Royal Society.)

Like  $f$ ,  $E$  is a function of  $\sin \theta/\lambda$ , and the relation between the two is shown graphically in Fig. 24-1, for oxygen, where both  $E$  and  $f$  have been plotted by Mott. Equations (16-36) to (16-38) and (18-3) show that the intensity of scattered x-rays is proportional to  $f^2$ . Similarly, the intensity of scattered electrons is proportional to  $E^2$ , to a sufficient degree of accuracy for ordinary work.<sup>3</sup> Although  $f$  is a pure number,  $E$  has the dimensions of an area, and it is plotted in arbitrary units in Fig. 24-1. For this reason, the  $1/16\pi^2$  has little or no significance in equation 24-1; it is only the relative values of  $E$  at different values of  $\sin \theta/\lambda$  that have practical interest. In comparing  $E$  with  $f$ , however, one should include a factor of the order of  $10^4$  between the two, to take care of the fact that the intensities of scattered cathode rays, proportional to  $E^2$ , are some  $10^7$  times those of scattered x-rays, proportional to  $f^2$ .

<sup>1</sup> J. C. Slater, *Rev. Modern Phys.*, **6**, 209 (1934).

<sup>2</sup> N. F. Mott, *Proc. Roy. Soc. (London) A*, **127**, 658 (1930).

<sup>3</sup> For more details, see M. Blackman, *Proc. Roy. Soc. (London) A*, **173**, 77 (1939)

In Fig. 24-1, it is noticed that the scattering decreases with angle more rapidly for electrons than for x-rays.

c. Although homogeneous electron beams generated at potentials of only a few volts or a few hundred volts can be diffracted, the practical applications of electron diffraction have thus far employed electrons having energies ranging from about 20 to 80 kv., as a rule. Application of equation (4-24) to such electrons shows that  $\lambda$  for the phase waves is of the order of 0.05 Å., which is roughly one-tenth or one-twentieth of the wave length of the x-rays ordinarily employed in diffraction work.

d. The shorter wave length of the phase waves as compared with x-rays used for diffraction work results in values of the Bragg angle  $\theta$  of the order of  $1^\circ$  instead of  $10^\circ$  as with x-ray transmission patterns. Consequently, a considerably longer specimen-to-film distance is preferred for an electron diffraction camera than for a comparable x-ray diffraction camera. Another consequence is that one is justified in making the approximation  $2 \sin \theta = 2\theta = \tan 2\theta$  in calculating  $d$  values from ring diameters by Bragg's law for work of ordinary accuracy. Such an approximation is very inexact with x-ray patterns. If  $D$  is the specimen-to-film distance and  $r$  is the radius of a ring in the transmission pattern, one has, as with x-rays,  $r/D = \tan 2\theta$ , and from Bragg's law,

$d = \frac{\lambda}{2 \sin \theta}$ . The above approximation then permits one to write

$$d = D \frac{\lambda}{r} \quad (24-2)$$

where  $d$  and  $\lambda$  are ordinarily in angstrom units and  $D$  and  $r$  in inches, centimeters, or millimeters.

e. Another result of the short wave length is the elimination of back-reflection patterns as one of the practical techniques. Back-reflection patterns have been obtained, especially from single crystals, with "slow" electron beams at potentials of the order of 100 volts; in fact, Davisson and Germer discovered electron diffraction by conducting experiments of this sort. Such beams have a long wave length, corresponding to cobalt  $K_\alpha$ , and similar x-ray wave lengths suitable for back reflection. The diffraction of such low-voltage electron beams is grossly affected by layers of adsorbed gases on the surface of the specimen and by other anomalies that have discouraged their use in ordinary practical work. Unsuccessful attempts have been made to obtain back-reflection patterns of graphite, gold, and iron with 50-kv. electron beams.<sup>1</sup> The reason for the failure is discernible in Sec. 21-3.

f. Another consequence of the shorter wave length is that, with very thin single crystals like a mica sheet  $5 \times 10^{-6}$  cm. thick, a so-called

<sup>1</sup> R. Jackson and A. G. Quarrell, *Proc. Phys. Soc. (London)*, **50**, 779 (1938).

“cross-grating” pattern can be obtained, as though the specimen were only one unit cell (20 Å.) thick. Figure 24-2 shows such a pattern by Finch, Quarrell, and Wilman.<sup>1</sup> The array of spots appears as though only two of the three Laue equations (15-1) to (15-3), were to be satisfied, without regard for the third. This can be explained on the basis of Ewald’s reciprocal lattice (page 384) on the grounds that the reflecting sphere, having a radius  $G^2/\lambda$ , will be about twenty times as large as in x-ray diffraction, since  $\lambda$  is only about one-twentieth as great. Therefore, when the sphere is tangent to one of the planes of reciprocal lattice points perpendicular to the primary beam, the effect is like laying a basketball on a screen wire, instead of a golf ball. Such a large ball will intersect all the wire intersections (reciprocal lattice points) over quite a “spot of tangency,” considering the fact that the “skin” of the ball has finite thickness, because  $\lambda$  varies over a range of a small fraction of a per cent, and that the points have a slight extent corresponding to the slight width of a diffraction maximum.

*g.* In x-ray diffraction, the wavelength of the primary rays is ordinarily found by looking it up in a table (0.71 Å. for molybdenum target, 1.54 Å. for copper, etc.) but this is not true with electron diffraction. The alternative method used in x-ray diffraction, of photographing a “standard” pattern from some substance like rock salt on the same film for comparison with the pattern in question, is suitable for electron diffraction, however. Gold foil is a favorite reference substance for electron diffraction work. If  $d$ ,  $D$ , and  $r$  are known, then  $\lambda$  can be calculated from equation (24-2). Of course,  $\lambda$  can be calculated from the voltage at which the beam is generated, by equation (4-24), if this voltage is known quite accurately, but it usually is not. For such a calculation, the next section will be found helpful.

*h.* Earlier chapters have emphasized the great penetrating power of x-rays as contrasted with cathode rays. Generally speaking, the prob-

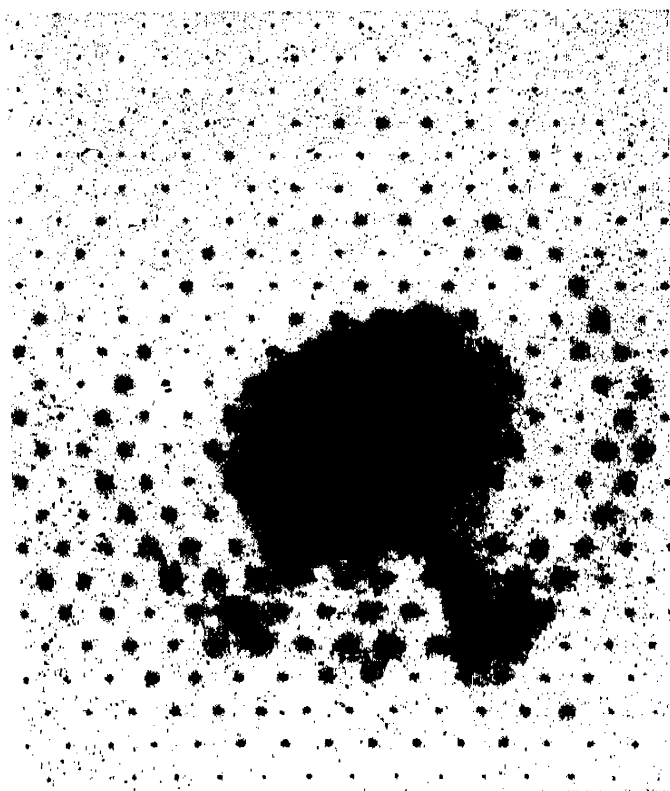


FIG. 24-2.—Electron diffraction cross-grating pattern of very thin mica crystal. (By G. I. Finch, A. G. Quarrell, and H. Wilman; courtesy of The Faraday Society.)

<sup>1</sup> G. I. Finch, A. G. Quarrell, and H. Wilman, *Trans. Faraday Soc.*, **31**, 1051 (1935).

ability that an electron with 50,000 electron volts energy will suffer an elastic collision when it encounters an atom is of the order of  $10^7$  times as great as the probability that an x-ray photon of ordinary energy or hardness will be scattered when it encounters such an atom.

i. The tendency for electrons to scatter rather than penetrate when they strike matter accounts for the fact that the proper thickness of a solid or liquid sample for transmission patterns is about a millionth of an inch for electron diffraction instead of about a thousandth of an inch, as for x-ray diffraction.

j. This also accounts for the fact that electron diffraction is superior to x-ray diffraction in most respects when the sample is a gas or vapor. With x-rays, it is difficult to get enough gas in a small space in the primary beam to scatter a measurable fraction of the rays, but this difficulty does not occur with electrons. Of course, a homogeneous electron beam calls for a good vacuum, and the problem of localizing a gas at one spot in a vacuum seems insuperable at first thought. However, the amount of gas required is so small that it can be introduced slowly into the vacuum chamber at the desired spot through a tiny jet, and fast pumps will still maintain a satisfactory vacuum in the rest of the chamber in spite of it. For details, see Sec. 3 and Fig. 24-5.

k. The very slight penetration of the electrons also makes them better suited than x-rays for the study of the crystal structure and chemical composition of thin surface coatings less than a ten-thousandth of an inch thick, say. In such cases, electrons give the pattern of the coating, whereas x-rays penetrate and give the pattern of the underlying material. For this type of work, the electron beam is made to impinge upon the sample at grazing incidence, producing a semicircular arc pattern in a manner analogous to that shown for x-rays in Figs. 23-8 and 23-9. In taking an x-ray pattern by this method, the surface may be regarded as smooth and flat, since the penetration is of the order of a thousandth of an inch. However, very few surfaces are smooth and flat from the standpoint of a homogeneous electron beam incident at a grazing angle of about  $1^\circ$ . Such a beam is capable of penetrating only about a millionth of an inch without losing its homogeneity through inelastic collisions. The formation of a transmission pattern from such a surface depends upon the existence of a few peaks or ridges here and there projecting a millionth of an inch or so above the plane of the surface.

l. The great increase in scattering power of the sample for electrons as compared with x-rays results in comparatively short exposure times. An electron diffraction pattern is ordinarily photographed in a few seconds, and often in a fraction of a second, as contrasted with minutes or hours for x-ray patterns. However, the time saved by the shorter

exposure is offset by the time required to evacuate the camera and by the more time-consuming technique of sample preparation.

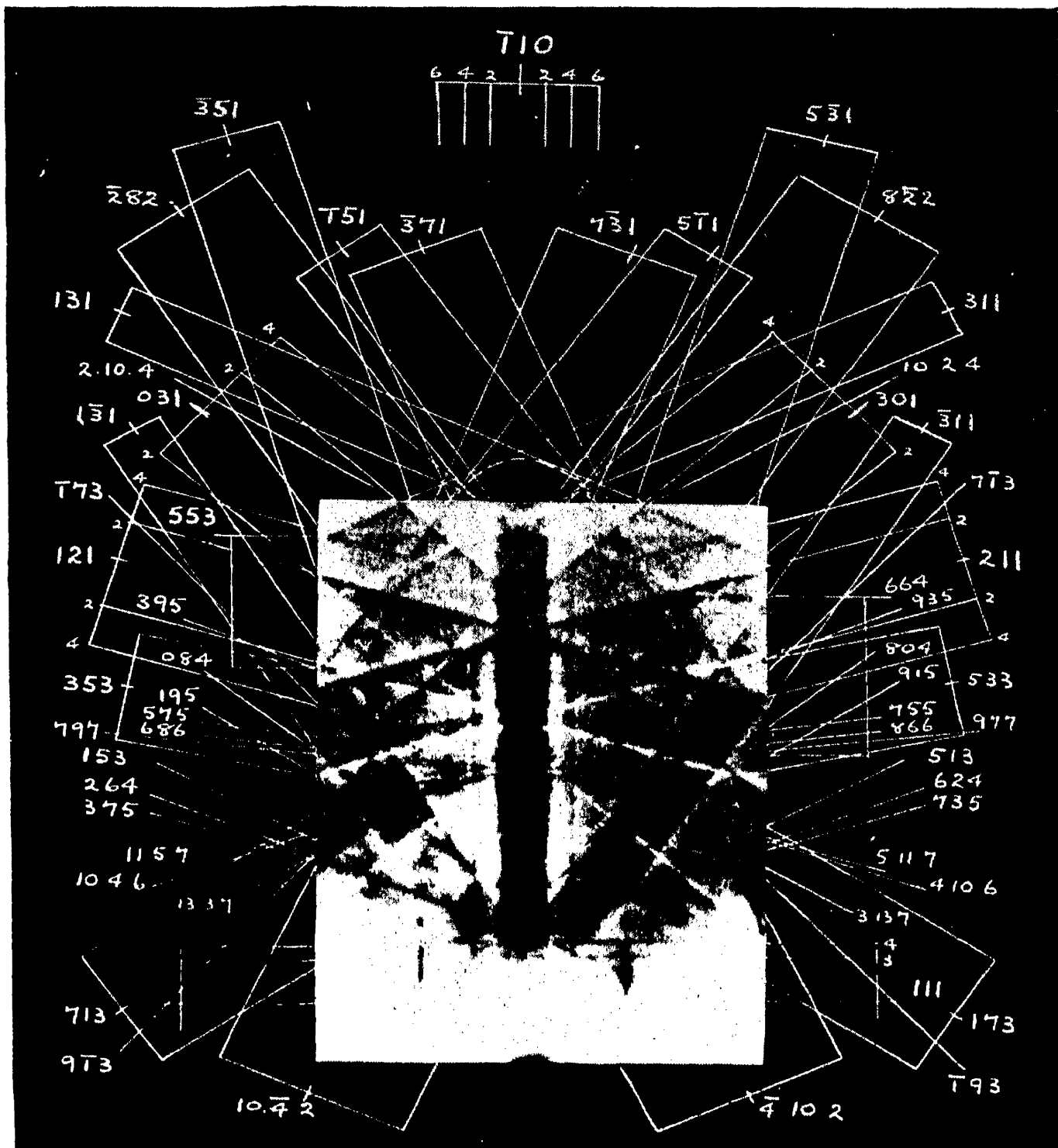


FIG. 24-3.—Kikuchi lines in the electron diffraction pattern from the (111) face of a fluorite crystal. (By G. I. Finch, A. G. Quarrell, and H. Wilman; courtesy of The Faraday Society.)

*m.* With thicker single crystal specimens, the character of the electron transmission pattern changes because many of the electrons are scattered before they experience Bragg reflection. These “thick” crystal patterns often display pairs of nearly straight lines, as in the pattern of a fluorite

crystal, taken by Finch, Quarrell, and Wilman, at  $60^\circ$  to the (111) plane (Fig. 24-3). Such lines are called "Kikuchi lines" because they were discovered by Kikuchi<sup>1</sup> in 1928, in patterns of mica. Kikuchi's explanation of these lines may be understood from Fig. 24-4. If  $XP$  is the primary beam incident normally upon a thin crystal slab at  $P$ , a considerable fraction of the beam will be scattered elastically but diffusely from a small region around  $P$ . Some of these rays  $PH$  and  $PJ$  will have the proper directions to satisfy Bragg's law for the set of crystal planes

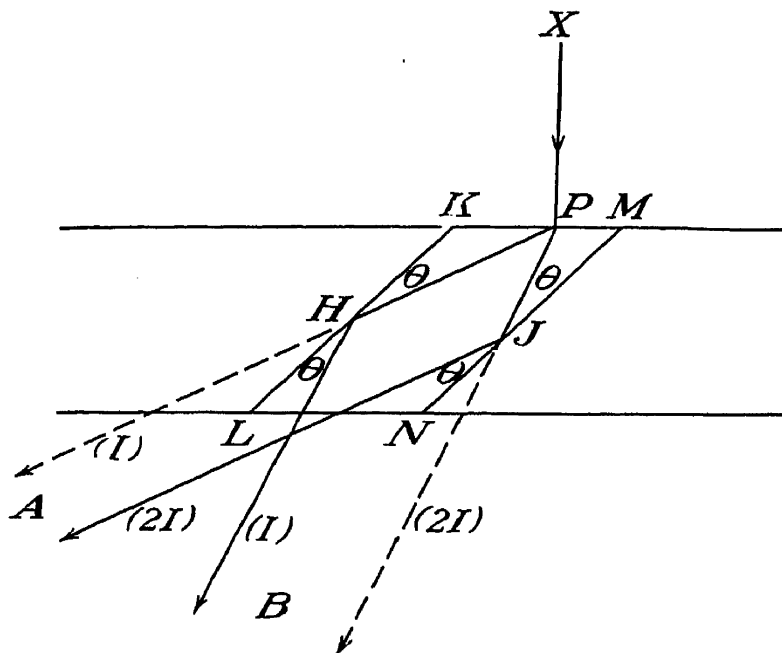


FIG. 24-4.—Kikuchi's explanation of the Kikuchi lines. (Figure by G. P. Thomson; courtesy of Macmillan & Company, Ltd., and The Macmillan Company.)

$KL$ ,  $MN$ . Since the intensity of scattered rays decreases with angle, it may be supposed, for illustration, that ray  $PJ$  is twice as intense as ray  $PH$ , or that their intensities are  $4I$  and  $2I$ , respectively. It may then be supposed that half of  $PH$  undergoes Bragg reflection, emerging in direction  $HB$  with intensity  $I$ , the other half being transmitted and emerging in direction  $HA$  with intensity  $I$ . Similar assumptions for ray  $PJ$  indicate that rays  $JA$  and  $JB$  both have intensity  $2I$ . On this basis, beams  $A$  and  $B$  are equally intense, both having intensity  $3I$ . If the Bragg reflections had not occurred, the rays in direction  $A$  would have had intensity  $2I$  and those in direction  $B$  would have had intensity  $4I$ . This explanation accounts for the fact that the Kikuchi lines appear in parallel pairs, the line farther from the primary beam being light and the one closer to the primary beam being dark. It is seen that an imaginary line on the pattern halfway between such a pair of Kikuchi lines represents the intersection of the corresponding crystallographic planes ( $KL$ ,  $MN$ ) with the photographic plate or film. The

<sup>1</sup> S. K. Kikuchi, *Proc. Imp. Acad. Japan*, **4**, 271, 354 (1928); *Japan. J. Phys.*, **5**, 83 (1928); *Physik. Z.*, **31**, 777 (1930).

Bragg reflections involved are often of higher order than the first, as indicated by the identifying marks surrounding the pattern of Fig. 24-3. This simple theory of the Kikuchi lines is not entirely adequate. For more details, see the book by Thomson and Cochran.<sup>1</sup>

*n.* In "powder" transmission patterns with high-voltage electrons, polycrystalline samples sometimes yield patterns having "extra," or "forbidden," rings. For example, in the pattern of gold foil, Finch, Quarrell, and Wilman<sup>2</sup> observed such extra rings at  $d = 4.81, 4.00, 2.79, 1.83, 1.61,$  and  $1.49$  Å., whereas gold should have only the following reflections, taken from the Hanawalt-Rinn-Frevel table:  $2.35, 2.03, 1.439, 1.227, 1.173, 1.019, 0.935, 0.910$  Å., etc. Investigation of these rings has shown that they are due to absorbed gas entering the metal lattice and forming an interstitial solid solution in the surface layers. Thorough outgassing of the sample eliminates the extra rings. They do not ordinarily appear in x-ray patterns because of the small scattering of x-rays by gas atoms and the much deeper penetration of x-rays.

*o.* In Chap. 6 it was found that the index of refraction of x-rays in matter is usually less than 1 by an amount of the order of  $10^{-6}$ , which is negligible in ordinary work but worthy of consideration in precision work (Sec. 15-5). If electrons are thought of as negatively charged particles, for the moment, it can be seen that they should undergo refraction when they enter a solid or liquid because the increase in electric potential at the boundary will give the electron an acceleration normal to the surface toward the interior as it enters, the reverse occurring when it emerges. This increase in electric potential [often thought of as a decrease in (negative) potential, since electrons are negative] within matter, as compared with the potential outside, may be regarded as a barrier to be hurdled by electrons in escaping from a metal. It is well known that a metal must be heated until the thermal energy of some of the free electrons within reaches a value sufficient to enable them to hurdle this barrier and escape, in the form of "thermionic emission" (pages 10 to 12).

The theory of this barrier in metals has been developed by Sommerfeld.<sup>3</sup> According to this, some of the free electrons in the metal have energy  $W_i$  even at absolute zero temperature, owing to the filling up of the lower energy levels by the Pauli principle (page 63), forcing some of the electrons into higher levels. The "height" of the potential barrier (in volts) to be hurdled at the surface is designated as  $W_a$ . Then the thermionic, or photoelectric, work function  $\Phi$ , with which most

<sup>1</sup> Footnote 1, p. 536.

<sup>2</sup> G. I. Finch, A. G. Quarrell, and H. Wilman, *Trans. Faraday Soc.*, **31**, 1051 (1935).

<sup>3</sup> A. Sommerfeld, *Naturwissenschaften*, **16**, 374 (1928); *Z. Physik*, **47**, 1, 43 (1928). See also L. A. DuBridge, *Am. J. Phys. (Am. Phys. Teacher)*, **7**, 357 (1939).

electrical engineers are familiar, is given by

$$\Phi = W_a - W_i \quad (24-3)$$

On this basis, the index of refraction  $\mu$  of a homogeneous electron beam generated at a potential difference of  $V$  volts is given by

$$\mu = \sqrt{1 + \frac{W_a}{V}} \quad (24-4)$$

Since  $W_a$  for most solids is of the order of 10 volts (usually between 5 and 20, at any rate), it is seen that  $\mu$  exceeds unity by a negligible<sup>1</sup> amount when one is using 30 or 50 kilovolt electrons, but its variation from unity becomes important for beams generated at a few hundred volts or less. In such cases, equation (24-4), combined with (4-24), Bragg's law, and Snell's law ( $\mu = \sin i / \sin r$ ) will enable one to make the proper correction, as on page 328 for x-rays.

**2. Relationship of Voltage to Wave-length.** Beginning with the pioneer work of Davisson and Germer and of G. P. Thomson, the experimental results have confirmed de Broglie's equation giving  $\lambda$  in centimeters,

$$\lambda = \frac{h}{mv} \quad (4-24) \text{ or } (24-5)$$

Since the velocity attained by 50-kv. electrons is not a negligible fraction of the velocity of light, one should not lose sight of the fact that

$$m = \frac{m_0}{\sqrt{1 - \frac{v^2}{c^2}}} \quad (4-14) \text{ or } (24-6)$$

so that

$$\lambda = \frac{h \sqrt{1 - \frac{v^2}{c^2}}}{m_0 v} \quad (4-23) \text{ or } (24-7)$$

where  $v$  is the velocity of the electrons in centimeters per second. This velocity is in turn related to the potential difference  $V$  (in volts) applied to the electron gun by the equation

$$\text{Kinetic energy} = \frac{eV}{300} = \frac{m_0 c^2}{\sqrt{1 - \frac{v^2}{c^2}}} - m_0 c^2 \quad (24-8)$$

(see page 56). Solving this for  $v$ , substituting the result in (24-7), making suitable approximations, and noting that  $h/\sqrt{em_0} = 10^{-8}$ ,

<sup>1</sup> A case where the refraction is significant has been reported by L. Sturkey and L. K. Frevel, *Phys. Rev.*, **68**, 56 (1945).



$$\lambda = \frac{h \sqrt{150/Vem_0}}{\sqrt{1 + \frac{eV}{600m_0c^2}}} = \frac{12.21}{\sqrt{V}} \frac{1}{\sqrt{1 + 0.98 \times 10^{-6}V}} \quad (24-9)$$

where  $\lambda$  is now in angstrom units, not centimeters, when  $V$  is in volts. Neglect of the relativity correction leaves merely

$$\lambda = \sqrt{\frac{150}{V}} \quad (24-10)$$

This simple equation can be derived directly from (24-5) and the classical equation for kinetic energy:

$$\frac{eV}{300} = \frac{1}{2}mv^2 \quad (24-11)$$

When  $V = 20$  kv., it is seen that the use of (24-10) instead of (24-9) results in an error of about 1 per cent, representing the relativity correction.

**3. Cameras.** As already stated, most applications of electron diffraction to "practical" problems have employed high-voltage electrons (above 20 kv.). High-voltage cameras will therefore be the main topic of discussion in this section. The youthful character of electron diffraction as a method of investigation is indicated by the fact that it is still customary for each experimenter to construct his own camera, in accordance with his own ideas, and adapted especially to the particular problems he has in mind. The RCA Manufacturing Co., Camden, N.J., sells electron microscopes and adapters that permit them to be used as electron diffraction cameras.<sup>1</sup> High-voltage cameras may be divided into two groups: (1) those intended for solid or nonvolatile liquid specimens (like mercury); (2) those intended for gaseous, vaporized, or volatile liquid specimens (like carbon tetrachloride). In group (1), those cameras deserving most attention are probably the ones developed by the pioneers in the field who have had longer experience than others. Therefore, the cameras developed by Germer and by Thomson and Fraser<sup>2</sup> are cited especially. There is a wide variety of such cameras,<sup>3</sup>

<sup>1</sup> R. G. Picard, *J. Applied Phys.*, **15**, 678 (1944). General Electric has just announced a new camera as this book goes to press; see C. H. Bachman, *Gen. Elec. Rev.*, **48**, 7 (November, 1945).

<sup>2</sup> L. H. Germer, *Rev. Sci. Instruments*, **6**, 138 (1935). G. P. Thomson and C. G. Fraser, *Proc. Roy. Soc. (London) A*, **128**, 641 (1930); *Trans. Faraday Soc.*, **31**, 1049 (1935). G. P. Thomson and W. Cochran, "Theory and Practice of Electron Diffraction," p. 216, Macmillan & Company, Ltd., London, 1939.

<sup>3</sup> G. I. Finch and A. G. Quarrell, *Proc. Phys. Soc. (London)*, **46**, 148 (1934); *Trans. Faraday Soc.*, **31**, 1051 (1935). H. J. Yecarian, *Phys. Rev.*, **48**, 631 (1935). J. A. Darbyshire and E. R. Cooper, *J. Sci. Instruments*, **12**, 10 (1935). H. R. Nelson, *J. Applied Phys.*, **9**, 623 (1938). D. H. Clewell, *Ind. Eng. Chem.*, **29**, 650 (1937). J. E. Ruedy, *Rev. Sci. Instruments*, **11**, 292 (1940). E. A. Gulbransen, *Electronics*, January, 1944, p. 126.

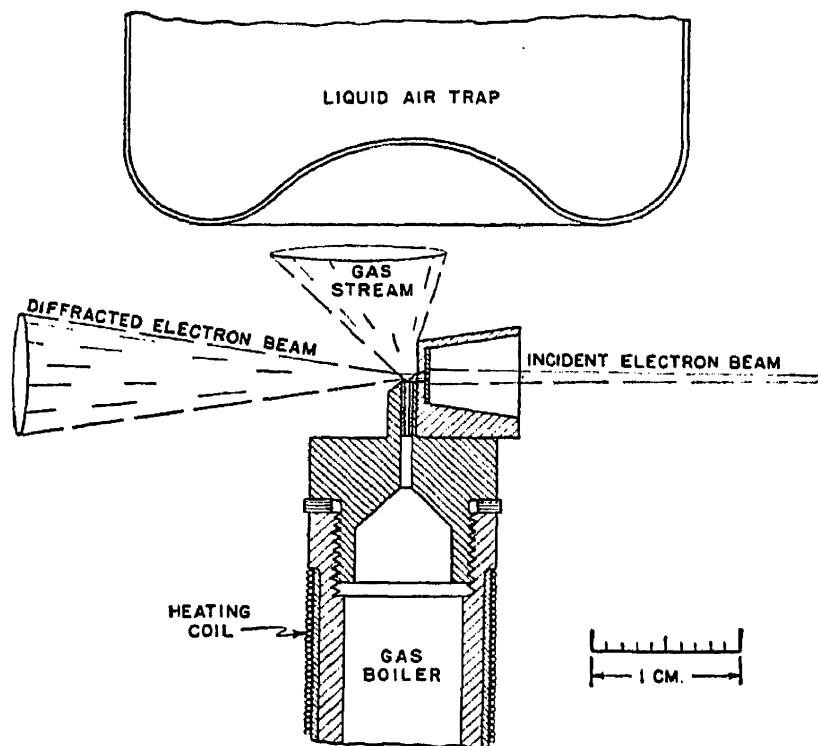


FIG. 24-5.—Method of obtaining an electron diffraction pattern of a gas or vapor. (By L. R. Maxwell, S. B. Hendricks, and V. M. Mosley; courtesy of the American Institute of Physics.)

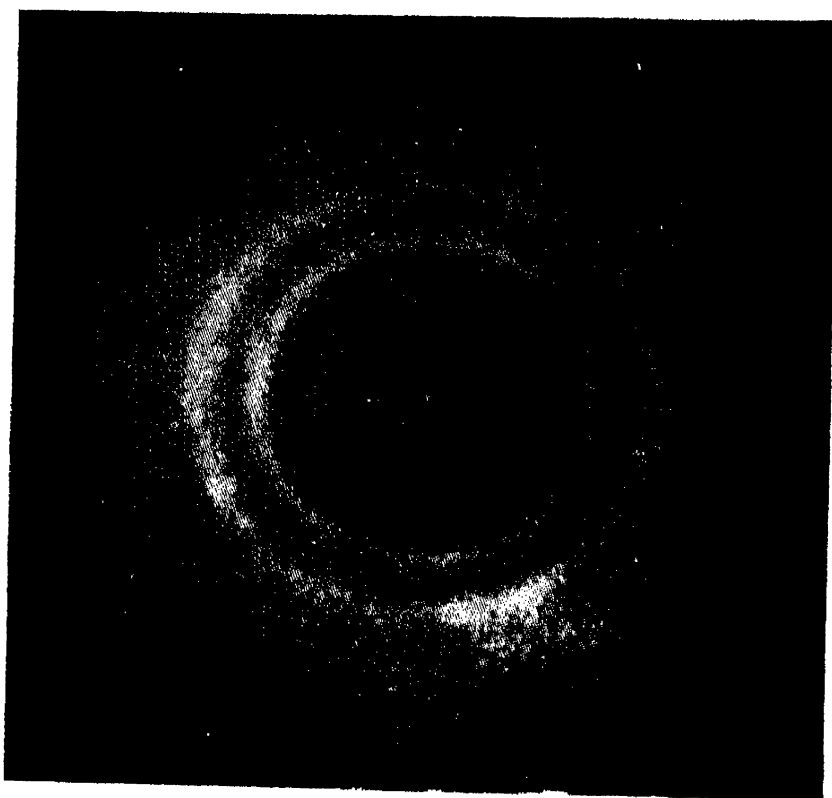


FIG. 24-6.—Electron diffraction pattern of arsenic vapor ( $\text{As}_4$ ). de Broglie wavelength 0.0617 Å. Plate distance 10 cm. Magnified 2 ×. This is a (reversed) print. (By L. R. Maxwell, S. B. Hendricks, and V. M. Mosley; courtesy of the American Institute of Physics.)

some being designed especially for high-temperature work,<sup>1</sup> etc. In group (2), there are also numerous cameras described in the literature.<sup>2</sup> The only essential difference between groups (1) and (2) is that for gases and vapors a jet of the proper size must be provided, its axis accurately intersecting the electron beam axis. It is helpful to have the jet impinge on a liquid air trap to help maintain the vacuum. A boiler for vaporizing the material may be necessary. Such a unit is illustrated in Fig. 24-5, as designed by Maxwell, Hendricks, and Mosley. Figure 24-6 shows a pattern of arsenic ( $\text{As}_4$ ) vapor obtained by the same workers. Since the scattering from gases or vapors rises to a maximum at zero angle, Debye<sup>3</sup> has improved upon the quality of such electron patterns by installing a rotating sector in front of the photographic plate that makes the exposure time proportional to  $r^4$  where  $r$  is the distance of any point on the plate from the center of the pattern.

Figure 24-7 is a photograph of a group (1) camera constructed and operated by W. W. Beeman and the author. Figure 24-8 is a section drawing of the camera. The plate or film holder *D* is somewhat different from the usual construction. Its principal part is a turntable that can be rotated by means of a tapered seal like the plug in a stopcock. On the underside of the turntable, radial rails are fastened so that six plates or films can be slid in through the port *C*, much as a drawer slides on rails attached to the underside of a table top. A sector is cut out of the

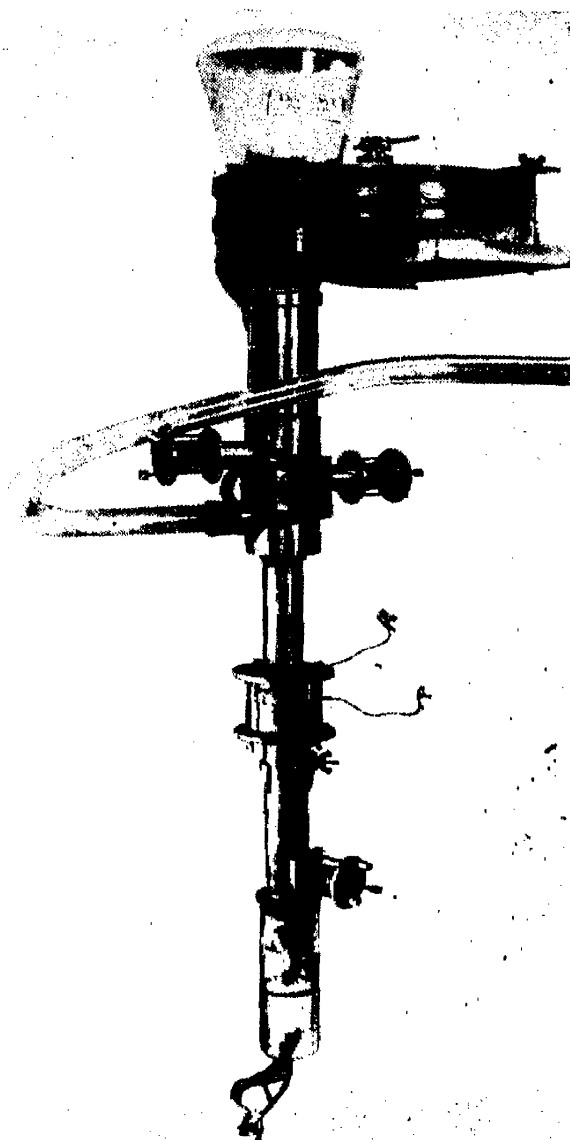


FIG. 24-7. Photograph of electron diffraction camera in use at General Motors Research Laboratories.

<sup>1</sup> G. L. Clark and E. Wolthuis, *J. Applied Phys.*, **8**, 630 (1937). R. Jackson and A. G. Quarrell, *Proc. Phys. Soc. (London)*, **51**, 237 (1939); *Automotive and Aviation Ind.*, **91**, 35 (Sept. 1, 1944).

<sup>2</sup> R. Wierl, *Ann. Physik*, **8**, 521 (1931); H. de Laszlo, *Proc. Roy. Soc. (London) A*, **146**, 672 (1934); L. R. Maxwell, S. B. Hendricks, and V. M. Mosley, *J. Chem. Phys.*, **3**, 705 (1935); L. O. Brockway, *Rev. Modern Phys.*, **8**, 231 (1936).

<sup>3</sup> P. P. Debye, *Physik Z.*, **40**, 66, 404 (1939).

turntable so that when the cutout portion is turned into the electron stream it is able to proceed unhindered to the fluorescent screen *A*, which was cut off of a discarded cathode-ray oscilloscope tube. Although the turntable type of plateholder has the advantage of being very simple and dependable, it is not so easily adapted to cameras mounted horizontally, as many are. Aside from these minor items, there are no features of the camera worth special mention; it is a typical camera.

Electron guns were mentioned in Sec. 7-4*e*. Electron diffraction workers seem to be divided almost equally into those who prefer a gas-discharge type of electron gun working on the principle of the gas-filled x-ray tube and those who prefer a hot-cathode high-vacuum gun. After using both types, the author feels that the advantages and disadvantages of the two are quite evenly balanced and that there are no grounds for a strong preference for either. For detailed drawings and instructions on the construction of a cold-cathode gun for electron diffraction work, one may refer to an article by Moss.<sup>1</sup> A good article to introduce one to the subject of an electron-gun design has been published by Pierce.<sup>2</sup>

In Fig. 24-8, the electrons emitted by the 12-mil tungsten wire filament *N* are accelerated to the diaphragm *M* by a potential difference of about 90 volts supplied by a radio B battery. After passing through the pinhole, they find themselves in a focusing cup like that of an x-ray tube (hot) cathode. As in an x-ray tube, they are then accelerated to the diaphragm *L* by a potential difference of some 50 kv. The electron current is much smaller than in an x-ray tube, however, being a few microamperes, rather than milliamperes. All the apparatus above *L*, including *L*, is at ground potential. The main framework of the camera consists of sections of brass tubing (about  $\frac{3}{16}$  in. wall thickness) soldered together. The gun is maintained at  $-50$  kv. or thereabouts by a transformer-kenotron-condenser circuit of the type shown and described in Fig. 7-22. The condenser has a capacity of about  $0.1 \mu\text{f}$ . To minimize the danger of electric shock, a 1-megohm resistor is placed in the high-voltage line before it enters the camera room where someone might touch it. Since the filament *N* is at high voltage, its heating current is supplied by a filament transformer of the type shown in Fig. 7-8. This transformer should be placed 10 ft. or more from the camera so that its alternating magnetic field will not cause the electron beam to wave back and forth as in a cathode-ray oscilloscope.

The tantalum diaphragm *L* is mounted on a brass bellows as shown, so that the 0.01-in. pinhole in the center of *L* can be aligned with the electron beam. *K* is a second stationary pinhole,  $\frac{1}{8}$  in. in diameter. *J* is a "magnetic lens." This consists of about 800 turns of No. 20

<sup>1</sup> H. Moss, *J. Sci. Instruments*, **18**, 8 (1941).

<sup>2</sup> J. R. Pierce, *J. Applied Phys.*, **11**, 548 (1940).

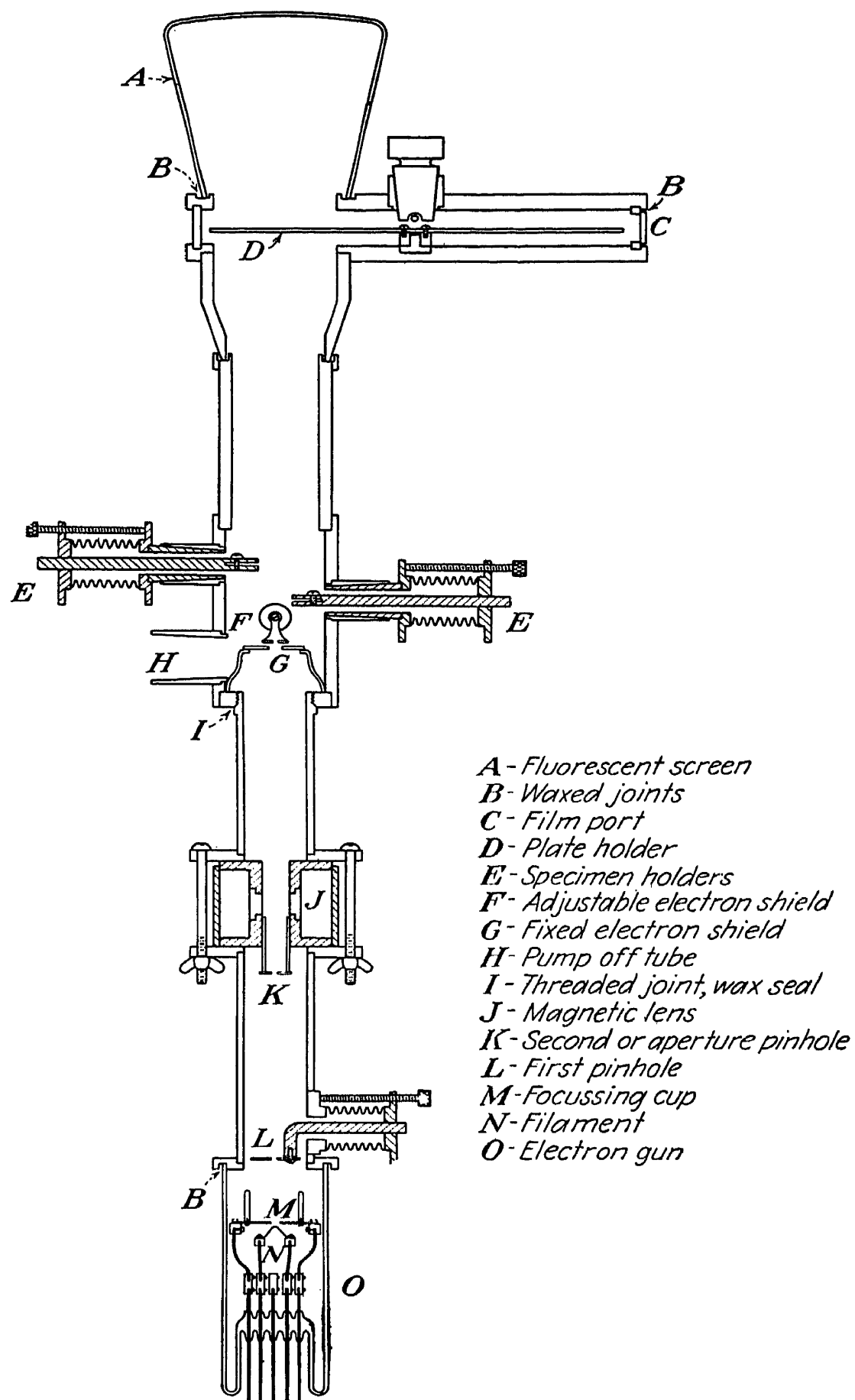


FIG. 24-8.—Section drawing of the camera in Fig. 24-7.

insulated copper wire wound on an iron spool, which fits snugly inside an enclosing iron cylinder after the winding is finished. The  $\frac{1}{2}$ -in.-diameter core of the spool contains a brass equatorial ring, represented by the white gap in the crosshatched iron lens case. Since brass is nonmagnetic, the ring acts as an air "flux gap," which permits the magnetic field set up in the iron to leak out into the region of the electron beam at the center. This lens affects the cathode-ray beam much as a glass converging lens affects a beam of light rays. Its focal length decreases as the (steady direct) current through the coil of wire is increased. Thus a storage battery and rheostat permit one to adjust the focal length of the lens until the clearest pattern appears on the screen *A*. The lens current is about  $\frac{1}{2}$  amp., and a 12-volt storage battery supplies it.

The design of electron guns, magnetic and electrostatic electron lenses, etc., comes in the field of "electron optics," which has developed rapidly in the last 15 years because of its importance in vacuum tubes, electron microscopes, television, cathode-ray oscilloscopes, etc. Space limitations will not permit even an outline of this subject here, but it has been covered elsewhere.<sup>1</sup> A most useful equation applying to magnetic lenses of the type shown in Fig. 24-8 is

$$\frac{1}{f} = \frac{0.022}{V} \int_{-\infty}^{\infty} H^2 dz \quad (24-12)$$

where  $f$  is the focal length of the lens in centimeters,  $V$  is the energy of the electrons in the beam in electron volts,  $H$  is the magnetic field strength in oersteds at any point  $P$  on the axis  $ZZ$ , and  $z$  is the distance of  $P$  from the lens center  $O$  (Fig. 24-9).

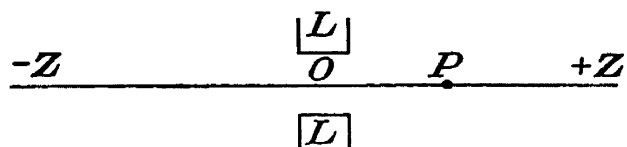


FIG. 24-9.—To explain formula (24-12) for a magnetic lens.

In Fig. 24-8, the electron beam emerging from the lens  $J$  passes through the shields  $F$  and  $G$ , which play a role equivalent to that of the guard pinhole  $C$  (Fig. 17-1) in an x-ray collimator. The beam strikes the surface of the specimen, mounted on  $H$  (Fig. 24-8), at a grazing angle of the order of  $1^\circ$ . The diffracted rays then strike the photographic plate or film at  $D$  or the fluorescent screen at  $A$ , so that the pattern may be observed visually and photographed.

The use of a magnetic lens  $J$  does not mean that one can permit a broad beam of electrons to pass through the lens and merely adjust the

<sup>1</sup> See, for example, E. Brüche and O. Scherzer, "Geometrische Elektronenoptik," Verlag Julius Springer, Berlin, 1934, especially pp. 82-142 for the theory and design of simple magnetic and electrostatic lenses; also, symposium, *Z. tech. Physik*, **17**, 584 ff. (1936); F. Gray, *Bell System Tech. J.*, **18**, 1 (1939) (electrostatic lenses only); footnote, 2, p. 548; A. L. Hughes, *Am. J. Phys.*, **9**, 204 (1941) (magnetic-lens theory).

lens current until the beam is brought to a focus on the plate *D*. The reason why this scheme will not work is understandable from Fig. 24-10. In the left-hand diagram, suppose a lens at the bottom causes the (light) rays to converge so that they will focus on the plate, as indicated by the dotted lines, when the specimen is absent. If the specimen, represented by a mirror, is introduced, then the reflected rays will still focus on the

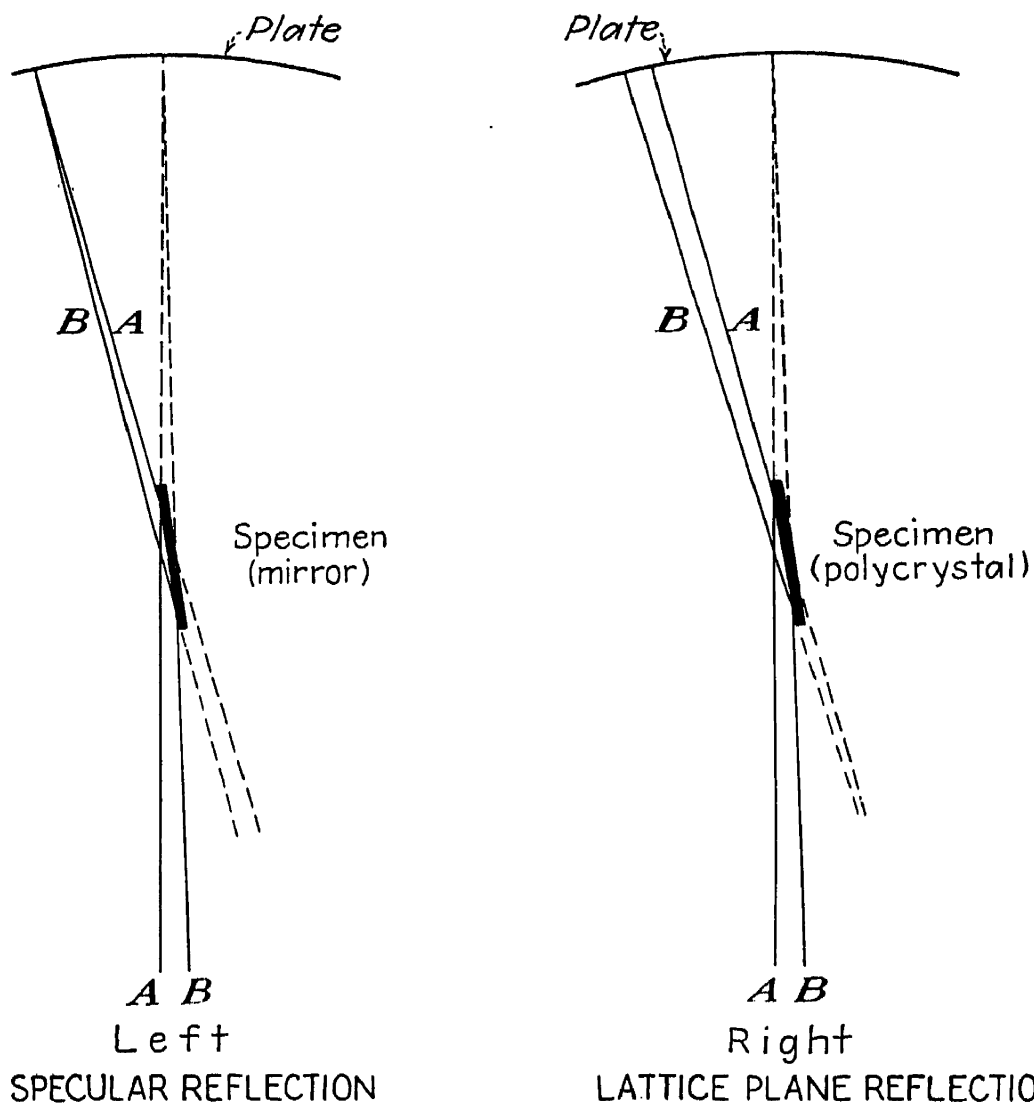


FIG. 24-10.—Showing difference in focusing between true reflection and Bragg reflection.

plate, as desired. Since the rays are really cathode rays, however, and their “reflection” in the specimen obeys Bragg’s law, the situation in the electron diffraction camera is as illustrated in the right-hand diagram of Fig. 24-10. Since each ray is deviated through a fixed angle and the rays trade sides in the beam after reflection, a converging primary beam will generate a diverging diffracted beam. The purpose of the magnetic lens is merely to compensate for the slight divergence of the rays passing through holes *L* and *K* (Fig. 24-8, or through *A* and *B*, Fig. 17-1) and render them accurately parallel so that a fine homogeneous beam of parallel rays strikes the specimen.

The two bellows *E* permit two or more specimens to be manipulated into or out of the beam while the camera is evacuated; the best angle of incidence can be found by adjusting the specimen while observing the pattern on the screen *A*. Process film or slow contrasty lantern-slide plates are suitable for photographing the patterns; as already stated, the exposure time is a matter of a second or so. A shutter controlled through a bellows (not shown) may be used to control the exposure by interrupting the beam between *K* and *L*.

The above discussion has assumed that reflection patterns are being taken. Thin film samples for transmission patterns may be supported on a copper disk with a  $\frac{3}{4}$ -mm. hole in the center or by a wire screen, the disk or screen being mounted on support *E* (Fig. 24-8) as before. The port *H* leads to the vacuum pumps, which should be capable of evacuating the camera to the necessary pressure of about  $10^{-5}$  mm. of mercury in a few minutes. For a discussion of such pumps and their operation, one may consult the book by Strong<sup>1</sup> and his coworkers.

Low-voltage equipment for the diffraction of electrons of a few hundred electron volts energy or less is even more individualistic in design than the high-voltage cameras. The original papers of Davisson and Germer include a description of their low-voltage camera. Such apparatus usually detects the diffracted electrons by a movable Faraday cage connected to an electrometer, rather than by photographic methods. Among numerous types of such apparatus built and described by others, one has also been built and described by the author.<sup>2</sup>

**4. Specimen Preparation.** The principal requirement for transmission specimens is that their thickness be of the order of a millionth of an inch. Such thin films may be picked up by floating them on water and bringing the supporting screen or disk (see preceding section) up under the film gently. Although commercial gold foil is very thin, it is not thin enough. It may be made so by floating it on a strong solution of KCN in water until it is on the point of disintegrating.

Reflection specimens must be prepared with much greater care than for x-ray diffraction. The specimen should be about 1 cm. square and 1 to 3 or 4 mm. thick. One of the centimeter square surfaces to be exposed to the beam should be ground quite flat with a fine abrasive, followed by etching. The extremely slight penetration of the rays makes it quite likely that the pattern from a piece of bright etched copper will be found to be the pattern of some grease from a fingerprint or from some invisible oxide layer like  $\text{Cu}_2\text{O}$  rather than the pattern of

<sup>1</sup> J. Strong, H. V. Neher, A. E. Whitford, C. H. Cartwright, and R. Hayward, "Procedures in Experimental Physics," Chap. III, Prentice-Hall, Inc., New York, 1939.

<sup>2</sup> W. T. Sproull, *Rev. Sci. Instruments*, **4**, 193 (1933).



copper. Grease coatings may usually be removed by immersing the specimen in ether, benzene, distilled water, etc., or by re-etching. Sometimes a reflection pattern can be obtained even though the specimen surface is not so very flat and smooth, but the patterns are usually disappointing. Iron specimens may be etched in 5 per cent nitric acid in pure ethyl alcohol, then 5 per cent picric acid in pure ethyl alcohol. For copper, 10 per cent ammonium sulfate in distilled water is suitable.

**5. General Fields of Application.** Space limitations will permit only an outline of the applications of electron diffraction here, with references for the reader interested in details.

*a. Applications to Solids and Liquids.* Some of the limitations of the method will be mentioned, followed by a list of applications for which the method is adaptable and helpful to a greater or less degree. First the very slight penetration of the electrons limits one to the grazing-incidence method, illustrated for x-rays in Fig. 23-8, or else to films only about a millionth of an inch thick, for transmission patterns. In the former case, the small values of the Bragg angle  $\theta$  rule out the study of concave surfaces, corrosion pits, etc.; in the latter case, it is obvious that comparatively few practical specimens are obtainable as millionth-inch-thick films. The extreme sensitivity of the method is often a handicap: a very slight contamination suffices to give patterns that have no significance in the work at hand. A clean sample lying on a table for an hour will acquire a film of grease from the air thick enough to change the pattern. The need for a vacuum eliminates volatile liquids from consideration as such; only their vapors may be examined. Many surfaces give patterns that are too faint to analyze accurately or, sometimes, no pattern at all. Even when a good pattern is obtained, it may not be one in the Hanawalt-Rinn-Prevel table, and it may be impossible to identify the coating that gave the pattern. However, such a pattern will give information about the grain size and orientation, and it will tell the experimenter that the coating is *not* any of the ones he might have guessed.

Among applications that have been discussed in the literature, often with very helpful results, there are (1) the chemical identity of thin surface films, the growth and orientation of the crystals in such films (for example, coatings sputtered or evaporated in vacuum), and hence the study of corrosion and oxidation of surfaces;<sup>1</sup> (2) measurement of the

<sup>1</sup> H. R. Nelson, *J. Applied Phys.*, **9**, 623 (1938); O. Rüdiger, *Ann. Physik*, **30**, 505 (1937); E. N. C. Andrade, *Trans. Faraday Soc.*, **31**, 1137 (1935); R. O. Jenkins, *Proc. Phys. Soc. (London)*, **47**, 109 (1935); G. I. Finch and A. G. Quarrell, *Proc. Roy. Soc. (London) A*, **141**, 398 (1933); G. P. Thomson, N. Stuart, and C. A. Murison, *Proc. Phys. Soc. (London)*, **45**, 381 (1933); F. Kirchner, *Z. Physik*, **76**, 576 (1932); J. J. Trillat and I. v. Hirsch, *J. phys. radium*, **3**, 185 (1932); I. Iitaka and S. Yama-

electrical conductivity of surface layers;<sup>1</sup> (3) the physical nature of the polishing process and the "Beilby layer,"<sup>2</sup> electrolytic polishing,<sup>3</sup> wear,

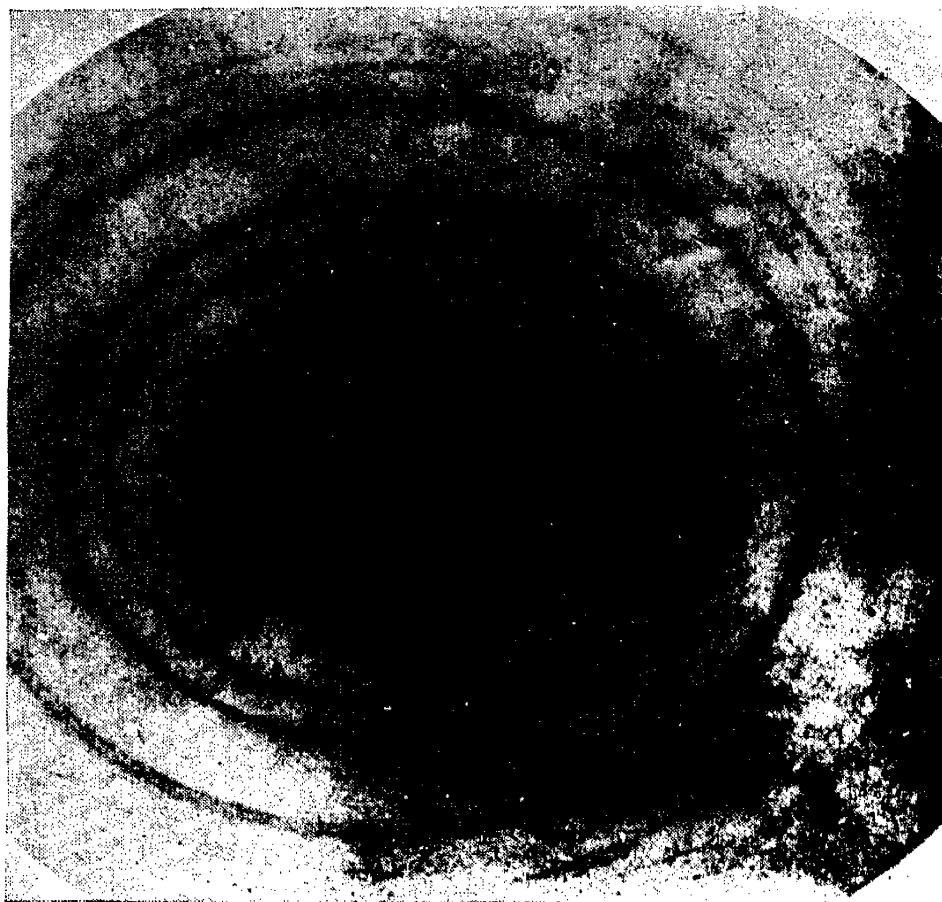


FIG. 24-11.—Transmission pattern of gold foil.

and "running in" of bearings and machinery;<sup>4</sup> (4) lubrication, grease and oil films,<sup>5</sup> graphite as a lubricant,<sup>6</sup> etc.; (5) thin organic and inorganic

guchi, *Nature*, **144**, 1090 (1939); G. D. Preston and L. L. Bircumshaw, *Phil. Mag.*, **22**, 654 (1936); *Automotive and Aviation Ind.*, **91**, 35 (Sept. 1, 1944).

<sup>1</sup> E. I. Alessandrini, *J. Applied Phys.*, **16**, 94 (1945); D. G. Brubaker and M. L. Fuller, *J. Applied Phys.*, **16**, 128 (1945).

<sup>2</sup> P. E. Axon, *Proc. Phys. Soc. (London)*, **52**, 312 (1940); E. Plessing, *Z. Physik*, **113**, 36 (1939); W. Cochrane, *Proc. Roy. Soc. (London) A*, **166**, 228 (1938); J. T. Burwell, *J. Chem. Phys.*, **6**, 749 (1938); S. Dobinski, *Phil. Mag.*, **23**, 397 (1937); L. H. Germer, *Phys. Rev.*, **49**, 163 (1936); G. I. Finch, A. G. Quarrell, and J. S. Roebuck, *Proc. Roy. Soc. (London) A*, **145**, 676 (1934); R. C. French, *Proc. Roy. Soc. (London) A*, **140**, 637 (1933); H. Raether, *Z. Physik*, **86**, 82 (1933); J. A. Darbyshire and K. R. Dixit, *Phil. Mag.*, **16**, 961 (1932).

<sup>3</sup> H. R. Nelson, *Phys. Rev.*, **57**, 559 (1940).

<sup>4</sup> G. I. Finch, A. G. Quarrell, and H. Wilman, *Trans. Faraday Soc.*, **31**, 1078 (1935).

<sup>5</sup> L. T. Andrew, *Trans. Faraday Soc.*, **32**, 607 (1936); H. R. Nelson, *Phys. Rev.*, **44**, 717 (1933); L. H. Germer and K. H. Storks, *J. Chem. Phys.*, **6**, 280 (1938); C. A. Murison, *Phil. Mag.*, **17**, 201 (1934).

<sup>6</sup> R. O. Jenkins, *Phil. Mag.*, **17**, 457 (London) (1934); G. I. Finch and H. Wilman, *Proc. Roy. Soc. (London) A*, **155**, 345 (1936).

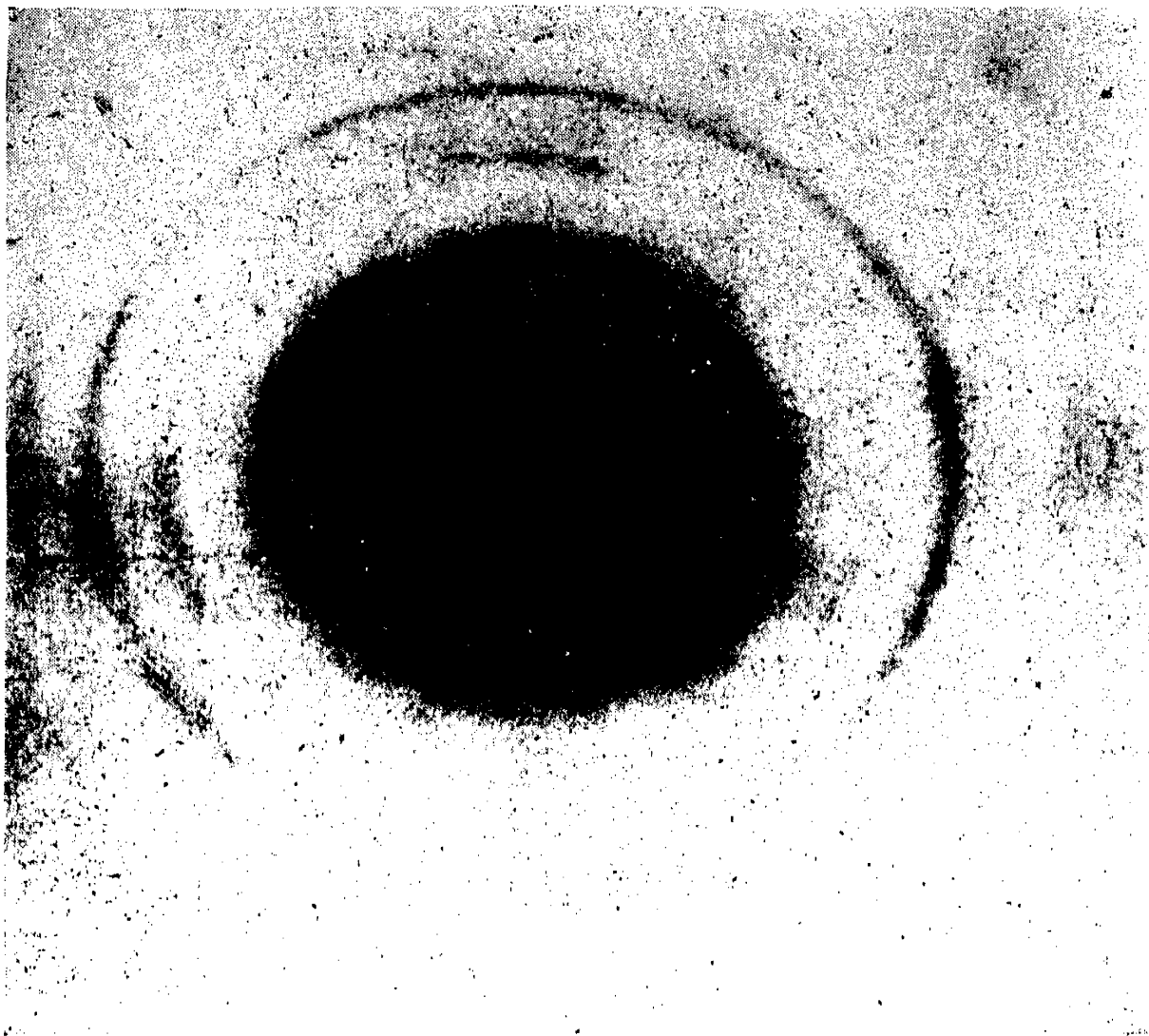


FIG. 24-12. Transmission pattern of oxidized copper foil.

films;<sup>1</sup> (6) study of polymers (vinyl acetate, methyl methacrylate, etc.);<sup>2</sup> (7) electroplating;<sup>3</sup> (8) surface catalysis;<sup>4</sup> (9) mercury<sup>5</sup> and amalgams;<sup>6</sup>

<sup>1</sup> A. Cameron, G. D. Coumoulos, and E. K. Rideal, *Proc. Roy. Soc. (London) A*, **178**, 415, 421 (1941); G. I. Finch, *J. Chem. Soc.*, **140**, 1137 (1938); G. I. Finch and S. Fordham, *Chemistry & Industry*, **56**, 632 (1937); L. H. Germer, *J. Applied Phys.*, **9**, 143 (1938); G. I. Finch and H. Wilman, *Trans. Faraday Soc.*, **33**, 337 (1937); S. Hill and A. H. Woodcock, *Proc. Roy. Soc. (London) A*, **155**, 331 (1936).

<sup>2</sup> G. D. Coumoulos, *Proc. Roy. Soc. (London) A*, **182**, 166 (1943).

<sup>3</sup> Footnote 4, p. 554; A. G. Quarrell, *Proc. Phys. Soc. (London)*, **49**, 279 (1937); G. I. Finch and C. H. Sun, *Trans. Faraday Soc.*, **32**, 852 (1936); G. I. Finch and A. L. Williams, *Trans. Faraday Soc.*, **33**, 564 (1937); W. Cochrane, *Proc. Phys. Soc. (London)*, **48**, 723 (1936).

<sup>4</sup> O. Beeck, A. E. Smith, and A. Wheeler, *Proc. Roy. Soc. (London) A*, **177**, 62 (1941); G. I. Finch, C. A. Murison, N. Stuart, and G. P. Thomson, *Proc. Roy. Soc. (London) A*, **141**, 414 (1933); O. Beeck, *Rev. Mod. Phys.*, **17**, 64 (1945).

<sup>5</sup> G. L. J. Bailey, S. Fordham, and J. T. Tyson, *Proc. Phys. Soc. (London)*, **50**, 63 (1938).

<sup>6</sup> A. E. Aylmer, G. I. Finch, and S. Fordham, *Trans. Faraday Soc.*, **32**, 864 (1936).



FIG. 24-13.—Reflection pattern showing gamma  $\text{Fe}_2\text{O}_3$  on surface of steel.

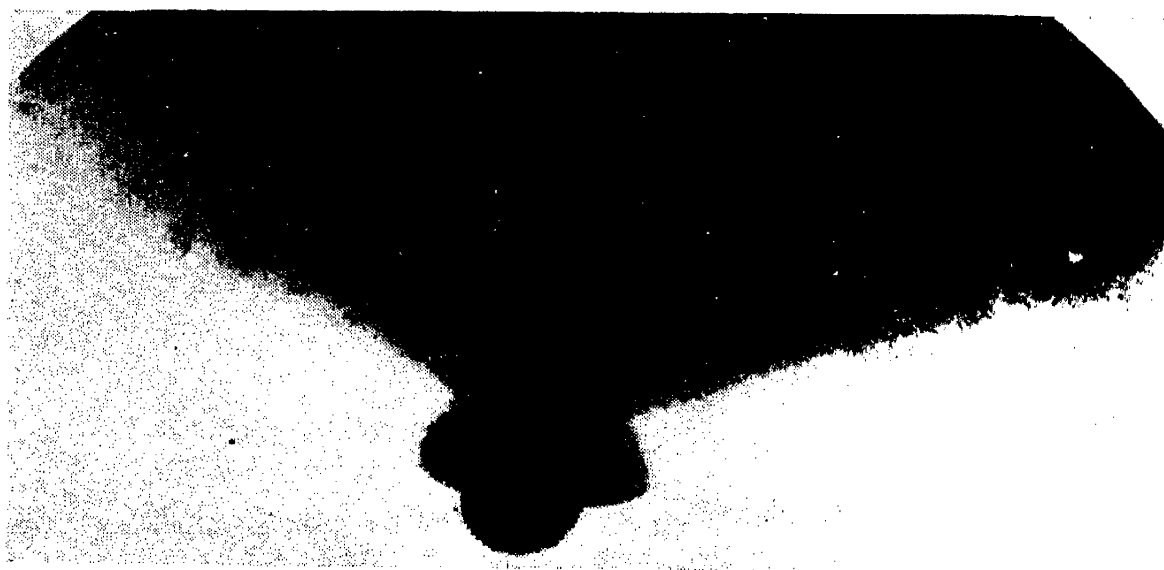


FIG. 24-14.—Reflection pattern of copper showing presence of  $\text{Cu}_2\text{O}$ .

(10) thermionic and photoelectric emitting surfaces;<sup>1</sup> (11) miscellaneous.<sup>2</sup>

*b. Applications to Gases and Vapors.* The applications of electron diffraction to gases and vapors are similar to those outlined for x-ray diffraction in Chap. 22, but they go beyond the capabilities of x-rays for reasons mentioned in Sec. 1*j*. Examples are (1) structure of benzene<sup>3</sup> and other molecules;<sup>4</sup> (2) atomic separations in molecules of  $\text{Br}_2$ ,  $\text{CO}_2$ ,

<sup>1</sup> H. Gaertner, *Phil. Mag.*, **19**, 82 (1935); J. A. Darbyshire, *Proc. Phys. Soc. (London)*, **50**, 635 (1938); J. E. Ruedy, *Rev. Sci. Instruments*, **11**, 292 (1940).

<sup>2</sup> G. P. Thomson and W. Cochran, "Theory and Practice of Electron Diffraction," Chap. XV, p. 211, Macmillan & Company, Ltd., London, 1939.

<sup>3</sup> R. Wierl, *Ann. Physik*, **8**, 521 (1931); L. Pauling and L. O. Brockway, *J. Chem. Phys.*, **2**, 867 (1934); P. L. F. Jones, *Trans. Faraday Soc.*, **31**, 1036 (1935).

<sup>4</sup> J. Y. Beach, *J. Chem. Phys.*, **9**, 54 (1941); S. H. Bauer and J. Y. Beach, *J. Am.*



FIG. 24-15.—Reflection pattern of polished nickel.

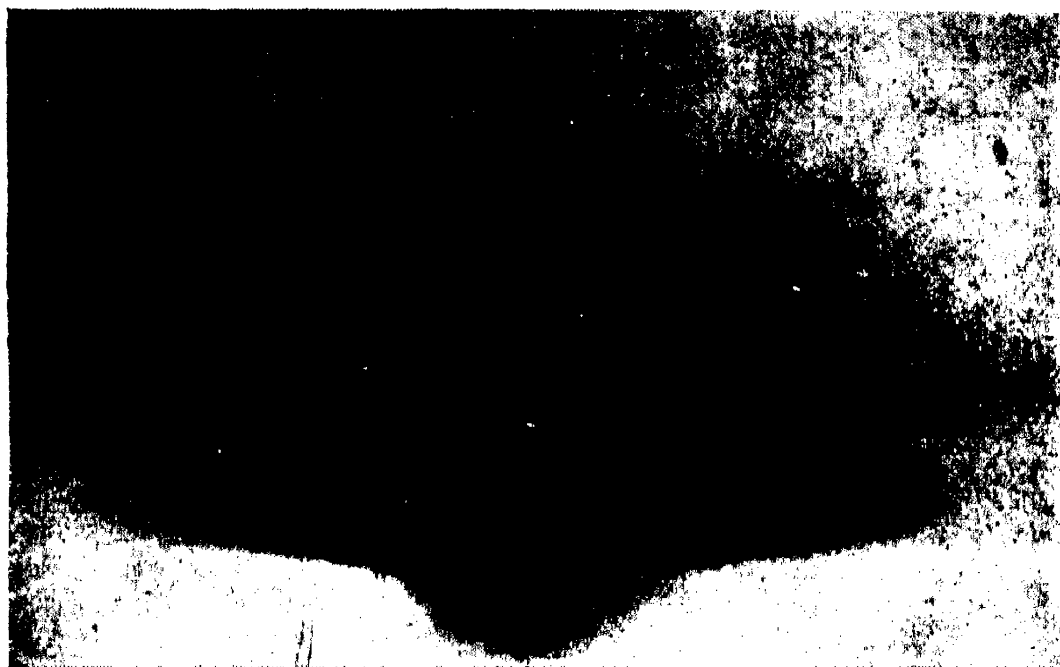


FIG. 24-16.—Reflection pattern of same specimen as in Fig. 24-15, after a light etch.

CS<sub>2</sub>, CCl<sub>4</sub>, cyclohexane, pentane, etc.;<sup>1</sup> (3) comparison of cis  $\begin{array}{c} \text{H}-\text{C}-\text{Cl} \\ \parallel \\ \text{H}-\text{C}-\text{Cl} \end{array}$  and trans  $\begin{array}{c} \text{H}-\text{C}-\text{Cl} \\ \parallel \\ \text{Cl}-\text{C}-\text{H} \end{array}$  dichloroethylene;<sup>2</sup> (4) configuration and atomic

*Chem. Soc.*, **63**, 1934 (1941); M. W. Lister and L. E. Sutton, *Trans. Faraday Soc.*, **37**, 393, 406 (1941).

<sup>1</sup> R. Wierl, *Ann. Physik*, **8**, 521 (1931); S. H. Bauer, *J. Chem. Phys.*, **4**, 406 (1936); A. Becker and E. Kipphan, *Ann. Physik*, **28**, 471 (1937).

<sup>2</sup> R. Wierl, *Ann. Physik*, **13**, 453 (1932).

separations (covalent bonds) in various molecules;<sup>1</sup> (5) radial distribution of electrons in atoms and molecules.<sup>2</sup>

**6. A Few Common Patterns.** A typical electron diffraction pattern of a vapor (arsenic) has already been shown in Fig. 24-6. Figure 24-11 shows the transmission pattern of gold foil, used by most investigators as a wave-length calibration standard, as explained on page 539. The arcing of some of the rings reveals preferential orientation, as with x-rays (Fig. 20-15). In surface films, the direction of preferential orientation is often normal to the surface and parallel to the primary beam. This condition, when present, is revealed by abnormal ring intensities, not arcing, as explained in Sec. 20-7.

Figure 24-12 is a transmission pattern of copper foil, showing that it has oxidized almost completely to  $\text{Cu}_2\text{O}$  at the spot where the pattern was taken. Figure 24-13 is a reflection pattern of 1020 steel etched in nitric acid, showing the presence of a surface coat of "gamma  $\text{Fe}_2\text{O}_3$ ," which has a pattern like  $\text{Fe}_3\text{O}_4$ . Figure 24-14 is a reflection pattern of oxidized copper, showing the presence of  $\text{Cu}_2\text{O}$ . Figure 24-15 is a reflection pattern of polished nickel, showing the amorphous type of pattern characteristic of many polished surfaces. Figure 24-16 is a pattern of the same surface after a light etch with nitric acid, showing some of the rings for Ni and  $\text{NiO}$ .

### QUESTIONS AND PROBLEMS

1. If one arbitrarily says that the atomic-scattering cross section  $E$  for a beam of 50-kv. cathode rays is 100 for copper when the Bragg angle  $\theta$  is  $1^\circ$ , then what is the value of  $E$  when  $\theta$  is  $2^\circ$ ? Ans. 38.2.

2. Does the result of Problem 1 indicate that the intensity at  $\theta = 2^\circ$  is about 38 per cent of the intensity at  $\theta = 1^\circ$ , or should you say that 14.6 per cent is a more accurate figure? Can you suggest how the latter figure was calculated? Is a homogeneous beam of electrons passing through a thin film scattered principally by the atoms, the electrons, the nuclei, or what is the fundamental nature of the electron diffraction process within a crystal?

3. A good specimen for a transmission pattern with 50-kv. electrons should be roughly how thick? Answer the same question for molybdenum  $K_\alpha$  x-rays (order of magnitude only). What property of cathode rays accounts for the large difference between your two answers? Does this property make cathode rays more suitable than x-rays for the study of the molecular structure of gases and vapors? Explain your answer.

4. What property of 50-kv. cathode rays renders them unsuited for taking back-reflection patterns? Is it possible to obtain back-reflection patterns with cathode rays of any sort? With the high-voltage rays, what two types of patterns are obtainable from solids? What is the order of magnitude of the exposure time for such patterns?

5. The lattice constant of gold is 4.07 Å. With a gold-foil specimen, one of the rings in its 50-kv. electron pattern has a radius of 0.7 cm. If the specimen-to-film

<sup>1</sup> L. O. Brockway, *Rev. Modern Phys.*, **8**, 231 (1936).

<sup>2</sup> J. Walter and J. Y. Beach, *J. Chem. Phys.*, **8**, 601 (1940).

distance is 30 cm., find the Miller indices of the  $d$  spacing involved, without using any trigonometric functions. (Gold is face-centered cubic.) *Ans.* (111).

6. If the high voltage is not known more accurately than about  $\pm 10$  kv., how does one determine the  $d$  spacings from the pattern of an unknown material? How should you account for the appearance of a ring at  $d = 4.00$  Å. in the electron pattern of gold foil?

7. What are Kikuchi lines? What is a cross-grating electron pattern? What sort of specimens give patterns in which they may be found? Briefly outline the theory accounting for their appearance.

8. Are electron beams refracted? Is the index of refraction more or less than 1? Is its departure from 1 negligible for high-voltage rays? For low-voltage rays? How is it related to the photoelectric work function? What is the work function  $W_a$ ?

9. Calculate the wave-length of 50-kv. cathode rays, neglecting the relativity correction. Including the correction. *Ans.* 0.548 Å; 0.534 Å.

10. With  $\frac{1}{2}$  amp. direct current flowing through its coil, the axial magnetic field strength at the center of a magnetic lens of the type shown in Fig. 24-8 is 200 oersteds. At 1 cm. from the center along the axis, it is 50 oersteds; at 2 cm., 25 oersteds; at 3 cm., 10 oersteds; at 4 cm., 5 oersteds; at 5 cm., 2 oersteds; beyond 5 cm., it is negligible. What is the focal length of such a lens for 44-kv. cathode rays, roughly? What is the purpose of such a lens in an electron diffraction camera? *Ans.* 42 cm.

11. Name two types of electron gun commonly used for electron diffraction. Are the patterns usually recorded on x-ray film? If not, on what kind are they recorded? Should you expect x-rays to be generated in a high-voltage electron diffraction camera? If so, what can be said regarding their intensity? Explain.

12. Outline the technique of sample preparation. What degree of vacuum is required in an electron diffraction camera? How can gases or vapors be studied in such a vacuum?

13. What are some of the limitations of the electron diffraction method in practical work? Name the more important fields to which it has been applied. Who discovered electron diffraction? When?





# APPENDIX

TABLE I.—MISCELLANEOUS DATA FOR THE X-RAY WORKER

1 radian = 57.29578 degrees      1 degree = 0.017453 radian  
 Napierian log base  $e = 2.7182818$        $\pi = 3.14159265$   
 $\sqrt{2} = 1.41421$        $\sqrt{3} = 1.73205$        $1/\pi = 0.31831$   
 1 centimeter = 0.39370 inch =  $10^8$  angstroms =  $10^4$  microns  
 1,000 x-units = 1.00203 angstroms.      1 inch = 2.540005 centimeters  
 1 electron volt =  $1.6008 \times 10^{-12}$  ergs, equivalent to  $1.16 \times 10^4$  degrees Kelvin  
 1 e.s.u. of potential = 300 volts  
 1 coulomb =  $2.9978 \times 10^9$  e.s.u. of charge  
 1 microfarad =  $8.98776 \times 10^5$  e.s.u. of capacity  
 $c = 2.9978 \times 10^{10}$  cm./sec. Avogadro's number  $N_0 = 6.023 \times 10^{23}$  per mole  
 Electronic charge  $e = 4.8021 \times 10^{-10}$  e.s.u. =  $1.602 \times 10^{-20}$  e.m.u.  
 $e/m = 5.2736 \times 10^{17}$  e.s.u./g.       $h = 6.624 \times 10^{-27}$  erg-sec.  
 Mass of electron  $m = 9.1066 \times 10^{-28}$  gram  
 Mass of atom of unit atomic weight =  $M_0 = 1.66035 \times 10^{-24}$  gram  
 Compton shift at 90 degrees =  $h/mc = 0.024265$  angstrom  
 Boltzmann constant  $k = 1.38 \times 10^{-16}$  erg/°C.  
 Zero degrees centigrade = 273.16 degrees Kelvin.  
 Rydberg constant for infinite mass = 109,737.3 per centimeter  
 True calcite grating space (20 degrees centigrade) = 3,029.512 x-units

	g./cm. <sup>3</sup>
Density of commercial aluminum alloy.....	2.71
Density of 1 per cent carbon steel.....	7.83
Brass, 67 per cent Cu, 33 per cent Zn.....	8.4
95 per cent zinc, 5 per cent aluminum.....	6.80
Copper.....	8.95
Magnesium.....	1.74
Rock salt.....	2.165

TABLE II.—DATA IN THE TEXT

	Table	Page
Electromagnetic spectrum.....	3-1	23
Quantum numbers.....	4-2	62
Electron volts to angstroms.....	(Eq.)	66
Lindemann glass versus beryllium windows.....	7-1	111
Characteristics of constant-voltage transformer.....	7-2	144
X-ray films.....	9-1	176
Recommended thicknesses, lead protection.....	10-1	203-204
Radiographic technique.....	12-1	241, 242, 244
Blocking material.....	12-2	255
Penetrameter dimensions.....	12-3	260
Linear absorption coefficients.....	13-1	290
Schoenflies notation.....	14-3	308
Grating spacings in x-units.....	16-1	338
Grating spacings in angstroms.....	16-2	339
Wave lengths of K lines of Mo and Cu.....	16-3	339
Atomic-structure factors.....	16-4	356
Inclination of cubic lattice planes to zone axes.....	20-1	454
Angles between crystallographic planes in cubic crystals...	20-2	459
Incoherent x-ray scattering function.....	22-1	501
Ionic radii.....	....	517
Interatomic distances.....	....	506, 518, 519
Metal classification.....	....	520
Beta and gamma superstructures.....	....	524

TABLE III.—PRINCIPAL EMISSION LINES OF X-RAY SPECTRA\*  
 (Compiled by J. M. Cork)  
 (Emission Wave Lengths in the K and L Series,  $\lambda$  in x-units  $\times 1000$ )  
 For calcite  $d = 3.02904 \times 10^3$  X.U.

At. no.	Element	K series				L series								
		$\alpha_2$	$\alpha_1$	$\beta_1$	$\beta_2$	$l$	$\alpha_2$	$\alpha_1$	$\eta$	$\beta_1$	$\beta_4$	$\beta_3$	$\beta_2$	$\gamma_1$
11	Sodium.....	11.885		11.594										
12	Magnesium.....	9.869		9.539										
13	Aluminum.....	8.320		7.965										
14	Silicon.....	7.111		6.7545										
15	Phosphorus.....	6.142		5.7921										
16	Sulfur.....	5.3637	5.3613	5.0211										
17	Chlorine.....	4.7212	4.7182	4.3942										
18	Argon.....													
19	Potassium.....	3.7371	3.7337	3.4468										
20	Calcium.....	3.3549	3.3517	3.0834										
21	Scandium.....	3.0284	3.0250	2.7739										
22	Titanium.....	2.7468	2.7432	2.5090										
23	Vanadium.....	2.5021	2.4984	2.2797			24.3							
24	Chromium.....	2.2889	2.2850	2.0806			21.52			21.19				
25	Manganese.....	2.1015	2.0975	1.9062			19.39			19.04				
26	Iron.....	1.9360	1.9321	1.7530		20.12	17.58		19.65	17.22	15.61			
27	Cobalt.....	1.7892	1.7853	1.6174		18.20	15.94		17.77	15.62	.....			
28	Nickel.....	1.6584	1.6545	1.4970	1.4856	16.55	14.53		16.17	14.24	13.14			
29	Copper.....	1.5412	1.5374	1.3894	1.3782	15.19	13.306		14.83	13.03	12.10			
30	Zinc.....	1.4360	1.4322	1.2926	1.2811	13.95	12.23		13.61	11.95	11.16			
31	Gallium.....	1.3409	1.3372	1.2052	1.1938	12.89	11.27		12.56	11.01	.....			
32	Germanium.....	1.2552	1.2513	1.1267	1.1146	11.922	10.415		11.587	10.153				

TABLE III.—PRINCIPAL EMISSION LINES OF X-RAY SPECTRA. \*—(Continued)

At. no.	Element	K series				L series								
		$\alpha_2$	$\alpha_1$	$\beta_1$	$\beta_2$	$l$	$\alpha_2$	$\alpha_1$	$\eta$	$\beta_1$	$\beta_4$	$\beta_3$	$\beta_2$	$\gamma_1$
33	Arsenic.....	1.1774	1.1734	1.0551	1.0428	11.048	9.652	10.711	.....	.....	.....	.....	.....	.....
34	Selenium.....	1.1065	1.1025	0.99013	0.97791	10.272	8.972	9.939	8.718	.....	.....	.....	.....	.....
35	Bromine.....	1.0417	1.0376	0.93087	0.91853	9.564	8.358	9.235	8.109	.....	.....	.....	.....	.....
37	Rubidium.....	0.9278	0.9236	0.82696	0.81476	.....	.....	.....	.....	6.801	6.769	.....	.....	.....
38	Strontium.....	0.8776	0.8734	0.78130	0.76921	7.822	6.849	7.506	6.610	6.392	6.358	.....	.....	.....
39	Yttrium.....	0.8313	0.8271	0.73919	0.72713	.....	6.436	7.031	6.204	6.008	5.974	.....	.....	.....
40	Zirconium.....	0.7885	0.7843	0.70028	0.68850	6.899	6.057	6.594	5.824	5.652	5.619	.....	5.574	5.374
41	Columbium.....	0.7489	0.7446	0.66438	0.65280	6.510	5.718	6.196	5.480	5.330	5.297	.....	5.226	5.024
42	Molybdenum.....	0.71210	0.70783	0.63098	0.61970	.....	5.401	5.836	5.166	5.041	5.005	.....	4.910	.....
44	Ruthenium.....	0.64606	0.64174	0.57131	0.56051	5.486	4.843	.....	4.611	4.513	4.476	.....	4.362	4.173
45	Rhodium.....	0.61637	0.61202	0.54449	0.53396	5.2070	4.5956	4.9112	4.3640	4.2802	4.2447	.....	4.1221	3.9357
46	Palladium.....	0.58860	0.58422	0.51961	0.50928	4.9396	4.3666	4.6502	4.1373	4.0623	4.0257	.....	3.9007	3.7164
47	Silver.....	0.56265	0.55824	0.49622	0.48607	4.6976	4.1538	4.4101	3.9266	3.8611	3.8245	.....	3.6938	3.5149
48	Cadmium.....	0.53831	0.53388	0.47413	0.46429	4.4713	3.9564	4.1875	3.7301	3.6743	3.6364	.....	3.5064	3.3280
49	Indium.....	0.51547	0.51104	0.45365	0.44408	4.2593	3.7724	3.9761	3.5478	3.4990	3.4619	.....	3.3312	3.1513
50	Tin.....	0.49404	0.48961	0.43430	0.42507	4.0633	3.6011	3.7818	3.3779	3.3363	3.2989	.....	3.1679	2.9949
51	Antimony.....	0.47394	0.46943	0.41630	0.40715	3.8803	3.4408	3.5996	3.2184	3.1843	3.1451	.....	3.0166	2.8451
52	Tellurium.....	0.45496	0.45045	0.39928	0.39043	3.7101	3.2910	.....	3.0700	3.0400	3.0013	.....	2.8761	2.7065
53	Iodine.....	0.43698	0.43246	0.38315	0.37466	3.5497	3.1509	.....	2.9309	2.9059	2.8682	.....	2.7461	2.5775
54	Xenon.....	.....	.....	.....	.....	.....	.....	.....	.....	.....	.....	.....	.....	.....
55	Cesium.....	0.40404	0.39953	0.35362	0.34516	3.2596	2.8956	2.9833	2.6778	2.6605	2.6299	.....	2.5064	2.3425
56	Barium.....	0.38891	0.38438	0.34022	0.33222	3.1287	2.7790	2.8571	2.5622	2.5498	2.5110	.....	2.3993	2.2366
57	Lanthanum.....	0.37463	0.37000	0.32726	0.31966	3.0000	2.6688	2.7340	2.4533	2.4438	2.4053	.....	2.2980	2.1372
58	Cerium.....	0.36103	0.35642	0.31501	0.30770	2.8857	2.5651	2.6147	2.3510	2.3442	2.3059	.....	2.2041	2.0443
59	Praesodymium.....	0.34805	0.34340	0.30360	0.29625	2.7781	2.4676	2.5070	2.2539	2.2501	2.2124	.....	2.1148	1.9568

TABLE III.—PRINCIPAL EMISSION LINES OF X-RAY SPECTRA.\*—(Continued)

At. no.	Element	K series					L series							
		$\alpha$		$\beta_1$	$\beta_2$	$l$	$\alpha_1$	$\eta$	$\beta_1$	$\beta_4$	$\beta_3$	$\beta_2$	$\gamma_1$	
		$\alpha_2$	$\alpha_1$											
60	Neodymium.....	0.33596	0.33128	0.29275	0.28573	2.6703	2.3756	2.3653	2.4042	2.1622	2.1622	2.1222	2.0314	1.8738
62	Samarium.....	0.31311	0.30844	0.27250	0.26575	2.4770	2.2057	2.1950	2.2140	1.9936	1.9964	1.9580	1.8781	1.7231
63	Europium.....	0.30267	0.29795	0.26307	0.25645	2.3903	2.1273	2.1163	.....	1.9163	1.9221	1.8827	1.8082	1.6543
64	Gadolinium.....	0.29251	0.28778	0.25394	0.24762	2.3071	2.0526	2.0419	.....	1.8425	1.8493	1.8109	1.7419	1.5886
65	Terbium.....	0.28294	0.27820	0.24551	0.23912	2.2290	1.9823	1.9715	.....	1.7727	1.7814	1.7425	1.6790	1.5266
66	Dysprosium.....	0.27369	0.26895	0.23710	0.23128	2.1540	1.9156	1.9046	1.8922	1.7066	1.7167	1.6777	1.6198	1.4697
67	Holmium.....	0.26499	0.26030	.....	.....	2.0821	1.8521	1.8521	1.8220	1.6435	1.6553	1.6160	1.5637	1.4142
68	Erbium.....	0.25669	0.25198	0.22215	0.21671	2.0151	1.7914	1.7804	1.7548	1.5834	1.5964	1.5579	1.5106	1.3623
69	Thulium.....	0.24861	0.24387	0.21487	.....	1.9511	1.7339	1.7228	1.6923	1.5268	1.5412	1.5023	1.4602	1.3127
70	Ytterbium.....	0.24099	0.23625	0.20834	0.20322	1.8900	1.6789	1.6678	1.6310	1.4725	1.4882	1.4494	1.4128	1.2648
71	Lutecium.....	0.23358	0.22882	0.20171	0.19649	1.8318	1.6264	1.6155	1.5738	1.4207	1.4372	1.3982	1.3672	1.2203
72	Hafnium.....	0.22653	0.22173	0.19515	0.19042	1.7774	1.5770	1.5660	1.5197	1.3711	1.3893	1.3497	1.3235	1.1765
73	Tantalum.....	0.21973	0.21488	0.18911	0.18451	1.7249	1.5298	1.5188	1.4679	1.3242	1.3431	1.3041	1.2819	1.1356
74	Tungsten.....	0.21345	0.20862	0.18422	0.17898	1.6750	1.4844	1.4734	1.4181	1.2792	1.2988	1.2599	1.2420	1.0963
76	Osmium.....	0.20131	0.19645	0.17361	0.16875	.....	1.3987	1.3886	.....	1.1949	.....	.....	1.1688	1.0229
77	Iridium.....	0.19550	0.19065	0.16850	0.16376	.....	1.3598	1.3485	1.2817	1.1554	1.1771	1.1385	1.1329	0.98876
78	Platinum.....	0.19004	0.18523	0.16370	0.15887	1.4964	1.3215	0.3103	1.2403	1.1176	1.1398	1.1016	1.0997	0.95599
79	Gold.....	0.18483	0.17996	0.15902	0.15426	1.4569	1.2850	1.2737	1.2003	1.0813	1.1042	1.0655	1.0680	0.9246
80	Mercury.....	.....	.....	.....	.....	1.4184	1.2495	1.2386	1.1616	1.0465	1.0692	1.0305	1.0377	0.8946
81	Thalium.....	0.17466	0.16980	0.15011	0.14539	1.3819	1.2163	1.2049	1.1254	1.0130	1.0370	0.9985	1.0082	0.8657
82	Lead.....	0.17004	0.16516	0.14606	0.14125	1.3474	1.1841	1.1726	1.0900	0.9808	0.0056	0.9672	0.9808	0.8380
83	Bismuth.....	0.16525	0.16041	0.14025	.....	1.3137	1.1530	1.1415	1.0565	0.9500	0.9750	0.9367	0.9532	0.8114
90	Thorium.....	0.1368	0.1323	0.1169	0.1134	1.1128	0.9658	0.9540	0.8528	0.7636	0.7919	0.7532	0.7919	0.6517
92	Uranium.....	0.1309	0.1264	0.1119	0.1084	1.0649	0.9206	0.9087	0.8035	0.7185	0.7464	0.7088	0.7531	0.6136

\* Reprinted from the "Handbook of Chemistry and Physics" by C. D. Hodgman by permission of the Chemical Rubber Company.

TABLE IV.—EXCITATION POTENTIAL IN KILOVOLTS FOR CHARACTERISTIC X-RAY SPECTRA \*

At. no.	Element	K	L	M	N
11	Sodium.....	1.07			
12	Magnesium.....	1.30			
13	Aluminum.....	1.55			
14	Silicon.....	1.83			
15	Phosphorus.....	2.14			
16	Sulfur.....	2.46			
17	Chlorine.....	2.82			
19	Potassium.....	3.59			
20	Calcium.....	4.03			
21	Scandium.....	4.49			
22	Titanium.....	4.95			
23	Vanadium.....	5.45			
24	Chromium.....	5.98			
25	Manganese.....	6.54			
26	Iron.....	7.10			
27	Cobalt.....	7.71			
28	Nickel.....	8.29			
29	Copper.....	8.86			
30	Zinc.....	9.65	1.20		
31	Gallium.....	10.4	1.31		
32	Germanium.....	11.1	1.41		
33	Arsenic.....	11.9	1.52		
34	Selenium.....	12.7	1.64		
35	Bromine.....	13.5	1.77		
37	Rubidium.....	15.2	2.05		
38	Strontium.....	16.1	2.19		
39	Yttrium.....	17.0	2.36		
40	Zirconium.....	18.0	2.51	0.43	0.05
41	Columbium.....	19.0	2.68	0.48	0.05
42	Molybdenum.....	20.0	2.87	0.51	0.06
44	Ruthenium.....	22.1	3.24	0.59	0.06
45	Rhodium.....	23.2	3.43	0.62	0.07
46	Palladium.....	24.4	3.64	0.67	0.08
47	Silver.....	25.5	3.79	0.72	0.10
48	Cadmium.....	26.7	4.07	0.77	0.11
49	Indium.....	27.9	4.28	0.83	0.12
50	Tin.....	29.1	4.49	0.88	0.13
51	Antimony.....	30.4	4.69	0.94	0.15
52	Tellurium.....	31.8	4.93	1.01	0.17
53	Iodine.....	33.2	5.18	1.08	0.19
55	Cesium.....	35.9	5.71	1.21	0.23
56	Barium.....	37.4	5.99	1.29	0.25
57	Lanthanum.....	38.7	6.26	1.36	0.27

TABLE IV.—EXCITATION POTENTIAL IN KILOVOLTS FOR CHARACTERISTIC X-RAY SPECTRA.\*—(Continued)

At. no.	Element	K	L	M	N
58	Cerium.....	40.3	6.54	1.43	0.29
59	Praeseodymium.....	41.9	6.83	1.51	0.30
60	Neodymium.....	43.6	7.12	1.58	0.32
62	Samarium.....	46.8	7.73	1.72	0.35
63	Europium.....	48.6	8.04	1.80	0.36
64	Gadolinium.....	50.3	8.37	1.88	0.38
65	Terbium.....	52.0	8.70	1.96	0.40
66	Dysprosium.....	53.8	9.03	2.04	0.42
67	Holmium.....	55.8	9.38	2.13	0.43
68	Erbium.....	57.5	9.73	2.22	0.45
69	Thulium.....	59.5	10.1	2.31	0.47
70	Ytterbium.....	61.4	10.5	2.41	0.50
71	Lutecium.....	63.4	10.9	2.50	0.51
72	Hafnium.....	65.4	11.3	2.60	0.54
73	Tantalum.....	67.4	11.7	2.71	0.57
74	Tungsten.....	69.3	12.1	2.81	0.59
76	Osmium.....	73.8	13.0	3.05	0.64
77	Iridium.....	76.0	13.4	3.17	0.67
78	Platinum.....	78.1	13.9	3.30	0.71
79	Gold.....	80.5	14.4	3.43	0.79
80	Mercury.....	82.9	14.8	3.57	0.82
81	Thallium.....	85.2	15.3	3.71	0.86
82	Lead.....	87.6	15.8	3.85	0.89
83	Bismuth.....	90.1	16.4	4.01	0.96
90	Thorium.....	109.	20.5	5.17	1.33
92	Uranium.....	115.	21.7	5.54	1.44

\* M. Siegbahn, "Spectroscopie der Röntgenstrahlen," Verlag Julius Springer, Berlin, 1924.

TABLE V.—ABSORPTION COEFFICIENTS FOR X-RAYS AND GAMMA RAYS\*  
 Mass Absorption Coefficients  
 $\lambda = 2.50 - 0.005 \times 10^3 \text{ X.U.}$

$\lambda, \text{X.U.} \times 1000$	H	Li	Be	B	C	N	O	Ne	Na	Mg	Al
2.50	0.52	4.0	6.1	9.1	17.8	.....	44.5	100	128	.....	.....
2.29	.....	.....	.....	.....	15.0	.....	36.4	75.5	.....	.....	.....
1.93	0.50	2.10	3.05	4.7	8.75	14.0	21.7	49.0	61.3	.....	.....
1.74	.....	.....	.....	.....	.....	.....	.....	.....	.....	See	See
1.656	.....	.....	.....	.....	.....	.....	.....	.....	.....	.....	.....
1.539	0.48	1.10	1.60	2.45	4.52	7.45	11.1	24.0	32.1	.....	.....
1.484	.....	.....	.....	.....	.....	.....	.....	.....	.....	.....	.....
1.432	.....	.....	.....	.....	.....	.....	.....	.....	.....	.....	.....
1.389	0.47	0.86	1.25	1.87	3.35	5.50	8.1	17.0	23.4	.....	.....
1.377	.....	.....	.....	.....	.....	.....	.....	.....	.....	next	next
1.293	.....	.....	.....	.....	.....	.....	.....	.....	.....	.....	.....
1.280	.....	.....	.....	.....	.....	.....	.....	.....	.....	.....	.....
1.235	0.46	0.67	0.95	1.35	2.42	3.95	5.7	12.4	17.1	.....	.....
1.104	.....	.....	.....	.....	.....	.....	.....	.....	.....	.....	.....
1.071	.....	.....	.....	.....	.....	.....	.....	.....	.....	.....	.....
1.038	.....	.....	.....	.....	.....	.....	.....	.....	.....	page	page
1.000	0.45	0.43	0.55	0.76	1.36	2.10	3.13	6.5	8.8	.....	.....
0.980	.....	.....	.....	.....	1.20	.....	.....	.....	.....	.....	.....
0.949	.....	.....	.....	.....	.....	.....	.....	.....	.....	.....	.....
0.932	.....	.....	.....	.....	1.05	.....	.....	.....	.....	.....	.....
0.900	.....	.....	.....	.....	.....	.....	.....	.....	.....	.....	.....
0.892	.....	.....	.....	.....	.....	.....	.....	.....	.....	.....	.....
0.880	0.440	0.350	0.425	0.580	0.990	1.50	2.20	4.55	6.10	8.34	9.75
0.862	.....	.....	.....	.....	.....	.....	.....	.....	.....	.....	.....
0.850	.....	.....	.....	.....	0.907	.....	.....	.....	.....	.....	8.85
0.814	.....	.....	.....	.....	0.814	.....	.....	.....	.....	.....	7.85
0.780	.....	.....	.....	.....	0.750	.....	.....	.....	.....	.....	6.86
0.710	0.435	0.260	0.315	0.365	0.598	0.870	1.22	2.50	3.30	4.30	5.22
0.680	.....	.....	.....	.....	0.550	.....	.....	.....	.....	.....	4.52
0.631	0.435	0.225	0.255	0.305	0.467	0.610	0.900	1.80	2.30	3.0	3.73
0.618	.....	.....	.....	.....	.....	.....	.....	.....	.....	.....	.....
0.560	.....	.....	.....	.....	0.370	.....	.....	.....	.....	.....	2.60
0.497	0.435	0.198	0.210	0.220	0.315	0.400	0.520	0.930	1.18	1.52	1.90
0.485	.....	.....	.....	.....	0.308	.....	.....	.....	.....	.....	1.77
0.476	0.430	.....	.....	0.215	0.304	.....	0.485	.....	.....	.....	1.74
0.424	.....	.....	.....	.....	.....	.....	.....	.....	.....	.....	1.23
0.417	0.390	0.180	0.185	0.198	0.256	0.310	0.372	0.580	0.750	0.940	1.170
0.383	.....	.....	.....	.....	0.230	.....	.....	.....	.....	.....	0.950
0.331	.....	.....	.....	.....	.....	.....	.....	.....	.....	.....	.....
0.260	0.385	0.156	0.166	0.175	0.185	0.200	0.210	0.270	0.305	0.343	0.402
0.220	.....	.....	.....	.....	0.178	.....	.....	.....	.....	.....	0.300
0.200	0.375	0.151	0.160	0.165	0.175	0.180	0.183	0.210	0.225	0.250	0.270
0.184	.....	.....	.....	.....	0.166	.....	.....	.....	.....	.....	0.246
0.178	.....	.....	.....	.....	0.164	.....	.....	.....	.....	.....	0.235
0.175	0.360	0.144	0.150	0.155	0.163	0.166	0.169	0.185	0.195	0.205	0.228
0.158	.....	.....	.....	.....	0.160	.....	.....	.....	.....	.....	0.208
0.155	.....	.....	.....	.....	.....	.....	.....	.....	.....	.....	.....
0.146	0.340	.....	.....	.....	0.155	.....	0.162	.....	0.170	0.176	0.195
0.142	0.330	.....	.....	.....	0.153	.....	.....	.....	.....	.....	0.191
0.130	0.320	0.132	.....	0.149	0.152	.....	0.157	.....	0.160	0.168	0.186
0.120	.....	.....	.....	.....	0.150	.....	0.154	.....	.....	0.163	0.172
0.113	0.310	.....	.....	.....	0.147	.....	0.153	.....	0.155	0.160	0.166
0.107	.....	.....	.....	.....	.....	.....	.....	.....	.....	.....	.....
0.098	0.280	0.125	.....	0.138	0.142	.....	0.144	.....	0.150	0.152	0.156
0.080	0.255	.....	.....	.....	0.137	.....	.....	.....	.....	.....	0.146
0.072	0.250	0.118	.....	0.132	0.136	.....	0.137	.....	0.139	0.140	0.143
0.064	0.245	0.110	.....	0.126	0.130	.....	0.130	.....	0.130	0.130	0.130
0.050	.....	.....	.....	.....	.....	0.120	.....	.....	.....	.....	0.115
0.040	0.205	.....	.....	.....	0.110	.....	.....	.....	.....	.....	0.105
0.030	0.180	.....	.....	.....	0.095	.....	.....	.....	.....	.....	0.093
0.024	0.165	.....	.....	.....	0.080	.....	.....	.....	.....	.....	0.079
0.010	0.117	.....	.....	.....	0.059	.....	.....	.....	.....	.....	0.058
0.005	0.078	.....	.....	.....	0.0385	.....	.....	.....	.....	.....	0.0380

\* Reprinted from the "Handbook of Chemistry and Physics" by permission of the Chemical Rubber Company.



TABLE V.—ABSORPTION COEFFICIENTS FOR X-RAYS AND GAMMA RAYS.\*—(Continued)

$\lambda$ , X.U. $\times 1000$	Mg	Al	S	Cl	A	Ca	Fe	Ni	Cu	Zn	Br	Sr	Mo
2.50	161	193	355	400	475	620	147	180	197	.....	.....	.....	.....
2.29	.....	150	285	315	355	480	115	137	153	.....	.....	.....	.....
1.93	77.2	93.5	173	198	235	306	71.2	89.5	96.2	.....	.....	.....	.....
1.74	.....	83.0	.....	.....	.....	.....	54	.....	.....	.....	.....	.....	.....
1.656	.....	60.7	110	126	143	195	465	59.2	63.5	See	See	.....	See
1.539	40.8	49.0	91	103	114	163	410	48.0	50.9	.....	.....	.....	.....
1.484	.....	.....	.....	.....	.....	.....	325	40.5	.....	.....	.....	.....	.....
1.432	.....	40.0	75	85	93	130	338	325	42	.....	.....	.....	.....
1.389	31.5	36.8	68.5	76.7	85.7	125	285	275	38.5	.....	.....	.....	.....
1.377	.....	.....	.....	.....	.....	.....	252	275	37.0	.....	.....	.....	.....
1.293	.....	29.8	55.3	60	72	102	212	233	307	next	next	.....	next
1.280	.....	28.8	.....	.....	.....	.....	.....	225	260	.....	.....	.....	.....
1.235	21.4	26.3	49.5	55.5	62.5	90	181	208	252	.....	.....	.....	.....
1.104	.....	18.6	38.0	44	50	67	135	155	230	.....	.....	.....	.....
1.071	.....	.....	.....	.....	.....	.....	.....	.....	175	.....	.....	.....	.....
1.038	.....	.....	.....	.....	.....	.....	.....	.....	.....	.....	.....	.....	.....
1.000	11.8	14.12	26.7	29.7	34.5	49	100	121	130	page	page	.....	page
0.980	.....	.....	.....	.....	.....	.....	.....	.....	.....	.....	.....	.....	.....
0.949	.....	12.0	22.0	24.5	.....	42	86	99	114	.....	.....	.....	.....
0.932	.....	.....	.....	.....	.....	.....	.....	.....	.....	.....	.....	.....	.....
0.900	.....	10.4	.....	.....	.....	.....	74.5	86.5	98.5	.....	.....	.....	.....
0.892	.....	.....	.....	.....	.....	.....	.....	.....	.....	.....	.....	.....	.....
0.880	.....	.....	18.2	20.7	24.0	34.8	69.5	82	91.2	103	.....	.....	36.0
0.862	.....	.....	.....	.....	.....	.....	.....	.....	.....	.....	.....	.....	.....
0.850	.....	.....	.....	.....	.....	.....	63.5	74	84.5	96.5	.....	.....	.....
0.814	See	.....	.....	.....	.....	.....	57	66	75.7	86	.....	.....	28
0.780	.....	.....	.....	.....	.....	.....	50.5	59.5	67.5	77	.....	.....	.....
0.710	.....	.....	9.90	11.6	13.0	18.6	38.5	48.1	51.0	59.0	80	106	19.9
0.680	.....	.....	.....	.....	.....	.....	32.7	41	45.3	52.7	.....	.....	.....
0.631	.....	.....	6.90	8.40	9.80	13.3	27.0	34	36.2	41.0	56.8	72.5	15.0
0.618	.....	.....	.....	.....	.....	.....	.....	.....	.....	.....	.....	.....	12.5
0.500	.....	.....	.....	.....	.....	.....	18.2	24	25.5	30.7	.....	.....	88.0
0.497	.....	.....	3.50	4.20	5.50	6.60	13.9	17.9	18.4	21.0	32.0	40.5	50.2
0.485	.....	.....	.....	.....	.....	.....	12.4	15.4	16.9	19.5	.....	.....	.....
0.476	.....	.....	.....	.....	.....	.....	.....	.....	16.6	.....	.....	.....	42
0.424	.....	.....	.....	.....	.....	.....	.....	.....	.....	.....	.....	.....	.....
0.417	.....	.....	2.10	2.47	2.95	3.97	8.45	10.5	11.45	12.3	19.0	24.0	30.0
0.380	.....	.....	.....	.....	.....	.....	6.32	7.70	8.42	9.95	.....	.....	22
0.331	preceding	.....	.....	.....	.....	.....	.....	.....	.....	.....	.....	.....	.....
0.260	.....	.....	0.650	0.750	0.850	1.10	2.28	2.89	3.16	3.58	5.30	6.50	8.20
0.220	.....	.....	.....	.....	.....	.....	1.42	1.80	2.00	2.32	.....	.....	.....
0.200	.....	.....	0.400	0.445	0.500	0.630	1.10	1.45	1.55	1.78	2.4	3.32	4.30
0.184	.....	.....	.....	.....	.....	.....	.....	1.24	.....	.....	.....	.....	.....
0.178	.....	.....	.....	.....	.....	.....	.....	.....	1.15	.....	.....	.....	.....
0.175	.....	.....	0.335	0.341	0.400	0.460	0.800	1.05	1.12	1.26	1.90	2.24	2.95
0.158	.....	.....	.....	.....	.....	.....	0.640	0.815	0.862	0.990	.....	.....	.....
0.155	.....	.....	.....	.....	.....	.....	.....	.....	.....	.....	.....	.....	.....
0.146	.....	.....	0.249	0.280	.....	0.345	0.520	.....	0.680	.....	.....	.....	.....
0.142	.....	.....	.....	.....	.....	.....	0.515	0.630	0.670	0.780	.....	.....	1.55
0.130	.....	.....	0.220	0.230	.....	0.290	0.424	.....	0.551	.....	.....	.....	.....
0.120	.....	.....	0.200	.....	.....	.....	0.368	0.430	0.455	0.537	.....	.....	.....
0.113	.....	page	0.189	0.195	.....	0.230	0.337	.....	0.422	.....	.....	.....	.....
0.107	.....	.....	.....	.....	.....	.....	.....	.....	.....	.....	.....	.....	.....
0.098	.....	.....	0.166	0.176	.....	0.200	0.265	.....	0.325	.....	.....	.....	0.790
0.080	.....	.....	.....	0.164	.....	.....	0.235	0.264	0.268	0.308	.....	.....	.....
0.072	.....	.....	0.150	0.158	.....	0.180	0.202	.....	0.232	.....	.....	.....	.....
0.064	.....	.....	0.139	0.142	.....	0.155	0.178	.....	0.193	.....	.....	.....	0.413
0.050	.....	.....	.....	.....	.....	.....	0.140	.....	0.155	.....	.....	.....	.....
0.040	.....	.....	.....	.....	.....	.....	0.118	.....	0.126	.....	.....	.....	.....
0.030	.....	.....	.....	.....	.....	.....	0.095	.....	0.100	.....	.....	.....	.....
0.024	.....	.....	.....	.....	.....	.....	0.080	.....	0.081	.....	.....	.....	.....
0.010	.....	.....	.....	.....	.....	.....	0.058	.....	0.057	.....	.....	.....	.....
0.005	.....	.....	.....	.....	.....	.....	.....	.....	0.0380	.....	.....	.....	.....

\* Reprinted from the "Handbook of Chemistry and Physics" by permission of the Chemical Rubber Company.

TABLE V.—ABSORPTION COEFFICIENTS FOR X-RAYS AND GAMMA RAYS.\*—(Continued)

$\lambda$	Zn	Br	Mo	Ag	Sn	I	Ba	Ta	W	Pt	Au	Pb	Bi	U
2.50	228	...	...	710	850	...	...	...	...	596	...	...	...	...
2.29	180	...	...	550	670	...	...	...	...	480	...	...	...	...
1.93	110	...	...	405	470	...	...	...	300	358	385	428	...	...
1.74	...	...	...	...	...	...	...	...	...	...	...	...	...	...
1.656	72.5	...	...	285	...	...	...	...	...	228	...	...	...	...
1.539	58.6	89	...	217	247	290	...	...	176	202	213	230	...	...
1.484	...	...	...	...	...	...	...	...	...	...	...	...	...	...
1.432	49.3	...	...	192	220	...	...	...	130	172	179	202	...	...
1.389	45.2	...	...	174	209	...	...	...	...	155	166	185	...	...
1.377	...	...	...	...	...	...	...	...	...	...	...	...	...	...
1.293	30	...	...	146	176	...	...	...	...	132	138	154	...	...
1.280	36	...	...	127	146	...	...	...	...	...	...	...	...	...
...	287	...	...	...	...	...	...	...	...	...	...	...	...	...
1.235	250	...	...	125	140	...	...	...	95	115	122	137	...	...
1.104	208	...	...	96.5	115	...	...	...	...	99	107	120	...	...
1.071	...	...	...	...	...	...	...	...	...	77.5	...	...	...	...
...	...	...	...	...	...	...	...	...	...	198	...	...	...	...
1.038	...	...	...	...	...	...	...	...	...	...	76.5	...	...	...
...	...	...	...	...	...	...	...	...	...	...	184	...	...	...
1.000	145	...	52	73.0	86.0	...	...	...	...	165	174	75	...	...
0.980	...	...	...	...	...	...	...	...	...	155	168	73	...	...
0.949	129	...	...	63.0	75.5	...	...	...	...	146	156	68	...	...
...	...	...	...	...	...	...	...	...	...	...	168	...	...	...
0.932	...	...	...	...	...	...	...	...	...	136	148	159	...	...
...	...	...	...	...	...	...	...	...	...	184	...	...	...	...
0.900	112	150	...	54.2	65.0	...	...	...	...	168	134	145	...	...
...	...	...	...	...	...	...	...	...	...	...	182	...	...	...
0.892	...	...	...	...	...	...	...	...	...	165	178	142	...	...
...	...	...	...	...	...	...	...	...	...	201	...	...	...	...
0.880	...	...	...	50	60	...	...	...	...	195	170	135	...	...
0.862	...	...	...	...	...	...	...	...	...	185	163	130	...	...
...	See	...	...	...	...	...	...	...	...	...	193	...	...	...
0.850	...	...	...	46	56	...	...	...	...	179	186	124	...	...
0.814	...	...	...	41	49.5	...	...	...	...	160	167	111	...	...
...	...	...	...	...	...	...	...	...	...	...	...	150	...	...
0.780	...	...	...	36	44.5	...	...	...	...	144	150	136	...	...
...	...	...	...	...	...	...	...	...	...	...	...	166	...	...
0.710	...	...	...	27.5	34.0	38.5	42.0	100	104	115	120	136	...	...
0.680	...	...	...	23.5	28.4	...	...	...	...	102	108	120	...	...
0.631	...	...	...	19.6	23.0	26.4	31.1	72	75	84.5	87	98	...	...
0.618	...	...	...	...	...	...	...	...	...	...	...	...	...	...
0.560	...	...	...	13.3	16.2	...	...	...	...	62	66	75	...	...
0.497	...	...	...	10.5	11.8	15.6	17.8	36	38	47	48.5	52.8	...	...
0.485	...	...	...	9.8	11.1	...	...	...	...	...	...	...	...	...
...	...	...	...	62.5	...	...	...	...	...	...	...	...	...	...
0.476	...	...	...	60	...	...	...	...	...	42	...	47.5	...	...
0.424	...	...	...	43.5	8.0	...	...	...	...	...	...	...	...	...
...	...	...	...	...	46.0	...	...	...	...	...	...	...	...	...
0.417	...	...	...	41	45	9.2	10.5	21.5	22.5	27.4	28.4	32.0	...	...
0.380	...	...	...	31.2	34	...	...	...	17.3	21.1	22	26.4	27.8	...
0.331	...	...	...	21.7	24.5	...	5.4	...	...	...	...	18.1	19.5	...
...	preceeding	...	...	...	...	...	28.0	...	...	...	...	...	...	...
0.260	...	...	...	11.4	12.8	14.2	16.1	6.7	6.85	8.0	8.3	10.0	11.0	...
0.220	...	...	...	7.05	7.80	...	...	...	4.25	5.25	5.50	5.92	6.4	...
0.200	...	...	...	5.48	6.20	7.0	8.0	3.4	3.50	4.25	4.40	4.90	5.1	5.40
0.184	...	...	...	4.45	...	...	...	2.8	...	3.45	3.60	4.05	4.2	...
...	...	...	...	...	...	...	...	11.8	...	...	...	...	...	...
0.178	...	...	...	...	...	...	...	...	2.7	3.16	3.30	3.55	...	...
...	...	...	...	...	...	...	...	...	11.3	...	...	...	...	...
0.175	...	...	...	3.96	4.50	5.10	5.70	10.0	10.5	2.97	3.13	3.48	...	3.95
0.158	...	...	...	3.00	3.40	...	...	...	8.6	2.45	2.43	2.60	...	...
...	...	...	...	...	...	...	...	...	...	9.40	...	...	...	...
0.155	...	...	...	...	...	...	...	...	...	...	2.30	...	...	...
...	...	...	...	...	...	...	...	...	...	...	8.80	...	...	...
0.146	...	...	...	2.48	2.66	...	...	6.75	...	7.60	7.85	2.35	...	2.70
0.142	...	...	...	2.31	2.64	...	...	...	6.75	7.20	7.32	2.10	...	...
...	...	...	...	...	...	...	...	...	...	...	...	7.75	...	...
0.130	...	...	...	1.97	2.12	...	...	5.10	...	6.30	6.40	6.55	...	2.20
0.120	...	...	...	1.61	1.77	...	2.20	...	4.60	4.92	4.98	5.20	...	1.90
0.113	...	...	...	1.47	1.60	...	...	3.80	...	4.40	4.50	4.75	...	...
0.107	...	...	...	...	...	...	...	...	...	...	...	...	...	...
...	...	...	page	...	...	...	...	...	...	...	...	...	...	1.02
0.098	...	...	...	1.05	1.17	...	...	2.80	...	3.15	3.21	3.50	...	4.65
0.080	...	...	...	0.73	0.79	...	...	...	2.30	2.40	2.42	2.50	...	3.90
0.072	...	...	...	0.584	0.614	...	...	1.75	...	2.00	2.05	2.10	...	2.70
0.064	...	...	...	0.465	0.490	...	...	1.35	...	1.52	1.55	1.64	...	2.25
0.050	...	...	...	...	0.320	...	...	...	...	0.86	0.88	1.00	...	1.80
0.040	...	...	...	...	0.21	...	...	...	...	...	...	0.62	...	...
0.030	...	...	...	...	0.13	...	...	...	...	...	...	0.38	...	...
0.024	...	...	...	...	0.10	...	...	...	...	...	...	0.21	...	...
0.010	...	...	...	...	0.060	...	...	...	...	...	...	0.071	...	0.082
0.005	...	...	...	...	0.0385	...	...	...	...	...	...	0.0425	...	0.044

\* Reprinted from the "Handbook of Chemistry and Physics" by permission of the Chemical Rubber Company.

TABLE V.—ABSORPTION COEFFICIENTS FOR X-RAYS AND GAMMA RAYS.\*—(Continued)  
 Atomic Absorption Coefficients  
 See Eq. (5-13), p. 79  
 Values multiplied by  $10^{23}$

A.	H 1	Li 3	C 6	N 7	O 8	Al 13	Fe 26	Cu 29	Mo 42	Ag 47	Pb 82	H <sub>2</sub> O (H)
0.025	.....	.....	.....	.....	.....	0.317	0.625	.....	.....	.....	2.60	.....
0.100	.....	.....	0.285	.....	.....	0.724	.....	3.3	.....	.....	.....	.....
0.125	0.04	.....	0.305	.....	0.385	0.792	3.67	4.8	21.3	.....	103.	0.478
0.150	0.05	.....	0.323	0.376	0.430	0.889	5.38	8.3	31.0	.....	53.6	0.534
0.175	0.06	.....	0.329	0.395	0.459	1.04	7.55	11.8	44.7	66.5	86.1	0.578
0.20	0.05	.....	0.343	0.409	0.482	1.19	9.75	16.4	63.5	107.	157.	0.591
0.25	0.05	.....	0.370	0.446	0.546	1.62	17.3	29.0	117.	203.	290.	0.650
0.30	0.04	0.197	0.400	0.518	0.641	2.34	28.4	47.2	201.	323.	485.	0.730
0.35	0.04	0.215	0.433	0.580	0.763	3.31	43.9	72.9	302.	483.	772.	0.840
0.40	0.05	0.238	0.475	.....	0.886	4.56	64.5	106.	422.	686.	1,150.	0.992
0.50	0.08	0.280	0.602	.....	1.29	8.44	127.	197.	769.	204.	2,070.	1.458
0.60	0.09	0.350	0.780	.....	1.92	14.0	208.	332.	1,277	348.	.....	2.11
0.70	0.10	0.462	1.052	.....	2.85	22.1	325.	512.	297.	.....	.....	3.04
0.80	0.17	.....	1.40	.....	4.03	32.4	466.	.....	430.	.....	.....	4.38
1.00	.....	.....	2.51	.....	.....	61.6	830.	.....	438.	2,000.	.....	8.01

\* Reprinted from the "Handbook of Chemistry and Physics" by permission of the Chemical Rubber Company.

TABLE VI.—WAVE LENGTHS OF THE K ABSORPTION LIMITS IN X-UNITS  $\times 1,000$ \*

Element	K limit	Element	K limit	Element	K limit
12Mg	9.51	35Br	0.918	60Nd	0.284
13Al	7.95	37Rb	0.814	62Sm	0.264
15P	5.76	38Sr	0.770	63Eu	0.254
16S	5.01	39Y	0.725	64Gd	0.246
17Cl	4.38	40Zr	0.687	65Tb	0.239
18A	3.87	41Cb	0.650	66Dy	0.230
19K	3.43	42Mo	0.618	67Ho	0.221
20Ca	3.06	44Ru	0.558	69Tm	0.208
21Sc	2.75	45Rh	0.533	70Yb	0.201
22Ti	2.49	46Pd	0.507	71Lu	0.195
23V	2.27	47Ag	0.485	72Hf	0.190
24Cr	2.07	48Cd	0.463	73Ta	0.184
25Mn	1.89	49In	0.443	74W	0.178
26Fe	1.74	50Sn	0.424	76Os	0.168
27Co	1.60	51Sb	0.406	78Pt	0.158
28Ni	1.49	52Te	0.388	79Au	0.153
29Cu	1.38	53I	0.371	80Hg	0.148
30Zn	1.30	55Cs	0.344	81Tl	0.144
31Ga	1.19	56Ba	0.331	82Pb	0.140
32Ge	1.11	57La	0.319	83Bi	0.136
33As	1.04	58Ce	0.306	90Th	0.113
34Se	0.98	59Pr	0.295	92U	0.107

\* M. Siegbahn, "Spectroscopie der Röntgenstrahlen," Verlag Julius Springer, Berlin, 1924.

TABLE VII.—MENDELYEV'S PERIODIC TABLE OF THE ELEMENTS

Group of elements												
Shell	I		II		III		IV		V		VI	
	a	b	a	b	a	b	a	b	a	b	a	b
K	1 hydrogen H 1.0081											
L	3 lithium Li 6.940	4 beryllium Be 9.02			5 boron B 10.82	6 carbon C 12.010			7 nitrogen N 14.008	8 oxygen O 16.000		
M	11 sodium Na 22.997	12 magnesium Mg 24.32	13 aluminum Al 26.97	14 silicon Si 28.06	15 phosphorus P 30.98	16 sulfur S 32.06			17 chlorine Cl 35.457	18 argon A 39.944		
N	19 potassium K 39.096	20 calcium Ca 40.08	21 scandium Sc 45.10	22 titanium Ti 47.90	23 vanadium V 50.95	24 chromium Cr 52.01	25 manganese Mn 54.93	26 iron Fe 55.84	27 cobalt Co 58.94	28 nickel Ni 58.69		
	29 copper Cu 63.57	30 zinc Zn 65.38	31 gallium Ga 69.72	32 germanium Ge 72.60	33 arsenic As 74.91	34 selenium Se 78.96	35 bromine Br 79.916	36 krypton Kr 83.7				
O	37 rubidium Rb 85.48	38 strontium Sr 87.63	39 yttrium Y 88.92	40 zirconium Zr 91.22	41 columbium Cb 92.91	42 molybdenum Mo 95.95	43 masurium Ma	44 ruthenium Ru 101.7	45 rhodium Rh 102.91	46 palladium Pd 106.7		
	47 silver Ag 107.880	48 cadmium Cd 112.41	49 indium In 114.76	50 tin Sn 118.70	51 antimony Sb 121.76	52 tellurium Te 127.61	53 iodine I 126.92	54 xenon Xe 131.1				
P	55 cesium Cs 132.91	56 barium Ba 137.36	Rare Earths	72 hafnium Hf 178.6	73 tantalum Ta 180.88	74 tungsten W 183.92	75 rhenium Re 186.31	76 osmium Os 190.2	77 iridium Ir 193.1	78 platinum Pt 195.23		
	79 gold Au 197.2	80 mercury Hg 200.61	81 thallium Tl 204.39	82 lead Pb 207.21	83 bismuth Bi 209.00	84 polonium Po 210	85	86 radon Rn 222				
	87	88 radium Ra 226.05	89 actinium Ac 227	90 thorium Th 232.12	91 protoactinium Pa 231	92 uranium U 238.07						
Q												

Rare				Earths			
62 samarium Sm 150.43	63 europium Eu 152.0	57 lanthanum La 138.92	58 cerium Ce 140.13	59 praseodymium Pr 140.92	60 neodymium Nd 144.27	61 illinium II 146	68 erbium Er 167.2
69 thulium Tm 169.4	70 ytterbium Yb 173.04	64 gadolinium Gd 156.9	65 terbium Tb 159.2	66 dysprosium Dy 162.46	67 holmium Ho 163.5		
		71 lutetium Lu 175.0					

TABLE VIII.—ARRANGEMENT OF ELECTRONS IN ORBITS\*

The following table gives, for each element, the atomic number and the arrangement of electrons in orbits. For a complete explanation of the significance of the data presented, see text.

Element	At. no.	Shell																
		K	L	M			N				O			P			Q	
		Orbit																
		1s	2s	2p	3s	3p	3d	4s	4p	4d	4f	5s	5p	5d	6s	6p	6d	7s
H	1	1																
He	2	2																
Li	3	2	1															
Be	4	2	2															
B	5	2	2	1														
C	6	2	2	2														
N	7	2	2	3														
O	8	2	2	4														
F	9	2	2	5														
Ne	10	2	2	6	(3s)	(3p)	(3d)											
Na	11	2	2	6	1													
Mg	12				2													
Al	13				2	1												
Si	14				2	2												
P	15	(10, Ne core)			2	3												
S	16				2	4												
Cl	17				2	5												
A	18				2	6		(4s)	(4p)	(4d)	(4f)							
K	19	2	2	6	2	6	....	1										
Ca	20						....	2										
Sc	21						1	2										
Ti	22						2	2										
V	23						3	2										
Cr	24	(18, A core)					5	1										
Mn	25						5	2										
Fe	26						6	2										
Co	27						7	2										
Ni	28						8	2										
Cu	29	2	2	6	2	6	10	1										
Zn	30						....	2										
Ga	31						....	2	1									
Ge	32						....	2	2									
As	33	(28, Cu core)					2	3										
Se	34						....	2	4									
Br	35						....	2	5									
Kr	36						....	2	6			(5s)	(5p)	(5d)				
Rb	37	2	2	6	2	6	10	2	6	....	....	1						
Sr	38						....					2						
Y	39						....				1							
Zr	40						....				2							
Cb	41						....				4							
Mo	42	(36, Kr core)					5				1							
Ma	43						....				6							
Ru	44						....				7							
Rh	45						....				8							
Pd	46						....			10								

\* Reprinted from the "Handbook of Chemistry and Physics" by permission of Chemical Rubber Company.

TABLE VIII.—ARRANGEMENT OF ELECTRONS IN ORBITS.\*—(Continued)

Ele- ment	At. no.	Shell																	
		K	L	M			N				O			P			Q		
		Orbit																	
		1s	2s	2p	3s	3p	3d	4s	4p	4d	4f	5s	5p	5d	6s	6p	6d	7s	
Ag	47	2	2	6	2	6	10	2	6	10	.....	1							
Cd	48	.....										2							
In	49	.....										2	1						
Sn	50	.....										2	2						
Sb	51	(46, Ag core).....										2	3						
Te	52	.....										2	4						
I	53	.....										2	5						
Xe	54	.....										2	6		(6s)	(6p)	(6d)		
Cs	55	2	2	6	2	6	10	2	6	10		2	6	.....	1				
Ba	56	(54, Xe core).....														2			
La	57	.....												1		2			
Ce	58	2	2	6	2	6	10	2	6	10	1	2	6	1	2				
Pr	59	.....										2			1	2			
Nd	60	.....										3			1	2			
Il...	61	.....										4			1	2			
Sa	62	.....										5			1	2			
Eu	63	.....										6			1	2			
Gd	64	.....										7			1	2			
Tb	65	(46, La).....										8	(8, La)	1	2				
Ds	66	.....										9			1	2			
Ho	67	.....										10			1	2			
Er	68	.....										11			1	2			
Tu	69	.....										12			1	2			
Yb	70	.....										13			1	2			
Lu	71	.....										14			1	2			
Hf	72	2	2	6	2	6	10	2	6	10	14	2	6	2	2				
Ta	73	.....													3	2			
W	74	.....													4	2			
Re	75	.....													5	2			
		.....													6	1			
Os	76	(68, Hf core).....													6	2			
		.....													7	1			
Ir	77	.....													7	1			
		.....													8	1			
Pt	78	.....													9	1			
		.....													10				
Au	79	2	2	6	2	6	10	2	6	10	14	2	6	10	1				
Hg	80	.....														2			
Tl	81	.....														2	1		
Pb	82	.....														2	2		
Bi	83	(78, Au core).....														2	3		
Po	84	.....														2	4		
—	85	.....														2	5		
Rn	86	.....														2	6		
—	87	2	2	6	2	6	10	2	6	10	14	2	6	10	2	6	(7s)		
Ra	88	.....																	1
Ac	89	.....																	2
Th	90	(86, Rn core).....																3	
Pa	91	.....																	3
U	92	.....																	4

\* Reprinted from the "Handbook of Chemistry and Physics" by permission of Chemical Rubber Company.

TABLE IX.—INTERNATIONAL TABLE OF THE RADIOACTIVE ELEMENTS AND THEIR CONSTANTS\*

Name	Symbol	Atomic weight	Atomic number	Half period $T$	Average life $\theta = \frac{1}{\lambda}$	Fraction transformed per sec., $\lambda$	Radiation ( ) weak radiation	Isotope
Uranium and radium series:								
Uranium I.....	UI	238	92	$4.67 \times 10^9$ yr.	$6.75 \times 10^9$ yr.	$4.7 \times 10^{-18}$	$\alpha$	U
Uranium X <sub>1</sub> .....	U-X <sub>1</sub>	234	90	24.6 days	35.5 days	$3.26 \times 10^{-7}$	$\beta$	Th
Uranium X <sub>2</sub> .....	U-X <sub>2</sub>	234	91	1.15 min.	1.65 min.	0.010	$\beta(\gamma)$	Pa
Uranium II (brevium).....	UII	234	92	$2 \times 10^6$ yr.	$3 \times 10^6$ yr.	$10^{-14}$ (?)	$\alpha$	U
Ionium.....	Io	230	90	$6.9 \times 10^4$ yr.	$10^5$ yr.	$3.2 \times 10^{-13}$	$\alpha$	Th
Radium.....	Ra	226	88	1690 yr.	2440 yr.	$1.30 \times 10^{-11}$	$\alpha(\beta + \gamma)$	Ra
Radon (radium emanation, niton).....	Rn	222	86	3.85 days	5.55 days	$2.085 \times 10^{-6}$	$\alpha$	Rn
Radium A.....	Ra-A	218	84	3.0 min.	4.32 min.	$3.85 \times 10^{-3}$	$\alpha$	Po
Radium B.....	Ra-B	214	82	26.8 min.	38.7 min.	$4.30 \times 10^{-4}$	$\beta(\gamma)$	Pb
Radium C.....	Ra-C	214	83	19.5 min.	28.1 min.	$5.92 \times 10^{-4}$	99.97% $\beta$ and $\gamma$	Bi
Radium C'.....	Ra-C'	214	84	$10^{-6}$ sec.	$10^{-6}$ sec.	$10^6$ (?)	$\alpha$	Po
Radium D (radiolead).....	Ra-D	210	82	16.5 yr.	23.8 yr.	$1.33 \times 10^{-9}$	( $\beta$ and $\gamma$ )	Pb
Radium E.....	Ra-E	210	83	5.0 days	7.2 days	$1.61 \times 10^{-6}$	$\beta$	Bi
Radium F (polonium).....	Ra-F	210	84	136 days	196 days	$5.90 \times 10^{-8}$	$\alpha(\gamma)$	Po
Radium G'.....	Ra G'	206	82	.....	.....	.....	.....	Pb
(Lead).....	Pb <sup>206</sup>							
Radium C.....	Ra-C	214	83	.....	.....	$1.8 \times 10^{-7}$	0.03% $\alpha$	Bi
Radium C''.....	Ra-C''	210	81	1.4 min.	2.0 min.	$8.3 \times 10^{-3}$	$\beta$	Tl
(Radium C <sub>2</sub> ).....								
Radium G''.....	Ra G''	210	82	.....	.....	.....	.....	Pb
Actinium series:								
Uranium ?.....	.....	?	92	.....	.....	.....	$\alpha$	U
Uranium Y.....	U-Y	?	90	1.04 days	1.5 days	$7.8 \times 10^{-6}$	$\beta$	Th
Protoactinium (ekatantalum).....	Pa	231	91	$1.2 \times 10^4$ yr.	$1.7 \times 10^4$ yr.	$1.9 \times 10^{-12}$	$\alpha$	Pa
Actinium.....	Ac	?	89	20 yrs.	28.8 yr.	$1.1 \times 10^{-9}$	.....	Ac
Radioactinium.....	Rd-Ac	?	90	19.5 days	28.1 days	$4.11 \times 10^{-7}$	$\alpha(\beta)$	Th
Actinium X.....	Ac-X	?	88	11.4 days	16.4 days	$7.06 \times 10^{-7}$	$\alpha$	Ra

\* Reprinted from the "Handbook of Chemistry and Physics" by permission of the Chemical Rubber Company.

TABLE X.—CRYSTALLOGRAPHIC DATA\*

(f.c. = face centered; b.c. = body centered; c.p. = close packed; c. = cubic; tet. = tetragonal; hh. = hexagonal division, hexagonal system; hr. = rhombohedral division, hexagonal system; o. = orthorhombic; m. = monoclinic; tri. = triclinic)

Compound	Crystal system	Type	a b c	Axial angle	Space group	Mole/cell
A (−235°C.) Spacings: 2.36 A.(100%); 2.04 A.(53%); 1.232 A.(53%); 1.445 A. (27%)	c.f.c.	Cu	5.43		$O_h^5$	4
Ag 2.36(1st reading always 100%); 2.04(53); 1.232(53); 1.445(27)	c.f.c.	Cu	4.0776		$O_h^5$	4
AgBr 2.88; 2.03(60); 1.66(20); 1.289(20)	c.	NaCl	5.755		$O_h^5$	4
AgNO <sub>3</sub> 3.00; 4.51(50); 4.08(50); 3.66(38)	o.		6.97, 7.34, 10.14	$111-111$		8
Ag <sub>2</sub> O 2.72; 2.36(40); 1.67(24); 1.422(16)	c.	Cu <sub>2</sub> O	4.72		$O_h^4$	2
Al 2.33; 2.02(40); 1.43(30); 1.219(30)	c.f.c.	Cu	4.041		$O_h^5$	4
Al <sub>2</sub> O <sub>3</sub> (corundum) 2.08; 1.59(100); 2.55(75); 3.47(50)	hr.	Fe <sub>2</sub> O <sub>3</sub>	5.12	$\omega = 55^\circ 17'$	$D_{3d}^6$	2
As 2.76; 1.88(20); 2.04(13); 1.56(8)	hr.	As	4.151	$\omega = 53^\circ 49'$	$D_{3d}^5$	2
Au 2.35; 2.03(53); 1.227(40); 1.439(33)	c.f.c.	Cu	4.070		$O_h^5$	4
Ba 3.54; 2.04(100); 2.51(50); 1.77(50)	c.b.c.	W	5.015		$O_h^9$	2
Ba(NO <sub>3</sub> ) <sub>2</sub> 2.44; 4.69(75); 2.34(50); 1.86(40)	c.	Ba(NO <sub>3</sub> ) <sub>2</sub>	8.11		$T_h^6$	4
BaO 3.20; 2.75(88); 1.95(75); 1.66(50)	c.	NaCl	5.50		$O_h^5$	4
Be 1.73; 1.97(20); 1.79(14); 1.328(12)	hh. c.p.	Mg	2.27 . . . 3.61		$D_{6h}^4$	2
Bi 3.28; 2.35(50); 2.27(50); 1.86(30)	hr.	As	4.749	$\omega = 57^\circ 16'$	$D_{6h}^5$	2

\* Compiled from *Ind. Eng. Chem., Anal. Ed.* **30**, 457–512 (1938) and from the "Handbook of Chemistry and Physics," by permission of J. D. Hanawalt, the American Chemical Society, and the Chemical Rubber Company.



TABLE X.—CRYSTALLOGRAPHIC DATA.\*—(Continued)

Compound	Crystal system	Type	<i>a b c</i>	Axial angle	Space group	Mole/cell
C (diamond) 2.05; 1.26(50); 1.072(40); 0.721(40)	c.	diamond	3.5597		$O_h^7$	8
C (graphite) 3.37; 2.02(60); 1.155(50); 1.227(35)	hh.		2.45 . . . 6.70		$D_{6h}^4$	4
$C_{12}H_{22}O_{11}H_2O$ spacings: 4.51; 5.4(35); 4.20(30); 3.73(25)						
$C_{29}H_{60}$ (nonicosane)	o.		7.45, 4.97, 77.2		$V_h^{16}$	4
$CH_3(CH_2)_{16}COOH$ ( $\beta$ )(stearic acid)	m. m.	5.546, 7.381, 48.84 5.68, 7.39, 50.7	$\beta = 63^\circ 38'$ $\beta = 60^\circ$		$C_{2h}^5$ or $C_{2h}^4$	4 4
Ca 3.21; 2.80(30); 1.97(20); 1.68(20)	e.f.c.	Cu	5.56		$O_h^5$	4
$CaCl_2$ 2.74, 3.18(50); 2.08(44); 1.93(31)	tet.		3.87 . . . 6.37		$C_{4h}^{17}$	2
$CaCO_3$ 3.04; 1.92(32); 2.28(24); 1.87(24)	hr.	$NaNO_3$	6.361	$\omega = 46^\circ 6'$	$D_{3d}^6$	2
$CaCl_2$ 4.49; 3.05(80); 2.33(60); 1.90(36)						
$CaF_2$ 1.93; 3.16(67); 1.65(50); 1.117(30)	c.	$CaF_2$	5.451		$O_h^5$	4
$Ca(OH)_2$ 2.63; 4.93(50); 1.93(50); 1.79(40)	hh.	$CdI_2$	3.58 . . . 4.90		$D_{3d}^3$	1
$CaO$ 2.39; 1.69(63); 2.76(40); 1.071(25)	c.	$NaCl$	4.797		$O_h^5$	4
Cl 2.33; 1.34(32); 1.65(20); 1.041(10)	e.b.c.	W	3.03		$O_h^9$	2
Cd 2.34; 2.80(40); 2.58(30); 1.310(27)	hh.c.p.	Mg	2.97 . . . 5.61		$D_{6h}^4$	2
$\alpha$ -Ce	e.f.c.	Cu	5.12		$O_h^5$	4
$\beta$ -Ce 3.20; 2.81(72); 1.85(40); 1.96(24)	hh.c.p.	Mg	3.65 . . . 5.91		$D_{6h}^4$	2

\* Compiled from *Ind. Eng. Chem., Anal. Ed.* **30**, 457–512 (1938) and from the "Handbook of Chemistry and Physics," by permission of J. D. Hanawalt, the American Chemical Society, and the Chemical Rubber Company.

TABLE X.—CRYSTALLOGRAPHIC DATA.\*—(Continued)

Compound	Crystal system	Type	<i>a b c</i>	Axial angle	Space group	Mole/cell
$\alpha$ -Co 2.04; 1.77(44); 1.253(22); 1.066(22)	c.f.c.	Cu	3.554		$O_h^5$	4
$\beta$ -Co	hh.c.p.	Mg	2.514 . . . 4.105		$D_{6h}^4$	2
$\alpha$ -Cr 2.03; 1.174(30); 1.437(17); 1.018(3)	c.b.c.	W	2.878		$O_h^9$	2
$\beta$ -Cr	hh.c.p.	Mg	2.717 . . . 4.418		$D_{6h}^4$	2
$\gamma$ -Cr	c.	$\alpha$ -Mn	8.717		$T_d^3$	58
Cs(−173°C.)	c.b.c.	W	6.05		$O_h^9$	2
Cu 2.08; 1.81(53); 1.277(33); 1.089(33)	c.f.c.	Cu	3.608		$O_h^5$	4
Cu <sub>2</sub> O 2.45; 1.51(44); 2.12(31); 1.283(31)	c.	Cu <sub>2</sub> O	4.27		$O_h^4$	2
CuO 2.51; 2.31(100); 1.85(20); 1.408(20)	tri. $\alpha = 85^\circ 21' \beta = 86^\circ 25' \gamma = 93^\circ 35'$		3.74; 4.67, 4.67			4
CuSO <sub>4</sub> ·5H <sub>2</sub> O 4.70; 4.00(58); 3.70(50); 5.6(42)	tri. $\beta = 107^\circ 8'; \gamma = 102^\circ 41'$		6.07, 10.78, 5.89	$\alpha = 82^\circ 5'$		2
CuZn	c.	CsCl	2.945		$O_h^1$	1
Cu <sub>5</sub> Zn <sub>8</sub>	c.		8.85		$T_d^3$	52
Er	hh.c.p.	Mg	3.74 . . . 6.09		$D_{6h}^4$	2
$\alpha$ -Fe 2.01; 1.166(38); 1.428(15); 1.010(10)	c.b.c.	W	2.861		$O_h^9$	2
$\beta$ -Fe(800°C.)	c.b.c.	W	2.90		$O_h^9$	2
$\gamma$ -Fe(1100°C.)	c.f.c.	Cu	3.63		$O_h^5$	4
$\delta$ -Fe(1425°C.)	c.b.c.	W	2.93		$O_h^9$	2

\* Compiled from *Ind. Eng. Chem., Anal. Ed.* **30**, 457–512 (1938) and from the "Handbook of Chemistry and Physics," by permission of J. D. Hanawalt, the American Chemical Society, and the Chemical Rubber Company.

TABLE X.—CRYSTALLOGRAPHIC DATA.\*—(Continued)

Compound	Crystal system	Type	<i>a b c</i>	Axial angle	Space group	Mole/cell
Fe <sub>3</sub> C(cementite)	o.	4.518, 5.069, 6.736			$V_h^{16}$	4
Fe <sub>4</sub> N 2.18; 1.88(40); 1.136(30); 1.332(20)	c.f.c.		3.789			1
Fe <sub>2</sub> O <sub>3</sub> (hematite) 2.69; 2.51(75); 1.84(63); 1.69(63)	hr.		5.42	$\omega = 55^\circ 17'$	$I_{3d}^6$	2
$\gamma$ -Fe <sub>2</sub> O <sub>3</sub> (magnetic)	c.		8.30			
Fe <sub>3</sub> O <sub>4</sub> (magnetite) 2.53; 1.483(80); 1.61(64); 2.10(32)	c.	MgAl <sub>2</sub> O <sub>4</sub>	8.37		$O_h^7$	8
FeS <sub>2</sub> (pyrite) 1.63; 2.70(75); 2.42(45); 1.91(45)	c.	FeS <sub>2</sub>	5.41		$T_h^6$	4
Ga	simple tet.		4.51 . . . 7.6		$D_{4h}^{16}$	8
Ga	o.		4.517, 4.511, 7.645		$V_h^{18}$	
Ge	c.	diamond	5.65		$O_h^7$	8
H <sub>2</sub> (−271°C.)	hh.		3.75 . . . 6.11			4
H <sub>3</sub> BO <sub>3</sub> 3.16; 5.9(17.5); 2.23(13), 2.62(6)						
H <sub>2</sub> O(ice, −20°C.) 3.67; 2.065(50); 3.44(20); 1.368(20)	hh.		4.535 . . . 7.41		$D_{6h}^4$	4
Hg(−46°C.)	hr.		2.997	$\omega = 70^\circ 32'$	$D_{3d}^5$	1
Hg	hr.f.c.		4.578	$\omega = 98^\circ 13'$		4
HgCl <sub>2</sub> 4.35; 3.00(75); 2.70(50); 3.40(38)	o.	4.307, 5.936, 12.67			$V_h^{16}$	4
Hg <sub>2</sub> Cl <sub>2</sub> 4.16; 3.17(100); 1.97(80); 2.06(60)	tet.		4.47 . . . 10.89		$D_{4h}^{17}$	2
HgS(cinnabar) 2.85; 3.36(83); 1.97(33); 3.16(27)	hh.		4.14 . . . 9.49		$D_3^4$ or $D_3^6$	3
HgS 3.37; 2.06(30); 1.76(30); 2.92(16)	c.	ZnS	5.84		$T_d^2$	4

\* Compiled from *Ind. Eng. Chem., Anal. Ed.*, **30**, 457–512 (1938) and from the "Handbook of Chemistry and Physics," by permission of J. D. Hanawalt, the American Chemical Society, and the Chemical Rubber Company.

TABLE X.—CRYSTALLOGRAPHIC DATA.\*—(Continued)

Compound	Crystal system	Type	<i>a b c</i>	Axial angle	Space group	Mole/cell
Hf	hh.c.p.	Mg	3.20 . . . 5.08		$D_{6h}^4$	2
I <sub>2</sub> 3.69; 3.09(100); 1.97(30); 2.02(20)	o.	4 I <sub>2</sub> groups	4.795, 7.255, 9.780		$V_h^{18}$	8
In 2.72; 2.29(40); 1.68(30); 1.395(30)	tet. f.c.		4.583 . . . 4.936		$D_{4h}^{17}$	4
Ir 2.20; 1.91(50); 1.153(36); 1.352(28)	c.f.c.	Cu	3.823		$O_h^5$	4
K 3.75; 2.16(30); 2.56(16); 1.87(4)	c.b.c.	W	5.333		$O_h^9$	2
KH <sub>2</sub> Al <sub>2</sub> Si <sub>3</sub> AlO <sub>12</sub> (mica)	m.	5.18, 9.02, 20.04		$\beta = 95^\circ 30'$		
KCl(sylvine) 3.13; 2.21(60); 1.81(14); 1.401(12)	c.	NaCl	6.28		$O_h^5$	4
$\alpha$ -K <sub>2</sub> Cr <sub>2</sub> O <sub>7</sub> 3.29; 3.02(75); 2.85(63); 3.68(50)	tri. $\beta = 96^\circ 13', \gamma = 90^\circ 51'$	7.50, 7.38, 13.40		$\alpha = 82^\circ 0'$		4
$\beta$ -K <sub>2</sub> Cr <sub>2</sub> O <sub>7</sub>	m.	7.47, 7.35, 12.97		$\beta = 91^\circ 55'$		4
K <sub>2</sub> SO <sub>4</sub> 2.88; 3.00(80); 2.08(40); 4.19(24)	o.	K <sub>2</sub> SO <sub>4</sub>	5.731, 10.01, 7.42			4
KClO <sub>3</sub> 3.45; 2.79(40); 2.86(30); 2.10(30)	m.	4.647, 5.585, 7.085		$\beta = 109^\circ 38'$	$C_{2h}^2$	2
KBr 3.29; 2.33(42); 1.468(17); 1.89(10)	c.	NaCl	6.578		$O_h^5$	4
KI 3.53; 2.50(80); 4.08(40); 2.03(32)	c.	NaCl	7.052		$O_h^5$	4
KCN 3.26; 2.30(63); 1.96(13); 3.77(10)	c.	NaCl	6.55		$O_h^5$	4
KOH 2.69; 1.98(83); 2.93(67); 3.13(23)						
Kr(−252.5°C.)	c.f.c.	Cu	5.59	.	$O_h^5$	4

\* Compiled from *Ind. Eng. Chem., Anal. Ed.* **30**, 457–512 (1938) and from the "Handbook of Chemistry and Physics," by permission of J. D. Hanawalt, the American Chemical Society, and the Chemical Rubber Company.

TABLE X.—CRYSTALLOGRAPHIC DATA.\*—(Continued)

Compound	Crystal system	Type	<i>a b c</i>	Axial angle	Space group	Mole/cell
La	hh.c.p.	Mg	3.72 . . . 6.06		$D_{6h}^4$	2
$\beta$ -La	c.f.c.		5.296			
Li 2.48; 1.430(20); 1.75(17); 1.240(3)	c.b.c.	W	3.50		$O_h^3$	2
LiF 2.00; 2.32(67); 1.419(23); 1.211(3)	c.	NaCl	4.01		$O_h^5$	4
Mg 2.45; 2.77(30); 2.60(25); 1.90(20)	hh.c.p.	Mg	3.203 . . . 5.196		$D_{2h}^4$	2
MgO 2.10; 1.485(75); 1.213(15); 2.42(6)	c.	NaCl	4.203		$O_h^5$	4
MgSO <sub>4</sub> ·7H <sub>2</sub> O(epsom salts) 4.22; 2.66(40), 5.9(20), 5.3(20)	o.		11.91, 12.02, 6.87		$V^4$	4
MgCl <sub>2</sub> 1.80; 5.9(63); 2.53(63); 2.94(31)	hr.	CdCl <sub>2</sub>	6.22 $\omega = 33^\circ 36'$		$D_{3d}^5$	1
$\alpha$ -Mn 2.09; 1.210(28); 1.89(20); 1.74(16)	c.b.c.	$\alpha$ -Mn	8.894		$T_d^3$	58
$\beta$ -Mn 2.10; 2.00(66); 1.237(30); 1.90(27)	c.		6.300		$O^6$ or $O^7$	20
$\gamma$ -Mn	tet. f.c.	In	3.774 . . . 3.526		$D_{4h}^{17}$	4
MnO 2.22; 2.56(66); 1.57(66); 1.339(23)	c.	NaCl	4.435		$O_h^5$	4
MnO <sub>2</sub> 3.11; 2.40(50); 1.62(50); 2.12(12)	tet.	SnO <sub>2</sub>	4.44 . . . 2.89		$D_{4h}^{14}$	2
KMnO <sub>4</sub> 3.22; 2.95(80), 3.57(60), 4.55(50)	o.	BaSO <sub>4</sub>	9.10, 5.69, 7.40		$V_h^{16}$	4

\* Compiled from *Ind. Eng. Chem., Anal. Ed.* **30**, 457–512 (1938) and from the "Handbook of Chemistry and Physics," by permission of J. D. Hanawalt, the American Chemical Society, and the Chemical Rubber Company.

TABLE X.—CRYSTALLOGRAPHIC DATA.\*—(Continued)

Compound	Crystal system	Type	<i>a b c</i>	Axial angle	Space group	Mole/cell
MnCl <sub>2</sub> 5.8; 1.84(80); 2.57(70); 3.12(50)	hr.	CdCl <sub>2</sub>	6.20	$\omega = 34^\circ 35'$	$D_{3d}^5$	1
Mo 2.22; 1.281(57); 1.57(36); 0.995(23)	c.b.c.	W	3.140		$O_h^9$	2
N <sub>2</sub> (−252°C.)(4N <sub>2</sub> )	c.		5.66		$T^4$	8
NH <sub>4</sub> Cl 2.72; 1.57(25); 3.85(15); 1.92(12)	c.	CsCl	3.866		$O_h^1$	1
Na 3.02; 1.75(20); 2.13(15); 1.51(5)	c.b.c.	W	4.30		$O_h^9$	2
NaBr 2.96; 2.09(63); 3.44(45); 1.329(35)	c.	NaCl	5.94		$O_h^5$	4
NaHCO <sub>3</sub> 2.94; 2.58(48); 3.49(16); 3.04(16)	m.	7.51, 9.70, 3.53		$\beta = 93^\circ 19'$	$C_{2h}^6$	4
NaCl 2.81; 1.99(83); 1.63(33); 1.260(33)	c.	NaCl	5.628		$O_h^5$	4
NaF 2.32; 1.64(60); 1.336(16); 1.035(8)	c.	NaCl	4.62		$O_h^5$	4
NaOH 2.35; 1.70(30); 1.65(25); 2.85(20)						
NaI 3.22; 3.74(83); 2.29(83); 1.95(58)	c.	NaCl	6.46		$O_h^5$	4
NaNO <sub>2</sub> 2.97; 2.78(40); 2.02(40); 2.00(23)	o.		3.55, 5.56, 5.37			2
NaNO <sub>3</sub> 3.03; 2.31(30); 1.89(25); 2.11(8)	hr.	NaNO <sub>3</sub>	6.32	$\omega = 47^\circ 15'$	$D_{3d}^6$	2
Na <sub>3</sub> PO <sub>4</sub> 2.55; 4.25(48); 2.70(48); 1.91(48)						
Na <sub>2</sub> SO <sub>2</sub> 2.78; 1.87(53); 4.66(40); 3.18(33)	o.		5.85, 12.29, 9.75		$V_h^{24}$	8
Ne(−268°C.)	c.f.c.	Cu	4.52		$O_h^5$	4

\* Compiled from *Ind. Eng. Chem., Anal. Ed.* **30**, 457–512 (1938) and from the "Handbook of Chemistry and Physics," by permission of J. D. Hanawalt, the American Chemical Society, and the Chemical Rubber Company.

TABLE X.—CRYSTALLOGRAPHIC DATA.\*—(Continued)

Compound	Crystal system	Type	a b c	Axial angle	Space group	Mole/cell
$\alpha$ Ni	hh.c.p.	Mg	2.66 . . . 4.29		$D_{6h}^4$	2
$\beta$ -Ni	c.f.c.	Cu	3.517		$O_h^5$	4
2.03; 1.76(50); 1.244(32); 1.061(32)						
NiSO <sub>4</sub> ·7H <sub>2</sub> O	o.	MgSO <sub>4</sub> ·7H <sub>2</sub> O	11.86, 12.08, 6.81		$V^4$	4
4.20; 5.3(60); 2.85(25); 3.75(16)						
O <sub>2</sub> (−252°C.)	o.b.c.		5.50, 3.82, 3.44			4
O <sub>2</sub>	hr.		6.19	$\omega = 99.1^\circ$		6
O <sub>2</sub> (−233°C.)	c.		6.83		$T_h^6$	8
Os	hh.c.p.	Mg	2.724 . . . 4.314		$D_{6h}^4$	2
2.07; 2.36(20); 2.16(15); 1.363(13)						
P (metallic)	hr.	As	5.14	$\omega = 34^\circ 7'$	$D_{3d}^5$	2
P (metallic)	hr. f.c.		5.96	$\omega = 60^\circ 47'$		8
P (black or red)	o.f.c.		3.31, 4.38, 10.50		$V_h^{18}$	8
P(−35°C.; yellow)	c.	(4P <sub>4</sub> )	7.17			16
P <sub>2</sub> O <sub>5</sub>	hh.		11.12 . . . 1.12			12
5.4; 5.2(53); 3.02(53); 3.27(33)						
Pb	c.f.c.	Cu	4.941		$O_h^5$	4
2.85; 2.47(50); 1.74(50); 1.49(50)						
PbCl <sub>2</sub>	o.	HgCl <sub>2</sub>	4.496, 7.667, 9.153		$V_h^{16}$	4
3.57; 3.87(88); 2.77(75); 2.50(50)						
PbO(red)	tet.	PbO	3.98 . . . 5.01		$D_{4h}^7$	2
PbO(yellow)	o.		5.50, 4.72, 5.88		$V_h^{10}$	4
3.06; 2.93(25), 2.72(25); 1.71(25)						
Pb <sub>2</sub> O	c.	CuO	5.38		$O_h^4$	2
PbO <sub>2</sub>	tet.	SnO <sub>2</sub>	4.97 . . . 3.40		$D_{4h}^{14}$	2
3.49; 2.78(100); 1.84(100); 2.46(28)						
Pb <sub>3</sub> O <sub>4</sub> 3.35; 2.88(43); 2.76(43); 2.62(28)						
2PbCO <sub>3</sub> ·Pb(OH) <sub>2</sub> 3.28; 2.62(100); 3.61(83); 4.45(33)						
Pd	c.f.c.	Cu	3.879		$O_h^5$	4
2.23; 1.94(50); 1.371(27); 1.170(27)						

\* Compiled from *Ind. Eng. Chem., Anal. Ed.* **30**, 457–512 (1938) and from the "Handbook of Chemistry and Physics," by permission of J. D. Hanawalt, the American Chemical Society, and the Chemical Rubber Company.

TABLE X.—CRYSTALLOGRAPHIC DATA.\*—(Continued)

Compound	Crystal system	Type	<i>a b c</i>	Axial angle	Space group	Mole/cell
Pt 2.25; 1.95(30); 1.382(16); 1.178(16)	c.f.c.	Cu	3.9142		$O_h^5$	4
Rb(−173°C.)	c.b.c.	W	5.62		$O_h^9$	2
Re 2.10; 2.38(33); 2.22(20); 1.379(17)	hh. c.p.	Mg	2.765 . . . 4.470		$D_{6h}^4$	2
Rh 2.20; 1.90(50); 1.146(40); 1.345(30)	c.f.c.	Cu	3.7944		$O_h^5$	4
Ru 2.04; 2.33(40); 2.13(30); 1.213(30)	hh.c.p.	Mg	2.695 . . . 4.273		$D_{6h}^4$	2
S 3.85; 3.21(50); 3.10(38); 2.85(38)	o.f.c.		10.48, 12.92, 24.55		$V_h^{24}$	128
Sb 3.10, 2.24(63); 2.14(63); 1.76(44)	hr.	As	4.501	$\omega = 57^\circ 5'$	$D_{3d}^5$	2
Sb	hr. f.c.		6.226	$\omega = 87^\circ 24'$		8
Se 3.02; 2.07(40); 3.78(33); 2.00(33)	hh.		4.377 . . . 4.944		$D_3^4$ or $D_3^6$	3
$\alpha$ -Se (4Se <sub>8</sub> )	m.		8.99, 8.97, 11.52		$C_{2h}^2$	32
			$\beta = 91^\circ 34'$			
$\beta$ -Se	m.		12.74, 8.04, 9.25	$\beta = 93^\circ 04'$	$C_{2h}^5$	32
Si 3.12; 1.91(100); 1.63(63); 1.104(40)	c.	diamond	5.42		$O_h^7$	8
SiO <sub>2</sub> ( $\alpha$ -cristobalite)			4.04; 2.48(32); 2.85(20); 3.13(16)			
SiO <sub>2</sub> ( $\beta$ -cristobalite)	c.		7.12		$O_h^7$	8
SiO <sub>2</sub> ( $\alpha$ -quartz)	hh.		4.903 . . . 5.393		$D_3^4$ or $D_3^6$	3
			3.35; 4.25(25); 1.82(25); 1.375(25)			
SiC (commercial)			2.51; 1.54(80); 1.312(60); 2.36(40)			

\* Compiled from *Ind., Eng. Chem., Anal. Ed.* **30**, 457–512 (1938) and from the "Handbook of Chemistry and Physics," by permission of J. D. Hanawalt, the American Chemical Society, and the Chemical Rubber Company.



TABLE X.—CRYSTALLOGRAPHIC DATA.\*—(Continued)

Compound	Crystal system	Type	<i>a b c</i>	Axial angle	Space group	Mole/cell
$\alpha$ -Sn (gray)	c.	diamond	6.46		$O_h^7$	8
$\beta$ -Sn (white)	tet.	double b.c.	5.818 . . .	3.174	$D_{4h}^{19}$	4
2.91; 2.79(80); 2.01(80); 2.05(32)						
SnO <sub>2</sub>	tet.	SnO <sub>2</sub>	4.72 . . .	3.16	$D_{4h}^{14}$	2
3.34; 2.64(63); 1.75(63); 2.36(18)						
Sr	c.f.c.	Cu	6.075		$O_h^5$	4
3.50; 1.83(100); 3.03(60); 2.14(20)						
Ta	c.b.c.	W	3.281		$O_h^9$	2
2.33; 1.346(30); 1.65(20); 1.165(5)						
Te	hh.	Se	4.495 . . .	5.912	$D_3^4$ or $D_3^6$	3
3.24; 2.34(48); 2.22(32); 1.83(28)						
Th	c.f.c.	Cu	5.074		$O_h^5$	4
2.92; 2.53(50); 1.79(38); 1.52(31)						
Ti	hh.c.p.	Mg	2.951 . . .	4.692	$D_{6h}^4$	2
2.23; 2.54(27); 2.34(20); 1.72(13)						
TiO <sub>2</sub> (anatase)	tet.		3.73 . . .	9.37	$D_{4h}^{19}$	4
3.52; 1.88(40); 1.70(28); 2.37(24)						
TiO <sub>2</sub> (rutile)	tet.	SnO <sub>2</sub>	4.58 . . .	2.95	$D_{4h}^{14}$	2
1.69; 3.24(80); 2.49(60); 2.19(30)						
$\alpha$ -Tl	hh.c.p.	Mg	3.450 . . .	5.520	$D_{6h}^4$	2
2.62; 3.00(40); 1.73(29); 1.56(29)						
U	c.b.c.	W	3.43		$O_h^9$	2
V	c.b.c.	W	3.011		$O_h^9$	2
2.14; 1.236(20); 1.51(7); 1.072(3)						
W	c.b.c.	W	3.1583		$O_h^9$	2
2.23; 1.290(71); 0.846(34); 1.58(29)						
WC	hh.		2.901 . . .	2.830		1
Xe(−173°C.)	c.f.c.	Cu	6.18		$O_h^5$	4

\* Compiled from *Ind. Eng. Chem., Anal. Ed.* **30**, 457–512 (1938) and from the "Handbook of Chemistry and Physics," by permission of J. D. Hanawalt, the American Chemical Society, and the Chemical Rubber Company.

TABLE X.—CRYSTALLOGRAPHIC DATA.\*—(Continued)

Compound	Crystal system	Type	<i>a b c</i>	Axial angle	Space group	Mole/cell
Zn 2.08; 2.46(25); 2.30(20); 1.33(18)	hh.c.p.	Mg	2.66 . . .	4.93	$D_{6h}^4$	2
ZnO 2.46; 2.81(50); 2.61(30); 1.61(30)	hh.		3.25 . . .	5.23	$C_{6v}^4$	2
ZnSO <sub>4</sub> ·7H <sub>2</sub> O 4.20; 5.3(60); 3.44(30); 2.87(30)	o.	MgSO <sub>2</sub> ·7H <sub>2</sub> O	11.85, 12.09, 6.83		$V^4$	4
ZnCl <sub>2</sub> 3.06; 4.79(67); 1.86(33); 2.34(20)	hr.	CdCl <sub>2</sub>	6.31	$\omega = 34^\circ 48'$	$D_{3d}^5$	1
Zr 2.44; 2.78(31); 2.56(20); 1.88(18)	hh.c.p.	Mg	3.223 . . .	5.123	$D_{6h}^4$	2

\* Compiled from *Ind. Eng. Chem., Anal. Ed.* **30**, 457–512 (1938) and from the "Handbook of Chemistry and Physics," by permission of J. D. Hanawalt, the American Chemical Society, and the Chemical Rubber Company.

TABLE XI.—CRYSTAL TYPES; UNIT-CELL CONFIGURATION  
(After Wyckoff.)

Face-centered cubic (copper)	000; $\frac{1}{2}\frac{1}{2}0$ ; $\frac{1}{2}0\frac{1}{2}$ ; $0\frac{1}{2}\frac{1}{2}$	
Hexagonal close-packed (magnesium)	000; $\frac{2}{3}\frac{1}{3}\frac{1}{3}$	
	$c/a = 1.63$ for true close packing	
	For zinc and cadmium, $c/a =$ about 1.86	
Body-centered cubic (tungsten)	000; $\frac{1}{2}\frac{1}{2}\frac{1}{2}$	
Diamond cubic (diamond)	000, $\frac{1}{2}\frac{1}{2}0$ , $\frac{1}{2}0\frac{1}{2}$ ; $0\frac{1}{2}\frac{1}{2}$ ; $\frac{1}{4}\frac{1}{4}\frac{1}{4}$ ; $\frac{3}{4}\frac{3}{4}\frac{3}{4}$ ; $\frac{3}{4}\frac{1}{4}\frac{3}{4}$ ; $\frac{1}{4}\frac{3}{4}\frac{3}{4}$	
Arsenic (rhombohedral)	000; $uuu$	For As, $u = 0.452$ ; for Sb, $u = 0.446$ , for Bi, $u = 0.452$ ; for red P, $u = 0.17$
Indium (face-centered tetragonal)	000; $\frac{1}{2}\frac{1}{2}0$ ; $\frac{1}{2}0\frac{1}{2}$ ; $0\frac{1}{2}\frac{1}{2}$	
NaCl (cubic)	Na—000; $\frac{1}{2}\frac{1}{2}0$ ; $\frac{1}{2}0\frac{1}{2}$ ; $0\frac{1}{2}\frac{1}{2}$ Cl— $\frac{1}{2}\frac{1}{2}\frac{1}{2}$ ; 00 $\frac{1}{2}$ ; $0\frac{1}{2}0$ , $\frac{1}{2}00$	
CsCl (cubic)	Cs—000      Cl— $\frac{1}{2}\frac{1}{2}\frac{1}{2}$	
ZnS (cubic)	Zn—000; $\frac{1}{2}\frac{1}{2}0$ ; $\frac{1}{2}0\frac{1}{2}$ ; $0\frac{1}{2}\frac{1}{2}$ S— $\frac{1}{4}\frac{1}{4}\frac{1}{4}$ ; $\frac{3}{4}\frac{3}{4}\frac{3}{4}$ ; $\frac{3}{4}\frac{1}{4}\frac{3}{4}$ ; $\frac{1}{4}\frac{3}{4}\frac{3}{4}$	
Cu <sub>2</sub> O (cubic)	Cu—000; $\frac{1}{2}\frac{1}{2}\frac{1}{2}$ O— $\frac{1}{4}\frac{1}{4}\frac{1}{4}$ ; $\frac{1}{4}\frac{3}{4}\frac{3}{4}$ ; $\frac{3}{4}\frac{1}{4}\frac{3}{4}$ ; $\frac{3}{4}\frac{3}{4}\frac{1}{4}$	
CdCl <sub>2</sub> (rhbdrl.)	Cd—000      Cl— $uuu$ ; $\bar{u}\bar{u}\bar{u}$	For CdCl <sub>2</sub> , $u = 0.25$
CaF <sub>2</sub> (cubic)	Ca—000; $0\frac{1}{2}\frac{1}{2}$ ; $\frac{1}{2}0\frac{1}{2}$ ; $\frac{1}{2}\frac{1}{2}0$ F— $\frac{1}{4}\frac{1}{4}\frac{1}{4}$ ; $\frac{1}{4}\frac{3}{4}\frac{3}{4}$ ; $\frac{3}{4}\frac{1}{4}\frac{3}{4}$ ; $\frac{3}{4}\frac{3}{4}\frac{1}{4}$ ; $\frac{1}{4}\frac{1}{4}\frac{3}{4}$ ; $\frac{1}{4}\frac{3}{4}\frac{1}{4}$ ; $\frac{3}{4}\frac{1}{4}\frac{1}{4}$ ; $\frac{3}{4}\frac{3}{4}\frac{1}{4}$	
CdI <sub>2</sub> (hex.)	Cd—000      I— $\frac{1}{3}\frac{2}{3}u$ ; $\frac{2}{3}\frac{1}{3}u$	
SnO <sub>2</sub> (cassiterite)	Sn—000; $\frac{1}{2}\frac{1}{2}\frac{1}{2}$	(tetragonal)
	O— $uu0$ ; $\bar{u}\bar{u}0$ ; $\frac{1}{2} - u$ , $u + \frac{1}{2}$ , $\frac{1}{2}$ ; $u + \frac{1}{2}$ , $\frac{1}{2} - u$ , $\frac{1}{2}$	
FeS <sub>2</sub>	Fe—000; $\frac{1}{2}\frac{1}{2}0$ ; $\frac{1}{2}0\frac{1}{2}$ ; $0\frac{1}{2}\frac{1}{2}$	(cubic)
	S— $uuu$ ; $u + \frac{1}{2}$ ; $\frac{1}{2} - u$ ; $\bar{u}$ ; $\bar{u}$ , $u + \frac{1}{2}$ , $\frac{1}{2} - u$ ; $\frac{1}{2} - u$ , $\bar{u}$ , $u + \frac{1}{2}$ ; $\bar{u}\bar{u}\bar{u}$ ; $\frac{1}{2} - u$ , $u + \frac{1}{2}$ , $u$ ; $u$ , $\frac{1}{2} - u$ , $u + \frac{1}{2}$ ; $u + \frac{1}{2}$ , $u$ , $\frac{1}{2} - u$	
Fe <sub>2</sub> O <sub>3</sub>	Fe— $uuu$ ; $\bar{u}\bar{u}\bar{u}$ ; $\frac{1}{2} - u$ , $\frac{1}{2} - u$ , $\frac{1}{2} - u$ ; $u + \frac{1}{2}$ , $u + \frac{1}{2}$ , $u + \frac{1}{2}$ (rhombohedral) O— $v\bar{v}0$ ; $\bar{v}0v$ ; $\frac{1}{2} - v$ , $v + \frac{1}{2}$ , $\frac{1}{2}$ ; $v + \frac{1}{2}$ , $\frac{1}{2}$ , $\frac{1}{2} - v$ ; $\frac{1}{2}$ , $\frac{1}{2} - v$ , $v + \frac{1}{2}$	
Cu <sub>5</sub> Zn <sub>8</sub> (see p. 523)	(cubic)	
NaNO <sub>3</sub> ,	Na— $\frac{1}{4}\frac{1}{4}\frac{1}{4}$ ; $\frac{3}{4}\frac{3}{4}\frac{3}{4}$	(rhombohedral)
	N—000; $\frac{1}{2}\frac{1}{2}\frac{1}{2}$	$u = 0.25$ to $0.27$
	O: $u\bar{u}0$ ; $\bar{u}0u$ ; $0u\bar{u}$ ; $\frac{1}{2} - u$ , $u + \frac{1}{2}$ , $\frac{1}{2}$ ; $u + \frac{1}{2}$ , $\frac{1}{2}$ , $\frac{1}{2} - u$ ; $\frac{1}{2}$ , $\frac{1}{2} - u$ , $u + \frac{1}{2}$	

TABLE XII.—NATURAL TRIGONOMETRIC FUNCTIONS FOR DECIMAL FRACTIONS OF A DEGREE\*

Deg.	sin	cos	tan	cot	Deg.	Deg.	sin	cos	tan	cot	Deg.
0.0	.00000	1.0000	.00000	$\infty$	90.0	6.0	.10453	0.9945	.10510	9.514	84.0
.1	.00175	1.0000	.00175	573.0	.9	.1	.10626	.9943	.10687	9.357	.9
.2	.00349	1.0000	.00349	286.5	.8	.2	.10800	.9942	.10863	9.205	.8
.3	.00524	1.0000	.00524	191.0	.7	.3	.10973	.9940	.11040	9.058	.7
.4	.00698	1.0000	.00698	143.24	.6	.4	.11147	.9938	.11217	8.915	.6
.5	.00873	1.0000	.00873	114.59	.5	.5	.11320	.9936	.11394	8.777	.5
.6	.01047	0.9999	.01047	95.49	.4	.6	.11494	.9934	.11570	8.643	.4
.7	.01222	.9999	.01222	81.85	.3	.7	.11667	.9932	.11747	8.513	.3
.8	.01396	.9999	.01396	71.62	.2	.8	.11840	.9930	.11924	8.386	.2
.9	.01571	.9999	.01571	63.66	.1	.9	.12014	.9928	.12101	8.264	.1
1.0	.01745	0.9998	.01746	57.29	89.0	7.0	.12187	0.9925	.12278	8.144	83.0
.1	.01920	.9998	.01920	52.08	.9	.1	.12360	.9923	.12456	8.028	.9
.2	.02094	.9998	.02095	47.74	.8	.2	.12533	.9921	.12633	7.916	.8
.3	.02269	.9997	.02269	44.07	.7	.3	.12706	.9919	.12810	7.806	.7
.4	.02443	.9997	.02444	40.92	.6	.4	.12880	.9917	.12988	7.700	.6
.5	.02618	.9997	.02619	38.19	.5	.5	.13053	.9914	.13165	7.596	.5
.6	.02792	.9996	.02793	35.80	.4	.6	.13226	.9912	.13343	7.495	.4
.7	.02967	.9996	.02968	33.69	.3	.7	.13399	.9910	.13521	7.396	.3
.8	.03141	.9995	.03143	31.82	.2	.8	.13572	.9907	.13698	7.300	.2
.9	.03316	.9995	.03317	30.14	.1	.9	.13744	.9905	.13876	7.207	.1
2.0	.03490	0.9994	.03492	28.64	88.0	8.0	.13917	0.9903	.14054	7.115	82.0
.1	.03664	.9993	.03667	27.27	.9	.1	.14090	.9900	.14232	7.026	.9
.2	.03839	.9993	.03842	26.03	.8	.2	.14263	.9898	.14410	6.940	.8
.3	.04013	.9992	.04016	24.90	.7	.3	.14436	.9895	.14588	6.855	.7
.4	.04188	.9991	.04191	23.86	.6	.4	.14608	.9893	.14767	6.772	.6
.5	.04362	.9990	.04366	22.90	.5	.5	.14781	.9890	.14945	6.691	.5
.6	.04536	.9990	.04541	22.02	.4	.6	.14954	.9888	.15124	6.612	.4
.7	.04711	.9989	.04716	21.20	.3	.7	.15126	.9885	.15302	6.535	.3
.8	.04885	.9988	.04891	20.45	.2	.8	.15299	.9882	.15481	6.460	.2
.9	.05059	.9987	.05066	19.74	.1	.9	.15471	.9880	.15660	6.386	.1
3.0	.05234	0.9986	.05241	19.081	87.0	9.0	.15643	0.9877	.15838	6.314	81.0
.1	.05408	.9985	.05416	18.464	.9	.1	.15816	.9874	.16017	6.243	.9
.2	.05582	.9984	.05591	17.886	.8	.2	.15988	.9871	.16196	6.174	.8
.3	.05756	.9983	.05766	17.343	.7	.3	.16160	.9869	.16376	6.107	.7
.4	.05931	.9982	.05941	16.832	.6	.4	.16333	.9866	.16555	6.041	.6
.5	.06105	.9981	.06116	16.350	.5	.5	.16505	.9863	.16734	5.976	.5
.6	.06279	.9980	.06291	15.895	.4	.6	.16677	.9860	.16914	5.912	.4
.7	.06453	.9979	.06467	15.464	.3	.7	.16849	.9857	.17093	5.850	.3
.8	.06627	.9978	.06642	15.056	.2	.8	.17021	.9854	.17273	5.789	.2
.9	.06802	.9977	.06817	14.669	.1	.9	.17193	.9851	.17453	5.730	.1
.40	.06976	0.9976	.06993	14.301	86.0	10.0	.1736	0.9848	.1763	5.671	80.0
.1	.07150	.9974	.07168	13.951	.9	.1	.1754	.9845	.1781	5.614	.9
.2	.07324	.9973	.07344	13.617	.8	.2	.1771	.9842	.1799	5.558	.8
.3	.07498	.9972	.07519	13.300	.7	.3	.1788	.9839	.1817	5.503	.7
.4	.07672	.9971	.07695	12.996	.6	.4	.1805	.9836	.1835	5.449	.6
.5	.07846	.9969	.07870	12.706	.5	.5	.1822	.9833	.1853	5.396	.5
.6	.08020	.9968	.08046	12.429	.4	.6	.1840	.9829	.1871	5.343	.4
.7	.08194	.9966	.08221	12.163	.3	.7	.1857	.9826	.1890	5.292	.3
.8	.08368	.9965	.08397	11.909	.2	.8	.1874	.9823	.1908	5.242	.2
.9	.08542	.9963	.08573	11.664	.1	.9	.1891	.9820	.1926	5.193	.1
5.0	.08716	0.9962	.08749	11.430	85.0	11.0	.1908	0.9816	.1944	5.145	79.0
.1	.08889	.9960	.08925	11.205	.9	.1	.1925	.9813	.1962	5.097	.9
.2	.09063	.9959	.09101	10.988	.8	.2	.1942	.9810	.1980	5.050	.8
.3	.09237	.9957	.09277	10.780	.7	.3	.1959	.9806	.1998	5.005	.7
.4	.09411	.9956	.09453	10.579	.6	.4	.1977	.9803	.2016	4.959	.6
.5	.09585	.9954	.09629	10.385	.5	.5	.1994	.9799	.2035	4.915	.5
.6	.09758	.9952	.09805	10.199	.4	.6	.2011	.9796	.2053	4.872	.4
.7	.09932	.9951	.09981	10.019	.3	.7	.2028	.9792	.2071	4.829	.3
.8	.10106	.9949	.10158	9.845	.2	.8	.2045	.9789	.2089	4.787	.2
.9	.10279	.9947	.10334	9.677	.1	.9	.2062	.9785	.2107	4.745	.1
6.0	.10453	0.9945	.10510	9.514	84.0	12.0	.2079	0.9781	.2126	4.705	78.0
Deg.	cos	sin	cot	tan	Deg.	Deg.	cos	sin	cot	tan	Deg.

TABLE XII.—NATURAL TRIGONOMETRIC FUNCTIONS FOR DECIMAL FRACTIONS OF A DEGREE.\*—(Continued)

Deg.	sin	cos	tan	cot	Deg.	Deg.	sin	cos	tan	cot	Deg.
12.0	0.2079	0.9781	0.2126	4.705	78.0	18.0	0.3090	0.9511	0.3249	3.078	72.0
.1	.2096	.9778	.2144	4.665	.9	.1	.3107	.9505	.3269	3.060	.9
.2	.2113	.9774	.2162	4.625	.8	.2	.3123	.9500	.3283	3.042	.8
.3	.2130	.9770	.2180	4.586	.7	.3	.3140	.9494	.3307	3.024	.7
.4	.2147	.9767	.2199	4.548	.6	.4	.3156	.9489	.3327	3.006	.6
.5	.2164	.9763	.2217	4.511	.5	.5	.3173	.9483	.3346	2.989	.5
.6	.2181	.9759	.2235	4.474	.4	.6	.3190	.9478	.3365	2.971	.4
.7	.2198	.9755	.2254	4.437	.3	.7	.3206	.9472	.3385	2.954	.3
.8	.2215	.9751	.2272	4.402	.2	.8	.3223	.9466	.3404	2.937	.2
.9	.2233	.9748	.2290	4.366	.1	.9	.3239	.9461	.3424	2.921	.1
13.0	0.2250	0.9744	0.2309	4.331	77.0	19.0	0.3256	0.9455	0.3443	2.904	71.0
.1	.2267	.9740	.2327	4.297	.9	.1	.3272	.9449	.3463	2.888	.9
.2	.2284	.9736	.2345	4.264	.8	.2	.3289	.9444	.3482	2.872	.8
.3	.2300	.9732	.2364	4.230	.7	.3	.3305	.9438	.3502	2.856	.7
.4	.2317	.9728	.2382	4.198	.6	.4	.3322	.9432	.3522	2.840	.6
.5	.2334	.9724	.2401	4.165	.5	.5	.3338	.9426	.3541	2.824	.5
.6	.2351	.9720	.2419	4.134	.4	.6	.3355	.9421	.3561	2.808	.4
.7	.2368	.9715	.2438	4.102	.3	.7	.3371	.9415	.3581	2.793	.3
.8	.2385	.9711	.2456	4.071	.2	.8	.3387	.9409	.3600	2.778	.2
.9	.2402	.9707	.2475	4.041	.1	.9	.3404	.9403	.3620	2.762	.1
14.0	0.2419	0.9703	0.2493	4.011	76.0	20.0	0.3420	0.9397	0.3640	2.747	70.0
.1	.2436	.9699	.2512	3.981	.9	.1	.3437	.9391	.3659	2.733	.9
.2	.2453	.9694	.2530	3.952	.8	.2	.3453	.9385	.3679	2.718	.8
.3	.2470	.9690	.2549	3.923	.7	.3	.3469	.9379	.3699	2.703	.7
.4	.2487	.9686	.2568	3.895	.6	.4	.3486	.9373	.3719	2.689	.6
.5	.2504	.9681	.2586	3.867	.5	.5	.3502	.9367	.3739	2.675	.5
.6	.2521	.9677	.2605	3.839	.4	.6	.3518	.9361	.3759	2.660	.4
.7	.2538	.9673	.2623	3.812	.3	.7	.3535	.9354	.3779	2.646	.3
.8	.2554	.9668	.2642	3.785	.2	.8	.3551	.9348	.3799	2.633	.2
.9	.2571	.9664	.2661	3.758	.1	.9	.3567	.9342	.3819	2.619	.1
15.0	0.2588	0.9659	0.2679	3.732	75.0	21.0	0.3584	0.9336	0.3839	2.605	69.0
.1	.2605	.9655	.2698	3.706	.9	.1	.3600	.9330	.3859	2.592	.9
.2	.2622	.9650	.2717	3.681	.8	.2	.3616	.9323	.3879	2.578	.8
.3	.2639	.9646	.2736	3.655	.7	.3	.3633	.9317	.3899	2.565	.7
.4	.2656	.9641	.2754	3.630	.6	.4	.3649	.9311	.3919	2.552	.6
.5	.2672	.9636	.2773	3.606	.5	.5	.3665	.9304	.3939	2.539	.5
.6	.2689	.9632	.2792	3.582	.4	.6	.3681	.9298	.3959	2.526	.4
.7	.2706	.9627	.2811	3.558	.3	.7	.3697	.9291	.3979	2.513	.3
.8	.2723	.9622	.2830	3.534	.2	.8	.3714	.9285	.4000	2.500	.2
.9	.2740	.9617	.2849	3.511	.1	.9	.3730	.9278	.4020	2.488	.1
16.0	0.2756	0.9613	0.2867	3.487	74.0	22.0	0.3746	0.9272	0.4040	2.475	68.0
.1	.2773	.9608	.2886	3.465	.9	.1	.3762	.9265	.4061	2.463	.9
.2	.2790	.9603	.2905	3.442	.8	.2	.3778	.9259	.4081	2.450	.8
.3	.2807	.9598	.2924	3.420	.7	.3	.3795	.9252	.4101	2.438	.7
.4	.2823	.9593	.2943	3.398	.6	.4	.3811	.9245	.4122	2.426	.6
.5	.2840	.9588	.2962	3.376	.5	.5	.3827	.9239	.4142	2.414	.5
.6	.2857	.9583	.2981	3.354	.4	.6	.3843	.9232	.4163	2.402	.4
.7	.2874	.9578	.3000	3.333	.3	.7	.3859	.9225	.4183	2.391	.3
.8	.2890	.9573	.3019	3.312	.2	.8	.3875	.9219	.4204	2.379	.2
.9	.2907	.9568	.3038	3.291	.1	.9	.3891	.9212	.4224	2.367	.1
17.0	0.2924	0.9563	0.3057	3.271	73.0	23.0	0.3907	0.9205	0.4245	2.356	67.0
.1	.2940	.9558	.3076	3.251	.9	.1	.3923	.9198	.4265	2.344	.9
.2	.2957	.9553	.3096	3.230	.8	.2	.3939	.9191	.4286	2.333	.8
.3	.2974	.9548	.3115	3.211	.7	.3	.3955	.9184	.4307	2.322	.7
.4	.2990	.9542	.3134	3.191	.6	.4	.3971	.9178	.4327	2.311	.6
.5	.3007	.9537	.3153	3.172	.5	.5	.3987	.9171	.4348	2.300	.5
.6	.3024	.9532	.3172	3.152	.4	.6	.4003	.9164	.4369	2.289	.4
.7	.3040	.9527	.3191	3.133	.3	.7	.4019	.9157	.4390	2.278	.3
.8	.3057	.9521	.3211	3.115	.2	.8	.4035	.9150	.4411	2.267	.2
.9	.3074	.9516	.3230	3.096	.1	.9	.4051	.9143	.4431	2.257	.1
18.0	0.3090	0.9511	0.3249	3.078	72.0	24.0	0.4067	0.9135	0.4452	2.246	66.0
Deg.	cos	sin	cot	tan	Deg.	Deg.	cos	sin	cot	tan	Dg.

TABLE XII.—NATURAL TRIGONOMETRIC FUNCTIONS FOR DECIMAL FRACTIONS OF A DEGREE.\*—(Continued)

Deg.	sin	cos	tan	cot	Deg.	Deg.	sin	cos	tan	cot	Deg.
24.0	0.4067	0.9135	0.4452	2.246	66.0	30.0	0.5000	0.8660	0.5774	1.7321	60.0
.1	.4083	.9128	.4473	2.236	.9	.1	.5015	.8652	.5797	1.7251	.9
.2	.4099	.9121	.4494	2.225	.8	.2	.5030	.8643	.5820	1.7182	.8
.3	.4115	.9114	.4515	2.215	.7	.3	.5045	.8634	.5844	1.7113	.7
.4	.4131	.9107	.4536	2.204	.6	.4	.5060	.8625	.5867	1.7045	.6
.5	.4147	.9100	.4557	2.194	.5	.5	.5075	.8616	.5890	1.6977	.5
.6	.4163	.9092	.4578	2.184	.4	.6	.5090	.8607	.5914	1.6909	.4
.7	.4179	.9085	.4599	2.174	.3	.7	.5105	.8599	.5938	1.6842	.3
.8	.4195	.9078	.4621	2.164	.2	.8	.5120	.8590	.5961	1.6775	.2
.9	.4210	.9070	.4642	2.154	.1	.9	.5135	.8581	.5985	1.6709	.1
25.0	0.4226	0.9063	0.4663	2.145	65.0	31.0	0.5150	0.8572	0.6009	1.6643	59.0
.1	.4242	.9056	.4684	2.135	.9	.1	.5165	.8563	.6032	1.6577	.9
.2	.4258	.9048	.4706	2.125	.8	.2	.5180	.8554	.6056	1.6512	.8
.3	.4274	.9041	.4727	2.116	.7	.3	.5195	.8545	.6080	1.6447	.7
.4	.4289	.9033	.4748	2.106	.6	.4	.5210	.8536	.6104	1.6383	.6
.5	.4305	.9026	.4770	2.097	.5	.5	.5225	.8526	.6128	1.6319	.5
.6	.4321	.9018	.4791	2.087	.4	.6	.5240	.8517	.6152	1.6255	.4
.7	.4337	.9011	.4813	2.078	.3	.7	.5255	.8508	.6176	1.6191	.3
.8	.4352	.9003	.4834	2.069	.2	.8	.5270	.8499	.6200	1.6128	.2
.9	.4368	.8996	.4856	2.059	.1	.9	.5284	.8490	.6224	1.6066	.1
26.0	0.4384	0.8988	0.4877	2.050	64.0	32.0	0.5299	0.8480	0.6249	1.6003	58.0
.1	.4399	.8980	.4899	2.041	.9	.1	.5314	.8471	.6273	1.5941	.9
.2	.4415	.8973	.4921	2.032	.8	.2	.5329	.8462	.6297	1.5880	.8
.3	.4431	.8965	.4942	2.023	.7	.3	.5344	.8453	.6322	1.5818	.7
.4	.4446	.8957	.4964	2.014	.6	.4	.5358	.8443	.6346	1.5757	.6
.5	.4462	.8949	.4986	2.006	.5	.5	.5373	.8434	.6371	1.5697	.5
.6	.4478	.8942	.5008	1.997	.4	.6	.5388	.8425	.6395	1.5637	.4
.7	.4493	.8934	.5029	1.988	.3	.7	.5402	.8415	.6420	1.5577	.3
.8	.4509	.8926	.5051	1.980	.2	.8	.5417	.8406	.6445	1.5517	.2
.9	.4524	.8918	.5073	1.971	.1	.9	.5432	.8396	.6469	1.5458	.1
27.0	0.4540	0.8910	0.5095	1.963	63.0	33.0	0.5446	0.8387	0.6494	1.5399	57.0
.1	.4555	.8902	.5117	1.954	.9	.1	.5461	.8377	.6519	1.5340	.9
.2	.4571	.8894	.5139	1.946	.8	.2	.5476	.8368	.6544	1.5282	.8
.3	.4586	.8886	.5161	1.937	.7	.3	.5490	.8358	.6569	1.5224	.7
.4	.4602	.8878	.5184	1.929	.6	.4	.5505	.8348	.6594	1.5166	.6
.5	.4617	.8870	.5206	1.921	.5	.5	.5519	.8339	.6619	1.5108	.5
.6	.4633	.8862	.5228	1.913	.4	.6	.5534	.8329	.6644	1.5051	.4
.7	.4648	.8854	.5250	1.905	.3	.7	.5548	.8320	.6669	1.4994	.3
.8	.4664	.8846	.5272	1.897	.2	.8	.5563	.8310	.6694	1.4938	.2
.9	.4679	.8838	.5295	1.889	.1	.9	.5577	.8300	.6720	1.4882	.1
28.0	0.4695	0.8829	0.5317	1.881	62.0	34.0	0.5592	0.8290	0.6745	1.4826	56.0
.1	.4710	.8821	.5340	1.873	.9	.1	.5606	.8281	.6771	1.4770	.9
.2	.4726	.8813	.5362	1.865	.8	.2	.5621	.8271	.6796	1.4715	.8
.3	.4741	.8805	.5384	1.857	.7	.3	.5635	.8261	.6822	1.4659	.7
.4	.4756	.8796	.5407	1.849	.6	.4	.5650	.8251	.6847	1.4605	.6
.5	.4772	.8788	.5430	1.842	.5	.5	.5664	.8241	.6873	1.4550	.5
.6	.4787	.8780	.5452	1.834	.4	.6	.5678	.8231	.6899	1.4496	.4
.7	.4802	.8771	.5475	1.827	.3	.7	.5693	.8221	.6924	1.4442	.3
.8	.4818	.8763	.5498	1.819	.2	.8	.5707	.8211	.6950	1.4388	.2
.9	.4833	.8755	.5520	1.811	.1	.9	.5721	.8202	.6976	1.4335	.1
29.0	0.4848	0.8746	0.5543	1.804	61.0	35.0	0.5736	0.8192	0.7002	1.4281	55.0
.1	.4863	.8738	.5566	1.797	.9	.1	.5750	.8181	.7028	1.4229	.9
.2	.4879	.8729	.5589	1.789	.8	.2	.5764	.8171	.7054	1.4176	.8
.3	.4894	.8721	.5612	1.782	.7	.3	.5779	.8161	.7080	1.4124	.7
.4	.4909	.8712	.5635	1.775	.6	.4	.5793	.8151	.7107	1.4071	.6
.5	.4924	.8704	.5658	1.767	.5	.5	.5807	.8141	.7133	1.4019	.5
.6	.4939	.8695	.5681	1.760	.4	.6	.5821	.8131	.7159	1.3968	.4
.7	.4955	.8686	.5704	1.753	.3	.7	.5835	.8121	.7186	1.3916	.3
.8	.4970	.8678	.5727	1.746	.2	.8	.5850	.8111	.7212	1.3865	.2
.9	.4985	.8669	.5750	1.739	.1	.9	.5864	.8100	.7239	1.3814	.1
30.0	0.5000	0.8660	0.5774	1.732	60.0	36.0	0.5878	0.8090	0.7265	1.3764	54.0
Deg.	cos	sin	cot	tan	Deg.	Deg.	cos	sin	cot	tan	Deg.

TABLE XII.—NATURAL TRIGONOMETRIC FUNCTIONS FOR DECIMAL FRACTIONS OF A DEGREE.\*—(Continued)

Deg.	sin	cos	tan	cot	Deg.	Deg.	sin	cos	tan	cot	Deg.
36.0	0.5878	0.8090	0.7265	1.3764	54.0	40.5	0.6494	0.7604	0.8541	1.1708	49.5
.1	.5892	.8080	.7292	1.3713	.9	.6	.6508	.7593	.8571	1.1667	.4
.2	.5906	.8070	.7319	1.3663	.8	.7	.6521	.7581	.8601	1.1626	.3
.3	.5920	.8059	.7346	1.3613	.7	.8	.6534	.7570	.8632	1.1585	.2
.4	.5934	.8049	.7373	1.3564	.6	.9	.6547	.7559	.8662	1.1544	.1
.5	.5948	.8039	.7400	1.3514	.5	41.0	0.6561	0.7547	0.8693	1.1504	49.0
.6	.5962	.8028	.7427	1.3465	.4	.1	.6574	.7536	.8724	1.1463	.9
.7	.5976	.8018	.7454	1.3416	.3	.2	.6587	.7524	.8754	1.1423	.8
.8	.5990	.8007	.7481	1.3367	.2	.3	.6600	.7513	.8785	1.1383	.7
.9	.6004	.7997	.7508	1.3319	.1	.4	.6613	.7501	.8816	1.1343	.6
37.0	0.6018	0.7986	0.7536	1.3270	53.0	.5	.6626	.7490	.8847	1.1308	.5
.1	.6032	.7976	.7563	1.3222	.9	.6	.6639	.7478	.8878	1.1263	.4
.2	.6046	.7965	.7590	1.3175	.8	.7	.6652	.7466	.8910	1.1224	.3
.3	.6060	.7955	.7618	1.3127	.7	.8	.6665	.7455	.8941	1.1184	.2
.4	.6074	.7944	.7646	1.3079	.6	.9	.6678	.7443	.8972	1.1145	.1
.5	.6088	.7934	.7673	1.3032	.5	42.0	0.6691	0.7431	0.9004	1.1106	48.0
.6	.6101	.7923	.7701	1.2985	.4	.1	.6704	.7420	.9036	1.1067	.9
.7	.6115	.7912	.7729	1.2938	.3	.2	.6717	.7408	.9067	1.1028	.8
.8	.6129	.7902	.7757	1.2892	.2	.3	.6730	.7396	.9099	1.0990	.7
.9	.6143	.7891	.7785	1.2846	.1	.4	.6743	.7385	.9131	1.0951	.6
38.0	0.6157	0.7880	0.7813	1.2799	52.0	.5	.6756	.7373	.9163	1.0913	.5
.1	.6170	.7869	.7841	1.2753	.9	.6	.6769	.7361	.9195	1.0875	.4
.2	.6184	.7859	.7869	1.2708	.8	.7	.6782	.7349	.9228	1.0837	.3
.3	.6198	.7848	.7898	1.2662	.7	.8	.6794	.7337	.9260	1.0799	.2
.4	.6211	.7837	.7926	1.2617	.6	.9	.6807	.7325	.9293	1.0761	.1
.5	.6225	.7826	.7954	1.2572	.5	43.0	0.6820	0.7314	0.9325	1.0724	47.0
.6	.6239	.7815	.7983	1.2527	.4	.1	.6833	.7302	.9358	1.0686	.9
.7	.6252	.7804	.8012	1.2482	.3	.2	.6845	.7290	.9391	1.0649	.8
.8	.6266	.7793	.8040	1.2437	.2	.3	.6858	.7278	.9424	1.0612	.7
.9	.6280	.7782	.8069	1.2393	.1	.4	.6871	.7266	.9457	1.0575	.6
39.0	0.6293	0.7771	0.8098	1.2349	51.0	.5	.6884	.7254	.9490	1.0538	.5
.1	.6307	.7760	.8127	1.2305	.9	.6	.6896	.7242	.9523	1.0501	.4
.2	.6320	.7749	.8156	1.2261	.8	.7	.6909	.7230	.9556	1.0464	.3
.3	.6334	.7738	.8185	1.2218	.7	.8	.6921	.7218	.9590	1.0428	.2
.4	.6347	.7727	.8214	1.2174	.6	.9	.6934	.7206	.9623	1.0392	.1
.5	.6361	.7716	.8243	1.2131	.5	44.0	0.6947	0.7193	0.9657	1.0355	46.0
.6	.6374	.7705	.8273	1.2088	.4	.1	.6959	.7181	.9691	1.0319	.9
.7	.6388	.7694	.8302	1.2045	.3	.2	.6972	.7169	.9725	1.0283	.8
.8	.6401	.7683	.8332	1.2002	.2	.3	.6984	.7157	.9759	1.0247	.7
.9	.6414	.7672	.8361	1.1960	.1	.4	.6997	.7145	.9793	1.0212	.6
40.0	0.6428	0.7660	0.8391	1.1918	50.0	.5	.7009	.7133	.9827	1.0176	.5
.1	.6441	.7649	.8421	1.1875	.9	.6	.7022	.7120	.9861	1.0141	.4
.2	.6455	.7638	.8451	1.1833	.8	.7	.7034	.7108	.9896	1.0105	.3
.3	.6468	.7627	.8481	1.1792	.7	.8	.7046	.7096	.9930	1.0070	.2
.4	.6481	.7615	.8511	1.1750	.6	.9	.7059	.7083	.9965	1.0035	.1
40.5	0.6494	0.7604	0.8541	1.1708	49.5	45.0	0.7071	0.7071	1.0000	1.0000	45.0
Deg.	cos	sin	cot	tan	Deg.	Deg.	cos	sin	cot	tan	Deg.

\* Reprinted from the "Handbook of Chemistry and Physics" by permission of the Chemical Rubber Company.





# INDEX

## A

- Abbott, F. R., 117  
Absorption, 71  
    chemical analysis by, 423  
    coefficient, 71, 164, 290  
        atomic, 79, 571  
        mass, 72, 568  
    edges, 73, 82, 288, 571  
    fluorescent, 76, 77  
    in powder patterns, 414  
    true, 76, 77  
Acceleration, of electrons, 36  
Accelerator, induction, 150  
Activator, 170  
Adams, G. D., 80  
Afterglow, 169  
Age hardening, 478  
Air-wall chamber, 191  
Albumen, 533  
Alcock, T. C., 533  
Allen, J. S., 157, 196  
Allessandrini, E. I., 554  
Allison, S. K., 39, 40, 43, 48, 84, 334, 357,  
    360, 367, 496, 499  
Allotropy, 417  
Allowed levels, 82  
Allowed lines, 67  
Allowed orbits, 58  
Allowed values, 62  
Alloys, 435, 520  
Alpha angle, 301  
Alpha brass, 522  
Alpha iron, 418  
Alpha particles and rays, 49, 154, 158  
    definition of, 158, 160  
    spectrum, 166  
Aluminum, extruded, 272  
    fibering in, 452  
    rolled, 272, 456  
    spot welds in, 273  
Aluminum castings, 269  
Aluminum wire, 452  
Amalgams, 555  
Amoroso, E. C., 228  
Amorphous materials, 406, 430, 496, 507,  
    511  
Amplifier, 30  
Analysis, chemical, 420  
    crystal, 340, 371, 378, 410  
Anderson, C. D., 79  
Andrade, E. N. C., 553  
Andrew, L. T., 554  
Angle, Bragg ( $\theta$ ), 324, 402  
    between planes, 459  
    scattering, ( $\phi$ ), 332  
Angstrom, 22, 66, 561  
Angular intensity distribution, 39  
Angular momentum, 58, 61  
Angular scattering, intensity, 78, 333  
Anita, D. P., 526  
Anode, 6, 112, 117  
    hooded, 108  
    rotating, 16, 18, 105, 116  
    tungsten, 14  
Anticathode, 6  
Apparatus, generating, 6, 105, 296  
    arrangement of, 147  
Ares, diffraction, 404, 527, 556  
    goniometer, 372, 380  
    orientation, 452, 457, 554  
Armstrong, E. J., 530  
Arneson, A. N., 201  
Artificial radioactivity, 165  
Astbury, W. T., 533  
Asterism, 474  
A.S.T.M. recommendations, 431  
Atlee, Z. J., 18, 105  
Atom, 7, 11, 49  
Atomic absorption coefficient, 79, 571  
Atomic bomb, 56, 167  
Atomic nuclei, 157, 536  
Atomic number, 14, 34, 47, 49, 158  
    and scattering, 78  
Atomic planes, 303, 459  
Atomic scattering coefficient, 79  
Atomic separations, 506, 517, 519, 557

- Atomic structure, 55, 352, 356, 500, 504
    - factor, 352, 356, 500, 537
  - Atomic weight, 47, 158, 572
  - Auger, P., 81
  - Auger effect, 81
  - Auger electrons, 81
  - Auger tracks, 81, 91
  - Austenite, 526
  - Automatic inspection, 286
  - Autotransformer, 138
  - Avogadro number, 79, 104, 337, 561
  - Axes, crystal, 301
    - fiber, 451, 455
    - principal, 487
    - of symmetry, 311
    - zone, 317
  - Axial ratio, 314
  - Axon, P. E., 554
  - Aylmer, A. E., 555
  - Azimuthal quantum number, 59, 61
- B
- Bachman, C. H., 545
  - Back-reflection patterns, 400, 538
    - best radiation for, 471
    - and strain, 470
  - Bäcklin, E., 103
  - Bailey, G. L. J., 555
  - Bain, E. C., 526
  - Baker, R. F., 182
  - Ballard, J. W., 433, 435, 533
  - Bands, diffraction, 496
    - energy level, 82
  - Barclay, A. E., 225
  - Barkla, C. G., 42, 46, 51, 90
  - Barkow, A. G., 458
  - Barlow, W., 312, 317
  - Barnes, R. B., 159
  - Barnes, R. J., 398
  - Barrell, C. W., 292
  - Barrett, C. S., 309, 462, 474, 482, 485, 499, 506
  - Bartlett, J. H., 152
  - Barytron, 157
  - Basart, J. C. M., 456
  - Bauer, S. H., 143, 556
  - Baxter, A., 433
  - Bayley, P. L., 293
  - Beach, J. Y., 557, 558
  - Bearden, J. A., 49, 99, 103, 338
  - Bearing journals, 527
  - Bearing lubrication, 554
  - Bearing radiography, 268
  - Bearing wear, 554
  - Beatty, R. T., 14, 34, 40, 51
  - Beatty's equation, 14
  - Beck, J., 105
  - Becker, A., 557
  - Becquerel, A. H., 160
  - Beeck, O., 555
  - Beeman, W. W., 82, 83, 547
  - Beese, N. C., 112
  - Beevers, C. A., 361
  - Beilby layer, 554
  - Bell, G. E., 179-181
  - Bellows, brass, 456, 552
  - Bémont, G., 160
  - Benson focus, 18, 112
  - Benzene, 519, 556
  - Berkelhamer, L. H., 533
  - Berkley, E. E., 433
  - Bernal, J. D., 384, 388
  - Bernal chart, 388
  - Bernet, E. J., 118, 146, 149
  - Beryllium windows, 106, 111
  - Beta angle, 301
  - Beta brass, 522
  - Beta iron, 418
  - Beta particles and rays, 49, 160
    - secondary, 76, 81, 292
    - spectrum, 166
  - Betatron, 5, 150, 237
  - Bewilogua, L., 501, 505, 506
  - Binders, 406
  - Binding, chemical, 517-519
  - Binding energy, 52, 61, 159
  - Bircumshaw, L. L., 554
  - Birge, R. T., 22, 26, 27, 159, 340
  - Biscoe, J., 391, 512
  - Bjurström, T., 417
  - Black body, 25
  - Black paper, 117, 291, 394, 473
  - Blackett, P. M. S., 166
  - Blackman, M., 537
  - Bloch, F., 83
  - Blocking material, 253
    - liquid, 255
  - Blodgett, K. B., 286
  - Blow holes, 262
  - Blurring, 215, 217, 243
  - Boardman, B. F., 42
  - Body-centered lattices, 306
  - Body-centered reflections (diagram), 401
  - Böhm, K., 37

- Bohlin, H., 397  
Bohr, N., 4, 39, 49, 50, 52, 53, 58, 166  
Bollman, V. L., 338  
Boltzmann constant, 12, 365, 561  
Bomb, atomic, 56, 167  
  radium, 233  
Bombardment, electron, 7  
  ion, 8, 110  
Bond, W. L., 530  
Bonding, 267  
Bonds, carbon, 518  
  covalent, 517  
  double, 518  
  homopolar, 517  
  hydrogen, 518  
  ionic, 517  
  metallic, 519  
  resonance of, 519  
  single, 518  
  triple, 518  
  Van der Waals, 519  
Booth, A. D., 364  
Born, M., 60, 478  
Bouguer, 71  
Bowers, A., 222  
Bozorth, R. M., 398, 450, 459  
Bradley, A. J., 400, 405, 523  
Bragg, W. H., 4, 28, 51, 79, 109, 322, 361, 474, 478, 517, 520  
Bragg, W. L., 4, 109, 336, 361-364, 369, 469, 474, 517, 520, 527  
Bragg angle, ( $\theta$ ), 324, 402  
Bragg method, 331, 340  
Bragg reflection, 327, 346, 373, 472, 551  
Bragg spectrometer, 333  
Bragg's law, 99, 322, 324, 328, 477, 538  
Brass, cold work in, 449, 456, 478  
  drawing, 456  
  rolling, 456  
  structure of, 522  
Brass bellows, 456, 552  
Brass castings, 276  
Bravais, A., 299, 301  
Breadth (*see* Width)  
Breit, G., 154, 500  
Brentano, J., 432, 433  
Brindley, G. W., 355, 356, 365, 504  
Broadening, 448  
  and microstrain, 478  
Brockway, L. O., 547, 556, 558  
Bronze castings, 276  
Brooks, H. B., 123  
Brown, S. C., 163, 195  
Brubaker, D. G., 554  
Brüche, E., 17, 550  
Brytex leaf, 171  
Bucky, G., 216  
Bucky grid, 216, 257  
Buerger, M. J., 347, 383, 389, 399  
Bunn, C. W., 533  
Bunsen-Roscoe law, 179  
Burger, H. C., 68  
Burgers, W. G., 456, 485  
Burwell, J. T., 554
- C
- Cables, shockproof, 127  
Calcite, 338  
Cam, 380  
Cameras, back-reflection, 396  
  cylindrical, 395, 404  
  electron, 545  
  Laue, 372  
  microradiographic, 290  
  miniature, 533  
  Phragmen, 520  
  reflection, 527  
  rotation, 379  
  Seemann-Bohlin, 397  
  simple powder, 392  
Cameron, A., 555  
Cameron, G. H., 448  
Camsell, C., 160  
Cancer, 226, 235  
Carcinoma, 235  
Cartwright, C. H., 286, 552  
Cascading transformer, 126  
Case hardening, 525  
Cassen, B., 232  
Cassette, 3, 173, 186, 214, 245, 392, 396  
  in electron diffraction, 549  
  motion of, 220, 223  
  rotation of, 396, 494  
Castings, aluminum, 269  
  brass, 276  
  bronze, 276  
  die, 275  
  ferrous, 261  
  magnesium, 269  
  zinc, 275  
Catalysis, 555  
Cathode, 6, 109, 111, 120  
  cold, 109  
  for field emission, 296

- Cathode, hot, 111  
Cathode ray, 6, 118, 237, 551  
    therapy, 237  
    tubes, 118  
Cell, 312  
    configuration, 351, 587  
    primitive, 315  
    unit, 312  
Cellophane, 533  
Cellulose, 530  
Cementite, 526  
Center of symmetry, 311, 362, 376  
Cetrone, V. C., 273, 291  
Chadwick, J., 160, 164, 166  
Chamber, cloud, 90  
    ionization, 29, 187, 286, 336  
Characteristic curves, 178  
Characteristic radiation, 48  
Characteristic spectra, 45  
    notation of, 67  
Charge, electronic, 104, 338, 561  
    nuclear, 7, 49, 158  
    space, 116, 121  
Charlesby, A., 179  
Charlton, E. E., 105, 106, 127, 150, 282  
Chemical analysis, 420  
    by Hanawalt method, 423  
    of surface films, 553  
    by x-ray spectroscopy, 421  
Chemistry, 420, 516, 519  
Chesley, F. G., 109  
Chilton, L. V., 288  
Chubb, L. W., 144  
Cinemaradiography, 224, 272  
Circuits, 128  
    Gratz, 136  
    Greinacher, 133  
    La Tour, 133  
    mechanically rectified, 130  
    primary rectified, 129  
    scaling, 195  
    self-rectifying, 128  
    Villard, 131  
    voltage doubling, 131, 133  
Cis form, 506, 557  
Clark, G. L., 290, 291, 474, 478, 517, 531, 547  
Clark, H., 48, 147  
Clark, J. C., 393  
Clark, R. K., 81  
Clarke, H., 478  
Clausen, G. E., 106  
Cleavage, 300  
Clewell, D. H., 545  
Close packing, 312, 315  
Cloud, R. W., 232, 237  
Cloud chamber, 90, 91  
Coatings, 553  
Cochrane, W., 536, 554, 555  
Cockroft, J. D., 154, 165, 236  
Coefficient, absorption, 71, 164, 290  
    atomic, 79, 571  
    linear, 71  
    mass, 72, 568  
    of reflection, 360  
    scattering, 75  
        atomic, 79  
Cohen, M., 526  
Coherent scattering, 77, 83, 88, 320, 496  
Cold shut, 262  
Cold work, 449, 450, 478  
Collector, 120  
Collimation, 334, 372, 379, 392, 396  
Coloration, 292  
Combination principle (Ritz), 52  
Compounds, chemical analysis of, 420  
    geometrical, 435  
    intermetallic, 435, 522  
    interstitial, 525  
    simple, 417  
Compton, A. H., 4, 39, 40, 43, 77, 84, 85, 88, 90, 96, 101, 299, 325, 357, 360, 496, 499, 503  
Compton, K. T., 149  
Compton effect, 83  
Compton scattering, 83  
Condensers, 132, 134, 141  
Conduction, electrical, of surfaces, 554  
    gas, 7  
    in metals, 11  
Cone, of rays, 320, 402  
    treatment, 213, 229  
Configuration, electronic, 69, 502, 504  
    unit cell, 314, 316, 351, 557, 587  
Constant, grating, 103  
    lattice, 316  
        calculation of, 337  
    physical, 561  
    Rydberg, 65, 561  
    screening, 54  
Constant potential (*see c.p.d.c.*)  
Constant-voltage transformer, 143  
Continuous radiation, spectrum, 29, 31, 35

- Continuous radiation, intensity of, 34  
Contour lines, 362  
Contrast, 244  
    film, 179  
    and voltage, 213, 244  
Control of current and voltage, 138  
Convection cooling, 15  
Cook, M., 456  
Coolidge, W. D., 4, 10, 105, 119  
Coolidge tube, 4, 10  
Cooling, 14, 105, 116  
Cooper, E. R., 545  
Cork, J. M., 48, 563  
Corona, 149, 199, 206  
Correspondence principle, 39  
Corrigan, K. E., 232  
Corrosion, 553  
Cosmic rays, 23, 80, 157  
Coster, D., 421  
Cotton, F. W., 433  
Cotton, 533  
Coulson, C. A., 504  
Couloulos, G. D., 555  
Counter, G-M, 163, 193, 336, 409  
Coupling, *jj*, 62  
    Russel-Saunders, 62  
Coutard, H., 234  
Covalent bond, 517  
c.p.d.c., 116, 117, 133, 136  
Crack, 249, 250, 261, 262, 265  
    crater, 248  
Cristobalite, 533  
Crookes, W., 1  
Cross-grating pattern, 539  
Crowther, J. A., 83, 239, 294  
Crystal, axes of, 301  
    chemistry, 517  
    holohedral, 308  
    ionic, 346, 517  
    lattice, 300, 302  
    models, 313, 450  
    mosaic, 366  
    nomenclature, 309  
    perfect, 366  
    piezoelectric, 528  
    planes or faces, 303, 459  
    quartz, 528, 533  
    standard, 336  
    structure factor, 357  
        examples of, 358  
    systems, 305  
    texture, 300, 462  
Crystal, twins, 368  
    types, 417, 576, 587  
Crystal analysis, 340, 371, 378, 410  
Crystallite, 449, 527  
Crystallography, 299, 517  
Cup, focusing, 10, 548  
Curie, I., 165, 236  
Curie, M. S., 160  
Curie, P., 160  
Curie, 162  
Curie point, 418  
Current, control, 138  
    electrical, 11  
    tube, 8  
Cybotaxis, 497  
Cyclohexane, 519, 557  
Cyclotron, 154, 236  
Cylinders, 257, 263, 268, 279  
Czochralski, 477
- D
- d* spacings, 324, 348, 401, 412  
Dana, E. S., 309  
Daniels, F., 119  
Dänzer, H., 154  
Darbyshire, J. A., 545, 554, 556  
Darkroom technique, 183, 431  
Darrow, K. K., 93  
Darwin, C. G., 328, 367  
Dauvillier, A., 32, 34  
Davey, W. P., 194, 335, 336, 380, 407, 409, 415  
Davis, B., 99, 100  
Davisson, C. J., 59, 538  
de Abreu, M., 222  
Debiere, A., 160  
de Broglie, L., 57, 59  
de Broglie, M., 73, 74, 378  
de Broglie waves, 57, 536  
Debye, P., 329, 365, 391, 501, 504–507  
Debye, P. P., 547  
Debye-Scherrer method, 391  
Decker, B. F., 462  
Definition, 215, 244  
Deformation, 448, 449, 468  
de Graaf, J. E., 106, 107  
Dehlinger, U., 11  
de Jong and Bouman method, 389  
de Laszlo, H., 547  
Delisa, J., 186  
den Hoed, D., 293

- Densitometer, 185, 432  
 Density, 432, 561  
     electron, 361  
     x-ray film, 177  
 Dershem, E., 289  
 de Smedt, J., 507  
 Detection of x-rays, 168  
 Deuterium, 158  
 Deuteron or deutron, 158  
 Developers, 183  
 Diagnostic opaques, 219  
 Diagnostic radiology, 211  
 Diagnostic work, 202  
 Diagram, energy level, 64  
     fiber, 455  
     reflection, 401  
 Diamond, 350, 359, 401, 412, 518  
 Diaphragm, Potter-Bucky, 216  
 Die castings, 275  
 Diffraction, by amorphous solids, 496  
     by crystals, 320  
     definition of, 103  
     discovery of, 3  
     electron, 59, 536  
     by gases, 496  
     by liquids, 496  
     mechanism of, 331  
     protection, 205  
     by ruled gratings, 96, 100  
     tubes, 109, 111  
 Diffraction pattern, 299, 554  
     temperature effect on, 364  
 Diffuse reflections, 474, 496  
 Diffuse rings, 446, 478, 496, 507  
 Diffuse scattering, 329, 496  
 Dilution of sample, 407  
 Diode, 119  
 Dirac, P. A. M., 500  
 Direction, crystal, 317, 454  
 Discharge, gaseous, 7  
 Discovery, of electron diffraction, 59  
     of x-ray diffraction, 299  
     of x-rays, 1  
 Disintegration, 158  
 Dispersion, 96  
 Distance (*see* Separation; Spacing)  
 Distortion, radiographic, 214, 243  
 Dixit, K. R., 554  
 Doan, R. L., 102, 299  
 Dobinski, S., 554  
 Documents, 292  
 Donnay, J. D. H., 399  
 Dorgelo, H. B., 68  
 Dose, 188  
     curves, 227, 229, 230  
     definition of, 188  
     and intensity, 189, 229  
     measurement, 190, 227  
     percentage depth, 228  
     from radium, 191  
     threshold (erythema), 201  
 Doublet, 68  
 Drawing, deep, 456  
     wire, 451  
 Draws, 262  
 Dresser, R., 232  
 Driffield, V. C., 178  
 Drosophila, 226, 294  
 Dross, 269  
 Drude, P., 97, 102  
 Dual nature of matter and radiation, 93  
 Duane, W., 27, 163, 325  
 Duane-Hunt limit, 27  
 DuBridge, L. A., 12, 543  
 Duffy, J. J., 201  
 Duggar, B. M., 295  
 DuMond, J. W. M., 28, 86, 105, 334, 338  
 Duncanson, W. E., 504  
 Duplicating, radiographs, 184  
     templates, 297  
 Dushman, S., 12  
 Dusts, 530  
 Dwight, C. H., 293
- E
- Eckart, C., 82  
 Eddy, C. E., 422  
 Edges, absorption, 73, 74, 82  
 Edmunds, G., 456  
 Edmunds, I. G., 179  
 Effect, Auger, 81  
     Compton, 83  
     intermittency, 179  
     wall, 190  
 Efficiency, 14, 34, 154  
     of fluorescence, 171  
 Ehrhardt, F., 506  
 Ehrke, L. F., 107, 296  
 Einstein, A., 55  
 Eisenstein, A., 107, 194, 196  
 Eisl, A., 187  
 Elastic waves, 365, 478  
 Elasticity theory, 486  
 Electromagnetic pulse, 35

- Electromagnetic spectrum, 20, 23  
Electromagnetic vectors, 36  
Electrometer, 30  
Electron (*see* K, L, M, etc.)  
  acceleration, 35  
  bombardment, 7  
  charge, 104, 339, 561  
  configuration, 69  
  density, 362  
  diffraction, 59, 536  
  distribution, 502, 504, 558  
  gun, 114, 548  
  induction accelerator, 150  
  lens, 114, 550  
  multiplier, 195  
  optics, 17, 112, 550  
  orbits, 49  
  patterns, 554  
  shells, 51, 63, 497, 504  
  spin, 61  
  structure factor, 500, 501  
Electrons, Auger, 81  
  free, 10, 82, 522  
  heavy, 157  
  K, L, M, etc., 51  
  photo, 28, 30, 90  
  recoil, 30, 90  
  valence, 69, 517  
Electron-volt, 27, 66, 187, 561  
Electroplating, 464, 555  
Elements, 47, 49, 63, 417, 572, 573, 576  
Elliott, L. G., 163, 195  
Ellis, C. D., 160  
Elwert, G., 41  
Emission, field, 107, 296  
  limited, 115, 120  
  thermionic, 10  
Emulsion, Lippmann, 177, 288  
  photographic, 173  
Enantiomorphic, 308  
Energy, bands, 82  
  binding, 52, 61, 159  
  kinetic, 56  
  levels, 50, 52, 63, 64, 66  
    bands of, 82  
    optical, 69  
  and matter, 56  
  packing, 159  
  and *r* unit, 189  
  of radiation, 26, 37, 93  
Epsilon brass, 524  
Epstein, D. W., 17  
Equipment, arrangement of, 147  
  generating, 105, 296, 399  
  mobile, 148  
  portable, 148  
Erf, L. A., 236  
Erythema, 199  
Erythematous dose, 201  
Esling, R. H., 393  
Evans, R. D., 163, 195, 236  
Eve, A. S., 160, 163, 233  
Ewald, P. P., 299, 367, 384  
Ewald sphere, 386  
Excitation potentials, 48, 69, 423, 566  
Exclusion principle, 60, 61, 63, 543  
Exograph, 17, 173  
Exposure, calculation of, 177, 243  
  definition of, 177  
  in electron diffraction, 540  
  safety test, 199, 200  
  in x-ray diffraction, 409  
Extinction, 365  
  micrographs, 482  
  space group, 347
- F
- Face-centered cubic structure, 315  
  reflections of, 401  
Face-centered lattices, 306  
Facets, 380  
Failla, G., 163, 207, 231, 235  
Fankuchen, I., 399, 533  
Faraday, M., 1  
Faraday, 338  
Fatigue failure, 458  
Fatty acids, 510, 516  
Faxen, H., 478  
Fermi, E., 355, 504  
Fermi statistics, 82  
Fernico, 117  
Ferrite, 526  
Fiber, axis, 451, 455  
  diagrams, 455  
  patterns, 452, 531  
Fibering, 449  
  limited, 451, 455  
Fibers, 530  
Field, J. E., 530-532  
Field emission, 107, 296  
Filament, 10, 111, 112  
  transformer, 122  
Files, G. W., 211, 213, 218

- Film (x-ray), 173
    - density, 177
    - development, 183, 431
    - duplication, 184
    - duplitized, 173
    - fast, 178
    - flaws, 246, 249
    - gamma, 179
    - grain, 174, 181
    - hard, 179
    - kinds of, 176
    - moving, 224, 389
    - no screen or nonscreen, 173
    - opacity, 177
    - reversal, 179
    - sizes, 183
    - slow, 179
    - soft, 179
    - solarization, 179
    - speed, 179
  - Film holder, 173, 182, 186, 245, 392, 396, 549
  - Filmer, J. C., 18
  - Filmer, P. G., 297
  - Films, surface, 554
  - Filter, 181, 201, 202, 216, 228, 231, 256, 335, 379, 393, 476
    - Ross, 433
  - Filtration, inherent, 231
  - Finch, G. I., 539, 543, 545, 553-555
  - Fink, D. G., 296
  - Fish tracks, 90
  - Fission, 166
  - Fixer, 184
  - Flaws, casting, 262
    - film, 246, 249
    - minimum size, 259
    - weld, 247, 248
  - Flax, 533
  - Fluorescence, 168
    - radiation, 76
    - theory of, 171
  - Fluorescent absorption, 76
  - Fluorescent materials, 169
  - Fluorescent x-rays, 76
  - Fluorite, 411
  - Fluoroscope, 172, 202, 285
  - Fluoroscopic screen, 168, 550
  - Fluoroscopy, 168, 202, 205, 285
  - Focal spot, 8, 10, 16, 18, 112
    - best size, 16, 212
    - line (Benson-Goetze), 18, 112
  - Focusing, cathode rays, 17, 110, 112
    - cup, 10, 17, 548
    - magnetic, 114, 550
  - Fog, 178, 253, 550
  - Forbidden lines, 67
  - Forbidden rings, 543
  - Fordham, S., 555
  - Forgings, 266
  - Form, 305
  - Formula, Klein-Nishina, 89
    - Scherrer, 446
    - Sellmeier, 97
  - Fortescue, C., 144
  - Fourier series, 21
    - representation of, 361
  - Francis, D. S., 228
  - Franklin, K. J., 225
  - Fraser, C. G., 545
  - Free electrons, 10, 82, 519, 543
  - French, R. C., 554
  - Freon, 118, 127, 149
  - Frequency, betatron, 154
    - definition of, 21
    - and energy, 26
    - power supply, 125, 127, 143
    - x-rays, 21
  - Frevet, L. K., 424, 544
    - (see also Hanawalt-Rinn-Frevet method)
  - Friedel's law, 376
  - Friedman, H., 82, 83
  - Friedrich, W., 3, 299, 477
  - Frommer, L., 456, 457, 482, 485, 493, 494
  - Fronzel, C., 293
  - Fry, S. L., 225
  - Fuller, M. L., 456, 554
- ( )
- Gaertner, H., 556
  - Gaertner, O., 171
  - Gajewski, H., 506
  - Gamertsfelder, C., 170, 173
  - Gamma, photographic, 179
    - superlattice, 522
  - Gamma angle, 301
  - Gamma brass, 522
  - Gamma iron, 418
  - Gamma-ray absorption, 164
  - Gamma-ray radiography, 258, 278
  - Gamma-ray spectrum, 163
  - Gamma rays, 160
  - Gap, 144



- Gardner, F. S., 526  
 Garvin, E. L., 288  
 Gas tubes, 6, 8, 109  
 Gases, conduction in, 7  
     electron diffraction by, 540, 546, 547, 556  
     x-ray diffraction by, 496  
         monatomic, 499  
         polyatomic, 504  
         technique of, 498  
 Gasifier, 9  
 Gassy tubes, 115  
 Gehman, S. D., 530-532  
 Geiger, H., 160, 193  
 Geiger-Müller counter, 163, 193, 336, 409, 410  
 Generation of x-rays, 6, 20, 45, 105  
 Genevèse, F., 48  
 Gensamer, M., 485  
 Germer, L. H., 59, 536, 545, 554  
 Gilbert, C. W., 165, 236  
 Gingrich, N. S., 170, 173, 194, 196, 363, 507, 509  
 Gisen, F., 485  
 Glass, coloration of, 292  
     Lindemann, 111  
     protective, 202, 286  
     structure of, 512  
 Glasser, O., 2, 192, 197  
 Glocker, R., 422, 453, 477, 485  
 Gnomonic projection, 374  
 Goetze focus, 18, 111  
 Gold, 523, 539, 554  
     pattern of, 554  
     standard, 493, 539  
 Göler, v., 462  
 Goniometer arcs, 372, 380  
 Goss, N. P., 450, 474  
 Goss, W. H., 145  
 Grain, crystal, distortion, 468  
     orientation, 449, 455, 463  
     size, 300, 438  
         above  $5 \times 10^{-3}$  mm., 440  
         below  $2 \times 10^{-4}$  mm., 446  
     photographic, development, 181  
     size, 174, 215, 288  
 Graphite, 391, 519, 554  
 Grating, constant, 103  
     cross, 539  
     ruled, 100  
 Gratz circuit, 136  
 Gray, F., 17, 550  
 Gray, J. A., 83  
 Gray, L. H., 187  
 Grazing incidence, 527, 540  
 Grease, 514, 554  
 Green, A. E. S., 28  
 Greenland, K. M., 286  
 Greenwood, W. H., 183  
 Greinacher circuit, 133  
 Grenz rays, 34, 287  
 Grid, industrial, 257  
     Potter-Bucky, 216  
     in x-ray tube, 107  
 Grimmitt, L. G., 163, 233  
 Gross, S. T., 289, 290, 432, 531  
 Groth, P., 309  
 Ground connection, 126  
 Group, point, 308  
     space, 309, 576  
 Group velocity, 98  
 Guellich, G. E., 526  
 Guggenheimer, K. M., 164  
 Guinier, A. J., 478  
 Gulbransen, E. A., 545  
 Gun, electron, 114, 548  
 Gunn, R., 146  
 Günther, P., 293, 421  
  

H

 H and D curve, 178  
 Hadding, A., 109  
 Hafnium, 421  
 Hagenow, C. F., 90, 92  
 Hahn, O., 160  
 Half life, 161  
 Half-value breadth, 446, 480  
 Half-value layer, 233  
 Hall, H., 75  
 Hamilton, J. G., 236  
 Hanawalt, J. D., 424, 455, 576-586  
 Hanawalt-Rinn-Frevel method, 420, 423, 576  
 Hard film, 179  
 Hard x-rays, 34  
 Hardening, age, 478  
     case, 525  
     precipitation, 478  
 Harding, S. W., 194, 336, 409  
 Hare, D. C. C., 297  
 Hartree, D. R., 355, 504  
 Harworth, K., 37  
 Hastings, J. M., 143  
 Hatley, C. C., 100

- Haüy, M. A., 300  
 Haworth, F. E., 398  
 Hayden, H. S., 232  
 Hayward, R., 552  
 Heat-treatment, 300, 450, 470, 478  
 Heisenberg, W., 60, 501  
 Heitler, W., 157  
 Hemihedry, 308  
 Hemimorphic, 308  
 Hemoglobin, 533  
 Hemp, 533  
 Henderson, J. E., 145  
 Hendricks, S. B., 295, 546, 547  
 Henshaw, P. S., 228  
 Herb, R. G., 118, 146, 149  
 Herbein, S. D., 184  
 Herzog, G., 499  
 Hevesy, G. v., 421  
 Hexagonal close packing, 312  
 Hexagonal and rhombohedral lattices, 351  
 Heydenburg, N. P., 166  
 Hicks, V., 105  
 High voltage, 7, 10  
     protection, 198  
     (See also Potential)  
 Hight, E. K., 255  
 Hill, S., 555  
 Hillier, J., 182  
 Hirsch, F. R., 68  
 Hirsch, I. S., 222  
 Hirsch, I. v., 553  
 History of x-rays, 1  
 Hittorf, 1  
 Hodgman, C. D., 145, 417, 565  
 Hoffman, R. M., 119  
 Hoisington, L. E., 118  
 Holohedry, 308  
 Holzapfel, L., 293  
 Holzknecht, G., 293  
 Homogeneous electron beam, 536  
 Homopolar bond, 517  
 Honerjäger, R., 37, 39, 42  
 Hönl, H., 100  
 Hooded anode, 108  
 Houston, V. W., 82  
 Houstoun, R. A., 97  
 H-R-F (see Hanawalt-Rinn-Frevel)  
 Hudson, C. M., 118  
 Huggins, M. L., 364  
 Hughes, A. L., 550  
 Hull, A. W., 391, 408, 515  
 Hull-Davey charts, 415  
 Hull-Debye-Scherrer method, 391  
 Hume, O. F., 220  
 Hume-Rothery, W., 400, 524  
 Hume-Rothery's law, 524  
 Hummell, A. D., 220  
 Hunt, F. L., 27  
 Hurter, F., 178  
 Hutchison, D. A., 337  
 Huyghens, C., 300  
 Hydrocarbons, 509, 514, 557  
 Hydrogen, 52, 158, 518  
  
 I  
 Identification, 260  
 Ievins, A., 404  
 Iitaka, I., 553  
 Illuminators, 185, 225  
 Inclusions, 262  
 Incoherent scattering, 77, 83, 496  
     function, 501  
 Incomplete fusion, 247  
 Incomplete penetration, 247  
 Index of microstrain, 480  
 Index of refraction, 97-99, 327  
     of electrons, 543  
 Index book, 426  
 Indices, of Bragg reflection, 346  
     Miller, 303  
     Miller-Bravais, 315  
     unmixed, 348  
 Induction coils, 125  
 Industrial fluoroscopy, 285  
 Industrial grid, 257  
 Industrial radiography, 239  
 Inglestam, E., 421  
 Inner precession, 61  
 Inner quantum number, 61  
 Inspection, automatic, 286  
     fluoroscopic, 168, 172, 202, 205, 285  
     radiographic, 239  
 Integrated reflections, 359, 367  
 Intensifying screen, 168  
     lead, 181  
 Intensity, characteristic radiation, 48, 68  
     continuous radiation, 32, 34  
     definition of, 33  
     of diffraction lines, 359, 414  
     distribution, angular, 39, 78, 332  
     wave length, 31, 41, 45  
     and dosage rate, 189  
     scale, 432

Intercepts, 304  
 Interference, 103, 320, 322  
 Intermetallic compound, 435, 522  
 Intermittency effect, 179  
 Interstitial compound, 525  
 Interstitial solid solution, 435, 525  
 Inverse-square law, 20, 207, 208  
 Ion bombardment, 8, 110  
 Ion pair, 187  
 Ionic bond, 517  
 Ionic crystals, 346  
 Ionic radii, 517  
 Ionization, 7, 187  
   potential, 66  
 Ionization chamber, 29, 187, 191, 336  
   air wall, 190  
   corrections for, 33  
   for inspection, 286  
   standard, 191  
   thimble, 191  
 Ions, 7  
 Iron, allotropic forms, 418  
 Irradiation sickness, 201, 235  
 Isenburger, H. R., 468  
 Isotopes, 158  
   radioactive, 165  
 Iwanenko, D., 150, 153

## J

Jackson, R., 538, 547  
 Jaeger, R., 210  
 James, R. W., 355, 356, 365, 504  
 Jassinsky, W. W., 154  
 Jauncey, G. E. M., 505  
 Jay, A. H., 433  
 Jeffries, Z., 451  
 Jenkins, F. A., 99, 353  
 Jenkins, R. O., 553, 554  
*jj* coupling, 62  
 Jönsson, A., 48  
 Johnson, R. P., 171  
 Joliot, F., 165, 236  
 Jones, F. W., 447  
 Jones, P. L. F., 556  
 Jones, R., 293  
 Jordan, P., 60  
 Jupnik, H., 421

## K

K edge, 73, 177, 571  
 K electrons, 51, 573

K electrons, capture of, 166  
 K excitation, 48, 69, 423, 566  
 K limit, 73, 177, 571  
 K lines, 46, 64, 67, 423, 563  
 K shell, 51, 573  
 Karlsson, H., 421  
 Katz, J. R., 507  
 Katzoff, S., 498, 510  
 Kaufman, J., 220  
 Kavanau, J. L., 518  
 Kearsley, W. K., 129  
 Kearsley stabilizer, 144  
 Keesom, W. H., 505, 507  
 Keesom's equation, 505, 511  
 Keller, F., 273  
 Kelvin temperature, 25, 561  
 Kemnitz, G., 485  
 Kenna, L. P., 286  
 Kennard, E. H., 29, 65, 365  
 Kenotrons, 119, 206  
 Kerst, D. W., 5, 149, 150, 152, 237  
 Kersten, H., 193, 293  
 Kikuchi, S. K., 542  
 Kikuchi lines, 541, 542  
 Kilovolts, crest or peak, 115  
 Kingdon, K. H., 107  
 Kipphan, E., 557  
 Kirchner, F., 88, 92, 553  
 Kirkpatrick, P., 14, 33, 34, 37, 41, 42,  
   92, 146, 367, 433  
 Kirkpatrick voltmeter, 146  
 Klein, O., 89  
 Klein-Nishina formula, 89  
 Knipping, P., 3, 299  
 Koch, P. P., 299  
 Kolkmeijer, N. H., 170  
 Koller, P. C., 295  
 Konopinski, E. J., 48, 157  
 Kossel, W., 50, 51  
 Koster, H., 220  
 Kramers, H. A., 39, 41, 164  
 Krebs, R. P., 193  
 Krom, C. J., 170  
 Kronhaus, A., 293  
 Kronig, R. L., 83  
 Krutter, H., 83, 512  
 Kryptoscreen paper, 171  
 Kulenkampff, H., 33, 34, 41  
 Kunst, H., 170  
 Kurbatov, J. D., 166  
 Kymograph, 221

## L

- L edge, 74
- L electron, 51, 573
- L series, 46, 64, 67, 563
- L shell, 51, 573
- Laby, T. H., 422
- Lacassagne, A., 234
- Lagsdin, J. B., 10, 110
- Lambert, J. H., 71
- Lambert's absorption law, 71
- Lambert's cosine law, 19
- Lampblack, 391
- Lane, T. B., 293
- Langmuir, D. B., 313
- Larkin, J. C., 236
- Larsson, A., 99
- Latitude, 257, 271
- La Tour circuit, 133
- Lattice, 300
  - classification, 305
- Lattice, crystal, 302
  - line, 301
  - models, 313, 450
  - point, 301
  - reciprocal, 384, 539
  - space, 301, 305
  - super, 436, 522
- Lattice constants, 316
  - calculation of, 337
- Laub, J., 83
- Laue, M. v., 3, 299, 320, 447
- Laue equations, 320, 324
- Laue method, 371
- Laue pattern, 377
- Laue spot, 375
- Law, Bunsen-Roscoe, 179
  - Bragg's, 322, 324, 327, 329, 477
  - Friedel's, 376
  - Hume-Rothery's, 524
  - of inverse square, 20
  - Lambert's absorption, 71
  - Lambert's cosine, 19
  - Moseley's, 47
  - of rational indices, 300
  - Snell's, 100, 328, 544
  - Stefan-Boltzmann, 15
  - of wave motion, 22
- Lawrence, J. H., 236
- Layer lines, 381, 383
- Lead backing, 81, 254
- Lead glass, 202, 286
- Lead letters, 246, 260
- Lead partitions, 203, 205
- Lead screens, 181
- Leak valve, 9, 110
- Le Galley, D. P., 195
- Leibmann, H., 293, 294
- Lenard, P., 1, 119
- Lenard tube, 119
- Lens, magnetic, 114, 550
- Levels, energy, 50, 52, 63-65, 82, 164
  - optical, 69
  - weight, 68
- Levy, L., 169
- Liebhafsky, H. A., 423
- Liebig, 309
- Life, half, 161
- Life of tubes, 115, 128, 135
- Light, velocity of, 20, 561
- Lilienfeld tube, 113
- Limit (*see* K, L, M, etc.)
  - absorption, 73, 82, 288, 571
  - Duane-Hunt, 27, 28
  - short wave-length, 27, 28
- Limited emission, 12, 115, 120
- Limited fibering, 455
- Limited space charge, 116, 121
- Lind, S. C., 160
- Lindemann glass, 111
- Lindsay, G. A., 100, 109, 421
- Line (*see* K, L, M, etc.)
  - broadening, 447, 448, 478
  - focus, 18, 111
  - forbidden, 67
  - intensity of, 48, 68, 432
  - Kikuchi, 541, 542
  - layer, 381, 383
  - shift, 468, 470, 482, 522
  - spectral, 45, 47, 423
- Linnik, W., 477
- Lipson, H., 339, 400, 405, 441
- Liquids, diffraction by, 496, 507
  - technique of, 498
  - electron diffraction in, 545, 555
  - x-rays affect, 293
- Lister, M. W., 557
- Livingston, M. S., 48, 155
- Livingston, R., 163, 293
- Lloyd, E. H., 482, 485, 493, 494
- Locher, G. L., 166, 195
- Long-chain compounds, 497, 509, 514
- Lonsdale, K., 412, 478
- Lorenz, H. A., 97

- Love, A. E. H., 486  
Lubrication, 514, 554  
    rotating anode, 16, 18  
Lummer, O., 24
- M
- M edges, 75  
M electrons, 51, 52, 573  
M series, 48, 64, 67  
M shell, 51, 573  
MacComb, W. S., 201  
Macdonald, P. A., 163  
Macewan, D., 361  
Machlett, R. R., 106, 150  
Mackenzie, K., 196  
MacMillan, D. P., 143  
Macrostrain, 468  
Macrostress, 468  
Maddigan, S. E., 288, 291  
Magnesium, extruded, 455  
    rolled, 456  
Magnesium castings, 269  
Magnetic lens, 114, 550  
Maloff, I. G., 17  
Malter, L., 196  
Manufacturers, 108, 109, 127, 177, 192,  
    194, 205, 240, 280, 287, 336, 399, 410,  
    422, 529, 545  
Margenau, H., 93  
Margolese, M. S., 163  
Mark, H., 531, 533  
Marlow, D., 334  
Martensite, 526  
Martin, C. L., 201, 235  
Martin, D. E., 432  
Mass absorption coefficient, 72, 568  
Mass number, 158, 575  
Mass scattering coefficient, 75  
Matrix mechanics, 60  
Mauguin notation, 311  
Maxwell, J. C., 1  
Maxwell, L. R., 295, 546, 547  
May, A., 179  
Mayneord, W. V., 189, 193, 228, 229  
McCue, J. J. G., 114  
McCutcheon, D. M., 291  
McKenna, J. F., 184  
McKibben, J. L., 118, 146, 149  
Mean free path, 7, 8  
Measurement of x-rays, 168  
Mechanical rectifier, 124, 130  
Medical applications of x-rays, 211  
Mellor, J. W., 160  
Mendelyev, D. I., 47  
Mendelyev, D. I., periodic table of, 63,  
    520, 572  
Menke, H., 507  
Mercury, 507, 509, 555  
Merrill, F. H., 150  
Mesham, P., 83  
Meson or mesotron, 157  
Metallic binding, 519  
Metallography, 438, 468, 520  
Metals, 11, 239, 422, 520, 543  
Meters, 140, 193  
Meyer, K. H., 531  
Meyer, St., 160  
Micrography, 288, 482  
Micron, 25, 561  
Micropatterns, 533  
Microphotometer, 185, 432  
    record, 433  
Microradiography, 175, 205, 287  
Microscope, x-ray, 363  
Microstrain, 468  
    index, 480  
Microstress, 468  
Miers, H. A., 309  
Mill, C. C., 294  
Miller, C. W., 194  
Miller, W. H., 304  
Miller indices, 303  
Miller-Bravais indices, 315  
Million volt equipment, 126, 147  
Million volt radiography, 281, 282  
Million volt tubes, 117, 118  
Mobile equipment, 148, 205  
Mobility, electrophoretic, 294  
Models, crystal, 313, 450  
Molecular weight, 337  
Molecules, 7, 496, 508, 509, 517, 531,  
    555-557, 607  
Möller, H., 485  
Momentum of electrons, angular, 58, 61  
Monochromatic x-rays, 72  
Monochromator, 335, 399  
    bent crystal, 398  
Montgomery, C. G., 195  
Montgomery, D. D., 195  
Moore, S., 220  
Moreland, H. D., 222  
Moriarty, C. D., 253  
Morningstar, O., 512  
Morrow, R. M., 510, 511

Mosaic structure, 366  
 Moseley, H. G. J., 4, 46, 47, 50, 336  
 Moseley's law, 4, 47  
 Mosley, V. M., 546, 547  
 Moss, H., 548  
 Motion pictures, 224, 272  
 Motor-generator set, 125, 127, 135, 143  
 Mott, N. F., 537  
 Moving film analysis, 389  
 Moyer, H. P., 297  
 Müller, A., 514–516  
 Müller, E. A. W., 107  
 Müller, W., 193  
 Muller, H. J., 294  
 Multiplier, electron, 195  
     photo, 287  
 Murison, C. A., 553–555  
 Mutation, 294

## N

N electrons, 51, 52, 573  
 N series, 48, 64, 67  
 N shell, 51, 573  
 Nardroff, R. v., 100  
 Neddermeyer, S. H., 79  
 Neher, H. V., 552  
 Nelson, H. R., 545, 553, 554  
 Nelson, J. B., 415  
 Nelson, R. B., 313  
 Neptunium, 167  
 Neutrino, 157  
 Neutron, 157, 164  
     therapy, 236  
 Nicholas, W. W., 37  
 Nielsen, D. M., 468  
 Niemann, F., 449, 478, 480  
 Nilakantan, P., 478  
 Nishina, Y., 89  
 Nitriding, 525  
 Nitrogen oxides, 206  
 Nix, F. C., 522  
 Northrup, D. L., 118, 150  
 Notation, for characteristic lines, 67  
     Schoenflies, 309  
     *s p d f*, 69  
 Nucleus, 10, 49, 157, 536  
 Number, atomic, 34, 49, 158, 572, 573  
     Avogadro, 79, 104, 337, 338, 561  
     mass, 158  
     quantum, 53, 59, 61–63  
     wave, 65  
 Nurnberger, C. E., 293

## O

Occhialini, G. P. S., 166  
 Ohlin, P., 28  
 Oils, 509, 554  
 Olds, J. W., 231, 236  
 Olson, C. M., 423  
 Omega angle, 305, 351  
 Opacity, 177, 433  
 Opaques, diagnostic, 219  
     industrial, 253  
 Orbits, allowed, 58  
     electronic, 49  
 Order, definition of, 103, 321  
 Orientation, in films, 553  
     parallel to beam, 463  
     of piezoelectric crystals, 528  
     preferential, 449, 455, 463  
     recrystallization in, 451  
 Oshry, H. I., 433, 553  
 Osswald, E., 485  
 Owen, E. A., 179  
 Oxidation, 533  
 Oxtail tube, 113  
 Ozone protection, 206

## P

Packard, C., 227  
 Packing energy, 159  
 Paintings, 292  
 Pair formation, 79  
 Pair of ions, 187  
 Paneth, F. A., 47  
 Panofsky, W. K. H., 28  
 Paper, 533  
     black, 177, 291, 373, 394, 473  
     x-ray, 171, 175, 222  
 Parameters, 349  
 Parkes, A. S., 228  
 Parkinson, D. B., 118, 146, 149  
 Pascoe, K. J., 441  
 Pastille, 197  
 Pattern, back-reflection, 395, 404, 538  
     cross grating, 539  
     diffraction, 299, 377, 383, 402  
     electron, 554–557  
     fiber, 452, 455  
     Hull-Debye-Scherrer, 402, 403  
     Laue, 377  
     liquid, 507  
     micro, 533

- Pattern, powder, 402, 403  
  absorption in, 414  
  reflection, 527, 551  
  rotation, 383  
  transmission, 400, 540  
Patterson, A. L., 363, 447, 448  
Patterson, C. V. S., 169  
Pauli, W., 60, 62, 82  
Pauli exclusion principle, 60, 63, 543  
Pauling, L., 355, 556  
Pearlite, 526  
Peckham, R. H., 186, 433  
Penetrameters, 259, 297  
Penetron, 297  
Periodic table, 47, 63, 572  
Petch, N. J., 400, 405, 526  
Petersen, M., 478  
Phantom, 230  
Phase, in alloys, 523  
  definition of, 103  
  velocity, 98  
  waves, 57, 536  
Phosphor, 168, 287  
Phosphorescence, 169  
Phosphorogen, 170  
Phosphorus, radioactive, 165, 236  
Photocell, 196  
Photoelectric absorption, 77  
Photoelectric effect, 28, 73, 75, 90  
Photoelectric emission, 556  
Photoelectric work function, 543  
Photofluorography, 222  
Photographic emulsion, 173  
Photography, 173  
  x-ray screen in, 222  
Photomultiplier tube, 287  
Photons, 21, 27, 28  
Photoroentgenology, 222  
Phragmen, G., 520  
Picard, R. G., 545  
Pierce, J. R., 196, 548  
Pierce, S. E., 79  
Pierce, W. G., 423  
Piezoelectric oscillators, 293, 528  
Pike, E. W., 32  
Pinholes (*see* Collimation)  
Pish, G., 478  
Piston, D. S., 42  
Pitchblende, 160  
Pitting of target, 17, 117  
Planck, M., 1, 25, 50  
Planck constant, 12, 26, 50, 561  
Planes, angles between, 459  
  atomic, 302  
  cleavage, 300  
  cooperating, 400, 442  
  equivalent, 400  
  rational, 302  
  reciprocal lattice, 386  
  spacings of, 323, 348, 350, 400, 412  
Planigraphs, 220  
Plastics, 530, 555  
Pleomorphic forms, 417  
Plessing, E., 554  
Plutonium, 167  
Podasevskij, M., 293  
Pohl, R., 299  
Point, group, 308  
  lattice, 301  
Poisson's ratio, 486  
Polanyi, M., 378, 453, 456, 531  
Polarity, 9, 141  
Polarization, 37, 42, 49, 90  
  factor, 354  
Pole figures, 460, 462  
Polishing, 554  
Polychromatic x-rays, 29  
Polymers, 533, 555  
Polymorphic forms, 417  
Polythene, 533  
Pomeranchuk, I., 150, 153  
Pool, M. L., 166  
Popp, W. C., 231, 236  
Population of planes, 323  
Porosity, 246, 251, 261, 268, 269  
Portable equipment, 148, 399  
Positrons, 79, 157  
Potential, 26  
  control, 138  
  excitation, 48, 69, 423, 566  
  ionization, 66  
  measurement, 144  
  peak, 115  
  root mean square, 115  
  within a solid, 83, 536, 543  
  stabilization, 142  
  tube, 8, 115  
  and wave-length, 34, 66, 544  
Potter, H. E., 216  
Potter-Bucky grid, 216  
Powder, cameras, 392, 395, 396  
  method, 391, 410  
Power rating, 115, 126  
Precession, 61

Precipitation hardening, 478  
 Preferential and preferred (*see* Orientation)  
 Prescott, J., 486  
 Preston, G. D., 412, 477, 478, 554  
 Principal axes, 487  
 Principle, combination (Ritz), 52  
   correspondence, 39  
   Pauli exclusion, 60, 63, 543  
   relativity, 55, 57  
 Pringsheim, E., 24, 25  
 Prins, J. A., 508  
 Protection, 198  
   gamma ray, 206  
   high voltage, 198, 548  
   of meters, 140  
   ozone, 206  
   x-ray, 201  
 Proteins, 533  
 Protons, 154, 157  
 Pulse, electromagnetic, 35  
 Pumps, 8, 552  
 Pyrites, 350, 351

## Q

Quanta, 20  
   energy of, 26  
 Quantized states, 58, 325  
 Quantized vectors, 62  
 Quantum mechanics, 41, 42, 60  
 Quantum number, 53, 58, 59, 61, 62, 63  
   azimuthal, 59, 61  
   inner, 61  
   principal, 61  
   spin, 61  
 Quantum theory, 26, 39, 50, 73, 325  
 Quarrell, A. G., 538, 539, 541, 543, 545, 547, 553-555  
 Quartz, 293, 433, 528, 533  
 Quimby, E. H., 201, 228

## R

r-meter, 192  
 r unit, 188, 189  
 Radian, 561  
 Radiation and rays, alpha, 160  
   for back-reflection, 471  
   beta, 160  
   cathode, 6, 118, 550  
   characteristic, 46

Radiation and rays, characteristic,  
   theory of, 49  
   continuous, 32  
   cosmic, 23, 80, 157  
   dual nature of, 93  
   electromagnetic, 21, 35  
   gamma, 23, 160  
   grenz, 34, 287  
   heat, 15, 24  
   infrared, 21, 24  
   Lenard, 119  
   stray, 114  
   ultraviolet, 21  
   visible, 21  
   and voltage, 34  
   x-, 20  
 Radii, atomic, 519  
   ionic, 517  
 Radio waves, 21  
 Radioactivity, 157  
   artificial, 165  
   induced, 165  
   natural, 157  
 Radiograph, 3, 17, 173  
   duplication of, 184  
   stereoscopic, 219  
 Radiographic definition, 215  
 Radiographic distortion, 214  
 Radiographic motion pictures, 224, 272  
 Radiographic sensitivity, 433  
 Radiographic standards, 431  
 Radiographic technique, 212, 241, 244, 255, 268, 287, 292, 296  
 Radiography, 3, 17, 173  
   of castings, 261, 269, 275, 276  
   indirect, 222-224  
   industrial, 239  
   instantaneous, 108, 225, 296  
   medical, 211  
   micro, 175, 287  
   million volt, 281  
   production, 283  
   with radium, 266, 278  
   of welds, 245, 272  
 Radiology, 211  
   diagnostic, 211  
   therapeutic, 225  
 Radium, 160  
   A, 161  
   B, 161  
   beam therapy, 233  
   bomb, 233



- Radium, C, 161  
C', 161  
container, 208  
dosage rate, 191  
emanation, 161  
F, 166  
handling, 207, 208  
precautions, 207, 208  
radiography, 266, 278  
safe, 207  
shipment, 207  
slide rule, 280  
therapy, 225, 227, 233, 234
- Radon, 160-162
- Raether, H., 554
- Raman, C. V., 85, 478, 499
- Ramberg, E. G., 182
- Randall, J. T., 496
- Rare earths, 64, 572
- Rating, of kenotrons, 122  
of transformers, 126  
of tubes, 115
- Rayon, 533
- Rays (*see* Radiation)
- Reciprocal lattice, 384, 539
- Reck, F. M., 273
- Recoil, electrons, 30, 86, 89, 90  
factor, 500
- Recrystallization, 451, 521
- Rectification, 9, 10, 13, 116, 117  
full wave, 124, 136, 137  
mechanical (Snook), 124, 130  
primary, 129  
tube, 119, 129
- Rectigon, 129
- Reflection, Bragg, 327, 346, 373, 472, 551  
coefficient, 359  
diagram, 401  
diffuse, 474, 478  
integrated, 359, 367  
from lead glass, 286  
for seven crystal systems, 348, 349  
suppressed, 346  
true, 96, 100, 551
- Refraction, of electrons, 544  
of x-rays, 96, 97, 327
- Registration, 168
- Regulation, 8, 12, 138
- Reinhard, M. C., 293
- Relativity, 55-57
- Resolving power, 321, 335, 471
- Resonance of bonds, 519
- Resonance neutrons, 165
- Reynolds, P. W., 400
- Reynolds, R., 224
- Rhombohedral and hexagonal lattices, 351
- Richards, T. L., 456
- Richardson, O. W., 12
- Richtmyer, F. K., 29, 64, 73, 75, 79, 365
- Rideal, E. K., 555
- Riley, D. P., 339, 415, 518
- Rings, diffraction, 402, 403, 554  
diffuse, 440, 446, 496, 507  
electronic, 50  
extra, 543  
forbidden, 543
- Rinn, H. W., 424  
(*See also* Hanawalt-Rinn-Frevel method)
- Rinne, F., 378
- Robb, G. P., 221
- Roberts, J. E., 164
- Roberts, R. B., 166
- Robertson, J. M., 363, 432, 433
- Robinson, H., 28, 81
- Rock salt, 336, 340
- Roebuck, J. S., 554
- Röntgen, W. C., 1, 2, 96, 99
- Roentgen, 188
- Rogers, T. H., 128
- Rolling, 455
- Ronnebeck, H. R., 433
- Root mean square potential, 115
- Rose, J. E., 145
- Ross, P. A., 367, 433
- Rotating crystal method, 378
- Rotating target, 16, 18, 105, 116
- Rotation, camera, 379  
pattern, 383  
of powder specimen, 405
- Royt, L. E., 118
- Rubber, 511, 512, 530-532
- Rüdiger, O., 553
- Ruedy, J. E., 545, 556
- Rugh, R., 228
- Rules, screen, 244  
selection, 60, 67  
slide, 280, 413  
sum, 68
- Rump, W., 14, 34
- Russel-Saunders coupling, 62
- Rutherford, E., 4, 49, 160, 193
- Rydberg constant, 65, 561

## S

- Sachs, G., 462, 478, 485  
 Sadler, C. A., 83  
 Safford, F. J., 146, 150  
 Salley, D. J., 159  
 Sample (*see* Specimen)  
 Sampson, L. H., 193  
 Sarcoma, 235  
 Sarsfield, L. G. H., 133, 134, 138, 141  
 Satellites, 68  
 Sauter, F., 41  
 Sauter method, 389  
 Scale, intensity, 432  
     Wyckoff, 377  
 Scanograph, 221  
 Scattering, 71, 77, 88, 331  
     angle  $\phi$ , 86, 332  
     and atomic number, 78  
     classical, 331  
     coefficient of, 75–77  
         atomic, 79  
     coherent (unmodified), 77, 83, 88, 496  
     diffuse, 329, 496  
     electron, 536, 537  
     function, 501  
     incoherent (modified or Compton), 77,  
         83, 88, 496  
     intensity, 78, 333  
     and polarization, 90  
     Thomson, 331  
 Scharf, K., 196  
 Scherrer, P., 391, 446  
 Scherrer formula, 446  
 Scherzer, O., 17, 39, 41, 550  
 Schiebold, E., 378  
 Schiebold method, 389  
 Schmidt, W., 456  
 Schoenflies, A., 309  
 Schoenflies notation, 309, 311  
 Schreiner, B. F., 293  
 Schrenk, H. H., 433, 435, 533  
 Schrödinger, E., 60, 88  
 Schwartzschild, M., 221  
 Schweidler, E., 160  
 Scott, G. W., 273  
 Scott, K. G., 236  
 Screen rule, 244  
 Screening constant, 54  
 Screens, efficiency of, 171  
     Fluorazure, 170, 432  
     fluoroscopic, 168, 548  
     Screens, intensifying, 168, 221  
         lead, 181  
         type B, 169  
 Seaborg, G. T., 159, 165  
 Seabury, R., 478  
 Secondary beta particles, 76, 81, 292  
 Secondary-electron multiplier, 195  
 Secondary x-rays, 71, 76  
 Seemann, H., 378, 397  
 Seemann, H. E., 179, 181  
 Seemann-Bohlin camera, 397, 520  
 Seitz, F., 171  
 Selection rules, 60, 67  
 Seljakow, N., 447  
 Sellmeier formula, 97  
 Sensitivity, radiographic, 259, 261  
 Separation, atomic, 506, 517, 519, 557  
 Serber, R., 5, 152  
 Series K, L, M, etc., 46, 64, 67, 563  
 Serioscopy, 220  
 Setty, R., 528, 530  
 Shadowgraph, 17, 173  
 Shafer, W. M., 289  
 Shearer tube, 109  
 Shells, electronic, 51, 63, 497, 504, 573  
 Shimizu, S., 293  
 Shockproof cables, 127  
 Shockproof tubes, 106, 113  
 Shore, S. X., 530  
 Shot, 253  
 Shrinkage, in castings, 261, 264, 269, 270,  
     272  
     film, 405  
 Siegbahn, M., 47, 48, 99, 109, 337, 339,  
     421, 567, 571  
 Silberstein, L., 181  
 Silica gel, 533  
 Silicosis, 533  
 Silk, 533  
 Simard, G. L., 512  
 Sinclair, H., 415  
 Singer, G., 190, 202, 207  
 Sisson, W. A., 532, 533  
 Skehan, J. W., 106  
 Skobeltzyn, D., 166  
 Slack, C. M., 99, 107, 119, 296  
 Slag, 247  
 Slater, J. C., 83, 537  
 Slide rule, for cubic structures, 413  
     for radium exposures, 280  
 Slits (*see* Collimation)  
 Smith, A. E., 555

- Smith, C. S., 398, 441, 449, 478, 480  
Smith, D. W., 273  
Smith, F. R., 194, 409  
Smith, H., 478  
Smith, H. M., 287  
Smith, S. L., 478  
Smithells, C. J., 233  
Snapshots, 107, 108, 225, 296  
Snell's law, 100, 328, 544  
Snoek, J. L., 450  
Snook, C. S., 125  
Snook rectifier, 124, 125, 130  
Soft x-rays, 34  
Solid solution, 435, 525  
    interstitial, 435, 525  
Soller, W., 398  
Soller slits, 398, 499  
Sommerfeld, A., 38, 41, 42, 82, 299, 325, 543  
Sommerfeld theory of metals, 543  
Sorbite, 526  
Space charge, 116, 121  
    limited, 116, 121  
Space group, 309, 576  
    extinction, 347  
Space-lattice, 301, 305  
Spacings,  $d$ , 324, 348, 401, 412  
Spear, F. G., 236  
Specifications, welding, 258-261  
Specimen, preparation, 405, 431, 521, 552  
    rotation, 405  
    thickness, 408  
Spectrometer or spectrograph, bent crystal, 421  
    Bragg, 333  
    double crystal, 334  
    infrared, 24  
    magnetic, 28  
    vacuum, 423  
    x-ray, 29, 46, 333, 422  
Spectroscopy, 46, 336, 421  
Spectrum, alpha and beta ray, 166  
    characteristic, 45, 46, 74, 423  
    continuous, 29, 31, 35, 74  
    electromagnetic, 23  
    gamma ray, 163, 164  
    infrared, 25  
    optical, 69  
Speed of film, 179  
Spencer, E. W., 220  
Spencer, R. G., 458  
Sphere, Ewald, 386  
Sphere, limiting, 387  
    of reflection, 387  
Sphere gap, 145  
Spiegel-Adolf, M., 186, 433  
Spiers, C. W. F., 293  
Spin of electron, 61  
Spot, focal, 8, 10, 16, 18, 112, 212  
Spot welds, 272-274  
Sproull, W. T., 547, 552  
Stabilization of current and voltage, 142  
Stadler, L. J., 294  
Stafford, J., 222  
Standards, radiographic, 258, 261  
    safety, 200  
Steadman, L. T., 164  
Steel, 245, 261, 296, 297, 418, 435, 438, 476, 484, 526  
Steenbeck, M., 107  
Stefan-Boltzmann law, 15  
Steinberg, I., 221  
Stenström, W., 97, 99, 329  
Stepanowa, E., 166  
Stephen, R. A., 398  
Stephenson, S. T., 421, 449, 478, 480  
Steps, H., 222  
Stereographic projection, 378, 460  
Stereoscope, 219  
Stereoscopic radiography, 219, 223, 263  
Stewart, G. W., 497, 509, 510  
Stickley, E. E., 441, 449, 478, 480  
Stintzing, H., 422  
Stoker, R., 193  
Stokes, A. R., 441  
Storks, K. H., 554  
Strain, 468  
    and line broadening, 478  
    and line shift, 482  
    principal, 487  
Stranski, I. N., 421  
Straumanis, M., 404  
Stress, 468  
    principal, 487  
    relief, 468, 470  
    surface, 474  
Strong, J., 552  
Structure of absorption edge, 82  
Structure factor, atomic, 55, 352, 356, 500, 504  
    crystal, 357  
    examples of, 358, 412  
    electronic, 500  
Sturkey, L., 544

- Sullivan, H. M., 194  
 Sum rules, 68  
 Sun, C. H., 555  
 Superlattice and superstructure, 436, 522, 523  
 Suppressed reflections, 346, 351  
     cubic diagram, 401  
 Surface, catalysis, 555  
     conductivity, 554  
     pattern, 527  
     strains, 474  
     structure, 540, 553  
 Survival curves, 227, 228, 235  
 Sutton, L. E., 557  
 Sutton, L. G., 273  
 Symmetry, axes, 311  
 Symmetry center, 311, 362, 376  
 Symmetry operations, 311  
 Symmetry plane, 311  
 Systems, crystal, 305
- T
- Tanis, H. E., 107  
 Target, 6, 14, 15, 17, 18, 106, 109, 111, 112, 473  
     bevel, 14  
     hooded, 108  
     rotating, 16, 18, 105, 116  
     thin, 37-41, 106  
 Tasker, H. S., 292  
 Taylor, A., 408, 414, 415  
 Taylor, L. S., 109, 204, 207  
 Taylor, R., 273, 278  
 Technique, casting, 262  
     charts, 241, 242  
     darkroom, 183, 431  
     diagnostic, 212, 217  
     radiographic, 212, 241, 244, 255, 268, 287, 292, 296  
     Straumanis, 404  
     therapeutic, 234, 235  
 Telecurietherapy, 233  
 Temperature effect, 364, 377, 478  
 Templates, 297  
 Terms, spectral, 52  
 Terrill, H. M., 138  
 Textiles, 530  
 Texture, 300, 392, 449, 455  
 Therapeutic equipment, 147, 203, 225-238  
 Therapy, 3, 225-238  
     cathode ray, 236, 237  
     deep, 211, 231  
     Therapy, neutron, 236  
         radioactive phosphorus, 236  
         superficial, 211, 231  
         x-ray and radium, 225, 233, 234  
 Thermal effects, 364, 377, 478  
 Thermal neutrons, 166  
 Thermal velocity, 11, 355  
 Thermonic emission, 10, 543, 556  
 Thermionic work function, 12, 543  
 Thermocouple, thermopile, 24, 29, 33  
 Thewlis, J., 523  
 Thickness, measurement, 297  
     of diffraction specimen, 408  
 Thilo, E. R., 107, 296  
 Thimble chamber, 191, 192  
 Thin films, 540, 553, 554  
 Thin layer absorption, 71  
 Thin target, 37-41, 106  
 Thomas, D. E., 456, 485, 492, 493  
 Thomas, H. A., 146  
 Thomas, L. H., 355, 504  
 Thomson, G. P., 59, 77, 331, 536, 553, 555  
 Thomson, J. J., 36, 50, 61, 77, 331  
 Thoroczkay, N. v., 235  
 Threshold dose, 201  
 Timoshenko, S., 486  
 Tolerance, x-ray dose, 199  
 Tomograph, 220  
 Towers, S. W., 292  
 Tracks, cloud chamber, 90, 91  
 Trans forms, 506, 557  
 Transformers, 125  
     auto, 138  
     cascading, 126  
     constant voltage, 143, 144  
     core type, 151  
     filament, 122, 145, 548  
     insulating, 122, 126  
     shell type, 151  
 Transmission cameras, 392, 395, 399  
 Transmission patterns, 402, 403, 405, 411  
 Treatment cone, 229  
 Trillat, J. J., 553  
 Triode tube, 107  
 Triplett, T., 149  
 Trivelli, A. P. H., 181  
 Troostite, 526  
 Trost, A., 210  
 Trump, J. G., 119, 125, 146, 149, 237  
 Tube, construction, 13, 111  
     current, 8  
     life, 115, 128, 135

Tube, motion, 212, 220  
   potential, 8, 115, 138, 142, 144  
   rating, 115  
   vibration, 212, 240  
 Tubes, 6-19, 105-118  
   cathode ray, 118  
   for chemical analysis, 422  
   Coolidge, 4, 10, 13, 105, 111  
   diagnostic, 13-19, 107  
   dental, 16  
   diffraction, 109, 111  
   field emission, 107, 108, 296  
   gas, 6, 9, 109  
   Hadding, 109  
   kinds of, 105  
   Lenard ray, 119  
   Lilienfeld, 114  
   million volt, 117  
   oxtail, 114  
   radiographic, 10, 107  
   rectifying, 9, 119, 128  
   rotating anode, 16, 18, 105, 116  
   Shearer, 109  
   shockproof, 113  
   therapeutic, 107, 112  
   triode, 107  
   Universal, 13, 15  
   valve, 119, 128  
 Tucker, C. W., 478  
 Tungar rectifier, 128  
 Tungsten anode, 14, 106, 112  
 Tungsten cathode, 111  
 Tungsten target, 14, 106, 112  
 Tuning up, 245  
 Turner, A. F., 286  
 Turner, A. H., 422  
 Turner, L. A., 166  
 Tuttle, L. W., 236  
 Tuve, M. A., 154  
 Twinning, 368  
 Tyson, J. T., 555

## U

Ulrey, C. T., 31-34, 45, 138  
 Undercutting, 248  
 Unit cell, 312  
 Unit configuration, 351, 587  
 Uranium fission, 166

## V

Vacuum, 6, 8, 10, 541, 552  
   camera, 289, 400, 549

Vacuum, spectrograph, 423  
 Valence, 524  
 Valence bond, 518  
 Valence electron, 69, 517  
 Valve, leak, 9, 110  
 Valve rectifier, 119  
 van Arkel, A. E., 485  
 Van Atta, L. C., 118, 149, 150  
 van den Broek, A., 49  
 Van de Graaff, R. J., 119, 125, 146, 149, 237  
 Van de Graaff generator, 125, 149  
 van de Maele, M., 224  
 Van der Waals binding, 519  
 Vapors, 540, 547, 556  
 Vectors, electromagnetic, 36, 90  
   quantized, 61  
 Velocity, group, 98  
   phase, 98  
   x-ray, 20, 98, 561  
 Versed sine, definition of, 89  
 Vibration, atomic, 365, 478  
   tube, 212, 240  
 Victoreen, J., 192  
 Victoreen Minometer, 193  
 Victoreen r-meter, 192  
 Viewers, 185, 225  
 Vilella, J. R., 526  
 Villard, P., 131, 292  
 Villard circuit, 131  
 Voke, E. L., 201  
 Voltage doubling, 131, 133  
   measurement, 144  
   stabilization, 142  
   tube, 8, 115  
   (*See also* Potential)  
 Voltmeter, 139, 140, 146

## W

Wadlund, A. P. R., 477  
 Waller, I., 355, 365  
 Waller, T., 99  
 Walter, B., 299  
 Walter, J., 558  
 Walton, E. T. S., 154, 165, 236  
 Wang, T. J., 150  
 Warburton, F. W., 79  
 Warhurst, E., 519  
 Warping of atomic planes, 474  
 Warren, B. E., 363, 391, 414, 509, 511, 512  
 Watson, B. B., 421

- Wave-length, 21, 65, 103, 339, 563  
 definition of, 21  
 of phase waves, 58, 544  
 and potential, 34, 66  
 range, 23
- Wave mechanics, 60
- Wave number, 65
- Waves, 21  
 de Broglie, 57, 536  
 elastic, 365, 478  
 electron, 55, 536  
 law of, 22  
 and particles, 55  
 phase, 57, 536  
 radio, 21
- Wear, 554
- Webster, D. L., 48
- Weerts, J., 468, 485
- Weight, atomic, 47, 158, 572  
 of a level, 68  
 molecular, 337
- Weigle, J., 478
- Weimer, P. K., 166
- Weinbaum, O., 196
- Weinstock, R., 41
- Weissenberg, K., 378, 456
- Weissenberg method, 389
- Weisz, P., 195
- Welds, butt, 245  
 fillet, 251  
 specifications, 258-261  
 spot, 272-274  
 in tubes, 257
- Wells, A. F., 517
- Wentzel, G., 499, 501
- West, D. W., 169
- Westendorp, W. F., 106, 127, 150, 282
- Westgren, A. F., 520, 521
- Wever, F., 456, 460, 485
- Wheeler, A., 555
- Wheeler, D., 220
- Wheeler, J. A., 166
- Whiddington, R., 51
- White, H. E., 99, 353
- White x-rays, 475
- Whitford, A. E., 552
- Whitmer, R. M., 100
- Wideröe, R., 154
- Widmyer, J. H., 273
- Width of diffraction maximum, 367, 441, 446-448, 478, 480
- Wiedmann, L., 14, 41, 42
- Wierl, R., 547, 556, 557
- Wightman, A., 93
- Wildhagen, A. R., 81, 150, 232
- Williams, A. L., 555
- Wilman, H., 539, 543, 554
- Wilson, A. J. C., 480
- Wilson, C. T. R., 90, 91
- Wilson, J. T., 18
- Wilson, W., 325
- Windows, 106, 109, 111, 113
- Winnek, D. F., 223
- Winslow, E. H., 423
- Wires, 128, 450
- Wollan, E. O., 49, 498, 499, 502-504, 506
- Wolthuis, E., 547
- Woo, Y. H., 84, 85, 505, 506
- Wood, F. C., 235
- Wood, W. A., 448, 465, 478
- Wood, 533
- Woodcock, A. H., 555
- Woods, R. C., 255, 273, 286, 291
- Woodyard, O. C., 433
- Wool, 533
- Work function, photoelectric, 543  
 Sommerfeld, 543  
 thermionic, 12, 543
- Wrede, W., 75
- Wrinch, D. M., 533
- Wyckoff, R. W. G., 10, 110, 346, 371, 377, 417, 587
- Wyckoff notation, 311
- Wyckoff scale, 377

## X

- X-ograph, 173
- X-ray or x-rays, absorption, 71  
 detection, 168  
 diffraction, 96, 320  
 film, 173  
 frequency, 21  
 generation, 6, 20, 45, 105  
 hard, 34  
 measurement, 168  
 in medicine, 211  
 micrography, 288, 482  
 microscope, 363  
 monochromatic, 72  
 nature of, 20  
 as particles, 24  
 photography, 173  
 polarized, 37, 49, 90

X-ray or x-rays, protection, 198, 201  
  refraction, 96, 97, 327  
  registration, 168  
  scattering, 71, 77, 88, 331  
  secondary, 71, 76  
  soft, 34  
  therapy, 3, 225-238  
  tubes, 6-19, 105-118  
  velocity of, 20, 98, 561  
  as waves, 21  
X-unit, 337, 339

## Y

Yamaguchi, S., 553  
Yearian, H. J., 545  
Yield point, 468, 478, 479, 483

Youtz, J. P., 105  
Yukawa particle, 157

## Z

Z-section method, 528, 529  
Zachariasen, W. H., 478, 512  
Zavalles, C. T., 107, 296  
Zener, C., 478  
Zernike, F., 508  
Zinc, 472, 473, 524  
  die castings, 275  
Zone, 317  
Zone axes, 317  
Zucker, M., 148, 193  
Zwicky, F., 368  
Zworykin, V. K., 196